REFERENCE DATA

for RADIO ENGINEERS

fourth edition

INTERNATIONAL
TELEPHONE AND TELEGRAPH CORPORATION
320 Park Avenue, New York 22, New York

Fourth Edition

First Printing; September, 1956
Second Printing; January, 1957
Third Printing; March, 1957
Fourth Printing; July, 1957
Fifth Printing; December, 1959
Sixth Printing; November, 1960
Seventh Printing; July, 1961
Eighth Printing; September, 1962

Printed in United States of America by
American Book—Stratford Press Incorporated
New York, New York

55

Foreword

E. Washington Stewart III

The first American edition of Reference Data for Radio Engineers was published by Federal Telephone and Radio Corporation in 1943. It was suggested by a 60-page brochure of that title issued in 1942 by Standard Telephones and Cables Limited, an English subsidiary of the International Telephone and Telegraph Corporation.

Expanded American editions published in 1946 and 1949 were stimulated by the widespread acceptance of the book by practicing engineers and by universities, technical schools, and colleges, in many of which it has become an accepted text. This fourth edition is sponsored by the International Telephone and Telegraph Corporation in behalf of its research, engineering, and manufacturing companies throughout the world.

Federal Telecommunication Laboratories Division of International Telephone and Telegraph Corporation has continued its major role of directing and approving the technical contents of all the editions published in the United States.

While dominantly the cooperative efforts of engineers in the International System, some of the material was obtained from other sources. Acknowledgement is made of contributions to the third and fourth editions by J. G. Truxal of the Polytechnic Institute of Brooklyn; J. R. Ragazzini and L. A. Zadeh of Columbia University; C. L. Hogan and H. R. Mimno of Harvard University; P. T. Demos, E. J. Eppling, A. G. Hill, and L. D. Smullin of Massachusetts Institute of Technology, and by A. Abbot, M. S. Buyer, J. J. Caldwell, Jr., M. J. DiToro, S. F. Frankel, G. H. Gray, R. E. Houston, H. P. Iskenderian, R. W. Kosley, George Lewis, R. F. Lewis, E. S. McLarn, S. Moskowitz, J. J. Nail, E. M. Ostlund, B. Parzen, Haraden Pratt, A. M. Stevens, and A. R. Vallarino.

Special credit is due to W. L. McPherson, who compiled the original British editions, and to H. T. Kohlhaas and F. J. Mann, editors of the first two and the third American editions, respectively. The present members of the International System who contributed to the fourth edition are listed on the following page.

Editorial Board

H. P. Westman, ***editor***

J. E. Schlaikjer, ***assistant editor***

International Telephone and Telegraph Corporation

H. H. Buttner
E. M. Deloraine
E. D. Phinney

Farnsworth Electronics Company

A. Henderson
H. Salinger

Federal Telecommunication Laboratories

R. T. Adams
F. J. Altman
C. R. Brown
T. G. Brown
J. H. Brundage
T. F. Buck
F. X. Bucher
H. G. Busignies
A. G. Clavier
L. A. deRosa
G. A. Deschamps
M. Dishal
D. S. Duguid
L. Feit
R. E. Gray
J. F. Heney
R. B. Hoffman
J. L. Jatlow
A. G. Kandoian
S. Klein
P. P. Lantzy
G. R. Leef
D. J. LeVine
W. W. Macalpine
T. J. Marchese
M. Masonson
C. R. Muller
F. A. Muller
H. G. Nordlin
P. F. Panter
H. A. Peretko
R. L. Plouffe
L. Pollock
J. H. Reynolds
P. C. Sandretto
E. J. Setescak
W. Sichak
H. R. Terhune
N. S. Tierney
M. W. Wallace
R. L. Whittle
A. K. Wing, Jr.

Federal Telephone and Radio Company

W. F. Bonner
M. Enderlin
R. A. Felmly
W. H. Hawk
M. Lilienstein
K. R. Stephanz

Kellogg Switchboard and Supply Company

B. E. Swanson
C. E. Wood

Mackay Radio and Telegraph Company

R. McSweeny
G. T. Royden
C. E. Scholz
L. Spangenberg

Standard Telecommunication Laboratories, Limited

A. H. W. Beck

Standard Telephones and Cables, Limited

W. L. McPherson
E. A. Richards
C. E. Strong

Contents

frequency spectrum

Reference Data for Radio Engineers — Fourth Edition

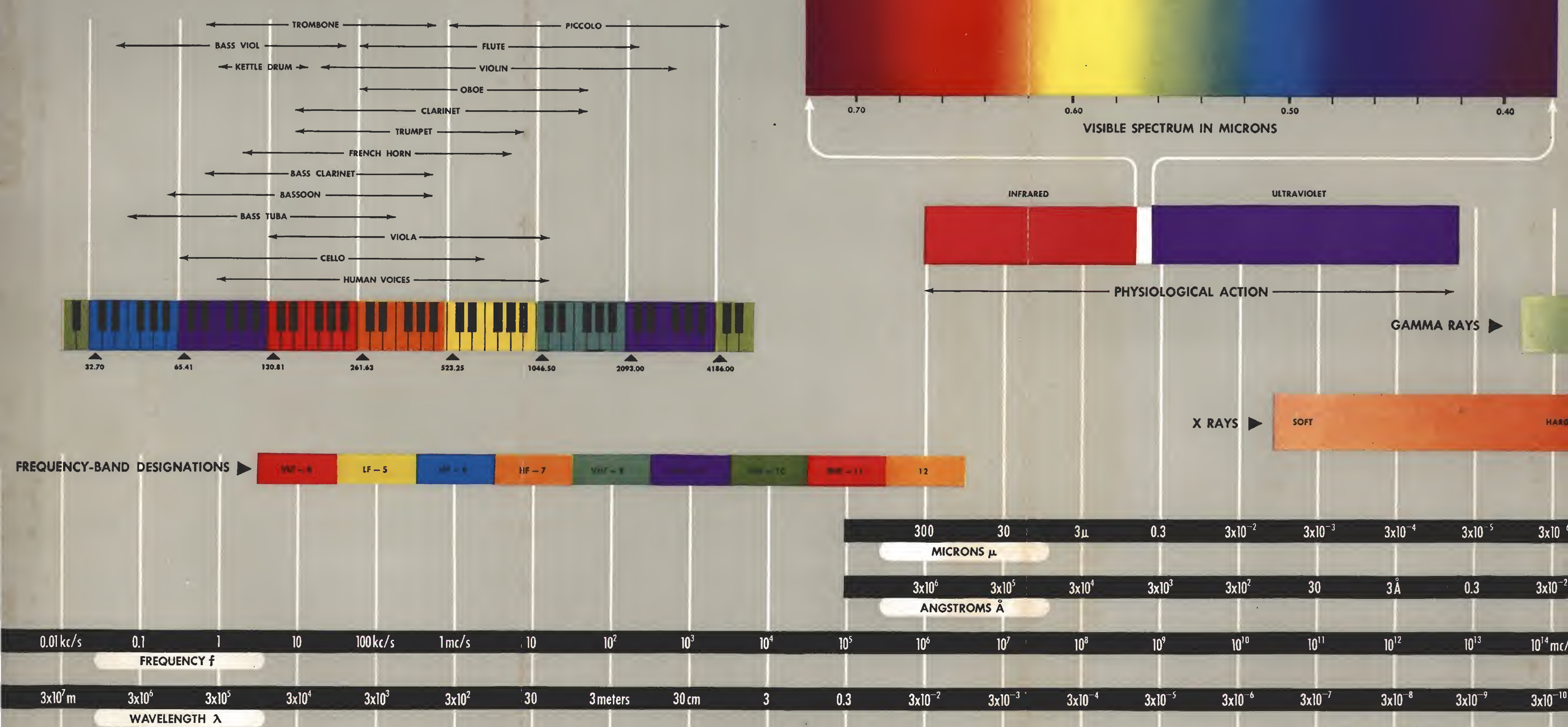

Frequency data

Wavelength–frequency conversion

The graph given below permits conversion between frequency and wavelength; by use of multiplying factors such as those at the bottom of the page, this graph will cover any portion of the electromagnetic-wave spectrum.

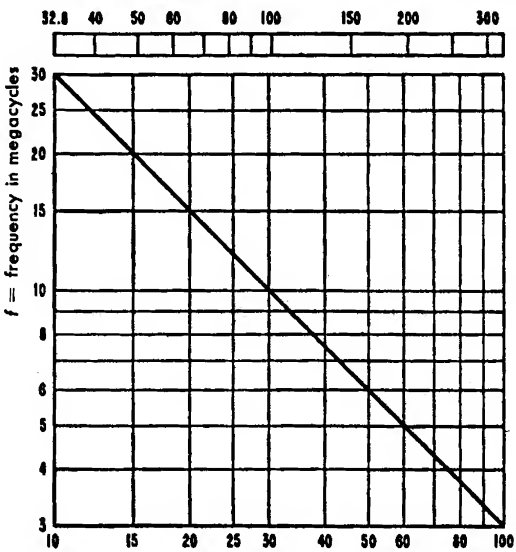

for frequencies from	multiply f by	multiply λ by
0.03 – 0.3 megacycles	0.01	100
0.3 – 3.0 megacycles	0.1	10
3.0 – 30 megacycles	1.0	1.0
30 – 300 megacycles	10	0.1
300 – 3,000 megacycles	100	0.01
3,000 – 30,000 megacycles	1,000	0.001
30,000 –300,000 megacycles	10,000	0.0001

Wavelength–frequency conversion *continued*

Conversion formulas

Propagation velocity $c \approx 3 \times 10^8$ meters/second

$$\text{Wavelength in meters } \lambda_m = \frac{300{,}000}{f \text{ in kilocycles}} = \frac{300}{f \text{ in megacycles}}$$

$$\text{Wavelength in feet } \lambda_{ft} = \frac{984{,}000}{f \text{ in kilocycles}} = \frac{984}{f \text{ in megacycles}}$$

$$\begin{aligned} 1 \text{ Angstrom unit } \mathring{A} &= 3.937 \times 10^{-9} \text{ inch} \\ &= 1 \times 10^{-10} \text{ meter} \\ &= 1 \times 10^{-4} \text{ micron} \end{aligned}$$

$$\begin{aligned} 1 \text{ micron } \mu &= 3.937 \times 10^{-5} \text{ inch} \\ &= 1 \times 10^{-6} \text{ meter} \\ &= 1 \times 10^{4} \text{ Angstrom units} \end{aligned}$$

Nomenclature of frequency bands

In accordance with the Atlantic City Radio Convention of 1947, frequencies should be expressed in kilocycles/second at and below 30,000 kilocycles, and in megacycles/second above this frequency. The band designations as decided upon at Atlantic City and as later modified by Comite Consultatif International Radio Recommendation No. 142 in 1953 are as follows

band number	frequency range	metric subdivision	Atlantic City frequency subdivision	
4	3– 30 kc	Myriametric waves	VLF	Very-low frequency
5	30– 300 kc	Kilometric waves	LF	Low frequency
6	300– 3,000 kc	Hectometric waves	MF	Medium frequency
7	3,000– 30,000 kc	Decametric waves	HF	High frequency
8	30– 300 mc	Metric waves	VHF	Very-high frequency
9	300– 3,000 mc	Decimetric waves	UHF	Ultra-high frequency
10	3,000– 30,000 mc	Centimetric waves	SHF	Super-high frequency
11	30,000– 300,000 mc	Millimetric waves	EHF	Extremely-high frequency
12	300,000–3,000,000 mc	Decimillimetric waves	—	—

Note that band "N" extends from 0.3×10^N to 3×10^N cy; thus band 4 designates the frequency range 0.3×10^4 to 3×10^4 cy. The upper limit is included in each band; the lower limit is excluded.

Description of bands by means of adjectives is arbitrary and the CCIR recommends that it be discontinued, e.g., "ultra-high frequency" should not be used to describe the range 300 to 3000 mc.

Nomenclature of frequency bands *continued*

Letter designations for frequency bands: Letters such as *X* have been employed in the past to indicate certain bands. These terms were originally used for military secrecy, but they were later mentioned in general technical literature. Those most often used are shown in Fig. 4 of the chapter "Radar fundamentals."

The letter designations have no official standing and the limits of the band associated with each letter are not accurately defined.

Frequency allocations by international treaty

For purposes of frequency allocations, the world has been divided into regions as shown in the figure.

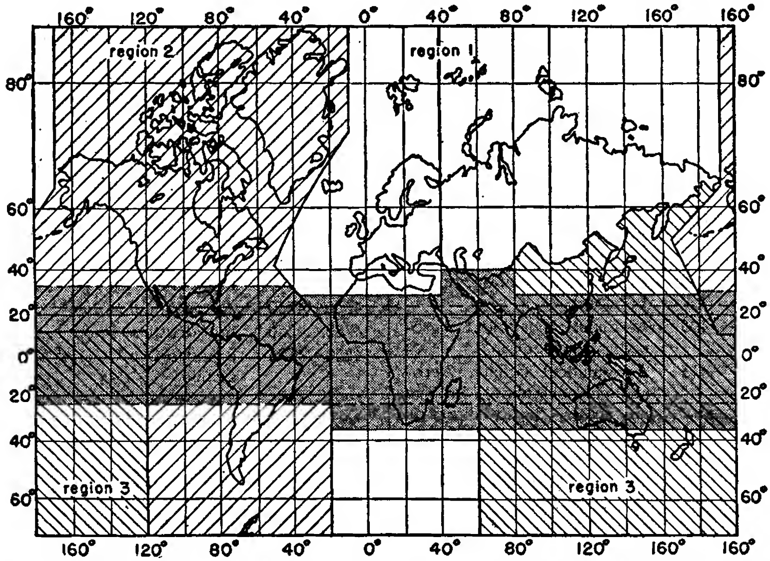

Regions defined in table of frequency allocations. Shaded area is the tropical zones

The following table of frequency allocations pertains to the western hemisphere (region 2). This allocation was adopted by the International Telecommunications Conference at Atlantic City in 1947 and was confirmed by the similar conference in Buenos Aires in 1952.

An asterisk (*) following a service designation indicates that the allocation has been made on a world-wide basis. All explanatory notes covering region 2 as well as other regions have been omitted. For these explanatory notes consult the texts of the Atlantic City and Buenos Aires Conventions

Frequency allocations by international treaty *continued*

which may be purchased from the Secretary General, International Telecommunications Union, Palais Wilson, Geneva, Switzerland.

Frequency assignments in the U.S.A. below 25 mc are in general accord with the following table. Above 25 mc, the U.S.A. assignments comply with the table, but the various bands have been subdivided among many services as shown in the listings on pages 12 to 15.

Assignments of frequencies in each country are subject to many special conditions. For the U.S.A. consult the Rules and Regulations of the Federal Communications Commission, which may be purchased from the Superintendent of Documents, Government Printing Office, Washington 25, D.C.

kilocycles	service
10– 14	Radio navigation*
14– 70	Fixed,* Maritime mobile*
70– 90	Fixed, Maritime mobile
90– 110	Fixed,* Maritime mobile,* Radio navigation*
110– 160	Fixed, Maritime mobile
160– 200	Fixed
200– 285	Aeronautical mobile, Aeronautical navigation
285- 325	Maritime navigation (radio beacons)
325– 405	Aeronautical mobile,* Aeronautical navigation*
405– 415	Aeronautical mobile, Aeronautical navigation, Maritime navigation (radio direction finding)
415– 490	Maritime mobile*
490– 510	Mobile (distress and calling)*
510– 535	Mobile
535– 1605	Broadcasting*
1605– 1800	Aeronautical navigation, Fixed, Mobile
1800– 2000	Amateur, Fixed, Mobile except aeronautical, Radio navigation
2000– 2065	Fixed, Mobile
2065– 2105	Maritime mobile
2105– 2300	Fixed, Mobile
2300– 2495	Broadcasting, Fixed, Mobile
2495– 2505	Standard frequency
2505– 2850	Fixed, Mobile
2850– 3155	Aeronautical mobile*
3155– 3200	Fixed,* Mobile except aeronautical mobile*
3200– 3400	Broadcasting,* Fixed,* Mobile except aeronautical mobile*
3400– 3500	Aeronautical mobile*
3500– 4000	Amateur, Fixed, Mobile except aeronautical
4000– 4063	Fixed*
4063– 4438	Maritime mobile*
4438– 4650	Fixed, Mobile except aeronautical
4650– 4750	Aeronautical mobile*
4750– 4850	Broadcasting, Fixed
4850– 4995	Broadcasting,* Fixed,* Land mobile*
4995– 5005	Standard frequency*
5005– 5060	Broadcasting,* Fixed*
5060– 5250	Fixed*
5250– 5450	Fixed, Land mobile
5450– 5480	Aeronautical mobile
5480– 5730	Aeronautical mobile*
5730– 5950	Fixed*
5950– 6200	Broadcasting*
6200– 6525	Maritime mobile*
6525– 6765	Aeronautical mobile*
6765– 7000	Fixed*
7000– 7100	Amateur*
7100– 7300	Amateur
7300– 8195	Fixed*
8195– 8815	Maritime mobile*
8815– 9040	Aeronautical mobile*
9040– 9500	Fixed*
9500– 9775	Broadcasting*
9775– 9995	Fixed*
9995–10005	Standard frequency*

Frequency allocations by international treaty *continued*

kilocycles	service
10005–10100	Aeronautical mobile*
10100–11175	Fixed*
11175–11400	Aeronautical mobile*
11400–11700	Fixed*
11700–11975	Broadcasting*
11975–12330	Fixed*
12330–13200	Maritime mobile*
13200–13360	Aeronautical mobile*
13360–14000	Fixed*
14000–14350	Amateur*
14350–14990	Fixed*
14990–15010	Standard frequency*
15010–15100	Aeronautical mobile*
15100–15450	Broadcasting*
15450–16460	Fixed*
16460–17360	Maritime mobile*
17360–17700	Fixed*
17700–17900	Broadcasting*
17900–18030	Aeronautical mobile*
18030–19990	Fixed*
19990–20010	Standard frequency*
20010–21000	Fixed*
21000–21450	Amateur*
21450–21750	Broadcasting*
21750–21850	Fixed*
21850–22000	Aeronautical fixed, Aeronautical mobile*
22000–22720	Maritime mobile*
22720–23200	Fixed*
23200–23350	Aeronautical fixed,* Aeronautical mobile*
23350–24990	Fixed,* Land mobile*
24990–25010	Standard frequency*
25010–25600	Fixed,* Mobile except aeronautical*
25600–26100	Broadcasting*
26100–27500	Fixed,* Mobile except aeronautical*
27500–28000	Fixed, Mobile
28000–29700	Amateur*

megacycles	service
29.7– 44	Fixed, Mobile
44 – 50	Broadcasting, Fixed, Mobile
50 – 54	Amateur
54 – 72	Broadcasting, Fixed, Mobile
72 – 76	Fixed, Mobile
76 – 88	Broadcasting, Fixed, Mobile
88 – 100	Broadcasting*
100 – 108	Broadcasting
108 – 118	Aeronautical navigation*
118 – 132	Aeronautical mobile*
132 – 144	Fixed, Mobile
144 – 146	Amateur*
146 – 148	Amateur
148 – 174	Fixed, Mobile
174 – 216	Broadcasting, Fixed, Mobile .
216 – 220	Fixed, Mobile
220 – 225	Amateur
225 – 235	Fixed, Mobile
235 – 328.6	Fixed,* Mobile*
328.6– 335.4	Aeronautical navigation*
335.4– 420	Fixed,* Mobile*
420 – 450	Aeronautical navigation,* Amateur*
450 – 460	Aeronautical navigation, Fixed, Mobile
460 – 470	Fixed,* Mobile*
470 – 585	Broadcasting*
585 – 610	Broadcasting
610 – 940	Broadcasting*
940 – 960	Fixed
960 – 1215	Aeronautical navigation*
1215 – 1300	Amateur*
1300 – 1660	Aeronautical navigation
1660 – 1700	Meteorological aids (radiosonde)
1700 – 2300	Fixed,* Mobile*
2300 – 2450	Amateur*
2450 – 2700	Fixed,* Mobile*
2700 – 2900	Aeronautical navigation*
2900 – 3300	Radio navigation*
3300 – 3500	Amateur
3500 – 3900	Fixed, Mobile
3900 – 4200	Fixed,* Mobile*
4200 – 4400	Aeronautical navigation*
4400 – 5000	Fixed,* Mobile*
5000 – 5250	Aeronautical navigation*
5250 – 5650	Radio navigation*
5650 – 5850	Amateur*
5850 – 5925	Amateur
5925 – 8500	Fixed,* Mobile*
8500 – 9800	Radio navigation*
9800 –10000	Fixed,* Radio navigation*
10000 –10500	Amateur*
Above 10500	Not allocated by Atlantic City Convention

Frequency allocations above 25 mc in U.S.A.

The following listings show the frequency bands above 25 mc allocated to various services in the U.S.A. as of 21 November 1956.* Note that many of these bands are shared by more than one service.

Government

Armed forces and other departments of the national government.

24.99 – 25.01	34.00 – 35.00	162.00 – 174.00	4400 – 5000
25.33 – 25.85	36.00 – 37.00	216.00 – 220.00	7125 – 8500
26.48 – 26.95	38.00 – 39.00	225.00 – 328.60	9800 – 10000
27.54 – 28.00	40.00 – 42.00	335.40 – 400.00	13225 – 16000
29.89 – 29.91	132.00 – 144.00	406.00 – 420.00	18000 – 21000
30.00 – 30.56	148.00 – 152.00	1700 –1850	22000 – 26000
32.00 – 33.00	157.05 – 157.25	2200 –2300	above 30000

Public safety

Police, fire, forestry, highway, and emergency services.

27.23 – 27.28	42.00 – 42.96	453 – 454	3500 – 3700
30.84 – 32.00	44.60 – 47.68	458 – 459	6425 – 6875
33.00 – 33.12	72.00 – 76.00	890 – 940	10550 – 10700
33.40 – 34.00	153.74 – 154.46	952 – 960	11700 – 12700
37.00 – 37.44	154.61 – 157.50	1850 – 1990	13200 – 13225
37.88 – 38.00	158.70 – 162.00	2110 – 2200	16000 – 18000
39.00 – 40.00	166.00 – 172.40	2450 – 2700	26000 – 30000

Industrial

Power, petroleum, pipe line, forest products, motion picture, press relay, builders, ranchers, factories, etc.

25.01 – 25.33	42.96 – 43.20	171.80 – 172.00	2110 – 2200
27.255	47.68 – 50.00	173.20 – 173.40	2450 – 2700
27.28 – 27.54	72.00 – 76.00	406.00 – 406.40	3500 – 3700
29.70 – 29.80	152.84 – 153.74	412.40 – 412.80	6425 – 6875
30.56 – 30.84	154.46 – 154.61	451.00 – 452.00	10550 – 10700
33.12 – 33.40	158.10 – 158.46	456.00 – 457.00	11700 – 12700
35.00 – 35.20	169.40 – 169.60	890 – 940	13200 – 13225
35.72 – 35.96	170.20 – 170.40	952 – 960	16000 – 18000
37.44 – 37.88	171.00 – 171.20	1850 –1990	26000 – 30000

Land transportation

Taxicabs, railroads, buses, trucks.

27.255	152.24 – 152.48	952 – 960	6425 – 6875
30.64 – 31.16	157.45 – 157.74	1850 – 1990	10550 – 10700
35.68 – 35.72	159.48 – 161.85	2110 – 2200	11700 – 12700
35.96 – 36.00	452 – 453	2450 – 2700	13200 – 13225
43.68 – 44.60	457 – 458	3500 – 3700	16000 – 18000
72.00 – 76.00	890 – 940		26000 – 30000

* These allocations are revised at frequent intervals. Specific information can be obtained from the Frequency Allocation and Treaty Division of the Federal Communications Commission; Washington 25, D. C.

Frequency allocations above 25 mc in U.S.A. *continued*

Domestic public

Message or paging services to persons and to individual stations, primarily mobile.

35.20 – 35.68	157.74 – 158.10	2450 – 2500	11700 – 12200
43.20 – 43.68	158.46 – 158.70	3500 – 3700	13200 – 13225
152.00 – 152.24	454 – 455	6425 – 6575	16000 – 18000
152.48 – 152.84	459 – 460	10550 –10700	26000 – 30000

Citizens radio

Personal radio services.

27.255
460 – 470

Common carrier fixed

Point-to-point telephone, telegraph, and program transmission for public use.

26.955	*76.00 – 88.00	2450 – 2500	10700 – 11700
29.80 – 29.89	†88 – 100	3700 – 4200	13200 – 13225
29.91 – 30.00	‡98 – 108	5925 – 6425	16000 – 18000
72.00 – 76.00	716 – 940	10550 –10700	26000 – 30000

* Territories of Alaska and Hawaii only.
† Territory of Alaska only.
‡ Territory of Hawaii only.

International control

Links between stations used for international communication and their associated control centers.

952 – 960	2100 – 2200	6575 – 6875
1850 – 1990	2500 – 2700	12200 – 12700

Television broadcasting

54 – 72	76 – 88	174 – 216	470 – 890

Frequency-modulation broadcasting

88 – 108

Television pickup, links, and intercity relay

Studio-to-transmitter links, etc.

890 – 940 (Sound only)	1990 – 2110	6875 – 7125	12700 – 13200

Frequency allocations above 25 mc in U.S.A. *continued*

FM and standard broadcasting links and intercity relay

Studio-to-transmitter links, etc.

890 – 952

Standard broadcasting remote pickup

25.85 – 26.48	166.0 – 170.2	455 – 456
152.84 – 153.38	450.0 – 451.0	

Aeronautical fixed

29.80 – 29.89	2500 – 2700	12200 – 12700
29.91 – 30.00	6575 – 6875	13200 – 13225
72.00 – 76.00	10550 – 10700	16000 – 18000
2450 – 2500		26000 – 30000

Aeronautical, air-to-ground

108 – 132	6425 – 6575	13200 – 13225
2450 – 2500	10550 – 10700	16000 – 18000
3500 – 3700	11700 – 12200	26000 – 30000

Flight-test telemetering

217.4 – 217.7	219.3 – 219.6

Aeronautical radio navigation

Instrument landing systems, ground control of approach, very-high-frequency omnidirectional range, tacan, etc.

75.0	960 – 1215	2700 – 3300	5000 – 5650
108.0 – 118.0	1300 – 1660	4200 – 4400	8500 – 9800
328.6 – 335.4			

Radio navigation and radio location

Civilian radar, racon, etc.

2900 – 3300	5250 – 5650	8500 – 9800

Meteorological aids

Radiosondes, etc.

400 – 406	1660 – 1700	2700 – 2900

Frequency allocations above 25 mc in U.S.A. *continued*

Maritime

Communication between ships and/or coastal stations.

27.255	43.0 – 43.2	*72.0 – 76.0	156.25 – 157.45
35.04 – 35.20			161.85 – 162.00

* For point-to-point use only.

Amateur

26.96 – 27.23	220 – 225	2300 – 2450	10000 – 10500
28.00 – 29.70	420 – 450	3300 – 3500	21000 – 22000
50.00 – 54.00	1215 – 1300	5650 – 5925	Above 30000
144.00 – 148.00			

Industrial, scientific, and medical equipment

27.12	915	5850	18000
40.68	2450		

International call-sign prefixes

AAA–ALZ	United States of America
AMA–AOZ	Spain
APA–ASZ	Pakistan
ATA–AWZ	India
AXA–AXZ	Commonwealth of Australia
AYA–AZZ	Republic of Argentina
BAA–BZZ	China
CAA–CEZ	Chile
CFA–CKZ	Canada
CLA–CMZ	Cuba
CNA–CNZ	Morocco
COA–COZ	Cuba
CPA–CPZ	Bolivia
CQA–CRZ	Portuguese Colonies
CSA–CUZ	Portugal
CVA–CXZ	Uruguay
CYA–CZZ	Canada
DAA–DMZ	Germany
DNA–DQZ	Belgian Congo – Ruanda-Urundi
DRA–DTZ	Byelorussian Soviet Socialist Republic
DUA–DZZ	Republic of the Philippines
EAA–EHZ	Spain
EIA–EJZ	Ireland
EKA–EKZ	Union of Soviet Socialist Republics
ELA–ELZ	Republic of Liberia
EMA–EOZ	Union of Soviet Socialist Republics
EPA–EQZ	Iran
ERA–ERZ	Union of Soviet Socialist Republics
ESA–ESZ	Estonia
ETA–ETZ	Ethiopia
EUA–EZZ	Union of Soviet Socialist Republics
FAA–FZZ	France and Colonies and Protectorates
GAA–GZZ	Great Britain
HAA–HAZ	Hungary
HBA–HBZ	Switzerland
HCA–HDZ	Ecuador
HEA–HEZ	Switzerland
HFA–HFZ	Poland
HGA–HGZ	Hungary
HHA–HHZ	Republic of Haiti
HIA–HIZ	Dominican Republic
HJA–HKZ	Republic of Colombia
HLA–HMZ	Korea
HNA–HNZ	Iraq
HOA–HPZ	Republic of Panama
HQA–HRZ	Republic of Honduras
HSA–HSZ	Siam
HTA–HTZ	Nicaragua
HUA–HUZ	Republic of El Salvador
HVA–HVZ	Vatican City State
HWA–HYZ	France and Colonies and Protectorates
HZA–HZZ	Kingdom of Saudi Arabia
IAA–IZZ	Italy and Colonies
JAA–JSZ	Japan
JTA–JVZ	Mongolian People's Republic
JWA–JXZ	Norway
JYA–JYZ	Hashimite Kingdom of Jordan
JZA–JZZ	Netherlands New Guinea
KAA–KZZ	United States of America

International call-sign prefixes 'continued

LAA–LNZ	Norway
LOA–LWZ	Argentine Republic
LXA–LXZ	Luxembourg
LYA–LYZ	Lithuania
LZA–LZZ	Bulgaria
MAA–MZZ	Great Britain
NAA–NZZ	United States of America
OAA–OCZ	Peru
ODA–ODZ	Republic of Lebanon
OEA–OEZ	Austria
OFA–OJZ	Finland
OKA–OMZ	Czechoslovakia
ONA–OTZ	Belgium and Colonies
OUA–OZZ	Denmark
PAA–PIZ	Netherlands
PJA–PJZ	Netherlands Antilles
PKA–POZ	Republic of Indonesia
PPA–PYZ	Brazil
PZA–PZZ	Surinam
QAA–QZZ	(Service abbreviations)
RAA–RZZ	Union of Soviet Socialist Republics
SAA–SMZ	Sweden
SNA–SRZ	Poland
SSA–SUZ	Egypt
SVA–SZZ	Greece
TAA–TCZ	Turkey
TDA–TDZ	Guatemala
TEA–TEZ	Costa Rica
TFA–TFZ	Iceland
TGA–TGZ	Guatemala
THA–THZ	France and Colonies and Protectorates
TIA–TIZ	Costa Rica
TJA–TZZ	France and Colonies and Protectorates
UAA–UQZ	Union of Soviet Socialist Republics
URA–UTZ	Ukranian Soviet Socialist Republic
UUA–UZZ	Union of Soviet Socialist Republics
VAA–VGZ	Canada
VHA–VNZ	Commonwealth of Australia
VOA–VOZ	Canada
VPA–VSZ	British Colonies and Protectorates
VTA–VWZ	India
VXA–VYZ	Canada
VZA–VZZ	Commonwealth of Australia
WAA–WZZ	United States of America
XAA–XIZ	Mexico
XJA–XOZ	Canada
XPA–XPZ	Denmark
XQA–XRZ	Chile
XSA–XSZ	China
XTA–XTZ	France and Colonies and Protectorates
XUA–XUZ	Cambodia
XVA–XVZ	Viet-Nam
XWA–XWZ	Laos
XXA–XXZ	Portuguese Colonies
XYA–XZZ	Burma
YAA–YAZ	Afghanistan
YBA–YHZ	Indonesia
YIA–YIZ	Iraq
YJA–YJZ	New Hebrides
YKA–YKZ	Syria
YLA–YLZ	Latvia
YMA–YMZ	Turkey
YNA–YNZ	Nicaragua
YOA–YRZ	Roumania
YSA–YSZ	Republic of El Salvador
YTA–YUZ	Yugoslavia
YVA–YYZ	Venezuela
YZA–YZZ	Yugoslavia
ZAA–ZAZ	Albania
ZBA–ZJZ	British Colonies and Protectorates
ZKA–ZMZ	New Zealand
ZNA–ZOZ	British Colonies and Protectorates
ZPA–ZPZ	Paraguay
ZQA–ZQZ	British Colonies and Protectorates
ZRA–ZUZ	Union of South Africa
ZVA–ZZZ	Brazil
2AA–2ZZ	Great Britain
3AA–3AZ	Principality of Monaco
3BA–3FZ	Canada
3GA–3GZ	Chile
3HA–3UZ	China
3VA–3VZ	Tunisia
3WA–3WZ	Viet-Nam
3YA–3YZ	Norway
3ZA–3ZZ	Poland
4AA–4CZ	Mexico
4DA–4IZ	Republic of the Philippines
4JA–4LZ	Union of Soviet Socialist Republics
4MA–4MZ	Venezuela
4NA–4OZ	Yugoslavia
4PA–4SZ	Ceylon
4TA–4TZ	Peru
4UA–4UZ	United Nations
4VA–4VZ	Republic of Haiti
4WA–4WZ	Yemen
4XA–4XZ	Israel
4YA–4YZ	International Civil Aviation Organization
5AA–5AZ	Libya
5CA–5CZ	Morocco
6AA–6ZZ	(Not allocated)
7AA–7ZZ	(Not allocated)
8AA–8ZZ	(Not allocated)
9AA–9AZ	San Marino
9NA–9NZ	Nepal
9SA–9SZ	Saar

Frequency tolerances *Atlantic City, 1947*

frequency band	type of service and power	tolerance in percent
10–535 kc	Fixed stations	
	10–50 kc	0.1
	50 kc–end of band	0.02
	Land stations	
	Coast stations	
	Power > 200 watts	0.02
	Power < 200 watts	0.05
	Aeronautical stations	0.02
	Mobile stations	
	Ship stations	0.1
	Aircraft stations	0.05
	Emergency (reserve) ship transmitters, and lifeboat, lifecraft, and survival-craft transmitters	0.5
	Radionavigation stations	0.02
	Broadcasting stations	20 cycles
535–1605 kc	Broadcasting stations	20 cycles
1605–4000 kc	Fixed stations	
	Power > 200 watts	0.005
	Power < 200 watts	0.01
	Land stations	
	Coast stations	
	Power > 200 watts	0.005
	Power < 200 watts	0.01
	Aeronautical stations	
	Power > 200 watts	0.005
	Power < 200 watts	0.01
	Base stations	
	Power > 200 watts	0.005
	Power < 200 watts	0.01
	Mobile stations	
	Ship stations	0.02
	Aircraft stations	0.02
	Land mobile stations	0.02
	Radionavigation stations	
	Power > 200 watts	0.005
	Power < 200 watts	0.01
	Broadcasting stations	0.005

Frequency tolerances *continued*

frequency band	type of service and power	tolerance in percent
4000–30,000 kc	Fixed stations	
	Power > 500 watts	0.003
	Power < 500 watts	0.01
	Land stations	
	Coast stations	0.005
	Aeronautical stations	
	Power > 500 watts	0.005
	Power < 500 watts	0.01
	Base stations	
	Power > 500 watts	0.005
	Power < 500 watts	0.01
	Mobile stations	
	Ship stations	0.02
	Aircraft stations	0.02
	Land mobile stations	0.02
	Transmitters in lifeboats, lifecraft, and survival craft	0.02
	Broadcasting stations	0.003
30–100 mc	Fixed stations	0.02
	Land stations	0.02
	Mobile stations	0.02
	Radionavigation stations	0.02
	Broadcasting stations	0.003
100–500 mc	Fixed stations	0.01
	Land stations	0.01
	Mobile stations	0.01
	Radionavigation stations	0.02
	Broadcasting stations	0.003
500–10,500 mc	———	0.75

Note: Requirements in the U.S.A. with respect to frequency tolerances are in all cases at least as restrictive (and for some services more restrictive) than the tolerances specified by the Atlantic City Convention. For details consult the Rules and Regulations of the Federal Communications Commission.

Intensity of harmonics *Atlantic City, 1947*

In the band 10–30,000 kilocycles, the power of a harmonic or a parasitic emission supplied to the antenna must be at least 40 decibels below the power of the fundamental. In no case shall it exceed 200 milliwatts (mean power). For mobile stations, endeavor will be made, as far as it is practicable, to reach the above figures.

Designation of emissions

Emissions are designated according to their classification and the width of the frequency band occupied by them. Classification is according to type of modulation, type of transmission, and supplementary characteristics.

type of modulation	type of transmission	supplementary characteristics	symbol
Amplitude modulation	Absence of any modulation	——	A0
	Telegraphy without the use of modulating audio frequency (on-off keying)	——	A1
	Telegraphy by the keying of a modulating audio frequency or audio frequencies, or by the keying of the modulated emission (Special case: An unkeyed modulated emission.)	——	A2
	Telephony	Double sideband, full carrier	A3
		Single sideband, reduced carrier	A3a
		Two independent sidebands, reduced carrier	A3b
	Facsimile	——	A4
	Television	——	A5
	Composite transmissions and cases not covered by the above	——	A9
	Composite transmissions	Reduced carrier	A9c
Frequency (or phase) modulation	Absence of any modulation	——	F0
	Telegraphy without the use of modulating audio frequency (frequency-shift keying)	——	F1
	Telegraphy by the keying of a modulating audio frequency or audio frequencies, or by the keying of the modulated emission (Special case: An unkeyed emission modulated by audio frequency.)	——	F2
	Telephony	——	F3
	Facsimile	——	F4
	Television	——	F5
	Composite transmissions and cases not covered by the above	——	F9

Designation of emissions *continued*

type of modulation	type of transmission	supplementary characteristics	symbol
Pulse modulation	Absence of any modulation intended to carry information	——	P0
	Telegraphy without the use of modulating audio frequency	——	P1
	Telegraphy by the keying of a modulating audio frequency or audio frequencies, or by the keying of the modulated pulse (Special case: An unkeyed modulated pulse.)	Audio frequency or audio frequencies modulating the pulse in amplitude	P2d
		Audio frequency or audio frequencies modulating the width of the pulse	P2e
		Audio frequency or audio frequencies modulating the phase (or position) of the pulse	P2f
	Telephony	Amplitude modulated	P3d
		Width modulated	P3e
		Phase (or position) modulated	P3f
	Composite transmission and cases not covered by the above	——	P9

Note: As an exception to the above principles, damped waves are designated by B.

Wherever the full designation of an emission is necessary, the symbol for that class of emission, as given above, is prefixed by a number indicating the necessary bandwidth in kilocycles occupied by it. Bandwidths of 10 kilocycles or less shall be expressed to a maximum of two significant figures after the decimal.

The necessary bandwidth is that required in the over-all system, including both the transmitter and the receiver, for the proper reproduction at the receiver of the desired information and does not necessarily indicate the interfering characteristics of an emission.

The following tables present some examples of the designation of emissions as a guide to the principles involved.

Designation of emissions *continued*

description	designation
Telegraphy 25 words/minute, international Morse code, carrier modulated by keying only	0.1AI
Telegraphy, 525-cycle tone, 25 words/minute, international Morse code, carrier and tone keyed or tone keyed only	1.15A2
Amplitude-modulated telephony, 3000-cycle maximum modulation, double sideband, full carrier	6A3
Amplitude-modulated telephony, 3000-cycle maximum modulation, single sideband, reduced carrier	3A3a
Amplitude-modulated telephony, 3000-cycle maximum modulation, two independent sidebands, reduced carrier	6A3b
Vestigial-sideband television (one sideband partially suppressed), full carrier (including a frequency-modulated sound channel)	6000A5, F3
Frequency-modulated telephony, 3000-cycle modulation frequency, 20,000-cycle deviation	46F3
Frequency-modulated telephony, 15,000-cycle modulation frequency, 75,000-cycle deviation	180F3
One-microsecond pulses, unmodulated, assuming a value of $K = 5$	10000P0

Determination of bandwidth *Atlantic City, 1947*

For the determination of the necessary bandwidth, the following table may be considered as a guide. In the formulation of the table, the following working terms have been employed:

B = telegraph speed in bauds (see pp. 541 and 846)

N/T = maximum possible number of black+white elements to be transmitted per second, in facsimile and television

M = maximum modulation frequency expressed in cycles/second

D = half the difference between the maximum and minimum values of the instantaneous frequencies; D being greater than $2M$, greater than N/T, or greater than B, as the case may be. Instantaneous frequency is the rate of change of phase

t = pulse length expressed in seconds

K = over-all numerical factor that differs according to the emission and depends upon the allowable signal distortion and, in television, the time lost from the inclusion of a synchronizing signal

Determination of bandwidth *continued*

Amplitude modulation

description and class of emission	necessary bandwidth in cycles/second	examples: details	examples: designation of emission
Continuous-wave telegraphy A1	Bandwidth = BK where K = 5 for fading circuits = 3 for nonfading circuits	Morse code at 25 words/minute, $B = 20$; bandwidth = 100 cycles	0.1A1
		Four-channel multiplex with 7-unit code, 60 words/minute/channel, $B = 170$, $K = 5$; bandwidth = 850 cycles	0.85A1
Telegraphy modulated at audio frequency A2	Bandwidth = $BK + 2M$ where K = 5 for fading circuits = 3 for nonfading circuits	Morse code at 25 words/minute, 1000-cycle tone, $B = 20$; bandwidth = 2100 cycles	2.1A2
Commercial telephony A3	Bandwidth = M for single sideband = $2M$ for double sideband	For ordinary single-sideband telephony, $M = 3000$	3A3a
		For high-quality single-sideband telephony, $M = 4000$	4A3a
Broadcasting A3	Bandwidth = $2M$	M is between 4000 and 10,000 depending upon the quality desired	8A3 to 20A3
Facsimile, carrier modulated by tone and by keying A4	Bandwidth = $\frac{KN}{T} + 2M$ where $K = 1.5$	Total number of picture elements (black+white) transmitted per second = circumference of cylinder (height of picture) × lines/unit length × speed of cylinder rotation (revolutions/second). If diameter of cylinder = 70 millimeters, lines/millimeter = 3.77, speed of rotation = 1/second, frequency of modulation = 1800 cycles; bandwidth = 3600 + 1242 = 4842 cycles	4.84A4
Television A5	Bandwidth = KN/T where K = 1.5 (This allows for synchronization and filter shaping.) *Note:* This band can be reduced when asymmetrical transmission is employed	Total picture elements (black+white) transmitted per second = number lines forming each image × elements/line × pictures transmitted/second. If lines = 500, elements/line = 500, pictures/second = 25; bandwidth ≈ 9 megacycles	9000A5

Determination of bandwidth *continued*

Frequency modulation

description and class of emission	necessary bandwidth in cycles/second	examples: details	examples: designation of emission
Frequency-shift telegraphy* F1	Bandwidth $= BK + 2D$ where $K = 5$ for fading circuits $= 3$ for nonfading circuits	Morse code at 100 words/ minute. $B = 80$, $K = 5$, $D = 425$; bandwidth $= 1250$ cycles	1.25F1
		Four-channel multiplex with 7-unit code, 60 words/minute/channel. Then, $B = 170$, $K = 5$, $D = 425$; bandwidth $= 1700$ cycles	1.7F1
Commercial telephony and broad-casting F3	Bandwidth $= 2M + 2DK$ For commercial telephony, $K = 1$. For high-fidelity transmission, higher values of K may be necessary	For an average case of commercial telephony, with $D = 15{,}000$ and $M = 3000$; bandwidth $= 36{,}000$ cycles	36F3
Facsimile F4	Bandwidth $= \frac{KN}{T} + 2M + 2D$ where $K = 1.5$	(See facsimile, amplitude modulation.) Cylinder diameter = 70 millimeters, lines/millimeter = 3.77, cylinder rotation speed = 1/second, modulation tone = 1800 cycles, $D = 10{,}000$ cycles; bandwidth $\approx 25{,}000$ cycles	25F4
Unmodulated pulse P0	Bandwidth $= 2K/t$ where K varies from 1 to 10 according to the permissible deviation in each particular case from a rectangular pulse shape. In many cases the value of K need not exceed 6	$t = 3 \times 10^{-6}$ and $K = 6$; bandwidth $= 4 \times 10^{6}$ cycles	4000P0
Modulated pulse P2 or P3	Bandwidth depends upon the particular types of modulation used	——	——

* CCIR Recommendation No. 87 (London, 1953) for F1 emission was
Bandwidth $= 0.5B + 2.5D$ for $2.5 < 2D/B < 8$
Bandwidth $= 2.5B + 2.0D$ for $8 < 2D/B < 20$

Standard frequencies and time signals

WWV and WWVH* *as of March, 1956*

The National Bureau of Standards operates radio stations WWV (near Washington, D.C.) and WWVH (Maui, Hawaii) which transmit standard radio frequencies, standard time intervals, time announcements, standard musical pitch, standard audio frequencies, and radio propagation notices.

Standard frequencies are transmitted continuously day and night except as follows:

WWV is silent for approximately 4 minutes beginning at 45 minutes ± 15 seconds after each hour.

WWVH is silent for 4 minutes following each hour and each half hour.

WWVH is silent for 34 minutes each day beginning at 1900 UT (Universal Time).

Vertical dipole antennas are employed and 100-percent amplitude double-sideband modulation is used for second pulses and announcements. The audio tones on WWV are transmitted as a single upper sideband with full carrier. Power output from the sideband transmitter is about one-third of the carrier power.

standard frequency in mc	WWV power in kw	WWVH power in kw
2.5	0.7	—
5	8.0	2.0
10	9.0	2.0
15	9.0	2.0
20	1.0	—
25	0.1	—

Audio frequencies and musical pitch: Two standard audio frequencies, 440 and 600 cycles per second, are broadcast on all carrier frequencies. The audio frequencies are given alternately, starting with 600 cycles on the hour for 3 minutes, interrupted 2 minutes, followed by 440 cycles for 3 minutes,

* Based on U.S. Dept. of Commerce, National Bureau of Standards, Letter Circular LC 1009 with corrections. Information on these services may be obtained from the Radio Standards Division, National Bureau of Standards; Boulder, Colorado.

Standard frequencies and time signals *continued*

and interrupted 2 minutes. Each 10-minute period is the same. The 440-cycle tone is the standard musical pitch A above middle C.

Time signals and standard time intervals: The audio frequencies are interrupted for intervals of precisely 2 minutes. They are resumed precisely on the hour and each 5 minutes thereafter. They are in agreement with the basic time service of the U.S. Naval Observatory so that they mark accurately the hour and the successive 5-minute periods.

Universal Time (Greenwich Civil Time or Greenwich Mean Time) is announced in international Morse code each five minutes starting with 0000 (midnight). Time announcements in Morse code are given just prior to and refer to the moment of return of the audio frequencies.

A voice announcement of Eastern Standard Time is given each 5 minutes from station WWV; this precedes and follows each telegraphic-code announcement.

A pulse or tick, of 0.005-second duration, occurs at intervals of precisely 1 second. Each pulse on WWV consists of 5 cycles of 1000-cycle tone and each pulse on WWVH consists of 6 cycles of 1200-cycle tone.

The tones of WWV are interrupted precisely 40 milliseconds each second except at the beginning and end of each 3-minute tone interval. The time pulse commences precisely 10 milliseconds after commencement of the 40-millisecond interruption. An additional pulse, 0.1 second later, is transmitted to identify the beginning of each minute. No pulse is transmitted at the beginning of the last second of each minute.

Accuracy: Frequencies transmitted from WWV and WWVH are accurate to within 1 part in 10^8; this is with reference to the mean solar second, 100-day interval, as determined by the U.S. Naval Observatory with a precision of better than 3 parts in 10^9. Time intervals, as transmitted, are accurate within $\pm$ 2 parts in 10^8 + 1 microsecond.

Frequencies received may be as accurate as those transmitted for several hours per day during total light or total darkness over the transmission path at locations in the service range. During the course of the day, errors in the received frequencies may vary approximately between -3 to $+3$

Standard frequencies and time signals *continued*

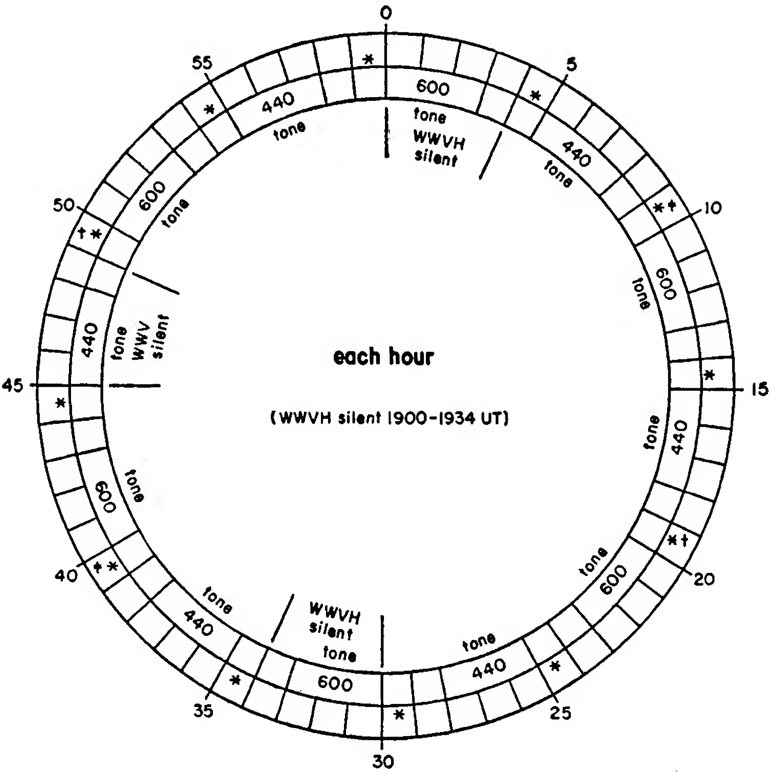

* One-minute announcement intervals:

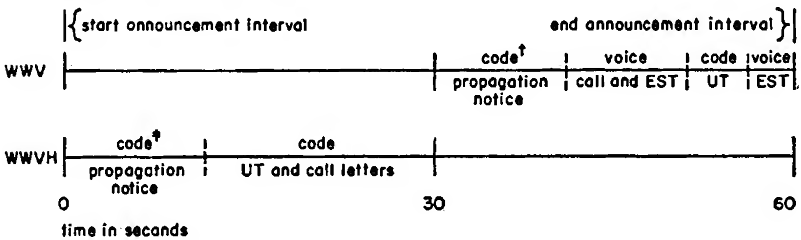

† North Atlantic propagation notice at 19.5 and 49.5 minutes past each hour.

‡ North Pacific propagation notice at 9 and 39 minutes past each hour.

Audio frequencies and announcements of WWV and WWVH.

Standard frequencies and time signals *continued*

parts in 10^7. During ionospheric storms, transient conditions in the propagating medium may cause momentary change as large as 1 part in 10^6.

Time intervals, as received, are normally accurate within $\pm$ 2 parts in $10^8 + 1$ millisecond. Transient conditions in the ionosphere at times cause received pulses to scatter by several milliseconds.

Radio propagation notices:* WWV broadcasts for the North Atlantic path at 19½ and 49½ minutes past every hour. The forecasts are changed daily at 0500, 1200, 1700, or 2300 Universal Time and remain unchanged for the following 6 hours. The letter–digit combination is sent as a modulated tone in international Morse code, the letter indicating conditions at 0500, 1200, 1700, or 2300 UT, respectively, and the digit the conditions forecast for the following 6-hour period. On WWVH, the forecasts as broadcast are changed at 0200 and 1800 UT and are for the next 9-hour period, these WWVH forecasts being broadcast at 9 and 39 minutes past each hour for the North Pacific path.

The letters and digits signify radio propagation quality as follows:

condition at 0500, 1200, 1700, or 2300 UT		forecast	propagation conditions
W	Disturbed	1	Useless
W		2	Very poor
W		3	Poor
W		4	Poor to fair
U	Unsettled	5	Fair
N	Normal	6	Fair to good
N		7	Good
N		8	Very good
N		9	Excellent

* Abstracted from, "North Atlantic Radio Warning Service," CRPL-RWS-31, March 19, 1956, National Bureau of Standards; Box 178, Fort Belvoir, Virginia and "North Pacific Radio Warning Service," CRPL-RWS-30, March 19, 1956, National Bureau of Standards; Box 1119, Anchorage, Alaska. The latest issues of these bulletins should be consulted for further information.

Standard frequencies and time signals *continued*

Other standard-frequency stations *as of August, 1954*

	Rugby	Tokyo	Torino	Johannesburg
Country	England	Japan	Italy	South Africa
Call sign	MSF	JJY	IBF	ZUO
Carrier power in kw	0.5	1	0.3	0.1
Days per week	7	7-2	Tuesday	7
Hours per day	24[a]	24	6[b]	24
Carriers in mc	2.5, 5, 10[c]	2.5[e], 5[f], 10[g] [d]	5	5
Modulations in c/s	1[h], 1000	1[i], 1000	1[h], 440, 1000	1[k]
Duration of tone modulation in minutes	5 in each 15	9 in each 20	5 in each 10[j]	—
Duration of time signals in minutes	5 in each 15	continuous	5 in each 10	continuous

[a] Total interruption of transmission from minute 15 to minute 20 of each hour.
[b] From 0800 to 1100 and from 1300 to 1600 UT.
[c] Transmissions are also made on 60 kc.
[d] Transmissions are also made on 4 and 8 mc.
[e] Daily from 0700 to 2300 UT.
[f] Mondays.
[g] Wednesdays.
[h] 5 cycles of 100-c/s modulation pulses.
[i] Interruptions for 20 milliseconds.
[j] 440- and 1000-c/s tones alternately.
[k] 100 cycles of 1000-c/s modulation pulses.

See also list of foreign radio time signals in "Radio Navigational Aids," U. S. Navy Hydrographic Office publication 205 for sale by the Hydrographic Office, Washington 25, D. C.

Units, constants, and conversion factors

Conversion factors

to convert	into	multiply by	conversely, multiply by
Acres	Square feet	4.356×10^{4}	2.296×10^{-5}
Acres	Square meters	4047	2.471×10^{-4}
Ampere-hours	Coulombs	3600	2.778×10^{-4}
Amperes per sq cm	Amperes per sq inch	6.452	0.1550
Ampere-turns	Gilberts	1.257	0.7958
Ampere-turns per cm	Ampere-turns per inch	2.540	0.3937
Atmospheres	Mm of mercury @ 0° C	760	1.316×10^{-3}
Atmospheres	Feet of water @ 4° C	33.90	2.950×10^{-2}
Atmospheres	Inches mercury @ 0° C	29.92	3.342×10^{-2}
Atmospheres	Kg per sq meter	1.033×10^{4}	9.678×10^{-5}
Atmospheres	Newtons per sq meter	1.0133×10^{5}	0.9869×10^{-5}
Atmospheres	Pounds per sq inch	14.70	6.804×10^{-2}
Btu	Foot-pounds	778.3	1.285×10^{-3}
Btu	Joules	1054.8	9.480×10^{-4}
Btu	Kilogram-calories	0.2520	3.969
Btu	Horsepower-hours	3.929×10^{-4}	2545
Bushels	Cubic feet	1.2445	0.8036
Centigrade (Celsius)	Fahrenheit	$C^\circ \times 9/5 = F^\circ - 32$ $(C^\circ + 40) \times 9/5 = (F^\circ + 40)$	
Chains (surveyor's)	Feet	66	1.515×10^{-2}
Circular mils	Square centimeters	5.067×10^{-6}	1.973×10^{5}
Circular mils	Square mils	0.7854	1.273
Cubic feet	Cords	7.8125×10^{-3}	128
Cubic feet	Gallons (liq US)	7.481	0.1337
Cubic feet	Liters	28.32	3.531×10^{-2}
Cubic inches	Cubic centimeters	16.39	6.102×10^{-2}
Cubic inches	Cubic feet	5.787×10^{-4}	1728
Cubic inches	Cubic meters	1.639×10^{-5}	6.102×10^{4}
Cubic inches	Gallons (liq US)	4.329×10^{-3}	231
Cubic meters	Cubic feet	35.31	2.832×10^{-2}
Cubic meters	Cubic yards	1.308	0.7646
Degrees (angle)	Radians	1.745×10^{-2}	57.30
Dynes	Pounds	2.248×10^{-6}	4.448×10^{5}
Ergs	Foot-pounds	7.376×10^{-8}	1.356×10^{7}
Fathoms	Feet	6	0.16667
Feet	Centimeters	30.48	3.281×10^{-2}
Feet	Varas	0.3594	2.782
Feet of water @ 4° C	Incnes of mercury @ 0° C	0.8826	1.133
Feet of water @ 4° C	Kg per sq meter	304.8	3.281×10^{-3}
Feet of water @ 4° C	Pounds per sq foot	62.43	1.602×10^{-2}
Foot-pounds	Horsepower-hours	5.050×10^{-7}	1.98×10^{6}
Foot-pounds	Kilogram-meters	0.1383	7.233
Foot-pounds	Kilowatt-hours	3.766×10^{-7}	2.655×10^{6}
Gallons (liq US)	Cubic meters	3.785×10^{-3}	264.2
Gallons (liq US)	Gallons (liq Br Imp) (Canada)	0.8327	1.201
Gausses	Lines per sq inch	6.452	0.1550

Conversion factors *continued*

to convert	into	multiply by	conversely, multiply by
Grains (for humidity calculations)	Pounds (avoirdupois)	1.429×10^{-4}	7000
Grams	Dynes	980.7	1.020×10^{-3}
Grams	Grains	15.43	6.481×10^{-2}
Grams	Ounces (avoirdupois)	3.527×10^{-2}	28.35
Grams	Poundals	7.093×10^{-2}	14.10
Grams per cm	Pounds per inch	5.600×10^{-3}	178.6
Grams per cu cm	Pounds per cu inch	3.613×10^{-2}	27.68
Grams per sq cm	Pounds per sq foot	2.0481	0.4883
Hectares	Acres	2.471	0.4047
Horsepower (boiler)	Btu per hour	3.347×10^{4}	2.986×10^{-5}
Horsepower (metric) (542.5 ft-lb per sec)	Btu per minute	41.83	2.390×10^{-2}
Horsepower (metric) (542.5 ft-lb per sec)	Foot-lb per minute	3.255×10^{4}	3.072×10^{-5}
Horsepower (metric) (542.5 ft-lb per sec)	Kg-calories per minute	10.54	9.485×10^{-2}
Horsepower (550 ft-lb per sec)	Btu per minute	42.41	2.357×10^{-2}
Horsepower (550 ft-lb per sec)	Foot-lb per minute	3.3×10^{4}	3.030×10^{-5}
Horsepower (550 ft-lb per sec)	Kilowatts	0.745	1.342
Horsepower (metric) (542.5 ft-lb per sec)	Horsepower (550 ft-lb per sec)	0.9863	1.014
Horsepower (550 ft-lb per sec)	Kg-calories per minute	10.69	9.355×10^{-2}
Inches	Centimeters	2.540	0.3937
Inches	Feet	8.333×10^{-2}	12
Inches	Miles	1.578×10^{-5}	6.336×10^{4}
Inches	Mils	1000	0.001
Inches	Yards	2.778×10^{-2}	36
Inches of mercury @ 0° C	Lbs per sq inch	0.4912	2.036
Inches of water @ 4° C	Kg per sq meter	25.40	3.937×10^{-2}
Inches of water @ 4° C	Ounces per sq inch	0.5782	1.729
Inches of water @ 4° C	Pounds per sq foot	5.202	0.1922
Inches of water @ 4° C	In of mercury	7.355×10^{-2}	13.60
Joules	Foot-pounds	0.7376	1.356
Joules	Ergs	10^{7}	10^{-7}
Kilogram-calories	Kilogram-meters	426.9	2.343×10^{-3}
Kilogram-calories	Kilojoules	4.186	0.2389
Kilograms	Tons, long (avdp 2240 lb)	9.482×10^{-4}	1016
Kilograms	Tons, short (avdp 2000 lb)	1.102×10^{-3}	907.2
Kilograms	Pounds (avoirdupois)	2.205	0.4536
Kilograms per kilometer	Pounds (avdp) per mile (stat)	3.548	0.2818
Kg per sq meter	Pounds per sq foot	0.2048	4.882
Kilometers	Feet	3281	3.048×10^{-4}
Kilowatt-hours	Btu	3413	2.930×10^{-4}
Kilowatt-hours	Foot-pounds	2.655×10^{6}	3.766×10^{-7}
Kilowatt-hours	Joules	3.6×10^{6}	2.778×10^{-7}

Conversion factors *continued*

to convert	into	multiply by	conversely, multiply by
Kilowatt-hours	Kilogram-calories	860	1.163×10^{-3}
Kilowatt-hours	Kilogram-meters	3.671×10^{5}	2.724×10^{-6}
Kilowatt-hours	Pounds carbon oxydized	0.235	4.26
Kilowatt-hours	Pounds water evaporated from and at 212° F	3.53	0.283
Kilowatt-hours	Pounds water raised from 62° to 212° F	22.75	4.395×10^{-2}
Knots* (naut mi per hour)	Feet per second	1.688	0.5925
Knots	Meters per minute	30.87	0.03240
Knots	Miles (stat) per hour	1.1508	0.8690
Lamberts	Candles per sq cm	0.3183	3.142
Lamberts	Candles per sq inch	2.054	0.4869
Leagues	Miles (approximately)	3	0.33
Links	Chains	0.01	100
Links (surveyor's)	Inches	7.92	0.1263
Liters	Bushels (dry US)	2.838×10^{-2}	35.24
Liters	Cubic centimeters	1000	0.001
Liters	Cubic meters	0.001	1000
Liters	Cubic inches	61.02	1.639×10^{-2}
Liters	Gallons (liq US)	0.2642	3.785
Liters	Pints (liq US)	2.113	0.4732
$\log_e N$ or $\ln N$	$\log_{10} N$	0.4343	2.303
Lumens per sq foot	Foot-candles	1	1
Lux	Foot-candles	0.0929	10.764
Meters	Yards	1.094	0.9144
Meters	Varas	1.179	0.848
Meters per min	Feet per minute	3.281	0.3048
Meters per min	Kilometers per hour	0.06	16.67
Microhms per cm cube	Microhms per inch cube	0.3937	2.540
Microhms per cm cube	Ohms per mil foot	6.015	0.1662
Miles (nautical)*	Feet	6076.1	1.646×10^{-4}
Miles (nautical)	Meters	1852	5.400×10^{-4}
Miles (nautical)	Miles (statute)	1.1508	0.8690
Miles (statute)	Kilometers	1.609	0.6214
Miles (statute)	Feet	5280	1.894×10^{-4}
Miles per hour	Kilometers per minute	2.682×10^{-2}	37.28
Miles per hour	Feet per minute	88	1.136×10^{-2}
Miles per hour	Kilometers per hour	1.609	0.6214
Millibars	Inches mercury (32° F)	0.02953	33.86
Millibars (10^3 dynes per sq cm)	Pounds per sq foot	2.089	0.4788
Nepers	Decibels	8.686	0.1151
Newtons	Dynes	10^{5}	10^{-5}
Newtons	Kilograms	0.1020	9.807
Newtons	Poundals	7.233	0.1383
Newtons	Pounds (avdp)	0.2248	4.448
Ounces (fluid)	Quarts	3.125×10^{-2}	32
Ounces (avoirdupois)	Pounds	6.25×10^{-2}	16
Pints	Quarts (liq US)	0.50	2
Pounds of water (dist)	Cubic feet	1.603×10^{-2}	62.38

Conversion factors *continued*

to convert	into	multiply by	conversely, multiply by
Pounds of water (dist)	Gallons	0.1198	8.347
Pounds per inch	Kg per meter	17.86	0.05600
Pounds per foot	Kg per meter	1.488	0.6720
Pounds per mile (statute)	Kg per kilometer	0.2818	3.548
Pounds per cu foot	Kg per cu meter	16.02	6.243×10^{-2}
Pounds per cu inch	Pounds per cu foot	1728	5.787×10^{-4}
Pounds per sq foot	Pounds per sq inch	6.944×10^{-3}	144
Pounds per sq foot	Kg per sq meter	4.882	0.2048
Pounds per sq inch	Kg per sq meter	703.1	1.422×10^{-3}
Poundals	Dynes	1.383×10^{4}	7.233×10^{-5}
Poundals	Pounds (avoirdupois)	3.108×10^{-2}	32.17
Quarts	Gallons (liq US)	0.25	4
Rods	Feet	16.5	6.061×10^{-2}
Slugs (mass)	Pounds (avoirdupois)	32.174	3.108×10^{-2}
Sq inches	Circular mils	1.273×10^{6}	7.854×10^{-7}
Sq inches	Sq centimeters	6.452	0.1550
Sq feet	Sq meters	9.290×10^{-2}	10.76
Sq miles	Sq yards	3.098×10^{6}	3.228×10^{-7}
Sq miles	Acres	640	1.562×10^{-3}
Sq miles	Sq kilometers	2.590	0.3861
Sq millimeters	Circular mils	1973	5.067×10^{-4}
(Temp rise, °C) × (U.S. gal water)/minute	Watts	264	3.79×10^{-3}
Tons, short (avoir 2000 lb)	Tonnes (1000 kg)	0.9072	1.102
Tons, long (avoir 2240 lb)	Tonnes (1000 kg)	1.016	0.9842
Tons, long (avoir 2240 lb)	Tons, short (avoir 2000 lb)	1.120	0.8929
Tons (US shipping)	Cubic feet	40	0.025
Watts	Btu per minute	5.689×10^{-2}	17.58
Watts	Ergs per second	10^{7}	10^{-7}
Watts	Foot-lb per minute	44.26	2.260×10^{-2}
Watts	Horsepower (550 ft-lb per sec)	1.341×10^{-3}	745.7
Watts	Horsepower (metric) (542.5 ft-lb per sec)	1.360×10^{-3}	735.5
Watts	Kg-calories per minute	1.433×10^{-2}	69.77
Watt-seconds (joules)	Gram-calories (mean)	0.2389	4.186
Webers per sq meter	Gausses	10^{4}	10^{-4}
Yards	Feet	3	0.3333

* Conversion factors for the nautical mile and, hence, for the knot, are based on the International Nautical Mile, which was adopted by the U.S. Department of Defense and the U.S. Department of Commerce, effective 1 July 1954. See, "Adoption of International Nautical Mile," *National Bureau of Standards Technical News Bulletin*, vol. 38, p. 122; August, 1954. The International Nautical Mile has been in use by many countries for various lengths of time.

Note: Pounds are avoirdupois in every entry except where otherwise indicated.

Examples

a. Required, the conversion factor for pounds (avoirdupois) to grams. Duplication of entries in the table has been reduced to the minimum. An entry will be found for kilograms to pounds, from which the required factor is obviously 453.6.

b. Convert inches per pound to meters per kilogram. A number of conversions have been collected under the name, pounds. The desired factor appears under pounds per inch. Since the reciprocal is tabulated, the factors must be interchanged, so the desired one is 0.05600.

Centigrade-to-fahrenheit conversion chart

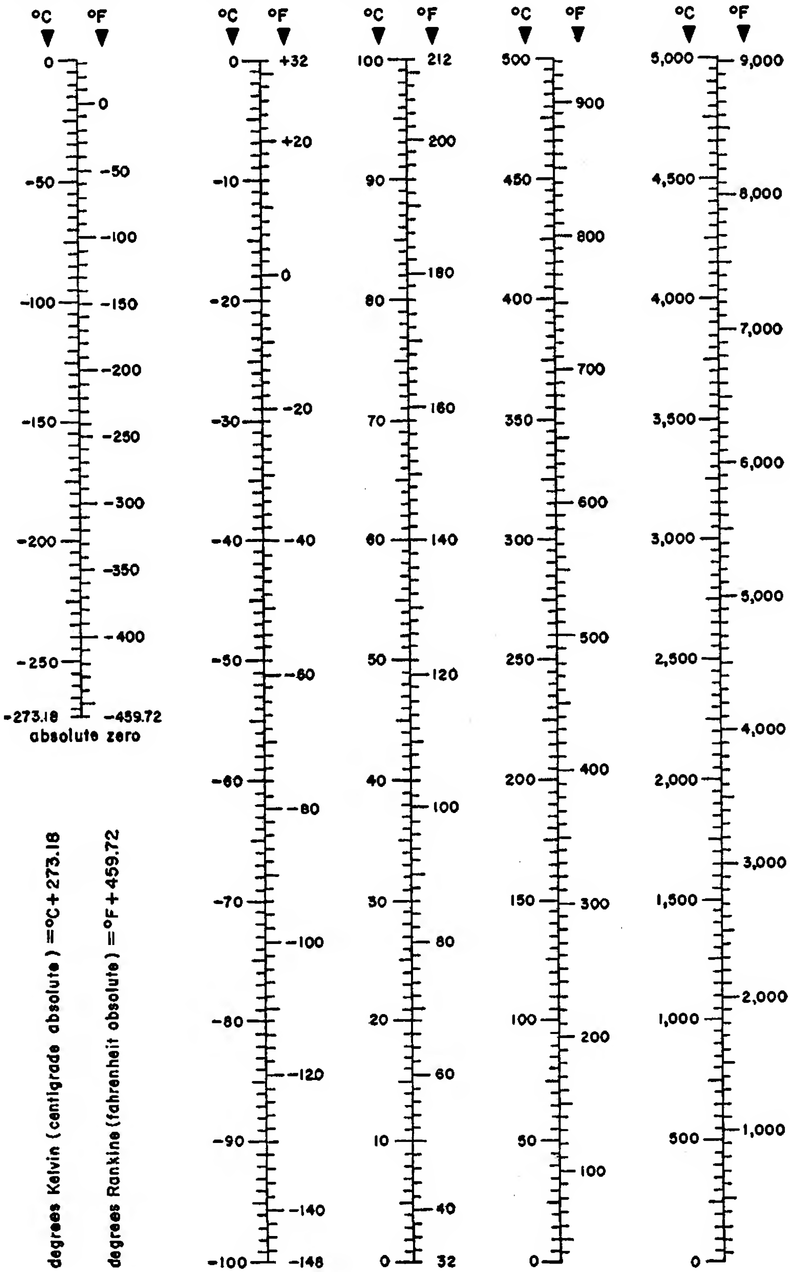

Principal physical atomic constants*

Centimeter-gram-second units

usual symbol	denomination	value and units
$F' = Ne/c$	Faraday's constant (physical scale)	9652.19 ± 0.11 emu (g mole)$^{-1}$
N	Avogadro's constant (physical scale)	$(6.02486 \pm 0.00016) \times 10^{23}$ (g mole)$^{-1}$
h	Planck's constant	$(6.62517 \pm 0.00023) \times 10^{-27}$ erg sec
m	Electron rest mass	$(9.1083 \pm 0.0003) \times 10^{-28}$ g
e	Electronic charge	$(4.80286 \pm 0.00009) \times 10^{-10}$ esu
$e' = e/c$		$(1.60206 \pm 0.00003) \times 10^{-20}$ emu
e/m	Charge-to-mass ratio of electron	$(5.27305 \pm 0.00007) \times 10^{17}$ esu g^{-1}
$e'/m = e/(mc)$		$(1.75890 \pm 0.00002) \times 10^{7}$ emu g^{-1}
c	Velocity of light in vacuum†	$299{,}793.0 \pm 0.3$ km sec^{-1}
$h/(mc)$	Compton wavelength of electron	$(24.2626 \pm 0.0002) \times 10^{-11}$ cm
$a_0 = h^2/(4\pi^2 me^2)$	First Bohr electron-orbit radius	$(5.29172 \pm 0.00002) \times 10^{-9}$ cm
$\sigma = \frac{\pi^2}{60}\frac{k^4}{c^2}\frac{8\pi^3}{h^3}$	Stefan-Boltzmann constant	$(0.56687 \pm 0.00010) \times 10^{-4}$ erg cm^{-2} deg^{-4} sec^{-1}
$\lambda_{max}T$	Wien displacement-law constant	(0.289782 ± 0.000013) cm deg
$\mu_0 = he/(4\pi mc)$	Bohr magneton	$(0.92731 \pm 0.00002) \times 10^{-20}$ erg gauss^{-1}
Nm	Atomic mass of the electron (physical scale)	$(5.48763 \pm 0.00006) \times 10^{-4}$
M_p/Nm	Ratio, proton mass to electron mass	1836.12 ± 0.02
$E_0 = e \cdot 10^8/c$	Energy associated with 1 ev	$(1.60206 \pm 0.00003) \times 10^{-12}$ erg
$(mc^2/E_0) \times 10^{-6}$	Energy equivalent of electron mass	(0.510976 ± 0.000007) Mev
$k = R_0/N$	Boltzmann's constant	$(1.38044 \pm 0.00007) \times 10^{-16}$ erg deg^{-1}
R_∞	Rydberg wave number for infinite mass	$(109{,}737.309 \pm 0.012)$ cm^{-1}
H	Hydrogen atomic mass (physical scale)	1.008142 ± 0.000003
R_0	Gas constant per mole (physical scale)	$(8.31696 \pm 0.00034) \times 10^{7}$ erg mole^{-1} deg^{-1}
V_0	Standard volume of perfect gas (physical scale)	$(22{,}420.7 \pm 0.6)$ cm^3 atmos mole^{-1}

* Extracted from: E. R. Cohen, J. W. M. DuMond, T. W. Layton, and J. S. Rollett, "Analysis of Variance of the 1952 Data on the Atomic Constants and a New Adjustment, 1955," *Reviews of Modern Physics*, vol. 27, pp. 363–380; October, 1955.

† Where c appears in the equations for other constants, it is the numerical value of the velocity in centimeters per second.

Principal physical atomic constants *continued*

Meter-kilogram-second rationalized units

The following table is derived from that on p. 34; for further details regarding symbols and probable errors, refer to that table.

usual symbol	denomination	value and units
F	Faraday's constant	9.652×10^{7} coulomb (kg-mole)$^{-1}$
N	Avogadro's constant	6.025×10^{26} (kg-mole)$^{-1}$
h	Planck's constant	6.625×10^{-34} joule sec
m	Electron rest mass	9.108×10^{-31} kg
e	Electronic charge	1.602×10^{-19} coulomb
e/m	Electron charge/mass	1.759×10^{11} coulomb kg^{-1}
c	Velocity of light in vacuum	2.998×10^{8} meters sec^{-1}
h/mc	Compton wavelength of electron	2.426×10^{-12} meter
a_0	First Bohr electron-orbit radius	5.292×10^{-11} meter
σ	Stefan-Boltzmann constant	5.669×10^{-8} watt meter^{-2} (deg K)$^{-4}$
$\lambda_{max}T$	Wien displacement-law constant	2.898×10^{-3} meter (deg K)
μ_0	Bohr magneton	9.273×10^{-24} joule meter^{2} weber^{-1}
Nm	Atomic mass of the electron	5.488×10^{-4}
M_p/Nm	Ratio, proton mass to electron mass	1836
v_0	Speed of 1-ev electron	5.932×10^{5} meter sec^{-1}
F_0	Energy associated with 1 ev	1.602×10^{-19} joule
mc^2/E_0	Energy equivalent of electron mass	0.5110×10^{6} ev
k	Boltzmann's constant	1.380×10^{-23} joule (deg K)$^{-1}$
R_∞	Rydberg wave number for infinite mass	1.097×10^{7} meter^{-1}
H	Hydrogen atomic mass	1.008
$R_0 = PV/MT$	Gas constant	8.317×10^{3} joule (kg-mole)$^{-1}$ (deg K)$^{-1}$ Note: joule = (newton/meter^{2}) meter^{3}
V_0	Standard volume of perfect gas at 0° C and 1 atmosphere (p. 29)	22.42 meter^{3} (kg-mole)$^{-1}$

Properties of free space

Velocity of light $= c = 1/(\mu_v\epsilon_v)^{1/2} = 2.998 \times 10^{8}$ meters per second
$= 186{,}280$ miles per second
$= 984 \times 10^{6}$ feet per second.

Permeability $= \mu_v = 4\pi \times 10^{-7} = 1.257 \times 10^{-6}$ henry per meter.

Permittivity $= \epsilon_v = 8.85 \times 10^{-12} \approx (36\pi \times 10^{9})^{-1}$ farad per meter.

Characteristic impedance $= Z_0 = (\mu_v/\epsilon_v)^{1/2} = 376.7 \approx 120\pi$ ohms.

Unit conversion table

quantity	symbol	equation in mks(r) units	mks(r) (rationalized) unit	equivalent number of: mks(nr) units	pract units	esu	emu	mks(nr) (nonrationalized) unit
length	l		meter (m)	1	10^2	10^2	10^2	meter (m)
mass	m		kilogram	1	10^3	10^3	10^3	kilogram
time	t		second	1	1	1	1	second
force	F	$F = ma$	newton	1	10^5	10^5	10^5	newton
work, energy	W	$W = Fl$	joule	1	1	10^7	10^7	joule
power	P	$P = W/t$	watt	1	1	10^7	10^7	watt
electric charge	q		coulomb	1	1	3×10^9	10^{-1}	coulomb
volume charge density	ρ	$\rho = q/v$	coulomb/m^3	1	10^{-6}	3×10^3	10^{-7}	coulomb/m^3
surface charge density	σ	$\sigma = q/A$	coulomb/m^2	1	10^{-4}	3×10^5	10^{-5}	coulomb/m^2
electric dipole moment	p	$p = ql$	coulomb-meter	1	10^2	3×10^{11}	10	coulomb-meter
polarization	P	$P = p/v$	coulomb/m^2	1	10^{-4}	3×10^5	10^{-5}	coulomb/m^2
electric field intensity	E	$E = F/q$	volt/m	1	10^{-2}	$10^{-4}/3$	10^6	volt/m
permittivity	ϵ	$F = q^2/4\pi\epsilon l^2$	farad/m	4π	$4\pi \times 10^{-9}$	$36\pi \times 10^9$	$4\pi \times 10^{-11}$	
displacement	D	$D = \epsilon E$	coulomb/m^2	4π	$4\pi \times 10^{-4}$	$12\pi \times 10^5$	$4\pi \times 10^{-5}$	
displacement flux	Ψ	$\Psi = DA$	coulomb	4π	4π	$12\pi \times 10^9$	$4\pi \times 10^{-1}$	
emf, electric potential	V	$V = El$	volt	1	1	$10^{-2}/3$	10^8	volt
current	I	$I = q/t$	ampere	1	1	3×10^9	10^{-1}	ampere
volume current density	J	$J = I/A$	ampere/m^2	1	10^{-4}	3×10^5	10^{-5}	ampere/m^2
surface current density	K	$K = I/l$	ampere/m	1	10^{-2}	3×10^7	10^{-3}	ampere/m
resistance	R	$R = V/I$	ohm	1	1	$10^{-11}/9$	10^9	ohm
conductance	G	$G = 1/R$	mho	1	1	9×10^{11}	10^{-9}	mho
resistivity	ρ	$\rho = RA/l$	ohm-meter	1	10^2	$10^{-9}/9$	10^{11}	ohm-meter
conductivity	γ	$\gamma = 1/\rho$	mho/meter	1	10^{-2}	9×10^9	10^{-11}	mho/meter
capacitance	C	$C = q/V$	farad	1	1	9×10^{11}	10^{-9}	farad
elastance	S	$S = 1/C$	daraf	1	1	$10^{-11}/9$	10^9	daraf
magnetic charge	m		weber	$1/4\pi$	$10^8/4\pi$	$10^{-2}/12\pi$	$10^8/4\pi$	
magnetic dipole moment	m	$m = ml$	weber-meter	$1/4\pi$	$10^{10}/4\pi$	$1/12\pi$	$10^{10}/4\pi$	
magnetization	M	$M = m/v$	weber/m^2	$1/4\pi$	$10^4/4\pi$	$10^{-6}/12\pi$	$10^4/4\pi$	
magnetic field intensity	H	$H = nI/l$	ampere-turn/m	4π	$4\pi \times 10^{-3}$	$12\pi \times 10^7$	$4\pi \times 10^{-3}$	
permeability	μ	$F = m^2/4\pi\mu l^2$	henry/m	$1/4\pi$	$10^7/4\pi$	$10^{-13}/36\pi$	$10^7/4\pi$	
induction	B	$B = \mu H$	weber/m^2	1	10^4	$10^{-6}/3$	10^4	weber/m^2
induction flux	Φ	$\Phi = BA$	weber	1	10^8	$10^{-2}/3$	10^8	weber
mmf, magnetic potential	M	$M = Hl$	ampere-turn	4π	$4\pi \times 10^{-1}$	$12\pi \times 10^9$	$4\pi \times 10^{-1}$	
reluctance	$\mathcal{R}$	$\mathcal{R} = M/\Phi$	amp-turn/weber	4π	$4\pi \times 10^{-9}$	$36\pi \times 10^{11}$	$4\pi \times 10^{-9}$	
permeance	$\mathcal{P}$	$\mathcal{P} = 1/\mathcal{R}$	weber/amp-turn	$1/4\pi$	$10^9/4\pi$	$10^{-11}/36\pi$	$10^9/4\pi$	
inductance	L	$L = \Phi/I$	henry	1	1	$10^{-11}/9$	10^9	henry

Compiled by J. R. Ragazzini and L. A. Zadeh, Columbia University, New York.
The velocity of light was taken as 3×10^{10} centimeters/second in computing the conversion factors.
Equations in the second column are for dimensional purposes only.

equivalent number of			practical (cgs) unit	equivalent number of		esu	equivalent number of emu units	emu
pract units	esu	emu		esu	emu			
10^2	10^2	10^2	centimeter (cm)	1	1	centimeter (cm) (G)	1	centimeter (cm)
10^3	10^3	10^3	gram	1	1	gram (G)	1	gram
1	1	1	second	1	1	second (G)	1	second
10^5	10^5	10^5	dyne	1	1	dyne (G)	1	dyne
1	10^7	10^7	joule	10^7	10^7	erg (G)	1	erg
1	10^7	10^7	watt	10^7	10^7	erg/second (G)	1	erg/second
1	3×10^9	10^{-1}	coulomb	3×10^9	10^{-1}	statcoulomb (G)	$10^{-10}/3$	abcoulomb
10^{-6}	3×10^3	10^{-7}	coulomb/cm^3	3×10^9	10^{-1}	statcoulomb/cm^3 (G)	$10^{-10}/3$	abcoulomb/cm^3
10^{-4}	3×10^5	10^{-5}	coulomb/cm^2	3×10^9	10^{-1}	statcoulomb/cm^2 (G)	$10^{-10}/3$	abcoulomb/cm^2
10^2	3×10^{11}	10	coulomb-cm	3×10^9	10^{-1}	statcoulomb-cm (G)	$10^{-10}/3$	abcoulomb-cm
10^{-4}	3×10^5	10^{-5}	coulomb/cm^2	3×10^9	10^{-1}	statcoulomb/cm^2 (G)	$10^{-10}/3$	abcoulomb/cm^2
10^{-2}	$10^{-4}/3$	10^6	volt/cm	$10^{-2}/3$	10^8	statvolt/cm (G)	3×10^{10}	abvolt/cm
10^{-9}	9×10^9	10^{-11}		9×10^{18}	10^{-2}	(G)	$10^{-20}/9$	
10^{-4}	3×10^5	10^{-5}		3×10^9	10^{-1}	(G)	$10^{-10}/3$	
1	3×10^9	10^{-1}		3×10^9	10^{-1}	(G)	$10^{-10}/3$	
1	$10^{-2}/3$	10^8	volt	$10^{-2}/3$	10^8	statvolt (G)	3×10^{10}	abvolt
1	3×10^9	10^{-1}	ampere	3×10^9	10^{-1}	statampere (G)	$10^{-10}/3$	abampere
10^{-4}	3×10^5	10^{-5}	ampere/cm^2	3×10^9	10^{-1}	statampere/cm^2 (G)	$10^{-10}/3$	abampere/cm^2
10^{-2}	3×10^7	10^{-3}	ampere/cm	3×10^9	10^{-1}	statampere/cm (G)	$10^{-10}/3$	abampere/cm
1	$10^{-11}/9$	10^9	ohm	$10^{-11}/9$	10^9	statohm (G)	9×10^{20}	abohm
1	9×10^{11}	10^{-9}	mho	9×10^{11}	10^{-9}	statmho (G)	$10^{-20}/9$	abmho
10^2	$10^{-9}/9$	10^{11}	ohm-cm	$10^{-11}/9$	10^9	statohm-cm (G)	9×10^{20}	abohm-cm
10^{-2}	9×10^9	10^{-11}	mho/cm	9×10^{11}	10^{-9}	statmho/cm (G)	$10^{-20}/9$	abmho/cm
1	9×10^{11}	10^{-9}	farad	9×10^{11}	10^{-9}	statfarad (cm) (G)	$10^{-20}/9$	abfarad
1	$10^{-11}/9$	10^9	daraf	$10^{-11}/9$	10^9	statdaraf (G)	9×10^{20}	abdaraf
10^8	$10^{-2}/3$	10^8		$10^{-10}/3$	1		3×10^{10}	unit pole (G)
10^{10}	1/3	10^{10}		$10^{-10}/3$	1		3×10^{10}	pole-cm (G)
10^4	$10^{-6}/3$	10^4		$10^{-10}/3$	1		3×10^{10}	pole/cm^2 (G)
10^{-3}	3×10^7	10^{-3}	oersted	3×10^{10}	1		$10^{-10}/3$	oersted (G)
10^7	$10^{-13}/9$	10^7	gauss/oersted	$10^{-20}/9$	1		9×10^{20}	gauss/oersted (G)
10^4	$10^{-6}/3$	10^4	gauss	$10^{-10}/3$	1		3×10^{10}	gauss (G)
10^8	$10^{-2}/3$	10^8	maxwell (line)	$10^{-10}/3$	1		3×10^{10}	maxwell (line) (G)
10^{-1}	3×10^9	10^{-1}	gilbert	3×10^{10}	1		$10^{-10}/3$	gilbert (G)
10^{-9}	9×10^{11}	10^{-9}	gilbert/maxwell	9×10^{20}	1		$10^{-20}/9$	gilbert/maxwell (G)
10^9	$10^{-11}/9$	10^9	maxwell/gilbert	$10^{-20}/9$	1		9×10^{20}	maxwell/gilbert (G)
1	$10^{-11}/9$	10^9	henry	$10^{-11}/9$	10^9	stathenry (G)	9×10^{20}	abhenry (cm) (G)

G = Gaussian unit.

Metric multiplier prefixes

Multiples and submultiples of fundamental units such as: meter, gram, liter, second, ohm, farad, henry, volt, ampere, and watt may be indicated by the following prefixes.

prefix	abbreviation	multiplier	prefix	abbreviation	multiplier
tera	T	10^{12}	deci	d	10^{-1}
giga	G	10^{9}	centi	c	10^{-2}
mega	M	10^{6}	milli	m	10^{-3}
myria	ma	10^{4}	micro	μ	10^{-6}
kilo	k	10^{3}	nano	n	10^{-9}
hecto	h	10^{2}	pico	p	10^{-12}
deca	da	10			

Fractions of an inch with metric equivalents

fractions of an inch		decimals of an inch	millimeters	fractions of an inch		decimals of an inch	millimeters
	1/64	0.0156	0.397		33/64	0.5156	13.097
1/32		0.0313	0.794	17/32		0.5313	13.494
	3/64	0.0469	1.191		35/64	0.5469	13.891
1/16		0.0625	1.588	9/16		0.5625	14.288
	5/64	0.0781	1.984		37/64	0.5781	14.684
3/32		0.0938	2.381	19/32		0.5938	15.081
	7/64	0.1094	2.778		39/64	0.6094	15.478
1/8		0.1250	3.175	5/8		0.6250	15.875
	9/64	0.1406	3.572		41/64	0.6406	16.272
5/32		0.1563	3.969	21/32		0.6563	16.669
	11/64	0.1719	4.366		43/64	0.6719	17.066
3/16		0.1875	4.763	11/16		0.6875	17.463
	13/64	0.2031	5.159		45/64	0.7031	17.859
7/32		0.2188	5.556	23/32		0.7188	18.256
	15/64	0.2344	5.953		47/64	0.7344	18.653
1/4		0.2500	6.350	3/4		0.7500	19.050
	17/64	0.2656	6.747		49/64	0.7656	19.447
9/32		0.2813	7.144	25/32		0.7813	19.844
	19/64	0.2969	7.541		51/64	0.7969	20.241
5/16		0.3125	7.938	13/16		0.8125	20.638
	21/64	0.3281	8.334		53/64	0.8281	21.034
11/32		0.3438	8.731	27/32		0.8438	21.431
	23/64	0.3594	9.128		55/64	0.8594	21.828
3/8		0.3750	9.525	7/8		0.8750	22.225
	25/64	0.3906	9.922		57/64	0.8906	22.622
13/32		0.4063	10.319	29/32		0.9063	23.019
	27/64	0.4219	10.716		59/64	0.9219	23.416
7/16		0.4375	11.113	15/16		0.9375	23.813
	29/64	0.4531	11.509		61/64	0.9531	24.209
15/32		0.4688	11.906	31/32		0.9688	24.606
	31/64	0.4844	12.303		63/64	0.9844	25.003
1/2		0.5000	12.700	—		1.0000	25.400

Greek alphabet

name	capital	small	commonly used to designate
ALPHA	A	α	Angles, coefficients, attenuation constant, absorption factor, area
BETA	B	β β	Angles, coefficients, phase constant
GAMMA	Γ	γ	Complex propagation constant (cap), specific gravity, angles, electrical conductivity, propagation constant
DELTA	Δ	δ	Increment or decrement (cap or small), determinant (cap) permittivity (cap), density, angles
EPSILON	E	ϵ	Dielectric constant, permittivity, base of natural logarithms, electric intensity
ZETA	Z	ζ	Coordinates, coefficients
ETA	H	η	Intrinsic impedance, efficiency, surface charge density, hysteresis, coordinates
THETA	Θ	ϑ θ	Angular phase displacement, time constant, reluctance, angles
IOTA	I	ι	Unit vector
KAPPA	K	κ	Susceptibility, coupling coefficient
LAMBDA	Λ	λ	Permeance (cap), wavelength, attenuation constant
MU	M	μ	Permeability, amplification factor, prefix micro
NU	N	ν	Reluctivity, frequency
XI	Ξ	ξ	Coordinates
OMICRON	O	o	
PI	Π	π	3.1416
RHO	P	ρ	Resistivity, volume charge density, coordinates
SIGMA	Σ	σ	Summation (cap), surface charge density, complex propagation constant, electrical conductivity, leakage coefficient
TAU	T	τ	Time constant, volume resistivity, time-phase displacement, transmission factor, density
UPSILON	Υ	υ	
PHI	Φ	ϕ φ	Scalar potential (cap), magnetic flux, angles
CHI	X	χ	Electric susceptibility, angles
PSI	Ψ	ψ	Dielectric flux, phase difference, coordinates, angles
OMEGA	Ω	ω	Resistance in ohms (cap), solid angle (cap), angular velocity

Small letter is used except where capital (cap) is indicated.

Decibels and power, voltage, and current ratios

The decibel, abbreviated db, is a unit used to express the ratio between two amounts of power, P_1 and P_2, existing at two points. By definition,

$$\text{number of db} = 10 \log_{10} \frac{P_1}{P_2}$$

It is also used to express voltage and current ratios;

$$\text{number of db} = 20 \log_{10} \frac{V_1}{V_2} = 20 \log_{10} \frac{I_1}{I_2}$$

Strictly, it can be used to express voltage and current ratios only when the voltages or currents in question are measured at places having identical impedances.

power ratio	voltage and current ratio	decibels	power ratio	voltage and current ratio	decibels
1.0233	1.0116	0.1	19.953	4.4668	13.0
1.0471	1.0233	0.2	25.119	5.0119	14.0
1.0715	1.0351	0.3	31.623	5.6234	15.0
1.0965	1.0471	0.4	39.811	6.3096	16.0
1.1220	1.0593	0.5	50.119	7.0795	17.0
1.1482	1.0715	0.6	63.096	7.9433	18.0
1.1749	1.0839	0.7	79.433	8.9125	19.0
1.2023	1.0965	0.8	100.00	10.0000	20.0
1.2303	1.1092	0.9	158.49	12.589	22.0
1.2589	1.1220	1.0	251.19	15.849	24.0
1.3183	1.1482	1.2	398.11	19.953	26.0
1.3804	1.1749	1.4	630.96	25.119	28.0
1.4454	1.2023	1.6	1000.0	31.623	30.0
1.5136	1.2303	1.8	1584.9	39.811	32.0
1.5849	1.2589	2.0	2511.9	50.119	34.0
1.6595	1.2882	2.2	3981.1	63.096	36.0
1.7378	1.3183	2.4	6309.6	79.433	38.0
1.8197	1.3490	2.6	10^4	100.000	40.0
1.9055	1.3804	2.8	$10^4 \times 1.5849$	125.89	42.0
1.9953	1.4125	3.0	$10^4 \times 2.5119$	158.49	44.0
2.2387	1.4962	3.5	$10^4 \times 3.9811$	199.53	46.0
2.5119	1.5849	4.0	$10^4 \times 6.3096$	251.19	48.0
2.8184	1.6788	4.5	10^5	316.23	50.0
3.1623	1.7783	5.0	$10^5 \times 1.5849$	398.11	52.0
3.5481	1.8836	5.5	$10^5 \times 2.5119$	501.19	54.0
3.9811	1.9953	6.0	$10^5 \times 3.9811$	630.96	56.0
5.0119	2.2387	7.0	$10^5 \times 6.3096$	794.33	58.0
6.3096	2.5119	8.0	10^6	1,000.00	60.0
7.9433	2.8184	9.0	10^7	3,162.3	70.0
10.0000	3.1623	10.0	10^8	10,000.0	80.0
12.589	3.5481	11.0	10^9	31,623	90.0
15.849	3.9811	12.0	10^{10}	100,000	100.0

To convert

Decibels to nepers multiply by 0.1151
Nepers to decibels multiply by 8.686

Where the power ratio is less than unity, it is usual to invert the fraction and express the answer as a decibel loss.

Properties of materials

Atomic weights*

element	symbol	atomic number	atomic weight	element	symbol	atomic number	atomic weight
Actinium	Ac	89	227	Lead	Pb	82	207.21
Aluminum	Al	13	26.98	Lithium	Li	3	6.940
Americium	Am	95	≈241	Lutetium	Lu	71	174.99
Antimony	Sb	51	121.76	Magnesium	Mg	12	24.32
Argon	A	18	39.944	Manganese	Mn	25	54.93
Arsenic	As	33	74.91	Mercury	Hg	80	200.61
Astatine	At	85	211	Molybdenum	Mo	42	95.95
Barium	Ba	56	137.36	Neodymium	Nd	60	144.27
Berklinium	Bk	97	≈243	Neon	Ne	10	20.183
Beryllium	Be	4	9.013	Neptunium	Np	93	≈239
Bismuth	Bi	83	209.00	Nickel	Ni	28	58.69
Boron	B	5	10.82	Niobium	Nb	41	92.91
Bromine	Br	35	79.916	Nitrogen	N	7	14.008
Cadmium	Cd	48	112.41	Osmium	Os	76	190.2
Calcium	Ca	20	40.08	Oxygen	O	8	16.0000
Californium	Cf	98	≈244	Palladium	Pd	46	106.7
Carbon	C	6	12.010	Phosphorus	P	15	30.975
Cerium	Ce	58	140.13	Platinum	Pt	78	195.23
Cesium	Cs	55	132.91	Plutonium	Pu	94	≈238
Chlorine	Cl	17	35.457	Polonium	Po	84	210.0
Chromium	Cr	24	52.01	Potassium	K	19	39.100
Cobalt	Co	27	58.94	Praseodymium	Pr	59	140.92
Copper	Cu	29	63.54	Promethium	Pm	61	147
Curium	Cm	96	≈242	Protactinium	Pa	91	231
Dysprosium	Dy	66	162.46	Radium	Ra	88	226.05
Erbium	Er	68	167.2	Radon	Rn	86	222
Europium	Eu	63	152.0	Rhenium	Re	75	186.31
Fluorine	F	9	19.00	Rhodium	Rh	45	102.91
Francium	Fr	87	223	Rubidium	Rb	37	85.48
Gadolinium	Gd	64	156.9	Ruthenium	Ru	44	101.7
Gallium	Ga	31	69.72	Samarium	Sm	62	150.43
Germanium	Ge	32	72.60	Scandium	Sc	21	44.96
Gold	Au	79	197.2	Selenium	Se	34	78.96
Hafnium	Hf	72	178.6	Silicon	Si	14	28.09
Helium	He	2	4.003	Silver	Ag	47	107.880
Holmium	Ho	67	164.94	Sodium	Na	11	22.997
Hydrogen	H	1	1.0080	Strontium	Sr	38	87.63
Indium	In	49	114.76	Sulfur	S	16	32.06
Iodine	I	53	126.91	Tantalum	Ta	73	180.88
Iridium	Ir	77	193.1	Technetium	Tc	43	98
Iron	Fe	26	55.85	Tellurium	Te	52	127.61
Krypton	Kr	36	83.80	Terbium	Tb	65	159.2
Lanthanum	La	57	138.92	Thallium	Tl	81	204.39

* From "Handbook of Chemistry and Physics," 34th edition, Chemical Rubber Publishing Company; Cleveland, Ohio.

Atomic weights *continued*

element	symbol	atomic number	atomic weight	element	symbol	atomic number	atomic weight
Thorium	Th	90	232.12	Vanadium	V	23	50.95
Thulium	Tm	69	169.4	Xenon	Xe	54	131.3
Tin	Sn	50	118.70	Ytterbium	Yb	70	173.04
Titanium	Ti	22	47.90	Yttrium	Y	39	88.92
Tungsten	W	74	183.92	Zinc	Zn	30	65.38
Uranium	U	92	238.07	Zirconium	Zr	40	91.22

Electromotive force

Series of the elements

element	volts	ion	element	volts	ion
Lithium	2.9595	Li^{+}	Tin	0.136	Sn^{++}
Rubidium	2.9259	Rb^{+}	Lead	0.122	Pb^{++}
Potassium	2.9241	K^{+}	Iron	0.045	Fe^{+++}
Strontium	2.92	Sr^{++}	Hydrogen	0.000	H^{+}
Barium	2.90	Ba^{++}	Antimony	−0.10	Sb^{+++}
Calcium	2.87	Ca^{++}	Bismuth	−0.226	Bi^{+++}
Sodium	2.7146	Na^{+}	Arsenic	−0.30	As^{+++}
Magnesium	2.40	Mg^{++}	Copper	−0.344	Cu^{++}
Aluminum	1.70	Al^{+++}	Oxygen	−0.397	O^{-}
Beryllium	1.69	Be^{++}	Polonium	−0.40	Po^{++++}
Uranium	1.40	U^{++++}	Copper	−0.470	Cu^{+}
Manganese	1.10	Mn^{++}	Iodine	−0.5345	I^{-}
Tellurium	0.827	Te^{--}	Tellurium	−0.558	Te^{++++}
Zinc	0.7618	Zn^{++}	Silver	−0.7978	Ag^{+}
Chromium	0.557	Cr^{++}	Mercury	−0.7986	Hg^{++}
Sulphur	0.51	S^{--}	Lead	−0.80	Pb^{++++}
Gallium	0.50	Ga^{+++}	Palladium	−0.820	Pd^{++}
Iron	0.441	Fe^{++}	Platinum	−0.863	Pt
Cadmium	0.401	Cd^{++}	Bromine	−1.0648	Br^{-}
Indium	0.336	In^{+++}	Chlorine	−1.3583	Cl^{-}
Thallium	0.330	Tl^{+}	Gold	−1.360	Au^{+++}
Cobalt	0.278	Co^{++}	Gold	−1.50	Au^{+}
Nickel	0.231	Ni^{++}	Fluorine	−1.90	F^{-}

Position of metals in the galvanic series

Corroded end (anodic, or least noble)

Magnesium
Magnesium alloys

Zinc

Aluminum 2S

Cadmium

Aluminum 17ST

Steel or Iron
Cast Iron

Chromium-iron (active)

Ni-Resist

18–8 Stainless (active)
18–8–3 Stainless (active)

Lead-tin solders
Lead
Tin

Nickel (active)
Inconel (active)

Brasses
Copper
Bronzes
Copper-nickel alloys
Monel

Silver solder

Nickel (passive)
Inconel (passive)

Chromium-iron (passive)
18–8 Stainless (passive)
18–8–3 Stainless (passive)

Silver

Graphite
Gold
Platinum

Protected end (cathodic, or most noble)

Note: Groups of metals indicate they are closely similar in properties.

Electromotive force *continued*

Periodic chart of work functions*

period	I A	I B	II A	II B	III A	III B	IV A	IV B	V A	V B	VI A	VI B	VII A	VII B	VIII	VIII	VIII
2	Li 2.39			Be 3.37		B 4.5		C 4.39									
3	Na 2.27			Mg 3.46		Al 3.74		Si 4.1		P —		S —					
4	K 2.15		Ca 2.76		Sc —		Ti 4.09		V 4.11		Cr 4.51		Mn 3.95		Fe 4.36	Co 4.18	Ni 4.84
		Cu 4.47		Zn 3.74		Ga 3.96		Ge 4.56		As 5.11		Se 4.72					
5	Rb 2.13		Sr 2.35		Y —		Zr 3.84		Cb 3.99		Mo 4.27		Tc —		Ru 4.52	Rh 4.65	Pd 4.82
		Ag 4.28		Cd 3.92		In —		Sn 4.11		Sb 4.08		Te 4.73					
6	Cs 1.89		Ba 2.29		La 3.3		Hf 3.53		Ta 4.12		W 4.50		Re 5.1		Os 4.55	Ir 4.57	Pt 5.29
		Au 4.58		Hg 4.52		Tl 3.76		Pb 4.02		Bi 4.28		Po —					
7	Fa —		Ra —		Ac —		Th 3.41		Pa —		U 3.74						
Rare earths	Ce 2.7	Pr 2.7	Nd 3.3	Sm 3.2													

* Mean of published data, 1924–1949. From, H. B. Michaelson, "Work Functions of the Elements," *Journal of Applied Physics*, vol. 21, pp. 536–540; June, 1950.

Temperature–emf characteristics of thermocouples*

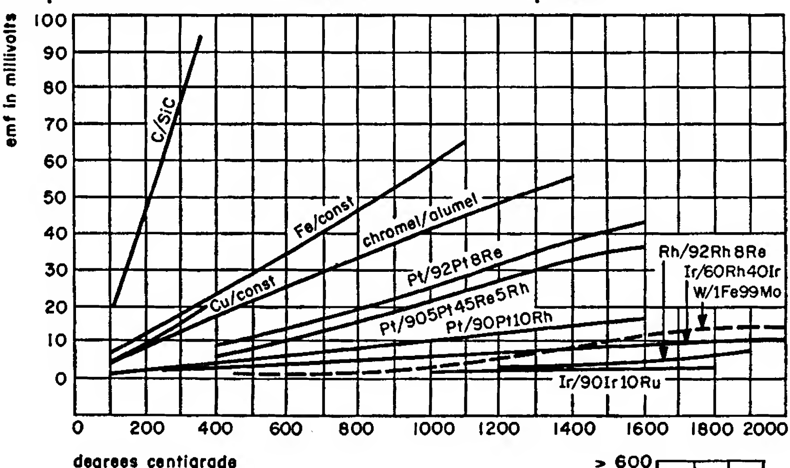

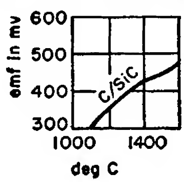

* From R. L. Weber, "Temperature Measurement and Control," Blakiston Co., Philadelphia, Pennsylvania; 1941: see pp. 68–71.

continued **Electromotive force**

Thermocouples and their characteristics

type	copper/constantan		iron/constantan		chromel/constantan		chromel/alumel		platinum/platinum rhodium (10)		platinum/platinum rhodium (13)		carbon/silicon carbide	
Composition, percent	100Cu	60Cu 40Ni	100Fe	60Cu 40Ni	90Ni 10Cr	55Cu 45Ni	90Ni 10Cr	94Ni 2Al 3Mn 1Si	Pt	90Pt 10Rh	Pt	87Pt 13Rh	C	SiC
*Range of application, °C	−200 to +300		−200 to +1382		0 to +1100		−200 to +1200		0 to +1450		0 to +1450		to +2000	
Resistivity, micro-ohm-cm	1.75	49	10	49	70	49	70	29.4	10	21				
Temperature coefficient of resistivity, per °C	0.0039	0.00001	0.005	0.00001	0.00035	0.0002	0.00035	0.000125	0.0030	0.0018				
Melting temperature, °C	1085	1190	1535	1190	1400	1190	1400	1430	1755	1700			3000	2700
emf in millivolts; reference junction at 0° C	100° C 200 300	4.24mv 9.06 14.42	100° C 200 400 600 800 1000	5.28mv 10.78 21.82 33.16 45.48 58.16	100° C 200 400 600	6.3mv 13.3 28.5 44.3	100° C 200 400 600 800 1000 1200 1400	4.1 mv 8.13 16.39 24.90 33.31 41.31 48.85 55.81	100° C 200 400 600 800 1000 1200 1400 1600	0.643mv 1.436 3.251 5.222 7.330 9.569 11.924 14.312 16.674	100° C 200 400 600 800 1000 1200 1400 1600	0.646mv 1.464 3.398 5.561 7.927 10.470 13.181 15.940 18.680	1210° C 1300 1360 1450	353.6mv 385.2 403.2 424.9
Influence of temperature and gas atmosphere	Subject to oxidation and alteration above 400° C due Cu, above 600° due constantan wire. Ni-plating of Cu tube gives protection, in acid-containing gas. Contamination of Cu affects calibration greatly. Resistance to oxid. atm. good. Resistance to reducing atm. good. Requires protection from acid fumes.		Oxidizing and reducing atmosphere have little effect on accuracy. Best used in dry atmosphere. Resistance to oxidation good to 400° C. Resistance to reducing atmosphere good. Protect from oxygen, moisture, sulphur.		Chromel attacked by sulphurous atmosphere. Resistance to oxidation good. Resistance to reducing atmosphere poor.		Resistance to oxidizing atmosphere very good. Resistance to reducing atmosphere poor. Affected by sulphur, reducing or sulphurous gas, SO_2 and H_2S.		Resistance to oxidizing atmosphere very good. Resistance to reducing atmosphere poor. Susceptible to chemical alteration by As, Si, P vapor in reducing gas (CO_2, H_2, H_2S, SO_2). Pt corrodes easily above 1000°. Used in gas-tight protecting tube.				Used as tube element. Carbon sheath chemically inert.	
Particular applications	Low temperature, industrial. Internal combustion engine. Used as a tube element for measurements in steam line.		Low temperature, industrial. Steel annealing, boiler flues, tube stills. Used in reducing or neutral atmosphere.				Used in oxidizing atmosphere. Industrial. Ceramic kilns, tube stills, electric furnaces.		International Standard 630 to 1065° C.		Similar to Pt/PtRh(10) but has higher emf.		Steel furnace and ladle temperatures. Laboratory measurements.	

* For prolonged usage; can be used at higher temperature for short periods.

Physical constants of various metals and alloys

material	relative resistance*	temp coeff of resistivity	specific gravity	coeff of thermal cond	avg coeff thermal expan (X10^{-6})	melting point °C
Advance (55 Cu, 45 Ni)	see	Constantan				
Aluminum	1.64	0.0039	2.70	2.03	28.7	660
Antimony	24.21	0.0036	6.7	0.187	10.9	630
Arsenic	19.33	0.0042	5.73	—	3.86	sublimes
Bismuth	69.8	0.004	9.8	0.0755	13.4	271
Brass (66 Cu, 34 Zn)	3.9	0.002	8.47	1.2	20.2	920
Cadmium	4.4	0.0038	8.64	0.92	31.6	321
Carbon, gas	2900	−0.0005	—	—	—	3500
Chromax (15 Cr, 35 Ni, balance Fe)	58.0	0.00031	7.95	0.130	—	1380
Cobalt	5.6	0.0033	8.9	—	12.4	1495
Columbium	see	Niobium				
Constantan (55 Cu, 45 Ni)	28.45	±0.0002	8.9	0.218	14.8	1210
Copper—annealed	1.00*	0.00393	8.89	3.88	16.1	1083
hard drawn	1.03	0.00382	8.94	—	—	1083
Duralumin	3.34	0.002	2.7	1.603	—	500–637
Eureka (55 Cu, 45 Ni)	see	Constantan				
Gallium	56.8	—	5.903-6.093	0.07-0.09	18.0	29.78
German silver	16.9	0.00027	8.7	0.32	18.4	1110
Germanium	≈65.0	—	5.35	—	—	958.5
Gold	1.416	0.0034	19.32	2.96	14.3	1063
Ideal (55 Cu, 45 Ni)	see	Constantan				
Indium	9.0	0.00498	7.30	0.057	33.0	156.4
Iron, pure	5.6	0.0052–0.0062	7.86	0.67	12.1	1535
Kovar A (29 Ni, 17 Co, 0.3 Mn, balance Fe)	28.4	—	8.2	0.193	6.2	1450
Lead	12.78	0.0039	11.34	0.344	29.4	327
Magnesium	2.67	0.004	1.74	1.58	29.8	651
Manganin (84 Cu, 12 Mn, 4 Ni)	26	±0.00002	8.5	0.63	—	910
Mercury	55.6	0.00089	13.55	0.063	—	−38.87
Molybdenum, drawn	3.3	0.0045	10.2	1.46	6.0	2630
Monel metal (67 Ni, 30 Cu, 1.4 Fe, 1 Mn)	27.8	0.002	8.8	0.25	16.3	1300–1350
Nichrome I (65 Ni, 12 Cr, 23 Fe)	65.0	0.00017	8.25	0.132	—	1350
Nickel	5.05	0.0047	8.9	0.6	15.5	1455
Nickel silver (64 Cu, 18 Zn, 18 Ni)	16.0	0.00026	8.72	0.33	—	1110
Niobium	13.2	0.00395	8.55	—	7.1	2500
Palladium	6.2	0.0033	12.0	0.7	11.0	1549
Phosphor-bronze (4 Sn, 0.5 P, balance Cu)	5.45	0.003	8.9	0.82	16.8	1050
Platinum	6.16	0.003	21.4	0.695	9.0	1774
Silicon	—	—	2.4	0.020	4.68	1420
Silver	0.95	0.0038	10.5	4.19	18.8	960.5
Steel, manganese (13 Mn, 1 C, 86 Fe)	41.1	—	7.81	0.113	—	1510
Steel, SAE 1045 (0.4–0.5 C, balance Fe)	7.6–12.7	—	7.8	0.59	15.0	1480
Steel, 18–8 stainless (0.1 C, 18 Cr, 8 Ni, balance Fe)	52.8	—	7.9	0.163	19.1	1410

* Resistivity of copper = 1.7241 × 10^{-6} ohm-centimeters.

Physical constants of various metals and alloys *continued*

material	relative resist-ance*	temp coeff of resistivity	specific gravity	coeff of thermal cond	avg coeff thermal expan ($\times 10^{-6}$)	melting point °C
Tantalum	9.0	0.003	16.6	0.545	6.6	2900
Thorium	18.6	0.0021	11.2	—	12.3	1845
Tin	6.7	0.0042	7.3	0.64	26.9	231.9
Titanium	47.8	—	4.5	0.41	8.5	1800
Tophet A (80 Ni, 20 Cr)	62.5	0.00014	8.4	0.136	—	1400
Tungsten	3.25	0.0045	19.3	1.6	4.6	3370
Uranium	32–40	0.0021	18.7	1.5	—	≈1150
Zinc	3.4	0.0037	7.14	1.12	26.3	419
Zirconium	2.38	0.0044	6.4	—	5.0	1900

Relative resistance: The table of relative resistances gives the ratio of the resistance of any material to the resistance of a piece of annealed copper of identical physical dimensions and temperature. The resistance of any substance of uniform cross-section is proportional to the length and inversely proportional to the cross-sectional area.

$$R = \rho L/A$$

where

ρ = resistivity, the proportionality constant
L = length
A = cross-sectional area
R = resistance in ohms

If L and A are measured in centimeters, ρ is in ohm-centimeters. If L is measured in feet, and A in circular mils, ρ is in ohm-circular-mils/foot.

Relative resistance = ρ divided by the resistivity of copper (1.7241×10^{-6} ohm-centimeters)

Temperature coefficient of resistivity gives the ratio of the change in resistivity due to a change in temperature of 1 degree centigrade relative to the resistivity at 20 degrees centigrade. The dimensions of this quantity are ohms/degree centigrade/ohm, or 1/degree centigrade.

The resistance at any temperature is

$$R = R_{20}\,[1 + \alpha_{20}\,(T - 20)]$$

where

R_{20} = resistance in ohms at 20 degrees centigrade
T = temperature in degrees centigrade
α_{20} = temperature coefficient of resistivity/degree centigrade at 20 degrees centigrade

Physical constants of various metals and alloys *continued*

Specific gravity of a substance is defined as the ratio of the weight of a given volume of the substance to the weight of an equal volume of water. In the cgs system, the specific gravity of a substance is exactly equal to the weight in grams of one cubic centimeter of the substance.

Coefficient of thermal conductivity is defined as the time rate of heat transfer through unit thickness, across unit area, for a unit difference in temperature. Expressing rate of heat transfer in watts, the coefficient of thermal conductivity

$$K = WL/A\Delta T$$

where

W = watts
L = thickness in centimeters
A = area in centimeters^2
ΔT = temperature difference in degrees centigrade

Coefficient of thermal expansion: The coefficient of linear thermal expansion is the ratio of the change in length per degree to the length at 0° C. It is usually given as an average value over a range of temperatures and is then called the average coefficient of thermal expansion.

Temperature charts of metals

On the following two pages are given centigrade and fahrenheit temperatures relating to the processing of metals and alloys.

Soldering, brazing, and welding: This chart has been prepared to provide, in a convenient form, the melting points and components of various common soldering and brazing alloys. The temperature limits of various joining processes are indicated with the type and composition of the flux best suited for the process. The chart is a compilation of present good practice and does not indicate that the processes and materials cannot be used in other ways under special conditions.

Melting points: The melting-point chart is a thermometer-type graph upon which are placed the melting points of metals, alloys, and ceramics most commonly used in electron tubes and other components in the electronics industry. Pure metals are shown opposite their respective melting points on the right side of the thermometer. Ceramic materials and metal alloys are similarly shown on the left. The melting temperature shown for ceramic bodies is that temperature above which no crystalline phase normally exists. No attempt has been made to indicate their progressive softening characteristic.

Temperature charts of metals *continued*

Soldering, brazing, and welding processes*

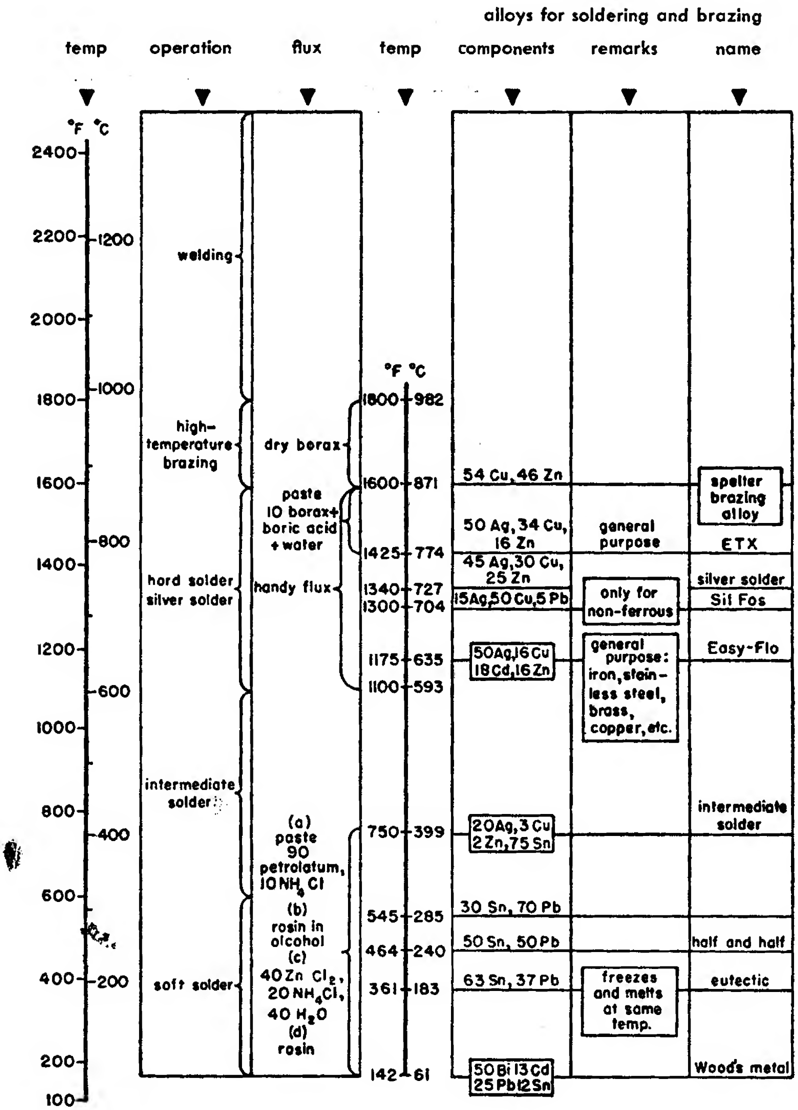

* By R. C. Hitchcock, Research Laboratories, Westinghouse Electric Corp., East Pittsburgh, Pa. Reprinted by permission from *Product Engineering*, vol. 18, p. 171; October, 1947.

Temperature charts of metals *continued*

Melting points of metals, alloys, and ceramics*

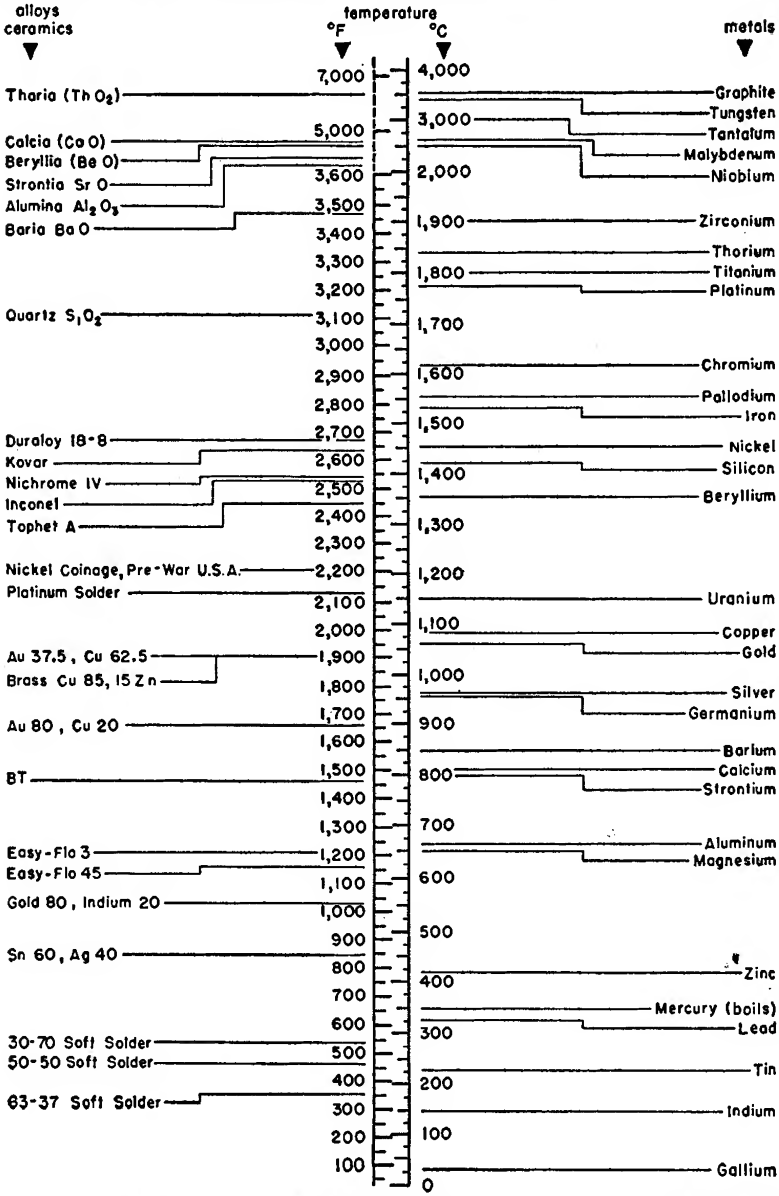

* By K. H. McPhee. Reprinted by permission from *Electronics*, vol. 21, p. 118; December, 1948.

Wire tables*

Solid copper—comparison of gauges

American (B & S) wire gauge	Birmingham (Stubs') iron wire gauge	British standard (NBS) wire gauge	diameter: mils	diameter: millimeters	circular mils	area: square millimeters	area: square inches	weight: per 1000 feet in pounds	weight: per kilometer in kilograms
–	0	–	340.0	8.636	115600	58.58	0.09079	350	521
0	–	–	324.9	8.251	105500	53.48	0.08289	319	475
–	–	0	324.0	8.230	105000	53.19	0.08245	318	472
–	1	1	300.0	7.620	90000	45.60	0.07069	273	405
1	–	–	289.3	7.348	83690	42.41	0.06573	253	377
–	2	–	284.0	7.214	80660	40.87	0.06335	244	363
–	–	–	283.0	7.188	80090	40.58	0.06290	242	361
–	–	2	276.0	7.010	76180	38.60	0.05963	231	343
–	3	–	259.0	6.579	67080	33.99	0.05269	203	302
2	–	–	257.6	6.544	66370	33.63	0.05213	201	299
–	–	3	252.0	6.401	63500	32.18	0.04988	193	286
–	4	–	238.0	6.045	56640	28.70	0.04449	173	255
–	–	4	232.0	5.893	53820	27.27	0.04227	163	242
3	–	–	229.4	5.827	52630	26.67	0.04134	159	237
–	5	–	220.0	5.588	48400	24.52	0.03801	147	217
–	–	5	212.0	5.385	44940	22.77	0.03530	136	202
4	–	–	204.3	5.189	41740	21.18	0.03278	126	188
–	6	–	203.0	5.156	41210	20.88	0.03237	125	186
–	–	6	192.0	4.877	36860	18.68	0.02895	112	166
5	–	–	181.9	4.621	33100	16.77	0.02600	100	149
–	7	–	180.0	4.572	32400	16.42	0.02545	98.0	146
–	–	7	176.0	4.470	30980	15.70	0.02433	93.6	139
–	8	–	165.0	4.191	27220	13.86	0.02138	86.2	123
6	–	–	162.0	4.116	26250	13.30	0.02062	79.5	118
–	–	8	160.0	4.064	25600	12.97	0.02011	77.5	115
–	9	–	148.0	3.759	21900	11.10	0.01720	66.3	98.6
7	–	–	144.3	3.665	20820	10.55	0.01635	63.0	93.7
–	–	9	144.0	3.658	20740	10.51	0.01629	62.8	93.4
–	10	–	134.0	3.404	17960	9.098	0.01410	54.3	80.8
8	–	–	128.8	3.264	16510	8.366	0.01297	50.0	74.4
–	–	10	128.0	3.251	16380	8.302	0.01267	49.6	73.8
–	11	–	120.0	3.048	14400	7.297	0.01131	43.6	64.8
–	–	11	116.0	2.946	13460	6.818	0.01057	40.8	60.5
9	–	–	114.4	2.906	13090	6.634	0.01028	39.6	58.9
–	12	–	109.0	2.769	11880	6.020	0.009331	35.9	53.5
–	–	12	104.0	2.642	10820	5.481	0.008495	32.7	48.7
10	–	–	101.9	2.588	10380	5.261	0.008155	31.4	46.8
–	13	–	95.00	2.413	9025	4.573	0.007088	27.3	40.6
–	–	13	92.00	2.337	8464	4.289	0.006648	25.6	38.1
11	–	–	90.74	2.305	8234	4.172	0.006467	24.9	37.1
–	14	–	83.00	2.108	6889	3.491	0.005411	20.8	31.0
12	–	–	80.81	2.053	6530	3.309	0.005129	19.8	29.4
–	–	14	80.00	2.032	6400	3.243	0.005027	19.4	28.8
–	15	15	72.00	1.829	5184	2.627	0.004072	16.1	23.4
13	–	–	71.96	1.828	5178	2.624	0.004067	15.7	23.3
–	16	–	65.00	1.651	4225	2.141	0.003318	12.8	19.0
14	–	–	64.08	1.628	4107	2.081	0.003225	12.4	18.5
–	–	16	64.00	1.626	4096	2.075	0.003217	12.3	18.4
–	17	–	58.00	1.473	3364	1.705	0.002642	10.2	15.1
15	–	–	57.07	1.450	3257	1.650	0.002558	9.86	14.7
–	–	17	56.00	1.422	3136	1.589	0.002463	9.52	14.1
16	–	–	50.82	1.291	2583	1.309	0.002028	7.82	11.6
–	18	–	49.00	1.245	2401	1.217	0.001886	7.27	10.8
–	–	18	48.00	1.219	2304	1.167	0.001810	6.98	10.4
17	–	–	45.26	1.150	2048	1.038	0.001609	6.20	9.23
–	19	–	42.00	1.067	1764	0.8938	0.001385	5.34	7.94
18	–	–	40.30	1.024	1624	0.8231	0.001276	4.92	7.32
–	–	19	40.00	1.016	1600	0.8107	0.001257	4.84	7.21
–	–	20	36.00	0.9144	1296	0.6567	0.001018	3.93	5.84
19	–	–	35.89	0.9116	1288	0.6527	0.001012	3.90	5.80
–	20	–	35.00	0.8890	1225	0.6207	0.0009621	3.71	5.52
–	21	21	32.00	0.8128	1024	0.5189	0.0008042	3.11	4.62
20	–	–	31.96	0.8118	1022	0.5176	0.0008023	3.09	4.60

* For information on insulated wire for inductor windings, see pp. 114 and 278.

Wire tables *continued*

Annealed copper (AWG)

AWG B & S gauge	diameter in mils	cross section circular mils	cross section square inches	ohms per 1000 ft at 20° C (68° F)	lbs per 1000 ft	ft per lb	ft per ohm at 20° C (68° F)	ohms per lb at 20° C (68° F)
0000	460.0	211,600	0.1662	0.04901	640.5	1.561	20,400	0.00007652
000	409.6	167,800	0.1318	0.06180	507.9	1.968	16,180	0.0001217
00	364.8	133,100	0.1045	0.07793	402.8	2.482	12,830	0.0001935
0	324.9	105,500	0.08289	0.09827	319.5	3.130	10,180	0.0003076
1	289.3	83,690	0.06573	0.1239	253.3	3.947	8,070	0.0004891
2	257.6	66,370	0.05213	0.1563	200.9	4.977	6,400	0.0007778
3	229.4	52,640	0.04134	0.1970	159.3	6.276	5,075	0.001237
4	204.3	41,740	0.03278	0.2485	126.4	7.914	4,025	0.001966
5	181.9	33,100	0.02600	0.3133	100.2	9.980	3,192	0.003127
6	162.0	26,250	0.02062	0.3951	79.46	12.58	2,531	0.004972
7	144.3	20,820	0.01635	0.4982	63.02	15.87	2,007	0.007905
8	128.5	16,510	0.01297	0.6282	49.98	20.01	1,592	0.01257
9	114.4	13,090	0.01028	0.7921	39.63	25.23	1,262	0.01999
10	101.9	10,380	0.008155	0.9989	31.43	31.82	1,001	0.03178
11	90.74	8,234	0.006467	1.260	24.92	40.12	794	0.05053
12	80.81	6,530	0.005129	1.588	19.77	50.59	629.6	0.08035
13	71.96	5,178	0.004067	2.003	15.68	63.80	499.3	0.1278
14	64.08	4,107	0.003225	2.525	12.43	80.44	396.0	0.2032
15	57.07	3,257	0.002558	3.184	9.858	101.4	314.0	0.3230
16	50.82	2,583	0.002028	4.016	7.818	127.9	249.0	0.5136
17	45.26	2,048	0.001609	5.064	6.200	161.3	197.5	0.8167
18	40.30	1,624	0.001276	6.385	4.917	203.4	156.6	1.299
19	35.89	1,288	0.001012	8.051	3.899	256.5	124.2	2.065
20	31.96	1,022	0.0008023	10.15	3.092	323.4	98.50	3.283
21	28.46	810.1	0.0006363	12.80	2.452	407.8	78.11	5.221
22	25.35	642.4	0.0005046	16.14	1.945	514.2	61.95	8.301
23	22.57	509.5	0.0004002	20.36	1.542	648.4	49.13	13.20
24	20.10	404.0	0.0003173	25.67	1.223	817.7	38.96	20.99
25	17.90	320.4	0.0002517	32.37	0.9699	1,031.0	30.90	33.37
26	15.94	254.1	0.0001996	40.81	0.7692	1,300	24.50	53.06
27	14.20	201.5	0.0001583	51.47	0.6100	1,639	19.43	84.37
28	12.64	159.8	0.0001255	64.90	0.4837	2,067	15.41	134.2
29	11.26	126.7	0.00009953	81.83	0.3836	2,607	12.22	213.3
30	10.03	100.5	0.00007894	103.2	0.3042	3,287	9.691	339.2
31	8.928	79.70	0.00006260	130.1	0.2413	4,145	7.685	539.3
32	7.950	63.21	0.00004964	164.1	0.1913	5,227	6.095	857.6
33	7.080	50.13	0.00003937	206.9	0.1517	6,591	4.833	1,364
34	6.305	39.75	0.00003122	260.9	0.1203	8,310	3.833	2,168
35	5.615	31.52	0.00002476	329.0	0.09542	10,480	3.040	3,448
36	5.000	25.00	0.00001964	414.8	0.07568	13,210	2.411	5,482
37	4.453	19.83	0.00001557	523.1	0.06001	16,660	1.912	8,717
38	3.965	15.72	0.00001235	659.6	0.04759	21,010	1.516	13,860
39	3.531	12.47	0.000009793	831.8	0.03774	26,500	1.202	22,040
40	3.145	9.888	0.000007766	1049.0	0.02993	33,410	0.9534	35,040

Temperature coefficient of resistance: The resistance of a conductor at temperature T in degrees centigrade is given by

$$R = R_{20}\,[1 + \alpha_{20}\,(T - 20)]$$

where R_{20} is the resistance at 20 degrees centigrade and α_{20} is the temperature coefficient of resistance at 20 degrees centigrade. For copper, $\alpha_{20} = 0.00393$. That is, the resistance of a copper conductor increases approximately 4/10 of 1 percent per degree centigrade rise in temperature.

Wire tables *continued*

Hard-drawn copper (AWG)*

AWG B & S gauge	wire diameter in inches	breaking load in pounds	tensile strength in lbs/in²	weight: pounds per 1000 feet	weight: pounds per mile	maximum resistance (ohms per 1000 feet at 68° F)	cross-sectional area: circular mils	cross-sectional area: square inches
4/0	0.4600	8143	49,000	640.5	3382	0.05045	211,600	0.1662
3/0	0.4096	6722	51,000	507.9	2682	0.06361	167,800	0.1318
2/0	0.3648	5519	52,800	402.8	2127	0.08021	133,100	0.1045
1/0	0.3249	4517	54,500	319.5	1687	0.1011	105,500	0.08289
1	0.2893	3688	56,100	253.3	1338	0.1287	83,690	0.06573
2	0.2576	3003	57,600	200.9	1061	0.1625	66,370	0.05213
3	0.2294	2439	59,000	159.3	841.2	0.2049	52,630	0.04134
4	0.2043	1970	60,100	126.4	667.1	0.2584	41,740	0.03278
5	0.1819	1591	61,200	100.2	529.1	0.3258	33,100	0.02600
–	0.1650	1326	62,000	82.41	435.1	0.3961	27,225	0.02138
6	0.1620	1280	62,100	79.46	419.6	0.4108	26,250	0.02062
7	0.1443	1030	63,000	63.02	332.7	0.5181	20,820	0.01635
–	0.1340	894.0	63,400	54.35	287.0	0.6006	17,956	0.01410
8	0.1285	826.0	63,700	49.97	263.9	0.6533	16,510	0.01297
9	0.1144	661.2	64,300	39.63	209.3	0.8238	13,090	0.01028
–	0.1040	550.4	64,800	32.74	172.9	0.9971	10,816	0.008495
10	0.1019	529.2	64,900	31.43	165.9	1.039	10,380	0.008155
11	0.09074	422.9	65,400	24.92	131.6	1.310	8,234	0.006467
12	0.08081	337.0	65,700	19.77	104.4	1.652	6,530	0.005129
13	0.07196	268.0	65,900	15.68	82.77	2.083	5,178	0.004067
14	0.06408	213.5	66,200	12.43	65.64	2.626	4,107	0.003225
15	0.05707	169.8	66,400	9.858	52.05	3.312	3,257	0.002558
16	0.05082	135.1	66,600	7.818	41.28	4.176	2,583	0.002028
17	0.04526	107.5	66,800	6.200	32.74	5.266	2,048	0.001609
18	0.04030	85.47	67,000	4.917	25.96	6.640	1,624	0.001276

*Courtesy of Copperweld Steel Co., Glassport, Pa. Based on ASA Specification H–4.2 and ASTM Specification B–1.

Modulus of elasticity is 17,000,000 lbs/inch². Coefficient of linear expansion is 0.0000094/degree Fahrenheit. Weights are based on a density of 8.89 grams/cm³ at 20 degrees centigrade (equivalent to 0.00302699 lbs/circular mil/1000 feet).
The resistances are maximum values for hard-drawn copper and are based on a resistivity of 10.674 ohms/circular-mil foot at 20 degrees centigrade (97.16 percent conductivity) for sizes 0.325 inch and larger, and 10.785 ohms/circular-mil foot at 20 degrees centigrade (96.16 percent conductivity) for sizes 0.324 inch and smaller.

Tensile strength of copper wire (AWG)*

AWG B & S gauge	wire diameter in inches	hard drawn: minimum tensile strength lbs/in²	hard drawn: breaking load in pounds	medium-hard drawn: minimum tensile strength lbs/in²	medium-hard drawn: breaking load in pounds	soft or annealed: maximum tensile strength lbs/in²	soft or annealed: breaking load in pounds
1	0.2893	56,100	3688	46,000	3024	37,000	2432
2	0.2576	57,600	3003	47,000	2450	37,000	1929
3	0.2294	59,000	2439	48,000	1984	37,000	1530
4	0.2043	60,100	1970	48,330	1584	37,000	1213
5	0.1819	61,200	1591	48,660	1265	37,000	961.9
–	0.1650	62,000	1326	—	—	—	—
6	0.1620	62,100	1280	49,000	1010	37,000	762.9
7	0.1443	63,000	1030	49,330	806.6	37,000	605.0
–	0.1340	63,400	894.0	—	—	—	—
8	0.1285	63,700	826.0	49,660	643.9	37,000	479.8
9	0.1144	64,300	661.2	50,000	514.2	37,000	380.5
–	0.1040	64,800	550.4	—	—	—	—
10	0.1019	64,900	529.2	50,330	410.4	38,500	314.0
11	0.09074	65,400	422.9	50,660	327.6	38,500	249.0
12	0.08081	65,700	337.0	51,000	261.6	38,500	197.5

*Courtesy of Copperweld Steel Co., Glassport, Pa.

continued **Wire tables**

Solid copperweld (AWG)

AWG B & S gauge	diam inch	cross-sectional area		weight			resistance ohms/1000 ft at 68° F		breaking load, pounds		attenuation in decibels/mile*				characteristic impedance*	
		circular mils	square inch	pounds per 1000 feet	pounds per mile	feet per pound	40% conduct	30% conduct	40% conduct	30% conduct	40% cond dry	40% cond wet	30% cond dry	30% cond wet	40% cond	30% cond
4	.2043	41,740	.03278	115.8	611.6	8.63	0.6337	0.8447	3,541	3,934	—	—	—	—	—	—
5	.1819	33,100	.02600	91.86	485.0	10.89	0.7990	1.065	2,938	3,250	—	—	—	—	—	—
6	.1620	26,250	.02062	72.85	384.6	13.73	1.008	1.343	2,433	2,680	.078	.086	.103	.109	650	686
7	.1443	20,820	.01635	57.77	305.0	17.31	1.270	1.694	2,011	2,207	.093	.100	.122	.127	685	732
8	.1285	16,510	.01297	45.81	241.9	21.83	1.602	2.136	1,660	1,815	.111	.118	.144	.149	727	787
9	.1144	13,090	.01028	36.33	191.8	27.52	2.020	2.693	1,368	1,491	.132	.138	.169	.174	776	852
10	.1019	10,380	.008155	28.81	152.1	34.70	2.547	3.396	1,130	1,231	.156	.161	.196	.200	834	920
11	.0907	8,234	.006467	22.85	120.6	43.76	3.212	4.28	896	975	.183	.188	.228	.233	910	1,013
12	.0808	6,530	.005129	18.12	95.68	55.19	4.05	5.40	711	770	.216	.220	.262	.266	1,000	1,120
13	.0720	5,178	.004067	14.37	75.88	69.59	5.11	6.81	490	530						
14	.0641	4,107	.003225	11.40	60.17	87.75	6.44	8.59	400	440						
15	.0571	3,257	.002558	9.038	47.72	110.6	8.12	10.83	300	330						
16	.0508	2,583	.002028	7.167	37.84	139.5	10.24	13.65	250	270						
17	.0453	2,048	.001609	5.684	30.01	175.9	12.91	17.22	185	205						
18	.0403	1,624	.001276	4.507	23.80	221.9	16.28	21.71	153	170						
19	.0359	1,288	.001012	3.575	18.87	279.8	20.53	27.37	122	135						
20	.0320	1,022	.0008023	2.835	14.97	352.8	25.89	34.52	100	110						
21	.0285	810.1	.0006363	2.248	11.87	444.8	32.65	43.52	73.2	81.1						
22	.0253	642.5	.0005046	1.783	9.413	560.9	41.17	54.88	58.0	64.3						
23	.0226	509.5	.0004002	1.414	7.465	707.3	51.92	69.21	46.0	51.0						
24	.0201	404.0	.0003173	1.121	5.920	891.9	65.46	87.27	36.5	40.4						
25	.0179	320.4	.0002517	0.889	4.695	1,125	82.55	110.0	28.9	32.1						
26	.0159	254.1	.0001996	0.705	3.723	1,418	104.1	138.8	23.0	25.4						
27	.0142	201.5	.0001583	0.559	2.953	1,788	131.3	175.0	18.2	20.1						
28	.0126	159.8	.0001255	0.443	2.342	2,255	165.5	220.6	14.4	15.9						
29	.0113	126.7	.0000995	0.352	1.857	2,843	208.7	278.2	11.4	12.6						
30	.0100	100.5	.0000789	0.279	1.473	3,586	263.2	350.8	9.08	10.0						
31	.0089	79.70	.0000626	0.221	1.168	4,521	331.9	442.4	7.20	7.95						
32	.0080	63.21	.0000496	0.175	0.926	5,701	418.5	557.8	5.71	6.30						
33	.0071	50.13	.0000394	0.139	0.734	7,189	527.7	703.4	4.53	5.00						
34	.0063	39.75	.0000312	0.110	0.582	9,065	665.4	887.0	3.59	3.97						
35	.0056	31.52	.0000248	0.087	0.462	11,430	839.0	1,119	2.85	3.14						
36	.0050	25.00	.0000196	0.069	0.366	14,410	1,058	1,410	2.26	2.49						
37	.0045	19.83	.0000156	0.055	0.290	18,180	1,334	1,778	1.79	1.98						
38	.0040	15.72	.0000123	0.044	0.230	22,920	1,682	2,243	1.42	1.57						
39	.0035	12.47	.00000979	0.035	0.183	28,900	2,121	2,828	1.13	1.24						
40	.0031	9.89	.00000777	0.027	0.145	36,440	2,675	3,566	0.893	0.986						

* DP insulators, 12-inch wire spacing at 1000 cycles/second.

Wire tables *continued*

Voltage drop in long circuits

The table below shows the conductor size (AWG or B&S gauge) necessary to limit the voltage drop to 2-percent maximum for various loads and distances. The calculations are for alternating-current circuits in conduit.

current in amperes	distance in feet									distance in feet								
	25	50	75	100	150	200	300	400	500	25	50	75	100	150	200	300	400	500
	single-phase—110 volts									**single-phase—220 volts**								
1	—	—	—	—	—	—	14	12	10	—	—	—	—	—	—	—	—	14
1.5	—	—	—	—	14	14	12	10	10	—	—	—	—	—	—	14	14	12
2	—	—	—	—	14	12	10	10	8	—	—	—	—	—	—	14	12	12
3	—	—	14	14	12	10	8	8	6	—	—	—	—	14	14	12	10	10
4	—	—	14	12	10	10	8	6	6	—	—	—	—	14	12	10	10	8
5	—	14	12	12	10	8	6	6	4	—	—	—	14	12	12	10	8	8
6	—	14	12	10	8	8	6	4	4	—	—	14	14	12	10	8	8	6
7	—	14	12	10	8	8	6	4	2	—	—	14	14	12	10	8	8	6
8	—	12	10	10	8	6	4	2	2	—	—	14	12	10	10	8	6	6
9	—	12	10	8	8	6	4	2	2	—	14	14	12	10	8	8	6	4
10	14	12	10	8	6	6	4	2	2	—	14	12	12	10	8	6	6	4
12	14	10	8	8	6	4	2	1	1	—	14	12	10	8	8	6	4	4
14	14	10	8	8	6	4	2	0	0	—	14	12	10	8	8	6	4	2
16	12	10	8	6	4	4	2	0	00	—	12	10	10	8	6	4	4	2
18	12	8	8	6	4	2	1	00	00	14	12	10	8	8	6	4	2	2
20	12	8	6	6	4	2	1	00	000	14	12	10	8	6	6	4	2	2
25	10	8	6	4	2	2	0	000	0000	14	10	8	8	6	4	2	2	1
30	10	6	4	4	2	1	00	—	—	12	10	8	6	4	4	2	1	0
35	10	6	4	2	2	0	000	—	—	12	10	8	6	4	2	2	0	00
40	8	6	4	2	1	00	0000	—	—	12	8	6	6	4	2	1	00	0000
45	8	4	4	2	0	00	—	—	—	10	8	6	4	4	2	0	00	0000
50	8	4	2	2	0	000	—	—	—	10	8	6	4	2	2	0	000	0000
60	6	4	2	1	00	0000	—	—	—	10	6	4	4	2	1	00	0000	—
70	6	2	2	0	000	—	—	—	—	10	6	4	2	2	0	000	—	—
80	6	2	1	00	0000	—	—	—	—	8	6	4	2	1	00	0000	—	—
90	4	2	0	00	—	—	—	—	—	8	4	4	2	0	00	—	—	—
100	4	2	0	000	—	—	—	—	—	8	4	2	2	0	000	—	—	—
120	4	1	00	0000	—	—	—	—	—	6	4	2	1	00	0000	—	—	—
	three-phase—220 volts									**three-phase—440 volts**								
1	—	—	—	—	—	—	—	—	—	—	—	—	—	—	—	—	—	—
1.5	—	—	—	—	—	—	—	14	14	—	—	—	—	—	—	—	—	—
2	—	—	—	—	—	—	14	14	12	—	—	—	—	—	—	—	—	—
3	—	—	—	—	—	14	12	12	10	—	—	—	—	—	—	—	14	14
4	—	—	—	—	14	14	12	10	10	—	—	—	—	—	—	14	14	12
5	—	—	—	—	14	12	10	10	8	—	—	—	—	—	—	14	12	12
6	—	—	—	14	12	12	10	8	8	—	—	—	—	—	14	12	12	10
7	—	—	14	14	12	10	8	8	6	—	—	—	—	14	14	12	10	10
8	—	—	14	14	12	10	8	6	6	—	—	—	—	14	14	12	10	10
9	—	—	14	12	10	10	8	6	6	—	—	—	—	14	12	10	10	8
10	—	—	14	12	10	10	8	6	6	—	—	—	—	14	12	10	10	8
12	—	14	12	12	10	8	6	6	4	—	—	—	14	12	12	10	8	8
14	—	14	12	10	8	8	6	4	4	—	—	14	14	12	10	8	8	6
16	—	14	12	10	8	8	6	4	2	—	—	14	14	12	10	8	8	6
18	—	12	10	10	8	6	4	4	2	—	—	14	12	10	10	8	6	6
20	—	12	10	10	8	6	4	2	2	—	—	14	12	10	10	8	6	6
25	14	12	10	8	6	6	4	2	1	—	14	12	12	10	8	6	6	4
30	14	10	8	8	6	4	2	2	0	—	14	12	10	8	8	6	6	4
35	12	10	8	6	4	4	2	1	0	—	12	10	10	8	6	4	4	4
40	12	10	8	6	4	2	2	0	00	—	12	10	10	8	6	4	2	2
45	12	8	6	6	4	2	1	0	000	14	12	10	8	6	6	4	2	2
50	12	8	6	4	4	2	0	00	000	14	12	10	8	6	6	4	2	1
60	10	8	6	4	2	2	0	000	—	14	10	8	8	6	4	2	2	0
70	10	6	4	4	2	1	00	0000	—	12	10	8	6	4	4	2	1	0
80	10	6	4	2	2	0	000	—	—	12	10	8	6	4	2	2	0	00
90	8	6	4	2	1	0	0000	—	—	12	8	6	6	4	2	1	0	000
100	8	6	4	2	0	00	—	—	—	12	8	6	6	4	2	0	00	000
120	8	4	2	2	0	0000	—	—	—	10	8	6	4	2	2	0	000	0000

Wire tables *continued*

Fusing currents of wires

The current I in amperes at which a wire will melt can be calculated from:

$$I = Kd^{3/2}$$

where d is the wire diameter in inches and K is a constant that depends on the metal concerned. The table below gives the fusing currents in amperes for 5 commonly used types of wire. Owing to the wide variety of factors that can influence the rate of heat loss, these figures must be considered as only approximations.

AWG B&S gauge	diam d in inches	copper (K = 10,244)	aluminum (K = 7585)	german silver (K = 5230)	iron (K = 3148)	tin (K = 1642)
40	0.0031	1.77	1.31	0.90	0.54	0.28
38	0.0039	2.50	1.85	1.27	0.77	0.40
36	0.0050	3.62	2.68	1.85	1.11	0.58
34	0.0063	5.12	3.79	2.61	1.57	0.82
32	0.0079	7.19	5.32	3.67	2.21	1.15
30	0.0100	10.2	7.58	5.23	3.15	1.64
28	0.0126	14.4	10.7	7.39	4.45	2.32
26	0.0159	20.5	15.2	10.5	6.31	3.29
24	0.0201	29.2	21.6	14.9	8.97	4.68
22	0.0253	41.2	30.5	21.0	12.7	6.61
20	0.0319	58.4	43.2	29.8	17.9	9.36
19	0.0359	69.7	51.6	35.5	21.4	11.2
18	0.0403	82.9	61.4	42.3	25.5	13.3
17	0.0452	98.4	72.9	50.2	30.2	15.8
16	0.0508	117	86.8	59.9	36.0	18.8
15	0.0571	140	103	71.4	43.0	22.4
14	0.0641	166	123	84.9	51.1	26.6
13	0.0719	197	146	101	60.7	31.7
12	0.0808	235	174	120	72.3	37.7
11	0.0907	280	207	143	86.0	44.9
10	0.1019	333	247	170	102	53.4
9	0.1144	396	293	202	122	63.5
8	0.1285	472	349	241	145	75.6
7	0.1443	561	416	287	173	90.0
6	0.1620	668	495	341	205	107

Courtesy of Automatic Electric Company; Chicago, Ill.

Wire tables *continued*

Physical properties of various wires*

property		copper annealed	copper hard-drawn	aluminum 99 percent pure
Conductivity, Matthiessen's standard in percent		99 to 102	96 to 99	61 to 63
Ohms/mil-foot at 68°F = 20°C		10.36	10.57	16.7
Circular-mil-ohms/mile at 68°F = 20°C		54,600	55,700	88,200
Pounds/mile-ohm at 68°F = 20°C		875	896	424
Mean temp coefficient of resistivity/°F		0.00233	0.00233	0.0022
Mean temp coefficient of resistivity/°C		0.0042	0.0042	0.0040
Mean specific gravity		8.89	8.94	2.68
Pounds/1000 feet/circular mil		0.003027	0.003049	0.000909
Weight in pounds/inch^3		0.320	0.322	0.0967
Mean specific heat		0.093	0.093	0.214
Mean melting point in °F		2,012	2,012	1,157
Mean melting point in °C		1,100	1,100	625
Mean coefficient of linear expansion/°F		0.00000950	0.00000950	0.00001285
Mean coefficient of linear expansion/°C		0.0000171	0.0000171	0.0000231
Solid wire (Values in pounds/in^2)	Ultimate tensile strength	30,000 to 42,000	45,000 to 68,000	20,000 to 35,000
	Average tensile strength	32,000	60,000	24,000
	Elastic limit	6,000 to 16,000	25,000 to 45,000	14,000
	Average elastic limit	15,000	30,000	14,000
	Modulus of elasticity	7,000,000 to 17,000,000	13,000,000 to 18,000,000	8,500,000 to 11,500,000
	Average modulus of elasticity	12,000,000	16,000,000	9,000,000
Concentric strand (Values in pounds/in^2)	Tensile strength	29,000 to 37,000	43,000 to 65,000	25,800
	Average tensile strength	35,000	54,000	—
	Elastic limit	5,800 to 14,800	23,000 to 42,000	13,800
	Average elastic limit	—	27,000	—
	Modulus of elasticity	5,000,000 to 12,000,000	12,000,000	Approx 10,000,000

* Reprinted by permission from "Transmission Towers," American Bridge Company, Pittsburgh, Pa.; 1925: p. 169.

Stranded copper (AWG)*

circular mils	AWG B & S gauge	number of wires	individual wire diam in inches	cable diam inches	area square inches	weight lbs per 1000 ft	weight lbs per mile	*maximum resistance ohms/1000 ft at 20° C
211,600	4/0	19	0.1055	0.528	0.1662	653.3	3,450	0.05093
167,800	3/0	19	0.0940	0.470	0.1318	518.1	2,736	0.06422
133,100	2/0	19	0.0837	0.419	0.1045	410.9	2,170	0.08097
105,500	1/0	19	0.0745	0.373	0.08286	325.7	1,720	0.1022
83,690	1	19	0.0664	0.332	0.06573	258.4	1,364	0.1288
66,370	2	7	0.0974	0.292	0.05213	204.9	1,082	0.1624
52,640	3	7	0.0867	0.260	0.04134	162.5	858.0	0.2048
41,740	4	7	0.0772	0.232	0.03278	128.9	680.5	0.2582
33,100	5	7	0.0688	0.206	0.02600	102.2	539.6	0.3256
26,250	6	7	0.0612	0.184	0.02062	81.05	427.9	0.4105
20,820	7	7	0.0545	0.164	0.01635	64.28	339.4	0.5176
16,510	8	7	0.0486	0.146	0.01297	50.98	269.1	0.6528
13,090	9	7	0.0432	0.130	0.01028	40.42	213.4	0.8233
10,380	10	7	0.0385	0.116	0.008152	32.05	169.2	1.038
6,530	12	7	0.0305	0.0915	0.005129	20.16	106.5	1.650
4,107	14	7	0.0242	0.0726	0.003226	12.68	66.95	2.624
2,583	16	7	0.0192	0.0576	0.002029	7.975	42.11	4.172
1,624	18	7	0.0152	0.0456	0.001275	5.014	26.47	6.636
1,022	20	7	0.0121	0.0363	0.0008027	3.155	16.66	10.54

* The resistance values in this table are trade maxima for soft or annealed copper wire and are higher than the average values for commercial cable. The following values for the conductivity and resistivity of copper at 20 degrees centigrade were used:

Conductivity in terms of International Annealed Copper Standard: 98.16 percent
Resistivity in pounds per mile-ohm: 891.58

The resistance of hard-drawn copper is slightly greater than the values given, being about 2 percent to 3 percent greater for sizes from 4/0 to 20 AWG.

iron (Ex BB)	steel (Siemens–Martin)	crucible steel, high strength	plow steel, extra-high strength	copper-clad 30% cond	copper-clad 40% cond
16.8	8.7	—	—	29.4	39.0
62.9	119.7	122.5	125.0	35.5	26.6
332,000	632,000	647,000	660,000	187,000	140,000
4,700	8,900	9,100	9,300	2.775	2.075
0.0028	0.00278	0.00278	0.00278	0.0024	—
0.0050	0.00501	0.00501	0.00501	0.0044	0.0041
7.77	7.85	7.85	7.85	8.17	8.25
0.002652	0.002671	—	—	0.00281	0.00281
0.282	0.283	0.283	0.283	0.298	0.298
0.113	0.117	—	—	—	—
2,975	2,480	—	—	—	—
1,635	1,360	—	—	—	—
0.00000673	0.00000662	—	—	0.0000072	0.0000072
0.0000120	0.0000118	—	—	0.0000129	0.0000129
50,000 to 55,000	70,000 to 80,000	—	—	—	—
55,000	75,000	125,000	187,000	60,000	100,000
25,000 to 30,000	35,000 to 50,000	—	—	—	—
30,000	38,000	69,000	130,000	30,000	50,000
22,000,000 to 27,000,000	22,000,000 to 29,000,000	—	—	—	—
26,000,000	29,000,000	30,000,000	30,000,000	19,000,000	21,000,000
—	74,000 to 98,000	85,000 to 165,000	140,000 to 245,000	70,000 to 97,000	—
—	80,000	125,000	180,000	80,000	—
—	37,000 to 49,000	—	—	—	—
—	40,000	70,000	110,000	—	—
—	12,000,000	15,000,000	15,000,000	—	—

Machine screws

Head styles—method of length measurement

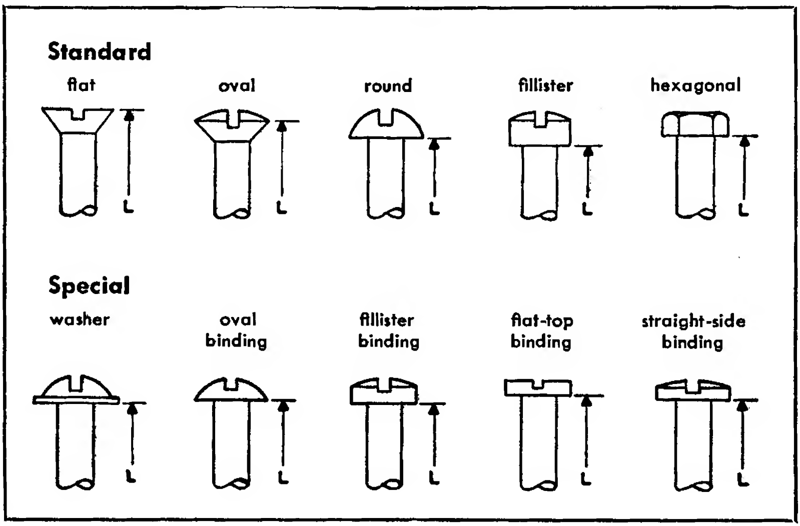

continued **Machine screws**

Dimensions and other data

screw		threads per inch		clearance drill*		tap drill†			head					hex nut			washer		
							diameter		round		flat	fillister							
no	dia	coarse	fine	no	dia	no	inches	mm	max OD	max height	max OD	max OD	max height	across flat	across corner	thickness	OD	ID	thickness
0	0.060	—	80	52	0.064	56	0.047	1.2	0.113	0.053	0.119	0.096	0.059	0.156	0.171	0.046	—	—	—
1	0.073	64	72	47	0.079	53	0.060	1.5	0.138	0.061	0.146	0.118	0.070	0.156	0.171	0.046	—	—	—
2	0.086	56	64	42	0.094	50	0.070	1.8	0.162	0.070	0.172	0.140	0.083	0.187	0.205	0.062	1/4	0.093	0.032
3	0.099	48	—	37	0.104	47	0.079	2.0	0.187	0.078	0.199	0.161	0.095	0.187	0.205	0.062	1/4	0.105	0.020
		—	56			45	0.082	2.1											
4	0.112	40	—	31	0.120	43	0.089	2.3	0.211	0.086	0.225	0.183	0.107	0.250	0.275	0.093	5/16	0.125	0.032
		—	48			42	0.094	2.4											
5	0.125	40	—	29	0.136	38	0.102	2.6	0.236	0.095	0.252	0.205	0.120	0.312	0.344	0.109	3/8	0.140	0.032
		—	44			37	0.104	2.6											
6	0.138	32	—	27	0.144	36	0.107	2.7	0.260	0.103	0.279	0.226	0.132	0.312	0.344	0.109	5/16	0.156	0.026
		—	40			33	0.113	2.9									3/8		0.046
8	0.164	32	—	18	0.170	29	0.136	3.5	0.309	0.119	0.332	0.270	0.156	0.344	0.373	0.125	3/8	0.186	0.032
		—	36			29	0.136	3.5									7/16		0.046
10	0.190	24	—	9	0.196	25	0.150	3.8	0.359	0.136	0.385	0.313	0.180	0.375	0.413	0.125	7/16	0.218	0.036
		—	32			21	0.159	4.0									1/2		0.063
12	0.216	24	—	2	0.221	16	0.177	4.5	0.408	0.152	0.438	0.357	0.205	0.437	0.488	0.156	1/2	0.250	0.063
		—	28			14	0.182	4.6									9/16		
¼	0.250	20	—	—	17/64	7	0.201	5.1	0.472	0.174	0.507	0.414	0.237	0.437	0.488	0.203	9/16	0.281	0.040
		—	28			3	0.213	5.5						0.500	0.577	0.250	5/8		0.063

All dimensions in inches except where noted.

* Clearance-drill sizes are practical values for use of the engineer or technician doing his own shop work.

† Tap-drill sizes are for use in hand tapping material such as brass or soft steel. For copper, aluminum, Norway iron, cast iron, bakelite, or for very thin material, the drill should be a size or two larger diameter than shown.

Drill sizes*

drill	inches	drill	inches	drill	inches	drill	inches
0.10 mm	0.003937	1.30 mm	0.051181	3.10 mm	0.122047	no 4	0.209000
0.15 mm	0.005905	no 55	0.052000	1/8 in	0.125000	5.40 mm	0.212598
0.20 mm	0.007874	1.35 mm	0.053149	3.20 mm	0.125984	no 3	0.213000
0.25 mm	0.009842	no 54	0.055000	3.25 mm	0.127952	5.50 mm	0.216535
0.30 mm	0.011811	1.40 mm	0.055118	no 30	0.128500	7/32 in	0.218750
no 80	0.013000	1.45 mm	0.057086	3.30 mm	0.129921	5.60 mm	0.220472
no 79½	0.013500	1.50 mm	0.059055	3.40 mm	0.133858	no 2	0.221000
0.35 mm	0.013779	no 53	0.059500	no 29	0.136000	5.70 mm	0.224409
no 79	0.014000	1.55 mm	0.061023	3.50 mm	0.137795	5.75 mm	0.226377
no 78½	0.014500	1/16 in	0.062500	no 28	0.140500	no 1	0.228000
no 78	0.015000	1.60 mm	0.062992	9/64 in	0.140625	5.80 mm	0.228346
1/64 in	0.015625	no 52	0.063500	3.60 mm	0.141732	5.90 mm	0.232283
0.40 mm	0.015748	1.65 mm	0.064960	no 27	0.144000	ltr A	0.234000
no 77	0.016000	1.70 mm	0.066929	3.70 mm	0.145669	15/64 in	0.234375
0.45 mm	0.017716	no 51	0.067000	no 26	0.147000	6.00 mm	0.236220
no 76	0.018000	1.75 mm	0.068897	3.75 mm	0.147637	ltr B	0.238000
0.50 mm	0.019685	no 50	0.070000	no 25	0.149500	6.10 mm	0.240157
no 75	0.020000	1.80 mm	0.070866	3.80 mm	0.149606	ltr C	0.242000
no 74½	0.021000	1.85 mm	0.072834	no 24	0.152000	6.20 mm	0.244094
0.55 mm	0.021653	no 49	0.073000	3.90 mm	0.153543	ltr D	0.246000
no 74	0.022000	1.90 mm	0.074803	no 23	0.154000	6.25 mm	0.246062
no 73½	0.022500	no 48	0.076000	5/32 in	0.156250	6.30 mm	0.248031
no 73	0.023000	1.95 mm	0.076771	no 22	0.157000	ltr E, 1/4 in	0.250000
0.60 mm	0.023622	5/64 in	0.078125	4.00 mm	0.157480	6.40 mm	0.251968
no 72	0.024000	no 47	0.078500	no 21	0.159000		
no 71½	0.025000	2.00 mm	0.078740	no 20	0.161000	6.50 mm	0.255905
0.65 mm	0.025590	2.05 mm	0.080708	4.10 mm	0.161417	ltr F	0.257000
no 71	0.026000	no 46	0.081000	4.20 mm	0.165354	6.60 mm	0.259842
no 70	0.027000	no 45	0.082000	no 19	0.166000	ltr G	0.261000
0.70 mm	0.027559	2.10 mm	0.082677	4.25 mm	0.167322	6.70 mm	0.263779
no 69½	0.028000	2.15 mm	0.084645	4.30 mm	0.169291	17/64 in	0.265625
no 69	0.029000	no 44	0.086000	no 18	0.169500	6.75 mm	0.265747
no 68½	0.029250	2.20 mm	0.086614	11/64 in	0.171875	ltr H	0.266000
0.75 mm	0.029527	2.25 mm	0.088582	no 17	0.173000	6.80 mm	0.267716
no 68	0.030000	no 43	0.089000	4.40 mm	0.173228	6.90 mm	0.271653
no 67	0.031000	2.30 mm	0.090551	no 16	0.177000	ltr I	0.272000
1/32 in	0.031250	2.35 mm	0.092519	4.50 mm	0.177165	7.00 mm	0.275590
0.80 mm	0.031496	no 42	0.093500	no 15	0.180000	ltr J	0.277000
no 66	0.032000	3/32 in	0.093750	4.60 mm	0.181102	7.10 mm	0.279527
no 65	0.033000	2.40 mm	0.094488	no 14	0.182000	ltr K	0.281000
0.85 mm	0.033464	no 41	0.096000	no 13	0.185000	9/32 in	0.281250
no 64	0.035000	2.45 mm	0.096456	4.70 mm	0.185039	7.20 mm	0.283464
0.90 mm	0.035433	no 40	0.098000	4.75 mm	0.187007	7.25 mm	0.285432
no 63	0.036000	2.50 mm	0.098425	3/16 in	0.187500	7.30 mm	0.287401
no 62	0.037000	no 39	0.099500	4.80 mm	0.188976	ltr L	0.290000
0.95 mm	0.037401	no 38	0.101500	no 12	0.189000	7.40 mm	0.291338
no 61	0.038000	2.60 mm	0.102362	no 11	0.191000	ltr M	0.295000
no 60½	0.039000	no 37	0.104000	4.90 mm	0.192913	7.50 mm	0.295275
1.00 mm	0.039370	2.70 mm	0.106299	no 10	0.193500	19/64 in	0.296875
no 60	0.040000	no 36	0.106500	no 9	0.196000	7.60 mm	0.299212
no 59	0.041000	2.75 mm	0.108267	5.00 mm	0.196850	ltr N	0.302000
1.05 mm	0.041338	7/64 in	0.109375	no 8	0.199000	7.70 mm	0.303149
no 58	0.042000	no 35	0.110000	5.10 mm	0.200787	7.75 mm	0.305117
no 57	0.043000	2.80 mm	0.110236	no 7	0.201000	7.80 mm	0.307086
1.10 mm	0.043307	no 34	0.111000	13/64 in	0.203125	7.90 mm	0.311023
1.15 mm	0.045275	no 33	0.113000	no 6	0.204000	5/16 in	0.312500
no 56	0.046500	2.90 mm	0.114173	5.20 mm	0.204724	8.00 mm	0.314960
3/64 in	0.046875	no 32	0.116000	no 5	0.205500	ltr O	0.316000
1.20 mm	0.047244	3.00 mm	0.118110	5.25 mm	0.206692	8.10 mm	0.318897
1.25 mm	0.049212	no 31	0.120000	5.30 mm	0.208661	8.20 mm	0.322834

* From New Departure Handbook.

Drill sizes *continued*

drill	inches	drill	inches	drill	inches	drill	inches
ltr P	0.323000	9.60 mm	0.377952	35/64 in	0.546875	25/32 in	0.781250
8.25 mm	0.324802	9.70 mm	0.381889	14.00 mm	0.551180	20.00 mm	0.787400
8.30 mm	0.326771	9.75 mm	0.383857	9/16 in	0.562500	51/64 in	0.796875
21/64 in	0.328125	9.80 mm	0.385826	14.50 mm	0.570865	20.50 mm	0.807085
8.40 mm	0.330708	ltr W	0.386000	37/64 in	0.578125	13/16 in	0.812500
ltr Q	0.332000	9.90 mm	0.389763	15.00 mm	0.590550	21.00 mm	0.826770
8.50 mm	0.334645	25/64 in	0.390625	19/32 in	0.593750	53/64 in	0.828125
8.60 mm	0.338582	10.00 mm	0.393700	39/64 in	0.609375	27/32 in	0.843750
ltr R	0.339000	ltr X	0.397000	15.50 mm	0.610235	21.50 mm	0.846455
8.70 mm	0.342519	ltr Y	0.404000	5/8 in	0.625000	55/64 in	0.859375
11/32 in	0.343750	13/32 in	0.406250	16.00 mm	0.629920	22.00 mm	0.866140
8.75 mm	0.344487	ltr Z	0.413000	41/64 in	0.640625	7/8 in	0.875000
8.80 mm	0.346456	10.50 mm	0.413385	16.50 mm	0.649605	22.50 mm	0.885825
ltr S	0.348000	27/64 in	0.421875	21/32 in	0.656250	57/64 in	0.890625
8.90 mm	0.350393	11.00 mm	0.433070	17.00 mm	0.669290	23.00 mm	0.905510
9.00 mm	0.354330	7/16 in	0.437500	43/64 in	0.671875	29/32 in	0.906250
ltr T	0.358000	11.50 mm	0.452755	11/16 in	0.687500	59/64 in	0.921875
9.10 mm	0.358267	29/64 in	0.453125	17.50 mm	0.688975	23.50 mm	0.925195
23/64 in	0.359375	15/32 in	0.468750	45/64 in	0.703125	15/16 in	0.937500
9.20 mm	0.362204	12.00 mm	0.472440	18.00 mm	0.708660	24.00 mm	0.944880
9.25 mm	0.364172	31/64 in	0.484375	23/32 in	0.718750	61/64 in	0.953125
9.30 mm	0.366141	12.50 mm	0.492125	18.50 mm	0.728345	24.50 mm	0.964565
ltr U	0.368000	1/2 in	0.500000	47/64 in	0.734375	31/32 in	0.968750
9.40 mm	0.370078	13.00 mm	0.511810	19.00 mm	0.748030	25.00 mm	0.984250
9.50 mm	0.374015	33/64 in	0.515625	3/4 in	0.750000	63/64 in	0.984375
3/8 in	0.375000	17/32 in	0.531250	49/64 in	0.765625	1 in	1.000000
ltr V	0.377000	13.50 mm	0.531495	19.50 mm	0.767715		

Sheet-metal gauges

Systems in use

Materials are customarily made to certain gauge systems. While materials can usually be had specially in any system, some usual practices are shown below.

material	sheet	wire
Aluminum	B&S	AWG (B&S)
Brass, bronze, sheet	B&S	—
Copper	B&S	AWG (B&S)
Iron, steel, band and hoop	BWG	—
Iron, steel, telephone and telegraph wire	—	BWG
Steel wire, except telephone and telegraph	—	W&M
Steel sheet	US	—
Tank steel	BWG	—
Zinc sheet	"Zinc gauge" proprietary	—

Sheet-metal gauges *continued*

Comparison of gauges*

The following table gives a comparison of various sheet-metal-gauge systems. Thickness is expressed in decimal fractions of an inch.

gauge	AWG B&S	Birmingham or Stubs BWG	Wash. & Moen W&M	British standard NBS SWG	London or old English	United States standard US	American Standard preferred thickness†
0000000	—	—	0.490	0.500	—	0.50000	—
000000	0.5800	—	0.460	0.464	—	0.46875	—
00000	0.5165	—	0.430	0.432	—	0.43750	—
0000	0.4600	0.454	0.3938	0.400	0.454	0.40625	—
000	0.4096	0.425	0.3625	0.372	0.425	0.37500	—
00	0.3648	0.380	0.3310	0.348	0.380	0.34375	—
0	0.3249	0.340	0.3065	0.324	0.340	0.31250	—
1	0.2893	0.300	0.2830	0.300	0.300	0.28125	—
2	0.2576	0.284	0.2625	0.276	0.284	0.265625	—
3	0.2294	0.259	0.2437	0.252	0.259	0.250000	0.224
4	0.2043	0.238	0.2253	0.232	0.238	0.234375	0.200
5	0.1819	0.220	0.2070	0.212	0.220	0.218750	0.180
6	0.1620	0.203	0.1920	0.192	0.203	0.203125	0.160
7	0.1443	0.180	0.1770	0.176	0.180	0.187500	0.140
8	0.1285	0.165	0.1620	0.160	0.165	0.171875	0.125
9	0.1144	0.148	0.1483	0.144	0.148	0.156250	0.112
10	0.1019	0.134	0.1350	0.128	0.134	0.140625	0.100
11	0.09074	0.120	0.1205	0.116	0.120	0.125000	0.090
12	0.08081	0.109	0.1055	0.104	0.109	0.109375	0.080
13	0.07196	0.095	0.0915	0.092	0.095	0.093750	0.071
14	0.06408	0.083	0.0800	0.080	0.083	0.078125	0.063
15	0.05707	0.072	0.0720	0.072	0.072	0.0703125	0.056
16	0.05082	0.065	0.0625	0.064	0.065	0.0625000	0.050
17	0.04526	0.058	0.0540	0.056	0.058	0.0562500	0.045
18	0.04030	0.049	0.0475	0.048	0.049	0.0500000	0.040
19	0.03589	0.042	0.0410	0.040	0.040	0.0437500	0.036
20	0.03196	0.035	0.0348	0.036	0.035	0.0375000	0.032
21	0.02846	0.032	0.03175	0.032	0.0315	0.0343750	0.028
22	0.02535	0.028	0.02860	0.028	0.0295	0.0312500	0.025
23	0.02257	0.025	0.02580	0.024	0.0270	0.0281250	0.022
24	0.02010	0.022	0.02300	0.022	0.0250	0.0250000	0.020
25	0.01790	0.020	0.02040	0.020	0.0230	0.0218750	0.018
26	0.01594	0.018	0.01810	0.018	0.0205	0.0187500	0.016
27	0.01420	0.016	0.01730	0.0164	0.0187	0.0171875	0.014
28	0.01264	0.014	0.01620	0.0148	0.0165	0.0156250	0.012
29	0.01126	0.013	0.01500	0.0136	0.0155	0.0140625	0.011
30	0.01003	0.012	0.01400	0.0124	0.01372	0.0125000	0.010
31	0.008928	0.010	0.01320	0.0116	0.01220	0.01093750	0.009
32	0.007950	0.009	0.01280	0.0108	0.01120	0.01015625	0.008
33	0.007080	0.008	0.01180	0.0100	0.01020	0.00937500	0.007
34	0.006305	0.007	0.01040	0.0092	0.00950	0.00859375	0.006
35	0.005615	0.005	0.00950	0.0084	0.00900	0.00781250	—
36	0.005000	0.004	0.00900	0.0076	0.00750	0.007031250	—
37	0.004453	—	0.00850	0.0068	0.00650	0.006640625	—
38	0.003965	—	0.00800	0.0060	0.00570	0.006250000	—
39	0.003531	—	0.00750	0.0052	0.00500	—	—
40	0.003145	—	0.00700	0.0048	0.00450	—	—

* Courtesy of Whitehead Metal Products Co., Inc.

† These thicknesses are intended to express the desired thickness in decimals. They have no relation to gauge numbers; they are approximately related to the AWG sizes 3–34.

Commercial insulating materials*

The tables on the following pages give a few of the important electrical and physical properties of insulating or dielectric materials. The dielectric constant and dissipation factor of most materials depend on the frequency and temperature of measurement. For this reason, these properties are given at a number of frequencies, but because of limited space, only the values at room temperature are given. The dissipation factor is defined as the ratio of the energy dissipated to the energy stored in the dielectric per cycle, or as the tangent of the loss angle. For dissipation factors less than 0.1, the dissipation factor may be considered equal to the power factor of the dielectric, which is the cosine of the phase angle by which the current leads the voltage.

Many of the materials listed are characterized by a peak dissipation factor occurring somewhere in the frequency range, this peak being accompanied by a rapid change in the dielectric constant. These effects are the result of a resonance phenomenon occurring in polar materials. The position of the dissipation-factor peak in the frequency spectrum is very sensitive to

* Most of the data listed in these tables have been taken from "Tables of Dielectric Materials," vols. I–IV, prepared by the laboratory for Insulation Research of the Massachusetts Institute of Technology, Cambridge, Massachusetts; January, 1953 and from, "Dielectric Materials and Applications," A. R. von Hipple, editor; John Wiley & Sons, Inc., New York, N. Y.: 1954.

material	composition	T °C	dielectric constant at (frequency in cycles/second)						
			60	10^3	10^6	10^8	3×10^9	2.5×10^{10}	60
ceramics									
AlSiMag A-35	Magnesium silicate	23	6.14	5.96	5.84	5.75	5.60	5.36	0.017
AlSiMag A-196	Magnesium silicate	25	5.90	5.88	5.70	5.60	5.42	5.18	0.0022
AlSiMag 211	Magnesium silicate	25	6.00	5.98	5.97	5.96	5.90	—	0.012
AlSiMag 228	Magnesium silicate	25	6.41	6.40	6.36	6.20	5.97	5.83	0.0013
AlSiMag 243	Magnesium silicate	22	6.32	6.30	6.22	6.10	5.78	5.75	0.0015
Ceramic NPOT96	—	25	—	29.5	29.5	29.5	—	—	—
Ceramic N750T96	—	25	—	83.4	83.4	83.4	83.4	—	—
Ceramic N1400T110	—	25	—	130.8	130.2	130.0	—	—	—
Coors AI-200	Aluminum oxide	25	—	8.83	8.80	8.80	8.79	—	—
Crolite 29	Oxides of aluminum, silicon, magnesium, calcium, barium	24	—	6.04	6.04	—	5.90	—	—
Magnesium oxide	—	25	—	9.65	9.65	9.65	—	—	—
Porcelain	Dry process	25	5.5	5.36	5.08	5.04	—	—	0.03
Porcelain	Wet process	25	6.5	6.24	5.87	5.80	—	—	0.03
Steatite 410	—	25	5.77	5.77	5.77	5.77	5.7	—	—
TamTicon B	Barium titanate†	26	1250	1200	1143	—	600	100	0.056
TamTicon MC	Magnesium titanate	25	—	13.9	13.9	13.9	13.8	13.7	—
TamTicon C	Calcium titanate	25	168	167.7	167.7	167.7	165	—	0.006
TamTicon S	Strontium titanate	25	—	233	232	232	—	—	—
TI-Pure R-200	Titanium dioxide (rutile)	26	—	100	100	100	—	—	—
Zirconium porcelain Zi-4	—	25	—	6.40	6.32	6.30	6.23	—	—

† Dielectric constant and dissipation factor are dependent on electrical field strength.

temperature. An increase in the temperature increases the frequency at which the peak occurs, as illustrated qualitatively in the sketch at the right. Nonpolar materials have very low losses without a noticeable peak; the dielectric constant remains essentially unchanged over the frequency range.

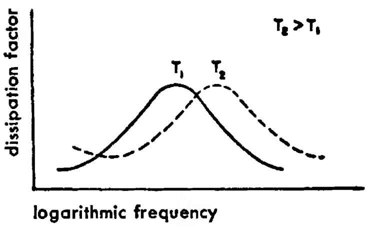

Another effect that contributes to dielectric losses is that of ionic or electronic conduction. This loss, if present, is important usually at the lower end of the frequency range only, and is distinguished by the fact that the dissipation factor varies inversely with frequency. Increase in temperature increases the loss due to ionic conduction because of increased ionic mobility.

The data given on dielectric strength are accompanied by the thickness of the specimen tested because the dielectric strength, expressed in volts/mil, varies inversely with the square root of thickness, approximately.

The direct-current volume resistivity of many materials is influenced by changes in temperature or humidity. The values given in the table may be reduced several decades by raising the temperature toward the higher end of the working range of the material, or by raising the relative humidity of the air surrounding the material to above 90 percent.

dissipation factor at (frequency in cycles/second)					dielectric strength in volts/mil at 25° C	dc volume resistivity in ohm-cm at 25° C	thermal expansion (linear) in parts/°C	softening point in °C	moisture absorption in percent
10^3	10^6	10^8	3×10^9	2.5×10^{10}					
0.0100	0.0038	0.0037	0.0041	0.0058	225 (1/8″)	$>10^{14}$	8.7×10^{-6}	1450	<0.1
0.0059	0.0031	0.0016	0.0018	0.0038	240 (1/4″)	$>10^{14}$	8.9×10^{-6}	1450	<0.1
0.0034	0.0005	0.0004	0.0012	—	—	$>10^{14}$	9.2×10^{-6}	1350	0.1–1
0.0020	0.0012	0.0010	0.0013	0.0042	—	—	$6\text{–}8 \times 10^{-6}$	1450	<0.05
0.00045	0.00037	0.0003	0.0006	0.0012	200 (1/8″)	$>10^{14}$	10.5×10^{-6}	1450	<0.1
0.00049	0.00016	0.0002	—	—	—	—	—	—	—
0.00045	0.00022	0.00046	—	—	—	—	—	—	—
0.00055	0.00030	0.00070	—	—	—	—	—	—	—
0.00057	0.00033	0.00030	0.0010	—	—	—	—	—	—
0.0019	0.0011	—	0.0024	—	—	—	7.7×10^{-6}	1325	—
<0.0003	<0.0003	<0.0003	—	—	—	—	—	—	—
0.0140	0.0075	0.0078	—	—	—	—	—	—	—
0.0180	0.0090	0.0135	—	—	—	—	—	—	—
0.0030	0.0007	0.0006	0 00089	—	—	—	—	—	—
0.0130	0.0105	—	0.30	0.60	75	10^{12}–10^{13}	—	1400–1430	0.1
0.0011	0.0004	0.0005	0.0017	0.0065	—	—	—	—	—
0.00044	0.0002	—	0.0023	—	100	10^{12}–10^{14}	—	1510	<0.1
0.0011	0.0002	0.0001	—	—	100	10^{12}–10^{14}	—	1510	0.1
0.0015	0.0003	0.00025	—	—	—	—	—	—	—
0.0040	0.0023	0.0025	0.0045	—	—	—	—	—	—

Commercial insulating materials *continued*

material	composition	T	dielectric constant at (frequency in cycles/second)						
		°C	60	10^3	10^6	10^8	3×10^9	2.5×10^{10}	60
glasses									
Corning 0010	Soda-potash-lead silicate ~20% lead oxide	24	6.70	6.63	6.43	6.33	6.10	5.87	0.0084
Corning 0120	Soda-potash-lead silicate	23	6.76	6.70	6.65	6.65	6.64	6.51	0.0050
Corning 1990	Iron-sealing glass	24	8.41	8.38	8.30	8.20	7.99	7.84	—
Corning 1991	—	24	8.10	8.10	8.08	8.00	7.92	—	0.0027
Corning 7040	Soda-potash-borosilicate	25	4.85	4.82	4.73	4.68	4.67	4.52	0.0055
Corning 7050	Soda-borosilicate	25	4.90	4.84	4.78	4.75	4.74	4.64	0.0093
Corning 7060 (Pyrex)	Soda-borosilicate	25	—	4.97	4.84	4.84	4.82	4.65	—
Corning 7070	Low-alkali, potash-lithiaborosilicate	23	4.00	4.00	4.00	4.00	4.00	3.9	0.0006
Corning 7720	Soda-lead borosilicate	24	4.75	4.70	4.62	—	4.60	—	0.0093
Corning 7750	Soda-borosilicate ~80% silicon dioxide	25	—	4.42	4.38	4.38	4.38	—	—
Corning 7900	96% silicon dioxide	20	3.85	3.85	3.85	3.85	3.84	3.82	0.0006
Fused silica 915c	Silicon dioxide	25	—	3.78	3.78	3.78	3.78	—	—
Quartz (fused)	100% silicon dioxide	25	3.78	3.78	3.78	3.78	3.78	3.78	0.0009
plastics									
Alkyd resin	Foamed diisocynate	25	—	1.223	1.218	1.20	1.20	—	—
Araldite CN-501	Epoxy resin	25	—	3.67	3.62	3.35	3.09	—	—
Araldite CN-504	Epoxy resin	25	—	3.99	3.69	3.39	3.15	—	—
Bakelite BM120	Phenol-formaldehyde	25	4.90	4.74	4.36	3.95	3.70	3.55	0.08
Bakelite BM250	Phenol-formaldehyde, 66% asbestos fiber, preformed and preheated	25	—	22	5.3	5.0	5.0	5.0	—
Bakelite BM262	Phenol-aniline-formaldehyde, 62% mica	25	4.87	4.80	4.67	4.65	—	4.5	0.010
Bakelite BT-48-306	100% phenol-formaldehyde	24	8.6	7.15	5.4	4.4	3.64	—	0.15
Beetle resin	Urea-formaldehyde, cellulose	27	6.6	6.2	5.65	5.1	4.57	—	0.032
Bureau of Standards casting resin	32.5% polystyrene, 53.5% poly-2,5-dichlorostyrene, 13% hydrogenated terphenyl, 0.5% divinyl-benzene	25	—	2.62	2.62	2.62	2.59	—	—
Catalin 200 base	Phenol-formaldehyde	22	8.8	8.2	7.0	—	4.89	—	0.05
Chemelec MI-405	75% Teflon, 25% calcium fluoride	25	—	2.50	2.50	2.50	2.50	—	—
Chemelec MI-407	88% Teflon, 12% ceramic	25	—	3.02	2.71	2.63	—	—	—
Chemelec MI-411	75% Teflon, 25% Fibreglas	25	—	2.14	2.14	2.14	—	—	—
Chemelec MI-422	80% Teflon, 20% titanium dioxide	25	—	2.72	2.72	2.72	—	—	—
Cibanite	100% aniline-formaldehyde	25	3.60	3.58	3.42	3.40	3.40	—	0.0030
DC 996	Methyl, phenyl, and methyl-phenyl polysiloxane resin	25	—	2.90	2.90	2.90	—	—	—
DC 2104 laminate XL-269	35% methyl and phenyl polysiloxane resin, 65% ECC-181 Fibreglas	25	—	4.14	4.13	4.10	4.07	—	—
Dilectene-100	100% aniline-formaldehyde	25	3.70	3.68	3.58	3.50	3.44	—	0.0033
Dilecto (Mecoboard)	45% cresol-phenol formaldehyde, 15% tung oil, 15% nylon	25	—	3.98	3.46	3.23	3.11	—	—
Dilecto (Teflon laminate GB-112T)	65-68% Teflon, 32-35% continuous-filament glass base	25	—	2.74	2.73	2.73	—	—	—
Durez 1601 natural	Phenol-formaldehyde, 67% mica	26	5.1	4.94	4.60	4.51	4.48	—	0.03
Durite 500	Phenol-formaldehyde, 65% mica, 4% lubricants	24	5.1	5.03	4.78	4.72	4.71	—	0.015
Epon resin RN-48	Epoxy resin	25	—	3.63	3.52	3.32	3.04	—	—
Formica FF-41	Melamine-formaldehyde, 55% filler	26	—	6.00	5.75	5.5	—	—	—
Formica XX	Phenol-formaldehyde, 50% paper laminate	26	5.25	5.15	4.60	4.04	3.57	—	0.025
Formvar E	Polyvinyl formal	26	3.20	3.12	2.92	2.80	2.76	2.7	0.003

dissipation factor at (frequency in cycles/second)					dielectric strength in volts/mil at 25° C	dc volume resistivity in ohm–cm at 25° C	thermal expansion (linear) in parts/°C	softening point in ° C	moisture absorption in percent
10^3	10^6	10^8	3×10^9	2.5×10^{10}					
0.00535	0.00165	0.0023	0.0060	0.0110	—	10^9 at 250°	90×10^{-7}	626	—
0.0030	0.0012	0.0018	0.0041	0.0127	—	10^{10} at 250°	87×10^{-7}	630	—
0.0004	0.0005	0.0009	0.00199	0.0112	—	10^{10} at 250°	132×10^{-7}	484	Poor
0.0009	0.0005	0.0012	0.0038	—	—	4×10^9 at 250°	128×10^{-7}	527	—
0.0034	0.0019	0.0027	0.0044	0.0073	—	5×10^9 at 250°	49×10^{-7}	697	—
0.0056	0.0027	0.0035	0.0052	0.0083	—	10^8 at 250°	46×10^{-7}	703	—
0.0055	0.0036	0.0030	0.0054	0.0090	—	7×10^7 at 250°	50×10^{-7}	693	—
0.0005	0.0008	0.0012	0.0012	0.0031	—	10^{11} at 250°	31×10^{-7}	746	—
0.0042	0.0020	—	—	—	—	6×10^8 at 250°	36×10^{-7}	756	—
0.0033	0.0018	—	0.0043	—	—	3×10^9 at 250°	42×10^{-7}	701	—
0.0006	0.0006	0.0006	0.00068	0.0013	—	5×10^9 at 250°	8×10^{-7}	1450	—
0.00026	0.00001	0.00003	0.0001	—	—	—	—	—	—
0.00075	0.0001	0.0002	0.00006	0.00025	410 (¼")	$>10^{19}$	5.7×10^{-7}	1667	—
0.00147	0.0041	0.0038	0.0034	—	—	—	—	—	—
0.0024	0.019	0.034	0.027	—	405 (⅛")	$>3.8 \times 10^7$	4.77×10^{-5}	109 (distortion)	0.14
0.0104	0.027	0.030	0.031	—	—	—	—	—	—
0.0220	0.0280	0.0380	0.0438	0.0390	300 (⅛")	10^{11}	$30–40 \times 10^{-6}$	<135 (distortion)	<0.6
0.370	0.125	—	—	0.032	—	—	—	145 (distortion)	—
0.0082	0.0055	0.0057	—	0.0089	325–375 (⅛")	2×10^{14}	$10–20 \times 10^{-6}$	100–115 (distortion)	0.3
0.082	0.060	0.077	0.052	—	277 (⅛")	—	$8.3–13 \times 10^{-5}$	50 (distortion)	0.42
0.024	0.027	0.050	0.0555	—	375 (0.085")	—	2.6×10^{-5}	152 (distortion)	2
0.00156	0.00047	0.0011	0.0005	—	—	—	—	—	—
0.0290	0.050	—	0.108	—	200 (⅛")	—	$7.5–15 \times 10^{-5}$	40–60 (distortion)	—
0.00051	0.0005	0.0009	0.00068	—	—	—	—	—	—
0.070	0.015	0.0158	—	—	—	—	—	—	—
0.00096	0.0007	0.0010	—	—	—	—	—	—	—
0.00077	0.00020	0.00024	—	—	—	—	—	—	—
0.0041	0.0078	0.0039	0.0029	—	600 (⅛")	—	6.49×10^{-5}	126	0.05–0.08
0.0015	0.0018	0.00165	—	—	—	—	—	—	—
0.0029	0.0022	0.0034	0.0071	—	—	—	—	—	—
0.0032	0.0061	0.0033	0.0026	—	810 (0.068")	$>10^{16}$	5.4×10^{-5}	125	0.06–0.08
0.0344	0.0263	0.0216	0.0220	—	—	—	—	—	—
0.00061	0.00058	0.00118	—	—	—	—	—	—	—
0.021	0.0080	0.0064	0.0062	—	—	—	—	—	—
0.0104	0.0082	0.0115	0.0126	—	—	—	—	—	—
0.0038	0.0142	0.0264	0.021	—	—	—	—	—	—
0.0119	0.0115	0.020	—	—	—	—	1.7×10^{-5}	—	0.6
0.0165	0.034	0.057	0.060	—	—	—	—	—	—
0.0100	0.019	0.013	0.0113	0.0115	860 (0.034")	$>5 \times 10^{16}$	7.7×10^{-5}	190	1.3

Commercial insulating materials *continued*

material	composition	T °C	dielectric constant at (frequency in cycles/second) 60	10^3	10^6	10^8	3×10^9	2.5×10^{10}	60
plastics—*continued*									
Geon 2046	59% polyvinyl-chloride, 30% dioctyl phosphate, 6% stabilizer, 5% filler	23	7.5	6.10	3.55	3.00	2.89	—	0.08
Hardman 51 Permo potting compound	Alkyd resin	25	—	2.95	2.70	2.59	2.53	—	—
Hydrogenated polystyrene	Polyvinylcyclohexane	24	—	2.25	2.25	2.25	2.25	—	—
Hysol 6020	Epoxy resin	25	—	3.90	3.54	3.29	3.01	—	—
Hysol 6030, flexible potting compound	Epoxy resin	25	—	6.15	4.74	3.61	3.20	—	—
Kel-F	Polychlorotrifluoroethylene	25	2.72	2.63	2.42	2.32	2.29	2.28	0.015
Kel-F, grade 300P25	Plasticized polychlorotrifluoroethylene	25	—	2.75	2.51	2.37	2.31	—	—
Koroseal 5CS-243	63.7% polyvinyl-chloride, 33.1% di-2-ethylhexyl-phthalate, lead silicate	27	6.2	5.65	3.60	2.9	2.73	—	0.07
Lumarith 22361	Ethylcellulose, 13% plasticizer	24	3.12	3.06	2.92	2.80	2.74	2.65	—
Marco resin MR-25C	Unsaturated polyester	25	—	3.24	3.10	2.90	2.77	—	—
Melmac molding compound 1500	Melamine-formaldehyde, 40% wood flour, 18% plasticizer	25	—	6.31	5.85	5.10	4.20	—	—
Melmac resin 592	Melamine-formaldehyde, mineral filler	27	8.0	6.25	5.20	4.70	4.67	—	0.08
Micarta 254	Cresylic acid—formaldehyde, 50% α-cellulose	25	5.45	4.95	4.51	3.85	3.43	3.21	0.098
Nylon 610	Polyhexamethylene-adipamide	25	3.7	3.50	3.14	3.0	2.84	2.73	0.018
Permafil 3256	Cross-linked addition polymer	24	—	4.22	3.86	3.5	—	3.0	—
Plaskon alkyd special electrical granular	Alkyd resin	25	—	5.10	4.76	4.55	4.50	—	—
Plaskon melamine	Melamine-formaldehyde, α-cellulose	24	—	7.57	7.00	6.0	4.93	—	—
Plaskon 911	Unsaturated polyester	24	—	3.81	3.56	3.25	3.07	—	—
Plasticell	Expanded polyvinyl chloride	25	—	1.04	1.04	1.04	1.04	—	—
Plastic CY-8	97% poly-2,5-dichlorostyrene	24	—	2.61	2.60	2.60	2.60	2.59	—
Plexiglass	Polymethyl methacrylate	27	3.45	3.12	2.76	—	2.60	—	0.064
Polyethylene DE-3401	0.1% antioxidant	25	2.26	2.26	2.26	2.26	2.26	2.26	<0.0002
Polyethylmethacrylate	—	22	—	2.75	2.55	2.52	2.51	2.5	—
Polyisobutylene	—	25	2.23	2.23	2.23	2.23	2.23	—	0.0004
Polystyrene	—	25	2.56	2.56	2.56	2.55	2.55	2.54	<0.00005
Polystyrene fibers Q-107	1-micron-diam fibers	26	—	2.14	2.14	2.14	2.11	—	—
Polyvinyl chloride W-174	65% Geon 101, 35% Paraplex G-25	25	—	4.77	3.52	3.00	—	—	—
Pyralin	Cellulose nitrate, 25% camphor	27	11.4	8.4	6.6	5.2	3.74	—	2.0
Red Glyptal 1201	Alkyd resin	25	—	4.5	3.9	—	—	—	—
Rexolite 1422	—	25	—	2.55	2.55	2.55	2.54	—	—
Saran B-115	Vinylidene-vinyl chloride copolymer	23	5.0	4.65	3.18	2.82	2.71	—	0.042
Styraloy 22	Copolymer of butadiene, styrene	23	2.4	2.4	2.4	2.4	2.4	2.40	0.001
Styrofoam 103.7	Foamed polystyrene, 0.25% filler	25	1.03	1.03	1.03	—	1.03	1.03	<0.0002
Teflon	Polytetrafluoroethylene	22	2.1	2.1	2.1	2.1	2.1	2.08	<0.0005
Tenite I (008A, H_4)	Cellulose acetate, plasticized	26	4.59	4.48	3.90	3.40	3.25	3.11	0.0075
Tenite II (205A, H_4)	Cellulose acetate-butyrate, plasticized	26	3.60	3.48	3.30	3.08	2.91	—	0.0045
Vibron 140	Cross-linked polystyrene	25	2.59	2.59	2.58	2.58	2.58	—	0.0004
Vinylite QYNA	100% polyvinyl-chloride	20	3.20	3.10	2.88	2.85	2.84	—	0.0115
Vinylite VG5901	62.5% polyvinyl-chloride-acetate, 29% plasticizer, 8.5% misc	25	—	5.5	3.4	3.0	2.88	—	—

dissipation factor at (frequency in cycles/second) 10^3	10^6	10^8	3×10^9	2.5×10^{10}	dielectric strength in volts/mil at 25° C	dc volume resistivity in ohm-cm at 25° C	thermal expansion (linear) in parts/°C	softening point in °C	moisture absorption in percent
0.110	0.089	0.030	0.0116	—	400 (0.075″)	8×10^{14}	—	60 (stable)	0.5
0.041	0.0124	0.0120	0.0125	—	—	—	—	—	—
0.0002	<0.0002	<0.0002	0.00018	—	—	—	—	—	—
0.0113	0.0272	0.0299	0.0274	—	—	—	—	—	—
0.048	0.084	0.090	0.038	—	—	—	—	—	—
0.0270	0.0082	—	0.0028	0.0053	—	10^{18}	—	—	—
0.0207	0.0175	0.0186	0.0093	—	—	—	—	—	—
0.100	0.093	0.030	0.0112	—	—	—	—	—	—
0.0048	0.0115	0.0160	0.0196	0.630	522 (⅛″)	5×10^{16}	—	51 (distortion)	1.50
0.0072	0.0138	0.0190	0.0130	—	—	—	—	—	—
0.0173	0.032	0.050	0.052	—	—	—	—	—	—
0.0470	0.0347	0.0360	0.0410	—	450 (⅛″)	3×10^{13}	3.5×10^{-5}	125 (distortion)	0.1
0.033	0.036	0.055	0.051	0.038	1020 (0.033″)	3×10^{13}	3×10^{-5}	>125	1.2
0.0186	0.0218	0.0200	0.0117	0.0105	400 (⅛″)	8×10^{14}	10.3×10^{-5}	65 (distortion)	1.5
0.0120	0.030	0.034	—	0.029	600 (0.060″)	—	$10\text{–}13 \times 10^{-5}$	>150 (distortion)	0.07
0.0236	0.0149	0.0138	0.0108	—	—	—	—	—	—
0.0122	0.041	0.085	0.103	—	300–400	—	—	99 (stable)	0.4–0.6
0.0125	0.0240	0.0220	0.0175	—	—	—	—	—	—
0.0011	0.0010	0.0010	0.0055	—	—	—	—	—	—
<0.0002	<0.0002	0.00025	0.00031	0.0029	—	—	—	—	—
0.0465	0.0140	—	0.0057	—	990 (0.030″)	$>5 \times 10^{16}$	$8\text{–}9 \times 10^{-5}$	70–75 (distortion)	0.3–0.6
<0.0002	<0.0002	0.0002	0.00031	0.0006	1200 (0.033″)	10^{17}	19×10^{-5} (varys)	95–105 (distortion)	0.03
0.0294	0.0090	—	0.0075	0.0083	—	—	—	60° (distortion)	Low
0.0001	0.0001	0.0003	0.00047	—	600 (0.010″)	—	—	25 (distortion)	Low
<0.00005	0.00007	<0.0001	0.00033	0.0012	500–700 (⅛″)	10^{18}	$6\text{–}8 \times 10^{-5}$	82 (distortion)	0.05
0.00063	0.0003	0.0004	0.00063	—	—	—	—	70–80° (distortion)	Slight
0.0930	0.0550	0.0415	—	—	—	—	—	—	—
0.100	0.064	0.103	0.165	—	—	—	9.8×10^{-5}	—	2.0
0.060	0.032	—	—	—	—	—	—	—	—
0.00011	0.00013	0.00038	0.00048	—	—	—	—	—	—
0.063	0.057	0.0180	0.0072	—	300 (⅛″)	$10^{14}\text{–}10^{16}$	15.8×10^{-5}	150	<0.1
0.0006	0.0012	0.0052	0.0032	0.0018	1070 (0.030″)	6×10^{14}	5.9×10^{-5}	125	0.2–0.4
<0.0001	<0.0002	—	0.0001	—	—	—	—	85	Low
<0.0003	<0.0002	<0.0002	0.00015	0.0006	1000–2000 (0.005″–0.012″)	10^{17}	9.0×10^{-5}	66 (distortion, stable to 300)	0.00
0.0175	0.039	0.038	0.031	0.030	290–600 (⅛″)	—	$8\text{–}16 \times 10^{-5}$	60–121	2.9
0.0097	0.018	0.017	0.028	—	250–400 (⅛″)	—	$11\text{–}17 \times 10^{-5}$	60–121	2.3
0.0005	0.0016	0.0020	0.0019	—	—	—	—	—	—
0.0185	0.0160	0.0081	0.0055	—	400 (⅛″)	10^{14}	6.9×10^{-5}	54 (distortion)	0.05–0.15
0.118	0.074	0.028	0.0106	—	—	—	—	—	—

Commercial insulating materials *continued*

material	composition	T °C	dielectric constant at (frequency in cycles/second) 60	10^3	10^6	10^8	3×10^9	2.5×10^{10}	60
plastics—*continued*									
Vinylite VG5904	54% polyvinyl-chloride-acetate, 41% plasticizer, 5% misc	25	—	7.5	4.3	3.3	2.94	—	—
Vinylite VYNW	Polymer of 95% vinyl-chloride, 5% vinyl-acetate	20	—	3.15	2.90	2.8	2.74	—	—
organic liquids									
Aroclor 1254	Pentachlorobiphenyl	25	5.05	5.05	3.70	2.75	2.70	—	0.0002
Aviation gasoline	100 octane	25	—	—	1.94	1.94	1.92	—	—
Bayol-D	77.6% paraffins, 22.4% naphthenes	24	2.06	2.06	2.06	2.06	2.06	—	0.0001
Benzene	Chemically pure, dried	25	2.28	2.28	2.28	2.28	2.28	2.28	<0.0001
Cable oil 5314	Aliphatic, aromatic hydrocarbons	25	2.25	2.25	2.25	2.25	2.22	—	0.0006
Carbon tetrachloride	—	25	2.17	2.17	2.17	2.17	2.17	—	0.007
DC-550	Methyl and methyl-phenyl polysiloxane	25	—	2.90	2.90	2.88	2.77	—	—
DC-710	Methyl and methyl-phenyl polysiloxane	25	—	2.98	2.98	2.95	2.79	—	—
Ethyl alcohol	Absolute	25	—	—	24.5	23.7	6.5	—	—
Ethylene glycol	—	25	—	—	41	41	12	—	—
Fraetol A	57.4% paraffins, 42.6% naphthenes	26	2.17	2.17	2.17	2.17	2.17	2.12	<0.0001
Halowax oil 1000	60% mon-, 40% di-, trichloronaphthalenes	25	4.80	4.77	4.74	—	3.52	—	0.30
Ignition-sealing compound 4	Organo-siloxane polymer	25	2.75	2.75	2.75	2.74	2.65	—	0.002
IN-420	Chlorinated Indan	24	5.77	5.71	—	—	—	—	0.00004
Jet fuel JP-3	—	25	—	—	2.08	2.08	2.04	—	—
Kel-F grease, grade 40	Polychlorotrifluoroethylene	25	—	2.88	2.78	—	2.20	—	—
Kel-F oil, grade 1	Polychlorotrifluoroethylene	25	—	2.61	2.61	2.58	2.34	—	—
Mareol	72.4% paraffins, 27.6% naphthenes	24	2.14	2.14	2.14	2.14	2.14	—	<0.002
Methyl alcohol	Absolute analytical grade	25	—	—	31.	31.0	23.9	—	—
Primol-D	49.4% paraffins, 50.6% naphthenes	24	2.17	2.17	2.17	2.17	2.17	—	<0.002
Pyranol 1467	Chlorinated benzenes, diphenyls	25	4.40	4.40	4.40	4.08	2.84	—	—
Pyranol 1476	Isomeric pentachlorodiphenyls	26	5.04	5.04	3.85	—	2.70	—	—
Pyranol 1478	Isomeric trichlorobenzenes	26	4.55	4.53	4.53	4.5	3.80	—	0.02
Silicone fluid SF96-40	—	25	—	2.71	2.71	2.71	2.70	—	—
Silicone fluid SF96-1000	—	25	—	2.73	2.73	2.73	2.71	—	—
Silicone fluid SC200	Methyl or ethyl siloxane polymer (1000 cs)	22	2.78	2.78	2.78	—	2.74	—	0.0001
Silicone fluid SC500	Methyl or ethyl siloxane polymer (0.65 cs)	22	2.20	2.20	2.20	2.20	2.20	2.13	<0.001
Styrene dimer	—	25	—	—	2.7	2.7	2.5	—	—
Styrene N-100	Monomeric styrene	22	2.40	2.40	2.40	2.40	2.40	—	0.01
Transil oil 10C	Aliphatic, aromatic hydrocarbons	26	2.22	2.22	2.22	2.20	2.18	—	0.001
Vaseline	—	25	2.16	2.16	2.16	2.16	2.16	—	0.0004
waxes									
Acrawax C	Cetylacetamide	24	2.60	2.58	2.54	2.52	2.48	2.44	0.025
Beeswax, yellow	—	23	2.76	2.66	2.53	2.45	2.39	—	—
Ceresin, white	Vegetable and mineral waxes	25	2.3	2.3	2.3	2.3	2.25	—	0.0009
Halowax 11-314	Dichloronaphthalenes	23	3.14	3.04	2.98	2.93	2.89	—	0.10
Halowax 1001, cold-molded	Tri- and tetrachloronaphthalenes	26	5.45	5.45	5.40	4.2	2.92	2.84	0.002
Kel-F-wax 150	Polychlorotrifluoroethylene	25	—	2.97	2.52	2.25	2.23	—	—
Opalwax	Mainly 12-hydroxystearin	24	14.2	10.3	3.2	2.7	2.55	2.5	0.12
Paraffin wax, 132° ASTM	Mainly C_{22} to C_{29} aliphatic, saturated hydrocarbons	25	2.25	2.25	2.25	2.25	2.25	2.2	<0.0002
Vistawax	Polybutene	25	2.34	2.34	2.34	2.30	2.27	—	0.0002

dissipation factor at (frequency in cycles/second) 10^3	10^6	10^8	3×10^9	2.5×10^{10}	dielectric strength in volts/mil at 25° C	dc volume resistivity in ohm-cm at 25° C	thermal expansion (linear) in parts/°C	softening point in ° C	moisture absorption in percent
0.071	0.140	0.067	0.034	—	—	—	—	—	—
0.0165	0.0150	0.0080	0.0059	—	—	—	—	—	—
0.00035	0.238	0.0170	0.0044	—	—	—	—	—	—
—	—	0.0001	0.0014	—	—	—	—	—	—
<0.0001	<0.0003	0.0005	0.00133	—	300 (0.100″)	—	1×10^{-3}	−26 (pour point)	Slight
<0.0001	<0.0001	<0.0001	<0.0001	<0.0001	—	—	—	—	—
<0.00004	0.0008	—	0.0018	—	300 (0.100″)	—	—	−40 (pour point)	—
0.0008	<0.00004	<0.0002	0.0004	—	—	—	—	—	—
0.0170	0.00038	—	0.021	—	—	—	—	—	—
0.00016	0.0010	—	0.014	—	—	—	—	—	—
—	0.090	0.062	0.250	—	—	—	—	—	—
—	0.030	0.045	1.00	—	—	—	—	—	—
<0.0001	<0.0003	0.0004	0.00072	0.0019	300 (0.100″)	—	7.06×10^{-4}	<−15 (pour point)	Slight
0.0050	<0.0002	—	0.25	—	—	—	2.1×10^{-4}	−38 (melts)	—
0.0006	0.0004	0.0015	0.0092	—	500 (0.010″)	1×10^{13}	63×10^{-5}	—	—
0.0010	—	—	—	—	—	10^{14}	—	10 (pour point)	—
—	0.0001	—	0.0055	—	—	—	—	—	—
0.00038	0.043	—	0.014	—	—	—	—	—	—
0.00023	0.00020	0.014	0.087	—	—	—	—	—	—
<0.0001	<0.0002	—	0.00097	—	300 (0.100″)	—	7.5×10^{-4}	−12 (pour point)	Slight
—	0.20	0.038	0.64	—	—	—	—	—	—
<0.0001	<0.0002	—	0.00077	—	—	—	6.91×10^{-4}	<−15 (pour point)	Slight
0.0003	0.0025	0.13	0.12	—	300 (0.100″)	—	—	—	—
0.0006	0.25	—	0.0042	—	—	—	—	10 (pour point)	—
0.0014	0.0002	0.014	0.23	—	—	—	—	—	—
<0.000003	<0.0001	—	0.0095	—	—	—	—	—	—
<0.000003	<0.0001	—	0.0106	—	—	—	—	—	—
0.00008	<0.0003	—	0.0096	—	—	—	—	—	—
<0.00004	<0.0003	0.00014	0.00145	0.0060	250–300 (0.100″)	—	1.598×10^{-3}	−68 (melts)	Nil
—	0.0003	0.0018	0.011	—	—	—	—	—	—
0.005	<0.0003	—	0.0020	—	300 (0.100″)	3×10^{12}	—	—	0.06
<0.00001	<0.0005	0.0048	0.0028	—	300 (0.100″)	—	—	−40 (pour point)	—
0.0002	<0.0001	<0.0004	0.00066	—	—	—	—	—	—
0.0068	0.0020	0.0012	0.0015	0.0021	—	—	—	137–139 (melts)	—
0.0140	0.0092	0.0090	0.0075	—	—	—	—	45–64 (melts)	—
0.0006	0.0004	0.0004	0.00046	—	—	—	—	57	—
0.0110	0.0003	0.0017	0.0037	—	—	—	—	35–63 (melts)	Nil
0.0017	0.0045	0.27	0.058	0.020	—	—	—	91–94	Low
0.0093	0.054	0.027	0.0113	—	—	—	—	—	—
0.21	0.145	0.027	0.0167	0.0160	—	—	—	86–88 (melts)	—
<0.0002	<0.0002	<0.0002	0.0002	<0.0003	1060 (0.027″)	$>5 \times 10^{16}$	13.0×10^{-5}	36	Very low
0.0003	0.00133	0.00133	0.0009	—	—	—	—	—	—

Commercial insulating materials *continued*

material	composition	T °C	dielectric constant at (frequency in cycles/second) 60	10^3	10^6	10^8	3×10^9	2.5×10^{10}	60
rubbers									
GR-I (butyl rubber)	Copolymer of 98–99% isobutylene, 1–2% isoprene	25	2.39	2.38	2.35	2.35	2.35	—	0.0034
GR-I compound	100 pts polymer, 5 pts zinc oxide, 1 pt tuads, 1.5 pts sulfur	25	2.43	2.42	2.40	2.39	2.38	—	0.005
GR-S (Buna S) cured	Styrene-butadiene copolymer, fillers, lubricants, etc.	25	2.96	2.96	2.90	2.82	2.75	—	0.0008
GR-S (Buna S) uncured	Copolymer of 75% butadiene, 25% styrene	26	2.5	2.5	2.50	2.45	2.45	—	0.0005
Gutta-percha	—	25	2.61	2.60	2.53	2.47	2.40	—	0.0005
Hevea rubber	Pale crepe	25	2.4	2.4	2.4	2.4	2.15	—	0.0030
Hevea rubber, vulcanized	100 pts pale crepe, 6 pts sulfur	27	2.94	2.94	2.74	2.42	2.36	—	0.005
Hycar OR Cell-tite	Based on butadiene polymer	25	—	1.40	1.38	1.38	1.38	—	—
Kralastic D Natural	Nitrile rubber	25	—	3.54	3.20	2.78	2.66	—	—
Neoprene compound	38% GN	24	6.7	6.60	6.26	4.5	4.00	4.0	0.018
Royalite 149–11	Polystyrene–acrylonitrile and polybutadiene–acrylonitrile	25	—	5.20	4.41	—	3.13	—	—
SE–450	Silicone-rubber compound	25	—	3.08	3.07	3.05	2.97	—	—
SE–972	Silicone-rubber compound	25	—	3.35	3.20	3.16	3.13	—	—
Silastic 120	50% siloxane elastomer, 50% titanium dioxide	25	5.78	5.76	5.75	5.75	5.73	—	0.056
Silastic 152	Siloxane elastomer	25	—	2.95	2.95	2.95	2.90	—	—
Silastic 181	45% siloxane elastomer, 55% silicon dioxide	25	—	3.30	3.20	3.18	3.11	—	—
Silastic 6167	33% siloxane elastomer, 67% titanium dioxide	25	—	10.1	10	10	10	—	—
Thiokol FA	Organic polysulfide, fillers	23	—	2260	110	30	16	13.6	—
woods*									
Balsawood	—	26	1.4	1.4	1.37	1.30	1.22	—	0.058
Douglas Fir	—	25	2.05	2.00	1.93	1.88	1.82	1.78	0.004
Douglas Fir, plywood	—	25	2.1	2.1	1.90	—	—	1.6	0.012
Mahogany	—	25	2.42	2.40	2.25	2.07	1.88	1.6	0.008
Yellow Birch	—	25	2.9	2.88	2.70	2.47	2.13	1.87	0.007
Yellow Poplar	—	25	1.85	1.79	1.75	—	1.50	1.4	0.004
miscellaneous									
Amber	Fossil resin	25	2.7	2.7	2.65	—	2.6	—	0.0010
Cenco Sealstix	DeKhotinsky cement	23	3.95	3.75	3.23	—	2.96	—	0.049
Plicene cement	—	25	2.48	2.48	2.48	2.47	2.40	—	0.005
Gilsonite	99.9% natural bitumen	26	2.69	2.66	2.58	2.56	—	—	0.006
Shellac (natural XL)	Contains ~ 3.5% wax	28	3.87	3.81	3.47	3.10	2.86	—	0.006
Mycalex 400	Mica, glass	25	—	7.45	7.39	—	—	—	—
Mycalex K10	Mica, glass, titanium dioxide	24	—	9.3	9.0	—	—	—	—
Mykroy, grade 8	Mica, glass	25	—	6.81	6.73	6.72	6.68	6.66	—
Ruby mica	Muscovite	26	5.4	5.4	5.4	5.4	5.4	—	0.005
Paper, Royalgrey	—	25	3.30	3.29	2.99	2.77	2.70	—	0.010
Selenium	Amorphous	25	—	6.00	6.00	6.00	6.00	6.00	—
Quinterra	Asbestos fiber, chrysotile	25	—	4.80	3.1	—	—	—	—
Quinorgo 3000	85% chrysotile asbestos, 15% organic material	25	—	6.4	3.3	—	—	—	—
Sodium chloride	Fresh crystals	25	—	5.90	5.90	—	—	5.90	—
Soil, sandy dry	—	25	—	2.91	2.59	2.55	2.55	—	—
Soil, loamy dry	—	25	—	2.83	2.53	2.48	2.44	—	—
Ice	From pure distilled water	−12	—	—	4.15	3.45	3.20	—	—
Snow	Freshly fallen snow	−20	—	3.33	1.20	1.20	1.20	—	—
Snow	Hard-packed snow followed by light rain	−6	—	—	1.55	—	1.5	—	—
Water	Distilled	25	—	—	78.2	78	76.7	34	—

* Field perpendicular to grain.

dissipation factor at (frequency in cycles/second) 10^3	10^6	10^8	3×10^9	2.5×10^{10}	dielectric strength in volts/mil at 25° C	dc volume resistivity in ohm-cm at 25° C	thermal expansion (linear) in parts/°C	softening point in ° C	moisture absorption in percent
0.0035	0.0010	0.0010	0.0009	—	—	—	—	—	—
0.0060	0.0022	0.0010	0.00093	—	—	—	—	—	—
0.0024	0.0120	0.0080	0.0057	—	870 (0.040″)	2×10^{15}	—	—	—
0.0009	0.0038	0.0071	0.0044	—	—	—	—	—	—
0.0004	0.0042	0.0120	0.0060	—	—	10^{15}	—	—	—
0.0018	0.0018	0.0050	0.0030	—	—	—	—	—	—
0.0024	0.0446	0.0180	0.0047	—	—	—	—	—	—
0.0058	0.0056	0.0047	0.0039	—	—	—	—	—	—
0.0052	0.053	0.027	0.0093	—	—	—	—	—	—
0.011	0.038	0.090	0.034	0.025	300 (⅛″)	8×10^{12}	—	—	Nil
0.0165	0.108	—	0.020	—	—	—	—	—	—
0.00072	0.0011	0.0030	0.0158	—	—	—	—	—	—
0.0067	0.0030	0.0032	0.0097	—	—	—	—	—	—
0.0030	0.0008	0.0027	0.0254	—	—	—	—	—	—
0.00052	0.00054	0.0020	0.0100	—	350 (⅛″)	—	—	—	—
0.0067	0.0037	0.0029	0.0100	—	450 (⅛″)	—	—	—	—
0.0026	0.00095	0.0027	0.045	—	—	—	—	—	—
1.29	0.39	0.28	0.22	0.10	—	—	—	—	—
0.0040	0.0120	0.0135	0.100	—	—	—	—	—	—
0.0080	0.026	0.033	0.027	0.032	—	—	—	—	—
0.0105	0.0230	—	—	0.0220	—	—	—	—	—
0.0120	0.025	0.032	0.025	0.020	—	—	—	—	—
0.0090	0.029	0.040	0.033	0.026	—	—	—	—	—
0.0054	0.019	—	0.015	0.017	—	—	—	—	—
0.0018	0.0056	—	0.0090	—	2300 (⅛″)	Very high	—	200	—
0.0335	0.024	—	0.021	—	—	—	9.8×10^{-5}	80–85	—
0.00355	0.00255	0.0015	0.00078	—	—	—	—	60–65	—
0.0035	0.0016	0.0011	—	—	—	—	—	155 (melts)	—
0.0074	0.031	0.030	0.0254	—	—	10^{16}	—	80	Low after baking
0.0019	0.0013	—	—	—	—	—	—	—	—
0.0125	0.0026	—	0.0040	—	—	—	—	400	<0.5
0.0066	0.0026	0.0025	0.0038	0.0081	—	—	—	—	—
0.0006	0.0003	0.0002	0.0003	—	3800-5600(.040″)	5×10^{13}	—	—	—
0.0077	0.038	0.066	0.056	—	202 (⅛″)	—	—	—	—
0.0004	<0.0003	<0.0002	0.00018	0.0013	—	—	—	—	—
0.15	0.025	—	—	—	—	—	—	—	—
0.231	0.087	—	—	—	—	—	—	—	—
<0.0001	<0.0002	—	—	<0.0005	—	—	—	—	—
0.08	0.017	—	0.0062	—	—	—	—	—	—
0.05	0.018	—	0.0011	—	—	—	—	—	—
—	0.12	0.035	0.0009	—	—	—	—	—	—
0.492	0.0215	—	0.00029	—	—	—	—	—	—
—	0.29	—	0.0009	—	—	—	—	—	—
—	0.040	0.005	0.157	0.2650	—	10^6	—	—	—

Ferrites

Ferrite is the common term that has come to be applied to a wide range of different ceramic ferromagnetic materials. Specifically, the term applies to those materials with the spinel crystal structures having the general formula XFe_2O_4, where X is any divalent metallic ion having the proper ionic radius to fit in the spinel structure. To date, ferrites have been prepared in which the divalent ion has been manganese, iron, cobalt, nickel, copper, cadmium, zinc, and magnesium. All of the known ferrites are mutually soluble in each other without limit; a wide range of magnetic and electrical properties can be obtained from specially formulated mixed ferrites that can be thought of as solid solutions of any two of the simple ferrites described above. Thus nickel–zinc ferrite can be prepared with the composition $Ni_{1-\delta}Zn_{\delta}Fe_2O_4$, where δ can take any value from zero to unity.

Several ceramic ferromagnetic materials have been prepared that do not have the basic formula XFe_2O_4 but common usage has included them in the family of ferrite materials. Thus, "lithium ferrite" has been prepared; the chemical formula of this material can be written as $(Li_{0.5}Fe_{0.5})Fe_2O_4$. It can be seen that in this compound, the divalent X ion has been replaced by equal amounts of monovalent lithium and trivalent iron. Certain microwave applications have made it important to obtain ferrites with high Curie temperatures and lower saturation moments than can be obtained from any of the mixed ferrites discussed above. This has been accomplished by replacing part of the trivalent iron by some other trivalent ion such as aluminum. Thus a typical composition might be $NiAl_xFe_{2-x}O_4$, where x could, in principle, vary from zero to two. Strictly speaking, these materials are not ferrites, but common usage includes them in the ever-growing list of ferrite materials. This substance can be thought of as a solid solution of nickel aluminate in nickel ferrite. Both materials have the spinel crystal structure and like all spinels, are completely soluble in each other.

The spinel crystal structure consists of a cubic close-packed oxygen lattice throughout which the metallic ions are distributed.* Two types of interstices exist in the oxygen lattice that will accommodate the metallic ions. In one of these interstices, the metallic ion is surrounded by four oxygen ions that occur at the corners of a regular tetrahedron. In the other, the metallic ion is surrounded by six oxygen ions occurring at the corners of a regular octahedron. The tetrahedral positions are commonly referred to as the *A* positions and the octahedral as the *B* positions, following the notation of Néel who developed the first satisfactory theory† explaining the mag-

* For a very clear and concise description of the spinel structure see: A. F. Wells, "Structural Inorganic Chemistry," Oxford University Press, London, England; 1946: pp. 85–87 and 379–385.

† L. Néel, "Magnetic Properties of Ferrites: Ferromagnetism and Antiferromagnetism," *Annales de Physique*, volume 3, pp. 137–198; 1948.

Ferrites *continued*

netic properties of these materials. There are twice as many *B* positions occupied in the spinel lattice as there are *A* positions; a spinel is known as a normal or inverse spinel depending upon how the metallic ions are distributed between the *A* and *B* positions. Thus, if both trivalent ions in the molecule are in the *B* positions and the divalent ion is in the *A* position, the spinel is normal. Many ferrites, however, are inverse spinels, and in these the trivalent iron ions are equally divided between the *A* and *B* positions, and the divalent metallic ion is in the *B* position. The distribution of ions can be inferred from magnetic data, but neutron-diffraction experiments give the most direct and unequivocal evidence available today for determining the ionic distribution. Evidence from both sources indicates that zinc, cadmium, and manganese ferrites are normal spinels, while all other known ferrites except magnesium are inverse. Magnesium is partially inverse and partially normal, the exact distribution of ions between the two sites depending upon the exact heat treatment of a particular sample.

The presently accepted theory of ferrites, verified to some extent by neutron-diffraction experiments, indicates that the magnetic moment of the ions in the *A* sites is aligned antiparallel to the magnetic moment of the ions in the *B* sites. Thus, basically, ferrites belong to the class of antiferromagnetic rather than ferromagnetic materials. However, they constitute a special class of antiferromagnetic substances, since the magnetic moment in one site normally is larger than that in the other site and hence there is a net magnetic moment in one direction. Thus, even though ferrites are fundamentally antiferromagnetic, macroscopically they exhibit the properties of ferromagnetism. Néel has suggested that materials that exhibit this property of uncompensated antiferromagnetism constitute a special class of materials and has proposed the name of ferrimagnetism to describe the phenomenon. In most of their important macroscopic properties, however, ferrites can be treated as ordinary ferromagnetic materials.

This theory quite accurately accounts for the saturation moment of most ferrites, and in addition, it explains how it is possible to add a diamagnetic ion such as divalent zinc to nickel ferrite and to increase the saturation moment of the material. Thus in pure nickel ferrite, half of the trivalent iron ions are in the *A* sites and half are in the *B* sites, while all of the divalent nickel is in the *B* sites. Since the magnetic moment of the ions in the *A* sites is aligned antiparallel to the moments in the *B* sites, the magnetic moments of the iron ions effectively cancel each other and the net saturation moment of nickel ferrite is due to the nickel ions alone. Since divalent nickel has two unpaired electrons, it is expected that the saturation moment of nickel ferrite should be 2 Bohr magnetons per molecule. It is experimentally measured to be 2.3 Bohr magnetons. When zinc is added to nickel ferrite

Ferrites *continued*

ferrite	saturation moment in gausses	Curie temperature in °C	saturation moment in Bohr magnetons n_B	X-ray density	lattice constant	first-order anisotropy constant K_1	saturation magnetostriction $\lambda_s \times 10^6$
$Ni\,Fe_2\,O_4$	3400	585	2.3	5.38	8.34	−0.06	−22
$Ni_{0.8}\,Zn_{0.2}\,Fe_2\,O_4$	4600	460	3.5	—	—	—	−18.5
$Ni_{0.6}\,Zn_{0.4}\,Fe_2\,O_4$	5800	360	4.8	—	—	—	−15.0
$Ni_{0.5}\,Zn_{0.4}\,Fe_2\,O_4$	5500	290	5.0	—	—	—	− 8.3
$Ni_{0.3}\,Zn_{0.5}\,Fe_2\,O_4$	2600	85	4.0	—	—	−0.004	− 1.0
$Mn\,Fe_2\,O_4$	5200	300	.0	5.00	8.50	−0.04	−14
$Mn_{0.5}\,Zn_{0.5}\,Fe_2\,O_4$	—	100	6.0	—	—	−0.004	—
$Fe\,Fe_2\,O_4$	6000	585	4.1	5.24	8.39	−0.135	+41
$Co\,Fe_2\,O_4$	5000	520	3.8	5.29	8.38	+2000	−250
$Cu\,Fe_2\,O_4$	1700	455	1.3	5.35	$\begin{cases} a = 8.24 \\ c = 8.68 \end{cases}$	—	—
$Li_{0.5}\,Fe_{2.5}\,O_4$	3900	670	2.6	4.75	8.33	—	—
$Mg\,Fe_2\,O_4$	1400	440	1.1	4.52	8.36	−0.05	—
$Mg\,Al\,Fe\,O_4$	—	—	0.3	—	—	—	—
$Ni\,Al_{0.25}\,Fe_{1.75}\,O_4$	1300	506	1.30	—	8.31	—	—
$Ni\,Al_{0.45}\,Fe_{1.55}\,O_4$	900	465	0.61	—	8.28	—	—
$Ni\,Al_{0.62}\,Fe_{1.38}\,O_4$	0	360	0	—	8.25	—	—
$Ni\,Al\,Fe\,O_4$	900	198	0.64	5.00	8.20	—	—

Ferrites *continued*

to form the mixed ferrite, $Ni_{1-\delta}Zn_{\delta}Fe_2O_4$, the zinc enters the *A* site and displaces δ ions of trivalent iron, forcing them over to the *B* sites. Thus in this material, the *A* sites are occupied by δ ions of zinc and $(1 - \delta)$ ions of iron per molecule and the *B* sites are occupied by $(1 + \delta)$ ions of iron and $(1 - \delta)$ ions of nickel. Since trivalent iron has 5 unpaired electrons, giving it a magnetic moment of 5 Bohr magnetons, it is to be expected that the saturation moment of nickel–zinc ferrite will be $(2 + 8\delta)$ Bohr magnetons per molecule. It is found experimentally that the moment of nickel–zinc ferrite follows this formula approximately until about half the nickel has been replaced by zinc (i.e., $\delta = 0.5$). On further additions of zinc, the exchange fields that account for the ferromagnetic property become so greatly weakened that the material rapidly becomes paramagnetic at room temperature.

The behavior of the conductivity and dielectric constant of ferrites is not well understood. They behave as if they consisted of large regions of fairly low-resistance material separated by thin layers of a relatively poor conductor. Therefore, the dielectric constant and conductivity show a relaxation as a function of frequency with the relaxation frequency varying from 1000 cycles/second to several megacycles/second. Most ferrites appear to have relatively high resistivities ($\approx 10^6$ ohm–centimeters) if they are prepared carefully so as to avoid the presence of any divalent iron in the material. However, if the ferrite is prepared with an appreciable amount of divalent iron, then both the conductivity and dielectric constant are very high. Relative dielectric constants as high as 100,000 and resistivities less than 1 ohm–centimeter have been measured in several ferrites having a small amount of divalent iron in their composition.

The accompanying table lists some of the pertinent information with respect to the more-important ferrites. Properties such as electrical conductivity and dielectric constant, which are extremely structure-sensitive, are not listed since slight changes in method of preparation can cause these properties to change by several orders of magnitude. Also not included in the table is the initial permeability of ferrite materials since this is also a structure-sensitive property. The initial permeability of most ferrites lies between 100 and 2000. In general, the ferrites listed in the table have the following properties in common.

Thermal conductivity = 1.5×10^{-2} calorie/second/centimeter^2/degree C

Specific heat = 0.2 calorie/gram/degree C

Young's modulus = 1.5×10^{12} dynes/centimeter^2

Components

Standards in general

Standardization of electronic components or parts is handled by several cooperating agencies. The Radio-Electronics-Television Manufacturers' Association (RETMA) and the American Standards Association (ASA) are active in the commercial field. Electron-tube standardization is handled by the Joint Electron Tube Engineering Council (JETEC), a cooperative effort of RETMA and the National Electrical Manufacturers Association (NEMA).

Military (MIL) standards are issued by the U. S. Department of Defense or one of its agencies such as the Armed Services Electro-Standards Agency (ASESA).

These organizations establish standards for electronic components or parts (and in some cases, for equipments) for the purpose of providing: interchangeability among different manufacturers' products as to size, performance, and identification; minimum number of sizes and designs; uniform testing of products for acceptance; and minimum manufacturing costs. In this chapter is presented a brief outline of the requirements, characteristics, and designations for the major types of component parts used in electronic equipment.

Color coding

The color code of Fig. 1 is used for marking electronic components.

Fig. 1—Standard electronics-industry color code.

color	significant figure	decimal multiplier	tolerance in percent*	voltage rating	characteristic
Black	0	1	±20 (M)	—	A
Brown	1	10	±1	100	B
Red	2	100	±2 (G)	200	C
Orange	3	1,000	±3	300	D
Yellow	4	10,000	GMV‡	400	E
Green	5	100,000	±5†	500	F
Blue	6	1,000,000	±6	600	G
Violet	7	10,000,000	±12.5	700	–
Gray	8	0.01†	±30	800	I
White	9	0.1†	±10†	900	J
Gold	–	0.1	±5 (J)	1000	–
Silver	–	0.01	±10 (K)	2000	–
No color	–	——	±20	500	–

* Letter symbol is used at end of type designations in RETMA standards and MIL specifications to indicate tolerance. ±3, ±6, ±12.5, and ±30 percent are tolerances for ASA 40-, 20-, 10-, and 5-step series.
† Optional coding where metallic pigments are undesirable.
‡ GMV is −0-to-+100-percent tolerance or Guaranteed Minimum Value.

Standards in general *continued*

Tolerance

The maximum deviation allowed from the specified nominal value is known as the tolerance. It is usually given as a percentage of the nominal value, though for very small capacitors, the tolerance may be specified in micro-microfarads ($\mu\mu$f). For critical applications it is important to specify the permissible tolerance; where no tolerance is specified, components are likely to vary by ± 20 percent from the nominal value.

Preferred values

To maintain an orderly progression of sizes, preferred numbers are frequently used for the nominal values. A further advantage is that all components manufactured are salable as one or another of the preferred values. Each preferred value differs from its predecessor by a constant multiplier, and the final result is conveniently rounded to two significant figures.

The ASA has adopted as an "American Standard" a series of preferred numbers based on $\sqrt[5]{10}$ and $\sqrt[10]{10}$ as listed in Fig. 2. This series has been widely used for fixed wire-wound power-type resistors and for time-delay fuses.

Because of the established practice of ± 20-, ± 10-, and ± 5-percent tolerances in the electronics-component industry, a series of values based on $\sqrt[6]{10}$, $\sqrt[12]{10}$, and $\sqrt[24]{10}$ has been adopted by the RETMA and is widely used for small electronics components, as fixed composition resistors and fixed ceramic, mica, and molded paper capacitors. These values are listed in Fig. 2.

Voltage rating

Distinction must be made between the breakdown-voltage rating (test volts) and the working-voltage rating. The maximum voltage that may be applied (usually continuously) over a long period of time without causing failure of the component determines the working-voltage rating. Application of the test voltage for more than a very few minutes, or even repeated applications of short duration, may result in permanent damage or failure of the component.

Characteristic

This term is frequently used to include various qualities of a component such as temperature coefficient of capacitance or resistance, Q value, maximum permissible operating termperature, stability when subjected to

Standards in general *continued*

repeated cycles of high and low temperature, and deterioration experienced when the component is subjected to moisture either as humidity or water immersion. One or two letters are assigned in RETMA or MIL type designations, and the characteristic may be indicated by color coding on the component. An explanation of the characteristics applicable to a component will be found in the following sections covering that component.

Fig. 2—ASA and RETMA preferred values. The RETMA series is standard in the electronics industry.

	American Standard		RETMA standard*		
Name of series	"5"	"10"	±20%	±10%	±5%
Percent step size	60	25	≈40	20	10
Step multiplier	$\sqrt[5]{10} = 1.58$	$\sqrt[10]{10} = 1.26$	$\sqrt[6]{10} = 1.46$	$\sqrt[12]{10} = 1.21$	$\sqrt[24]{10} = 1.10$
Values in the series	10	10	**10**	**10**	**10**
	–	12.5	–	–	**11**
	–	(12)	–	**12**	**12**
	–	–	–	–	**13**
	–	–	**15**	**15**	**15**
	16	16	–	–	**16**
	–	–	–	**18**	**18**
	–	20	–	–	**20**
	–	–	**22**	**22**	**22**
	–	–	–	–	**24**
	25	25	–	–	–
	–	–	–	**27**	**27**
	–	31.5	–	–	**30**
	–	(32)	–	–	–
	–	–	**33**	**33**	**33**
	–	–	–	–	**36**
	–	–	–	**39**	**39**
	40	40	–	–	–
	–	–	–	–	**43**
	–	–	**47**	**47**	**47**
	–	50	–	–	–
	–	–	–	–	**51**
	–	–	–	**56**	**56**
	–	–	–	–	**62**
	63	63	–	–	–
	–	–	**68**	**68**	**68**
	–	–	–	–	**75**
	–	80	–	–	–
	–	–	–	**82**	**82**
	–	–	–	–	**91**
	100	100	**100**	**100**	**100**

*Use decimal multipliers for smaller and larger values. Associate the tolerance ±20%, ±10%, or ±5% only with the values listed in the corresponding column: Thus, 1200 ohms may be either ±10 or ±5, but not ±20 percent; 750 ohms may be ±5, but neither ±20 nor ±10 percent.

Resistors—fixed composition

Color code

RETMA-standard and MIL-specification requirements for color coding of fixed composition resistors are identical (Fig. 3). The exterior body color of insulated axial-lead composition resistors is usually tan, but other colors, except black, are permitted. Noninsulated, axial-lead composition resistors have a black body color. Radial-lead composition resistors may have a body color representing the first significant figure of the resistance value.

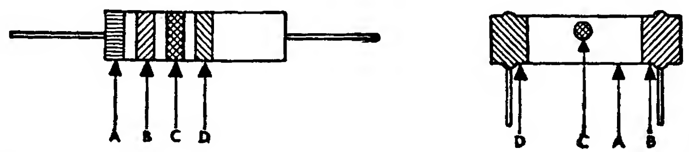

axial leads	color	radial leads
Band A	Indicates first significant figure of resistance value in ohms	Body A
Band B	Indicates second significant figure	End B
Band C	Indicates decimal multiplier	Band C or dot
Band D	If any, indicates tolerance in percent about nominal resistance value. If no color appears here, tolerance is ± 20%	Band D

Fig. 3—Resistor color coding. Colors of Fig. 1 determine values.

Examples: Code of Fig. 1 determines resistor values. Examples are

resistance in ohms and tolerance	band designation			
	A	B	C	D
3300 ± 20%	Orange	Orange	Red	Black or no band
510 ± 5%	Green	Brown	Brown	Gold
1.8 megohms ± 10%	Brown	Gray	Green	Silver

Tolerance

Standard resistors are furnished in ±20-, ±10-, and ±5-percent tolerances, and in the preferred-value series previously tabulated. "Even" values, such as 50,000 ohms, may be found in old equipment, but they are seldom used in new designs.

Resistors—fixed composition *continued*

Temperature and voltage coefficients

Resistors are rated for maximum wattage at an ambient temperature of 40 or 70 degrees centigrade; above these temperatures it is necessary to operate at reduced wattage ratings. Resistance values are found to be a function of voltage as well as temperature; current MIL specifications allow a maximum voltage coefficient of 0.035 percent/volt for $\frac{1}{4}$- and $\frac{1}{2}$-watt ratings, and 0.02 percent/volt for larger ratings. Specification MIL-R-11A permits a resistance-temperature characteristic as in Fig. 4.

Fig. 4—Temperature coefficient of resistance.

	characteristic	percent maximum allowable change from resistance at 25 degrees centigrade					
Nominal resistance in ohms		0 to 1000	>1000 to 10,000	>10,000 to 0.1 meg	>0.1 meg to 1.0 meg	>1 meg to 10 meg	>10 meg to 100 meg
At −55 deg cent ambient	F	±6.5	±10	±13	±20	±26	±35
At +105 deg cent ambient	F	±5	±6	±7.5	±10	±18	±22

The separate effects of exposure to high humidity, salt-water immersion (applied to immersion-proof resistors only), and a 1000-hour rated-load life test should not exceed a 10-percent change in the resistance value. Soldering the resistor in place may cause a maximum resistance change of ±3 percent. Simple temperature cycling between −55 and +85 degrees centigrade for 5 cycles should not change the resistance value as measured at 25 degrees centigrade by more than 2 percent. The above summary of composition-resistor performance indicates that tolerances closer than ±5 percent may not be satisfactorily maintained in service; for a critical application, other types of small resistors should be employed.

Resistors—fixed wire wound low power types

Color coding

Small wire-wound resistors in $\frac{1}{2}$-, 1-, or 2-watt ratings may be color coded as described in Fig. 3 for insulated composition resistors, but band A will be twice the width of the other bands.

Resistors—fixed wire wound low power types *continued*

Maximum resistance

For reliable continuous operation, it is recommended that the resistance wire used in the manufacture of these resistors be not less than 0.0015 inch in diameter. This limits the maximum resistance available in a given physical size or wattage rating as follows:

½-watt: 470 ohms   1-watt: 2200 ohms   2-watt: 3300 ohms

Wattage

Wattage ratings are determined for a temperature rise of 70 degrees in free air at a 40-degree-centigrade ambient. If the resistor is mounted in a confined area, or may be required to operate in higher ambient temperatures, the allowable dissipation must be reduced.

Temperature coefficient

The temperature coefficient of resistance over the range −55 to +110 degrees, referred to 25 degrees centigrade, may have maximums as follows:

value	RETMA	MIL
Above 10 ohms	± 0.025 percent/°C	± 0.030 percent/°C
10 ohms or less	± 0.15 percent/°C	± 0.065 percent/°C

Stability of these resistors is somewhat better than that of composition resistors, and they may be preferred except where a noninductive resistor is required.

Resistors—fixed film

Film-type resistors employ a thin layer of resistive material deposited on an insulating core. The low-power types are more stable than the usual composition resistors. Except for high-precision requirements, film-type resistors are a good alternative for accurate wire-wound resistors, being both smaller and less expensive.

The power types are similar in size and performance to conventional wire-wound power resistors. While their 200-degree-centigrade maximum operating temperature limits the power rating, the maximum resistance value available for a given physical size is much higher than that of the corresponding wire-wound resistor.

Resistors—fixed film *continued*

Construction

For low-resistance values, a continuous film is applied to the core, a range of values being obtained by varying the film thickness. Higher resistances are achieved by the use of a spiral pattern, a coarse spiral for intermediate values and a fine spiral for high resistance. Thus, the inductance is greater in high values, but it is likely to be far less than in wire-wound resistors. Special high-frequency units having greatly reduced inductance are available.

Resistive films

Resistive-material films currently used are microcrystalline carbon, boron–carbon, and various metallic oxides or precious metals.

Deposited-carbon resistors have a negative temperature coefficient of 0.01 to 0.05 percent/degree centigrade for low-resistance values and somewhat larger for higher values. Cumulative permanent resistance changes of 1 to 5 percent may result from soldering, overload, low-temperature exposure, and aging. Additional changes up to 5 percent are possible from moisture penetration and cyclic temperatures.

The introduction of a small percentage of boron in the deposited-carbon film results in a more stable unit. A negative temperature coefficient of 0.005 to 0.02 percent/degree centigrade is typical. Similarly, a metallic dispersion in the carbon film provides a negative coefficient of 0.015 to 0.03 percent/degree centigrade. In other respects, these materials are similar to standard deposited carbon. Carbon and boron–carbon resistive elements have the highest random noise of the film-type resistors.

Metallic oxide and precious-metal-alloy films permit higher operating temperatures. Their noise characteristics are excellent. Temperature coefficients are predominantly positive, varying from 0.03 to as little as 0.0025 percent/degree centigrade.

Applications

Power ratings of film resistors are based on continuous direct-current or on root-mean-square operation. Power derating is necessary for the standard units above 40 degrees centigrade; for hermetically-sealed resistors, above 70 degrees centigrade. In pulse applications, the power

Resistors—fixed film *continued*

dissipated during each pulse and the pulse duration are more significant than average power conditions. Short high-power pulses may cause instantaneous local heating sufficient to alter or destroy the film. Excessive peak voltages may result in flashover between turns of the film element. Derating under these conditions must be determined experimentally.

Film resistors are fairly stable up to about 10 megacycles. Because of the extremely thin resistive film, skin effect is small. At frequencies above 10 megacycles, it is advisable to use only unspiraled units if inductive effects are to be minimized (these are available in low resistance values only).

Under extreme exposure, deposited-carbon resistors deteriorate rapidly unless the element is protected. Encapsulated or hermetically sealed units are preferred for such applications. Open-circuiting in storage as the result of corrosion under the end-caps is frequently reported in all types of film resistors. Silver-plated caps and core-ends effectively overcome this problem.

Capacitors—fixed ceramic

Ceramic-dielectric capacitors of one grade are used for temperature compensation of tuned circuits and have many other applications. In certain styles, if the temperature coefficient is unimportant (i.e., general-purpose applications), they are competitive with mica capacitors. Another grade of ceramic capacitors offers the advantage of very high capacitance in a small physical volume; unfortunately this grade has other properties that limit its use to noncritical applications such as bypassing.

Color code

If the capacitance tolerance and temperature coefficient are not printed on the capacitor body (Fig. 5), the color code of Fig. 6 may be used.

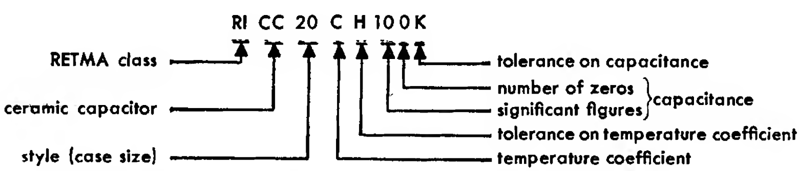

Fig. 5—Type designation for ceramic capacitors. RETMA class is omitted on MIL-specification capacitors.

Capacitors—fixed ceramic *continued*

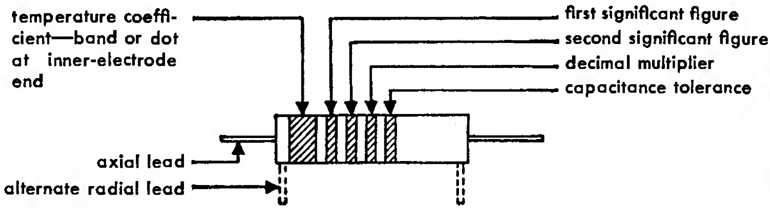

color	significant figure	decimal multiplier	capacitance tolerance in percent ($C > 10\ \mu\mu f$)	capacitance tolerance in $\mu\mu f$ ($C \leqslant 10\ \mu\mu f$)	temperature coefficient in parts/million/°C
Black	0	1	±20 (M)	2.0 (G)	0 (C)
Brown	1	10	±1 (F)	±0.1 (B)	−30 (H)
Red	2	100	±2 (G)	—	−80 (L)
Orange	3	1,000	—	—	−150 (P)
Yellow	4	10,000	—	—	−220 (R)
Green	5	—	±5 (J)	±0.5 (D)	−330 (S)
Blue	6	—	—	—	−470 (T)
Violet	7	—	—	—	−750 (U)
Gray	8	0.01	—	±0.25 (C)	+30
White	9	0.1	±10 (K)	1.0 (F)	+100 to −750 (RETMA general purpose)
Silver	-	—	—	—	See Fig. 7, (RETMA class 4)

Note: Letters in parentheses are used in type designations described in Fig. 5.

Fig. 6—Color code for fixed ceramic capacitors.

Capacitance and capacitance tolerance

Preferred-number values on RETMA and MIL specifications are standard for capacitors above 10 micromicrofarads ($\mu\mu f$). The physical size of a capacitor is determined by its capacitance, its temperature coefficient, and its class. Note that the capacitance tolerance is expressed in $\mu\mu f$ for nominal capacitance values below $10\mu\mu f$ and in percent for nominal capacitance values of 10 $\mu\mu f$ and larger.

Temperature coefficient

The change in capacitance per unit capacitance per degree centigrade is the temperature coefficient, usually expressed in parts per million parts per degree centigrade (ppm/°C). Preferred temperature coefficients are those listed in Fig. 6.

Capacitors—fixed ceramic *continued*

Temperature-coefficient tolerance: Because of the nonlinear nature of the temperature coefficient, specification of the tolerance requires a statement of the temperature range over which it is to be measured (usually −55 to +85 degrees centigrade, or +25 to +85 degrees centigrade), and a

Fig. 7—Quality of fixed ceramic capacitors. Summary of test requirements.

		specification MIL-C-20	RETMA class 1	RETMA class 2	RETMA class 3	RETMA class 4
Minimum initial insulation resistance in megohms		>7500	7500			
Minimum Q for C > 30 $\mu\mu f$ (See Fig. 8 for smaller C)		>1000	1000	500	350	250
Maximum allowable capacitance drift with temperature cycling (percent or $\mu\mu f$, whichever is greater)		0.2% or 0.25 $\mu\mu f$	0.3% or 0.25 $\mu\mu f$			—
Maximum capacitance change in percent over range − 55 to + 85 C		—	—	—	—	±25
Working voltage = sum of dc and peak ac		—	500			350
Humidity test		100 hours exposure at 40°C, 95% relative humidity				
Life test at 85°C		1000 hours, 750 vdc plus 250 vac at 100 cycles or less	1000 hours, 1000 volts			1000 hours, 750 volts
After humidity test or life test	Minimum Q (C > 30 $\mu\mu f$)	> ½ initial limits	350		170	50
After humidity test or life test	Minimum insulation resistance in megohms	>1000	1000			100
After life test	Maximum capacitance change	1%	1% or 0.5 $\mu\mu f$			
Application		Temperature compensation; stable, general-purpose uses		Intermediate quality		High-capacitance general-purpose, noncritical uses only
Volume efficiency ($\mu\mu f$/inch^3)		Low		Low		High

Capacitors—fixed ceramic *continued*

statement of the measuring procedure to be employed. Standard tolerances based on +25 to +85 degrees centigrade are symmetrical:

Tolerance in ppm/°C	±15	±30	±60	±120	±250	±500
Code	(F)	(G)	(H)	(J)	(K)	(L)

The smaller tolerances can be supplied only for capacitors of 10 $\mu\mu$f or larger, and only for the smaller temperature coefficients.

Quality

Insulation resistance, internal loss (conveniently expressed in terms of Q), capacitance drift with temperature cycling, together with the permissible effects of humidity and accelerated life tests, are summarized in Fig. 7. These data will be a guide to the probable performance under favorable or moderately severe ambient conditions.

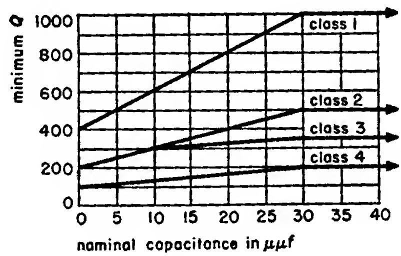

Fig. 8—Minimum Q requirements for ceramic capacitors where capacitance <30 $\mu\mu$f.

General-purpose ceramic capacitors

Ceramic materials suitable for temperature-compensating capacitors must have nearly linear temperature characteristics in the operating temperature range and high dielectric properties. Only low- and medium-*K* (dielectric-constant) ceramics meet these limitations.

For many circuit applications, nonlinear capacitance–temperature characteristics and power factors of 1 to 2 percent are not objectionable. Capacitors having high-*K* ceramic bodies (up to $K=6000$) fall in this class. The high dielectric constant results in an extremely small unit. Generally, the higher the *K*, the greater the nonlinearity and the greater the power factor.

Six basic styles are manufactured. In lead-mounted types, tubular and disc configurations are available. Feedthrough and standoff types are made in both tubular and discoidal constructions.

Inductance in the leads and element causes parallel resonance in the megacycle region. The user is advised to exercise care in their application

Capacitors—fixed ceramic *continued*

above about 50 megacycles for tubular styles and about 500 megacycles for disc types. Precise frequency limits cannot be cited because of the indeterminate inductive effects of lead length, lead dress, and variations in construction.

Capacitors—molded mica dielectric

Type designation

Small fixed mica capacitors in molded plastic cases are manufactured to performance standards established by the RETMA or in accordance with a MIL specification. A comprehensive numbering system, the *type designation,* is used to identify the component. The mica-capacitor type designations are of the form shown in Fig 9.

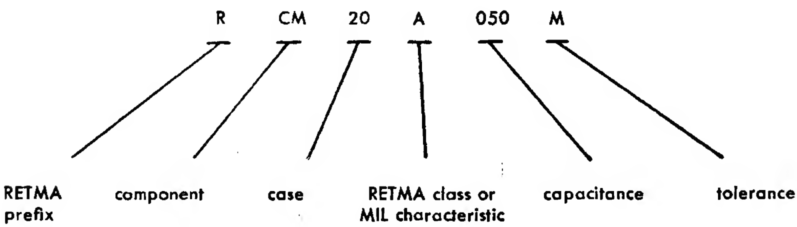

Fig. 9—Type designation for mica-dielectric capacitors.

Component designation: Fixed mica-dielectric capacitors are identified by the symbol CM for MIL specification, or RCM for RETMA standard.

Case designation: The case designation is a two-digit symbol that identifies a particular case size and shape.

Characteristic: The MIL characteristic or RETMA class is indicated by a single letter in accordance with Fig. 10.

Capacitance value: The nominal capacitance value in micromicrofarads is indicated by a 3-digit number. The first two digits are the first two digits of the capacitance value in micromicrofarads. The final digit specifies the number of zeros that follow the first two digits. If more than two significant figures are required, additional digits may be used, the last digit always indicating the number of zeros.

Capacitors—molded mica dielectric *continued*

Capacitance tolerance: The symmetrical capacitance tolerance in percent is designated by a letter as shown in Fig. 1.

Color coding

The significance of the various colored dots for RETMA-standard and MIL-specification mica capacitors is explained by Fig. 12. The meaning of each color may be interpreted from Fig. 1.

Fig. 10—Fixed-mica-capacitor requirements by MIL characteristic and RETMA class.*

	MIL-specification requirements†			RETMA-standard requirements			
MIL char or RETMA class	**maximum capacitance drift in percent**	**maximum range of temperature coefficient (ppm/°C)‡**	**minimum Q**	**maximum capacitance drift**	**maximum range of temperature coefficient (ppm/°C)‡**	**minimum insulation resistance in megohms**	**minimum Q**
A	—	—		±(5% + 1 μμf)	±1000	3000	30% of RETMA value in Fig. 11.
B	—	—	See Fig. 11, MIL values, for all capacitors not assigned specific current ratings	±(3% + 1 μμf)	±500	6000	See Fig. 11, RETMA values, applicable only up to 1000 μμf
C	±0.5	±200		±(0.5% + 0.5 μμf)	±200		
I	—	—		±(0.3% + 0.2 μμf)	−50 to +150		
D	±0.3	±100		±(0.3% + 0.1 μμf)	±100		
J	—	—		±(0.2% + 0.2 μμf)	−50 to +100		
E	±(0.1% + 0.1 μμf)	−20 to +100		±(0.1% + 0.1 μμf)	−20 to +100		
F	±(0.05% + 0.1 μμf)	0 to +70		—	—	—	—

* Where no data are given, such characteristics are not included in that particular standard.

† Insulation resistance of all MIL capacitors *must* exceed 7500 megohms.

‡ ppm/°C = parts/million/degree centigrade.

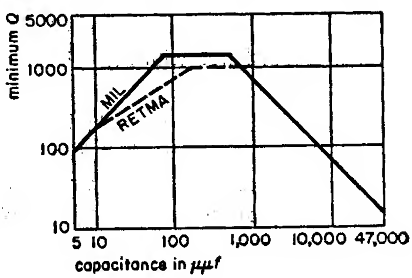

Fig. 11—Minimum Q versus capacitance for MIL mica capacitors (Q measured at 1.0 megacycle), and for RETMA mica capacitors (Q measured at 0.5 to 1.5 megacycles).

Capacitors—molded mica dielectric *continued*

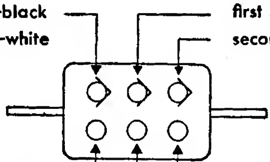

Fig. 12—Standard code for fixed mica capacitors. See color code, Fig. 1.

Examples

	top row			bottom row			
type	left	center	right	left	tolerance center	multiplier right	description
RCM20A221M	white	red	red	black	black	brown	220 $\mu\mu f \pm 20\%$, RETMA class A
CM30C681J	black	blue	gray	red	gold	brown	680 $\mu\mu f \pm 5\%$, characteristic C

Capacitance

Measured at 500 kilocycles for capacitors of 1000 $\mu\mu$f or smaller; larger capacitors are measured at 1 kilocycle.

Temperature coefficient

Measurements to determine the temperature coefficient of capacitance and the capacitance drift are based on one cycle over the following temperature values (all in degrees centigrade).

MIL: +25, −40, −10, +25, +45, +65, +85, +25

RETMA: +25, −20, +25, +85, +25

Dielectric strength

Molded-mica capacitors are subjected to a test potential of twice their direct-current voltage rating.

Humidity and thermal-shock resistance

RETMA-standard capacitors must withstand a 120-hour humidity test: Five cycles of 16 hours at 40 degrees centigrade, 90-percent relative humidity, and 8 hours at standard ambient. Units must pass capacitance and dielectric-strength tests, but insulation resistance may be as low as 1000 megohms for class A, and 2000 megohms for other classes.

Capacitors—molded mica dielectric *continued*

MIL specification capacitors must withstand 5 cycles of +25, +85, +25, −55, +25 degree-centigrade thermal shock followed by 2 cycles of water immersion at +65 and +20 degrees centigrade. Units must pass capacitance and dielectric-strength tests, but insulation resistance may be as low as 3000 megohms.

Life

Capacitors are given accelerated life tests at 85 degrees centigrade with 150 percent of rated voltage applied. No failures are permitted before: 1000 hours for MIL specification; or 500 hours for RETMA standard.

Capacitors—fixed mica dielectric button style

Color code

"Button" mica capacitors are color coded in several different ways, of which the two most widely used methods are shown in Fig. 13.

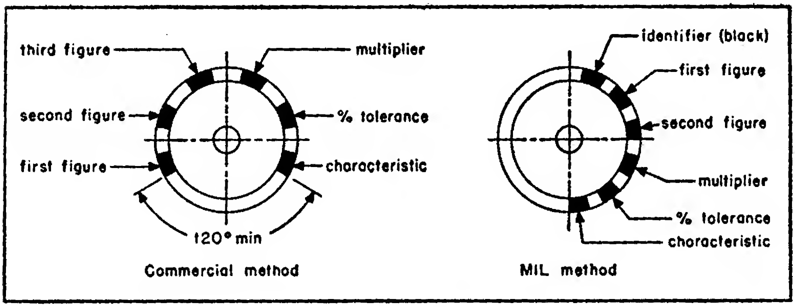

Fig. 13—Color coding of button-mica capacitors. See Fig. 1 for color code. Commercial color code for characteristic not standardized; varies with manufacturer.

Characteristic

The table of characteristics for button-style mica capacitors is given in Fig. 14. Insulation resistance after moisture-resistance test should be at least 100 megohms for characteristic X capacitors; at least 500 megohms for all other MIL or commercial characteristics.

Capacitors—fixed mica dielectric button style *continued*

Initial Q values should exceed 500 for capacitors 5 to 50 $\mu\mu$f; 700 for capacitors 51 to 100 $\mu\mu$f; and 1000 for capacitors 101 to 5000 $\mu\mu$f. Initial insulation resistance should exceed 10,000 megohms. Dielectric-strength tests should be made at twice rated voltage.

Fig. 14—Requirements for button-style mica capacitors.

characteristic		max range of temp coeff (ppm/°C)	maximum capacitance drift
MIL	commercial		
—	C	±200	±0.5%
D or X	—	±100	±0.3% or 0.3 $\mu\mu$f, whichever is greater
—	D	±100 + 0.05 $\mu\mu$f	±(0.3% + 0.05 $\mu\mu$f)
—	E	(−20 to +100) + 0.05 $\mu\mu$f	±(0.1% + 0.05 $\mu\mu$f)
—	F	(0 to +70) + 0.05 $\mu\mu$f	±(0.05% + 0.05 $\mu\mu$f)

Thermal-shock and humidity tests

These are commercial requirements. After 5 cycles of +25, −55, +85, +25 degrees centigrade, followed by 96 hours at 40 degrees centigrade and 95-percent relative humidity, capacitors should have an insulation resistance of at least 500 megohms; a Q of at least 70 percent of initial minimum requirements; a capacitance change of not more than 2 percent of initial value; and should pass the dielectric-strength test.

Capacitors—impregnated paper dielectric

The proper application of paper capacitors is a complex problem requiring consideration of the equipment duty cycle, desired capacitor life, ambient temperature, applied voltage and waveform, and the capacitor-impregnant characteristics. From the data below, a suitable capacitor rating may be determined for a specified life under normal use.

Life—voltage and ambient temperature

Normal paper-dielectric-capacitor voltage ratings are for an ambient temperature of 40 degrees centigrade, and provide a life expectancy of approximately 1 year continuous service. For ambient temperatures outside

Capacitors—impregnated paper dielectric *continued*

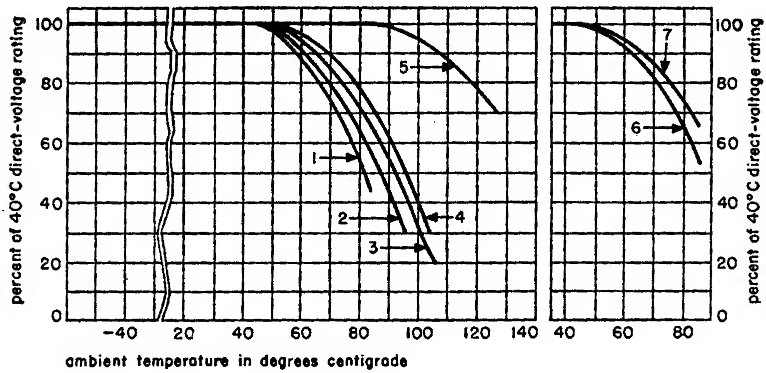

MIL specification

MIL char	watt-second rating	voltage rating	curve
D E F	>50	All	1
	5–50	All	2
	0.5–5	All, plus those excluded from group of curve 4	3
	0–0.5	1500 v and below—small cased tubular styles; 1000 v and below—other styles	4
K	0–0.8	600 v and below—small cased tubular styles; 400 v and below—other styles	5

RETMA standard

watt-second rating	voltage rating	curve
>50	1500 and over	6
5–50	2000 and below	6
5–50	2500 and above	7
0–5	All	7

Fig. 15—Life-expectancy rating for paper capacitors as a function of ambient temperature.

Capacitors—impregnated paper dielectric *continued*

the range 0 to +40 degrees centigrade, the applied voltage must be reduced in accordance with Fig. 15.

The energy content of a capacitor may be found from

$W = CE^2/2$ watt-seconds

where

C = capacitance in farads

E = applied voltage in volts

In multiple-section capacitors, the sum of the watt-second ratings should be used to determine the proper derating of the unit.

Longer life in continuous service may be secured by operating at voltages lower than those determined from Fig. 15. Experiment has shown that the life of paper-dielectric capacitors having the usual oil or wax impregnants is approximately inversely proportional to the 5th power of the applied voltage:

desired life in years (at ambient ≈ 45°C)	1	2	5	10	20
applied voltage in percent of rated voltage	100	85	70	60	53

The above life derating is to be applied together with the ambient-temperature derating to determine the adjusted-voltage rating of the paper capacitor for a specific application.

Waveform

Normal filter capacitors are rated for use with direct current. Where alternating voltages are present, the adjusted-voltage rating of the capacitor should be calculated as the sum of the direct voltage and the peak value of the alternating voltage. The alternating component must not exceed 20 percent of the rating at 60 cycles, 15 percent at 120 cycles, 6 percent at 1000 cycles, or 1 percent at 10,000 cycles.

Where alternating-current rather than direct-current conditions govern, this fact must be included in the capacitor specification, and capacitors specially designed for alternating-current service should be procured.

Where heavy transient or pulse currents are present, standard capacitors may not give satisfactory service unless an allowance is made for the unusual conditions.

Capacitors — impregnated paper dielectric *continued*

Fig. 16—Characteristics of impregnants for paper capacitors.

property			castor oil		mineral oil		askarels* (chlorinated synthetic)		Halowax (chlorinated naphthalene synthetic)	mineral wax	polyisobutenes, silicone fluids, or polyesters
Characteristic		From Specification MIL–C–25A	D	—	E†	—	F†	—	—	—	K
		From RETMA standard	—	C	—	A	—	B	—	—	—
Measurements at 25°C ambient	Megohms × microfarads‡	Nominal	1500		7000		6000		3000	15,000	20,000
		Specification minimum	**500**		**2000**	**3000**	**1500**	**1000**	**2000**	—	**4000**
	Minimum insulation resistance in megohms		**1500**		**6000**		**4500**	**1500**	**6000**	—	**12,000**
	Power factor in percent	60 c/s	<0.2		0.3		<0.3		0.5 to 3	0.5 to 1.5	≈0.5
		1000 c/s	—		≈1		—		≈2	—	≈1
Measurements at high-ambient temperature	High-ambient test temperature in degrees centigrade		**85**		**85**		**85**		**55**	85	**125**
	Megohms × microfarads‡	Nominal	10		40		30		100	50	20
		Specification minimum	**5**		**20**	**30**	**15**	**10**	**100**	—	**10**
	Minimum insulation resistance in megohms		**150**		**600**		**450**	**150**	**1000**	—	**150**
	Power factor in percent		2 to 6		0.3 to 1.6		1 to 5		1 to 3	0.2 to 1.5	≈1.5
	Percent capacitance change from value at 25 degrees centigrade		±5		±5		±5		−4.5 to 0	−10 to −6	+1 to +3

Measurements at low-ambient temperature	Low-ambient test temperature in degrees centigrade		**−55**	**−40**	**−55**	**−40**	**−55**	**−40**	**−20**	−55	**−55**
	Power factor in percent		1.5 to 4		0.5 to 3		0.8 to 3		0.5 to 4	3 to 4	≈3
	Percent capacitance change from value at 25 degrees centigrade	Nominal	−20 to +4		−10 to +2		−30 to −20		−10 to −5	−6 to −2	−5 to −2
		Specification maximum	**−30**	**+5 to −30**	**−15**	**±5**	**−30**	**+5 to −30**	**−10**	—	**−10**
Application data	Recommended ambient temperature range in degrees centigrade		−55 to +85		−55 to +85		−55 to +85		−20 to +55	to +85	−55 to +125
	Relative capacitor volume (for units of equal capacitance)		100		135		100		100	135	135
	Recommended uses		General-purpose dc. Also ac if temperature range is imited		General-purpose dc and ac; high-temp. applications. High-stability requirements		General-purpose dc and ac. Non-inflammable		General-purpose dc over limited temperature range	General-purpose dc over wider temp. range than Halowax units allow	General-purpose dc; high-temp. applications

Bold figures in tabulation are Specification MIL–C–25A or RETMA-standard limits for that property.

* Trade names Aroclor, Pyranol, Dykanol A, Inerteen etc.

† MIL–C–25A characteristics *A* and *B* (not tabulated above) are essentially long-life versions of MIL characteristics *E* and *F*, respectively.

‡ At 25 degrees centigrade, applies to capacitors of approximately $\frac{1}{3}$ microfarad or larger. At any test temperature, capacitors are not expected to show megohm × microfarad products in excess of the insulation-resistance requirements.

Capacitors—impregnated paper dielectric *continued*

Capacitor impregnants

Fig. 16 lists the various impregnating materials in common use together with their distinguishing properties. At the bottom will be found recommendations for application of capacitors according to their impregnating material.

Insulation resistance

For ordinary electronic circuits, the exact value of capacitor insulation resistance is unimportant. In many circuits little difference in performance is observed when the capacitor is shunted by a resistance as low as 5 megohms. In the very few applications where insulation resistance is important (e.g., some *RC*-coupled amplifiers), the capacitor value is usually small and megohm×microfarad products of 10 to 20 are adequate.

The insulation resistance of a capacitor is a function of the impregnant; its departure from maximum value is an indication of the care taken in manufacture to avoid undesirable contamination of the impregnant. For example, if an askarel-impregnated capacitor has the same insulation resistance as a good castor-oil-impregnated capacitor of equal rating, the askarel impregnant is strongly contaminated, and the capacitor life will be considerably reduced.

Measurements are made with potentials between 100 and 500 volts, and a maximum charging time of 2 minutes.

Power factor

This is a function of the capacitor impregnant. In most filter applications where a specified maximum capacitor impedance at a known frequency may not be exceeded, the determining factor is the capacitor reactance and not the power factor. A power factor of 14 percent will increase the impedance only 1 percent, a negligible amount.

For alternating-current applications, however, the power factor determines the capacitor internal heating. Consideration must be given to the alternating voltage and the operating temperature. Power factor is a function of the voltage applied to the capacitor; any specification should include actual capacitor operating conditions, rather than arbitrary bridge-measurement conditions.

For manufacturing purposes, power factor is measured at room temperature ($\approx$25 degrees centigrade), with 1000 cycles applied to capacitors of 1 μf or less, rated 3000 volts or less; and with 60 cycles applied to capacitors

Capacitors—impregnated paper dielectric *continued*

larger than 1 μf, or rated higher than 3000 volts. Under these conditions the power factor should not exceed 1 percent.

Temperature coefficient of capacitance

Depending upon the impregnant characteristics, low temperature may cause an appreciable drop in capacitance. Due allowance for this must be made if low-temperature operation of the equipment is to be satisfactory. This temperature effect is nonlinear.

Life tests

Accelerated life tests run on paper capacitors are based on 250-hour operation at the high-ambient-temperature limit shown in Fig. 16 with an applied direct voltage determined by the watt-second and 40-degree-centigrade voltage ratings.

Capacitors—metalized paper

When dielectric breakdown occurs in conventional paper–foil capacitors, conducting particles or carbonized areas in the paper establish conduction between the foils. Since the foils are capable of carrying substantial current, sustained conduction results, carbonizing a large area of paper, and permanently short-circuiting the capacitor.

In the metalized-paper capacitor (construction shown in Fig. 17), the metallic film is extremely thin. On breakdown, this film immediately burns away, leaving the capacitor operable, but with slightly reduced capacitance. This phenomena results in self-healing capacitors.

Minor defects (pin holes, thin spots, and conducting particles) are unavoidably present in all capacitor papers. Therefore, conventional paper capacitors employ not less than two layers of paper. Since the metalized-paper types are self healing, a single layer may be used. Metalized-paper capacitors designed to operate just below the dielectric-breakdown potential are appreciably smaller than conventional-construction paper capacitors.

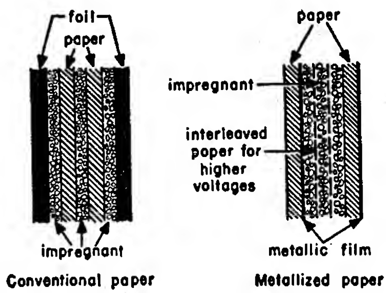

Fig. 17—Construction of conventional and metalized-type paper capacitors.

Capacitors—metalized paper *continued*

Characteristics

Characteristics of metalized-paper capacitors may best be illustrated by comparing them with conventional paper capacitors.

The space saving possible with metalized-paper capacitors is their outstanding characteristic. At 200-volts rating they are one-quarter the volume

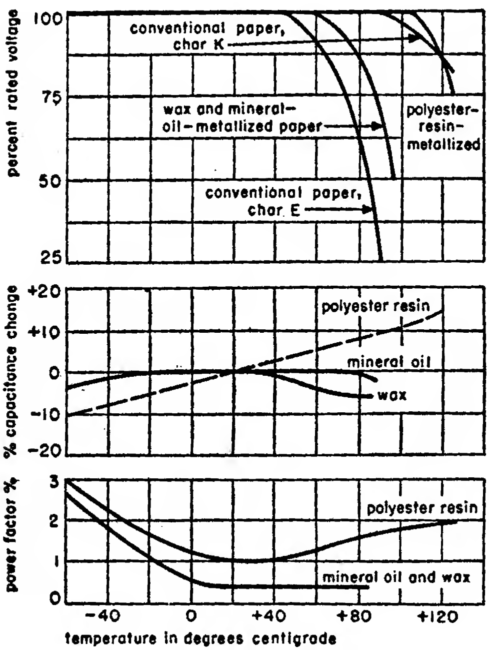

Fig. 18—From top to bottom, voltage derating, capacitance change, and power factor as a function of temperature for metalized-paper capacitors.

of conventional paper construction; at 600-volts rating, the ratio increases to 0.8. Above 600-volts rating, metalized-paper capacitors provide no size advantages.

Electrical performance, including temperature characteristics, depends largely on the impregnant. Since an occasional arcover is normal, the impregnant must be one that does not break down as the result of arcing. This limits impregnants to mineral waxes and oils and, for high-temperature use, certain polyester resins. Except for upper-temperature operation, these impregnants give similar results.

Capacitors—metalized paper *continued*

The insulation resistance is significantly lower than that of paper–foil construction, being in the order of 500 megohm–microfarads, compared to 6000 for paper–foil. Capacitance change at high- and low-temperature limits normally does not exceed 5 to 6 percent for mineral-wax- or oil-impregnated capacitors and 10 to 20 percent for polyester-resin-impregnated capacitors. The power factor at 1000 cycles/second is about 0.03 at low temperature and 0.01 to 0.02 at room temperature and above. For operation at elevated temperatures, voltage derating is recommended; see Fig. 18. The variation of capacitance and power factor is also indicated in Fig. 18.

Applications

Internal noise is probably the greatest deterrent to the general use of metalized-paper capacitors. This characteristic limits their use to bypassing and filtering. When operated at 75 percent of rated voltage, random arcing is negligible, but space advantage is less significant.

To be sure that faults will burn out, it is important that sufficient volt–amperes be available in the circuit. Similarly, it is necessary to limit the resistance in series with the capacitor. Most faults have a resistance of between 1 and 100 ohms. While a voltage of about 4 volts or a current of 10 milliamperes will eventually clear the capacitor, higher values are recommended for reliable performance.

Capacitors—plastic film

Where extreme-stability, low-loss, high-temperature, or high-frequency operation is required, paper capacitors offer, at best, marginal performance. Mica capacitors in high-capacitance values are large and expensive. One or more of these operating characteristics are obtainable in a superior degree, in certain of the plastic-film capacitors. Other plastic-film capacitors are practical for general use, because of space factor, price, and performance under moderate conditions.

Fig. 19 shows capacitance–temperature and voltage-derating curves, while Fig. 20 lists general characteristics of the various film types. Since some conflict exists between sources, the information is conservatively stated.

Capacitors—plastic film *continued*

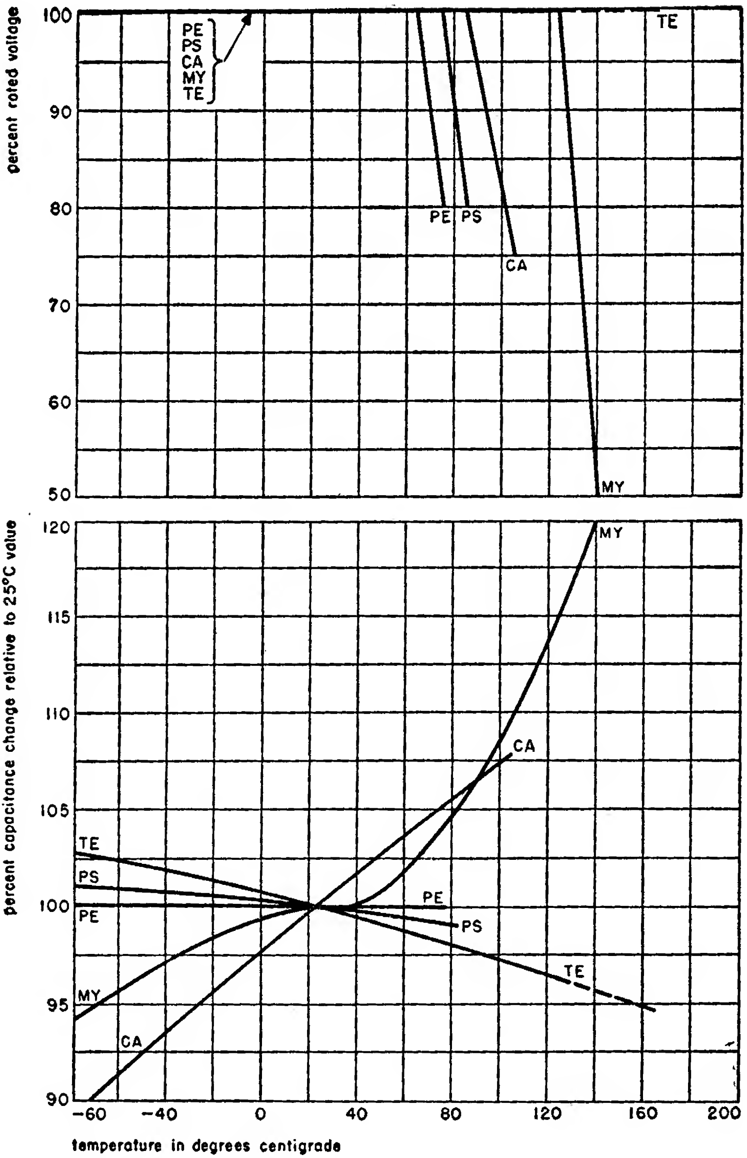

Fig. 19—Top, voltage derating and below, capacitance variation as a function of temperature for plastic-film capacitors, CA = cellulose acetate, MY = Mylar, PE = polyethylene, PS = polystyrene, and TE = Teflon.

Capacitors—plastic film *continued*

Fig. 20—Characteristics of hermetically sealed plastic-film capacitors.

property		cellulose acetate	poly-ethylene	poly-styrene	Mylar	Teflon
Operating temperature range in °C		−60 to +105	−60 to +75	−90 to +85	−60 to +140	−60 to +200
Relative size compared to paper	Below 1000 V	1.25	2.50	4.50 to 6.50	0.75	1.70 to 2.10
	Above 1000 V	0.80 to 0.85	0.50 to 0.75	—	0.30 to 0.35	0.70 to 1.60
Voltage range in volts		600 to 30,000	1000 to 30,000	100 to 1000	300 to 8000	200 to 30,000
Insulation resistance in megohms × microfarads	25°C	4000	10^5	3.5×10^7	10^5	2.5×10^5
	High temp	10	10^4	4×10^5	6.5×10^3	10^5
Power factor at o0 cycles/second	Low temp	0.02	0.0003	0.0002	0.015	0.0005
	25°C	0.01	0.0005	0.0002	0.005	0.0005
	High temp	0.01	0.001	0.00075	0.015	0.002
Dielectric absorption in percent	Low temp	5	0.01 to 0.02	0.05	0.5	0.01 to 0.05
	High temp	—	0.3	0.35 to 1.1	8	—
Normal life at rated voltage		10,000 hrs at 85°C	10,000 hrs at 65°C	2000 hrs at 75°C	2000 hrs at 125°C	10,000 hrs at 150°C

Capacitors—electrolytic

The electrolytic capacitor consists essentially of two electrodes immersed in an electrolyte with a chemical film that constitutes the dielectric on one (Fig. 21) or both electrodes. Extremely thin dielectric films are practical because of the substantial dielectric properties and the uniformity of this chemical layer. Since the electrolyte is conductive, the effective electrode spacing is small and the capacitance correspondingly large. An electrolytic capacitor is characterized by a very-high volume efficiency.

Capacitors—electrolytic *continued*

Construction

The dielectric film, which is formed by applying a potential between electrodes, is unidirectional, having high resistance in one direction and being conductive in the other. Thus, when only one plate is "formed," the capacitor is polarized and must be operated with one electrode positive with respect to the other. By forming both plates, a nonpolar unit results. This unit, because of the double film, has half the capacitance of the equivalent polar type.

For a given case size, the capacitance can be increased by a factor of 2 to 4 by etching the formed electrode prior to assembly. By substituting metalized cloth gauze or a porous slug for the conventional foil electrode, similar results are obtained. These units are electrically inferior to plain foil (unetched), having larger power factors, higher low-temperature impedances, and greater capacitance change with temperature.

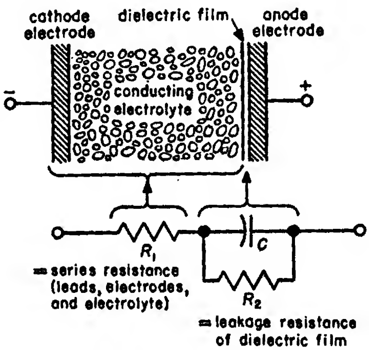

Fig. 21—Basic cell and simplified equivalent circuit for polar electrolytic capacitor.

Types

The ideal electrode metal is one whose dielectric film provides perfect "valve" action; that is, has zero direct-current resistance in one direction and infinite resistance in the other. This metal must also be completely insoluble in the electrolyte and have high conductivity. While not ideal, aluminum and tantalum approach these requirements, with tantalum being superior to aluminum.

Aluminum-foil electrolytic capacitors have a space factor of approximately 1/6 that of paper capacitors. For low voltages (under 100 volts), this space advantage is even greater. Single aluminum e ectrolytic cells are practical up to 450 direct volts, above which cells must be used in series and the space factor then approaches that of paper capacitors.

By using tantalum in place of aluminum, further size reduction is achieved, the space factor being only 1/20 that of paper capacitors. The performance of these exceeds the aluminum type in such characteristics as film stability, temperature range, leakage current, power factor, and life.

Capacitors—electrolytic *continued*

In one type of tantalum capacitor, foil construction and a neutral electrolyte are employed. These units will operate at temperatures up to 125 degrees centigrade and are available in polar and nonpolar types. A single cell is not practical above 150 volts. Their outstanding feature is the reduced possibility of leakage and danger of corrosion.

Another type of tantalum electrolytic capacitor employs a porous slug of tantalum as the anode (formed electrode), the cathode being the silver-plated can. In these, sulphuric acid is the electrolyte. Only polar construction is feasible, with single-cell voltages up to about 80 volts. Because of the type of electrolyte, operation up to 175 degrees centigrade is possible, provided voltage is derated and a substantial life reduction can be tolerated.

A third type of tantalum capacitor has a coiled tantalum wire as the anode. It is a low-voltage, polar device being useful primarily for microminiature assemblies where temperature fluctuations are small and operating conditions moderate.

Performance

Electrolytic capacitors have definite limitations. Compared to other types of capacitors, losses are large (large leakage currents and high power factor). The capacitance change with temperature is large. With increasing frequency, the capacitance decreases, while power factor becomes greater.

At subzero temperatures, the series resistance increases sharply, while capacitance falls off. (See Figs. 22 and 23.) Thus, at low temperatures,

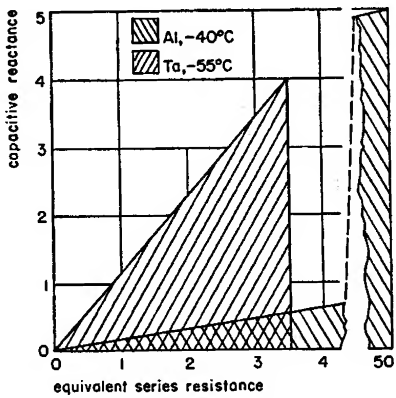

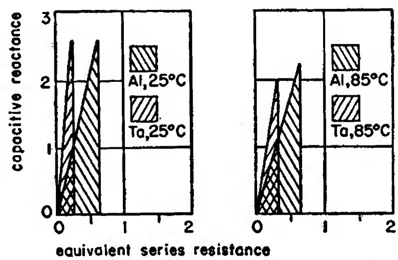

Fig. 22—Typical 120-cycle/second impedance diagrams for aluminum (Al) and tantalum (Ta) plain-foil polar electrolytic capacitors of 150-volt rating at low, high, and room temperatures. Resistance and reactance are drawn to same arbitrary scale for all charts.

Capacitors—electrolytic *continued*

the impedance (Fig. 23) is substantially larger than at room temperature. Aside from electrical considerations, the freezing and boiling temperatures of the electrolyte determine absolute temperature limits.

Referring to Fig. 21, R_1 represents the lumped series resistance of leads, electrodes, and electrolyte. In a well-constructed unit, only the resistance

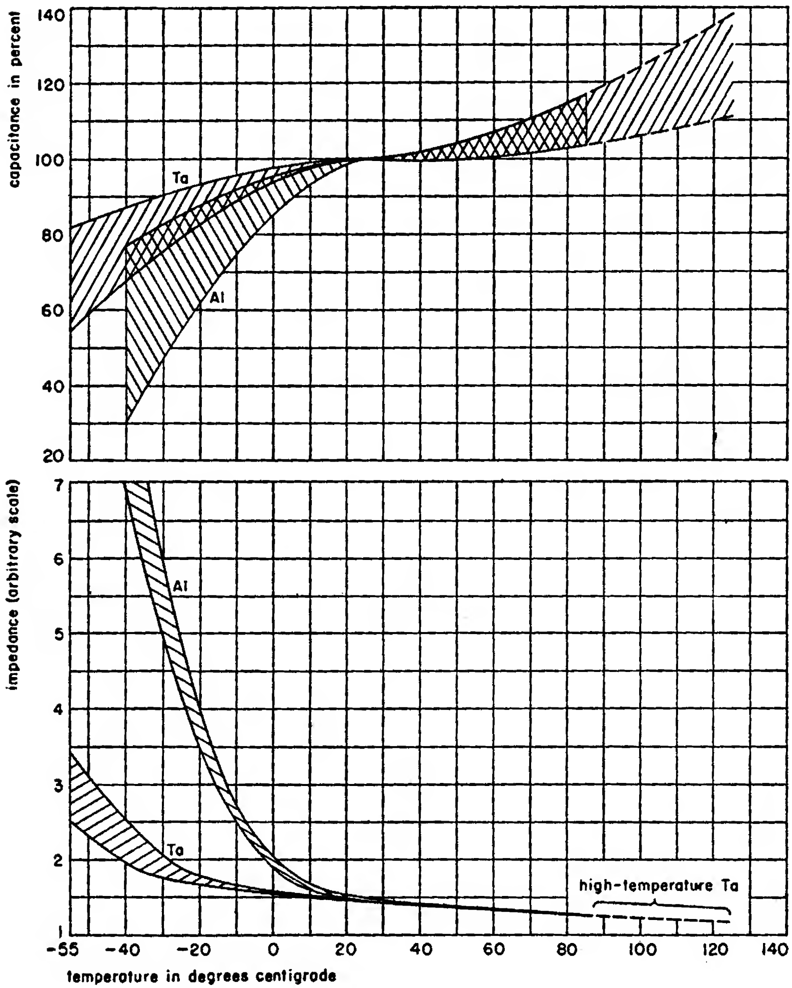

Fig. 23—Top, capacitance and below, 120-cycle/second impedance as a function of temperature for aluminum (Al) and tantalum (Ta) electrolytic capacitors.

Capacitors—electrolytic *continued*

of the electrolyte is significant. Resistance R_2, which is many times greater than R_1, represents the leakage path through the imperfect dielectric.

With direct voltage impressed on the capacitor, leakage current through R_2 accounts for practically all the internal heating. However, when an alternating-current component is present, the resultant charging current flowing through R_1 generates additional heat in the electrolyte. The effect of ripple heating, therefore, is determined by the ripple current. Heat tolerance and heat dissipation (the latter, largely a factor of case size) determine ripple-current limits

Applications

Space factor and price account for the extensive use of electrolytic capacitors. Electrical performance usually limits electrolytic capacitors to circuit applications such as bypassing at power and audio frequencies where circuit requirements are satisfied by minimum rather than precise capacitance values.

For the polar type, when operated within maximum ripple-current limits, the large power factor and associated losses generally present no problem. Except for some reduction in maximum operating temperature, the resultant internal heating is not serious. However, for the nonpolar unit, internal heating, when operated in alternating-current circuits, limits the capacitor to an intermittant cycle. A duty cycle of twenty 3-second periods/hour is typical.

The dielectric film is not completely stable, particularly in aluminum electrolytics. Therefore, some film deterioration occurs in storage. When voltage is applied, the film reforms; but, while reforming, high leakage current flows. In extreme cases, the resultant heating may generate vapor and burst the case.

Because of the film instability, extensive voltage derating of electrolytics is impractical. A 450-volt capacitor operated on 300 volts eventually becomes a 300-volt capacitor. Surge-voltage limitations must also be observed, since high leakage (and heating) will occur during surges. Where such limits may be exceeded, protective circuitry must be provided or another type of capacitor substituted.

When these capacitors are used in series, it is imperative that equalizing resistors be provided. An equalizing resistor, shunted across each capacitor, prevents unequal voltage distribution across the capacitor chain.

Capacitors—electrolytic *continued*

Since the case is in contact with the electrolyte, there is a conducting path between the case and the element. This condition makes necessary external insulation between the case and the chassis, whenever the chassis and the negative terminal are not at the same potential.

IF transformer frequencies[1]

Recognized standard frequencies for receiver intermediate-frequency transformers are

Standard broadcast (540 to 1600 kilocycles)	**455**, 260 kilocycles
Standard broadcast (vehicular)	**262.5** kilocycles
Very-high-frequency broadcast	**10.7** megacycles
Very-, ultra-, and super-high-frequency equipment	**30**, 60, 100 megacycles (common practice)
Television: sound carrier	**41.25** megacycles
picture carrier	**45.75** megacycles

Color codes for transformer leads

Radio power transformers[2]

Primary	Black
If tapped:	
Common	Black
Tap	Black-Yellow
Finish	Black-Red
Rectifier	
Plate	Red
Center tap	Red-Yellow
Filament	Yellow
Center tap	Yellow-Blue

General Use	
Filament No. 1	Green
Center tap	Green-Yellow
Filament No. 2	Brown
Center tap	Brown-Yellow
Filament No. 3	Slate
Center tap	Slate-Yellow

Intermediate-frequency transformers[3]

Primary	
Plate	Blue
B+	Red
Secondary	
Grid or diode	Green
Grid return	White

For full-wave transformer:

Second diode	Violet

Old standard[4] is same as above, except:

Grid return	Black
Second diode	Green-Black

[1] RETMA Standard REC–109–C.
[2] Old RMA Standard M4–505.
[3] RETMA Standard REC–114.
[4] Old RMA Standard M4–506.

Printed circuits

A printed circuit consists of a conductive circuit pattern applied to one or both sides of an insulating base. Printed circuits have several advantages over conventional methods of assembly using chassis and wiring harnesses.

Soldering is done in one operation instead of connection-by-connection.

Uniformity: A more uniform product is produced because wiring errors are eliminated and because distributed capacitances are constant from one production unit to another.

Automation: The printed-circuit method of construction lends itself to automatic assembly and testing machinery.

Flexibility: The printed circuit consists of printed wiring but may also include printed components such as capacitors and inductors. Capacitors may be produced by printing conducting areas on opposite sides of the wiring board, using the board material as the dielectric. Spiral-type inductors may also be printed. Both types of components are illustrated in Fig. 24.

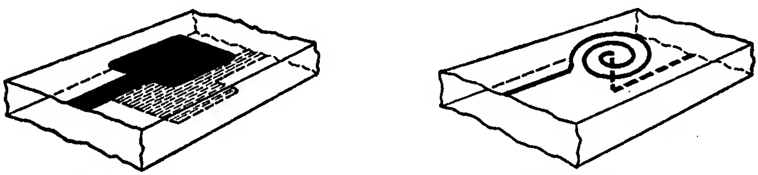

Printed-circuit capacitor   Printed-circuit inductor

Fig. 24—Formation of reactive elements by printed-circuit methods.

Printed-circuit base materials

Printed-circuit base materials are available in thicknesses varying from 1/64 to 1/2 inch. The important properties of the usual materials are tabulated in Fig. 25. For special applications, other laminates are available having base insulation of:

a. Glass-cloth Teflon (polytetrafluoroethylene).
b. Kel-F (polymonochlorotrifluoroethylene).
c. Silicone rubber (flexible).
d. Glass-mat–polyester-resin.

The most widely used base material is NEMA-XXXP paper-base phenolic.

Printed circuits *continued*

Fig. 25—Properties of typical printed-circuit dielectric base materials.

material	punch-ability	me-chanical strength	mois-ture resist-ance	insula-tion	arc resist-ance	abra-sive action on tools	maxi-mum temper-ature in deg C
NEMA type-P paper-base phenolic	Good	Good	Poor	Fair	Poor	No	—
NEMA type-XXXP paper-base phenolic	Fair	Good	Good	Good	Fair	No	125
NEMA type-G5 glass-cloth melamine	Fair	Excellent	Poor*	Good	Good	Yes	135
NEMA type-G6 glass-cloth silicone	Fair	Good	Good	Excellent	Good	Yes	200
NEMA type-G7 glass-cloth silicone	Fair	Good	Poor*	Excellent	Good	Yes	200
Glass-cloth epoxy resin	—	—	Excellent	Excellent	Good	Yes	160

* Along glass fibers.

Conductor materials

Conductor materials available are silver, brass, aluminum, and copper; copper is the most widely used. Laminates are available with copper foil on one or both sides and are furnished in the thicknesses of foil listed in Fig. 26. The current-carrying capacity in amperes for copper conductors 1/16-inch wide are also listed in Fig. 26.

Fig. 26—Weight of foil and current-carrying capacity.

inches thickness	weight in ounces/foot^2	current-carrying capacity in amperes		
		for 10°C rise	for 20°C rise	for 40°C rise
0.0013	1	2	4	6
0.0027	2	3.5	6	8

Printed circuits *continued*

Manufacturing processes

The most widely used production methods are:

Etching process, wherein the desired circuit is printed on the metal-clad laminate by photographic, silk-screen, photo-offset, or other means, using an ink or lacquer resistant to the etching bath. The board is then placed in an etching bath that removes all of the unprotected metal (ferric chloride is a commonly used mordant for copper-clad laminates). After the etching is completed, the ink or lacquer is removed to leave the conducting pattern exposed.

Plating process, wherein the designed circuit pattern is printed on the unclad base material using an electrically conductive ink and, by electroplating, the conductor is built up to the desired thickness. This method lends itself to plating through punched holes in the board for the purpose of making connections from one side of the board to the other.

Other processes, including metal spraying and die stamping.

Circuit-board finishes

Conductor protective finishes are required on the circuit pattern to improve shelf-storage life of the circuit boards and to facilitate soldering. Some of the most widely used finishes are:

a. Hot-solder coating (done by dip-soldering in a solder bath) is a low-cost method and gives good results where coating thickness is not critical.

b. Silver plating is used as a soldering aid but is subject to tarnishing and has a limited shelf life.

c. Hot-rolled or plated solder coat gives good solderability and uniform coating thickness.

d. Other finishes for special purposes are: Gold plate for corrosion resistance and solderability and electroplated rhodium over nickel for wear resistance. Nonmetallic finishes, such as acrylic sprays and epoxy and silicone-resin coatings, are sometimes applied to circuit boards to improve moisture resistance. On two-sided circuit boards, where the possibility of components shorting out the circuit patterns exists, a thin sheet of insulating material is sometimes laminated over the circuit before the parts are inserted.

Printed circuits *continued*

Design considerations

Diameter of punched holes in circuit boards should not be less than 2/3 the thickness of the base material.

Distance between punched holes or between holes and the edge of the material should not be less than the material thickness.

Punched-hole tolerance should not be less than ±0.005 inch on the diameters.

Hole sizes should be approximately 0.010 inch larger than the diameter of the wire to be inserted in the hole.

Tolerances on fractional dimensions under 12 inches should not be less than ±1/64 inch; over 12 inches, not less than ±1/32 inch. Copper-conductor widths should not be less than 1/16 inch unless absolutely necessary.

Conductor spacing should not be less than 1/16 inch unless absolutely necessary. In spacing conductors carrying high voltages, a good rule of thumb is to allow 5000 volts/inch for XXXP phenolic.

Preparation of art work

Workmanship: In preparing the master art work for printed circuits, careful workmanship and accuracy are important. When circuits are reproduced by photographic means, considerable retouching time is saved if care is taken with the original art work.

Materials: Art work should be prepared on a dimensionally stable glass-cloth tracing cloth using a good grade of permanent black ink. Where tolerances will permit, a less stable material such as good-quality tracing paper or high-grade bristol board may be used for the art work.

Scale: Art work should be prepared to a scale that is two to five times oversize. Photographic reduction to final negative size should be possible, however, in one step.

Bends: Avoid the use of sharp corners when laying out the circuit. See Fig. 27.

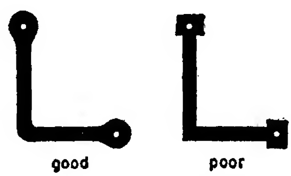

Fig. 27—Proper design of bends for printed-circuit conductors.

Printed circuits *continued*

Holes to be drilled or punched in the circuit board should have their centers indicated by a circle of 1/32-inch diameter (final size after reduction). See Fig. 28.

Fig. 28—Indication for hole.

Registration of reverse side: When drawing the second side of a printed circuit board, corresponding centers should be taken directly from the back of the drawing of the first side.

Reference marks: In addition to the illustration of the circuit pattern, the trim line, registration marks, and two scale dimensions at right angles should be shown. Nomenclature, reference designations, operating instructions, and other information may also be added.

Assembly

All components should be inserted on one side of the board if practicable. In the case of boards with the circuit on one side only, the components should be inserted on the side opposite the circuit. This allows all connections to be soldered simultaneously by dip-soldering.

Dip-soldering consists of applying a flux, usually a rosin–alcohol mixture, to the circuit pattern and then placing the board in contact with molten solder. Slight agitation of the board will insure good fillets around the wire leads. A five-second dip in a 60/40 tin–lead solder bath maintained at a temperature of 450 degrees fahrenheit will give satisfactory results.

After solder-dipping, the residual flux should be removed by a suitable solvent.

Fundamentals of networks

Inductance of single-layer solenoids*

The approximate value of the *low-frequency* inductance of a single-layer solenoid is†

$L = Fn^2d$ microhenries

where

F = form factor, a function of the ratio d/l. Value of F may be read from the accompanying chart, Fig. 1.

n = number of turns

d = diameter of coil (inches), between centers of conductors

l = length of coil (inches)

= n times the distance between centers of adjacent turns.

The formula is based on the assumption of a uniform current sheet, but the correction due to the use of spaced round wires is usually negligible for practical purposes. For higher frequencies, skin effect alters the inductance slightly. This effect is not readily calculated, but is often negligibly small. However, it must be borne in mind that the formula gives approximately the *true* value of inductance. In contrast, the *apparent* value is affected by the shunting effect of the distributed capacitance of the coil.

Example: Required a coil of 100 microhenries inductance, wound on a form 2 inches diameter by 2 inches winding length. Then $d/l = 1.00$, and $F = 0.0173$ in Fig. 1.

$$n = \sqrt{\frac{L}{Fd}} = \sqrt{\frac{100}{0.0173 \times 2}} = 54 \text{ turns}$$

Reference to magnet-wire data, Fig. 2, will assist in choosing a desirable size of wire, allowing for a suitable spacing between turns according to the application of the coil. A slight correction may then be made for the increased diameter (diameter of form plus two times radius of wire), if this small correction seems justified.

Approximate formula

For single-layer solenoids of the proportions normally used in radio work, the inductance is given to an accuracy of about 1 percent by

$$L = n^2 \frac{r^2}{9r + 10l} \text{ microhenries}$$

where $r = d/2$.

* Calculation of copper losses in single-layer solenoids is treated in F. E. Terman, "Radio Engineers Handbook," 1st edition, McGraw-Hill Book Company, Inc., New York, N. Y.; 1943: pp. 77–80.

† Formulas and chart (Fig. 1) derived from equations and tables in Bureau of Standards Circular No. C74.

Inductance of single-layer solenoids *continued*

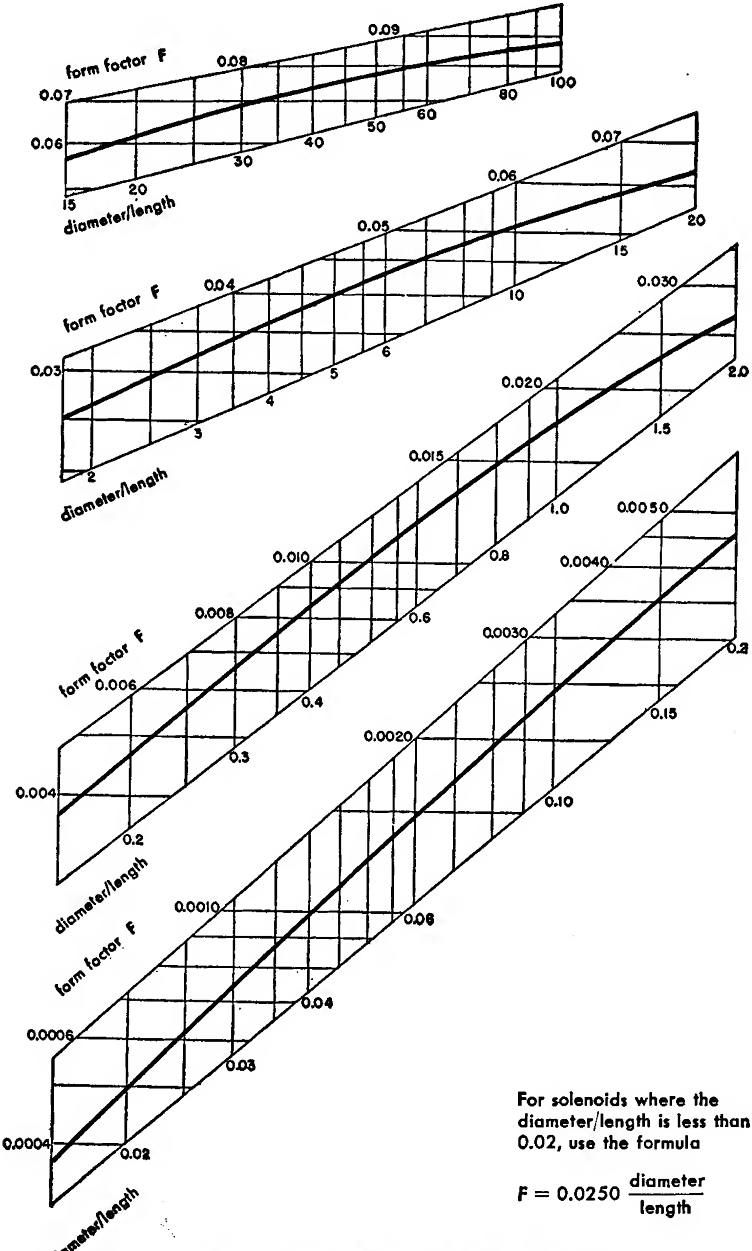

For solenoids where the diameter/length is less than 0.02, use the formula

$$F = 0.0250\ \frac{\text{diameter}}{\text{length}}$$

Fig. 1—Inductance of a single-layer solenoid, form factor = F.

Inductance of single-layer solenoids *continued*

General remarks

In the use of various charts, tables, and calculators for designing inductors, the following relationships are useful in extending the range of the devices. They apply to coils of any type or design.

a. If all dimensions are held constant, inductance is proportional to n^2.

b. If the proportions of the coil remain unchanged, then for a given number of turns the inductance is proportional to the dimensions of the coil. A

Fig. 2—Magnet-wire data.

AWG B & S gauge	bare nom diam in inches	enam nom diam in inches	SCC* diam in inches	DCC* diam in inches	SCE* diam in inches	SSC* diam in inches	DSC* diam in inches	SSE* diam in inches	bare min diam inches	bare max diam inches	enameled min diam inches	enameled diam* in inches
10	.1019	.1039	.1079	.1129	.1104	—	—	—	.1009	.1029	.1024	.1044
11	.0907	.0927	.0957	.1002	.0982	—	—	—	.0898	.0917	.0913	.0932
12	.0808	.0827	.0858	.0903	.0882	—	—	—	.0800	.0816	.0814	.0832
13	.0720	.0738	.0770	.0815	.0793	—	—	—	.0712	.0727	.0726	.0743
14	.0641	.0659	.0691	.0736	.0714	—	—	—	.0634	.0647	.0648	.0664
15	.0571	.0588	.0621	.0666	.0643	.0591	.0611	.0613	.0565	.0576	.0578	.0593
16	.0508	.0524	.0558	.0603	.0579	.0528	.0548	.0549	.0503	.0513	.0515	.0529
17	.0453	.0469	.0503	.0548	.0523	.0473	.0493	.0493	.0448	.0457	.0460	.0473
18	.0403	.0418	.0453	.0498	.0472	.0423	.0443	.0442	.0399	.0407	.0410	.0422
19	.0359	.0374	.0409	.0454	.0428	.0379	.0399	.0398	.0355	.0363	.0366	.0378
20	.0320	.0334	.0370	.0415	.0388	.0340	.0360	.0358	.0316	.0323	.0326	.0338
21	.0285	.0299	.0335	.0380	.0353	.0305	.0325	.0323	.0282	.0287	.0292	.0303
22	.0253	.0266	.0303	.0343	.0320	.0273	.0293	.0290	.0251	.0256	.0261	.0270
23	.0226	.0238	.0276	.0316	.0292	.0246	.0266	.0262	.0223	.0228	.0232	.0242
24	.0201	.0213	.0251	.0291	.0266	.0221	.0241	.0236	.0199	.0203	.0208	.0216
25	.0179	.0190	.0224	.0264	.0238	.0199	.0219	.0213	.0177	.0181	.0186	.0193
26	.0159	.0169	.0204	.0244	.0217	.0179	.0199	.0192	.0158	.0161	.0166	.0172
27	.0142	.0152	.0187	.0227	.0200	.0162	.0182	.0175	.0141	.0144	.0149	.0155
28	.0126	.0135	.0171	.0211	.0183	.0146	.0166	.0158	.0125	.0128	.0132	.0138
29	.0113	.0122	.0158	.0198	.0170	.0133	.0153	.0145	.0112	.0114	.0119	.0125
30	.0100	.0108	.0145	.0185	.0156	.0120	.0140	.0131	.0099	.0101	.0105	.0111
31	.0089	.0097	.0134	.0174	.0144	.0109	.0129	.0119	.0088	.0090	.0094	.0099
32	.0080	.0088	.0125	.0165	.0135	.0100	.0120	.0110	.0079	.0081	.0085	.0090
33	.0071	.0078	.0116	.0156	.0125	.0091	.0111	.0100	.0070	.0072	.0075	.0080
34	.0063	.0069	.0108	.0148	.0116	.0083	.0103	.0091	.0062	.0064	.0067	.0071
35	.0056	.0061	.0101	.0141	.0108	.0076	.0096	.0083	.0055	.0057	.0059	.0063
36	.0050	.0055	.0090	.0130	.0097	.0070	.0090	.0077	.0049	.0051	.0053	.0057
37	.0045	.0049	.0085	.0125	.0091	.0065	.0085	.0071	.0044	.0046	.0047	.0051
38	.0040	.0044	.0080	.0120	.0086	.0060	.0080	.0066	.0039	.0041	.0042	.0046
39	.0035	.0038	.0075	.0115	.0080	.0055	.0075	.0060	.0034	.0036	.0036	.0040
40	.0031	.0034	.0071	.0111	.0076	.0051	.0071	.0056	.0030	.0032	.0032	.0036
41	.0028	.0031	—	—	—	—	—	—	.0027	.0029	.0029	.0032
42	.0025	.0028	—	—	—	—	—	—	.0024	.0026	.0026	.0029
43	.0022	.0025	—	—	—	—	—	—	.0021	.0023	.0023	.0026
44	.0020	.0023	—	—	—	—	—	—	.0019	.0021	.0021	.0024

* Nominal bare diameter plus maximum additions.

For additional data on copper wire, see pp. 50–57 and p. 278.

Inductance of single-layer solenoids *continued*

coil with all dimensions m times those of a given coil (having the same number of turns) has m times the inductance of the given coil. That is, inductance has the dimensions of *length*.

Decrease of solenoid inductance by shielding*

When a solenoid is enclosed in a cylindrical shield, the inductance is re-

* RCA Application Note No. 48; June 12, 1935.

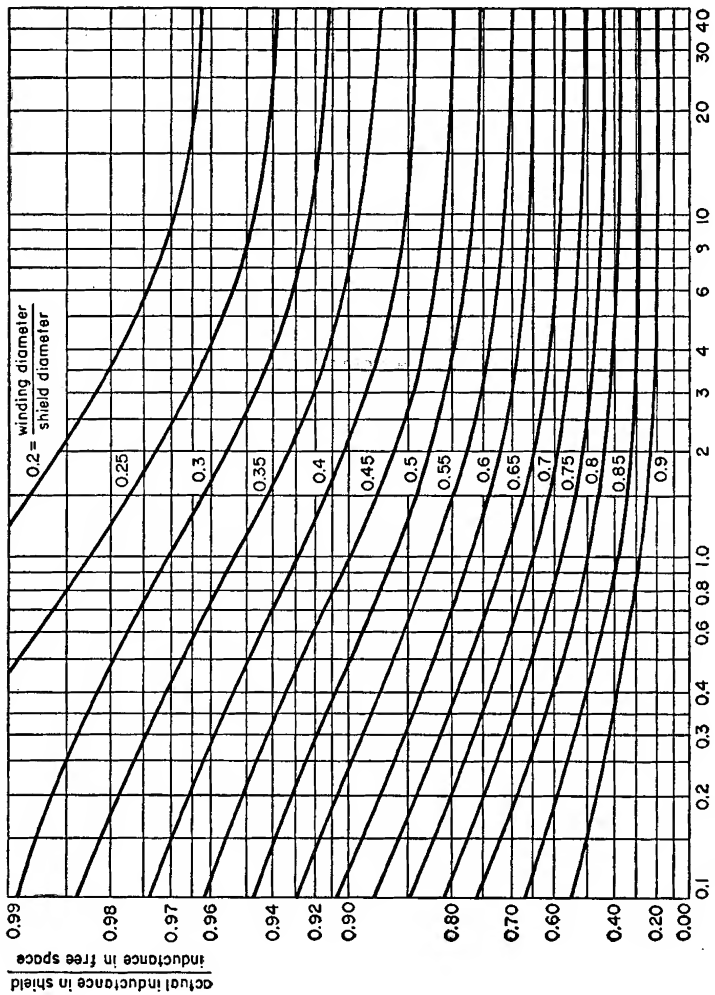

By Permission of RCA, copyright proprietor.

Fig. 3—Curves for determination of inductance decrease when a solenoid is shielded.

Inductance of single-layer solenoids *continued*

duced by a factor given in the accompanying chart, Fig. 3. This effect has been evaluated by considering the shield to be a short-circuited single-turn secondary. The curves in Fig. 3 are reasonably accurate provided the clearance between each end of the coil winding and the corresponding end of the shield is at least equal to the radius of the coil. For square shield cans, take the equivalent shield diameter (for Fig. 3) as being 1.2 times the width of one side of the square.

Example: Let the coil winding length be 1.5 inches and its diameter 0.75 inch, while the shield diameter is 1.25 inches. What is the reduction of inductance due to the shield? The proportions are

(winding length)/(winding diameter) = 2.0

(winding diameter)/(shield diameter) = 0.6

Referring to Fig. 3, the actual inductance in the shield is 72 percent of the inductance of the coil in free space.

Reactance charts

Figs. 4, 5, and 6 give the relationships of capacitance, inductance, reactance, and frequency. Any one value may be determined in terms of two others by use of a straight edge laid across the correct chart for the frequency under consideration.

Example: Given a capacitance of 0.001 μf, find the reactance at 50 kilocycles and inductance required to resonate. Place a straight edge through these values and read the intersections on the other scales, giving 3180 ohms and 10.1 millihenries. See Fig. 5.

Reactance charts *continued*

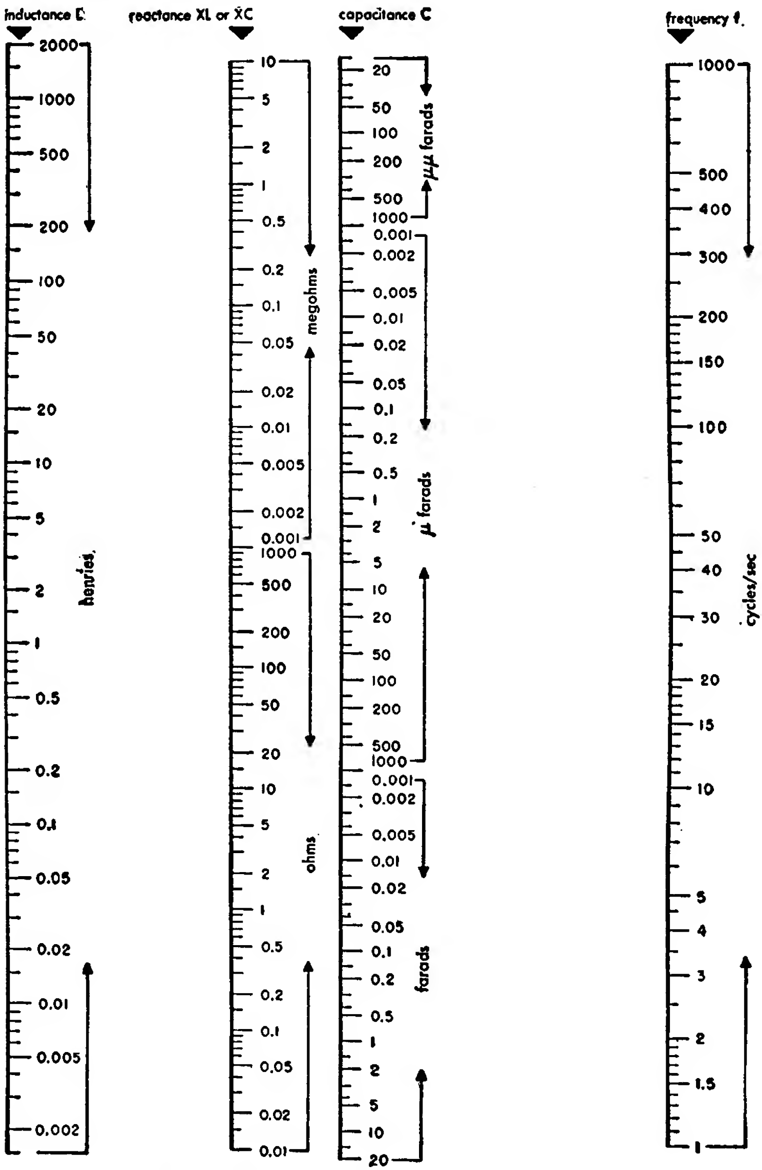

Fig. 4—Chart covering 1 cycle to 1000 cycles.

Reactance charts *continued*

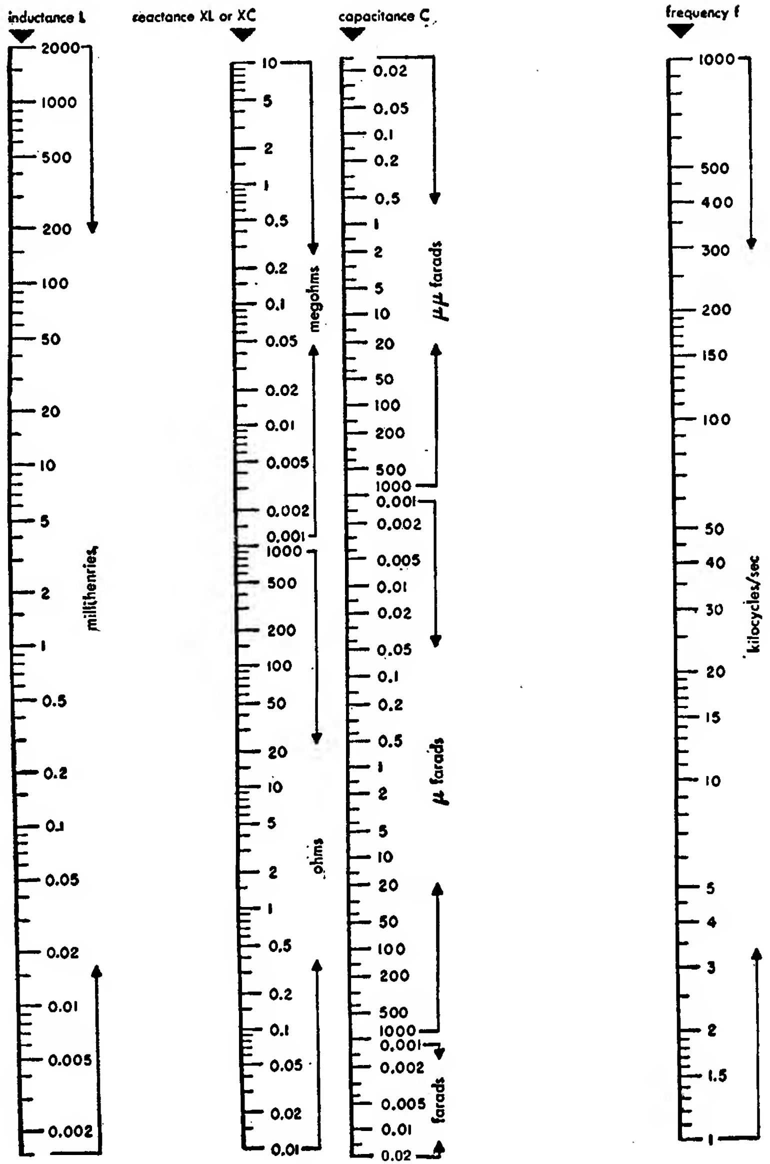

Fig. 5—Chart covering 1 kilocycle to 1000 kilocycles.

Reactance charts *continued*

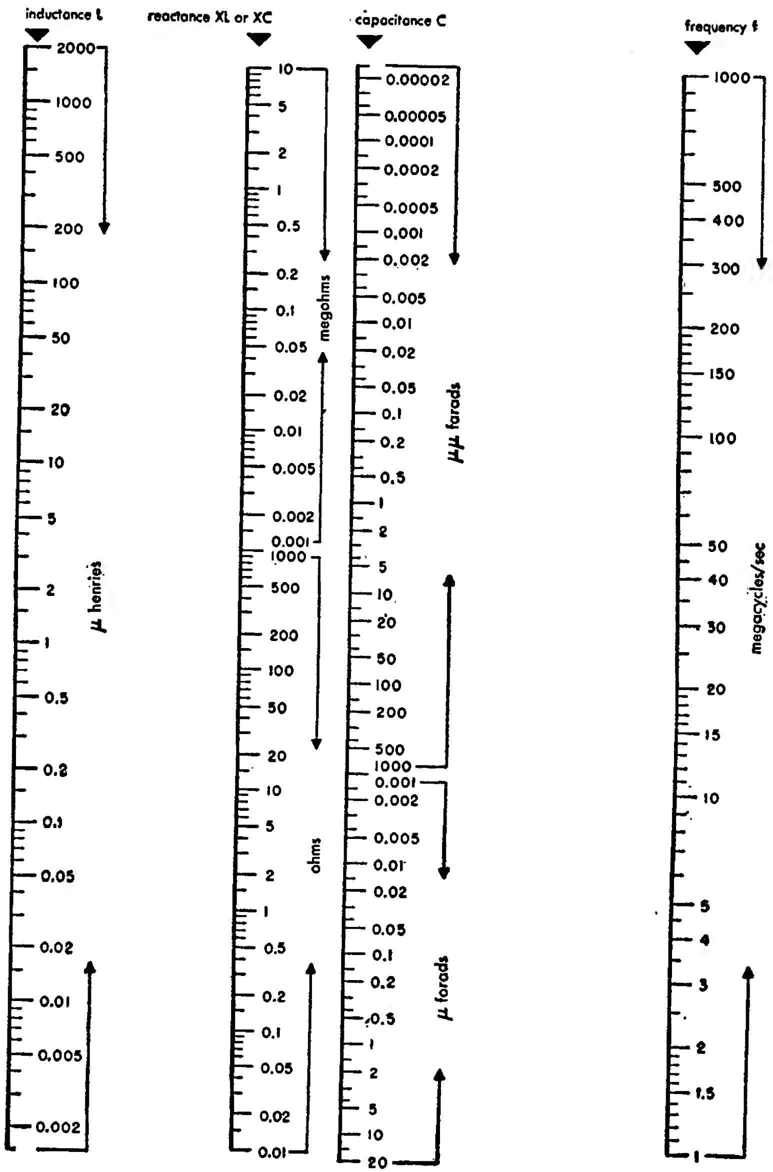

Fig. 6—Chart covering 1 megacycle to 1000 megacycles.

Impedance formulas

Parallel and series circuits and their equivalent relationships

Parallel circuit

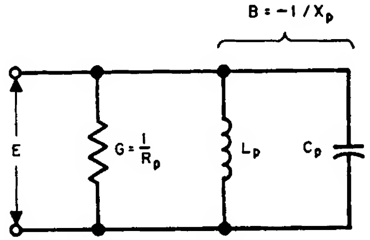

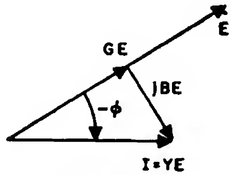

parallel circuit

Conductance $G = \dfrac{1}{R_p}$

Susceptance $B = -\dfrac{1}{X_p}$

$$= \omega C_p - \frac{1}{\omega L_p}$$

$$\omega = 2\pi f$$

Reactance $X_p = \dfrac{\omega L_p}{1 - \omega^2 L_p C_p}$

Admittance $Y = \dfrac{I}{E} = \dfrac{1}{Z} = G + jB$

$$= \sqrt{G^2 + B^2}\ \angle -\phi = |Y|\ \angle -\phi$$

Impedance $Z = \dfrac{E}{I} = \dfrac{1}{Y}$

$$= \frac{R_p X_p}{R_p^2 + X_p^2}(X_p + jR_p)$$

$$= \frac{R_p X_p}{\sqrt{R_p^2 + X_p^2}}\ \angle \phi = |Z|\ \angle \phi$$

Phase angle $-\phi = \tan^{-1} \dfrac{B}{G}$

$$= \cos^{-1} \frac{G}{|Y|} = -\tan^{-1} \frac{R_p}{X_p}$$

Impedance formulas *continued*

Series circuit

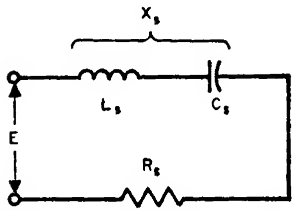

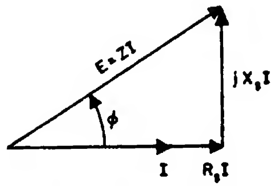

equivalent series circuit

Resistance $= R_s$

Reactance $X_s = \omega L_s - \dfrac{1}{\omega C_s}$

Impedance $Z = \dfrac{E}{I} = R_s + jX_s = \sqrt{R_s^2 + X_s^2}\ \angle\phi = |Z|\ \angle\phi$

Phase angle $\phi = \tan^{-1}\dfrac{X_s}{R_s} = \cos^{-1}\dfrac{R_s}{|Z|}$

For both circuits

Vectors E and I, phase angle ϕ, and Z, Y are identical for the parallel circuit and its equivalent series circuit

$$Q = |\tan\phi| = \frac{|X_s|}{R_s} = \frac{R_p}{|X_p|} = \frac{|B|}{G}$$

$$(\text{pf}) = \cos\phi = \frac{R_s}{|Z|} = \frac{|Z|}{R_p} = \frac{G}{|Y|} = \sqrt{\frac{R_s}{R_p}} = \frac{1}{\sqrt{Q^2+1}} = \frac{(\text{kw})}{(\text{kva})}$$

$$Z^2 = R_s^2 + X_s^2 = \frac{R_p^2X_p^2}{R_p^2 + X_p^2} = R_sR_p = X_sX_p$$

$$Y^2 = G^2 + B^2 = \frac{1}{R_p^2} + \frac{1}{X_p^2} = \frac{G}{R_s}$$

$$R_s = \frac{Z^2}{R_p} = \frac{G}{Y^2} = R_p\frac{X_p^2}{R_p^2 + X_p^2} = R_p\frac{1}{Q^2+1}$$

$$X_s = \frac{Z^2}{X_p} = -\frac{B}{Y^2} = X_p\frac{R_p^2}{R_p^2 + X_p^2} = X_p\frac{1}{1 + 1/Q^2}$$

Impedance formulas *continued*

$$R_p = \frac{1}{G} = \frac{Z^2}{R_s} = \frac{R_s^2 + X_s^2}{R_s} = R_s\,(Q^2 + 1)$$

$$X_p = -\frac{1}{B} = \frac{Z^2}{X_s} = \frac{R_s^2 + X_s^2}{X_s} = X_s\left(1 + \frac{1}{Q^2}\right) = \frac{R_s R_p}{X_s} = \pm R_p \sqrt{\frac{R_s}{R_p - R_s}}$$

Approximate formulas

Reactor $R_s = \dfrac{X^2}{R_p}$ and $X = X_s = X_p$ (See Note 1, p. 123)

Resistor $R = R_s = R_p$ and $X_s = \dfrac{R^2}{X_p}$ (See Note 2, p. 123)

Simplified parallel and series circuits

$$X_p = \omega L_p \qquad B = -\frac{1}{\omega L_p} \qquad X_s = \omega L_s$$

$$\tan\phi = \frac{\omega L_s}{R_s} = \frac{R_p}{\omega L_p}$$

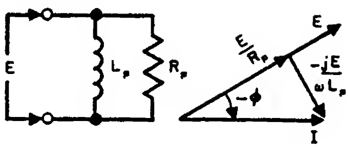

$$Q = \frac{\omega L_s}{R_s} = \frac{R_p}{\omega L_p}$$

$$(\text{pf}) = \frac{R_s}{\sqrt{R_s^2 + \omega^2 L_s^2}}$$

$$= \frac{\omega L_p}{\sqrt{R_p^2 + \omega^2 L_p^2}}$$

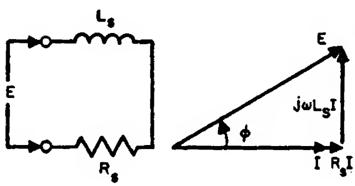

$(\text{pf}) = \dfrac{1}{Q}$ approx (See Note 3, p. 123)

$$R_s = R_p \frac{1}{Q^2 + 1} \qquad R_p = R_s\,(Q^2 + 1) \qquad Z = R_p \frac{1 + jQ}{1 + Q^2}$$

$$L_s = L_p \frac{1}{1 + 1/Q^2} \qquad L_p = L_s\left(1 + \frac{1}{Q^2}\right) \qquad Y = \frac{1}{R_s}\frac{1 - jQ}{1 + Q^2}$$

Impedance formulas *continued*

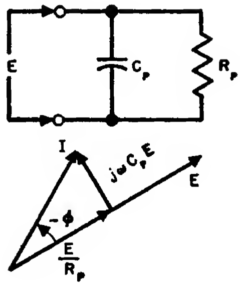

$$X_p = \frac{-1}{\omega C_p} \qquad B = \omega C_p \qquad X_s = \frac{-1}{\omega C_s}$$

$$\tan\phi = \frac{-1}{\omega C_s R_s} = -\omega C_p R_p$$

$$Q = \frac{1}{\omega C_s R_s} = \omega C_p R_p$$

$$\text{(pf)} = \frac{\omega C_s R_s}{\sqrt{1 + \omega^2 C_s^2 R_s^2}} = \frac{1}{\sqrt{1 + \omega^2 C_p^2 R_p^2}}$$

$$\text{(pf)} \approx \frac{1}{Q} \quad \text{(See Note 3)}$$

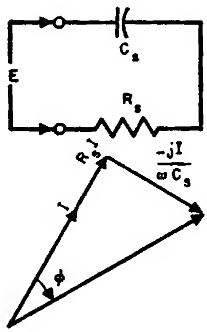

$$R_s = R_p \frac{1}{Q^2 + 1} \qquad R_p = R_s\,(Q^2 + 1)$$

$$C_s = C_p\left(1 + \frac{1}{Q^2}\right) \qquad C_p = C_s \frac{1}{1 + 1/Q^2}$$

$$Z = R_p \cdot \frac{1 - jQ}{1 + Q^2} \qquad Y = \frac{1}{R_s}\frac{1 + jQ}{1 + Q^2}$$

Approximate formulas

Inductor $R_s = \omega^2 L^2/R_p$ and $L = L_p = L_s$ (See Note 1)

Resistor $R = R_s = R_p$ and $L_p = R^2/\omega^2 L_s$ (See Note 2)

Capacitor $R_s = 1/\omega^2 C^2 R_p$ and $C = C_p = C_s$ (See Note 1)

Resistor $R = R_s = R_p$ and $C_s = 1/\omega^2 C_p R^2$ (See Note 2)

Note 1: (Small resistive component) Error in percent $= -\ 100/Q^2$
(for $Q = 10$, error $= 1$ percent low)

Note 2: (Small reactive component) Error in percent $= -\ 100\,Q^2$
(for $Q = 0.1$, error $= 1$ percent low)

Note 3: Error in percent $= +\ 50/Q^2$ approximately
(for $Q = 7$, error $= 1$ percent high)

Impedance formulas *continued*

impedance $Z = R + jX$ ohms

magnitude $|Z| = [R^2 + X^2]^{\frac{1}{2}}$ ohms

phase angle $\phi = \tan^{-1} \frac{X}{R}$

admittance $Y = \frac{1}{Z}$ mhos

diagram	impedance Z	magnitude $\|Z\|$	phase angle ϕ	admittance Y
	R	R	0	$\frac{1}{R}$
	$j\omega L$	ωL	$+\frac{\pi}{2}$	$-j\frac{1}{\omega L}$
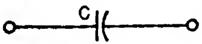	$-j\frac{1}{\omega C}$	$\frac{1}{\omega C}$	$-\frac{\pi}{2}$	$j\omega C$
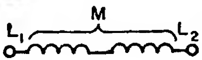	$j\omega\,(L_1 + L_2 \pm 2M)$	$\omega(L_1 + L_2 \pm 2M)$	$+\frac{\pi}{2}$	$-j\frac{1}{\omega\,(L_1 + L_2 \pm 2M)}$
	$-j\frac{1}{\omega}\left(\frac{1}{C_1} + \frac{1}{C_2}\right)$	$\frac{1}{\omega}\left(\frac{1}{C_1} + \frac{1}{C_2}\right)$	$-\frac{\pi}{2}$	$j\omega\frac{C_1 C_2}{C_1 + C_2}$
	$R + j\omega L$	$[R^2 + \omega^2 L^2]^{\frac{1}{2}}$	$\tan^{-1}\frac{\omega L}{R}$	$\frac{R - j\omega L}{R^2 + \omega^2 L^2}$
	$R - j\frac{1}{\omega C}$	$\frac{1}{\omega C}[1 + \omega^2 C^2 R^2]^{\frac{1}{2}}$	$-\tan^{-1}\frac{1}{\omega CR}$	$\frac{R + j\frac{1}{\omega C}}{R^2 + \frac{1}{\omega^2 C^2}}$
	$j\left(\omega L - \frac{1}{\omega C}\right)$	$\left(\omega L - \frac{1}{\omega C}\right)$	$\pm\frac{\pi}{2}$	$j\frac{\omega C}{1 - \omega^2 LC}$
	$R + j\left(\omega L - \frac{1}{\omega C}\right)$	$\left[R^2 + \left(\omega L - \frac{1}{\omega C}\right)^2\right]^{\frac{1}{2}}$	$\tan^{-1}\frac{\left(\omega L - \frac{1}{\omega C}\right)}{R}$	$\frac{R - j\left(\omega L - \frac{1}{\omega C}\right)}{R^2 + \left(\omega L - \frac{1}{\omega C}\right)^2}$

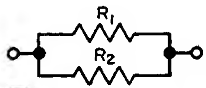	$\frac{R_1 R_2}{R_1 + R_2}$	$\frac{R_1 R_2}{R_1 + R_2}$	0	$\left(\frac{1}{R_1} + \frac{1}{R_2}\right)$
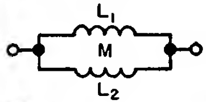	$j\omega\left[\frac{L_1 L_2 - M^2}{L_1 + L_2 \mp 2M}\right]$	$\omega\left[\frac{L_1 L_2 - M^2}{L_1 + L_2 \mp 2M}\right]$	$+\frac{\pi}{2}$	$-j\frac{1}{\omega}\left[\frac{L_1 + L_2 \mp 2M}{L_1 L_2 - M^2}\right]$
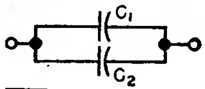	$-j\frac{1}{\omega\ (C_1 + C_2)}$	$\frac{1}{\omega\ (C_1 + C_2)}$	$-\frac{\pi}{2}$	$j\omega(C_1 + C_2)$
	$\omega LR\left[\frac{\omega L + jR}{R^2 + \omega^2 L^2}\right]$	$\frac{\omega LR}{[R^2 + \omega^2 L^2]^{\frac{1}{2}}}$	$\tan^{-1}\frac{R}{\omega L}$	$\frac{1}{R} - j\frac{1}{\omega L}$
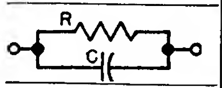	$\frac{R(1 - j\omega CR)}{1 + \omega^2 C^2 R^2}$	$\frac{R}{[1 + \omega^2 C^2 R^2]^{\frac{1}{2}}}$	$-\tan^{-1}\omega CR$	$\frac{1}{R} + j\omega C$
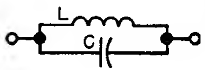	$j\frac{\omega L}{1 - \omega^2 LC}$	$\frac{\omega L}{1 - \omega^2 LC}$	$\pm\frac{\pi}{2}$	$j\left(\omega C - \frac{1}{\omega L}\right)$
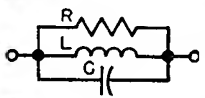	$\frac{\frac{1}{R} - j\left(\omega C - \frac{1}{\omega L}\right)}{\left(\frac{1}{R}\right)^2 + \left(\omega C - \frac{1}{\omega L}\right)^2}$	$\frac{1}{\left[\left(\frac{1}{R}\right)^2 + \left(\omega C - \frac{1}{\omega L}\right)^2\right]^{\frac{1}{2}}}$	$\tan^{-1} R\left(\frac{1}{\omega L} - \omega C\right)$	$\frac{1}{R} + j\left(\omega C - \frac{1}{\omega L}\right)$
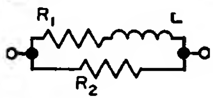	$R_2\frac{R_1(R_1 + R_2) + \omega^2 L^2 + j\omega LR_2}{(R_1 + R_2)^2 + \omega^2 L^2}$	$R_2\left[\frac{R_1^2 + \omega^2 L^2}{(R_1 + R_2)^2 + \omega^2 L^2}\right]^{\frac{1}{2}}$	$\tan^{-1}\frac{\omega LR_2}{R_1\ (R_1 + R_2) + \omega^2 L^2}$	$\frac{R_1(R_1 + R_2) + \omega^2 L^2 - j\omega LR_2}{R_2(R_1^2 + \omega^2 L^2)}$

Impedance formulas *continued*

impedance $Z = R + jX$ ohms

phase angle $\phi = \tan^{-1}\dfrac{X}{R}$

magnitude $|Z| = [R^2 + X^2]^{\frac{1}{2}}$ ohms

admittance $Y = \dfrac{1}{Z}$ mhos

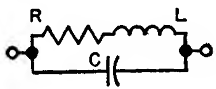	impedance Z	$\dfrac{R + j\omega[L(1 - \omega^2LC) - CR^2]}{(1 - \omega^2LC)^2 + \omega^2C^2R^2}$
	magnitude $\|Z\|$	$\left[\dfrac{R^2 + \omega^2L^2}{(1 - \omega^2LC)^2 + \omega^2C^2R^2}\right]^{\frac{1}{2}}$
	phase angle ϕ	$\tan^{-1}\dfrac{\omega[L(1 - \omega^2LC) - CR^2]}{R}$
	admittance Y	$\dfrac{R - j\omega[L(1 - \omega^2LC) - CR^2]}{R^2 + \omega^2L^2}$
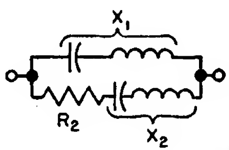	impedance Z	$X_1\dfrac{X_1 R_2 + j[R_2^2 + X_2(X_1 + X_2)]}{R_2^2 + (X_1 + X_2)^2}$
	magnitude $\|Z\|$	$X_1\left[\dfrac{R_2^2 + X_2^2}{R_2^2 + (X_1 + X_2)^2}\right]^{\frac{1}{2}}$
	phase angle ϕ	$\tan^{-1}\dfrac{R_2^2 + X_2(X_1 + X_2)}{X_1R_2}$
	admittance Y	$\dfrac{R_2X_1 - j(R_2^2 + X_2^2 + X_1X_2)}{X_1(R_2^2 + X_2^2)}$

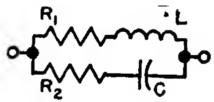	**Impedance Z**	$\dfrac{R_1R_2(R_1+R_2)+\omega^2L^2R_2+\dfrac{R_1}{\omega^2C^2}}{(R_1+R_2)^2+\left(\omega L-\dfrac{1}{\omega C}\right)^2}+j\dfrac{\omega LR_2^2-\dfrac{R_1^2}{\omega C}-\dfrac{L}{C}\left(\omega L-\dfrac{1}{\omega C}\right)}{(R_1+R_2)^2+\left(\omega L-\dfrac{1}{\omega C}\right)^2}$ **Note:** When $R_1=R_2=\sqrt{L/C}$, then $Z=R_1=R_2$, a pure resistance at any frequency where the given conditions hold. Compare Case 3a, p. 156.
	magnitude $\lvert Z\rvert$	$\left[\dfrac{(R_1^2+\omega^2L^2)\left(R_2^2+\dfrac{1}{\omega^2C^2}\right)}{(R_1+R_2)^2+\left(\omega L-\dfrac{1}{\omega C}\right)^2}\right]^{\frac{1}{2}}$
	phase angle ϕ	$\tan^{-1}\left[\dfrac{\omega LR_2^2-\dfrac{R_1^2}{\omega C}-\dfrac{L}{C}\left(\omega L-\dfrac{1}{\omega C}\right)}{R_1R_2(R_1+R_2)+\omega^2L^2R_2+\dfrac{R_1}{\omega^2C^2}}\right]$
	admittance Y	$\dfrac{R_1+\omega^2C^2R_1R_2(R_1+R_2)+\omega^4L^2C^2R_2}{(R_1^2+\omega^2L^2)(1+\omega^2C^2R_2^2)}+j\omega\left[\dfrac{CR_1^2-L+\omega^2LC(L-CR_2^2)}{(R_1^2+\omega^2L^2)(1+\omega^2C^2R_2^2)}\right]$
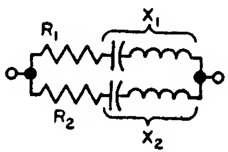	**Impedance Z**	$\dfrac{(R_1R_2-X_1X_2)+j(R_1X_2+R_2X_1)}{(R_1+R_2)+j(X_1+X_2)}$
	magnitude $\lvert Z\rvert$	$\left[\dfrac{(R_1^2+X_1^2)(R_2^2+X_2^2)}{(R_1+R_2)^2+(X_1+X_2)^2}\right]^{\frac{1}{2}}$
	phase angle ϕ	$\tan^{-1}\dfrac{X_1}{R_1}+\tan^{-1}\dfrac{X_2}{R_2}-\tan^{-1}\dfrac{X_1+X_2}{R_1+R_2}$
	admittance Y	$\dfrac{1}{R_1+jX_1}+\dfrac{1}{R_2+jX_2}$

Skin effect

Symbols

A = correction coefficient

D = diameter of conductor in inches

f = frequency in cycles/second

R_{ac} = resistance at frequency f

R_{dc} = direct-current resistance

R_{sq} = resistance per square

T = thickness of tubular conductor in inches

T_1 = depth of penetration of current

δ = skin depth

λ = free-space wavelength in meters

μ_r = relative permeability of conductor material ($\mu_r = 1$ for copper and other nonmagnetic materials)

ρ = resistivity of conductor material at any temperature

ρ_c = resistivity of copper at 20 degrees centigrade
= 1.724 microhm-centimeter

Skin depth

The skin depth is that distance below the surface of a conductor where the current density has diminished to $1/e$ of its value at the surface. The thickness of the conductor is assumed to be several (perhaps at least three) times the skin depth. Imagine the conductor replaced by a cylindrical shell of the same surface shape but of thickness equal to the skin depth; with uniform current density equal to that which exists at the surface of the actual conductor. Then the total current in the shell and its resistance are equal to the corresponding values in the actual conductor.

The skin depth and the resistance per square (of any size), in meter–kilogram–second (rationalized) units, are

$$\delta = (\lambda/\pi\sigma\mu c)^{1/2} \text{ meter}$$

$$R_{sq} = 1/\delta\sigma \text{ ohm}$$

where

c = velocity of light in vacuo = 2.998×10^8 meters/second

$\mu = 4\pi \times 10^{-7} \mu_r$ henry/meter

$1/\sigma = 1.724 \times 10^{-8} \rho/\rho_c$ ohm-meter

Skin effect *continued*

For numerical computations:

$$\delta = (3.82 \times 10^{-4}\ \lambda^{1/2})\ k_1 = (6.61/f^{1/2})k_1 \text{ centimeter}$$

$$\delta = (1.50 \times 10^{-4}\ \lambda^{1/2})\ k_1 = (2.60/f^{1/2})k_1 \text{ inch}$$

$$\delta_m = (2.60/f_{mc}{}^{1/2})\ k_1 \text{ mils}$$

$$R_{sq} = (4.52 \times 10^{-3}/\lambda^{1/2})\ k_2 = (2.61 \times 10^{-7}\ f^{1/2})\ k_2 \text{ ohm}$$

where

$$k_1 = [(1/\mu_r)\ \rho/\rho_c]^{1/2}$$

$$k_2 = (\mu_r\rho/\rho_c)^{1/2}$$

$k_1, k_2 =$ unity for copper

Example: What is the resistance/foot of a cylindrical copper conductor of diameter D inches?

$$R = \frac{12}{\pi D} R_{sq} = \frac{12}{\pi D} \times 2.61 \times 10^{-7}\ (f)^{1/2}$$

$$= 0.996 \times 10^{-6}\ (f)^{1/2}/D \text{ ohm/foot}$$

If

$$D = 1.00 \text{ inch}$$

$$f = 100 \times 10^6 \text{ cycles/second,}$$

$$R = 0.996 \times 10^{-6} \times 10^4 \approx 1 \times 10^{-2} \text{ ohm/foot.}$$

General considerations

Fig. 7 shows the relationship of R_{ac}/R_{dc} versus $D\sqrt{f}$ for copper, or versus $D\sqrt{f}\ \sqrt{\mu_r\rho_c/\rho}$ for any conductor material, for an isolated straight solid conductor of circular cross section. Negligible error in the formulas for R_{ac} results when the conductor is spaced at least $10D$ from adjacent conductors. When the spacing between axes of parallel conductors carrying the same current is $4D$, the resistance R_{ac} is increased about 3 percent, when the depth of penetration is small. The formulas are accurate for concentric lines due to their circular symmetry.

For values of $D\sqrt{f}\ \sqrt{\mu_r\rho_c/\rho}$ greater than 40,

$$\frac{R_{ac}}{R_{dc}} = 0.0960\ D\sqrt{f}\ \sqrt{\mu_r\rho_c/\rho} + 0.26 \qquad (1)$$

Skin effect *continued*

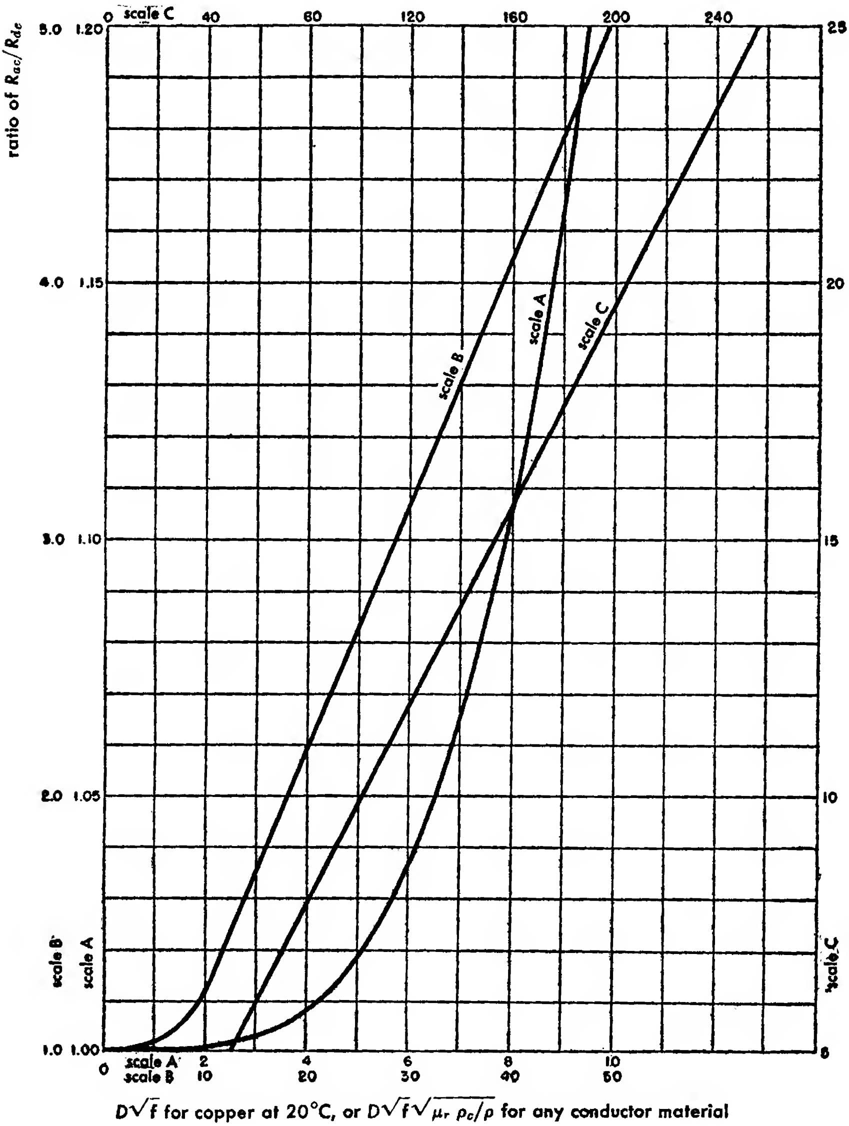

Fig. 7—Resistance ratio for isolated straight solid conductors of circular cross section.

Skin effect *continued*

The high-frequency resistance of an isolated straight conductor: either solid or tubular for $T < D/8$ or $T_1 < D/8$; is given in equation (2). If the current flow is along the inside surface of a tubular conductor, D is the inside diameter.

$$R_{ac} = A\frac{\sqrt{f}}{D}\sqrt{\mu_r\frac{\rho}{\rho_c}} \times 10^{-6} \text{ ohm/foot} \tag{2}$$

The values of the correction coefficient A for solid conductors and for tubular conductors are shown in Fig. 8.

Fig. 8—Skin-effect correction coefficient *A* for solid and tubular conductors.

solid conductors

$D\sqrt{f}\sqrt{\mu_r\frac{\rho_c}{\rho}}$	A
> 370	1.000
220	1.005
160	1.010
98	1.02
48	1.05
26	1.10
13	1.20
9.6	1.30
5.3	2.00
< 3.0	$R_{ac} \approx R_{dc}$

$$R_{dc} = \frac{10.37}{D^2}\frac{\rho}{\rho_c} \times 10^{-6} \text{ ohm/foot}$$

tubular conductors

$T\sqrt{f}\sqrt{\mu_r\frac{\rho_c}{\rho}}$	A	R_{ac}/R_{dc}
$= B$ where $B > 3.5$	1.00	0.384 B
3.5	1.00	1.35
3.15	1.01	1.23
2.85	1.05	1.15
2.60	1.10	1.10
2.29	1.20	1.06
2.08	1.30	1.04
1.77	1.50	1.02
1.31	2.00	1.00
$= B$ where $B < 1.3$	$\frac{2.60}{B}$	1.00

The value of $T\sqrt{f}\sqrt{\mu_r\rho_c/\rho}$ that just makes $A = 1$ indicates the penetration of the currents below the surface of the conductor. Thus, approximately,

$$T_1 = \frac{3.5}{\sqrt{f}}\sqrt{\frac{\rho}{\mu_r\rho_c}} \text{ inches.} \tag{3}$$

When $T_1 < D/8$ the value of R_{ac} as given by equation (2) (but not the value of R_{ac}/R_{dc} in Fig. 8, "tubular conductors") is correct for any value $T \geqslant T_1$.

Under the limitation that the radius of curvature of all parts of the cross section is appreciably greater than T_1, equations (2) and (3) hold for isolated

Skin effect *continued*

straight conductors of any shape. In this case the term D = (perimeter of cross section)/π.

Examples

a. At 100 megacycles, a copper conductor has a depth of penetration $T_1 = 0.00035$ inch.

b. A steel shield with 0.005-inch copper plate, which is practically equivalent in R_{ac} to an isolated copper conductor 0.005-inch thick, has a value of $A = 1.23$ at 200 kilocycles. This 23-percent increase in resistance over that of a thick copper sheet is satisfactorily low as regards its effect on the losses of the components within the shield. By comparison, a thick aluminum sheet has a resistance $\sqrt{\rho/\rho_c} = 1.28$ times that of copper.

Network theorems

Reciprocity theorem

If an emf of any character whatsoever located at one point in a linear network produces a current at any other point in the network, the same emf acting at the second point will produce the same current at the first point.

Corollary: If a given current flowing at one point of a linear network produces a certain open-circuit voltage at a second point of the network, the same current flowing at the second point will produce a like open-circuit voltage at the first point.

Thévenin's theorem

If an impedance Z is connected between two points of a linear network, the resulting steady-state current I through this impedance is the ratio of the potential difference V between the two points prior to the connection of Z, and the sum of the values of (1) the connected impedance Z, and (2) the impedance Z_1 of the network measured between the two points, when all generators in the network are replaced by their internal impedances:

$$I = \frac{V}{Z + Z_1}$$

Corollary: When the admittance of a linear network is Y_{12} measured be-

Network theorems *continued*

tween two points with all generators in the network replaced by their internal impedances, and the current which would flow between the points if they were short-circuited is I_{sc}, the voltage between the points is $V_{12} = I_{sc}/Y_{12}$.

Principle of superposition

The current that flows at any point in a network composed of constant resistances, inductances, and capacitances, or the potential difference that exists between any two points in such a network, due to the simultaneous action of a number of emf's distributed in any manner throughout the network, is the sum of the component currents at the first point, or the potential differences between the two points, that would be caused by the individual emf's acting alone. (Applicable to emf's of any character.)

In the application of this theorem, it is to be noted that for any impedance element Z through which flows a current I, there may be substituted a virtual source of voltage of value $-ZI$.

Formulas for simple R, L, and C networks*

1. Self-inductance of circular ring of round wire at radio frequencies, for nonmagnetic materials

$$L = \frac{a}{100}\left[7.353 \log_{10} \frac{16a}{d} - 6.386\right] \text{ microhenries}$$

where

a = mean radius of ring in inches
d = diameter of wire in inches

$$\frac{a}{d} > 2.5$$

2. Capacitance

a. For parallel-plate capacitor

$$C = 0.0885\epsilon_r \frac{(N-1)\,A}{t} = 0.225\,\epsilon_r \frac{(N-1)\,A''}{t''} \text{ micromicrofarads}$$

* Many formulas for computing capacitance, inductance, and mutual inductance will be found in Bureau of Standards Circular No. C74, obtainable from the Superintendent of Documents, Government Printing Office, Washington 25, D.C.

Formulas for simple R, L, and C networks *continued*

where

A = area of one side of one plate in square centimeters
A'' = area in square inches
N = number of plates
t = thickness of dielectric in centimeters
t'' = thickness in inches
ϵ_r = dielectric constant relative to air

This formula neglects "fringing" at the edges of the plates.

b. For coaxial cylindrical capacitor. Per unit axial length,

$$C = \frac{2\pi\epsilon_r\epsilon_v}{\log_e (b/a)}$$

$$= \frac{5 \times 10^6\ \epsilon_r}{c^2 \log_e (b/a)} \text{ farad/meter}$$

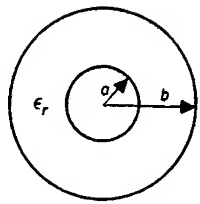

where

c = velocity of light in vacuo, meters per second (see pp. 34–35)

ϵ_r = dielectric constant relative to air

ϵ_v = permittivity of free space in farad/meter (see p. 35)

$$C = \frac{0.2416\ \epsilon_r}{\log_{10} (b/a)} \text{ micromicrofarad/centimeter}$$

$$= \frac{0.614\ \epsilon_r}{\log_{10} (b/a)} \text{ micromicrofarad/inch}$$

$$= \frac{7.36\ \epsilon_r}{\log_{10} (b/a)} \text{ micromicrofarad/foot}$$

When $1.0 < (b/a) < 1.4$, then with accuracy of one percent or better,

$$C = 8.50\ \epsilon_r \frac{(b/a) + 1}{(b/a) - 1} \text{ micromicrofarad/foot}$$

3. Reactance of an inductor

$X = 2\pi fL$ ohms

Formulas for simple R, L, and C networks *continued*

where

f = frequency in cycles/second
L = inductance in henries

or f in kilocycles and L in millihenries; or f in megacycles and L in microhenries.

At 159.2 megacycles, 1.00 microhenry has
$X = 1000$ ohms

At 60 cycles, 1.00 henry has
$X = 377.0$ ohms

4. Reactance of a capacitor

$$X = -\frac{1}{2\pi f C} \text{ ohms}$$

where

f = frequency in cycles/second
C = capacitance in farads

This may be written $X = -\dfrac{159.2}{fC}$ ohms

where

f = frequency in kilocycles/second
C = capacitance in microfarads
or f in megacycles and C in millimicrofarads ($0.001\mu f$).

At 159.2 megacycles, 1.00 micromicrofarad has
$X = -1000$ ohms

At 60 cycles, 1.00 microfarad has
$X = -2653$ ohms

5. Resonant frequency of a series-tuned circuit

$$f = \frac{1}{2\pi\sqrt{LC}} \text{ cycles/second}$$

where

L = inductance in henries
C = capacitance in farads

Formulas for simple R, L, and C networks *continued*

This may be written $LC = \dfrac{25{,}330}{f^2}$

f = frequency in kilocycles
L = inductance in millihenries
C = capacitance in millimicrofarads ($0.001\mu f$)
or f in megacycles, L in microhenries, and C in micromicrofarads;
or f in cycles, L in henries, and C in microfarads.

At 60 cycles
$LC = 7.036$ henries $\times$ microfarads

6. Dynamic resistance of a parallel-tuned circuit at resonance

$$r = \frac{X^2}{R} = \frac{L}{CR} \text{ ohms}$$

where

$X = \omega L = 1/\omega C$
$R = r_1 + r_2$
= resistance in ohms
L = inductance in henries
C = capacitance in farads

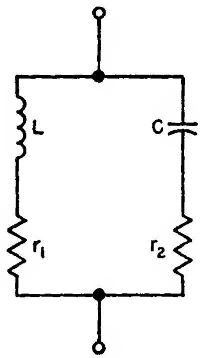

The formula is accurate for engineering purposes provided $X/R > 10$.

7. Parallel impedances

If Z_1 and Z_2 are the two impedances that are connected in parallel, then the resultant impedance is

$$Z = \frac{Z_1 Z_2}{Z_1 + Z_2}$$

Refer also to page 127.

Given one impedance Z_1 and the desired resultant impedance Z, the other impedance is

$$Z_2 = \frac{Z Z_1}{Z_1 - Z}$$

Formulas for simple R, L, and C networks *continued*

8. Input impedance of a 4-terminal network*

$Z_{11} = R_{11} + jX_{11}$

is the impedance of the first circuit, measured at terminals 1 — 1 with terminals 2 — 2 open-circuited.

$Z_{22} = R_{22} + jX_{22}$

is the impedance of the second circuit, measured at terminals 2 — 2 with load Z_2 removed and terminals 1 — 1 open-circuited.

$Z_{12} = R_{12} + jX_{12}$

is the transfer impedance between the two pairs of terminals, i.e., the open-circuit voltage appearing at either pair when unit current flows at the other pair.

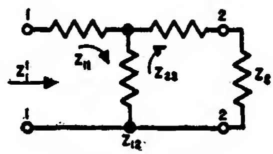

equivalent circuit

Then the impedance looking into terminals 1 — 1 with load Z_2 across terminals 2 — 2 is

$$Z_1' = R_1' + jX_1' = Z_{11} - \frac{Z^2_{12}}{Z_{22} + Z_2} = R_{11} + jX_{11} - \frac{R^2_{12} - X^2_{12} + 2jR_{12}X_{12}}{R_{22} + R_2 + j(X_{22} + X_2)}$$

When

$R_{12} = 0$

$$Z_1' = R_1' + jX_1' = Z_{11} + \frac{X^2_{12}}{Z_{22} + Z_2}$$

Example: A transformer with tuned secondary and negligible primary resistance.

$Z_{11} = j\omega L_1$

$Z_{22} + Z_2 = R_2$ since $X_{22} + X_2 = 0$

$Z_{12} = j\omega M$

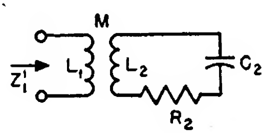

Then $Z_1' = j\omega L_1 + \dfrac{\omega^2 M^2}{R_2}$

* **Scope and limitations:** The formulas for 4-terminal networks, given in paragraphs 8 to 12 inclusive, are applicable to any such network composed of linear passive elements. The elements may be either lumped or distributed, or a combination of both kinds.

Formulas for simple R, L, and C networks *continued*

9. Input admittance of a 4-terminal network*

Y_{11} = admittance measured at terminals 1 — 1 with terminals 2 —2 short-circuited.

Y_{22} = admittance measured at terminals 2 — 2 with load Y_2 disconnected, and terminals 1 — 1 short-circuited.

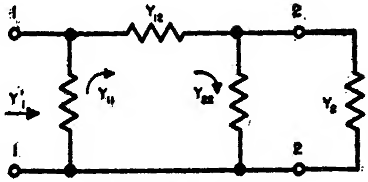

equivalent circuit

Y_{12} = transfer admittance, i.e., the short-circuit current that would flow at one pair of terminals when unit voltage is impressed across the other pair.

Then the admittance looking into terminals 1 — 1 with load Y_2 connected across 2 — 2 is

$$Y_1' = G_1' + jB_1' = Y_{11} - \frac{Y^2_{12}}{Y_{22} + Y_2}$$

10. 4-terminal network with loads equal to image impedances*

When Z_1 and Z_2 are such that $Z' = Z_1$ and $Z'' = Z_2$ they are called the *image impedances*. Let the input impedance measured at terminals 1 — 1 with terminals 2 — 2 open-circuited be Z'_{oc} and with 2 — 2 short-circuted be Z'_{sc}. Similarly Z''_{oc} and Z''_{sc} measured at terminals 2 — 2. Then

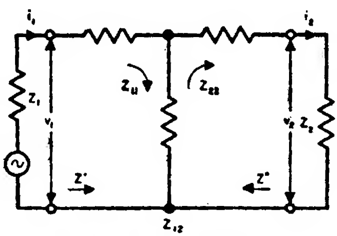

equivalent circuit

$$Z' = [Z'_{oc}Z'_{sc}]^{1/2} = \left[Z_{11}\left(Z_{11} - \frac{Z^2_{12}}{Z_{22}}\right)\right]^{1/2} = \left[Y_{11}\left(Y_{11} - \frac{Y^2_{12}}{Y_{22}}\right)\right]^{-1/2} = \left(\frac{AB}{CD}\right)^{1/2}$$

$$Z'' = [Z''_{oc}Z''_{sc}]^{1/2} = \left[Z_{22}\left(Z_{22} - \frac{Z^2_{12}}{Z_{11}}\right)\right]^{1/2} = \left[Y_{22}\left(Y_{22} - \frac{Y^2_{12}}{Y_{11}}\right)\right]^{-1/2} = \left(\frac{BD}{AC}\right)^{1/2}$$

$$\tanh\,(\alpha + j\beta) = \pm\left[\frac{Z'_{sc}}{Z'_{oc}}\right]^{1/2} = \pm\left[\frac{Z''_{sc}}{Z''_{oc}}\right]^{1/2} = \pm\left[1 - \frac{Z^2_{12}}{Z_{11}Z_{22}}\right]^{1/2}$$

$$= \pm\left[1 - \frac{Y^2_{12}}{Y_{11}Y_{22}}\right]^{1/2} = \pm\left(\frac{BC}{AD}\right)^{1/2}$$

* See footnote on p. 137.

Formulas for simple R, L, and C networks *continued*

The quantities Z_{11}, Z_{22}, and Z_{12} are defined in paragraph 8, above, while Y_{11}, Y_{22}, and Y_{12} are defined in paragraph 9.

$(\alpha + j\beta)$ is called the *image transfer constant,* defined by

$$\left(\frac{\text{complex volt-amperes into load from 2–2}}{\text{complex volt-amperes into network at 1–1}}\right) = \frac{v_2 i_2}{v_1 i_1} = \frac{v_2^2 Z_1}{v_1^2 Z_2} = \frac{i_2^2 Z_2}{i_1^2 Z_1}$$

$$= \epsilon^{-2(\alpha+j\beta)} = \epsilon^{-2\alpha}\underline{/-2\beta}$$

when the load is equal to the image impedance. The quantities α and β are the same irrespective of the direction in which the network is working.

When Z_1 and Z_2 have the same phase angle, α is the attenuation in nepers and β is the angle of lag of i_2 behind i_1.

11. Currents in a 4-terminal network*

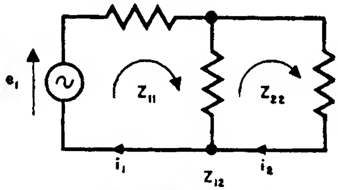

equivalent circuit

$$i_1 = \frac{e_1}{Z_1'}$$

$$= e_1 \frac{Z_{22}}{Z_{11}Z_{22} - Z^2_{12}}$$

$$= e_1 \frac{R_{22} + jX_{22}}{(R_{11}R_{22} - X_{11}X_{22} - R^2_{12} + X^2_{12}) + j(R_{11}X_{22} + R_{22}X_{11} - 2R_{12}X_{12})}$$

$$i_2 = e_1 \frac{Z_{12}}{Z_{11}Z_{22} - Z^2_{12}}$$

12. Voltages in a 4-terminal network*

Let

i_{1sc} = current that would flow between terminals 1–1 when they are short-circuited.

Y_{11} = admittance measured across terminals 1 — 1 with generator replaced by its internal impedance, and with terminals 2 — 2 short-circuited.

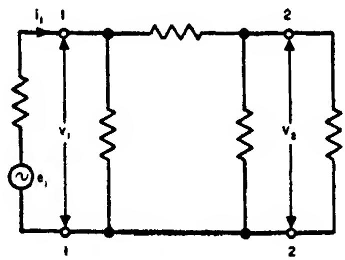

equivalent circuit

* See footnote on p. 137.

Formulas for simple R, L, and C networks *continued*

Y_{22} = admittance measured across terminals 2 — 2 with load connected and terminals 1 — 1 short-circuited.

Y_{12} = transfer admittance between terminals 1 — 1 and 2 — 2 (defined in paragraph 9 above).

Then the voltage across terminals 1 — 1, which are on the end of the network nearest the generator, is

$$v_1 = \frac{i_{1sc} Y_{22}}{Y_{11} Y_{22} - Y^2_{12}}$$

The voltage across terminals 2 — 2, which are on the load end of the network is

$$v_2 = \frac{i_{1sc} Y_{12}}{Y_{11} Y_{22} - Y^2_{12}}$$

13. Power transfer between two impedances connected directly

Let $Z_1 = R_1 + jX_1$ be the impedance of the source, and $Z_2 = R_2 + jX_2$ be the impedance of the load.

The maximum power transfer occurs when

$R_2 = R_1$ and $X_2 = -X_1$

$$\frac{P}{P_m} = \frac{4R_1R_2}{(R_1 + R_2)^2 + (X_1 + X_2)^2}$$

P = power delivered to the load when the impedances are connected directly.

P_m = power that would be delivered to the load were the two impedances connected through a perfect impedance-matching network.

14. Power transfer between two meshes coupled reactively

In the general case, X_{11} and X_{22} are not equal to zero and X_{12} may be any reactive coupling. When only one of the quantities X_{11}, X_{22}, and X_{12} can be varied, the best power transfer under the circumstances is given by:

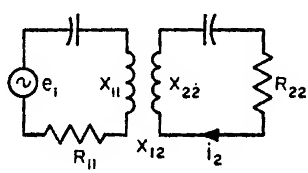

Formulas for simple R, L, and C networks *continued*

For X_{22} variable

$$X_{22} = \frac{X^2_{12}X_{11}}{R^2_{11} + X^2_{11}} \quad \text{(zero reactance looking into load circuit)}$$

For X_{11} variable

$$X_{11} = \frac{X^2_{12}X_{22}}{R^2_{22} + X^2_{22}} \quad \text{(zero reactance looking into source circuit)}$$

For X_{12} variable

$$X^2_{12} = \sqrt{(R^2_{11} + X^2_{11})\ (R^2_{22} + X^2_{22})}$$

When two of the three quantities can be varied, a perfect impedance match is attained and maximum power is transferred when

$$X^2_{12} = \sqrt{(R^2_{11} + X^2_{11})\ (R^2_{22} + X^2_{22})}$$

and

$$\frac{X_{11}}{R_{11}} = \frac{X_{22}}{R_{22}} \quad \text{(both circuits of same Q or phase angle)}$$

For perfect impedance match the current is

$$i_2 = \frac{e_1}{2\sqrt{R_{11}R_{22}}} \angle \tan^{-1}\frac{R_{11}}{X_{11}}$$

In the most common case, the circuits are tuned to resonance $X_{11} = 0$ and $X_{22} = 0$. Then $X^2_{12} = R_{11}R_{22}$ for perfect impedance match.

15. Optimum coupling between two circuits tuned to the same frequency

From the last result in paragraph 14, maximum power transfer (or an impedance match) is obtained for $\omega^2M^2 = R_1R_2$ where M is the mutual inductance between the circuits, and R_1 and R_2 are the resistances of the two circuits.

16. Coefficient of coupling—geometrical consideration

By definition, coefficient of coupling k is

$$k = \frac{M}{\sqrt{L_1L_2}}$$

where M = mutual inductance, and L_1 and L_2 are the inductances of the two coupled circuits.

Formulas for simple R, L, and C networks *continued*

Coefficient of coupling of two coils is a geometrical property, being a function of the proportions of the configuration of coils, including their relationship to any nearby objects that affect the field of the system. As long as these proportions remain unchanged, the coefficient of coupling is independent of the physical size of the system, and of the number of turns of either coil.

17. T$-\pi$ or Y$-\Delta$ transformation

The two networks are equivalent, as far as conditions at the terminals are concerned, provided the following equations are satisfied. Either the impedance equations or the admittance equations may be used:

$Y_1 = 1/Z_1$, $Y_c = 1/Z_c$, etc.

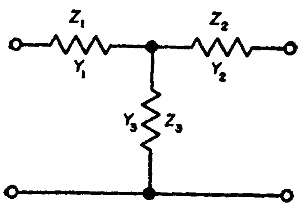

T or Y network

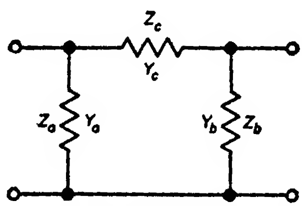

π or Δ network

Impedance equations

$$Z_c = \frac{Z_1Z_2 + Z_1Z_3 + Z_2Z_3}{Z_3}$$

$$Z_a = \frac{Z_1Z_2 + Z_1Z_3 + Z_2Z_3}{Z_2}$$

$$Z_b = \frac{Z_1Z_2 + Z_1Z_3 + Z_2Z_3}{Z_1}$$

$$Z_1 = \frac{Z_aZ_c}{Z_a + Z_b + Z_c}$$

$$Z_2 = \frac{Z_bZ_c}{Z_a + Z_b + Z_a}$$

$$Z_3 = \frac{Z_aZ_b}{Z_a + Z_b + Z_c}$$

Admittance equations

$$Y_c = \frac{Y_1Y_2}{Y_1 + Y_2 + Y_3}$$

$$Y_a = \frac{Y_1Y_3}{Y_1 + Y_2 + Y_3}$$

$$Y_b = \frac{Y_2Y_3}{Y_1 + Y_2 + Y_3}$$

$$Y_1 = \frac{Y_aY_b + Y_aY_c + Y_bY_c}{Y_b}$$

$$Y_2 = \frac{Y_aY_b + Y_aY_c + Y_bY_c}{Y_a}$$

$$Y_3 = \frac{Y_aY_b + Y_aY_c + Y_bY_c}{Y_c}$$

Formulas for simple R, L, and C networks *continued*

These relationships can be written as six equations in matrix form. Included are the transformations between the open-circuit impedances and short-circuit admittances, paragraphs 8, 9, and 19.

$$\begin{bmatrix} Z_1 & Z_2 & Z_3 \\ Z_{11} & Z_{22} & Z_{12} \end{bmatrix} = \begin{bmatrix} Y_b & Y_a & Y_c \\ Y_{bb} & Y_{aa} & Y_{ab} \end{bmatrix} \div |Y|$$

and $|Y| = 1/|Z|$

where the determinants $|Y|$ and $|Z|$ are given in the tabulations of T and π sections, paragraph 19.

18. General circuit parameters

Linear passive four-terminal network with source and load.

$$\begin{cases} V_1 = AV_2 + BI_2 \\ I_1 = CV_2 + DI_2 \end{cases}$$

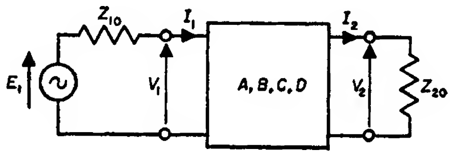

$$\begin{bmatrix} V_1 \\ I_1 \end{bmatrix} = \begin{bmatrix} A & B \\ C & D \end{bmatrix} \times \begin{bmatrix} V_2 \\ I_2 \end{bmatrix}$$

$$V_1 = E_1 - Z_{10} I_1$$

$$V_2 = Z_{20} I_2$$

$$\begin{cases} V_2 = DV_1 + B(-I_1) \\ (-I_2) = CV_1 + A(-I_1) \end{cases}$$

$$\begin{bmatrix} V_2 \\ -I_2 \end{bmatrix} = \begin{bmatrix} D & B \\ C & A \end{bmatrix} \times \begin{bmatrix} V_1 \\ -I_1 \end{bmatrix}$$

The determinant of the matrix of the general circuit parameters is equal to unity

$AD - BC = 1$

When a network is symmetrical

$A = D$

Formulas for simple R, L, and C networks *continued*

Two two-terminal-pair networks in cascade

$$\begin{bmatrix} V_1 \\ I_1 \end{bmatrix} = \begin{bmatrix} A & B \\ C & D \end{bmatrix} \times \begin{bmatrix} A' & B' \\ C' & D' \end{bmatrix} \times \begin{bmatrix} V_3 \\ I_3 \end{bmatrix}$$

The expansion of this product and other operations of matrix algebra are given in the section, "Matrix algebra", of chapter "Mathematical formulas", pp. 1090-1097.

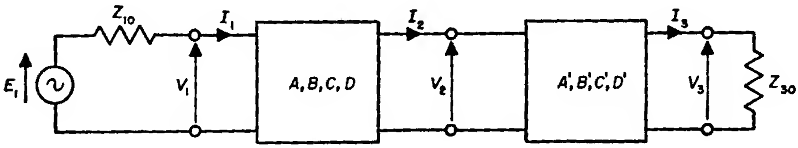

19. Tabulation of matrixes

description	diagram	matrix
Series impedance	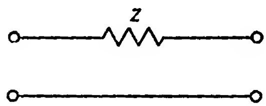	$\begin{bmatrix} A & B \\ C & D \end{bmatrix} = \begin{bmatrix} 1 & Z \\ 0 & 1 \end{bmatrix}$
Shunt admittance	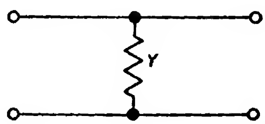	$\begin{bmatrix} 1 & 0 \\ Y & 1 \end{bmatrix}$
Ideal transformer n = turns ratio	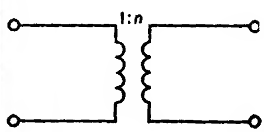	$\begin{bmatrix} 1/n & 0 \\ 0 & n \end{bmatrix}$

Formulas for simple R, L, and C networks *continued*

description	diagram	matrix
Inductively coupled elements	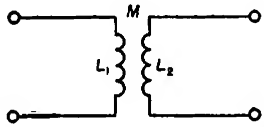	$\begin{bmatrix} L_1/M & j\omega(L_1L_2-M^2)/M \\ -j/\omega M & L_2/M \end{bmatrix}$
Symmetrical lattice or bridge section	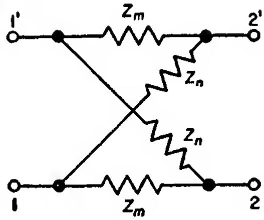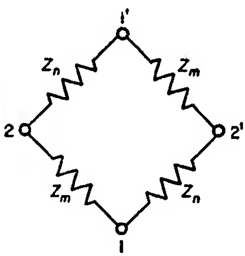	$\begin{bmatrix} \dfrac{Z_n+Z_m}{Z_n-Z_m} & \dfrac{2Z_mZ_n}{Z_n-Z_m} \\ \dfrac{2}{Z_n-Z_m} & \dfrac{Z_n+Z_m}{Z_n-Z_m} \end{bmatrix}$
T section $\begin{cases} V_1 = Z_{11}I_1 + Z_{12}(-I_2) \\ V_2 = Z_{21}I_1 + Z_{22}(-I_2) \end{cases}$ Determinant of the impedances: $\lvert Z \rvert = Z_{11}Z_{22} - Z_{12}^2$ $= Z_1Z_2 + Z_1Z_3 + Z_2Z_3$ $= (Y_1+Y_2+Y_3)/Y_1Y_2Y_3$ $= 1/\lvert Y \rvert = B/C$	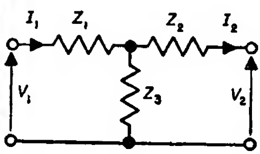$Z_{11} = Z_1 + Z_3 = A/C$ $Z_{22} = Z_2 + Z_3 = D/C$ $Z_{12} = Z_{21} = Z_3 = 1/C$	$\begin{bmatrix} A & B \\ C & D \end{bmatrix} =$ $\begin{bmatrix} (1+Z_1/Z_3) & \lvert Z\rvert/Z_3 \\ 1/Z_3 & (1+Z_2/Z_3) \end{bmatrix}$ $= \begin{bmatrix} Z_{11}/Z_{12} & \lvert Z\rvert/Z_{12} \\ 1/Z_{12} & Z_{22}/Z_{12} \end{bmatrix}$

Formulas for simple R, L, and C networks *continued*

description	diagram	matrix
π section $\begin{cases} I_1 = Y_{aa}V_1 + Y_{ab}(-V_2) \\ I_2 = Y_{ba}V_1 + Y_{bb}(-V_2) \end{cases}$ Determinant of the admittances: $\lvert Y \rvert = Y_{aa}Y_{bb} - Y_{ab}^2$ $= Y_aY_b + Y_aY_c + Y_bY_c$ $= (Z_a+Z_b+Z_c)/Z_aZ_bZ_c$ $= 1/\lvert Z \rvert = C/B$	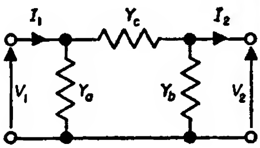 $Y_{aa} = Y_a + Y_c = D/B$ $Y_{bb} = Y_b + Y_c = A/B$ $Y_{ab} = Y_{ba} = Y_c = 1/B$	$\begin{bmatrix} A & B \\ C & D \end{bmatrix} =$ $\begin{bmatrix} (1+Y_b/Y_c) & 1/Y_c \\ \lvert Y \rvert/Y_c & (1+Y_a/Y_c) \end{bmatrix}$ $= \begin{bmatrix} Y_{bb}/Y_{ab} & 1/Y_{ab} \\ \lvert Y \rvert/Y_{ab} & Y_{aa}/Y_{ab} \end{bmatrix}$
Transmission line		See pp. 555 and 557

Example 1: Determine the *ABCD* parameters for a T section.

Method 1: Consider the section under open- or short-circuit conditions at either pair of terminals. The parameters in the equations for V_1 and I_1 at the beginning of paragraph 18 can then be found by inspection.

With output open-circuited, $I_2 = 0$ and

$$A = V_1/V_2 = (Z_1 + Z_3)/Z_3$$

$$C = I_1/V_2 = 1/Z_3$$

With input open-circuited, $I_1 = 0$ and

$$D = CV_2/(-I_2) = (Z_2 + Z_3)/Z_3$$

With input short-circuited, $V_1 = 0$ and

$$B = AV_2/(-I_2) = \frac{Z_1 + Z_3}{Z_3}\left(Z_2 + \frac{Z_1Z_3}{Z_1 + Z_3}\right)$$

$$= (Z_1Z_2 + Z_2Z_3 + Z_1Z_3)/Z_3$$

Method 2: Start with the impedance equations for V_1 and V_2 in terms of I_1 and I_2. Translate into the *ABCD* form for V_1 and I_1 in terms of V_2 and I_2.

Method 3: Combine the individual series-impedance and shunt-admittance elements by multiplication of the matrixes.

Formulas for simple R, L, and C networks *continued*

Example 2: Determine the *ABCD* parameters for a symmetrical lattice section. Refer to the diagrams of the lattice in the tabulation of matrixes. In accordance with the definitions in paragraph 8, page 137, the open-circuit input and transfer impedances are

$$Z_{11} = Z_{22} = (Z_m + Z_n)/2$$

$$Z_{12} = (Z_n - Z_m)/2$$

When these are substituted in the *ABCD* matrix for the T section, the matrix for the lattice results.

20. Elementary R-C, R-L, and L-C filters and equalizers

Simple attenuating sections of broad frequency-discriminating characteristics, as used in power supplies, grid-bias feed, etc. are shown in Figs. 9 and 10. The output load impedance is assumed to be high compared to the impedance of the shunt element of the filter. The phase angle ϕ is that of E_{out} with respect to E_{in}.

The relationships for low-pass filters are plotted in Figs. 11 and 12.

R-C Section (Figs. 10A and B)

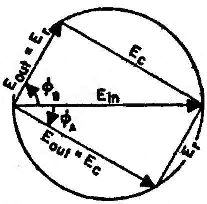

R-L Section (Figs. 10C and D)

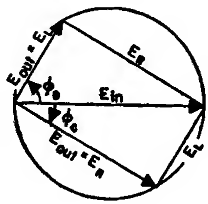

Fig. 9—Circle diagrams for *R-L* and *R-C* filter sections.

Examples of low-pass R-C filters

a. $R = 100{,}000$ ohms

$C = 0.1 \times 10^{-6}$ (0.1 μf)

Then $T = RC = 0.01$ second

At $f = 100$ cps: $E_{out}/E_{in} = 0.16-$

At $f = 30{,}000$ cps: $E_{out}/E_{in} = 0.00053$

Formulas for simple R, L, and C networks *continued*

Fig. 10—Simple filter sections containing R, L, and C. See also Fig. 9.

diagram	type	time constant or resonant freq	formula and approximation
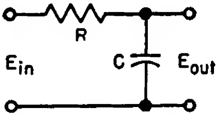	**A** low-pass R-C	$T = RC$	$\frac{E_{out}}{E_{in}} = \frac{1}{\sqrt{1+\omega^2T^2}} \approx \frac{1}{\omega T}$ $\phi_A = -\tan^{-1}(R\omega C)$
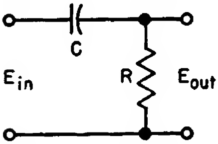	**B** high-pass R-C	$T = RC$	$\frac{E_{out}}{E_{in}} = \frac{1}{\sqrt{1+\frac{1}{\omega^2T^2}}} \approx \omega T$ $\phi_B = \tan^{-1}(1/R\omega C)$
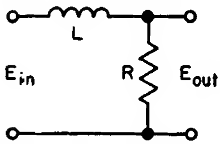	**C** low-pass R-L	$T = \frac{L}{R}$	$\frac{E_{out}}{E_{in}} = \frac{1}{\sqrt{1+\omega^2T^2}} \approx \frac{1}{\omega T}$ $\phi_C = -\tan^{-1}(\omega L/R)$
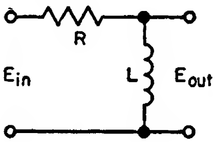	**D** high-pass R-L	$T = \frac{L}{R}$	$\frac{E_{out}}{E_{in}} = \frac{1}{\sqrt{1+\frac{1}{\omega^2T^2}}} \approx \omega T$ $\phi_D = \tan^{-1}(R/\omega L)$
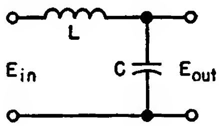	**E** low-pass L-C	$f_0 = \frac{0.1592}{\sqrt{LC}}$	$\frac{E_{out}}{E_{in}} = \frac{1}{1-\omega^2LC} = \frac{1}{1-f^2/f_0^2}$ $\approx -\frac{1}{\omega^2LC} = -\frac{f_0^2}{f^2}$ $\phi = 0$ for $f < f_0$; $\phi = \pi$ for $f > f_0$
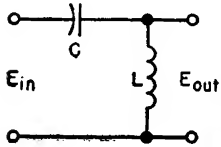	**F** high-pass L-C	$f_0 = \frac{0.1592}{\sqrt{LC}}$	$\frac{E_{out}}{E_{in}} = \frac{1}{1-1/\omega^2LC} = \frac{1}{1-f_0^2/f^2}$ $\approx -\omega^2LC = -\frac{f^2}{f_0^2}$ $\phi = 0$ for $f > f_0$; $\phi = \pi$ for $f < f_0$

R in ohms; L in henries; C in farads ($1\mu f = 10^{-6}$ farad).

T = time constant (seconds), f_0 = resonant frequency (cps), $\omega = 2\pi f$,

$2\pi = 6.28$, $1/2\pi = 0.1592$, $4\pi^2 = 39.5$, $1/4\pi^2 = 0.0253$.

Formulas for simple R, L, and C networks *continued*

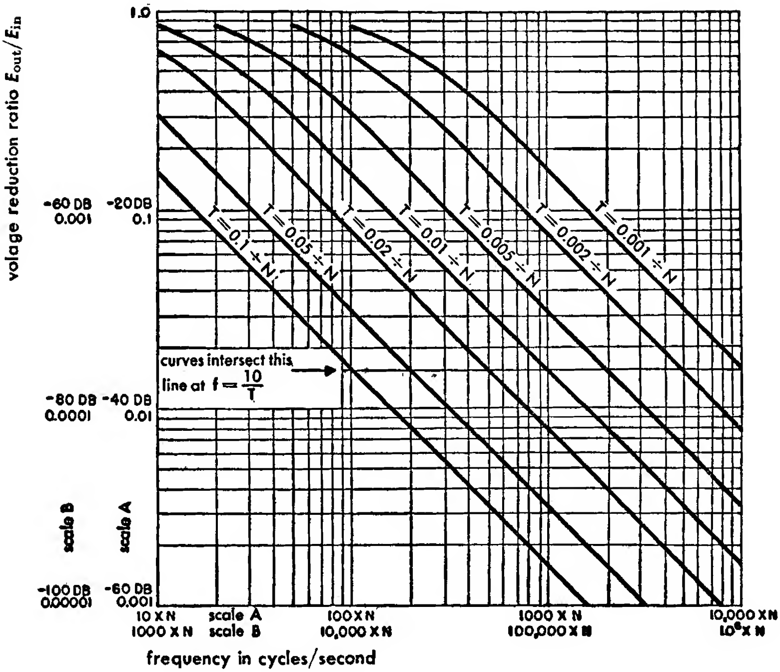

Fig. 11—Low-pass *R-C* and *R-L* filters. *N* is any convenient factor, usually taken as an integral power of 10.

b. $R = 1{,}000$ ohms

$C = 0.001 \times 10^{-6}$ farad

$T = 1 \times 10^{-6}$ second $= 0.1/N$, where $N = 10^5$

At $f = 10$ megacycles $= 100 \times N$: $E_{out}/E_{in} = 0.016-$

Example of low-pass L-C filter

At $f = 120$ cps, required $E_{out}/E_{in} = 0.03$

Then from curves: $LC = 6 \times 10^{-5}$ approximately.

Whence, for $C = 4\ \mu f$, we require $L = 15$ henries.

Formulas for simple R, L, and C networks *continued*

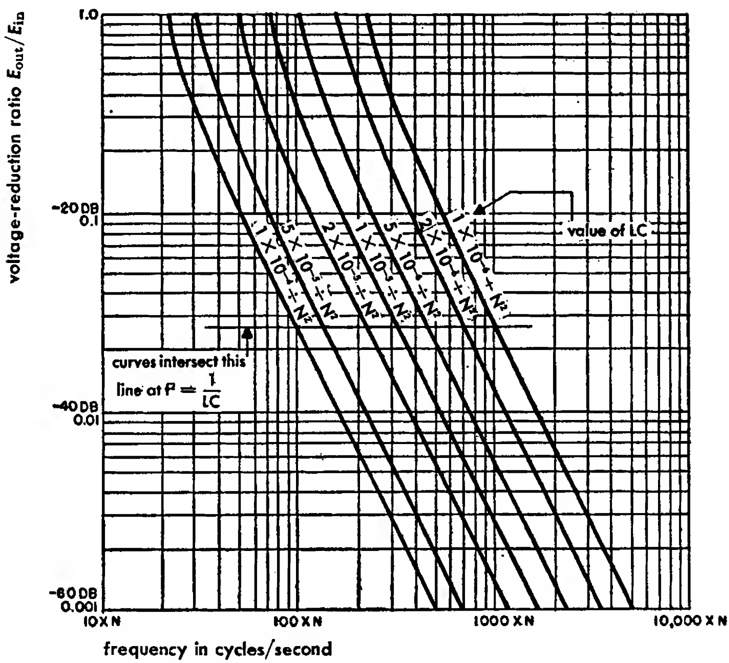

Fig. 12—Low-pass *L-C* filters. *N* is any convenient factor, usually taken as an integral power of 10.

Effective and average values of alternating current

(Similar equations apply to ac voltages)

$i = I \sin \omega t$

Average value $I_{av} = \frac{2}{\pi} I$

which is the direct current that would be obtained were the original current fully rectified, or approximately proportional to the reading of a rectifier-type meter.

Effective or root-mean-square (rms) value $I_{eff} = \frac{I}{\sqrt{2}}$

which represents the heating or power effectiveness of the current, and is proportional to the reading of a dynamometer or thermal-type meter.

Effective and average values of alternating current *continued*

When

$i = I_0 + I_1 \sin \omega_1 t + I_2 \sin \omega_2 t + \ldots .$

$I_{eff} = \sqrt{I_0^2 + \frac{1}{2}(I_1^2 + I_2^2 + \ldots .)}$

Note: The average value of a complex current is *not* equal to the sum of the average values of the components.

Power

The power at a point in an alternating-current network is

$P = (\text{real})\ \boldsymbol{V}\,\boldsymbol{I}^* = (\text{real})\ \boldsymbol{V}^*\,\boldsymbol{I}$

the first form of which is the real part of the product of the root-mean-square complex sinusoidal voltage by the conjugate of the corresponding current. This expression is useful in analytical work.

Example: Let $\boldsymbol{V} = V\underline{/\phi}$ and $\boldsymbol{I} = I\underline{/\psi}$

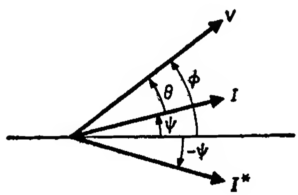

Then

$\boldsymbol{I}^* = I\underline{/-\psi}$

and

$P = (\text{real})\ V\,I\,\underline{/\phi - \psi} = V\,I\cos\theta$

Transients—elementary cases

The complete transient in a linear network is, by the principle of superposition, the sum of the individual transients due to the store of energy in each inductor and capacitor and to each external source of energy connected to the network. To this is added the steady-state condition due to each external source of energy. The transient may be computed as starting from any arbitrary time $t = 0$ when the initial conditions of the energy of the network are known.

Time constant (designated T): Of the discharge of a capacitor through a resistor is the time $t_2 - t_1$ required for the voltage or current to decay to $1/\epsilon$ of its value at time t_1. For the charge of a capacitor the same definition applies, the voltage "decaying" toward its steady-state value. The time constant of discharge or charge of the current in an inductor through a resistor follows an analogous definition.

Transients—elementary cases *continued*

Energy stored in a capacitor $= \frac{1}{2} CE^2$ joules (watt-seconds)

Energy stored in an inductor $= \frac{1}{2} LI^2$ joules (watt-seconds)

$\epsilon = 2.718$ $1/\epsilon = 0.3679$ $\log_{10}\epsilon = 0.4343$ T and t in seconds

R in ohms L in henries C in farads E in volts I in amperes

Capacitor charge and discharge

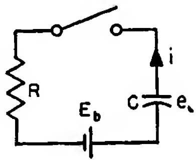

Closing of switch occurs at time $t = 0$

Initial conditions (at $t = 0$): Battery $= E_b$; $e_c = E_o$.

Steady state (at $t = \infty$): $i = 0$; $e_c = E_b$.

Transient:

$$i = \frac{E_b - E_0}{R} \epsilon^{-t/RC} = I_0 \epsilon^{-t/RC}$$

$$\log_{10}\left(\frac{i}{I_0}\right) = -\frac{0.4343}{RC} t$$

$$e_c = E_0 + \frac{1}{C}\int_0^t i dt = E_0 \epsilon^{-t/RC} + E_b (1 - \epsilon^{-t/RC})$$

Time constant: $T = RC$

Fig. 13 shows current: $i/I_0 = \epsilon^{-t/T}$

Fig. 13 shows discharge (for $E_b = 0$): $e_c/E_0 = \epsilon^{-t/T}$

Fig. 14 shows charge (for $E_0 = 0$): $e_c/E_b = 1 - \epsilon^{-t/T}$

These curves are plotted on a larger scale in Fig. 15.

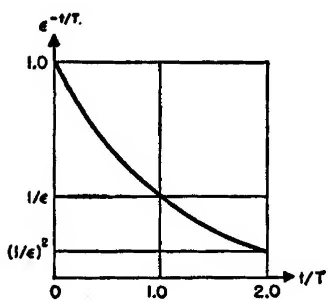

Fig. 13—Capacitor discharge.

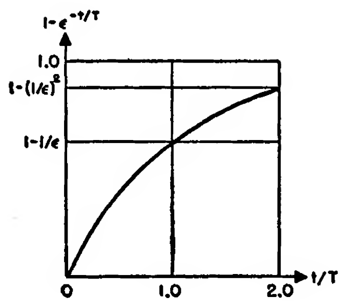

Fig. 14—Capacitor charge.

Transients—elementary cases *continued*

Two capacitors

Closing of switch occurs at time $t = 0$

Initial conditions (at $t = 0$):

$e_1 = E_1$; $e_2 = E_2$.

Steady state (at $t = \infty$):

$e_1 = E_f$; $e_2 = -E_f$; $i = 0$.

$$E_f = \frac{E_1C_1 - E_2C_2}{C_1 + C_2} \qquad C' = \frac{C_1C_2}{C_1 + C_2}$$

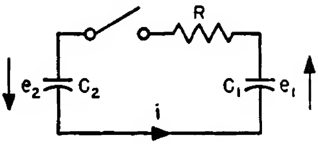

Transient:

$$i = \frac{E_1 + E_2}{R}\,\epsilon^{-t/RC'}$$

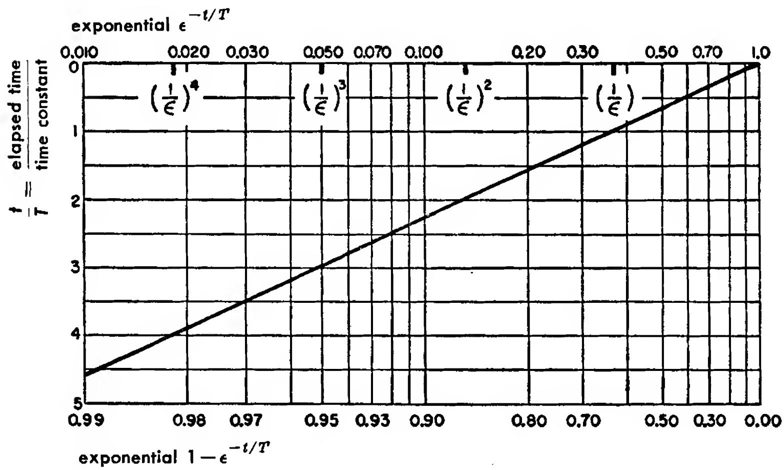

Use exponential $\epsilon^{-t/T}$ for charge or discharge of capacitor or discharge of inductor:

$$\frac{\text{(current at time } t)}{\text{(initial current)}}$$

Discharge of capacitor:

$$\frac{\text{(voltage at time } t)}{\text{(initial voltage)}}$$

Use exponential $1 - \epsilon^{-t/T}$ for charge of capacitor:

$$\frac{\text{(voltage at time } t)}{\text{(battery or final voltage)}}$$

Charge of inductor:

$$\frac{\text{(current at time } t)}{\text{(final current)}}$$

Fig. 15—Exponential functions $\epsilon^{-t/T}$ and $1-\epsilon^{-t/T}$ applied to transients in *R-C* and *L-R* circuits.

Transients—elementary cases *continued*

$$e_1 = E_f + (E_1 - E_f)\ \epsilon^{-t/RC'} = E_1 - (E_1 + E_2)\frac{C'}{C_1}(1 - \epsilon^{-t/RC'})$$

$$e_2 = -E_f + (E_2 + E_f)\ \epsilon^{-t/RC'} = E_2 - (E_1 + E_2)\frac{C'}{C_2}(1 - \epsilon^{-t/RC'})$$

Original energy $= \frac{1}{2}(C_1E_1^2 + C_2E_2^2)$ joules

Final energy $= \frac{1}{2}(C_1 + C_2)\ E_f^2$ joules

Loss of energy $= \int_0^\infty i^2 R dt = \frac{1}{2} C' (E_1 + E_2)^2$ joules

(Loss is independent of the value of R.)

Inductor charge and discharge

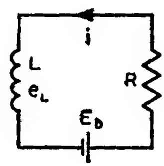

Initial conditions (at $t = 0$):
Battery $= E_b$; $i = I_0$

Steady state (at $t = \infty$): $i = I_f = E_b/R$

Transient, plus steady state:

$$i = I_f\ (1 - \epsilon^{-Rt/L}) + I_0\ \epsilon^{-Rt/L}$$

$$e_L = -L\,di/dt = -(E_b - RI_0)\epsilon^{-Rt/L}$$

Time constant: $T = L/R$

Fig. 13 shows discharge (for $E_b = 0$): $i/I_0 = \epsilon^{-t/T}$

Fig. 14 shows charge (for $I_0 = 0$): $i/I_f = (1 - \epsilon^{-t/T})$

These curves are plotted on a larger scale in Fig. 15.

Series R-L-C circuit charge and discharge

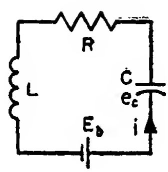

Initial conditions (at $t = 0$):
Battery $= E_b$; $e_c = E_0$; $i = I_0$
Steady state (at $t = \infty$): $i = 0$; $e_c = E_b$

Differential equation:

$$E_b - E_0 - \frac{1}{C}\int_0^t i dt - Ri - L\frac{di}{dt} = 0$$

Transients—elementary cases *continued*

when $L\frac{d^2i}{dt^2} + R\frac{di}{dt} + \frac{i}{C} = 0$

Solution of equation:

$$i = \epsilon^{-Rt/2L}\left[\frac{2(E_b - E_0) - RI_0}{R\sqrt{D}} \sinh \frac{Rt}{2L}\sqrt{D} + I_0 \cosh \frac{Rt}{2L}\sqrt{D}\right]$$

where $D = 1 - \frac{4L}{R^2C}$

Case 1: When $\frac{L}{R^2C}$ is small

$$i = \frac{1}{(1 - 2A - 2A^2)}\left\{\left[\frac{E_b - E_0}{R} - I_0\,(A + A^2)\right]\epsilon^{-\frac{t}{RC}(1+A+2A^2)} + \left[I_0(1 - A - A^2) - \frac{E_b - E_0}{R}\right]\epsilon^{-\frac{Rt}{L}(1-A-A^2)}\right\}$$

where $A = \frac{L}{R^2C}$

For practical purposes, the terms A^2 can be neglected when $A<0.1$. The terms A may be neglected when $A<0.01$.

Case 2: When $\frac{4L}{R^2C} <1$ for which $\sqrt{D}$ is real

$$i = \frac{\epsilon^{-Rt/2L}}{\sqrt{D}}\left\{\left[\frac{E_b - E_0}{R} - \frac{I_0}{2}\left(1 - \sqrt{D}\right)\right]\epsilon^{\frac{Rt}{2L}\sqrt{D}} + \left[\frac{I_0}{2}\left(1 + \sqrt{D}\right) - \frac{E_b - E_0}{R}\right]\epsilon^{-\frac{Rt}{2L}\sqrt{D}}\right\}$$

Case 3: When D is a small positive or negative quantity

$$i = \epsilon^{-Rt/2L}\left\{\frac{2(E_b - E_0)}{R}\left[\frac{Rt}{2L} + \frac{1}{6}\left(\frac{Rt}{2L}\right)^3 D\right] + I_0\left[1 - \frac{Rt}{2L} + \frac{1}{2}\left(\frac{Rt}{2L}\right)^2 D - \frac{1}{6}\left(\frac{Rt}{2L}\right)^3 D\right]\right\}$$

This formula may be used for values of D up to ± 0.25, at which values the error in the computed current i is approximately 1 percent of I_0 or of $\frac{E_b - E_0}{R}$.

Transients—elementary cases *continued*

Case 3a: When $4L/R^2C = 1$ for which $D = 0$, the formula reduces to

$$i = \epsilon^{-Rt/2L}\left[\frac{E_b - E_0}{R}\frac{Rt}{L} + I_0\left(1 - \frac{Rt}{2L}\right)\right]$$

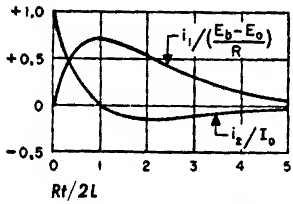

Fig. 16—Transients for $4L/R^2C = 1$.

or $i = i_1 + i_2$, plotted in Fig. 16. For practical purposes, this formula may be used when $4L/R^2C = 1 \pm 0.05$ with errors of 1 percent or less.

Case 4: When $\dfrac{4L}{R^2C} > 1$ for which $\sqrt{D}$ is imaginary

$$i = \epsilon^{-Rt/2L}\left\{\left[\frac{E_b - E_0}{\omega_0 L} - \frac{RI_0}{2\omega_0 L}\right]\sin\omega_0 t + I_0\cos\omega_0 t\right\}$$

$$= I_m\epsilon^{-Rt/2L}\sin(\omega_0 t + \psi)$$

where $\omega_0 = \sqrt{\dfrac{1}{LC} - \dfrac{R^2}{4L^2}}$

$$I_m = \frac{1}{\omega_0 L}\sqrt{\left(E_b - E_0 - \frac{RI_0}{2}\right)^2 + \omega_0^2L^2I_0^2} \qquad \psi = \tan^{-1}\frac{\omega_0 L\, I_0}{E_b - E_0 - \dfrac{RI_0}{2}}$$

The envelope of the voltage wave across the inductor is:

$$\pm\epsilon^{-Rt/2L}\frac{1}{\omega_0\sqrt{LC}}\sqrt{\left(E_b - E_0 - \frac{RI_0}{2}\right)^2 + \omega_0^2L^2I_0^2}$$

Example: Relay with transient-suppressing capacitor.

Switch closed till time $t = 0$, then opened.

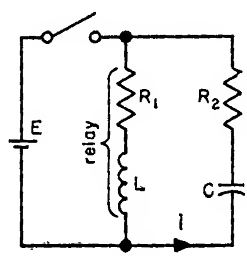

Let $L = 0.10$ henry, $R_1 = 100$ ohms,

$E = 10$ volts

Suppose we choose

$C = 10^{-6}$ farads

$R_2 = 100$ ohms

Transients—elementary cases *continued*

Then

$R = 200$ ohms
$I_0 = 0.10$ ampere
$E_0 = 10$ volts
$\omega_0 = 3 \times 10^3$
$f_0 = 480$ cps

Maximum peak voltage across L (envelope at $t = 0$) is approximately 30 volts. Time constant of decay of envelope is 0.001 second.

It is preferable that the circuit be just nonoscillating (Case 3a) and that it present a pure resistance at the switch terminals for any frequency (see note on p. 127).

$$R_2 = R_1 = R/2 = 100 \text{ ohms}$$

$$4L/R^2C = 1$$

$$C = 10^{-5} \text{ farad} = 10 \text{ microfarads}$$

At the instant of opening the switch, the voltage across the parallel circuit is $E_0 - R_2 I_0 = 0$.

Series R-L-C circuit with sinusoidal applied voltage

By the principle of superposition, the transient and steady-state conditions are the same for the actual circuit and the equivalent circuit shown in the accompanying illustrations, the closing of the switch occurring at time $t = 0$. In the equivalent circuit, the steady state is due to the source e acting continuously from time $t = -\infty$, while the transient is due to short-circuiting the source $-e$ at time $t = 0$.

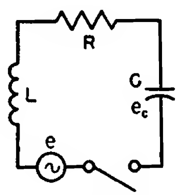

actual circuit

Source: $e = E \sin (\omega t + \alpha)$

Steady state: $i = \dfrac{e}{Z} \angle -\phi = \dfrac{E}{Z} \sin (\omega t + \alpha - \phi)$

where

$$Z = \sqrt{R^2 + \left(\omega L - \frac{1}{\omega C}\right)^2}$$

$$\tan \phi = \frac{\omega^2 LC - 1}{\omega CR}$$

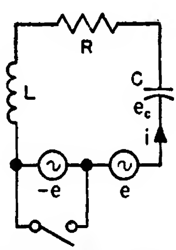

equivalent circuit

The transient is found by determining current $i = I_0$

Transients—elementary cases *continued*

and capacitor voltage $e_c = E_0$ at time $t = 0$, due to the source $-e$. These values of I_0 and E_0 are then substituted in the equations of Case 1, 2, 3, or 4, above, according to the values of R, L, and C.

At time $t = 0$, *due to the source* $-e$:

$$i = I_0 = -\frac{E}{Z} \sin (\alpha - \phi)$$

$$e_c = E_0 = \frac{E}{\omega CZ} \cos (\alpha - \phi)$$

This form of analysis may be used for any periodic applied voltage e. The steady-state current and the capacitor voltage for an applied voltage $-e$ are determined, the periodic voltage being resolved into its harmonic components for this purpose, if necessary. Then the instantaneous values $i = I_0$ and $e_c = E_0$ at the time of closing the switch are easily found, from which the transient is determined. It is evident, from this method of analysis, that the waveform of the transient need bear no relationship to that of the applied voltage, depending only on the constants of the circuit and the hypothetical initial conditions I_0 and E_0.

Transients—operational calculus and Laplace transforms

Among the various methods of operational calculus used to solve transient problems, one of the most efficient makes use of the Laplace transform.

If we have a function $v = f(t)$, then by *definition* the Laplace transform is $\mathcal{L}[f(t)] = F(p)$, where

$$F(p) = \int_0^\infty \epsilon^{-pt} f(t)\, dt \tag{4}$$

The inverse transform of $F(p)$ is $f(t)$. Most of the mathematical functions encountered in practical work fall in the class for which Laplace transforms exist. Transforms of functions are given on pages 1081 to 1083.

In the following, an abbreviated symbol such as $\mathcal{L}[i]$ is used instead of $\mathcal{L}[i(t)]$ to indicate the Laplace transform of the function $i(t)$.

The electrical (or other) system for which a solution of the differential equation is required, is considered only in the time domain $t \geqslant 0$. Any currents or voltages existing at $t = 0$, before the driving force is applied, constitute initial conditions. Driving force is assumed to be 0 when $t < 0$.

Transients—operational calculus and Laplace transforms *continued*

Example

Take the circuit of Fig. 17, in which the switch is closed at time $t = 0$. Prior to the closing of the switch, suppose the capacitor is charged; then at $t = 0$, we have $v = V_0$. It is required to find the voltage v across capacitor C as a function of time.

Writing the differential equation of the circuit in terms of voltage, and since $i = dq/dt = C(dv/dt)$, the equation is

$$e(t) = v + Ri = v + RC(dv/dt) \tag{5}$$

where $e(t) = E_b$

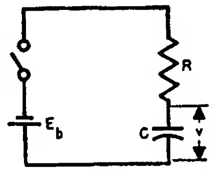

Fig. 17.

Referring to the table of transforms, the applied voltage is E_b multiplied by unit step, or $E_bS_{-1}(t)$; the transform for this is E_b/p. The transform of v is $\mathcal{L}[v]$. That of $RC(dv/dt)$ is $RC[p\mathcal{L}[v] - v(0)]$, where $v(0) = V_0$ = value of v at $t = 0$. Then the transform of (5) is

$$\frac{E_b}{p} = \mathcal{L}[v] + RC[p\mathcal{L}[v] - V_0]$$

Rearranging, and resolving into partial fractions,

$$\mathcal{L}[v] = \frac{E_b}{p(1 + RCp)} + \frac{RCV_0}{1 + RCp} = E_b\left(\frac{1}{p} - \frac{1}{p + 1/RC}\right) + \frac{V_0}{p + 1/RC} \tag{6}$$

Now we must determine the equation that would transform into (6). The inverse transform of $\mathcal{L}[v]$ is v, and those of the terms on the right-hand side are found in the table of transforms. Then, in the time domain $t \geqslant 0$,

$$v = E_b(1 - \epsilon^{-t/RC}) + V_0\,\epsilon^{-t/RC} \tag{7}$$

This solution is also well known by classical methods. However, the advantages of the Laplace-transform method become more and more apparent in reducing the labor of solution as the equations become more involved.

Circuit response related to unit impulse

Unit impulse is defined on page 1081. It has the dimensions of time^{-1}. For example, suppose a capacitor of one microfarad is suddenly connected to a battery of 100 volts, with the circuit inductance and resistance negligibly small. Then the current flow is 10^{-4} coulombs multiplied by unit impulse.

The general transformed equation of a circuit or system may be written

$$\mathcal{L}[i] = \phi(p)\,\mathcal{L}[e] + \psi(p) \tag{8}$$

Here $\mathcal{L}[i]$ is the transform of the required current (or other quantity), $\mathcal{L}[e]$ is the transform of the applied voltage or driving force $e(t)$. The transform of the initial conditions, at $t = 0$, is included in $\psi(p)$.

First considering the case when the system is initially at rest, $\psi(p) = 0$. Writing i_a for the current in this case,

$$\mathcal{L}[i_a] = \phi(p)\, \mathcal{L}[e] \tag{9}$$

Now apply unit impulse $S_0(t)$ (multiplied by one volt-second), and designate the circuit current in this case by $B(t)$ and its transform by $\mathcal{L}[B]$. By pair 13, page 1083, the transform of $S_0(t)$ is 1, so

$$\mathcal{L}[B] = \phi(p) \tag{10}$$

Equation (9) becomes, for any driving force

$$\mathcal{L}[i_a] = \mathcal{L}[B]\, \mathcal{L}[e] \tag{11}$$

Applying pair 4, page 1082,

$$i_a = \int_0^t B(t - \lambda)\, e(\lambda)\, d\lambda = \int_0^t B(\lambda)\, e(t - \lambda)\, d\lambda \tag{12}$$

To this there must be added the current i_0 due to any initial conditions that exist. From (8),

$$\mathcal{L}[i_0] = \psi(p) \tag{13}$$

Then i_0 is the inverse transform of $\psi(p)$.

Circuit response related to unit step

Unit step is defined and designated $S_{-1}(t) = 0$ for $t < 0$ and equals unity for $t > 0$. It has no dimensions. Its transform is $1/p$ as given in pair 12, page 1083. Let the circuit current be designated $A(t)$ when the applied voltage is $e = S_{-1}(t) \times$ (1 volt). Then, the current i_a for the case when the system is initially at rest, and for any applied voltage $e(t)$, is given by any of the following formulas:

$$\left.\begin{aligned} i_a &= A(t)\, e(0) + \int_0^t A(t - \lambda)\, e'(\lambda)\, d\lambda \\ &= A(t)\, e(0) + \int_0^t A(\lambda)\, e'(t - \lambda)\, d\lambda \\ &= A(0)\, e(t) + \int_0^t A'(t - \lambda)\, e(\lambda)\, d\lambda \\ &= A(0)\, e(t) + \int_0^t A'(\lambda)\, e(t - \lambda)\, d\lambda \end{aligned}\right\} \tag{14}$$

where A' is the first derivative of A and similarly for e' of e.

Transients—operational calculus and Laplace transforms *continued*

As an example, consider the problem of Fig. 17 and (5) to (7) above. Suppose $V_0 = 0$, and that the battery is replaced by a linear source

$$e(t) = Et/T_1$$

where T_1 is the duration of the voltage rise in seconds. By (7), setting $E_b = 1$,

$$A(t) = 1 - \epsilon^{-t/RC}$$

Then using the first equation in (14) and noting that $e(0) = 0$, and $e'(t) = E/T_1$ when $0 \leqslant t \leqslant T_1$, the solution is

$$v = \frac{Et}{T_1} - \frac{ERC}{T_1}(1 - \epsilon^{-t/RC})$$

This result can, of course, be found readily by direct application of the Laplace transform to (5) with $e(t) = Et/T_1$.

Heaviside expansion theorem

When the system is initially at rest, the transformed equation is given by (9) and may be written

$$\mathcal{L}[i_a] = \frac{M(p)}{G(p)}\mathcal{L}[e] \tag{15}$$

$M(p)$ and $G(p)$ are rational functions of p. In the following, $M(p)$ must be of lower degree than $G(p)$, as is usually the case. The roots of $G(p) = 0$ are p_r, where $r = 1, 2, \ldots.\ n$, and there must be no repeated roots. The response may be found by application of the *Heaviside expansion theorem.*

For a force $e = E_{max}\,\epsilon^{j\omega t}$ applied at time $t = 0$,

$$\frac{i_a(t)}{E_{max}} = \frac{M(j\omega)}{G(j\omega)}\epsilon^{j\omega t} + \sum_{r=1}^{n}\frac{M(p_r)\,\epsilon^{p_r t}}{(p_r - j\omega)\,G'(p_r)} \tag{16a}$$

$$= \frac{\epsilon^{j\omega t}}{Z(j\omega)} + \sum_{r=1}^{n}\frac{\epsilon^{p_r t}}{(p_r - j\omega)\,Z'(p_r)} \tag{16b}$$

The first term on the right-hand side of either form of (16) gives the steady-state response, and the second term gives the transient. When $e = E_{max}\cos\omega t$, take the real part of (16), and similarly for $\sin\omega t$ and the imaginary part. $Z(p)$ is defined in (19) below. If the applied force is the unit step, set $\omega = 0$ in (16).

Application to linear networks

The equation for a single mesh is of the form

$$A_n\frac{d^n i}{dt^n} + \ldots. + A_1\frac{di}{dt} + A_0 i + B\int i\,dt = e(t) \tag{17}$$

System initially at rest: Then, (17) transforms into

$$(A_n p^n + \ldots + A_1 p + A_0 + Bp^{-1})\,\mathcal{L}[i] = \mathcal{L}[e] \tag{18}$$

where the expression in parenthesis is the operational impedance, equal to the alternating-current impedance when we set $p = j\omega$.

If there are m meshes in the system, we get m simultaneous equations like (17) with m unknowns $i_1, i_2, \ldots, i_m$. The m algebraic equations like (18) are solved for $\mathcal{L}[i_1]$, etc., by means of determinants, yielding an equation of the form of (15) for each unknown, with a term on the right-hand side for each mesh in which there is a driving force. Each such driving force may of course be treated separately and the responses added.

Designating any two meshes by the letters h and k, the driving force $e(t)$ being in either mesh and the mesh current $i(t)$ in the other, then the fraction $M(p)/G(p)$ in (15) becomes

$$\frac{M_{hk}(p)}{G(p)} = \frac{1}{Z_{hk}(p)} = Y_{hk}(p) \tag{19}$$

where $Y_{hk}(p)$ is the operational transfer admittance between the two meshes. The determinant of the system is $G(p)$, and $M_{hk}(p)$ is the cofactor of the row and column that represent $e(t)$ and $i(t)$.

System not initially at rest: The transient due to the initial conditions is solved separately and added to the above solution. The driving force is set equal to zero in (17), $e(t) = 0$, and each term is transformed according to

$$\mathcal{L}\left[\frac{d^n i}{dt^n}\right] = p^n \mathcal{L}[i] - \sum_{r=1}^{n} p^{n-r}\left[\frac{d^{r-1} i}{dt^{r-1}}\right]_{t=0} \tag{20a}$$

$$\mathcal{L}\left[\int_0^t i\,dt\right] = \frac{1}{p}\mathcal{L}[i] + \frac{1}{p}\left[\int i\,dt\right]_{t=0} \tag{20b}$$

where the last term in each equation represents the initial conditions. For example, in (20b) the last term would represent, in an electrical circuit, the quantity of electricity existing on a capacitor at time $t = 0$, the instant when the driving force $e(t)$ commences to act.

Resolution into partial fractions: The solution of the operational form of the equations of a system involves rational fractions that must be simplified before finding the inverse transform. Let the fraction be $h(p)/g(p)$ where $h(p)$ is of lower degree than $g(p)$, for example $(3p + 2)/(p^2 + 5p + 8)$. If $h(p)$ is of equal or higher degree than $g(p)$, it can be reduced by division.

The reduced fraction can be expanded into partial fractions. Let the factors of the denominator be $(p - p_r)$ for the n nonrepeated roots p_r of the equation $g(p) = 0$, and $(p - p_a)$ for a root p_a repeated m times.

Transients—operational calculus and Laplace transforms *continued*

$$\frac{h(p)}{g(p)} = \sum_{r=1}^{n} \frac{A_r}{p - p_r} + \sum_{r=1}^{m} \frac{B_r}{(p - p_a)^{m-r+1}} \tag{21a}$$

There is a summation term for each root that is repeated. The constant coefficients A_r and B_r can be evaluated by reforming the fraction with a common denominator. Then the coefficients of each power of p in $h(p)$ and the reformed numerator are equated and the resulting equations solved for the constants. More formally, they may be evaluated by

$$A_r = \frac{h(p_r)}{g'(p_r)} = \left[\frac{h(p)}{g(p)/(p - p_r)}\right]_{p=p_r} \tag{21b}$$

$$B_r = \frac{1}{(r-1)!} f^{(r-1)}(p_a) \tag{21c}$$

where

$$f(p) = (p - p_a)^m \frac{h(p)}{g(p)}$$

and $f^{(r-1)}(p_a)$ indicates that the $(r-1)$th derivative of $f(p)$ is to be found, after which we set $p = p_a$.

Fractions of the form $\dfrac{A_1 p + A_2}{p^2 + \omega^2}$ or, more generally,

$$\frac{A_1 p + A_2}{p^2 + 2ap + b} = \frac{A(p + a) + B\omega}{(p + a)^2 + \omega^2} \tag{22a}$$

where $b > a^2$ and $\omega^2 = b - a^2$, need not be reduced further. By pairs 8 23, and 24 of the table on pages 1082 and 1083, the inverse transform of (22a) is

$$\epsilon^{-at}(A \cos \omega t + B \sin \omega t) \tag{22b}$$

where

$$A = \frac{h(-a + j\omega)}{g'(-a + j\omega)} + \frac{h(-a - j\omega)}{g'(-a - j\omega)} \tag{22c}$$

$$B = j\left[\frac{h(-a + j\omega)}{g'(-a + j\omega)} - \frac{h(-a - j\omega)}{g'(-a - j\omega)}\right] \tag{22d}$$

Similarly, the inverse transform of the fraction $\dfrac{A(p + a) + B\alpha}{(p + a)^2 - \alpha^2}$ is $\epsilon^{-at}(A \cosh \alpha t + B \sinh \alpha t)$, where A and B are found by (22c) and (22d), except that $j\omega$ is replaced by α and the coefficient j is omitted in the expression for B.

Filters, image-parameter design

General

The basic filter half section and the full sections derived from it are shown in Fig. 1. The fundamental filter equations follow, with filter characteristics and design formulas next. Also given is the method of building up a composite filter and the effect of the design parameter *m* on the image-impedance characteristic. An example of the design of a low-pass filter completes the chapter. It is to be noted that while the impedance characteristics and design formulas are given for the half sections as shown, the attenuation and phase characteristics are for full sections, either T or π.

Fundamental filter equations

Image impedances Z_T and Z_π

The element-value design equations to be given are derived by assuming that the network is terminated with impedances that change with frequency in accordance with the following image-impedance equations. Unfortunately, this assumption can be only approximately satisfied.

Z_T = mid-series image impedance
= impedance looking into 1–2 (Fig. 1A) with Z_π connected across 3–4.

Z_π = mid-shunt image impedance
= impedance looking into 3–4 (Fig. 1A) with Z_T connected across 1–2.

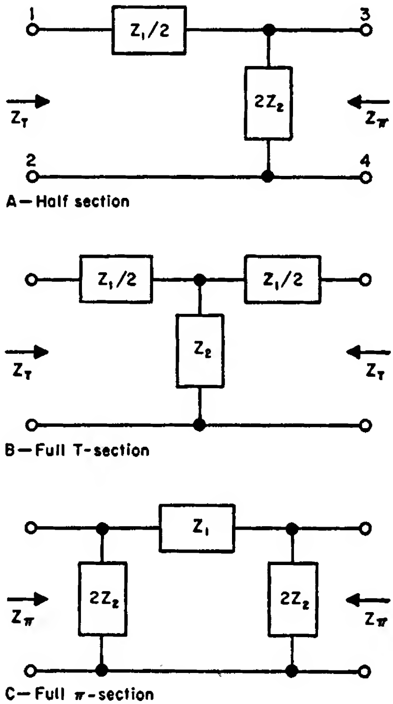

Fig. 1—Basic filter sections.

Fundamental filter equations *continued*

Formulas for the above are

$$Z_T = \sqrt{Z_1Z_2 + Z_1^2/4}$$

$$= \sqrt{Z_1Z_2}\sqrt{1 + Z_1/4Z_2} \text{ ohms}$$

$$Z_\pi = \frac{Z_1Z_2}{\sqrt{Z_1Z_2 + Z_1^2/4}}$$

$$= \frac{\sqrt{Z_1Z_2}}{\sqrt{1 + Z_1/4Z_2}} \text{ ohms}$$

$$Z_TZ_\pi = Z_1Z_2$$

Image transfer constant θ

The transfer constant $\theta = \alpha + j\beta$ of a network is defined as one-half the natural logarithm of the complex ratio of the steady-state volt-amperes entering and leaving the network when the latter is terminated in its image impedance. The real part α of the transfer constant is called the image attenuation constant, and the imaginary part β is called the image phase constant.

Formulas in terms of full sections are

$$\cosh\theta = 1 + Z_1/2Z_2$$

Pass band

$\alpha = 0$, for frequencies making $-1 \leqslant Z_1/4Z_2 \leqslant 0$

$\beta = \cos^{-1}(1 + Z_1/2Z_2) = \pm 2\sin^{-1}\sqrt{-Z_1/4Z_2}$ radians

Image impedance = pure resistance

Stop band

$$\begin{cases} \alpha = \cosh^{-1}|1 + Z_1/2Z_2| = 2\sinh^{-1}\sqrt{Z_1/4Z_2} \text{ nepers} & \text{for } Z_1/4Z_2 > 0 \\ \beta = 0 \text{ radians} \end{cases}$$

$$\begin{cases} \alpha = \cosh^{-1}|1 + Z_1/2Z_2| = 2\cosh^{-1}\sqrt{-Z_1/4Z_2} \text{ nepers} & \text{for } Z_1/4Z_2 < -1 \\ \beta = \pm\pi \text{ radians} \end{cases}$$

Image impedance = pure reactance

The above formulas are based on the assumption that the impedance arms are pure reactances with zero loss.

Low-pass filter design

type and half section	impedance characteristics

Constant-k

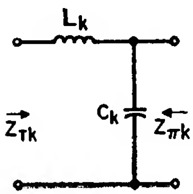

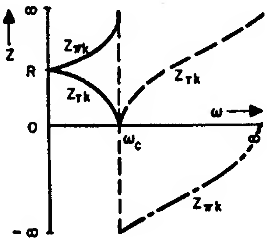

$$Z_{Tk} = R\sqrt{1 - \omega^2/\omega_c^2}$$

$$Z_{\pi k} = \frac{R}{\sqrt{1 - \omega^2/\omega_c^2}}$$

Series m-derived

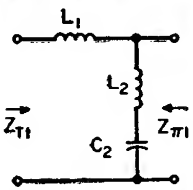

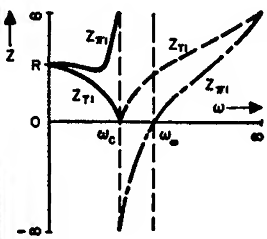

$$Z_{T1} = Z_{Tk}$$

$$Z_{\pi 1} = \frac{R\,(1 - \omega^2/\omega_\infty^2)}{\sqrt{1 - \omega^2/\omega_c^2}}$$

$$= \frac{R\left[1 - \dfrac{\omega^2}{\omega_c^2}(1 - m^2)\right]}{\sqrt{1 - \omega^2/\omega_c^2}}$$

Shunt m-derived

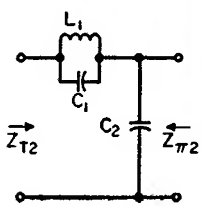

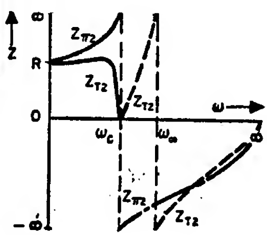

$$Z_{T2} = \frac{R\sqrt{1 - \omega^2/\omega_c^2}}{1 - \omega^2/\omega_\infty^2}$$

$$= \frac{R\sqrt{1 - \omega^2/\omega_c^2}}{1 - \dfrac{\omega^2}{\omega_c^2}(1 - m^2)}$$

$$= R^2/Z_{\pi 1}$$

$$Z_{\pi 2} = Z_{\pi k}$$

Notations:

Z in ohms, α in nepers, and β in radians

$\omega_c = 2\pi f_c$ = angular cutoff frequency

$= 1/\sqrt{L_k C_k}$

$\omega_\infty = 2\pi f_\infty$ = angular frequency of peak attenuation

$m = \sqrt{1 - \omega_c^2/\omega_\infty^2}$

R = nominal terminating resistance

$= \sqrt{L_k/C_k}$

$= \sqrt{Z_{Tk} Z_{\pi k}}$

<table>
<tr><th rowspan="2">full-section
attenuation α and phase β characteristics</th><th colspan="2">design formulas</th></tr>
<tr><th>half-section
series arm</th><th>half-section
shunt arm</th></tr>
<tr><td>


When $0 \leqslant \omega \leqslant \omega_c$
$\alpha = 0$
$\beta = 2 \sin^{-1} \frac{\omega}{\omega_c}$

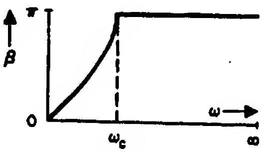

When $\omega_c < \omega < \infty$
$\beta = \pi$
$\alpha = 2 \cosh^{-1} \frac{\omega}{\omega_c}$
</td><td>$L_k = \frac{R}{\omega_c}$</td><td>$C_k = \frac{1}{\omega_c R}$</td></tr>
<tr><td>


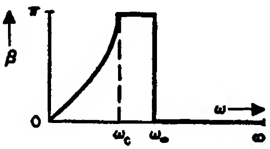

</td><td>$L_1 = mL_k$</td><td>$L_2 = \frac{1 - m^2}{m} L_k$

$C_2 = mC_k$</td></tr>
<tr><td>
When $\omega_c < \omega < \omega_\infty$, $\beta = \pi$ and

$$\alpha = \cosh^{-1} \left[2 \frac{1/\omega_\infty^2 - 1/\omega_c^2}{1/\omega_\infty^2 - 1/\omega^2} - 1 \right] = \cosh^{-1} \left[2 \frac{m^2}{\omega_c^2/\omega^2 - (1 - m^2)} - 1 \right]$$

When $0 \leqslant \omega \leqslant \omega_c$, $\alpha = 0$ and

$$\beta = \cos^{-1} \left[1 - 2 \frac{1/\omega_\infty^2 - 1/\omega_c^2}{1/\omega_\infty^2 - 1/\omega^2} \right] = \cos^{-1} \left[1 - 2 \frac{m^2}{\omega_c^2/\omega^2 - (1 - m^2)} \right]$$

When $\omega_\infty < \omega < \infty$, $\beta = 0$ and

$$\alpha = \cosh^{-1} \left[1 - 2 \frac{1/\omega_\infty^2 - 1/\omega_c^2}{1/\omega_\infty^2 - 1/\omega^2} \right] = \cosh^{-1} \left[1 - 2 \frac{m^2}{\omega_c^2/\omega^2 - (1 - m^2)} \right]$$
</td><td>$L_1 = mL_k$

$C_1 = \frac{1 - m^2}{m} C_k$</td><td>$C_2 = mC_k$</td></tr>
<tr><td></td><td colspan="2">
For constant-k type
$R^2 = Z_{1k} Z_{2k} = k^2$

For m-derived type
Curves drawn for $m \approx 0.6$
$R^2 = Z_{T2} Z_{\pi 1}$
$= Z_{1(\text{series-}m)} Z_{2(\text{shunt-}m)}$
$= Z_{1(\text{shunt-}m)} Z_{2(\text{series-}m)}$
</td></tr>
</table>

High-pass filter design

type and half section	impedance characteristics

Constant-*k*

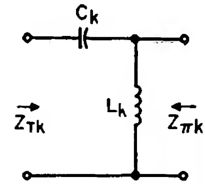

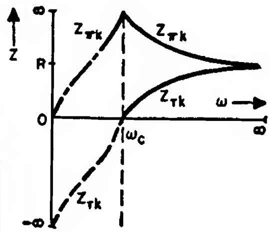

$$Z_{Tk} = R\sqrt{1 - \frac{\omega_c^2}{\omega^2}}$$

$$Z_{\pi k} = \frac{R}{\sqrt{1 - \dfrac{\omega_c^2}{\omega^2}}}$$

Series *m*-derived

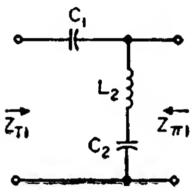

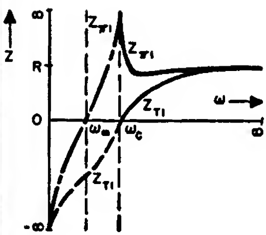

$$Z_{T1} = Z_{Tk}$$

$$Z_{\pi 1} = \frac{R\left(1 - \dfrac{\omega_\infty^2}{\omega^2}\right)}{\sqrt{1 - \omega_c^2/\omega^2}} = \frac{R\left[1 - \dfrac{\omega_c^2}{\omega^2}(1 - m^2)\right]}{\sqrt{1 - \omega_c^2/\omega^2}}$$

Shunt *m*-derived

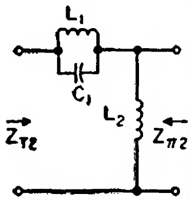

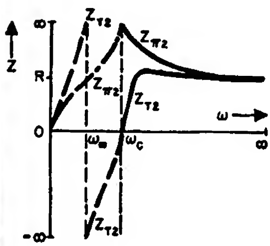

$$Z_{T2} = \frac{R\sqrt{1 - \omega_c^2/\omega^2}}{1 - \omega_\infty^2/\omega^2} = \frac{R\sqrt{1 - \omega_c^2/\omega^2}}{1 - \dfrac{\omega_c^2}{\omega^2}(1 - m^2)} = R^2/Z_{\pi 1}$$

$$Z_{\pi 2} = Z_{\pi k}$$

Notations:

Z in ohms, α in nepers, and β in radians

$\omega_c = 2\pi f_c$ = angular cutoff frequency $= 1/\sqrt{L_k C_k}$

$\omega_\infty = 2\pi f_\infty$ = angular frequency of peak attenuation

$m = \sqrt{1 - \omega_\infty^2/\omega_c^2}$

R = nominal terminating resistance $= \sqrt{L_k/C_k} = \sqrt{Z_{Tk} Z_{\pi k}}$

full-section attenuation α and phase β characteristics	design formulas: half-section series arm	design formulas: half-section shunt arm
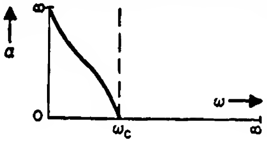 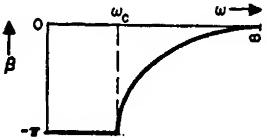 When $0 < \omega < \omega_c$ $\alpha = 2 \cosh^{-1} \frac{\omega_c}{\omega}$ $\beta = -\pi$ When $\omega_c < \omega < \infty$ $\alpha = 0$ $\beta = -2 \sin^{-1} \frac{\omega_c}{\omega}$	$C_k = \frac{1}{\omega_c R}$	$L_k = \frac{R}{\omega_c}$
 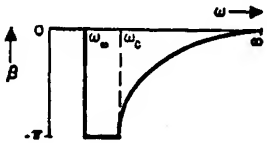	$C_1 = \frac{C_k}{m}$	$L_2 = \frac{L_k}{m}$ $C_2 = \frac{m}{1 - m^2} C_k$
When $\omega_\infty < \omega < \omega_c$, $\beta = -\pi$ and $\alpha = \cosh^{-1}\left[2 \frac{\omega_c^2 - \omega_\infty^2}{\omega^2 - \omega_\infty^2} - 1\right] = \cosh^{-1}\left[2 \frac{m^2}{\frac{\omega^2}{\omega_c^2} - (1 - m^2)} - 1\right]$ When $0 < \omega < \omega_\infty$, $\beta = 0$ and $\alpha = \cosh^{-1}\left[1 - 2 \frac{\omega_\infty^2 - \omega_c^2}{\omega_\infty^2 - \omega^2}\right] = \cosh^{-1}\left[1 + 2 \frac{m^2}{(1 - m^2) - \frac{\omega^2}{\omega_c^2}}\right]$ When $\omega_c < \omega < \infty$, $\alpha = 0$ and $\beta = \cos^{-1}\left[1 - 2 \frac{\omega_\infty^2 - \omega_c^2}{\omega_\infty^2 - \omega^2}\right] = \cos^{-1}\left[1 + 2 \frac{m^2}{(1 - m^2) - \frac{\omega^2}{\omega_c^2}}\right]$	$L_1 = \frac{m}{1 - m^2} L_k$ $C_1 = \frac{C_k}{m}$	$L_2 = \frac{L_k}{m}$

For constant-*k* type

$R^2 = Z_{1k} Z_{2k} = k^2$

For *m*-derived type

Curves drawn for $m \approx 0.6$

$R^2 = Z_{T2} Z_{\pi 1}$
$= Z_{1(\text{series-m})} Z_{2(\text{shunt-m})}$
$= Z_{1(\text{shunt-m})} Z_{2(\text{series-m})}$

Band-pass filter design

Notations:

The following notations apply to the charts on band-pass filter design that appear on pp. 170–179.

Z in ohms, α in nepers, and β in radians

$\omega_1 = 2\pi f_1$ = lower cutoff angular frequency

$\omega_2 = 2\pi f_2$ = upper cutoff angular frequency

$\omega_0 = \sqrt{\omega_1 \omega_2}$ = midband angular frequency

$\omega_2 - \omega_1$ = width of pass band

R = nominal terminating resistance

$\omega_{1\infty} = 2\pi f_{1\infty}$ = lower angular frequency of peak attenuation

$\omega_{2\infty} = 2\pi f_{2\infty}$ = upper angular frequency of peak attenuation

$$m_1 = \frac{\dfrac{\omega_1\omega_2}{\omega_{2\infty}^2} g + h}{1 - \dfrac{\omega_{1\infty}^2}{\omega_{2\infty}^2}}$$

$$m_2 = \frac{g + h\dfrac{\omega_{1\infty}^2}{\omega_1\omega_2}}{1 - \dfrac{\omega_{1\infty}^2}{\omega_{2\infty}^2}}$$

type and half section	impedance characteristics

Constant-k

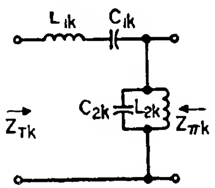

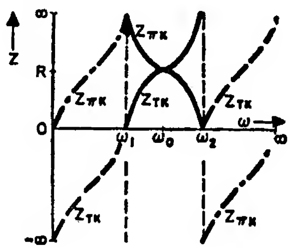

$$Z_{Tk} = \frac{R\sqrt{(\omega_2^2 - \omega^2)(\omega^2 - \omega_1^2)}}{\omega(\omega_2 - \omega_1)}$$

$$Z_{\pi k} = \frac{R\,\omega(\omega_2 - \omega_1)}{\sqrt{(\omega_2^2 - \omega^2)(\omega^2 - \omega_1^2)}}$$

$$g = \sqrt{\left(1 - \frac{\omega_{1\infty}^2}{\omega_1^2}\right)\left(1 - \frac{\omega_{1\infty}^2}{\omega_2^2}\right)}$$

$$h = \sqrt{\left(1 - \frac{\omega_1^2}{\omega_{2\infty}^2}\right)\left(1 - \frac{\omega_2^2}{\omega_{2\infty}^2}\right)}$$

$$L_{1k}C_{1k} = L_{2k}C_{2k} = \frac{1}{\omega_1\omega_2} = \frac{1}{\omega_0^2}$$

$$R^2 = \frac{L_{1k}}{C_{2k}} = \frac{L_{2k}}{C_{1k}}$$

$$= Z_{1k}\,Z_{2k} = k^2$$

$$= Z_{\mathrm{T}k}\,Z_{\pi k}$$

$$\left.\begin{aligned} &= Z_{1(\text{series-}m)}\,Z_{2(\text{shunt-}m)} \\ &= Z_{2(\text{series-}m)}\,Z_{1(\text{shunt-}m)} \\ &= Z_{\mathrm{T}(\text{shunt-}m)}\,Z_{\pi(\text{series-}m)} \\ Z_{\mathrm{T}(\text{series-}m)} &= Z_{\mathrm{T}k} \\ Z_{\pi(\text{shunt-}m)} &= Z_{\pi k} \end{aligned}\right\} \text{for any one pair of } m\text{-derived half-sections}$$

full-section attenuation α and phase β characteristics	frequencies of peak α	design formulas: half-section series arm	design formulas: half-section shunt arm
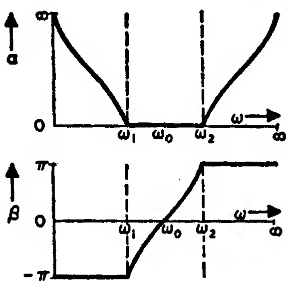 When $\omega_2 < \omega < \infty$, $\beta = \pi$ and $\alpha = 2\cosh^{-1}\left[\frac{\omega^2 - \omega_0^2}{\omega(\omega_2 - \omega_1)}\right]$ When $0 < \omega < \omega_1$, $\beta = -\pi$ and $\alpha = 2\cosh^{-1}\left[\frac{\omega_0^2 - \omega^2}{\omega(\omega_2 - \omega_1)}\right]$ When $\omega_1 < \omega < \omega_2$, $\alpha = 0$ and $\beta = 2\sin^{-1}\left[\frac{\omega^2 - \omega_0^2}{\omega(\omega_2 - \omega_1)}\right]$	$\omega_{1\infty} = 0$ $\omega_{2\infty} = \infty$	$L_{1k} = \frac{R}{\omega_2 - \omega_1}$ $C_{1k} = \frac{\omega_2 - \omega_1}{R\omega_0^2}$	$L_{2k} = \frac{R(\omega_2 - \omega_1)}{\omega_0^2}$ $C_{2k} = \frac{1}{R(\omega_2 - \omega_1)}$

Band-pass filter design* *continued*

type and half section	impedance characteristics

3-element series I

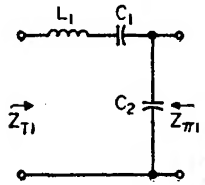

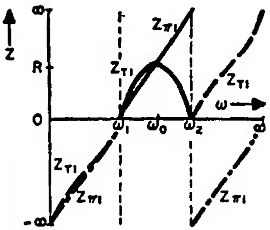

$$Z_{T1} = Z_{Tk}$$

$$Z_{\pi 1} = \frac{R(\omega_2 + \omega_1)}{\omega} \sqrt{\frac{\omega^2 - \omega_1^2}{\omega_2^2 - \omega^2}}$$

3-element shunt I

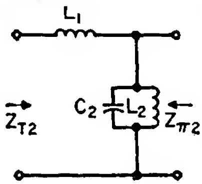

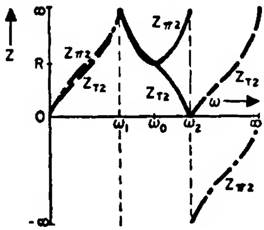

$$Z_{T2} = \frac{R\omega}{(\omega_2 + \omega_1)} \sqrt{\frac{\omega_2^2 - \omega^2}{\omega^2 - \omega_1^2}}$$

$$= R^2/Z_{\pi 1}$$

$$Z_{\pi 2} = Z_{\pi k}$$

3-element series II

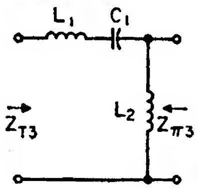

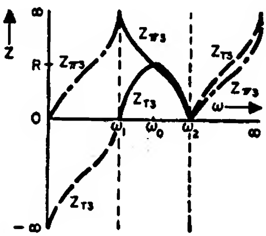

$$Z_{T3} = Z_{Tk}$$

$$Z_{\pi 3} = \frac{R\omega(\omega_2 + \omega_1)}{\omega_2^2} \sqrt{\frac{\omega_2^2 - \omega^2}{\omega^2 - \omega_1^2}}$$

3-element shunt II

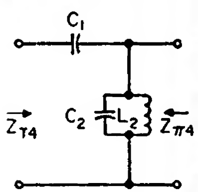

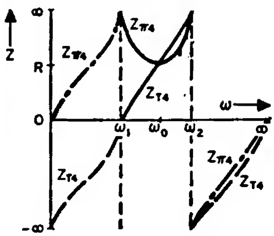

$$Z_{T4} = \frac{R\omega_2^2}{\omega(\omega_2 + \omega_1)} \sqrt{\frac{\omega^2 - \omega_1^2}{\omega_2^2 - \omega^2}}$$

$$= R^2/Z_{\pi 3}$$

$$Z_{\pi 4} = Z_{\pi k}$$

* See notations on pp. 170–171.

full-section attenuation α and phase β characteristics	conditions	frequencies of peak α	design formulas: half-section series arm	design formulas: half-section shunt arm
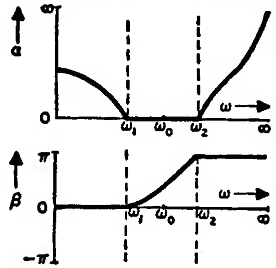 When $0 < \omega < \omega_1$, $\beta = 0$ and $\alpha = \cosh^{-1}\left[1 - 2\frac{\omega^2 - \omega_1^2}{\omega_2^2 - \omega_1^2}\right]$ When $\omega_1 < \omega < \omega_2$, $\alpha = 0$ and $\beta = \cos^{-1}\left[1 - 2\frac{\omega^2 - \omega_1^2}{\omega_2^2 - \omega_1^2}\right]$ When $\omega_2 < \omega < \infty$, $\beta = \pi$ and $\alpha = \cosh^{-1}\left[2\frac{\omega^2 - \omega_1^2}{\omega_2^2 - \omega_1^2} - 1\right]$	$m_1 = 1$ $m_2 = \frac{\omega_1}{\omega_2}$	$\omega_{2\infty} = \infty$	$L_1 = L_{1k}$ $C_1 = \frac{C_{1k}}{m_2}$	$C_2 = \frac{1-m_2}{1+m_2} C_{2k}$
			$L_1 = \frac{1-m_2}{1+m_2} L_{1k}$	$L_2 = \frac{L_{2k}}{m_2}$ $C_2 = C_{2k}$
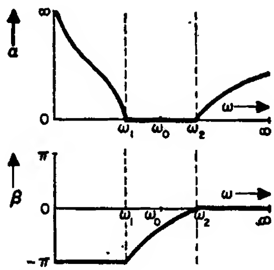 When $0 < \omega < \omega_1$, $\beta = -\pi$ and $\alpha = \cosh^{-1}\left[2\frac{\omega_1^2(\omega_2^2 - \omega^2)}{\omega^2(\omega_2^2 - \omega_1^2)} - 1\right]$ When $\omega_1 < \omega < \omega_2$, $\alpha = 0$ and $\beta = \cos^{-1}\left[1 - 2\frac{\omega_1^2(\omega_2^2 - \omega^2)}{\omega^2(\omega_2^2 - \omega_1^2)}\right]$ When $\omega_2 < \omega < \infty$, $\beta = 0$ and $\alpha = \cosh^{-1}\left[1 - 2\frac{\omega_1^2(\omega_2^2 - \omega^2)}{\omega^2(\omega_2^2 - \omega_1^2)}\right]$	$m_1 = \frac{\omega_1}{\omega_2}$ $m_2 = 1$	$\omega_{1\infty} = 0$	$L_1 = m_1 L_{1k}$ $C_1 = C_{1k}$	$L_2 = \frac{1+m_1}{1-m_1} L_{2k}$
			$C_1 = \frac{1+m_1}{1-m_1} C_{1k}$	$L_2 = L_{2k}$ $C_2 = m_1 C_{2k}$

Band-pass filter design* *continued*

type and half section	impedance characteristics	
4-element series I 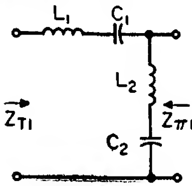	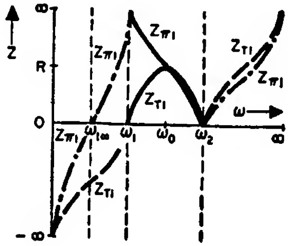	$Z_{T1} = Z_{Tk}$ $Z_{\pi 1} = \dfrac{R}{\omega(\omega_2 - \omega_1)} \sqrt{\dfrac{\omega_2^2 - \omega^2}{\omega^2 - \omega_1^2}} \times [(\omega^2 - \omega_1^2) + m_1^2(\omega_2^2 - \omega^2)]$
4-element shunt I 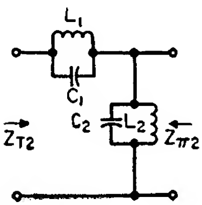	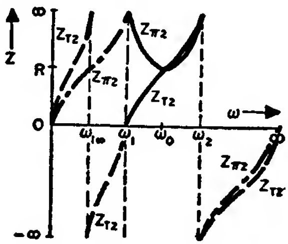	$Z_{T2} = \dfrac{R\omega(\omega_2-\omega_1)}{(\omega^2-\omega_1^2)+m_1^2(\omega_2^2-\omega^2)} \times \sqrt{\dfrac{\omega^2 - \omega_1^2}{\omega_2^2 - \omega^2}}$ $= R^2/Z_{\pi 1}$ $Z_{\pi 2} = Z_{\pi k}$
4-element series II 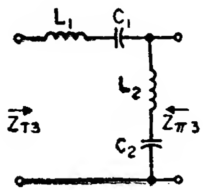	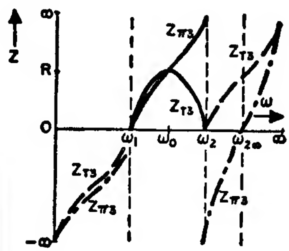	$Z_{T3} = Z_{Tk}$ $Z_{\pi 3} = \dfrac{R}{\omega(\omega_2 - \omega_1)} \sqrt{\dfrac{\omega^2 - \omega_1^2}{\omega_2^2 - \omega^2}} \times [(\omega_2^2-\omega^2)+m_1^2(\omega^2-\omega_1^2)]$
4-element shunt II 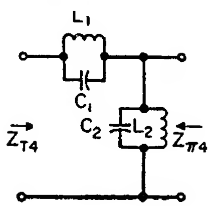	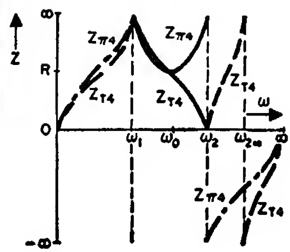	$Z_{T4} = \dfrac{R\omega(\omega_2-\omega_1)}{(\omega_2^2-\omega^2)+m_1^2(\omega^2-\omega_1^2)} \times \sqrt{\dfrac{\omega_2^2 - \omega^2}{\omega^2 - \omega_1^2}}$ $= R^2/Z_{\pi 3}$ $Z_{\pi 4} = Z_{\pi k}$

* See notations on pp. 170–171.

full-section attenuation α and phase β characteristics	conditions	frequency of peak α	design formulas: half-section series arm	design formulas: half-section shunt arm
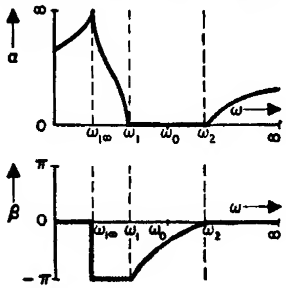	$\frac{m_1}{m_2}=\frac{\omega_1}{\omega_2}$ $m_2=\sqrt{\frac{1-\frac{\omega_{1\infty}^2}{\omega_1^2}}{1-\frac{\omega_{1\infty}^2}{\omega_2^2}}}$	$\omega_{1\infty}=\sqrt{\frac{\omega_1^2-\omega_2^2 m_1^2}{1-m_1^2}}$	$L_1=m_1L_{1k}$ $C_1=\frac{C_{1k}}{m_2}$	$L_2=\frac{1-m_1^2}{m_1}L_{1k}$ $C_2=\frac{m_2}{1-m_2^2}C_{1k}$
When $\omega_1<\omega<\omega_2$, $\alpha=0$ and $\beta=\cos^{-1}A$ When $0<\omega<\omega_{1\infty}$, $\beta=0$ and $\alpha=\cosh^{-1}A$ When $\omega_{1\infty}<\omega<\omega_1$, $\beta=-\pi$ and $\alpha=\cosh^{-1}(-A)$ When $\omega_2<\omega<\infty$, $\beta=0$ and $\alpha=\cosh^{-1}A$	$A=1-\frac{2}{1+\frac{(\omega^2-\omega_1^2)}{m_1^2(\omega_2^2-\omega^2)}}$		$L_1=\frac{m_2}{1-m_2^2}L_{2k}$ $C_1=\frac{1-m_1^2}{m_1}C_{2k}$	$L_2=\frac{L_{2k}}{m_2}$ $C_2=m_1C_{2k}$
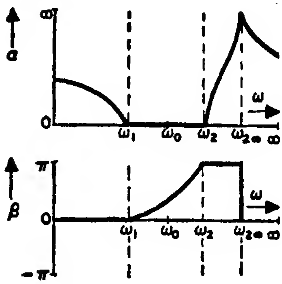	$\frac{m_1}{m_2}=\frac{\omega_2}{\omega_1}$ $m_1=\sqrt{\frac{1-\frac{\omega_2^2}{\omega_{2\infty}^2}}{1-\frac{\omega_1^2}{\omega_{2\infty}^2}}}$	$\omega_{2\infty}=\sqrt{\frac{m_1^2\omega_1^2-\omega_2^2}{m_1^2-1}}$	$L_1=m_1L_{1k}$ $C_1=\frac{C_{1k}}{m_2}$	$L_2=\frac{1-m_1^2}{m_1}L_{1k}$ $C_2=\frac{m_2}{1-m_2^2}C_{1k}$
When $\omega_2<\omega<\omega_{2\infty}$, $\beta=\pi$ and $\alpha=\cosh^{-1}(-B)$ When $0<\omega<\omega_1$, $\beta=0$ and $\alpha=\cosh^{-1}B$ When $\omega_1<\omega<\omega_2$, $\alpha=0$ and $\beta=\cos^{-1}B$ When $\omega_{2\infty}<\omega<\infty$, $\beta=0$ and $\alpha=\cosh^{-1}B$	$B=1-\frac{2}{1+\frac{(\omega_2^2-\omega^2)}{m_1^2(\omega^2-\omega_1^2)}}$		$L_1=\frac{m_2}{1-m_2^2}L_{2k}$ $C_1=\frac{1-m_1^2}{m_1}C_{2k}$	$L_2=\frac{L_{2k}}{m_2}$ $C_2=m_1C_{2k}$

Band-pass filter design* *continued*

type and half section | **impedance characteristics**

5-element series I

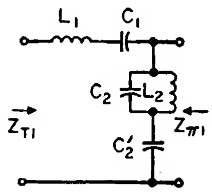

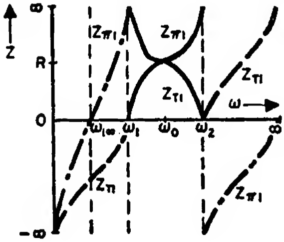

$Z_{T1} = Z_{Tk}$

$$Z_{\pi 1} = R\left[\frac{\omega^2(\omega_2^2+\omega_1^2-2\omega_0^2 m_2)+\omega_0^4(m_2^2-1)}{\omega(\omega_2-\omega_1)\sqrt{(\omega_2^2-\omega^2)(\omega^2-\omega_1^2)}}\right]$$

5-element shunt I

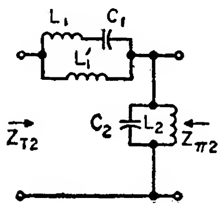

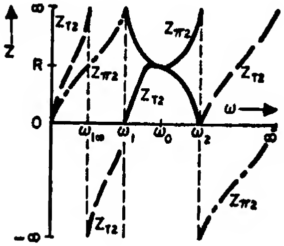

$Z_{T2} = R^2/Z_{\pi 1}$

$Z_{\pi 2} = Z_{\pi k}$

5-element series II

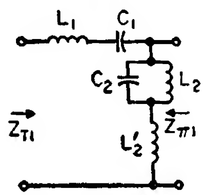

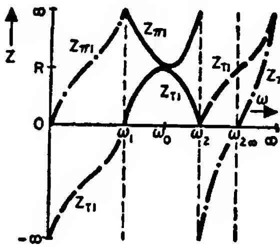

$Z_{T1} = Z_{Tk}$

$$Z_{\pi 1} = \frac{\omega R}{(\omega_2-\omega_1)} \times \frac{\omega_2^2+\omega_1^2-2\omega_0^2 m_1+\omega^2(m_1^2-1)}{\sqrt{(\omega_2^2-\omega^2)(\omega^2-\omega_1^2)}}$$

5-element shunt II

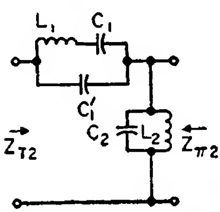

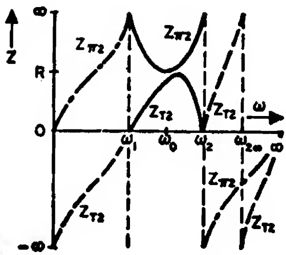

$Z_{T2} = R^2/Z_{\pi 1}$

$Z_{\pi 2} = Z_{\pi k}$

* See notations on pp. 170–171.

full-section attenuation α and phase β characteristics	conditions	frequency of peak α	design formulas: half-section series arm	design formulas: half-section shunt arm
 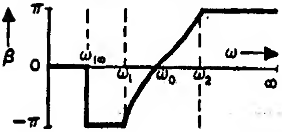 When $\omega_1 < \omega < \omega_2$, $\alpha = 0$ and $\beta = \cos^{-1}\left[1 - \frac{2(\omega^2 - \omega_0^2 m_2)^2}{\omega^2(\omega_2^2+\omega_1^2-2\omega_0^2 m_2)+\omega_0^4(m_2^2-1)}\right]$ When $0 < \omega < \omega_{1\infty}$, $\beta = 0$ and $\alpha = \cosh^{-1}\left[1 - \frac{2(\omega^2 - \omega_0^2 m_2)^2}{\omega^2(\omega_2^2+\omega_1^2-2\omega_0^2 m_2)+\omega_0^4(m_2^2-1)}\right]$ When $\omega_{1\infty} < \omega < \omega_1$, $\beta = -\pi$ and $\alpha = \cosh^{-1}\left[\frac{2(\omega^2 - \omega_0^2 m_2)^2}{\omega^2(\omega_2^2+\omega_1^2-2\omega_0^2 m_2)+\omega_0^4(m_2^2-1)} - 1\right]$ When $\omega_2 < \omega < \infty$, $\beta = \pi$ and α = same formula as for $0 < \omega < \omega_{1\infty}$	$m_1 = 1$ $m_2 = \frac{\omega_{1\infty}^2}{\omega_0^2} + \sqrt{\left(1 - \frac{\omega_{1\infty}^2}{\omega_1^2}\right)\left(1 - \frac{\omega_{1\infty}^2}{\omega_2^2}\right)}$	$\omega_{1\infty} = \omega_0^2\sqrt{\frac{1 - m_2^2}{\omega_2^2 + \omega_1^2 - 2\omega_0^2 m_2}}$ $\omega_{2\infty} = \infty$	$L_1 = L_{1k}$ $C_1 = \frac{C_{1k}}{m_2}$	$L_2 = \frac{L_{1k}}{m_2}\left[\frac{(\omega_2-\omega_1)^2}{\omega_0^2} - \frac{(1-m_2)^2}{m_2}\right]$ $C_2 = C_{1k}\Big/\left[\frac{(\omega_2-\omega_1)^2}{\omega_0^2} - \frac{(1-m_2)^2}{m_2}\right]$ $C_2' = \frac{m_2}{1-m_2^2}C_{1k}$
			$L_1 = L_{2k}\Big/\left[\frac{(\omega_2-\omega_1)^2}{\omega_0^2} - \frac{(1-m_2)^2}{m_2}\right]$ $C_1 = \frac{C_{2k}}{m_2}\left[\frac{(\omega_2-\omega_1)^2}{\omega_0^2} - \frac{(1-m_2)^2}{m_2}\right]$ $L_1' = \frac{m_2}{1-m_2^2}L_{2k}$	$L_2 = \frac{L_{2k}}{m_2}$ $C_2 = C_{2k}$
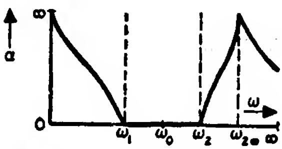 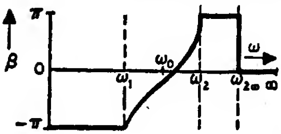 When $\omega_2 < \omega < \omega_{2\infty}$, $\beta = \pi$ and $\alpha = \cosh^{-1}\left\{1 - \frac{2(\omega^2 m_1 - \omega_0^2)^2}{\omega^2[\omega_2^2+\omega_1^2-2\omega_0^2 m_1+\omega^2(m_1^2-1)]}\right\}$ When $0 < \omega < \omega_1$, $\beta = -\pi$ and $\alpha = \cosh^{-1}\left\{\frac{2(\omega^2 m_1 - \omega_0^2)^2}{\omega^2[\omega_2^2+\omega_1^2-2\omega_0^2 m_1+\omega^2(m_1^2-1)]} - 1\right\}$ When $\omega_1 < \omega < \omega_2$, $\alpha = 0$ and $\beta = \cos^{-1}\left\{1 - \frac{2(\omega^2 m_1 - \omega_0^2)^2}{\omega^2[\omega_2^2+\omega_1^2-2\omega_0^2 m_1+\omega^2(m_1^2-1)]}\right\}$ When $\omega_{2\infty} < \omega < \infty$, $\beta = 0$ and α = same formula as for $0 < \omega < \omega_1$	$m_1 = \frac{\omega_0^2}{\omega_{2\infty}^2} + \sqrt{\left(1 - \frac{\omega_1^2}{\omega_{2\infty}^2}\right)\left(1 - \frac{\omega_2^2}{\omega_{2\infty}^2}\right)}$ $m_2 = 1$	$\omega_{1\infty} = 0$ $\omega_{2\infty} = \sqrt{\frac{\omega_2^2 + \omega_1^2 - 2\omega_0^2 m_1}{1 - m_1^2}}$	$L_1 = m_1 L_{1k}$ $C_1 = C_{1k}$	$L_2 = L_{1k}\left[\frac{(\omega_2-\omega_1)^2}{\omega_0^2} - \frac{(m_1-1)^2}{m_1}\right]$ $C_2 = m_1 C_{1k}\Big/\left[\frac{(\omega_2-\omega_1)^2}{\omega_0^2} - \frac{(m_1-1)^2}{m_1}\right]$ $L_1' = \frac{1-m_1^2}{m_1}L_{1k}$
			$L_1 = m_1 L_{2k}\Big/\left[\frac{(\omega_2-\omega_1)^2}{\omega_0^2} - \frac{(m_1-1)^2}{m_1}\right]$ $C_1 = C_{2k}\left[\frac{(\omega_2-\omega_1)^2}{\omega_0^2} - \frac{(m_1-1)^2}{m_1}\right]$ $C_1' = \frac{1-m_1^2}{m_1}C_{2k}$	$L_2 = L_{2k}$ $C_2 = m_1 C_{2k}$

Band-pass filter design* *continued*

type and half section	impedance characteristics

6-element series

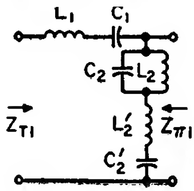

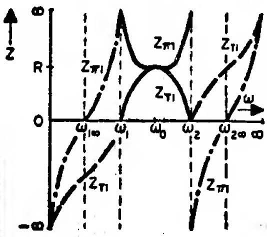

$$Z_{T1} = Z_{Tk}$$

$$Z_{\pi 1} = \frac{R}{\omega(\omega_2 - \omega_1)} \times \frac{(\omega_2^2-\omega^2)(\omega^2-\omega_1^2)+(\omega_0^2 m_2-\omega^2 m_1)^2}{\sqrt{(\omega_2^2-\omega^2)(\omega^2-\omega_1^2)}}$$

6-element shunt

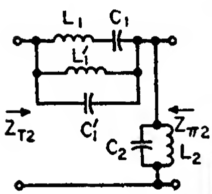

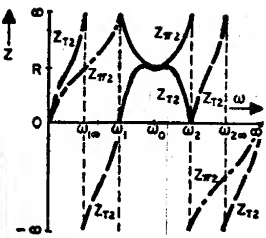

$$Z_{T2} = R^2/Z_{\pi 1}$$

$$Z_{\pi 2} = Z_{\pi k}$$

full-section attenuation α and phase β characteristics

When $\omega_1 < \omega < \omega_2$, $\alpha = 0$ and

$$\beta = \cos^{-1}\left[1 - \frac{2(\omega^2 m_1 - \omega_0^2 m_2)^2}{(\omega^2 m_1 - \omega_0^2 m_2)^2 + (\omega_2^2 - \omega^2)(\omega^2 - \omega_1^2)}\right]$$

When $\omega_2 < \omega < \omega_{2\infty}$, $\beta = \pi$ and

$$\alpha = \cosh^{-1}\left[\frac{2(\omega^2 m_1 - \omega_0^2 m_2)^2}{(\omega^2 m_1 - \omega_0^2 m_2)^2 + (\omega_2^2 - \omega^2)(\omega^2 - \omega_1^2)} + 1\right]$$

When $0 < \omega < \omega_{1\infty}$, $\beta = 0$ and

$$\alpha = \cosh^{-1}\left[1 - \frac{2(\omega^2 m_1 - \omega_0^2 m_2)^2}{(\omega^2 m_1 - \omega_0^2 m_2)^2 + (\omega_2^2 - \omega^2)(\omega^2 - \omega_1^2)}\right]$$

When $\omega_{1\infty} < \omega < \omega_1$, $\beta = -\pi$ and

$$\alpha = \cosh^{-1}\left[\frac{2(\omega^2 m_1 - \omega_0^2 m_2)^2}{(\omega^2 m_1 - \omega_0^2 m_2)^2 + (\omega_2^2 - \omega^2)(\omega^2 - \omega_1^2)} - 1\right]$$

When $\omega_{2\infty} < \omega < \infty$, $\beta = 0$ and
α = same formula as for $0 < \omega < \omega_{1\infty}$

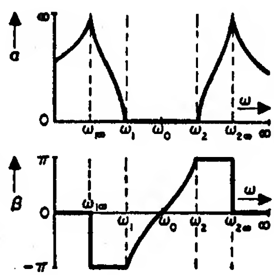

* See notations on pp. 170–171.

design formulas

half-section series arm	half-section shunt arm
	$L_2 = \frac{L_{1k}}{m_2}\left[\frac{(\omega_2-\omega_1)^2}{\omega_0^2} - \frac{(m_1-m_2)^2}{m_1 m_2}\right]$
$L_1 = m_1 L_{1k}$	$L_2' = \frac{1-m_1^2}{m_1} L_{1k}$
$C_1 = \frac{C_{1k}}{m_2}$	$C_2 = \frac{m_1 C_{1k}}{\frac{(\omega_2-\omega_1)^2}{\omega_0^2} - \frac{(m_1-m_2)^2}{m_1 m_2}}$
	$C_2' = \frac{m_2}{1-m_2^2} C_{1k}$
$L_1 = \frac{m_1 L_{2k}}{\frac{(\omega_2-\omega_1)^2}{\omega_0^2} - \frac{(m_1-m_2)^2}{m_1 m_2}}$	
$C_1 = \frac{C_{2k}}{m_2}\left[\frac{(\omega_2-\omega_1)^2}{\omega_0^2} - \frac{(m_1-m_2)^2}{m_1 m_2}\right]$	$L_2 = \frac{L_{2k}}{m_2}$
$L_1' = \frac{m_2}{1-m_2^2} L_{2k}$	$C_2 = m_1 C_{2k}$
$C_1' = \frac{1-m_1^2}{m_1} C_{2k}$	

conditions	frequency of peak α
$m_1 = \frac{g\frac{\omega_0^2}{\omega_{2\infty}^2} + h}{1 - \frac{\omega_{1\infty}^2}{\omega_{2\infty}^2}}$ $\quad m_2 = \frac{g + h\frac{\omega_{1\infty}^2}{\omega_0^2}}{1 - \frac{\omega_{1\infty}^2}{\omega_{2\infty}^2}}$	$\omega_{1\infty}^2 + \omega_{2\infty}^2 = \frac{\omega_2^2 + \omega_1^2 - 2\omega_0^2 m_1 m_2}{1 - m_1^2}$ $\omega_{1\infty}^2 \times \omega_{2\infty}^2 = \omega_0^4\left(\frac{1-m_2^2}{1-m_1^2}\right)$

Band-stop filter design

Notations

Z in ohms, α in nepers, and β in radians

ω_1 = lower cutoff angular frequency

ω_2 = upper cutoff angular frequency

$\omega_0 = \sqrt{\omega_1\omega_2} = 1/\sqrt{L_{1k}C_{1k}}$
$= 1/\sqrt{L_{2k}C_{2k}}$

$\omega_2 - \omega_1$ = width of stop band

$\omega_{1\infty}$ = lower angular frequency of peak attenuation

$\omega_{2\infty}$ = upper angular frequency of peak attenuation

R = nominal terminating resistance

$R^2 = \frac{L_{1k}}{C_{2k}} = \frac{L_{2k}}{C_{1k}}$
$= Z_{1k}Z_{2k} = Z_{Tk}Z_{\pi k} = k^2$
$= Z_{1(\text{series-}m)}\, Z_{2(\text{shunt-}m)}$
$= Z_{2(\text{series-}m)}\, Z_{1(\text{shunt-}m)}$
$= Z_{T2}\, Z_{\pi 1}$

Band-stop filter design* *continued*

type and half section	impedance characteristics

Constant-k

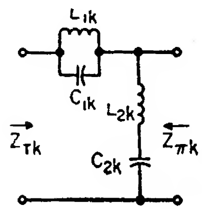

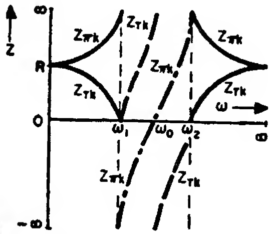

$$Z_{Tk} = \frac{R\sqrt{(\omega^2 - \omega_1^2)(\omega^2 - \omega_2^2)}}{(\omega_0^2 - \omega^2)}$$

$$Z_{\pi k} = \frac{R(\omega_0^2 - \omega^2)}{\sqrt{(\omega^2 - \omega_1^2)(\omega^2 - \omega_2^2)}}$$

For the pass bands, use $|\omega_0^2 - \omega^2|$ in the above formulas

Series *m*-derived

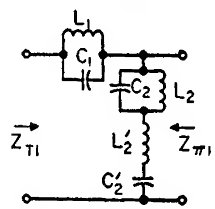

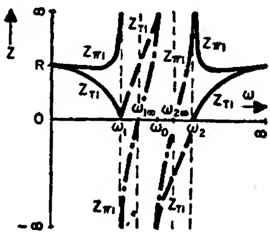

curves drawn for $m = 0.6$

$$Z_{T1} = Z_{Tk}$$

$$Z_{\pi 1} = R\left\{\frac{1 - (1 - m^2)\left[\dfrac{\omega(\omega_2 - \omega_1)}{\omega_0^2 - \omega^2}\right]^2}{\sqrt{1 - \left[\dfrac{\omega(\omega_2 - \omega_1)}{\omega_0^2 - \omega^2}\right]^2}}\right\}$$

Shunt *m*-derived

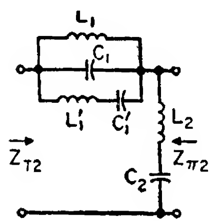

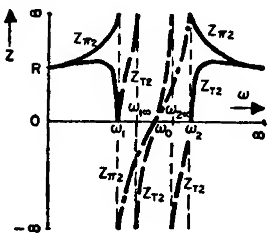

curves drawn for $m = 0.6$

$$Z_{T2} = \frac{R^2}{Z_{\pi 1}}$$

$$Z_{\pi 2} = Z_{\pi k}$$

* See notations on preceding page.

<table>
<tr><th rowspan="2">full-section attenuation α and phase β characteristics</th><th rowspan="2">conditions</th><th rowspan="2">freq of peak α</th><th colspan="2">design formulas</th></tr>
<tr><th>half-section series arm</th><th>half-section shunt arm</th></tr>
<tr><td>
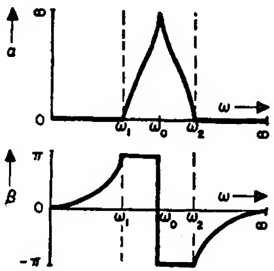

When $\omega = \omega_0$
$\alpha = \infty$

When $\omega_0 < \omega < \omega_2$
$\alpha = 2\cosh^{-1}\dfrac{\omega(\omega_2-\omega_1)}{\omega^2-\omega_0^2}$
$\beta = -\pi$

When $\omega_2 < \omega < \infty$
$\alpha = 0$
$\beta = 2\sin^{-1}\dfrac{\omega(\omega_2-\omega_1)}{\omega_0^2-\omega^2}$

When $\omega_1 < \omega < \omega_0$
$\alpha = 2\cosh^{-1}\dfrac{\omega(\omega_2-\omega_1)}{\omega_0^2-\omega^2}$
$\beta = \pi$

When $0 < \omega < \omega_1$
$\alpha = 0$
$\beta = 2\sin^{-1}\dfrac{\omega(\omega_2-\omega_1)}{\omega_0^2-\omega^2}$
</td><td></td><td>$\omega_\infty = \omega_0$</td><td>$L_{1k} = \dfrac{R(\omega_2-\omega_1)}{\omega_1\omega_2}$

$C_{1k} = \dfrac{1}{R(\omega_2-\omega_1)}$</td><td>$L_{2k} = \dfrac{R}{\omega_2-\omega_1}$

$C_{2k} = \dfrac{\omega_2-\omega_1}{\omega_1\omega_2 R}$</td></tr>
<tr><td rowspan="2">
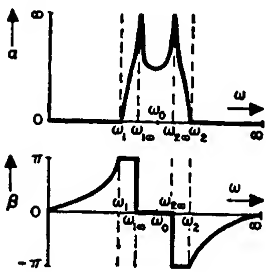

curves drawn for $m = 0.6$

When $\omega_2 < \omega < \infty$, $\alpha = 0$ and
β = same formula as for $0 < \omega < \omega_1$

When $\omega_{2\infty} < \omega < \omega_2$, $\beta = -\pi$ and
α = same formula as for $\omega_1 < \omega < \omega_{1\infty}$

When $0 < \omega < \omega_1$, $\alpha = 0$ and
$\beta = \cos^{-1}\left[1 - \dfrac{2\omega^2m^2(\omega_2-\omega_1)^2}{(\omega^2-\omega_1^2)(\omega^2-\omega_2^2)+\omega^2m^2(\omega_2-\omega_1)^2}\right]$

When $\omega_1 < \omega < \omega_{1\infty}$, $\beta = \pi$ and
$\alpha = \cosh^{-1}\left[\dfrac{2\omega^2m^2(\omega_2-\omega_1)^2}{(\omega^2-\omega_1^2)(\omega^2-\omega_2^2)+\omega^2m^2(\omega_2-\omega_1)^2} - 1\right]$

When $\omega_{1\infty} < \omega < \omega_{2\infty}$, $\beta = 0$ and
$\alpha = \cosh^{-1}\left[1 - \dfrac{2\omega^2m^2(\omega_2-\omega_1)^2}{(\omega^2-\omega_1^2)(\omega^2-\omega_2^2)+\omega^2m^2(\omega_2-\omega_1)^2}\right]$
</td><td rowspan="2">$m = \sqrt{1 - \dfrac{(\omega_{2\infty}-\omega_{1\infty})^2}{(\omega_2-\omega_1)^2}}$</td><td rowspan="2">$\omega_{1\infty}\,\omega_{2\infty} = \omega_0^2$</td><td>$L_1 = mL_{1k}$

$C_1 = \dfrac{C_{1k}}{m}$</td><td>$L_2 = \dfrac{1-m^2}{m}L_{1k}$

$C_2 = \dfrac{m}{1-m^2}C_{1k}$

$L_2' = \dfrac{L_{2k}}{m}$

$C_2' = mC_{2k}$</td></tr>
<tr><td>$L_1 = mL_{1k}$

$C_1 = \dfrac{C_{1k}}{m}$

$L_1' = \dfrac{m}{1-m^2}L_{2k}$

$C_1' = \dfrac{1-m^2}{m}C_{2k}$</td><td>$L_2 = \dfrac{L_{2k}}{m}$

$C_2 = mC_{2k}$</td></tr>
</table>

Building up a composite filter

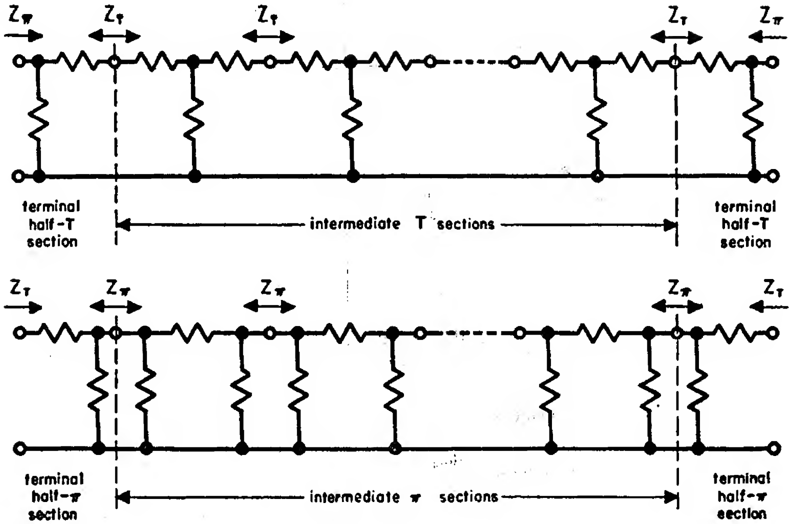

Fig. 2—Method of building up a composite filter.

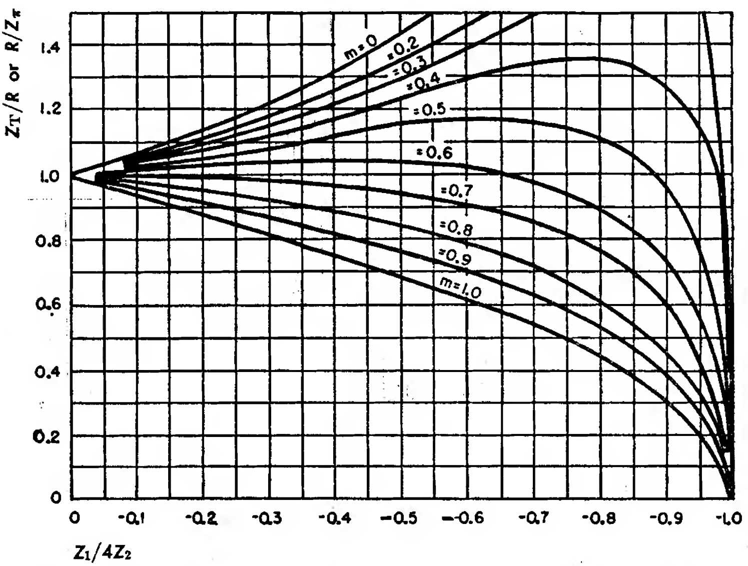

Fig. 3—Effect of design parameter *m* on the image-impedance characteristics in the pass band.

Building up a composite filter *continued*

The intermediate sections (Fig. 2) are matched on an image-impedance basis, but the attenuation characteristics of the sections may be varied by suitably choosing the infinite attenuation frequencies of each section. Thus, the frequencies attenuated only slightly by one section may be strongly attenuated by other sections. However, the image impedance will be far from constant in the passband and therefore the use of true resistors for terminations will change the attenuation shape.

Some improvement in the uniformity of the image impedance is obtained by using suitably designed terminating half sections. For these terminating sections, a value of $m \approx 0.6$ is usually used (Fig. 3).

Example of low-pass image-parameter design

To cut off at 15 kilocycles/second; to give peak attenuation at 30 kilocycles; with a load resistance of 600 ohms; and using a constant-k midsection and an m-derived midsection. Full T-sections will be used.

Constant-k midsection

$$L_k = \frac{R}{\omega_c} = \frac{600}{(6.28)\ (15 \times 10^3)} = 6.37 \times 10^{-3} \text{ henry}$$

$$C_k = \frac{1}{\omega_c R} = \frac{1}{(6.28)\ (15 \times 10^3)\ (600)} = 0.0177 \times 10^{-6} \text{ farad}$$

$$\alpha = 2 \cosh^{-1} \frac{\omega}{\omega_c} = 2 \cosh^{-1} \frac{f}{15}$$

$$\beta = 2 \sin^{-1} \frac{\omega}{\omega_c} = 2 \sin^{-1} \frac{f}{15}$$

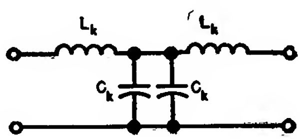

where α is in nepers, β in radians, and f in kilocycles.

m-derived midsection

$$m = \sqrt{1 - \omega_c^2/\omega_\infty^2} = \sqrt{1 - 15^2/30^2}$$
$$= \sqrt{0.75} = 0.866$$

$$L_1 = mL_k = 0.866\ (6.37 \times 10^{-3})$$
$$= 5.52 \times 10^{-3} \text{ henry}$$

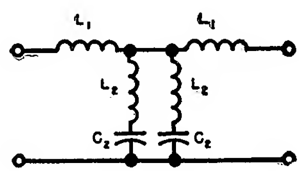

Example of low-pass image-parameter design *continued*

$$L_2 = \frac{1-m^2}{m} L_k = \left[\frac{1-(0.866)^2}{0.866}\right](6.37 \times 10^{-3}) = 1.84 \times 10^{-3} \text{ henry}$$

$$C_2 = mC_k = 0.866\ (0.0177 \times 10^{-6}) = 0.0153 \times 10^{-6} \text{ farad}$$

$$\alpha = \cosh^{-1}\left[1 - \frac{2m^2}{\frac{\omega_c^2}{\omega^2} - (1-m^2)}\right] = \cosh^{-1}\left[1 - \frac{1.5}{\frac{225}{f^2} - 0.25}\right]$$

$$\beta = \cos^{-1}\left[1 - \frac{2m^2}{\frac{\omega_c^2}{\omega^2} - (1-m^2)}\right] = \cos^{-1}\left[1 - \frac{1.5}{\frac{225}{f^2} - 0.25}\right]$$

End sections m = 0.6

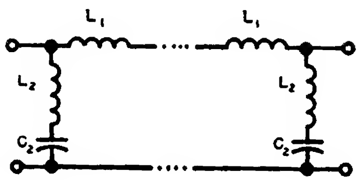

$$L_1 = mL_k = 0.6\ (6.37 \times 10^{-3})$$
$$= 3.82 \times 10^{-3} \text{ henry}$$

$$L_2 = \frac{1-m^2}{m} L_k$$
$$= \left[\frac{1-(0.6)^2}{0.6}\right](6.37 \times 10^{-3}) = 6.80 \times 10^{-3} \text{ henry}$$

$$C_2 = mC_k = 0.6\ (0.0177 \times 10^{-6}) = 0.0106 \times 10^{-6} \text{ farad}$$

Frequency of peak attenuation f_∞

$$f_\infty = \sqrt{\frac{f_c^2}{1-m^2}} = \sqrt{\frac{(15 \times 10^3)^2}{1-(0.6)^2}} = 18.75 \text{ kilocycles}$$

Filter showing individual sections

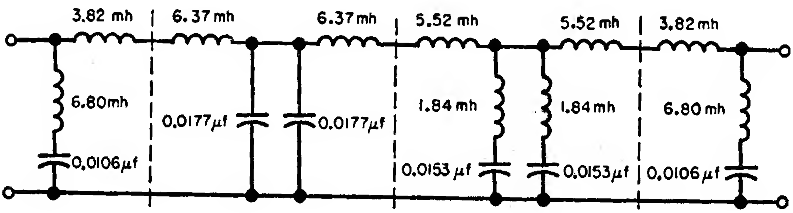

Example of low-pass image-parameter design *continued*

Filter after combining elements

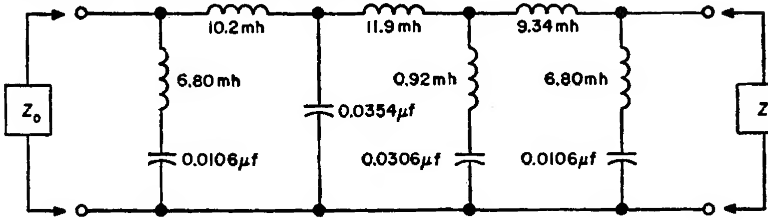

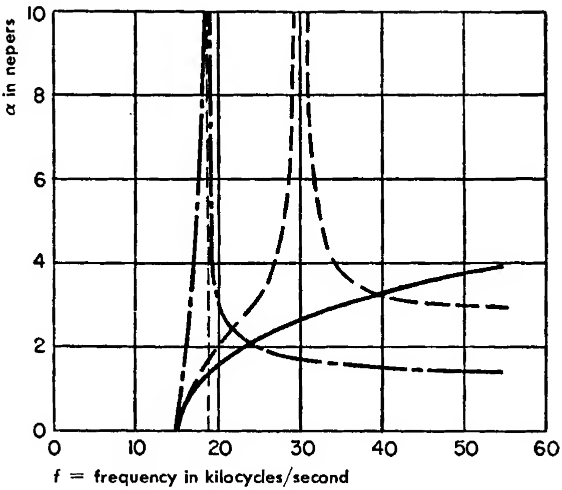

Image-terminated attenuation of each section. Solid line = constant-*k* midsection. Dashed = *m*-derived midsection. Dash-dot = *m*-derived ends.

Image attenuation and phase characteristics

Given at the right and on the following page are the image-terminated attenuation and phase characteristics. These shapes are not obtainable when 600-ohm resistors are used in place of the terminating Z_0.

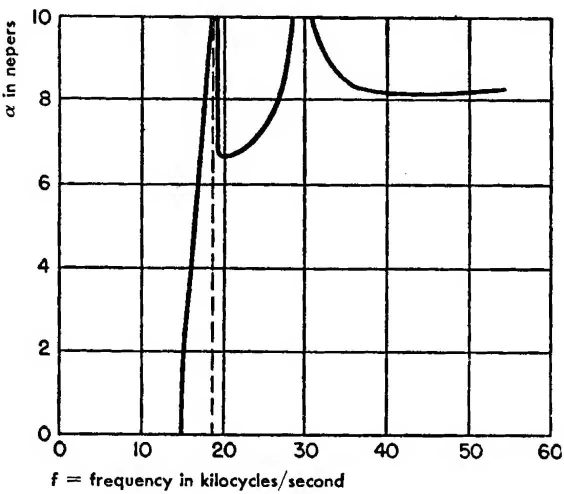

Image-terminated attenuation of composite filter.

Example of low-pass image-parameter design *continued*

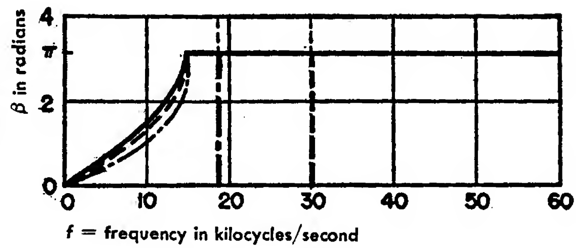

Image-terminated phase characteristic of each section. Solid line = constant-k midsection. Dashed = M-derived midsection. Dash — dot = m-derived ends.

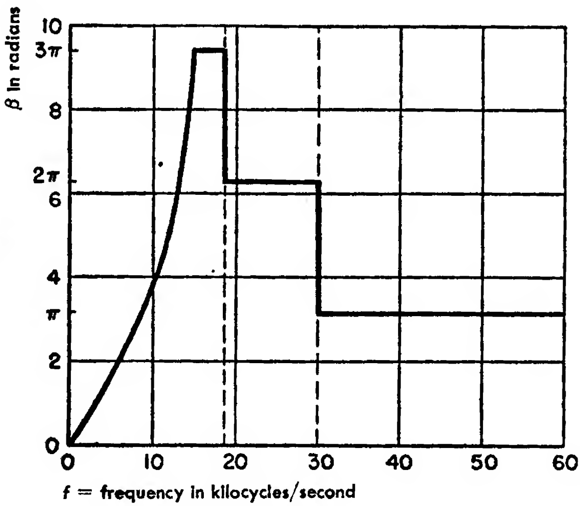

Image-terminated phase characteristic of composite filter.

Impedance required for proper termination

$$Z_o = \frac{R\left[1 - \dfrac{\omega^2}{\omega_c^2}(1 - m^2)\right]}{\sqrt{1 - \omega^2/\omega_c^2}}$$

$$= \frac{600\,[1 - 0.64\,(f/15)^2]}{\sqrt{1 - (f/15)^2}}$$

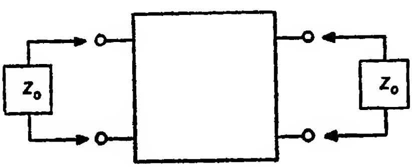

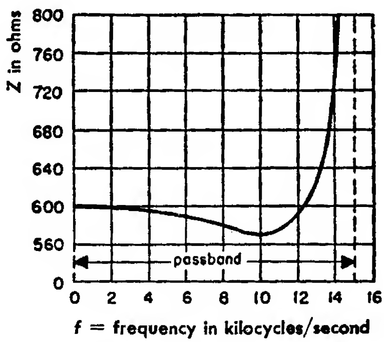

Filters, modern-network-theory design

The design information in this chapter results from the application of modern network theory to electric wave filters. Only design *results* are supplied and a careful study of the references cited will be required for an understanding of the synthesis procedures that underlie these results.

Limitations of image-parameter theory

Consider the simple low-pass ladder network of Fig. 1A. Two simultaneous design equations, (1) and (2), are provided by classical image-parameter theory (p. 165).

$$(Z_1/4Z_2)_{f=f_c} = -1 \text{ and } 0 \tag{1}$$

$$Z_{0T} = (Z_1 Z_2)^{1/2} [1 + (Z_1/4Z_2)]^{1/2} \tag{2}$$

Z_1 and Z_2, the full series- and shunt-arm impedances, respectively, must be suitably related to make (1) true at the desired cutoff frequencies and the generator and load impedance must satisfy (2). Under the image-parameter theory, the resulting attenuation for the low-pass case is

$$\left.\begin{aligned} V_p/V &= 1.0, & (\omega/\omega_c) &< 1 \\ &= \exp[(n-1)\cosh^{-1}(\omega/\omega_c)], & (\omega/\omega_c) &> 1 \end{aligned}\right\} \tag{3}$$

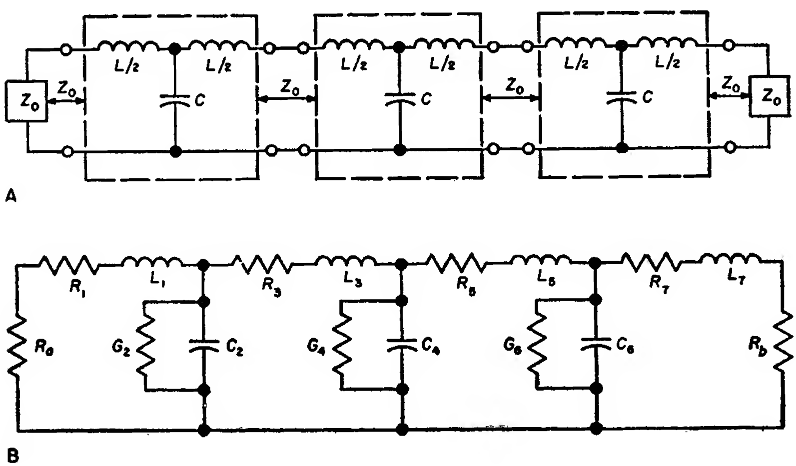

Fig. 1—A 7-element low-pass filter considered on the basis of image-parameter theory at A and of modern network theory at B.

Limitations of image-parameter theory *continued*

where n is the number of arms in the network of Fig. 1 and V_p/V and ω are as in Fig. 3. It is this attenuation shape that is plotted in the tabulations of chapter 6.

Equation (1) offers no problems. The application of (2) to Fig. 1 demands *terminating impedances that are physically impossible with a finite number of elements*. The generator and load impedances for Fig. 1A must be pure resistances of $(L/C)^{1/2}$ ohms at zero frequency. As frequency increases, the value of resistance must decrease to a short-circuit at the cutoff frequency, and with further increase in frequency must behave like a pure inductance starting at zero value at the cutoff frequency and increasing to $L/2$ at infinite frequency.

The physical impracticability of devising such terminating impedances is why element values obtained by (1) cannot simultaneously satisfy (2). The relative attenuation indicated by (3) is similarly incorrect and cannot be realized in practice.

Lattice-configuration filters also require impractical terminating impedances when designed by image-parameter theory. (Constant-resistance lattices are an exception but are seldom used for filtering.) The practical use of resistive terminations automatically makes element values computed on the basis of ideal impedance terminations incorrect.

For more than three decades, filters have been designed according to the image-parameter theory. Their commercial acceptance is due in no small part to the highly approximate requirements for most filters. Where more-exact characteristics are required, shifting of element values in the actual filter has usually resulted in an acceptable design. For precise amplitude and phase response in the pass band, the simple and approximate solutions obtained through image-parameter theory must give way to equations based on modern network theory.

Modern-network-theory design

Relative attenuation

A typical low-pass filter with resistive generator and load is shown in Fig. 1B. It is composed of lumped inductors, capacitors, and the resistive elements unavoidably associated therewith. The circuit equations for the complete network can be written by the application of Kirchhoff's laws. Modern network theory does just this and then solves the equations to find the network parameters that will produce optimum performance in some desired respect.

Modern-network-theory design *continued*

A block diagram of a generalized filter is illustrated in Fig. 2. This may be of low-pass, high-pass, band-pass, band-rejection, phase-compensating, or other type. The elements of the filter include resistors, capacitors, self- and mutual-inductors, and possibly coupling elements such as electron tubes or transistors, all according to the design. The terminations shown are a constant-voltage generator (the same voltage at all frequencies) with a series resistor at the input and a resistive load. (Frequently it is preferable to stipulate a constant-current generator with a shunt conductance.) The generator and load resistors need not be equal and they can be assigned any value between zero and infinity. Characteristic impedance plays no part in the modern network theory of filters.

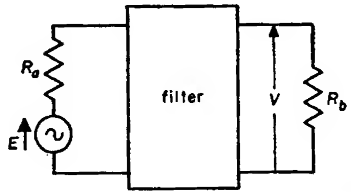

Fig. 2—Block diagram of a filter with generator and load.

Either or both the generator or load can be reactive, in which case the reactances are absorbed inside the block of Fig. 2 as specified parts of the filter. Either, but not both, R_a or R_b can be zero or infinite.

The term *bandwidth* as used herein has two different meanings, according to the type of filter. For low- or high-pass filters, it is synonymous with the actual frequency of the point in question, or equivalent to the number of cycles per second in a band terminated on one side by zero frequency and on the other by the actual frequency. The actual frequency can be anywhere in the pass or the reject region. For symmetrical band-pass (Fig. 4) and band-reject filters, it is the difference in cycles per second between two particular frequencies (anywhere in the pass or reject regions) with the requirement that their geometrical mean be equal to the geometrical midfrequency f_0 of the pass or reject band.

A typical filter characteristics is plotted in Fig. 3 for a low-pass filter. In Fig. 3A, the magnitude of the output voltage V is plotted against radian bandwidth ω. Several specific points are indicated on the diagram. V_p is the peak voltage output, while V_m is the maximum voltage that could be developed across the load were it matched to the generator through an ideal network. Symbol ω_β designates a specified frequency or bandwidth where some particular characteristic is exhibited by the filter, such as the point where the response is 3 decibels down from the peak, for example.

Modern-network-theory design *continued*

The characteristic of major interest to the filter engineer is the plot, shown in Fig. 3B, of relative attenuation versus relative bandwidth. Relative attenuation is defined as the ratio of the peak output voltage V_p to the voltage output V at the frequency being considered. Relative bandwidth is defined as the ratio of the bandwidth being considered to a clearly specified reference bandwidth (e.g., the 3-decibel-down bandwidth).

It should be noted that the elements of a filter are not uniquely fixed if only a certain relative attenuation shape is specified; in general it is possible also to demand that at one frequency the absolute magnitude of some transfer function be optimized.

The complex relative attenuation of a complete filter (including generator and load) composed of lumped linear passive elements is always equal to a constant multiplied by the ratio of two polynomials in $(j\omega)$. Modern filter theory has derived various expressions for optimum relative attenuation shapes that can be physically realized from these complex expressions. The shapes are optimum in that they give the maximum possible rate of cutoff between the accept and reject bands for a given number of filter components, with a specified allowable equal ripple in the accept band, and a specified required equal ripple in the reject band. See Fig. 4 for typical shapes of attenuation characteristic for band-pass filters.

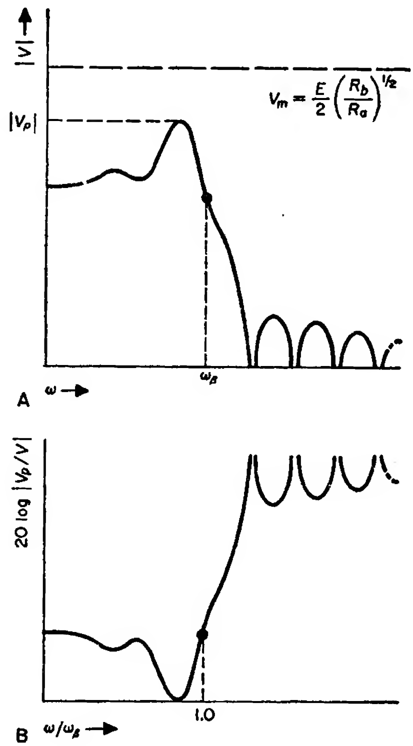

Fig. 3—Low-pass-filter output voltage versus frequency at *A*; attenuation versus normalized frequency at *B*. *A* is the actual voltage across the load as a function of frequency and is for the low-pass case. *B* uses the information in *A* to produce a plot of *relative* attenuation against *relative* bandwidth.

The phase and transient response, in a majority of filter applications, are not as important as the amplitude response. Most of the following treatment refers to this latter type of problem.

Chebishev and Butterworth performance with constant-K and equivalent configurations

The attenuation-curve shapes illustrated in Figs. 4A and 4B are termed Chebishev and that in Fig. 4C is termed Butterworth. The equations for these

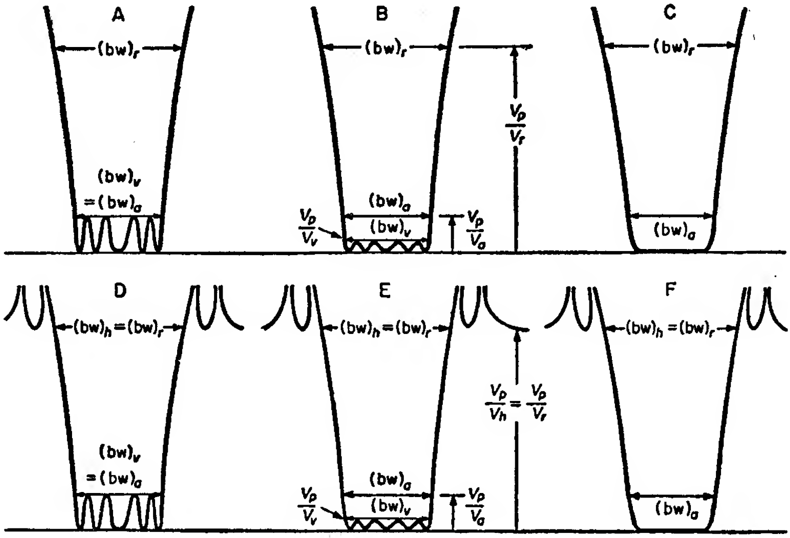

Fig. 4—*A, B, C,* are the optimum relative attenuation shapes of (4) and (5) that can be produced by constant-K-type networks. *D, E, F,* are the optimum relative attenuation shapes of (8), (12), (13), (16) that can be derived by M-derived-type networks.

shapes are (4) and (5), respectively. The Butterworth shape is the same as the limiting case of the Chebishev shape when we set $V_p/V_v = 1.0$.

Chebishev:

$$\left(\frac{V_p}{V}\right)^2 = 1 + \left[\left(\frac{V_p}{V_v}\right)^2 - 1\right] \cosh^2\left(n \cosh^{-1} \frac{x}{x_v}\right) \tag{4}$$

Butterworth:

$$\left(\frac{V_p}{V}\right)^2 = 1 + \left(\frac{x}{x_{3\text{db}}}\right)^{2n} \tag{5}$$

where

V = output voltage at point x

V_p = peak output voltage in pass band

Chebishev and Butterworth performance with constant-K and equivalent configurations *continued*

V_v = valley output voltage in pass band

n = number of poles, equal to the number of arms in the ladder network being used. For low-pass and high-pass filters, n = number of reactances in the filter. For band-pass and band-reject, n = total number of resonators in the filter.

x = a variable found in the following tabulations.

x_v = value of x at point on skirt where attenuation equals valley attenuation.

x_{3db} = value of x at point on skirt where attenuation is 3 decibels below V_p.

Significance of x

Low-pass filters:

$x = \omega = 2\pi f$

High-pass filters:

$x = -1/\omega = -1/2\pi f$

Symmetrical band-pass filters:

$x = (\omega/\omega_0 - \omega_0/\omega) = (f_2 - f_1)/f_0 = (\text{bw})/f_0$

Symmetrical band-reject filters:

$x = -1/(\omega/\omega_0 - \omega_0/\omega) = -f_0/(\text{bw})$

where

$f_0 = (f_1 f_2)^{1/2}$ = midfrequency of the pass or reject band

f_1, f_2 = two frequencies where the characteristic exhibits the same attenuation.

Working charts for these filters, derived from (4) and (5) are presented in Figs. 5 to 10 for value of n from 2 to 7, respectively.

These curves give

$(V_p/V)_{db} = 20 \log_{10} (V_p/V)$

versus x/x_{3db}

For low-pass and band-pass filters,

$x/x_{3db} = (\text{bw})/(\text{bw})_{3db}$

Chebishev and Butterworth performance with constant-K and equivalent configurations *continued*

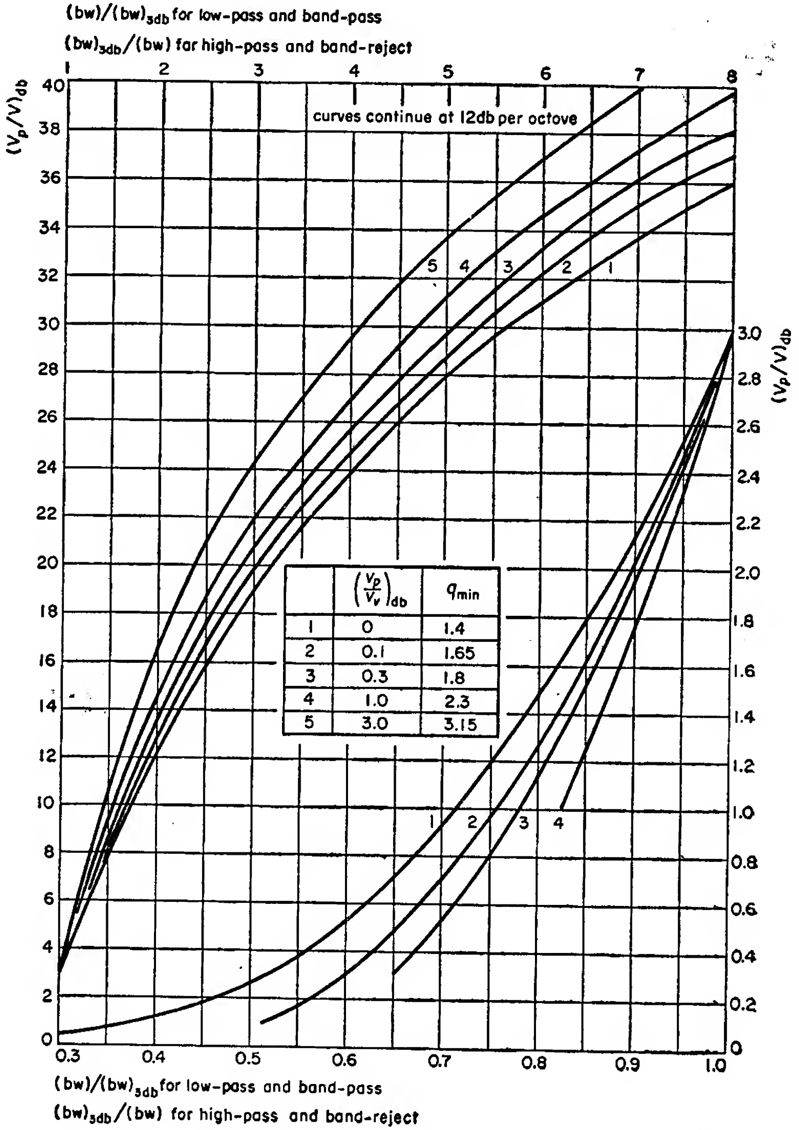

Fig. 5—Relative attenuation for a 2-pole network.

Chebishev and Butterworth performance with constant-K and equivalent configurations *continued*

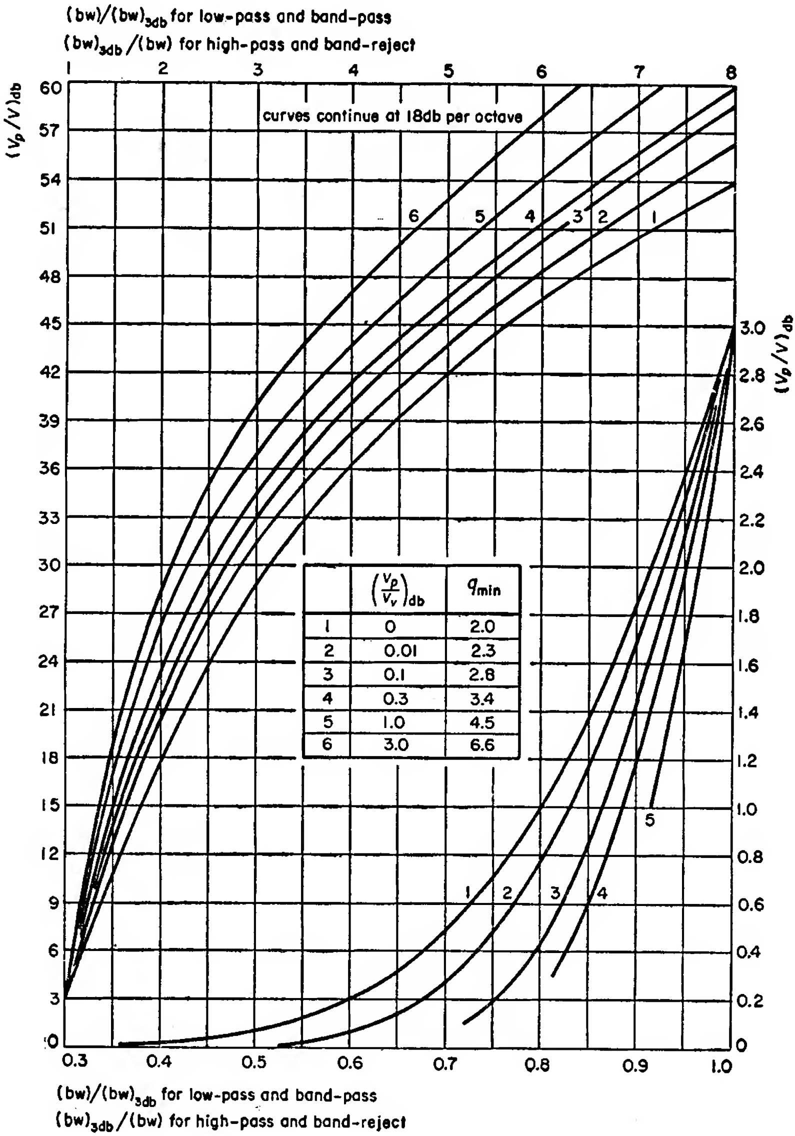

	$\left(\frac{V_p}{V_v}\right)_{db}$	q_{min}
1	0	2.0
2	0.01	2.3
3	0.1	2.8
4	0.3	3.4
5	1.0	4.5
6	3.0	6.6

Fig. 6—Relative attenuation for a 3-pole network.

Chebishev and Butterworth performance with constant-K and equivalent configurations *continued*

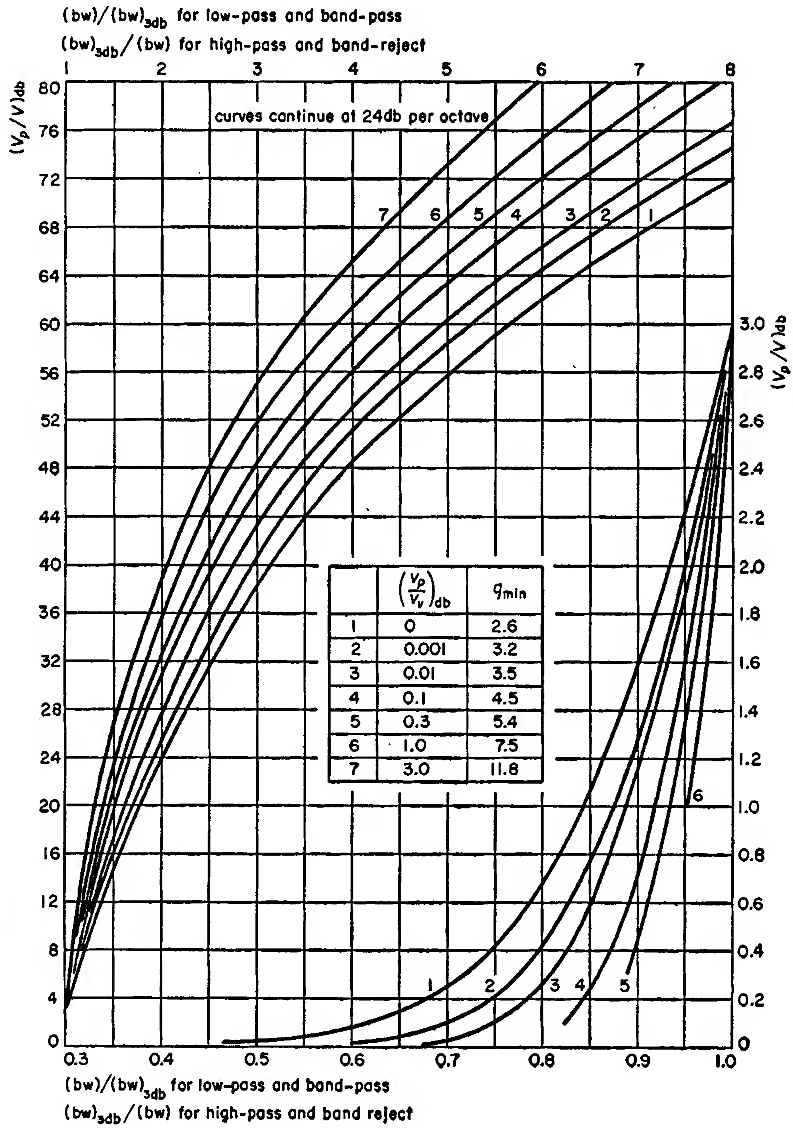

	$\left(\frac{V_p}{V_v}\right)_{db}$	q_{min}
1	0	2.6
2	0.001	3.2
3	0.01	3.5
4	0.1	4.5
5	0.3	5.4
6	1.0	7.5
7	3.0	11.8

Fig. 7—Relative attenuation for a 4-pole network.

Chebishev and Butterworth performance with constant-K and equivalent configurations *continued*

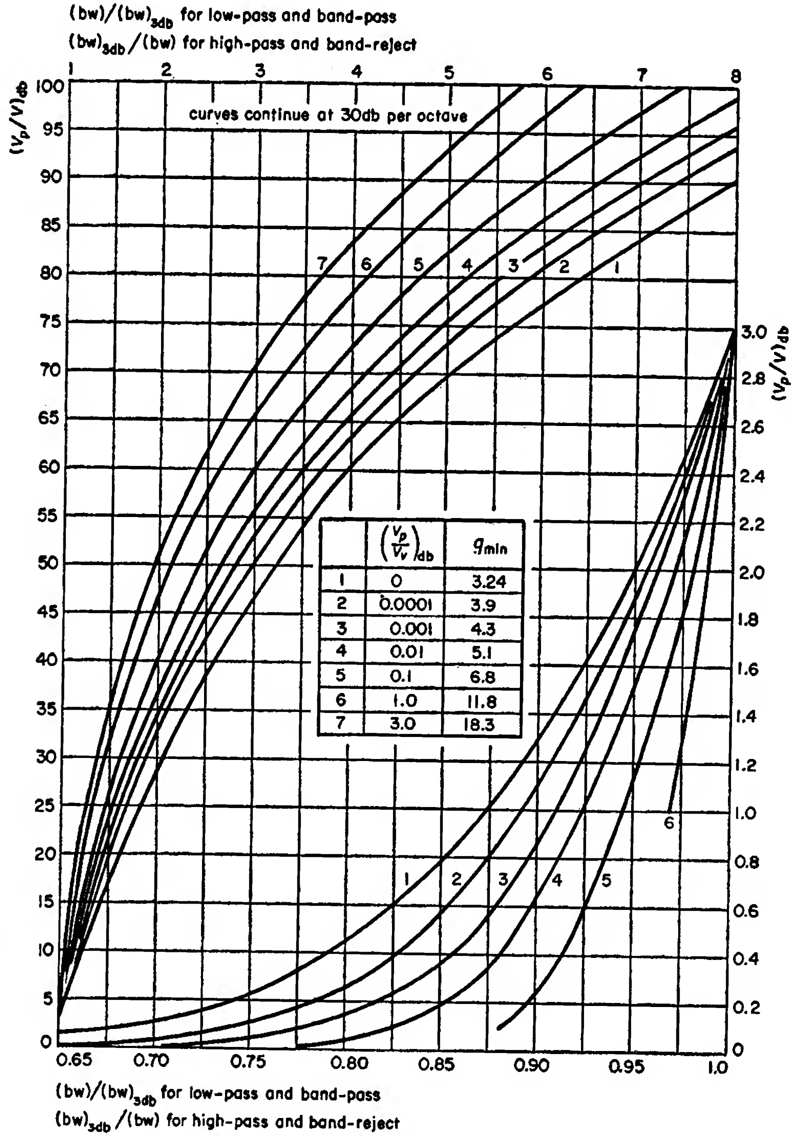

	$\left(\frac{V_p}{V_v}\right)_{db}$	g_{min}
1	0	3.24
2	0.0001	3.9
3	0.001	4.3
4	0.01	5.1
5	0.1	6.8
6	1.0	11.8
7	3.0	18.3

Fig. 8—Relative attenuation for a 5-pole network.

Chebishev and Butterworth performance with constant-K and equivalent configurations *continued*

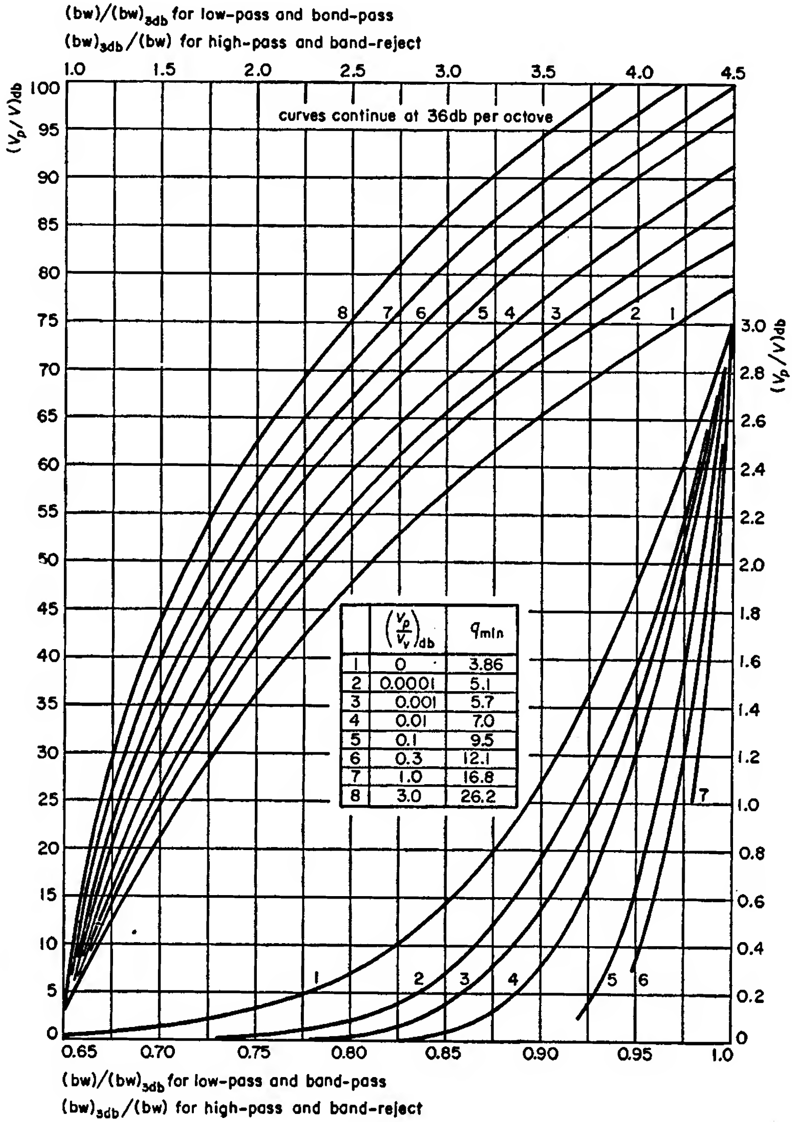

	$\left(\frac{V_p}{V_v}\right)_{db}$	q_{min}
1	0	3.86
2	0.0001	5.1
3	0.001	5.7
4	0.01	7.0
5	0.1	9.5
6	0.3	12.1
7	1.0	16.8
8	3.0	26.2

Fig. 9—Relative attenuation for a 6-pole network.

Chebishev and Butterworth performance with constant-K and equivalent configurations *continued*

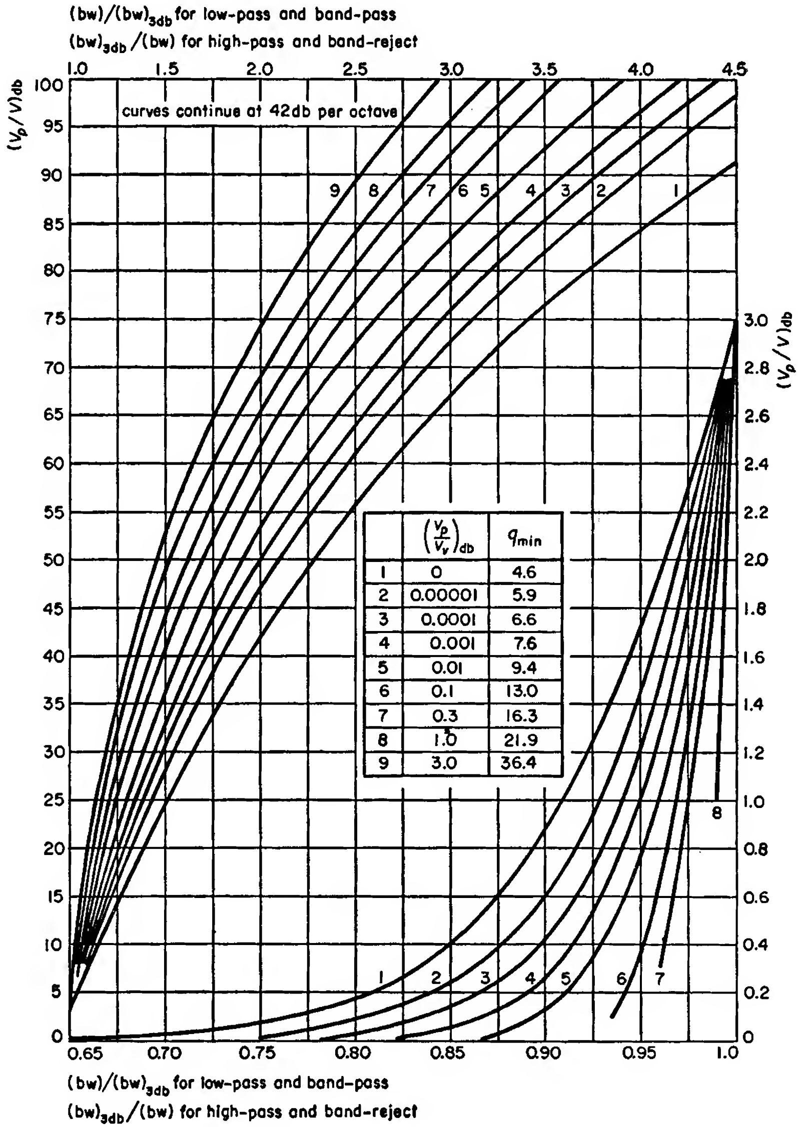

	$\left(\frac{V_p}{V_v}\right)_{db}$	q_{min}
1	0	4.6
2	0.00001	5.9
3	0.0001	6.6
4	0.001	7.6
5	0.01	9.4
6	0.1	13.0
7	0.3	16.3
8	1.0	21.9
9	3.0	36.4

Fig. 10—Relative attenuation for a 7-pole network.

Chebishev and Butterworth performance with constant-K and equivalent configurations *continued*

For high-pass and band-reject filters, the scale of the abscissa gives

$(\text{bw})_{3\text{db}}/(\text{bw})$

On each chart, Figs. 5 to 10, the family of curves toward the right side gives the attenuation shape for points where it is less than 3 decibels, while those toward the left are for the reject band (greater than 3 decibels). Each curve of the former family has been stopped where the attenuation is equal to that of the peak-to-valley ratio.

Thus, in Fig. 5, curve 3 has been stopped at 0.3 decibel, which is the value of $(V_p/V_v)_{\text{db}}$ for which the curve was computed. (See table on chart, Fig. 5).

The curves give actual optimum attenuation characteristics based on rigorous computation of the ladder network. In contrast, the commonly used attenuation curves based on "image-parameter theory" are approximations that are actually unattainable in practice.

Low- and band-pass filters—required unloaded Q

Constant-K and equivalent filters can be constructed that will actually give the attenuation shapes predicted by modern network theory. To attain this result, it is required that the unloaded Q of each element be greater than a certain minimum value*. The q_{min} column on each chart is used in the following manner to obtain this minimum allowable value: For the internal reactances of low-pass circuits,

$$Q_{\text{min}} = q_{\text{min}}$$

For the internal resonators of band-pass circuits,

$$Q_{\text{min}} = q_{\text{min}}\,[f_0/(\text{bw})_{3\text{db}}]$$

* S. Darlington, "Synthesis of Reactance 4-Poles," *Journal of Mathematics and Physics*, vol. 18, pp. 257-353; September, 1939. Also, M. Dishal, "Design of Dissipative Band-Pass Filters Producing Desired Exact Amplitude-Frequency Characteristics," *Proceedings of the IRE*, vol. 37, pp. 1050-1069; September, 1949: also, *Electrical Communication*, vol. 27, pp. 56–81; March, 1950. Also, M. Dishal, "Concerning the Minimum Number of Resonators and the Minimum Unloaded Q Needed in a Filter," *Transactions of the IRE Professional Group on Vehicular Communication*, vol. PGVC–3, pp. 85–117; June, 1953: also, *Electrical Communication*, vol. 31, pp. 257–277; December, 1954.

Chebishev and Butterworth performance with constant-K and equivalent configurations *continued*

Examples

a. In a low-pass filter without any peaks of infinite attenuation at a finite frequency, how few elements are required to satisfy the following specifications, and what minimum Q must they have? Response to be 1 decibel down at 30 kilocycles, and 50 decibels down at not more than 75 kilocycles, compared to the peak response.

The allowable ripple is 1 decibel in the pass band.

Then,

$(\mathrm{bw})_{50\mathrm{db}}/(\mathrm{bw})_{1\mathrm{db}} < 75/30 = 2.5$

$(V_p/V_v)_{\mathrm{db}} \leqslant 1.0$ decibel

Since $(\mathrm{bw})_{1\mathrm{db}}$ will be slightly less than $(\mathrm{bw})_{3\mathrm{db}}$, we must have $(\mathrm{bw})_{50\mathrm{db}}/(\mathrm{bw})_{3\mathrm{db}}$ a little less than 2.5 when $(V_p/V)_{\mathrm{db}} = 50$ decibels. Consulting the charts, Figs. 5 to 10, and examining curves for $(V_p/V_v)_{\mathrm{db}} = 1.0$, it is found that a 5-pole network (Fig. 8) is the least that will meet the requirements. Here, curve 6 gives

$(\mathrm{bw})_{50\mathrm{db}}/(\mathrm{bw})_{3\mathrm{db}} = 2.14$

while

$(\mathrm{bw})_{1\mathrm{db}}/(\mathrm{bw})_{3\mathrm{db}} = 0.97.$

Then

$(\mathrm{bw})_{50\mathrm{db}}/(\mathrm{bw})_{1\mathrm{db}} = 2.14/0.97 = 2.20$

The 3-decibel frequency will be

$30\ (\mathrm{bw})_{3\mathrm{db}}/(\mathrm{bw})_{1\mathrm{db}} = 30/0.97 = 31$ kilocycles

At this frequency, the Q of each capacitor and inductor must be at least equal to $Q_{\min} = 11.8$ as shown in the table on Fig. 8.

b. Consider a band-pass filter with requirements similar to the above: bandwidth 1-decibel down to be 30 kilocycles, 50 decibels down at 75 kilocycles bandwidth, and 1-decibel allowable ripple. Further, let the midfrequency be $f_0 = 500$ kilocycles. The solution at first is the same as above, and a 5-pole network is required.

Chebishev and Butterworth performance with constant-K and equivalent configurations *continued*

The 3-decibel bandwidth is 31 kilocycles and the Q of each resonator must be at least

$11.8\ f_0/(\text{bw})_{3\text{db}} = 11.8 \times 500/31 = 190$

where 11.8 is $q_{\min}$ as read from the table on Fig. 8. If a Q of 190 is not practical to attain, a greater number of resonators can be used. Suppose 7 resonators or poles are tried, per Fig. 10. Then curve 2 gives

$(\text{bw})_{50\text{db}}/(\text{bw})_{1\text{db}} = 2.10/0.93 = 2.26.$

The table shows the peak-to-valley ratio of 10^{-5} decibel and $q_{\min} = 5.9$. The 3-decibel bandwidth is $30/0.93 = 32.2$ kilocycles. Then, the minimum Q of each resonator can be $5.9 \times 500/32.2 = 92$, which is less than half that required if 5 resonators are used.

c. In the band-pass filter, suppose the filter is subdivided into N identical stages in cascade, isolated by electron tubes or decoupling capacitors or resistors. For each stage the response requirements are the original number of decibels divided by N. For $N = 2$ stages,

$(\text{bw})_{25\text{db}}/(\text{bw})_{0.5\text{db}} < 2.5$

$(V_p/V_v)_{\text{db}} \leqslant 0.5$ decibel

Proceeding as before, it is found that a 3-pole network (Fig. 6) for each stage will just suffice, curve 4 giving

$(V_p/V_v)_{\text{db}} = 0.3$

and

$(\text{bw})_{25\text{db}}/(\text{bw})_{0.5\text{db}} = 2.1/0.84 = 2.5$

To find the required minimum Q of each of the 6 resonators, the 3-decibel bandwidth of each stage is

$30/0.84 = 35.8$ kilocycles

For curve 4, $q_{\min} = 3.4$, so the minimum allowable Q for each resonator is

$3.4 \times 500/35.8 = 47.5$

Maximally linear phase response

In the design of filters where the linearity of the phase characteristic inside the pass band is important, certain changes in design are necessary compared

Chebishev and Butterworth performance with constant-K and equivalent configurations *continued*

to the previously considered cases. For constant-K-type filters, rate of change of phase with frequency becomes more-and-more linear as the number of arms is increased, provided the design produces a complex relative attenuation characteristic given by the polynomical of (6*).

$$\frac{V_p}{V} = \frac{n!}{(2n)!}\sum_{r=0}^{n} \frac{2^r\,(2n-r)!}{r!\,(n-r)!}\left(j\frac{x}{x_\beta}\right)^r \tag{6}$$

where r is a series of integers and the other symbols are described under (5). The magnitude of (6) is plotted in Figs. 11 and 12 for several values of n.

The former is for the relative attenuation inside the 3-decibel points and the latter for the response outside these points. The curves for $n = \infty$ are plotted from (7), which is the Gaussian shape that the attenuation characteristic approaches as n approaches infinity.

$$10 \log (V_p/V)^2 = 3\ (x/x_{3db})^2 \tag{7}$$

With a constant-K-configuration network that produces only poles, a maximally linear phase response can be produced only at the limitation of a rounded attenuation shape in the pass band as illustrated in Figs. 11 and 12.

The column labeled q_{min} on Fig. 11 gives the minimum allowable Q, measured at the 3-decibel-down frequency, of the inductors and capacitors of a low-pass filter. For band-pass filters, the minimum allowable unloaded Q at the midfrequency f_0 is $q_{min}\ f_0/(\mathrm{bw})_{3db}$. For the phase response figures on Fig. 11, the symbols are as follows.

Low-pass filter

$t_0 = d\theta/d\omega$
 = slope of phase characteristic at zero frequency in radians per radian per second.

t_{3db} = slope at f_{3db}

f_{3db} = frequency of 3-decibel-down response

Band-pass filter

t_0 = slope at midfrequency

t_{3db} = slope at 3-decibel-down bandwidth

$f_{3db} = \frac{1}{2}\ (\mathrm{bw})_{3db}$
 = one-half the total 3-decibel bandwidth

* W. E. Thomson, "Networks with Maximally Flat Delay," *Wireless Engineer*, vol. 29, pp. 256–263; October, 1952.

Chebishev and Butterworth performance with constant-K and equivalent configurations *continued*

The column $(t_0 - t_{3db})\ f_{3db}$ shows the *group-delay* distortion over the pass band. It shows numerically that the phase slope becomes much more constant as the number of elements is increased, in a filter designed for this purpose.

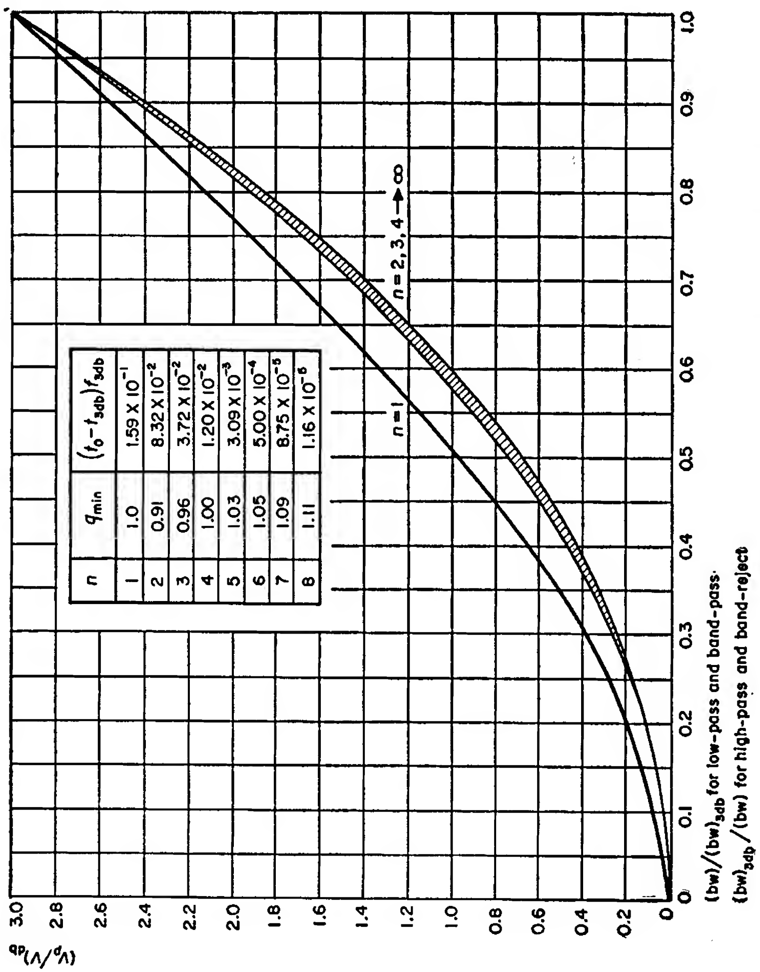

n	q_{min}	$(t_0 - t_{3db})f_{3db}$
1	1.0	1.59×10^{-1}
2	0.91	8.32×10^{-2}
3	0.96	3.72×10^{-2}
4	1.00	1.20×10^{-2}
5	1.03	3.09×10^{-3}
6	1.05	5.00×10^{-4}
7	1.09	8.75×10^{-5}
8	1.11	1.16×10^{-6}

Fig. 11—Attenuation shape within the 3-decibel-down pass band for *n*-pole flat-time-delay filters.

Chebishev and Butterworth performance with constant-K and equivalent configurations *continued*

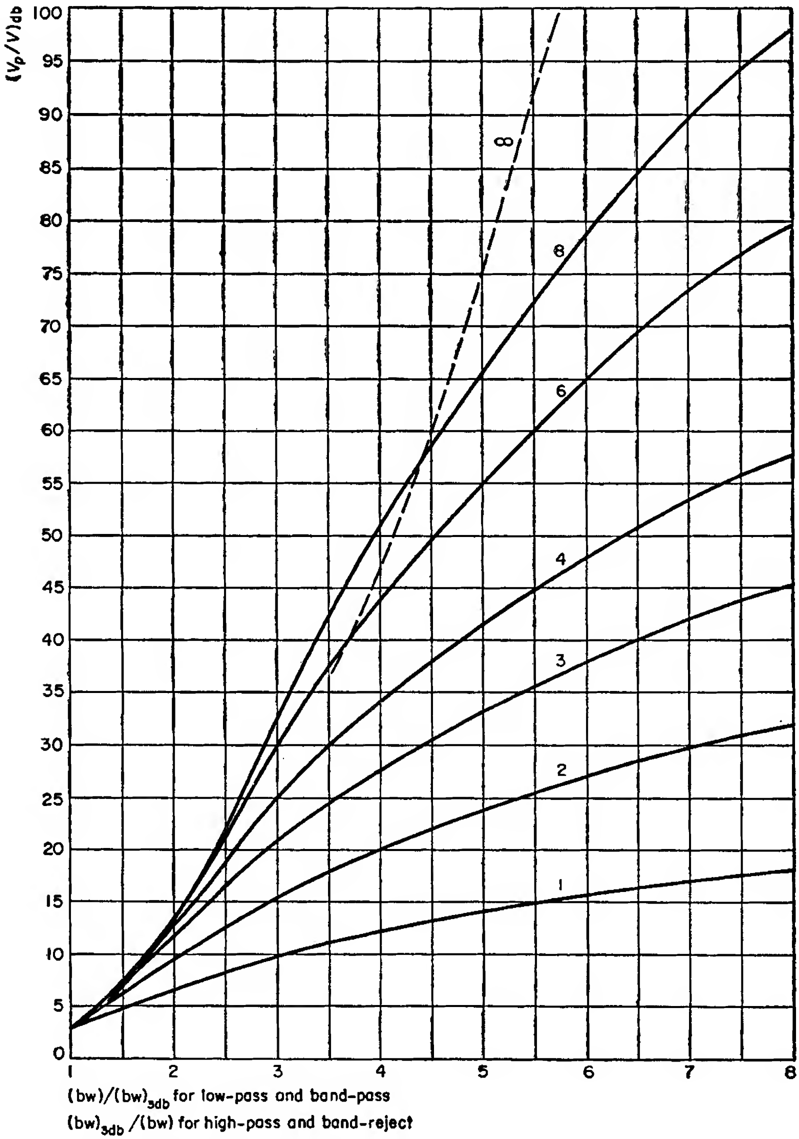

Fig. 12—Attenuation shape beyond 3-decibel-down pass band for n-pole flat-time-delay filters.

M-derived and equivalent filters

Typical attenuation curves for M-derived filters are shown in Figs. 4D, E, F. The modern network theory of these filters has been treated by Norton and Darlington.* The attenuation shapes produced may be called elliptic and inverse-hyperbolic and are optimum in the sense that the rate of cutoff between the accept and reject bands is a maximum. Equation (8) gives the elliptic-function shape.

$$\left(\frac{V_p}{V}\right)^2 = 1 + \left[\left(\frac{V_p}{V_v}\right)^2 - 1\right] cd_v{}^2\left[n\frac{K_v}{K_f}\,cd_f{}^{-1}\left(\frac{x}{x_v}\right)\right] \tag{8}$$

where

cd = (cn/dn), the ratio of the two elliptic functions cn and dn†

n = number of poles, or arms in the M-derived configuration

x = a bandwidth variable described under (5)

K_v, K_f = complete elliptic integrals of the first kind, evaluated for the modulus value given by the respective subscript.

Referring to the symbols on Fig. 4, the moduli v and f are given in (9) and (10).

$$v = \left[\frac{(V_p/V_v)^2 - 1}{(V_p/V_h)^2 - 1}\right]^{1/2} \tag{9}$$

$$f = x_v/x_n = (\mathrm{bw})_v/(\mathrm{bw})_h \tag{10}$$

These are not independent, but must satisfy the equation

$$\log q_v = n \log q_f \tag{11}$$

where q_k is called the modular constant of the modulus value k, the latter being equal to v or f, respectively. A tabulation of log q is available in the literature.‡

In the limit, when $V_p/V_v = 1.0$ or zero decibels (Fig. 4F), the ripples in the accept band vanish. Then (8) reduces to the inverse hyperbolic shape of (12).

$$\left(\frac{V_p}{V}\right)^2 = 1 + \frac{(V_p/V_h)^2 - 1}{\cosh^2\left[n \cosh^{-1}(x_h/x)\right]} \tag{12}$$

Curves plotted from (8) and (12) are presented in Figs. 13 to 18. Those labeled $V_p/V_v = 0$ decibels, for n poles, m zeros, are plotted from (12)

* S. Darlington, "Synthesis of Reactance 4-Poles" *Journal of Mathematics and Physics,* vol. 18, pp. 257–353; September, 1939.

† G. W. and R. M. Spencely, "Smithsonian Elliptic Function Tables," (Publication 3863), Smithsonian Institution; Washington, D. C.: 1947.

‡ E. Jahnke and F. Emde, "Table of Functions with Formulas and Curves," 4th Edition, Dover Publications; New York, N. Y., 1945: see pp. 49–51.

M-derived and equivalent filters *continued*

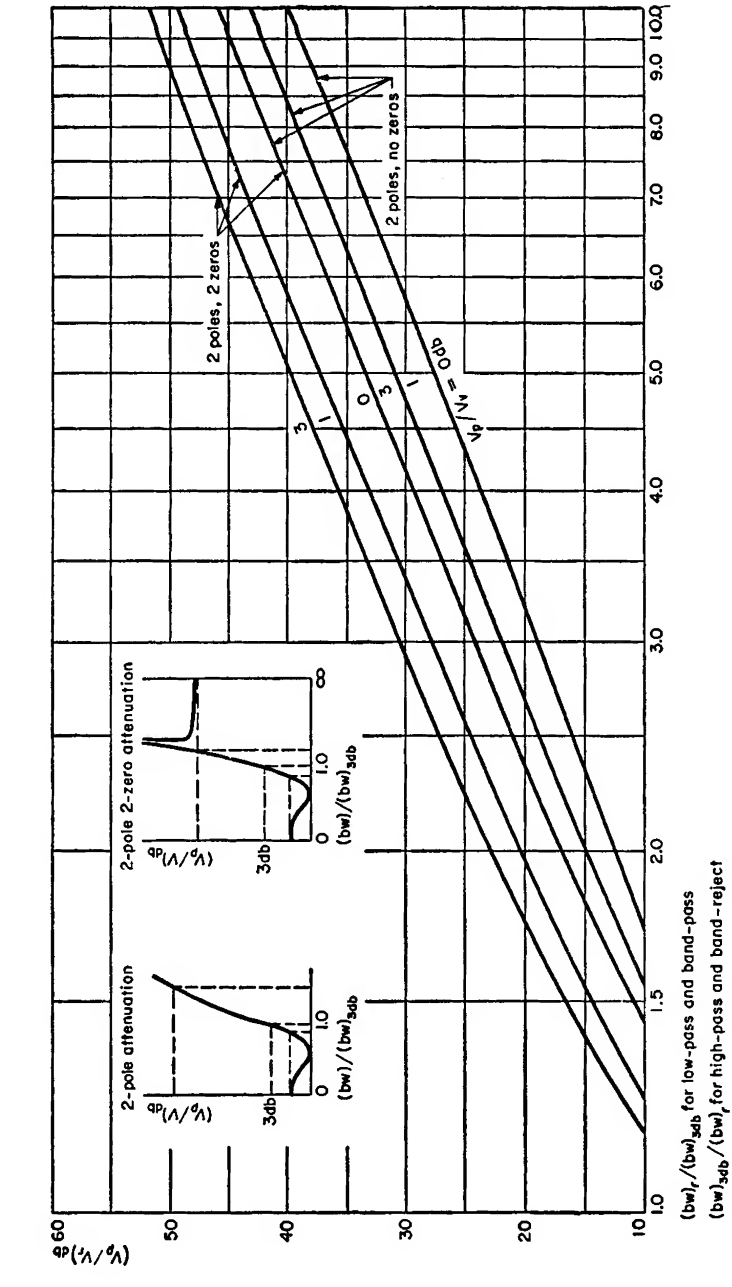

Fig. 13—Maximum rate of cutoff for 2-pole and for 2-pole 2-zero filters.

M-derived and equivalent filters *continued*

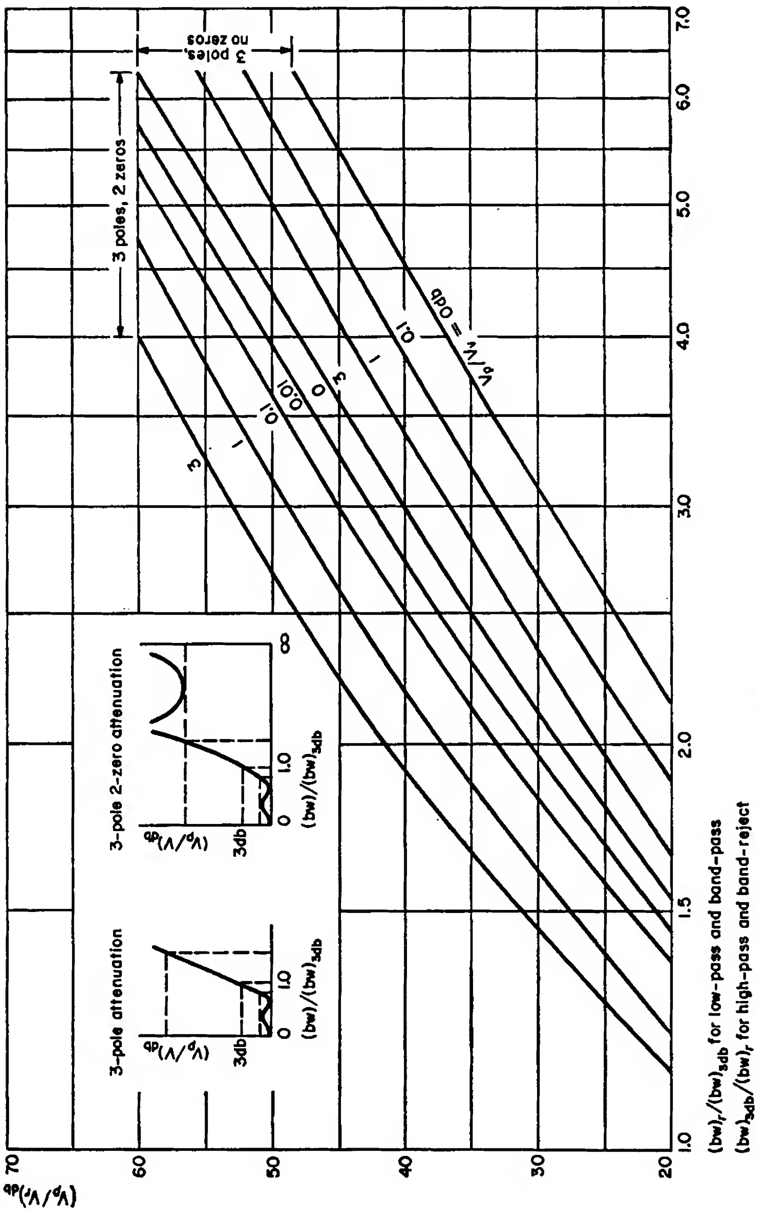

Fig. 14—Maximum rate of cutoff for 3-pole and for 3-pole 2-zero filters.

M-derived and equivalent filters *continued*

while the others are from (8). For the M-derived shapes, n = the number of poles = the number of arms in the ladder network. When n is an even number, the number of zeros $m = n$. When n is odd, $m = n - 1$. The following description of Fig. 13 can be extended to cover the entire group of figures mentioned above.

The maximum rates of cutoff obtainable with 2-pole no-zero and 2-pole

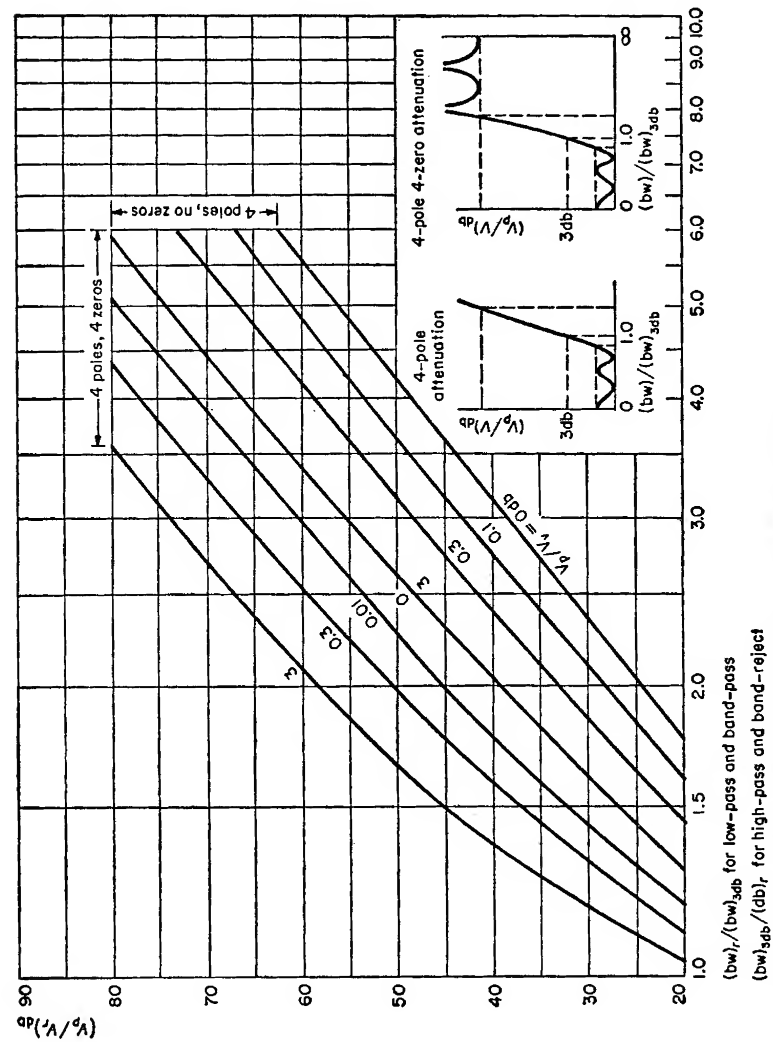

Fig. 15—Maximum rate of cutoff for 4-pole and for 4-zero filters.

M-derived and equivalent filters *continued*

2-zero networks are plotted in Fig. 13 for several ratios of V_p/V_v. Two insert sketches drawn in the figure show typical shapes of the attenuation curves for these two cases. The main curves give the relative coordinates of only two points on the skirt of the attenuation curve. These two points are the 3-decibel-down bandwidth and the "hill bandwidth" (where the response first equals that of the "response hills", where occur the uniform minimum

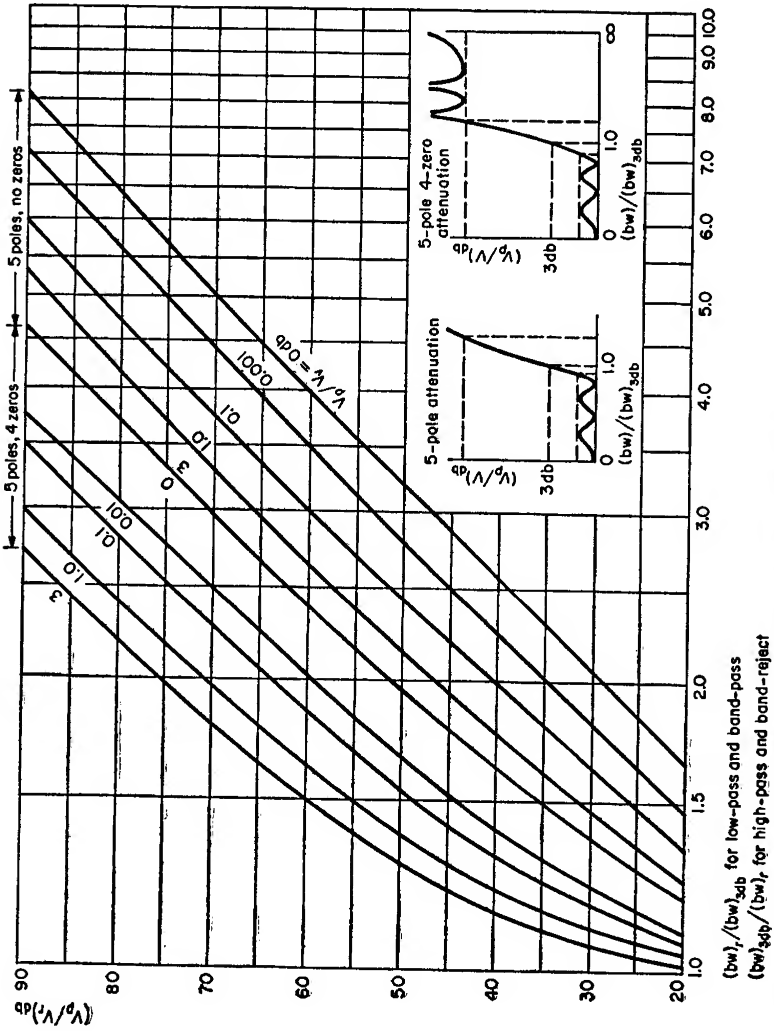

Fig. 16—Maximum rate of cutoff for 5-pole and for 5-pole 4-zero filters.

M-derived and equivalent filters *continued*

attenuation in the reject band). Thus each point specifies a different relative attenuation shape.

Comparison of the curves for 2-poles no-zero with those for 2 poles 2 zeros shows the improvement in cutoff rate that is obtainable when zeros are correctly added to the network. More complete attenuation information on the 2-pole no-zero configuration has been presented on Fig. 5. Again, it is stressed that data of Figs. 5 and 13 represent the actual attenuation

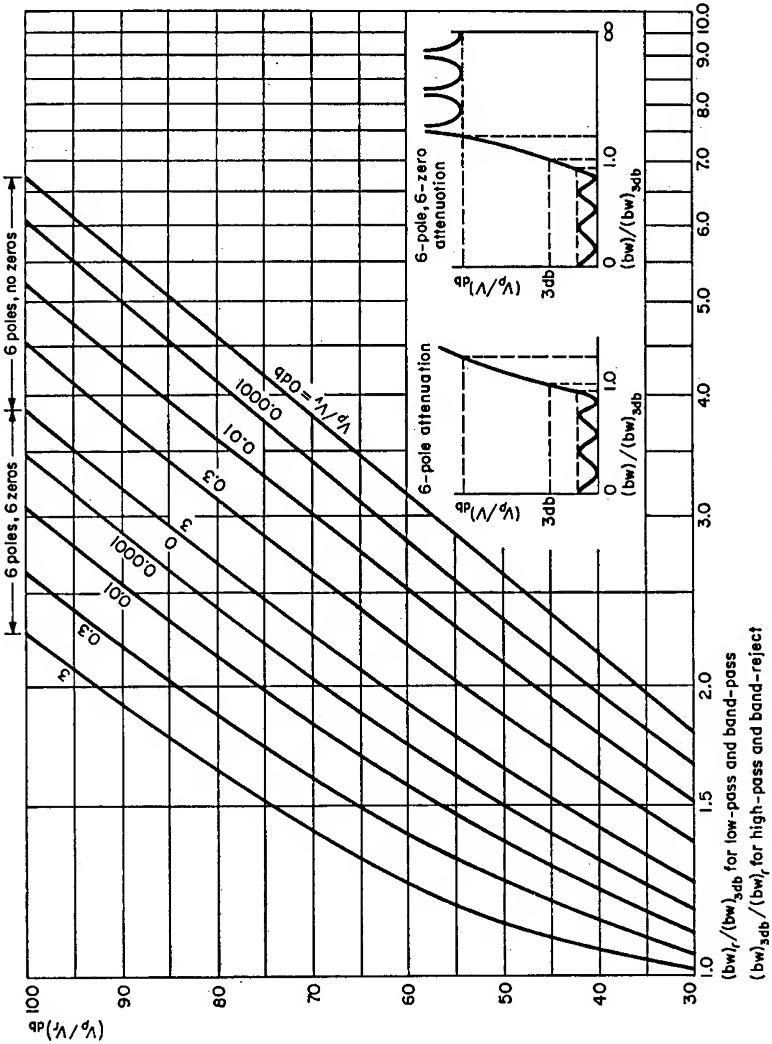

Fig. 17—Maximum rate of cutoff for 6-pole and for 6-pole 6-zero filters.

M-derived and equivalent filters *continued*

shapes and rate of cutoff attainable with filters using finite-Q elements (except for a rounding off of the infinite attenuation peaks). In contrast, the rates of cutoff and the attenuation shapes predicted by the simple "image" theory are unobtainable in physically realizable networks.

The rates of cutoff shown are the best that are possible of attainment with the specified number of poles and zeros, and with equal-ripple-type behavior.

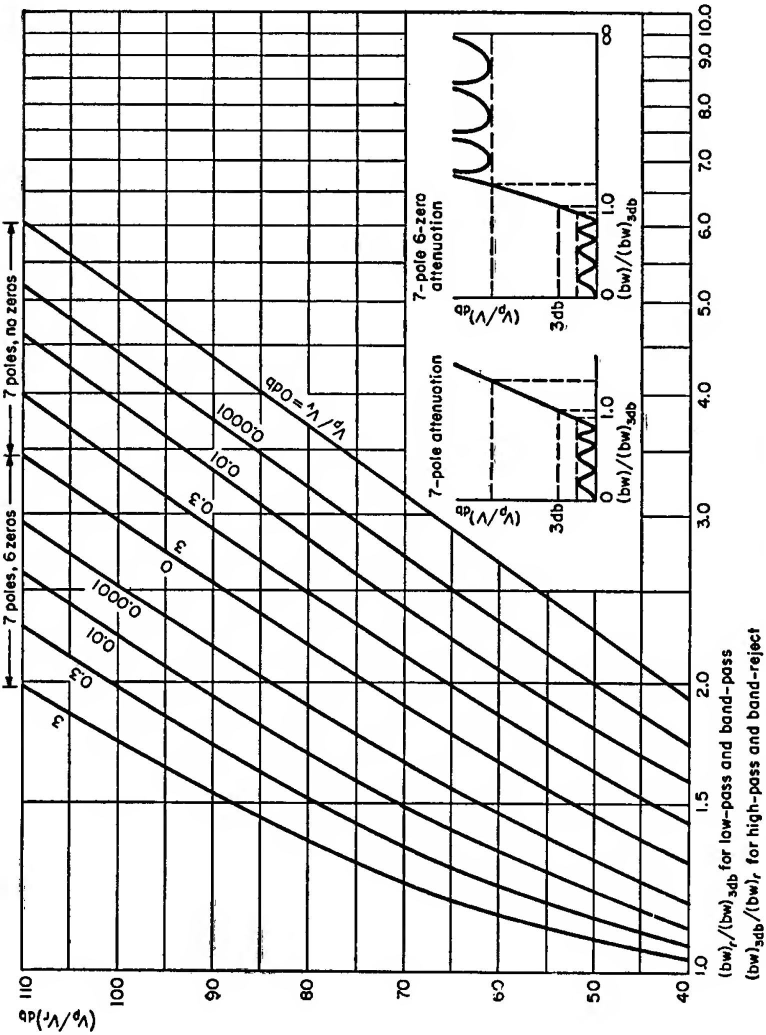

Fig. 18—Maximum rate of cutoff for 7-pole and 7-pole 6-zero filters.

M-derived and equivalent filters *continued*

Resistive terminations and *n* even

It is evident from the attenuation shapes of Figs. 13, 15, and 17 that for an *M*-derived network having an even number of arms, the optimum shape

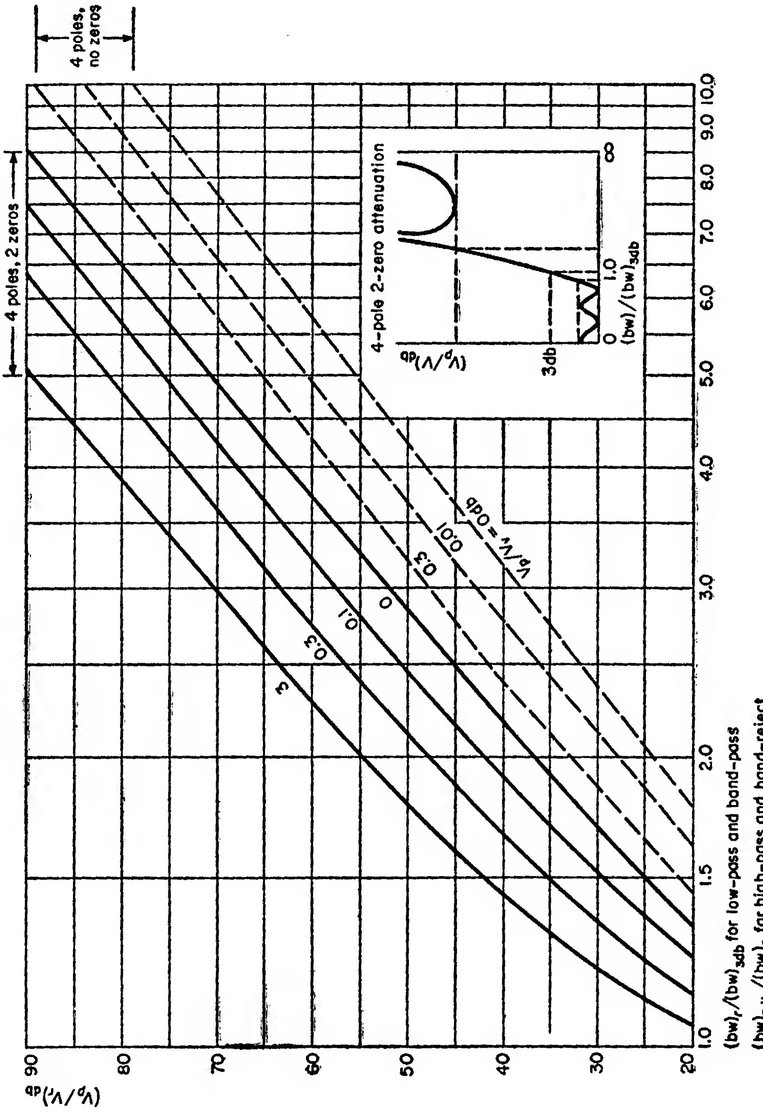

Fig. 19—Maximum rate of cutoff for 4-pole and 4-pole 2-zero filters.

M-derived and equivalent filters *continued*

given by (8) produces a finite attenuation at an infinite frequency. This requires a completely reactive termination at one end of the network. If resistive terminations must be used, then the optimum shape that is practically realizable with an even number of arms is given by

$$\left(\frac{V_p}{V}\right)^2 = 1 + \left[\left(\frac{V_p}{V_v}\right)^2 - 1\right] cd_v{}^2\left(n\,\frac{K_v\,u}{K_f}\right) \tag{13}$$

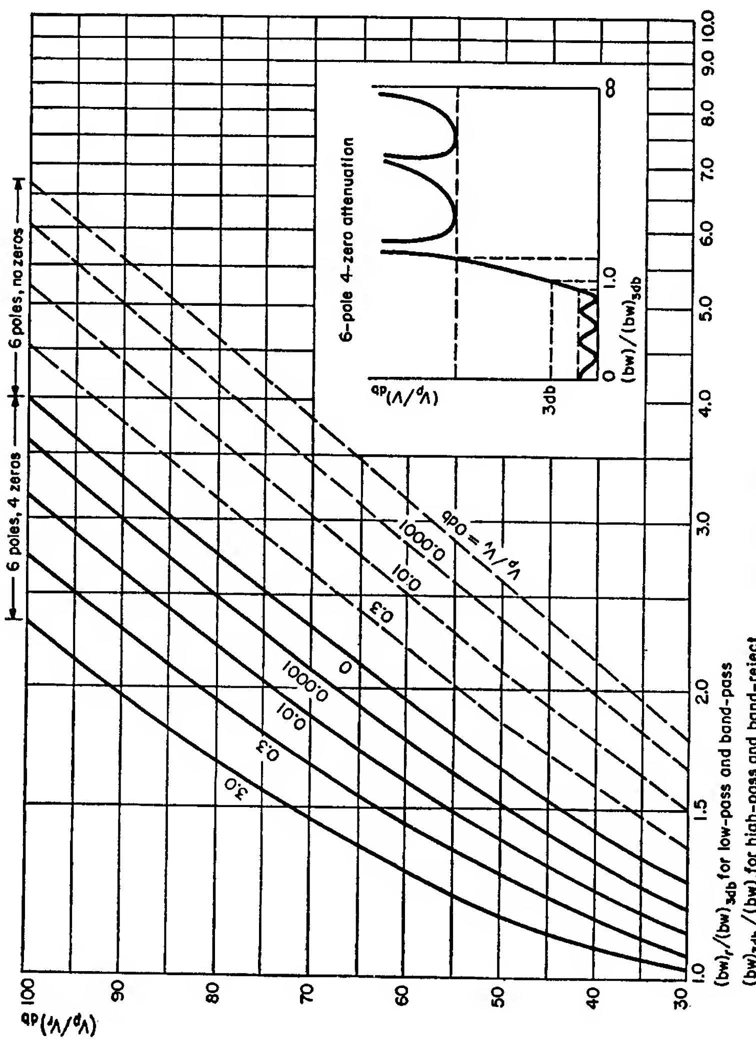

Fig. 20—Maximum rate of cutoff for 6-pole and 6-pole 4-zero filters.

M-derived and equivalent filters *continued*

where

$$u = sc_f^{-1}\left\{\left[\left(\frac{x_v}{x}\right)^2 - 1\right]^{1/2} \frac{dn_f\ (K_f/n)}{f'}\right\} \tag{14}$$

The modulus v is given by (9) and the modulus f by (10).

Solving (13) then gives the ratio of hill-to-valley bandwidth as

$$\frac{x_h}{x_v} = \frac{1}{f\ cd_f\ (K_f/n)} \tag{15}$$

This optimum attenuation shape (13) produces two fewer points of infinite rejection, or response zeros than response poles. In contrast, (8) requires an equal number of zeros and poles.

If the ripples in the pass band approach zero decibels ($V_p/V_v = 1$) then, as a limit, (13) becomes

$$\left(\frac{V_p}{V}\right)^2 = 1 + \frac{(V_p/V_h)^2 - 1}{\cosh^2 (n \cosh^{-1} y)} \tag{16}$$

where

$$y = \left[\left(\frac{x_h}{x} \cos \frac{90}{n}\right)^2 + \sin^2 \frac{90}{n}\right]^{1/2}$$

Based on (13) and (16), the rates of cutoff have been plotted in Figs. 19 and 20 for 4-pole 2-zero and for 6-pole 4-zero filters. Fig. 5 already has presented the data for a 2-pole no-zero network, the simplest case. An increase in rate of cutoff results when $n - 2$ response zeros are suitably added to n response poles as shown by the dotted curves in Figs. 19 and 20; the data being derived from Figs. 7 and 9.

Circuit-element values

This section concerns the values of the circuit elements required to produce the optimum relative-attenuation shapes of constant-K-configuration filters. There are two convenient ways of expressing the element values for these ladder networks.

a. The reactive and resistive components of each element may be related to one of the terminating resistances (or to a completely arbitrary normalizing resistance R_0) and also to a definite bandwidth, usually the 3-decibels-down

Circuit-element values *continued*

value. The numerical results are called ladder-network coefficients or singly loaded Q's.

b. The reactive component of each element may be related to the reactive part of the immediately preceding element, and to a definite bandwidth such as the 3-decibel-down value. These numerical results are called the normalized coefficients of coupling. The resistive component of each element is related to its reactive part and the numerical values are called normalized decrements or, when inverted, normalized Q's.

The latter form of normalized coefficients of coupling k and normalized Q's $(= q)$ will be used because the numerical values may be applied directly to the adjustment and checking of actual filters.

Figs. 21–24 relate the normalized k and q to the inductance, capacitance, and resistance values for various types of filters.

For low-pass filters, Fig. 21 shows that k gives the ratio of resonant frequency

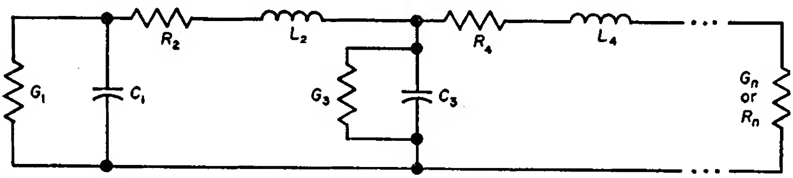

A

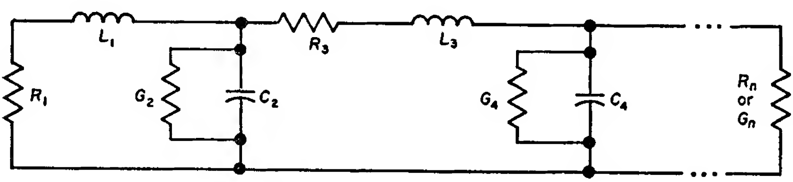

B

Fig. 21—Relations among normalized k and q and values of inductance, capacitance, and resistance for low-pass and large-percentage-band-pass circuits.
A—Shunt arm at one end. $1/(C_1L_2)^{1/2}=k_{12}\omega_{3db}$, $1/(L_2C_3)^{1/2}=k_{23}\omega_{3db}$, $1/(C_3L_4)^{1/2}=k_{34}\omega_{3db}$, etc. $G_1/C_1=(1/q_1)\omega_{3db}$, $q_2 = (\omega_{3db}\, L_2)/R_2$, $q_3 = (\omega_{3db}\, C_3)/G_3$, $q_4 = (\omega_{3db}\, L_4)/R_4$, etc.

B—Series arm at one end, $1/(L_1C_2)^{1/2} = k_{12}\omega_{3db}$, $1/(C_2L_3)^{1/2} = k_{23}\omega_{3db}$, $1/(L_3C_4)^{1/2} = k_{34}\omega_{3db}$, etc. $R_1/L_1 = (1/q_1)\omega_{3db}$, $q_2 = (\omega_{3db}\, C_2)/G_2$, $q_3 = (\omega_{3db}\, L_3)/R_3$, $q_4 = (\omega_{3db}\, C_4)/G_4$, etc.

To design a bandpass circuit, the total required 3-decibel-down bandwidth should replace ω_{3db}, an inductor should be connected across each shunt capacitor, and a capacitor put in series with each series inductor; each such circuit being resonated to the geometric mean frequency $f_0 = (f_1\, f_2)^{1/2}$

Circuit-element values *continued*

of two immediately adjacent elements to the over-all 3-decibels-down frequency. The resonant frequency of C_1 and L_2 in this example must be k_{12} times the required over-all 3-decibels-down bandwidth.

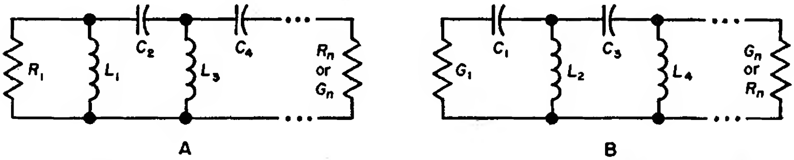

Fig. 22—Relations among normalized k and q and values of inductance, capacitance, and resistance for high-pass and large-percentage-band-reject circuits.

A—Shunt arm at one end. $1/(L_1C_2)^{1/2} = (1/k_{12})\omega_{3db}$, $(1/C_2L_3)^{1/2} = (1/k_{23})\omega_{3db}$, $1/(L_3\ C_4)^{1/2} = (1/k_{34})\omega_{3db}$, etc. $(R_1/L_1) = q_1\omega_{3db}$. All reactances are assumed to be lossless.

B—Series arm at one end. $1/(C_1L_2)^{1/2} = (1/k_{12})\omega_{3db}$, $1/(L_2C_3)^{1/2} = (1/k_{23})\omega_{3db}$, $1/(C_3L_4)^{1/2} = (1/k_{34})\omega_{3db}$, etc. $(G_1/C_1) = q_1\omega_{3db}$. All reactances are assumed to be lossless. To design a band-reject circuit, the total required 3-decibel-down bandwidth should replace ω_{3db}, a capacitor should be placed in series with each shunt inductor, and an inductor in shunt of each series capacitor; each such circuit being resonated to the geometric mean frequency $f_0 = (f_1\ f_2)^{1/2}$.

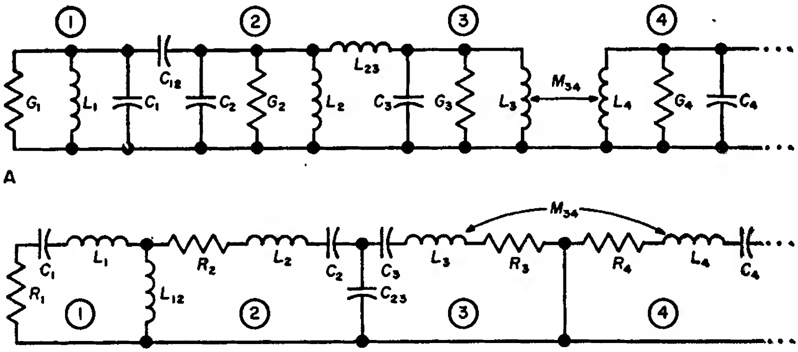

Fig. 23—Relations among normalized k and q and values of inductance, capacitance, and resistance for small-percentage-band-pass circuits.

A—Parallel-resonant circuits. $C_{12}/(C_1C_2)^{1/2} \doteq k_{12}[(bw)_{3db}/f_0]$, $(L_2\ L_3)^{1/2}/L_{23} \doteq k_{23}[(bw)_{3db}/f_0]$, $M_{34}/(L_3L_4)^{1/2} \doteq k_{34}[(bw)_{3db}/f_0]$, etc. $Q_1 = q_1\ [f_0/(bw)_{3db}]$, $q_2 = Q_2/[f_0/(bw)_{3db}]$, $q_3 = Q_3/[f_0/(bw)_{3db}]$, $q_4 = Q_4/(f_0/(bw)_{3db})$, etc. Any adjacent pair of resonators may be coupled by any of the three methods shown. Each node must resonate at f_0 with all other nodes short-circuited.

B—Series-resonant circuits. $L_{12}/(L_1L_2)^{1/2} \doteq k_{12}[(bw)_{3db}/f_0]$, $(C_2C_3)^{1/2}/C_{23} \doteq k_{23}[(bw)_{3db}/f_0]$, $M_{34}/(L_3L_4)^{1/2} \doteq k_{34}[(bw)_{3db}/f_0]$, etc. $Q_1 = q_1[f_0/(bw)_{3db}]$, $q_2 = Q_2/[f_0/(bw)_{3db}]$, $q_3 = Q_3/[f_0/(bw)_{3db}]$, $q_4 = Q_4[f_0/(bw)_{3db}]$. Any adjacent pair or resonators may be coupled by any of the three methods shown. Each mesh must resonate at f_0 with all other meshes open-circuited.

Circuit-element values *continued*

Fig. 21 also gives as the inverse of q, the ratio of the 3-decibels-down bandwidth of a single element resulting from the resistive load and losses associated with it, to the required 3-decibels-down bandwidth of the over-all filter. Thus, $1/R_1C_1$ is the 3-decibels-down radian bandwidth of C_1 and the conductance G_1 that must be shunted across it. If C_1 and G_1 are properly chosen, the measured bandwidth of these elements at their 3-decibels-down point will be $1/q_1$ times the required over-all 3-decibels-down bandwidth of the filter.

The legend of Fig. 21 shows how it is applicable also to large-percentage band-pass filters.

Fig. 22 gives the required information for high-pass and large-percentage band-reject filters.

Similar data are given in Fig. 23 for small-percentage bandpass filters. It should be noted that the required *actual* coefficient of coupling between resonant circuits, $M_{ab}/(L_aL_b)^{1/2}$ for example, may be obtained by multiplying the required over-all fractional 3-decibels-down bandwidth by the nor-

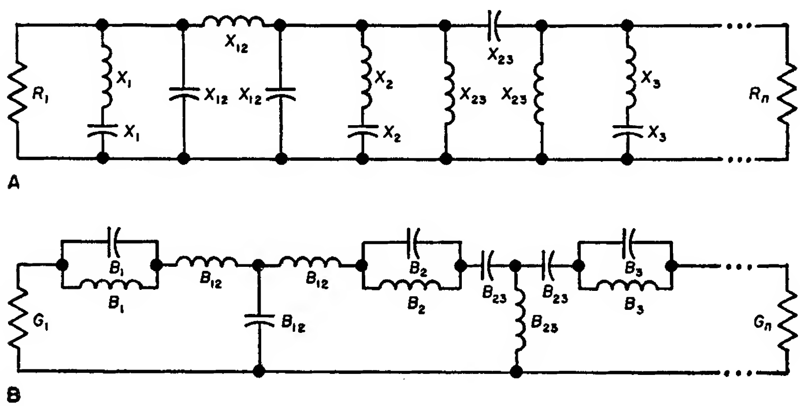

Fig. 24—Relations among normalized k and q and values of inductance, capacitance, and resistance for small-percentage-band-reject circuits.

A—Series-resonant circuits. $X_{12}/(X_1X_2)^{1/2} = (1/k_{12})[(\mathrm{bw})_{3db}/f_0]$, $X_{23}/(X_2X_3)^{1/2} = (1/k_{23})[(\mathrm{bw})_{3db}/f_0]$, etc. $X_1/R_1 = (1/q_1)\ [f_0(\mathrm{bw})_{3db}]$, $X_n/R_n = (1/q_n)\ [f_0/(\mathrm{bw})_{3db}]$. All resonant circuits are assumed to be lossless. Any adjacent pair of resonators may be coupled by either of the two π (or their dual T) couplings shown. The reactances X are measured at the midfrequency of the reject band.

B—Parallel-resonant circuits. $B_{12}/(B_1B_2)^{1/2} = (1/k_{12})[(\mathrm{bw})_{3db}/f_0]$, $B_{23}/(B_2B_3)^{1/2} = (1/k_{23})[(\mathrm{bw})_{3db}/f_0]$, etc. $B_1/G_1 = (1/q_1)\ [f_0/(\mathrm{bw})_{3db}]$, $B_n/G_n = (1/q_n)\ [f_0/(\mathrm{bw})_{3db}]$.

All resonant circuits are assumed to be lossless. Any adjacent pair of resonators may be coupled by either of the two T (or their dual π) couplings shown. The susceptances B are measured at the midfrequency of the reject band.

Circuit-element values *continued*

malized coefficient of coupling. The required *actual* resonant-circuit Q results from multiplying the fractional midfrequency by q. An experimental procedure for checking k and q values is available.* Fractional midfrequency $f_0/(\mathrm{bw})_{3\mathrm{db}}$ = reciprocal of fractional 3-decibels-down bandwidth.

Fig. 24 supplies the data for small-percentage band-reject filters.

Butterworth, Chebishev, and maximally linear phase designs

Elegant closed-form equations for k and q values producing optimum Chebishev and Butterworth response shapes for filters having any number of total arms may be obtained if lossless reactances are used.† The design data in Figs. 25–30 are based on such equations. The k and q values for the maximally linear phase shape result from the Darlington synthesis procedure applied to (6). The tables provide data for two limiting cases of terminations; equal resistive loading at the two ends of the filter and resistive loading at only one end.

For Figs. 25–30, the $(V_p/V_v)_{\mathrm{db}}$ column gives the ripple in decibels in the passband, and the corresponding curves on Figs. 5–10 give the complete attenuation shape.

For low-pass circuits, $q_{2,3,4}\ldots$ is the required unloaded Q, measured at the required 3-decibel-down frequency, of the internal inductors and capacitors to be used. For band-pass circuits, the unloaded resonator Q required in the internal resonators is obtained by multiplying the required 3-decibel fractional midfrequency $[f_0/(\mathrm{bw})_{3\mathrm{db}}]$ by $q_{2,3,4}\ldots$

Fig. 25—2-pole no-zero filter 3-decibel-down k and q values.

$(V_p/V_v)_{\mathrm{db}}$	q_1	k_{12}	q_2
Equal resistive terminations			
Linear phase	0.576	0.899	2.15
0	1.414	0.707	1.414
0.3	1.82	0.717	1.82
1.0	2.21	0.739	2.21
3.0	3.13	0.779	3.13
Resistive termination at only one end			
Linear phase	0.455	1.27	>10
0	0.707	1.00	>14
0.3	0.910	0.904	>18
1.0	1.11	0.866	>23
3.0	1.56	0.840	>32

* M. Dishal, "Alignment and Adjustment of Synchronously Tuned Multiple-Resonant-Circuit Filters," *Proceedings of the IRE*, vol. 39, pp. 1448–1455; November, 1951: Also, *Electrical Communication*, vol. 29, pp. 154–164; June, 1952.

† V. Belevitch, "Tchebyshev Filters and Amplifier Networks," *Wireless Engineer*, vol. 29, pp. 106–110; April, 1952. H. J. Orchard, "Formulae for Ladder Filters," *Wireless Engineer*, vol. 30, pp. 3–5; January, 1953. E. Green, "Exact Amplitude–Frequency Characteristics of Ladder Networks," *Marconi Review*, vol. 16, no. 108, pp. 25–68; 1953. M. Dishal, "Two New Equations for the Design of Filters," *Electrical Communication*, vol. 30, pp. 324–337; December, 1952.

Circuit-element values *continued*

It should be realized that designs can be made that call for unloaded Q's that are *one-tenth* of those called for in these designs.

For the detailed way in which the q and k columns fix the required element values see Figs. 21, 22, 23, and 24 and related discussion.

The first column of the tables gives the peak-to-valley ratio within the pass band.

Except for Fig. 25, the second column gives the unloaded q of the elements on which the remaining design values are based. Proceeding across the table, figuratively from the left end of the filter, the next column gives q_1

Fig. 26—3-pole no-zero filter 3-decibel-down k and q values.

$(V_p/V_v)_{db}$	q_2	q_1	k_{12}	k_{23}	q_3
Equal resistive terminations					
Linear phase	>10	0.338	1.74	0.682	2.21
0	>20	1.00	0.707	0.707	1.00
0.1	>29	1.43	0.665	0.665	1.43
1.0	>45	2.21	0.645	0.645	2.21
3.0	>67	3.36	0.647	0.647	3.36
Resistive termination at only one end					
Linear phase	>10	0.293	2.01	0.899	>10
0	>20	0.500	1.22	0.707	>20
0.1	>29	0.714	0.961	0.661	>29
1.0	>45	1.11	0.785	0.645	>45
3.0	>67	1.68	0.714	0.649	>67

Fig. 27—4-pole no-zero filter 3-decibel-down k and q values.

$(V_p/V_v)_{db}$	$q_{2,3}$	q_1	k_{12}	k_{23}	k_{34}	q_4
Equal resistive terminations						
Linear phase	>10	2.24	0.644	1.175	2.53	0.233
0	>26	0.766	0.840	0.542	0.840	0.766
0.01	>36	1.05	0.737	0.541	0.737	1.05
0.1	>46	1.34	0.690	0.542	0.690	1.34
1.0	>76	2.21	0.638	0.546	0.638	2.21
3.0	>118	3.45	0.624	0.555	0.624	3.45
Resistive termination at only one end						
Linear phase	>10	0.211	2.78	1.29	0.828	>10
0	>26	0.383	1.56	0.765	0.644	>26
0.01	>36	0.524	1.20	0.666	0.621	>36
0.1	>46	0.667	1.01	0.626	0.618	>46
1.0	>76	1.10	0.781	0.578	0.614	>76
3.0	>118	1.72	0.692	0.567	0.609	>118

Circuit-element values *continued*

from which with the aid of Figs. 21–24 the relation between the terminating resistance R_1 and the first reactance element is obtained. The next column for k_{12} with Figs. 21–24 provides for the relation between the first and second reactances. Continuing across the table, all relations between adjacent elements will be obtained including that of the right-hand terminating resistance.

Example

Reverting to the previous example, a filter is required having $(bw)_{50db}/(bw)_{1db}$

Fig. 28—5-pole no-zero filter 3-decibel-down k and q values.

$(V_p/V_v)_{db}$	$q_{2,3,4}$	q_1	k_{12}	k_{23}	k_{34}	k_{45}	q_5
Equal resistive terminations							
0	>32	0.618	1.0	0.556	0.556	1.0	0.618
0.001	>43	0.822	0.845	0.545	0.545	0.845	0.822
0.1	>68	1.29	0.703	0.535	0.535	0.703	1.29
1.0	>118	2.21	0.633	0.535	0.538	0.633	2.21
3.0	>182	3.47	0.614	0.538	0.538	0.614	3.47
Resistive termination at only one end							
Linear phase	>10	0.162	3.62	1.68	1.14	0.804	>10
0	>32	0.309	1.90	0.900	0.655	0.619	>32
0.001	>43	0.412	1.48	0.760	0.603	0.606	>43
0.1	>68	0.649	1.044	0.634	0.560	0.595	>68
1.0	>118	1.105	0.779	0.570	0.544	0.595	>118
3.0	>182	1.74	0.679	0.554	0.542	0.597	>182

Fig. 29—6-pole no-zero filter 3-decibel-down k and q values.

$(V_p/V_v)_{db}$	$q_{2,3,4,5}$	q	k_{12}	k_{23}	k_{34}	k_{45}	k_{56}	q_6
Equal resistive terminations								
0	>39	0.518	1.17	0.606	0.518	0.606	1.17	0.518
0.001	>51	0.679	0.967	0.573	0.518	0.573	0.967	0.679
0.01	>69	0.936	0.810	0.550	0.518	0.550	0.810	0.936
0.1	>95	1.27	0.716	0.539	0.518	0.539	0.716	1.27
1.0	>168	2.25	0.631	0.531	0.510	0.531	0.631	2.25
3.0	>261	3.51	0.610	0.582	0.524	0.582	0.610	3.51
Resistive termination at only one end								
Linear phase	>11	0.129	4.55	2.09	1.42	1.09	0.803	>11
0	>39	0.259	2.26	1.05	0.732	0.606	0.606	>39
0.001	>51	0.340	1.76	0.689	0.650	0.573	0.596	>51
0.01	>69	0.468	1.34	0.725	0.591	0.550	0.591	>69
0.1	>95	0.637	1.06	0.642	0.560	0.539	0.589	>95
1.0	>168	1.12	0.771	0.566	0.533	0.531	0.589	>168
3.0	>261	1.75	0.673	0.546	0.529	0.531	0.591	>261

Circuit-element values *continued*

= 2.5 and $V_p/V_v < 1$ decibel. The 5-pole no-zero response with a pass-band peak-to-valley ratio of 1 decibel in Fig. 8 satisfied the requirement.

Fig. 28 is for 5-pole networks and if the terminations are to be equal resistive loads, the upper part of the table should be used. If a shunt capacitance is to appear at one end of the low-pass filter, Fig. 21A will apply.

Reading along the fourth row for $(V_p/V_v)_{db} = 1$, the second column requires normalized unloaded Q's of at least 118 at the over-all 3-decibels-down frequency, which for this example is 31 kilocycles. Realize that much-lower unloaded-Q designs can be accomplished.

The required value of $q_1 = 2.21$ is found in the third column. From Fig. 21A, $1/R_1C_1 = 0.451\omega_{3db}$ from which R_1 or C_1 may be obtained. Experimentally, the 3-decibels-down bandwidth of R_1C_1 must measure 0.451 times the required 3-decibels-down bandwidth or $31 \times 0.451 = 14$ kilocycles.

From the table, a value of 0.633 is obtained for k_{12} and from Fig. 21A it is found that $1/(C_1L_2)^{1/2} = 0.633\omega_{3db}$. This means that a resonant circuit made up of C_1 and L_2 must tune to 0.633 times the required 3-decibels-down bandwidth or $31 \times 0.633 = 19.7$ kilocycles.

In this fashion, all the remaining elements are determined. Any one of them may be set arbitrarily (for instance, the input load resistance R_1), but once it has been set, all other values are rigidly determined by the k and q factors.

Fig. 30—7-pole no-zero filter 3-decibel-down k and q values.

$(V_p/V_v)_{db}$	$q_{2,3,4,5,6}$	q_1	k_{12}	k_{23}	k_{34}	k_{45}	k_{56}	k_{67}	q_7
Equal resistive termination									
0	>45	0.445	1.34	0.669	0.528	0.528	0.669	1.34	0.445
0.00001	>59	0.580	1.10	0.611	0.521	0.521	0.611	1.10	0.580
0.001	>75	0.741	0.930	0.579	0.519	0.519	0.579	0.930	0.741
0.01	>93	0.912	0.830	0.560	0.519	0.519	0.560	0.830	0.912
0.1	>127	1.26	0.723	0.541	0.517	0.517	0.541	0.723	1.26
1.0	>223	2.25	0.631	0.530	0.517	0.517	0.530	0.631	2.25
3.0	>353	3.52	0.607	0.529	0.519	0.519	0.529	0.607	3.52
Resistive termination at only one end									
Linear phase	>11	0.105	5.53	2.53	1.72	1.33	1.08	0.804	>11
0	>45	0.223	2.62	1.20	0.824	0.659	0.579	0.598	>45
0.00001	>59	0.290	2.05	0.981	0.710	0.601	0.552	0.589	>58
0.001	>75	0.370	1.64	0.830	0.642	0.570	0.541	0.588	>75
0.01	>93	0.456	1.38	0.744	0.602	0.551	0.538	0.588	>93
0.1	>127	0.629	1.08	0.648	0.560	0.531	0.530	0.587	>127
1.0	>223	1.12	0.770	0.564	0.530	0.521	0.527	0.587	>223
3.0	>353	1.76	0.669	0.542	0.523	0.520	0.528	0.588	>353

Circuit-element values *continued*

Elements of lower Q

Designs may be based on elements having unloaded Q's of only 1/10th those given in Figs. 25–30. These designs are necessary for small-percentage band-pass filters. As is evident from Fig. 23, the Q of the internal resonators measured at the midfrequency must be the normalized q multiplied by the fractional midfrequency $f_0/(\text{bw})_{3\text{db}}$. If the bandwidth percentage is small, the fractional midfrequency and therefore the actually required Q will be large.

Practical values of end q's and all k's will result if the internal elements have finite q's above the minimum values given in Figs. 5–10. For a required response shape, such as for 0.1-decibel pass-band ripple, the resulting data can be expressed as in Figs. 31–36. These curves are for zero-decibel ripple (Butterworth) and for the maximally linear phase shape.

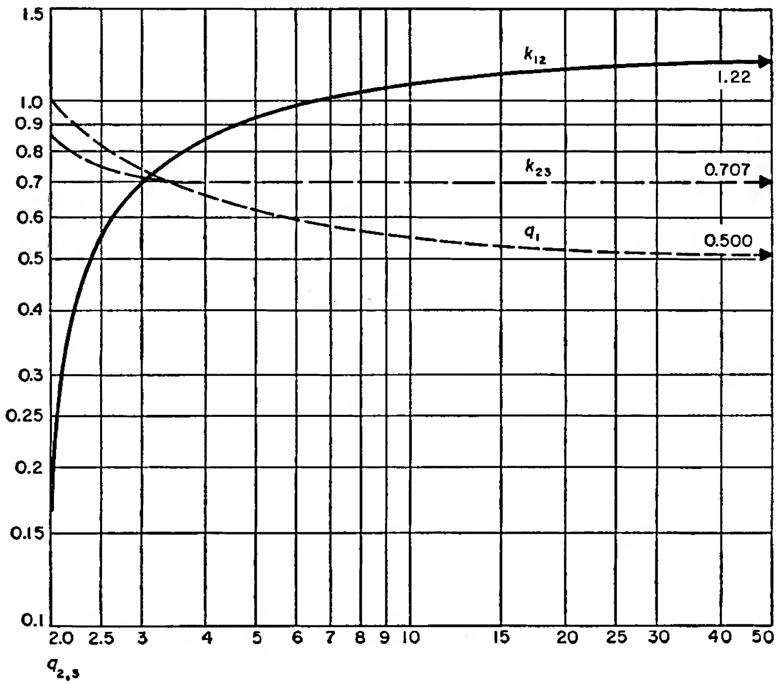

Fig. 31—3-pole filter of finite-Q elements producing a maximally flat amplitude shape. See curve 1 of Fig. 5.

Circuit-element values *continued*

Example

a. The filter to be designed must have a relative attenuation of $(bw)_{70db}/(bw)_{3db} = 5$ and there must be no ripple in the pass band. Curve 1 of Fig. 8 satisfies these conditions and calls for a 5-pole network.

b. The specified fractional midfrequency is 20 (pass band = 5 percent of the midfrequency), the Q_{min} from Fig. 8 becomes $3.24 \times 20 = 65$. Assume further that resonators with unloaded midfrequency Q's of 100 are available. As the normalized unloaded q is the actual unloaded Q divided by the fractional midfrequency, the filter must produce a Butterworth shape with 5 resonators having normalized unloaded q's of $100/20 = 5$.

c. There are three possible generator and load conditions.

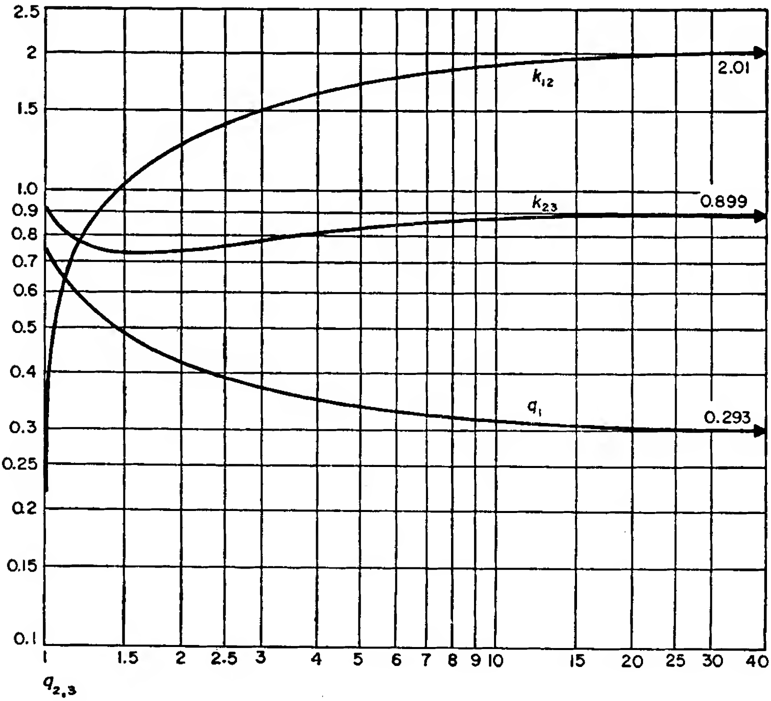

Fig. 32—3-pole filter of finite-Q elements producing a maximally linear phase shape. See Figs. 11 and 12.

Circuit-element values *continued*

1. Resistive generator and resistive load. It is usually desirable to maximize the ratio of the power delivered to the load to that available from the generator. The generator resistance and the load resistances will have to be tapped onto their associated resonators to obtain the required q_1 and q_n.

2. Resistive generator and reactive load or vice versa. The function to be considered here is the transfer impedance or admittance. Again the resistive impedance must be transformed by tapping it onto the associated resonator.

3. Reactive generator and load. The transfer impedance or admittance is the significant factor and a loading resistance must be added to either or both end resonators.

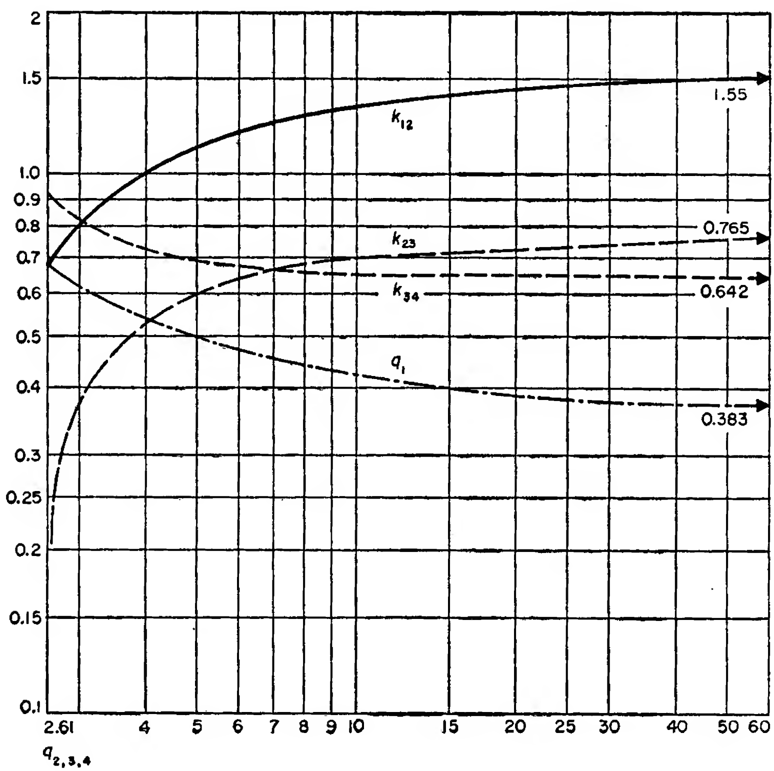

Fig. 33—4-pole filter of finite-Q elements producing a maximally flat amplitude shape. See curve 1 of Fig. 6.

Circuit-element values *continued*

Figs. 31–36 provide optimum design data for cases (2) and (3).

Assuming a high-impedance filter to be required, the network of Fig. 37 might well be used. High-side capacitance coupling will be employed and the element values will be obtained from Fig. 35.

a. The q_1 curve of Fig. 35 intersects the abscissa value of 5 at 0.405. By tapping a resistive generator or load onto it, or placing a resistor across it, the resonator C_1L_1 must be loaded to produce an actual Q of $0.405\, f_0/(\mathrm{bw})_{3db} = 8.1$ (see Fig. 23A).

b. As a convenience, the same size of inductor may be used for resonating each node, say 4 millihenries. For a required midfrequency of 80 kilocycles

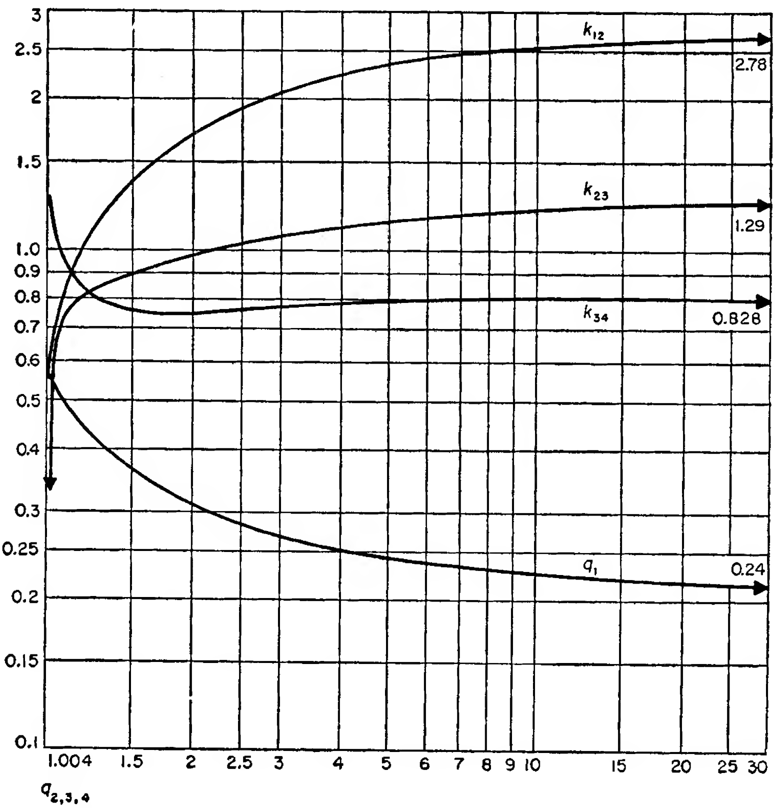

Fig. 34—4-pole filter of finite-Q elements producing a maximally linear phase shape. See Figs. 11 and 12.

Circuit-element values *continued*

for this example, each node total capacitance will be 1000 micromicrofarads.

c. Again from Fig. 35, we get k_{12} of 1.35 for an abscissa value of 5. From Fig. 23, $C_{12} = 1.35\,[(\text{bw})_{3\text{db}}/f_0]\,(C_1C_2)^{1/2} = 1.35 \times 0.05 \times 1000 = 67.5$ micromicrofarads. At the midfrequency of 80 kilocycles, node 1 must be resonant when all other nodes are short-circuited. To produce the required capacitance in shunt of L_1, C_a must be $1000 - 67.5 = 933$ micromicrofarads.

d. From Fig. 35, a value of 0.67 is obtained for k_{23}, and $C_{23} = 0.67 \times 0.05 \times 1000 = 33.5$ micromicrofarads. To resonate node 2 at the midfrequency with all other nodes short-circuited $C_b = 1000 - 33.5 - 67.5 = 899$ micromicrofarads.

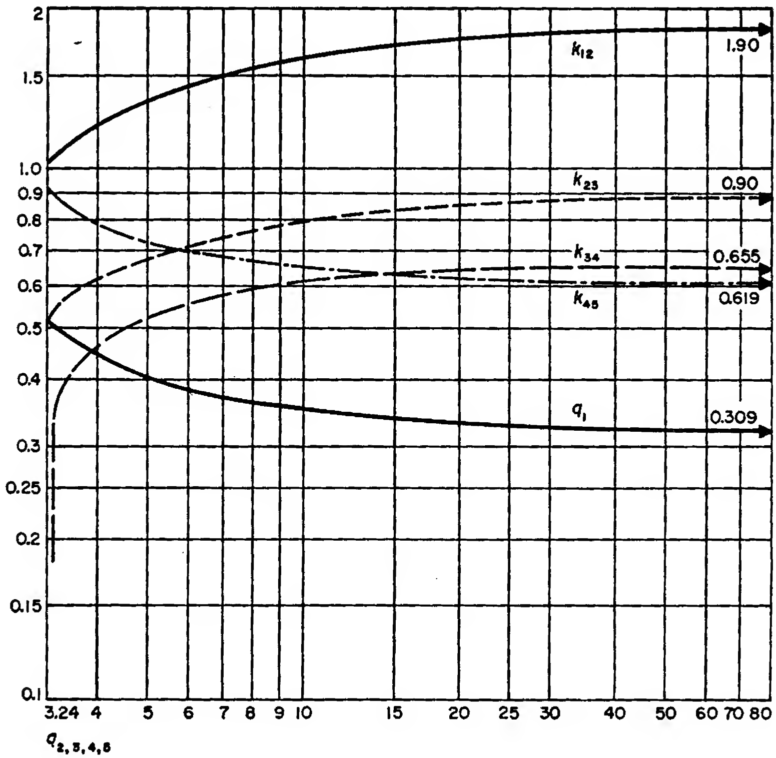

Fig. 35—5-pole filter of finite-Q elements producing a maximally flat amplitude shape. See curve 1 of Fig. 7.

Circuit-element values *continued*

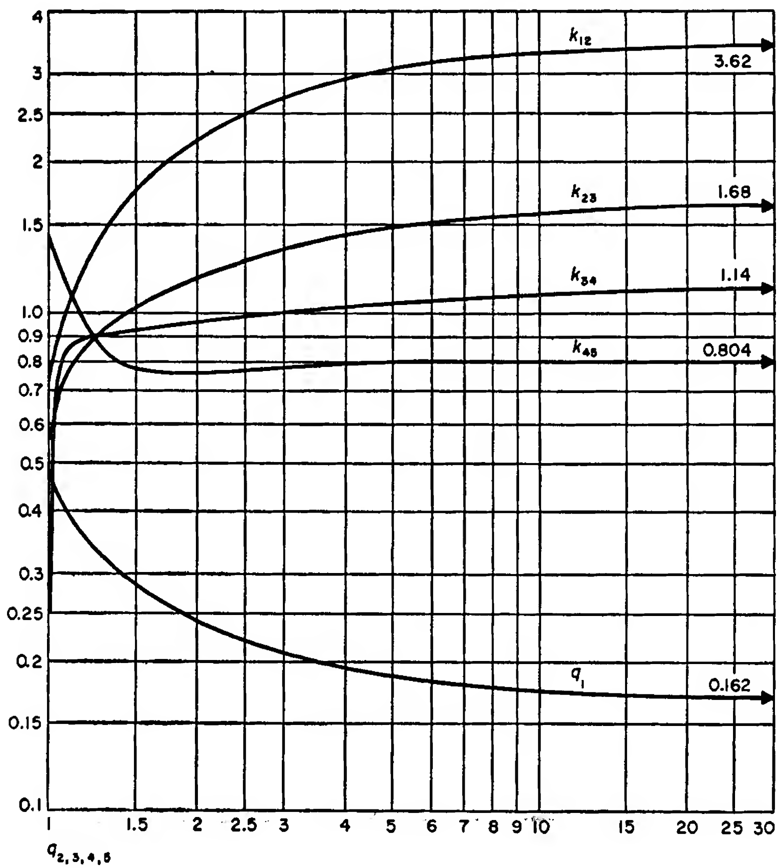

Fig. 36—5-pole filter of finite-Q elements producing a maximally linear phase shape. See Figs. 11 and 12.

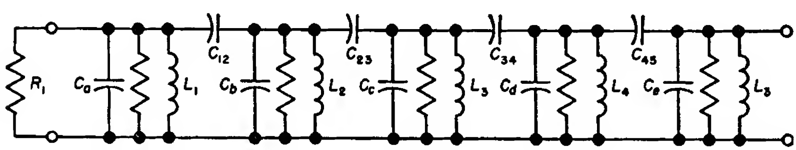

Fig. 37—5-resonator filter with high-side capacitance coupling.

Circuit-element values *continued*

e. Additional computations give values for C_{34} of $0.53 \times 0.05 \times 1000 = 26.5$ micromicrofarads, $C_c = 1000 - 33.5 - 26.5 = 940$, $C_{45} = 0.73 \times 0.05 \times 1000 = 36.5$, $C_d = 1000 - 36.5 - 26.5 = 937$, and $C_e = 1000 - 36.5 = 963.5$ micromicrofarads.

All inductances will be identical and of 4 millihenries and there will be no inductive coupling among them.

Stagger tuning of single-tuned interstages

Butterworth response *(Figs. 4 and 38)*

The required Q's are given by

$$\frac{1}{Q_m} = \frac{(\mathrm{bw})_\beta/f_0}{\sqrt[2n]{(V_p/V_\beta)^2 - 1}} \sin\left(\frac{2m-1}{n}\,90°\right)$$

The required stagger tuning is given by

$$(f_a - f_b)_m = \frac{(\mathrm{bw})_\beta}{[(V_p/V_\beta)^2 - 1]^{1/2n}} \cos\left(\frac{2m-1}{n}\,90°\right)$$

$$(f_a + f_b)_m = 2f_0$$

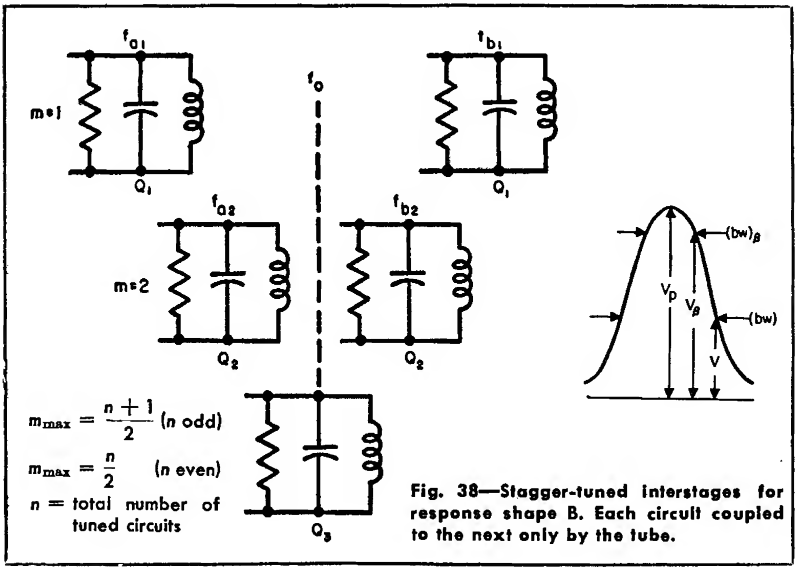

Fig. 38—Stagger-tuned interstages for response shape B. Each circuit coupled to the next only by the tube.

Stagger tuning of single-tuned interstages *continued*

The amplitude response is given by

$$V_p/V = \{1 + [(V_p/V_\beta)^2 - 1]\,[(\mathrm{bw})/(\mathrm{bw})_\beta]^{2n}\}^{1/2}$$

$$\frac{(\mathrm{bw})}{(\mathrm{bw})_\beta} = \left[\frac{(V_p/V)^2 - 1}{(V_p/V_\beta)^2 - 1}\right]^{1/2n}$$

$$n = \frac{\log\left[\dfrac{(V_p/V)^2 - 1}{(V_p/V_\beta)^2 - 1}\right]}{2\log[(\mathrm{bw})/(\mathrm{bw})_\beta]}$$

$$\text{Stage gain} = \frac{g_m}{2\pi(\mathrm{bw})_\beta C}\,[(V_p/V_\beta)^2 - 1]^{1/2n}$$

or

$$n = \frac{\log\left\{\dfrac{(\text{total gain})}{[(V_p/V_\beta)^2 - 1]^{1/2}}\right\}}{\log\left(\dfrac{g_m}{2\pi(\mathrm{bw})_\beta C}\right)}$$

where

g_m = geometric-mean transconductance of n tubes
C = geometric-mean capacitance

Chebishev response *(Figs. 4 and 39)*

The required Q's are given by

$$\frac{1}{Q_m} = \frac{(\mathrm{bw})_\beta}{f_0} S_n \sin\left[\frac{2m - 1}{n} 90°\right]$$

$$S_n = \sinh\left\{\frac{1}{n}\sinh^{-1}\frac{1}{[(V_p/V_\beta)^2 - 1]^{1/2}}\right\}$$

The required stagger tuning is given by

$$(f_a - f_b)_m = (\mathrm{bw})_\beta C_n \cos\left(\frac{2m - 1}{n} 90°\right)$$

$$(f_a + f_b)_m = 2f_0$$

$$C_n = \cosh\left\{\frac{1}{n}\sinh^{-1}\frac{1}{[(V_p/V_\beta)^2 - 1]^{1/2}}\right\}$$

Stagger tuning of single-tuned interstages *continued*

Shape outside pass band is

$$\frac{V_p}{V} = \left\{1 + \left[\left(\frac{V_p}{V_\beta}\right)^2 - 1\right]\left\{\cosh^2\left[n \cosh^{-1} \frac{(\mathrm{bw})}{(\mathrm{bw})_\beta}\right]\right\}\right\}^{1/2}$$

$$\frac{(\mathrm{bw})}{(\mathrm{bw})_\beta} = \cosh\left\{\frac{1}{n}\cosh^{-1}\left[\frac{(V_p/V)^2 - 1}{(V_p/V_\beta)^2 - 1}\right]^{1/2}\right\}$$

$$n = \frac{\cosh^{-1}\left[\dfrac{(V_p/V)^2 - 1}{(V_p/V_\beta)^2 - 1}\right]^{1/2}}{\cosh^{-1}\left[(\mathrm{bw})/(\mathrm{bw})_\beta\right]}$$

Shape inside pass band is

$$\frac{V_p}{V} = \left\{1 + \left[\left(\frac{V_p}{V_\beta}\right)^2 - 1\right]\left\{\cos^2\left[n \cos^{-1} \frac{(\mathrm{bw})}{(\mathrm{bw})_\beta}\right]\right\}\right\}^{1/2}$$

$$\frac{(\mathrm{bw})_{\mathrm{crest}}}{(\mathrm{bw})_\beta} = \cos\left(\frac{2m-1}{n} 90°\right)$$

$$\frac{(\mathrm{bw})_{\mathrm{trough}}}{(\mathrm{bw})_\beta} = \cos\left(\frac{2m}{n} 90°\right)$$

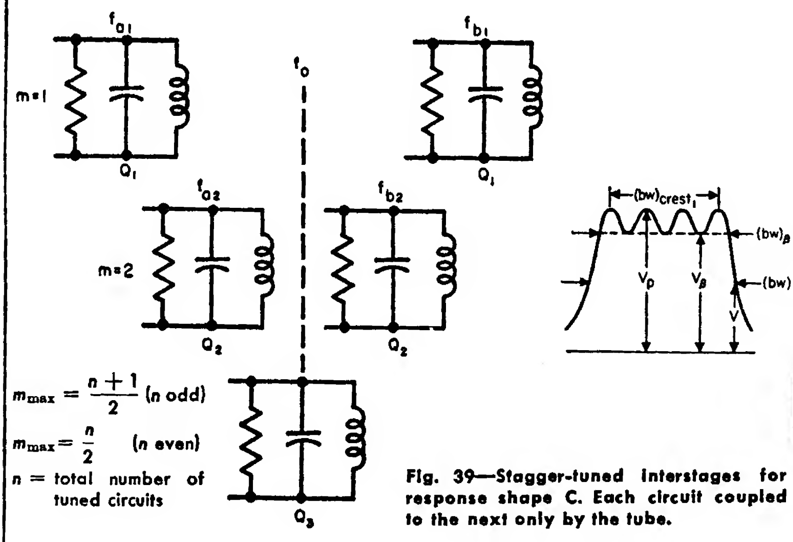

$m_{max} = \frac{n+1}{2}$ (n odd)

$m_{max} = \frac{n}{2}$ (n even)

n = total number of tuned circuits

Fig. 39—Stagger-tuned interstages for response shape C. Each circuit coupled to the next only by the tube.

Stagger tuning of single-tuned interstages *continued*

$$\text{Stage gain} = \frac{g_m}{2^{1/n}\pi(\mathrm{bw})_\beta C}\left[(V_p/V_\beta)^2 - 1\right]^{1/2n}$$

$$n = \frac{\log\left[\dfrac{(\text{total gain})}{\frac{1}{2}\left[(V_p/V_\beta)^2 - 1\right]^{1/2}}\right]}{\log\left[\dfrac{g_m}{\pi(\mathrm{bw})_\beta C}\right]}$$

where

g_m = geometric-mean transconductance of n tubes

C = geometric-mean capacitance

Quartz-crystal band-pass filters

When a filter requires a small-percentage bandwidth as well as a high rate of cutoff, it is not practical to obtain sufficiently high unloaded Q in ordinary L-C resonators. Such filters can be constructed utilizing piezoelectric quartz crystals or mechanically resonant rods of some low-mechanical-loss material such as NiSpan-C.

The design information presented in Figs. 25–31 can be applied to filters of the constant-K type using rods. However, frequent use is made of quartz crystals in a lattice structure, to which the following design information is applicable.

High-impedance lattice filters

An "open-circuited" lattice is shown in Fig. 40. The arrangements of the impedance arms Z_A and Z_B are shown in Fig. 41. In each arm there is an L-C parallel-resonant circuit shunted by $(n/2) - 1$ quartz crystals. The number of complex poles in the transfer function is equal the n. The L-C circuit is loaded by R_p to give the required $Q_p = \omega_0 C_p R_p$. Its capacitance includes those of the crystal holders and it is resonant to $(f_0 + \Delta f_p)$ as shown in the diagrams. The motional capacitance C_1, C_2, C_3, etc., must have a particular value, and each crystal must be resonant to a particular frequency, $(f_0 \pm \Delta f_1)$, $(f_0 \pm \Delta f_2)$, etc.

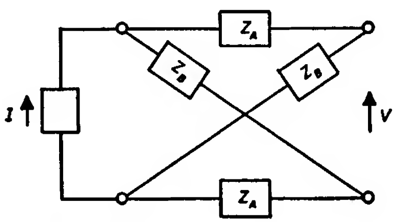

Fig. 40—High-impedance lattice section.

Quartz-crystal band-pass filters *continued*

Frequently, divided-electrode crystals are used so one crystal can be used for the identical resonators in the two series arms, and likewise in the lattice arms.

The structure can be modified by converting the lattice to its equivalent in accordance with Fig. 42. The elements Z that are lifted out of the arms and shunted across the terminals consist of L_p, R_p, and most of C_p.

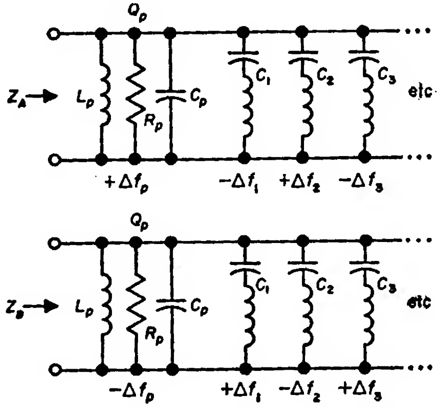

Fig. 41—Detailed structure of the lattice arms indicated in Fig. 40.

Design information

The data of Fig. 43 is for the Chebishev and Butterworth response shapes of 4-pole no-zero networks for which the relative attenuation is plotted in Fig. 7. Similarly, Fig. 44 is for 6-pole no-zero networks, plotted in Fig. 9.

Examination of the tables shows that the required Q_p of the L-C parallel-resonant circuit is roughly the same as the fractional midfrequency. This

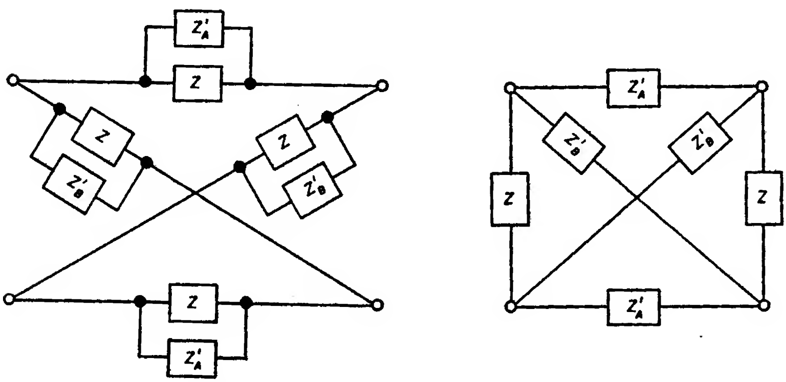

Fig. 42—Equivalent lattices.

limits the practical design to $f_0/(\text{bw})_{3db}$ less than about 250. A lower limit to the $f_0/(\text{bw})_{3db}$ is of the order of 10 due to the fact that C_p/C_1 is roughly equal to the square of $f_0/(\text{bw})_{3db}$, and C_p includes those of the crystal

Quartz-crystal band-pass filters *continued*

holders and coil and stray distributed capacitances, so cannot be reduced indefinitely.

The impedance Z in (Fig. 42), must include the equivalent-generator and equivalent-load impedances. Since R_p often comes to some hundreds of

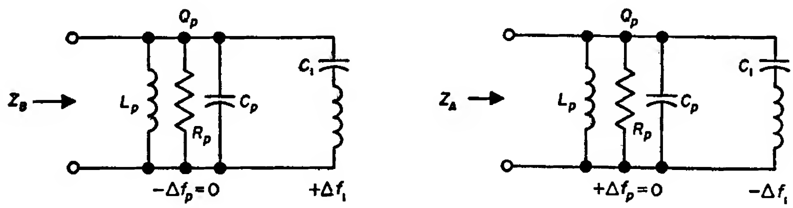

$(V_p/V_v)_{db}$	$\Delta f_1/\Delta f_{3db}$	C_p/C_1 $[f_0/(bw)_{3db}]^2$	Q_p $f_0/(bw)_{3db}$
0	0.542	1.414	0.766
0.001	0.541	1.66	0.912
0.01	0.540	1.84	1.05
0.1	0.541	2.10	1.34
1.0	0.546	2.46	2.21
3.0	0.552	2.57	3.44

Fig. 43—4-pole no-zero lattice-filter design for Chebishev response. Note that Δf_{3db} is one-half the total 3-decibel bandwith, or, $2\Delta f_{3db} = (bw)_{3db}$.

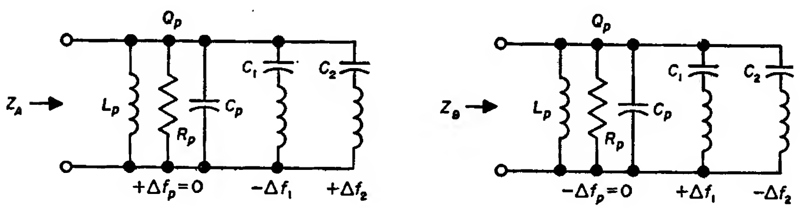

$(V_p/V_v)_{db}$	$\Delta f_1/\Delta f_{3db}$	C_1/C_2	$\Delta f_2/\Delta f_{3db}$	C_p/C_1 $[f_0/(bw)_{3db}]^2$	Q_p $f_0/(bw)_{3db}$
0	0.400	2.30	0.920	1.05	0.518
0.0001	0.370	2.40	0.889	1.51	0.680
0.01	0.350	2.47	0.869	2.14	0.936
0.1	0.339	2.53	0.859	2.73	1.28
1.0	0.330	2.57	0.850	3.49	2.25
3.0	0.332	2.58	0.858	3.72	3.51

Fig. 44—6-pole no-zero lattice-filter design for Chebishev response. Note that Δf_{3db} is one-half the total 3-decibel bandwith, or, $2\Delta f_{3db} = (bw)_{3db}$.

Quartz-crystal band-pass filters *continued*

thousands of ohms, it is obvious that this type of filter requires a very-high-impedance equivalent generator and load.

Example

Required, a filter for $f_0 = 175$ kilocycles, $(bw)_{3db} = 2.0$ kilocycles, $(bw)_{60db} < 5.0$ kilocycles, $(V_p/V_v)_{db} < 0.3$.

Then, $f_0/(bw)_{3db} = 87.5$ and $(bw)_{60db}/(bw)_{3db} < 2.5$. The latter requirement is satisfied by the curve for $(V_p/V_v)_{db} = 0.1$-decibel ripple on Fig. 9 with a 6-pole, no-zero network. The internal resonators must have $q_{min}\, f_0/(bw)_{3db} = 9.5 \times 87.5 = 831$. This is far beyond L-C possibilities, but crystal unloaded Q usually exceeds 25,000.

In Fig. 44, let $C_1 = 0.020$ micromicrofarads, which can be obtained. Lower values for C_2 can also be realized.

$C_2 = C_1/2.53 = 0.00800$ micromicrofarads.

$\Delta f_1 = 0.339 \Delta f_{3db} = 0.339 \times 1000 = 339$ cycles

Then the first crystal in arm A is series-resonant at 175 kilocycles minus 339 cycles. In arm B, it is plus 339 cycles.

Similarly, $\Delta f_2 = 0.859 \times 1000 = 859$ cycles.

In the parallel-resonant circuits,

$C_p = 2.73\, C_1 [f_0/(bw)_{3db}]^2 = 2.73 \times 0.020 \times (87.5)^2 = 422$ micromicrofarads

Since $F_p = 0$, they are parallel-resonant at 175 kilocycles. The loaded $Q_p = 1.28 \times 87.5 = 112$. The equivalent

$R_p = Q_p/2\pi f\, C_p = 112/2\pi \times 175 \times 422 \times 10^{-9} = 240{,}000$ ohms

If the unloaded Q of the inductor L_p is 200, the added loading due to generator or load must be in excess of one-half megohm.

Low-impedance generator and load

A low-impedance generator and/or load may be used with above filter design by the following procedure:

After the arms of Fig. 41 have been designed, convert the resulting lattice of Fig. 40 to the configuration of Fig. 42 so that the Z across each end of the filter consists of L_p, R_p, and most of C_p. Then use either of the following two steps:

Quartz-crystal band-pass filters *continued*

a. Couple the generator to one L_p and load to the other L_p via mutual inductance, with an effective turns ratio that transforms the low impedance to the value required to produce the proper R_p across each Z.

b. In each Z, across the filter ends, open the inductor L_p at its midpoint and connect directly in series with L_p a generator and load of the proper resistance R_s to produce the required Q_p. The required terminal resistances R_s can be calculated from the simple relationship that, with series loading, $Q_p = X_p/R_s$.

With practical crystals, the value of R_s is some tens of ohms for percentage bandwidths around 1 percent, and some hundreds of ohms for bandwidths around 5 percent.

Lattice equivalent*

An important lattice equivalent (Fig. 45) halves the number of crystals required for the full-lattice filter. After the full-lattice design is completed, it is merely necessary to double the reactances of one L-C resonator and to center-tap it; halve the reactances of the second L-C resonator and ground its bottom side; and then, as shown in Fig. 45B, two arms of the full lattice may be omitted. This equivalence is valid when dealing with small-percentage bandwidths and with high L-C-resonator loaded Q's (Q_p).

For large-percentage bandwidths and/or low loaded Q's, it is necessary to use an inductive center tap with a coupling coefficient between the two sides of the coil (L_p) approaching unity. The use of a capacitive center tap greatly simplifies the problem of "trimming-in" the tap point, which is always necessary in practice.

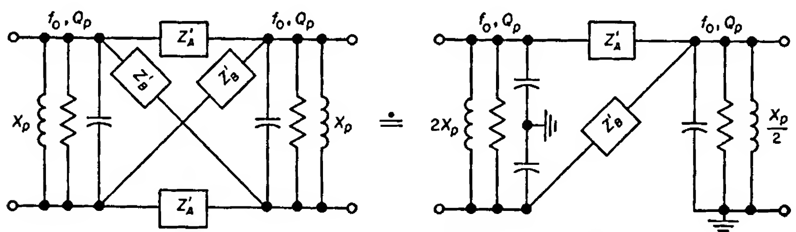

A. Full-lattice crystal filter.

B. Modified equivalent crystal filter.

Fig. 45—Modification of L-C resonators to halve the required number of crystals.

* This late development was added in the fourth printing of "Reference Data for Radio Engineers," fourth edition. It also appears in a paper by M. Dishal, "Practical Modern Network Theory Design Data for Crystal Filters," *IRE 1957 National Convention Record*, Part 8.

Filters, simple bandpass design

Coefficient of coupling*

Several types of coupled circuits are shown in Figs. 1B to F, together with formulas for the coefficient of coupling in each case. Also shown is the dependence of bandwidth on resonance frequency. This dependence is only a rough approximation to show the trend and may be altered radically if L_m, M, or C_m are adjusted as the circuits are tuned to various frequencies.

$k = X_{120}/\sqrt{X_{10}X_{20}}$ = coefficient of coupling

X_{120} = coupling reactance at resonance frequency f_0

X_{10} = reactance of inductor (or capacitor) of first circuit at f_0

X_{20} = reactance of similar element of second circuit at f_0

$(\text{bw})_C$ = bandwidth with capacitive tuning

$(\text{bw})_L$ = bandwidth with inductive tuning

Gain at resonance

Single circuit

In Fig. 1A,

$$\frac{E_0}{E_g} = -g_m\,|X_{10}|\,Q$$

where

E_0 = output volts at resonance frequency f_0

E_g = input volts to grid of driving tube

g_m = transconductance of driving tube

Pair of coupled circuits *(Figs. 2 and 3)*

In any figure—Figs. 1B to F,

$$\frac{E_0}{E_g} = jg_m\sqrt{X_{10}X_{20}}\,Q\,\frac{kQ}{1 + k^2Q^2}$$

This is maximum at critical coupling, where $kQ = 1$.

$Q = \sqrt{Q_1Q_2}$ = geometric-mean Q for the two circuits, as loaded with the tube grid and plate impedances

* See also "Coefficient of coupling—geometrical consideration," pp. 141–142.

Fig. 1—Several types of coupled circuits, showing coefficient of coupling and selectivity formulas in each case.

diagram	coefficient of coupling	approximate bandwidth variation with frequency	selectivity far from resonance: formula*	selectivity far from resonance: curve in Fig. 4
A 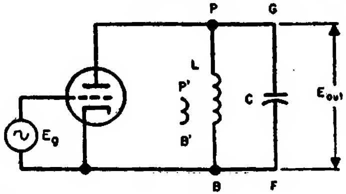			Input to *PB* or to *P'B'*: $\frac{E_0}{E} = jQ\left(\frac{f}{f_0} - \frac{f_0}{f}\right)$	A
B 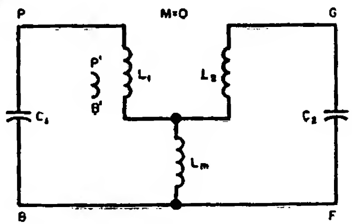	$k = L_m/\sqrt{(L_1 + L_m)(L_2 + L_m)}$ $= \omega_0^2 L_m \sqrt{C_1C_2}$ $\approx L_m/\sqrt{L_1L_2}$	$(bw)_C \propto f_0$ $(bw)_L \propto f_0^3$	Input to *PB*: $\frac{E_0}{E} = -A\frac{f}{f_0}$	C
			Input to *P'B'*: $\frac{E_0}{E} = -A\frac{f_0}{f}$	D
C 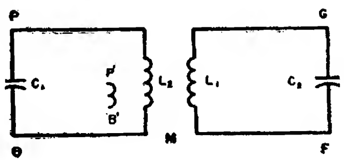	$k = M/\sqrt{L_1L_2}$ $= \omega_0^2 M\sqrt{C_1C_2}$ *M* may be positive or negative	$(bw)_C \propto f_0$ $(bw)_L \propto f_0^3$	Input to *PB*: $\frac{E_0}{E} = -A\frac{f}{f_0}$	C
			Input to *P'B'*: $\frac{E_0}{E} = -A\frac{f_0}{f}$	D

* Where $A = \frac{Q^2}{1 + k^2Q^2}\left(\frac{f}{f_0} - \frac{f_0}{f}\right)^2$

Table continued on next page.

Fig. 1—*continued*

	diagram	coefficient of coupling	approximate bandwidth variation with frequency	selectivity far from resonance: formula*	selectivity far from resonance: curve in Fig. 4
D	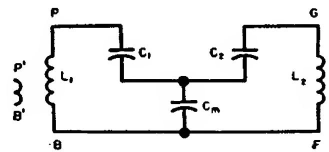	$k = -\left[\frac{C_1C_2}{(C_1+C_m)(C_2+C_m)}\right]^{\frac{1}{2}}$ $= -1/\omega_0^2 C_m\sqrt{L_1L_2}$ $\approx -\sqrt{C_1C_2}/C_m$	$(bw)_C \propto 1/f_0$ $(bw)_L \propto f_0$	Input to *PB* or to *P'B'*: $\frac{E_0}{E} = -A\frac{f_0}{f}$	D
E	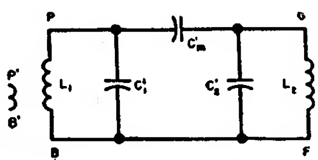	$k = \frac{-C_m'}{\sqrt{(C_1'+C_m')(C_2'+C_m')}}$ $= -\omega_0^2 C_m'\sqrt{L_1L_2}$ $\approx -C_m'/\sqrt{C_1'C_2'}$	$(bw)_C \propto f^3$ $(bw)_L \propto f$	Input to *PB* or to *P'B'*: $\frac{E_0}{E} = -A\frac{f_0}{f}$	D
F	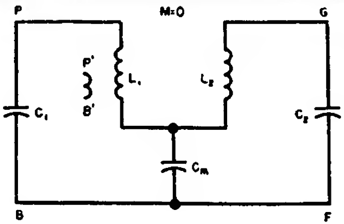	$k = -\left[\frac{C_1C_2}{(C_1+C_m)(C_2+C_m)}\right]^{\frac{1}{2}}$ $= -1/\omega_0^2 C_m\sqrt{L_1L_2}$ $\approx -\sqrt{C_1C_2}/C_m$	$(bw)_C \propto 1/f_0$ $(bw)_L \propto f_0$	Input to *PB*: $\frac{E_0}{E} = -A\left(\frac{f}{f_0}\right)^2$	B
				Input to *P'B'*: $\frac{E_0}{E} = -A\frac{f}{f_0}$	C

* Where $A = \frac{Q^2}{1+k^2Q^2}\left(\frac{f}{f_0}-\frac{f_0}{f}\right)^2$

Gain at resonance *continued*

For circuits with critical coupling and over coupling, the approximate gain is

$$\left|\frac{E_0}{E_g}\right| \approx \frac{0.1\, g_m}{\sqrt{C_1C_2}\ (\text{bw})}$$

where (bw) is the useful pass band in megacycles, g_m is in micromhos, and C is in micromicrofarads.

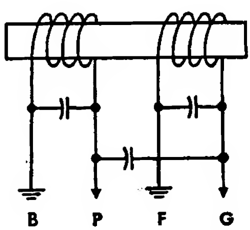

Fig. 2—Connection wherein k_m opposes k_c. (k_c may be due to stray capacitance.) Peak of attenuation is at $f = f_0\sqrt{-k_m/k_c}$. Reversing connections or winding direction of one coil causes k_m to aid k_c.

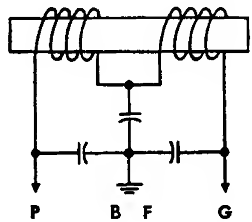

Fig. 3—Connection wherein k_m aids k_c. If mutual-inductance coupling is reversed, k_m will oppose k_c and there will be a transfer minimum at $f = f_0\sqrt{-k_m/k_c}$.

Selectivity far from resonance

The selectivity curves of Fig. 4 are based on the presence of only a single type of coupling between the circuits. The curves are useful beyond the peak region treated on pp. 241-246.

In the equations for selectivity in Fig. 1

E = output volts at signal frequency f for same value of E_g as that producing E_0

For inductive coupling

$$A = \frac{Q^2}{1 + k^2Q^2}\left[\left(\frac{f}{f_0} - \frac{f_0}{f}\right)^2 - k^2\left(\frac{f}{f_0}\right)^2\right] \approx \frac{Q^2}{1 + k^2Q^2}\left(\frac{f}{f_0} - \frac{f_0}{f}\right)^2$$

For capacitive coupling

A is defined by a similar equation, except that the neglected term is $-k^2(f_0/f)^2$. The 180-degree phase shift far from resonance is indicated by the minus sign in the expression for E_0/E.

Selectivity far from resonance *continued*

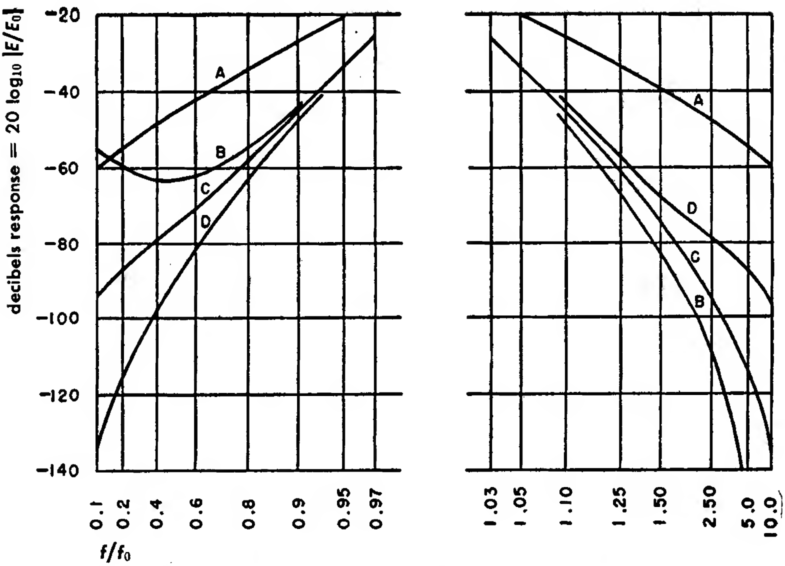

Fig. 4—Selectivity for frequencies far from resonance. $Q = 100$ **and** $|k|\,Q = 1.0$.

Example: The use of the curves, Figs. 4, 5, and 6, is indicated by the following example. Given the circuit of Fig. 1C with input to *PB*, across capacitor C_1. Let $Q = 50$, $kQ = 1.50$, and $f_0 = 16.0$ megacycles. Required is the response at $f = 8.0$ megacycles.

Here $f/f_0 = 0.50$ and curve C, Fig. 4, gives -75 decibels. Then applying the corrections from Figs. 5 and 6 for Q and *kQ*, we find

Response $= -75 + 12 + 4 = -59$ decibels

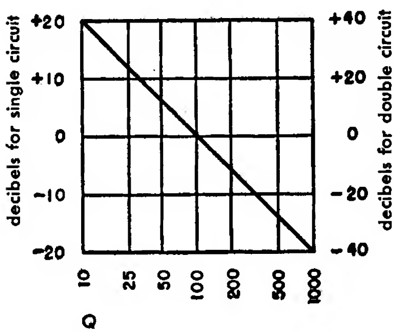

Fig. 5—Correction for $Q \neq 100$.

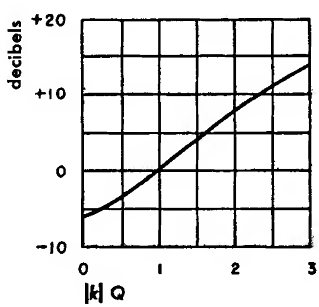

Fig. 6—Correction for $|k|Q \neq 1.0$.

Selectivity of single- and double-tuned circuits near resonance

Formulas and curves are presented for the selectivity and phase shift:

Of n single-tuned circuits
Of m pairs of coupled tuned circuits

The conditions assumed are

a. All circuits are tuned to the same frequency f_0.

b. All circuits have the same Q, or each pair of circuits includes one circuit having Q_1 and the other having Q_2.

c. Otherwise the circuits need not be identical.

d. Each successive circuit or pair of circuits is isolated from the preceding and following ones by tubes, with no regeneration around the system.

Certain approximations have been made in order to simplify the formulas. In most actual applications of the types of circuits treated, the error involved is negligible from a practical standpoint. Over the narrow frequency band in question, it is assumed that

a. The reactance around each circuit is equal to $2X_0\,\Delta f/f_0$.

b. The resistance of each circuit is constant and equal to X_0/Q.

c. The coupling between two circuits of a pair is reactive and constant. (When an untuned link is used to couple the two circuits, this condition frequently is far from satisfied, resulting in a lopsided selectivity curve.)

d. The equivalent input voltage, taken as being in series with the tuned circuit (or the first of a pair), is assumed to bear a constant proportionality to the grid voltage of the input tube or other driving source, at all frequencies in the band.

e. Likewise, the output voltage across the circuit (or the final circuit of a pair) is assumed to be proportional only to the current in the circuit.

The following symbols are used in the formulas in addition to those defined on pages 236 and 239.

$$\frac{\Delta f}{f_0} = \frac{f - f_0}{f_0} = \frac{\text{(deviation from resonance frequency)}}{\text{(resonance frequency)}}$$

(bw) = bandwidth = $2\Delta f$
X_0 = reactance at f_0 of inductor in tuned circuit
n = number of single-tuned circuits
m = number of pairs of coupled circuits
ϕ = phase shift of signal at f relative to shift at f_0 as signal passes through cascade of circuits

Selectivity of single- and double-tuned circuits near resonance *continued*

$p = k^2Q^2$ or $p = k^2Q_1Q_2$, a parameter determining the form of the selectivity curve of coupled circuits

$$B = p - \frac{1}{2}\left(\frac{Q_1}{Q_2} + \frac{Q_2}{Q_1}\right)$$

Selectivity and phase shift of single-tuned circuits

$$\frac{E}{E_0} = \left[\frac{1}{\sqrt{1 + \left(2Q\frac{\Delta f}{f_0}\right)^2}}\right]^n$$

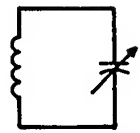

single-tuned circuit

$$\frac{\Delta f}{f_0} = \pm \frac{1}{2Q}\sqrt{\left(\frac{E_0}{E}\right)^{\frac{2}{n}} - 1}$$

$$\text{Decibel response} = 20 \log_{10}\left(\frac{E}{E_0}\right)$$

(db response of n circuits) $= n \times$ (db response of single circuit)

$$\phi = n \tan^{-1}\left(-2Q\frac{\Delta f}{f_0}\right)$$

These equations are plotted in Figs. 7 and 8, following.

Q determination by 3-decibel points

For a single-tuned circuit, when

$E/E_0 = 0.707$ (3 decibels down)

$$Q = \frac{f_0}{2\Delta f} = \frac{\text{(resonance frequency)}}{\text{(bandwidth)}_{3db}}$$

Selectivity and phase shift of pairs of coupled tuned circuits

Case 1: When $Q_1 = Q_2 = Q$

These formulas can be used with reasonable accuracy when Q_1 and Q_2 differ by ratios up to 1.5 or even 2 to 1. In such cases use the value $Q = \sqrt{Q_1Q_2}$.

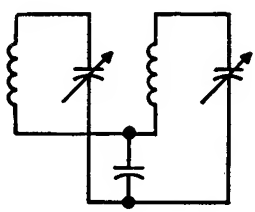

one of several types of coupling

$$\frac{E}{E_0} = \left[\frac{p+1}{\sqrt{\left[\left(2Q\frac{\Delta f}{f_0}\right)^2 - (p-1)\right]^2 + 4p}}\right]^m$$

Selectivity of single- and double-tuned circuits

near resonance *continued*

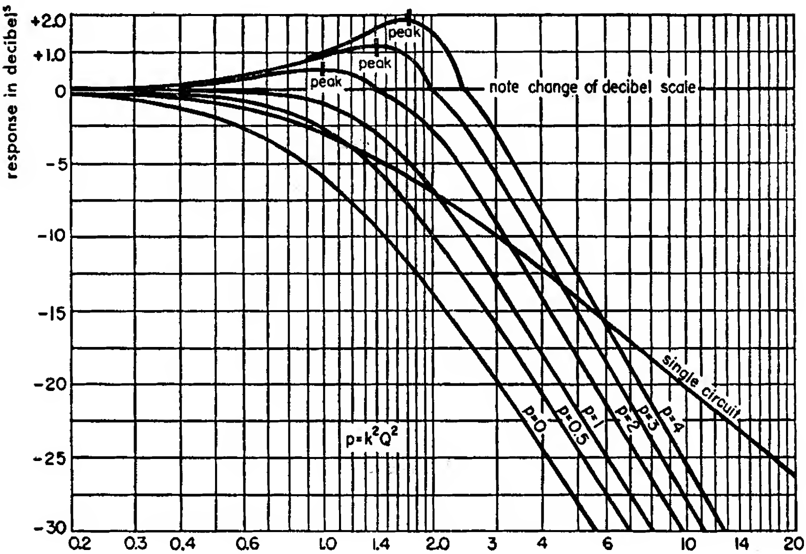

$$Q\frac{2\Delta f}{f_0} = Q\frac{(bw)}{f_0}$$

Fig. 7—Selectivity curves showing response of a single circuit $n = 1$, and a pair of coupled circuits $m = 1$.

The selectivity curves are symmetrical about the axis $Q\frac{\Delta f}{f_0} = 0$ for practical purposes.

Extrapolation beyond lower limits of chart:

Δ response for doubling Δf	circuit	useful limit at $\frac{(bw)}{f_0}$	useful limit error becomes
− 6 db	← single →	0.6	1 to 2 db
− 12 db	← pair →	0.4	3 to 4 db

Example: Of the use of Figs. 7 and 8. Suppose there are three single-tuned circuits ($n = 3$). Each circuit has a $Q = 200$ and is tuned to 1000 kilocycles. The results are shown in the following table:

abscissa $Q\frac{(bw)}{f_0}$	bandwidth kilocycles	ordinate db response for $n = 1$	decibels response for $n = 3$	ϕ* for $n = 1$	ϕ* for $n = 3$
1.0	5.0	−3.0	−9	∓45°	∓135°
3.0	15	−10.0	−30	∓71½°	∓215°
10.0	50	−20.2	−61	∓84°	∓252°

* ϕ is negative for $f > f_0$, and vice versa.

Selectivity of single- and double-tuned circuits near resonance *continued*

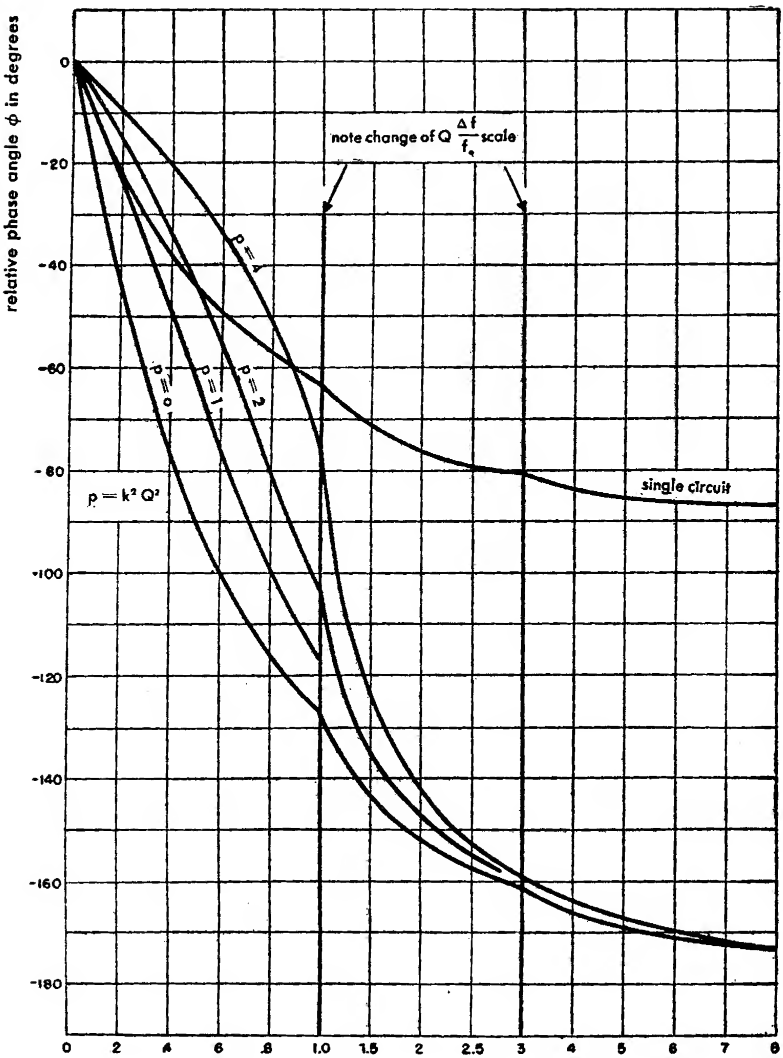

$$Q\frac{\Delta f}{f_0} = Q\frac{f - f_0}{f_0}$$

Fig. 8—Phase-shift curves for a single circuit $n = 1$ and a pair of coupled circuits $m = 1$.

For $f > f_0$, ϕ is negative, while for $f < f_0$, ϕ is positive. The numerical value is identical in either case for the same $|f - f_0|$.

Selectivity of single- and double-tuned circuits near resonance *continued*

$$\frac{\Delta f}{f_0} = \pm \frac{1}{2Q}\sqrt{(p-1) \pm \sqrt{(p+1)^2\left(\frac{E_0}{E}\right)^{\frac{2}{m}} - 4p}}$$

For very small values of E/E_0 the formulas reduce to

$$\frac{E}{E_0} = \left[\frac{p+1}{\left(2Q\frac{\Delta f}{f_0}\right)^2}\right]^m$$

Decibel response $= 20 \log_{10} (E/E_0)$

(db response of m pairs of circuits) $= m \times$ (db response of one pair)

$$\phi = m \tan^{-1}\left[\frac{-4Q\frac{\Delta f}{f_0}}{(p+1) - \left(2Q\frac{\Delta f}{f_0}\right)^2}\right]$$

As p approaches zero, the selectivity and phase shift approach the values for n single circuits, where $n = 2m$ (gain also approaches zero).

The above equations are plotted in Figs. 7 and 8.

For overcoupled circuits ($p > 1$)

Location of peaks: $$\frac{f_{peak} - f_0}{f_0} = \pm \frac{1}{2Q}\sqrt{p-1}$$

Amplitude of peaks: $$\frac{E_{peak}}{E_0} = \left(\frac{p+1}{2\sqrt{p}}\right)^m$$

Phase shift at peaks: $$\phi_{peak} = m \tan^{-1}(\mp\sqrt{p-1})$$

Approximate pass band (where $E/E_0 = 1$) is

$$\frac{f_{unity} - f_0}{f_0} = \sqrt{2}\,\frac{f_{peak} - f_0}{f_0} = \pm \frac{1}{Q}\sqrt{\frac{p-1}{2}}$$

Case 2: General formula for any Q_1 and Q_2

$$\frac{E}{E_0} = \left[\frac{p+1}{\sqrt{\left[\left(2Q\frac{\Delta f}{f_0}\right)^2 - B\right]^2 + (p+1)^2 - B^2}}\right]^m$$

(For B see top of p. 242.)

Selectivity of single- and double-tuned circuits near resonance *continued*

$$\frac{\Delta f}{f_0} = \pm \frac{1}{2Q}\sqrt{B \pm \left[(p+1)^2\left(\frac{E_0}{E}\right)^{\frac{2}{m}} - (p+1)^2 + B^2\right]^{\frac{1}{2}}}$$

$$\phi = m \tan^{-1}\left[-\frac{2Q\dfrac{\Delta f}{f_0}\left(\sqrt{\dfrac{Q_1}{Q_2}} + \sqrt{\dfrac{Q_2}{Q_1}}\right)}{(p+1) - \left(2Q\dfrac{\Delta f}{f_0}\right)^2}\right]$$

For overcoupled circuits

Location of peaks: $\dfrac{f_{\text{peak}} - f_0}{f_0} = \pm \dfrac{\sqrt{B}}{2Q} = \pm \dfrac{1}{2}\sqrt{k^2 - \dfrac{1}{2}\left(\dfrac{1}{Q_1^2} + \dfrac{1}{Q_2^2}\right)}$

Amplitude of peaks: $\dfrac{E_{\text{peak}}}{E_0} = \left[\dfrac{p+1}{\sqrt{(p+1)^2 - B^2}}\right]^m$

Case 3: Peaks just converged to a single peak

Here $B = 0$ or $k^2 = \dfrac{1}{2}\left(\dfrac{1}{Q_1^2} + \dfrac{1}{Q_2^2}\right)$

$$\frac{E}{E_o} = \left[\frac{2}{\sqrt{\left(2Q'\dfrac{\Delta f}{f_0}\right)^4 + 4}}\right]^m$$

where $Q' = \dfrac{2Q_1Q_2}{Q_1 + Q_2}$

$$\frac{\Delta f}{f_0} = \pm \frac{\sqrt{2}}{4}\left(\frac{1}{Q_1} + \frac{1}{Q_2}\right)\sqrt[4]{\left(\frac{E_0}{E}\right)^{\frac{2}{m}} - 1}$$

$$\phi = m \tan^{-1}\left[-\frac{4Q'\dfrac{\Delta f}{f_0}}{2 - \left(2Q'\dfrac{\Delta f}{f_0}\right)^2}\right]$$

The curves of Figs. 7 and 8 may be applied to this case, using the value $p = 1$, and substituting Q' for Q.

Attenuators

Definitions

An attenuator is a network designed to introduce a known loss when working between resistive impedances Z_1 and Z_2 to which the input and output impedances of the attenuator are matched. Either Z_1 or Z_2 may be the source and the other the load. The attenuation of such networks expressed as a power ratio is the same regardless of the direction of working.

Three forms of resistance network that may be conveniently used to realize these conditions are shown on page 252. These are the T section, the π section, and the bridged-T section. Equivalent balanced sections also are shown. Methods are given for the computation of attenuator networks, the hyperbolic expressions giving rapid solutions with the aid of tables of hyperbolic functions on pages 1103-1105. Tables of the various types of attenuators are given on pages 255 to 262.

Ladder attenuator

Ladder attenuator, Fig. 1, input switch points P_0, P_1, P_2, P_3 at shunt arms. Also intermediate point P_m tapped on series arm. May be either unbalanced, as shown, or balanced.

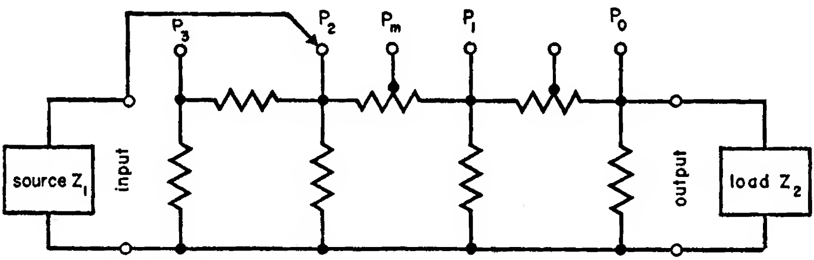

Fig. 1—Ladder attenuator.

Ladder, for design purposes, Fig. 2, is resolved into a cascade of π sections by imagining each shunt arm split into two resistors. Last section matches Z_2 to $2Z_1$. All other sections are symmetrical, matching impedances $2Z_1$, with a terminating resistor $2Z_1$ on the first section. Each section is designed for the loss required between the switch points at the ends of that section.

Input to P_0: Loss in decibels $= 10 \log_{10} \dfrac{(2Z_1 + Z_2)^2}{4Z_1Z_2}$

Input impedance $Z_1' = \dfrac{Z_2}{2}$ Output impedance $= \dfrac{Z_1Z_2}{Z_1 + Z_2}$

Ladder attenuator *continued*

Input to P_1, P_2, or P_3: Loss in decibels $= 3 +$ (sum of **losses of** π sections between input and output). Input impedance $Z_1' = Z_1$

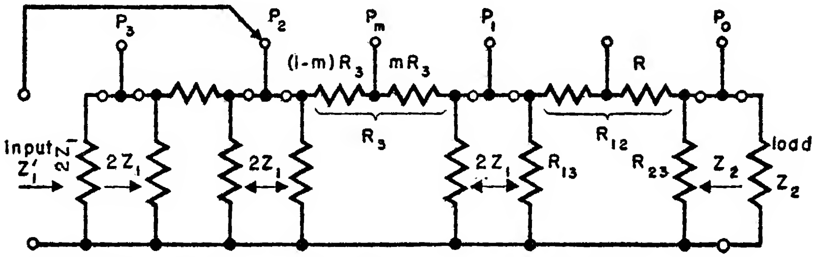

Fig. 2—Ladder attenuator resolved into a cascade of π sections.

Input to P_m (on a symmetrical π section):

$$\frac{e_0}{e_m} = \frac{1}{2}\,\frac{m(1-m)\,(K-1)^2 + 2K}{K - m\,(K-1)}$$

where

e_0 = output voltage when $m = 0$ (switch on P_1)

e_m = output voltage with switch on P_m

K = current ratio of the section (from P_1 to P_2) $\quad K > 1$

Input impedance $Z_1' = Z_1\left[m(1-m)\,\dfrac{(K-1)^2}{K} + 1\right]$

Maximum $\quad Z_1' = Z_1\left[\dfrac{(K-1)^2}{4K} + 1\right]$ for $m = 0.5$.

The unsymmetrical last section may be treated as a system of voltage-dividing resistors. Solve for the resistance R from P_0 to the tap, for each value of

$$\left(\frac{\text{output voltage with input on } P_0}{\text{output voltage with input on tap}}\right)$$

A useful case

When $Z_1 = Z_2 = 500$ ohms.

Then loss on P_0 is 3.52 decibels.

Let the last section be designed for loss of 12.51 decibels. Then

Ladder attenuator *continued*

R_{13} = 2444 ohms (shunted by 1000 ohms)
R_{23} = 654 ohms (shunted by 500 ohms)
R_{12} = 1409 ohms

The table shows the location of the tap and the input and output impedances for several values of loss, relative to the loss on P_0:

relative loss in decibels	tap R ohms	input impedance ohms	output impedance ohms
0	0	250	250
2	170	368	304
4	375	478	353
6	615	562	394
8	882	600	428
10	1157	577	454
12	1409	500	473

Input to P_0: Output impedance = 0.6 Z (See Fig. 3.)

Input to P_0, P_1, P_2, or P_3: Loss in decibels = 6 + (sum of losses of π sections between input and output). Input impedance = Z

Input to P_m:

$$\frac{e_0}{e_m} = \frac{1}{4}\,\frac{m(1-m)(K-1)^2 + 4K}{K - m(K-1)}$$

Input impedance:

$$Z' = Z\left[\frac{m(1-m)(K-1)^2}{2K} + 1\right]$$

$$\text{Maximum } Z' = Z\left[\frac{(K-1)^2}{8K} + 1\right] \text{ for } m = 0.5$$

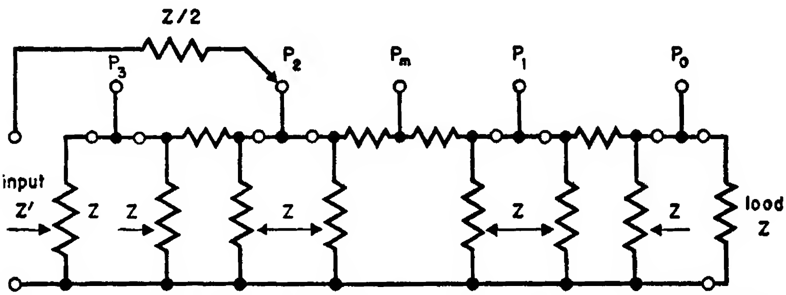

Fig. 3—A variation of the ladder attenuator, useful when $Z_1 = Z_2 = Z$. Simpler in design, with improved impedance characteristics, but having minimum insertion loss 2.5 decibels higher than attenuator of Fig. 2. All π sections are symmetrical.

Load impedance

Effect of incorrect load impedance on operation of an attenuator

In the applications of attenuators, the question frequently arises as to the effect upon the input impedance and the attenuation by the use of a load impedance which is different from that for which the network was designed. The following results apply to all resistive networks that, when operated between resistive impedances Z_1 and Z_2, present matching terminal impedances Z_1 and Z_2, respectively. The results may be derived in the general case by the application of the network theorems and may be readily confirmed mathematically for simple specific cases such as the T section.

For the designed use of the network, let

Z_1 = input impedance of properly terminated network

Z_2 = load impedance that properly terminates the network

N = power ratio from input to output

K = current ratio from input to output

$K = \frac{i_1}{i_2} = \sqrt{\frac{NZ_2}{Z_1}}$ (different in the two directions except when $Z_2 = Z_1$)

For the actual conditions of operation, let

$$(Z_2 + \Delta Z_2) = Z_2\left(1 + \frac{\Delta Z_2}{Z_2}\right) = \text{actual load impedance}$$

$$(Z_1 + \Delta Z_1) = Z_1\left(1 + \frac{\Delta Z_1}{Z_1}\right) = \text{resulting input impedance}$$

$$(K + \Delta K) = K\left(1 + \frac{\Delta K}{K}\right) = \text{resulting current ratio}$$

While Z_1, Z_2, and K are restricted to real quantities by the assumed nature of the network, ΔZ_2 is not so restricted, e.g.,

$$\Delta Z_2 = \Delta R_2 + j\Delta X_2$$

As a consequence, ΔZ_1 and ΔK can become imaginary or complex. Furthermore, ΔZ_2 is not restricted to small values.

Load impedance *continued*

The results for the actual conditions are

$$\frac{\Delta Z_1}{Z_1} = \frac{2\,\Delta Z_2/Z_2}{2N + (N-1)\dfrac{\Delta Z_2}{Z_2}} \quad \text{and} \quad \frac{\Delta K}{K} = \left(\frac{N-1}{2N}\right)\frac{\Delta Z_2}{Z_2}$$

Certain special cases may be cited

Case 1: For small $\Delta Z_2/Z_2$

$$\frac{\Delta Z_1}{Z_1} = \frac{1}{N}\frac{\Delta Z_2}{Z_2} \quad \text{or} \quad \Delta Z_1 = \frac{1}{K^2}\Delta Z_2$$

$$\frac{\Delta i_2}{i_2} = -\frac{1}{2}\frac{\Delta Z_2}{Z_2}$$

but the error in insertion power loss of the attenuator is negligibly small.

Case 2: Short-circuited output

$$\frac{\Delta Z_1}{Z_1} = \frac{-2}{N+1}$$

$$\text{or input impedance} = \left(\frac{N-1}{N+1}\right) Z_1 = Z_1 \tanh \theta$$

where θ is the designed attenuation in nepers.

Case 3: Open-circuited output

$$\frac{\Delta Z_1}{Z_1} = \frac{2}{N-1}$$

$$\text{or input impedance} = \left(\frac{N+1}{N-1}\right) Z_1 = Z_1 \coth \theta$$

Case 4: For $N = 1$ (possible only when $Z_1 = Z_2$ and directly connected)

$$\frac{\Delta Z_1}{Z_1} = \frac{\Delta Z_2}{Z_2}$$

$$\frac{\Delta K}{K} = 0$$

Case 5: For large N

$$\frac{\Delta K}{K} = \frac{1}{2}\frac{\Delta Z_2}{Z_2}$$

Attenuator network design

see page 254 for symbols

description	configuration: unbalanced	configuration: balanced
Unbalanced T and balanced H (see Fig. 8)	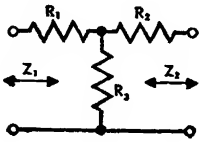	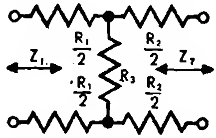
Symmetrical T and H ($Z_1 = Z_2 = Z$) (see Fig. 4)	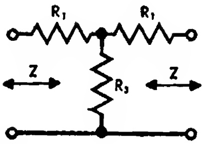	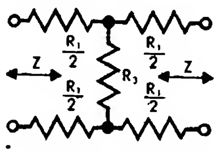
Minimum-loss pad matching Z_1 and Z_2 ($Z_1 > Z_2$) (see Fig. 7)	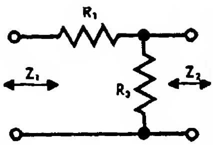	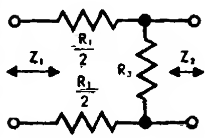
Unbalanced π and balanced 0	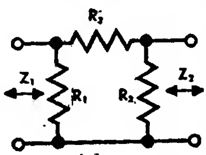	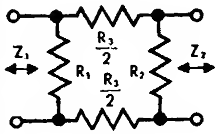
Symmetrical π and 0 ($Z_1 = Z_2 = Z$) (see Fig. 5)	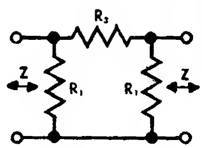	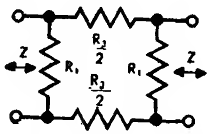
Bridged T and bridged H (see Fig. 6)	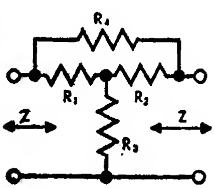	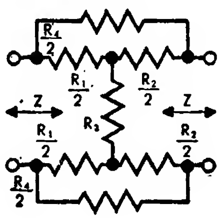

design equations		
hyperbolic	**arithmetical**	**checking equations**
$R_3=\frac{\sqrt{Z_1Z_2}}{\sinh\theta}$ $R_1=\frac{Z_1}{\tanh\theta}-R_3$ $R_2=\frac{Z_2}{\tanh\theta}-R_3$	$R_3=\frac{2\sqrt{NZ_1Z_2}}{N-1}$ $R_1=Z_1\left(\frac{N+1}{N-1}\right)-R_3$ $R_2=Z_2\left(\frac{N+1}{N-1}\right)-R_3$	
$R_3=\frac{Z}{\sinh\theta}$ $R_1=Z\tanh\frac{\theta}{2}$	$R_3=\frac{2Z\sqrt{N}}{N-1}=\frac{2ZK}{K^2-1}$ $=\frac{2Z}{K-1/K}$ $R_1=Z\frac{\sqrt{N}-1}{\sqrt{N}+1}=Z\frac{K-1}{K+1}$ $=Z[1-2/(K+1)]$	$R_1R_3=\frac{Z^2}{1+\cosh\theta}=Z^2\frac{2K}{(K+1)^2}$ $\frac{R_1}{R_3}=\cosh\theta-1=2\sinh^2\frac{\theta}{2}$ $=\frac{(K-1)^2}{2K}$ $Z=R_1\sqrt{1+2\frac{R_3}{R_1}}$
$\cosh\theta=\sqrt{\frac{Z_1}{Z_2}}$ $\cosh 2\theta=2\frac{Z_1}{Z_2}-1$	$R_1=Z_1\sqrt{1-\frac{Z_2}{Z_1}}$ $R_3=\frac{Z_2}{\sqrt{1-\frac{Z_2}{Z_1}}}$	$R_1R_3=Z_1Z_2$ $\frac{R_1}{R_3}=\frac{Z_1}{Z_2}-1$ $N=\left(\sqrt{\frac{Z_1}{Z_2}}+\sqrt{\frac{Z_1}{Z_2}-1}\right)^2$
$R_3=\sqrt{Z_1Z_2}\sinh\theta$ $\frac{1}{R_1}=\frac{1}{Z_1\tanh\theta}-\frac{1}{R_3}$ $\frac{1}{R_2}=\frac{1}{Z_2\tanh\theta}-\frac{1}{R_3}$	$R_3=\frac{N-1}{2}\sqrt{\frac{Z_1Z_2}{N}}$ $\frac{1}{R_1}=\frac{1}{Z_1}\left(\frac{N+1}{N-1}\right)-\frac{1}{R_3}$ $\frac{1}{R_2}=\frac{1}{Z_2}\left(\frac{N+1}{N-1}\right)-\frac{1}{R_3}$	
$R_3=Z\sinh\theta$ $R_1=\frac{Z}{\tanh\frac{\theta}{2}}$	$R_3=Z\frac{N-1}{2\sqrt{N}}=Z\frac{K^2-1}{2K}$ $=Z(K-1/K)/2$ $R_1=Z\frac{\sqrt{N}+1}{\sqrt{N}-1}=Z\frac{K+1}{K-1}$ $=Z[1+2/(K-1)]$	$R_1R_3=Z^2(1+\cosh\theta)=Z^2\frac{(K+1)^2}{2K}$ $\frac{R_3}{R_1}=\cosh\theta-1=\frac{(K-1)^2}{2K}$ $Z=\frac{R_1}{\sqrt{1+2\frac{R_1}{R_3}}}$
	$R_1=R_2=Z$ $R_4=Z(K-1)$ $R_3=\frac{Z}{K-1}$	$R_3R_4=Z^2$ $\frac{R_4}{R_3}=(K-1)^2$

Four-terminal networks: The hyperbolic equations above are valid for passive linear four-terminal networks in general, working between input and output impedances matching the respective image impedances. In this case: Z_1 and Z_2 are the image impedances; R_1, R_2 and R_3 become complex impedances; and θ is the image transfer constant. $\theta=\alpha+j\beta$, where α is the image attenuation constant and β is the image phase constant.

Attenuator network design *continued*

Symbols

Z_1 and Z_2 are the terminal impedances (resistive) to which the attenuator is matched.

N is the ratio of the power absorbed by the attenuator from the source to the power delivered to the load.

K is the ratio of the attenuator input current to the output current into the load. When $Z_1 = Z_2$, $K = \sqrt{N}$. Otherwise K is different in the two directions.

Attenuation in decibels $= 10 \log_{10} N$

Attenuation in nepers $= \theta = \frac{1}{2} \log_e N$

For a table of decibels versus power and voltage or current ratio, see page 40. Factors for converting decibels to nepers, and nepers to decibels, are given at the foot of that table.

Notes on error formulas

The formulas and figures for errors, given in Figs. 4 to 8, are based on the assumption that the attenuator is terminated approximately by its proper terminal impedances Z_1 and Z_2. They hold for deviations of the attenuator arms and load impedances up to $\pm$ 20 percent or somewhat more. The error due to each element is proportional to the deviation of the element, and the total error of the attenuator is the sum of the errors due to each of the several elements.

When any element or arm R has a reactive component ΔX in addition to a resistive error ΔR, the errors in input impedance and output current are

$$\Delta Z = A(\Delta R + j\Delta X)$$

$$\frac{\Delta i}{i} = B\left(\frac{\Delta R + j\Delta X}{R}\right)$$

where A and B are constants of proportionality for the elements in question. These constants can be determined in each case from the figures given for errors due to a resistive deviation ΔR.

The reactive component ΔX produces a quadrature component in the output current, resulting in a phase shift. However, for small values of ΔX, the error in insertion loss is negligibly small.

For the errors produced by mismatched terminal load impedance, refer to Case 1, page 251.

Symmetrical T or H attenuators

Interpolation of symmetrical T or H attenuators *(Fig. 4)*

Column R_1 may be interpolated linearly. Do not interpolate R_3 column. For 0 to 6 decibels interpolate the $1000/R_3$ column. Above 6 decibels, interpolate the column $\log_{10} R_3$ and determine R_3 from the result.

Fig. 4—Symmetrical T and H attenuator values. $Z = 500$ ohms resistive (diagram on page 252).

attenuation in decibels	series arm R_1 ohms	shunt arm R_3 ohms	$1000/R_3$	$\log_{10} R_3$
0.0	0.0	inf	0.0000	——
0.2	5.8	21,700	0.0461	——
0.4	11.5	10,850	0.0921	——
0.6	17.3	7,230	0.1383	——
0.8	23.0	5,420	0.1845	——
1.0	28.8	4,330	0.2308	——
2.0	57.3	2,152	0.465	——
3.0	85.5	1,419	0.705	——
4.0	113.1	1,048	0.954	——
5.0	140.1	822	1.216	——
6.0	166.1	669	1.494	2.826
7.0	191.2	558	——	2.747
8.0	215.3	473.1	——	2.675
9.0	238.1	405.9	——	2.608
10.0	259.7	351.4	——	2.546
12.0	299.2	268.1	——	2.428
14.0	333.7	207.8	——	2.318
16.0	363.2	162.6	——	2.211
18.0	388.2	127.9	——	2.107
20.0	409.1	101.0	——	2.004
22.0	426.4	79.94	——	1.903
24.0	440.7	63.35	——	1.802
26.0	452.3	50.24	——	1.701
28.0	461.8	39.87	——	1.601
30.0	469.3	31.65	——	1.500
35.0	482.5	17.79	——	1.250
40.0	490.1	10.00	——	1.000
50.0	496.8	3.162	——	0.500
60.0	499.0	1.000	——	0.000
80.0	499.9	0.1000	——	−1.000
100.0	500.0	0.01000	——	−2.000

Symmetrical T or H attenuators *continued*

Errors in symmetrical T or H attenuators

Series arms R_1 and R_2 in error: Error in input impedances:

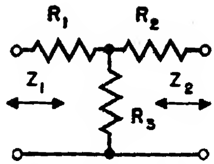

nominally $R_1 = R_2$
$Z_1 = Z_2$

$$\Delta Z_1 = \Delta R_1 + \frac{1}{K^2}\Delta R_2$$

and

$$\Delta Z_2 = \Delta R_2 + \frac{1}{K^2}\Delta R_1$$

Error in insertion loss, in decibels,

$$\text{db} = 4\left(\frac{\Delta R_1}{Z_1} + \frac{\Delta R_2}{Z_2}\right) \text{ approximately}$$

Shunt arm R_3 in error (10 percent high)

designed loss, in decibels	error in insertion loss, in decibels	error in input impedance $100\frac{\Delta Z}{Z}$ percent
0.2	−0.01	0.2
1	−0.05	1.0
6	−0.3	3.3
12	−0.5	3.0
20	−0.7	1.6
40	−0.8	0.2
100	−0.8	0.0

Error in input impedance:

$$\frac{\Delta Z}{Z} = 2\frac{K-1}{K(K+1)}\frac{\Delta R_3}{R_3}$$

Error in output current:

$$\frac{\Delta i}{i} = \frac{K-1}{K+1}\frac{\Delta R_3}{R_3}$$

See notes on page 254.

Symmetrical π and O attenuators

Interpolation of symmetrical π and O attenuators (Fig. 5).

Column R_1 may be interpolated linearly above 16 decibels, and R_3 up to 20 decibels. Otherwise interpolate the $1000/R_1$ and $\log_{10} R_3$ columns, respectively.

Fig. 5—Symmetrical π and O attenuator. Z = 500 ohms resistive (diagram, page 252).

attenuation in decibels	shunt arm R_1 ohms	$1000/R_1$	series arm R_3 ohms	$\log_{10} R_3$
0.0	∞	0.000	0.0	—
0.2	43,400	0.023	11.5	—
0.4	21,700	0.046	23.0	—
0.6	14,500	0.069	34.6	—
0.8	10,870	0.092	46.1	—
1.0	8,700	0.115	57.7	—
2.0	4,362	0.229	116.1	—
3.0	2,924	0.342	176.1	—
4.0	2,210	0.453	238.5	—
5.0	1,785	0.560	304.0	—
6.0	1,505	0.665	373.5	—
7.0	1,307	0.765	448.0	—
8.0	1,161.4	0.861	528.4	—
9.0	1,049.9	0.952	615.9	—
10.0	962.5	1.039	711.5	—
12.0	835.4	1.197	932.5	—
14.0	749.3	1.335	1,203.1	—
16.0	688.3	1.453	1,538	—
18.0	644.0	—	1,954	—
20.0	611.1	—	2,475	3.394
22.0	586.3	—	3,127	3.495
24.0	567.3	—	3,946	3.596
26.0	552.8	—	4,976	3.697
28.0	541.5	—	6,270	3.797
30.0	532.7	—	7,900	3.898
35.0	518.1	—	14,050	4.148
40.0	510.1	—	25,000	4.398
50.0	503.2	—	79,100	4.898
60.0	501.0	—	2.50×10^5	5.398
80.0	500.1	—	2.50×10^6	6.398
100.0	500.0	—	2.50×10^7	7.398

Symmetrical π and 0 attenuators *continued*

Errors in symmetrical π and 0 attenuators

Error in input impedance:

$$\frac{\Delta Z'}{Z'} = \frac{K-1}{K+1}\left(\frac{\Delta R_1}{R_1} + \frac{1}{K^2}\frac{\Delta R_2}{R_2} + \frac{2}{K}\frac{\Delta R_3}{R_3}\right)$$

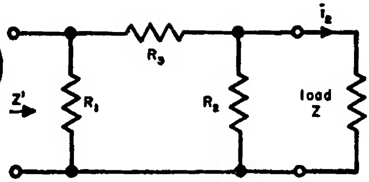

nominally $R_1 = R_2$ and $Z' = Z$

Error in insertion loss,

$$\text{decibels} = -8\frac{\Delta i_2}{i_2} \text{ (approximately)}$$

$$= 4\frac{K-1}{K+1}\left(-\frac{\Delta R_1}{R_1} - \frac{\Delta R_2}{R_2} + 2\frac{\Delta R_3}{R_3}\right)$$

See notes on page 254.

Bridged T or H attenuators

Interpolation of bridged T or H attenuators *(Fig. 6)*

Bridge arm R_4: Use the formula $\log_{10}(R_4 + 500) = 2.699 +$ decibels/20 for $Z = 500$ ohms. However, if preferred, the tabular values of R_4 may be interpolated linearly, between 0 and 10 decibels only.

Fig. 6—Values for bridged T or H attenuators. $Z = 500$ ohms resistive, $R_1 = R_2 = 500$ ohms (diagram on page 252).

attenuation in decibels	bridge arm R_4 ohms	shunt arm R_3 ohms	attenuation in decibels	bridge arm R_4 ohms	shunt arm R_3 ohms
0.0	0.0	∞	12.0	1,491	167.7
0.2	11.6	21,500	14.0	2,006	124.6
0.4	23.6	10,610	16.0	2,655	94.2
0.6	35.8	6,990	18.0	3,472	72.0
0.8	48.2	5,180	20.0	4,500	55.6
1.0	61.0	4,100	25.0	8,390	29.8
2.0	129.5	1,931	30.0	15,310	16.33
3.0	206.3	1,212	40.0	49,500	5.05
4.0	292.4	855	50.0	157,600	1.586
5.0	389.1	642	60.0	499,500	0.501
6.0	498	502	80.0	5.00×10^6	0.0500
7.0	619	404	100.0	50.0×10^6	0.00500
8.0	756	331	—	—	—
9.0	909	275.0	—	—	—
10.0	1,081	231.2	—	—	—

Bridged T or H attenuators *continued*

Shunt arm R_3: Do not interpolate R_3 column. Compute R_3 by the formula $R_3 = 10^6/4R_4$ for $Z = 500$ ohms.

Note: For attenuators of 60 db and over, the bridge arm R_4 may be omitted provided a shunt arm is used having twice the resistance tabulated in the R column. (This makes the input impedance 0.1 of 1 percent high at 60 db.)

Errors in bridged T or H attenuators

Resistance of any one arm 10 percent higher than correct value

designed loss decibels	A decibels*	B percent*	C percent*
0.2	0.01	0.005	0.2
1	0.05	0.1	1.0
6	0.2	2.5	2.5
12	0.3	5.6	1.9
20	0.4	8.1	0.9
40	0.4	10	0.1
100	0.4	10	0.0

* Refer to following tabulation.

element in error (10 percent high)	error in loss	error in terminal impedance	remarks
Series arm R_1 (analogous for arm R_2)	Zero	B, for adjacent terminals	Error in impedance at opposite terminals is zero
Shunt arm R_3	$-$A	C	Loss is lower than designed loss
Bridge arm R_4	A	C	Loss is higher than designed loss

Error in input impedance:

$$\frac{\Delta Z_1}{Z_1} = \left(\frac{K-1}{K}\right)^2 \frac{\Delta R_1}{R_1} + \frac{K-1}{K^2}\left(\frac{\Delta R_3}{R_3} + \frac{\Delta R_4}{R_4}\right)$$

For $\Delta Z_2/Z_2$ use subscript 2 in formula in place of subscript 1.

Error in output current:

$$\frac{\Delta i}{i} = \frac{K-1}{2K}\left(\frac{\Delta R_3}{R_3} - \frac{\Delta R_4}{R_4}\right)$$

See notes on page 254.

Minimum-loss pads

Interpolation of minimum-loss pads *(Fig. 7)*

This table may be interpolated linearly with respect to Z_1, Z_2, or Z_1/Z_2 except when Z_1/Z_2 is between 1.0 and 1.2. The accuracy of the interpolated value becomes poorer as Z_1/Z_2 passes below 2.0 toward 1.2, especially for R_3.

For other terminations

If the terminating resistances are to be Z_A and Z_B instead of Z_1 and Z_2, respectively, the procedure is as follows. Enter the table at $\frac{Z_1}{Z_2} = \frac{Z_A}{Z_B}$ and

Fig. 7—Values for minimum-loss pads matching Z_1 and Z_2, both resistive (diagram on page 252).

Z_1 ohms	Z_2 ohms	Z_1/Z_2	loss in decibels	series arm R_1 ohms	shunt arm R_3 ohms
10,000	500	20.00	18.92	9,747	513.0
8,000	500	16.00	17.92	7,746	516.4
6,000	500	12.00	16.63	5,745	522.2
5,000	500	10.00	15.79	4,743	527.0
4,000	500	8.00	14.77	3,742	534.5
3,000	500	6.00	13.42	2,739	547.7
2,500	500	5.00	12.54	2,236	559.0
2,000	500	4.00	11.44	1,732	577.4
1,500	500	3.00	9.96	1,224.7	612.4
1,200	500	2.40	8.73	916.5	654.7
1,000	500	2.00	7.66	707.1	707.1
800	500	1.60	6.19	489.9	816.5
600	500	1.20	3.77	244.9	1,224.7
500	400	1.25	4.18	223.6	894.4
500	300	1.667	6.48	316.2	474.3
500	250	2.00	7.66	353.6	353.6
500	200	2.50	8.96	387.3	258.2
500	160	3.125	10.17	412.3	194.0
500	125	4.00	11.44	433.0	144.3
500	100	5.00	12.54	447.2	111.80
500	80	6.25	13.61	458.3	87.29
500	65	7.692	14.58	466.4	69.69
500	50	10.00	15.79	474.3	52.70
500	40	12.50	16.81	479.6	41.70
500	30	16.67	18.11	484.8	30.94
500	25	20.00	18.92	487.3	25.65

Minimum-loss pads *continued*

read the loss and the tabular values of R_1 and R_3. Then the series and shunt arms are, respectively, MR_1 and MR_3, where $M = \frac{Z_A}{Z_1} = \frac{Z_B}{Z_2}$.

Errors in minimum-loss pads

impedance ratio Z_1/Z_2	D decibels*	E percent*	F percent*
1.2	0.2	+4.1	+1.7
2.0	0.3	7.1	1.2
4.0	0.35	8.6	0.6
10.0	0.4	9.5	0.25
20.0	0.4	9.7	0.12

* Notes

Series arm R_1 10 percent high: Loss is increased by D decibels from above table. Input impedance Z_1 is increased by E percent. Input impedance Z_2 is increased by F percent.

Shunt arm R_3 10 percent high: Loss is decreased by D decibels from above table. Input impedance Z_2 is increased by E percent. Input impedance Z_1 is increased by F percent.

Errors in input impedance

$$\frac{\Delta Z_1}{Z_1} = \sqrt{1 - \frac{Z_2}{Z_1}}\left(\frac{\Delta R_1}{R_1} + \frac{1}{N}\frac{\Delta R_3}{R_3}\right)$$

$$\frac{\Delta Z_2}{Z_2} = \sqrt{1 - \frac{Z_2}{Z_1}}\left(\frac{\Delta R_3}{R_3} + \frac{1}{N}\frac{\Delta R_1}{R_1}\right)$$

Error in output current, working either direction

$$\frac{\Delta i}{i} = \frac{1}{2}\sqrt{1 - \frac{Z_2}{Z_1}}\left(\frac{\Delta R_3}{R_3} - \frac{\Delta R_1}{R_1}\right)$$

See notes on page 254.

Miscellaneous T and H pads (Fig. 8)

Fig. 8—Values for miscellaneous T and H pads (diagram on page 252).

resistive terminations		loss decibels	attenuator arms		
Z_1 ohms	Z_2 ohms		series R_1 ohms	series R_2 ohms	shunt R_3 ohms
5,000	2,000	10	3,889	222	2,222
5,000	2,000	15	4,165	969	1,161
5,000	2,000	20	4,462	1,402	639
5,000	500	20	4,782	190.7	319.4
2,000	500	15	1,763	165.4	367.3
2,000	500	20	1,838	308.1	202.0
2,000	200	20	1,913	76.3	127.8
500	200	10	388.9	22.2	222.2
500	200	15	416.5	96.9	116.1
500	200	20	446.2	140.2	63.9
500	50	20	478.2	19.07	31.94
200	50	15	176.3	16.54	36.73
200	50	20	183.8	30.81	20.20

Errors in T and H pads

Series arms R_1 and R_2 in error: Errors in input impedances are

$$\Delta Z_1 = \Delta R_1 + \frac{1}{N}\frac{Z_1}{Z_2}\Delta R_2 \quad \text{and} \quad \Delta Z_2 = \Delta R_2 + \frac{1}{N}\frac{Z_2}{Z_1}\Delta R_1$$

Error in insertion loss, in decibels $= 4\left(\frac{\Delta R_1}{Z_1} + \frac{\Delta R_2}{Z_2}\right)$ approximately

Shunt arm R_3 in error (10 percent high)

Z_1/Z_2	designed loss decibels	error in loss decibels	error in input impedance	
			$100\frac{\Delta Z_1}{Z_1}$	$100\frac{\Delta Z_2}{Z_2}$
2.5	10	−0.4	1.1%	7.1%
2.5	15	−0.6	1.2	4.6
2.5	20	−0.7	0.9	2.8
4.0	15	−0.5	0.8	6.0
4.0	20	−0.65	0.6	3.6
10	20	−0.6	0.3	6.1

$$\frac{\Delta Z_1}{Z_1} = \frac{2}{N-1}\left(\sqrt{\frac{NZ_2}{Z_1}} + \sqrt{\frac{Z_1}{NZ_2}} - 2\right)\frac{\Delta R_3}{R_3}$$

{for $\Delta Z_2 Z_2$ interchange subscripts 1 and 2

$$\frac{\Delta i}{i} = \frac{N + 1 - \sqrt{N}\left(\sqrt{\frac{Z_1}{Z_2}} + \sqrt{\frac{Z_2}{Z_1}}\right)}{N-1}\,\frac{\Delta R_3}{R_3}$$

{where i is the output current.

Bridges and impedance measurements

In the diagrams of bridges below, the source is shown as a generator, and the detector as a pair of headphones. The positions of these two elements may be interchanged as dictated by detailed requirements in any individual case, such as location of grounds, etc. For all but the lowest frequencies, a shielded transformer is required at either the input or output (but not usually at both) terminals of the bridge. This is shown in some of the following diagrams. The detector is chosen according to the frequency of the source. When insensitivity of the ear makes direct use of headphones impractical, a simple radio receiver or its equivalent is essential. Some selectivity is desirable to discriminate against harmonics, for the bridge is often frequency sensitive. The source may be modulated in order to obtain an audible signal, but greater sensitivity and discrimination against interference are obtained by the use of a continuous-wave source and a heterodyne detector. An amplifier and oscilloscope or an output meter are sometimes preferred for observing nulls. In this case it is convenient to have an audible output signal available for the preliminary setup and for locating trouble, since much can be deduced from the quality of the audible signal that would not be apparent from observation of amplitude only.

Fundamental alternating-current or Wheatstone bridge

Balance condition is $Z_x = Z_s Z_a / Z_b$
Maximum sensitivity when Z_d is the conjugate of the bridge output impedance and Z_g the conjugate of its

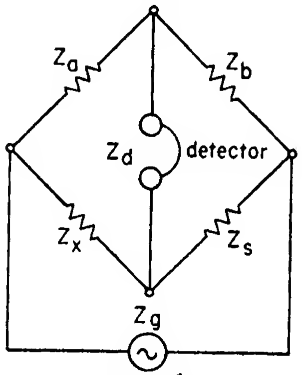

input impedance. Greatest sensitivity when bridge arms are equal, e.g., for resistive arms,

$Z_d = Z_a = Z_b = Z_x = Z_s = Z_g$

Bridge with double-shielded transformer

Shield on secondary may be floating, connected to either end, or to center of secondary winding. It may be in two equal parts and connected to opposite ends of the winding. In any case, its capacitance to ground must be kept to a minimum.

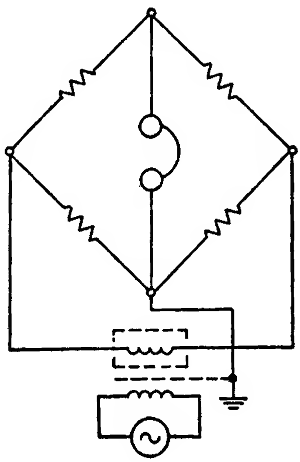

Wagner earth connection

None of the bridge elements are grounded directly. First balance bridge with switch to *B*. Throw switch to G and rebalance by means of *R* and C. Recheck bridge balance and repeat as required. The capacitor balance C is necessary only when the

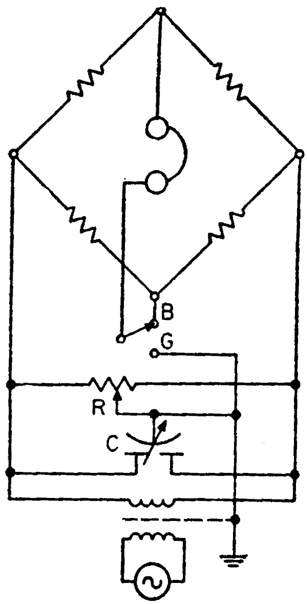

frequency is above the audio range. The transformer may have only a single shield as shown, with the capacitance of the secondary to the shield kept to a minimum.

Capacitor balance

Useful when one point of bridge must be grounded directly and only a simple shielded transformer is used. Balance bridge, then open the two arms at *P* and Q. Rebalance by auxiliary capacitor C. Close *P* and Q and check balance.

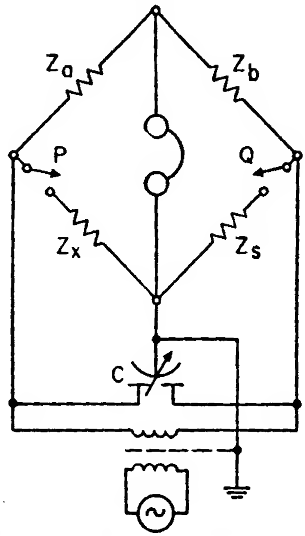

Series-resistance-capacitance bridge

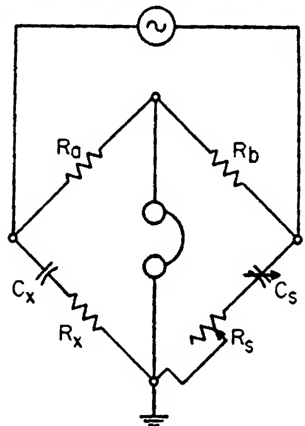

$$C_x = C_s R_b/R_a$$

$$R_x = R_s R_a/R_b$$

Wien bridge

$$\frac{C_x}{C_s} = \frac{R_b}{R_a} - \frac{R_s}{R_x}$$

$$C_s C_x = 1/\omega^2 R_s R_x$$

Wien bridge *continued*

For measurement of frequency, or in a frequency-selective application, if

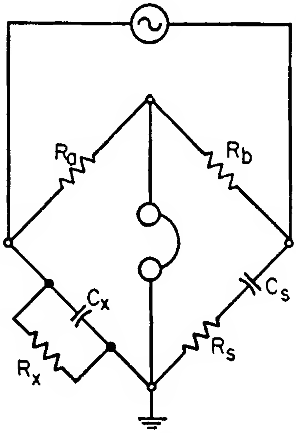

we make $C_x = C_s$, $R_x = R_s$, and $R_b = 2R_a$, then

$$f = \frac{1}{2\pi C_s R_s}$$

Owen bridge

$$L_x = C_b R_a R_d$$

$$R_x = \frac{C_b R_a}{C_d} - R_c$$

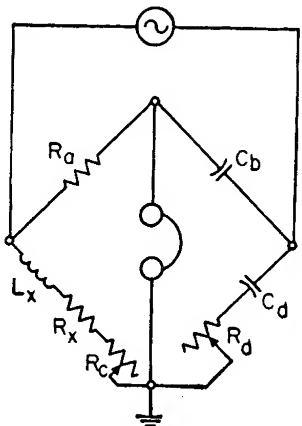

Resonance bridge

$$\omega^2 LC = 1$$

$$R_x = R_s R_a / R_b$$

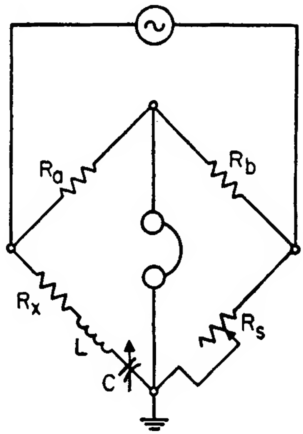

Maxwell bridge

$$L_x = R_a R_b C_s$$

$$R_x = \frac{R_a R_b}{R_s}$$

$$Q_x = \omega \frac{L_x}{R_x} = \omega C_s R_s$$

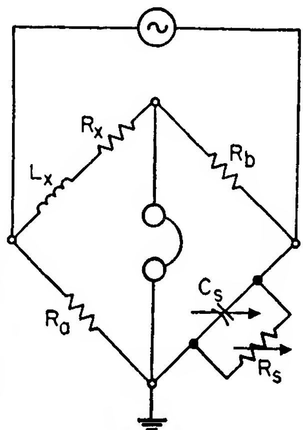

Hay bridge

For measurement of large inductance.

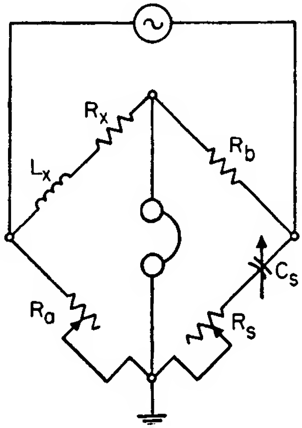

$$L_x = \frac{R_a R_b C_s}{1 + \omega^2 C_s^2 R_s^2}$$

$$Q_x = \frac{\omega L_x}{R_x} = \frac{1}{\omega C_s R_s}$$

Schering bridge

$$C_x = C_s R_b / R_a$$

$$1/Q_x = \omega C_x R_x = \omega C_b R_b$$

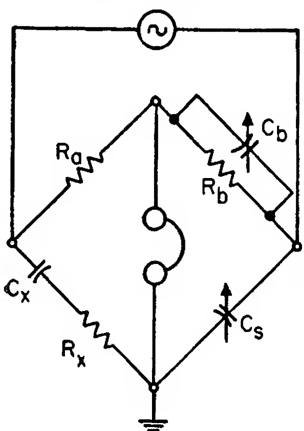

Substitution method for high impedances

Initial balance (unknown terminals $x - x$ open):

C_s' and R_s'

Final balance (unknown connected to $x - x$):

C_s'' and R_s''

Then when $R_x > 10/\omega C_s'$, there results, with error < 1 percent,

$$C_x = C_s' - C_s''$$

The parallel resistance is

$$R_x = \frac{1}{\omega^2 C_s'^2 (R_s' - R_s'')}$$

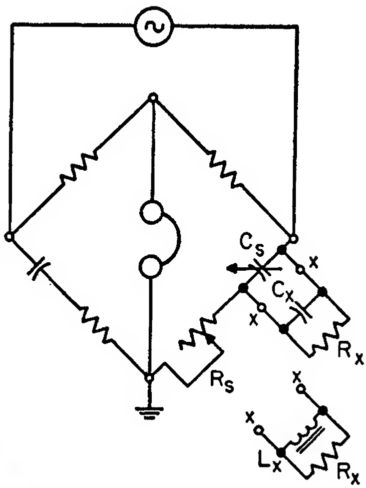

If unknown is an inductor,

$$L_x = -\frac{1}{\omega^2 C_x} = \frac{1}{\omega^2 (C_s'' - C_s')}$$

Measurement with capacitor in series with unknown

Initial balance (unknown terminals x–x short-circuited):

C_s' and R_s'

Final balance (x — x un-shorted):

C_s'' and R_s''

Then the series resistance is

$$R_x = (R_s'' - R_s')R_a/R_b$$

$$C_x = \frac{R_b C_s' C_s''}{R_a(C_s' - C_s'')}$$

$$= \frac{R_b}{R_a} C_s' \left(\frac{C_s'}{C_s' - C_s''} - 1\right)$$

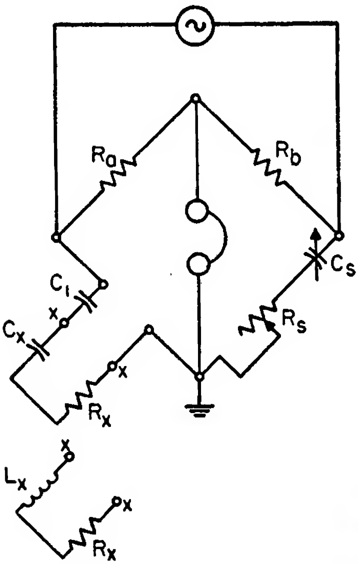

When $C_s'' > C_s'$,

$$L_x = \frac{1}{\omega^2} \frac{R_a}{R_b C_s'} \left(1 - \frac{C_s'}{C_s''}\right)$$

Measurement of direct capacitance

Connection of N to N' places C_{nq} across phones, and C_{np} across R_b which requires only a small re-adjustment of R_s.

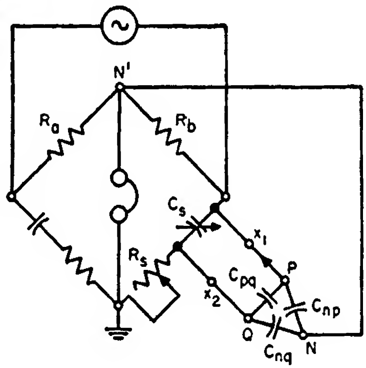

Initial balance: Lead from P disconnected from X_1 but lying as close to connected position as practical.

Final balance: Lead connected to X_1.

By the substitution method above, $C_{pq} = C_s' - C_s''$

Felici mutual-inductance balance

At the null:

$$M_x = -M_s$$

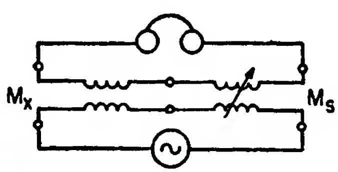

Useful at lower frequencies where capacitive reactances associated with windings are negligibly small.

Mutual-inductance capacitance balance

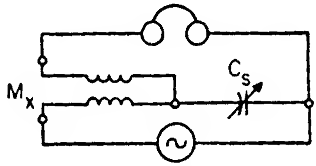

Using low-loss capacitor. At the null

$M_x = 1/\omega^2 C_s$

Hybrid-coil method

At null:

$Z_1 = Z_2$

The transformer secondaries must be accurately matched and balanced to

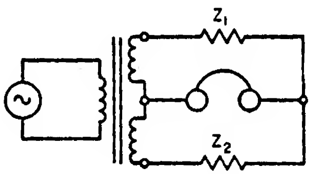

ground. Useful at audio and carrier frequencies.

Q of resonant circuit by bandwidth

For 3-decibel or half-power points. Source loosely coupled to circuit. Adjust frequency to each side of resonance, noting bandwidth when

$v = 0.71 \times$ (v at resonance)

$$Q = \frac{\text{(resonance frequency)}}{\text{(bandwidth)}}$$

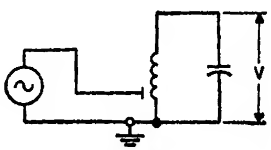

Q-meter (Boonton Radio Type 160A)

R_1 = 0.04 ohm

R_2 = 100 megohms

V = vacuum-tube voltmeter

I = thermal milliammeter

$L_x R_x C_0$ = unknown coil plugged into COIL terminals for measurement.

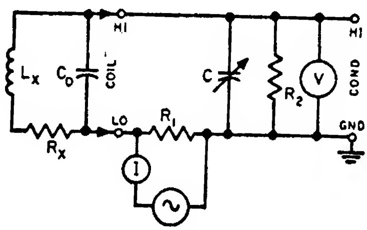

Correction of Q reading

For distributed capacitance C_0 of coil

$$Q_{\text{true}} = Q\,\frac{C + C_0}{C}$$

where

Q = reading of Q-meter (corrected for internal resistors R_1 and R_2 if necessary)

C = capacitance reading of Q-meter

Measurement of C_0 and true L_x

C plotted vs $1/f^2$ is a straight line.

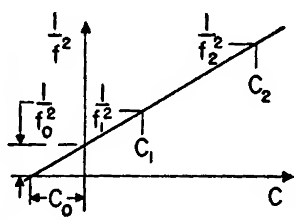

Measurement of C_0 and true L_x *continued*

L_x = true inductance

$$= \frac{1/f^2_2 - 1/f^2_1}{4\pi^2\ (C_2 - C_1)}$$

C_0 = negative intercept

f_0 = natural frequency of coil

When only two readings are taken and $f_1/f_2 = 2.00$,

$C_0 = (C_2 - 4C_1)/3$

Using μh, mc, and $\mu\mu$f,

$L_x = 19{,}000/f^2_2\ (C_2 - C_1)$

Measurement of admittance

Initial readings $C'Q'$ (LR_p is any suitable coil)

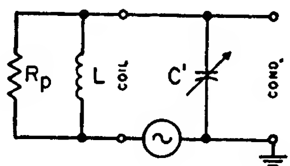

Final readings $C''\ Q''$

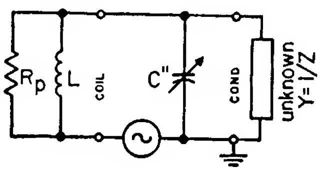

$1/Z = Y = G + jB = 1/R_p + j\omega C$

Then

$C = C' - C''$

$1/Q = G/\omega C$

$$= \frac{C'}{C}\left(\frac{1000}{Q''} - \frac{1000}{Q'}\right) \times 10^{-3}$$

If Z is inductive, $C'' > C'$

Measurement of impedances lower than those directly measurable

For the initial reading, $C'Q'$, COND terminals are open.

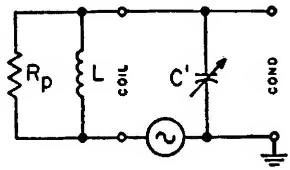

On second reading, $C''Q''$, a capacitive divider C_aC_b is connected to the COND terminals.

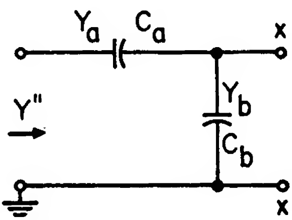

Final reading, $C'''Q'''$, unknown connected to $x-x$.

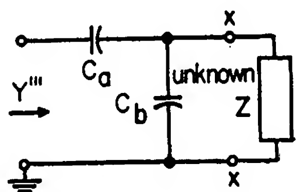

$Y_a = G_a + j\omega C_a \quad Y_b = G_b + j\omega C_b$

G_a and G_b not shown in diagrams.

Then the unknown impedance is

$$Z = \left(\frac{Y_a}{Y_a + Y_b}\right)^2 \frac{1}{Y''' - Y''} - \frac{1}{Y_a + Y_b} \text{ ohms}$$

where, with capacitance in micromicrofarads and $\omega = 2\pi \times$ (frequency in megacycles/second):

Measurement of impedances lower than those directly measurable *continued*

$$\frac{1}{Y''' - Y''} = \frac{10^6/\omega}{C'\left(\frac{1000}{Q'''} - \frac{1000}{Q''}\right) \times 10^{-3} + j(C'' - C''')}$$

Usually G_a and G_b may be neglected, when there results

$$Z = \left(\frac{1}{1 + C_b/C_a}\right)^2 \frac{1}{Y''' - Y''} + j\frac{10^6}{\omega(C_a + C_b)} \text{ ohms}$$

For many measurements, C_a may be 100 micromicrofarads. $C_b = 0$ for very low values of Z and for highly reactive values of Z. For unknowns that are principally resistive and of low or medium value, C_b may take sizes up to 300 to 500 micromicrofarads. When $C_b = 0$

$$Z = \frac{1}{Y''' - Y''} + j\frac{10^6}{\omega C_a} \text{ ohms}$$

and the "second" reading above becomes the "initial", with $C' = C''$ in the formulas.

Parallel-T (symmetrical)

Conditions for zero transfer are

$$\omega^2 C_1 C_2 = 2/R_2{}^2$$
$$\omega^2 C_1{}^2 = 1/2R_1R_2$$
$$C_2R_2 = 4\, C_1R_1$$

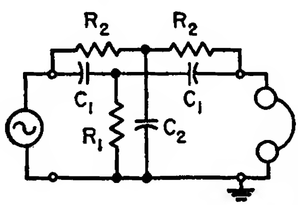

When used as a frequency-selective network, if we make $R_2 = 2R_1$ and $C_2 = 2C_1$ then

$$f = 1/2\pi C_1R_2 = 1/2\pi C_2R_1$$

For additional information, see G. E. Valley, Jr. and H. Wallman, "Vacuum Tube Amplifiers," McGraw-Hill Book Company, Inc., New York, N. Y.; 1948: pp. 387–389.

Twin-T admittance-measuring circuit (General Radio Co. Type 821-A)

This circuit may be used for measuring admittances in the range somewhat exceeding 400 kilocycles to 40 megacycles. It is applicable to the special measuring techniques described above for the Q-meter.

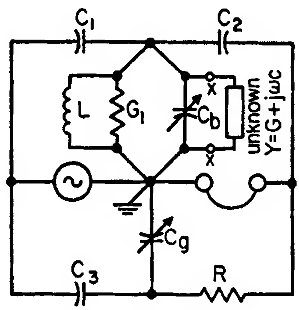

Conditions for null in output

$$G + G_l = R\omega^2 C_1C_2(1 + C_g/C_3)$$
$$C + C_b = 1/\omega^2 L - C_1C_2\left(\frac{1}{C_1} + \frac{1}{C_2} + \frac{1}{C_3}\right)$$

With the unknown disconnected, call the initial balance C_b' and C_g'.

With unknown connected, final balance is C_b'' and C_g''.

Then the components of the unknown $Y = G + j\omega C$ are

$$C = C_b' - C_b''$$
$$G = \frac{R\omega^2 C_1C_2}{C_3}(C_g'' - C_g')$$

Iron-core transformers and reactors

Iron-core transformers are, with few exceptions, closely coupled circuits for transmitting alternating-current energy and matching impedances. The equivalent circuit of a generalized transformer is shown in Fig. 1.

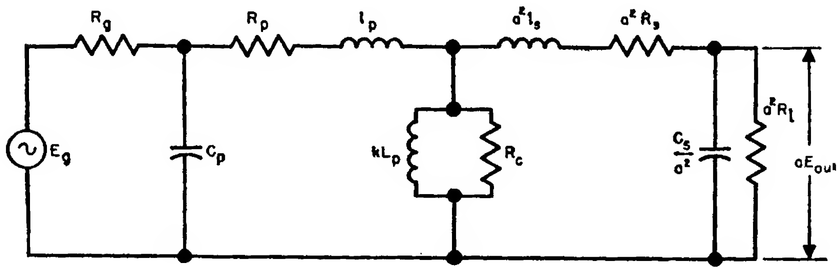

a = turns ratio = N_p/N_s
C_p = primary equivalent shunt capacitance
C_s = secondary equivalent shunt capacitance
E_g = root-mean-square generator voltage
E_{out} = root-mean-square output voltage
k = coefficient of coupling
L_p = primary inductance
l_p = primary leakage inductance
l_s = secondary leakage inductance
R_c = core-loss equivalent shunt resistance
R_g = generator impedance
R_l = load impedance
R_p = primary-winding resistance
R_s = secondary-winding resistance

Fig. 1—Equivalent network of a transformer.

Major transformer types used in electronics

Power transformers

Power transformers operate from a source of nearly zero impedance at a single low frequency, primarily to transfer power at convenient voltages.

Rectifier plate and/or filament: Power rectifiers and tube heaters.

Vibrator power supply: Permit the operation of radio receivers from direct-current sources, such as automobile batteries, when used in conjunction with vibrator inverters.

Scott connection: Serve to transmit power from 2-phase to 3-phase systems, or vice versa.

Autotransformer: Is a special case of the usual isolation type in that a part of the primary and secondary windings are physically common. The size, voltage regulation, and leakage inductance are, for a given rating, less than those for an isolation-type transformer handling the same power.

Major transformer types used in electronics *continued*

Audio-frequency transformers

Match impedances and transmit audio frequencies.

Output: Couple the plate(s) of an amplifier to an output load.

Input or interstage: Couple a magnetic pickup, microphone, or plate of a tube to the grid of another tube.

Driver: Couple the plate(s) of a driver stage (preamplifier) to the grid(s) of an amplifier stage where grid current is drawn.

Modulation: Couple the plate(s) of an audio-output stage to the grid or plate of a modulated amplifier.

High-frequency transformers

Match impedances and transmit a band of frequencies in the carrier or higher-frequency ranges.

Power-line carrier-amplifier: Couple different stages, or couple input and output stages to the line.

Intermediate-frequency: Are coupled tuned circuits used in receiver intermediate-frequency amplifiers to pass a band of frequencies (these units may, or may not have magnetic cores).

Pulse: Transform energy from a pulse generator to the impedance level of a load with, or without, phase inversion. Also serve as interstage coupling or inverting devices in pulse amplifiers. Pulse transformers may be used to obtain low-level pulses of a certain repetition rate in regenerative-pulse-generating circuits (blocking oscillators).

Sawtooth-amplifier: Provide a linear sweep to the horizontal plates of a cathode-ray oscilloscope.

Major reactor types used in electronics

Filter: Smooth out ripple voltage in direct-current supplies. Here, swinging chokes are the most economical design in providing adequate filtering, in most cases, with but a single filtering section.

Audio-frequency: Supply plate current to a vacuum tube in parallel with the output circuit.

Radio-frequency: Pass direct current and present high impedance at the high frequencies.

Wave-filter: Used as filter components to aid in the selection or rejection of certain frequencies.

Special nonlinear transformers and reactors

These make use of nonlinear properties of magnetic cores by operating near the knee of the magnetization curve. See pp. 323–326.

Peaking transformers: Produce steeply peaked waveforms, for firing thyratrons.

Saturable-reactor elements: Used in tuned circuits; generate pulses by virtue of their saturation during a fraction of each half cycle.

Saturable reactors: Serve to regulate voltage, current, or phase in conjunction with glow-discharge tubes of the thyratron type. Used as voltage-regulating devices with dry-type rectifiers. Also used in mechanical vibrator rectifiers and magnetic amplifiers.

Design of power transformers for rectifiers

The equivalent circuit of a power transformer is shown in Fig. 2.

a. Determine total output volt-amperes, and compute the primary and secondary currents from

$$E_pI_p \times 0.9 = \frac{1}{\eta}\left[(E_sI_{dc})_{pl}K + (EI)_{fil}\right]$$

$$I_s = K'I_{dc}$$

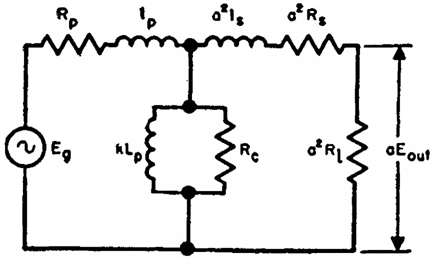

Fig. 2—Equivalent network of a power transformer. l_p and l_s may be neglected when there are no strict requirements on voltage regulation.

where the numeric 0.9 is the power factor, and the efficiency η and the K, K' factors are listed in Figs. 3 and 4. E_pI_p is the input volt-amperes, I_{dc} refers to the total direct-current component drawn by the supply; and

Fig. 3—Factors K and K' for single-phase-rectifier supplies. See pp. 306-307 for more complex circuits.

filter	K	K′
Full-wave:		
Capacitor input	0.717	1.06
Reactor input	0.5	0.707
Half-wave:		
Capacitor input	1.4	2.2
Reactor input	1.06	1.4

Fig. 4—Efficiency of various sizes of power supplies.*

watts output	approximate efficiency in percent
20	70
30	75
40	80
80	85
100	86
200	90

* From "Radio Components Handbook," Technical Advertising Associates; Cheltenham, Pa., May, 1948: p. 92.

Design of power transformers for rectifiers *continued*

the subscripts *pl* and *fil* refer to the volt-amperes drawn from the plate-supply and filament-supply (if present) windings, respectively. E_s is the total voltage across the secondary of the transformer.

$E_s = 2.35\ E_{dc}$
for single-phase full-wave rectifier.

E_{dc} is the direct-current output voltage of the rectifier. Factor 2.35 is twice the ratio of root-mean-square to average values plus an allowance for 5-percent regulation.

Where a transformer is operated at different loads according to a regular duty cycle, the equivalent volt–ampere $(VA)_{eq}$ rating is computed as follows:

$$(VA)_{eq} = \left[\frac{(VA)^2{}_1t_1 + (VA)^2{}_2t_2 + (VA)^2{}_3t_3 + \ldots (VA)^2{}_nt_n}{t_1 + t_2 + t_3 + \ldots t_n}\right]^{1/2}$$

where $(VA)_1$ = output during time (t_1), etc.

Example: 5 kilovolt–ampere output, 1 minute on, 1 minute off.

$$(VA)_{eq} = \left[\frac{(5000)^2\ (1) + (0)^2\ (1)}{1+1}\right]^{1/2} = \left[\frac{(5000)^2}{2}\right]^{1/2}$$

$$= 5000/(2)^{1/2} = 3535 \text{ volt–amperes}$$

b. Compute the size of wire of each winding, on the basis of current densities given by

For 60-cycle sealed units,

amperes/inch^2 = $2470 - 585 \log W_{out}$

$$\text{or, inches diameter} \approx 1.13 \left[\frac{I \text{ (in amperes)}}{2470 - 585 \log W_{out}}\right]^{1/2}$$

For 60-cycle open units, uncased,

amperes/inch^2 = $2920 - 610 \log W_{out}$

$$\text{or, inches diameter} \approx 1.13 \left[\frac{I \text{ (in amperes)}}{2920 - 610 \log W_{out}}\right]^{1/2}$$

c. Compute, roughly, the net core area

$$A_c = \frac{\sqrt{W_{out}}}{5.58}\sqrt{\frac{60}{f}} \text{ inches}^2$$

Design of power transformers for rectifiers *continued*

where f is in cycles (see also Fig. 5). Select a lamination and core size from the manufacturer's data book that will nearly meet the space requirements, and provide core area for a flux density B_m not to exceed the values shown in Fig. 10. Further information on available core materials is given in Fig. 6.

d. Compute the primary turns N_p from the transformer equation

$$E_p = 4.44\ fN_pA_cB_m \times 10^{-8}$$

with A_c in square centimeters and B_m in gausses. Then the secondary turns

$$N_s = 1.05(E_s/E_p)N_p$$

(this allows 5 percent for IR drop of windings).

e. Calculate the number of turns per layer that can be placed in the lamination window space, deducting from the latter the margin space given in Fig. 7 (see also Fig. 8).

Fig. 5—Equivalent LI^2 and EI ratings of power transformers: B_m = flux density in gausses: EI = volt-amperes. This table gives the maximum values of LI^2 and EI ratings at 60 and 400 cycles for various size cores. Ratings are based on a 50-degree-centigrade rise above ambient. These values can be reduced to obtain a smaller temperature rise. EI ratings are based on a two-winding transformer with normal operating voltage. When three or more windings are required, the EI ratings should be decreased slightly.

	at 60 cycles		at 400 cycles			tongue width of E	stack height	amperes per
LI^2	EI	B_m*	EI	B_m*	EI-type punchings	in inches	in inches	inch²
0.0195	3.9	14,000	9.5	5000	21	$\frac{1}{2}$	$\frac{1}{2}$	3200
0.0288	5.8	14,000	15.0	4900	62.5	$\frac{5}{8}$	$\frac{5}{8}$	2700
0.067	13.0	14,000	30.0	4700	75	$\frac{3}{4}$	$\frac{3}{4}$	2560
0.088	17.0	14,000	38.0	4600	75	$\frac{3}{4}$	1	2560
0.111	24.0	13,500	50.0	4500	11	$\frac{7}{8}$	$\frac{7}{8}$	2330
0.200	37.0	13,000	80.0	4200	12	1	1	2130
0.300	54.0	13,000	110.0	4000	12	1	$1\frac{1}{2}$	2030
0.480	82.0	12,500	180.0	3900	12.5	$1\frac{1}{4}$	$1\frac{1}{4}$	1800
0.675	110.0	12,000	230.0	3900	12.5	$1\frac{1}{4}$	$1\frac{3}{4}$	1770
0.850	145.0	12,000	325.0	3700	13	$1\frac{1}{2}$	$1\frac{1}{2}$	1600
1.37	195.0	11,000	420.0	3500	13	$1\frac{1}{2}$	2	1500
3.70	525.0	10,500	1100.0	3200	19	$1\frac{3}{4}$	$1\frac{3}{4}$	1220

From "Radio Components Handbook," Technical Advertising Associates; Cheltenham, Pa.; May, 1948: see p. 92.

* B_m refers to 29-gauge silicon steel, 14 mils thick.

Fig. 6—Data on metallic core materials.[4]

metal or alloy	material or trade name	composition in percent (remainder is iron)	characteristic property or application	permeability: initial	permeability: maximum	direct-current saturation in kilogausses	residual induction in kilogausses	coercive force in oersteds	resistivity in microhm-centimeters	curie temperature in degrees centigrade
Silicon–iron	Silicon–Iron	4 Si	Transformer	400	7,000	20	12	0.5	60	690
	Hypersil	3.5 Si	Grain oriented	1,500	35,000	20	13.7	0.1 to 0.3	50	750
	Trancor 3X									
	Silectron									
	Sendust	9.5 Si, 5.5 Al	High-frequency powder	30,000	120,000	10	5	0.05	80	—
Cobalt–iron	Hyperco	35 Co, 0.5 Cr	High saturation	650	10,000	24	> 13	> 1	28	970
	Permendur 2V	49 Co, 2 V		800	4,500		14	2	25	980
Nickel–iron	Perminvar 45–25	45 Ni, 25 Co	"Constant" permeability	400	2,000	15.5	3.3	1.2	20	715
	Perminvar 7–70	70 Ni, 7 Co		850	4,000	12.5	2.4	0.6	15	650
	Conpernik	50 Ni		1,500	2,000	16	—	—	45	—
	Isoperm 36	36 Ni, 9 Cu	High frequency	60	65	—	—	—	70	300
	Isoperm 50	50 Ni		90	100	16	—	—	40	500
	Permalloy 45	45 Ni	Combine good permeability and flux density	2,700	23,000	16.5	8	0.3	45	440
	Allegheny 4750	47 to 50 Ni		9,000	50,000	16	6.2†	0.08†	52	430
	Armco 48	48 Ni		—	—		—	—	—	—
	Nicaloi	49 Ni		—	—		—	—	—	—
	High Perm 49			5,000	50,000		6.5	0.03	43	475
	Hipernik	50 Ni, Si, Mn		4,000	100,000		8†	0.03†	45	500

Nickel–iron *cont.*	Monimax	47 Ni, 3 Mo	High resistivity	2,000	38,000	15	—	0.06	80	390
	Sinimax	42 Ni, 3 Si		3,500	30,000	11	—	0.1	90	290
	Permenorm *5000Z*	45 to 50 Ni	Rectangular hysteresis loop	400 to 1,700	40,000 to 100,000	15.5 to 16	13 to 15	0.2 to 0.4	40 to 50	450 to 500
	Permenite									
	Deltamax									
	Hypernik *V*									
	Orthonik									
	Orthonol									
	Permalloy *65*	65 to 68 Ni		1,500	250,000 to 600,000	13	13	0.03	20	600
	Alloy *1040*	72 Ni, 14 Cu, 3 Mo	Highest permea-bility, low saturation	40,000		6	2.5	0.02	55	290
	Mumetal	77 Ni, 5 Cu, 2 Cr		20,000	100,000	8	6		60	400
	Permalloy *78*	78 Ni, 0.6 Mn		9,000		10.7	6	0.05	16	580
	Mo-Permalloy *4–79*	79 Ni, 4 Mo		20,000	75,000	8	5.5		55	—
	Supermalloy	79 Ni, 5 Mo		55,000 to 150,000	500,000 to 1,000,000	6.8 to 7.8	—	0.002 to 0.05	65	400
	Hymu *80*	80 Ni		10,000	100,000	8	—	0.06	58	460

* Reprinted by permission from an article by S. R. Hoh, "Evaluation of High-Performance Magnetic Core Materials (Part 1)," *Tele-Tech and Electronic Industries*, vol. 12, pp. 86–89, 154–156; October, 1953.

† B_{max} = 10,000 gausses.

Note 1—The table shows characteristics as listed by the manufacturers. The parameters of different lots of material may vary considerably from the above values. In the cases of residual induction and coercive force, the difference may amount to 50 percent.

Note 2—For information on ferrite materials, see page 74.

continued **Design of power transformers for rectifiers**

Fig. 7—Wire table for transformer design. The resistance R_T at any temperature T is given by $R_T = \frac{234.5 + T}{234.5 + t} \times r$, where t = reference temperature of winding, and r = resistance of winding at temperature t, all in degrees centigrade.

AWG B&S gauge	diameter in inches: bare	single formvar*	double formvar	turns per inch (formvar)	space factor	ohms per 1000 ft†	pounds per 1000 ft	margin m in inches	interlayer insulation‡ t	AWG B&S gauge
10	0.1019	0.1039	0.1055	8	90	0.9989	31.43	0.25	0.010K	10
11	0.0907	0.0927	0.0942	9	90	1.260	24.92	0.25	0.010K	11
12	0.0808	0.0827	0.0842	10	90	1.588	19.77	0.25	0.010K	12
13	0.0719	0.0738	0.0753	12	90	2.003	15.68	0.25	0.010K	13
14	0.0641	0.0659	0.0673	13	90	2.525	12.43	0.25	0.010K	14
15	0.0571	0.0588	0.0602	15	90	3.184	9.858	0.25	0.010K	15
16	0.0508	0.0524	0.0538	17	90	4.016	7.818	0.1875	0.010K	16
17	0.0453	0.0469	0.0482	19	90	5.064	6.200	0.1875	0.007K	17
18	0.0403	0.0418	0.0431	21	90	6.385	4.917	0.1875	0.007K	18
19	0.0359	0.0374	0.0386	23	90	8.051	3.899	0.1562	0.007K	19
20	0.0320	0.0334	0.0346	26	90	10.15	3.092	0.1562	0.005K	20
21	0.0285	0.0299	0.0310	30	90	12.80	2.452	0.1562	0.005K	21
22	0.0253	0.0266	0.0277	33	90	16.14	1.945	0.125	0.003K	22
23	0.0226	0.0239	0.0249	37	90	20.36	1.542	0.125	0.003K	23
24	0.0201	0.0213	0.0223	42	90	25.67	1.223	0.125	0.002G	24
25	0.0179	0.0190	0.0200	47	90	32.37	0.9699	0.125	0.002G	25
26	0.0159	0.0169	0.0179	52	89	40.81	0.7692	0.125	0.002G	26
27	0.0142	0.0152	0.0161	57	89	51.47	0.6100	0.125	0.002G	27
28	0.0126	0.0135	0.0145	64	89	64.90	0.4837	0.125	0.0015G	28
29	0.0113	0.0122	0.0131	71	89	81.83	0.3836	0.125	0.0015G	29
30	0.0100	0.0109	0.0116	80	89	103.2	0.3042	0.125	0.0015G	30
31	0.0089	0.0097	0.0104	88	88	130.1	0.2413	0.125	0.0015G	31
32	0.0080	0.0088	0.0094	98	88	164.1	0.1913	0.0937	0.0013G	32
33	0.0071	0.0079	0.0084	110	88	206.9	0.1517	0.0937	0.0013G	33
34	0.0063	0.0070	0.0075	124	88	260.9	0.1203	0.0937	0.001G	34
35	0.0056	0.0062	0.0067	140	88	329.0	0.0954	0.0937	0.001G	35
36	0.0050	0.0056	0.0060	155	87	414.8	0.0757	0.0937	0.001G	36
37	0.0045	0.0050	0.0054	170	87	523.1	0.0600	0.0937	0.001G	37
38	0.0040	0.0045	0.0048	193	87	659.6	0.0476	0.0625	0.001G	38
39	0.0035	0.0040	0.0042	215	86	831.8	0.0377	0.0625	0.0007G	39
40	0.0031	0.0036	0.0038	239	86	1049	0.0299	0.0625	0.0007G	40

*Dimensions very nearly the same as for enamelled wire.
†Values are at 20 degrees centigrade.
‡K = kraft paper, G = glassine.

Additional data on wire will be found on pp. 50–57 and p. 114.

Design of power transformers for rectifiers *continued*

A_c = core area = $(gp)k$
a = height of coil
= coil-build
b = coil width
g = width of lamination tongue
l_c = average length of magnetic-flux path
k = stacking factor
≈ 0.90 for 14-mil lamination
≈ 0.80 for 2-mil lamination or ribbon-wound core
m = marginal space given in Fig. 7
p = height of lamination stack
t = thickness of interlayer insulation
w = width of core window
τ = window length tolerance
= 1/16 inch, total

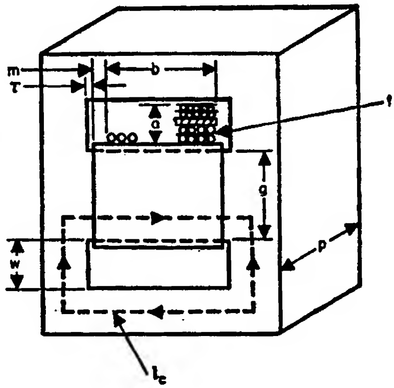

Fig. 8—Dimensions relating to the design of a transformer coil-build and core.

f. From (d) and (e) compute the number of layers n_l for each winding. Use interlayer insulation of thickness t as given in Fig. 7, except that the voltage stress should be limited to 40 volts/mil.

g. Calculate the coil-build a:

$$a = 1.1[n_l(D + t) - t + t_c]$$

for each winding from (b) and (f), where D = diameter of insulated wire and t_c = thickness of insulation under and over the winding; the numeric 1.1 allows for a 10-percent bulge factor. The total coil-build should not exceed 85–90 percent of the window width. (Note: Insulation over the core may vary from 0.025 to 0.050 inches for core-builds of $\frac{1}{2}$ to 2 inches.)

h. Compute the mean length per turn (MLT), of each winding, from the geometry of core and windings as shown in Fig. 9. Compute length of each winding N(MLT).

$$(\mathrm{MLT})_1 = 2(r + J) + 2(s + J) + \pi a_1$$
$$(\mathrm{MLT})_2 = 2(r + J) + 2(s + J) + \pi(2a_1 + a_2)$$

where

a_1 = build of first winding
a_2 = build of second winding
J = thickness of winding form
r,s = winding-form dimensions

Design of power transformers for rectifiers *continued*

i. Calculate the resistance of each winding from (h) and Fig. 7, and determine IR drop and I^2R loss for each winding.

j. Make corrections, if required, in the number of turns of the windings to allow for the IR drops, so as to have the required E_s:

$$E_s = (E_p - I_pR_p)\ N_s/N_p - I_sR_s$$

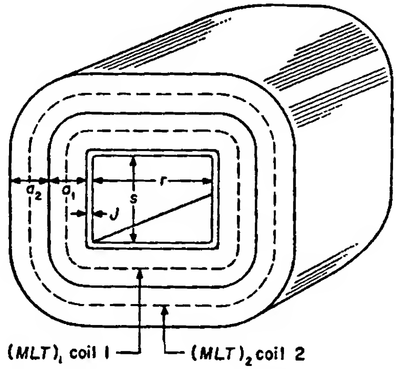

Fig. 9—Dimensions relating to coil mean length of turn (MLT).

k. Compute core losses from weight of core and the table on core materials, Fig. 10, or the graph, Fig. 11.

l. Determine the percent efficiency η and voltage regulation (vr) from

$$\eta = \frac{W_{out} \times 100}{W_{out} + (\text{core loss}) + (\text{copper loss})}$$

$$(vr) = \frac{I_s[R_s + (N_s/N_p)^2R_p]}{E_s}$$

m. For a more accurate evaluation of voltage regulation, determine leakage-reactance drop $= I_{dc}\omega l_{sc}/2\pi$, and add to the above (vr) the value of $(I_{dc}\omega l_{sc})/2\pi E_{dc}$. Here, l_{sc} = leakage inductance viewed from the secondary; see "Methods of winding transformers", p. 299 to evaluate l_{sc}.

Fig. 10—Typical operating conditions for core materials at various frequencies.

frequency in cycles	lamination thickness in inches	core material	core flux density B_{max} in gausses	approximate core loss in watts/lb	approximate exciting (VA)/lb
25	0.025	2.5-percent silicon	14,000	0.65	4.0
60	0.014	4-percent silicon	12,000	0.80	6.0
60	0.014	Grain-orient. silicon	15,000	1.0	6.0
400	0.004	Grain-orient. silicon	10,000	4.5	10.0
800	0.004	Grain-orient. silicon	6,000	4.5	10.0
16,000	—	Ferrite	1,000	5.0	—

Design of power transformers for rectifiers *continued*

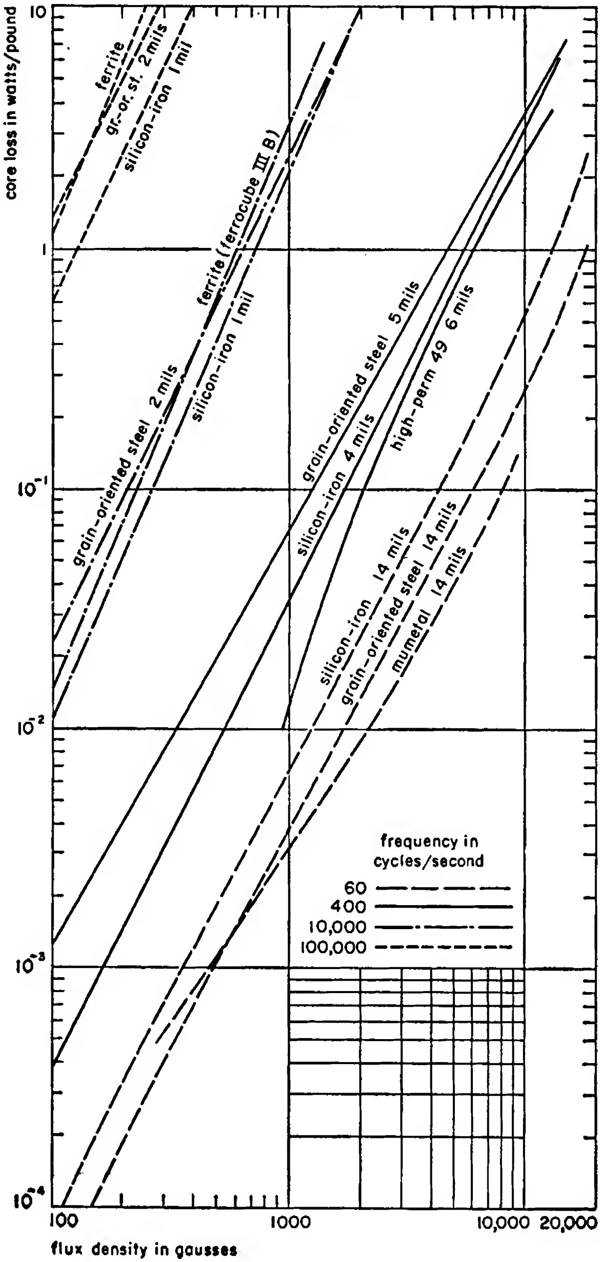

Fig. 11—Typical core losses.

Design of power transformers for rectifiers *continued*

n. Bring out all terminal leads using the wire of the coil, insulated with suitable sleevings, for all sizes of wire heavier than 21; and by using 7–30 stranded and insulated wire for smaller sizes.

Effect of power frequency on design: Design procedure is similar to that described above for 60-cycle transformers except for the flux density at which the core is operated. Operation at lower frequencies requires a larger core (see equation in paragraph (c) above) although reduction of core loss partially compensates the size increase. As an example, a 25-cycle transformer is approximately twice as large as its 60-cycle equivalent.

High-frequency operation (Fig. 10) normally results in size and weight reduction and is used primarily in aircraft applications where power-supply frequencies are usually 400 or 800 cycles. A smaller core results from increased frequency; but greatly increased losses (Fig. 11) prevent proportional size decrease from 60-cycle equivalent. Use of thinner laminations partially compensates the effects of losses permitting further reduction in size. Voltage drop due to leakage reactance has greater effect than at 60 cycles and may require interleaved winding.

Television flyback transformers supply power at 16 kilocycles, where normal core materials are not satisfactory since extremely thin, (0.001- to 0.002-inch) and expensive laminations are required. Molded ferrite cores are normally used due to their excellent loss characteristics at these frequencies.

Design of filter reactors for rectifiers and plate-current supply

These reactors carry direct current and are provided with suitable air-gaps. Optimum design data may be obtained from Hanna curves, Fig. 12. These curves relate direct-current energy stored in core per unit volume, LI_{dc}^2/V to magnetizing field NI_{dc}/l_c (where l_c = average length of flux path in core), for an appropriate air-gap. Heating is seldom a factor, but direct-current-resistance requirements affect the design; however, the transformer equivalent volt-ampere ratings of chokes (Fig. 5) should be useful in determining their sizes. This is based on the empirical relationship $(VA)_{eq} = 188LI_{dc}^2$.

As an example, take the design of a choke that is to have an inductance of 10 henries with a superimposed direct current of 0.225 amperes, and a direct-current resistance $\leqslant$ 125 ohms. This reactor shall be used for suppressing harmonics of 60 cycles, where the alternating-current ripple voltage (2nd harmonic) is about 35 volts.

Design of filter reactors for rectifiers *continued*

a. $LI^2 = 0.51$. Based on data of Fig. 5, try 4-percent silicon-steel core, type EI–12.5 punchings, with a core-build of 1.5 inches. From manufacturer's data, volume $= 13.7$ inches^3; $l_c = 7.5$ inches; $A_c = 1.69$ inches^2.

b. Compute $LI_{dc}^2/V = 0.037$; from Fig. 12, $NI_{dc}/l_c = 85$; hence, by substitution, $N = 2840$ turns. Also, gap ratio $l_g/l_c = 0.003$, or, total gap $l_g = 22$ mils.

Alternating-current flux density $B_m = \dfrac{E \times 10^8}{4.44fNA_c} = 210$ gausses, where A_c is in square centimeters.

c. Calculate from the geometry of the core, the mean length/turn, (MLT) $= 0.65$ feet, and the length of coil $= N(\text{MLT}) = 1840$ feet, which is to have a maximum direct-current resistance of 125 ohms. Hence, $R_{dc}/N(\text{MLT}) = 0.068$ ohms/foot. From Fig. 7, the nearest size is No. 28.

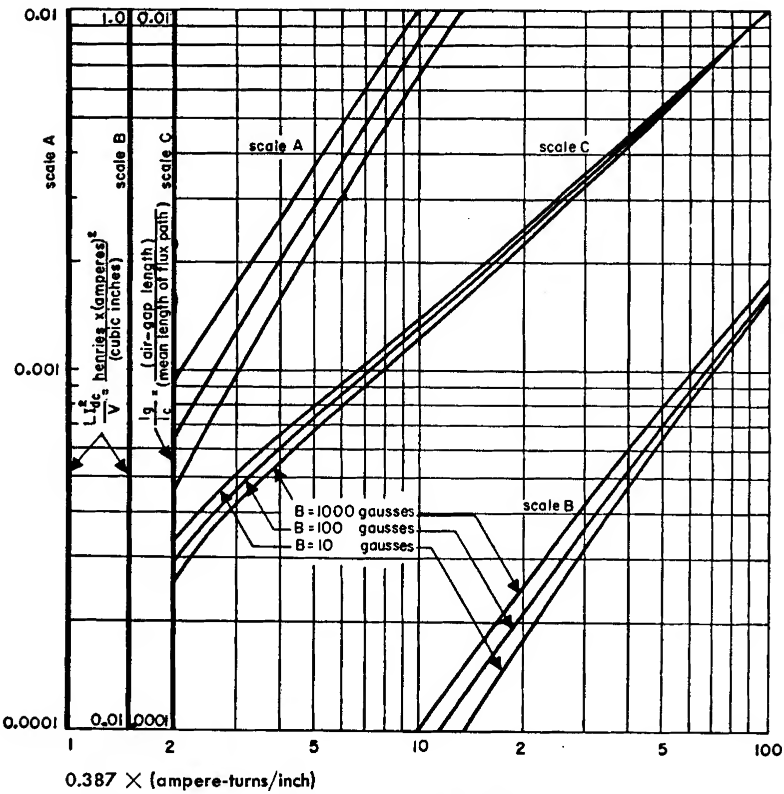

Fig. 12—Hanna curves for 4-percent silicon-steel core material.

Design of filter reactors for rectifiers *continued*

d. Now see if 2840 turns of No. 28 single-Formex wire will fit in the window space of the core. (Determine turns per layer, number of layers, and coil-build, as explained in the design of power transformers.)

e. This is an actual coil design; in case lamination window space is too small (or too large) change stack of laminations, or size of lamination, so that the coil meets the electrical requirements, and the total coil-build $\approx$ 0.85 to 0.90 $\times$ (window width).

Note: To allow for manufacturing variations in permeability of cores and resistance of wires, use at least 10-percent tolerance.

Swinging reactors: Used where direct current in rectifier circuit varies. Reactor is designed to saturate under full-load current while providing adequate inductance for filtering. At light-load current, higher inductance is available to perform proper filtering and prevent "capacitor effect." Equivalent size to 60-cycle power transformer is approximated as

$$(VA)_{eq} = 188(L_{max} \times L_{min})^{1/2} I^2_{dc\ (max)}$$

Design is similar to normal reactor and is based on meeting both L and I_{dc} extremes. Typical swing in inductance is 4:1 for a current swing of 10:1.

Design of wave-filter reactors

Wave-filter reactors must have high Q to provide attenuation at frequencies immediately off the pass band. Materials listed in Fig. 6 having both high initial permeability and high resistivity are generally suitable. Additional data on a few materials is given in Fig. 13.

Cores are usually molded from powdered materials or wound from very thin strips to reduce eddy-current losses. They are usually of toroidal or "pot" form to minimize leakage flux. Maximum Q is obtained when:

(copper loss) $\approx$ (core loss)

The inductance is given by

$$L \approx \frac{1.25N^2A_c}{l_g + l_c/\mu_0} 10^{-8} \quad \text{henries}$$

where dimensions are in centimeters and μ_0 = initial permeability. This relationship is valid primarily where the air-gap l_g is small. Where large gaps are encountered, the effects of fringing flux at the gaps must be considered since the effective gap is generally smaller than the physical gap.*

* P. K. McElroy, "Those Iron-Cored Coils Again", *General Radio Experimenter,* vol. 21, pp. 2–8; January, 1947.

continued **Design of wave-filter reactors**

Fig. 13—Characteristics of some core materials for wave-filter reactors.* $R_c/fL = \mu_0(aB_m + c) + \mu_0 ef$, where R_c = ohms resistance due to core loss.

alloy		initial permeability μ_0	resistivity in microhms/centimeter	hysteresis coefficient ($a \times 10^6$)	residual coefficient ($c \times 10^6$)	eddy-current coefficient ($e \times 10^9$)	gauge in mils	uses (frequencies in kilocycles)
4-percent silicon steel		400	60	120	75	870	14	Rectifier filters
Nicalloy		3,500 to 5,000	43 to 45	0.4	14	1550	14	Wave filters up to 0.1–0.2
						284	6	Wave filters up to 10
Hymu		10,000 to 20,000	55 to 58	0.05	0.05	950	14	Wave filters up to 0.1–0.2
						175	6	Wave filters up to 10
2–81 molybdenum-permalloy dust†		125	1 ohm/cm	1.6	30	19	—	Wave filters 0.2 to 7
		60	—	3.2	50	10	—	Wave filters 5–20
		26	—	6.9	96	7.7	—	Wave filters 15–60
		14	—	11.4	143	7.1	—	Wave filters 40–150
Carbonyl types	C	55	—	9	80	7	—	Wave filters
	P	26	—	3.4	220	27	—	Wave filters
	Th	16	—	2.5	80	8	—	Wave filters 40–high

*Additional data on metallic core materials will be found on p. 276. Ferrite materials are listed on p. 74.

†Data on molybdenum-permalloy dust and definition of constants a, c, and e are from an article by V. E. Legg, and F. J. Given, "Compressed Powdered Molybdenum-Permalloy for High-Quality Inductance Coils," *Bell System Technical Journal*, v. 19, pp. 385–406; July, 1940.

Design of wave-filter reactors *continued*

When using molybdenum-permalloy-dust toroidal cores, the inductance is given by

$$L \approx \frac{1.25N^2A_c}{l_c}\,\mu_{ef} \times 10^{-8} \qquad \text{for } \mu_{ef} = 125$$

$$L \approx 0.85\,\frac{1.25N^2A_c}{l_c}\,\mu_{ef} \times 10^{-8} \qquad \text{for } \mu_{ef} = 65$$

Ferrite cores may be used, but many ferrites have high temperature coefficients of resistance and low curie temperatures (see page 74).

Small gaps in filter cores will reduce losses, improve Q, stabilize constants for varying alternating voltage, and reduce the effects of temperature changes in the case of ferrite cores.

Design of audio-frequency transformers

Important parameters are: generator and load impedances R_g, R_l, respectively, generator voltage E_g, frequency band to be transmitted, efficiency (output transformers only), harmonic distortion, and operating voltages (for adequate insulation).

At mid-frequencies: The relative low- and high-frequency responses are taken with reference to mid-frequencies, where

$$\frac{aE_{out}}{E_g} = \frac{1}{(1 + R_s/R_l) + R_1/a^2R_l}$$

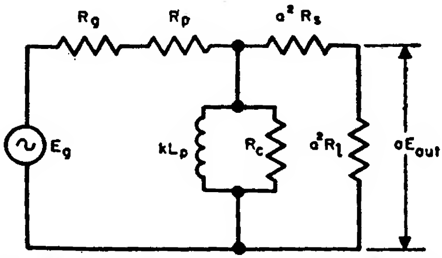

Fig. 14—Equivalent network of an audio-frequency transformer at low frequencies. $R_1 = R_g + R_p$ and $R_2 = R_s + R_l$. In a good output transformer, R_p, R_s, and R_c may be neglected. In input or interstage transformers, R_c may be omitted.

At low frequencies: The equivalent unity-ratio network of a transformer becomes approximately as shown in Fig. 14:

$$\text{Amplitude} = \frac{1}{\sqrt{1 + (R'_{par}/X_m)^2}}$$

$$\text{Phase angle} = \tan^{-1}\frac{R'_{par}}{X_m}$$

where

$$R'_{par} = \frac{R_1R_2a^2}{R_1 + R_2a^2} \qquad R_1 = R_g + R_p \qquad R_2 = R_l + R_s \qquad X_m = 2\pi f L_p$$

Design of audio-frequency transformers *continued*

At high frequencies: Neglecting the effect of winding and other capacitances (as in low-impedance-level output transformers), the equivalent unity-ratio network becomes approximately as in Fig. 15:

$$\text{Amplitude} = \frac{1}{\sqrt{1 + (X_l/R'_{se})^2}}$$

$$\text{Phase angle} = \tan^{-1}\frac{X_l}{R'_{se}}$$

where

$$R'_{se} = R_1 + R_2 a^2$$

$$X_l = 2\pi f l_{scp}$$

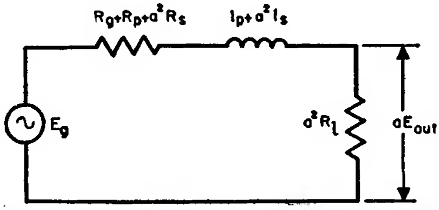

Fig. 15—Equivalent network of an audio-frequency transformer at high frequencies, neglecting the effect of the winding shunt capacitances.

l_{scp} = inductance measured across primary with secondary short-circuited $= l_p + a^2 l_s$

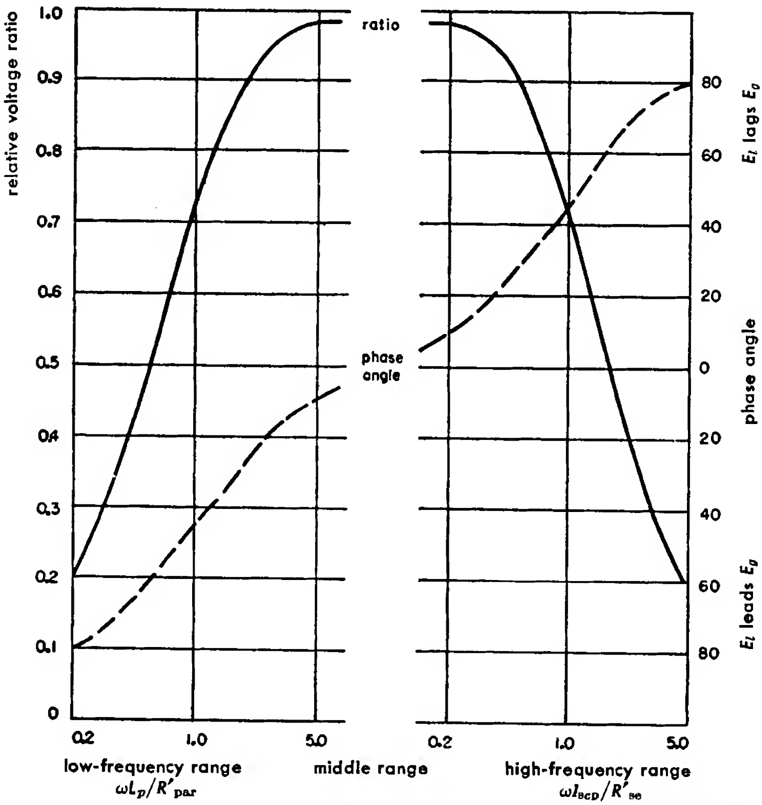

Courtesy of McGraw-Hill Publishing Company

Fig. 16—Universal frequency and phase response of output transformers.

Design of audio-frequency transformers *continued*

These low- and high-frequency responses are shown on the curves of Fig. 16.

If at high frequencies, the effect of winding and other capacitances is appreciable, the equivalent network on a 1:1-turns-ratio basis becomes as shown in Fig. 17. The relative high-frequency response of this network is given by

$$\frac{(R_1 + R_2)/R_2}{\sqrt{\left(\frac{R_1}{X_c}+\frac{X_l}{R_l}\right)^2 + \left(\frac{X_l}{X_c}-\frac{R_g}{R_l}-1\right)^2}}$$

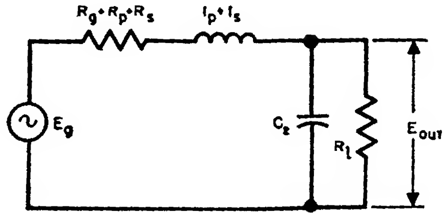

Fig. 17—Equivalent network of a 1:1-turns-ratio audio-frequency transformer at high frequencies when effect of winding shunt capacitances is appreciable. In a step-up transformer, C_2 = equivalent shunt capacitances of both windings. In a step-down transformer, C_2 shunts both leakage inductances and R_2.

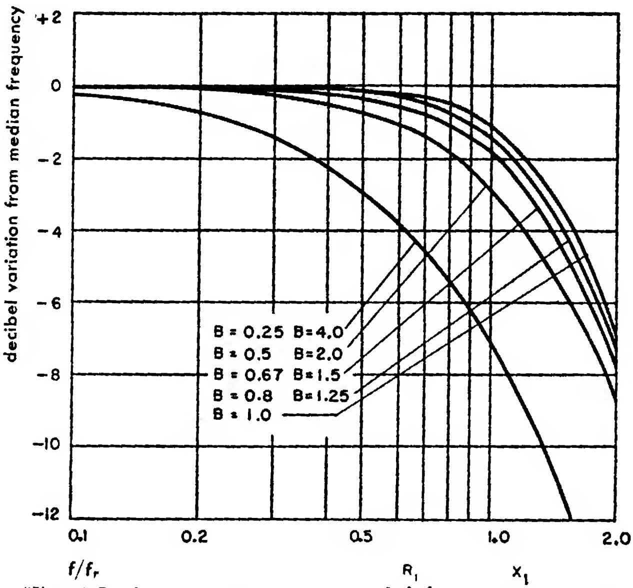

Reprinted from "Electronic Transformers and Circuits," by R. Lee, 2nd ed., p. 151, 1955; by permission, John Wiley & Sons, N. Y.

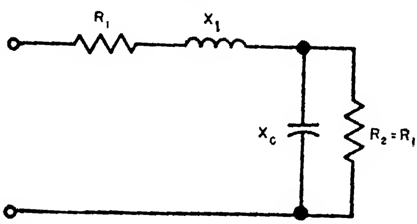

Fig. 18—Transformer characteristics at high frequencies for matched impedances. At frequency f_r, $X_l = X_c$ and $B = X_c/R_1$.

Design of audio-frequency transformers *continued*

This high-frequency response is plotted in Figs. 18 and 19 for $R_1 = R_2$ (matched impedances), and $R_2 = \infty$ (input and interstage transformers) based on simplified equivalent networks as indicated.

Harmonic distortion requirements may constitute a deciding factor in the design of transformers. Such distortion is caused by either variations in load impedance or nonlinearity of magnetizing current. The percent harmonic voltage appearing in the output of a loaded transformer is given by*

$$(\text{percent harmonics}) = \frac{E_h}{E_f} = \frac{I_h}{I_f}\frac{R'_{\text{par}}}{X_m}\left(1 - \frac{R'_{\text{par}}}{4X_m}\right)$$

where $100\,I_h/I_f$ = percent of harmonic current measured with zero-impedance source (values in Fig. 20 are for 4-percent silicon-steel core).

*N. Partridge, "Harmonic Distortion in Audio-Frequency Transformers," *Wireless Engineer*, v. 19; September, October, and November, 1942.

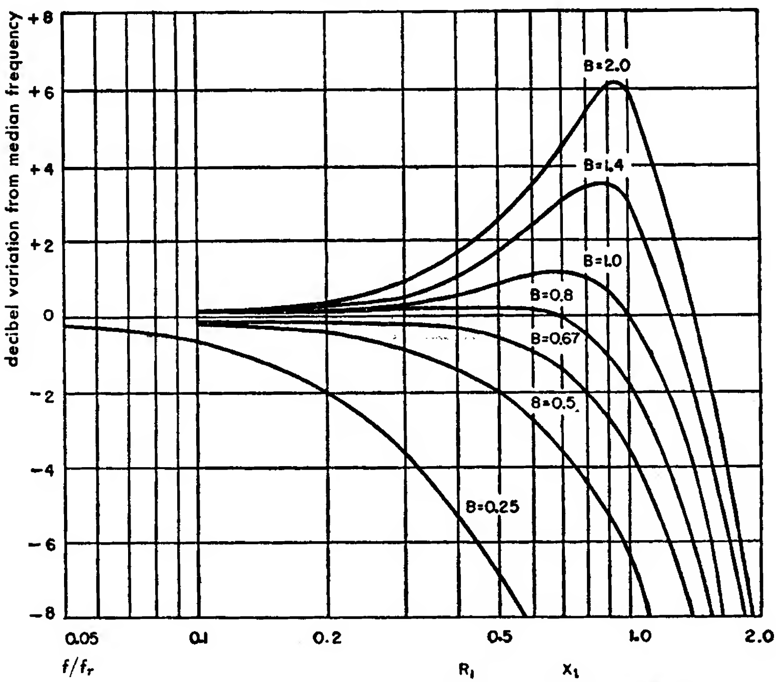

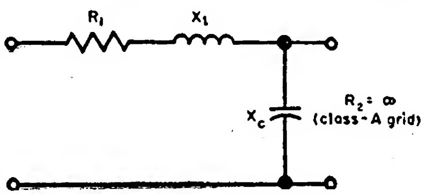

Reprinted from "Electronic Transformers and Circuits," by R. Lee, 2nd ed., p. 153, 1955, by permission, John Wiley & Sons, N. Y.

Fig. 19—Input- or interstage-transformer characteristics at high frequencies. At f_r, $X_l = X_c$ and $B = X_c/R_1$.

Design of audio-frequency transformers *continued*

Fig. 20—Harmonics produced by various flux densities B_m in a 4-percent silicon-steel-core audio transformer.

B_m	percent 3rd harmonic	percent 5th harmonic
100	4	1.0
500	7	1.5
1,000	9	2.0
3,000	15	2.5
5,000	20	3.0
10,000	30	5.0

Insertion loss: Loss introduced in circuit by addition of transformer. At midband, loss is caused by winding resistance and core loss. Frequency discrimination adds to this at low and high frequencies. Insertion loss is input divided by output expressed in decibels or, in terms of measured voltages and impedance:

$$\text{(db insertion loss)} = 10 \log \frac{E_g^2 R_l}{4 E_0^2 R_g}$$

Impedance match: For maximum power transfer, the reflected load impedance should equal generator impedance. Winding resistance should be included in this calculation: For matching,

$$R_g = a^2 (R_l + R_s) + R_p$$

Also, in properly matched transformer,

$$R_g = a^2 R_l = (Z_{oc} \times Z_{sc})^{1/2}$$

where

Z_{oc} = transformer primary open-circuit impedance.

Z_{sc} = transformer primary impedance with secondary winding short-circuited.

Where more than one secondary is used, the turns ratio to match impedances properly depends on the power delivered from each winding.

$$\frac{N_s}{N_p} = \left(\frac{R_n}{R_g} \times \frac{w_n}{w_p}\right)^{1/2}$$

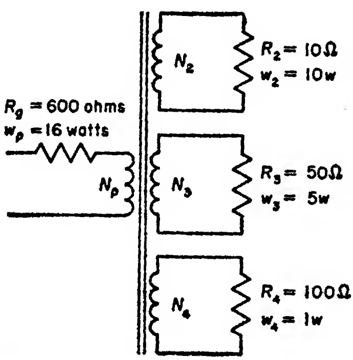

Fig. 21—Multisecondary audio transformer.

Design of audio-frequency transformers *continued*

Example: Using Fig. 21,

$$\frac{N_2}{N_p} = \left(\frac{10}{600} \times \frac{10}{16}\right)^{1/2} = 0.102$$

$$\frac{N_3}{N_p} = \left(\frac{50}{600} \times \frac{5}{16}\right)^{1/2} = 0.161$$

$$\frac{N_4}{N_p} = \left(\frac{100}{600} \times \frac{1}{16}\right)^{1/2} = 0.102$$

Example of audio-output-transformer design

This transformer is to operate from a 4000-ohm impedance; to deliver 5 watts to a matched load of 10 ohms; to transmit frequencies of 60 to 15,000 cycles with a V_{out}/V_{in} ratio of 71 percent of that at mid-frequencies (400 cycles); and the harmonic distortion is to be less than 2 percent. (See Figs. 14 and 15.)

a. We have: $E_s = (W_{out}R_l)^{1/2} = 7.1$ volts

$$I_s = W_{out}/E_s = 0.7 \text{ amperes}$$

$$a = (R_g/R_l)^{1/2} = 20$$

Then

$I_p \approx 1.1\, I_s/a = 0.039$ amperes, and $E_p \approx 1.1\, aE_s = 156$

b. To evaluate the required primary inductance to transmit the lowest frequency of 60 cycles, determine $R'_{se} = R_1 + a^2R_2$ and $R'_{par} = \dfrac{R_1R_2a^2}{R_1 + R_2a^2}$, where $R_1 = R_g + R_p$ and $R_2 = R_l + R_s$. We choose winding resistances $R_s = R_p/a^2 \approx 0.05R_l = 0.5$

(for a copper efficiency $= \dfrac{R_la^2 \times 100}{(R_l + R_s)a^2 + R_p} = 91$ percent). Then,

$R'_{se} = 2R_1 = 8400$ ohms, and $R'_{par} = R_1/2 = 2100$ ohms.

c. In order to meet the frequency-response requirements, we must have according to Fig. 16, $\dfrac{\omega_{low}L_p}{R'_{par}} = 1 = \dfrac{\omega_{high}l_{scp}}{R'_{se}}$, which yield

$L_p \approx 5.6$ henries and $l_{scp} = 0.089$ henries

Example of audio-output-transformer design *continued*

d. Harmonic distortion is usually a more important factor in determining the minimum inductance of output transformers than is the attenuation requirement at low frequencies. Compute now the number of turns and inductance for an assumed $B_m = 5000$ for 4-percent silicon-steel core with type EI–12 punchings in square stack. From manufacturer's catalog, A_c (net) = 5.8 centimeters², $l_c = 15.25$ centimeters. From Fig. 22, $\mu_{ac} \approx 5000$.

$$N_p = \frac{E_p \times 10^8}{4.44 f A_c B_m} = 2020$$

$$N_s = 1.1 N_p / a = 111$$

$$L_p \approx \frac{1.25 N_p^2 \mu_{ac} A_c}{l_c} \times 10^{-8} = 97 \text{ henries}$$

At 60 cycles, $X_m = \omega L_p = 36{,}600$ and $R'_{par}/X_m \approx 0.06$.

From values of I_h/I_f for 4-percent silicon-steel (See Fig. 20):

$$\frac{E_h}{E_f} = \frac{I_h}{I_f}\frac{R'_{par}}{X_m}\left(1 - \frac{R'_{par}}{4X_m}\right) \approx 0.012 \text{ or } 1.2 \text{ percent}$$

e. Now see if core window is large enough to fit windings. Assuming a simple method of winding (secondary over the primary), compute from geometry of core the approximate (MLT), for each winding (Fig. 9).

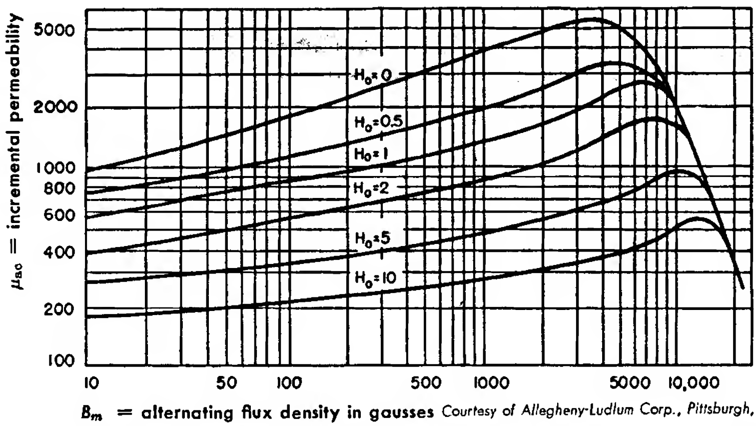

Courtesy of Allegheny-Ludlum Corp., Pittsburgh, Pa.

Fig. 22—Incremental permeability μ_{ac} characteristics of Allegheny audio-transformer "A" sheet steel at 60 cycles/second. No. 29 U.S. gauge, L-7 standard laminations stacked 100 percent, interleaved. This is 4-percent silicon-steel core material. H_0 = magnetizing field in oersteds.

Example of audio-output-transformer design *continued*

For the primary, (MLT) $\approx$ 0.42 feet and N_p(MLT) $\approx$ 850 feet.

For the secondary, (MLT) $\approx$ 0.58 feet and N_s(MLT) $\approx$ 65 feet.

For the primary, then, the size of wire is obtained from R_p/N_p(MLT) = 0.236 ohms/foot; and from Fig. 7, use No. 33.
For the secondary, R_s/N_s(MLT) $\approx$ 0.008, and size of wire is No. 18.

f. Compute the turns/layer, number of layers, and total coil-build, as for power transformers. For an efficient design, (total coil-built) $\approx$ (0.85 to 0.90) $\times$ (window width)

g. To determine if leakage inductance is within the required limit of (c) above, evaluate

$$l_{scp} = \frac{10.6 N_p^2 (\mathrm{MLT}) (2nc + a)}{n^2 b \times 10^9} = 0.036 \text{ henries}$$

which is less than the limit 0.089 henries of (c). The symbols of this equation are defined in Fig. 28. If leakage inductance is high, interleave windings as indicated under "Methods of winding transformers", p. 298.

Example of audio-input-transformer design

This transformer must couple a 500-ohm line to the grids of 2 tubes in class-A push-pull. Attenuation to be flat to 0.5 decibel over 100 to 15,000 cycles; step-up = 1:10; and input to primary is 2 volts.

a. Due to low input power, use core material of high permeability, such as *4750* in Fig. 6. To allow for possible variation from manufacturer's stated value of 9000, assume μ_0 = 4000. Interleave primary between halves of secondary. Use No. 40 wire for secondary. For interwinding insulation use 0.010 paper. Use winding-space tolerance of 10 percent.

b. Total secondary load resistance $= R'_{\mathrm{par}} = \dfrac{a^2 R_1 R_2}{a^2 R_1 + R_2} \approx a^2 R_1$

$$= 500 \times 10^2 = 50{,}000 \text{ ohms}$$

From universal-frequency-response curves of Fig. 16 for 0.5 decibel down at 100 cycles (voltage ratio = 0.95),

$$\frac{\omega_{\mathrm{low}} L_s}{R'_{\mathrm{par}}} = 3, \text{ or } L_s = 240 \text{ henries}$$

c. Try Allegheny type EI–68 punchings, square stack. From manufacturer's catalog, A_c = 3.05 centimeters, l_c = 10.5 centimeters, and window dimensions = $\frac{11}{32} \times 1\frac{1}{32}$ inches, interleaved singly: l_a = 0.0005.

Example of audio-input-transformer design *continued*

From formula $L = \dfrac{1.25N^2A_c}{l_g + l_c/\mu_0} \times 10^{-8}$ and above constants, compute

$N_s = 4400$
$N_p = N_s/a = 440$

d. Choose size of wire for primary winding, so that $R_p \approx 0.1R_g = 50$ ohms. From geometry of core, (MLT) ≈ 0.29 feet; also, $R_p/N_p\,(\text{MLT}) = 0.392$, or No. 35 wire ($D = 0.0062$ for No. 35F).

e. Turns per layer of primary $= 0.9b/d = 110$; number of layers $n_p = N_p/110 = 4$; turns per layer of secondary $0.9b/d = 200$; number of layers $n_s = N_s/200 = 22$.

f. Secondary leakage inductance

$$l_{scs} = \frac{10.6N^2_s\,(\text{MLT})\,(2nc + a) \times 10^{-9}}{n^2b} = 0.35 \text{ henries}$$

g. Secondary effective layer-to-layer capacitance

$$C_e = \frac{4C_l}{3n_l}\left(1 - \frac{1}{n_l}\right)$$

(see p. 299) where $C_l = 0.225A\epsilon/t = 1770$ micromicrofarads. Substituting this value of C_l into above expression of C_e, we find

$C_e = 107$ micromicrofarads

h. Winding-to-core capacitance $= 0.225A\epsilon/t \approx 63$ micromicrofarads (using 0.030-inch insulation between winding and core). Assuming tube and stray capacitances total 30 micromicrofarads, total secondary capacitance

$C_s \approx 200$ micromicrofarads

i. Series-resonance frequency of l_{sc} and C_s is

$$f_r = \frac{1}{2\pi\sqrt{l_{sc}C_s}} = 19{,}200 \text{ cycles,}$$

At f_r, $B = X_c/R_1 = 1/2\pi f_r C_s R_1 = 0.83$; at 15,000 cycles, $f/f_r = 0.78$.

From Fig. 18, decibels variation from median frequency is seen to be less than 0.5.

If it is required to extend the frequency range, use Mumetal core material for its higher μ_0 (20,000). This will reduce the primary turns, the leakage inductance, and the winding shunt capacitance.

Considerations in audio-transformer design

Output transformers

These are step-down low-impedance transformers in which the high-frequency response is governed mainly by leakage inductance since distributed capacitance has little effect on the low load impedance. Commonly used in the plate circuit of vacuum-tube amplifiers and thus has direct current in the primary unless shunt feeding or push-pull operation is employed. Usually employ silicon steel with gapped construction. Since transmission of power is concerned, the efficiency should be high.

Input and interstage transformers

Such transformers are usually step-up type to obtain as much voltage gain as possible to drive the grid of the following tube. The secondary works into a high impedance represented either by a shunt resistor or the grid itself. High-frequency response is analyzed in Fig. 19.

When direct current is present in the primary, the incremental permeability is reduced as indicated in Fig. 22. This increases the number of winding turns required and the resulting increase in shunt capacitance makes it difficult to obtain good high-frequency response. When direct current is not present, high-permeability core material should be used. Since no power is transferred, the secondary wire size is limited only by winding techniques and is as small as possible. Low-frequency response can be manipulated where a coupling capacitor exists by applying filter theory to the coupling capacitance and to the inductances of the choke and primary winding as indicated in Fig. 23.

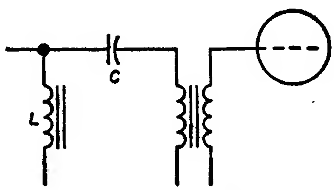

Fig. 23—Equivalent filter used in determining the low-frequency response of shunt-fed interstage transformers.

Interstage transformers usually have ratios of 1 : 1 or slightly higher. Both primary and secondary impedances are rather high and are thus susceptible to shunt capacitances.

Modulation transformers

These transformers are treated similarly to output transformers except that high power and low distortion must be given special consideration. This transformer usually works from a class-*B* push–pull amplifier and it is essential that the load impedance remain fairly constant with a power factor near unity. Such a condition can be obtained in the normal modulation

Considerations in audio-transformer design *continued*

circuit by treating the inductance of the transformer secondary, the coupling capacitance, and the inductance of the modulation choke as a high-pass filter with a cutoff frequency of $\frac{1}{2}$ to $\frac{1}{3}$ of the lowest frequency to be passed as indicated in Fig. 24A.

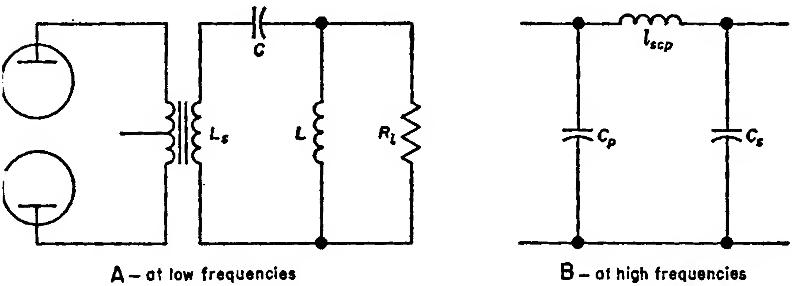

Fig. 24—Equivalent filters used in determining the low- and high-frequency responses of modulation transformers.

For the high-frequency end, the transformer primary capacitance, leakage inductance, and secondary capacitance are treated as a low-pass filter with cutoff frequency from 2 to 3 times the highest frequency to be transmitted (Fig. 24B). Modulation transformers commonly used in low-power circuits dispense with the modulation choke and coupling capacitor as indicated in Fig. 25.

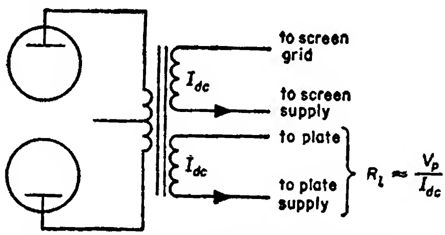

Fig. 25—Typical low-power modulation circuit.

Driver transformers

These transformers are used to drive high-power class-*B* amplifiers where the grids draw current over part of a cycle and thus require some power. Good regulation is a requirement to prevent poor waveform. The best way to do this is to employ a step-down ratio that will supply the necessary grid swing with adequate margin of safety. Low winding resistances and low leakage inductance in each half of the secondary are required to maintain good regulation.

Considerations in audio-transformer design *continued*

Class-A-amplifier transformers

These transformers are used in common single-tube amplifier stages coupled by transformers. Since the tube is operated over the linear portion of its characteristic, minimum distortion is experienced, provided the transformer reflects the proper load to the tube. Unless shunt feed is used, the primary winding of the transformer carries the direct plate current. The alternating-current output consists of variations in the plate direct current. Input transformers are essentially unloaded except for tube capacitance or shunt resistance since the grid never draws current.

Class-B-amplifier transformers

Class-*B* amplifiers operate over a greater range of the tube characteristic than in class A and distortion is greater since part of the characteristic is nonlinear. Plate current flows essentially $\frac{1}{2}$ cycle at a time since negative swings of the grid cutoff plate current resulting in slightly lower average current than in the class-*A* case. The primary of transformer-coupled amplifiers carries direct current. The internal tube resistance varies greatly with grid voltage, thus the high-frequency response is difficult to predict. Input transformers have to supply some grid power and driver-transformer theory applies to them.

Push-pull-amplifier transformers

Class-*A*: Both tubes draw plate current at all times and thus contribute to output. For this reason, primary balance or coupling of the transformer is not too important and one-half of the winding may be placed over the other. Turns ratio of entire primary winding to secondary is equal to the square root of the impedance ratio (Fig. 26). Average direct current of primary is balanced out due to center feeding, although generally 5-percent unbalance should be allowable to take care of tube variations.

Class-*B*: In contrast to class-*A* operation, only one tube conducts at a time since the other is biased off. Good coupling between primary halves and the entire secondary is a requirement. Primary-to-primary leakage inductance causes nicks in output wave because of transients as operation switches from one tube to the other. Since only one tube operates at a time, the turns ratio of each half of the primary to the whole secondary, equals the square root of one tube impedance to the secondary impedance (Fig. 27). Variations in tube impedance, which may become quite large, affect the high-frequency response.

Considerations in audio-transformer design *continued*

Class-AB_1: An intermediate case where the bias voltage is slightly higher than class A but the grids draw no current. Coupling transformers are similar to class A.

Class-AB_2: The tubes are biased near cutoff but not as far as class B. Grid current is drawn and for a portion of each cycle the tubes act independently. Class B transformer design applies.

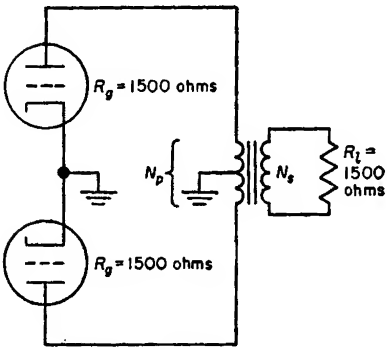

$$\frac{N_p}{N_s} = \left(\frac{3000}{1500}\right)^{1/2} = 1.4$$

Fig. 26—Push-pull class-A amplifier with a 1.4:1 turns ratio.

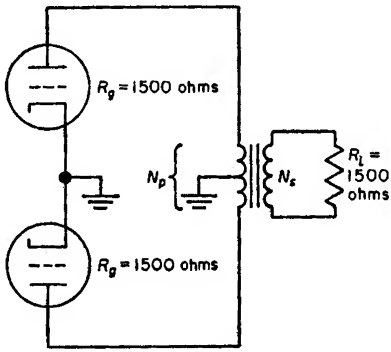

$$\frac{\frac{1}{2}N_p}{N_s} = \left(\frac{1500}{1500}\right)^{1/2} = 1 \text{ (for each half of primary)}$$

$$N_p/N_s = 2$$

Fig. 27—Push-pull class-B amplifier with a 2:1 turns ratio.

Methods of winding transformers

Most common methods of winding transformers are shown in Fig. 28. Leakage

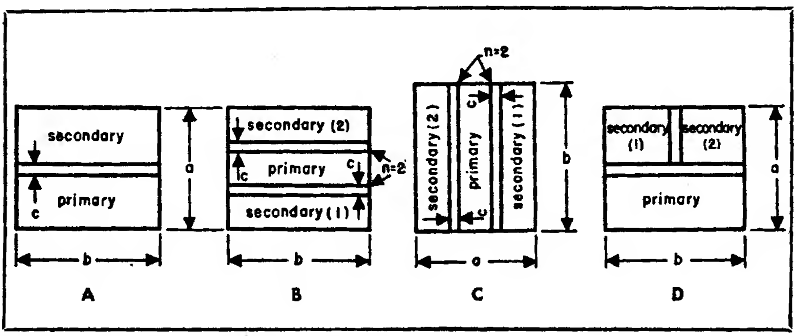

Fig. 28—Methods of winding transformers.

Methods of winding transformers *continued*

inductance is reduced by interleaving, i.e., by dividing the primary or secondary coil in two sections, and placing the other winding between the two sections. Interleaving may be accomplished by concentric and by coaxial windings, as shown on Figs. 28B and C; reduction of leakage inductance is computed from the equation

$$l_{sc} = \frac{10.6N^2(\text{MLT})(2nc + a)}{n^2 b \times 10^9} \text{ henries}$$

(dimensions in inches) to be the same for both Figs. 28B and C.

Means of reducing leakage inductance are

a. Minimize turns by using high-permeability core.

b. Reduce build of coil.

c. Increase winding width.

d. Minimize spacing between windings.

e. Use bifilar windings.

Means of minimizing capacitance are

a. Increase dielectric thickness (t).

b. Reduce winding width b and thus area A.

c. Increase number of layers.

d. Avoid large potential differences between winding sections as the effect of capacitance is proportional to applied potential.

Note: Leakage inductance and capacitance requirements must be compromised in practice since corrective measures are opposites.

Effective interlayer capacitance of a winding may be reduced by sectionalizing it as shown in D. This can be seen from the formula

$$C_e = \frac{4C_l}{3n_l}\left(1 - \frac{1}{n_l}\right) \text{ micromicrofarads}$$

where

n_l = number of layers

C_l = capacitance of one layer to another

$$= \frac{0.225A\epsilon}{t} \text{ micromicrofarads}$$

where

Methods of winding transformers *continued*

A = area of winding layer
 = (MLT)b inches^2
t = thickness of interlayer insulation in inches
ϵ = dielectric constant
 ≈ 3 for paper

Pulse transformers

Pulse transformers are designedto transmit square waves or trains of pulses as described in Fig. 7, page 538, while maintaining as closely as possible the original shape. Fourier analysis shows that such pulse waveforms consist of a wide range of frequency components. Thus the transformer must have suitable bandwidth to maintain fidelity.

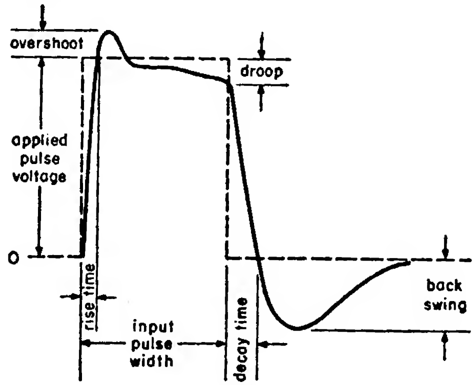

Fig. 29—Output pulse shape. In the strictest sense, pulse rise and decay times are measured between the 10- and 90-percent values; width between the 50-percent values.

Pulse transformers can be analyzed by considering the leading edge, top, and trailing edge of the pulse separately. Fig. 29 portrays a typical transformer output pulse compared to input pulse. Refer to page 541 for pulse terminology. Fig. 30 shows the fundamental circuit and Fig. 31 illustrates equivalent circuits for the various transient conditions.

Leading-edge reproduction requires transmission of a wide band of frequencies and is controlled by leakage inductance l_{scp} and winding capacitances C_p and C_s as indicated in Fig. 31A, B, and C. Analysis for step-up and step-down transformers varies slightly as shown. Leakage inductance and winding capacitance must be minimized to achieve a sharp rise; however, output voltage may overshoot input voltage and oscillation may be encountered where very abrupt rise times are involved.

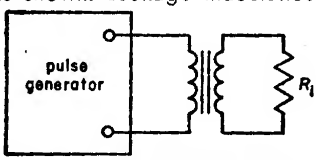

Fig. 30—Pulse-transformer circuit.

Pulse transformers *continued*

Pulse-top response is dependent on the magnitude of the open-circuit inductance of the transformer as indicated in Fig. 31D. The greater the inductance L_p, the smaller the droop from input voltage level.

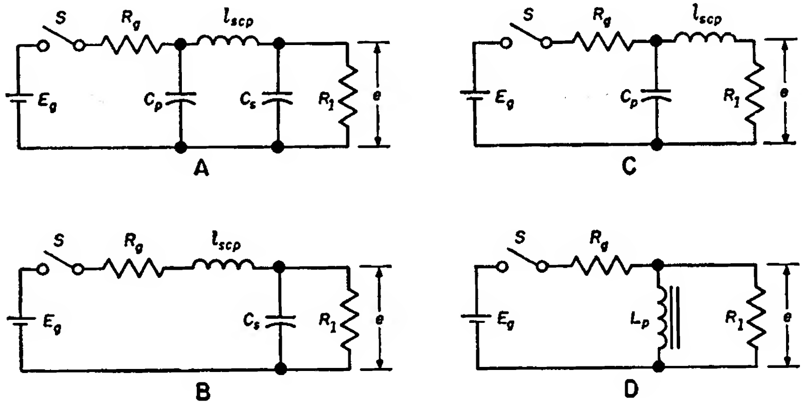

Fig. 31—Pulse-transformers equivalent circuits. *A*—Leading-edge equivalent circuit. *B*—Leading-edge equivalent circuit for step-up-ratio transformer. C—Leading edge equivalent circuit step-down-ratio transformer. *D*—Top-of-pulse equivalent circuit. *E*—Trailing-edge equivalent circuit.

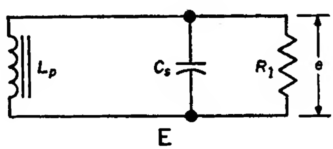

Control of the trailing edge of the pulse is dependent on the open-circuit inductance and secondary winding capacitance as shown in Fig. 31E. The lower the capacitance, the faster the rate of voltage decay. Negative backswing depends on the magnitude of the transformer magnetizing current. The greater the magnetizing current, the greater the backswing.

Pulse-transformer design involves analysis of transient effects and thus direct solution is complex. Empirical or graphical solution* is usually used.

Low-loss core materials such as grain-oriented silicon-steel loop cores or nickel–iron alloys in 2-mil thickness are normally used. Small air gaps are commonly used to reduce remanent magnetism in core due to unidirectional pulses. Windings are normally interleaved to reduce leakage reactance. Where load impedance is high, single-layer primary and secondary windings are best; where low, interleaved windings are best.

*R. Lee, "Electronic Transformers and Circuits," 2nd edition, John Wiley & Sons, Inc., New York; New York; 1955: chapter 10, p. 292.

Pulse transformers *continued*

Special winding techniques may be required to reduce winding capacitances. Construction is normally of core type, single or double coil, since capacitance may be more easily controlled.

Temperature and humidity

Fig. 32—Classification of electrical insulating materials.*

class	insulating material	limiting insulation temperature (hottest spot) in °C	permissible rise in °C above 40°C ambient: by thermometer	permissible rise in °C above 40°C ambient: by resistance or imbedded detector
O	Cotton, silk, paper and similar organic materials when neither impregnated nor immersed in a liquid dielectric	90	35	45
A	(1) Cotton, silk, paper, and similar organic materials when either impregnated or immersed in a liquid dielectric; or (2) molded and laminated materials with cellulose filler, phenolic resins and other resins of similar properties;or (3) films and sheets of cellulose acetate and other cellulose derivatives of similar properties; or (4) varnishes (enamel) as applied to conductors	105	50	60
B	Mica, glass fiber, asbestos, etc., with suitable binding substances. Other materials or combinations of materials, not necessarily inorganic, may be included in this class if by experience or acceptance tests they can be shown to be capable of operation at class-*B* temperature limits	130	70	80
H	Silicone elastomer, mica, glass fiber, asbestos, etc., with suitable binding substances such as appropriate silicone resins. Other materials or combinations of materials may be included in this class if by experience or acceptance tests they can be shown to be capable of operation at class-*H* temperature limits	180	100	120
C	Entirely mica, porcelain, glass, quartz, and similar inorganic materials	No limit selected	—	—

*Abridged from, "General Principles Upon Which Temperature Limits Are Based In the Rating of Electrical Machines and Other Equipment," American Institute of Electrical Engineers Standard No. 1, with revisions proposed in a paper, "Problems of Revising AIEE Standard No. 1," *Electrical Engineering*, vol. 75, pp. 344-348; April, 1956.

Temperature and humidity *continued*

Standard classes of insulating materials and their limiting operating temperatures are listed in Fig. 32. A comparison of the properties of five high-temperature wire insulating coatings is shown in Fig. 33.

Fig. 33—Comparison of five high-temperature wire-insulating materials.*

characteristic	modified teflon	teflon	silicone enamel DC1360	formvar (vinyl acetal)	plain enamel
Upper temp. limit	+250°C	+250°C	+180°C	+105°C	+80°C
Lower temp. limit	−100°C	−100°C	−40°C	−40°C	−40°C
Dielectric strength	Excellent	Very good	Very good	Good	Good
Dielectric constant (60cy—30,000mc)	2.0—2.05†	2.0—2.05†	Inferior	Inferior	Inferior
Power factor (60cy—10,000mc)	0.0002†	0.0002†	Inferior, about 0.006—0.007	Inferior	Inferior
Space factor	Excellent	Excellent	Excellent	Excellent	Excellent
Solvent resistance	Excellent	Excellent	Fair	Fair	Poor
Abrasion resistance	Good	Fair	Very good	Excellent	Good
Thermoplastic flow	Good	Fair	Excellent	Excellent	Good
Crazing resistance	Excellent	Very good	Fair	Fair	Fair
Flame resistance	Excellent	Excellent	Fair	Poor	Poor
Fungus resistance	Excellent	Excellent	Good	Good	Poor
Moisture resistance	Excellent	Excellent	Good	Good	Good
Continuity of insul.	Excellent	Excellent	Good	Good	Good
Arc resistance	Excellent	Excellent	Good	Good	Good
Flexibility	Excellent	Very good	Good	Good	Good

* Taken from, J. Holland, "Choosing Wire Insulation For High Temperatures," *Electronic Design*, vol. 2, p. 14; July, 1954.
† Stable at temperatures up to 250° C.

Open-type constructions generally permit greater cooling than enclosed types, thus allowing smaller sizes for the same power ratings. Moderate humidity protection may be obtained by impregnating and dip-coating or molding transformers in polyester or epoxy resins; these units provide good heat dissipation but are not as good in this respect as completely open transformers.

Protection against the detrimental effects of humidity is commonly obtained by enclosing transformers in hermetically sealed metallic cases. This is particularly important if very-fine wire, high output voltage, or direct-current potentials are involved. Heat conductivity to the case exterior may be improved by the use of asphalt or thermosetting resins as filling materials. Best conductivity is obtained with high-melting-point silica-filled asphalts or resins of the polyester or epoxy types. Coils impregnated with these resins dissipate heat best since voids in the heat path may be eliminated.

Temperature and humidity *continued*

Immersion in oil is an excellent means of removing heat from transformers. An air space or bellows must be provided to accommodate expansion of oil when heated.

Dielectric insulation and corona

For class-A, a maximum dielectric strength of 40 volts/mil is considered safe for small thicknesses of insulation. At high operating voltages, due regard must be paid to corona that occurs prior to dielectric breakdown and will in time deteriorate insulation and cause dielectric failure. Best practice is to operate insulation at least 25 percent below the corona starting voltage. Approximate 60-cycle root-mean-square corona voltage V is:

$$\log \frac{V \text{ (in volts)}}{800} = \frac{2}{3} \log (100t)$$

where t = total insulation thickness in inches. This may be used as a guide in determining the thickness of insulation. With the use of varnishes that require no solvents, but solidify by polymerization, the bubbles present in the usual varnishes are eliminated, and much higher operating voltages and, hence, reduction in the size of high-voltage units may be obtained. Fosterite, and some polyesters, such as the Intelin 211 compound, belong in this group. In the design of high-voltage transformers, the creepage distance required between wire and core may necessitate the use of insulating channels covering the high-voltage coil, or taping of the latter. For units operating at 10 kilovolts or higher, oil insulation will greatly reduce creepage and, hence, size of the transformer.

■ Rectifiers and filters

Rectifier basic circuits

Half-wave rectifier (Fig. 1): Most applications are for low-power direct conversion of the type necessary in small ac-dc radio receivers (without an intermediary transformer), and often with the use of a metallic rectifier. Not generally used in high-power circuits due to the low frequency of the ripple voltage and a large direct-current polarization effect in the transformer, if used.

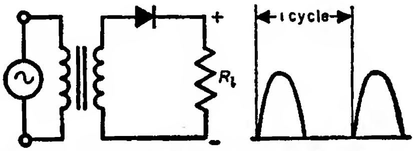

Fig. 1—Half-wave single-phase rectifier.

Full-wave rectifier (Fig. 2): Extensively used due to higher frequency of ripple voltage and absence of appreciable direct-current polarization of transformer core because transformer-secondary halves are balanced.

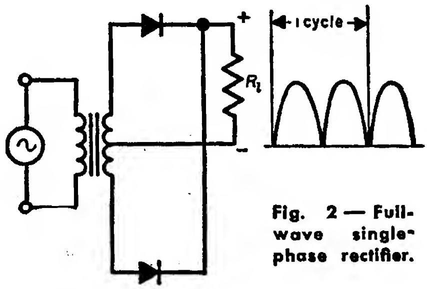

Fig. 2 — Full-wave single-phase rectifier.

Bridge rectifier (Fig. 3): Transformer utilization better than in circuit of Fig. 2. Extensively used with semiconductor rectifiers (p. 311). Not often used with tube rectifiers: requiring 4 tubes and 3 well-insulated filament-transformer secondaries. Peak inverse voltage is half that of Fig. 2, but rectifier voltage drop is doubled (for same tube type).

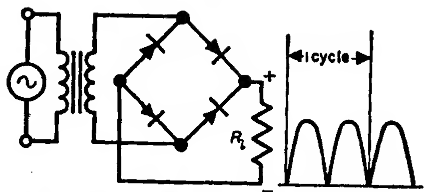

Fig. 3—Bridge rectifier.

Voltage multiplier (Fig. 4): May be used with or without a line transformer. Without the transformer, it develops sufficiently high output voltage for low-power equipment; however, lack of electrical insulation from the power line may be objectionable. May also be used for obtaining high voltages from a transformer having relatively low step-up ratio.

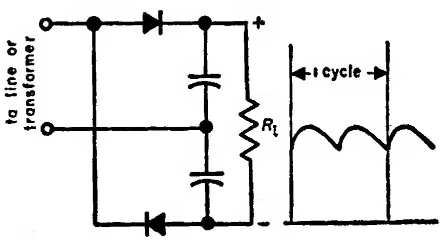

Fig. 4—Voltage-doubler rectifier.

Typical power rectifier circuit connections and circuit data

type of circuit	single-phase full-wave	single-phase full-wave (bridge)	3-phase half-wave	3-phase half-wave
transformer	single-phase center-tap	single-phase	delta–wye	delta–zig zag
circuit: secondary, primary	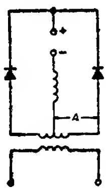	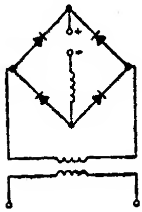	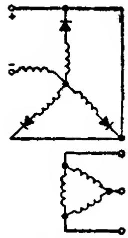	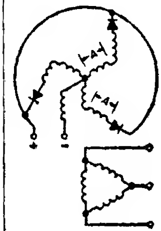
Number of phases of supply	1	1	3	3
Number of rectifiers*	2	4	3	3
Ripple voltage	0.48	0.48	0.18	0.18
Ripple frequency	2f	2f	3f	3f
Line voltage	1.11	1.11	0.855	0.855
Line current	1	1	0.816	0.816
Line power factor †	0.90	0.90	0.826	0.826
Transformer primary volts per leg	1.11	1.11	0.855	0.855
Transformer primary amperes per leg	1	1	0.471	0.471
Transformer primary kilovolt–amperes	1.11	1.11	1.21	1.21
Transformer average kilovolt–amperes	1.34	1.11	1.35	1.46
Transformer secondary volts per leg	1.11A	1.11	0.855	0.493A
Transformer secondary amperes per leg	0.707	1	0.577	0.577
Transformer secondary kilovolt-amperes	1.57	1.11	1.48	1.71
Peak inverse voltage per rectifier	3.14	1.57	2.09	2.09
Peak current per rectifier	1	1	1	1
Average current per rectifier	0.5	0.5	0.333	0.333

Unless otherwise stated, factors shown express the ratio of the root-mean-square value of the circuit quantities designated to the average direct-current-output values of the rectifier.

Factors are based on a sine-wave voltage input, infinite-inductance choke, and no transformer or rectifier losses.

6-phase half-wave	6-phase half-wave	6-phase (double 3-phase) half-wave	3-phase full-wave	3-phase full-wave
delta–star	delta–6-phase fork	delta–double-wye with balance coil	delta–wye	delta–delta
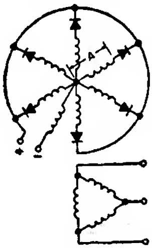	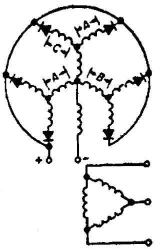	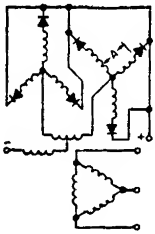	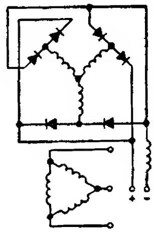	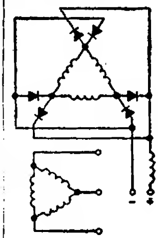
3 6	3 6	3 6	3 6	3 6
0.042 6*f*	0.042 6*f*	0.042 6*f*	0.042 6*f*	0.042 6*f*
0.740 0.816 0.955	0.428 1.41 0.955	0.855 0.707 0.955	0.428 1.41 0.955	0.740 0.816 0.955
0.740 0.577 1.28	0.428 0.816 1.05	0.855 0.408 1.05	0.428 0.816 1.05	0.740 0.471 1.05
1.55 0.740A 0.408 1.81	1.42 0.428A { 0.577B } { 0.408C } 1.79	1.26 0.855A 0.289 1.48	1.05 0.428 0.816 1.05	1.05 0.740 0.471 1.05
2.09 1 0.167	2.09 1 0.167	2.42 0.5 0.167	1.05 1 0.333	1.05 1 0.333

* These circuit factors are equally applicable to electron-tube or metallic-plate rectifiers.

† (Line power factor) = (direct-current output watts)/(line volt–amperes.)

Semiconductor rectifiers

Applications

Foremost in the category of semiconductor- or dry-type rectifiers are selenium, germanium, silicon, and copper-oxide rectifiers. The various fields of application for the different types are governed by their basic voltage and current characteristics, environmental conditions, size and weight considerations, and cost.

The uses of semiconductor rectifiers cover a wide range of applications that include battery chargers; radio, television, and miscellaneous direct-current power supplies; magnetic amplifiers; servomechanism circuits; and many special applications such as arc suppression, polarization of alternating-current circuits (direct-current restorers), drainage rectifiers (for cathodic protection), and many others.

Equivalent circuit

Semiconductor rectifiers may be regarded as resistive devices having low electrical resistance in the forward direction and high resistance in the reverse direction. (For high-impedance circuits, the capacitance across the rectifying layer may become important.) The voltage drop in the forward direction must be taken into account when the alternating-current input voltage of a rectifier is to be determined.

Aging

Some semiconductor rectifiers exhibit a phenomenon known as aging, which manifests itself in an increase of forward as well as reverse resistance with usage. The degree of aging is different for the various types. Depending on the application, means for compensating for the aging effect may or may not be required.

Rating of a rectifier cell

It is common practice to rate a rectifier cell on the basis of the root-mean-square sinusoidal voltage that it can withstand in the reverse direction and on the average forward current that it will pass at a certain current density. For *selenium-rectifier cells*, typical ratings at 35 degrees centigrade ambient are:

26 root-mean-square volts per cell

320 direct-current milliamperes per square inch of active rectifying area

The cell voltage ratings for *copper-oxide rectifiers* are lower than for selenium; such rectifiers are used mostly in low-voltage circuits.

Semiconductor rectifiers *continued*

Voltage ratings of *germanium* and *silicon* rectifiers are higher than for selenium, so such rectifiers can be employed more advantageously in high-voltage circuits.

Forward voltage drop

Typical dynamic forward voltage-drop characteristics for selenium rectifiers are shown in Fig. 5. The forward voltage drop per rectifying element or plate is highest for battery-charging and capacitive load applications, due to the high ratio of root-mean-square current to average direct current.

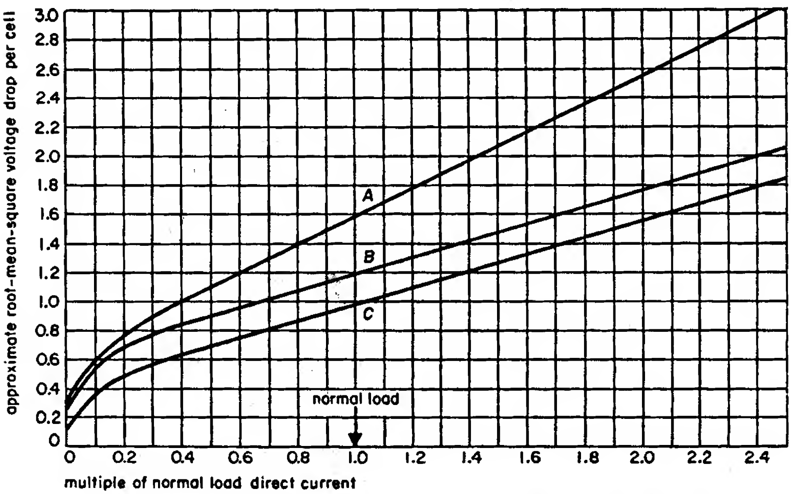

Fig. 5—Typical dynamic forward voltage-drop curves for selenium-rectifier cells, at 65-degree-centigrade cell temperature. A—Battery or capacitive loads: Single-phase half-wave, bridge, or center-tap. B—Resistive or inductive loads: Single-phase half-wave, bridge, or center-tap; and 3-phase half-wave. C—All types of loads: 3-phase bridge or center-tap.

Rating of a selenium rectifier stack

Stacks are operated at a given temperature that is a safe value with allowance for aging. Catalog rating is in most cases based on an ambient temperature of 35 degrees centigrade. Ratings for higher temperatures than that (Fig. 6) are based on reduction in forward current to reduce forward-current losses, reduction in reverse voltage to reduce reverse-current losses, or a combination of both forward-current and reverse-voltage reductions to obtain the desired operating temperature with good electrical

Semiconductor rectifiers *continued*

efficiency. The forward voltage drop and consequent heating depend to a small degree on the temperature of the rectifier cell, as does also the reverse current.

The 35-degree-centigrade rating of a rectifier is based on a current density for a cell of about 320 milliamperes per square inch of active rectifying area. While each cell has this basic rating, it is common practice to increase the current density for the same temperature rise by increasing the space between cells or by using forced-air or oil cooling. The increase in spacing allows for current density increases from 20 to 50 percent; the higher percentage applies to smaller-size cells. This causes some reduction in efficiency due to higher voltage drop.

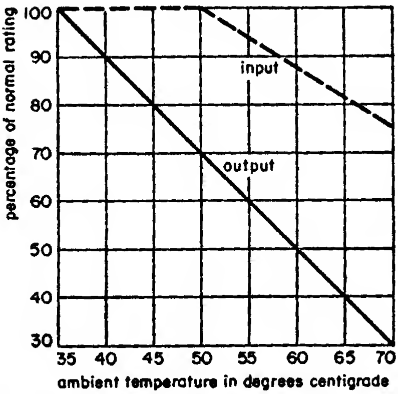

Fig. 6—Selenium-rectifier temperature derating curves (approximate), for root-mean-square alternating input voltage and average direct output current based on 35-degree-centigrade ambient.

The cells at each end of a stack have the lowest temperature due to greatest cooling there. Cell temperatures rise successively from each end toward the center of the stack. In a long stack, the temperatures of a number of the central cells are practically identical. As a consequence, some manufacturers raise the rating of stacks of 1 to 8 cells as much as 50 percent, and of stacks of 9 to 16 cells as much as 25 percent. These increases apply only to the normal-spaced convection-cooled ratings and not to the wide-spaced or forced-air- or oil-cooled ratings.

Past practice for forced-air- or oil-cooled rectifiers has been to rate them up to 2.5-times normal rating with adequate cooling. Experience shows that up to 2-times normal is a better design figure to use when long life and good efficiency and voltage regulation are factors.

Development of new techniques in selenium-rectifier manufacture permit operating at higher reverse voltages, higher current densities, and higher cell temperatures. This is in addition to ratings that may be given to regular production stacks, which permit greater output or increased-temperature operation coincident with a reduction in life expectancy. New processes may also carry a reduction in life expectancy subject to further experience in use and in the laboratory.

Semiconductor rectifiers *continued*

Circuit design for semiconductor power rectifiers

For most applications, particularly with single-phase input, full-wave bridge circuits are used, although half-wave and center-tap rectifiers are frequently used where low direct voltage is required. However, when direct-voltage requirements exceed the output of a single series rectifier element, use of the full-wave bridge circuit is preferred, since the same number of rectifier plates are then required for half-wave or center-tap connections as for a full-wave bridge connection. A half-wave rectifier has a relatively poor power factor, high ripple content in the output, and requires a larger transformer than a full-wave bridge circuit. A center-tap rectifier requires a somewhat larger transformer than an equivalent full-wave bridge rectifier, with the added complication of bringing out the center tap.

The table on pages 306 and 307 for typical power-rectifier circuit connections and circuit data show the theoretical values of direct and alternating voltages, current, and power for the basic rectifier and transformer elements of single-phase and polyphase conversion circuits, based on perfect rectifiers and transformers.

The information in Figs. 7 and 8 can be used to determine the input values of alternating voltages and output direct currents and the number of rectifier cells for various basic rectifier circuits.

The formulas and the values of the constants K and I_{ac} are approximate, but are sufficiently accurate for practical design purposes.

Symbols for Figs. 7 and 8

I_{ac} = transformer secondary current in root-mean-square amperes

I_{dc} = average load direct current in amperes

K = circuit form factor

n = number of cells in series in each arm of rectifier

V_{ac} = alternating root-mean-square input voltage per secondary winding (see diagrams)

$V_{ac\Delta}$ = phase-to-phase alternating input voltage for 3-phase full-wave bridge

V_{dc} = average value of direct-current output voltage

V_p = reverse root-mean-square voltage per plate (rating of rectifier cell)

ΔV = root-mean-square voltage drop per cell at I_{dc} (see Fig. 5)

Semiconductor rectifiers *continued*

Fig. 7—Single-phase-rectifier circuits, formulas, and design constants.

constant		half-wave	full-wave center tap	full-wave bridge
Circuit		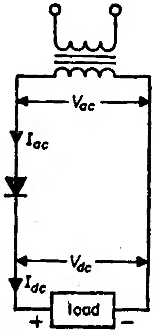	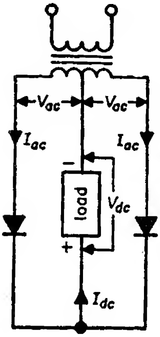	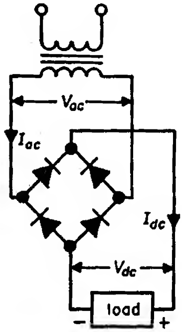
V_{ac}		$KV_{dc} + n\Delta V$	$KV_{dc} + n\Delta V$	$KV_{dc} + 2n\Delta V$
Resistive and inductive loads	n	$KV_{dc}/(V_p - \Delta V)$	$2KV_{dc}/(V_p - 2\Delta V)$	$KV_{dc}/(V_p - 2\Delta V)$
	V_p	V_{ac}/n	$2V_{ac}/n$	V_{ac}/n
	K	2.26	1.13	1.13
	$I_{ac,rms}$	1.57 $I_{dc,avg}$	0.785 $I_{dc,avg}$	1.11 $I_{dc,avg}$
Battery and capacitive loads	n	$2KV_{dc}/(V_p - 2\Delta V)$	$2KV_{dc}/(V_p - 2\Delta V)$	$KV_{dc}/(V_p - 2\Delta V)$
	V_p	$2V_{ac}/n$	$2V_{ac}/n$	V_{ac}/n
	K	1.0	0.85	0.85
	$I_{ac,rms}$	2.3 $I_{dc,avg}$	1.15 $I_{dc,avg}$	1.65 $I_{dc,avg}$

Semiconductor rectifiers *continued*

Fig. 8—Three-phase-rectifier circuits, formulas, and design constants. For all loads.

constant	half-wave	full-wave bridge
Circuit	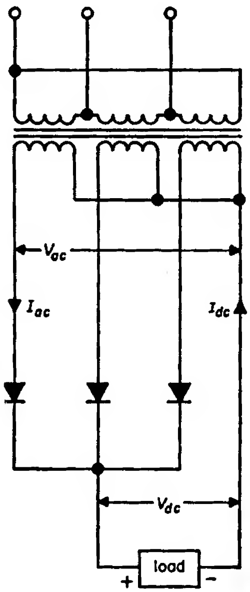	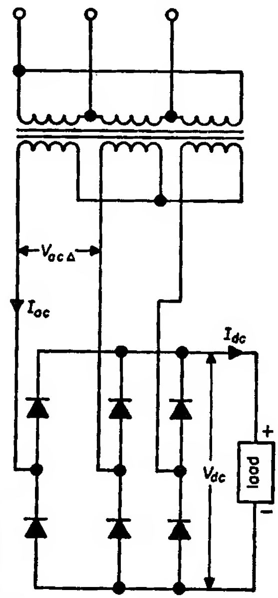
Input	$V_{ac} = KV_{dc} + n\Delta V$	$V_{ac\Delta} = KV_{dc} + 2n\Delta V$
n	$1.73\ KV_{dc}/(V_p - 1.73\Delta V)$	$KV_{dc}/(V_p - 2\Delta V)$
V_p	$1.73\ V_{ac}/n$	$V_{ac\Delta}/n$
K	0.855	0.74
$I_{ac,rms}$	$0.577\ I_{dc,avg}$	$0.816\ I_{dc,avg}$

Semiconductor rectifiers *continued*

Rectifiers for magnetic amplifiers

Rectifiers used in conjunction with magnetic amplifiers (chapter 13) must have low reverse leakage currents to obtain as high a gain as possible with a given set of components. Rectifier leakage current behaves like negative feedback, thus reducing amplification. Changes in the rectifier operating temperature, which result in changes in the reverse leakage current, may also result in objectionable unbalances between associated amplifiers. For best amplifier performance the reverse leakage of rectifiers for magnetic-amplifier applications should be held to approximately 0.2 percent of the required forward current. This can be achieved by reducing the operating voltage per plate below the normal value.

Grid-controlled gaseous rectifiers

Grid-controlled rectifiers are used to obtain closely controlled voltages and currents. They are commonly used in the power supplies of high-power radio transmitters. For low voltages, gas-filled tubes, such as argon (those that are unaffected by temperature changes) are used. For higher voltages, mercury-vapor tubes are used to avoid flash-back (conduction of current when plate is negative). These circuits permit large power to be handled, with smooth and stable control of voltage, and permit the control of short-circuit currents through the load by automatic interruption of the rectifier output for a period sufficient to permit short-circuit arcs to clear, followed by immediate reapplication of voltage.

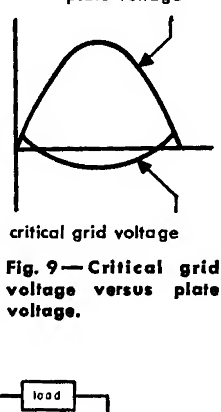

Fig. 9—Critical grid voltage versus plate voltage.

In a thyratron, the grid has a one-way control of conduction, and serves to fire the tube at the instant that it acquires a critical voltage. Relationship of the critical voltage to the plate voltage is shown in Fig. 9. Once the tube is fired, current flow is generally determined by the external circuit conditions; the grid then has no control, and plate current can be stopped only when the plate voltage drops to zero.

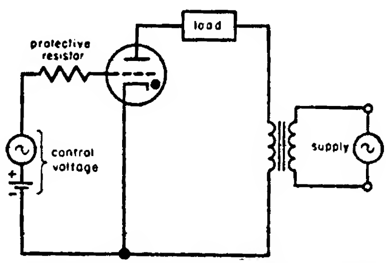

Fig. 10—Basic thyratron circuit. The grid voltage has direct- and alternating-current components.

Grid-controlled gaseous rectifiers *continued*

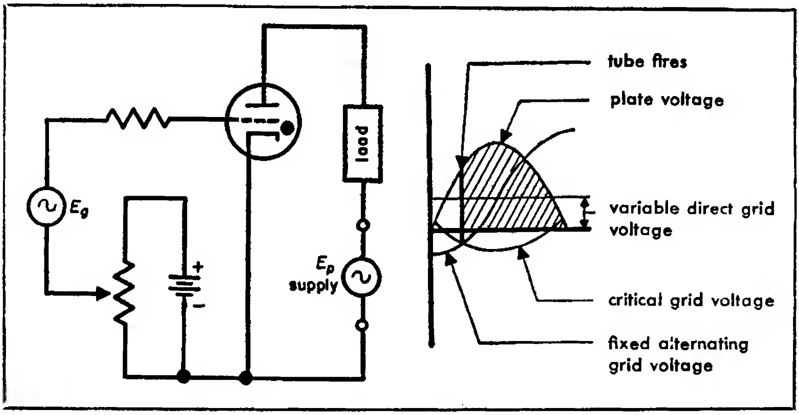

Fig. 11—Control of plate-current conduction period by means of variable direct grid voltage. E_g lags E_p by 90 degrees.

Basic circuit

The basic circuit of a thyratron with alternating-current plate and grid excitation is shown in Fig. 10. The average plate current may be controlled by maintaining

a. A variable direct grid voltage plus a fixed alternating grid voltage that lags the plate voltage by 90 degrees (Fig. 11).

b. A fixed direct grid voltage plus an alternating grid voltage of variable phase (Fig. 12).

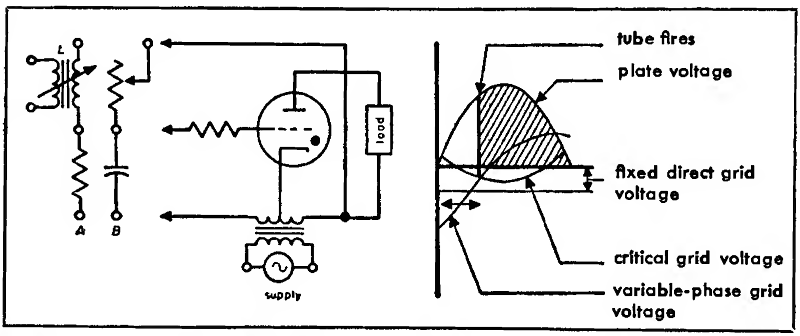

Fig. 12—Control of plate-current conduction period by fixed direct grid voltage (not indicated in schematic) and alternating grid voltage of variable phase. Either inductance-resistance or capacitance-resistance phase-shift networks (*A* and *B*, respectively) may be used. *L* may be a variable inductor of the saturable-reactor type.

Grid-controlled gaseous rectifiers *continued*

Phase shifting

The phase of the grid voltage may be shifted with respect to the plate voltage by:

a. Varying the indicated resistor in Fig. 12.

b. Variation of the inductance of the saturable reactor in Fig. 12.

c. Varying the capacitor in Fig. 13.

On multiphase circuits, a phase-shifting transformer may be used.

Fig. 13—Full-wave thyratron rectifier. The capacitor is the variable element in the phase-shifting network, and hence gives control of output voltage.

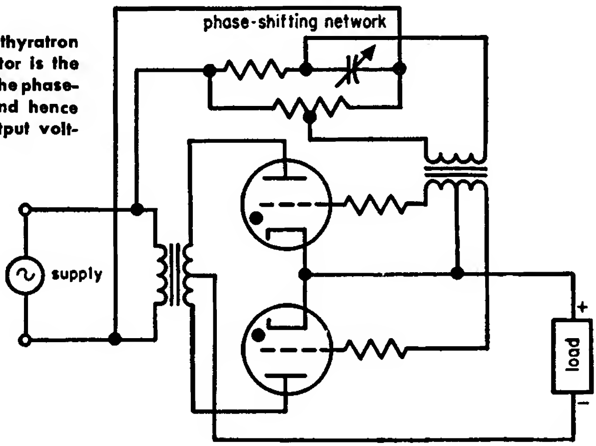

For a stable output with good voltage regulation, it is necessary to use an inductor-input filter in the load circuit. The value of the inductance is critical, increasing with the firing angle. The design of the plate-supply transformer of a full-wave circuit (Fig. 13) is the same as that of an ordinary full-wave rectifier, to which the circuit of Fig. 13 is closely similar. Grid-controlled rectifiers yield larger harmonic output than ordinary rectifier circuits.

Filters for rectifier circuits

Rectifier filters may be classified into three types:

Inductor input (Fig. 14): Have good voltage regulation, high transformer-utilization factor, and low rectifier peak currents, but also give relatively low output voltage.

Filters for rectifier circuits *continued*

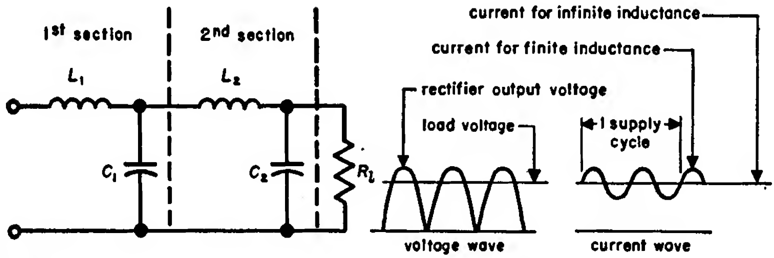

Fig. 14—Inductor-input filter.

Capacitor input (Fig. 15): Have high output voltage, but poor regulation, poor transformer-utilization factor, and high peak currents. Used mostly in radio receivers.

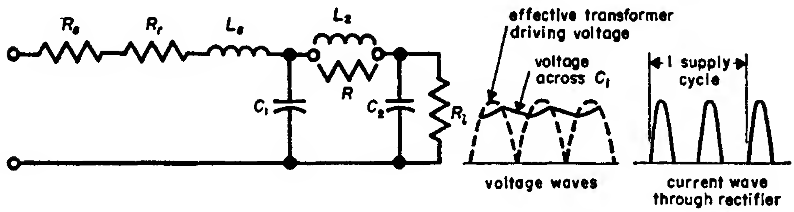

R_s = ½ × (secondary-winding resistance)
L_s = leakage inductance viewed from ½ secondary winding
R_r = equivalent resistance of tube IR drop

Fig. 15—Capacitor-input filter. C_1 is the input capacitor.

Resistor input (Fig. 16): Used for low-current applications.

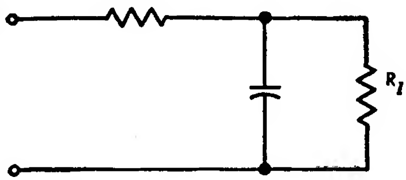

Fig. 16—Resistor-input filter.

Design of inductor-input filters

The constants of the first section (Fig. 14) are determined from the following considerations:

a. There must be sufficient inductance to insure continuous operation of rectifiers and good voltage regulation. Increasing this critical value of inductance by a 25-percent safety factor, the minimum value becomes

Filters for rectifier circuits *continued*

$$L_{\min} = \frac{K}{f_s} R_l \text{ henries} \quad (1)$$

where

f_s = frequency of source in cycles/second

R_l = maximum value of total load resistance in ohms

K = 0.060 for full-wave single-phase circuits

= 0.0057 for full-wave two-phase circuits

= 0.0017 for full-wave three-phase circuits

At 60 cycles, single-phase full-wave,

$$L_{\min} = R_l/1000 \text{ henries} \quad (1A)$$

b. The LC product must exceed a certain minimum, to insure a required ripple factor

$$r = \frac{E_r}{E_{dc}} = \frac{\sqrt{2}}{p^2-1} \frac{10^6}{(2\pi f_s p)^2 L_1 C_1} = \frac{K'}{L_1 C_1} \quad (2)$$

where, except for single-phase half-wave,

p = effective number of phases of rectifier

E_r = root-mean-square ripple voltage appearing across C_1

E_{dc} = direct-current voltage on C_1

L_1 is in henries and C_1 in microfarads.

For single-phase full-wave, $p = 2$ and

$$r = \frac{0.83}{L_1 C_1}\left(\frac{60}{f_s}\right)^2 \quad (2A)$$

For three-phase, full-wave, $p = 6$ and

$$r = (0.0079/L_1 C_1)(60/f_s)^2 \quad (2B)$$

Equations (1) and (2) define the constants L_1 and C_1 of the filter, in terms of the load resistor R_l and allowable ripple factor r.

Filters for rectifier circuits *continued*

Swinging chokes: Swinging chokes have inductances that vary with the load current. When the load resistance varies through a wide range, a swinging choke, with a bleeder resistor R_b (10,000 to 20,000 ohms) connected across the filter output, is used to guarantee efficient operation; i.e., $L_{min} = R_l'/1000$ for all loads, where $R_l' = (R_l R_b)/(R_l + R_b)$. Swinging chokes are economical due to their smaller relative size, and result in adequate filtering in many cases.

Second section: For further reduction of ripple voltage E_{r1}, a smoothing section (Fig. 14) may be added, and will result in output ripple voltage E_{r2}:

$$E_{r2}/E_{r1} \approx 1/(2\pi f_r)^2 L_2 C_2 \tag{3}$$

where f_r = ripple frequency

Design of capacitor-input filters

The constants of the input capacitor (Fig. 15) are determined from:

a. Degree of filtering required.

$$r = \frac{E_r}{E_{dc}} = \frac{\sqrt{2}}{2\pi f_r C_1 R_l} = \frac{0.00188}{C_1 R_l}\left(\frac{120}{f_r}\right) \tag{4}$$

where $C_1 R_l$ is in microfarads × megohms, or farads × ohms.

b. A maximum-allowable C_1 so as not to exceed the maximum allowable peak-current rating of the rectifier.

Unlike the inductor-input filter, the source impedance (transformer and rectifier) affects output direct-current and ripple voltages, and the peak currents. The equivalent network is shown in Fig. 15.

Neglecting leakage inductance, the peak output ripple voltage E_{r1} (across the capacitor) and the peak plate current for varying effective load resistance are given in Fig. 17. If the load current is small, there may be no need to add the L-section consisting of an inductor and a second capacitor. Otherwise, with the completion of an L_2C_2 or RC_2 section (Fig. 15), greater

Filters for rectifier circuits *continued*

filtering is obtained, the peak output-ripple voltage E_{r2} being given by (3) or

$$E_{r2}/E_{r1} \approx 1/\omega RC_2 \tag{5}$$

respectively.

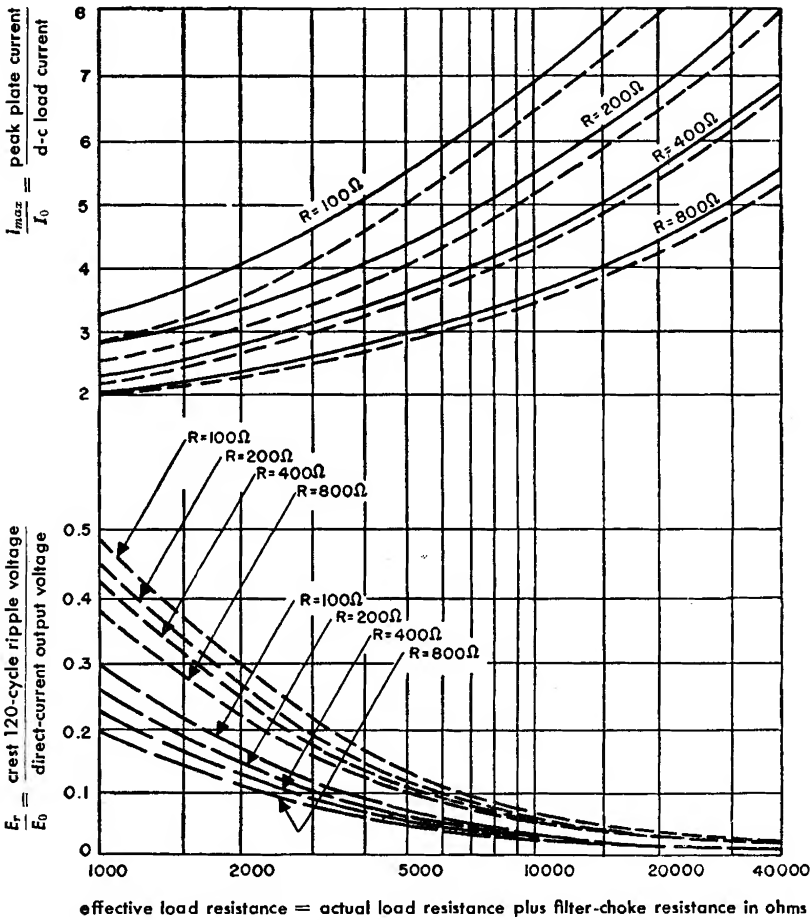

Reprinted from "Radio Engineers Handbook" by F. E. Terman, 1st ed., p. 672, 1943; by permission, McGraw-Hill Book Co., N. Y.

$R = R_s + R_T$ (see Fig. 15)

———	input capacitance = ∞
—— ——	= 8μf
— — — —	= 4μf

Fig. 17—Performance of capacitor-input filter for 60-cycle full-wave rectifier, assuming negligible leakage-inductance effect.

Surge suppression and contact protection *

When the current in an inductive circuit is suddenly interrupted, the resulting surge can have several undesirable effects:

a. Contact arcing, producing deterioration that eventually results in circuit failure due to mechanical locking or snagging, or to high contact resistance.

b. High-voltage transients resulting in insulation breakdown.

c. Wide-band electrical interference.

One method of suppressing surges is to shunt a selenium rectifier across the inductor as shown in Figs. 18 and 19.

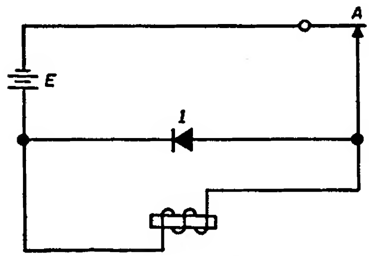

Fig. 18—Conventional method of using the selenium rectifier as a spark suppressor.

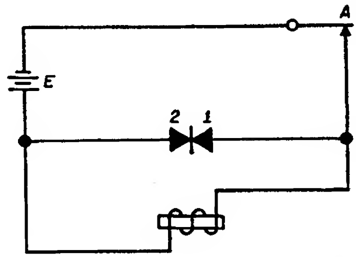

Fig. 19—Method of improving the release time by adding a second rectifier.

The rectifier in Fig. 18 appreciably lengthens the release time (as when the electromagnet is a relay coil). By connecting the rectifier across the contact *A* instead of across the coil, a release time only slightly lengthened is secured. This, however, is usually a less desirable connection, especially when there are several contacts controlling the same coil. Also, when contact *A* is open, a small reverse current flows, of the order of 0.5 milliampere. The system of Fig. 18 is applicable to direct-current circuits only.

The system of Fig. 19 gives good protection with only a small lengthening of the release time over that when no protection is used. It is applicable to both alternating and direct-current circuits. When contact *A* is closed, rectifier 1 blocks current flow from the battery. Upon opening contact *A*, the reverse-resistance characteristic of rectifier 2 comes into play. It is high at low voltages and decreases as the voltage is increased. The voltage rise due to the inductive surge is thus limited to a value insufficient to

* H. F. Herbig and J. D. Winters, "Investigation of the Selenium Rectifier for Contact Protection," *Transactions of the American Institute of Electrical Engineers*, vol. 70, part 2, pp. 1919–1923; 1951: Also, *Electrical Communication*, vol. 30, pp. 96–105; June, 1953.

Surge suppression and contact protection *continued*

cause arcing at the contact. However, the inductor is not immediately short-circuited, so the current decays rapidly.

Typical performance data are shown in Fig. 20. For comparison, data are included for cases where a capacitor with series resistor is shunted across the coil; also for a silicon-carbide varistor in place of the rectifier shown in Fig. 18.

Fig. 20—Peak voltages and release times for electromagnets with different contact protections.*

	telephone clutch magnet $L = 0.485$ henry $R = 164$ ohms $I = 0.293$ ampere		telephone relay $L = 3.45$ henries $R = 1650$ ohms $I = 0.029$ ampere	
contact protection	release time in milli-seconds	peak voltage at contact	release time in milli-seconds	peak voltage at contact
Three 9/32-inch-diameter cells (Figure 18)	4.0	83	55.0	57
Two 9/32-inch-diameter cells (Figure 19)†	1.3	180	12.0	150
Three 1-inch square cells (Figure 19)†	1.3	192	10.9	169
Silicon-carbide varistor	1.3	210	12.8	140
0.5 microfarad + 510 ohms	—	arcing	10.9	160
0.1 microfarad + 510 ohms	—	arcing	7.9	259
Unprotected	1.0	400 to 900	7.6	450 to 750

* Courtesy of *Transactions of the AIEE.*
† For each rectifier, 1 and 2.

■ Magnetic amplifiers

Elementary theory

The simple magnetic amplifiers of Figs. 1A and 1B consist of an iron-core reactor T with windings 1–2 and 3–4, an inductor L, and a load resistor R_l. E_p is the power supply, which must be an alternating voltage; $E_{c,dc}$ is the control voltage; $I_{c,dc}$ is the control current; and I_l is the load current. In Fig. 1B, rectifier RE permits unidirectional I_l to flow only during half-cycles of E_p. The practical magnetic amplifier of Fig. 1C uses two separate reactors T_1 and T_2 to secure fullwave I_l. The intermittent flow of I_l induces voltages in the control windings and the inductor restricts flow of resulting alternating current in the control circuit. Amplification occurs because relatively small variations in $E_{c,dc}$ or $I_{c,dc}$ cause larger changes of E_l or I_l.

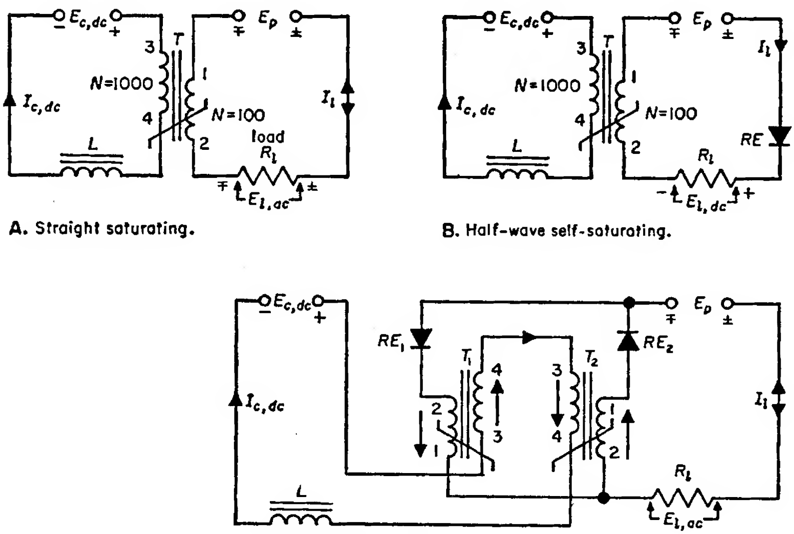

A. Straight saturating.

B. Half-wave self-saturating.

C. Full-wave self-saturating.

Fig. 1—Simple magnetic-amplifier circuits. In *A* and *B*, symbol *N* = number of turns on the reactors. In the circuits, arrows and ± signs indicate instantaneous directions.

Referring to Fig. 1A, when $E_{c,dc}$ is zero, the inductive impedance of winding 1–2 is much greater than R_l and most of E_p appears across 1–2. When $E_{c,dc}$ increases until $I_{c,dc}$ magnetically saturates the core, no further change of flux can occur. Since an inductive voltage drop occurs only where there is change in flux, only a small voltage drop then occurs across the resistance of 1–2 and practically all of E_p appears across R_l.

Elementary theory *continued*

In Fig. 1B, assume $E_{c,dc}$ to be zero and assume the core material of T to have a hysteresis loop similar to Fig. 2A. During part of each positive half-cycle of E_p, current flows in 1–2 and the flux density in T rises to $+B_{max}$. Winding 1–2 now offers only a low impedance and I_l is limited only by R_l. During the negative half-cycle, the flux density returns to $+B_r$.

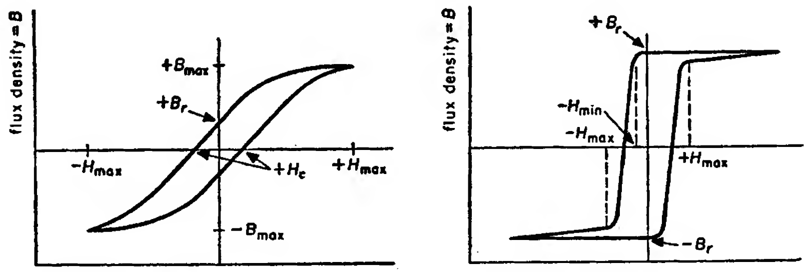

A. Conventional core material.

B. Magnetic-amplifier core.

Fig. 2—Hysteresis loops for magnetic core materials.

If now some value of $E_{c,dc}$ is applied in Fig. 1B, resulting in sufficient ampere–turns to produce $+H_{max}$, the core becomes saturated. During negative half-cycles, current in 1–2 is blocked by *RE* and the iron remains saturated. Thus, no change in flux can occur and winding 1–2 absorbs only a small voltage due to its resistance. Maximum possible I_l flows through R_l.

If $I_{c,dc}$ is in the direction of and of a magnitude corresponding to $-H_{max}$ while the flow of I_l in 1–2 during positive half-cycles is sufficient to overcome this and to saturate the core in the opposite direction, then flux density varies from $-B_{max}$ to $+B_{max}$. Then maximum voltage drop occurs across T and minimum current flows through R_l.

The ampere–turns needed for control depend on the B–H characteristic of the iron, assuming an ideal rectifier. Smaller H_{max} values require less control current. H_{max} is usually made as small as possible by employing gapless toroidal cores wound of thin tape made from high-nickel-content alloys or from grain-oriented steels. Hysteresis loops of such cores have quasirectangular shapes as in Fig. 2B. In reactors using these materials, maximum I_l will flow even when $E_{c,dc}$ is zero. To secure control, $I_{c,dc}$ must produce magnetizing forces between $-H_{min}$ and $-H_{max}$. In practice, rectifier *RE* has some reverse leakage and an increase in the ideal control current is needed to overcome this.

Elementary theory *continued*

When $I_{c,dc}$ is such that it produces a magnetizing force in the control range between $-H_{max}$ and $-H_{min}$ in Fig. 2B, a rapid transition of the magnetic state of the iron from partial desaturation to saturation occurs during each positive half-cycle of E_p. The reactor ceases to provide counter-electromotive force very suddenly, since the change in flux stops abruptly as B_{max} is reached. At this instant, the full voltage and current appear on the load and continue for the remaining portion of the half-cycle. The action is similar to that of a thyratron tube. The time at which the transition occurs is called the firing point or firing angle and is expressed in degrees of a cycle. The firing point depends upon $I_{c,dc}$.

In straight saturating amplifiers, illustrated in their simplest form by Fig. 1A, the ampere–turns of the control winding must be equal to the ampere–turns of the output winding. Such amplifiers act as constant-current generators and the voltage across the load depends on its impedance. Output current is controlled by $I_{c,dc}$.

The more-common self-saturating amplifiers, illustrated by Figs. 1B and 1C act as constant-voltage generators. Voltage across the load is virtually independent of load impedance. Output voltage is controlled by $I_{c,dc}$.

Control curves

A typical curve of output load voltage E_l against signal current $I_{c,dc}$ for a self-saturating magnetic amplifier using nickel-alloy cores is shown in Fig. 3A. The solid curve is for an amplifier with ideal rectifiers while the

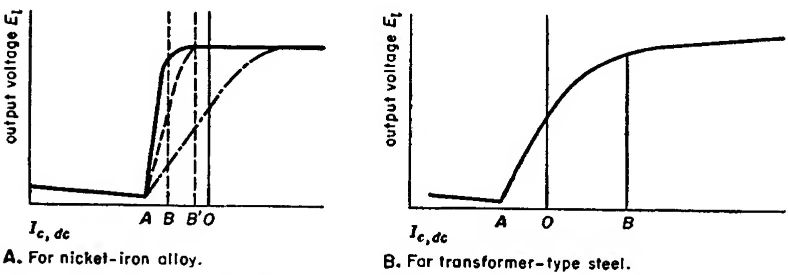

Fig. 3—Typical control curves for different core materials.

dashed curves are for practical amplifiers using rectifiers having appreciable leakage.

Control generally occurs when $I_{c,dc}$ has a value between AO and BO on this curve. The difference AB should be as small as possible for maximum

Control curves *continued*

sensitivity. Values of *OB* and *AB* for typical cores are listed in Fig. 4. The values are nearly independent of core dimensions for toroidal cores smaller than 2 to 3 inches outside diameter.

To obtain control in the region *AB*, the relative directions of the magnetizing forces due to the control and load windings must be as indicated by the arrows in Fig. 1C.

To the left of point *A*, the control curve for amplifiers operating at low frequencies, such as 60 cycles/second, slopes slightly upward as shown in Fig. 3. At higher frequencies such as 400 cycles/second, there is a greater upward slope to the left.

Fig. 4—Characteristics of cores for magnetic amplifiers. For toroidal cores up to 3 inches outside diameter for groups *A* and *B* and up to 2 inches for groups *C* and *D* materials.*

control range and flux	group *A* Hypersil Magnesil Silectron	group *B* Deltamax Hipernik V Orthonic Orthonol Permeron	group *C* HY-MU-80 4-79 Mo Permalloy Squaremu	group *D* Supermalloy
OB (bias) in milliampere–turns (Fig. 3A)	1,000 to 2,500	500 to 1,500	100 to 150	50 to 80
AB (signal) in milliampere–turns (Fig. 3A)	750 to 1,500	500 to 1,000	80 to 200	50 to 80
Saturation flux density in gausses	18,000 to 20,000	13,500 to 15,500	7,000 to 8,000	6,800 to 7,800

* See pp. 276-277 for other similar materials.

To the right of point *A*, the voltage across the load is practically independent of load impedance and is determined by signal ampere–turns and the core material. It is generally not desirable to operate self-saturating amplifiers in the region to the left of point *A*, since their characteristics then become similar to straight saturating amplifiers, i.e., ampere–turns of the output winding approximates the ampere–turns of the control winding on this portion of the curve.

Fig. 3B is a typical control curve for a magnetic amplifier using cores of grain-oriented or transformer-grade steel laminations. When using reactors of transformer steel, rectifier leakage usually may be disregarded. In large magnetic-amplifier cores including gaps, *AB* is about 5 ampere–turns/inch of magnetic path for grain-oriented steels and up to 10 ampere–turns/inch for lower grades of transformer steel.

Bias winding

When the control curve of the magnetic amplifier is similar to the full line of Fig. 3A, energy required from the control source can be reduced by biasing the amplifier to point *B*. The full signal can then be used to produce changes in $I_{c,dc}$ from point *B* to point *A* in the control region. A separate direct-current bias winding capable of producing the *OB* ampere–turns (listed in Fig. 4 for small cores) is used for this purpose.

Due to rectifier leakage or due to the shape of the hysteresis loop of the core material, point *B* may fall on the zero axis or to the right of zero as shown by the lower dashed line in Fig. 3A. In such cases, the bias winding may be omitted, or it may be retained if available $I_{c,dc}$ or $E_{c,dc}$ does not have the magnitude and polarity needed for operation at the desired initial point on the hysteresis loop.

Control inductor

Referring to Fig. 1C, while one core is firing, the other is desaturating due to the action of the control current. The voltages induced in the control windings by these two actions oppose each other. Theoretically, the voltages would be equal and opposite if the signal source had zero impedance and the cores and rectifiers were perfectly matched. In practice, the net voltage induced in the control windings is a function of the impedance of the signal source, of the control point at which the amplifier is operating, and of the mismatch of cores and rectifiers.

For design purposes, it may be assumed that the maximum total induced voltage will not exceed the voltage that would be induced in one core alone. The frequency of this voltage is equal to the power-supply frequency for half-wave amplifiers like Fig. 1B and to twice the power-supply frequency for full-wave amplifiers like Fig. 1C and Fig. 5.

It is good practice to put an inductor *L* in series with the control winding. If this choke is omitted, additional control ampere–turns may be required to offset alternating current circulating in the control circuit.

Direct-current loads

The circuits of Figs. 5A, B, or C may be used for direct-current loads. If $E_{l,dc}$ is the required voltage across the load, the required E_p will depend partially on the forward voltage drop through the rectifiers. Power-supply voltage may be approximated for design purposes as in Fig. 6.

Direct-current loads *continued*

The peak inverse voltage across the rectifiers is also given in Fig. 6. The lower reverse leakage of Fig. 5C permits higher gains with this circuit, but the speed of response of Fig. 5C is less than that of Fig. 5A.

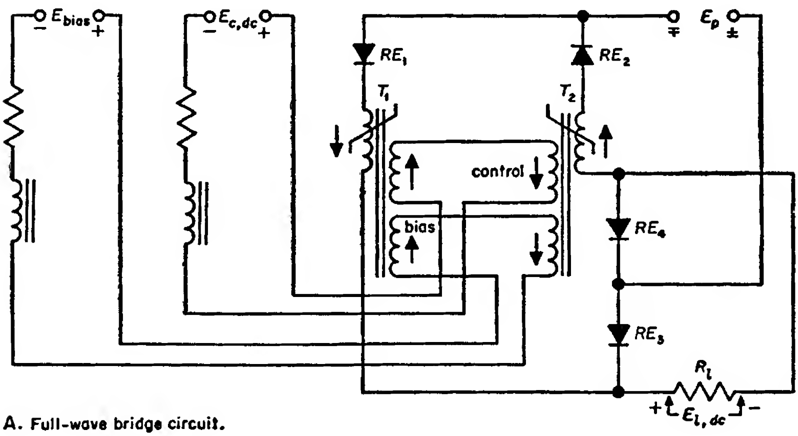

A. Full-wave bridge circuit.

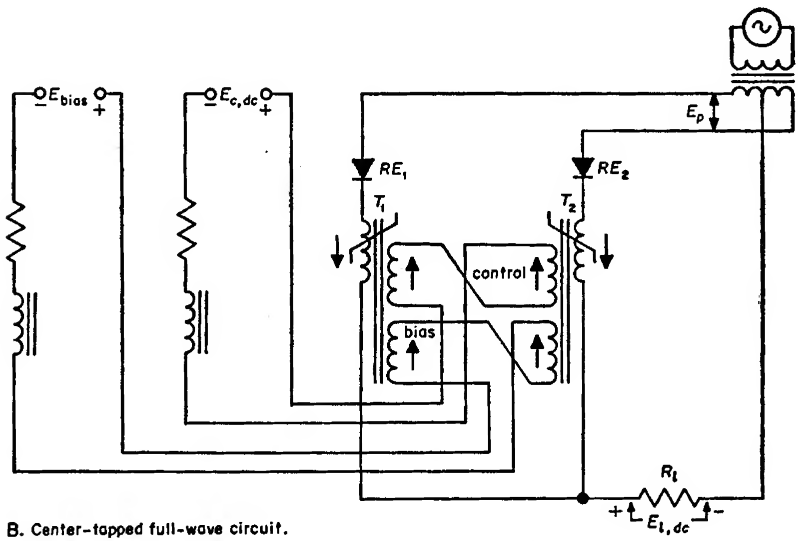

B. Center-tapped full-wave circuit.

Fig. 5—Practical magnetic-amplifier circuits for direct-current output. Polarity of $E_{c,dc}$ depends on value of I_{bias}.

Direct-current loads *continued*

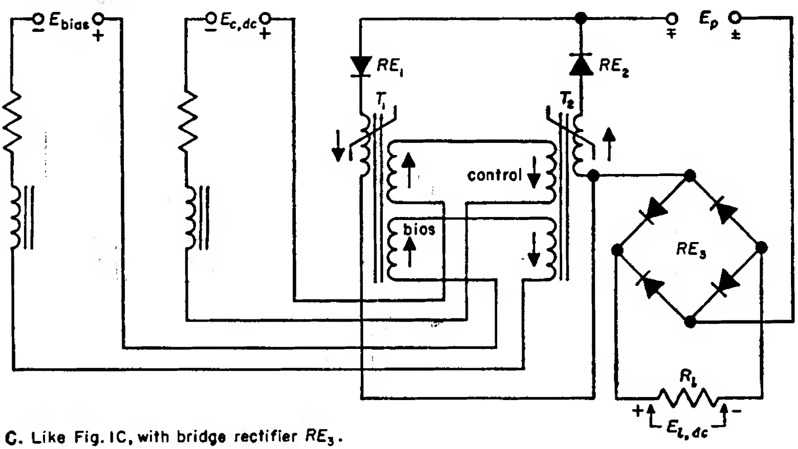

C. Like Fig. 1C, with bridge rectifier RE_3.

Fig. 5—*Continued.*

Fig. 6—Required supply voltage and inverse rectifier voltage for circuits of Fig. 5.

circuit, Fig. 5	E_p using selenium rectifiers	E_p using germanium or silicon diodes	peak inverse voltage across rectifiers $RE_{1,2}$
A	1.6 $E_{l,dc}$	1.4 $E_{l,dc}$	1.4 E_p
B	3.2 $E_{l,dc}$	2.9 $E_{l,dc}$	1.4 E_p
C	1.7 $E_{l,dc}$	1.6 $E_{l,dc}$	0.5 E_p

Fig. 7 is a 3-phase amplifier with direct-current output. Six separate reactors are used. The bias windings have been omitted in the figure. This circuit may produce ripple $E_{l,ac}$ across the load as high as 0.3 $E_{l,dc}$. Frequency of the induced voltage across inductor L is 6 times the supply frequency. Output turns required on each reactor can be calculated by assuming a voltage across the reactor of $E_p/(3)^{1/2}$. Control ampere–turns required in a 3-phase amplifier are higher than in a single-phase amplifier partly because the inverse voltage across the rectifiers is higher for a longer portion of each cycle and the effect of rectifier leakage is thus more pronounced. The control curve of the Fig. 7 amplifier with selenium rectifiers is similar to that of Fig. 3B. Using cores of group-B materials Fig. 4, AO would be approximately 2 to 3 ampere–turns and OB would be between 1 and 7 ampere–turns.

Direct-current loads *continued*

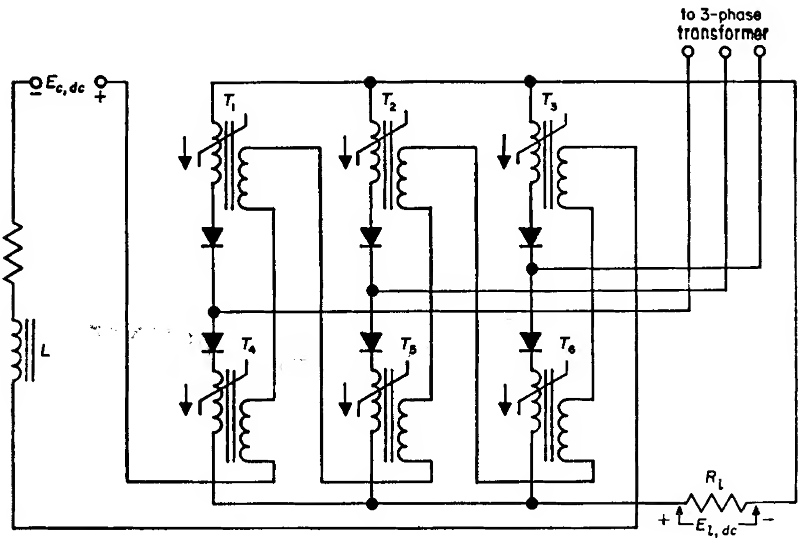

Fig. 7—Three-phase bridge magnetic amplifier.

Two-stage amplifiers

Fig. 8 shows a two-stage amplifier with direct-current output. This circuit is useful where small control signals are available and high outputs are required. Cores of the first stage may be made of materials listed under

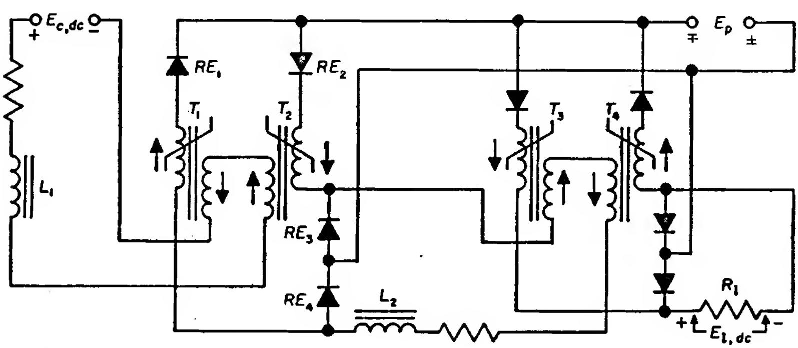

Fig. 8—Two-stage magnetic amplifier. The bias circuit is omitted for simplicity.

Two-stage amplifiers *continued*

groups C or D in Fig. 4, while cores of the second stage are generally of group-A or -B materials. Inductor L_2 has the same function as L_1 and, in addition, it prevents alternating currents induced in control windings of the second stage from flowing through rectifiers RE_1 to RE_4, thereby causing unwanted direct currents in the control windings of the second stage and the output windings of the first stage.

Fig. 9 is a push-pull amplifier driving a single stage. If well designed and if the preamplifier push-pull stage uses group-D core material, the power stage can be driven to full output with the application of 10 milliampere–turns of signal at the preamplifier. In this balanced circuit, $E_{c,dc}$ may assume either polarity.

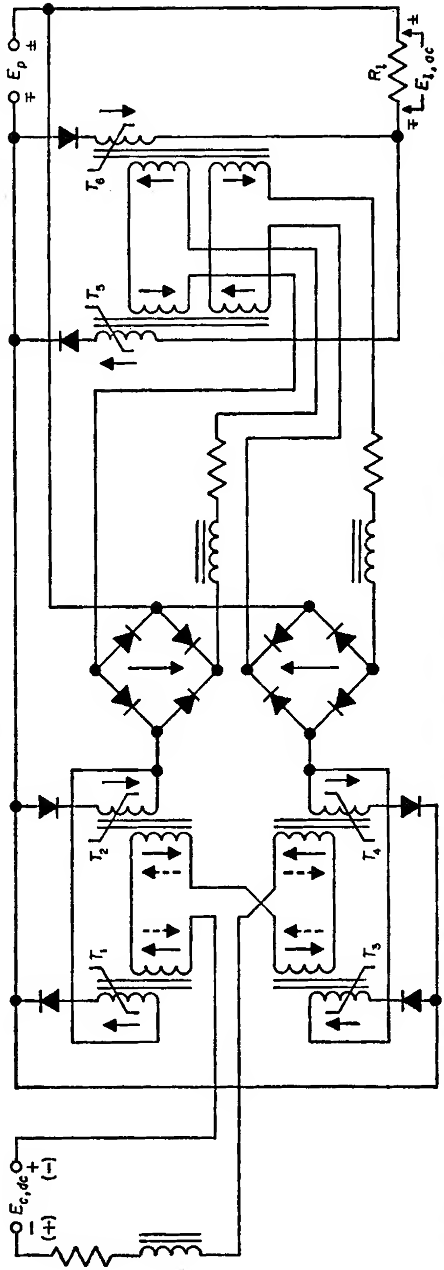

Fig. 9—Push-pull magnetic amplifier driving a single-stage magnetic amplifier. The bias circuits are not shown.

AC control signal

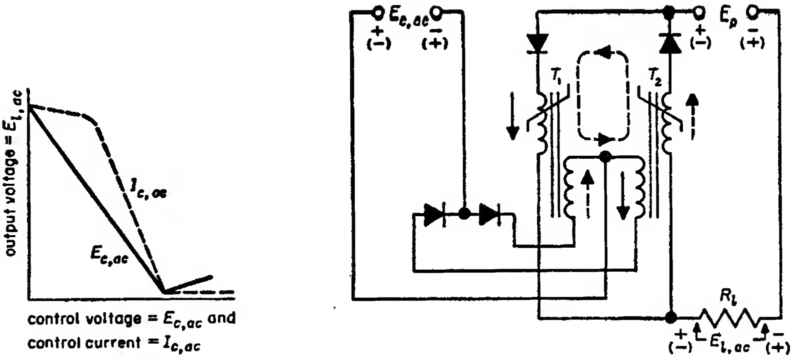

Fig. 10—Magnetic amplifier controlled by alternating-current signal. The operating characteristic of the circuit is also given.

Fig. 10 is the basic circuit of a magnetic amplifier controlled by an alternating-current signal. Control and supply voltages are of the same frequency and their phase relationship must be as shown in the figure. The + and − signs indicate relative instantaneous polarities of the two waves.

The relationship between the output voltage $E_{l,ac}$, control voltage $E_{c,ac}$, and control current $I_{c,ac}$ is shown in Fig. 10. With no voltage applied to the control winding, the amplifier operates at maximum output. When a signal is applied, the output is reduced as indicated.

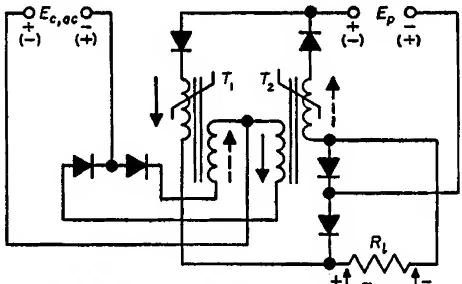

A. Bridge rectification of output.

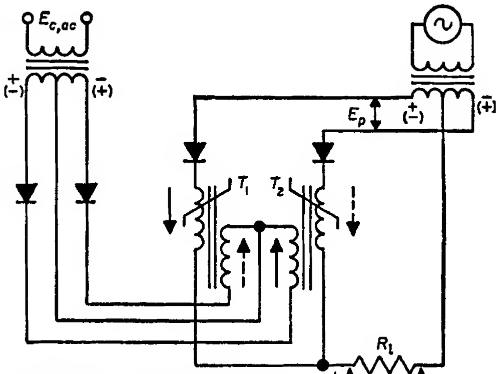

B. Center-tap rectification of output.

Fig. 11—Amplifiers with alternating-current control and direct-current output are shown at the right.

AC control signal *continued*

The basic circuit of Fig. 10 can be modified for direct-current output as shown in Figs. 11A and B. The response times τ of the three amplifiers are: For Fig. 10, $1 \leqslant \tau \leqslant 4$ cycles, for Fig. 11A, $0.5 \leqslant \tau \leqslant 2$ cycles, and for Fig. 11B, $0.5 \leqslant \tau \leqslant 1$ cycle.

The poor response time of Fig. 10 is due to circulating currents that may occur in the reactors-and-rectifiers circuit indicated by the dashed oval. Any circulating currents in Figs. 11A and B must flow through the load impedance and they are thus minimized.

Combination transistor–magnetic amplifiers

To control a magnetic amplifier with an alternating-current signal, the signal must be strong enough to change the flux of the core completely during a half-cycle of the power-supply voltage. When the available signal is too small, a transistor preamplifier may be used.

Figs. 12 and 13 show two methods of coupling transistors to magnetic amplifiers. Instead of the single-stage transistor amplifiers shown, there may be several transistor stages in cascade.

In Fig. 12, an $E_{c,ac}$ of power-line frequency is impressed on a single-ended transistor circuit. The transistor is biased on the emitter electrode to act as a class-A amplifier and its output is coupled to the magnetic amplifier by the inductor L and capacitor C. The control signal of the magnetic amplifier is then the amplified version of the $E_{c,ac}$ signal received by the transistor.

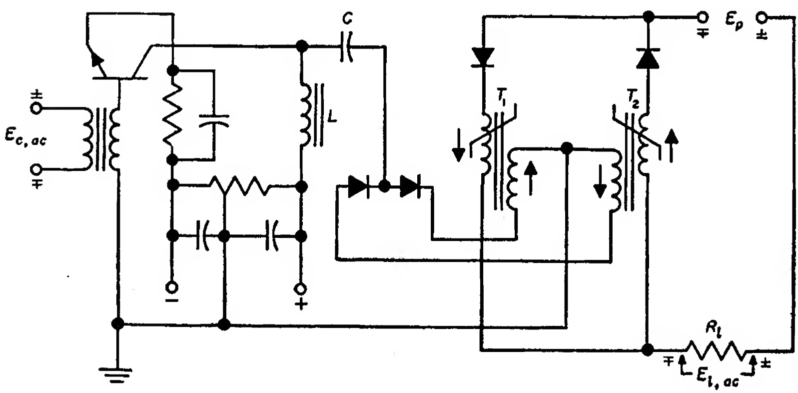

Fig. 12—Transistor coupled to alternating-current-controlled magnetic amplifier.

Combination transistor-magnetic amplifiers *continued*

Output of the magnetic amplifier is dependent on phase and amplitude of the output of the transistor and thus of the initial signal.

In Fig. 13, the transistor stage has a push-pull output that feeds a double-ended diode phase discriminator (demodulator). Alternatively, conventional ring demodulators or transistor demodulators* might be used to secure control direct current for this type of magnetic amplifier. Output of the magnetic amplifier will depend on both the phase and amplitude of the initial signal.

When very-low-level direct-current signals have to be used, a mechanical vibrator or diode chopper or transistor chopper† may be employed to convert the direct into alternating current. The resulting $E_{c,ac}$ is passed through a transistor stage to drive the magnetic amplifier.

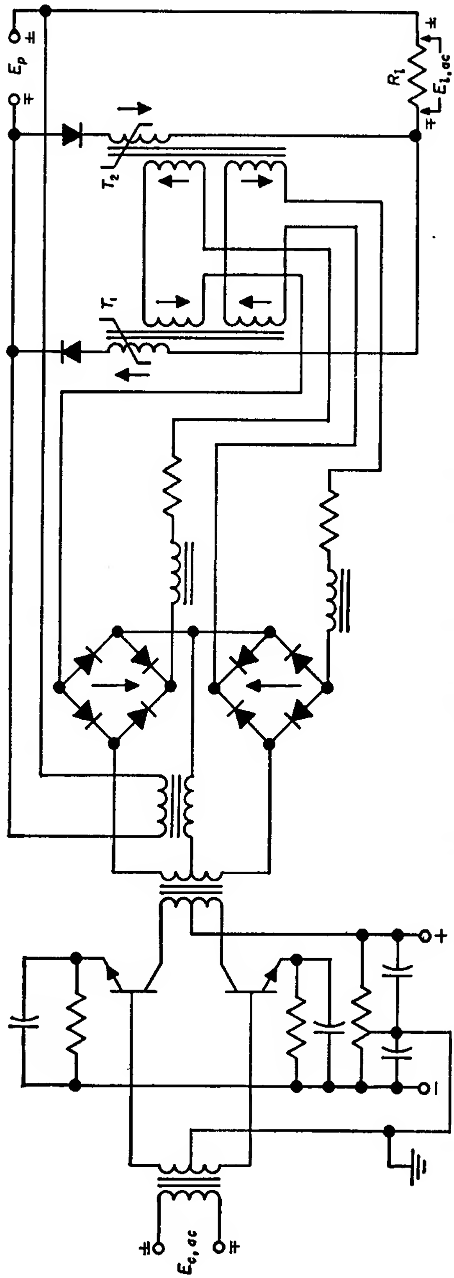

Fig. 13—Push-pull transistors coupled to direct-current-controlled magnetic amplifier. The bias circuit is not shown.

*R. O. Decker, "Transistor Demodulator for High-Performance Magnetic Amplifiers in A-C Servo Applications," *Communication and Electronics*, no. 17, pp. 121–123; March, 1955.

† A. P. Kruper, "Switching Transistors Used as a Substitute for Mechanical Low-Level Choppers," *Communication and Electronics*, no. 17, pp. 141–144; March, 1955.

Feedback

Control curves of standard magnetic amplifiers as shown in Fig. 3 are generally not linear. If a linear relationship between signal current and load current or voltage is desired, negative feedback must be used. Fig. 14 shows typical feedback circuits. It is desirable to use an inductor in series with the feedback winding as indicated.

Note that the direction of I_c has been reversed; since the feedback has a polarity such that it tends to reduce the output.

To illustrate the design of a feedback circuit, assume that the control curve of an amplifier without feedback is shown by the solid curve of Fig. 3A and that 1 ampere–turn of control current is needed for full output. Further, assume that the maximum departure of this control curve from a straight line is 0.5 ampere–turn while the desired linearity should be better than 10 percent. The intrinsic nonlinearity cannot be changed since it is dependent principally on the core material. However, if control ampere–turns can be increased to 5 while keeping the nonlinearity at 0.5 ampere–turn, the desired result will be achieved. The feedback winding in this case would be designed to produce 5 ampere–turns in the negative direction when the amplifier gives full output. Since these negative ampere–turns must be counteracted by

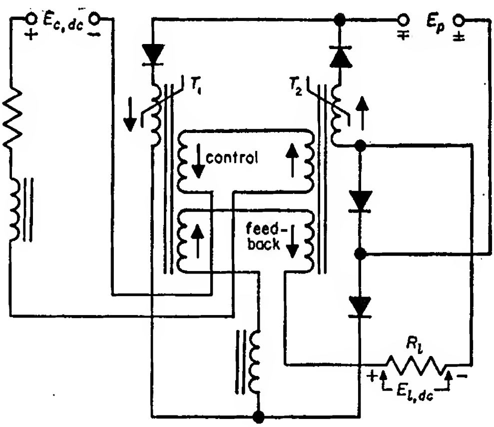

A. Current feedback.

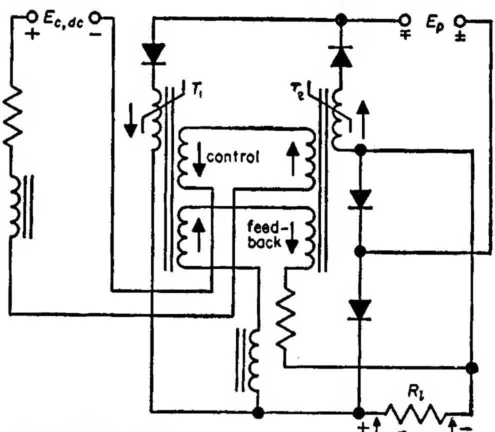

B. Voltage feedback.

Fig. 14—Circuits employing negative feedback for improving linearity of control curve.

Feedback *continued*

the control current, a signal of approximately 5 ampere-turns is now required for full output.

Volts per turn

Voltage/turn of winding is a function of B_{max} and the cross-sectional area of the core. It may be expressed as follows for toroidal cores:

$$\text{Millivolts/turn} = (D_o - D_i)\, H\, K_1\, K_2$$
$$= 2\, A_i\, K_1\, K_2$$
$$= 0.4\, A_c\, K_1\, K_2$$

where

A_c = cross-sectional area* of core in centimeters^2

A_i = cross-sectional area of core in inches^2

* In the equations there is an apparent discrepancy between areas in square inches and square centimeters. Cross-sectional areas in square inches are $[(D_o - D_i)/2] \times H$. The housing is excluded but the space occupied by insulating coatings between turns of the iron tape is included in square-inch areas. Cross-sectional areas in square centimeters are actual net iron areas and include a stacking factor of approximately 80 percent. This different method of computing square inches and square centimeters is followed in most commercial catalogs of cores.

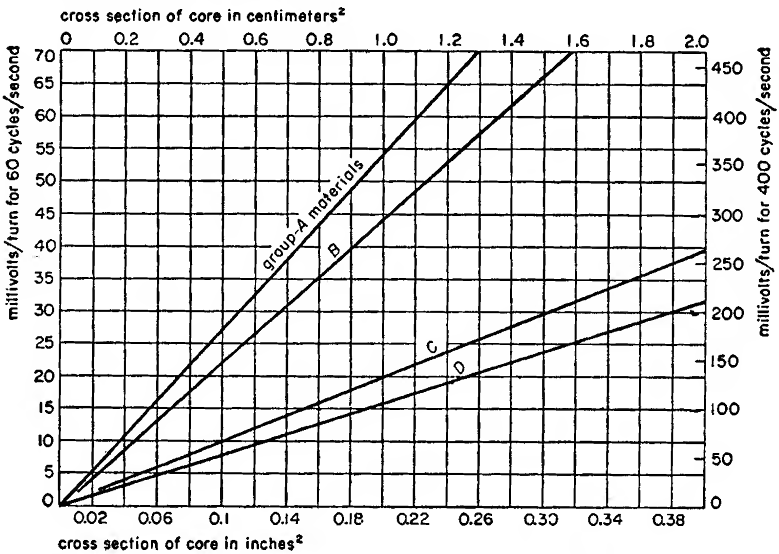

Fig. 15—Approximate induced voltage/winding-turn for toroidal cores.

Volts per turn *continued*

D_i = inside diameter in inches of core having a rectangular section

D_o = outside diameter in inches of core having a rectangular section

H = height in inches of core having a rectangular section

K_1 = 136 for group-*A* core materials (Fig. 4)

= 111 for group-*B* core materials (Fig. 4)

= 50 for group-C core materials (Fig. 4)

= 40 for group-*D* core materials (Fig. 4)

K_2 = 1.0 for 60 cycles/second

= 6.7 for 400 cycles/second

The relationships are plotted in Fig. 15.

Design procedure

The following pertains to a single-stage full-wave self-saturating magnetic amplifier using toroidal cores in circuits similar to Fig. 1C for alternating-current output or to Fig. 5A for direct-current output. The same procedures can be used to design each part of more-complex circuits.

a. Choose a supply voltage approximately 1.2 $E_{l,ac}$ or from 1.4 to 1.6 $E_{l,dc}$ see "Direct-current loads" above.

If there is any choice of frequency, choose the highest available power-supply frequency.

b. Make a preliminary selection of core material. If P_c is the power available from the signal source, materials listed in Fig. 4 may be chosen for toroidal cores as follows:

For $P_c >$ 100 milliwatts, use group-*A* materials
For 100 milliwatts $> P_c >$ 1 milliwatt, use group-*B* materials
For 1 milliwatt $> P_c >$ 0.01 milliwatt, use group-C materials
For 0.01 milliwatt $> P_c$ use group-*D* materials

The choice will depend to some extent on the required response time. For

Design procedure *continued*

equal gains and outputs, the response time becomes progressively shorter from group-*A* to group-*D* materials.

c. Determine the P_l that the load will absorb and the power range over which the load will have to be controlled. Use these data to make a preliminary choice of core size. The following empirical relationship is an aid to choice.

$$D_i^2 \times A_i \approx \frac{0.5 \times P_l \times 10^5}{B_{max} \times f}$$

where

D_i = inside diameter of toroidal core in inches

A_i = cross-sectional area of core in inches²

P_l = load in watts

B_{max} = saturation flux density in gausses (Fig. 4)

f = supply frequency in cycles/second

Another aid is the fact that a core with $D_i = 2$ inches, $D_o = 2.5$ inches, and $H = 0.5$ inch, of group-*B* material, is good for 8-watts output at 60 cycles/second. Output is approximately proportional to volume of the core, to frequency, and to B_{max}.

These relationships are rough guides only and final selection may be a core differing by a factor of as much as 2 or 3 from these rules. If the designer has experience with amplifiers somewhat similar to the one to be designed, it is preferable to rely on the experience rather than on these empirical rules in selecting core sizes.

d. Toroidal cores for magnetic amplifiers are a commercial product. If ready-made cores are to be used, consult manufacturers catalogs and choose a core with parameters close to those estimated in (*b*) and (*c*). Most commercial cores have molded housings. Note the inside diameter and clear inside area of the housing.

e. From the table on p. 51 select a wire size for the output winding on the basis of 1 circular mil/milliampere. In full-wave circuits, take the root-mean-square current in the output winding of each reactor as 0.707 × (average I_l).

Design procedure *continued*

f. Determine millivolts/turn from Fig. 15 and calculate the number of output turns. Increase the calculated turns by 10 percent for safety.

g. From the tables on p. 114 and p. 278, calculate cross-sectional area of output winding. Increase this area by 75 percent to provide for control and bias windings, insulation, winding clearances, etc. To the estimated area of all windings, add the clearance hole for the shuttle of the winding machine. (Shuttle rings vary in thickness from 1/4 inch for small cores with small wire to 1 inch for the larger core and wire sizes.)

The total required area obtained in this way should be checked against the clear inside area of the core. If there is not sufficient space, select another core.

h. Select rectifiers on the basis of load current, forward voltage drop, reverse leakage, and mechanical mounting arrangements.

i. Rectifier reverse leakage current in percent of I_l may be estimated as follows:

0.25 to 1.0 percent for selenium rectifiers operating at their full rated inverse voltage (26 to 36 volts/plate, depending on type of plate).

0.10 to 0.25 percent for selenium rectifiers with extra plates or at reduced voltage so that inverse voltage does not exceed 10 to 15 volts/plate.

0.1 to 0.5 percent for germanium diodes, depending on type and inverse voltage.

0.01 to 0.10 percent for silicon diodes.

j. Calculate leakage ampere–turns due to the output winding by multiplying the leakage current of (i) by the turns of (f). From Fig. 4, obtain the control ampere–turns *AB* required on the assumption of perfect rectifiers. Add the two figures to obtain total control ampere–turns required (*AB* in Fig. 3).

k. Knowing the $I_{c,dc}$ that the signal source is capable of supplying, calculate the turns on the control winding and select the wire size.

l. Calculate the resistance of the control winding and check that the signal source can produce the required control current through both reactors in series. If not, select a core requiring less control ampere–turns or secure rectifiers of lower leakage.

m. Design the bias winding. It should be capable of at least the *OB* ampere–turns shown in Fig. 4. Number of turns will depend on the current that the bias source is capable of delivering.

Design procedure *continued*

n. Calculate the voltages induced in the control and bias windings by multiplying the number of turns of the respective windings by the volts/turn of Fig. 15.

o. Calculate the maximum alternating-current component to be permitted in the control and bias circuits as 30 percent of the respective direct currents.

p. On the assumption that control and bias sources and windings offer negligible impedance to the induced voltage, compute the inductance of chokes to be used in series with the signal and bias windings to limit the current to the value of (o) above when an assumed voltage of one coil per (n) above is applied at twice the supply frequency.

Sample design

An $E_{l,dc}$ is to be controlled from zero to 18 volts with an $I_{l,dc}$ between 0 and 30 milliamperes. The available $E_{c,dc}$ varies from zero to 0.25 volt at zero to 400 microamperes. Power supply of 60 cycles/second is available.

A circuit similar to Fig. 5A is chosen and E_p of $1.4 \times 18 = 25$ volts is assumed. Maximum available P_c is 0.1 milliwatt and group-C core material is selected. Cores with $D_i = 1$, $D_o = 1\frac{3}{8}$, and $H = \frac{1}{4}$ (inch) are selected from a manufacturers catalog. Iron cross-sectional area of each core is 0.047 inch. From Fig. 15, induced voltage is approximately 4.7 millivolts/turn. The catalog shows the inside diameter of the housing of these cores as 0.93 inch, which provides a winding space of 0.67 inch^2.

Effective load current in each reactor is $0.707 \times 30 = 21$ milliamperes. A suitable wire size for the output winding is 37 AWG with a copper cross-section of 19.8 circular mils. The output windings require $25/0.0047 = 5300$ turns.

Peak inverse voltage across the rectifiers is $1.4 \times 25 = 35$ and forward current is 21 milliamperes/rectifier. Germanium diodes type *1N54* are specified for the rectifiers. Reverse leakage current is estimated at approximately (0.1 percent) $\times$ (21 milliamperes) $\approx$ 20 microamperes.

Leakage ampere–turns $= 20 \times 10^{-6} \times 5300 \approx 100$ milliampere–turns.

Fig. 4 indicates that the reactor can be controlled with about 140 milliampere–turns. Control windings of $100 + 140 = 240$ milliampere–turns are therefore required. Since 400 microamperes are available from the source, 600 turns are needed on each control winding.

Sample design *continued*

Estimating $1\frac{1}{2}$ inches of wire/turn, total length of each control winding is 75 feet. Permissible resistance of the control winding on each reactor is $(0.5) \times (0.25/400) \times 10^{-6} = 310$ ohms. Since 75 feet of 37 AWG wire has a resistance of only 39 ohms, this size may be used for both control and output windings.

The leakage of 100 milliampere–turns is about the same as the value *OB* for group-C cores shown in Fig. 4. Therefore, a bias winding will be omitted. (If a bias winding were used, 150 turns with a current of 1 milliampere would be sufficient.)

Using 37 AWG wire for both windings, we have 5900 turns on each core. Double-formvar-insulated 37 AWG wire has a diameter 0.0054 inch and a space factor of 0.87 as shown on p. 278. Inside diameter 0.93 inch of the core housing will permit approximately $\pi \times 0.93 \times (0.87/0.0054) = 500$ close-wound turns on the first layer and less on the remaining layers. There will be at least 12 layers of winding having a total thickness of about $12 \times (0.0054/0.87)$, say, 0.10 inch. Area remaining for the shuttle of the winding machine is $(\pi/4)\ (0.93 - 2 \times 0.10)^2 = 0.42$ inch^2 which is sufficient.

The induced voltage in each control winding will be (600 turns) $\times$ (4.7 millivolts) = 2.8 volts. This voltage at 120 cycles/second will be applied across the inductor in series with the control supply. Permissible alternating current in the control circuit is $0.3 \times 400 = 120$ microamperes. Impedance required in the inductor is $2.8/(120 \times 10^{-6} = 23{,}500$ ohms. At 120 cycles/second, the inductor should have a reactance of 31 henries.

Calculation of response time

Speed of response τ is defined as the time necessary for a magnetic amplifier to reach 63 percent of ultimate output upon application of a step signal voltage in the control circuit. It includes the time required to change the flux in the control-circuit inductor. Response is fairly independent of the number of turns on the output windings. It depends only upon the number of turns N_c of the control winding, the type and cross-section of the core, and the voltage E_c available from the signal source.

Response time in cycles can be approximated from the following empirical formula. It yields results which may be in error by ± 50 percent.

$$\tau \approx \frac{N_c \times (\text{volts/turn})}{2E_c}$$

Volts/turn may be obtained from Fig. 15.

Calculation of response time *continued*

For example, the response time of the amplifier in the above sample design would be:

$$\tau \approx \frac{600 \times 4.7 \times 10^{-3}}{2 \times 0.25} = 6 \text{ cycles}$$

With 60-cycle/second supply, this would be 0.10 second.

Practical considerations

In amplifiers using two or more cores and rectifiers, the components should be carefully matched. If this is not done, I_c requirements may be 50-percent higher than estimated.

For high-sensitivity amplifiers with moderate output, toroidal cores should not be larger than $D_o = 2$ to 3 inches. If selenium rectifiers are used, the number of turns on the output winding should be held to a maximum of 3500 and the rectifiers should have enough plates so that inverse voltage/plate will not exceed 10 to 15 volts. If germanium diodes with high leakage resistance such as types *1N54, 1N67,* or *1N81* are used, the number of output turns may be increased to 7000.

For highest sensitivity, amplifiers should be equipped with cores of group-C or group-*D* materials listed in Fig. 4. Silicon-diode rectifiers having a reverse leakage of a few microamperes and relatively high inverse-voltage ratings should be used with such cores. The number of turns on the output winding should not exceed 10,000 in this case for 60-cycle operation or 2500 for 400-cycle operation because of intrawinding capacitance effects.

E_l/I_c of high-sensitivity amplifiers may change by from 2 to 10 percent during their lifetime. This should be anticipated in the design.

For alternating-current-controlled amplifiers, optimum design usually consists in employing as thin and narrow a core as possible because the smaller the core cross-section, the lower the required signal.

Triggering

This phenomena occurs quite often in high-performance amplifiers having very-low-leakage rectifiers. Referring to the control curve in Fig. 16A, the action is as follows: when I_c increases in the negative direction, the amplifier cuts off at point *A*; then when I_c decreases, the amplifier remains at cutoff up to point *R*, where the output suddenly shoots up to point *S*. The amplifier can be cut off again along the line *SA*. The area enclosed by *SAR* is the triggering region.

Practical considerations *continued*

Triggering may be used to advantage in certain bistable switching circuits, but it is usually undesirable. The simplest way to minimize the phenomena is to use rectifiers with more leakage or to shunt a resistor across the

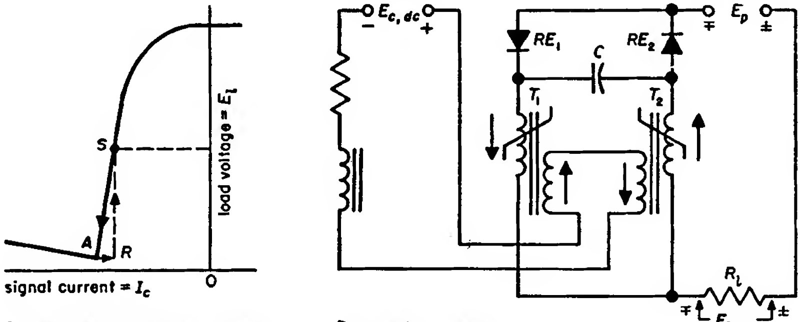

A. Characteristic showing triggering B. Capacitor *C* added

Fig. 16—The effect of triggering on magnetic amplifier output. Capacitor C across the rectifiers prevents triggering.

rectifiers, but both these cures reduce the gain of the amplifier. Triggering can be eliminated without diminishing amplifier gain by placing a capacitor C across RE_1 and RE_2 as shown in Fig. 16B. In general, the size of C cannot be predetermined. Minimum C is desirable for least response time and the value can be determined experimentally by starting with about 1 microfarad and substituting smaller values until triggering starts.

Feedback control systems

Introduction*

A feedback control system (Fig. 1) is one in which the difference between a reference input and some function of the controlled variable is used to supply an actuating error signal to the control elements and the controlled system. The amplified actuating error signal is applied in a manner tending to reduce this difference to zero. A supplemental source of power is available in such systems to provide amplification at one or more points.

The two most common types of feedback control systems are regulators and servomechanisms. Fundamentally, the systems are similar, the difference in names arising from the different natures of the types of reference inputs, the disturbances to which the control is subjected, and the number of integrating elements in the control. Thus, regulators are designed primarily to maintain the controlled variable or system output very nearly equal to a desired value in the presence of output disturbances. Generally, a regulator does not contain any integrating elements.

A servomechanism is a feedback control system in which the controlled variable is a position (or velocity). Ordinarily in a servomechanism, the reference input is the input signal of primary importance; load disturbances, while they may be present, are of secondary importance. Generally, one or more integrating elements are contained in the forward transfer function of a servomechanism.

Types of systems

The various types of feedback control systems can be described most effectively in terms of the simple closed-loop direct feedback system. Fig. 2 shows such a system. $R(s)$, $C(s)$, and $E(s)$ are the Laplace transforms of the reference input, controlled variable, and error signal, respectively.

Note: The complex variable s instead of p will be employed in this chapter to conform with the general practice in the literature on feedback control systems.

* H. Chestnut and R. W. Mayer, "Servomechanisms and Regulating System Design," John Wiley & Sons, Inc., New York, N. Y.; 1951 and 1955: vols. 1 and 2. Also, W. R. Evans, "Control System Dynamics," McGraw-Hill Book Company, Inc., New York, N. Y.; 1954. Also, J. G. Truxal, "Automatic Feedback Control System Synthesis," McGraw-Hill Book Company, Inc., New York, N. Y.; 1955. Also, H. S. Tsien, "Engineering Cybernetics," McGraw-Hill Book Company, Inc., New York, N. Y.; 1954.

For a typical linear system, $G(s)$ might appear as

$$\frac{C(s)}{E(s)} = G(s) = \frac{K(T_1s+1)\ (T_3s+1)}{s^n(T_2s+1)\ (T_4s+1)}$$

The value of the exponent n, an integer, designates the type of the system. This in turn reveals the nature of the steady-state performance of the system as outlined below.

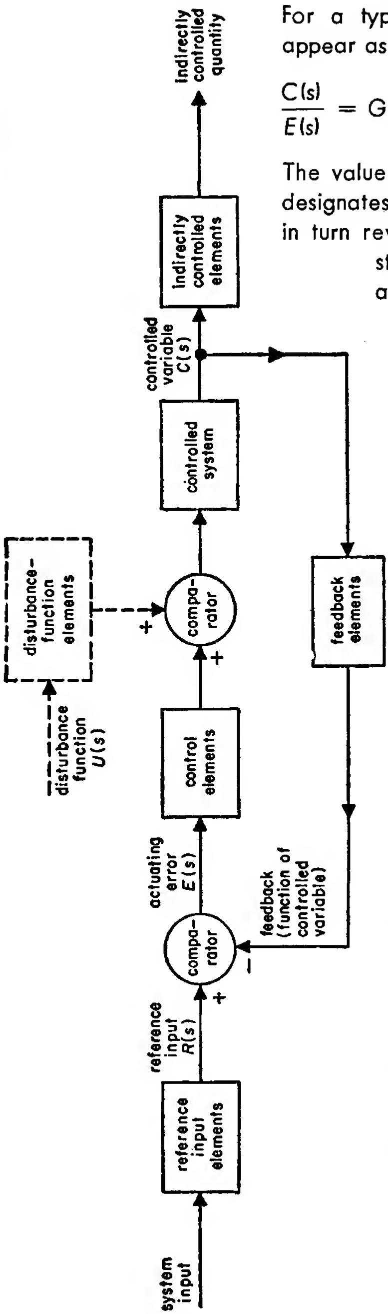

Fig. 1—Block diagram of feedback control system.

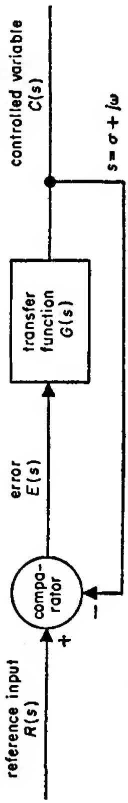

Fig. 2—Single-loop system.

Types of systems *continued*

Type-0 system: A constant value of the controlled variable requires a constant error signal under steady-state conditions. A feedback control system of this type is generally referred to as a regulator system.

Type-1 system: A constant rate of change of the controlled variable requires a constant error signal under steady-state conditions. A type-1 feedback control system is generally referred to as a servomechanism system. For reference inputs that change with time at a constant rate, a constant error is required to produce the same steady-state rate of the controlled variable. When applied to position control, type-1 systems may also be referred to as a "zero-displacement-error" system. Under steady-state conditions, it is possible for the reference signal to have any desired constant position or displacement and the feedback signal or controlled variable to have the same displacement.

Type-2 system: A constant acceleration of the controlled variable requires a constant error under steady-state conditions for a type-2 system. Since these systems can maintain a constant value of controlled variable and a constant controlled variable speed with no actuating error, they are sometimes referred to as "zero-velocity-error" systems.

Stability of systems

A linear control system is unstable when its response to any aperiodic, bounded signal increases without bound. Mathematically, instability may be investigated by analysis of the closed-loop response of the system shown in Fig. 2.

$$\frac{C}{R}(s) = \frac{G(s)}{1 + G(s)}$$

$$s = \sigma + j\omega$$

The stability of the system depends upon the location of the poles of $C(s)/R(s)$ or the zeros of $[1 + G(s)]$ in the complex s plane. Several methods of stability determination can be employed.

Routh's criterion

A method due to Routh is constructed as follows. Let D = numerator polynomial of $1 + G(s)$. Then form

$$D = \sum_{i=0}^{i=n} a_i s^i$$

Stability of systems *continued*

where $a_n > 0$.

a. Construct the table shown below, with the first two rows formed directly from the coefficients and succeeding rows found as indicated.

$$
\begin{array}{ccccccc}
a_n & a_{n-2} & a_{n-4} & a_{n-6} & \cdot & \cdot & \cdot \\
a_{n-1} & a_{n-3} & a_{n-5} & a_{n-7} & \cdot & \cdot & \cdot \\
b_1 & b_2 & b_3 & b_4 & \cdot & \cdot & \cdot \\
c_1 & c_2 & c_3 & c_4 & \cdot & \cdot & \cdot \\
d_1 & d_2 & d_3 & \cdot & \cdot & \cdot & \cdot \\
e_1 & e_2 & \cdot & \cdot & \cdot & \cdot & \cdot \\
f_1 & \cdot & \cdot & \cdot & \cdot & \cdot & \cdot \\
\cdot & \cdot & \cdot & \cdot & \cdot & \cdot & \cdot \\
\cdot & \cdot & \cdot & \cdot & \cdot & \cdot & \cdot \\
\cdot & \cdot & \cdot & \cdot & \cdot & \cdot & \cdot
\end{array}
$$

where

$$b_1 = \frac{a_{n-1}\,a_{n-2} - a_{n-3}\,a_n}{a_{n-1}}$$

$$b_2 = \frac{a_{n-1}\,a_{n-4} - a_{n-5}\,a_n}{a_{n-1}}$$

$$b_3 = \frac{a_{n-1}\,a_{n-6} - a_{n-7}\,a_n}{a_{n-1}}$$

$$c_1 = \frac{b_1\,a_{n-3} - b_2\,a_{n-1}}{b_1}$$

$$c_2 = \frac{b_1\,a_{n-5} - b_3\,a_{n-1}}{b_1}$$

Stability of systems *continued*

$$c_3 = \frac{b_1 a_{n-7} - b_4 a_{n-1}}{b_1}$$

$$d_1 = \frac{c_1 b_2 - b_1 c_2}{c_1}$$

$$d_2 = \frac{c_1 b_3 - b_1 c_3}{c_1}$$

$$d_3 = \frac{c_1 b_4 - b_1 c_4}{c_1}$$

.

.

.

The table will consist of n rows.

b. The system is stable; i.e., the polynomial has no right-half-plane zeros if every entry in the first column of the table is positive. If any complete row is zero, the rest of the table cannot be formed. In such a case the polynomial always has zeros in the right-half-plane or on the imaginary axis.

Nyquist stability criterion

A second method for determining stability is known as Nyquist stability criterion. This method consists in obtaining the locus of the transfer function G(s) in the complex G plane for values of $s = j\omega$ for ω from $-\infty$ to $+\infty$. For single-loop systems, if the locus thus described encloses the point $-1+j0$, the system is unstable; otherwise it is stable. Since the locus is always symmetrical about the real axis, it is sufficient to draw the locus for positive values of ω only. Fig. 3 shows loci for several simple systems. Curves A and C represent stable systems and are typical of the type-1 system; curve B is an unstable system. Curve D is conditionally stable; that is, for a particular range of values of gain K it is unstable. The system is stable both for larger and smaller values of gain. Note: it is unstable as shown.

Phase margin θ_p and gain margin g are also illustrated in Fig. 3A. The former is the angle between the negative real axis and G $(j\omega)$ at the point where the locus intersects the unit-gain circle. It is positive when measured as shown.

Gain margin g is the negative db value of $G(j\omega)$ corresponding to the frequency at which the phase angle is 180 degrees (i.e., where $G(j\omega)$ intersects the negative real axis). The gain margin is often expressed in decibels,

Stability of systems *continued*

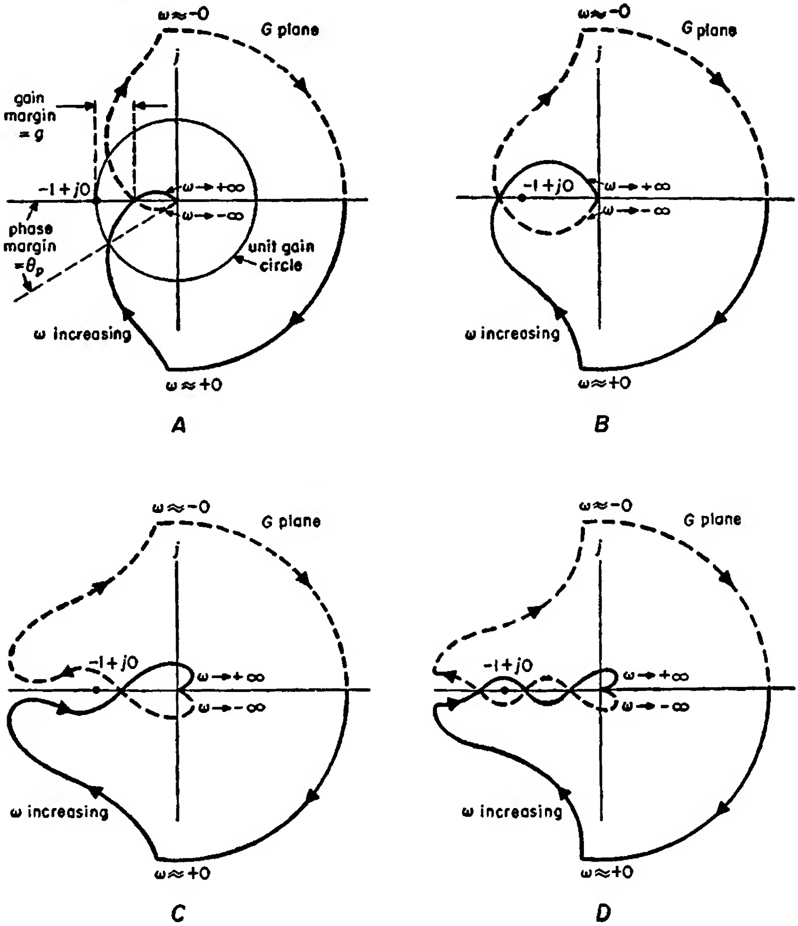

Fig. 3—Typical Nyquist loci.

so that $g = -20 \log_{10} G(j\omega)$. Typical satisfactory values are -10 db for g and an angle of 30° for θ_p. These values are selected on the basis of a good compromise between speed of response and reasonable overshoot. Note that for conditionally stable systems, the terms gain margin and phase margin are without their usual significance.

Logarithmic plots

The transfer function of a feedback control system can be described by separate plots of attenuation and phase versus frequency. This provides a

Stability of systems *continued*

very simple method for constructing a Nyquist diagram from a given transfer function. Use of logarithmic frequency scale permits simple straight-line (asymptotic) approximations for each curve. Fig. 4 illustrates the method for a transfer function with a single time constant. A comparison between approximate and actual values is included.

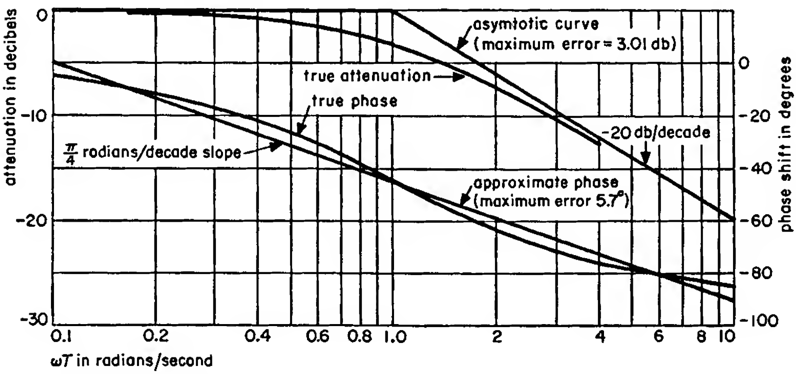

Fig. 4—Transfer-function plot. $G(j\omega) = 1/(1 + j\omega T)$

Transfer functions of the form $G = (1 + j\omega T)$ have similar approximations except that the attenuation curve slope is inverted upward (+ 20 db/decade) and the values of phase shift are positive.

The transfer function of feedback control systems can often be expressed as a fraction with the numerator and denominator each composed of linear factors of the form $(Ts + 1)$. Certain types of control systems such as hydraulic motors where compressibility of the oil in the pipes is appreciable or some steering problems where the viscous damping is small give rise to transfer functions in which quadratic factors occur in addition to the linear factors. The process of taking logarithms (as in making a db plot) facilitates computation because only the addition of product terms is involved. The associated phase angles are directly additive.

For example

$$G(j\omega) = \frac{K(1 + j\omega T_2)}{[T^2(j\omega)^2 + 2\zeta T(j\omega) + 1]\,(1 + j\omega T_1)\,(1 + j\omega T_3)}$$

where $s = j\omega$. The exact magnitude of G in decibels is

$$20\log_{10}|G| = 20\log_{10}K + 20\log_{10}|1 + j\omega T_2| - 20\log_{10}|1 + j\omega T_1|$$
$$- 20\log_{10}|1 + j\omega T_3| - 20\log_{10}|T^2(j\omega)^2 + 2\zeta T(j\omega) + 1|$$

Stability of systems *continued*

Plots of attenuation and phase for quadratic factors as a function of the relative damping ratio ζ are given in Fig. 5. The low-frequency asymptote is 0 db, but the high-frequency asymptote has a slope of $\pm$ 40 db/decade (the positive slope applies to zero quadratic factors), twice the slope of the simple pole or zero case. The two asymptotes intersect at

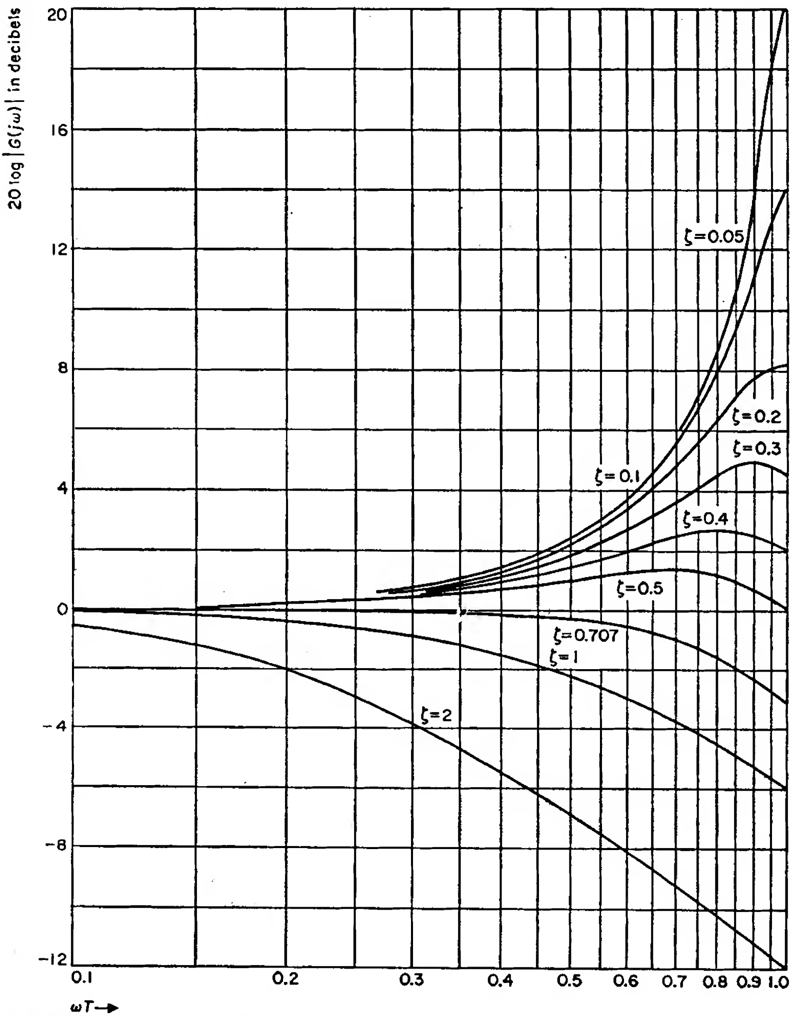

Fig. 5A—Attenuation curve for quadratic factor. $G(j\omega) = 1/[T^2(j\omega^2) + 2\zeta T(j\omega) + 1]$. *By permission from "Automotic Feedbock Control System Synthesis," by J. G. Truxal. Copyright 1955. McGraw-Hill Book Company, Inc.*

Stability of systems *continued*

$\omega = 1/T$

The difference between the asymptotic plot and the actual curves depends on the value of ζ with a variety of shapes realizable for the actual curve. Regardless of the value of ζ, the actual curve approaches the asymptotes at both low and high frequencies. In addition, the error between the asymptotic plot and the actual curve is geometrically symmetrical about the break frequency $\omega = 1/T$. As a result of this symmetry, the curves of Fig. 5A

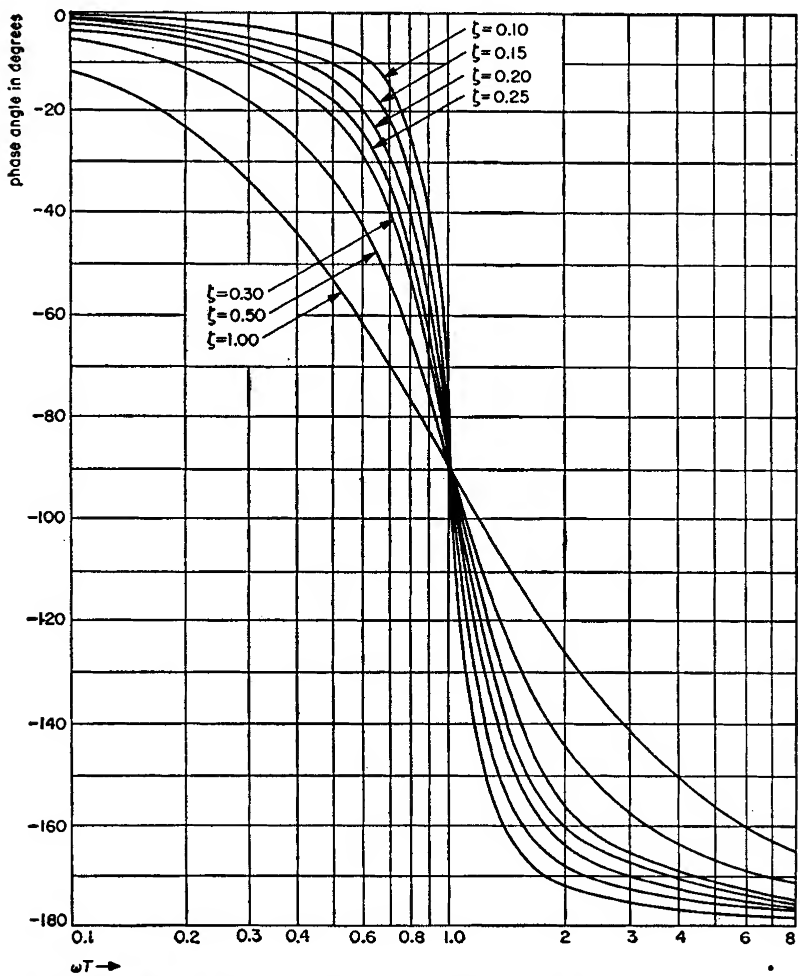

Fig. 5B—Phase characteristic. *By permission from "Theory of Servomechanisms," by H. M. James, N. B. Nichols, and R. S. Phillips. Copyright 1947. McGraw-Hill Book Company, Inc.*

Stability of systems *continued*

are plotted only for $\omega T \leqslant 1$. The error for $\omega = \alpha/T$ is identical with the error at $\omega = 1/\alpha T$.

Log plots applied to transfer functions

Nyquist's method, although yielding satisfactory results, has undesirable limitations when applied to system synthesis because the quantitative effect of parameter changes is not readily apparent. The use of attenuation–phase plots yields a more direct approach to the problem. The method* is based upon the relation between phase and the rate of change of gain with frequency of networks. As a first approximation, which is valid for simple systems, a gain rate of change of 20 db/decade corresponds to a phase shift of 90°. Since the stability of a system can be determined from its phase margin at unity gain (0 db), simple criteria for the slope of the attenuation curve can be established. Thus it is obvious that to avoid instability, the slope

* A theorem due to Bode shows that the phase angle of a network at any desired frequency is dependent on the rate of change of gain with frequency, where the rate of change of gain at the desired frequency has the major influence on the value of the phase angle at that frequency.

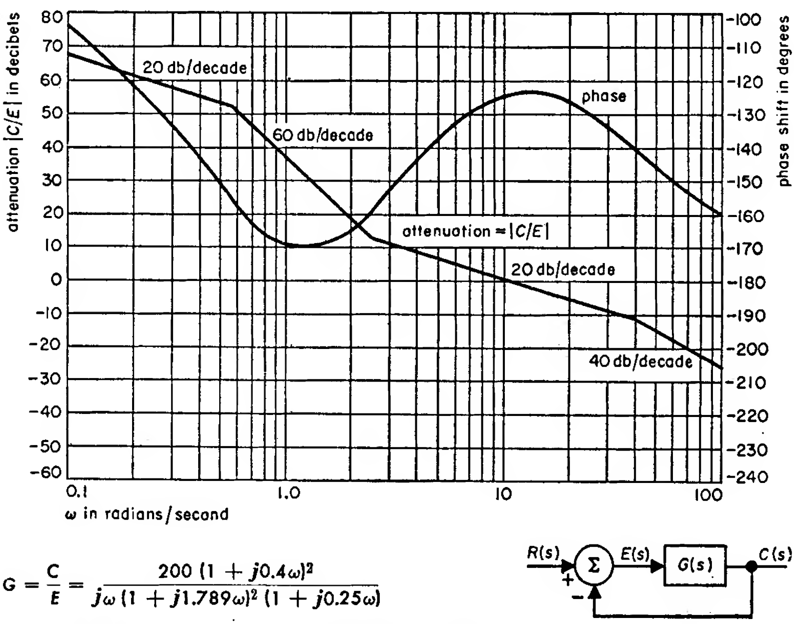

$$G = \frac{C}{E} = \frac{200\,(1 + j0.4\omega)^2}{j\omega\,(1 + j1.789\omega)^2\,(1 + j0.25\omega)}$$

Fig. 6—Attenuation and phase shift for a stable system.

Stability of systems *continued*

of the attenuation curve at unity gain must be appreciably less than -40 db/decade (commonly about -33 db/decade).

The design procedure is to construct asymptotic attenuation–phase curves as a first approximation. From this it can be determined whether the stability requirements are met. Refinements can be made by using the actual instead of asymptotic values for the curve as outlined in Fig. 4.

Figs. 6 and 7 are examples of transfer functions plotted in this manner. In Fig. 6 a positive phase margin exists and the system is stable. Associated with the first-order pole at the origin is a uniform (low-frequency) slope of -20 db/decade and $-90°$ phase shift. This may be considered characteristic of the integrating action of a type-1 control system. Fig. 7 is an unstable system. It has a negative phase margin (as a result of the steep slope of the attenuation curve). The former is stable, the latter is unstable.

Root-locus method

Root-locus is a method of design due to Evans, based upon the relation between the poles and zeros of the closed-loop system function and those of the open-loop transfer function. The rapidity and ease with which the

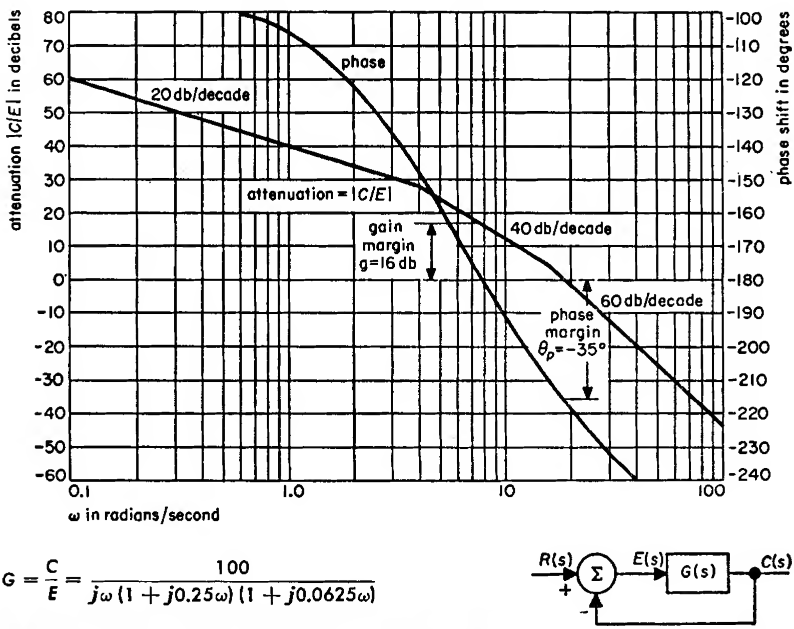

$$G = \frac{C}{E} = \frac{100}{j\omega(1 + j0.25\omega)(1 + j0.0625\omega)}$$

Fig. 7—Attenuation and phase shift for an unstable system.

Stability of systems *continued*

loci can be constructed form the basis for the success of root-locus design methods, in much the same way that the simplicity of the gain and phase plots (Bode diagrams) makes design in the frequency domain so attractive. The root-locus plots can be used to adjust system gain, guide the design of compensation networks, or study the effects of changes in system parameters.

In the usual feedback control system, G(s) is a rational algebraic function, the ratio of two polynomials in s; thus,

$$G(s) = m(s)/n(s)$$

From Fig. 2

$$\frac{C}{R}(s) = \frac{G(s)}{1+G(s)} = \frac{m(s)/n(s)}{1+[m(s)/n(s)]} = \frac{m(s)}{m(s)+n(s)}$$

The zeros of the closed-loop system are identical with those of the open-loop system function.

The closed-loop poles are the values of s at which $m(s)/n(s) = -1$. The root-locus method is a graphical technique for determination of the zeros of $m(s) + n(s)$ from the zeros of $m(s)$ and $n(s)$. Root loci are plots in the complex s plane of the variations of the poles of the closed-loop-system function with changes in the open-loop gain. For the single-loop system of Fig. 2, the root loci constitute all s-plane points at which

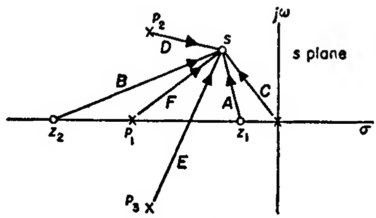

Fig. 8—Graphical interpretation of G(s).

$$G(s) = K(AB/CDEF) = \underline{/A} + \underline{/B} - \underline{/C} - \underline{/D} - \underline{/E} - \underline{/E}$$

$$\underline{/G(s)} = 180° + n\,360°$$

where n is any integer including zero. For a type-1 feedback control system

$$G(s) = \frac{K\,(s+z_1)\,(s+z_2)}{s\,(s+p_1)\,(s+p_2)\,(s+p_3)}$$

A graphical interpretation is given in Fig. 8. Examples are given in Figs. 9 and 10.

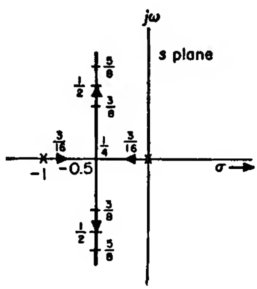

Fig. 9—Root loci for $G(s) = K/[s(s+1)]$

Values of K as indicated by fractions.

Stability of systems *continued*

Gain K_1, Fig. 10, produces the case of critical damping. An increase in gain somewhat beyond this value causes a damped oscillation to appear. The latter increases in frequency (and decreases in damping) with further increase in gain. At gain K_3 a sustained oscillation will result. Instability exists for gain greater than K_3, as at K_4. This corresponds to poles in the right half of the s plane for the closed-loop transfer function.

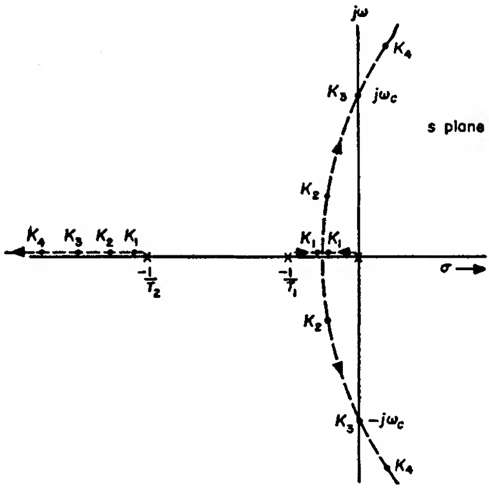

Fig. 10—Root loci for $G(s) = K/[s(T_1s + 1)(T_2s + 1)]$.

Aids in sketching root-locus plots

a. The simplest portions of the plot to establish are the intervals along the negative real $(-\sigma)$ axis, because then all angles are either 0° or 180°.

Complex pairs of zeros or poles contribute no net angle for points along the real axis.

Along the real axis, the locus will exist for intervals that have an *odd* number of zeros and poles to the right of the interval (Fig. 11).

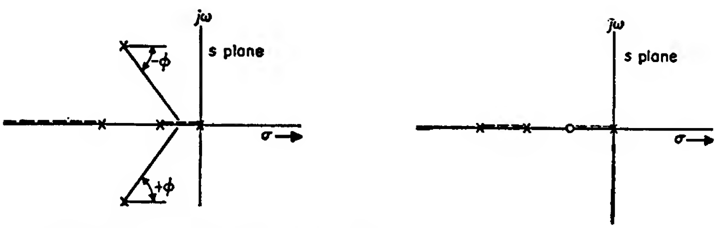

Fig. 11—Root-locus intervals along the real axis

b. For very large values of s, all angles are essentially equal. The locus will thus finally approach asymptotes at the angles (Fig. 12), given by

Stability of systems *continued*

$$\frac{180^\circ + n\,360^\circ}{(\text{number of poles}) - (\text{number of zeros})}$$

These asymptotes meet at a point s_1 (on the negative real axis) given by

$$s_1 = \frac{\Sigma(\text{poles}) - \Sigma(\text{zeros})}{(\text{number of finite poles}) - (\text{number of finite zeros})}$$

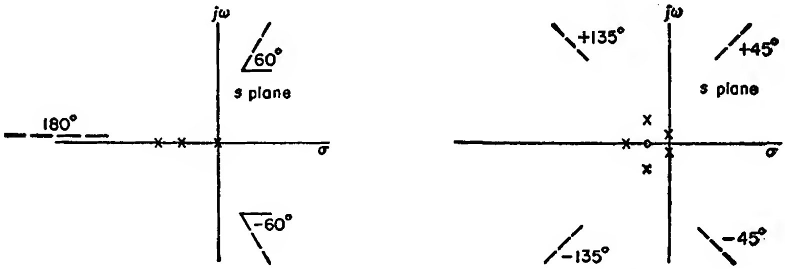

Fig. 12—Final asymptotes for root loci. Left, 60° asymptotes for system having 3 poles. Right, 45° asymptotes for system having an excess of 4 poles over zeros.

c. Breakaway points from the real axis occur where the net change in angle caused by a small vertical displacement is zero. In Fig. 13 the point p satisfies this condition at $1/x_0 = (1/x_1) + (1/x_2)$.

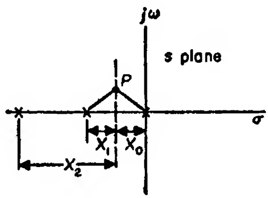

Fig. 13—Breakaway points.

d. Intersections with $j\omega$ axis. Routh's test applied to the polynomial $m(s) + n(s)$ frequently permits rapid determination of the points at which the loci cross the $j\omega$ axis and the value of gain at these intersections.

e. Angles of departure and arrival. The angles at which the loci leave the poles and arrive at the zeros are readily evaluated from the following equation

$$\Sigma\underline{/\text{vectors from zeros to } s} - \Sigma\underline{/\text{vectors from poles to } s} = 180^\circ + n360^\circ.$$

For example, consider Fig. 14. The angle of departure of the locus from the pole at $(-1 + j1)$ is desired. If a test point is assumed only slightly displaced from the pole, the angles contributed by all critical frequencies (except the pole in question) are determined approximately by the vectors from these

Stability of systems *continued*

poles and zeros to $(-1 + j1)$. The angle contributed by the pole at $(-1 + j1)$ is then just sufficient to make the total angle 180°. In the example shown in the figure the departure angle is found from the relation:

$$\underbrace{+\,45^\circ}_{s+2} - (\underbrace{135^\circ}_{s} + \underbrace{90^\circ}_{s+1+j1} + \underbrace{26.6^\circ}_{s+3} + \underbrace{\theta_1}_{s+1-j1} = 180^\circ + n\,360^\circ$$

Hence $\theta = -26.6^\circ$, the angle at which the locus leaves $(-1 + j1)$.

Fig. 14—Loci for $G(s) = \dfrac{K(s+2)}{s(s+3)(s^2+2s+2)}$

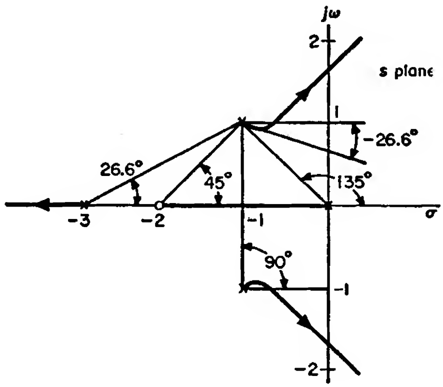

Methods of stabilization

Methods of stabilization for improving feedback-control-system response fall into the following basic categories:

a. Series (cascade) compensation.

b. Feedback (parallel) compensation.

c. Load compensation.

In many cases any one of the above methods may be used to advantage and it is largely a question of practical considerations as to which is selected. Fig. 15 illustrates the three methods.

Networks for series stabilization

Common networks for stabilization are shown in Fig. 16 with the transfer functions. The bridged-T network can be used for stabilization of ac systems although it has the disadvantage of requiring close control of the carrier frequency. Asymptotic attenuation and phase curves for the first

Methods of stabilization *continued*

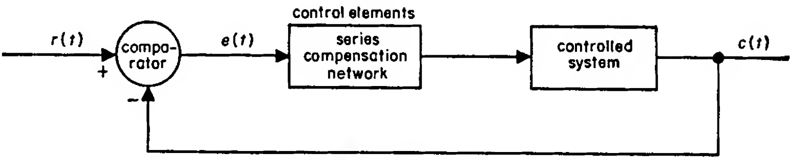

Series compensation.

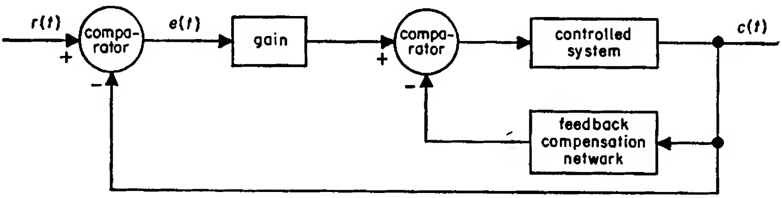

Feedback compensation.

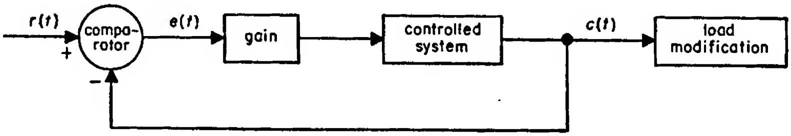

Load compensation.

Fig. 15—Simple schemes for compensation.

Phase-lag network

$$\frac{E_o}{E_i} = \frac{(T_2 s + 1)}{(T_1 s + 1)}$$

where

$T_2 = R_2 C_2$

$T_1 = (R_1 + R_2)\ C_2$

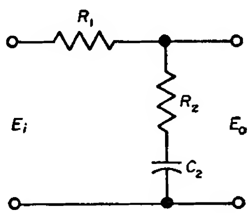

Phase-lead network

$$\frac{E_o}{E_i} = \frac{T_2}{T_1}\left(\frac{T_1 s + 1}{T_2 s + 1}\right)$$

where

$T_1 = R_1 C_1$

$$T_2 = \frac{R_2 R_1 C}{R_1 + R_2}$$

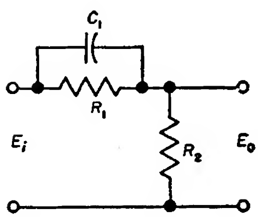

Fig. 16—Networks for series stabilization. *Continued on next page.*

Methods of stabilization *continued*

Lead-lag network

$$\frac{E_o}{E_i} = \frac{(T_1 s + 1)\ (T_2 s + 1)}{T_1 T_2 s^2 + (T_1 + T_2 + T_{12})\ s + 1}$$

where

$T_1 = R_1 C_1$

$T_2 = R_2 C_2$

$T_{12} = R_1 C_2$

$$G_1 = \frac{T_1 + T_2}{T_1 + T_2 + T_{12}}$$

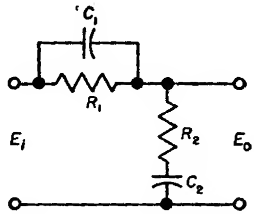

Bridged-T network

$$\frac{E_o}{E_i} = \frac{T_1 T_3 s^2 + 2T_1 s + 1}{T_1 T_3 s^2 + (2T_1 + T_3) s + 1}$$

where

$T_1 = R_1 C$

$T_3 = R_3 C$

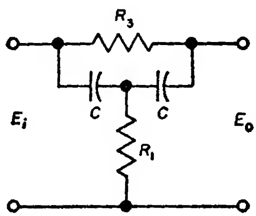

Fig. 16—Networks for series compensation. *Continued*

three networks are shown in Figs. 17 and 18. The positive values of phase angle are to be associated with the phase-lead network whereas the negative values are to be applied to the phase-lag network. Fig. 19 is a plot of the maximum phase shift for lag and lead networks as a function of the time-constant ratio.

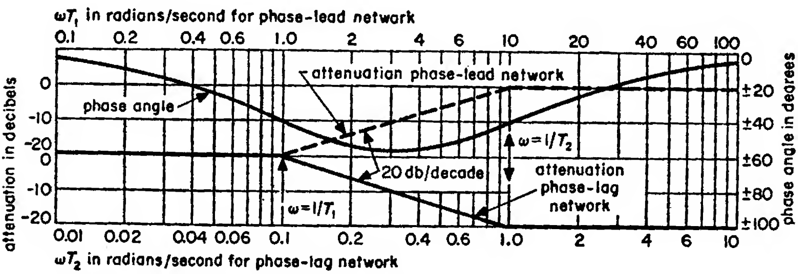

Fig. 17—Phase and attenuation for phase-lead and phase-lag networks. $T_1 = 10T_2$.

Methods of stabilization *continued*

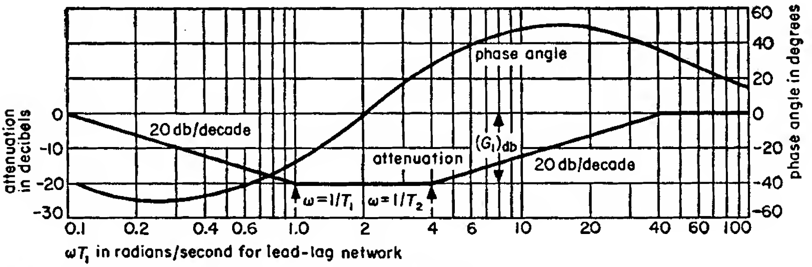

Fig. 18—Phase and attenuation for lead-lag network.

$G_1 = (T_1 + T_2)/(T_1 + T_2 + T_{12})$.

$T_2 = T_1/4$ and $T_{12} = 11.25T_1$.

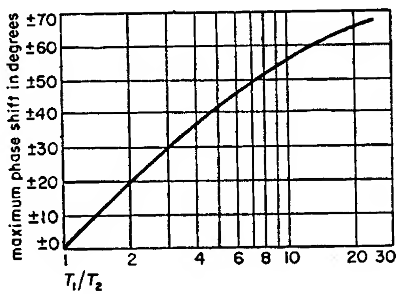

Fig. 19—Maximum phase shift for phase-lead (use positive angles) and phase-lag (negative angles) networks.

Instead of direct feedback, the feedback connection may contain frequency-sensitive elements. Typical of such frequency-sensitive elements are tachometers or other rate- or acceleration-sensitive devices that may be fed back directly or through suitable stabilizing means.

Load stabilization

The commonest form of load stabilization involves the addition of an oscillation damper (tuned or untuned) to change the apparent characteristics of the load. Oscillation dampers can be used to obtain the equivalent of tachometric feedback. The primary advantages of load stabilization are the simplicity of instrumentation and the fact that the compensating action is independent of drift of the carrier frequency in ac systems.

Error coefficients

Of major importance in feedback control systems, along with stability, is system accuracy. *Static accuracy* refers to the accuracy of a system after the steady state is reached and is ordinarily measured with the system input constant or slowly varying. *Dynamic accuracy* refers to the ability of the

Methods of stabilization *continued*

system to follow rapid changes of the input. The following refers to a system such as Fig. 2.

Static-error coefficients

Position error constant:

$$K_p = \lim_{s\to 0} \frac{C(s)}{E(s)} = \lim_{s\to 0} G(s) = \frac{\text{(controlled variable)}}{\text{(actuating error)}}$$

for a constant value of controlled variable.

Velocity error constant:

$$K_v = \lim_{s\to 0} \frac{sC(s)}{E(s)} = \lim_{s\to 0} sG(s) = \frac{\text{(velocity of controlled variable)}}{\text{(actuating error)}}$$

for a constant velocity of controlled variable.

Acceleration error constant:

$$K_a = \lim_{s\to 0} \frac{s^2C(s)}{E(s)} = \lim_{s\to 0} s^2G(s) = \frac{\text{(acceleration of controlled variable)}}{\text{(actuating error)}}$$

for constant acceleration of the controlled variable.

Multiple inputs and load disturbances

Frequently systems are subjected to unwanted signals entering the system at points other than the input. Examples are load-torque disturbances, noise generated at a point within the system, etc. These may be represented as additional inputs to the system. Fig. 20 is a block diagram of such a condition.

For linear operation,

a. $$\frac{C}{R} = \frac{G_1G_2}{1 + HG_1G_2}$$

b. $$\frac{C}{U} = \frac{G_2}{1 + HG_1G_2}$$

Combining (a) and (b),

$$\frac{C}{U} = \frac{1}{G_1}\left(\frac{C}{R}\right)$$

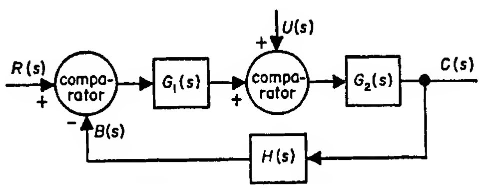

Fig. 20—Multiple-input control system.

Multiple inputs and load disturbances *continued*

If it is desired that the sum of R and U be reproduced in the output (controlled variable), then G_1 should be equal to unity. If U is a disturbance to be minimized, then G_1 should be as large as possible. An example of such a disturbance is the torque produced on a radar antenna by wind forces.

Practical application

An example of a common application is the positioning-type servomechanism shown in Fig. 21. Such a system ordinarily includes the following components: a comparator to measure the error, an amplifier, a second comparator or mixer to measure $(E_1 - B)$, a motor, and a tachometer.

For this system,

$$\frac{C(s)}{E(s)} = \frac{G_1(s)\,G_2(s)}{1 + H(s)\,G_2(s)}$$

$$\frac{C(s)}{R(s)} = \frac{G_1(s)\,G_2(s)}{1 + H(s)\,G_2(s) + G_1(s)\,G_2(s)}$$

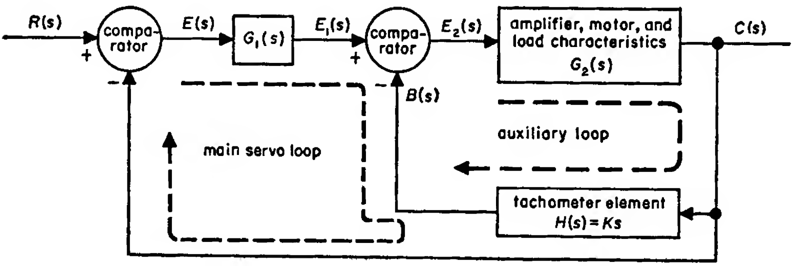

Fig. 21—Positioning-type servo.

Control-system components

Error-measuring systems: potentiometers, synchros

Commonly used error-measuring systems or comparators are shown in Fig. 22.

For synchros whose primary excitation is 115 volts, the error sensitivity is approximately 1 volt/degree for a load resistance of 10,000 ohms across the control-transformer rotor.

Control-system components *continued*

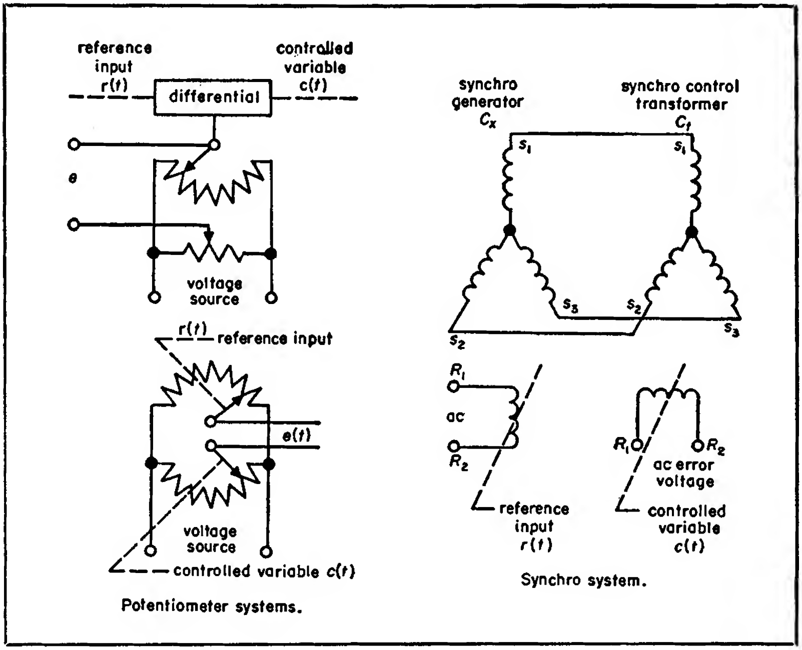

Fig. 22—Error-measuring systems.

The static error of a synchro transmitter and control transformer combination is of the order of 18 minutes maximum and is a function of the rotor position. In some precision units, this error may be reduced to a few minutes of arc. In synchro-control transformers, a very undesirable characteristic is the presence of residual voltages at the null position. In well-designed units this voltage will be less than 30 millivolts.

Synchro errors can be materially reduced by the utilization of double-speed systems. Such systems consist of a dual set of synchro units whose shafts are geared in such a manner as to provide a "fine" and a "coarse" control. The synchro error can be effectively reduced by the factor of the gear ratio employed. Synchronizing networks are employed to provide for proper switching between the two sets of synchros.

Linear motor and load characteristics

In the following, subscript *m* refers to motor, *l* refers to load, and 0 refers to combined motor and load.

Control-system components *continued*

θ = angular position in radians
r = angular velocity in radians/sec = $d\theta/dt$
T_m = motor-developed torque in pound–feet
J_m = motor moment of inertia in slug–feet^2
E_m = impressed volts
k_t = motor stalled-torque constant in pound–feet/volt
$= [\Delta T_m/\Delta E_m]_{r_m}$
f_m = motor internal-damping characteristic in pound–feet–seconds/radian
$= -[\Delta T_m/\Delta_{rm}]_{E_m}$
r_m = motor torque–inertia constant in 1/second
$= T_m/J_m$
J_l = load inertia in slug–feet^2
f_l = load viscous-friction coefficient in pound–feet–seconds/radian
F_l = load coulomb friction in pound–feet
N = motor-to-load gear ratio
$= \theta_m/\theta_l$
f_0 = over-all viscous-friction coefficient referred to load shaft
$= f_l + N^2 f_m$
J_0 = over-all inertia referred to load shaft
$= J_l + N^2 J_m$
T_0 = over-all time constant in seconds
$= J_0/f_0$

The ideal motor characteristics of Fig. 23 are quite representative of dc shunt motors. For alternating-current two-phase servomotors, one phase of

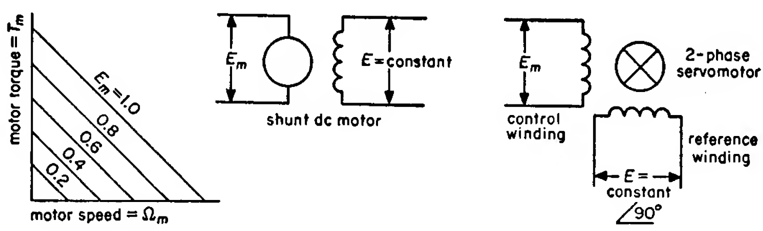

Fig. 23—Ideal motor curves.

which is excited from a constant-voltage source (the reference winding), the curves are approximately valid up to about 40-percent of synchronous speed.

The speed and load-transfer characteristics are given by

Control-system components *continued*

$$\theta_0(s) = \frac{k_t N\, E_m(s) - F_l(s)}{J_0 s^2 + f_0 s}$$

When the coulomb friction F_l can be neglected,

$$G(s) = \frac{\theta_0(s)}{E_m(s)} = \frac{k_t N}{f_0 s\,(T_0 s + 1)}$$

Rate generators

A rate generator (or tachometer generator) is a precision electromechanical component resembling a small motor and having an output voltage proportional to its shaft rotational speed. Rate generators have extensive applications both as computing instruments and as stabilizing components of feedback control systems. An example of the latter is illustrated in Fig. 21. The use of the rate generator produces an effective viscous damping and also tends to linearize the servomechanism by inserting damping of a linear nature and of such magnitude that it swamps out the rather large nonlinear damping of the motor. To eliminate the backlash between rate generators and servomotors, they are often constructed as integral units having a common shaft. These units are available for dc or ac (either 400- or 60-cycle) operation.

Linearity considerations

The preceding material applies strictly to linear systems. Actually all systems are nonlinear to some extent. This nonlinearity may cause serious deterioration in performance. Common sources of nonlinearity are:

a. Nonlinear motor characteristics.

b. Overloading of amplifiers by noise.

c. Static friction.

d. Backlash in gears, potentiometers, etc. For good performance it is recommended that the total backlash should not exceed 20 percent of the expected static error.

e. Low-efficiency gear or worm drives that cause locking action.

Electron tubes

General data*

Cathode emission

The cathode of an electron tube is the primary source of the electron stream. Available emission from the cathode must be at least equal to the sum of the instantaneous peak currents drawn by all of the electrodes. Maximum current of which a cathode is capable at the operating temperature is known as the saturation current and is normally taken as the value at which the current first fails to increase as the three-halves power of the voltage causing the current to flow. Thoriated-tungsten filaments for continuous-wave operation are usually assigned an available emission of approximately one-half the saturation value; oxide-coated emitters do not have a well-defined saturation point and are designed empirically. In Fig. 1, the values refer to the saturation current.

Fig. 1—Commonly used cathode materials.

type	efficiency in milliamperes/watt	specific emission I_s in amp/cm²	emissivity in watts/cm²	operating temp in deg K	ratio hot/cold resistance
Bright tungsten (W)	5–10	0.25–0.7	70–84	2500–2600	14/1
Thoriated tungsten (Th-W)	40–100	0.5–3.0	26–28	1950–2000	10/1
Tantalum (Ta)	10–20	0.5–1.2	48–60	2380–2480	6/1
Oxide coated (Ba-Ca-Sr)	50–150	0.5–2.5	5–10	1100–1250	2.5 to 5.5/1

Operation of cathodes: Thoriated-tungsten and oxide-coated emitters should be operated close to specified temperature. A customary allowable heating-voltage deviation is ± 5 percent. Bright-tungsten emitters may be operated at the minimum temperature that will supply required emission as determined by power-output and distortion measurements. Life of a bright-tungsten emitter is lengthened by lowering the operating temperature. Fig. 2 shows a typical relationship between filament voltage and temperature, life, and emission.

Mechanical stresses in filaments due to the magnetic field of the heating current are proportional to I_f^2. Current flow through a cold filament should be limited to 150 percent of the normal operating value for large tubes, and

* J. Millman, and S. Seely, "Electronics," 1st ed., McGraw-Hill Book Company, New York' New York; 1941. K. R. Spangenberg, "Vacuum Tubes," 1st ed., McGraw-Hill Book Company, New York, New York; 1948. A. H. W. Beck, "Thermionic Valves, Their Theory and Design," Cambridge University Press, London, England; 1953. "Standards on Electron Tubes: Definitions of Terms, 1950," Institute of Radio Engineers, New York, New York.

General data *continued*

250 percent for medium types. Excessive starting current may easily warp or break a filament.

Thoriated-tungsten filaments may sometimes be restored to useful activity by applying filament voltage (only) in accordance with one of the following schedules:

a. Normal filament voltage for several hours or overnight.

b. If the emission fails to respond; at 30 percent above normal for 10 minutes, then at normal for 20 to 30 minutes.

c. In extreme cases, when *a* and *b* have failed to give results, and at the risk of burning out the filament; at 75 percent above normal for 3 minutes followed by schedule *b*.

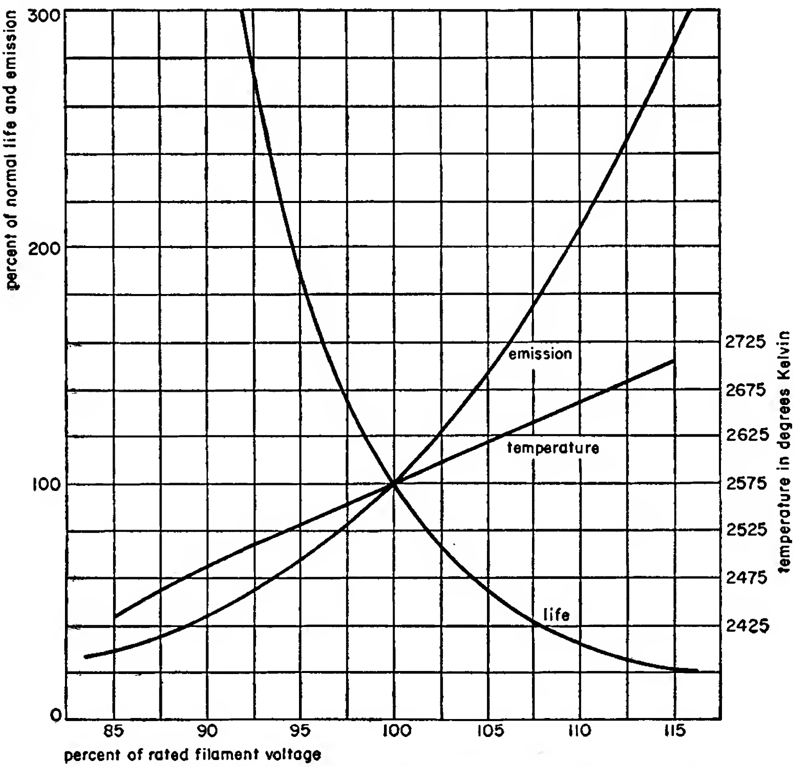

Fig. 2—Effect of change in filament voltage on the temperature, life, and emission of a bright-tungsten filament (based on 2575-degree-Kelvin normal temperature).

General data *continued*

Electrode dissipation

In computing cooling-medium flow, a minimum velocity sufficient to insure turbulent flow at the dissipating surface must be maintained. The figures for specific dissipation (Fig. 3) apply to clean cooling surfaces and may be reduced to a small fraction of the values shown by heat-insulating coatings such as scale or dust.

Fig. 3—Typical operating data for common types of cooling.

type	average cooling-surface temperature in degrees centigrade	specific dissipation in watts/centimeter^2 of cooling surface	cooling-medium supply
Radiation	400–1000	4–10	
Water	30–150	30–110	0.25–0.5 gallons/minute/kilowatt
Forced-air	150–200	0.5–1	50–150 feet^3/minute/kilowatt

Operation temperature of a radiation-cooled surface for a given dissipation is determined by the relative total emissivity of the anode material. Temperature and dissipation are related by the expression,

$$P = \epsilon_t \, \sigma (T^4 - T_0^4)$$

where

P = radiated power in watts/centimeter^2

ϵ_t = total thermal emissivity of the surface

σ = Stefan-Boltzmann constant

= 5.67×10^{-12} watt-centimeters^{-2} $\times$ degrees Kelvin^{-4}

T = temperature of radiating surface in degrees Kelvin

T_0 = temperature of surroundings in degrees Kelvin

Total thermal emissivity varies with the degree of roughness of the surface of the material, and the temperature. Values for typical surfaces are in Fig. 4.

Fig. 4—Total thermal emissivity ϵ_t of electron-tube materials.

material	temp. in deg. Kelvin	thermal emissivity	material	temp. in deg. Kelvin	thermal emissivity
Aluminum	450	0.1	Molybdenum, quartz-blasted	1300	0.5
Anode graphite	1000	0.9	Nickel	600	0.09
Copper	300	0.07	Tantalum	1400	0.18
Molybdenum	1300	0.13	Tungsten	2600	0.30

Except where noted, the surface of the metals is as normally produced.

General data *continued*

Dissipation and temperature rise for water cooling

$$P = 264\, Q_W (T_2 - T_1)$$

where

P = power in watts

Q_W = flow in gallons/minute

T_2, T_1 = outlet and inlet water temperatures in degrees Kelvin, respectively

Dissipation and temperature rise for forced-air cooling

$$P = 169\, Q_A \left(\frac{T_2}{T_1} - 1\right)$$

where Q_A = air flow in feet^3/minute, other quantities as above. Fig. 5 shows the method of measuring air flow and temperature rise in forced-air-cooled systems. A water manometer is used to determine the static pressure against which the blower must deliver the required air flow. Air velocity and outlet air temperature must be weighted over the cross-section of the air stream.

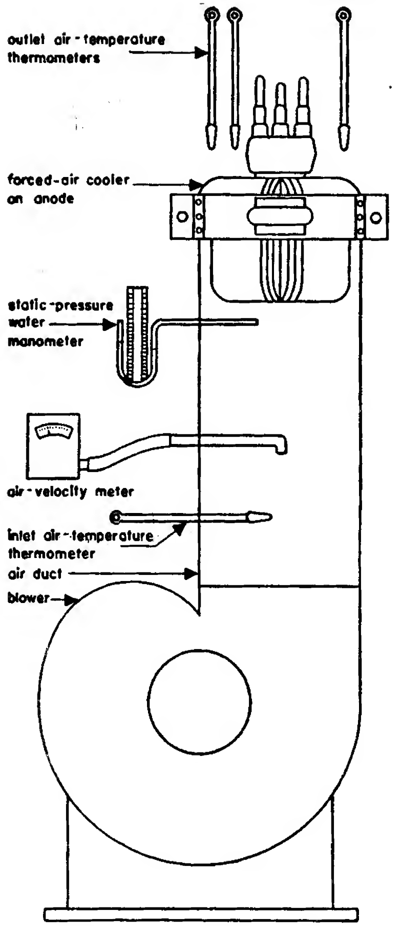

Fig. 5—Measurement of air flow and temperature rise in a forced-air-cooled system is shown at the right.

Grid temperature: Operation of grids at excessive temperatures will result in one or more harmful effects: liberation of gas, high primary (thermal) emission, contamination of the other electrodes by deposition of grid material, and melting of the grid may occur. Grid-current ratings should not be exceeded, even for short periods.

Nomenclature

Application of the standard nomenclature* to a typical electron-tube circuit is shown in Fig. 6. A typical oscillogram is given in Fig. 7 to illustrate the designation of the various components of a current. By logical extension of these principles, any tube, circuit, or electrical quantity may be covered.

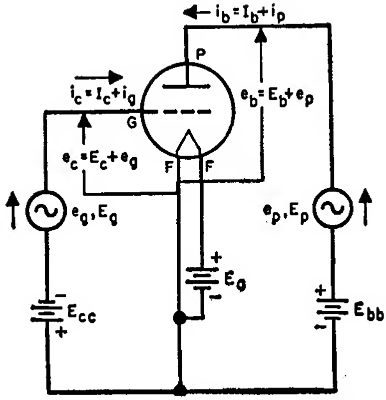

Fig. 6 —Typical electron-tube circuit.

e_c = instantaneous total grid voltage
e_b = instantaneous total plate voltage
i_c = instantaneous total grid current
E_c = average or quiescent value of grid voltage
E_b = average or quiescent value of plate voltage
I_c = average or quiescent value of grid current
e_g = instantaneous value of varying component of grid voltage
e_p = instantaneous value of varying component of plate voltage

* "Standards on Abbreviations, Graphical Symbols, Letter Symbols, and Mathematical Signs," The Institute of Radio Engineers; 1948.

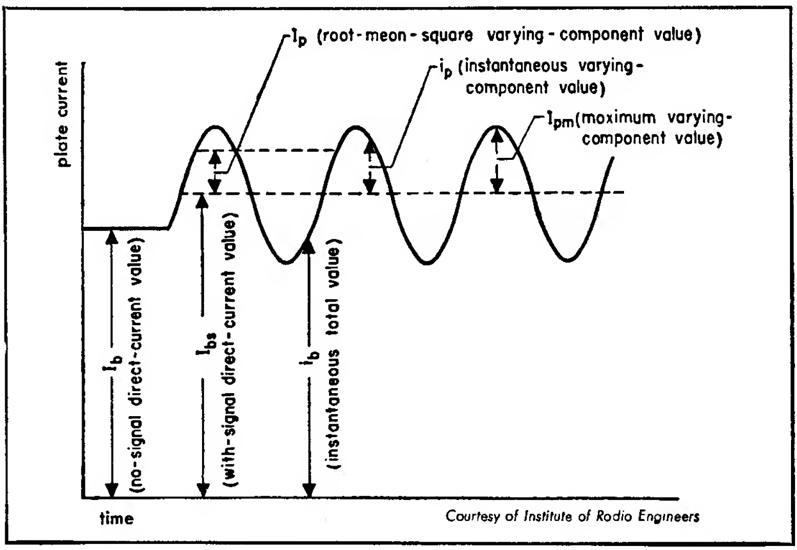

Fig. 7—Nomenclature of the various components of a current.

Nomenclature *continued*

i_g = instantaneous value of varying component of grid current
E_g = effective or maximum value of varying component of grid voltage
E_p = effective or maximum value of varying component of plate voltage
I_g = effective or maximum value of varying component of grid current
I_f = filament or heater current
I_s = total electron emission from cathode
C_{gp} = grid-plate direct capacitance
C_{gk} = grid-cathode direct capacitance
C_{pk} = plate-cathode direct capacitance
θ_p = plate-current conduction angle
r_l = external plate load resistance
r_p = variational (ac) plate resistance

Noise in tubes*

There are several sources of noise in electron tubes, some associated with the nature of electron emission and some caused by other effects in the tube.

Shot effect

The electric current emitted from a cathode consists of a large number of electrons and consequently exhibits fluctuations that produce tube noise and set a limitation to the minimum signal voltage that can be amplified.

Shot effect in temperature-limited case: The root-mean-square value I_n of the fluctuating (noise) component of the plate current is given in amperes by

$$I_n^2 = 2\epsilon I \cdot \Delta f$$

where

I = plate direct current in amperes
ϵ = electronic charge = 1.6×10^{-19} coulombs
Δf = bandwidth in cycles/second

* B. J. Thompson, D. O. North, and W. A. Harris, "Fluctuations in Space-Charge-Limited Currents at Moderately High Frequencies," *RCA Review*: Part I—January, 1940; Part II—July, 1940; Part III—October, 1940; Part IV—January, 1941; Part V—April, 1941. J. L. Lawson and G. E. Uhlenbeck, "Threshold Signals," McGraw-Hill Book Company, Inc., New York, New York; 1950: see Chapter 4. H. Goldberg, "Some Notes on Noise Figures," *Proceedings of the IRE*, vol. 36, pp. 1025–1214; October, 1948: also, vol. 37, p. 40; January, 1949.

Noise in tubes *continued*

Shot effect in space-charge-controlled region: The space charge tends to eliminate a certain amount of the fluctuations in the plate current. The following equations are generally found to give good approximations of the plate-current root-mean-square noise component in amperes.

For diodes:

$$I_n^2 = 4\,k \times 0.64\, T_c g \cdot \Delta f$$

For negative-grid triodes:

$$I_n^2 = 4\,k \times \frac{0.64}{\sigma}\, T_c g_m \cdot \Delta f$$

where

k = Boltzmann's constant = 1.38×10^{-23} joules/degree Kelvin

T_c = cathode temperature in degrees Kelvin

g = diode plate conductance

g_m = triode transconductance

σ = tube parameter varying between 0.5 and 1.0

Δf = bandwidth in cycles/second

Partition noise

Excess noise appears in multicollector tubes due to fluctuations in the division of the current between the different electrodes. Let a pentode be considered, for instance, and let e_g be the root-mean-square noise voltage that, if applied on the grid, would produce the same noise component in the plate current. Let e_t be the same quantity when the tube is operated as a triode. North has given

$$e_g^2 = \left(1 + 8.7\,\sigma \frac{I_{c2}}{g_m} \frac{1000}{T_c}\right) e_t^2$$

where

I_{c2} = screen current in amperes

g_m = pentode transconductance

σ, T_c = as above

Noise in tubes *continued*

Evaluation of tube performance

Equivalent noise input-resistance values: A common way of expressing the properties of electron tubes with respect to noise is to determine the *equivalent noise input resistance;* that is to say, the value of a resistance that, if considered as a source of thermal noise applied to the driving grid, would produce the same noise component in the anode circuit.

The information below has been given by Harris,* and is found to give practical approximations.

For triode amplifiers:

$$R_{eg} = 2.5/g_m$$

For pentode amplifiers:

$$R_{eg} = \frac{I_b}{I_b + I_{c2}}\left(\frac{2.5}{g_m} + \frac{20\,I_{c2}}{g_m{}^2}\right)$$

For triode mixers:

$$R_{eg} = 4/g_c$$

For pentode mixers:

$$R_{eg} = \frac{I_b}{I_b + I_{c2}}\left(\frac{4}{g_c} + \frac{20\,I_{c2}}{g_c{}^2}\right)$$

For multigrid converters and mixers:

$$R_{eg} = \frac{19\,I_b(I_a - I_b)}{g_c{}^2\,I_a}$$

where

R_{eg} = equivalent grid noise resistance in ohms

g_m = transconductance in mhos

I_b = average plate current in amperes

I_{c2} = average screen-grid current in amperes

* W. A. Harris, "Fluctuations in Space-Charge-Limited Currents at Moderately High Frequencies, Part V—Fluctuations in Vacuum-Tube Amplifiers and Input Systems," *RCA Review* vol. 5, pp. 505–524; April, 1941: and vol. 6, pp. 114–124, July, 1941.

Noise in tubes *continued*

g_c = conversion conductance in mhos

I_a = sum of currents from cathode to all other electrodes in amperes

The cathode temperature is assumed to be 1000 degrees Kelvin in the foregoing formulas, and the equivalent-noise-resistance temperature is assumed to be 293 degrees Kelvin.

Low-noise triode amplifiers have noise resistances of the order of 200 ohms; low-noise pentode amplifiers, 700 ohms; pentode mixers, 3000 ohms. Frequency converters have much higher noise resistances, of the order of 200,000 ohms.

Noise factor or noise figure: Another common way of expressing the properties of electron tubes with respect to noise is by means of noise factor. This quantity is defined as the ratio of the available signal-to-noise ratio at the signal-generator (input) terminals to the available signal-to-noise ratio at the output terminals.

Other sources of electron-tube noise

Flicker effect due to variations in the activity of the cathode, is most common in oxide-coated emitters. It varies as f^{-1} and is thus important only at low frequencies.

Collision ionization causes noise when ionized gas atoms or molecules liberate bursts of electrons on striking the cathode.

Induced noise: At ultra-high frequencies it is not necessary for electrons to reach an electrode for induced current to flow in the electrode leads. Noise due to fluctuations in this induced current is called induced noise.

Miscellaneous noises due to microphonics, hum, leakage, charges on insulators, and poor contacts.

Low- and medium-frequency tubes

This section applies particularly to triodes and multigrid tubes operated at frequencies where electron-inertia effects are negligible. The construction illustrated in Fig. 8 is typical of that used in small transmitting tubes at these frequencies.

Low- and medium-frequency tubes *continued*

Coefficients

Amplification factor, μ: Ratio of incremental plate voltage to control-electrode voltage change at a fixed plate current with constant voltage on other electrodes

$$\mu = \left[\frac{\delta e_b}{\delta e_{c1}}\right]_{\substack{I_b \\ E_{c2} \ldots E_{cn} \\ r_l = 0}} \text{constant}$$

Transconductance, s_m: Ratio of incremental plate current to control-electrode voltage change at constant voltage on other electrodes

$$s_m = \left[\frac{\delta i_b}{\delta e_{c1}}\right]_{\substack{E_b,\ E_{c2} \ldots E_{cn} \text{ constant} \\ r_l = 0}}$$

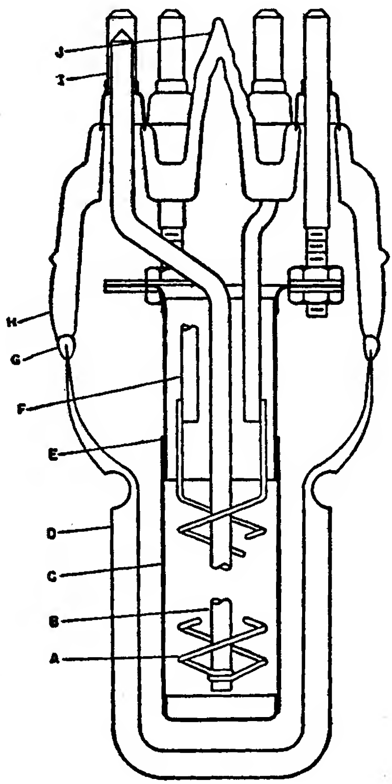

Fig. 8—Electrode arrangement of a small external-anode triode. Overall length is 4 1/16 inches. A—filament, B—filament central-support rod, C—grid wires, D—anode, E—grid-support sleeve, F—filament-leg support rods, G—metal-to-glass seal, H—glass envelope, I—filament and grid terminals, J—exhaust tubulation.

Low- and medium-frequency tubes *continued*

When electrodes are plate and control grid, the ratio is the mutual conductance, g_m

$$g_m = \frac{\mu}{r_p}$$

Variational (ac) plate resistance, r_p: Ratio of incremental plate voltage to current change at constant voltage on other electrodes

$$r_p = \left[\frac{\delta e_b}{\delta i_b}\right]_{\substack{E_{c1} \ldots E_{cn} \text{ constant} \\ r_l = 0}}$$

Total (dc) plate resistance, R_p: Ratio of total plate voltage to current for constant voltage on other electrodes

$$R_p = \left[\frac{E_b}{I_b}\right]_{\substack{E_{c1} \ldots E_{cn} \text{ constant} \\ r_l = 0}}$$

Amplification factor $\mu = \dfrac{e_{b2} - e_{b1}}{e_{c2} - e_{c1}}$

Mutual conductance $g_m = \dfrac{i_{b2} - i_{b1}}{e_{c2} - e_{c1}}$

Total plate resistance $R_p = \dfrac{e_{b2}}{i_{b2}}$

Variational plate resistance $r_p = \dfrac{e_{b2} - e_{b1}}{i_{b2} - i_{b1}}$

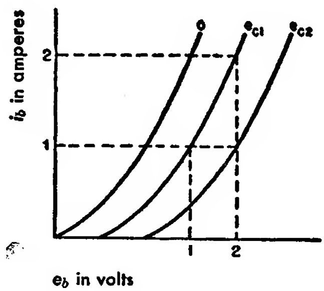

Fig. 9—Graphical method of determining coefficients.

A useful approximation of these coefficients may be obtained from a family of anode characteristics, Fig. 9. Relationships between the actual geometry of a tube and its coefficients are roughly illustrated by Fig. 10.

Low- and medium-frequency tubes *continued*

Fig. 10—Tube characteristics for unipotential cathode and negligible saturation of cathode emission.

function	parallel-plane cathode and anode	cylindrical cathode and anode
Diode anode current (amperes)	$G_1 e_b^{\frac{3}{2}}$	$G_1 e_b^{\frac{3}{2}}$
Triode anode current (amperes)	$G_2 \left(\frac{e_b + \mu e_c}{1 + \mu}\right)^{\frac{3}{2}}$	$G_2 \left(\frac{e_b + \mu e_c}{1 + \mu}\right)^{\frac{3}{2}}$
Diode perveance G_1	$2.3 \times 10^{-6} \frac{A_b}{d_b^2}$	$2.3 \times 10^{-6} \frac{A_b}{\beta^2 r_b^2}$
Triode perveance G_2	$2.3 \times 10^{-6} \frac{A_b}{d_b d_c}$	$2.3 \times 10^{-6} \frac{A_b}{\beta^2 r_b r_c}$
Amplification factor μ	$\dfrac{2.7\, d_c \left(\frac{d_b}{d_c} - 1\right)}{\rho \log \frac{\rho}{2\pi r_g}}$	$\dfrac{2\pi d_c}{\rho} \dfrac{\log \frac{d_b}{d_c}}{\log \frac{\rho}{2\pi r_g}}$
Mutual conductance g_m	$1.5 G_2 \frac{\mu}{\mu + 1} \sqrt{E'_g}$ $E'_g = \frac{E_b + \mu E_c}{1 + \mu}$	$1.5 G_2 \frac{\mu}{\mu + 1} \sqrt{E'_g}$ $E'_g = \frac{E_b + \mu E_c}{1 + \mu}$

where

A_b = effective anode area in square centimeters
d_b = anode-cathode distance in centimeters
d_c = grid-cathode distance in centimeters
β = geometrical constant, a function of ratio of anode-to-cathode radius; $\beta^2 \approx 1$ for $r_b/r_k > 10$ (see curve, Fig. 11)
ρ = pitch of grid wires in centimeters
r_g = grid-wire radius in centimeters
r_b = anode radius in centimeters
r_k = cathode radius in centimeters
r_c = grid radius in centimeters

Note: These formulas are based on theoretical considerations and do not provide accurate results for practical structures; however, they give a fair idea of the relationship between the tube geometry and the constants of the tube.

Low- and medium-frequency tubes *continued*

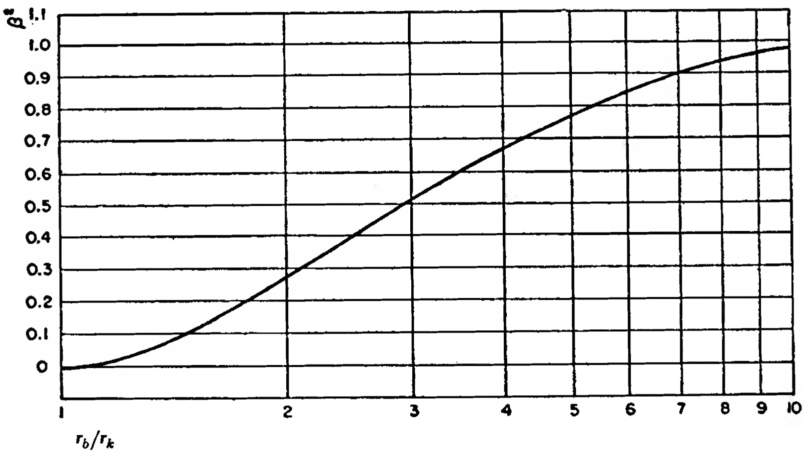

Fig. 11—Values of β^2 for values of $r_b/r_k < 10$.

High-frequency triodes and multigrid tubes*

When the operating frequency is increased, the operation of triodes and multigrid tubes is affected by electron-inertia effects. The design features that distinguish the high-frequency tube shown in Fig. 12 from the lower-frequency tube (Fig. 8) are, reduced cathode-to-grid and grid-to-anode spacings, high emission density, high power density,

* D. R. Hamilton, J. K. Knipp, and J. B. Kuper, "Klystrons and Microwave Triodes," 1st ed., McGraw-Hill Book Company, New York, New York; 1948.

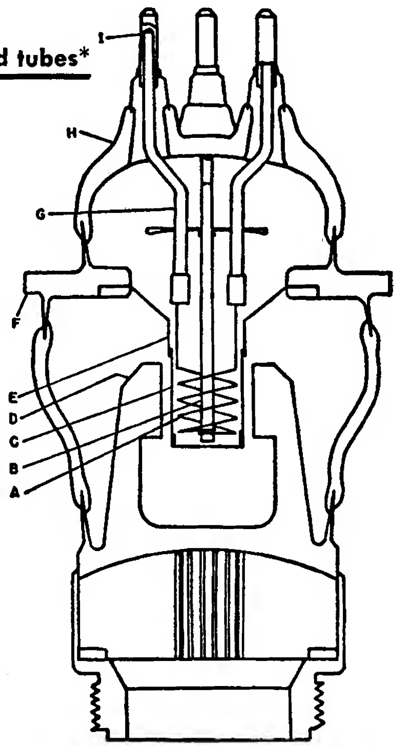

Fig. 12—Electrode arrangement of external-anode ultra-high-frequency triode. Overall length is $4\frac{9}{16}$ inches. A—filament, B—filament central-support rod, C—grid wires, D—anode, E—grid-support cone, F—grid terminal flange, G—filament-leg support rods, H—glass envelope, I—filament terminals.

High-frequency triodes and multigrid tubes *continued*

small active and inactive capacitances, heavy terminals, short support leads, and adaptability to a cavity circuit.

Factors affecting ultra-high-frequency operation

Electron inertia: The theory of electron-inertia effects in small-signal tubes has been formulated;* no comparable complete theory is now available for large-signal tubes.

When the transit time of the electrons from cathode to anode is an appreciable fraction of one radio-frequency cycle:

a. Input conductance due to reaction of electrons with the varying field from the grid becomes appreciable. This conductance, which increases as the square of the frequency, results in lowered gain, an increase in driving-power requirement, and loading of the input circuit.

b. Grid-anode transit time introduces a phase lag between grid voltage and anode current. In oscillators, the problem of compensating for the phase lag by design and adjustment of a feedback circuit becomes difficult. Efficiency is reduced in both oscillators and amplifiers.

c. Distortion of the current pulse in the grid-anode space increases the anode-current conduction angle and lowers the efficiency.

Electrode admittances: In amplifiers, the effect of cathode-lead inductance is to introduce a conductance component in the grid circuit. This effect is serious in small-signal amplifiers because the loading of the input circuit by the conductance current limits the gain of the stage. Cathode-grid and grid-anode capacitive reactances are of small magnitude at ultra-high frequencies. Heavy currents flow as a result of these reactances and tubes must be designed to carry the currents without serious loss. Coaxial cavities are often used in the circuits to resonate with the tube reactances and to minimize resistive and radiation losses. Two circuit difficulties arise as operating frequencies increase:

a. The cavities become physically impossible as they tend to take the dimensions of the tube itself.

b. Cavity Q varies inversely as the square root of the frequency, which makes the attainment of an optimum Q a limiting factor.

* A. G. Clavier, "Effect of Electron Transit-Time in Valves," *L'Onde Electrique,* v. 16, pp. 145–149; March, 1937: also, A. G. Clavier, "The Influence of Time of Transit of Electrons in Thermionic Valves," *Bulletin de la Societe Francaise des Electriciens,* v. 19, pp. 79–91; January, 1939. F. B. Llewellyn, "Electron-Inertia Effects," 1st ed., Cambridge University Press, London; 1941.

High-frequency triodes and multigrid tubes *continued*

Scaling factors: For a family of similar tubes, the dimensionless magnitudes such as efficiency are constant when the parameter

$$\phi = fd/V^{\frac{1}{2}}$$

is constant, where

f = frequency in megacycles

d = cathode-to-anode distance in centimeters

V = anode voltage in volts

Based upon this relationship and similar considerations, it is possible to derive a series of factors that determine how operating conditions will vary as the operating frequency or the physical dimensions are varied (see table, Fig. 13). If the tube is to be scaled exactly, all dimensions will be reduced inversely as the frequency is increased, and operating conditions will be as given in the "size-frequency scaling" column. If the dimensions of the tube are to be changed, but the operating frequency is to be maintained, operation will be as in the "size scaling" column. If the dimensions are to be maintained, but the operating frequency changed, operating conditions will be as in the "frequency scaling" column. These factors apply in general to all types of tubes.

Fig. 13—Scaling factors for ultra-high-frequency tubes.

quantity	ratio	size-frequency scaling	size scaling	frequency scaling
Voltage	V_2/V_1	1	d^2	f^2
Field	E_2/E_1	f	d	f^2
Current	I_2/I_1	1	d^3	f^3
Current density	J_2/J_1	f^2	d	f^3
Power	P_2/P_1	1	d^5	f^5
Power density	h_2/h_1	f^2	d^3	f^5
Conductance	G_2/G_1	1	d	f
Magnetic-flux density	B_2/B_1	f	1	f

d = ratio of scaled to original dimensions
f = ratio of original to scaled frequency

With present knowledge and techniques, it has been possible to reach certain values of power with conventional tubes in the ultra- and super-high-frequency regions. The approximate maximum values that have been obtained are plotted in Fig. 14.

High-frequency triodes and multigrid tubes *continued*

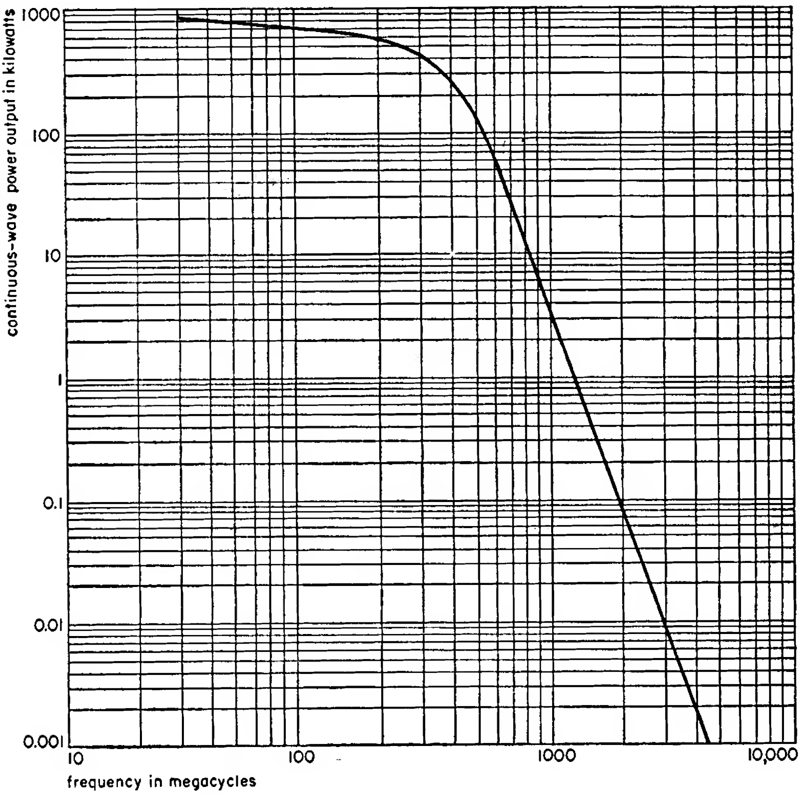

Fig. 14—Maximum ultra-high-frequency continuous-wave power obtainable from a single triode or tetrode. These data are based on 1956 knowledge and techniques.

Microwave tubes

The reduced performance of triodes and multigrid tubes in the microwave region has fostered the development of other types of tubes for use as oscillators and amplifiers at microwave frequencies. The three principal varieties are the magnetron, the klystron, and the traveling-wave amplifier.

Terminology

Anode strap: Metallic connector between selected anode segments of a multicavity magnetron.

Microwave tubes *continued*

Beam-coupling coefficient: Ratio of the amplitude of the velocity modulation produced by a gap, expressed in volts, to the radio-frequency gap voltage.

Bunching: Any process that introduces a radio-frequency conduction-current component into a velocity-modulated electron stream as a direct result of the variation in electron transit time that the velocity modulation produces.

Cavity impedance: The impedance of the cavity that appears across the gap.

Cavity resonator: Any region bounded by conducting walls within which resonant electromagnetic fields may be excited.

Circuit efficiency: The ratio of (*a*) the power of the desired frequency delivered to the output terminals of the circuit of an oscillator or amplifier to (*b*) the power of the desired frequency delivered by the electron stream to the circuit.

Coherent-pulse operation: Method of pulse operation in which the phase of the radio-frequency wave is maintained through successive pulses.

Conduction-current modulation: Periodic variation in the conduction current passing any one point, or the process of producing such a variation.

Drift space: In an electron tube, a region substantially free of externally applied alternating fields in which a relative repositioning of the electrons is determined by their velocity distributions and the space-charge forces.

Duty: The product of the pulse duration and the pulse-repetition rate.

Electronic efficiency: The ratio of (*a*) the power of the desired frequency delivered by the electron stream to the circuit in an oscillator or amplifier to (*b*) the direct power supplied to the stream.

End shields limit the interaction space in the direction of the magnetic field.

End spaces: In a multicavity magnetron, the two cavities at either end of the anode block terminating all of the anode-block cavity resonators.

External Q: The reciprocal of the difference between the reciprocals of the loaded and unloaded Q's. For a magnetron it is equal to

$$Q_{external} = (\text{total stored energy})/(\text{output energy})$$

Microwave tubes *continued*

Frequency pulling: Of an oscillator, is the change in the generated frequency caused by a change of the load impedance.

Frequency pushing: Of an oscillator, is the change in frequency due to change in anode current (or in anode voltage).

Input gap: Gap in which the initial velocity modulation of the electron stream is produced. This gap is also known as the buncher gap.

Interaction gap: Region between electrodes in which the electron stream interacts with a radio-frequency field.

Interaction space: Region between anode and cathode.

Loaded Q: Of a specific mode of resonance of a system, is the Q when there is external coupling to that mode. Note: When the system is connected to the load by means of a transmission line, the loaded Q is customarily determined when the line is terminated in its characteristic impedance. For a magnetron it is equal to

$$Q_{loaded} = \text{(total stored energy)}/\text{(output + cavity-dissipation energies)}$$

Magnet gap: Space between the pole faces of a magnet.

Mode: One of the components of a general configuration of a vibrating system. A mode is characterized by a particular geometrical pattern and a resonant frequency (or propagation constant).

Mode number (klystron): Number of whole cycles that a mean-speed electron remains in the drift space of a reflex klystron.

Mode number *n* (magnetron): The number of radians of phase shift in going once around the anode, divided by 2π. Thus, n can have integral values 1, 2, 3 . . . $N/2$, where N is the number of anode segments.

Output gap: Gap in which variations in the conduction current of the electron stream are subjected to opposing electric fields in such a manner as to extract usable radio-frequency power from the electron beam. This gap is also known as the catcher gap.

π mode: Of a multicavity magnetron, is the mode of resonance for which the phase difference between any two adjacent anode segments is π radians. For an N-cavity magnetron, the π mode has the mode number $N/2$.

Microwave tubes *continued*

Pulling figure: Of an oscillator, is the difference in megacycles/second between the maximum and minimum frequencies of oscillation obtained when the phase angle of the load-impedance reflection coefficient varies through 360 degrees, while the absolute value of this coefficient is constant and is normally equal to 0.20.

Pulse: Momentary flow of energy of such short time duration that it may be considered as an isolated phenomenon.

Pulse operation: Method of operation in which the energy is delivered in pulses.

Pushing figure: Of an oscillator, is the rate of frequency pushing in megacycles/second/ampere (or megacycles/second/volt).

Q: Of a specific mode of resonance of a system, is 2π times the ratio of the stored electromagnetic energy to the energy dissipated per cycle when the system is excited in this mode.

RF pulse duration: Time interval between the points at which the amplitude of the envelope of the radio-frequency pulse is 70.7 percent of the maximum amplitude of the envelope.

Reflector: Electrode whose primary function is to reverse the direction of an electron stream. It is also called a repeller.

Reflex bunching: Type of bunching that occurs when the velocity-modulated electron stream is made to reverse its direction by means of an opposing direct-current field.

Space-charge debunching: Any process in which the mutual interactions between electrons in the stream disperses the bunched electrons.

Transit angle: The product of angular frequency and time taken for an electron to traverse the region under consideration. This time is known as the transit time.

Unloaded Q: Of a specific mode of resonance of a system, is the Q of the mode when there is no external coupling to it. For a magnetron it is equal to

$Q_{unloaded}$ = (total stored energy)/(cavity-dissipation energy)

Velocity modulation: Process whereby a periodic time variation in velocity is impressed on an electron stream; also, the condition existing in the stream subsequent to such a process.

Microwave tubes *continued*

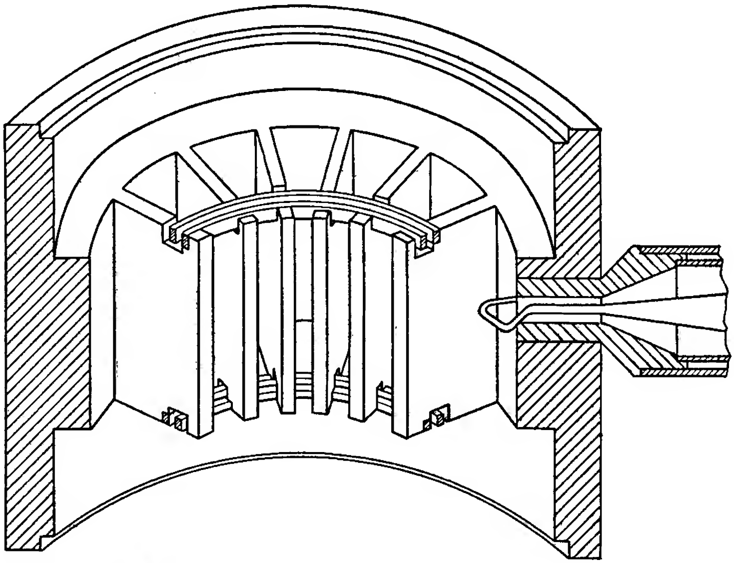

A. Strapped vane type.

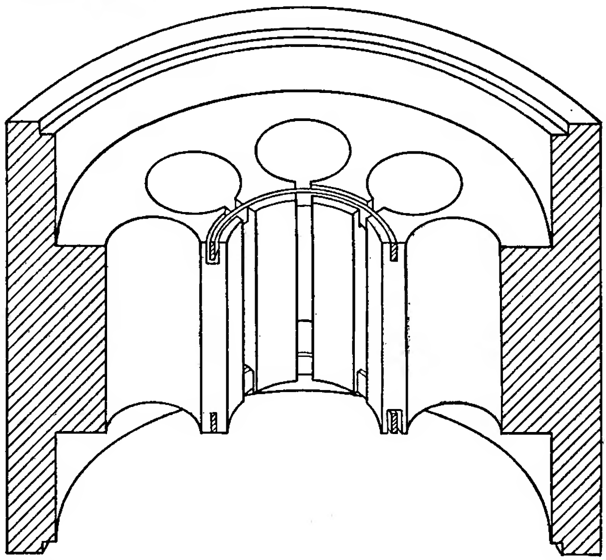

B. Strapped hole-and-slot type.

Fig. 15—Basic anode structures of typical multicavity microwave magnetrons.

Microwave tubes *continued*

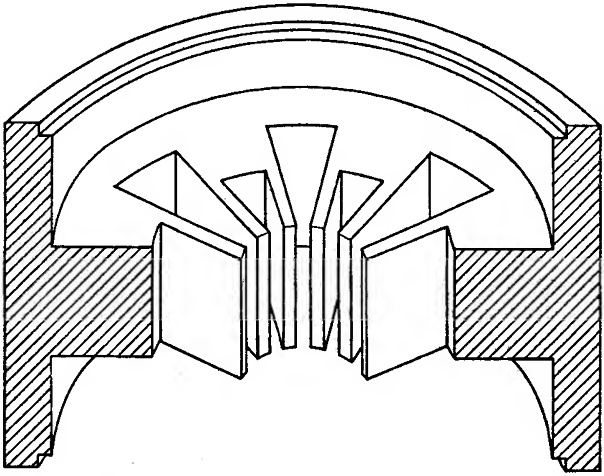

C. Rising-sun type.

Fig. 15—*Continued.*

Magnetrons*

A magnetron is a high-vacuum tube containing a cathode and an anode, the latter usually divided into two or more segments, in which tube a constant magnetic field modifies the space-charge distribution and the current-voltage relations. In modern usage, the term "magnetron" refers to the magnetron oscillator in which the interaction of the electronic space charge with the resonant system converts direct-current power into alternating-current power, usually of microwave frequencies.

Many forms of magnetrons have been made in the past and several kinds of operation have been employed. The type of tube that is now almost universally employed is the multicavity magnetron generating traveling-wave oscillations. It possesses the advantages of good efficiency at high frequencies, capability of high outputs either in pulsed or continuous-wave operation, moderate magnetic-field requirements, and good stability of operation. A section through the basic anode structure of a typical magnetron is shown in Fig. 15A.

* G. B. Collins, "Microwave Magnetrons," vol. 6, Radiation Laboratory Series, 1st ed., McGraw-Hill Book Company, New York, New York; 1948. J. B. Fisk, H. D. Hagstrum, and P. L. Hartman, "The Magnetron as a Generator of Centimeter Waves," *Bell System Technical Journal*, v. 25, pp. 167–348; April, 1946.

Microwave tubes *continued*

In magnetrons, the operating frequency is determined by the resonant frequency of the separate cavities arranged around the central cylindrical cathode and parallel to it. A high direct-current potential is placed between the cathode and the cavities and radio-frequency output is brought out through a suitable transmission line or waveguide usually coupled to one of the resonator cavities. Under the action of the radio-frequency voltages across these resonators and the axial magnetic field, the electrons from the cathode form a bunched space-charge cloud that rotates around the tube axis, exciting the cavities and maintaining their radio-frequency voltages. Most efficient operation occurs in the π mode; that is, in such a fashion that the phase difference between the voltages across each adjacent resonator is 180 degrees. Since other modes of operation are possible, it is often desirable to provide means for suppressing them. A common method is to strap alternating anode segments together conductively so that large circulating currents flow in the unwanted modes of operation, thus damping them. This is illustrated in Figs. 15A and B. Fig. 15C shows another example of a resonant multicavity system that is known as a rising-sun type. It should be noted that the anode segments are not strapped and mode suppression is accomplished by maintaining the proper size ratio between the large and small cavities. One definite advantage of this type of resonant system is its application for very-high microwave frequency operation where the physical size of the cavity is small and its fabrication becomes increasingly difficult.

Magnetron performance data

The performance data for a magnetron is usually given in terms of two diagrams, the performance chart and the Rieke diagram.

Performance chart: Is a plot of anode current along the abscissa and anode voltage along the ordinate of rectangular-coordinate paper. For a fixed typical tube load, pulse duration, pulse-repetition rate, and setting of the tuner of tunable tubes, lines of constant magnetic field, power output, efficiency, and frequency, may be plotted over the complete operating range of the tube. Regions of unsatisfactory operation are indicated by cross hatching. For tunable tubes, it is customary to show performance

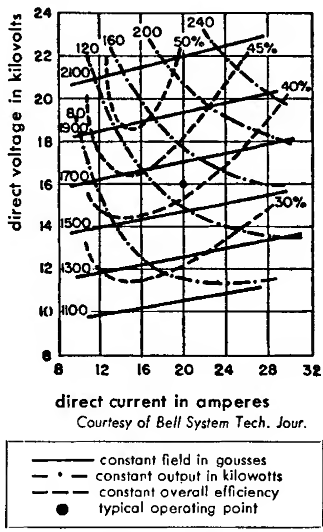

Courtesy of Bell System Tech. Jour.

Fig. 16—Performance chart for pulsed magnetron.

Microwave tubes *continued*

charts for more than one setting of the tuner. In the case of magnetrons with attached magnets, curves showing the variation of anode voltage, efficiency, frequency, and power output with change in anode current are given. A typical chart for a magnetron having eight resonators is given in Fig. 16.

Rieke diagram: Shows the variation of power output, anode voltage, efficiency, and frequency with changes in the voltage standing-wave ratio and phase angle of the load for fixed typical operating conditions such as magnetic field, anode current, pulse duration, pulse-repetition rate, and the setting of the tuner for tunable tubes. The Rieke diagram is plotted on polar coordinates, the radial coordinate being the reflection coefficient measured in the line joining the tube to the load and the angular coordinate being the angular distance of the voltage standing-wave minimum from a suitable reference plane on the output terminal. On the Rieke diagram, lines of constant frequency, anode voltage, efficiency, and output may be drawn (Fig. 17).

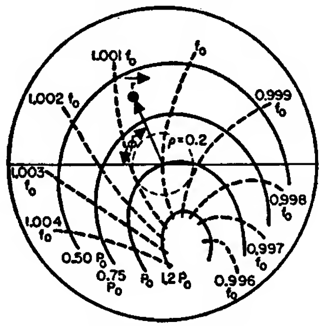

Courtesy of Bell System Tech. Jour.

——— constant power output
— — — constant frequency

Fig. 17—Rieke diagram.

Magnetron design data

The design of a new magnetron is usually begun by scaling from an existing magnetron having similar characteristics. Normalized operating parameters have been defined in such a way that a family of magnetrons scaled from the same parent have the same electronic efficiency for like values of $I/\mathcal{J}$, $V/\mathcal{V}$, and $B/\mathcal{B}$,

where the normalized parameters $\mathcal{J}$, $\mathcal{V}$, and $\mathcal{B}$ for the π mode are

$$\mathcal{J} = \frac{2\pi a_1}{(1-\sigma^2)^2\,(1/\sigma+1)}\,\frac{m}{e}\left(\frac{4\pi c}{N\lambda}\right)^3 r_a^2\,\epsilon_0 h$$

$$= \frac{8440 a_1}{(1-\sigma^2)\,(1/\sigma+1)}\left(\frac{4\pi r_a}{N\lambda}\right)^3 \frac{h}{r_a}\ \text{amperes}$$

$$\mathcal{V} = \frac{1}{2}\,\frac{m}{e}\left(\frac{4\pi c}{N\lambda}\right)^2 r_a^2 = 253{,}000\left(\frac{4\pi r_a}{N\lambda}\right)^2\ \text{volts}$$

Microwave tubes *continued*

$$\mathcal{B} = 2\frac{m}{e}\left(\frac{4\pi c}{N\lambda}\right)\frac{1}{(1-\sigma^2)} = \frac{42{,}400}{N\lambda(1-\sigma^2)} \text{ gausses}$$

where

a_1 = a slowly varying function of r_a/r_c approximately equal to one in the range of interest
r_a = radius of anode in meters
r_c = radius of cathode in meters
h = anode height in meters
N = number of resonators
n = mode number
λ = wavelength in meters
m = mass of an electron in kilograms
e = charge on an electron in coulombs
c = velocity of light in free space in meters/second
ϵ_0 = permittivity of free space

and I, V, and B are the operating conditions. Scaling may be done in any direction or in several directions at the same time. For reasonable performance it has been found empirically that

$$\frac{V}{\mathcal{V}} \geqslant 6, \quad \frac{B}{\mathcal{B}} \geqslant 4, \quad \text{and} \quad \frac{1}{3} < \frac{I}{\mathcal{I}} < 3$$

The minimum voltage required for oscillation has been named the "Hartree" voltage and is given by

$$V_H = \mathcal{V}\left(2\frac{B}{\mathcal{B}} - 1\right)$$

Slater's rule gives the relation between cathode and anode radius as

$$\sigma = \frac{r_c}{r_a} \approx \frac{N-4}{N+4}$$

Magnetrons for pulsed operation have been built to deliver peak powers varying from 3 megawatts at 3000 megacycles to 100 kilowatts at 30,000 megacycles. Continuous-wave magnetrons having outputs ranging from one kilowatt at 3000 megacycles to a few watts at 30,000 megacycles have been produced. Operation efficiencies up to 60 percent at 3000 megacycles are obtained, falling to 30 percent at 30,000 megacycles.

Microwave tubes *continued*

Klystrons*

A klystron is an electron tube in which the following processes may be distinguished.

a. Periodic variations of the longitudinal velocities of the electrons forming the beam in a region confining a radio-frequency field.

b. Conversion of the velocity variation into conduction-current modulation by motion in a region free from radio-frequency fields.

c. Extraction of the radio-frequency energy from the beam in another confined radio-frequency field.

The transit angles in the confined fields are made short ($\delta \doteqdot \pi/2$) so that there is no appreciable conduction-current variation while traversing them.

Several variations of the basic klystron exist. Of these, the simplest is the two-cavity amplifier or oscillator. The most important is the reflex klystron that is used as a low-power oscillator. The multicavity high-power amplifier is now also becoming important.

Two-cavity klystron amplifiers

An electron beam is formed in an electron gun and passed through the gaps associated with the two cavities (Fig. 18). After emerging from the second gap, the electrons pass to a collector designed to dissipate the remaining beam power without the production of secondary electrons. In the first gap, the electron beam is alternately accelerated and decelerated in succeeding half-periods of the radio-frequency cycle, the magnitude of the change in speed depending upon the magnitude of the alternating voltage impressed upon the cavity. The electrons then move in a drift space where there are no radio-frequency fields. Here, the electrons that were accelerated in the input gap catch up with those that were decelerated in the preceding half-cycle and a local increase of current density occurs in the beam. Analysis shows that the maximum of the current-density wave occurs at the position, in time and space, of those electrons that passed the center of the input gap as the field changed from negative to positive. There is therefore a phase difference of $\pi/2$ between the current wave and the voltage wave that produced it. Thus at the end of the drift space,

* D. R. Hamilton, J. K. Knipp, and J. B. H. Kuper, "Klystrons and Microwave Triodes," McGraw-Hill Book Company, New York, New York; 1948. A. H. W. Beck, "Velocity-Modulated Thermionic Valves," Cambridge University Press, London, England; 1948. A. H. W. Beck, "Thermionic Valves, Their Theory and Design," Cambridge University Press, London, England; 1953.

Microwave tubes *continued*

the initially uniform electron beam has been altered into a beam showing periodic density variations. This beam now traverses the output gap and the variations in density induce an amplified voltage wave in the output circuit, phased so that the negative maximum corresponds with the phase of the bunch center. The increased radio-frequency energy has been gained by conversion from the direct-current beam energy.

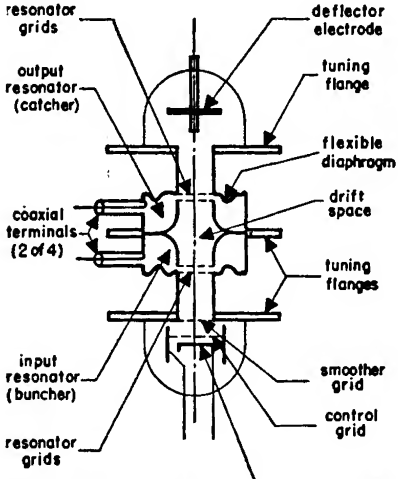

Courtesy of Sperry Gyroscope Co.

Fig. 18—Diagram of a 2-cavity klystron.

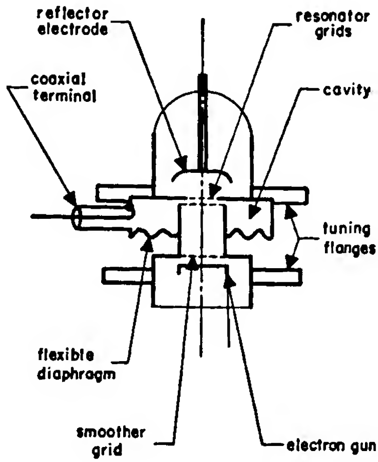

Fig. 19—Diagram of a reflex klystron.

The two-cavity amplifier can be made to oscillate by providing a feedback loop from the output to the input cavity, but a much simpler structure results if the electron beam direction is reversed by a negative electrode, termed the reflector.

Reflex klystrons*

A representative reflex klystron is shown schematically in Fig. 19. The velocity-modulation process takes place as before, but analysis shows that in the retarding field used to reverse the direction of electron motion, the phase of the current wave is exactly opposite to that in the two-cavity klystron. When the bunched beam returns to the cavity gap, a positive field extracts maximum energy from the beam, since the direction of electron motion has now been reversed. Consideration of the phase conditions shows that for a fixed cavity potential, the reflex klystron will oscillate only

Microwave tubes *continued*

near certain discrete values of reflector voltage for which the transit time measured from the gap center to the reflection point and back is given by

$$\omega\tau = 2\pi(N + 3/4)$$

where N is an integer called the mode number.

By varying the reflector voltage around the value corresponding with the mode center, it is possible to vary the oscillation frequency by a small percentage and this fact is made use of in providing automatic frequency control or in frequency-modulation transmission.

Reflex klystron performance data

The performance data for a reflex klystron are usually given in the form of a reflector-characteristic chart. This chart displays power output and frequency deviation as a function of reflector voltage. Several modes are often displayed on the same chart. A typical chart is shown in Fig. 20.

There are two rather distinct classes of reflex klystron in current large-scale manufacture (Fig. 21).

a. Tubes for local oscillators in radar systems. These have power outputs designed to operate crystal mixers with the necessary degree of isolation, i.e., 10–100 milliwatts. The electronic tuning range required is about 50 megacycles independent of center frequency, but the linearity of the Δf versus ΔV_r characteristic is relatively unimportant.

b. Tubes as frequency modulators in microwave links. These usually require considerably greater power, up to about 10 watts, and the linearity of Δf

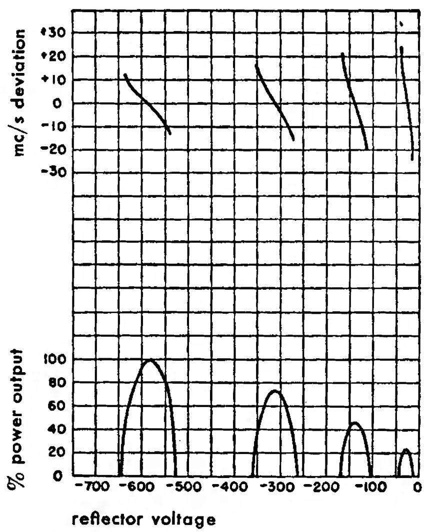

Courtesy of Sperry Gyroscope Co.

Fig. 20—Klystron reflector-characteristic chart.

* J. R. Pierce and W. G. Shepherd, "Reflex Oscillators" *Bell System Technical Journal*, vol. 26, pp. 460–681; July, 1947.

Microwave tubes *continued*

versus ΔVr characteristic over a limited (e.g., 10-megacycle) excursion is of primary importance as this parameter determines the harmonic margins in the system. Second-harmonic margins of −96 decibels for deviations of 125 kilocycles have been observed; the third-harmonic margins are about −120 decibels.

Fig. 21—Typical reflex klystrons.

frequency in megacycles	power output in milliwatts	useful mode width Δf_{3db} in megacycles	operating voltage
	local oscillators		
3,000	150	40	300
9,000	40	40	350
24,000	35	120	750
35,000	>15	50	2000
50,000	10–20	60–140	600
	frequency-modulation transmitters		
4,000	1000	40	1100
7,000	1000	37	750
9,000	600	60	500

Multicavity klystrons

More recently, multicavity klystrons have been perfected for use in two rather different fields of application: applications requiring extremely high pulse powers* and continuous-wave systems in which moderate powers† (tens of kilowatts) are required. An example of the first application is a power source for nuclear-particle acceleration, while ultra-high-frequency television is an example of the latter.

A multicavity klystron amplifier is shown schematically in Fig. 22. The example shown has three cavities all coupled to the same beam. The radio-frequency input modulates the beam as before. The bunched beam induces an

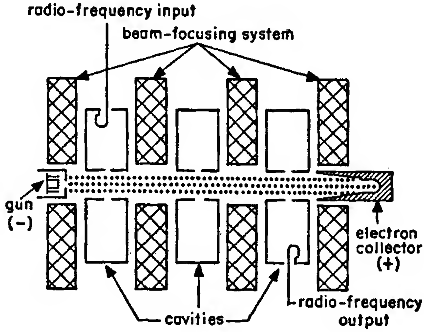

Fig. 22—Three-cavity klystron.

* M. Chodorow, E. L. Ginzton, I. R. Neilson, and S. Sonkin, "Design and Performance of a High-Power Pulsed Klystron." *Proceedings of the IRE*, vol. 41, pp. 1584–1602; November, 1953.

† D. H. Priest, C. E. Murdock, and J. J. Woerner, "High-Power Klystrons at U.H.F." *Proceedings of the IRE*, vol. 41, pp. 20–25; January, 1953.

Microwave tubes *continued*

amplified voltage across the second cavity, which is tuned to the operating frequency. This amplified voltage remodulates the beam with a certain phase-shift and the now more-strongly bunched beam excites a highly amplified wave in the output circuit. It is found that the optimum power output is obtained when the second cavity is slightly detuned. Moreover, when increased bandwidth is required, the second cavity may be loaded with a resultant lowering in overall gain. Modern multicavity klystrons use magnetically focused, high-perveance beams and under these conditions, high gains, large power outputs, and reasonable values of efficiency are readily obtained.

Continuous-wave multicavity klystrons are available with outputs of around 10 kilowatts at frequencies up to 2400 megacycles. The efficiencies are of the order of 30 percent and the gains vary between 20 and 40 decibels, according to the number of cavities, bandwidth, etc. Pulsed tubes have been designed for outputs of 30 megawatts and with efficiencies of over 40 percent at frequencies near 3000 megacycles.

Traveling-wave tubes*

The traveling-wave tube is a relatively new type of microwave tube in which a longitudinal electron beam interacts continuously with the field of a wave traveling along a wave-propagating structure. In its most common form it is an amplifier, although there are related types of tubes that are basically oscillators.

* J. R. Pierce, "Traveling-Wave Tubes," D. Van Nostrand Co., Inc., New York, New York; 1950. R. Kompfner, "Reports on Progress in Physics," vol. 15, pp. 275–327, The Physical Society, London, England; 1952. R. G. E. Hutter, "Traveling-Wave Tubes," *Advances in Electronics and Electron Physics*, vol. 6, Academic Press, Inc., New York, New York; 1954. A bibliography is given in a survey paper by J. R. Pierce, "Some Recent Advances in Microwave Tubes," *Proceedings of the IRE*, vol. 42, pp. 1735–1747; December, 1954.

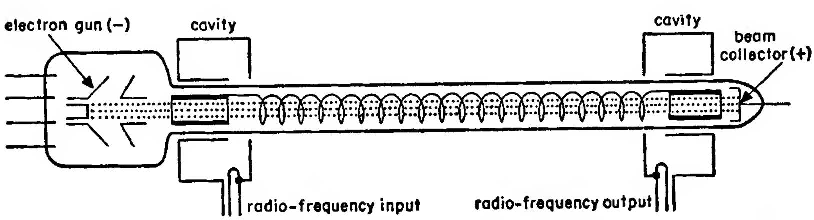

Fig. 23—Basic helical traveling-wave tube. The magnetic beam-focusing system between input and output cavities is not shown here.

Microwave tubes *continued*

The principle of operation may be understood by reference to the schematic diagram representing a typical tube, Fig. 23. An electron stream is produced by an electron gun, travels along the axis of the tube, and is finally collected by a suitable electrode. Spaced closely around the beam is a circuit, in this case a helix, capable of propagating a slow wave. The circuit is proportioned so that the phase velocity of the wave is small with respect to the velocity of light. In typical low-power tubes, a value of the order of one-tenth of the velocity of light is used; for higher-power tubes the phase velocity may be two or three times higher. Suitable means are provided to couple an external radio-frequency circuit to the slow-wave structure at the input and output. The velocity of the electron stream is adjusted to be approximately the same as the phase velocity of the wave on the circuit.

When a wave is launched on the circuit, the longitudinal component of its field interacts with the electrons traveling along in approximate synchronism with it. Some electrons will be accelerated and some decelerated, resulting in a progressive rearrangement in phase of the electrons with respect to the wave. The electron stream, thus modulated, in turn induces additional waves on the helix. This process of mutual interaction continues along the length of the tube with the net result that direct-current energy is given up by the electron stream to the circuit as radio-frequency energy, and the wave is thus amplified.

By virtue of the continuous interaction between a wave traveling on a broadband circuit and an electron stream, traveling-wave tubes do not suffer the gain–bandwidth limitation of ordinary types of electron tubes. By proper circuit design, such tubes are made to have bandwidths of an octave in frequency, and even more in special cases.

The helix* is an extremely useful form of slow-wave circuit because the impedance that it presents to the wave is relatively high and because when properly proportioned, its phase velocity is almost independent of frequency over a wide range.

An essential feature of this type of tube is the approximate synchronism between the electron stream and the wave. For this reason, the traveling-wave tube will operate correctly only over a limited range in voltage. Practical considerations require that the operating voltages be kept as low as is consistent with obtaining the necessary beam input power; the voltage, in turn, dictates the phase velocity of the circuit. The electron velocity v in

* S. Sensiper, "Electromagnetic Wave Propagation on Helical Structures," *Proceedings of the IRE*, vol. 43, pp. 149–161; February, 1955.

Microwave tubes *continued*

centimeters/second is determined by the accelerating voltage V in accordance with the relationship

$$v = 5.93 \times 10^7 V^{1/2}$$

Fig. 24 shows a typical relationship between gain and beam voltage.

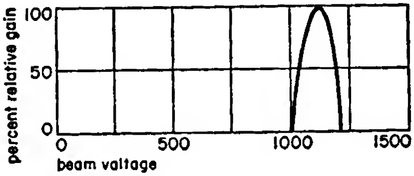

Fig. 24—Traveling-wave-tube gain versus accelerating voltage.

The gain of a traveling-wave tube is given approximately by

$$G = A + BCN$$

in decibels where

A = the initial loss due to the establishment of the modes on the helix and lies in the range from -6 to -9 decibels.

B = a gain coefficient that accounts for the effect of circuit attenuation and space charge.

C = a gain parameter that depends upon the impedances of the circuit and the electron stream

$$= \left[\frac{E^2}{(\omega/v)^2 P} \times \frac{I_0}{8V_0}\right]^{1/3}$$

I_0 = beam current

V_0 = beam voltage

N = number of active wavelengths in tube

$= (l/\lambda_0)\ (c/v)$

l = axial length of the helix

λ_0 = free-space wavelength

v = phase velocity of wave along tube

c = velocity of light

The term $E^2/(\omega/v)^2P$ is a normalized wave impedance that may be defined in a number of ways.

In practice, the attenuation of the circuit will vary along the tube and the gain per unit length will consequently not be constant. The total gain will be a summation of the gains of various sections of the tube.

Microwave tubes *continued*

Commonly, C is of the order of 0.02 to 0.2 in helix traveling-wave tubes. The gain of low- and medium-power tubes varies from 20 to 50 decibels with 30 decibels being a common value. The gain in a tube designed to produce appreciable power will vary somewhat with signal level when the beam voltage is adjusted for optimum operation. Fig. 25 shows a typical characteristic.

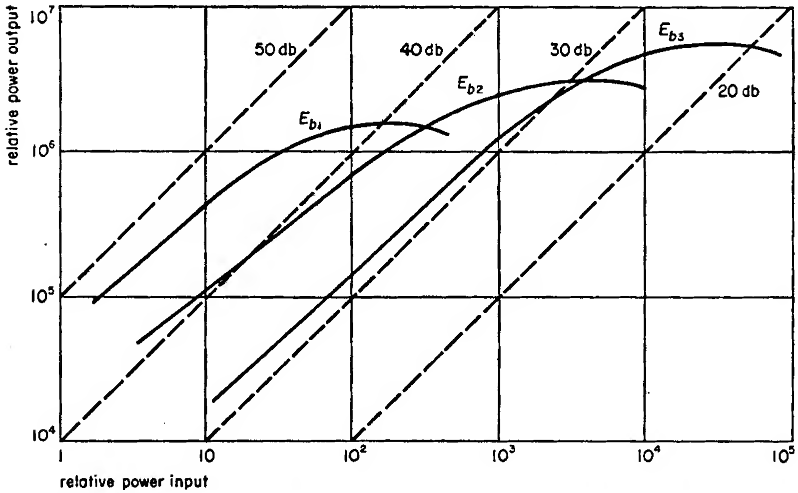

Fig. 25—Gain of traveling-wave tube as a function of input level and beam voltage. $E_{b1} < E_{b2} < E_{b3}$.

To restrain the physical size of the electron stream as it travels along the tube, it is necessary to provide a longitudinal magnetic field of a strength appropriate to overcome the space-charge forces that would otherwise cause the beam to spread. In most cases, an electromagnet is used to provide the field, but permanent-magnet structures have been used experimentally.

Other types of slow-wave circuit in addition to the helix are possible, including a number of periodic structures. In general, such designs are capable of operation at higher power levels but at the expense of bandwidth.

Traveling-wave-tube performance data

Traveling-wave tubes are designed to emphasize particular inherent characteristics for specific applications. Three general classes are distinguished.

Low-noise amplifiers: Tubes of this class are intended for the first stage of

Microwave tubes *continued*

a receiver and are proportioned to have the best possible noise figure. This requires that the random variations in the electron stream be minimized and that steps be taken also to minimize partition noise. Tubes have been made with noise figures of around 7 decibels in the frequency range from 3000 to 11,000 megacycles. Gains of the order of 20 to 25 decibels are customary. The maximum output power will be of the order of a few milliwatts.

Intermediate power amplifiers: These tubes are intended to provide power gain under conditions where neither noise nor large values of power output are of importance. Gains of 30 or more decibels are customary and the maximum output power is usually in the range from 100 milliwatts to 1 watt.

Power amplifiers: For this class of tubes, the application is usually the output stage of a transmitter; the power output, either continuous-wave or pulsed, is of primary importance. Much active development continues in this area and the values of power that can be obtained are expected to change. At this writing, continuous-wave powers range from a few kilowatts in the ultra-high-frequency region to approximately 10 watts at 9000 megacycles. Tubes especially designed for pulsed operation provide considerably higher powers. Efficiencies in excess of 30 percent have been obtained, with 20 percent being a usual value. Power gains of 30 or more decibels are usual.

Backward-wave oscillators*

Although the traveling-wave tube can be made to oscillate by the provision of a suitable feedback circuit from output to input, a new type of tube that is designed for this purpose gives improved performance for many applications. The backward-wave oscillator resembles closely the traveling-wave tube except for the fundamental difference that the electron stream interacts with a wave whose phase and group velocities are in opposite directions.

The backward-wave oscillator has a number of useful properties: it may be tuned electronically over a wide range of frequencies, an octave or more; its frequency is relatively unaffected by the load; and it is stable. In the first two respects, it is superior to the reflex klystron.

* R. Kompfner and N. T. Williams, "Backward-Wave Tubes," *Proceedings of the IRE*, vol. 41, pp. 1602–1611; November, 1953. H. R. Johnson, "Backward-Wave Oscillators," *Proceedings of the IRE*, vol. 43, pp. 684–697; June, 1955. R. R. Warnecke, P. Guénard, O. Doehler, and B. Epsztein, "The 'M'-type Carcinotron Tube," *Proceedings of the IRE*, vol. 43, pp. 413–424; April, 1955.

Microwave tubes *continued*

Backward-wave oscillator tubes are of two general types: low-power types suitable for local-oscillator or signal-generator use, having a wide tuning range and a power output of from one to tens of milliwatts; and high-power types, generally of the transverse-magnetic-field type, having power outputs of a hundred watts or more.

Photometry

Photometric units

Light flux is the quantity of light transmitted through a given area/unit time. It is expressed in lumens.

Light intensity $I = \phi/\omega$, or better, $I = d\phi/d\omega$ = light flux emitted into unit solid angle. It is expressed in candles. Experimentally, the candle is defined (since 1948) by specifying the brightness of a black body at the temperature of freezing platinum (2042 degrees kelvin) as 60 stilb. In German literature, the Hefner-candle (HK) is used; 1 (HK) = 0.92 candle.

Illumination E = light flux incident/unit projected area, expressed in lumens/foot^2, or lux = lumens/meter^2, or phots = lumens/centimeter^2. These are commonly called foot-candles, meter-candles, etc., but the word candle must here be regarded as a misnomer.

Brightness B = light intensity/unit projected area, equivalent to light flux/unit projected area/steradian. Expressed in (*a*) candles/foot^2 or stilbs = candles/centimeter^2. Also expressed in (*b*) 1 lambert = $(1/\pi)$ stilb, or 1 foot-lambert = $(1/\pi)$ candle/foot^2, or 1 apostilb = 10^{-4} lambert, etc. Various derived units as 1 candle/meter^2, or 1 milli- or microlambert (= 10^{-3} or 10^{-6} lambert) occur in the literature. The units under (*b*) are so chosen that they assume the value 1 for a diffuse emitting surface radiating 1 lumen/unit area.

Photometric relations

Illumination: A point light source of intensity 1 candle illuminating perpendicularly a screen at a distance of r feet causes an illumination of I/r^2 foot-candles on it.

Lambert's law: (Not always valid.) A diffusely radiating plane surface radiates into a direction forming an angle θ with its normal, a flux proportional to $\cos\theta$. A surface obeying Lambert's law has the same brightness when viewed from any direction.

Photometry *continued*

Brightness of illuminated surfaces: If a diffusely reflecting area of A feet^2 is illuminated from any direction with E foot-candles, it reradiates REA lumens into a hemisphere: R is the reflection factor; $R = 1$ for an ideal white area. Its brightness then is RE/π candles/foot^2 or RE foot-lamberts.

Optical imaging: In an optical system of light-gathering diameter D and focal length f, the ratio $f/D = n_f$ is called the f-number. If a surface of brightness B candles/foot^2 is imaged by the system with a linear magnification m, the image is illuminated by

$$E = \frac{\pi}{4} \frac{B}{n_f^2 (m + 1)^2}$$

foot-candles, disregarding lens losses. For an object at infinity, the same formula applies with $m = 0$. Thus, while the amount of flux intercepted by the system depends on D, the illumination and brightness depend only on n_f.

The brightness of an image can never exceed that of the object; it becomes equal to it if the system has no losses and is sharply focussed. This applies to the case where object and image lie in the same optical medium; otherwise, if n_o and n_i are the refractive indices of the object and image space,

$$n_i B_i \leqslant n_o B_o.$$

General data

Spectral response of the eye: The relative visibility of different wavelengths as experienced by the eye in bright light (cone vision) is given in Fig. 26.

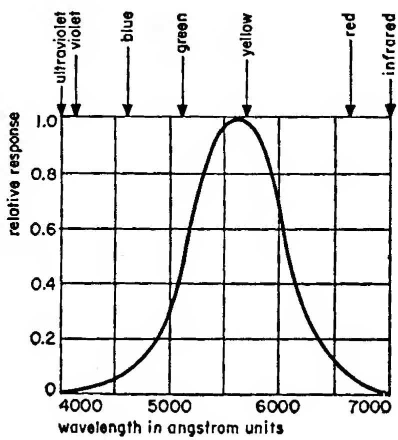

Fig. 26—Spectral response of human eye.

Mechanical equivalent of light: A light source having a spectral distribution as given by Fig. 26 and emitting 1 lumen, radiates 0.00147 watts.

Illumination at Earth's surface:

Sun at zenith = 10,000 foot-candles

Full moon = 0.03 foot-candles

Photometry *continued*

Approximate brightness values:

Highlights, 35-millimeter movie	0.004 lamberts
Page brightness for reading fine print	0.011 lamberts
November football field	0.054 lamberts
Surface of moon seen from Earth	1.6 lamberts
Summer baseball field	3 lamberts
Surface of 40-watt vacuum bulb, frosted	8 lamberts
Crater of carbon arc	45,000 lamberts
Sun seen from Earth	520,000 lamberts

Colorimetry: This subject is treated with special emphasis on color-television requirements in the literature. Two books and three papers are of particular interest.*

Cathode-ray tubes†

A cathode-ray tube is a vacuum tube in which an electron beam, deflected by applied electric and/or magnetic fields, indicates by a trace on a fluorescent screen the instantaneous value of the actuating voltages

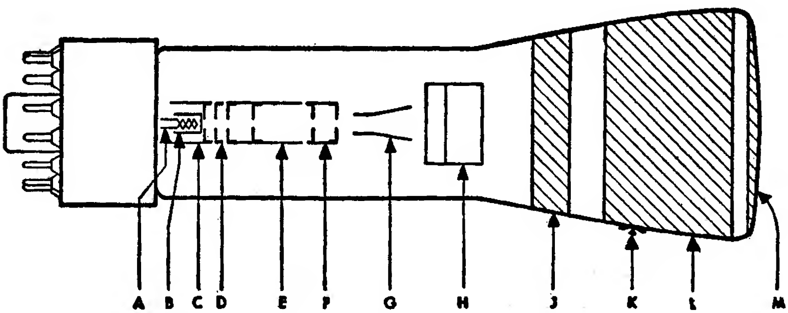

Fig. 27—Electrode arrangement of typical electrostatic focus and deflection cathode-ray tube. A–heater, B–cathode, C–control electrode, D–screen grid or pre-accelerator, E–focusing electrode, F–accelerating electrode, G–deflection-plate pair, H–deflection-plate pair, J–conductive coating connected to accelerating electrode, K–intensifier-electrode terminal, L–intensifier electrode (conductive coating on glass), M–fluorescent screen.

* D. G. Fink, "Television Engineering," 2nd edition, McGraw-Hill Book Company, Inc., New York, New York; 1952. M. S. Kiver, "Color Television Fundamentals," McGraw-Hill Book Company, Inc., New York, New York; 1955. F. J. Bingley, "Colorimetry in Television," *Proceedings of the IRE*, vol. 41, pp. 838–851; July, 1953: vol. 42, pp. 48–51 and 51–57; January, 1954.

† K. R. Spangenberg, "Vacuum Tubes," 1st ed., McGraw-Hill Book Company, Inc., New York, New York; 1948.

Cathode-ray tubes *continued*

and/or currents. A typical high-intensity cathode-ray tube with post-deflection acceleration is shown in Fig. 27.

Formulas for deflection

Electric-field deflection: Is proportional to the deflection voltage, inversely proportional to the accelerating voltage, and deflection is in the direction of the applied field (Fig. 28). For structures using straight and parallel deflection plates, it is given by

$$D = \frac{E_d L l}{2 E_a A}$$

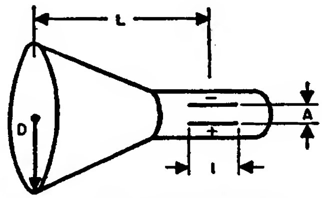

Fig. 28—Electrostatic deflection.

where

D = deflection in centimeters
E_a = accelerating voltage
E_d = deflection voltage
l = length of deflecting plates or deflecting field in centimeters
L = length from center of deflecting field to screen in centimeters
A = separation of plates

Magnetic-field deflection: Is proportional to the flux or the current in the coil, inversely proportional to the square root of the accelerating voltage, and deflection is at right angles to the direction of the applied field (Fig. 29).

Deflection is given by

$$D = \frac{0.3 L l H}{\sqrt{E_a}}$$

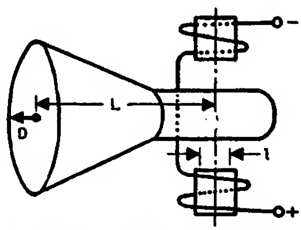

Fig. 29—Magnetic deflection.

where H = flux density in gausses
l = length of deflecting field in centimeters

Deflection sensitivity: Is linear up to frequency where the phase of the deflecting voltage begins to reverse before an electron has reached the end of the deflecting field. Beyond this frequency, sensitivity drops off, reaching

Cathode-ray tubes *continued*

zero and then passing through a series of maxima and minima as n = 1, 2, 3, ... Each succeeding maximum is of smaller magnitude.

$$D_{zero} = n\lambda\, v/c$$

$$D_{max} = (2n - 1)\,\frac{\lambda}{2}\,\frac{v}{c}$$

where

D = deflection in centimeters

v = electron velocity in centimeters/second

c = speed of light (3×10^{10} centimeters/second)

λ = free-space wavelength in centimeters

Magnetic focusing: There is more than one value of current that will focus. Best focus is at minimum value. For an average coil

$$IN = 220\,(V_0 d/f)^{1/2}$$

IN = ampere turns

V_0 = accelerating voltage in kilovolts

d = mean diameter of coil

f = focal length

d and f are in the same units. A well-designed, shielded coil will require fewer ampere turns.

Example of good shield design (Fig. 30):

$$X = d_1/20$$

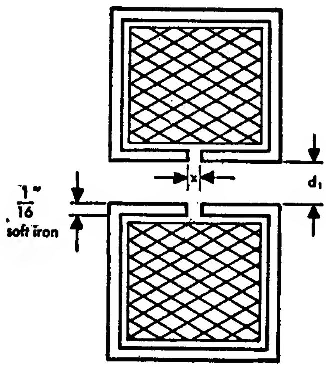

Fig. 30—Magnetic focusing.

Cathode-ray tubes *continued*

Cathode-ray tube phosphors*

designation	color: fluorescent	color: phosphorescent	spectral range between 10% points in angstrom units	spectral peak in angstron units	persistance (approximate time to decay to 10% of peak)
P1	Green	Green	4900–5800	5250	20 milliseconds
P2	Blue-green	Green	4500–6400	5430	Long
P3	Yellow	Yellow	5040–7000	6020	13 milliseconds
P4	White	White	3900–6630	2 components: 5650, 4400	Not over 7% of peak in 33 milliseconds
P4, silicate	White	Blue	3260–7040	2 components: 5400, 4100	
P4, silicate–sulfide	White	Yellow	3300–6990	2 components: 5400, 4350	
P5	Blue	Blue	3480–5750	4300	18 microseconds
P6	White	White	4160–6950	2 components: 5630, 4600	800 microseconds
P7	Blue-white	Yellow	3900–6500	2 components: 5580, 4400	One long, one short
P10	Dark-trace: color depends on absorption characteristics, type of illumination		4000–5500	—	Very long
P11	Blue	Blue	4000–5500	4600	2 milliseconds
P12	Orange	Orange	5450–6800	5900	Medium long
P14	Purple	Orange	3900–7100	2 components: 6010, 4400	One short, one medium long
P15	Blue-green	Blue-green	3700–6050	2 components: 5040, 3910	3 microseconds
P16	Violet and near ultraviolet	Violet and near ultraviolet	3350–4370	3700	5 microseconds
P17	Greenish-yellow	Yellow	3800–6350	2 components: 4500, 5540	One long, one extremely short
P18	White	Blue	3260–7040	2 components: 5400, 4100	13 milliseconds
P19	Orange	Orange	5450–6650	5950	Very long
P20	Yellow-green	Yellow-green	4600–6490	5550	2 milliseconds
P21	Yellow	Yellow	5540–6500	6060	Very long
P22	Tricolor	—	3900–6800	3 components: 6430, 5260, 4500	One short, two medium
P23	White	White	4000–7200	2 components: 5750, 4600	Short
P24	Blue-green	Blue-green	4260–6400	5070	1.5 microseconds
P25	Orange	Orange	5300–7100	6100	Very long

* Source: Joint Electron Tube Engineering Council, Committee 6 on Cathode-Ray Tubes.

Photosensitive tubes*

Photoemission

If monochromatic light impinges on a cathode, electrons are emitted. Such electrons are known as photoelectrons. Their number is proportional to the incoming light flux, while their energy is independent of it. The energy expressed in volts V depends on the wavelength λ according to Einstein's law:

$$e\,(V + \phi) = hc/\lambda$$

where

e = electronic charge

$= 1.6 \times 10^{-19}$ coulomb

ϕ = work function in volts

h = Planck's constant

$= 6.6 \times 10^{-34}$ joule–seconds

c = velocity of light

$= 3 \times 10^{10}$ centimeters/second

If a threshold wavelength λ_0 is defined by

$$e\phi = hc/\lambda_0$$

V is seen to be zero (except for thermal velocities) at the wavelength λ_0; for $\lambda > \lambda_0$, there is no electron emission.

The photosurfaces most in use are

S1 (silver–cesium): λ_0 = 12,000 angstrom units

yield = 20 microamperes/lumen

S4 (antimony–cesium): λ_0 = 6,000 angstrom units

yield = 50 microamperes/lumen

where the yield data give the representative response to white light (2870-degree-Kelvin tungsten filament). Another way of specifying the yield, applicable only for monochromatic light, is the quantum equivalent Q; i.e., the number of electrons emitted/incoming photon (hc/λ). For the *S1* surface, Q is approximately 1.5 percent at 4000 angstrom units and

* Only photoemissive electron tubes are considered here. Photoconductive and photovoltaic devices are usually not built in the form of tubes.

Photosensitive tubes *continued*

0.8 percent at 8000 angstrom units. *S4* layers have a peak response near 4500 angstrom units, with Q = 16 percent. The quantum equivalent decreases, in all surfaces, to very low values at the threshold wavelength. Pure metals are photoemissive in the ultraviolet and all substances will emit electrons under X-ray irradiation.

Vacuum phototubes

The cathode is a solid metal plate or a translucent layer on the glass wall. The anode may be a plate, rod, or wire screen. Except for very-strong light or unfavorable circuit conditions, a few volts suffice to saturate the photocurrent. The battery *E*, Fig. 31, has to provide, besides this accelerating potential, the voltage drop across resistor R_l. The familiar graphical load-line method applies in this case.

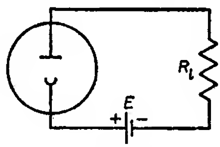

Fig. 31—Phototube circuit.

The saturation current is proportional to the incoming light flux. Exceptions may occur at the very-lowest light levels (dark current from thermionic emission at room temperature, important only in *S1* surfaces) and at the highest ones, where space charge may prevent saturation or, in translucent cathodes, the conductivity of the cathode may not suffice to provide the full photocurrent. The most important noise source (other than light fluctuations or background illumination) is the shot effect accompanying the photocurrent.

Gas phototubes

In tubes not containing a high vacuum, ionization by collision of electrons with neutral molecules may occur so that more than one electron reaches the anode for each originally emitted photoelectron. This "gas amplification factor" has a value of between 3 and 5; a higher factor causes instabilities. Gas tubes operation is restricted to frequencies below 10,000 cycles/second.

Secondary electron emission from metals

If a metal is bombarded with electrons of *V* volts velocity, it reemits electrons that can be detected if the field near the surface is such as to accelerate these electrons away from the metal. This is the process of secondary emission and the electrons are termed secondary electrons. The returning electrons form two groups: one with velocities equal or almost equal to that of the primaries (reflected electrons) and one with a velocity of 2–10

Photosensitive tubes *continued*

volts for $20 < V < 1000$ volts (true secondaries). The two groups cannot be distinguished at $V < 20$ volts.

The secondary-emission factor K is defined as the ratio (true secondaries)/(primaries). Factor K has a maximum at $V = V_m$ (400–1000 volts, depending on the material). This maximum may range from < 1 (for carbon) to < 2 for most pure metals, but in some alloys, K rises to as much as 12. At higher values of V, factor K decreases and goes below 1 at a few thousand volts. At $V < V_m$, there is a decrease again and K reaches the value 1 at about 25–50 volts for good secondary-emitting alloys.

Where high secondary emission is desired, one of the following alloys is commonly used: silver–cesium, antimony–cesium, silver–magnesium, beryllium–copper. These show at 100 volts, values of K from 2.5 to 4.

Multiplier phototubes

Secondary-emission multiplication is used to provide amplification of weak currents in multiplier phototubes. A typical structure is shown in Fig. 32. Photoelectrons from the photocathode are focussed electrostatically onto the first secondary-emitting dynode, *1*. The resulting secondary electrons are then focussed on dynode 2, and so on. With each successive dynode, the current is amplified by the secondary emission factor, K, or a total of K^n times for n stages. The current is finally collected on an output electrode, usually called the collector.

Multiplier circuits: The voltage steps from stage to stage are usually made equal. Occasionally, the first or last step (cathode to 1st dynode or last dynode to collector) is made larger; the former has the effect of increasing the first-stage gain which reduces the noise, while the latter is done to relieve space-charge limitations at the output.

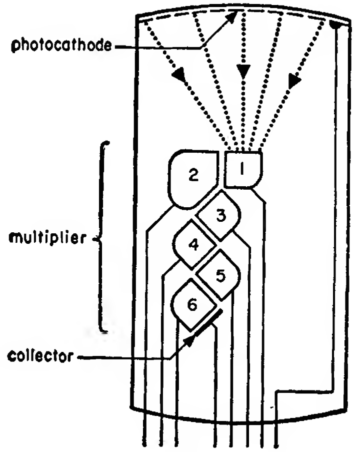

Fig. 32—Six-stage multiplier phototube.

The electrons hitting stage j (Fig. 33) constitute a current I_j leaving stage j, while $I_{j+1} = KI_j$ flows into stage j. It is seen from the figure that these

Photosensitive tubes *continued*

currents are completed through the divider. It is common practice to make the divider current at least 10 times the output signal, or in an n-stage multiplier,

$$R_d < E/10\,(n+1)\,i_c$$

The load resistor R_l is determined by bandwidth considerations. It is parallelled by the output capacitance of the multiplier (3–5 micromicrofarads) and the input capacitance of the following stage.

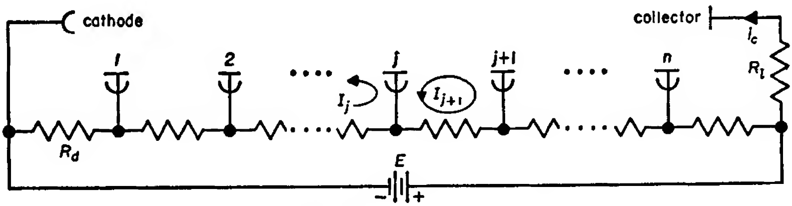

Fig. 33—Circuit of multiplier phototube.

Multiplier signal and noise: The upper frequency limit of a multiplier (usually about 30 megacycles) is determined by the transit-time spread, i.e., the differences in transit times between the individual electrons.

If the photocathode receives L lumens and emits S amperes/lumen, then LS amperes flow into the first stage and the output current at the collector is LSK^n. Even if the light flux is free of fluctuations, the cathode current LS will carry shot-effect noise, with a root-mean-square value of

$$I_{cn} = (2\,LS\,eF)^{1/2}$$

where

e = electronic charge

F = bandwidth in cycles/second

The output noise current is then

$$I_n = kK^n I_{cn}$$

where the factor k arises from the fact that secondary emission is itself a random process. Approximately,

$$k = [K/(K-1)]^{1/2}$$

This assumes that no other noise sources are present, such as leakage, positive ions, or a ripple in the applied voltage. In the neighborhood of

Photosensitive tubes *continued*

$V_s = 100$ V/stage, factor K is proportional to V_s^{α}, where α lies between 0.5 and 0.7; hence p-percent ripple on the applied voltage E would give $n\alpha p$-percent ripple in the collector current.

Image dissector

The image dissector is a television camera tube having a continuous photocathode on which is formed a photoelectric emission pattern that is scanned by moving its electron-optical image over an aperture.

Principle of dissector operation: From the optical image focused on the photocathode (Fig. 34), an electro-optical image is derived that is focused in the plane containing the aperture. Two sets of scanning coils sweep this image over the aperture. At any instant, only the electrons entering the electron multiplier through the aperture are utilized. The output signal is taken from the multiplier collector.

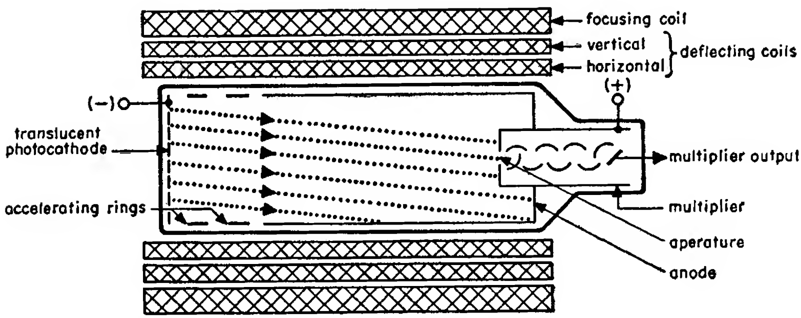

Fig. 34—Image dissector.

No storage means are used, and therefore, the dissector is not suitable at very-low light levels. But the output signal is proportional to the light, free from shading, and, within reasonable limits, independent of temperature.

With a long focus coil (as in Fig. 34), the electron-optical magnification from cathode to aperture is unity. With a short focus coil it is possible to obtain a magnification m with $\frac{1}{3} < m < 3$. If a is the aperture area, a picture element on the cathode has a size a/m^2; this determines the resolution.

S1 or *S4* photocathodes may be used.

Dissector focusing and scanning fields: If the aperture is distant from the

Photosensitive tubes *continued*

cathode by d centimeters and has a voltage of V volts above cathode potential, a focusing field of

$$H_0 = c\,V^{1/2}/d$$

oersteds is needed; $c = 15$ (approximately) for first focus.

To bring into the aperture electrons that originate at a point on the cathode r centimeters from center, the instantaneous transverse scanning field has to be

$$H_t = H_0 r/d$$

Dissector signal and noise: Let

S = sensitivity of cathode in amperes/lumen

E = illumination on cathode in foot-candles

e = electronic charge

$= 1.6 \times 10^{-19}$ coulomb

F = bandwidth in cycles/second

k = noise contribution of multiplier (see "Multiplier phototubes", p. 409)

$= 1.25$ (approximately)

G = multiplier gain

a = aperture area in feet^2

m = magnification

Then, signal output current

$$I_s = SE\,(a/m^2)\,G$$

and the noise output current

$$I_n = k[2\,SEe\,(a/m^2)\,F]^{1/2}\,G$$

To take account of the dark noise, E should be replaced by $E + E_0$ in the noise formula, where E_0 is about 0.01 footcandles for an $S1$ photocathode and about 5×10^{-6} footcandles for $S4$.

For a frame of area A_f and a frame time T_f, containing N picture elements,

$$a = A_f m^2/N$$

$$F = N/2T_f$$

Photosensitive tubes *continued*

Image orthicon

The image orthicon is a television camera tube having a sensitivity and spectral response approaching that of the eye. Commercially acceptable pictures can be obtained with incident illumination levels $\geqslant$ 10 foot–candles.

As shown in Fig. 35, the tube comprises three sections: an image section, a scanning section, and a multiplier section.

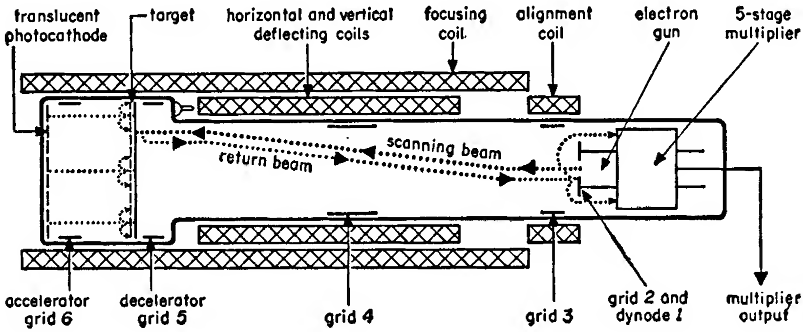

Fig. 35—Image orthicon. *By Permission of RCA, copyright proprietor.*

Principle of orthicon operation: From the light image focused on the photocathode, an electron image is derived that is accelerated to and magnetically focused in the plane of the target. These primary electrons striking the glass target (thickness of the order of a ten-thousandth of an inch and a lateral electrical resistivity of between 3×10^{11} and 10^{12} ohm-centimeter) cause the emission of secondary electrons that are collected by an adjacent mesh screen held at a small positive potential with respect to target-voltage cutoff. The photocathode side of the target thus has a pattern of positive charges that corresponds to the light pattern from the scene being televised; since the glass target is very thin, the charges set up a similar potential pattern on the opposite or scanned side of the glass.

In the scanning section, the target is scanned by a low-velocity electron beam produced by an electron gun. The beam is focused at the target by means of the axial magnetic field of the external focusing coiland the electrostatic field of grid 4. The decelerating field between grids 4 and 5 is shaped such that the electron beam always approaches normal to the plane of the target and is at a low velocity. If the elemental area on the target is positive, then electrons from the scanning beam deposit until the charge is neutralized; if the elemental area is at cathode potential (i.e., corresponding to a black

Photosensitive tubes *continued*

picture area), no electrons are deposited. In both cases the excess beam electrons are turned back and focused into a 5-stage signal multiplier. The charges existing on either side of the target glass will by conductivity neutralize each other in less than one frame time. Electrons turned back at the target form a return beam that has been amplitude-modulated in accordance with the charge pattern of the target.

Alignment of the electron beam is accomplished by the transverse magnetic field of the external alignment coil. Deflection of the beam is produced by the transverse magnetic fields of the external horizontal and vertical deflecting coils.

In the multiplier section, the return beam is directed to the first stage of the electrostatically focused, 5-stage multiplier where secondary electrons are emitted in quantities greater than the striking primary electrons. Grid 3 facilitates a more complete collection by dynode 2 of the secondary electrons from dynode 1. The gain of the multiplier is high enough that the limiting noise in the use of the tube is the random noise of the electron beam rather than the input noise of the video amplifier.

For highlights in the scene, the grid of the first video-amplifier stage will swing positive.

Orthicon operating considerations: The temperature of the entire bulb should be held between 45 and 60 degrees centigrade since low target temperatures are characterized by a rapidly disappearing "sticking picture" of opposite polarity from the original when the picture is moved; high temperatures will cause loss of resolution and damage to the tube.

An over-all potential of 1750 volts is necessary to operate the tube (+1250 volts at 1 milliampere, −500 volts at 1 milliampere, and +330 volts at 90 milliamperes for the voltage divider and typical focusing and alignment coils).

The video amplifier should be designed to accept a range of alternating-current signal voltages corresponding to signal-output currents of 1 to 30 microamperes (depending on the tube type) in the load resistor. Resolution of 300 lines at 70-percent modulation and 600 lines at 15 percent can be produced when the photocathode highlight illumination from a Radio-Electronics-Television Manufacturers Association Standard Test Chart is above the knee of the output-current versus photocathode-illumination curve.

The maximum band pass of the amplifier can be determined* as follows:

* D. G. Fink, "Television Engineering," 2nd edition, McGraw-Hill Book Company, Inc., New York, New York; 1952.

Photosensitive tubes *continued*

$f_{max} = \frac{1}{2} kmn^2 f \, (w/h) \; (k_v/k_h)$

where

f_{max} = amplifier band pass in cycles/second

k = vertical resolution factor, representing the effect of random positioning of the picture elements with respect to the transmitter scanning lines, usually 70.7 percent

m = horizontal resolution divided by the vertical resolution

n = number of lines in the picture

f = number of picture frames/second

w/h = aspect ratio
= (picture width)/(picture height)

k_v = fraction of total field time devoted to scanning picture elements

k_h = fraction of line-scanning time during which the scanning lines are active

Full-size scanning of the target should always be used during operation. The blanking signal, a series of negative-voltage pulses, should be supplied to the target to prevent the electron beam from striking the target during retrace. In the event of scanning failure, the beam must not reach the target.

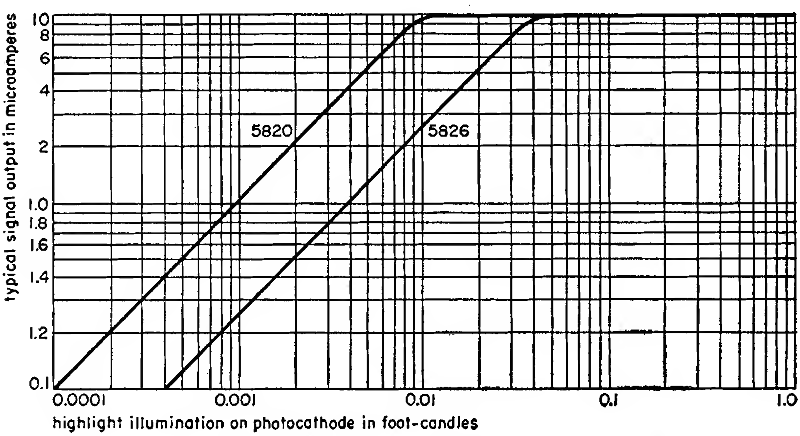

Fig. 36—Basic light-transfer characteristic for types *5820* and *5826* image orthicons. The curves are for small-area highlights illuminated by tungsten light, white fluorescent light, or daylight.

By Permission of RCA, copyright proprietor.

Photosensitive tubes *continued*

It is necessary to add a shading-correction signal, of sawtooth shape and of horizontal-scan frequency, to the video signal after it has been clamped to obtain a uniformly shaded picture.

The illumination on the photocathode is related to the scene illumination by the formula for optical imaging given on p. 401.

Orthicon signal and noise: Typical signal output current for the types *5820* and *5826* are shown in Fig. 36.

The tubes should be operated so that the highlights on the photocathode bring the signal output slightly over the knee of the signal-output curve.

The spectral response of the types *5820* and *5826* is shown in Fig. 37. It will be noted that when a Wratten 6 filter is used with the tube, a spectral curve closely approximating that of the human eye is obtained.

From the standpoint of noise, the total television system can be represented as shown in Fig. 38 where the following definitions hold:

F = bandwidth in cycles/second

I_s = signal current

I_n = total image-orthicon noise current

e = electronic charge
= 1.6×10^{-19} coulombs

I = image-orthicon beam current

E_{nt} = thermal noise in R_1

E_{ns} = shot noise in the input amplifier tube

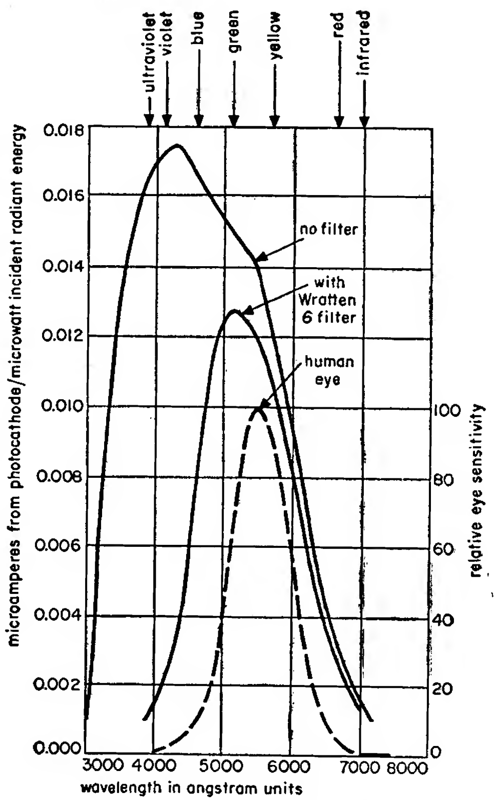

By Permission of RCA, copyright proprietor.

Fig. 37—Spectral sensitivity of image orthicon.

Photosensitive tubes *continued*

R_1 = input load

C_1 = total input shunt capacitance

R_t = shot-noise equivalent resistance of the input amplifier

$= 2.5/g_m$ for triode or cascode input

$$= \frac{I_b}{I_b + I_c}\left(\frac{2.5}{g_m} + \frac{20I_{c2}}{g_m{}^2}\right) \text{ for pentode input}$$

g_m = transconductance of input tube or cascode combination

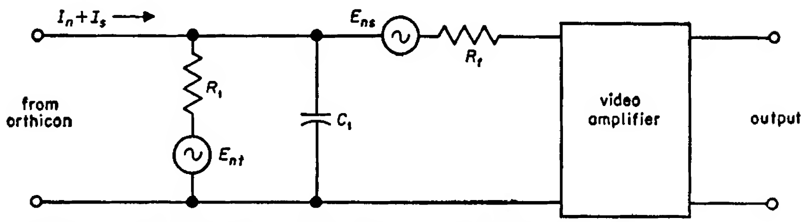

Fig. 38—Equivalent circuit for noise in orthicon and first amplifier stage.

I_b = amplifier direct plate current

I_c = amplifier direct screen-grid current

ΔN = electron-multiplier noise factor referred to multiplier input

m = multiplier gain

k_m = electron-multiplier noise factor, referred to multiplier output

$= m\Delta N$

σ = stage gain in the multiplier

k = Boltzmann's constant

$= 1.38 \times 10^{-23}$ joules/degree Kelvin

T = absolute temperature in degrees Kelvin

The noise added per stage is

$$\Delta n = [\sigma/(\sigma - 1)]^{1/2}$$

For a total multiplier noise figure to be directly usable, it must be referred to the first-dynode current, therefore, for 5 multiplier stages,

Photosensitive tubes *continued*

$$\overline{\Delta N} = \Delta n^2 + \frac{\Delta n^2}{\sigma^2} + \frac{\Delta n^2}{\sigma^4} + \frac{\Delta n^2}{\sigma^6} + \frac{\Delta n^2}{\sigma^8}$$

After combining all noise sources,

$$\frac{S}{N} = \frac{I_s}{\left\{F\left[2eIK_m^2 + 4KT\left(\frac{1}{R_1} + \frac{R_t}{R_1} + \frac{\omega^2 C_1^2 R_t}{3}\right)\right]\right\}^{1/2}}$$

The signal current is an alternating-current signal superimposed on a larger direct beam current. This can be thought of as a modulation of the beam current. Properly adjusted tubes obtain as much as 30-percent modulation.

$I_s = mMI$

where M is the percentage modulation.

If S/N is now rewritten,

$$\frac{S}{N} = \frac{I_s}{\left[4kTF\left(\frac{2eI_s m \overline{\Delta N}^2}{4KTM} + \frac{1}{R_1} + \frac{R_t}{R_1^2} + \frac{\omega^2 C_1^2 R_t}{3}\right)\right]^{1/2}}$$

In typical television operation, the thermal noise of the load resistor and the shot noise of the first amplifier can be neglected.

Orthicon focusing and scanning fields: The electron optics of the scanning section of the tube are quite complicated and space does not permit the

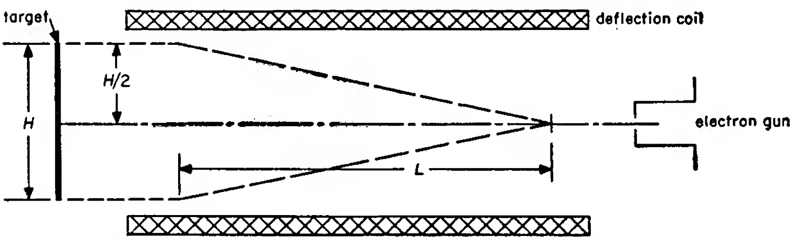

Fig. 39—Deflection in image orthicon.

inclusion of the complete formulas. A simple relationship between the strength of the magnetic focusing field and the magnetic deflection field is given below. It should be noted that the electron beam does not reach first focus at the target but rather considerably before it reaches the target; thus the beam is working at a higher-order focus. This means that the radii

Photosensitive tubes *continued*

of the focus helixes are kept small and all of the electrons in the beam approach the target perpendicular to its surface, thereby avoiding shading in the output video signal. Working at a higher-order focus not only demands more focus current but also more deflection current. Note the deflection path in Fig. 39. Let

H = horizontal dimension of scanned area or target

L = effective length of horizontal deflection field

H_d = horizontal deflection field (peak-to-peak value)

H_f = focusing field

then

$$H_d = H_f\, H/L$$

For the image orthicon,

$H \approx 1.25$ inches

$L \approx 4$ inches

$H_f \approx 75$ gausses

then

$H_d \approx 23$ gausses

Vidicon

The vidicon is a small television camera tube that is used primarily in industrial television and studio film pickup because of its 600-line resolution, small size, simplicity, and spectral response approaching that of the human

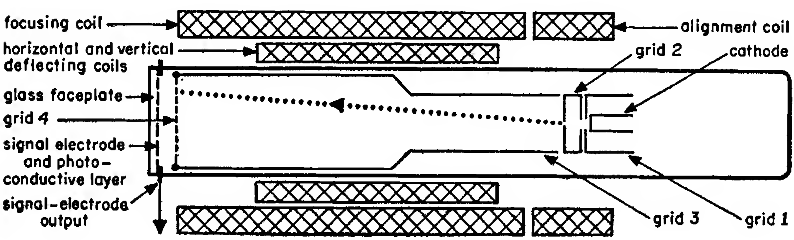

Fig. 40—Vidicon construction. *By Permission of RCA, copyright proprietor.*

Photosensitive tubes *continued*

eye. As shown in Fig. 40, the tube consists of a signal electrode composed of a transparent conducting film on the inner surface of the faceplate; a thin layer (a few microns) of photoconductive material deposited on the signal electrode; a fine mesh screen, grid *4*, located adjacent to the photoconductive layer; a focusing electrode, grid *3*, connected to grid *4*; and an electron gun.

Principle of vidicon operation: Each elemental area of the photoconductor can be likened to a leaky capacitor with one plate electrically connected to the signal electrode that is at some positive voltage (usually about 20 volts) with respect to the thermionic cathode of the electron gun and the other plate floating except when commutated by the electron beam. Initially, the gun side of the photoconductive surface is charged to cathode potential by the electron gun, thus leaving a charge on each elemental capacitor. During the frame time, these capacitors discharge in accordance with the value of their leakage resistance, which is determined by the amount of light falling on that elemental area. Hence, there appears on the gun side of the photoconductive surface a positive-potential pattern corresponding to the pattern of light from the scene imaged on the opposite surface of the layer. Even those areas that are dark discharge slightly, since the dark resistivity of the material is not infinite.

The electron beam is focused at the surface of the photoconductive layer by the combined action of the uniform magnetic field and the electrostatic field of grid *3*. Grid *4* serves to provide a uniform decelerating field between itself and the photoconductive layer such that the electron beam always approaches the surface normally and at a low velocity. When the beam scans the surface, it deposits electrons where the potential of the elemental area is more positive than that of the electron-gun cathode and at this moment the electrical circuit is completed through the signal-electrode circuit to ground. The amount of signal current flowing at this moment depends upon the amount of discharge in the elemental capacitor, which in turn depends upon the amount of light falling on this area. The signal polarity is such that highlights in the scene swing the first video-amplifier-tube grid negative.

Alignment of the beam is accomplished by a transverse magnetic field produced by external coils located at the base end of the focusing coil.

Deflection of the beam is accomplished by the transverse magnetic fields produced by external deflecting coils.

Photosensitive tubes *continued*

Vidicon operating considerations: The temperature of the faceplate of the tube should never exceed 60 degrees centigrade in either operation or storage. As the temperature increases, both the signal output current and the dark current (current that flows when the photoconductive surface receives no light) increase; however, the dark current increases faster and shading (unequalness of dark current at different points on the surface) in the output signal current becomes a serious problem. Further, as the signal-electrode voltage is increased, the signal output-current-to-dark-current ratio decreases, thus increasing the shading problem.

Shielding of both the signal electrode and signal lead from external fields is highly important.

A blanking signal should be furnished to grid *1* or to the cathode to prevent the electron beam from striking the photoconductive surface during retrace of the horizontal and vertical sweeps. Failure of scanning for a few minutes may permanently damage the photoconductive surface. Full-size scanning of the surface should always be used.

The video amplifier should be capable of handling input signals of from 0.02 to 0.4 microampere through the signal-electrode load resistor. Typical signal output current versus illumination on the tube face is shown in Fig. 41.

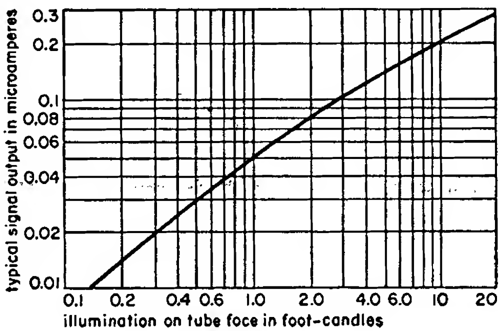

Fig. 41—Typical vidicon signal output for 2870-degree-Kelvin light uniformly distributed over photoconductive layer. Scanned area was ½ by ⅜ inches.

By Permission of RCA, copyright proprietor.

It will be noted from the curve that the gamma of the tube is less than one. The illumination falling on the tube face can be computed from the formula for optical imaging given on p. 401.

Vidicon signal and noise: Since the vidicon acts as a constant-current generator as far as signal current is concerned, the value of the load resistor is determined by band-pass and noise considerations in the input circuit of the video amplifier. The band pass is determined the same as for

Photosensitive tubes *continued*

the image orthicon on p. 413. Where the signal current is less than 1 microampere and the band pass is relatively wide, the principal noise in the system is contributed by the input circuit and first tube of the video amplifier. To minimize the thermal noise of the load resistor, its resistance is made much higher than the flat-band-pass considerations would indicate, since the signal voltage increases directly and the noise voltage increases as the square root. To correct for the attenuation of the signal with increasing frequency, the amplitude response of the video amplifier must have the following form:

$$G = G_0 \frac{(1 + 4\pi^2 F^2 C_1^2 R_1^2)^{1/2}}{R_1}$$

where G_0 = unequalized amplifier gain, Fig. 42.

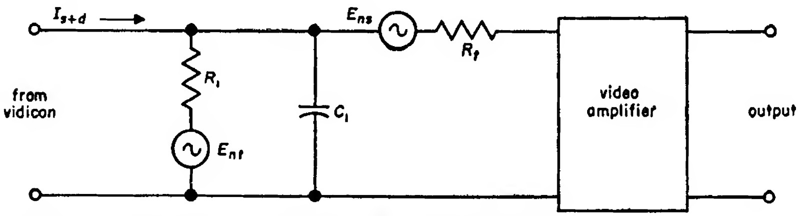

Fig. 42—Input circuit for first-stage amplifier in vidicon circuit.

The signal-to-noise ratio is

$$\frac{S}{N} = \frac{I_t}{\left[4kTF\left(\frac{1}{R_1} + \frac{R_t}{R_1^2} + \frac{4\pi^2 C_1^2 F^2 R_t}{3} + 20 I_{s+d}\right)\right]^{1/2}}$$

where

I_s = vidicon signal current

I_d = vidicon dark current

E_{nt} = thermal noise in input resistor

E_{ns} = shot noise of input amplifier tube

R_1 = input load

C_1 = total input shunt capacitance

R_t = shot-noise equivalent resistance of input amplifier

For triode or cascode input,

$R_t = 2.5/g_m$

Photosensitive tubes *continued*

and for pentode input,

$$R_t = \frac{I_b}{I_b + I_{c2}}\left(\frac{2.5}{g_m} + \frac{20 I_{c2}}{g_m^2}\right)$$

where

g_m = transconductance

I_b = direct plate current

I_{c2} = direct screen current

e = electronic charge

= 1.6×10^{-19} coulombs

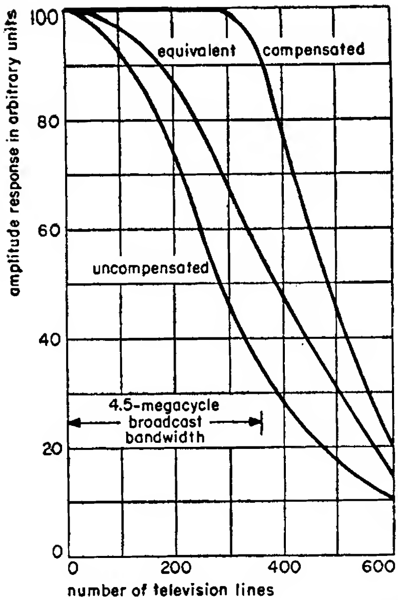

By Permission of RCA, copyright proprietor.

Fig. 43—Vidicon resolution, showing uncompensated and compensated horizontal responses and equivalent amplitude response. Highlight signal-electrode microamperes = 0.35; test pattern = transparent square-wave resolution wedge; 80 television lines = 1-megacycle bandwidth.

It will be noted from the signal-to-noise equation that the shot noise of the first amplifier tube is amplified in a frequency-selective manner, whereas the thermal noise of the load resistor has a flat frequency distribution. For a given bandwidth, as the load resistor is increased in value, the frequency at which equalization starts becomes lower and thus the shot-noise power increases in proportion to the thermal-noise power. Finally, a point is reached where the required equalization ratio is physically difficult to achieve (about 50-to-1 is maximum for a typical industrial television applications).

The resolution of a typical tube is shown in Fig. 43. The equivalent amplitude response, which is shown, is expressed by the equation,

(Equivalent amplitude response) = $(R_v R_h)^{1/2}$

where R_v and R_h = vertical and horizontal amplitude responses, respectively.

The vidicon has such a high inherent signal-to-noise ratio that aperture equalization for the scanning beam can be used when high incident illumination is available. An expression of the form:

$\gamma = 1/(1 + k_1\omega^2 + k_2\omega^4 + \ldots)$

Photosensitive tubes *continued*

Fig. 44—Vidicon persistence characteristic. Scanned area of photoconductive layer = ½ by ⅜ inch; initial output = 0.2 microampere.

By Permission of RCA, copyright proprietor.

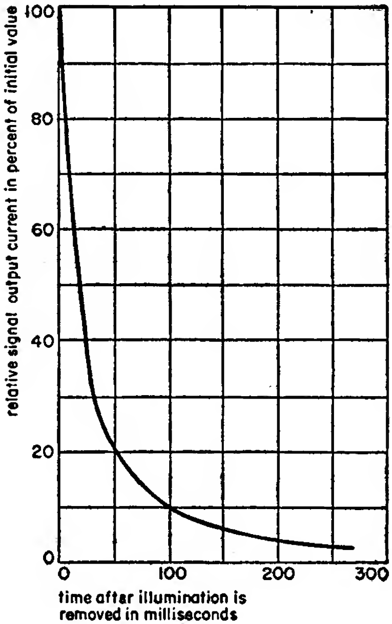

may be used to approximate the equivalent admittance of the tube. Since the scanning beam is symmetrical $(1 + \cos x)$, no phase distortion accompanies the reduction in amplitude of the higher-frequency components of the signal. In practice, the function is very nearly

$$\gamma = 1/(1 + k_1\omega^2)$$

and the correction circuit must then have the inverse response $= 1 + k_1\omega^2$. If the curve in Fig. 43 is fitted with asymptotes, one of which has a zero slope and the other a *12-decibels-per-octave slope*, then k_1 is found to be 0.0064×10^{-12}.

Aperture equalization amplifies high-frequency noise; the equation is

$$\frac{S}{N} = \frac{R_1^3 I_s^3}{(4kT\lambda)^{1/2}}$$

where

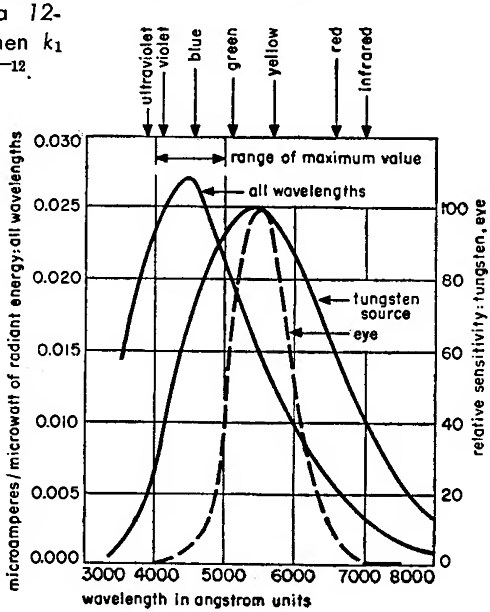

Fig. 45—Vidicon spectral response. Response with 2870-degree-Kelvin tungsten light compares to eye response. Scanned area of ½ by ⅜ inch gives 0.02-microampere output.

By Permission of RCA, copyright proprietor.

Photosensitive tubes *continued*

$$\lambda = (R_1 + R_t)\,F + (F^3/3)\,(8\pi^2C_2^2R_1^3 + 8\pi^2C_2^2R_1^2R_t + 4\pi^2C_1^2R_1^2R_t)$$
$$+ (F^5/5)\,(16\pi^4C_2^4R_1^5 + 16\pi^4C_2^4R_1^4R_t + 32\pi^4C_1^2C_2^2R_1^4R_t)$$
$$+ (F^7/7)\,(64\pi^6C_1^2C_2^4R_1^6R_t)$$

$$R_1C_2 = k_1^{1/3}$$

Persistence or lag of the photoconductive surface is shown in Fig. 44. More incident illumination and less signal-electrode voltage are helpful in reducing this effect. Fig. 45 shows the spectral response of the vidicon.

Gas tubes*

Ionization

A gas tube is an electron tube in which the pressure of the contained gas is such as to affect substantially the electrical characteristics of the tube. Such effects are caused by collisions between moving electrons and gas atoms. These collisions, if of sufficient energy, may dislodge an electron from the atom, thereby leaving the atom as a positive ion. The electronic space charge is effectively neutralized by these positive ions and comparatively high free-electron densities are easily created.

Fig. 46—Ionization properties of gases.

gas	ionization energy in volts	collision probability † P_c
Helium	24.5	12.7
Neon	21.5	17.5
Nitrogen	16.7	37.0
Hydrogen (H_2)	15.9	20.0
Argon	15.7	34.5
Carbon monoxide	14.2	23.8
Oxygen	13.5	34.5
Krypton	13.3	45.4
Water vapor	13.2	55.2
Xenon	11.5	62.5
Mercury	10.4	67.0

* J. D. Cobine, "Gaseous Conductors" 1st edition, McGraw-Hill Book Company, Inc., New York, New York; 1941.

† From, E. H. Kennard, "Kinetic Theory of Gases," McGraw-Hill Book Company, Inc., New York, New York; 1938: see p. 149.

Gas tubes *continued*

Fig. 46 gives the energy in electron–volts necessary to produce ionization. The column P_c is the kinetic-theory collision probability/centimeter of path length for an electron in a gas at 15 degrees centigrade at a pressure of 1 millimeter of mercury. The collision frequency is given by the expression

$$f_c = v\,P_c\,p$$

where

f_c = collisions/second

P_c = collision probability in collisions/centimeter/millimeter pressure

p = gas pressure in millimeters of mercury

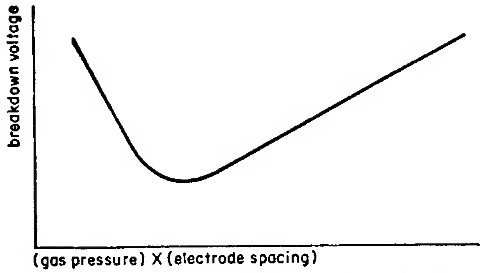

Fig. 47—Effect of gas pressure and tube geometry on gap voltage required for breakdown.

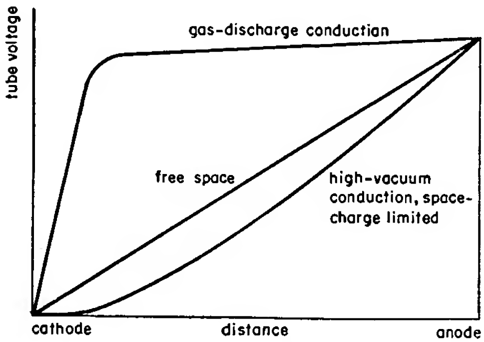

Fig. 48—Voltage distribution between plane parallel electrodes showing effect of space-charge neutralization.

Characteristics of gas tubes

The more-important parameters that determine the effect gas will have on tube operation are qualitatively described in Figs. 47–49.

Cathodes of gas tubes

Cold-cathode gas tubes require several hundreds of volts tube drop and

Gas tubes *continued*

operate with currents of tens of milliamperes. The discharge reflects the entire characteristic of Fig. 49. The advantages are simplicity of construction and circuit, long life, and reliability.

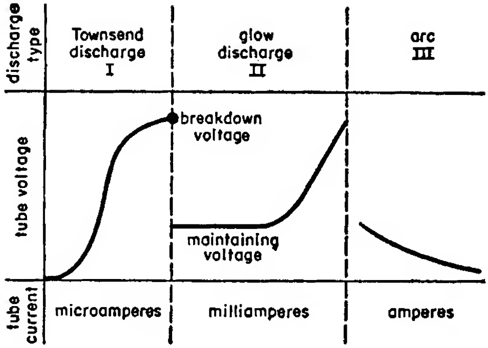

Fig. 49—Typical volt–ampere characteristic of gaseous discharge.

Hot-cathode gas tubes require several tens of volts tube drop and conduct currents that depend primarily on the cathode emission capabilities. In general, the discharge does not exhibit the characteristic of region I of Fig. 49. The advantages are high tube currents with low power losses.

Mercury-pool cathodes provide an electron supply from an arc spot on a pool of mercury. The discharge operates in region III of Fig. 49. The mercury vapor is ionized and can conduct hundreds of amperes at tube voltages of approximately 10 volts.

Fig. 50—Gas-tube regulator circuit at right and regulator-tube characteristics below.

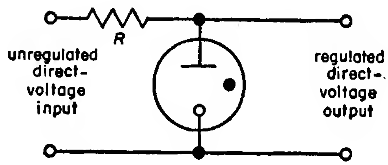

tube type	regulation level in volts	regulation current limits in milliamperes
OA2	150	5–30
OA3/VR75	75	5–40
OB2	105	5–30
OC3/VR105	105	5–40
OD3/VR150	150	5–40
874	90	10–50
991	60	0.4–2.0
5651	87	1.5–3.5

Applications of gas tubes

Relaxation oscillators, trigger tubes, and step switching tubes (see p. 476)

Gas tubes *continued*

all make use of the wide difference between the breakdown and maintaining voltages of a glow-discharge device.

Voltage-regulator tubes take advantage of the tube-current independence of tube voltage in the glow-discharge region of a cold-cathode tube (Fig. 50).

Low-impedance switching tubes are a new class under development. These tubes are glow-discharge devices that have static impedance levels of perhaps 10,000 ohms but have zero or even negative dynamic impedances. Thus the tube performs as a relay and transmits information with negligible loss as well.

Power rectifier and control tubes: Mercury-vapor rectifiers, thyratrons (see p. 314), and ignitrons employ the very-high current-carrying capacity of gas discharge tubes with low power losses for rectification and control in high-power equipment. The operation of mercury-vapor tubes is dependent on temperature insofar as tube voltage drop and peak inverse voltages are concerned (Fig. 51).

Fluorescent lamps employ the high efficiency of gas discharges in conjunction with fluorescent coatings, to produce radiation in varying parts of the visible spectrum.

Noise generators: These gas discharge tubes produce white noise throughout a large part of the microwave spectrum and are useful as standard noise sources for measurement purposes.

TR tubes: Transit–receive tubes are gas discharge devices designed to isolate the receiver section of radar equipment from the transmitter during the period of high power output. A typical tr tube and its circuit are illustrated in Fig. 52. The cones in the waveguide form a transmission cavity tuned to the transmitter frequency and the tube conducts received

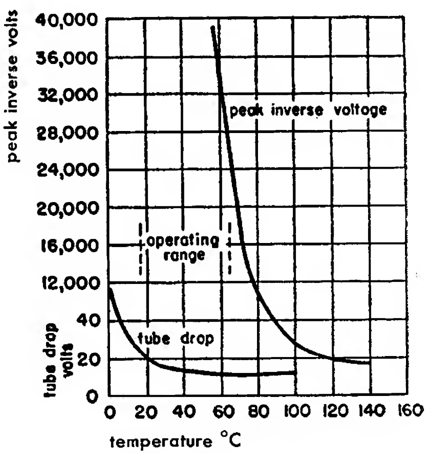

Courtesy of McGraw-Hill Book Co

Fig. 51—Tube drop and arcback voltages as a function of the condensed mercury temperature in a hot-cathode mercury-vapor tube.

Gas tubes *continued*

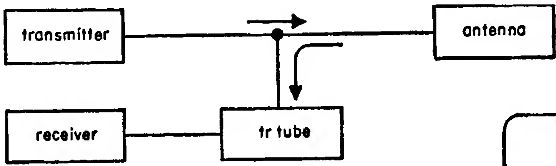

low-power-level signals from the antenna to the receiver. When the transmitter is operated, however, the high-power signal causes gas ionization between the cone tips, which detunes the structure and reflects all the transmitter power to the antenna. The receiver is protected from the destructively high level of power and all of the available transmitter power is useful output.

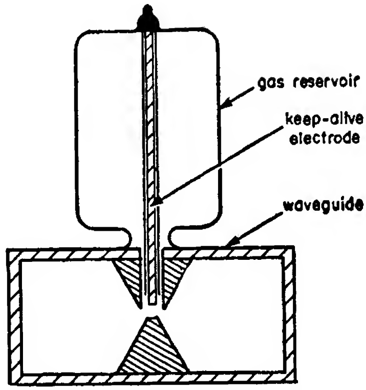

Fig. 52—Diagram of a tr tube and circuit.

Microwave gas discharge circuit elements: A new class of gas discharge devices under current development are microwave circuit control elements. The plasmas of gas discharges are capable, because of the high free-electron density, of strong interaction with electromagnetic waves in the microwave region. In general, microwave phase shift and/or absorption results. If used in conjunction with a magnetic field, these effects can be increased and made nonreciprocal. Phase shift is a result of the change in dielectric constant caused by the plasma according to the following equation.

$$\frac{\epsilon_p}{\epsilon_0} = 1 - \frac{0.8 \times 10^{-4} N_0}{f_s^2}$$

where

ϵ_p = dielectric constant in plasma

ϵ_0 = dielectric constant in free space

N_0 = electron density in electrons/centimeter^3

f_s = signal frequency in megacycles

Absorption of microwave energy results when electrons, having gained energy from the electric field of the signal, lose this energy in collisions with the tube envelope or neutral gas molecules. This absorption is a maximum when the frequency of collisions is equal to the signal frequency and the absolute magnitude is proportional to the free-electron density.

Armed Services list of standard electron tubes*

Receiving

filament voltage	diodes	triodes	twin triodes	pentodes: remote	pentodes: sharp	mixers and converters	power output: pentodes	power output: triodes	rectifiers
1.25 and 1.4	‡1A3	—	‡3A5	—	‡†1AD4 †1AH4	—	‡3B4 3V4 ‡†5672 ‡†6088	—	‡1B3GT ‡1Z2
5.0	—	—	—	—	—	—	—	—	‡5R4WGA ‡5Y3WGTA
6.3	2B22 ‡5726/6AL5W 5829WA ‡†5896	‡2C40 ‡6C4W †5703WA ‡†5718 ‡†5719 †5744WA	‡12AT7WA ‡5670 ‡5751 ‡5814A 6021 †6111 †6112	‡5749/6BA6W ‡†5899	‡6AH6 ‡6AU6WA ‡5654/6AK5W ‡†5639 †5702WA ‡†5840	†5636 ‡5725/6AS6W ‡5750/6BE6W †5784W	‡2E30 6AG7 6BG6G ‡6L6WGB 5686 ‡†5902 ‡6005/6AQ5W	‡5687 6080	‡6X4W ‡†5641

Transmitting

triodes	tetrodes	twin tetrodes	pulse modulation	magnetrons	rectifiers: vacuum	rectifiers: gas	rectifiers: grid control	clippers	gas switching: atr	gas switching: tr
‡2C39A ‡2C43 ‡100TH ‡250TH 450TL 811 880 5667 5794	‡4D21 ‡4-65A ‡4X150A ‡5D22 5933	‡829B ‡832A	‡3C45 ‡3D21A ‡3E29 ‡4C35 ‡4PR60A ‡5C22 1258 5948/1754 5949/1907	2J30–34 2J42 2J51 2J61A–62A 4J50 4J52 4J54–59 4J78 5J26 5586 5607 5657	‡2X2A ‡3B24WA 371B 836 1616 ‡8020	0Z4A/1003 3B ‡3B28 ‡4B26 ‡4B32 6C 16B 857B 869B 1005 1006 5517	‡C1K ‡884 ‡5684/C3J/A ‡5685/C6J ‡5696 ‡5727/2D21W	3B29 4B31 719A	1B35A 1B36 1B37A 1B44 1B51 1B52 1B53 1B56 1B57 5792 5793	1B23 1B26 1B27 1B50 1B58 1B63A 5853

Miscellaneous

cathode ray	crystals	klystrons	phototubes	voltage regulators
2BP1 3JP (1, 7, 12) 3WP1 5CP (1A, 7A, 12) 5FP (7A, 14) 5JP1A 5RP (7A, 11A) 5SP (1A, 7A) 7MP7 10KP7 12SP7	1N21B 1N23B 1N25 1N26 1N31 1N32 1N53 1N69 1N81 1N126	2K22 2K25 2K26 2K28 2K29 2K41 2K45 2K54 2K55 6BL6 726 A, B, C	1P21	‡0A2 ‡0B2 †5644 ‡5651 †5783WA

* From Specification MIL-STD-200B, Armed Services Electro-Standards Agency; Fort Monmouth, New Jersey: 2 February, 1955. This standard is revised at intervals; the latest issue should always be consulted.

† Subminiature type.

‡ Also United States tubes on North Atlantic Treaty Organization priority list of electronic tubes (valves).

Armed Services list of reliable eletcron tubes*

reliable type	lower-quality counterpart	description	comments on use
0A2WA	0A2, 6073	Miniature voltage regulator	—
0B2WA	0B2, 6074	Miniature voltage regulator	—
6AK5WA	6AK5, 6AK5W	Miniature sharp-cutoff pentode	—
†6AU6WA	6AU6	Miniature rf sharp-cutoff pentode	—
6SK7WA	6SK7, 6SK7W	Octal rf remote-cutoff pentode	—
†12AT7WA	12AT7	Miniature high-mu twin triode	—
†5636	—	Subminiature pentode mixer	—
†5639	—	Subminiature video-amplifier pentode	—
†5641	—	Subminiature half-wave rectifier	—
†5644	—	Subminiature voltage regulator	—
5647	—	Subminiature diode	—
†5654/6AK5W	6AK5, 6AK5W, 6AK5WA	Miniature sharp-cutoff rf pentode	Higher input capacitance
5654/6AK5W/6096	6AK5, 6AK5W, 6AK5WA	Miniature sharp-cutoff rf pentode	Higher input capacitance
†5670	2C51	Miniature medium-mu twin triode	5670 draws 1/6 more heater current than 2C51
5670WA	2C51	Miniature medium-mu twin triode	5670WA draws 1/6 more heater current than 2C51
†5686	—	Miniature rf beam-power pentode	—
†5702WA	5702	Subminiature rf sharp-cutoff pentode	—
†5703WA	5703	Subminiature medium-mu triode	—
†5718	—	Subminiature medium-mu triode	—
†5719	—	Subminiature high-mu triode	—
†5725/6AS6W	6AS6, 6AS6W	Miniature dual-control rf pentode	5725/6AS6W has 10% lower plate and screen dissipation than 6AS6, 6AS6W
5725/6AS6W/6187,	6AS6, 6AS6W	Miniature dual-control rf pentode	5725/6AS6W/6187 has different transconductances and dissipation ratings than 6AS6, 6AS6W
†5726/6AL5W	6AL5, 6AL5W	Miniature double diode	—
5726/6AL5W/6097	6AL5, 6AL5W	Miniature double diode	—
†5727/2D21W	2D21	Miniature thyratron gas tetrode	—
†5744WA	5744	Subminiature high-mu triode	—
†5749/6BA6W	6BA6	Miniature rf remote-cutoff pentode	—
†5750/6BE6W	6BE6	Miniature pentagrid converter	—
†5751	12AX7	Miniature high-mu twin triode	5751 draws 1/6 more heater current and has lower mu than 12AX7
5751WA	12AX7	Miniature high-mu twin triode	5751WA draws 1/6 more heater current and has lower mu than 12AX7
†5783WA	5783	Subminiature voltage-reference tube	5783WA has shorter bulb than 5783
5784WA	—	Subminiature dual-control rf pentode	—
5787WA	—	Subminiature voltage regulator	—
†5814A	12AU7, 5814	Miniature medium-mu twin triode	5814A draws 1/6 more heater current than 12AU7
5814WA	12AU7, 5814	Miniature medium-mu twin triode	5814WA draws 1/6 more heater current than 12AU7
†5829WA	5829	Subminiature double diode	5829WA has different interelectrode capacitance than 5829
5839	26-volt-version 6X5GT, 6X5WGT	Octal, full-wave rectifier	5839 has 26.5-volt filament and has longer envelope than 6X5GT, 6X5WGT
†5840	—	Subminiature rf sharp-cutoff pentode	—

5852	6X5GT, 6X5WGT	Octal, full-wave rectifier	5852 draws twice the heater current of 6X5GT and 6X5WGT and has longer envelope
†5896	—	Subminiature double diode	—
†5899	—	Subminiature semiremote-cutoff pentode	—
†5902	—	Subminiature audio beam-power pentode	—
5903	—	Subminiature double diode	—
5904	—	Subminiature medium-mu triode	—
5905	—	Subminiature rf sharp-cutoff pentode	—
5906	—	Subminiature rf sharp-cutoff pentode	—
5907	—	Subminiature rf semiremote-cutoff pentode	—
5908	—	Subminiature pentode mixer	—
5916	—	Subminiature pentode mixer	—
5977	—	Subminiature low-mu triode	—
5992	6V6GT, 6V6GTY, 6V6Y	Octal beam-power pentode	5992 draws 1/3 more heater current than 6V6GT family and has higher transconductance
5993	6X4, 6X4W	Miniature full-wave rectifier	5993 draws 1/3 more heater current and has different base and larger envelope than 6X4, 6X4W
†6005/6AQ5W	6AQ5, 6AQ5W	Miniature beam-power amplifier	—
6005/6AQ5W/6095	6AQ5, 6AQ5W	Miniature beam-power amplifier	—
†6021	6BF7, 6BF7W	Subminiature medium-mu twin triode	6021 is slightly shorter and has 14% higher transconductance than 6BF7, 6BF7W
6072	12AY7	Miniature medium-mu low-noise twin triode	6072 draws 1/6 more heater current than 12AY7
6094	6AQ5, 6AQ5W	Miniature beam-power amplifier	6094 has a 9-pin base, larger envelope and draws 1/3 more heater current than 6AQ5, 6AQ5W
6098/6AR6WA	6AR6	Octal beam-power amplifier	—
6099	6J6, 6J6W	Miniature medium-mu twin triode	6099 has slightly higher transconductance than 6J6, 6J6W
6100/6C4WA	6C4, 6C4W	Miniature medium-mu triode	6100/6C4WA envelope is 3/8-inch longer than 6C4W
6101/6J6WA	6J6, 6J6W	Miniature medium-mu twin triode	6101/6J6WA has a slightly higher transconductance than 6J6, 6J6W
6106	5Y3GT, 5Y3WGT, 5Y3WGTA	Octal full-wave rectifier	6106 draws 5% less heater current than 5Y3GT family. 6106 is a heater-cathode type
6110	—	Subminiature double diode	—
†6111	—	Subminiature medium-mu twin triode	—
†6112	—	Subminiature high-mu twin triode	—
6135	6C4, 6C4W	Miniature medium-mu triode	6135 draws 1/6 more heater current than 6C4, 6C4W and has 3/8-inch longer envelope than 6C4W
6184	—	Subminiature double diode	—
6186/6AG5WA	6AG5	Miniature sharp-cutoff pentode	—
6188/6SU7WGT	6SU7GT, 6SU7GTY, 6SL7GT, 6SL7WGT	Octal high-mu twin triode	6188/6SU7WGT envelope has larger maximum height
6189/12AU7WA	12AU7	Miniature medium-mu twin triode	—
6205	—	Subminiature rf sharp-cutoff pentode	—
6206	—	Subminiature semiremote-cutoff pentode	—

* From Specification MIL-E-1B, Armed Services Electro-Standards Agency; Fort Monmouth, New Jersey: 28 October 1954. This list is revised at intervals; the latest issue should always be consulted. *Note:* In many instances, the reliabilized version differs somewhat physically and electrically, from its lower-quality counterpart. This list is not to be confused with an interchangeability list. Individual specification sheets should be referred to when substitution is contemplated.

† These types are included in MIL-STD-200B.

Electron-tube circuits

Classification

It is common practice to differentiate between types of vacuum-tube circuits, particularly amplifiers, on the basis of the operating regime of the tube.

Class-A: Grid bias and alternating grid voltages such that plate current flows continuously throughout electrical cycle ($\theta_p = 360$ degrees).

Class-AB: Grid bias and alternating grid voltages such that plate current flows appreciably more than half but less than entire electrical cycle ($360° > \theta_p > 180°$).

Class-B: Grid bias close to cut-off such that plate current flows only during approximately half of electrical cycle ($\theta_p \approx 180°$).

Class-C: Grid bias appreciably greater than cut-off so that plate current flows for appreciably less than half of electrical cycle ($\theta_p < 180°$).

A further classification between circuits in which positive grid current is conducted during some portion of the cycle, and those in which it is not, is denoted by subscripts 2 and 1, respectively. Thus a class-AB_2 amplifier operates with a positive swing of the alternating grid voltage such that positive electronic current is conducted and accordingly in-phase power is required to drive the tube.

General design

For quickly estimating the performance of a tube from catalog data, or for predicting the characteristics needed for a given application, the ratios given below may be used.

The table gives correlating data for typical operation of tubes in the various amplifier classifications. From the table, knowing the maximum ratings of a tube, the maximum power output, currents, voltages, and corresponding load

Typical amplifier operating data. Maximum signal conditions—per tube.

function	class A	class B a-f (p-p)	class B r-f	class C r-f
Plate efficiency η (percent)	20–30	35–65	60–70	65–85
Peak instantaneous to d-c plate current ratio ${}^{M}i_b/I_b$	1.5–2	3.1	3.1	3.1–4.5
RMS alternating to d-c plate current ratio I_p/I_b	0.5–0.7	1.1	1.1	1.1–1.2
RMS alternating to d-c plate voltage ratio E_p/E_b	0.3–0.5	0.5–0.6	0.5–0.6	0.5–0.6
D-C to peak instantaneous grid current $I_c/{}^{M}i_c$		0.25–0.1	0.25–0.1	0.15–0.1

General design *continued*

impedance may be estimated. Thus, taking for example, a type F-124-A water-cooled transmitting tube as a class-C radio-frequency power amplifier and oscillator—the constant-current characteristics of which are shown in Fig. 1—published maximum ratings are as follows:

D-C plate voltage	E_b	$=$ 20,000 volts
D-C grid voltage	E_c	$=$ 3,000 volts
D-C plate current	I_b	$=$ 7 amperes
R-F grid current	I_g	$=$ 50 amperes
Plate input	P_i	$=$ 135,000 watts
Plate dissipation	P_p	$=$ 40,000 watts

Maximum conditions may be estimated as follows:

For $\eta = 75$ percent $\quad P_i = 135{,}000$ watts $\quad E_b = 20{,}000$ volts

Power output $P_0 = \eta P_i = 100{,}000$ watts

Average d-c plate current $I_b = P_i/E_b = 6.7$ amperes

From tabulated typical ratio ${}^{M}i_b/I_b = 4$, instantaneous peak plate current ${}^{M}i_b = 4I_b = 27$ amperes*

The rms alternating plate-current component, taking ratio $I_p/I_b = 1.2'$ $I_p = 1.2\ I_b = 8$ amperes

The rms value of the alternating plate-voltage component from the ratio $E_p/E_b = 0.6$ is $E_p = 0.6\ E_b = 12{,}000$ volts.

The approximate operating load resistance R_l is now found from

$R_l = E_p/I_p = 1500$ ohms

An estimate of the grid drive power required may be obtained by reference to the constant-current characteristics of the tube and determination of the peak instantaneous positive grid current ${}^{M}i_c$ and the corresponding instantaneous total grid voltage ${}^{M}e_c$. Taking the value of grid bias E_c for the given operating condition, the peak alternating grid drive voltage is

$${}^{M}E_g = ({}^{M}e_c - E_c)$$

from which the peak instantaneous grid drive power is

$${}^{M}P_c = {}^{M}E_g\ {}^{M}i_c$$

* In this discussion, the superscript M indicates the use of the maximum or peak value of the varying component, i.e., ${}^{M}i_b$ = maximum or peak value of the alternating component of the plate current.

General design *continued*

An approximation to the average grid drive power P_g, necessarily rough due to neglect of negative grid current, is obtained from the typical ratio

$$\frac{I_c}{{}^{M}i_c} = 0.2$$

of d-c to peak value of grid current, giving

$$P_g = I_cE_g = 0.2\ {}^{M}i_cE_g \text{ watts}$$

Plate dissipation P_p may be checked with published values since

$$P_p = P_i - P_0$$

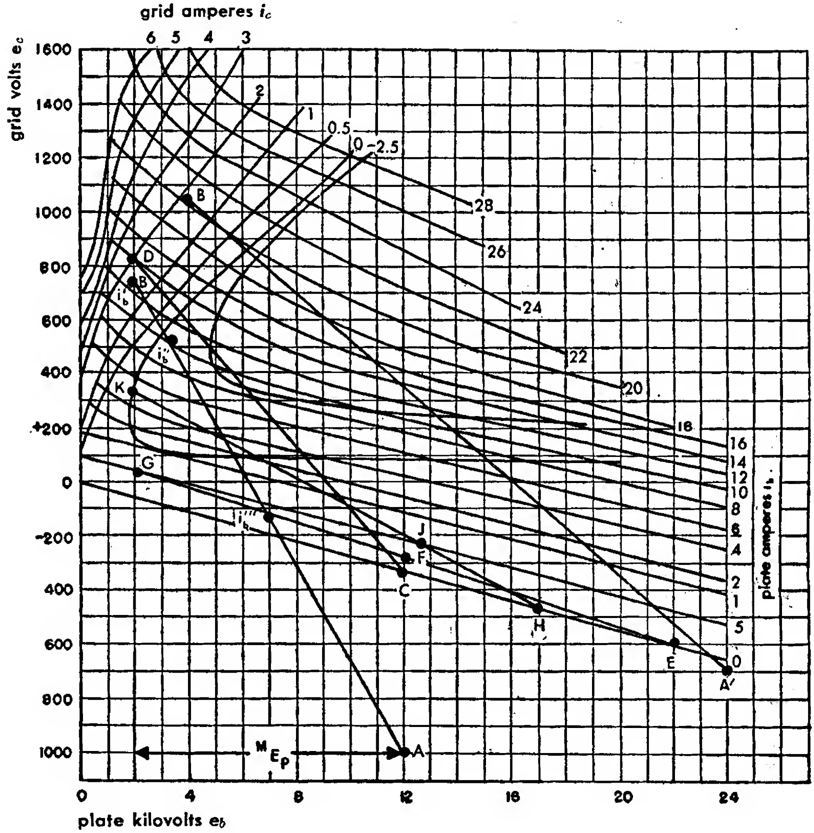

Fig. 1—Constant-current characteristics with typical load lines AB—class C, CD—class B, EFG—class A, and HJK—class AB.

General design *continued*

It should be borne in mind that combinations of published maximum ratings as well as each individual maximum rating must be observed. Thus, for example in this case, the maximum d-c plate operating voltage of 20,000 volts does not permit operation at the maximum d-c plate current of 7 amperes since this exceeds the maximum plate input rating of 135,000 watts.

Plate load resistance R_l may be connected directly in the tube plate circuit, as in the resistance-coupled amplifier, through impedance-matching elements as in audio-frequency transformer coupling, or effectively represented by a loaded parallel-resonant circuit as in most radio-frequency amplifiers. In any case, calculated values apply only to effectively resistive loads, such as are normally closely approximated in radio-frequency amplifiers. With appreciably reactive loads, operating currents and voltages will in general be quite different and their precise calculation is quite difficult.

The physical load resistance present in any given set-up may be measured by audio-frequency or radio-frequency bridge methods. In many cases, the proper value of R_l is ascertained experimentally as in radio-frequency amplifiers that are tuned to the proper minimum d-c plate current. Conversely, if the circuit is to be matched to the tube, R_l is determined directly as in a resistance-coupled amplifier or as

$$R_l = N^2 R_s$$

in the case of a transformer-coupled stage, where N is the primary-to-secondary voltage transformation ratio. In a parallel-resonant circuit in which the output resistance R_s is connected directly in one of the reactance legs,

$$R_l = \frac{X^2}{R_s} = \frac{L}{Cr_s} = QX$$

where X is the leg reactance at resonance (ohms), and L and C are leg inductance in henries and capacitance in farads, respectively;

$$Q = \frac{X}{R_s}$$

Graphical design methods

When accurate operating data are required, more precise methods must be used. Because of the nonlinear nature of tube characteristics, graphical methods usually are most convenient and rapid. Examples of such methods are given below.

A comparison of the operating regimes of class A, AB, B, and C amplifiers is given in the constant-current characteristics graph of Fig. 1. The lines

Graphical design methods

continued

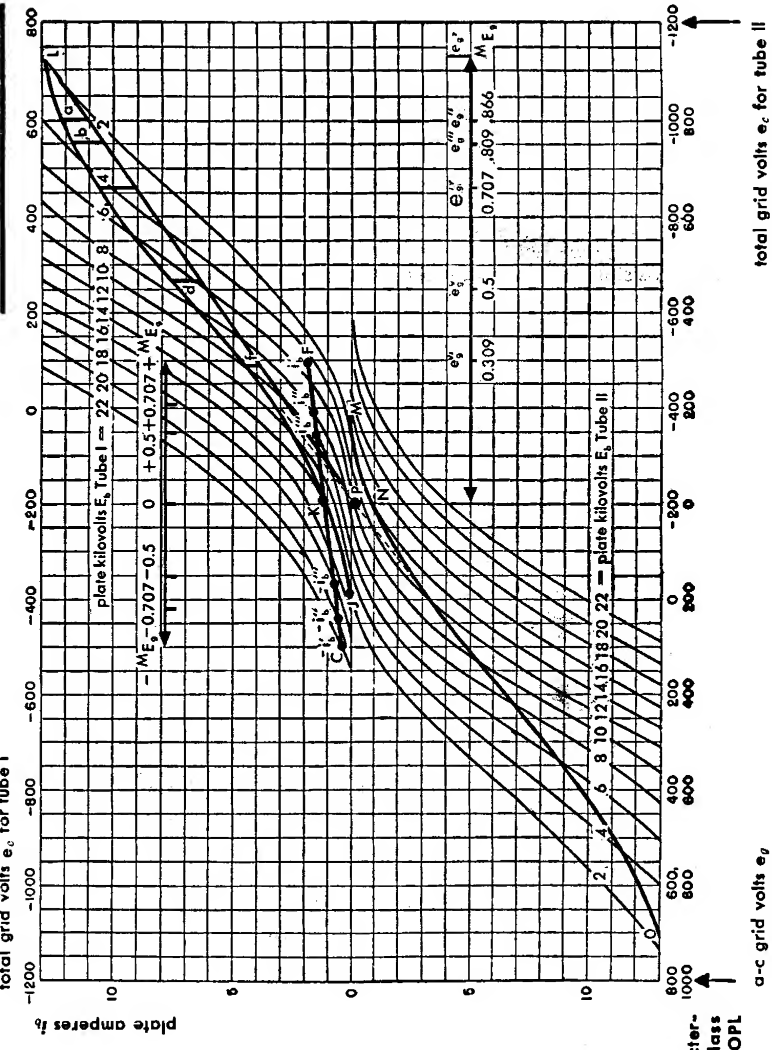

Fig. 2—Transfer characteristics i_b versus e_b with class A_2—CKF and class B—OPL load lines.

Graphical design methods *continued*

corresponding to the different classes of operation are each the locus of instantaneous grid e_c and plate e_b voltages, corresponding to their respective load impedances.

For radio-frequency amplifiers and oscillators having tuned circuits giving an effectively resistive load, plate and grid tube and load alternating voltages are sinusoidal and in phase (disregarding transit time), and the loci become straight lines.

For amplifiers having nonresonant resistive loads, the loci are in general nonlinear except in the distortionless case of linear tube characteristics (constant r_p), for which they are again straight lines.

Thus, for determination of radio-frequency performance, the constant-current chart is convenient. For solution of audio-frequency problems, however, it is more convenient to use the $(i_b - e_c)$ transfer characteristics of Fig. 2 on which a dynamic load line may be constructed.

Methods for calculation of the most important cases are given below.

Class-C radio-frequency amplifier or oscillator

Draw straight line from A to B (Fig. 1) corresponding to chosen d-c operating plate and grid voltages, and to desired peak alternating plate and grid voltage excursions. The projection of AB on the horizontal axis thus corresponds to ${}^{M}E_p$. Using Chaffee's 11-point method of harmonic analysis, lay out on AB points:

$$e_p' = {}^{M}E_p \qquad e_p'' = 0.866\ {}^{M}E_p \qquad e_p''' = 0.5\ {}^{M}E_p$$

to each of which correspond instantaneous plate currents i_b', i_b'' and i_b''' and instantaneous grid currents i_c', i_c'' and i_c'''. The operating currents are obtained from the following expressions:

$$I_b = \frac{1}{12}\,[i_b' + 2\,i_b'' + 2\,i_b'''] \qquad I_c = \frac{1}{12}\,[i_c' + 2\,i_c'' + 2\,i_c''']$$

$${}^{M}I_p = \frac{1}{6}\,[i_b' + 1.73\,i_b'' + i_b'''] \qquad {}^{M}I_g = \frac{1}{6}\,[i_c' + 1.73\,i_c'' + i_c''']$$

Substitution of the above in the following give the desired operating data.

Power output $P_0 = \dfrac{{}^{M}E_p\,{}^{M}I_p}{2}$

Power input $P_i = E_b\,I_b$

Average grid excitation power $= \dfrac{{}^{M}E_g\,{}^{M}I_g}{2}$

Graphical design methods *continued*

Peak grid excitation power $= {}^{M}E_g \, i'_c$

Plate load resistance $\quad R_l = \dfrac{{}^{M}E_p}{{}^{M}I_p}$

Grid bias resistance $\quad R_c = \dfrac{E_c}{I_c}$

Plate efficiency $\quad \eta = \dfrac{P_0}{P_i}$

Plate dissipation $\quad P_p = P_i - P_0$

The above procedure may also be applied to plate-modulated class-C amplifiers. Taking the above data as applying to carrier conditions, the analysis is repeated for ${}^{\text{crest}}E_b = 2E_b$ and ${}^{\text{crest}}P_0 = 4P_0$ keeping R_l constant. After a cut-and-try method has given a peak solution, it will often be found that combination fixed and self grid biasing as well as grid modulation is indicated to obtain linear operation.

To illustrate the preceding exposition, a typical amplifier calculation is given below:

Operating requirements (carrier condition)

$E_b = 12{,}000$ volts $\qquad P_0 = 25{,}000$ watts $\qquad \eta = 75$ percent

Preliminary calculation (refer to table below)

Class-C r-f amplifier data for 100-percent plate modulation.

symbol	preliminary carrier	detailed carrier	detailed crest
E_b (volts)	12,000	12,000	24,000
${}^{M}E_p$ (volts)	10,000	10,000	20,000
E_c (volts)	—	−1,000	−700
${}^{M}E_g$ (volts)	—	1,740	1,740
I_b (amp)	2.9	2.8	6.4
${}^{M}I_p$ (amp)	4.9	5.1	10.2
I_c (amp)	—	0.125	0.083
${}^{M}I_g$ (amp)	—	0.255	0.183
P_i (watts)	35,000	33,600	154,000
P_0 (watts)	25,000	25,5[illegible]0	102,000
P_g (watts)	—	220	160
η (percent)	75	76	66
R_l (ohms)	2,060	1,960	1,960
R_c (ohms)	—	7,100	7,100
E_{cc} (volts)	—	−110	−110

Graphical design methods *continued*

$$\frac{E_p}{E_b} = 0.6$$

$$E_p = 0.6 \times 12{,}000 = 7200 \text{ volts}$$

$$^{M}E_p = 1.41 \times 7200 = 10{,}000 \text{ volts}$$

$$I_p = \frac{P_o}{E_p}$$

$$I_p = \frac{25{,}000}{7200} = 3.48 \text{ amperes}$$

$$^{M}I_p = 4.9 \text{ amperes}$$

$$\frac{I_p}{I_b} = 1.2$$

$$I_b = \frac{3.48}{1.2} = 2.9 \text{ amperes}$$

$$P_i = 12{,}000 \times 2.9 = 35{,}000 \text{ watts}$$

$$\frac{^{M}i_b}{I_b} = 4.5$$

$$^{M}i_b = 4.5 \times 2.9 = 13.0 \text{ amperes}$$

$$R_l = \frac{E_p}{I_p} = \frac{7200}{3.48} = 2060 \text{ ohms}$$

Complete calculation

Lay out carrier operating line, AB on constant-current graph, Fig. 1, using values of E_b, $^{M}E_p$, and $^{M}i_b$ from preliminary calculated data. Operating carrier bias voltage, E_c, is chosen somewhat greater than twice cutoff value, 1000 volts, to locate point A.

The following data are taken along AB:

$i_b' = 13$ amp	$i_c' = 1.7$ amp	$E_c = -1000$ volts
$i_b'' = 10$ amp	$i_c'' = -0.1$ amp	$e_c' = 740$ volts
$i_b''' = 0.3$ amp	$i_c''' = 0$ amp	$^{M}E_p = 10{,}000$ volts

From the formulas, complete carrier data as follows are calculated:

$$^{M}I_p = \frac{1}{6}[13 + 1.73 \times 10 + 0.3] = 5.1 \text{ amp}$$

$$P_0 = \frac{10{,}000 \times 5.1}{2} = 25{,}500 \text{ watts}$$

$$I_b = \frac{1}{12}[13 + 2 \times 10 + 2 \times 0.3] = 2.8 \text{ amp}$$

$$P_i = 12{,}000 \times 2.8 = 33{,}600 \text{ watts}$$

Graphical design methods *continued*

$$\eta = \frac{25{,}500}{33{,}600} \times 100 = 76 \text{ percent}$$

$$R_l = \frac{10{,}000}{5.1} = 1960 \text{ ohms}$$

$$I_c = \frac{1}{12}[1.7 + 2(-0.1)] = 0.125 \text{ amp}$$

$$^{M}I_g = \frac{1}{6}[1.7 + 1.7(-0.1)] = 0.255 \text{ amp}$$

$$P_g = \frac{1740 \times 0.255}{2} = 220 \text{ watts}$$

Operating data at 100-percent positive modulation crests are now calculated knowing that here

$E_b = 24{,}000$ volts $\qquad R_l = 1960$ ohms

and for undistorted operation

$P_0 = 4 \times 25{,}500 = 102{,}000$ watts $\qquad {}^{M}E_p = 20{,}000$ volts

The crest operating line A′B′ is now located by trial so as to satisfy the above conditions, using the same formulas and method as for the carrier condition.

It is seen that in order to obtain full-crest power output, in addition to doubling the alternating plate voltage, the peak plate current must be increased. This is accomplished by reducing the crest bias voltage with resultant increase of current conduction period, but lower plate efficiency.

The effect of grid secondary emission to lower the crest grid current is taken advantage of to obtain the reduced grid-resistance voltage drop required. By use of combination fixed and grid resistance bias proper variation of the total bias is obtained. The value of grid resistance required is given by

$$R_c = \frac{-[E_c - {}^{\text{crest}}E_c]}{I_c - {}^{\text{crest}}I_c}$$

and the value of fixed bias by

$$E_{cc} = E_c - (I_c R_c)$$

Calculations at carrier and positive crest together with the condition of zero output at negative crest give sufficiently complete data for most purposes. If accurate calculation of audio-frequency harmonic distortion is necessary, the above method may be applied to the additional points required.

Graphical design methods *continued*

Class-B radio-frequency amplifiers

A rapid approximate method is to determine by inspection from the tube ($i_b - e_b$) characteristics the instantaneous current, i'_b and voltage e'_b corresponding to peak alternating voltage swing from operating voltage E_b.

A-C plate current $\quad {}^{M}I_p = \dfrac{i'_b}{2}$

D-C plate current $\quad I_b = \dfrac{i'_b}{\pi}$

A-C plate voltage $\quad {}^{M}E_p = E_b - e'_b$

Power output $\quad P_0 = \dfrac{(E_b - e'_b)\, i'_b}{4}$

Power input $\quad P_i = \dfrac{E_b i'_b}{\pi}$

Plate efficiency $\quad \eta = \dfrac{\pi}{4}\left(1 - \dfrac{e'_b}{E_b}\right)$

Thus $\eta \approx 0.6$ for the usual crest value of ${}^{M}E_p \approx 0.8\, E_b$.

The same method of analysis used for the class-C amplifier may also be used in this case. The carrier and crest condition calculations, however, are now made from the same E_b, the carrier condition corresponding to an alternating-voltage amplitude of ${}^{M}E_p/2$ such as to give the desired carrier power output.

For greater accuracy than the simple check of carrier and crest conditions, the radio-frequency plate currents ${}^{M}I_p{}'$, ${}^{M}I_p{}''$, ${}^{M}I_p{}'''$, ${}^{M}I_p{}^{o}$, $-{}^{M}I_p{}'''$, $-{}^{M}I_p{}''$, and $-{}^{M}I_p{}'$ may be calculated for seven corresponding selected points of the audio-frequency modulation envelope $+{}^{M}E_g$, $+0.707\,{}^{M}E_g$, $+0.5\,{}^{M}E_g$, 0, $-0.5{}^{M}E_g$, $-0.707{}^{M}E_g$, and $-{}^{M}E_g$, where the negative signs denote values in the negative half of the modulation cycle. Designating

$$S' = {}^{M}I'_p - (-{}^{M}I'_p)$$
$$D' = {}^{M}I'_p + (-{}^{M}I'_p) - 2{}^{M}I_p{}^{0}$$

the fundamental and harmonic components of the output audio-frequency current are obtained as

$${}^{M}I_{p1} = \frac{S'}{4} + \frac{S''}{2\sqrt{2}} \text{ (fundamental)} \qquad {}^{M}I_{p2} = \frac{5\,D'}{24} + \frac{D''}{4} - \frac{D'''}{3}$$

Graphical design methods *continued*

$$^{M}I_{p3} = \frac{S'}{6} - \frac{S'''}{3} \qquad ^{M}I_{p4} = \frac{D'}{8} - \frac{D''}{4}$$

$$^{M}I_{p5} = \frac{S'}{12} - \frac{S''}{2\sqrt{2}} + \frac{S'''}{3} \qquad ^{M}I_{p6} = \frac{D'}{24} - \frac{D''}{4} + \frac{D'''}{3}$$

This detailed method of calculation of audio-frequency harmonic distortion may, of course, also be applied to calculation of the class-C modulated amplifier, as well as to the class-A modulated amplifier.

Class-A and AB audio-frequency amplifiers

Approximate formulas assuming linear tube characteristics:

Maximum undistorted power output $^{M}P_0 = \dfrac{^{M}E_p\,^{M}I_p}{2}$

when plate load resistance $R_l = r_p \left[\dfrac{E_c}{\dfrac{^{M}E_p}{\mu} - E_c} - 1 \right]$

and

negative grid bias $E_c = \dfrac{^{M}E_p}{\mu}\left(\dfrac{R_l + r_p}{R_l + 2r_p}\right)$

giving

maximum plate efficiency $\eta = \dfrac{^{M}E_p\,^{M}I_p}{8E_b\,I_b}$

Maximum maximum undistorted power output $^{MM}P_0 = \dfrac{^{M}E^2_p}{16\,r_p}$

when

$$R_l = 2\,r_p \qquad E_c = \frac{3}{4}\,\frac{^{M}E_p}{\mu}$$

An exact analysis may be obtained by use of a dynamic load line laid out on the transfer characteristics of the tube. Such a line is CKF of Fig. 2 which is constructed about operating point K for a given load resistance r_l from the following relation:

$$i_b^{S} = \frac{e_b^{R} - e_b^{S}}{R_l} + i_b^{R}$$

where

R, S, etc., are successive conveniently spaced construction points.

Graphical design methods *continued*

Using the seven-point method of harmonic analysis, plot instantaneous plate currents i_b', i_b'', i_b''', i_b, $-i_b'''$, $-i_b''$, and $-i_b'$ corresponding to $+{}^{M}E_g$, $+0.707{}^{M}E_g$, $+0.5{}^{M}E_g$, 0, $-0.5{}^{M}E_g$, $-0.707{}^{M}E_g$, and $-{}^{M}E_g$, where 0 corresponds to the operating point K. In addition to the formulas given under class-B radio-frequency amplifiers:

$$I_b \text{ average} = I_b + \frac{D'}{8} + \frac{D''}{4}$$

from which complete data may be calculated.

Class-AB and B audio-frequency amplifiers

Approximate formulas assuming linear tube characteristics give (referring to Fig. 1, line CD) for a class-B audio-frequency amplifier:

$${}^{M}I_p = i_b'$$

$$P_0 = \frac{{}^{M}E_p\,{}^{M}I_p}{2}$$

$$P_i = \frac{2}{\pi} E_b\,{}^{M}I_p$$

$$\eta = \frac{\pi}{4}\frac{{}^{M}E_p}{E_b}$$

$$R_{pp} = 4\,\frac{{}^{M}E_p}{i'_b} = 4R_l$$

Again an exact solution may be derived by use of the dynamic load line JKL on the $(i_b - e_c)$ characteristic of Fig. 2. This line is calculated about the operating point K for the given R_l (in the same way as for the class-A case). However, since two tubes operate in phase opposition in this case, an identical dynamic load line MNO represents the other half cycle, laid out about the operating bias abscissa point but in the opposite direction (see Fig. 2).

Algebraic addition of instantaneous current values of the two tubes at each value of e_c gives the composite dynamic characteristic for the two tubes OPL. Inasmuch as this curve is symmetrical about point P, it may be analyzed for harmonics along a single half-curve PL by the Mouromtseff 5-point method. A straight line is drawn from P to L and ordinate plate-current differences a, b, c, d, f between this line and curve, corresponding to e_g'', e_g''', e_g^{IV}, e_g^{V}, and e_g^{VI}, are measured. Ordinate distances measured upward from curve PL are taken positive.

Graphical design methods *continued*

Fundamental and harmonic current amplitudes and power are found from the following formulas:

$$^{M}I_{p1} = i'_b - {}^{M}I_{p3} + {}^{M}I_{p5} - {}^{M}I_{p7} + {}^{M}I_{p9} - {}^{M}I_{p11}$$

$$^{M}I_{p3} = 0.4475\ (b + f) + \frac{d}{3} - 0.578\ d - \frac{1}{2}\,{}^{M}I_{p5}$$

$$^{M}I_{p5} = 0.4\ (a - f)$$

$$^{M}I_{p7} = 0.4475\ (b + f) - {}^{M}I_{p3} + 0.5\,{}^{M}I_{p5}$$

$$^{M}I_{p9} = {}^{M}I_{p3} - \frac{2}{3}\,d$$

$$^{M}I_{p11} = 0.707c - {}^{M}I_{p3} + {}^{M}I_{p5}.$$

Even harmonics are not present due to dynamic characteristic symmetry. The direct-current and power-input values are found by the 7-point analysis from curve PL and doubled for two tubes.

Classification of amplifier circuits

The classification of amplifiers in classes A, B, and C is based on the operating conditions of the tube.

Another classification can be used, based on the type of circuits associated with the tube.

A tube can be considered as a four-terminal network with two input terminals and two output terminals. One of the input terminals and one of the output terminals are usually common; this common junction or point is usually called "ground".

When the common point is connected to the filament or cathode of the tube, we can speak of a grounded-cathode circuit: the most-conventional type of vacuum-tube circuit. When the common point is the grid, we can speak of a grounded-grid circuit, and when the common point is the plate or anode, we can speak of the grounded-anode circuit.

This last type of circuit is most commonly known by the name of *cathode-follower.*

A fourth and most-general class of circuit is obtained when the common point or ground is not directly connected to any of the three electrodes of the tube. This is the condition encountered at uhf where the series impedances of the internal tube leads make it impossible to ground any of them. It is also encountered in such special types of circuits as the *phase-splitter,* in which the impedance from plate to ground and the impedance from cathode to ground are made equal in order to obtain an output between plate and cathode balanced with respect to ground.

Classification of amplifier circuits *continued*

<table>
<tr><th></th><th>grounded-cathode</th><th>grounded-grid</th><th>grounded-plate or cathode-follower</th></tr>
<tr><td>Circuit schematic</td>
<td>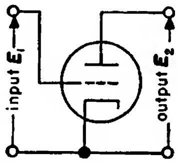
</td>
<td>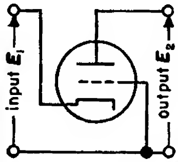
</td>
<td>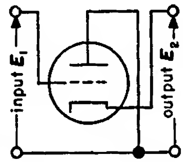
</td></tr>
<tr><td>Equivalent circuit, alternating current component, class-A operation</td>
<td>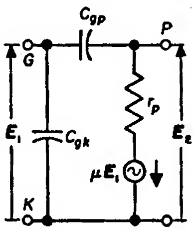
</td>
<td>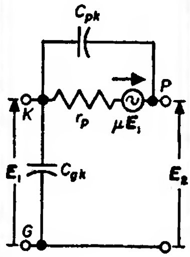
</td>
<td>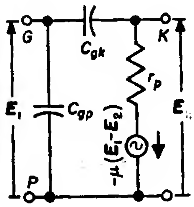
</td></tr>
<tr><td>Voltage gain, A for output load impedance $=Z_2$
$A=\frac{E_2}{E_1}$</td>
<td>$A=\frac{-\mu Z_2}{r_p+Z_2}$
$=-g_m\frac{r_pZ_2}{r_p+Z_2}$
neglecting C_{gp}
(Z_2 includes C_{pk})</td>
<td>$A=(1+\mu)\ \frac{Z_2}{r_p+Z_2}$
neglecting C_{pk}
(Z_2 includes C_{gp})</td>
<td>$A=\frac{\mu Z_2}{r_p+(1+\mu)Z_2}$
neglecting C_{gk}
(Z_2 includes C_{pk})</td></tr>
<tr><td>Input admittance
$Y_1=\frac{I_1}{E_1}$</td>
<td>$Y_1=j\omega[C_{gk}+(1-A)C_{gp}]$</td>
<td>$Y_1=j\omega[C_{gk}+(1-A)C_{pk}]+\frac{1+\mu}{r_p+Z_2}$</td>
<td>$Y_1=j\omega[C_{gp}+(1-A)C_{gk}]$</td></tr>
<tr><td>Equivalent generator seen by load at output terminals</td>
<td>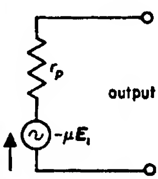

neglecting C_{gp}</td>
<td>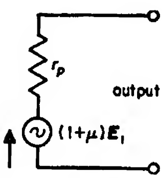

neglecting C_{pk}</td>
<td>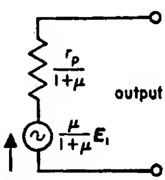

neglecting C_{gk}</td></tr>
</table>

Classification of amplifier circuits *continued*

Design information for the first three classifications is given in the table on page 445, where

Z_2 = load impedance to which output terminals of amplifier are connected

$\mathbf{E}_1$ = phasor input voltage to amplifier

$\mathbf{E}_2$ = phasor output voltage across load impedance Z_2

$\mathbf{A}$ = voltage gain of amplifier = $\mathbf{E}_2/\mathbf{E}_1$

Y_1 = input admittance to input terminals of amplifier

$\omega = 2\pi \times$ (frequency of excitation voltage $\mathbf{E}_1$)

$j = (-1)^{1/2}$

and the remaining notation is in accordance with the nomenclature of pages 371 and 372.

Amplifier pairs

The basic amplifier classes are often used in pairs, or combination forms' for special characteristics. The availability of dual triodes makes these combined forms especially useful.

Grounded-cathode–grounded-plate

This pairing provides the gain and 180-degree phase reversal of a grounded-plate stage with a low source impedance at the output terminals. It is especially useful in feedback circuits or for amplifiers driving a low or unknown load impedance. In tuned amplifiers, the possibility of oscillation must be considered (see note on cathode-followers with reactive source and load). Direct coupling is useful for pulse work, permitting large positive input and negative output excursions.

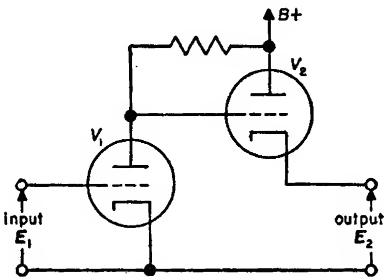

Grounded-plate–grounded-grid (cathode-coupled)

Direct coupling is usual, making a very simple structure. Several modified forms are possible with special characteristics.

Amplifier pairs *continued*

Cathode-coupled amplifier: As a simple amplifier, R_3 and input E_1' are short-circuited. Output E_2 is in phase with input E_1. Gain (with $R_1 \gg 1/g_m$) is given by $\mathbf{A} \approx g_m R_2/2$. Even-harmonic distortion is reduced by symmetry, as in a push-pull stage. Due to the in-phase input and output relations, this circuit forms the basis for various R–C oscillators and the class of cathode-coupled multivibrators.

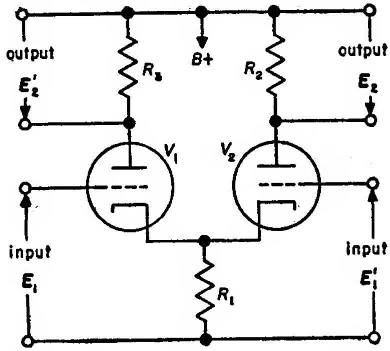

Symmetrical clipper: With suitable bias adjustment, symmetrical clipping or limiting occurs between V_1 cutoff and V_2 cutoff, without drawing grid current.

Differential amplifier: With input supplied to E_1 and E_1', the output E_2 responds (approximately) to the difference $E_1 - E_1'$. Balance is improved by constant-current supply to the cathode (long-tailed pair) such as a high value of R_1 (preferably connected from a highly negative supply) or a constant-current pentode. The signal to E_1' should be slightly attenuated for precise adjustment of balance.

Phase inverter: With R_3 and R_2 both used, approximately balanced (push–pull) outputs (E_2 and E_2') are obtained from either input E_1' or E_1. As a phase inverter (paraphase), one input (E_1) is used, the other being grounded, and R_3 is made slightly less than R_2 to provide exact balance.

Grounded-cathode–grounded-grid (cascode)

This circuit has characteristics somewhat resembling the pentode, with the advantage that no screen current is required. V_2 serves to isolate V_1 from the output load R_l, giving voltage gain equation

$$A = \frac{\mu_1 R_l}{r_{p1} + \dfrac{r_{p2} + R_l}{\mu_2 + 1}}$$

For $R_l \ll \mu r_p$, $\quad A \approx g_{m1} R_l$

For $R_l \gg \mu r_p$, $\quad A \approx \mu_1 \mu_2$

Amplifier pairs *continued*

As an rf amplifier, the grounded-grid stage V_2 drastically reduces capacitive feedback from output to input, without introducing partition noise (as produced by the screen current of a pentode). Shot noise contributed by V_2 is negligible due to the highly degenerative effect of r_{p1} in series with the cathode. The noise figure thus approaches the theoretical noise of V_1 used as a triode, without the undesirable effects of triode plate–grid capacitance.

Because of the 180° phase relation of input and output, this circuit is also valuable in audio feedback circuits, replacing a single stage with considerable increase in gain (for high values of R_l).

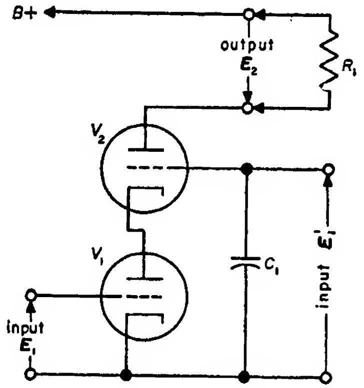

The grid of V_2 provides a second input connection E_1' useful for feedback or for gating. The voltage gain from E_1' to the output is considerably reduced, being given by

$$A = \frac{R_l \mu}{R_l + \mu r_p}$$

For $R_l \ll \mu r_p$, $\quad A_2 \approx R_l / r_{p1}$

For $R_l \gg \mu r_p$, $\quad A_2 \approx \mu$

Cathode-follower data

General characteristics

a. High-impedance input, low-impedance output.

b. Input and output have one side grounded.

c. Good wide-band frequency and phase response.

d. Output is in phase with input.

e. Voltage gain or transfer is always less than one.

f. A power gain can be obtained.

g. Input capacitance is reduced.

General case

$$\text{Transfer} = \frac{E_{out}}{E_{in}} = \frac{g_m R_l}{g_m R_l + 1 + R_l / r_p}$$

Cathode-follower data *continued*

R_{out} = output resistance

$$= \frac{r_p}{\mu + 1} \text{ or approximately } \frac{1}{g_m}$$

g_m = transconductance in mhos (1000 micromhos = 0.001 mhos)

R_l = total load resistance

$$\text{Input capacitance} = C_{gp} + \frac{C_{gk}}{1 + g_m R_l}$$

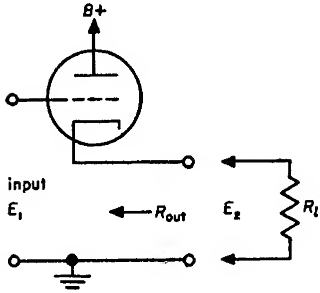

Specific cases

a. To match the characteristic impedance of the transmission line, R_{out} must equal Z_0.

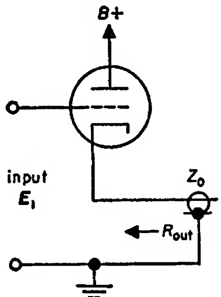

b. If R_{out} is less than Z_0, add resistor R_c' in series so that $R_c' = Z_0 - R_{out}$.

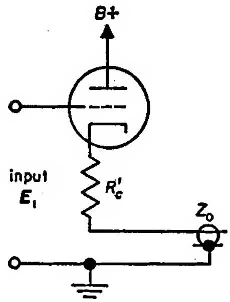

c. If R_{out} is greater than Z_0, add resistor R_c in parallel so that

$$R_c = \frac{Z_0 R_{out}}{R_{out} - Z_0}$$

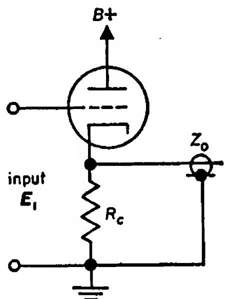

Note 1: Normal operating bias must be provided. For coupling a high imped-

Cathode-follower data *continued*

ance into a low-impedance transmission line, for maximum transfer choose a tube with a high g_m.

Note 2: Oscillation may occur in a cathode-follower if the source becomes inductive and load capacitive at high frequencies. The general expression for voltage gain of a cathode-follower (including C_{gk}) is given (see p. 445) by

$$\mathbf{A} = \frac{\mu Z_2 + Z_2 r_p/Z_{gk}}{r_p + Z_2\,(1 + \mu) + Z_2 r_p/Z_{gk}}$$

The input admittance

$$Y_1 = j\omega[C_{gp} + (1 - \mathbf{A})C_{gk}]$$

may contain negative-resistance terms causing oscillation at the frequency where an inductive grid circuit resonates the capacitive Y_1 component.

The use of a simple triode (or pentode) grounded-cathode circuit with c load resistor equal to Z_0 provides an equally good match with slightly higher gain ($g_m R_l$), but will overload at a lower maximum voltage. The anode-follower (see "Special applications of feedback") provides output approximating the cathode-follower without the risk of oscillation.

Resistance-coupled audio-amplifier design

Stage gain A*

Medium frequencies $= A_m = \dfrac{\mu R}{R + R_p}$

High frequencies $= A_h = \dfrac{A_m}{\sqrt{1 + \omega^2 C_1^2 r^2}}$

Low frequencies* $= A_l = \dfrac{A_m}{\sqrt{1 + \dfrac{1}{\omega^2 C_2^2 \rho^2}}}$

* The low-frequency stage gain also is affected by the values of the cathode bypass capacitor and the screen bypass capacitor.

Resistance-coupled audio-amplifier design *continued*

where

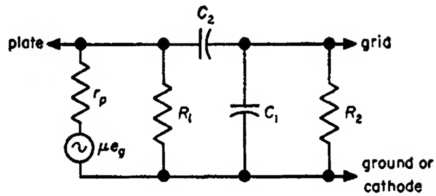

$$R = \frac{R_l R_2}{R_l + R_2}$$

$$r = \frac{R r_p}{R + r_p}$$

$$\rho = R_2 + \frac{R_l r_p}{R_l + r_p}$$

μ = amplification factor of tube
ω = $2\pi \times$ frequency
R_l = plate-load resistance in ohms
R_2 = grid-leak resistance in ohms
r_p = a-c plate resistance in ohms
C_1 = total shunt capacitance in farads
C_2 = coupling capacitance in farads

Given C_1, C_2, R_2, and X = fractional response required.

At highest frequency

$$r = \frac{\sqrt{1 - X^2}}{\omega C_1 X} \qquad R = \frac{r\, r_p}{r_p - r} \qquad R_l = \frac{R R_2}{R_2 - R}$$

At lowest frequency

$$C_2 = \frac{X}{\omega \rho \sqrt{1 - X^2}}$$

Cascaded stages

The 3-decibel-down frequencies for n cascaded identical R–C-amplifier stages

$$F = f/f_2 = f_1/f = (2^{1/n} - 1)^{1/2}$$

where

n = number of identical stages
f = 3-db-down frequency for n stages
f_1 = ower 3-db-down frequency of one stage
f_2 = upper 3-db-down frequency of one stage

Resistance-coupled audio-amplifier design *continued*

n	F	1/F
1	1	1
2	0.643	1.555
3	0.51	1.96

Example: $n = 3$, $f_1 = 51$ cycles, $f_2 = 100$ kilocycles:

Lower $f = (1/F)f_1 = 1.96 \times (51) = 200$ cycles

Upper $f = Ff_2 = 0.51 \times (100\text{kc}) = 51$ kilocycles

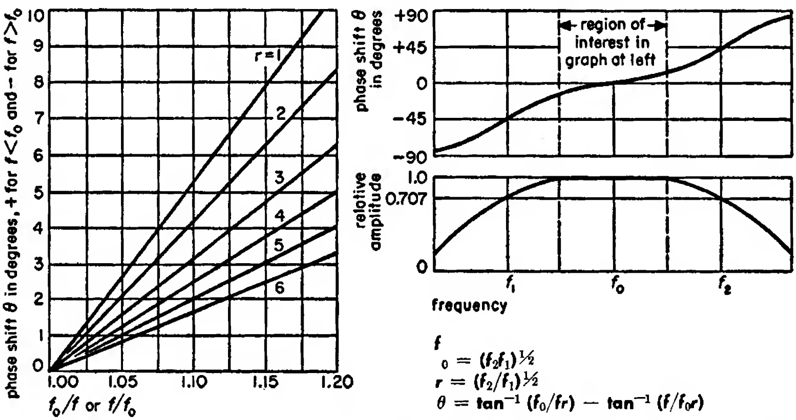

$f_0 = (f_2 f_1)^{1/2}$
$r = (f_2/f_1)^{1/2}$
$\theta = \tan^{-1}(f_0/fr) - \tan^{-1}(f/f_0 r)$

Phase shift in the vicinity of f_0 as a function of the ratio of the upper 3-decibel frequency f_2 to the lower 3-decibel frequency f_1.

Negative feedback

The following quantities are functions of frequency with respect to magnitude and phase:

E, N, D = signal, noise, and distortion output voltage with feedback

e, n, d = signal, noise, and distortion output voltage without feedback

A = voltage amplification magnitude of amplifier at a given frequency

$\mathbf{A}$ = amplification including phase angle (complex quantity)

$\vec{\beta}$ = fraction of output voltage fed back (complex quantity); for usual negative feedback, $\vec{\beta}$ is negative

ϕ = phase shift of amplifier and feedback circuit at a given frequency

Negative feedback *continued*

Reduction in gain caused by feedback

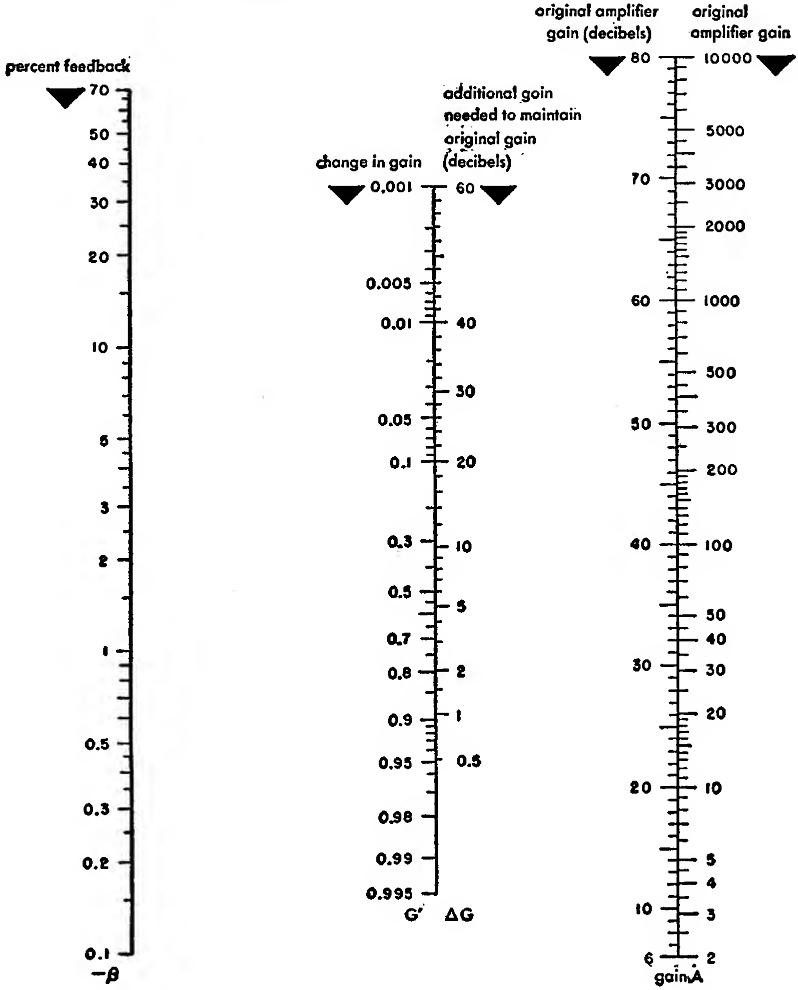

Fig. 3—In negative-feedback amplifier considerations $\vec{\beta}$, expressed as a percentage, has a negative value. A line across the β and A scales intersects the center scale to indicate change in gain. It also indicates the amount, in decibels, the input must be increased to maintain original output.

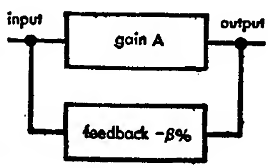

Negative feedback *continued*

The total output voltage with feedback is

$$E + N + D = e + \frac{n}{1 - \overrightarrow{A\beta}} + \frac{d}{1 - \overrightarrow{A\beta}} \tag{1}$$

It is assumed that the input signal to the amplifier is increased when negative feedback is applied, keeping $E = e$.

$(1 - \overrightarrow{A\beta})$ is a measure of the amount of feedback. By definition, the amount of feedback expressed in decibels is

$$20 \log_{10} |1 - \overrightarrow{A\beta}| \tag{2}$$

$$\text{Voltage gain with feedback} = \frac{\mathbf{A}}{1 - \overrightarrow{A\beta}} \tag{3}$$

$$\text{and change of gain} = \frac{1}{1 - \overrightarrow{A\beta}} \tag{4}$$

If the amount of feedback is large, i.e., $-\overrightarrow{A\beta} \gg 1$,

voltage gain becomes $-\overrightarrow{1/\beta}$ and so is independent of **A**. (5)

In the general case when ϕ is not restricted to 0 or π

$$\text{the voltage gain} = \frac{\mathbf{A}}{\sqrt{1 + |\overrightarrow{A\beta}|^2 - 2|\overrightarrow{A\beta}|\cos\phi}} \tag{6}$$

$$\text{and change of gain} = \frac{1}{\sqrt{1 + |\overrightarrow{A\beta}|^2 - 2|\overrightarrow{A\beta}|\cos\phi}} \tag{7}$$

Hence if $|\overrightarrow{A\beta}| \gg 1$, the expression is substantially independent of ϕ.

On the polar diagram relating $(\overrightarrow{A\beta})$ and ϕ (Nyquist diagram), the system is unstable if the point (1, 0) is enclosed by the curve. Examples of Nyquist diagrams for feedback amplifiers will be found in the chapter on "Feedback control systems".

Feedback amplifier with single beam-power tube

The use of the foregoing negative feedback formulas is illustrated by the amplifier circuit shown in Fig. 4.

The amplifier consists of an output stage using a 6V6-G beam-power tetrode with feedback, driven by a resistance-coupled stage using a 6J7-G

Negative feedback *continued*

in a pentode connection. Except for resistors R_1 and R_2 which supply the feedback voltage, the circuit constants and tube characteristics are taken from published data.

The fraction of the output voltage to be fed back is determined by specifying that the total harmonic distortion is not to exceed 4 percent. The plate supply voltage is taken as 250 volts. At this voltage, the 6V6-G has 8-percent

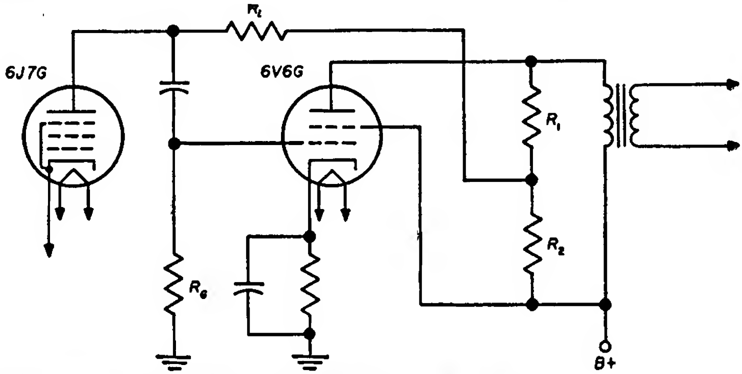

Fig. 4—Feedback amplifier with single beam-power tube.

total harmonic distortion. From equation (1), it is seen that the distortion output voltage with feedback is

$$D = \frac{d}{1 - \vec{\mathbf{A}\beta}}$$

This may be written as

$$1 - \vec{\mathbf{A}\beta} = \frac{d}{D}$$

where

$$\frac{d}{D} = \frac{8}{4} = 2 \qquad 1 - \vec{\mathbf{A}\beta} = 2 \qquad \vec{\beta} = -\frac{1}{\mathbf{A}}$$

and where $\mathbf{A}$ = the voltage amplification of the amplifier without feedback.

The peak a-f voltage output of the 6V6-G under the assumed conditions is

$$E_o = \sqrt{4.5 \times 5000 \times 2} = 212 \text{ volts}$$

This voltage is obtained with a peak a-f grid voltage of 12.5 volts so that the voltage gain of this stage without feedback is

$$\mathbf{A} = \frac{212}{12.5} = 17$$

Negative feedback *continued*

Hence $\vec{\beta} = -\frac{1}{\mathbf{A}} = -\frac{1}{17} = -0.0589$ or 5.9 percent, approximately.

The voltage gain of the output stage with feedback is computed from equation (3) as follows

$$\mathbf{A}' = \frac{\mathbf{A}}{1 - \mathbf{A}\vec{\beta}} = \frac{17}{2} = 8.5$$

and the change of gain due to feedback by equation (4) is thus

$$\frac{1}{1 - \mathbf{A}\vec{\beta}} = 0.5$$

The required amount of feedback voltage is obtained by choosing suitable values for R_1 and R_2. The feedback voltage on the grid of the 6V6-G is reduced by the effect of R_g, R_l and the plate resistance of the 6J7-G. The effective grid resistance is

$$R_g' = \frac{R_g r_p}{R_g + r_p}$$

where $R_g = 0.5$ megohm.

This is the maximum allowable resistance in the grid circuit of the 6V6-G with cathode bias.

$r_p = 4$ megohms = the plate resistance of the 6J7-G tube

$$R_g' = \frac{4 \times 0.5}{4 + 0.5} = 0.445 \text{ megohm}$$

The fraction of the feedback voltage across R_2 that appears at the grid of the 6V6-G is

$$\frac{R_g'}{R_g' + R_l} = \frac{0.445}{0.445 + 0.25} = 0.64$$

where $R_l = 0.25$ megohm.

Thus the voltage across R_2 to give the required feedback must be

$$\frac{5.9}{0.64} = 9.2 \text{ percent of the output voltage.}$$

This voltage will be obtained if $R_1 = 50{,}000$ ohms and $R_2 = 5000$ ohms. This resistance combination gives a feedback voltage ratio of

$$\frac{5000 \times 100}{50{,}000 + 5000} = 9.1 \text{ percent of the output voltage}$$

Negative feedback *continued*

In a transformer-coupled output stage, the effect of phase shift on the gain with feedback does not become appreciable until a noticeable decrease in gain without feedback also occurs. In the high-frequency range, a phase shift of 25 degrees lagging is accompanied by a 10-percent decrease in gain. For this frequency, the gain with feedback is computed from (6).

$$A' = \frac{A}{\sqrt{1 + (A\beta)^2 - 2(A\beta)\cos\phi}}$$

where $A = 15.3$, $\phi = 155°$, $\cos\phi = -0.906$, $\beta = 0.059$.

$$A' = \frac{15.3}{\sqrt{1 + 0.9^2 + 2 \times 0.9 \times 0.906}} = \frac{15.3}{\sqrt{3.44}} = \frac{15.3}{1.85} = 8.27$$

The change of gain with feedback is computed from (7).

$$\frac{1}{\sqrt{1 + (A\beta)^2 - 2(A\beta)\cos\phi}} = \frac{1}{1.85} = 0.541$$

if this gain with feedback is compared with the value of 8.5 for the case of no phase shift, it is seen that the effect of frequency on the gain is only 2.7 percent with feedback compared to 10 percent without feedback.

The change of gain with feedback is 0.541 times the gain without feedback whereas in the frequency range where there is no phase shift, the corresponding value is 0.5. This quantity is 0.511 when there is phase shift but no decrease of gain without feedback.

Special applications of feedback (anode follower)

For the basic circuit shown at the right, Z_l includes the plate capacitance, plate resistance r_p, load resistance R_l, and any external load coupled to the output terminals; Z_1 includes the source capacitance, Z_2 includes the plate–grid capacitance; the grid–ground capacitance is ignored; and the dc circuits are omitted for clarity. Then,

$E_2/E_1 \approx -Z_2/Z_1$

so long as

$$g_m Z_l \gg \left(\frac{Z_l}{Z_1} + \frac{Z_2}{Z_1} + 1\right)$$

and

$g_m Z_2 \gg 1$

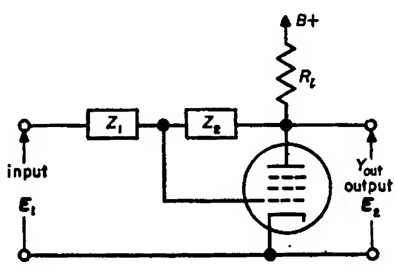

Negative feedback *continued*

The two inequalities shown above must be satisfied if the circuits shown in this section are to give satisfactory performance.

$$Y_{out} = \frac{Z_1}{Z_1 + Z_2} g_m + \frac{1}{Z_l} + \frac{1}{Z_1 + Z_2}$$

Integrator (Miller type)

$$\mathbf{E}_2 \approx -\frac{\mathbf{E}_1}{j\omega C_2 R_1}$$

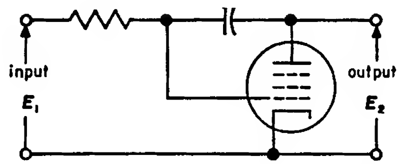

Differentiator

$$\mathbf{E}_2 \approx -j\omega R_2 C_1 \mathbf{E}_1$$

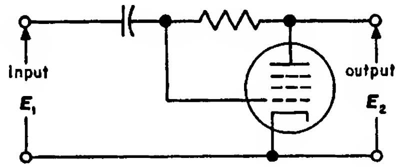

Adding network

$$\frac{\mathbf{E}_1}{Z_1} + \frac{\mathbf{E}_1'}{Z_1'} + \frac{\mathbf{E}''_1}{Z''_1} + \ldots \approx -\frac{\mathbf{E}_2}{Z_2}$$

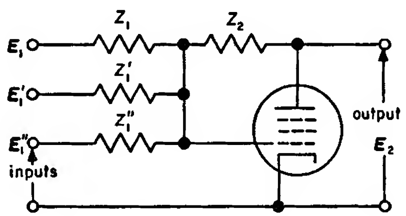

Phase inverter

$$Z_2 \approx Z_1$$

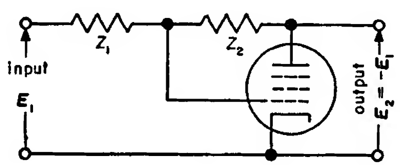

Negative feedback *continued*

Selective amplifier

$C = 1/2\pi f_0 R$

$R_1 \gg R$

$R_l \ll R$

$(bw)_{3db} = 4f_0/(\text{gain})$

$(\text{gain}) = [E_2/E_1]\, f_0$

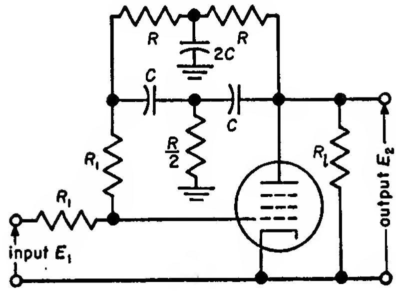

Phase shifter

$\theta \approx 2 \arctan (2\pi f R_3 C_1)$

$R_1 = R_2 \ll R_3$

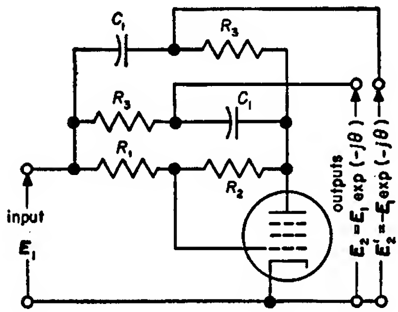

Distortion

A rapid indication of the harmonic content of an alternating source is given by the *distortion factor* which is expressed as a percentage.

$$\begin{pmatrix}\text{Distortion}\\ \text{factor}\end{pmatrix} = \sqrt{\frac{(\text{sum of squares of amplitudes of harmonics})}{(\text{square of amplitude of fundamental})}} \times 100 \text{ percent}$$

If this factor is reasonably small, say less than 10 percent, the error involved in measuring it,

$$\sqrt{\frac{(\text{sum of squares of amplitudes of harmonics})}{(\text{sum of squares of amplitudes of fundamental and harmonics})}} \times 100 \text{ percent}$$

is also small. This latter is measured by the *distortion-factor meter*.

Capacitive-differentiation amplifiers

Capacitive-differentiation systems employ a series-RC circuit (Fig. 5) with the output voltage e_2 taken across R_2. The latter includes the resistance of the load, which is assumed to have a negligible reactive component compared to R_2. In many applications the circuit time constant $RC \ll T$, where T is the period of the input pulse e_1. Thus, transients constitute a minor part of the response, which is essentially a steady-state phenomenon within the time domain of the pulse.

Differential equation

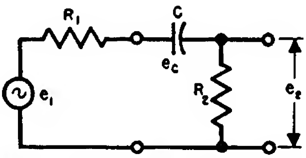

Fig. 5—Capacitive differentiation.

$$e_1 = e_c + RC\frac{de_c}{dt}$$

where $R = R_1 + R_2$. Then

$$e_2 = R_2C\frac{de_c}{dt} = \frac{R_2}{R}(e_1 - e_c)$$

When the rise and decay times of the pulse are each $\gg RC$.

$$e_2 \approx R_2C\frac{de_1}{dt}$$

Trapezoidal input pulse

When T_1, T_2, and T_3 are each much greater than RC, the output response e_2 is approximately rectangular, as shown in Fig. 6.

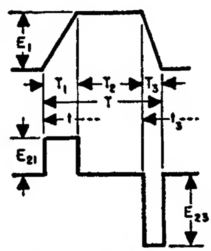

Fig. 6—Trapezoidal input pulse and principal response.

$$E_{21} = E_1R_2C/T_1$$

$$E_{23} = -E_1R_2C/T_3$$

More accurately, for any value of T, but for widely spaced input pulses,

If $\quad 0 < t < T_1$: $e_{21} = \dfrac{E_1R_2C}{T_1}\left[1 - \exp\left(-\dfrac{t}{RC}\right)\right]$

$$T_1 < t < (T_1 + T_2):\ e_{22} = \frac{E_1R_2C}{T_1}\left[\exp\left(\frac{T_1}{RC}\right) - 1\right]\exp\left(-\frac{t}{RC}\right)$$

Note: $\quad \exp\left(-\dfrac{t}{RC}\right) = \epsilon^{-t/RC}$

Capacitive-differentiation amplifiers *continued*

$$(T_1 + T_2) < t < T:\ e_{23} = -\frac{E_1R_2C}{T_3}\left\{1 - \left\{\frac{T_3}{T_1}\left[\exp\left(\frac{T_1}{RC}\right) - 1\right]\right.\right.$$
$$\left.\left. + \exp\left(\frac{T_1 + T_2}{RC}\right)\right\} \exp\left(-\frac{t}{RC}\right)\right\}$$

$$t > T:\quad e_{2x} = \frac{E_1R_2C}{T_3}\left\{\frac{T_3}{T_1}\left[\exp\left(\frac{T_1}{RC}\right) - 1\right]\right.$$
$$\left. + \exp\left(\frac{T_1 + T_2}{RC}\right) - \exp\left(\frac{T}{RC}\right)\right\} \exp\left(-\frac{t}{RC}\right)$$
$$= A \exp\left(-\frac{t}{RC}\right)$$

$$\text{when } T_2 \gg RC:\quad e_{23} = -\frac{E_1R_2C}{T_3}\left[1 - \exp\left(-\frac{t_3}{RC}\right)\right]$$

For a long train of identical pulses repeated at regular intervals of T_r between starting points of adjacent pulses, add to each of the above (e_{21}, e_{22}, e_{23}, and e_{2x}) a term

$$e_{20} = \frac{A}{\exp\left(\frac{T_r}{RC}\right) - 1} \exp\left(-\frac{t}{RC}\right)$$

where A is defined in the expression for e_{2x} above.

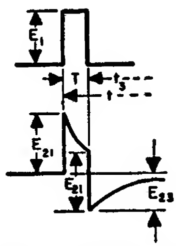

Fig. 7—Single rectangular pulse and response for T much shorter than in Fig. 6.

Rectangular input pulse

Fig. 7 is a special case of Fig. 6, with $T_1 = T_3 = 0$.

$$0 < t < T:\quad e_{21} = \frac{R_2}{R} E_1 \exp\left(-\frac{t}{RC}\right) = E_{21} \exp\left(-\frac{t}{RC}\right)$$

$$t > T:\quad e_{23} = -\frac{R_2}{R} E_1 \left[\exp\left(\frac{T}{RC}\right) - 1\right] \exp\left(-\frac{t}{RC}\right)$$
$$= E_{23} \exp\left(-\frac{t_3}{RC}\right)$$

$$\text{where } E_{23} = -\frac{R_2}{R} E_1 \left[1 - \exp\left(-\frac{T}{RC}\right)\right]$$

Capacitive-differentiation amplifiers *continued*

Triangular input pulse

Fig. 8 is a special case of the trapezoidal pulse, with $T_2 = 0$. The total output amplitude is approximately

$$|E_{21}| + |E_{23}| = |E_1| R_2C \frac{T_1 + T_3}{T_1T_3}$$

which is a maximum

when $T_1 = T_3$.

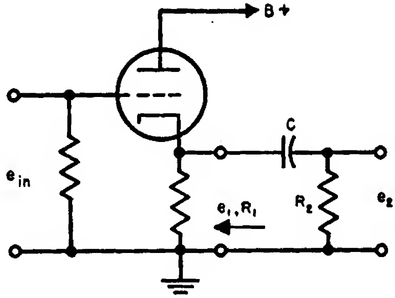

Fig. 9—Capacitive-differentiation circuit with cathode-follower source.

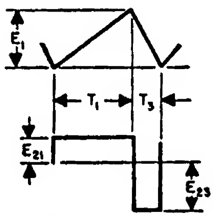

Fig. 8 — Triangular pulse—special case of Fig. 6.

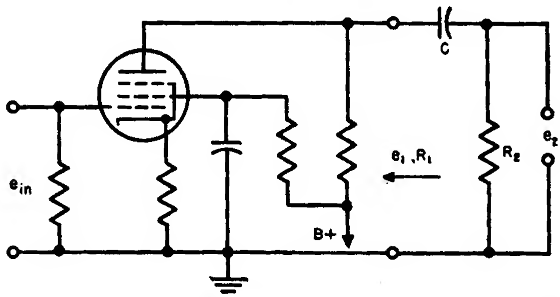

Fig. 10—Capacitive-differentiation circuit with plate-circuit source.

Schematic diagrams

Two capacitive-differentiation circuits using vacuum tubes as driving sources are given in Figs. 9 and 10.

Capacitive-integration amplifiers

Capacitive-integration circuits employ a series-RC circuit (Fig. 11) with the output voltage e_2 taken across capacitor C. The load admittance is accounted for by including its capacitance in C; while its shunt resistance is combined with R_1 and R_2 to form a voltage divider treated by Thevenin's theorem. In contrast with capacitive differentiation, time constant $RC \gg T$ in many applications. Thus, the output voltage is composed mostly of the early part of a transient response to the input voltage wave. For a long repeated train of identical input pulses, this repeated transient response becomes steady-state.

Capacitive-integration amplifiers *continued*

Circuit equations

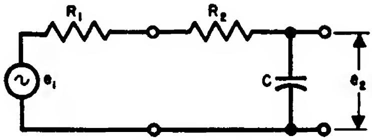

Fig. 11—Capacitive integration.

$$e_1 = e_2 + RC\frac{de_2}{dt}$$

where $R = R_1 + R_2$.

When $t \ll RC$ and E_{20} is very small compared to the amplitude of e_1,

$$e_2 \approx E_{20} + \frac{1}{RC}\int_0^t e_1\,dt$$

where E_{20} = value of e_2 at time $t = 0$.

Rectangular input-wave train

See Fig. 12.

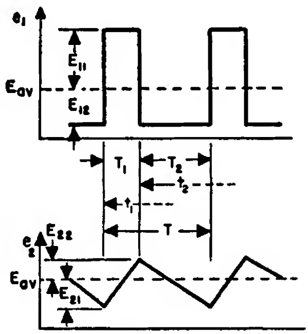

Fig. 12—Rectangular input-wave train at top Below, output wave on an exaggerated voltage scale.

$$E_{av} = \frac{1}{T}\int_0^T e_1\,dt$$

Then

$$E_{11}T_1 + E_{12}T_2 = 0$$

After equilibrium or steady-state has been established,

$$e_{21} = E_{av} + E_{11}\left[1 - \exp\left(-\frac{t_1}{RC}\right)\right] + E_{21}\exp\left(-\frac{t_1}{RC}\right)$$

$$e_{22} = E_{av} + E_{12}\left[1 - \exp\left(-\frac{t_2}{RC}\right)\right] + E_{22}\exp\left(-\frac{t_2}{RC}\right)$$

If the steady-state has not been established at time $t_1 = 0$, add to e_2 the term

$$(E_{20} - E_{av} - E_{21})\exp\left(-\frac{t_1}{RC}\right)$$

When $T_1 = T_2 = T/2$, then

$$E_{11} = -E_{12} = E_1$$
$$E_2 = E_{22} = -E_{21} = E_1 \tanh\ (T/4RC)$$

Capacitive-integration amplifiers *continued*

Approximately, for any T_1 and T_2, provided $T \ll RC$,

$0 < t_1 < T_1$: $e_{21} = E_{av} - E_2\,(1 - 2t_1/T_1)$

$0 < t_2 < T_2$: $e_{22} = E_{av} + E_2\,(1 - 2t_2/T_2)$

where $E_2 = E_{22} = -E_{21} = E_{11}T_1/2RC$
$= -E_{12}T_2/2RC$

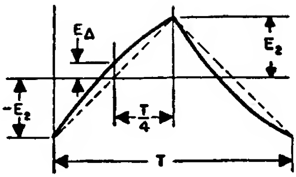

Fig. 13—Error E_Δ from assuming a linear output (dashed line).

Error due to assuming a linear output-voltage wave (Fig. 13) is

$E_\Delta/E_2 \approx T/8RC$

when $T_1 = T_2 = T/2$. The error in E_2 due to setting $\tanh\,(T/4RC) = T/4RC$ is comparatively negligible. When $T/RC = 0.7$, the approximate error in E_2 is only 1 percent. However, the error E_Δ is 1 percent of E_2 when $T/RC = 0.08$.

Biased rectangular input wave

In Fig. 14, when $(T_1 + T_2) \ll RC$, and $E_{20} = 0$ at $t = 0$, the output voltage approximates a series of steps.

$E_2 = E_1T_1/RC$

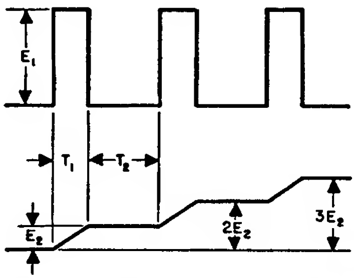

Fig. 14—Rectangular input wave gives stepped output.

Triangular input wave

In Fig. 15, when $(T_1 + T_2) \ll RC$, and after the steady-state has been established, then, approximately,

$0 < t_1 < T_1$:

$$e_{21} = E_{20} + E_{21} - 4E_{21}\left(\frac{t_1}{T_1} - \frac{1}{2}\right)^2$$

$0 < t_2 < T_2$:

$$e_{22} = E_{20} + E_{22} - 4E_{22}\left(\frac{t_2}{T_2} - \frac{1}{2}\right)^2$$

where

$E_{20} = E_1\,(T_2 - T_1)/6RC$

$E_{21} = E_1T_1/4RC$

$E_{22} = -E_1T_2/4RC$

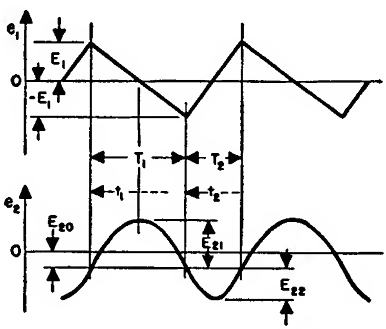

Fig. 15—Triangular input wave at top. Below, parabolic output wave on an exaggerated voltage scale.

Capacitive-integration amplifiers *continued*

Schematic diagrams

Two capacitive-integration circuits using vacuum tubes as sources are given in Figs. 16 and 17.

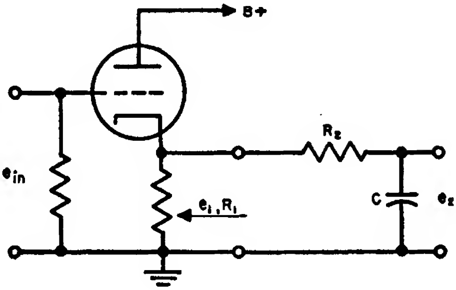

Fig. 16 (right)—Capacitive-integration circuit with cathode-follower source.

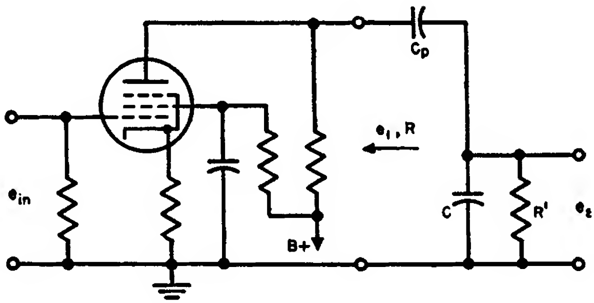

Fig. 17 (right)—Capacitive-integration circuit with plate-circuit source. $C_p \gg C$ and $R' \gg R$

Relaxation oscillators

Relaxation oscillators are a class of oscillator characterized by a large excess of positive feedback, causing the circuit to operate in abrupt transitions between two blocked or overloaded end-states. These end-states may be *stable*, the circuit remaining in such condition until externally disturbed; or *quasistable*, recovering (after a period determined by coupling time-constants and bias) and switching back to the opposite state. Relaxation oscillators are classified as *bistable*, *monostable*, or *astable* according to the number of stable end-states. Most circuits are adaptable to all three forms. Multistate devices are also possible. A wide variety of circuit arrangements is possible, including multivibrators, blocking oscillators, trigger circuits, counters, and circuits of the phantastron, sanotron, and sanophant class. Relaxation oscillators are often used for counting and frequency division, and to generate nonsinusoidal waveforms for timing, triggering, and similar applications.

Multivibrators

A number of multivibrator circuits are formed from three basic two-stage amplifiers (grounded-cathode–grounded-cathode, grounded-plate–grounded-

Relaxation oscillators *continued*

grid, and grounded-cathode–grounded-grid or combinations of these types), that readily provide the needed positive feedback with simple resistance or resistance–capacitance coupling. End-states may be any two of the four "blocked" conditions corresponding to cutoff or saturation in either stage. In general, the duration of a quasistable state will be determined by the exponential decay of charge stored in a coupling-circuit time-constant (the circuit switching back to the opposite state when the saturated or the cutoff tube recovers gain) while stable states are produced by direct coupling with bias sufficient to hold one tube inoperative. The memory effect of charge storage also operates in the case of stable end-states to ensure completion of transfer across the unstable region. The timing accuracy of an astable or quasistable multivibrator is considerably improved by supplying the grid resistors from a high positive voltage (B+). The recovery from a cutoff condition thereby becomes an exponential towards a voltage much higher than the operating point, terminating in switch-over when the cutoff tube conducts. Grid conduction serves to clamp the capacitor voltage during the conducting state, erasing residual charge from the previous state. The starting condition for the next transition is thus more precisely determined and the linearity of the exponential recovery is improved by the more nearly constant-current discharge (since the range from cutoff to zero bias represents a smaller fraction of total charge). The grid-circuit time-constant must be appropriately increased to obtain the same dwell time.

Bistable circuits

Bistable circuits are especially suited for binary counters and frequency dividers and as trigger circuits to produce a step or pulse when an input signal passes above or below a selected amplitude.

Symmetrical bistable multivibrator: The circuit is shown in Fig. 18. Trigger signal may be applied to both plates, both grids, or if pentodes are used, to both suppressor grids.

Binary counter stage: An adaptation of the symmetrical bistable multivibrator is shown in Fig. 19. Alternative trigger inputs are shown with corresponding outputs to drive a following stage. The use of coupling diodes (V_3, V_4) reduces the tendency of C_1, C_2 in the circuit of Fig. 18 to cause misfiring by unbalanced stored charge. Tubes V_5 and V_6 illustrate the application of clamping diodes, especially useful in high-speed circuits, to fix critical operating voltages. Pentodes with plate and grid clamping are suitable for very-high speeds.

Relaxation oscillators *continued*

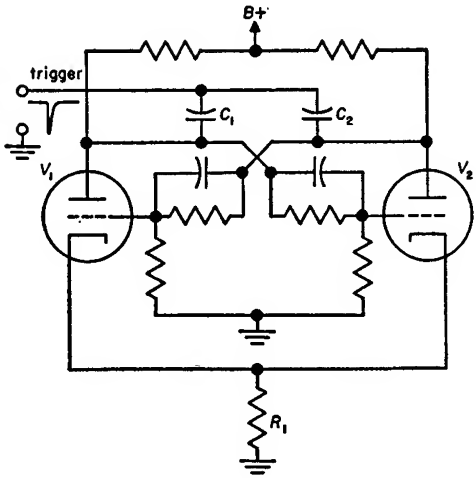

Fig. 18—Symmetrical bistable multivibrator (basic binary counter).

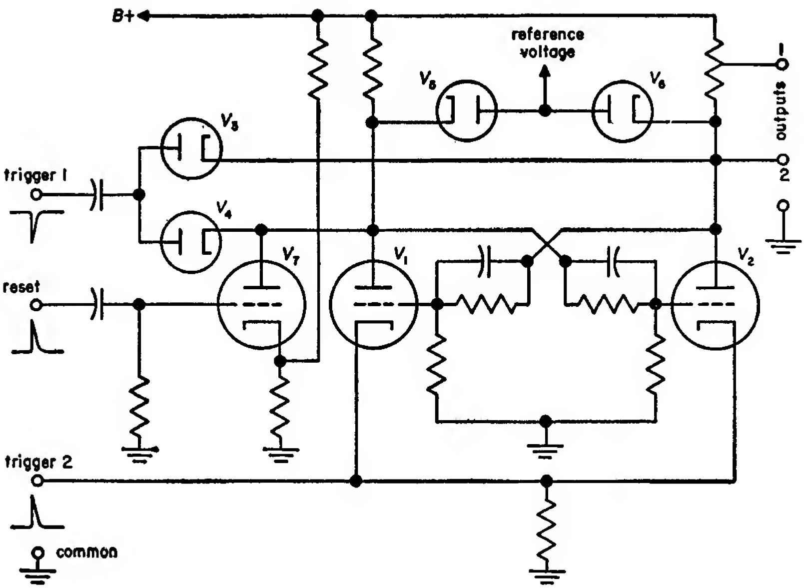

Fig. 19—Binary counter stage.

Relaxation oscillators *continued*

Schmitt trigger: The circuit of Fig. 20 has the property that an output of constant peak value (a flat-topped pulse) is obtained for the period that the input waveform exceeds a specific voltage.

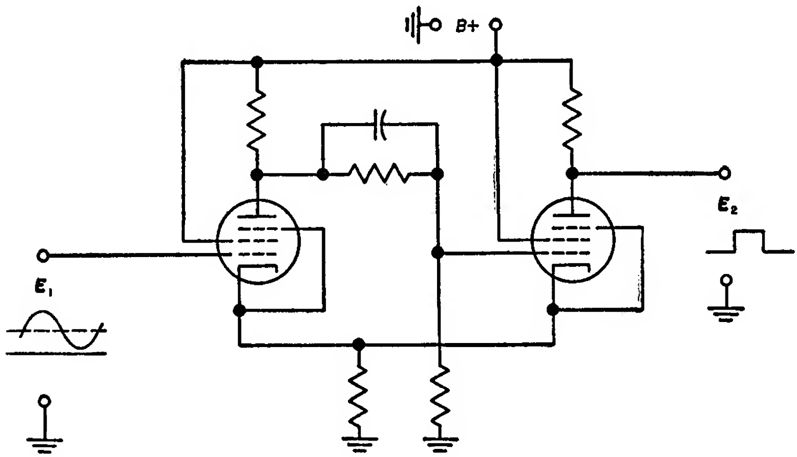

Fig. 20—Basic Schmitt trigger.

Monostable circuits

Monostable multivibrators are useful for driven-sweep, pulse, and timing-wave generators. The absence of time-constants and residual charge "memory" in the stable state reduces jitter when driven with irregularly spaced timing signals. Monostable versions may be derived from all of the foregoing bistable multivibrators by elimination of the direct (dc) coupling to one or the other grid. The circuit of Figure 21 with R omitted is commonly used for pulse generation.

Most astable circuits can be made monostable by sufficient inequality of bias. The circuit of Fig. 24 is an example.

Sweep waveforms can be produced by integration of pulse outputs. The phantastron class of Miller sweep generators are also particularly useful for this purpose.

Driven (one-shot) multivibrator: Circuit is given in Fig. 22. Equations are

Relaxation oscillators *continued*

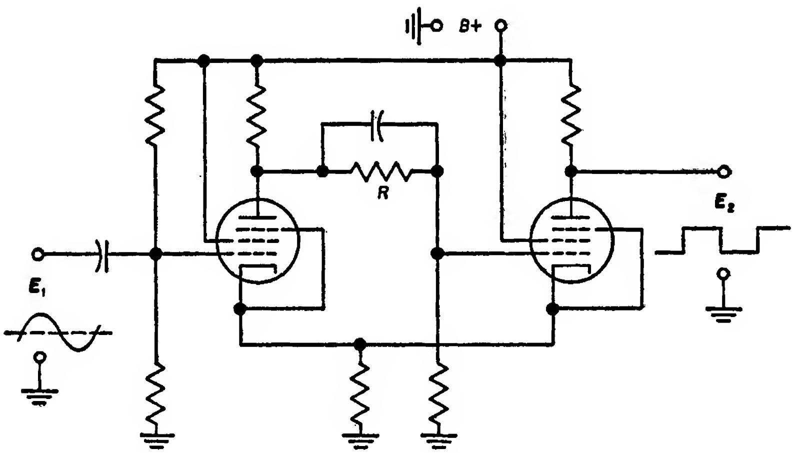

Fig. 21—Regenerative clipper (modified Schmitt trigger).

$f_{mv} = f_s$

f_{mv} = multivibrator frequency in cycles/second

f_s = synchronizing frequency in cycles/second

Conditions of operation are

$f_s > f_n$ or $\mathcal{T}_s < \mathcal{T}_n$

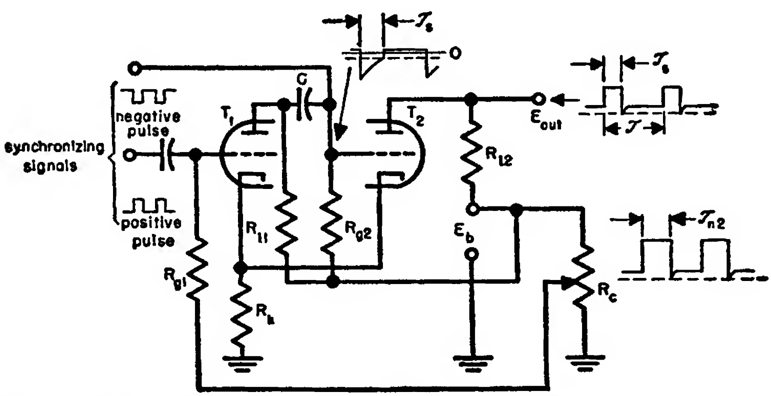

Fig. 22—Driven (one-shot) multivibrator schematic and waveforms.

Relaxation oscillators *continued*

where

f_n = free-running frequency in cycles/second

$\mathfrak{T}_s$ = synchronizing period in seconds

$\mathfrak{T}_n$ = free-running period in seconds

$$\mathfrak{T}_{n2} = R_{g2}C \log_e \left(\frac{E_{b1} - E_{m1} + E_{c2}}{E_{c2} + E_{x2}} \right)$$

Regenerative clipper: Bias on the first grid places the circuit of Fig. 21 in the center of the unstable region, giving regenerative clipping.

Phantastron: The phantastron circuit is a form of monostable multivibrator with similarities to the Miller sweep circuit. It is useful for generating very-short pulses and linear sweeps. It uses a characteristic of pentodes: that

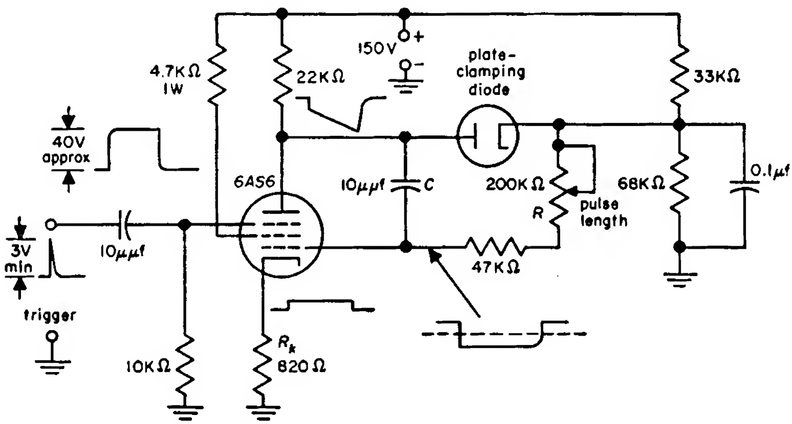

Fig. 23—Cathode-coupled phantastron.

while cathode current is determined mainly by control-grid potential, the screen-grid, suppressor-grid and plate potentials determine the division of current between plate and screen. In certain tubes, such as the 6AS6, the transconductance from suppressor grid to plate is sufficiently high so that the plate current may be cut off completely with a small negative bias on the suppressor.

A typical phantastron circuit is shown in Figure 23. During operation it switches between two states of interest.

Relaxation oscillators *continued*

a. *Stable:* the control grid is slightly positive and draws current. Cathode current is maximum and the suppressor is biased negatively to plate-current cutoff by the cathode current in R_k. The plate is at a high potential determined by the clamping diode and the screen potential is low.

b. *Unstable:* when a positive trigger is applied to the suppressor grid (or a negative trigger to the control grid, cathode, or plate) the plate conducts, driving the control grid negative, reducing the cathode current, and taking most of the screen current. The plate potential then runs down linearly as in the Miller circuit.

The end of this period comes when the control grid goes positive again, resulting in increase of cathode current, suppressor cutoff, and heavy screen current.

In the circuit shown, the pulse length is variable from 0.3 to 0.6 microseconds. For longer pulses, it is possible to get a wide range of control both by varying R and C and by varying the plate-clamping potential.

Decreasing R_k results in astable operation.

Astable circuits

The operating principles of the multivibrator and the exponential recovery from quasistable states are illustrated by the analysis of the free-running multivibrator.

Free-running zero-bias symmetrical multivibrator: Exact equation for semi-period (Figs. 24 and 25):

$$\mathcal{T}_1 = \left(R_{g1} + \frac{R_{l2} r_p}{R_{l2} + r_p}\right) C_1 \log_e \frac{E_b - E_m}{E_x}$$

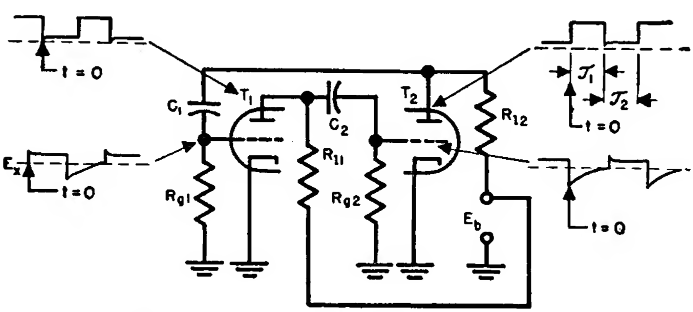

Fig. 24—Schematic diagram of symmetrical multivibrator and voltage waveforms on tube elements.

Relaxation oscillators *continued*

where

$\mathfrak{T} = \mathfrak{T}_1 + \mathfrak{T}_2 = 1/f,\ \mathfrak{T}_1 = \mathfrak{T}_2,\ R_{g1} = R_{g2},\ C_1 = C_2.$

f = repetition frequency in cycles/second

$\mathfrak{T}$ = period in seconds

$\mathfrak{T}_1$ = semiperiod in seconds

r_p = plate resistance of tube in ohms

E_b = plate-supply voltage

E_m = minimum alternating voltage on plate

E_x = cutoff voltage corresponding to E_b

C = capacitance in farads

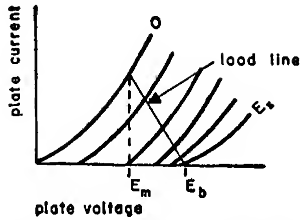

Fig. 25—Multivibrator potentials on plate-characteristic curve.

Approximate equation for semiperiod, where $R_{g1} \gg \dfrac{R_{l2}r_p}{R_{l2} + r_p}$, is

$$\mathfrak{T}_1 = R_{g1}C_1 \log_e\left(\frac{E_b - E_m}{E_x}\right)$$

Equation for buildup time is

$\mathfrak{T}_B = 4(R_l + r_p)C$ = 98 percent of peak value

Free-running zero-bias unsymmetrical multivibrator: See symmetrical multivibrator for circuit and terminology; the wave forms are given in Fig. 26.

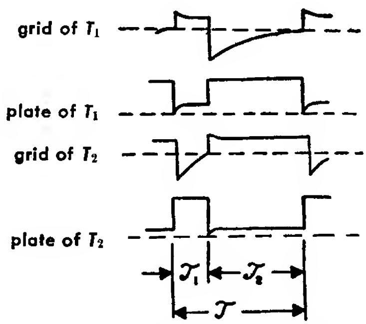

Fig. 26 — Unsymmetrical multivibrator waveforms.

Equations for fractional periods are

$$\mathfrak{T}_1 = \left(R_{g1} + \frac{R_{l2}r_p}{R_{l2} + r_p}\right) C_1 \log_e\left(\frac{E_{b2} - E_{m2}}{E_{x1}}\right)$$

$$\mathfrak{T}_2 = \left(R_{g2} + \frac{R_{l1}r_p}{R_{l1} + r_p}\right) C_2 \log_e\left(\frac{E_{b1} - E_{m1}}{E_{x2}}\right)$$

$$\mathfrak{T} = \mathfrak{T}_1 + \mathfrak{T}_2 = 1/f$$

Relaxation oscillators *continued*

Free-running positive-bias multivibrator: Equations for fractional period (Fig. 27) are

$$\mathfrak{I}_1 = \left(R_{g1} + \frac{R_{l2}r_p}{R_{l2} + r_p}\right) C_1 \log_e \left(\frac{E_{b2} - E_{m2} + E_{c1}}{E_{c1} + E_{x1}}\right)$$

$$\mathfrak{I}_2 = \left(R_{g2} + \frac{R_{l1}r_p}{R_{l1} + r_p}\right) C_2 \log_e \left(\frac{E_{b1} - E_{m1} + E_{c2}}{E_{c2} + E_{x2}}\right)$$

where

$\mathfrak{I} = \mathfrak{I}_1 + \mathfrak{I}_2 = 1/f$

E_c = positive bias voltage

R_c = bias control

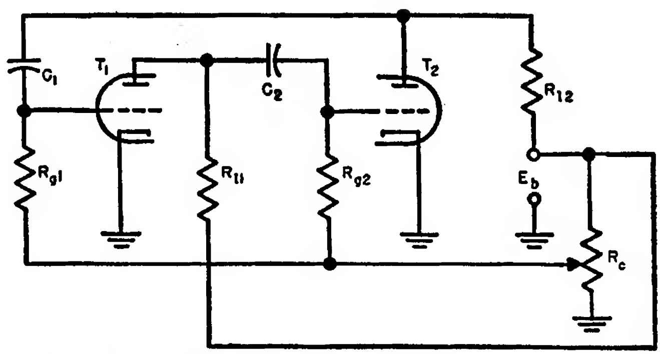

Fig. 27—Free-running positive-bias multivibrator.

Blocking oscillators

The blocking oscillator is a single-tube relaxation oscillator using a close-coupled (current) transformer that imposes a fixed current ratio between grid current and plate current, while also providing the polarity reversal for positive feedback. There are, therefore, two end-states that satisfy the requirement i_p/i_g = turns ratio: one in the positive-grid region, with large grid current, and one at cutoff, with both currents zero. Astable and monostable forms are illustrated in the following discussion.

Relaxation oscillators *continued*

Astable blocking oscillator: Conditions for blocking are

$E_1/E_0 < 1 - \epsilon^{1/\alpha f - \theta}$

where

E_0 = peak grid volts

E_1 = positive portion of grid swing in volts

E_c = grid bias in volts

f = frequency in cycles/second

α = grid time constant in seconds

ϵ = 2.718 = base of natural logs

θ = decrement of wave

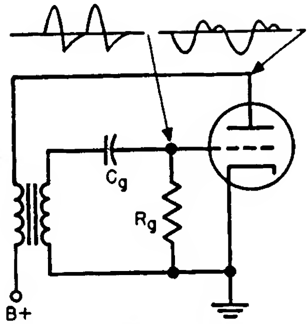

Fig. 28—Free-running blocking oscillator—schematic and waveforms.

a. Use strong feedback $= E_0$ is high

b. Use large grid time constant $= \alpha$ is large

c. Use high decrement (high losses) $= \theta$ is high

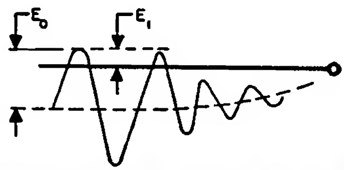

Fig. 29—Blocking-oscillator grid voltage.

Pulse width is $\mathfrak{J}_1 \approx 2\sqrt{LC}$

where

$\mathfrak{J}_1$ = pulse width in seconds

L = magnetizing inductance of transformer in henries

C = interwinding capacitance of transformer in farads

$$L = M\frac{n_1}{n_2}$$

where

M = mutual inductance between windings

n_1/n_2 = turns ratio of transformer

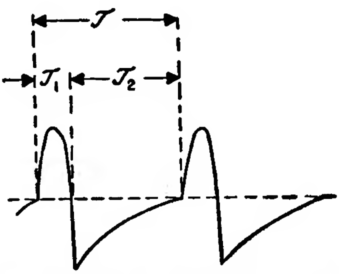

Fig. 30—Blocking oscillator pulse waveform.

Relaxation oscillators *continued*

Repetition frequency

$$\mathfrak{I}_2 \approx \frac{1}{f} \approx R_g C_g \log_e \frac{E_b + E_g}{E_b + E_x}$$

where

$\mathfrak{I}_2 \gg \mathfrak{I}_1$

f = repetition frequency in cycles/second

E_b = plate-supply voltage

E_g = maximum negative grid voltage

E_x = grid cutoff in volts

$\mathfrak{I} = \mathfrak{I}_1 + \mathfrak{I}_2 = 1/f$

Astable positive-bias wide-frequency-range blocking oscillator: Typical circuit values (Fig. 31) are

R = 0.5 to 5 megohms

C = 50 micromicrofarads to 0.1 microfarads

R_k = 10 to 200 ohms

R_b = 50,000 to 250,000 ohms

Δf = 100 cycles to 100 kilocycles

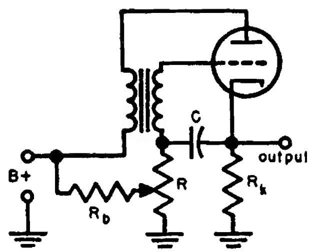

Fig. 31 — Free-running positive bias blocking oscillator.

Monostable blocking oscillator: Operating conditions (Fig. 32) are

a. Tube off unless positive voltage is applied to grid.

b. Signal input controls repetition frequency.

c. E_c is a high negative bias.

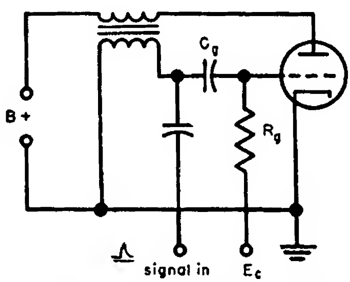

Fig. 32—Driven blocking oscillator.

Relaxation oscillators *continued*

Synchronized astable blocking oscillator: Operating conditions (Fig. 33) are

$f_n < f_s$ or $T_n > T_s$

where

f_n = free-running frequency in cycles/second

f_s = synchronizing frequency in cycles/second

T_n = free-running period in seconds

T_s = synchronizing period in seconds

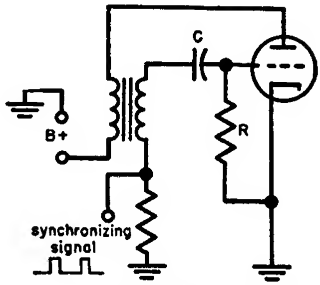

Fig. 33—Synchronized blocking oscillator.

Gas-tube oscillators

A simple relaxation oscillator is based on the negative-resistance characteristic of a glow discharge, the two end-states corresponding to ignition and extinction potential of the discharge. Two astable forms are discussed. The circuit of Fig. 34 may also be used with a simple diode (neon lamp), omitting the grid resistor and bias. The circuit of Fig. 35 may be made monostable if the supply voltage is less than the ignition voltage at the selected bias.

Astable gas-tube oscillator: This circuit is often used as a simple generator of the sawtooth waveform necessary for the horizontal deflection of a cathode-ray oscilloscope beam. Equation for period (Fig. 34)

$\mathfrak{T} = \alpha RC\ (1 + \alpha/2)$

where

$\mathfrak{T}$ = period in cycles/second

$$\alpha = \frac{E_i - E_x}{E - E_x}$$

E_i = ignition voltage

E_x = extinction voltage

E = plate-supply voltage

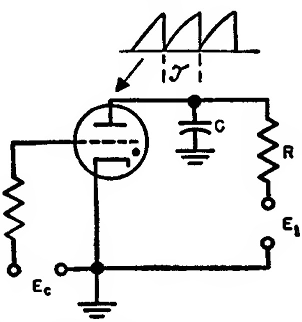

Fig. 34—Free-running gas-tube oscillator.

Gas-tube oscillators *continued*

Velocity error = change in velocity of cathode-ray-tube spot over trace-period.

Maximum percentage error = $\alpha \times 100$

if $\alpha \ll 1$.

Position error = deviation of cathode-ray-tube trace from linearity.

Maximum percentage error $= \frac{\alpha}{8} \times 100$

if $\alpha \ll 1$.

Synchronized astable gas-tube oscillator: Conditions for synchronization (Fig. 35) are

$f_s = Nf_n$

where

f_n = free-running frequency in cycles/second

f_s = synchronizing frequency in cycles/second

N = an integer

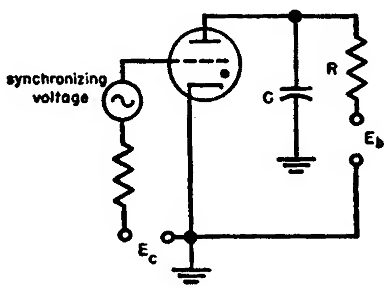

Fig. 35—Synchronized gas-tube oscillator.

For $f_s \neq Nf_n$, the maximum δf_n before slipping is given by

$$\frac{E_0}{E_s}\frac{\delta f_n}{f_s} = 1$$

where

$\delta f_n = f_n - f_s$

E_0 = free-running ignition voltage

E_s = synchronizing voltage referred to plate circuit

■ Semiconductors and transistors

Definitions

Acceptor impurity: An impurity that may induce hole conduction.

Base region: The interelectrode region of a *transistor* into which *minority carriers* are injected.

Bias: The quiescent direct emitter current or collector voltage of a transistor.

Breakdown voltage: The reverse voltage at which a *pn* junction draws a large current.

Carrier: In a semiconductor, a mobile *conduction electron* or *hole.*

Collector: An electrode through which a flow of minority carriers leaves the interelectrode region.

Conduction band: A range of states in the energy spectrum of a solid in which electrons can move freely.

Depletion layer, space-charge layer: A region in which the mobile *carrier* charge density is insufficient to neutralize the net fixed charge density of *donors* and *acceptors.*

Donor impurity: An impurity that may induce electronic conduction.

Doping: Addition of *impurities* to a semiconductor or production of a deviation from stoichiometric composition, to achieve a desired characteristic.

Electron: The electrons in the *conduction band* of a solid, which are free to move under the influence of an electric field.

Emitter: An *electrode* from which a flow of *minority carriers* enters the interelectrode region.

Energy gap: The energy range between the bottom of the *conduction band* and the top of the *valence band.*

Definitions *continued*

Hole: A mobile vacancy in the electronic valence structure of a semiconductor that acts like a positive electronic charge with a positive mass.

Interbase current: In a junction tetrode transistor, the current that flows from one base connection to the other through the base region.

***i*-type or intrinsic semiconductor:** A semiconductor in which the electrical properties are essentially not modified by *impurities* or *imperfections* within the crystal.

Junction: See *pn* junction.

Lifetime of minority carriers: The average time interval between the generation and recombination of *minority carriers* in a homogeneous semiconductor.

Majority carriers: The type of *carrier* constituting more than half of the total number of *carriers*.

Minority carriers: The type of *carrier* constituting less than half of the total number of *carriers*.

Mobility: The average drift velocity of *carriers* per unit electric field.

***n*-type semiconductor:** An *extrinsic semiconductor* in which the *conduction-electron* density exceeds the *hole* density.

Ohmic contact: A contact between two materials, possessing the property that the potential difference across it is proportional to the current passing through it.

Photodiode: A two-electrode semiconductor device sensitive to light. Photoconductive cells are photodiodes in which the resistance decreases when illuminated. Photoelectric cells are self-generating photodiodes.

Phototransistors: Photoconductive cells that have current-multiplying collectors.

***pn* junction:** A region of transition between *p*- and *n*-type semiconducting material.

p-type semiconductor: An *extrinsic semiconductor* in which the *hole* density exceeds the *conduction-electron* density.

Definitions *continued*

Punch-through: At sufficiently high collector voltage in a junction transistor with very narrow base region, the space-charge layer may extend completely across the base region, causing an emitter-to-collector breakdown that is called punch-through (see Fig. 21).

Saturation current: In a reverse-biased junction, the current due to thermally generated electrons or holes.

Semiconductor: An electronic conductor, with resistivity in the range between metals and insulators, in which the electrical charge *carrier* concentration increases with increasing temperature over some temperature range. Certain semiconductors possess 2 types of *carriers*, namely, negative electrons and positive *holes*.

Semiconductor device: An electronic device in which the characteristic distinguishing electronic conduction takes place within a semiconductor.

Semiconductor, extrinsic: A semiconductor with electrical properties dependent upon *impurities*.

Thermistor: An electronic device that makes use of the change of resistivity of a semiconductor with change in temperature.

Transistor: An active *semiconductor device* with 3 or more electrodes.

Valence band: The range of energy states in the spectrum of a solid crystal in which lie the energies of the valence electrons that bind the crystal together.

Varistor: A 2-electrode *semiconductor device* having a voltage-dependent nonlinear resistance.

Semiconductors

Semiconductor materials and applications

device	semiconductor	type	applications
Transistors	Germanium	Junction	General-purpose to 75° C
	Germanium	Point-contact	Computors
	Silicon	Junction	High-temperature use

Semiconductors *continued*

device	semiconductor	type	applications
Rectifiers	Germanium	Point-contact diode	Economical, useful to vhf
	Germanium	Junction diode	High-rectification-ratio diode
	Germanium	Junction diode	Power rectifier
	Silicon	Point-contact diode	Microwave detector, mixer
	Silicon	Junction diode	Very-high-rectification-ratio diode, voltage control or reference
	Silicon	Junction diode	Power rectifier
	Selenium	Dry-disk	Power-supply rectifier, low-frequency diode
	Copper oxide	Dry-disk	Meter rectifier, ring modulator
	Copper sulfide	Dry-disk	Low-voltage power rectifier
Varistors	Silicon carbide	Fired	Voltage surge suppressor, voltage limiter
	Selenium	Dry-disk	Contact protector
	Copper oxide	Dry-disk	Voltage surge suppressor
Thermistors	Mixed metallic oxides	Fired	Temperature sensing, current surge suppressor, temperature compensation
Photoconductive cells	Germanium	Junction	General-purpose
	Germanium	Point-contact	Phototransistor
	Lead sulfide	—	Infrared detector
	Lead telluride	—	Infrared detector
Photoelectric cells	Silicon	Junction	Power source for transistors
	Cadmium sulfide	Junction	Power source for transistors
	Selenium	Dry-disk	Light meter

Diodes, photodiodes, varistors, and thermistors

Diodes as discussed here denote rectifiers for rated currents of less than 1 ampere. These can be divided into three general classes:

a. *Point-contact diodes* are better for high frequencies than junction diodes due to reduced minority-carrier storage effects and smaller rectifying areas.

Semiconductors *continued*

b. *Junction diodes* have better rectifying characteristics than point-contact types, especially in the reverse direction, and they are generally less noisy.

c. *Selenium diodes* are small-area selenium rectifiers that have characteristics similar to selenium power rectifiers.

Photodiodes are junction germanium diodes constructed so that light can be directed onto the crystal surface at the *pn* junction. The diode is reverse-biased, the saturation current comprising the dark current. Incident light causes photo-generated hole-electron pairs, some of which are "collected" through the junction, adding to the current. Phototransistors are similar except that the diode has either a point-contact collector or a junction-hook collector, either of which "multiplies" collected current.

Varistors, or voltage-sensitive resistors, made of silicon carbide, have voltage–current characteristics that can be approximated by

$$I \approx AV^n$$

for $V > 5$ volts. Units are available for values of n between about 3.5 and 7.0.

Characteristics somewhat similar to this are obtained with pairs of dry-disk rectifiers wired in series, back-to-back (Fig. 1). Selenium rectifiers are used in this way for contact protection* in which service they offer a low resistance to high induced voltages but a high resistance to normal voltages. With this connection, the characteristic is essentially that of the reverse of one of the cells but is symmetrical in either direction. In the parallel front-to-back connection, the characteristic is like that of the forward of the individual cell, but symmetrical. Copper-oxide rectifiers are used in the latter way as symmetrical limiters for low voltages.

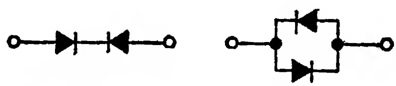
Series back-to-back. Parallel front-to-back.
Fig. 1—Connections for rectifier-type varistors.

Silicon junction diodes have very-sharp reverse voltage breakdown characteristics and hence are also useful as voltage limiters. (Nonsymmetrical unless two are used in series back-to-back.) They are available with breakdown voltages in 20-percent-range steps from 6.8 to 470 volts. They can be used in a way similar to gas discharge voltage-regulator tubes to give a constant-voltage supply with varying input voltage or varying load current.

* H. F. Herbig and J. D. Winters, "Investigation of the Selenium Rectifier for Contact Protection," *Transactions of the American Institute of Electrical Engineers*, vol. 70, part 2, pp. 1919–1923; 1951: also, *Electrical Communication*, vol. 30, pp. 96–105; June, 1953.

Semiconductors *continued*

Thermistors, or thermally sensitive resistors, are made of complex metallic-oxide compounds using oxides of manganese, nickel, copper, cobalt, and sometimes other metals. They are useful for temperature measurement and control, to compensate for positive temperature coefficient of resistance of metallic conductors, and for current surge suppression.*

Vacuum or gas-filled sealed units are usable up to about 300° centigrade and air-exposed units to about 120° centigrade. The resistance decreases with increasing temperature, varying approximately exponentially with inverse absolute temperature. Cold resistances are between 500 and 500,000 ohms.

pn junctions†

Single-crystal semiconductors like germanium and silicon have little conductivity when pure, such conductivity being called *intrinsic*. Intrinsic conductivity increases exponentially with absolute temperature T, being,‡ for germanium,

$$\sigma_i = 4.3 \times 10^4 \exp(-4350/T) \text{ ohm}^{-1} \text{ centimeter}^{-1}$$

and for silicon,

$$= 3.4 \times 10^4 \exp(-6450/T) \text{ ohm}^{-1} \text{ centimeter}^{-1}$$

If very-small amounts of impurities are built into the crystal, substitutionally replacing some atoms of the semiconductor in the crystal lattice, such impurities may increase the conductivity. One atom of impurity for 10^9 to 10^5 atoms of semiconductor is used for practical purposes to bring the conductivity within the range of about 0.2 to 2000 ohm^{-1} centimeters^{-1} (5 to 0.0005 ohm-centimeters resistivity). Pentavalent elements like antimony and arsenic (donors) make the semiconductor n-type and trivalent elements like indium and aluminum (acceptors) make the semiconductor p-type. When donor and acceptor impurities are both present in the same part of a single crystal, the effects tend to cancel. The conductivity becomes n- or p-type depending on whether the donors or acceptors, respectively, are present in excess.

* J. W. Howes, "Characteristics and Applications of Thermally Sensitive Resistors, or Thermistors," *Proceedings of the Institution of Radio Engineers, Australia*, vol. 13, pp. 123–131; May, 1952: also *Electrical Communication*, vol. 32, pp. 98–111; June, 1955.

† W. Shockley, "Electrons and Holes in Semiconductors," D. Van Nostrand Company, Inc., New York, N. Y.; 1950.

‡ E. M. Conwell, "Properties of Silicon and Germanium," *Proceedings of the IRE*, vol. 40, pp. 1327–1337; November, 1952.

Semiconductors *continued*

A single crystal of semiconductor may be n-type in one region and p-type in another region due to impurity density variation, the surface separating the two regions being called a *pn* junction. Nearly all of the interesting properties of semiconductors are associated with the electrical characteristics of *pn* junctions.

These *pn* junctions have rectifying properties. At room temperature, the current through such a junction is related to the voltage across it, as

$$I = I_s[(\exp 40V) - 1]$$

where

I_s = saturation current.

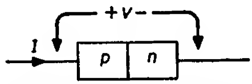

Fig. 2—Polarity for forward current in a *pn* junction.

When a *pn* junction is biased in the forward direction (Fig. 2) making the *p* region positive with respect to the *n* region, holes are readily emitted from the *p* region (where they are plentiful and are called majority carriers) into the *n* region (where they are referred to as minority carriers) and conversely, electrons are emitted into the *p* region to become minority carriers there. These minority carriers, the electrons in the *p* region and holes in the *n* region, will recombine with some of the larger number of opposite-type-charge carriers, but not instantaneously; the time required for the number injected to decay to 1/e of its original value is called the lifetime of minority carriers. This lifetime is a characteristic of a particular crystal and is generally between a fraction of a microsecond and a few milliseconds, more perfect crystals giving the longer lifetimes. In the forward conducting direction, the charge carriers are practically unimpeded in their flow across the junction.

When a *pn* junction is reverse-biased, the holes in the *p* region and the electrons in the *n* region are withdrawn away from the junction leaving a *depletion layer* that becomes wider as the voltage is increased. The only current that can flow arises from thermally generated electron–hole pairs that form in or near the junction. Electrons from such thermally generated pairs are drawn into the *n* region and holes into the *p* region. This reverse current is called the *saturation current* since it saturates at a very-low voltage and increases little with higher voltage (surface defects may cause reverse current to increase substantially with increase in voltage, but well-made semiconductor devices have junctions in which the current increases only slowly as the voltage is raised from about 0.1 to 40 volts). Being due to thermally generated electron–hole pairs, the saturation current increases exponentially with temperature.

Semiconductors *continued*

The theoretical breakdown voltage of a *pn* junction is approximately inversely proportional to the donor or acceptor density near the junction. Significant departures from this inverse relationship have been found. Nevertheless, an empirical relationship sometimes used as a guide is, for germanium,

$$V_b \approx 96\rho_n + 45\rho_p$$

and for silicon,

$$\approx 39\rho_n + 8\rho_p$$

where

ρ_n, ρ_p = resistivity of *n*, p, regions in ohm–centimeters

Surface leakage may cause breakdown at a considerably lower voltage.

Properties of germanium and silicon*

property	germanium	at °C	silicon	at °C
Atomic number	32	—	14	—
Atomic weight	72.60	—	28.08	—
Density in grams centimeter^{-3}	5.323	—	2.328	—
Energy gap in electron–volts	0.72	25	1.12	25
Temperature coefficient of energy gap in electron–volts °C^{-1}	−0.0001	—	−0.0003	—
Mobility of electrons in centimeters^2 volt^{-1} second^{-1}	3600	25	1200	25
Mobility of holes in centimeters^2 volt^{-1} second^{-1}	1700	25	250	25
Melting point in °C	936	—	1420	—
Linear thermal expansion coefficient in °C^{-1}	6.1×10^{-6}	0–300	4.2×10^{-6}	10–50
Thermal conductivity in calories second^{-1} centimeter^{-1} °C^{-1}	0.14	25	0.20	20
Specific heat in calories gram^{-1} °C^{-1}	0.074	0–100	0.181	20–90
Dielectric constant	16	—	12	—

* E. M. Conwell, "Properties of Silicon and Germanium," *Proceedings of the IRE*, vol. 40, pp. 1327–1337; November, 1952.

Transistors

List of symbols

V_c = collector voltage (quiescent value relative to base)
V_e = emitter voltage (quiescent value relative to base)
I_c = collector current (quiescent value)
I_e = emitter current (quiescent value)
I_{co} = collector cutoff current (I_c with $I_e = 0$)
r_e = emitter resistance (see Fig. 3)
r_b = base resistance (see Fig. 3)
r_c = collector resistance (see Fig. 3)
r_b' = high-frequency (or extrinsic) base resistance (see Fig. 18)
r_b'' = low-frequency component of base resistance (see Fig. 18)
α = alpha (current multiplication factor)
$= [\partial i_c / \partial i_e]_{V_c}$
α_0 = low-frequency alpha
β = beta
$= \alpha / (1 - \alpha)$
C_c = collector capacitance (see Fig. 3)
f_α = alpha cutoff frequency (at which $\alpha = \alpha_0 / (2)^{1/2}$)
f_β = beta cutoff frequency (at which $\beta = \alpha_0 / (2)^{1/2} (1 - \alpha_0)$)

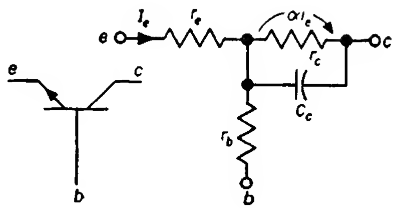

Fig. 3—Equivalent circuit for definition of r_e, r_b, and r_c.

Point-contact transistors

Point-contact transistors have two sharp pointed metal wires or whiskers pressed against the surface of a semiconductor, the contact points being in close juxtaposition. The whiskers are the emitter and collector connections and a soldered ohmic connection to the semiconductor is the base connection. The construction is shown in Fig. 4. The semiconductor is generally n-type germanium that requires biasing polarities the same as for pnp-junction types. They are less useful than junction types because they are more noisy (≈ 50-decibel noise figure), give less power gain at low frequencies, have higher collector

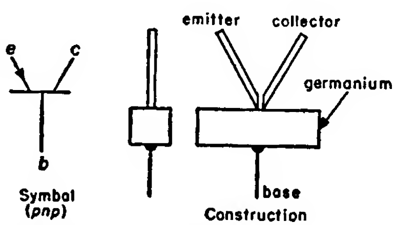

Fig. 4—Point-contact transistor.

Transistors *continued*

cutoff current, and tend to be unstable as amplifiers in common-emitter circuits because α is greater than unity. They are used principally in computer circuits where the latter characteristic and the high cutoff frequency are advantageous.

Junction transistors

Junction transistors are made in several different types, most of the differences arising out of the methods of manufacture. The basic type is the triode, which may be either *pnp* or *npn*.

pnp triode: The most-common junction transistor; made either by alloying (fusing) or by etching and electroplating (surface-barrier technique). Alloyed transistors are made by placing a thin wafer cut from a semiconductor crystal, usually *n*-type germanium, between two small pieces of a suitable metal such as indium; this assembly is heated until the wafers melt and alloy with the semiconductor. Wires are attached to the metal dots to serve as emitter and collector connections and a soldered ohmic contact to the semiconductor serves as the base connection. The collector is made larger than the emitter to improve the collector efficiency. Such a unit is shown diagrammatically in Fig. 5. Surface-barrier transistors are made by electrolytically etching a semiconductor wafer with two jet streams and immediately thereafter plating two metallic spots thereon. The appearance is similar to the alloyed type except that the dimensions, especially of the base thickness and the thickness of the metal spots, is much smaller in the surface-barrier type.

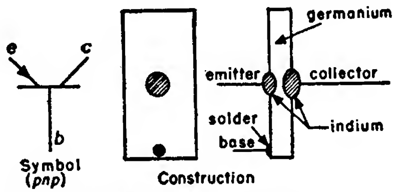

Fig. 5—Alloyed-junction transistor.

Power transistors are made by the alloying process. In this case the base connection is made in the form of a ring around the emitter and close to it and the collector is soldered to a heat-conducting stud.

Grown-junction npn triodes: Made with germanium and with silicon. Made by growing a single crystal, which is mainly *n*-type but has one or more thin layers that are *p*-type, cutting this into a number of small bars, each of which includes one *p*-layer separating two *n*-regions, and

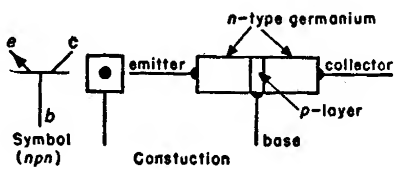

Fig. 6—Grown-junction *npn* transistor.

Transistors *continued*

making welded or soldered connections to each of the three regions. Such a unit is shown diagrammatically in Fig. 6.

Tetrodes: Germanium high-frequency tetrodes are made in the same way except that a second base connection is made to the same *p*-layer (Fig. 7). Interbase current lowers the base resistance to allow operation at considerably higher frequency than can be obtained with the same crystal used as a triode. Audio-frequency gain-control tetrodes also made in this way utilize the dependence of current gain α on interbase current for gain-control purposes.

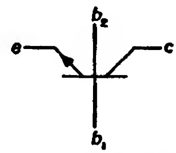

Fig. 7—Junction tetrode transistor symbol. (Construction of Fig. 6 with second connection to base.)

Special transistors

Several kinds of experimental junction transistors have been devised either for operation at higher frequencies or for negative-resistance characteristics useful in switching and pulse circuits.

Intrinsic-barrier transistor: (*pnip* or *npin*) functions in the same way as the *pnp* or *npn* transistor, except that the intrinsic layer between the *p* and *n* regions of the collector junction reduces collector capacitance and allows the use of a low-resistivity base region, and therefore low base resistance, without lowering the collector breakdown voltage. The high-frequency limit for oscillation has been estimated to be about 1500 megacycles. In Fig. 8, a germanium *ni* crystal is grown by pulling from a melt and the *p*-type emitter and collector are formed by alloying indium into the *n* and *i* regions.

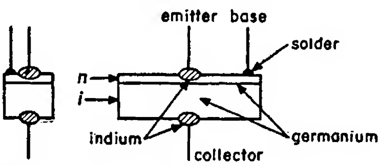

Fig. 8—Intrinsic-barrier transistor.

Unipolar transistor is so-called because its operation depends on the action of only one type of charge carrier, either electrons or holes, but not both, as does that of other junction transistors. Two ohmic connections called the *source* and *drain* are made to, say, *n*-type germanium, and these are connected in series with a direct-current power supply and load impedance. A *p* region called the *gate* surrounds the current path between source and drain where this path is very narrowly constricted, as shown in Fig. 9.

Transistors *continued*

The gate-to-source *pn* junction is biased in the reverse direction causing a depletion layer between them that still further constricts the current path from source to drain. The input signal voltage is superimposed on the gate bias. The varying gate voltage causes the cross-sectional area of the undepleted current path from source to drain to change, causing, in turn, a variation in output current. More like a vacuum tube than other transistors, with input voltage controlling output current, unipolar transistor gain is expressed as transconductance. The input impedance is high and output impedance is relatively low. Operation at high frequencies is possible because charge carriers move by drifting in an electric field, rather than by diffusion.

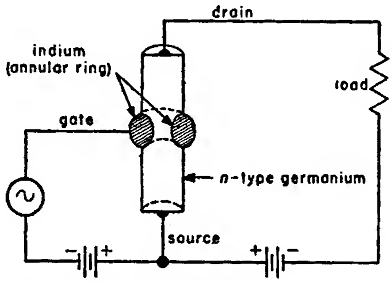

Fig. 9—Unipolar transistor.

Hook-collector transistors have an extra *pn* junction in the collector. The *hook* refers to the potential trap for electrons or holes caused by the *pn* junction, which results in current multiplication and an alpha greater than one. In one type of hook-collector transistor the *n*-type base region and the *pn* collector regions are grown into a crystal that is cut into small bars. The *p*-type emitter is formed by alloying a gold–gallium wire into the base region as shown in Fig. 10. Holes are emitted from the *p*-type emitter, diffuse through the *n*-type base, are collected in he *p*-type hook region, and (since they change the potential of this region with respect to the *n*-type collector), cause electrons to be emitted in the opposite direction. These electrons diffuse through the *p*-type hook region and are collected into the base region. Alpha increases with emitter current and reaches 20 or 30 before collector dissipation becomes excessive. Very-simple switching circuits are possible with this transistor since only one transistor is needed for a bistable flip-flop.

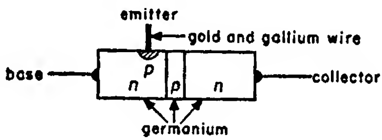

Fig. 10—Hook-collector transistor.

Double-base diode: Not usually referred to as a transistor, but is described briefly here because it exhibits negative-resistance effects similar to the hook-collector and point-contact transistors. Two ohmic base connections are made to an *n*-type crystal as shown in Fig. 11. A *p* region is formed

Transistors *continued*

by alloying with indium, for example. A bias voltage is applied between the base connections. Since the potential in the base region now varies with position, the *p* region can be biased positive with respect to a part of the base region in contact with it, but negative with respect to another part. The *p* region then emits holes in the former part and collects holes in the latter. This effect, and modulation of the conductivity of the *n*-region by injected holes, results in a negative-resistance region in the voltage–current characteristic between the *p*-region connection and one of the base-region connections. Simple switching circuits can be made with the double-base diode with the further possibility of relatively high power-dissipation capabilities*.

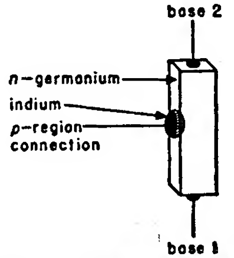

Fig. 11—Double-base diode.

Amplification in transistors

The *npn* junction-triode transistor consists of two *pn* junction diodes (as described above) within a single crystal, the middle, or base region being

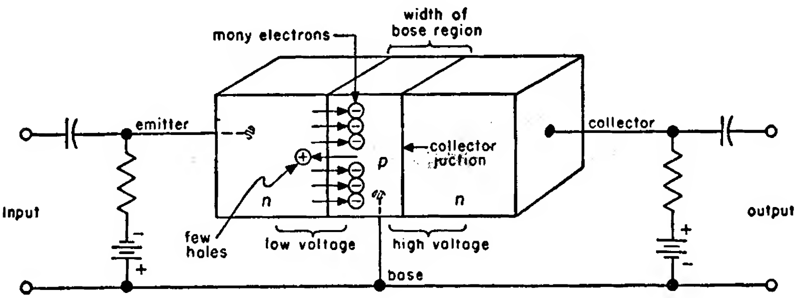

Fig. 12—Transistor amplification process.

common to both diodes (Fig. 12). The emitter-to-base junction is biased in the forward (highly conducting) direction and the collector-to-base junction is biased in the reverse (poorly conducting) direction.

Crossing the junction, the emitter-to-base current is composed of two parts, electrons emitted into the base region and holes into the emitter region.

* R. F. Shea, "Principles of Transistor Circuits," John Wiley & Sons, Inc., New York, N. Y.; 1953.

Transistors *continued*

Electrons in the base region wander randomly while repelling one another (diffusion), rapidly spreading throughout that region. Those that wander to the collector junction are attracted across that junction by the strong electric field there. If the base region is narrow, only a few reach the base connection and the rest are collected. Collected electrons comprise emitter-to-collector current, whereas those not collected comprise undesired emitter-to-base current.

Another source of undesired emitter-to-base current results from holes emitted from the base region into the emitter region. These would leave the base region negatively charged except that an equal number of electrons are forced out through the base lead to prevent such a charge buildup.

The ratio of the desired emitted electron current to the total emitter current (emitter efficiency) can be made nearly one by more-heavily doping the emitter than the base so that the emitter region is strongly *n*-type with a high density of electrons whereas the base region is weakly *p*-type with only few holes.

It can be seen that by proper design, the collector current can be nearly equal to the emitter current; small variations in emitter current (signal input) will then cause nearly equal variations in collector current.

The signal power required for any given signal current is small because the emitter-to-base voltage variations are small, being of the order of millivolts. The output power, however, is high since the load voltage variations can be large (of the order of volts). In this way, power amplification of the order of 30 decibels is obtained.

The action is the same in *pnp* transistors except that bias polarities are reversed and holes and electrons are interchanged.

In point-contact transistors, the action is believed to be similar to that in the *pnp*-junction type, but is not as well understood. Holes are emitted from the emitter point into the *n*-type germanium, diffuse through it and are collected by the collector point. The collector current, however, is larger than the emitter current, possibly due to a hook mechanism (as described above).

Typical transistor characteristic curves

The curves given in Figs. 13–17 are typical of the results obtained with various present-day transistors.

Transistors *continued*

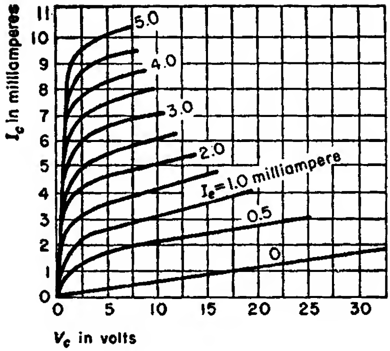

Fig. 13—Collector-family curves for point-contact-type transistor in common-base circuit.

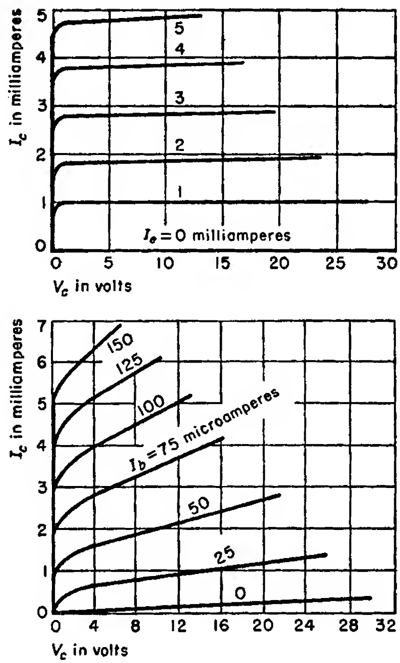

Fig. 14—Collector-family curves for germanium junction-type transistor in common-base (top) and common-emitter (below) circuits.

Transistors *continued*

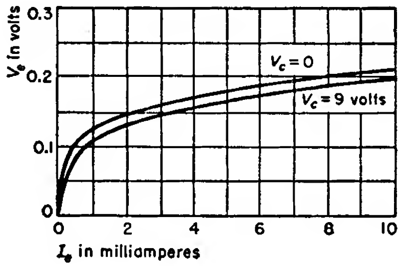

Fig. 15—Emitter-family curves for germanium junction transistor.

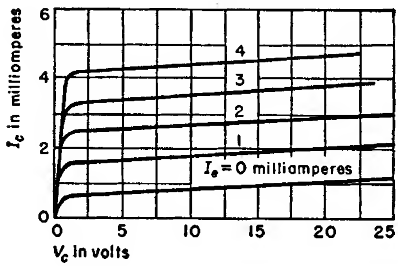

Fig. 16—Collector-family curves for germanium junction transistor in common-base circuit at high temperature (85° C).

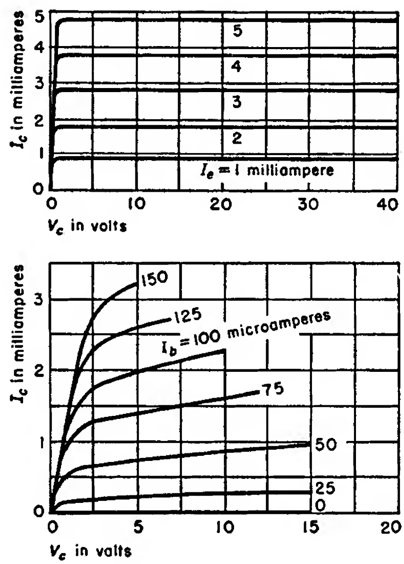

Fig. 17—Collector-family curves for silicon grown-junction-type transistor in common-base (top) and common-emitter (below) circuits.

Transistors *continued*

Variation of characteristics for junction transistors

Emitter resistance

$r_e \approx c/I_e$

in ohms, where c is a constant. If I_e is in milliamperes, useful empirical values for c are

$c = 12$ for low-power germanium alloyed types

$= 25$ for germanium grown types

$= 35$ for silicon grown types

The other variations of r_e are either unimportant or unpredictable.

Base resistance: Base resistance decreases with increasing I_e. The variation of base resistance with frequency can best be described by separating r_b into two parts, r_b' and r_b'' as shown in Fig. 18.

$r_b' + r_b''$ = low-frequency base resistance

r_b' = high-frequency base resistance ("extrinsic base resistance").

r_b' = generally $r_b''/4$ to $r_b''/10$

r_b' is an important criterion for high-frequency performance, ranking with f_α and C_c in this respect. For example, the maximum frequency at which oscillation can be obtained with alloyed transistors is

$f = (\alpha_0 f_\alpha / 8\pi r_b' C_c)^{1/2}$

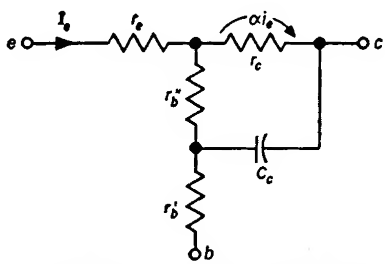

Fig. 18—Separation of two components of transistor base resistance.

The product $r_b'C_c$ also enters into the denominator of calculated power gain for band-pass amplifiers at high frequencies.*

Collector resistance: r_c decreases to half its 25-degree-centigrade value at about 85 degrees centigrade in most germanium types. In silicon the change is small. r_c decreases with increasing I_e.

* J. B. Angell and F. P. Keiper, "Circuit Applications of Surface-Barrier Transistors," *Proceedings of the IRE*, vol. 41, pp. 1709–1712; December, 1953.

Transistors *continued*

Current gain*: α and β increase to a maximum at I_e between 1 and 10 milliamperes, the increase at low currents being generally small. At high I_e, the decrease is more rapid, which is important when high output power is desired, especially at low V_c. Power transistors are designed to minimize this effect.

The magnitude of α decreases with increasing frequency and a phase shift is introduced. Magnitude and phase can be computed from the approximate formula

$$\alpha \approx \frac{\alpha_0}{1 + j\,(f/f_\alpha)}$$

which is fairly accurate up to $f = f_\alpha$. As an example of the application of this formula, in a transistor with $\alpha = 0.95$ and $f_\alpha = 2$ megacycles, the α at 1 megacycle and the phase shift between collector and emitter currents is

$$\alpha \approx \frac{0.95}{1 + j\,(1/2)} = 0.76 - j\,0.38 = 0.85 \underline{/ -26.6^\circ}$$

The cutoff frequency for β ($f_\beta = 0.707$ of low-frequency β) is approximately

$$f_\beta \approx (1 - \alpha_0)\, f_\alpha$$

which is much lower than f_α. In the example above, it is approximately

$$f_\beta \approx (1 - 0.95)\,2 = 0.1 \text{ megacycle}$$

and

$$\beta = \frac{0.95}{1 - 0.95}\,(0.707) = 19\,(0.707) = 13.4 \text{ at 100 kilocycles}$$

Current gain varies little with V_c as long as V_c is greater than 1 volt. Current gain generally increases with increasing temperature. In grown-junction silicon and germanium, β increases about 0.6 percent/degree centigrade between -40 and $+150$ degrees centigrade for silicon and between -40 and $+50$ degrees centigrade for germanium. At higher temperatures, β tends to increase more rapidly and α may exceed 1. In alloyed germanium above room temperature, β may rise slightly, remain constant, or fall, depending on the manufacturing process used, but α generally does not go above 1 at any temperature.

* R. L. Pritchard, "Frequency Variations of Current-Amplification Factor for Junction Transistors," *Proceedings of the IRE*, vol. 40, pp. 1476–1481; November, 1952.

Transistors *continued*

Collector cutoff current: I_{co} increases exponentially with temperature (see Fig. 19). In silicon at room temperature, it is about 2 decades lower than in germanium. It also increases with collector voltage, generally because of minute surface contamination.

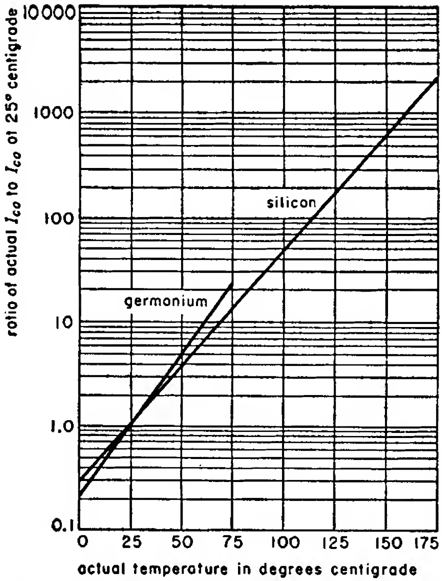

Fig. 19—Change of collector cutoff current with temperature.

Noise: Noise figure increases with emitter bias current and with collector bias voltages above about one volt and therefore low-noise amplifier stages should have $V_c \approx 1$ volt and I_e should be as low as I_{co} and stability considerations will permit. Noise figure is a minimum when the signal source resistance is approximately 1000 ohms, but the minimum is broad, so that resistances between 300 and 3000 ohms are usually satisfactory. Noise figure tends to decrease with increasing frequency as shown in Fig. 20. At low frequencies, the noise figure is inversely proportional to frequency (1/f noise) and differences between units becomes more pronounced. Quoted figures are usually measured at

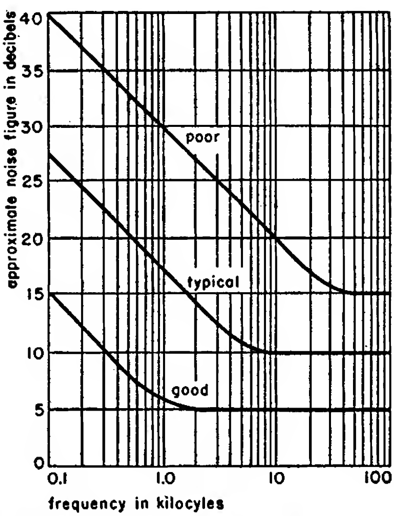

Fig. 20—Variation of noise figure with frequency.

$V_c = 1.5$ to 2.5 volts

$I_e = 0.5$ milliampere

$f = 1$ kilocycle

Typical values (1956) are between 10 and 20 decibels.

Transistors *continued*

Collector capacitance:

$C_c \propto V_c^{-n}$

where

n = 1/2 for step junctions (alloyed)

= 1/3 for graded junctions (grown)

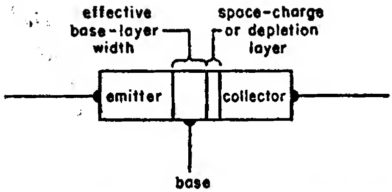

Fig. 21—Depletion layer and effective base-region width.

This effect is due to space-charge-layer widening (Fig. 21). C_c increases slowly with increasing I_e.

Cutoff frequency: f_α increases with increasing collector bias voltage because widening of the space-charge layer* decreases the effective base region width (Fig. 21) and for f_α in megacycles,

$f_\alpha = C/W^2$

where

W = width of base region in mils

C = 5.6 for germanium *npn*

= 1.9 for silicon *npn*

= 2.6 for germanium *pnp*

= 0.4 for silicon *pnp*

Basic principles of biasing

As in the electron-tube triode, the biasing of transistor triodes is fixed by two independent parameters but, whereas in the electron tube the simplest description of bias conditions results from considering the cathode electrode as common and the independent bias parameters as the grid voltage and plate voltage, in transistor triodes it is simplest to consider the base electrode as common and the independent bias parameters as the emitter *current* and

* J. M. Early, "Effects of Space Charge Layer Widening in Junction Transistors," *Proceedings of the IRE*, vol. 40, pp. 1401–1406; November, 1952.

Transistors *continued*

collector voltage. Collector voltage biasing of transistors using a constant-voltage source of supply is similar to plate-voltage biasing of tubes. Emitter biasing of transistors, however, since it requires a constant bias *current* to be obtained generally from a constant-voltage source, must be treated differently than any electron-tube biasing problem. Because the emitter-to-base junction is a forward-biased diode, the voltage required for any given current is small, generally a few tenths of a volt. For stable fixed emitter-current bias, a much larger supply voltage should be used together with a current-determining series resistor to provide, in effect, a constant-current source not seriously affected by transistor characteristics or supply-voltage variations.

For biasing purposes, the base electrode is considered common, and the emitter current and collector-to-base voltage are fixed whether the base electrode is common to input and output signals or not, just as in the analogous common-grid and common-plate (cathode-follower) operation of tubes. Common-emitter operation of junction transistors is used often and requires that the direct-current circuit consisting of resistors, inductors, and transformer windings hold the average emitter current and collector-to-base voltage substantially constant while the alternating-current circuit, which includes capacitors as well, supplies the signal alternating-current to the base and the output alternating-current is taken from the collector. Similar considerations apply for grounded-collector operation.

Transistor circuits

In this chapter are given in condensed form descriptions of the various types of circuits in which transistors are operated together with design information enabling the determination of the circuit parameters. The following symbols are used.

A_i = current amplification

A_v = voltage amplification

$a = r_m/r_c$

e_g = signal input voltage

G = power gain

i_{c0} = collector current with $i_e = 0$

i_l = load current

r_b = base resistance

r_c = collector resistance

r_e = emitter resistance

r_g = generator resistance

r_i = input resistance

r_l = load resistance

r_m = equivalent emitter–collector transresistance

r_o = output resistance

y_l = load admittance

z_l = load impedance

α = short-circuit current multiplication factor

Δ = determinant

Basic circuits *

The triode transistor is a 3-terminal device and is connected into a 4-terminal circuit in any of 3 possible methods, as illustrated by the charts of Figs. 1–3.

* R. F. Shea et al, "Principles of Transistor Circuits," John Wiley & Sons, Inc., New York, N. Y.: 1953. Also, Staff of Bell Telephone Laboratories, "The Transistor, Selected Reference Material," Bell Telephone Laboratories, New York, N. Y.: 1951. Also, W. H. Duerig, et al, "Transistor Physics and Electronics," Applied Physics Laboratory of Johns Hopkins University, Baltimore, Md.: 1953.

continued Basic circuits

Fig. 1—Common-base circuit.

$\Delta = r_b(r_c - r_m + r_l + r_e) + r_e\,(r_c + r_l)$

Stability criterion:

$$\frac{r_m}{r_c + r_l} < 1 + \frac{r_e + r_g}{r_b} + \frac{r_e + r_g}{r_c + r_l}$$

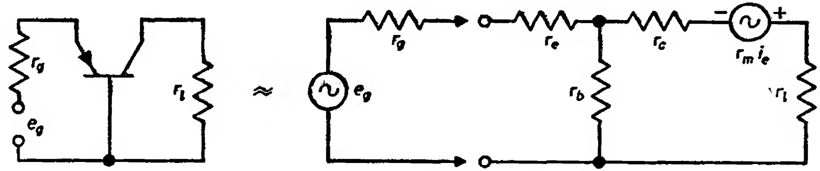

	exact formula	approximate formulas	
Conditions for validity	—	$r_e \ll r_c - r_m$ $r_b \ll r_c$	$r_e \ll r_c - r_m$ $r_b \ll r_c$ $r_b \ll r_l \ll r_c - r_m$
Input resistance $= r_i$	$r_e + r_b - \dfrac{r_b\,(r_b + r_m)}{r_l + r_c + r_b}$	$r_e + r_b \cdot \dfrac{r_c(1-a) + r_l}{r_c + r_l}$	$r_e + r_b\,(1-a)$
Output resistance $= r_o$	$r_c + r_b - \dfrac{r_b\,(r_b + r_m)}{r_g + r_e + r_b}$	$r_c \cdot \dfrac{r_e + r_b\,(1-a) + r_g}{r_e + r_b + r_g}$	$r_c \cdot \dfrac{r_e + r_b\,(1-a) + r_g}{r_e + r_b + r_g}$
Voltage amplification $= A_v$	$\dfrac{(r_m + r_b)\,r_l}{r_b(r_c - r_m + r_e + r_l) + r_e(r_c + r_l)}$	$\dfrac{a\,r_c\,r_l}{r_c[r_e + r_b(1-a)] + r_l(r_e + r_b)}$	$\dfrac{a\,r_l}{r_e + r_b\,(1-a)}$
Current amplification $= A_i$	$\dfrac{r_m + r_b}{r_b + r_c + r_l}$	$\dfrac{a}{1 + r_l/r_c}$	a
Power gain $= G$	$\dfrac{(r_m + r_b)^2\,r_l}{(r_b + r_c + r_l)\,[r_b(r_c - r_m + r_e + r_l) + r_e(r_c + r_l)]}$	$\dfrac{a^2\,r_c^2 r_l}{(r_c + r_l)\,r_c[r_e \times r_b(1-a) + r_l(r_e + r_b)]}$	$\dfrac{a^2\,r_l}{r_e + r_b\,(1-a)}$

continued **Basic circuits**

Fig. 2—Common-emitter circuit.

$$\Delta = r_b(r_c - r_m + r_e + r_l) + r_e(r_c + r_l)$$

Stability criterion:

$$\frac{r_m}{r_c + r_l} < 1 + \frac{r_e}{r_b + r_g} + \frac{r_e}{r_c + r_l}$$

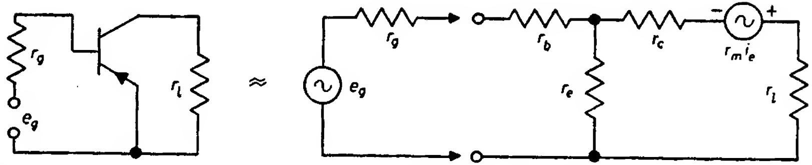

	exact formula	approximate formulas	
Conditions for validity	—	$r_e \ll r_c - r_m$ $r_b \ll r_c$	$r_c \ll r_c - r_m$ $r_b \ll r_c$ $r_e \ll r_l \ll r_c - r_m$
Input resistance $= r_i$	$r_e + r_b + \dfrac{r_e(r_m - r_e)}{r_l + r_e + r_c - r_m}$	$r_b + r_e \cdot \dfrac{r_c + r_l}{r_c(1-a) + r_l}$	$r_b + \dfrac{r_e}{1-a}$
Output resistance $= r_o$	$r_c + r_e - r_m + \dfrac{r_e(r_m - r_e)}{r_g + r_b + r_e}$	$r_c(1-a) + r_e \cdot \dfrac{r_m + r_g}{r_e + r_b + r_g}$	$r_c(1-a) + r_e \cdot \dfrac{r_m + r_g}{r_e + r_b + r_g}$
Voltage amplification $= A_v$	$\dfrac{-r_l(r_m - r_e)}{r_b(r_c - r_m + r_e + r_l) + r_e(r_c + r_l)}$	$\dfrac{-a\, r_c r_l}{r_c[r_e + r_b(1-a)] + r_l(r_e + r_b)}$	$\dfrac{-a\, r_l}{r_e + r_b(1-a)}$
Current amplification $= A_i$	$\dfrac{r_m - r_e}{r_c - r_m + r_e + r_l}$	$\dfrac{a}{1 - a + r_l/r_c}$	$\dfrac{a}{1-a}$
Power gain $= G$	$\dfrac{r_l(r_m - r_e)^2}{(r_c - r_m + r_e + r_l)[r_b(r_c - r_m + r_c + r_l) + r_e(r_c + r_l)]}$	$\dfrac{a^2 r_c^2 r_l}{[r_c(1-a) + r_l]\, r_c[r_e + r_b(1-a)] + r_l(r_e + r_b)}$	$\dfrac{a^2 r_l}{(1-a)[r_e + r_b(1-a)]}$

continued **Basic circuits**

Fig. 3—Common-collector circuit.

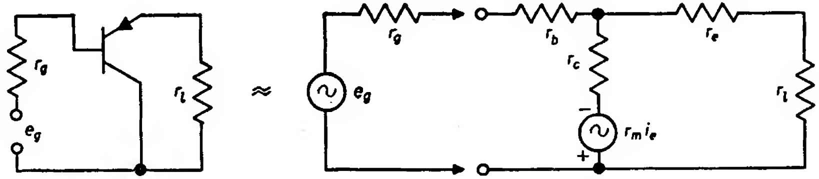

$$\Delta = r_b\,(r_c - r_m + r_l + r_e) + r_c\,(r_e + r_l)$$

Stability criterion:

$$\frac{r_m}{r_c} < 1 + \frac{r_c + r_l}{r_b + r_g} + \frac{r_e + r_l}{r_c}$$

	exact formula	approximate formulas	
Conditions for validity	—	$r_e \ll r_c - r_m$ $r_b \ll r_c$	$r_e \ll r_c - r_m$ $r_b \ll r_c$ $r_e \ll r_l \ll r_c - r_m$
Input resistance $= r_i$	$r_b + r_c + \dfrac{r_c\,(r_m - r_c)}{r_l + r_e + r_c - r_m}$	$r_b + r_c \cdot \dfrac{r_e + r_l}{r_c\,(1 - a) + r_l}$	$\dfrac{r_l}{1 - a}$
Output resistance $= r_o$	$r_e + r_c - r_m + \dfrac{r_e\,(r_m - r_c)}{r_g + r_b + r_c}$	$r_e + r_c\,(1 - a) \cdot \dfrac{r_g + r_b}{r_g + r_c}$	$r_e + (r_b + r_g)\,(1 - a)$
Voltage amplification $= A_v$	$\dfrac{r_c\,r_l}{r_b\,(r_c - r_m + r_e + r_l) + r_c\,(r_e + r_l)}$	$\dfrac{r_l}{r_e + r_b\,(1 - a) + r_l}$	1
Current amplification $= A_i$	$\dfrac{r_c}{r_c - r_m + r_e + r_l}$	$\dfrac{1}{(1 - a) + r_l/r_c}$	$\dfrac{1}{1 - a}$
Power gain $= G$	$\dfrac{r_c^2\,r_l}{(r_c - r_m + r_e + r_l)\,[r_b\,(r_c - r_m + r_e + r_l) + r_c\,(r_e + r_l)]}$	$\dfrac{r_l\,r_c}{[r_c\,(1 - a) + r_l]\,[r_e + r_b\,(1 - a) + r_l]}$	$\dfrac{1}{1 - a}$

Matrixes for transistor networks

Fig. 4 gives the properties of properly terminated 4-terminal networks in terms of their matrix coefficients, Fig. 5 gives transistor matrixes and Fig. 6 gives the matrixes of 3-terminal networks. In these figures,

z_l = load impedance

z_g = source impedance

$\Delta^z = z_{11}z_{22} - z_{12}z_{21}$

$\Delta^y = y_{11}y_{22} - y_{12}y_{21}$

$\Delta^h = h_{11}h_{22} - h_{12}, h_{21}$

$d = h_{11}h_{22} - h_{12}h_{23} - h_{12} + h_{21} + 1$

$\approx 1 + h_{21}$ for junction transistors

Note that for junction transistors,

$\Delta^h \ll -h_{21}$

and

$h_{12} \ll 1$

Matrixes for transistor networks *continued*

Fig. 4—Transistor terminal characteristics in terms of 4-terminal matrix coefficients.

	input impedance $= z_i$	output impedance $= z_o$	voltage amplification $= A_v$	current amplification $= A_i$
z	$\dfrac{\Delta^z + z_{11}z_l}{z_{22} + z_l}$	$\dfrac{\Delta^z + z_{22}z_g}{z_{11} + z_g}$	$\dfrac{z_{21}z_l}{\Delta^z + z_{11}z_l}$	$\dfrac{z_{21}}{z_{22} + z_l}$
y	$\dfrac{y_{22} + y_l}{\Delta^y + y_{11}y_l}$	$\dfrac{y_{11} + y_g}{\Delta^y + y_{22}y_g}$	$\dfrac{-y_{21}}{y_{22} + y_l}$	$\dfrac{-y_{21}y_l}{\Delta^y + y_{11}y_l}$
h	$\dfrac{\Delta^h + h_{11}y_l}{h_{22} + y_l}$	$\dfrac{h_{11} + z_g}{\Delta^h + h_{22}z_g}$	$\dfrac{-h_{21}z_l}{h_{11} + \Delta^h z_l}$	$\dfrac{-h_{21}y_l}{h_{22} + y_l}$
g	$\dfrac{g_{22} + z_l}{\Delta^g + g_{11}z_l}$	$\dfrac{\Delta^g + g_{22}y_g}{g_{11} + y_g}$	$\dfrac{g_{21}z_l}{g_{22} + z_l}$	$\dfrac{g_{21}}{\Delta^g + g_{11}z_l}$
a	$\dfrac{a_{11}z_l + a_{12}}{a_{21}z_l + a_{22}}$	$\dfrac{a_{22}z_g + a_{12}}{a_{21}z_g + a_{11}}$	$\dfrac{z_l}{a_{12} + a_{11}z_l}$	$\dfrac{1}{a_{22} + a_{21}z_l}$
b	$\dfrac{b_{22}z_l + b_{12}}{b_{21}z_l + b_{11}}$	$\dfrac{b_{11}z_g + b_{12}}{b_{21}z_g + b_{22}}$	$\dfrac{z_l\Delta^b}{b_{12} + b_{22}z_l}$	$\dfrac{\Delta^b}{b_{11} + b_{12}z_l}$

Matrixes for transistor networks *continued*

Fig. 5—Transistor matrixes.

$\Delta = r_e r_b + r_c[r_e + r_b (1 - a)]$

	common emitter	common base	common collector
z	$\begin{bmatrix} r_e + r_b & r_e \\ r_e - ar_c & r_e + r_c(1-a) \end{bmatrix}$	$\begin{bmatrix} r_e + r_b & r_b \\ r_b + ar_c & r_b + r_c \end{bmatrix}$	$\begin{bmatrix} r_b + r_c & r_c(1-a) \\ r_c & r_e + r_c(1-a) \end{bmatrix}$
y	$\frac{1}{\Delta}\begin{bmatrix} r_e + r_c(1-a) & -r_e \\ -(r_e - ar_c) & r_e + r_b \end{bmatrix}$	$\frac{1}{\Delta}\begin{bmatrix} r_b + r_c & -r_b \\ -(r_b + ar_c) & r_e + r_b \end{bmatrix}$	$\frac{1}{\Delta}\begin{bmatrix} r_e + r_c(1-a) & r_c(1-a) \\ -r_c & r_b + r_c \end{bmatrix}$
h	$\frac{1}{r_e + r_c(1-a)}\begin{bmatrix} \Delta & r_e \\ -(r_e - ar_c) & 1 \end{bmatrix}$	$\frac{1}{r_b + r_c}\begin{bmatrix} \Delta & r_b \\ -(r_b + ar_c) & 1 \end{bmatrix}$	$\frac{1}{r_e + r_c(1-a)}\begin{bmatrix} \Delta & r_c(1-a) \\ -r_c & 1 \end{bmatrix}$
g	$\frac{1}{r_e + r_b}\begin{bmatrix} 1 & -r_e \\ r_e - ar_c & \Delta \end{bmatrix}$	$\frac{1}{r_e + r_b}\begin{bmatrix} 1 & -r_b \\ r_b + ar_c & \Delta \end{bmatrix}$	$\frac{1}{r_b + r_c}\begin{bmatrix} 1 & -r_c(1-a) \\ r_c & \Delta \end{bmatrix}$
a	$\frac{1}{r_e - ar_c}\begin{bmatrix} r_e + r_b & \Delta \\ 1 & r_e + r_c(1-a) \end{bmatrix}$	$\frac{1}{r_b - ar_c}\begin{bmatrix} r_e + r_b & \Delta \\ 1 & r_b + r_c \end{bmatrix}$	$\frac{1}{r_c}\begin{bmatrix} r_b + r_c & \Delta \\ 1 & r_e + r_c(1-a) \end{bmatrix}$
b	$\frac{1}{r_e}\begin{bmatrix} r_e + r_c(1-a) & \Delta \\ 1 & r_e + r_b \end{bmatrix}$	$\frac{1}{r_b}\begin{bmatrix} r_b + r_c & \Delta \\ 1 & r_e + r_b \end{bmatrix}$	$\frac{1}{r_c(1-a)}\begin{bmatrix} r_e + r_c(1-a) & \Delta \\ 1 & r_b + r_c \end{bmatrix}$

Matrixes for transistor networks *continued*

Fig. 6—Matrixes of 3-terminal networks exactly expressed in terms of common-base *h* parameters.

	common base	common emitter	common collector
z	$\begin{matrix} \frac{\Delta^h}{h_{22}} & \frac{h_{12}}{h_{22}} \\ -\frac{h_{21}}{h_{22}} & \frac{1}{h_{22}} \end{matrix}$	$\begin{matrix} \frac{\Delta^h}{h_{22}} & \frac{\Delta^h - h_{12}}{h_{22}} \\ \frac{\Delta^h + h_{21}}{h_{22}} & \frac{d}{h_{22}} \end{matrix}$	$\begin{matrix} \frac{1}{h_{22}} & \frac{1 + h_{21}}{h_{22}} \\ \frac{1 - h_{12}}{h_{22}} & \frac{d}{h_{22}} \end{matrix}$
y	$\begin{matrix} \frac{1}{h_{11}} & -\frac{h_{12}}{h_{11}} \\ \frac{h_{21}}{h_{11}} & \frac{\Delta^h}{h_{11}} \end{matrix}$	$\begin{matrix} \frac{d}{h_{11}} & \frac{h_{12} - \Delta^h}{h_{11}} \\ -\frac{\Delta^h + h_{21}}{h_{11}} & \frac{\Delta^h}{h_{11}} \end{matrix}$	$\begin{matrix} \frac{d}{h_{11}} & -\frac{1 + h_{21}}{h_{11}} \\ \frac{h_{12} - 1}{h_{11}} & \frac{1}{h_{11}} \end{matrix}$
h	$\begin{matrix} h_{11} & h_{12} \\ h_{21} & h_{22} \end{matrix}$	$\begin{matrix} \frac{h_{11}}{d} & \frac{\Delta^h - h_{12}}{d} \\ -\frac{h_{21} - \Delta^h}{d} & \frac{h_{22}}{d} \end{matrix}$	$\begin{matrix} \frac{h_{11}}{d} & \frac{1 + h_{21}}{d} \\ \frac{h_{12} - 1}{d} & \frac{h_{22}}{d} \end{matrix}$
g	$\begin{matrix} \frac{h_{22}}{\Delta^h} & -\frac{h_{12}}{\Delta^h} \\ -\frac{h_{21}}{\Delta^h} & \frac{h_{11}}{\Delta^h} \end{matrix}$	$\begin{matrix} \frac{h_{22}}{\Delta^h} & \frac{h_{12} - \Delta^h}{\Delta^h} \\ \frac{h_{21} + \Delta^h}{\Delta^h} & \frac{h_{11}}{\Delta^h} \end{matrix}$	$\begin{matrix} h_{22} & -(1 + h_{21}) \\ 1 - h_{12} & h_{11} \end{matrix}$
a	$\begin{matrix} -\frac{\Delta^h}{h_{21}} & -\frac{h_{11}}{h_{21}} \\ -\frac{h_{22}}{h_{21}} & -\frac{1}{h_{21}} \end{matrix}$	$\begin{matrix} \frac{\Delta^h}{\Delta^h + h_{21}} & \frac{h_{11}}{\Delta^h + h_{21}} \\ \frac{h_{22}}{\Delta^h + h_{21}} & \frac{d}{\Delta^h + h_{21}} \end{matrix}$	$\begin{matrix} \frac{1}{1 - h_{12}} & \frac{h_{11}}{1 - h_{12}} \\ \frac{h_{22}}{1 - h_{12}} & \frac{d}{1 - h_{12}} \end{matrix}$
b	$\begin{matrix} \frac{1}{h_{12}} & \frac{h_{11}}{h_{12}} \\ \frac{h_{22}}{h_{12}} & \frac{\Delta^h}{h_{12}} \end{matrix}$	$\begin{matrix} \frac{d}{\Delta^h - h_{12}} & \frac{h_{11}}{\Delta^h - h_{12}} \\ \frac{h_{22}}{\Delta^h - h_{12}} & \frac{\Delta^h}{\Delta^h - h_{12}} \end{matrix}$	$\begin{matrix} \frac{d}{1 + h_{21}} & \frac{h_{11}}{1 + h_{21}} \\ \frac{h_{22}}{1 + h_{21}} & \frac{1}{1 + h_{21}} \end{matrix}$

Typical transistor characteristics

Typical values of impedances and gains for junction-type and point-contact-type transistors are given in Fig. 7.

Fig. 7—Transistor characteristics (as of 1956).

		common base		common emitter		common collector	
		point contact	junction	point contact	junction	point contact	junction
Maximum voltage amplification = A_v with $r_g = 0$ and $r_l = \infty$		1.9×10^2	1.7×10^4	-1.9×10^2	-1.7×10^5	1	1
Maximum current amplification = A_i with $r_l = 0$		+2.5	+0.95	−1.7	−19	+0.67	+19
Input resistance = r_i in ohms	$r_l = 0$	8	35	−5	750	−5	120
	$r_l = \infty$	200	270	200	270	1.5×10^4	5×10^6
Output resistance = r_o in ohms	$r_g = 0$	6×10^2	6.8×10^5	6×10^2	7×10^5	7.5	37
	$r_g = \infty$	1.5×10^3	5×10^6	-2.2×10^4	2.5×10^3	-2.2×10^4	2.5×10^5
Matched input resistance in ohms		37	100	Unstable	450	Unstable	6×10^4
Matched output resistance in ohms		3000	2×10^6	Unstable	4×10^5	Unstable	3×10^3
Typical equivalent generator resistance = r_g in ohms		300	300	300	300	2×10^4	2×10^4
Small-signal power gain = G with typical r_g and r_l		20	25	35	40	13	12

Cascade, series, and parallel circuits

Fig. 8 gives the 6 possible forms of equations relating the terminal voltages and currents of a 4-terminal network.

The definitions of the *z* and *h* matrix coefficients are also apparent from equations in Fig. 8A and C. The definitions of the *y*, *g*, *a*, and *b* matrix coefficients may be found from equations *B*, *D*, *E*, and *F*, respectively, of Fig. 8.

The use of matrices will frequently simplify the calculations required when combining networks, as indicated in the accompanying diagrams.

Cascade, series, and parallel circuits *continued*

Fig. 8—Use of matrixes in combining transistor circuits.

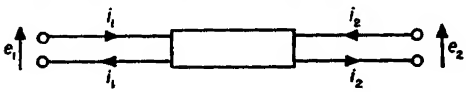

network configuration	4-pole equations
A. Series (add matrixes) 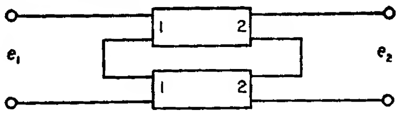	$e_1 = z_{11}i_1 + z_{12}i_2$ $e_2 = z_{21}i_1 + z_{22}i_2$
B. Parallel (add matrixes) 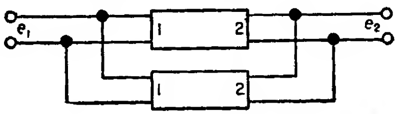	$i_1 = y_{11}e_1 + y_{12}e_2$ $i_2 = y_{21}e_1 + y_{22}e_2$
C. Series–parallel (add matrixes) 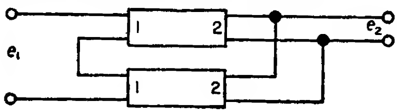	$e_1 = h_{11}i_1 + h_{12}e_2$ $i_2 = h_{21}e_1 + h_{22}e_2$
D. Parallel–series (add matrixes) 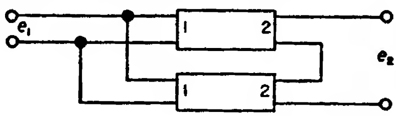	$i_1 = g_{11}e_1 + g_{12}i_2$ $e_2 = g_{21}e_1 + g_{22}i_2$
E. Cascade (multiply matrixes) 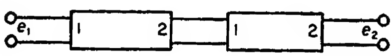	$e_1 = a_{11}e_2 - a_{12}i_2$ $i_1 = a_{21}e_2 - a_{22}i_2$
F. Cascade (multiply matrixes) 	$e_2 = b_{11}e_1 - b_{12}i_1$ $i_2 = b_{21}e_1 - b_{22}i_1$

Duality and electron-tube analogy

Fig. 9—Current-voltage duals.

Courtesy of Bell System Technical Journal.

voltage operation	current operation
A. Constant-voltage supply. 	Constant-current supply. 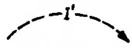 $I' = E/r$
B. Series battery and resistance. 	Constant-current supply and resistance in parallel. 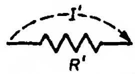 $I'=E/r \quad R'=r^2/R$
C. Series battery and resistance. 	Series battery and resistance. (Equivalent to constant-current supply *B* above by Thevenin's theorem). 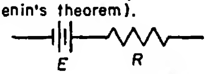 $E' = (r/R) \quad R' = r^2/R$
D. Resistance. 	Resistance.  $R'=r^2/R$
E. Power-sensitive resistance with positive temperature coefficient. 	Power-sensitive resistance with negative temperature coefficient 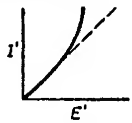 $I' = E/r \quad E' = rI$
F. Short-circuit-stable negative resistance. 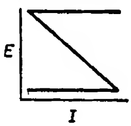	Open-circuit-stable negative resistance 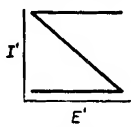 $I'=E/r \quad E'=rI$
G. Capacitance 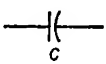	Inductance 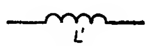 $L'=r^2C$
H. Ideal transformer of impedance ratio $1:a^2$ 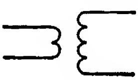 $1:a^2$	Ideal transformer of impedance ratio $a^2:1$ 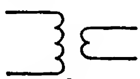 $a^2:1$

Duality and electron-tube analogy *continued*

Fig. 9—*Continued.*

voltage operation	current operation
I. Suitable electron-tube triode. 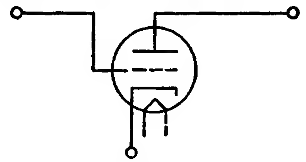	Transistor plus ideal phase reversing transformer. 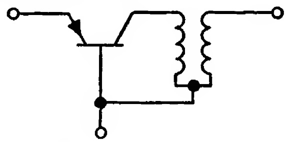
J. Any mid-series terminated constant-R filter section of design resistance R. 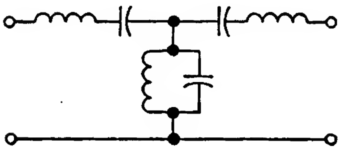	The same constant-r filter section mid-shunt terminated but with design resistance changed to r^2/R. 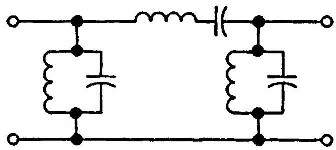

The transistor is current-operated, not voltage-operated. As a guide in circuit design, it is possible to replace the constant-voltage source of the electron tube with a current source. This principle (called duality) may be extended by replacing elements with given voltage characteristics by elements having equivalent current characteristics.*

Fig. 9 is a list of current–voltage duals.

It is sometimes possible, when consideration is given to loading effects, to convert electron-tube circuits directly to junction-transistor circuits by using the electron-tube analogy shown in Fig. 10.

* R. L. Wallace, Jr. and G. Raisbeck, "Duality as a Guide in Transitor Circuit Design," *Bell System Technical Journal,* vol. 30, pp. 381–417; April, 1951.

Fig. 10—The 3 basic transistor connections are at the left and the electron-tube equivalent circuits at the right.

transistor circuit	electron-tube equivalent
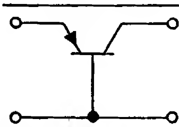 Common base.	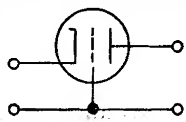 Grounded grid.
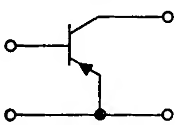 Common emitter.	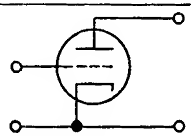 Grounded cathode.
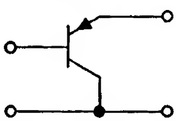 Common collector.	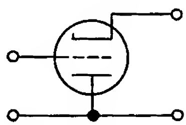 Cathode-follower.

Small-signal amplifiers

General

Small-signal amplifiers may be designed using the formulas in the preceeding section.

It must be remembered that the transistor is a bilateral device; any change in the output circuit will affect all preceeding stages.

In the application of point-contact transistors, care must be taken to insure stability. Junction transistors have $\alpha < 1$ and, therefore, should not cause instability troubles at low frequencies.

Biasing

In both Fig. 11A and B, battery polarity is shown for *pnp* transistors. The polarity is reversed for *npn* transistors.

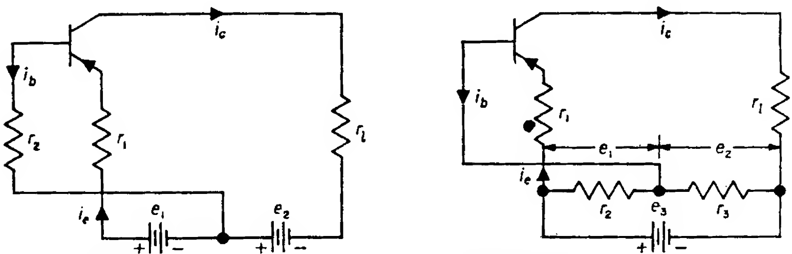

A. Two batteries.

B. One battery.

Fig. 11—Transistor biasing methods.

In Fig. 11,

$e_3 \equiv e_1 + e_2$

$e_1 \equiv e_3 r_2/(r_3 + r_2)$

$e_2 \equiv e_3 r_3/(r_3 + r_2)$

The branch currents in Fig. 11B are:

$$i_c = \frac{i_{c0}\,(1 + r_1/r_2 + r_1/r_3) + \alpha e/r_3}{1 - \alpha + r_1/r_2 + r_1/r_3}$$

$i_e = (i_c - i_{c0})/\alpha$

$i_b = i_e\,(1 - \alpha) - i_{c0}$

where i_{c0} = collector current when $i_e = 0$.

Small–signal amplifiers *continued*

Coupling circuits

Transistors may be cascaded in much the same manner as electron tubes. The common-base, common-emitter, or common-collector configurations may be used. The stages may be coupled by transformers or by *R–C* networks.

Unlike the unilateral electron tube, the transistor is bilateral and essentially a current-operated device. In addition, the transistor (except in common-collector circuits) generally has an input impedance that is comparable to or lower than the output impedance. It is important that care be taken to match impedances between stages. The common-collector stage is a useful impedance-matching device and in view of the efficiency of the transistor, it can be used for impedance matching in place of a transformer. The equations given in Figs. 1–3 may be used to determine the interstage transformation ratios.

Any analysis of a transistor amplifier on a stage-by-stage basis is at best but a rough approximation. For accurate analysis, the matrix methods described above are available.

Large-signal operation

Output stage *

The transistor output stage has two power limitations:

a. The maximum voltage that can be applied between the collector and base of the transistor.

b. The temperature rise in the transistor.

The second limitation is especially important, because it can lead to a "runaway" effect. The higher the temperature, the higher the i_{c0}, which, in turn, leads to higher temperature and ultimately to failure of the transistor.

It is possible to obtain efficiencies of the order of 47 percent with class-*A* transistor amplifiers. However, when transistors are used in power stages, it is advisable to use class-*B* amplification, since the output can approach 3 times the total dissipated power, which is equivalent to 6 times the allowable dissapation of each unit. Furthermore, the no-signal standby power is negligible in the class-*B* circuit.

The output circuit for the class-*B* transistor amplifier can be analyzed by the same methods used for the conventional electron-tube equivalents.

* P. I. Richards, "Power Transistors, Circuit Design and Data," Transistor Products, Inc., Waltham, Mass.

Large-signal operation *continued*

For a class-*B* transistor amplifier with sinusoidal driving voltage,

$$P = e_c^2/2r_l$$

where

P = power output

r_l = reflected load resistance to one-half the primary

$$\eta = \frac{\pi}{4(1 + \pi\, r_l i_{c0}/e_c)}$$

where η is the efficiency at maximum power-output levels. In actual cases η will be 65 to 75 percent.

The equivalent circuit for large-signal operation is given in Fig. 12.

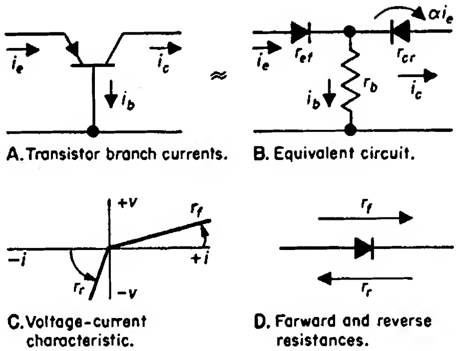

Fig. 12—Large-signal transistor operation. Symbol r_f is the dynamic resistance of the emitter diode biased in the forward conducting direction and r_r is the dynamic resistance of the collector diode biased in the reverse direction.

Complementary symmetry

A class-*B* transistor amplifier can be constructed without the need for a separate phase inverter or a push-pull output transformer. This can be done by using a *pnp* and an *npn* transistor as shown in Fig. 13.

The *pnp* unit will amplify the negative part of the input signal and the *npn* transistor will amplify the positive part. In this manner, phase inversion is automatically accomplished.

The positive and negative signals are combined by coupling the two outputs.

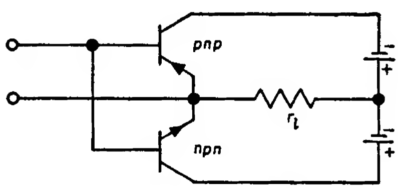

Fig. 13—Complementary symmetry for push-pull stage.

Negative resistance

Trigger circuits

Point-contact and hook-collector transistors have an α that is greater than unity.

Negative resistance *continued*

This can give rise to a negative input resistance that can be utilized in switching or regenerative circuits.

Fig. 14 illustrates the typical input characteristic of a common-base amplifier.

The "N" curve shown in Fig. 14 has counterparts for the common-emitter and the common-collector configurations. These are all the result of equivalent transistor properties and only the common-base curve will be considered in this discussion.

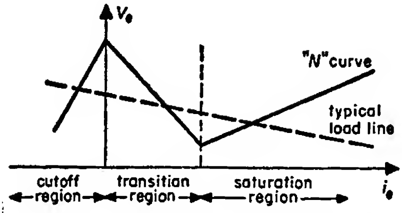

Fig. 14—Input resistance of a common-base transistor amplifier.

Monostable operation is obtained if the load line intersects a positive-resistance portion only once, either in the saturation region or in the cutoff region.

Bistable operation is obtained when the load line intersects a positive-, a negative-, and again a positive-resistance region.

Astable operation is obtained when the load line intersects only the negative-resistance part of the characteristic.

A circuit that may be used as an astable or monostable trigger is shown in Fig. 15.

The emitter current is:

$$i_e = \frac{r_c\, e_c}{r_l\,(r'_b + r_c + r_l}\exp - \frac{(r'_b + r_l)\, t}{r'_b\, r_l\, C}$$

The period of the pulse is:

$$t = \frac{r_b r_l\, C}{r'_b + r_l}\ln\frac{r_c[a\,(r_l + r'_b) - r_b]}{r_l\,(r'_b + r_c + r_l)}$$

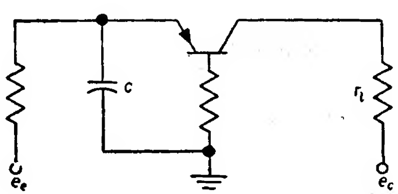

Fig. 15—Astable or monostable trigger circuit.

Negative resistance *continued*

Oscillators

Oscillators may be grouped into two classes:

a. Four-terminal or feedback oscillators.

b. Two-terminal or negative-resistance oscillators.

The feedback oscillators may be constructed with either point-contact or junction transistors.

The design may be based on electron-tube circuit theory and analogy or duality (described earlier).

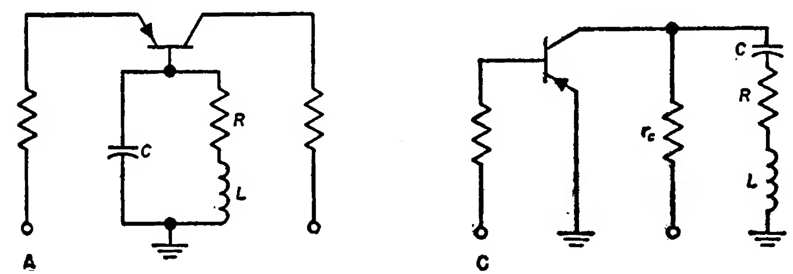

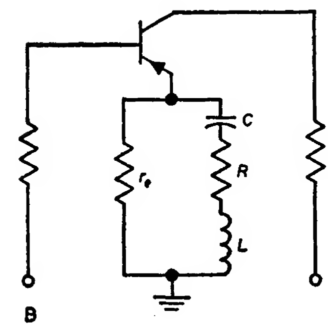

Fig. 16—Oscillator circuits using negative-resistance characteristic of transistor.

The point-contact and the hook-collector transistor can be used as a two-terminal oscillator by placing a resonant circuit in series with the base lead (Fig. 16A), or in parallel with the emitter resistance (Fig. 16B), or in parallel with the collector resistance (Fig. 16C).

Video-frequency amplifiers

Low-frequency compensation

A transistor amplifier may be compensated to give an improved low-frequency response by splitting the collector load and bypassing a portion of this split load. The condition for constant current flowing in the input resistance of the next stage is

$$\frac{r_1 + r_2/(1 + \omega^2 C_1^2 r_2^2)}{r_i} = \frac{\omega C}{(1 + \omega^2 C_1^2 r_2^2)\ (r_2^2 \omega C_1)}$$

where

r_1 = unbypassed portion of collector load

r_2 = bypassed portion of collector load

C_1 = bypass capacitor

C = coupling capacitor to following stage

r_i = input resistance of following stage

when $r_2 \approx r_1 \gg 1/\omega C_1$, the above equation becomes $r_1/r_i \approx C/C_1$

High-frequency compensation

Transistor video-frequency amplifiers are generally capacitor-coupled because of the bandwidth limitations of impedance-matching transformers. The common-emitter configuration permits reasonable impedance matching and is therefore best suited for this application.

The input equivalent circuit of a common-emitter stage for high frequencies is shown in Fig. 17.

The input impedance is approximately

$z_i = r_3 + r_3/[1 + j\ (10f/f_{\alpha 0})]$

where, for most transistors currently available for use as video amplifiers,

$r_3 = r_4$

$2\pi f_{\alpha 0} r_4 = 10$

$C_3 r_4 = 10/2\pi f_{\alpha 0}$

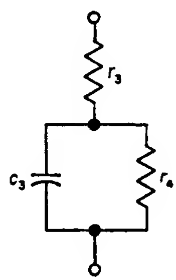

Fig. 17—Equivalent circuit.

High-frequency compensation may be obtained if an inductance L is placed in series with the collector load resistance r_1. The value of the compensating L may be obtained from the following equations.

Video-frequency amplifiers *continued*

$$|A_i| = \left(\frac{r_1^2 + \omega^2 L^2}{A^2 + B^2}\right)^{1/2} \times \frac{1}{\{[(1/\alpha_0) - 1]^2 + [(1/\alpha_0)\ (\omega/\omega_{\alpha 0})]^2\}^{1/2}}$$

where

$$A = r_1 + r_3 \frac{1}{1 + (10\omega/\omega_{\alpha 0})^2}\left[2 - 2\omega^2 C_2 L + (1 - \omega^2 C_2 L)^2 \frac{10\omega^2}{\omega_{\alpha 0}} + r_1 C_2 \omega \frac{10\omega}{\omega_{\alpha 0}}\right]$$

and

$$B = \omega L + \omega r_3 \frac{1}{1 + (10\omega/\omega_{\alpha 0})^2}\left(2C_2 r_1 + C_2 r_1 \left(\frac{10\omega}{\omega_{\alpha 0}}\right)^2 + \omega C_2 L \frac{\omega 10}{\omega_{\alpha 0}} - \frac{10}{\omega_{\alpha 0}}\right)$$

If $\omega \ll \omega_2$

$$|A_1| = \frac{r_1}{r_1 + 2r_3} \quad \frac{\alpha_0}{1 - \alpha_0}$$

where

ω_2 = cutoff frequency of amplifier

α_0 = low-frequency alpha

C_2 = capacitance across L and r_1

In addition to the shunt compensation described above, series inductance can be used to resonate with the input capacitance.

Another method of high-frequency compensation is available. The emitter resistance may be only partially bypassed, resulting in degeneration at lower frequencies. The compensation conditions are similar to that of electron-tube cathode compensation.

Intermediate-frequency amplifiers

Series-resonant interstages

For the series-resonant coupling circuit (Fig. 18), the power gain per stage is

$G \approx |b|^2\, r_{i2}/r_{i1}$

For iterated stages, $r_{i1} = r_{i2}$, and

$G \approx |b|^2$

For common-base stages,

$G \approx |a|^2\, r_{i2}/r_{i1}$

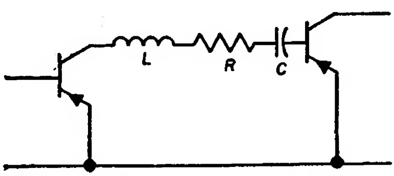

Fig. 18—Series-resonant interstage circuit.

Intermediate-frequency amplifiers *continued*

where

a = common-base current gain

$b = a/(1-a)$

r_{i1} = input resistance of stage

r_{i2} = input resistance of following stage

Junction transistors give less than unity gain in this circuit for common-base or common-collector connection. Point-contact transistors may be used in the common-base connection.

$f_0/\Delta f_{3db} = Q = \omega_0 L/(R + r_{i2})$

where

f_0 = center frequency

Δf_{3db} = 3-decibel bandwidth

Parallel-resonant interstages

If Q (> 10) includes the effect of the input impedance of the next stage for common-base stages (Fig. 19),

$G \approx |a|^2 Q^2 r_{i2}/r_{i1}$

For common-emitter stages,

$G \approx |b|^2 Q^2 r_{i2}/r_{i1}$

The formulas below apply also.

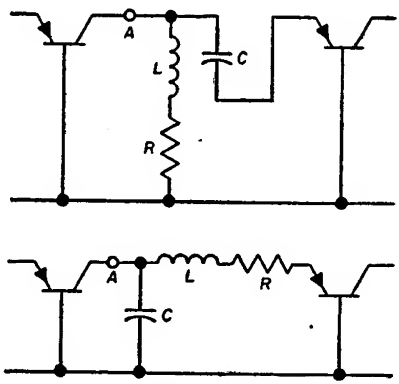

Fig. 19—Parallel-resonant interstage circuits.

Parallel-resonant interstage with impedance transformation:

Power gain per stage:

$G = A_i^2 (r_l/r_{i1}) \times$ (fraction of output power delivered to load)

Let:

r_{i1} = input resistance of stage

r_{i2} = input resistance of next stage

Intermediate-frequency amplifiers *continued*

g_i = conductance seen at A (Fig. 19) due to r_{i2}

g_n = conductance seen at A due to network losses R

g_o = output conductance of transistor

p = ratio of equivalent series resistance seen at A to input resistance of next stage

$= r_1/r_{i2}$

$z_l = r_l + jx_l$ = total load impedance seen at A

$$z_c = \frac{r_c\,(1 - j\omega\, r_c C_c)}{1 + \omega^2 r_c^2 C_c^2} = \text{collector impedance}$$

Then, for common-base stages, power gain is,

$$G = \left|\frac{a}{1 + z_l/z_c}\right|^2 p\,\frac{r_{i2}}{r_{i1}}\left(\frac{g_i}{g_i + g_n}\right)^2$$

For common-emitter connection,

$$G = \left|\frac{a}{1 - a + z_l/z_c}\right|^2 p\,\frac{r_{i2}}{r_{i1}}\left(\frac{g_i}{g_i + g_n}\right)^2$$

For common-collector stages,

$$G = \left|\frac{1}{1 - a + z_l/z_c}\right|^2 p\,\frac{r_{i2}}{r_{i1}}\left(\frac{g_i}{g_i + g_n}\right)^2$$

where C is the total C seen at A (Fig. 19) due to the transistor output, the coupling network, and the following stage.

$$\frac{f_0}{f_{3\text{db}}} = Q = \frac{\omega_0 C}{g_o + g_n + g_i}$$

If $z_l \ll z_c$ and $g_i \gg g_n$ (load not matched, network losses low) and successive stages are identical ($r_{i1} = r_{i2}$):

For common-base stages,

$G = |a|^2\, p$

For common-emitter stages,

$G = |b|^2\, p$

For common-collector stages,

$G = |b+1|^2\, p$

Intermediate-frequency amplifiers *continued*

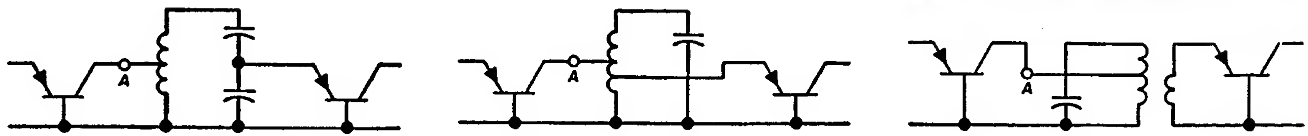

Fig. 20—Three types of single-tuned resonant interstage circuit.

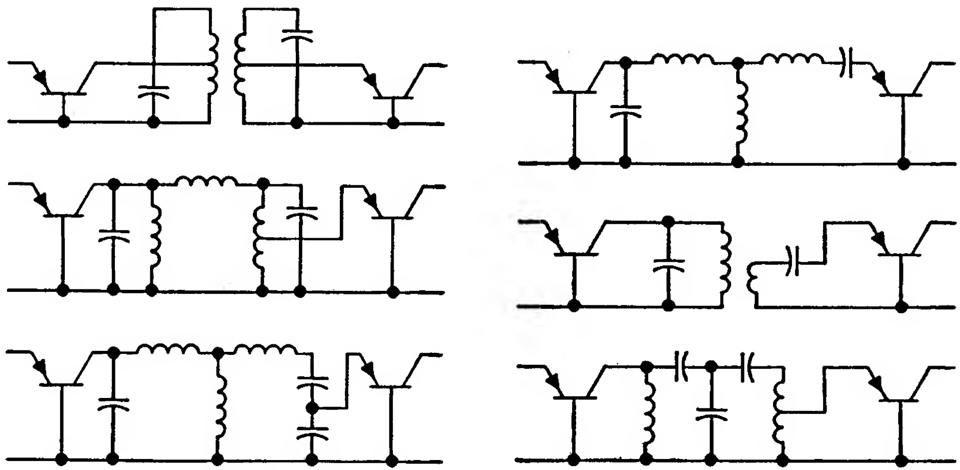

Fig. 21—Various double-tuned interstage circuits.

Intermediate-frequency amplifiers *continued*

Tuned-circuit interstages

Other configurations of single-tuned interstage are shown in Fig. 20. Any of the 3 transistor configurations may be used in these circuits.

Double-tuned interstages

For double-tuned interstages (Fig. 21), the same gain formulas apply as for the single-tuned case. For a given bandwidth, however, p may be made larger in the double-tuned case.

The T and π equivalents of the transformers will not always be physically realizable.

For large bandwidth, the condition $Q_1 \gg Q_2$ is desirable, since then loading resistors are not required with their accompanying power loss.

For $Q_1 \gg Q_2$, for transitional coupling (Fig. 22),

$$\Delta f_{3db}/f_0 = k = 1/Q_2\ (2)^{1/2}$$

where k = coefficient of coupling. If $z_i = r_i + jx_i$ = input impedance of next stage then,

$$Q_2 = \frac{\omega_0 L_2 + x_i}{r_i}$$

$$L_2 = \frac{Q_2 r_i - x_i}{\omega_0}$$

$$= \frac{r_i}{2\pi \Delta f_{3db}} - \frac{x_i}{\omega_0}$$

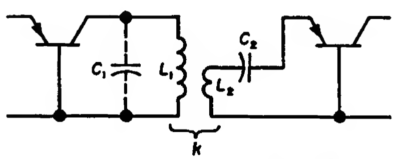

Fig. 22—Double-tuned interstage.

L_2, C_2, and x_i are series-resonant at f_0.

$$L_1C_1 = 1/\omega_0^2$$

$$p \approx Q_2^2 C_2/C_1$$

C_1 includes the transistor output capacitance.

Neutralization *

For neutralization (Fig. 23),

$r_b'C_c = r_nC_n$

Either point *A* or point *B* may be at ground potential. The choice will depend on the relative ease of isolating the source or the load from ground.

The effect of neutralization is to make the 12 term of the matrix equal to zero.

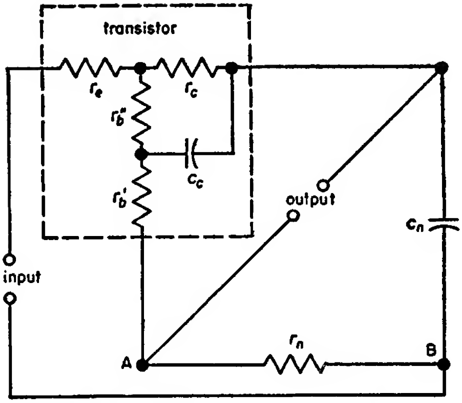

Fig. 23—Neutralization of common-base amplifier*

Temperature compensation

The i_c of a transistor may increase appreciably with temperature. This is objectionable since it increases the power dissipated in the transistor and so increases its temperature rise. Two possible methods for stabilizing i_c against temperature variations follow.

The circuit of Fig. 24A depends on negative feedback, similar to cathode bias in electron tubes, i_e being stabilized by the degeneration produced by R_1 at direct current. Capacitor C must bypass R_1 at the frequencies to be amplified.

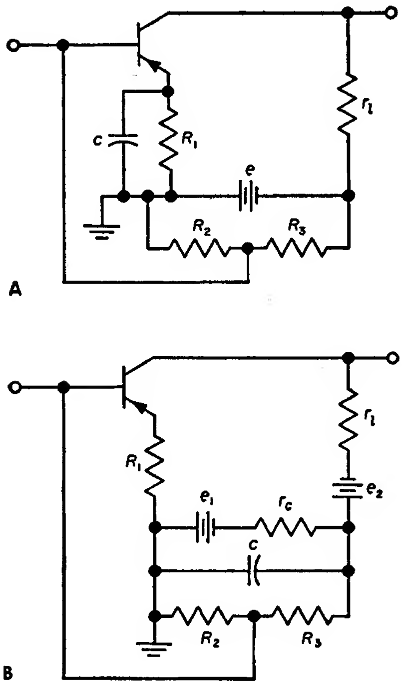

Fig. 24—Two types of temperature compensation for transistors.

* A. P. Stern, C. A. Aldrich, and W. F. Chou, "Internal Feedback and Neutralization of Transistor Amplifiers," *Proceedings of the IRE*, vol. 43, pp. 838–848; July, 1955.

Temperature compensation *continued*

For the circuit of Fig. 24A, with α being assumed constant over the operating range,

$$i_c = \frac{i_{c0}\,(1 + R_1/R_2 + R_1/R_3) + \alpha e/R_3}{1 - \alpha + R_1/R_2 + R_1/R_3}$$

When the variation with frequency of the phase shift resulting from R_1 and C is objectionable, or where C must be made inconveniently large, the circuit of Fig. 24B may be used. Since r_c and R_3 are higher resistances than R_1, a smaller C may be used for the same bypassing effect. Here stabilization is obtained by the drop in i_c influencing base potential and R_1 is made small to minimize degeneration of signal frequencies.

If $R_3 \gg R_1$ and $r_c \gg R_1$, then

$$i_c = \frac{i_{c0}[(r_c/R_3)\,(1 + R_1/R_2) + 1 + R_1/R_2 + R_1/R_3] + \alpha e_1/R_3}{1 - \alpha + R_1/R_2 + R_1/R_3 + (r_c/R_3)\,(1 + R_1/R_2)}$$

Pulse circuits

Transistors may be utilized for the generation, amplification, and shaping of pulse waveforms.

The Ebers and Moll* equivalent circuits of Figure 25 give the large-signal transient response of a junction transistor. The parameters are defined as follows:

i_{e0} = saturation current of emitter junction with zero collector current

i_{c0} = saturation current of collector junction with zero emitter current

α_n = transistor direct-current gain with the emitter functioning as an emitter and the collector functioning as a collector (normal α)

α_i = transistor direct-current gain with the collector functioning as an emitter and the emitter functioning as collector (inverted α)

$$\Phi_e = \frac{kT}{q} \ln\left[-\frac{i_e + \alpha_i i_c}{i_{e0}} + 1\right]$$

= emitter-to-junction voltage

$$\Phi_c = \frac{kT}{q} \ln\left[-\frac{i_c + \alpha_n i_e}{i_{c0}} + 1\right]$$

= collector-to-junction voltage

* J. J. Ebers and J. L. Moll, "Large-Signal Behavior of Junction Transistors:" also, J. L. Moll, "Large-Signal Transient Response of Junction Transistors," *Proceedings of the IRE*, vol. 42, pages 1761–1772, 1773–1784; December, 1954.

Pulse circuits *continued*

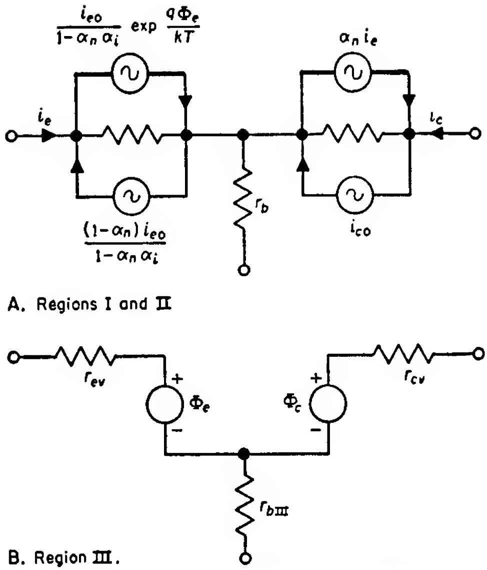

Fig. 25—Low-frequency large-signal equivalent circuit of a junction transistor.

The switching time can be calculated from the small-signal equivalent circuit parameters, the turn-on time, from cutoff to saturation, depends on the frequency response of the transistor in the active region. The turn-off time, from saturation to cutoff depends on minority carrier storage time and decay time. Carrier storage time is that required for the operating point to move out of the saturation region into the active region on removal of the drive current and is a function of the frequency response of the transistors in the saturation region. Decay time follows the storage time and returns the transistor to cutoff; it depends on the frequency response in the active region. Switching time of order $3/\omega_n$ is realized if carrier storage is avoided.

$$\text{Turn-on time} = \frac{1}{\omega_n}\ \frac{i_{e2}}{i_{e2} - 0.9\, i_c/\alpha_n}$$

$$\text{Storage time} = \frac{\omega_n + \omega_i}{\omega_n\omega_i(1-\alpha_n\alpha_i)} \ln \frac{i_{e2} - i_{e1}}{i_c/\alpha_n + i_{e2}}$$

$$\text{Decay time} = \frac{1}{\omega_n} \ln \frac{i_c + \alpha_n i_{e2}}{(i_c + \alpha_n i_{e2})/10}$$

where

ω_n = cutoff frequency of normal alpha

ω_i = cutoff frequency of inverted alpha

i_{e1}, i_{e2} = emitter current before and after switching step is applied

i_c = collector current in the saturation state.

k = Boltzmann's Constant

Pulse circuits *continued*

T = absolute temperature

q = charge on electron

Measurement of small-signal parameters

The small-signal parameters may be represented by ratios of small alternating voltages and currents if care is taken to keep the magnitudes of these signals small compared to direct-current condition. For instance,

$$z_{11} = r_e + r_b$$

$$= \left[\frac{\partial v_e}{\partial i_e}\right]_{i_c} \approx \left[\frac{\Delta v_e}{\Delta i_e}\right]_{i_c} \approx \left[\frac{v_e}{i_e}\right]_{i_c}$$

Also,

$z_{11} = e_1/i_1$ when $i_2 = 0$

$z_{12} = e_1/i_2$ when $i_1 = 0$

$z_{21} = e_2/i_1$ when $i_2 = 0$

$z_{22} = e_2/i_2$ when $i_1 = 0$

and

$h_{11} = e_1/i_1$ when $e_2 = 0$

$h_{12} = e_1/e_2$ when $i_1 = 0$

$h_{21} = i_2/i_1$ when $e_2 = 0$

$h_{22} = i_2/e_2$ when $i_1 = 0$

Fig. 26 indicates the use of matrixes for solution of transistor parameters, where

$z_{11} = r_e + r_b$

$z_{12} = r_b$

$z_{21} = r_b + \alpha r_c$

$z_{22} = r_c + r_b$

Measurement of small-signal parameters *continued*

and

$h_{11} = r_e + r_b + h_{21} r_b$

$h_{12} = r_b/(r_c + r_b)$

$h_{21} = -(r_b + \alpha r_c)/(r_e + r_b)$

$h_{22} = 1/(r_c + r_b)$

Fig. 26—Transistor parameters in terms of common-base matrix coefficients.

.	z	h
r_e	$z_{11} - z_{12}$	$h_{11} - \dfrac{h_{12}}{h_{22}}(1 + h_{21})$
r_c	$z_{22} - z_{12}$	$(1 - h_{12})/h_{22}$
r_b	z_{12}	h_{12}/h_{22}
r_m	$z_{21} - z_{12}$	$-\dfrac{h_{21} + h_{12}}{h_{22}}$
α	$\dfrac{z_{21} - z_{12}}{z_{22} - z_{12}}$	$\dfrac{h_{21} - h_{12}}{1 - h_{12}}$

Modulation

The material in this chapter is divided into two sections on continuous-wave (cw) and noncontinuous (pulse) relations.

Continuous-wave modulation

The process of continuous-wave modulation of a radio-frequency carrier $y = A(t) \cos \gamma(t)$ is treated under two main headings as follows:

a. Modification of its amplitude $A(t)$

b. Modification of its phase $\gamma(t)$

For a harmonic oscillation, $\gamma(t)$ is replaced by $(\omega t + \phi)$, so that

$$y = A(t) \cos (\omega t + \phi) = A(t) \cos \psi(t)$$

A is the amplitude. The whole argument of the cosine $\psi(t)$ is the phase.

Amplitude modulation

In amplitude modulation (Fig. 1), ω is constant. The signal intelligence $f(t)$ is made to control the amplitude parameter of the carrier by the relation

$$A(t) = [A_0 + a\, f(t)]$$
$$= A_0[1 + m_a\, f(t)]$$

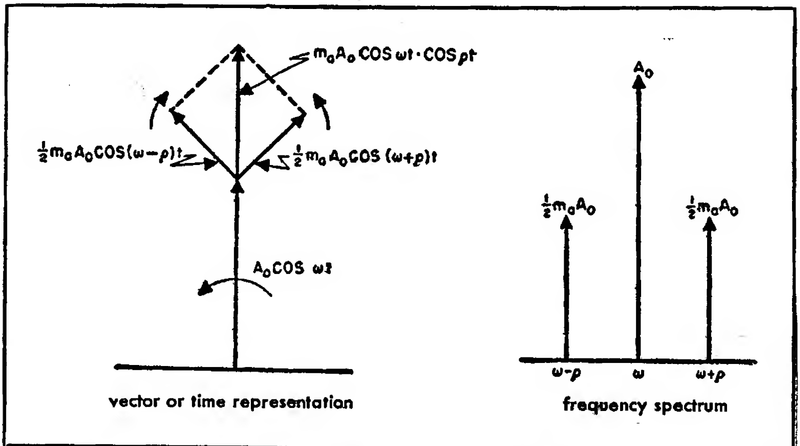

Fig. 1—Vector and sideband representation of amplitude modulation for a single sinusoidal modulation frequency ($a \cos pt$).

Continuous-wave modulation *continued*

where

$\psi(t) = \omega t + \phi$

ω = angular carrier frequency

ϕ = carrier phase constant

A_0 = amplitude of the unmodulated carrier

a = maximum amplitude of modulating function

$f(t)$ = generally, a continuous function of time representing the signal; $0 \leqslant f(t) \leqslant 1$

$m_a = a/A_0$ = degree of amplitude modulation; $0 \leqslant m_a < 1$

$y = A_0 [1 + m_a f(t)] \cos(\omega t + \phi)$

For a signal $f(t)$ represented by a sum of sinusoidal components

$$af(t) = \sum_{K=1}^{K=m} a_K \cos(p_K t + \theta_K)$$

where p_K is the angular frequency of the kth component of the modulating signal and θ_K is the constant part of its phase.

Assuming the system is linear, each frequency component p_K gives rise to a pair of sidebands $(\omega + p_K)$ and $(\omega - p_K)$ symmetrically located about the carrier frequency ω.

$$y = A_0 \left[1 + \frac{1}{A_0} \sum_{K=1}^{K=m} a_K \cos(p_K t + \theta_K) \right] \cos(\omega t + \phi)$$

The constant component of the carrier phase ϕ is dropped for simplification

$$y = \underbrace{A_0 \cos(\omega t)}_{\text{carrier}} + \underbrace{(\cos \omega t) \left[\sum_{K=1}^{K=m} a_K \cos(p_K t + \theta_K) \right]}_{\text{modulation vectors}}$$

$$= \underbrace{A_0 \cos \omega t}_{\text{carrier}} + \underbrace{\frac{a_1}{2} \cos[(\omega + p_1)t + \theta_1]}_{\text{upper sideband}} + \underbrace{\frac{a_1}{2} \cos[(\omega - p_1)t - \theta_1]}_{\text{lower sideband}} + \cdots$$

$$+ \underbrace{\frac{a_m}{2} \cos[(\omega + p_m)t + \theta_m]}_{\text{upper sideband}} + \underbrace{\frac{a_m}{2} \cos[(\omega - p_m)t - \theta_m]}_{\text{lower sideband}}$$

Continuous-wave modulation *continued*

$$\text{Degree of modulation} = \frac{1}{A_0}\sum_{K=1}^{K=m} a_K \quad \text{for } p\text{'s not harmonically related.}$$

$$\text{Percent modulation} = \frac{(\text{crest ampl}) - (\text{trough ampl})}{(\text{crest ampl}) + (\text{trough ampl})} \times 100$$

Percent modulation may be measured by means of an oscilloscope, the modulated carrier wave being applied to the vertical plates and the modulating voltage wave to the horizontal plates. The resulting trapezoidal pattern and a nomograph for computing percent modulation are shown in Fig. 2. The dimensions A and B in that figure are proportional to the crest amplitude and trough amplitude, respectively.

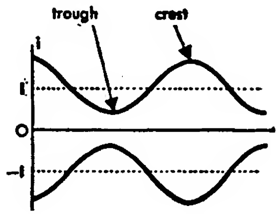

Peak voltage at crest for p's not harmonically related:

$$A_{\text{crest}} = A_{0,\,\text{rms}}\left[1 + \frac{1}{A_0}\sum_{K=1}^{K=m} a_K\right] \times (2)^{1/2}$$

Effective value of the modulated wave in general:

$$A_{\text{eff}} = A_{0,\,\text{rms}}\left[1 + \frac{1}{2A_0^2}\sum_{K=1}^{K=m} a_K^2\right]^{1/2}$$

In the design of some components of a system, such as capacitors and transmission lines, frequently all the signal is considered as being present in one pair of sidebands. Then the peak voltage and the kilovolt–amperes are as follows,

$$V_{\text{peak, crest}} = (1 + m_a)\, V_{\text{peak, carrier}}$$

$$(\text{kva}) = (1 + m_a^2/2)\ (\text{kva})_{\text{carrier}}$$

where m_a is the degree of amplitude modulation. For example, if the design is for a 1-kilowatt carrier, 100-percent modulated, $m_a = 1.00$ and the power at full modulation is 1.50 kilowatts. The effective current is $(1.50)^{1/2} = 1.225$ times the root-mean-square carrier current.

Continuous-wave modulation *continued*

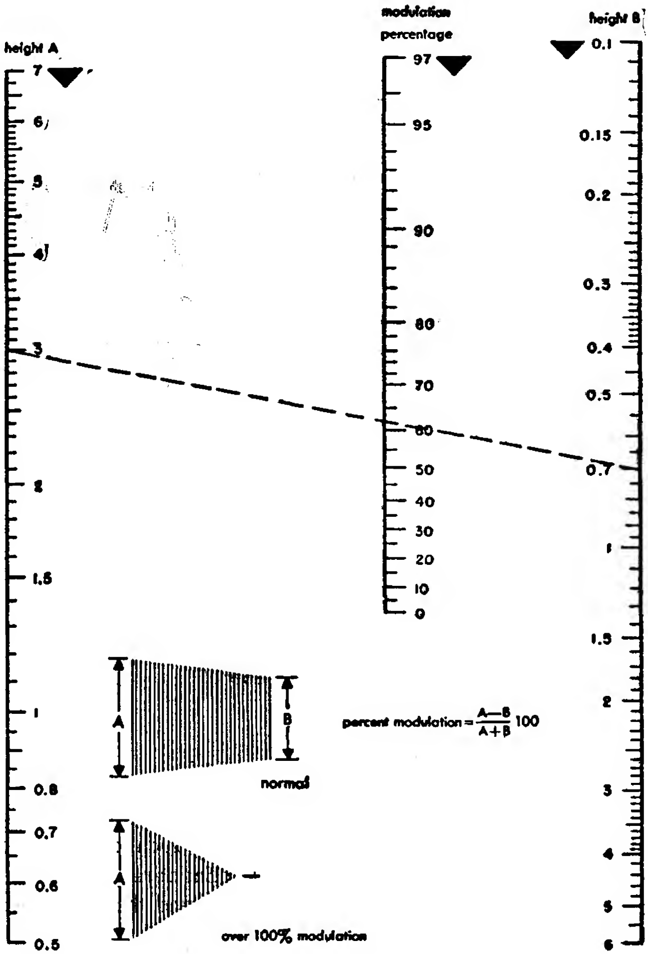

To determine the modulation percentage from an oscillogram of type illustrated apply measurements *A* and *B* to scales *A* and *B* and read percentage from center scale. Any units of measurement may be used.

Example: $A = 3$ inches, $B = 0.7$ inches; modulation = 62 percent.

Fig. 2—Modulation percentage from oscillograms.

Continuous-wave modulation *continued*

Systems of amplitude modulation

The above analysis shows how two sidebands are generated when the amplitude of a carrier signal is controlled by a modulation signal. It is apparent that the desired information is contained in the sidebands, and, in fact, in either sideband alone. Consequently, there have arisen three additional systems of amplitude modulation other than double-sideband with full carrier. These are: suppressed-carrier, single-sideband, and vestigial-sideband modulations.

Suppressed-carrier modulation: It is sufficient to transmit only enough carrier so that at the receiver this carrier can be used to control the frequency and phase of a locally generated carrier. The locally generated carrier may be made sufficiently large to reduce the effective percentage of modulation. This will aid in removing the distortion inherent in some types of detectors when the modulation percentage approaches or exceeds 100 percent.

Single-sideband modulation: Single-sideband systems are used to translate the spectrum of a modulation signal to a new space in the frequency domain with or without inversion. Substantially no carrier voltage is transmitted in this system. The principal advantage is that the effective bandwidth required for transmission is half that required for a double-sideband system. It is required, in order to demodulate this signal, that a locally generated carrier be supplied. This carrier must be very close to the frequency of the carrier used in the modulation process at the transmitter to preserve the spectral components in the derived modulation signal.

Vestigial-sideband modulation: Single-sideband systems are at a serious disadvantage when the modulation signal contains very-low frequencies. It becomes increasingly difficult as the low-frequency limit approaches zero frequency to suppress the adjacent portion of the unwanted sideband. However, it is not necessary to suppress the unwanted sideband completely. If the characteristic that modifies the two sidebands satisfies certain requirements, then the modulating wave can be recovered without distortion with a product demodulator. This is known as a vestigial-sideband system. Envelope detectors can also be employed provided that the modulation percentage is not too high. Excessive distortion will otherwise result.

Continuous-wave modulation *continued*

Angular modulation

All sinusoidal angular modulations derived from the harmonic oscillation $y = A \cos(\omega t + \phi)$ can be expressed in the form

$$y = A \cos \psi(t)$$
$$= A \cos(\omega_0 t + \Delta\theta \cos pt)$$

where the oscillating component $\Delta\theta \cos pt$ of the phase excursion is determined by the type of angular modulation used. In all angular modulations A is constant.

Frequency modulation

$$y = A_0 \cos \psi(t)$$

The signal intelligence $f(t)$ is made to control the instantaneous frequency parameter of the carrier by the relation

$$\omega(t) = \omega_0 + \Delta\omega\, f(t)$$

where

$\omega(t)$ = instantaneous frequency
$= d\psi(t)/dt$

$\psi(t) = \int \omega(t)\, dt$

ω_0 = frequency of unmodulated carrier

$\Delta\omega$ = maximum instantaneous frequency excursion from ω_0

For single-frequency modulation $f(t) = \cos pt$,

$$y = A \cos\left(\omega_0 t + \frac{\Delta\omega}{p} \sin pt\right)$$

$\Delta\omega/p = \Delta\theta$ (in radians) is the modulation index. The phase excursion $\Delta\theta$ is inversely proportional to the modulation frequency p. In general for broadcast applications, $\Delta\omega \ll \omega_0$ and $\Delta\theta \gg 1$.

Phase modulation

$$y = A_0 \cos \psi(t)$$

The signal intelligence $f(t)$ is made to control the instantaneous phase excursions of the carrier by the relation $\delta\theta = \Delta\theta\, f(t)$.

Continuous-wave modulation *continued*

$$\psi(t) = [\omega_0 t + \Delta\theta\, f(t)] = \int_0^t \omega(t)\, dt$$

$$y = A \cos [\omega_0 t + \Delta\theta\, f(t)]$$

For sinusoidal modulation $f(t) = \cos pt$,

$$y = A \cos (\omega_0 t + \Delta\theta \cos pt)$$

Maximum phase excursion is independent of the modulation frequency p.

The instantaneous frequency of the phase-modulated wave is given by the derivative of its total phase:

$$\omega(t) = d\psi(t)/dt = (\omega_0 - p\Delta\theta \sin pt)$$

$$\Delta\omega = \omega(t) - \omega_0 = -p\Delta\theta \sin pt$$

Maximum frequency excursion $\Delta\omega = -p\Delta\theta$ is proportional to the modulation frequency p.

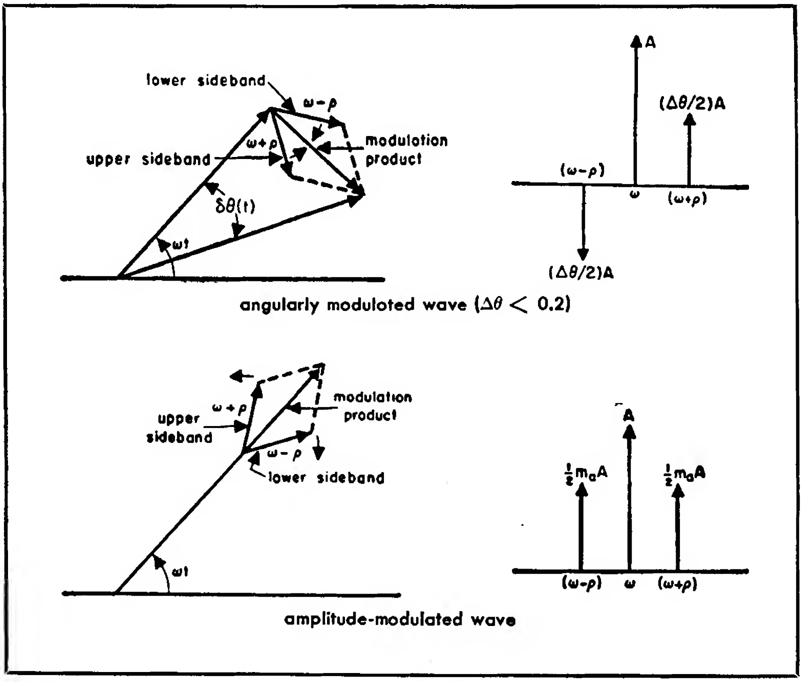

Fig. 3—Sideband and modulation vector representation of angular modulation for $\Delta\theta < 0.2$ as well as for amplitude modulation.

Continuous-wave modulation *continued*

Sideband energy distribution in angular modulation

$y = A \cos (\omega_0 t + \Delta\theta \cos pt)$

for $\Delta\theta < 0.2$ and a single sinusoidal modulation. See Fig. 3.

$$y = A(\underbrace{\cos \omega_0 t}_{\text{carrier}} - \underbrace{\Delta\theta \cos pt \sin \omega_0 t}_{\text{modulation vector}})$$

$$= A\left[\underbrace{\cos \omega_0 t}_{\text{carrier}} - \underbrace{\frac{\Delta\theta}{2} \sin (\omega_0 + p)t}_{\text{upper sideband}} - \underbrace{\frac{\Delta\theta}{2} \sin (\omega_0 - p)t}_{\text{lower sideband}}\right]$$

Frequency spectrum of angular modulation: No restrictions on $\Delta\theta$.

$$\begin{aligned} y &= A \cos (\omega_0 t + \Delta\theta \cos pt) \\ &= A[J_0(\Delta\theta) \cos \omega_0 t - 2J_1(\Delta\theta) \cos pt \sin \omega_0 t \\ &\qquad - 2J_2(\Delta\theta) \cos 2pt \cos \omega_0 t \\ &\qquad + 2J_3(\Delta\theta) \cos 3pt \sin \omega_0 t \\ &\qquad + \dots\dots\dots\dots\dots] \end{aligned}$$

This gives the carrier modulation vectors. See Fig. 4.

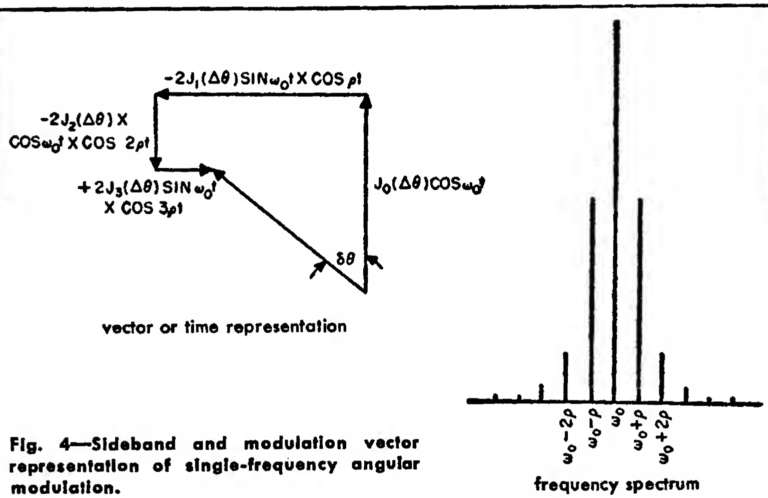

Fig. 4—Sideband and modulation vector representation of single-frequency angular modulation.

Continuous-wave modulation *continued*

The sideband frequencies are given by

$$y = A\{J_0(\Delta\theta)\cos\omega_0 t - J_1(\Delta\theta)[\sin(\omega_0+p)t + \sin(\omega_0-p)t]$$
$$- J_2(\Delta\theta)[\cos(\omega_0+2p)t + \cos(\omega_0-2p)t]$$
$$+ J_3(\Delta\theta)[\sin(\omega_0+3p)t + \sin(\omega_0-3p)t]\}$$

Here, $J_n(\Delta\theta)$ is the Bessel function of the first kind and nth order with argument $\Delta\theta$. An expansion of $J_n(\Delta\theta)$ in a series is given on page 1085, tables of Bessel functions are on pages 1118 to 1121; and a 3-dimensional representation of Bessel functions is given in Fig. 5. The carrier and sideband amplitudes are oscillating functions of $\Delta\theta$:

Carrier vanishes for $\Delta\theta$ radians $= 2.40;\ 5.52;\ 8.65 + n\pi$

First sideband vanishes for $\Delta\theta$ radians $= 3.83;\ 7.02;\ 10.17;\ 13.32 + n\pi$

The property of vanishing carrier is used frequently in the measurement of $\Delta\omega$ in frequency modulation. This follows from $\Delta\omega = (\Delta\theta)(p)$. Knowing $\Delta\theta$ and p, $\Delta\omega$ is computed.

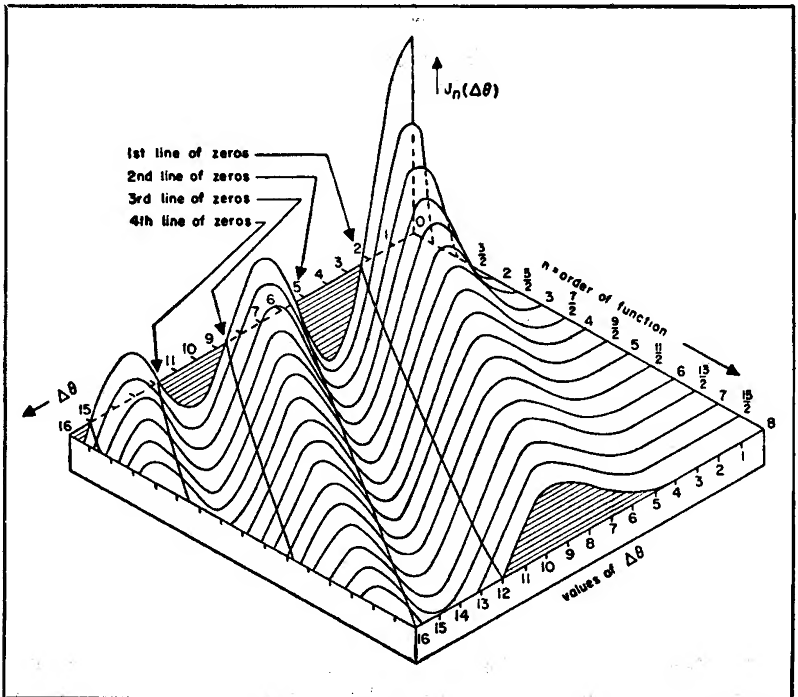

Fig. 5—Three-dimensional representation of Bessel functions.

Continuous-wave modulation *continued*

The approximate number of important sidebands and the corresponding bandwidth necessary for transmission are as follows, where $f = p/2\pi$ and $\Delta f = \Delta\omega/2\pi$,

	$\Delta\theta = 5$	$\Delta\theta = 10$	$\Delta\theta = 20$
Signal frequency	$0.2\ \Delta f$	$0.1\ \Delta f$	$0.05\ \Delta f$
Number of pairs of sidebands	7	13	23
Bandwidth	$14\ f$ $2.8\ \Delta f$	$26\ f$ $2.6\ \Delta f$	$46\ f$ $2.3\ \Delta f$

This table is based on neglecting sidebands in the outer regions where all amplitudes are less than $0.02A_0$. The amplitude below which the sidebands are neglected, and the resultant bandwidth, will depend on the particular application and the quality of transmission desired.

Interference and noise in am and fm

Interference rejection in amplitude and frequency modulations: Simplest case of interference; two unmodulated carriers:

e_0 = desired signal

$= E_0 \sin \omega_0 t$

e_1 = interfering signal

$= E_1 \sin \omega_1 t$

The vectorial addition of these two results in a voltage that has both amplitude and frequency modulation.

Amplitude-modulation interference

E_t = resultant voltage

$$\approx E_0\left[1 + \frac{E_1}{E_0}\cos(\omega_1 - \omega_0)t\right] \text{ for } E_1 \ll E_0$$

The interference results in the amplitude modulation of the original carrier by a beat frequency equal to $(\omega_0 - \omega_1)$ having a modulation index equal to E_1/E_0.

Continuous-wave modulation *continued*

Frequency-modulation interference

$\omega(t)$ = resultant instantaneous frequency

$$= \omega_0 + \frac{E_1}{E_0}(\omega_1 - \omega_0)\cos(\omega_1 - \omega_0)t \quad \text{for } E_1 \ll E_0$$

$$\Delta\omega_1 = \omega(t) - \omega_0 = \frac{E_1}{E_0}(\omega_1 - \omega_0)\cos(\omega_1 - \omega_0)t$$

The interference results in frequency modulation of the original carrier by a beat frequency equal to $(\omega_0 - \omega_1)$ having a frequency deviation ratio to maximum desired deviation equal to $E_1(\omega_1 - \omega_0)/E_0\Delta\omega$ and relative interference of

$$\left(\frac{\text{interference amplitude modulation}}{\text{interference frequency modulation}}\right) = \frac{\Delta\omega}{(\omega_1 - \omega_0)}$$

where $\Delta\omega$ is the desired frequency deviation.

Noise reduction in frequency modulation: The noise-suppressing properties of frequency modulation apply when the signal carrier level at the frequency discriminator is greater than the noise level. When the noise level exceeds the carrier signal level, the noise suppresses the signal. For a given amount of noise at a receiver there is a sharp threshold level of frequency-modulation signal above which the noise is suppressed and below which the signal is suppressed. This threshold has been defined as the improvement threshold. For the condition where the threshold level is exceeded:

Random noise: Assuming the receivers have uniform gain in the pass band, the resultant noise is proportional to the square of the voltage components over the spectrum of noise frequencies:

$$\left(\frac{\text{fm signal/random-noise ratio}}{\text{am signal/random-noise ratio}}\right) = (3)^{1/2}\frac{\Delta\omega}{p} = (3)^{1/2}\,\Delta\theta$$

Impulse noise: Noise voltages add directly:

$$\left(\frac{\text{fm signal/impulse-noise ratio}}{\text{am signal/impulse-noise ratio}}\right) = 2\frac{\Delta\omega}{p} = 2\,\Delta\theta$$

Continuous-wave modulation *continued*

The carrier signal required to reach the improvement threshold depends on the frequency deviation of the incoming signal. The greater the deviation, the greater the signal required to reach the improvement threshold, but the greater the noise suppression, once this level is reached. Fig. 6 illustrates this characteristic.

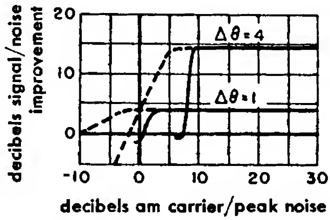

Fig. 6—Improvement threshold for frequency modulation. Deviation $\Delta\theta$ affects amount of signal required to reach threshold and also amount of noise suppression obtained. Solid line shows peak, and dotted line the root-mean-square noise in the output.
Courtesy of McGraw-Hill Book Company

In amplitude modulation, the presence of the carrier increases the background noise in a receiver. In frequency modulation, the presence of the carrier decreases the background noise, since the carrier effectively suppresses it.

Pulse modulation

The process of pulse modulation covers methods where either the amplitude or time of occurrence of some characteristic of a pulse carrier are controlled by instantaneous samples of the modulating wave.

Sampling

Instead of transmitting a continuous signal, it is sufficient to sample the signal at regular, discrete time intervals and to transmit information regarding the signal amplitudes at the sampling times only. This information may be put into any one of many different forms. It may be used to amplitude-modulate a pulse train (pam), time-modulate a pulse train

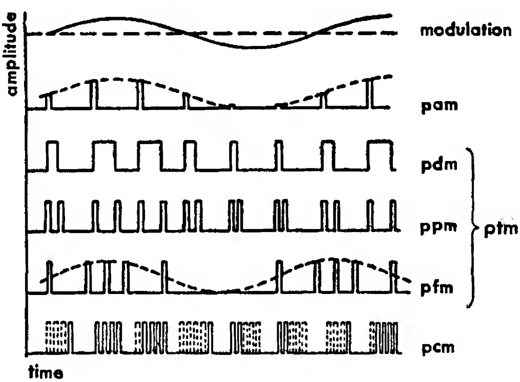

Fig. 7—Pulse trains of single channels for various pulse systems, showing effect of modulation on amplitude and time-spacing of subcarrier pulses. The modulation signal is at the top.

Pulse modulation *continued*

(ptm), etc., as shown in Fig. 7. The original signal can be recovered from the pulse-modulated signal provided that the sampling rate is sufficiently high. The minimum sampling frequency is given by

$$f_p = 2\, f_h/m$$

where

f_p = sampling frequency

m = largest integer not exceeding f_h/w

$w = (f_h - f_l)$ = modulation - frequency bandwidth

f_h = highest frequency limit of modulation-frequency band

f_l = lowest frequency limit of modulation-frequency band

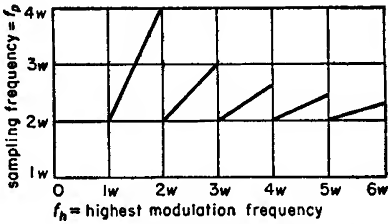

Fig. 8—Minimum sampling frequency versus highest frequency in the modulation-frequency band as a function of modulation-frequency bandwidth.

A plot of this relation in terms of the quantities f_p, f_h, and w is shown in Fig. 8. For example, if f_h = 7.5 kilocycles and f_l = 4.5 kilocycles, then w = 3 kilocycles or f_h = 2.5w. Then, f_p = 2.5w = 7.5 kilocycles.

In practice, a value of f_p 15-percent larger than that given in the above formula is utilized. This permits the sampling components to be separated from the voice components with a more-economical filter. Inherent spurious distortion is introduced by the modulation process in conventional pulse-time modulation (but not in pulse-amplitude modulation) and for distortion requirements of less than 1 percent, a factor of 2.5 to 3 in the above formula is recommended.

Basic modulating and encoding methods

Pulse-time modulation (ptm) in which the values of instantaneous samples of the modulating wave control the time of occurrence of some characteristic of a pulse carrier; the amplitude of the individual pulses being fixed.

Pulse-amplitude modulation (pam) in which the values of the instantaneous samples of the modulating wave control the amplitude of a pulse carrier; the time of occurrence of the individual pulses being fixed.

Pulse modulation *continued*

Pulse-code modulation (pcm) in which the modulating wave is sampled, quantized, and coded.

Pulse-time-modulation types

Pulse-position modulation (ppm) in which each instantaneous sample of a modulating wave controls the time position of a pulse in relation to the timing of a recurrent reference pulse.

Pulse-duration modulation (pdm) in which each instantaneous sample of the modulating wave controls the time duration of a pulse. Also called pulse-width modulation (pwm).

Pulse-frequency modulation (pfm) in which the modulating wave is used to frequency-modulate a carrier wave consisting of a series of pulses.

Additional methods that include modified-time-reference and pulse-shape modulation.

Pulse-amplitude-modulation types

Pulse-amplitude modulation (pam) used when the modulating wave is caused to amplitude-modulate a pulse carrier. Forms of this type of modulation include single-polarity pam and double-polarity pam.

Pulse-code-modulation types

Binary pulse-code modulation (pcm): Pulse-code modulation in which the code for each element of information consists of one of two distinct kinds or values, such as pulses and spaces. Fig. 9 shows a 32-level binary code raster. A level of 21 in decimal notation is represented in this method by  .

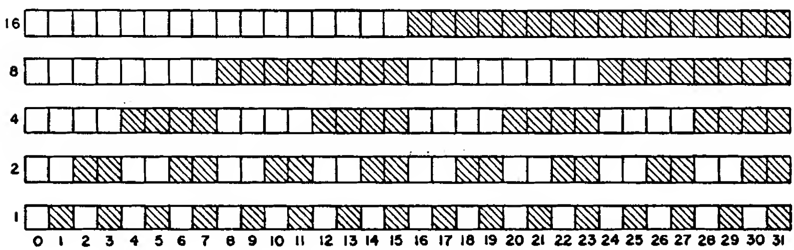

Fig. 9—Binary code raster for 32 levels.

Pulse modulation *continued*

Ternary pulse-code modulation (pcm): Pulse-code modulation in which the code for each element of information consists of any one of three distinct kinds or values, such as positive pulses, negative pulses, and spaces.

***N*-ary pulse-code modulation (pcm):** Pulse-code modulation in which the code for each element of information consists of any one of *N* distinct kinds or values.

Terminology

Baud: The unit of signaling speed equal to one code element per second. The signaling speed is sometimes measured in cycles per second. See p. 846.

Clipper: A device that gives output only when the input exceeds a critical value.

Code: A plan for representing each of a finite number of values as a particular arrangement of discrete events.

Code character: A particular arrangement of code elements used in a code to represent a single value.

Code element: One of the discrete events in a code.

Limiter: A device whose output is constant for all inputs above a critical value.

Noise improvement factor (nif): Ratio of receiver output signal-to-noise ratio to the receiver input signal-to-noise ratio. (Receiver is used in the broad sense and is taken to include pulse demodulators.)

PCM level: The number by which a given subrange of a quantized signal may be identified.

Pulse decay time: The time required for the instantaneous amplitude to go from 90 percent to 10 percent of the peak value.

Pulse duration: The time required for the instantaneous amplitude to go from the 50-percent point of the leading edge through the peak value and return to the 50-percent level of the trailing edge.

Pulse improvement threshold: In constant-amplitude pulse-modulation systems, the condition that exists when the ratio of peak pulse voltage to peak noise voltage exceeds 2 after selection and before any nonlinear process such as amplitude clipping and limiting. The ratio of peak to root-mean-square noise voltage is ordinarily taken to be 4. Therefore, at the improvement threshold, the ratio of peak to root-mean-square noise voltage is taken to be 8 (or 18 db).

Pulse regeneration: The process of replacing each code element by a new element standardized in timing and magnitude.

Pulse modulation *continued*

Pulse rise time: The time required for the instantaneous amplitude to go from 10 percent to 90 percent of the peak value.

Quantization: A process wherein the complete range of instantaneous values of a wave is divided into a finite number of smaller subranges, each of which is represented by an assigned or quantized value within the subranges.

Time gate: A device that gives output only during chosen time intervals.

Quantization distortion: The inherent distortion introduced in the process of quantization. This is sometimes referred to as quantization noise.

Pulse bandwidth

The bandwidth necessary to transmit a video pulse train is determined by the rise and decay times of the pulse. This bandwidth F_v is approximately given by

$$F_v \approx 1/2t_r$$

where t_r is the rise or decay time, whichever is the smaller.

The radio-frequency bandwidth F_R is then

$$F_R \approx 1/t_r$$

for amplitude-keyed radio-frequency carrier. Bandwidth is

$$F_R \approx \frac{1}{t_r}(m+1)$$

for frequency-keyed radio-frequency carrier where m is the index of modulation.

Time-division multiplex

Pulse modulation is commonly used in time-division-multiplex systems. Because of the time space available between the modulated pulses, other pulses corresponding to other signal channels can be inserted if they are

Fig. 10—Time-multiplex train of subcarrier pulses for 8 channels and marker pulse *M* for synchronization of receiver with transmitter.

Pulse modulation *continued*

in frequency synchronism. A multiplex train of pulses is shown in Fig. 10. It is common practice to use a channel or a portion of a channel for synchronization between the transmitter and the receiver. This pulse is shown as *M* in Fig. 10. This synchronizing pulse may be separated from the signal-carrying pulses by giving it some unique characteristic such as modulation at a submultiple of the sampling rate, wider duration, or by using two or more pulses with a fixed spacing.

Signal-to-noise ratio

The signal/noise improvement factors (nif) for the pulse subcarrier are as follows:

Pulse-amplitude modulation: If the minimum bandwidth is used for transmission of pam pulses, the signal/noise ratio at the receiver output is equal to that at the input to the receiver. The improvement factor is therefore unity.

Pulse-position modulation: By the use of wider bandwidths, an improvement in the signal/noise ratio at the receiver output may be obtained. This improvement is similar to that obtained by frequency modulation applied to a continuous-wave carrier. Since ppm is a constant-amplitude method of transmission, amplitude noise variations may be removed by limiting and clipping the pulses in the receiver. An improvement threshold is then established at which the signal/noise power ratio s/n at the receiver output is closely given in decibels by

$$s/n = 18 \text{ db} + (\text{nif})$$

where the noise improvement factor (nif) for pulse-position modulation is given by

$$(\text{nif in db}) = 20 \log_{10} (\delta/t_r)$$

where

δ = peak modulation displacement

t_r = rise time of received pulses

Pulse-code modulation: The output signal/noise ratio is extremely large after the improvement threshold is exceeded. However, because of the random nature of noise peaks, the exact threshold is indeterminate. The output signal/noise ratio in decibels can be closely given in terms of the input power ratio for a binary-pcm system by

$$(\text{decibels output } s/n) \approx 2.2 \times (\text{input } s/n)$$

Pulse modulation *continued*

For N-ary codes of orders greater than 2, the (nif) is less than that for the binary code, and decreases with larger values of N.

The over-all radio-frequency-transmission signal/noise ratio is determined by the product of the transmission and the pulse-subcarrier improvement factors. To calculate the over-all output s/n ratio, the pulse-subcarrier signal/noise ratio is first determined using the radio-frequency modulation-improvement formula. This value of pulse s/n is substituted as the input s/n in the above equations.

Quantization noise

In generating pulse-code modulation, the process of quantization is introduced to enable the transformation of the sampled signal amplitude into a pulse code. This process divides the signal amplitude into a number of discrete levels. Quantization introduces a type of distortion that, because of its random nature, resembles noise. This distortion varies with the number of levels used to quantize the signal. The percent distortion D is given by

$$D = [1/(6)^{1/2}L] \times 100$$

where L is the number of levels on one side of the zero axis.

Cross-talk

An important characteristic of a multiplex system is the interchannel cross-talk. Such cross-talk can be kept to a low value by preventing excessive carryover between channel pulses.

Pulse-amplitude modulation: The cross-talk is directly proportional to the amplitude of the decaying pulse at the time of occurrence of the following channel. If the pulse decays over a time T in an exponential manner, such as might be caused by transmission through a resistance-capacitance network, the cross-talk ratio is then

$$(\text{pam cross-talk ratio}) = \exp(2\pi F_v T)$$

where F_v is measured at the 3-decibel point.

Pulse-position modulation: The cross-talk ratio under the same conditions is

$$(\text{ppm cross-talk ratio}) = \frac{\exp(2\pi F_v T)}{\sinh(2\pi F_v \delta)} \frac{\delta}{t_r}$$

Pulse-code-modulation: Cross-talk between channels in a pcm system will arise if the carryover from the last pulse of a channel does not decay to one-half or less of the amplitude of the pulse at the time of the next channel.

Pulse modulation *continued*

Pulse-modulation spectrums

The approximations $J_n(x) \approx (x/2)^n/n!$ and $\sin x \approx x$ used in Figs. 11 and 12 are valid for small arguments typical of time-division-multiplex equipment. When in doubt, use the exact magnitudes that are listed first.

The following list defines the symbols used in expressing the spectrums of a sampled modulating signal.

A = average amplitude of pulse in peak volts

A_0 = magnitude of the direct-current component in volts

A_c = peak amplitude of radio-frequency carrier component in peak volts

A_{mp} = Peak magnitude of the mth sampling carrier-frequency harmonic component in peak volts

A_{mp+nq} = peak magnitude of the nth upper and lower audio sidebands about the mth sampling carrier-frequency harmonic component in peak volts

A_{nq} = peak magnitude of the nth-modulation-frequency harmonic component in peak volts

A_p = peak magnitude of the sampling carrier-frequency component in peak volts

A_q = peak magnitude of the modulation-frequency component in peak volts

A_v = peak amplitude of the modulating signal or peak excursions from the average pulse amplitude for pulse-amplitude modulation in peak volts

A_ω = peak magnitude of the radio-frequency carrier-frequency component in peak volts

$A_{\omega \pm q}$ = peak magnitude of the audio-frequency sidebands about the radio-frequency carrier-frequency component in peak volts

$A_{\omega \pm mp}$ = peak magnitude of the sampling carrier sidebands about the radio-frequency carrier-frequency component in peak volts

$A_{\omega \pm q \pm mp}$ = peak magnitude of the mth sampling-carrier sidebands about the audio sidebands of the radio-frequency carrier-frequency component in peak volts

$J_n(x)$ = Bessel function of the first kind, of nth order and argument x

m = harmonic order of the sampling carrier p

m_a = degree of amplitude modulation of radio-frequency carrier

Pulse modulation *continued*

Fig. 11—Video-frequency pulse-modulation spectrums.

component	symbol	natural ppm	uniform ppm	natural pdm (pwm)
Direct-current component	A_0	$\frac{A\Delta}{T}$	$\frac{A\Delta}{T}$	$\frac{A\Delta}{T}$
Modulation-frequency component	A_q	$\frac{2A\delta}{T}\sin\frac{q\Delta}{2} \approx \frac{A\Delta\delta q}{T}$	$\frac{4A}{qT}J_1(q\delta)\sin\frac{q\Delta}{2} \approx \frac{A\Delta\delta q}{T}$	$\frac{A\delta}{T}$
nth modulation-frequency harmonic component	A_{nq}	0	$\frac{4A}{nqT}J_n(nq\delta)\sin\frac{nq\Delta}{2} \approx \frac{2A\Delta}{Tn!}\left(\frac{nq\delta}{2}\right)^n$	0
Sampling carrier-frequency component	A_p	$\frac{2A}{\pi}J_0(p\delta)\sin\frac{p\Delta}{2} \approx \frac{2A\Delta}{T}$	$\frac{2A}{\pi}J_0(p\delta)\sin\frac{p\Delta}{2} \approx \frac{2A\Delta}{T}$	$\frac{A}{\pi}\left\lvert 1\underline{/0^\circ} - J_0(p\delta)\underline{/-p\Delta}\right\rvert \approx -\frac{2A}{\pi}\sin\frac{p\Delta}{2} \approx \frac{2A\Delta}{T}$
mth sampling carrier-frequency harmonic component	A_{mp}	$\frac{2A}{m\pi}J_0(mp\delta)\sin\frac{mp\Delta}{2} \approx \frac{2A\Delta}{T}$	$\frac{2A}{m\pi}J_0(mp\delta)\sin\frac{mp\Delta}{2} \approx \frac{2A\Delta}{T}$	$\frac{A}{m\pi}\left\lvert 1-\underline{/0^\circ} - J_0(mp\delta)\underline{/-mp\Delta}\right\rvert \approx \frac{2A}{m\pi}\sin\frac{mp\Delta}{2} \approx \frac{2A\Delta}{T}$
nth upper and lower audio sidebands about the mth sampling carrier-frequency component	$A_{mp\pm nq}$	$\frac{2A}{m\pi}J_n(mp\delta)\sin\left[(mp\pm nq)\frac{\Delta}{2}\right] \approx \frac{A\Delta}{m\pi n!}\left(\frac{mp\delta}{2}\right)^n(mp\pm nq)$	$\frac{2AJ_n[(mp\pm nq)\delta]}{m\pi(1\pm nq/mp)}\sin\left[(mp\pm nq)\frac{\Delta}{2}\right] \approx \frac{2A\Delta}{Tn!}\left(\frac{\delta}{2}\right)^n(mp\pm nq)^n$	$\frac{A}{m\pi}J_n(mp\delta) \approx \frac{A}{m\pi n!}\left(\frac{mp\delta}{2}\right)^n$

uniform pdm (pwm)	flat-topped double-polarity pam	flat-topped single-polarity pam	double-polarity pam or pulsed audio	single-polarity pam or gated audio
$\frac{A\Delta}{T}$	0	$\frac{A\Delta}{T}$	0	$\frac{A\Delta}{T}$
$\frac{2A}{qT} J_1 (q\delta)$ $\approx \frac{A\delta}{T}$	$\frac{2A_v}{qT} \sin \frac{q\Delta}{2}$ $\approx \frac{A_v\Delta}{T}$	$\frac{2A_v}{qT} \sin \frac{q\Delta}{2}$ $\approx \frac{A_v\Delta}{T}$	$\frac{A_v\Delta}{T}$	$\frac{A_v\Delta}{T}$
$\frac{2A}{nqT} J_n (nq\delta)$ $\approx \frac{2A}{qT}\left(\frac{q\delta}{2}\right)^n\left(\frac{n^{n-1}}{n!}\right)$	0	0	0	0
$\frac{A}{\pi}[1 - J_0 (p\delta)]$ ≈ 0	0	$\frac{2A}{\pi} \sin \frac{p\Delta}{2}$ $\approx \frac{2A\Delta}{T}$	0	$\frac{A}{\pi} \sin \frac{p\Delta}{2}$ $\approx \frac{A\Delta}{T}$
$\frac{A}{m\pi}[1 - J_0(mp\delta)]$ ≈ 0	0	$\frac{2A}{m\pi} \sin \frac{mp\Delta}{2}$ $\approx \frac{2A\Delta}{T}$	0	$\frac{A}{m\pi} \sin \frac{mp\Delta}{2}$ $\approx \frac{A\Delta}{T}$
$\frac{2A}{T}\frac{J_n[(mp\pm nq)\delta]}{mp\pm nq}$ $\approx \frac{2A}{T}\left(\frac{\delta}{2}\right)^n \frac{(mp\pm nq)^{n-1}}{n!}$	$\frac{2A_v}{T}\frac{\sin[(mp\pm q)\Delta/2]}{mp\pm q}$ $\approx \frac{A_v\Delta}{T}$	$\frac{2A_v}{T}\frac{\sin[(mp\pm q)\Delta/2]}{mp\pm q}$ $\approx \frac{A_v\Delta}{T}$	$\frac{A_v}{m\pi}\sin\frac{mp\Delta}{2}$ $\approx \frac{A_v\Delta}{T}$	$\frac{A_v}{m\pi}\sin\frac{mp\Delta}{2}$ $\approx \frac{A_v\Delta}{T}$

Pulse modulation *continued*

n = harmonic order of the modulation frequency q

p = angular sampling carrier or repetition frequency in radians/second

q = angular modulation frequency in radians/second

$T = 2\pi/p$ = average interval between samples or repetiton period in seconds

δ = peak excursion or deviation of entire ppm pulse or modulated pdm (or pwm) pulse edge from its average position in seconds

Δ = average pulse duration in seconds

θ_v = arbitrary phase shift of the modulating signal at time $t = 0$ with respect to the sampling pulse in radians

ω = angular radio-frequency carrier frequency in radians/second

Fig. 12—Radio-frequency pulse-modulation spectrums.

component	symbol	simple am	am (suppressed carrier)
Radio-frequency carrier-frequency component	A_ω	$\frac{A_c\Delta}{T}$	0
Audio sidebands about the rf carrier-frequency component	$A_{\omega\pm q}$	$\frac{m_aA_c\Delta}{2T}$	$\frac{m_aA_c\Delta}{2T}$
Sampling-carrier sidebands about rf carrier-frequency component	$A_{\omega\pm mp}$	$\frac{A_c}{m\pi}\sin\frac{mp\Delta}{2} \approx \frac{A_c\Delta}{T}$	0
mth sampling-carrier sidebands about audio sidebands of rf carrier-frequency component	$A_{\omega\pm q\pm mp}$	$\frac{m_aA_c}{2m\pi}\sin\frac{mp\Delta}{2} \approx \frac{m_aA_c\Delta}{2T}$	$\frac{m_aA_c}{2m\pi}\sin\frac{mp\Delta}{2} \approx \frac{m_aA_c\Delta}{2T}$

Transmission lines

General

The formulas and charts of this chapter are for transmission lines operating in the TEM mode.* At the beginning of several of the sections (e.g., "Fundamental quantities," "Voltage and current," "Impedance and admittance," "Reflection coefficient") there are accurate formulas, according to conventional transmission-line theory. These are applicable from the lowest power and communication frequencies, including direct current, up to the frequency where a higher mode begins to appear on the line.

Following the accurate formulas are others that are specially adapted for use in radio-frequency problems. In cases of small attenuation, the terms α^2x^2 and higher powers in the expansion of exp αx, etc., are neglected. Thus, when $\alpha x = (\alpha/\beta)\theta = 0.1$ neper (or about one decibel), the error in the approximate formulas is of the order of one percent.

Much of the information is useful also in connection with special lines, such as those with spiral (helical) inner conductors, which function in a quasi-TEM mode; likewise for microstrip.

It should be observed that Z_0 and Y_0 are complex quantities and the imaginary part cannot be neglected in the accurate formulas, unless preliminary examination of the problem indicates the contrary. Even when attenuation is small, $Z_0 = 1/Y_0$ must often be taken at its complex value, especially when the standing-wave ratio is high. In the first few pages of formulas, the symbol R_0 is used frequently. However, in later charts and special applications, the conventional symbol Z_0 is used where the context indicates that the quadrature component need not be considered for the moment.

Rule of subscripts and sign conventions

The formulas for voltage, impedance, etc., are generally for the quantities at the input terminals of the line in terms of those at the output terminals (Fig. 1). In case it is desired to find the quantities at the output in terms of those at the input, it is simply necessary to interchange the subscripts 1 and 2 in the formulas

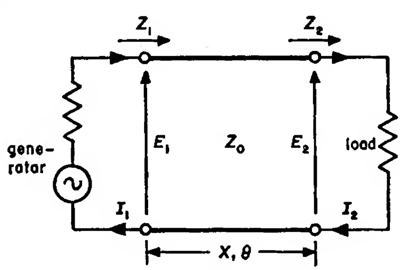

Fig. 1—Transmission line with generator, load.

* The information on pp. 549–583 is valid for single-mode waveguides in general, except for formulas where the symbols R, L, G, or C per unit length are involved.

General *continued*

and to place a minus sign before x or θ. The minus sign may then be cleared through the hyperbolic or circular functions; thus,

$\sinh(-\gamma x) = -\sinh \gamma x$, etc.

Symbols

Voltage and current symbols usually represent the alternating-current complex sinusoid, with magnitude equal to the root-mean-square value of the quantity.

Certain quantities, namely C, c, f, L, T, v, and ω are shown with an optional set of units in parentheses. Either the standard units or the optional units may be used, provided the same set is used throughout.

$A = 10 \log_{10} (1/\eta)$ = dissipation loss in a length of line in decibels

$A_0 = 8.686\alpha x$ = normal or matched-line attenuation of a length of line in decibels.

B_m = susceptive component of Y_m in mhos

C = capacitance of line in farads/unit length (microfarads/unit length)

c = velocity of light in vacuum in units of length/second (units of length/microsecond). See chapter 2

E = voltage (root-mean-square complex sinusoid) in volts

${}_fE$ = voltage of forward wave, traveling toward load

${}_rE$ = voltage of reflected wave

$|E_{\mathrm{flat}}|$ = root-mean-square voltage when standing-wave ratio = 1.0

$|E_{\max}|$ = root-mean-square voltage at crest of standing wave

$|E_{\min}|$ = root-mean-square voltage at trough of standing wave

e = instantaneous voltage

$F_p = G/\omega C$ = power factor of dielectric

f = frequency in cycles/second (megacycles/second)

G = conductance of line in mhos/unit length

G_m = conductive component of Y_m in mhos

Symbols *continued*

$g_a = Y_a/Y_0$ = normalized admittance at voltage standing-wave maximum

$g_b = Y_b/Y_0$ = normalized admittance at voltage standing-wave minimum

I = current (root-mean-square complex sinusoid) in amperes

${}_fI$ = current of forward wave, traveling toward load

${}_rI$ = current of reflected wave

i = instantaneous current

L = inductance of line in henries/unit length (microhenries/unit length)

P = power in watts

R = resistance of line in ohms/unit length

R_m = resistive component of Z_m in ohms

$r_a = Z_a/Z_0$ = normalized impedance at voltage standing-wave maximum

$r_b = Z_b/Z_0$ = normalized impedance at voltage standing-wave minimum

$S = |E_{max}/E_{min}|$ = voltage standing-wave ratio

T = delay of line in seconds/unit length (microseconds/unit length)

v = phase velocity of propagation in units of length/second (units of length/microsecond)

X_m = reactive component of Z_m in ohms

x = distance between points 1 and 2 in units of length (also used for normalized reactance = X/Z_0)

$Y_1 = G_1 + jB_1 = 1/Z_1$ = admittance in mhos looking toward load from point 1

$Y_0 = G_0 + jB_0 = 1/Z_0$ = characteristic admittance of line in mhos

$Z_1 = R_1 + jX_1$ = impedance in ohms looking toward load from point 1

$Z_0 = R_0 + jX_0$ = characteristic impedance of line in ohms

Z_{oc} = input impedance of a line open-circuited at the far end

Z_{sc} = input impedance of a line short-circuited at the far end

α = attenuation constant = nepers/unit length
= $0.1151 \times$ decibels/unit length

Symbols *continued*

β = phase constant in radians/unit length

$\gamma = \alpha + j\beta$ = propagation constant

ϵ = base of natural logarithms = 2.718; or dielectric constant of medium (relative to air), according to context

$\eta = P_2/P_1$ = efficiency (fractional)

$\theta = \beta x$ = electrical length or angle of line in radians

$\theta° = 57.3\theta$ = electrical angle of line in degrees

λ = wavelength in units of length

λ_0 = wavelength in free space

$\rho = |\rho|\underline{/2\psi}$ = voltage reflection coefficient

$\rho_{db} = -20 \log_{10} (1/\rho)$ = voltage reflection coefficient in decibels

ϕ = time phase angle of complex voltage at voltage standing-wave maximum

ψ = half the angle of the reflection coefficient = electrical angle to nearest voltage standing-wave maximum on the generator side

$\omega = 2\pi f$ = angular velocity in radians/second (radians/microsecond)

Fundamental quantities and line parameters

$$dE/dx = (R + j\omega L)I$$

$$d^2E/dx^2 = \gamma^2 E$$

$$dI/dx = (G + j\omega C)E$$

$$d^2I/dx^2 = \gamma^2 I$$

$$\gamma = \alpha + j\beta = \sqrt{(R + j\omega L)(G + j\omega C)}$$

$$= j\omega\sqrt{LC}\sqrt{(1 - jR/\omega L)(1 - jG/\omega C)}$$

$$\alpha = \{\tfrac{1}{2}[\sqrt{(R^2 + \omega^2L^2)(G^2 + \omega^2C^2)} + RG - \omega^2 LC]\}^{\frac{1}{2}}$$

$$\beta = \{\tfrac{1}{2}[\sqrt{(R^2 + \omega^2L^2)(G^2 + \omega^2C^2)} - RG + \omega^2 LC]\}^{\frac{1}{2}}$$

$$Z_0 = \frac{1}{Y_0} = \sqrt{\frac{R + j\omega L}{G + j\omega C}} = \sqrt{\frac{L}{C}} \times \sqrt{\frac{1 - jR/\omega L}{1 - jG/\omega C}} = R_0\left(1 + j\frac{X_0}{R_0}\right)$$

$$Y_0 = 1/Z_0 = G_0\,(1 + j\,B_0/G_0)$$

Fundamental quantities and line parameters *continued*

$$\alpha = \tfrac{1}{2}\,(R/R_0 + G/G_0)$$

$$\beta\, B_0/G_0 = \tfrac{1}{2}\,(R/R_0 - G/G_0)$$

$$R_0 = [M/2(G^2 + \omega^2C^2)]^{1/2}$$

$$G_0 = [M/2(R^2 + \omega^2L^2)]^{1/2}$$

$$B_0/G_0 = -X_0/R_0 = (\omega CR - \omega LG)/M$$

$$\text{where } M = [(R^2 + \omega^2L^2)\,(G^2 + \omega^2C^2)]^{1/2} + RG + \omega^2LC$$

$$1/T = v = f\lambda = \omega/\beta$$

$$\beta = \omega/v = \omega T = 2\pi/\lambda$$

$$\gamma x = \alpha x + j\beta x = \frac{\alpha}{\beta}\,\theta + j\theta$$

$$\theta = \beta x = 2\pi\, x/\lambda = 2\pi\, fTx$$

$$\theta^\circ = 57.3\theta = 360\, x/\lambda = 360\, fTx$$

a. Special case—distortionless line: when $R/L = G/C$, the quantities Z_0 and α are independent of frequency

$$X_0 = 0$$

$$\alpha = R/R_0$$

$$Z_0 = R_0 + j0 = \sqrt{L/C}$$

$$\beta = \omega\sqrt{LC}$$

b. For small attenuation: $R/\omega L$ and $G/\omega C$ are small

$$\gamma = j\omega\sqrt{LC}\left[1 - j\left(\frac{R}{2\omega L} + \frac{G}{2\omega C}\right)\right] = j\beta\left(1 - j\frac{\alpha}{\beta}\right)$$

$$\beta = \omega\sqrt{LC} = \omega L/R_0 = \omega CR_0$$

$$T = 1/v = \sqrt{LC} = R_0C$$

$$\frac{\alpha}{\beta} = \frac{R}{2\omega L} + \frac{G}{2\omega C} = \frac{R}{2\omega L} + \frac{F_p}{2} = \frac{Rv}{2\omega R_0} + \frac{F_p}{2} = \text{attenuation in nepers/radian}$$

$$= \frac{(\text{decibels per 100 feet})\ (\text{wavelength in line, meters})}{1663}$$

Fundamental quantities and line parameters *continued*

$$\alpha = \frac{R}{2}\sqrt{\frac{C}{L}} + \frac{G}{2}\sqrt{\frac{L}{C}} = \frac{R}{2R_0} + \pi\frac{F_p}{\lambda} = \frac{R}{2R_0} + \frac{F_p\beta}{2}$$

where R and G vary with frequency, while L and C are nearly independent of frequency.

$$Z_0 = \frac{1}{Y_0} = \sqrt{\frac{L}{C}}\left[1 - j\left(\frac{R}{2\omega L} - \frac{G}{2\omega C}\right)\right] = R_0\left(1 + j\frac{X_0}{R_0}\right)$$

$$= \frac{1}{G_0(1 + j\,B_0/G_0)} = \frac{1}{G_0}\left(1 - j\frac{B_0}{G_0}\right)$$

$$R_0 = 1/G_0 = \sqrt{L/C}$$

$$\frac{B_0}{G_0} = -\frac{X_0}{R_0} = \frac{R}{2\omega L} - \frac{F_p}{2} = \frac{\alpha}{\beta} - F_p$$

$$X_0 = -\frac{R}{2\omega\sqrt{LC}} + \frac{G}{2\omega C}\sqrt{\frac{L}{C}} = -\frac{R\lambda}{4\pi} + \frac{F_p}{2}\ R_0$$

c. With certain exceptions, the following few equations are for ordinary lines (e.g., not spiral delay lines) with the field totally immersed in a uniform dielectric of dielectric constant ϵ (relative to air). The exceptions are all the quantities not including the symbol ϵ, these being good also for special types such as spiral delay lines, microstrip, etc.

$$L = 1.016\ R_0\sqrt{\epsilon} \times 10^{-3} \text{ microhenries/foot}$$

$$= \tfrac{1}{3}\ R_0\sqrt{\epsilon} \times 10^{-4} \text{ microhenries/centimeter}$$

$$C = 1.016\ \frac{\sqrt{\epsilon}}{R_0} \times 10^{-3} \text{ microfarads/foot}$$

$$= \frac{\sqrt{\epsilon}}{3R_0} \times 10^{-4} \text{ microfarads/centimeter}$$

$v/c = 1016/R_0C' = 1/\sqrt{\epsilon} =$ velocity factor (with capacitance C' in micromicrofarads/foot)

$\lambda = \lambda_0\, v/c = c/f\sqrt{\epsilon} = \lambda_0/\sqrt{\epsilon}$

$T = 1/v = R_0C' \times 10^{-6} = 1.016 \times 10^{-3}/(v/c) = 1.016 \times 10^{-3}\sqrt{\epsilon}$ microseconds/foot (with capacitance C' in micromicrofarads/foot)

The line length is

$x/\lambda = xf\sqrt{\epsilon}/984$ wavelengths

$\theta = 2\pi x/\lambda = xf\sqrt{\epsilon}/156.5$ radians

where xf is the product of feet times megacycles.

Voltage and current

$$E_1 = {}_fE_1 + {}_rE_1 = {}_fE_2\epsilon^{\gamma x} + {}_rE_2\epsilon^{-\gamma x} = E_2\left(\frac{Z_2 + Z_0}{2Z_2}\epsilon^{\gamma x} + \frac{Z_2 - Z_0}{2Z_2}\epsilon^{-\gamma x}\right)$$

$$= \frac{E_2 + I_2Z_0}{2}\epsilon^{\gamma x} + \frac{E_2 - I_2Z_0}{2}\epsilon^{-\gamma x}$$

$$= E_2\,[\cosh \gamma x + (Z_0/Z_2)\sinh \gamma x] = E_2 \cosh \gamma x + I_2Z_0 \sinh \gamma x$$

$$= \frac{E_2}{1 + \rho_2}(\epsilon^{\gamma x} + \rho_2\epsilon^{-\gamma x})$$

$$I_1 = {}_fI_1 + {}_rI_1 = {}_fI_2\epsilon^{\gamma x} + {}_rI_2\epsilon^{-\gamma x} = Y_0({}_fE_2\epsilon^{\gamma x} - {}_rE_2\epsilon^{-\gamma x})$$

$$= I_2\left(\frac{Z_0 + Z_2}{2Z_0}\epsilon^{\gamma x} + \frac{Z_0 - Z_2}{2Z_0}\epsilon^{-\gamma x}\right) = \frac{I_2 + E_2Y_0}{2}\epsilon^{\gamma x} + \frac{I_2 - E_2Y_0}{2}\epsilon^{-\gamma x}$$

$$= I_2\left(\cosh \gamma x + \frac{Z_2}{Z_0}\sinh \gamma x\right)$$

$$= I_2 \cosh \gamma x + E_2Y_0 \sinh \gamma x = \frac{I_2}{1 - \rho_2}(\epsilon^{\gamma x} - \rho_2\epsilon^{-\gamma x})$$

$$E_1 = AE_2 + BI_2$$

$$I_1 = CE_2 + DI_2$$

where the general circuit parameters are

$$A = \cosh \gamma x$$

$$B = Z_0 \sinh \gamma x$$

$$C = Y_0 \sinh \gamma x$$

$$D = \cosh \gamma x$$

See section on "General circuit parameters" in chapter 5, and that on "Matrix algebra" in chapter 37.

a. When point 2 is at a voltage maximum or minimum; x' is measured from voltage maximum and x'' from voltage minimum (similarly for currents):

$$E_1 = E_{\max}\left[\cosh \gamma x' + \frac{1}{S}\sinh \gamma x'\right]$$

$$= E_{\min}\,[\cosh \gamma x'' + S \sinh \gamma x'']$$

$$I_1 = I_{\max}\left[\cosh \gamma x' + \frac{1}{S}\sinh \gamma x'\right]$$

$$= I_{\min}\,[\cosh \gamma x'' + S \sinh \gamma x'']$$

Voltage and current *continued*

When attenuation is neglected:

$$E_1 = E_{\max}\left[\cos\theta' + j\frac{1}{S}\sin\theta'\right]$$
$$= E_{\min}\left[\cos\theta'' + jS\sin\theta''\right]$$

b. Letting Z_l = impedance of load, l = distance from load to point 2, and x_l = distance from load to point 1:

$$E_1 = E_2\frac{\cosh\gamma x_l + (Z_0/Z_l)\sinh\gamma x_l}{\cosh\gamma l + (Z_0/Z_l)\sinh\gamma l}$$

$$I_1 = I_2\frac{\cosh\gamma x_l + (Z_l/Z_0)\sinh\gamma x_l}{\cosh\gamma l + (Z_l/Z_0)\sinh\gamma l}$$

c. $$e_1 = \sqrt{2}\,|_fE_2|\epsilon^{\alpha x}\sin\left(\omega t + 2\pi\frac{x}{\lambda} - \psi_2 + \phi\right) + \sqrt{2}\,|_rE_2|\,\epsilon^{-\alpha x}\sin\left(\omega t - 2\pi\frac{x}{\lambda} + \psi_2 + \phi\right)$$

$$i_1 = \sqrt{2}\,|_fI_2|\,\epsilon^{\alpha x}\sin\left(\omega t + 2\pi\frac{x}{\lambda} - \psi_2 + \phi + \tan^{-1}\frac{B_0}{G_0}\right) + \sqrt{2}\,|_rI_2|\epsilon^{-\alpha x}\sin\left(\omega t - 2\pi\frac{x}{\lambda} + \psi_2 + \phi + \tan^{-1}\frac{B_0}{G_0}\right)$$

d. For small attenuation:

$$E_1 = E_2\left[\left(1 + \frac{Z_0}{Z_2}\alpha x\right)\cos\theta + j\left(\frac{Z_0}{Z_2} + \alpha x\right)\sin\theta\right]$$

$$I_1 = I_2\left[\left(1 + \frac{Z_2}{Z_0}\alpha x\right)\cos\theta + j\left(\frac{Z_2}{Z_0} + \alpha x\right)\sin\theta\right]$$

e. When attenuation is neglected:

$$E_1 = E_2\cos\theta + jI_2Z_0\sin\theta$$
$$= E_2\left[\cos\theta + j(Y_2/Y_0)\sin\theta\right]$$
$$= {}_fE_2\epsilon^{j\theta} + {}_rE_2\epsilon^{-j\theta}$$

Voltage and current *continued*

$$I_1 = I_2 \cos\theta + jE_2Y_0 \sin\theta$$
$$= I_2 [\cos\theta + j(Z_2/Z_0) \sin\theta]$$
$$= Y_0({}_fE_2\epsilon^{j\theta} - {}_rE_2\epsilon^{-j\theta})$$

General circuit parameters (see p. 555) are:

$A = \cos\theta$

$B = jZ_0 \sin\theta$

$C = jY_0 \sin\theta$

$D = \cos\theta$

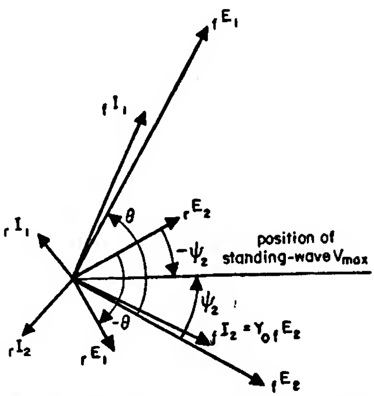

Fig. 2—Diagram of complex voltages and currents at two fixed points on a line with considerable attenuation. (Diagram rotates counterclockwise with time.)

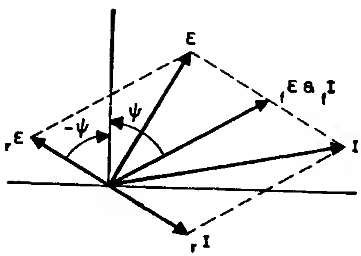

Fig. 3—Voltages and currents at time t = 0 at a point ψ electrical degrees toward the load from a voltage standing-wave maximum.

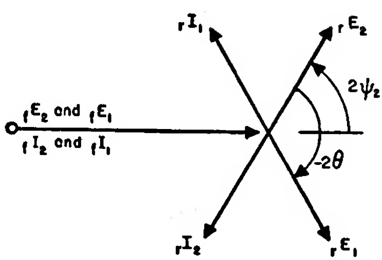

Fig. 4—Abbreviated diagram of a line with zero attenuation.

Impedance and admittance

$$\frac{Z_1}{Z_0} = \frac{Z_2 \cosh \gamma x + Z_0 \sinh \gamma x}{Z_0 \cosh \gamma x + Z_2 \sinh \gamma x}$$

$$\frac{Y_1}{Y_0} = \frac{Y_2 \cosh \gamma x + Y_0 \sinh \gamma x}{Y_0 \cosh \gamma x + Y_2 \sinh \gamma x}$$

a. By interchange of subscripts and change of signs (see p. 549), the load impedance is:

$$\frac{Z_2}{Z_0} = \frac{Z_1 \cosh \gamma x - Z_0 \sinh \gamma x}{Z_0 \cosh \gamma x - Z_1 \sinh \gamma x}$$

b. The input impedance of a line at a position of maximum or minimum voltage has the same phase angle as the characteristic impedance:

$$\frac{Z_1}{Z_0} = \frac{Z_b}{Z_0} = \frac{Y_0}{Y_b} = r_b + j0 = \frac{1}{S} \text{ at a voltage minimum (current maximum).}$$

$$\frac{Y_1}{Y_0} = \frac{Y_a}{Y_0} = \frac{Z_0}{Z_a} = g_a + j0 = \frac{1}{S} \text{ at a voltage maximum (current minimum).}$$

c. When attenuation is small:

$$\frac{Z_1}{Z_0} = \frac{\left(\frac{Z_2}{Z_0} + \alpha x\right) + j\left(1 + \frac{Z_2}{Z_0}\alpha x\right)\tan\theta}{\left(1 + \frac{Z_2}{Z_0}\alpha x\right) + j\left(\frac{Z_2}{Z_0} + \alpha x\right)\tan\theta}$$

For admittances, replace Z_0, Z_1, and Z_2 by Y_0, Y_1, and Y_2, respectively.

When A and B are real:

$$\frac{A \pm jB \tan\theta}{B \pm jA \tan\theta} = \frac{2AB \pm j(B^2 - A^2)\sin 2\theta}{(B^2 + A^2) + (B^2 - A^2)\cos 2\theta}$$

d. When attenuation is neglected:

$$\frac{Z_1}{Z_0} = \frac{Z_2/Z_0 + j\tan\theta}{1 + j(Z_2/Z_0)\tan\theta} = \frac{1 - j(Z_2/Z_0)\cot\theta}{Z_2/Z_0 - j\cot\theta}$$

and similarly for admittances.

e. When attenuation $\alpha x = \theta\alpha/\beta$ is small and standing-wave ratio is large (say > 10):

Impedance and admittance *continued*

For θ measured from a voltage minimum

$$\frac{Z_1}{Z_0} = \left(r_b + \frac{\alpha}{\beta}\theta\right)(1 + \tan^2\theta) + j\tan\theta = \left(r_b + \frac{\alpha}{\beta}\theta\right)\frac{1}{\cos^2\theta} + j\tan\theta$$

(See Note 1)

$$\left.\begin{aligned}\frac{Z_0}{Z_1} = \frac{Y_1}{Y_0} &= \left(r_b + \frac{\alpha}{\beta}\theta\right)(1 + \cot^2\theta) - j\cot\theta \\ &= \left(r_b + \frac{\alpha}{\beta}\theta\right)\frac{1}{\sin^2\theta} - j\cot\theta\end{aligned}\right\}$$

(See Note 2)

For θ measured from a voltage maximum

$$\frac{Z_0}{Z_1} = \frac{Y_1}{Y_0} = \left(g_a + \frac{\alpha}{\beta}\theta\right)(1 + \tan^2\theta) + j\tan\theta$$

(See Note 1)

$$\frac{Z_1}{Z_0} = \left(g_a + \frac{\alpha}{\beta}\theta\right)(1 + \cot^2\theta) - j\cot\theta$$

(See Note 2)

Note 1: Not valid when $\theta \approx \pi/2$, $3\pi/2$, etc., due to approximation in denominator $1 + (r_b + \theta\alpha/\beta)^2\tan^2\theta = 1$ (or with g_a in place of r_b).

Note 2: Not valid when $\theta \approx 0$, π, 2π, etc., due to approximation in denominator $1 + (r_b + \theta\alpha/\beta)^2\cot^2\theta = 1$ (or with g_a in place of r_b). For open- or short-circuited line, valid at $\theta = 0$.

f. When x is an integral multiple of $\lambda/2$ or $\lambda/4$. For $x = n\lambda/2$, or $\theta = n\pi$

$$\frac{Z_1}{Z_0} = \frac{\dfrac{Z_2}{Z_0} + \tanh n\pi\dfrac{\alpha}{\beta}}{1 + \dfrac{Z_2}{Z_0}\tanh n\pi\dfrac{\alpha}{\beta}}$$

For $x = n\lambda/2 + \lambda/4$, or $\theta = (n + \frac{1}{2})\pi$

$$\frac{Z_1}{Z_0} = \frac{1 + \dfrac{Z_2}{Z_0}\tanh(n + \frac{1}{2})\pi\dfrac{\alpha}{\beta}}{\dfrac{Z_2}{Z_0} + \tanh(n + \frac{1}{2})\pi\dfrac{\alpha}{\beta}}$$

g. For small attenuation, with any standing-wave ratio: For $x = n\lambda/2$, or $\theta = n\pi$, where n is an integer

Impedance and admittance *continued*

$$\frac{Z_1}{Z_0} = \frac{\dfrac{Z_2}{Z_0} + n\pi\dfrac{\alpha}{\beta}}{1 + \dfrac{Z_2}{Z_0}n\pi\dfrac{\alpha}{\beta}}$$

$$g_{a1} = \frac{g_{a2} + \alpha n\lambda/2}{1 + g_{a2}\alpha n\lambda/2} = \frac{1}{S_1}$$

For $x = (n + \frac{1}{2})\lambda/2$, or $\theta = (n + \frac{1}{2})\pi$, where n is an integer or zero:

$$\frac{Z_1}{Z_0} = \frac{1 + \dfrac{Z_2}{Z_0}(n + \frac{1}{2})\alpha\dfrac{\lambda}{2}}{\dfrac{Z_2}{Z_0} + (n + \frac{1}{2})\alpha\dfrac{\lambda}{2}}$$

$$g_{b1} = \frac{1 + g_{a2}(n + \frac{1}{2})\dfrac{\alpha}{\beta}\pi}{g_{a2} + (n + \frac{1}{2})\dfrac{\alpha}{\beta}\pi} = S_1$$

Subscript a refers to the voltage-maximum point and b to the voltage minimum. In the above formulas, the subscripts a and b may be interchanged, and/or r may be substituted in place of g, except for the relationships to standing-wave ratio.

Lines open- or short-circuited at the far end

Point 2 is the open- or short-circuited end of the line, from which x and θ are measured.

a. Voltages and currents:

Use formulas of "Voltages and currents" section p. 555 with the following conditions

Open-circuited line: $\rho_2 = 1.00\,\underline{/0^\circ} = 1.00$; ${}_rE_2 = {}_fE_2 = E_2/2$; ${}_rI_2 = -{}_fI_2$; $I_2 = 0$; $Z_2 = \infty$.

Short-circuited line: $\rho_2 = 1.00\,\underline{/180^\circ} = -1.00$; ${}_rE_2 = -{}_fE_2$; $E_2 = 0$; ${}_rI_2 = {}_fI_2 = I_2/2$; $Z_2 = 0$.

Lines open- or short-circuited at the far end *continued*

b. Impedances and admittances·

$Z_{oc} = Z_0 \coth \gamma x$

$Z_{sc} = Z_0 \tanh \gamma x$

$Y_{oc} = Y_0 \tanh \gamma x$

$Y_{sc} = Y_0 \coth \gamma x$

c. For small attenuation:

Use formulas for large (swr) in paragraph e, pp. 558–559, with the following conditions

Open-circuited line: $g_a = 0$

Short-circuited line: $r_b = 0$

d. When attenuation is neglected:

$Z_{oc} = -jR_0 \cot \theta$

$Z_{sc} = jR_0 \tan \theta$

$Y_{oc} = jG_0 \tan \theta$

$Y_{sc} = -jG_0 \cot \theta$

e. Relationships between Z_{oc} and Z_{sc}:

$$\sqrt{Z_{oc}Z_{sc}} = Z_0$$

$$\pm\sqrt{Z_{sc}/Z_{oc}} = \tanh \gamma x \approx \frac{\alpha}{\beta}\theta\,(1 + \tan^2 \theta) + j \tan \theta = \frac{\alpha\theta}{\beta \cos^2 \theta} + j \tan \theta$$

$$\approx j \tan \theta \left[1 - j\frac{\alpha}{\beta}\theta(\tan \theta + \cot \theta)\right] = j \tan \theta \left(1 - j\frac{\alpha}{\beta}\frac{2\theta}{\sin 2\theta}\right)$$

Note: Above approximations not valid for $\theta \approx \pi/2, 3\pi/2$, etc.

$$\pm\sqrt{Z_{oc}/Z_{sc}} = \coth \gamma x \approx \frac{\alpha}{\beta}\theta(1 + \cot^2 \theta) - j \cot \theta = \frac{\alpha\theta}{\beta \sin^2 \theta} - j \cot \theta$$

$$\approx -j \cot \theta \left[1 + j\frac{\alpha}{\beta}\theta(\tan \theta + \cot \theta)\right] = - j \cot \theta \left(1 + j\frac{\alpha}{\beta}\frac{2\theta}{\sin 2\theta}\right)$$

Note: Above approximations not valid for $\theta \approx \pi, 2\pi$, etc.

Lines open- or short-circuited at the far end *continued*

f. When attenuation is small (except for $\theta \approx n\pi/2$, $n = 1, 2, 3 \ldots$):

$$\pm\sqrt{\frac{Z_{sc}}{Z_{oc}}} = \pm\sqrt{\frac{Y_{oc}}{Y_{sc}}} = \pm j\sqrt{-\frac{C_{oc}}{C_{sc}}}\left[1 - j\tfrac{1}{2}\left(\frac{G_{oc}}{\omega C_{oc}} - \frac{G_{sc}}{\omega C_{sc}}\right)\right]$$

Where $Y_{oc} = G_{oc} + j\omega C_{oc}$ and $Y_{sc} = G_{sc} + j\omega C_{sc}$. The $+$ sign is to be used before the radical when C_{oc} is positive, and the $-$ sign when C_{oc} is negative.

g. $R/|X|$ component of input impedance of low-attenuation nonresonant line:

Short-circuited line (except when $\theta \approx \pi/2, 3\pi/2$, etc.)

$$\frac{R_1}{|X_1|} = \frac{G_1}{|B_1|} = \left|\frac{\alpha}{\beta}\,\theta(\tan\theta + \cot\theta) + \frac{B_0}{G_0}\right| = \left|\frac{\alpha}{\beta}\frac{2\theta}{\sin 2\theta} + \frac{B_0}{G_0}\right|$$

Open-circuited line (except when $\theta \approx \pi, 2\pi$, etc.)

$$\frac{R_1}{|X_1|} = \frac{G_1}{|B_1|} = \left|\frac{\alpha}{\beta}\,\theta(\tan\theta + \cot\theta) - \frac{B_0}{G_0}\right| = \left|\frac{\alpha}{\beta}\frac{2\theta}{\sin 2\theta} - \frac{B_0}{G_0}\right|$$

Voltage reflection coefficient and standing-wave ratio

$$\rho = \frac{{}_rE}{{}_fE} = -\frac{{}_rI}{{}_fI} = \frac{Z - Z_0}{Z + Z_0} = \frac{Y_0 - Y}{Y_0 + Y} = |\rho|\,\underline{/2\psi}$$

where ψ is the electrical angle to the nearest voltage maximum on the generator side of point where ρ is measured (Figs. 2, 3, and 4).

$$\rho_1 = \rho_2\epsilon^{-2\alpha x}\,\underline{/-2\theta}$$

$$|\rho_1| = |\rho_2|/10^{A_0/10}$$

Voltage reflection coefficient in decibels

$$\rho_{db} = -20\log_{10}|1/\rho|$$

The minus sign is frequently omitted.

$$|\rho_{db}\text{ at input}| = |\rho_{db}\text{ at load}| + 2A_0$$

These two relationships and standing-wave ratio versus reflection coefficient in decibels are shown in the alignment charts on pages 570–571.

$$Z = \frac{E}{I} = \frac{{}_fE + {}_rE}{{}_fI + {}_rI} = Z_0\frac{1+\rho}{1-\rho}$$

Voltage reflection coefficient and standing-wave ratio *continued*

$$\frac{Z}{Z_0} = \frac{1+\rho}{1-\rho} = \frac{1 + jS \cot \psi}{S + j \cot \psi}$$

$$S = \left|\frac{E_{\max}}{E_{\min}}\right| = \left|\frac{I_{\max}}{I_{\min}}\right| = \left|\frac{|{}_fE| + |{}_rE|}{|{}_fE| - |{}_rE|}\right| = \left|\frac{|{}_fI| + |{}_rI|}{|{}_fI| - |{}_rI|}\right|$$

$$= \frac{1+|\rho|}{1-|\rho|} = r_a = \frac{1}{g_a} = g_b = \frac{1}{r_b}$$

$$|\rho| = \frac{S-1}{S+1}$$

$$1/S_1 = \tanh\,[\alpha x + \tanh^{-1}(1/S_2)]$$

$$= \tanh\,[0.1151\,A_0 + \tanh^{-1}(1/S_2)]$$

a. For high standing-wave ratio. When the ratio is greater than 6/1, and for one-percent accuracy:

$$1/S_1 = 1/S_2 + \alpha x = 1/S_2 + 0.115\,A_0$$

$$|\rho_{\mathrm{db}}| = 17.4/S$$

Subject to the conditions below, the standing-wave ratio is given by one or the other of these equations:

$$S \approx (1 + x^2)/r$$

$$S \approx (1 + b^2)/g$$

where

$$r + jx = Z/Z_0 = (1/R_0)\,[R - (B_0/G_0)\,X + jX]$$

$$g + jb = Y/Y_0 = (1/G_0)\,[G + (B_0/G_0)\,B + jB]$$

Conditions, for one-percent accuracy:

$$r < 0.1\,|x + 1/x| \text{ when } |x| > 0.3$$

$$g < 0.1\,|b + 1/b| \text{ when } |b| > 0.3$$

The boundary of the one-percent-error region can be plotted on the Smith chart by use of the equation (for impedances)

$$|\cot \psi| = 0.1\,S^2/(S^2 - 1)^{1/2}$$

The same boundary line on the chart holds when reading admittances.

Power and efficiency

The net power flowing toward the load is

$$P = |{}_fE|^2 G_0 [1 - |\rho|^2 + 2 |\rho| (B_0/G_0) \sin 2\psi]$$

where $|E|$ is the root-mean-square voltage.

Example: Derive the power formula. By page 151:

$$P = \text{(real) } EI^*$$

When the following expressions are substituted in this equation, the power formula results:

$$E = {}_fE (1 + \rho)$$

$$I = {}_fEY_0 (1 - \rho)$$

$$I^* = {}_fE^*Y_0^* (1 - \rho^*)$$

$$Y_0^* = G_0 (1 - jB_0/G_0)$$

$$\rho = |\rho| \exp j2\psi$$

$$\rho^* = |\rho| \exp - j2\psi$$

a. When the angle B_0/G_0 of the characteristic admittance is negligibly small, the net power flowing toward the load is given by

$$P = G_0(|{}_fE|^2 - |{}_rE|^2) = |{}_fE|^2 G_0(1 - |\rho|^2) = |E_{\max}E_{\min}|/R_0$$

$$P_1 = |{}_fE_2|^2 G_0(\epsilon^{2(\alpha/\beta)\theta} - |\rho_2|^2 \epsilon^{-2(\alpha/\beta)\theta})$$

b. Efficiency, when B_0/G_0 is negligibly small:

$$\eta = \frac{P_2}{P_1} = \frac{1 - |\rho_2|^2}{\epsilon^{2(\alpha/\beta)\theta} - |\rho_2|^2 \epsilon^{-2(\alpha/\beta)\theta}}$$

$$= \frac{1 - |\rho_2|^2}{1 - |\rho_2|^2 \eta_{\max}^2} \eta_{\max} = \frac{1 - |\rho_2|^2}{1 - |\rho_1|^2} \epsilon^{-2\alpha x}$$

$$= \frac{1/|\rho_2| - |\rho_2|}{1/|\rho_1| - |\rho_1|} = \frac{S_1 - 1/S_1}{S_2 - 1/S_2}$$

The maximum error in the above expressions is

$$\pm 100 (S_2 - 1/S_2) B_0/G_0 \text{ percent}$$

$$\pm 4.34 (S_2 - 1/S_2) B_0/G_0 \text{ decibels}$$

Power and efficiency *continued*

When the load matches the line, $\rho_2 = 0$ and the efficiency is accurately

$$\eta_{max} = \exp\left[-2(\alpha/\beta)\theta\right] = \exp(-2\alpha x) = 10^{-A_0/10}$$

$$A - A_0 = 10 \log_{10}(\eta_{max}/\eta)$$

The alignment chart on p. 573 is drawn from the expressions in this paragraph.

c. Efficiency, when swr is high:

$$\eta = \frac{P_2}{P_1} = \frac{R_2}{R_1}\left(\frac{1 + x_1^2}{1 + x_2^2}\right) = \frac{G_2}{G_1}\left(\frac{1 + b_1^2}{1 + b_2^2}\right)$$

$$= \frac{R_2}{R_0^2 G_1}\left(\frac{1 + b_1^2}{1 + x_2^2}\right) = \frac{R_0^2 G_2}{R_1}\left(\frac{1 + x_1^2}{1 + b_2^2}\right)$$

where R is the ohmic resistance while x is the normalized reactance and similarly for G and b. It is important that the R's and G's be computed properly, using formulas in the section on "Transformation of impedance on lines with high swr," page 566. Note the identity of the efficiency formulas with the left-hand terms of the impedance formulas. The conditions for accuracy are the same as stated for the impedance formulas for high standing-wave ratio.

Example: Physical significance of formula for efficiency at high standing-wave ratio: Subject to stated conditions, approximately, $x = \cot\psi$ and $I = I_{max}\sin\psi$. I_{max} = current standing-wave maximum, practically constant along line when standing-wave ratio > 6. Then

$$P = I^2 R = I_{max}^2 R/(1 + x^2)$$

d. Attenuation in nepers $= \frac{1}{2}\log_e \frac{P_1}{P_2} = 0.1151 \times$ (attenuation in decibels)

For a matched line, attenuation $= (\alpha/\beta)\theta = \alpha x$ nepers.

Attenuation in decibels $= 10 \log_{10} \frac{P_1}{P_2} = 8.686 \times$ (attenuation in nepers)

When $2(\alpha/\beta)\theta$ is small,

$$\frac{P_1}{P_2} = 1 + 2\frac{\alpha}{\beta}\theta\frac{1 + |\rho_2|^2}{1 - |\rho_2|^2} \text{ and}$$

$$\text{decibels/wavelength} = 10 \log_{10}\left(1 + 4\pi\frac{\alpha}{\beta}\frac{1 + |\rho_2|^2}{1 - |\rho_2|^2}\right)$$

Power and efficiency *continued*

e. For the same power flowing in a line with standing waves as in a matched, or "flat," line:

$$P = |E_{\text{flat}}|^2/R_0$$

$$|E_{\text{max}}| = |E_{\text{flat}}|\, S^{1/2}$$

$$|E_{\text{min}}| = |E_{\text{flat}}|\, /S^{1/2}$$

$$|{}_fE| = \frac{|E_{\text{flat}}|}{2}\left(S^{1/2} + \frac{1}{S^{1/2}}\right)$$

$$|{}_rE| = \frac{|E_{\text{flat}}|}{2}\left(S^{1/2} - \frac{1}{S^{1/2}}\right)$$

When the loss is small, so that S is nearly constant over the entire length, then per half wavelength

$$\frac{\text{(power loss)}}{\text{(loss for flat line)}} \approx \tfrac{1}{2}\left(S + \frac{1}{S}\right)$$

f. The power dissipation per unit length, for unity standing-wave ratio, is

$$\Delta P_d/\Delta x = 2\,\alpha P$$

$$\frac{\text{(dissipation in watts/foot)}}{\text{(line power in kilowatts)}} = 2.30 \text{ (decibels/100 feet)}$$

where the decibels/100 feet is the normal attenuation for a matched line.

When swr > 1, the dissipation at a current maximum is S times that for swr = 1, assuming the attenuation to be due to conductor loss only. The multiplying factor for local heating reaches a minimum value of $(S + 1/S)/2$ all along the line when conductor loss and dielectric loss are equal.

g. Further considerations on power and efficiency are given in the section, "Mismatch and transducer loss," p. 569.

Transformation of impedance on lines with high swr*

When standing-wave ratio is greater than 10 or 20, resistance cannot be read accurately on the Smith chart, although it is satisfactory for reactance.

* W. W. Macalpine, "Computation of Impedance and Efficiency of Transmission Lines with High Standing-Wave Ratio," *Transactions of the AIEE,* vol. 72, part I, pp. 334-339; July, 1953: also *Electrical Communication,* vol. 30, pp. 238-246; September, 1953.

Transformation of impedance on lines with high swr *continued*

Use the formula:

$$R_1 = R_2 \frac{1 + x_1^2}{1 + x_2^2} + R_0 (1 + x_1^2) \left[\frac{\alpha}{\beta}\theta + \frac{B_0}{G_0}\left(\frac{x_1}{1 + x_1^2} - \frac{x_2}{1 + x_2^2}\right)\right]$$

where R = ohmic resistance

$x = X/R_0$ = normalized reactance.

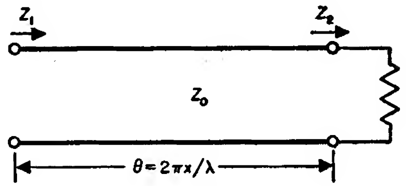

When admittance is given or required, similar formulas can be written with the aid of the following tabulation. The top row shows the terms in the above formula.

R_1	R_2	x_1^2	x_2^2	R_0	x_1	$-x_2$
G_1	G_2	b_1^2	b_2^2	$1/R_0$	$-b_1$	b_2
R_1	$G_2R_0^2$	x_1^2	b_2^2	R_0	x_1	b_2
G_1	R_2/R_0^2	b_1^2	x_2^2	$1/R_0$	$-b_1$	$-x_2$

For transforming R to G or vice versa:

$R = R_0^2\, G|x/b|$

where x and b are read on the Smith chart in the usual manner for transforming impedances to admittances.

The conditions for roughly one-percent accuracy of the formulas are:

Standing-wave ratio greater than 6/1 at input; $|B_0/G_0| < 0.1$; $r + jx$ or $g + jb$ (whichever is used, at each end of line) meet the requirements stipulated in paragraph *a* ("For high standing-wave ratio") on p. 563; and the line parameters and given impedance be known to one-percent accuracy.

The formula for resistance transformation is derived from expressions for high swr in paragraph *a*, just referred to.

Example: A load of $0.4 - j2000$ ohms is fed through a length of RG-17A/U cable at a frequency of 2.0 megacycles. What are the input impedance and the efficiency for a 24-foot length of cable and for a 124-foot length?

Transformation of impedance on lines with high swr *continued*

For RG-17A/U, the attenuation at 2.0 megacycles is 0.095 decibel/100 feet (see chart, p. 614). The dielectric constant $\epsilon = 2.26$ and F_p is negligibly small. Then, by formulas in paragraph b and c, pp. 553 and 554,

$$B_0/G_0 = \alpha/\beta = (\text{db}/100\ \text{ft})\ (\lambda_{\text{meters}})/1663$$
$$= [0.095 \times 150/(2.26)^{1/2}]/1663 = 0.0057$$

$$x/\lambda = xf\epsilon^{1/2}/984 = 24 \times 2.0 \times 1.5/984 = 0.073$$
$$\theta = 2\pi x/\lambda = 0.46 \text{ radian for 24-foot length.}$$

while

$$x/\lambda = 0.38 \text{ and } \theta = 2.4 \text{ for 124-foot length.}$$
$$Z_2/Z_0 \approx (0.4 - j2000)/50 = 0.008 - j40$$

For the 24-foot length, by the Smith chart,

$$x_1 = X_1/Z_0 = -1.9, \text{ or } X_1 = -95 \text{ ohms}$$

The conditions for accuracy of the resistance transformation formula are satisfied. Now,

$$1 + x_1^2 = 1 + (1.9)^2 = 4.6$$
$$1 + x_2^2 = 1 + (40)^2 = 1600$$
$$R_1 = 0.4\ (4.6/1600) + 50 \times 4.6 \times 0.0057\ [0.46 - (1.9/4.6) + (40/1600)]$$
$$= 0.0012 + 0.105 = 0.106 \text{ ohm}$$

The efficiency formula in paragraph c, "When swr is high," p. 565, gives

$$\eta = 0.0012/0.106 = 0.0113, \text{ or } 1.1 \text{ percent}$$

where the 0.0012 figure is taken directly from the first quantity on the right-hand side of the computation of R_1.

Similarly, for the 124-foot length, $x_1 = 1.1$, $X_1 = 55$ ohms, $1 + x_1^2 = 2.21$, $R_1 = 0.00055 + 1.83 = 1.83$ ohms

$$\eta = 0.00055/1.83 = 3.1 \times 10^{-4}, \text{ or } 0.03 \text{ percent}$$

Tabulating the results,

length in feet	input impedance in ohms	efficiency in percent	loss in decibels
24	0.106 − j95	1.1	19.6
124	1.8 + j55	0.03	35

Transformation of impedance on lines with high swr *continued*

The considerably greater loss for 124 feet compared to 24 feet is because the transmission passes through a current maximum where the loss per unit length is much higher than at a current minimum.

Mismatch and transducer loss

On the following pages are formulas and three alignment charts enabling the calculation of attenuation when impedance mismatch exists in a transmission-line system; also change in standing-wave ratio along a line due to attenuation.

One end mismatched

When either generator or load impedance is mismatched to the Z_0 of the line and the other is matched,

$$\text{(mismatch loss)} = \frac{P_m}{P} = \frac{1}{1 - |\rho|^2} = \frac{(S+1)^2}{4S} \quad (1)$$

where

P = power delivered to load

P_m = power that would be delivered were system matched

S = standing-wave ratio of mismatched impedance referred to Z_0

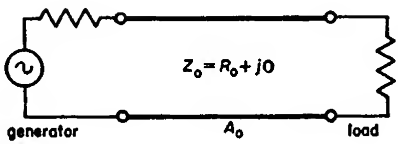

Compared to an ideal transducer (ideal matching network between generator and load):

$$\text{(transducer loss)} = A_0 + 10 \log_{10} (P_m/P) \text{ decibels} \quad (2)$$

where A_0 = normal attenuation of line.

Generator and load mismatched

$|X_0/R_0| \ll 1$

When mismatches exist at both ends of the system:

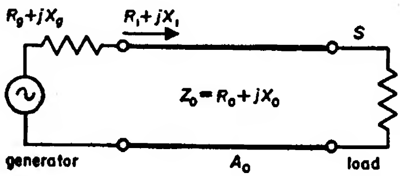

$$\text{(mismatch loss at input)} = \frac{P_m}{P} = \frac{(R_g + R_1)^2 + (X_g + X_1)^2}{4 R_g R_1} \quad (3)$$

$$\text{(transducer loss)} = (A - A_0) + A_0 + 10 \log_{10} (P_m/P) \text{ decibels} \quad (4)$$

Mismatch and transducer loss *continued*

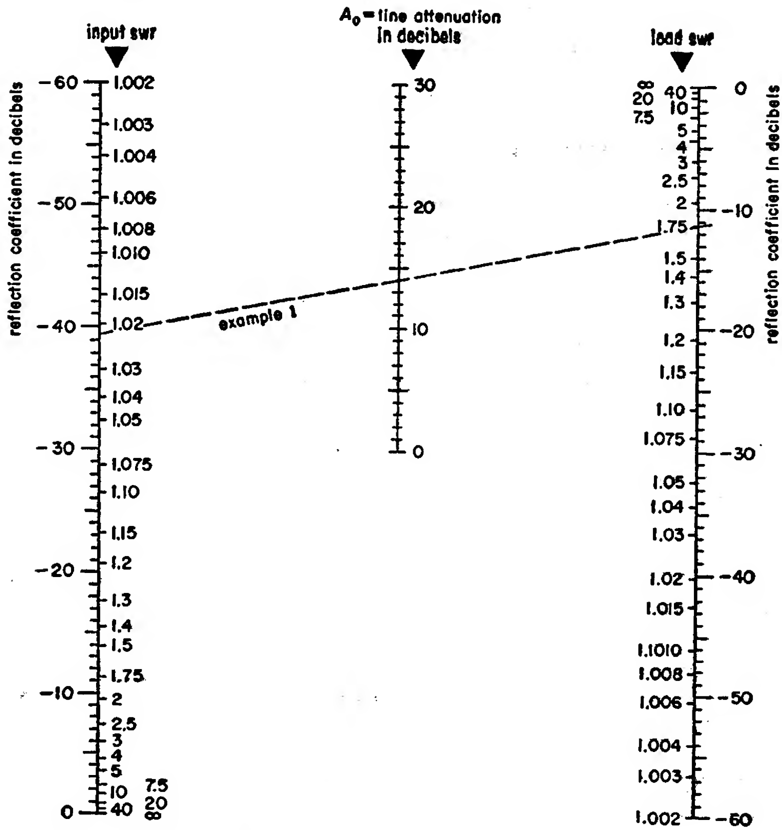

Line attenuation and voltage reflection coefficient for low swr.

where $(A - A_0)$ = standing-wave loss factor obtained from chart on p. 573 for S = standing-wave ratio at load.

Notes on (3):

a. This equation reduces to (1) when X_g and/or X_1 is zero.

b. In (3), the impedances can be either ohmic or normalized with respect to any convenient Z_0.

c. When determining input impedance $R_1 + jX_1$ on Smith chart, adjust radius arm for S at input, determined from that at output by aid of charts on pp. 570 and 571.

Mismatch and transducer loss *continued*

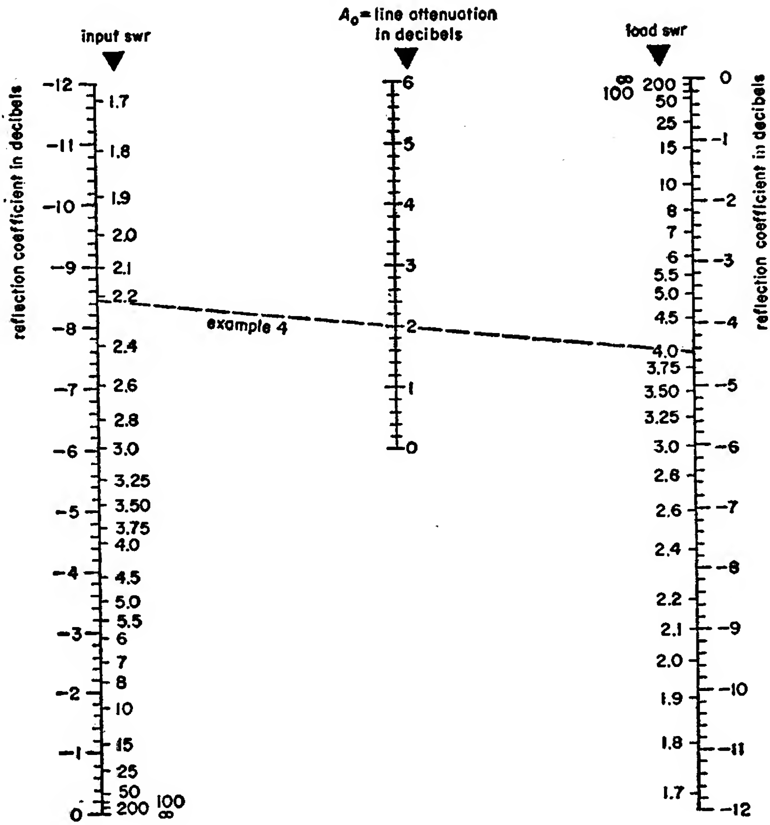

Line attenuation and voltage reflection coefficient for high swr.

d. For junction of two admittances, use (3) with G and B substituted for R and X, respectively.

e. Equation (3) is valid for a junction in any linear passive network. Likewise (1) when at least one of the impedances concerned is purely resistive. Determine S as if one impedance were that of a line.

Examples

Example 1: The swr at the load is 1.75 and the line has an attenuation of 14 decibels. What is the input swr?

Using the alignment chart, p. 570, set a straightedge through the 1.75

Mismatch and transducer loss *continued*

division on the "load swr" scale and the 14-decibel point on the middle scale. Read the answer on the "input swr" scale, which the straightedge intersects at 1.022.

Example 2: Readings on a reflectometer show the reflected wave to be 4.4 decibels below the incident wave. What is the swr?

Using chart, p. 571, locate the reflection coefficient 4.4 (or −4.4) decibels on either outside scale. Beside it, on the same horizontal line, read swr = 4.0+.

Example 3: A 50-ohm line is terminated with a load of $200 + j0$ ohms. The normal attenuation of the line is 2.00 decibels. What is the loss in the line?

Use alignment chart, p. 573. Align a straightedge through the points $A_0 = 2.0$ and swr = 4.0. Read $A - A_0 = 1.27$ decibels on the left-hand scale. Then the transmission loss in the line is:

$A = 1.27 + 2.00 = 3.27$ decibels

This is the dissipation or heat loss as opposed to the mismatch loss at the input, for which see example 4.

Example 4: In the preceding example, suppose the generator impedance is $100 + j0$ ohms, and the line is 5.35 wavelengths long. What is the mismatch loss between the generator and the line?

According to example 3, the load swr = 4.0 and the line attenuation is 2.0 decibels. Then, using chart, p. 571, the input swr is found to be 2.22. On the Smith chart, locate the point corresponding to 0.35 wavelength toward the generator from a voltage maximum, and swr = 2.22. Read the input normalized impedance as $0.62 + j0.53$ with respect to $Z_0 = 50$ ohms. Now the mismatch loss at the input can be determined by use of (3). However, since the generator impedance is nonreactive, (1) can be used, if desired. Refer to notes a and e above and the following paragraph.

With respect to $100 + j0$ ohms, the normalized impedance at the line input is $0.31 + j0.265$ which gives swr = 3.5 according to the Smith chart. Then by (1), $P_m/P = 1.45$, giving a mismatch loss of 1.62 decibels. The transducer loss is found by using the results of examples 3 and 4 in (4). This is

$1.27 + 2.00 + 1.62 = 4.9$ decibels

Mismatch and transducer loss *continued*

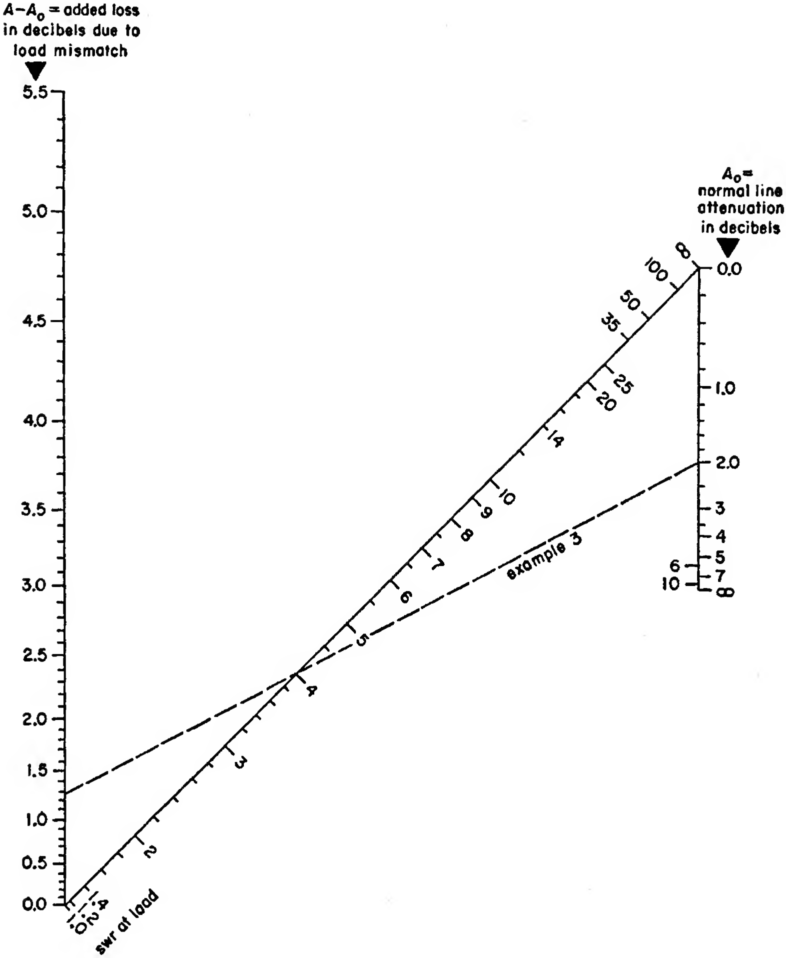

Due to load mismatch, an increase of loss in db as read from this chart must be added to normal line attenuation to give total dissipation loss in line. This does not include mismatch loss due to any difference of line *input* impedance from generator impedance.

Standing-wave loss factor.

Attenuation and resistance of transmission lines at ultra-high frequencies

The normal or matched-line attenuation in decibels/100 feet is:

$A_{100} = 4.34\ R_t/Z_0 + 2.78\ f\ \epsilon^{1/2}\ F_p$

where the total line resistance/100 feet (for perfect surface conditions of the conductors) is, for copper coaxial line,

$R_t = 0.1\ (1/d + 1/D)\ f^{1/2}$

and for copper two-wire open line,

$= (0.2/d)\ f^{1/2}$

where

D = diameter of inner surface of outer coaxial conductor in inches

d = diameter of conductors (coaxial-line center conductor) in inches

f = frequency in megacycles/second

ϵ = dielectric constant relative to air

F_p = power factor of dielectric at frequency f.

For other conductor materials, the resistance of conductor of diameter d (and similarly for D) is

$0.1\ (1/d)\ (f\mu_r\rho/\rho_{cu})^{1/2}$ ohms/100 feet

See the section on "Skin effect," p. 131.

Resonant lines

Symbols

f_0 = resonance frequency in megacycles

G_a = conductance load in mhos at voltage standing-wave maximum, equivalent to some or all of the actual loads

k = coefficient of coupling

n = integral number of quarter wavelengths

$p = k^2\ Q_{1s}\ Q_{2s}$ = load transfer coefficient or matching factor

P_c = power converted into heat in resonator

P_m = power capability of generator in watts

Resonant lines *continued*

P_x = power transferred when load is directly connected to generator (for single resonators); or an analogous hypothetical power (for two coupled resonators)

Q = figure of merit of a resonator as it exists, whether loaded or unloaded

Q_d = doubly loaded Q (all loads being included)

Q_s = singly loaded Q (all loads included except one). For a pair of coupled resonators, Q_{1s} is the value for the first resonator when isolated from the other. (Similarly for Q_{2s})

Q_u = unloaded Q

R_b = resistance load in ohms at voltage standing-wave minimum, equivalent to some or all of the actual loads

R_u = resistance similar to R_b except for unloaded resonator

R_1 = generator resistance, referred to short-circuited end

R_2 = load resistance

S_x = R_1/R_2 or R_2/R_1 = mismatch factor between generator and load

Z_{10} = characteristic impedance of the first of a pair of resonators

θ_1 = electrical angle from a voltage standing-wave minimum point

a. Q of a resonator (electrical, mechanical or any other) is:

$$Q = 2\pi \frac{\text{(energy stored)}}{\text{(energy dissipated per cycle)}}$$

$$= 2\pi f \frac{\text{(energy stored)}}{\text{(power dissipation)}}$$

In a freely oscillating system, the amplitude decays exponentially:

$$I = I_0 \exp\,(-\pi f t/Q)$$

b. Unloaded Q of a resonant line:

$$Q_u = \beta/2\alpha$$

the line length being n quarter-wavelengths, where n is a small integer. The losses in the line are equivalent to those in a hypothetical resistor at the short-circuited end (p. 558, paragraph e):

$$R_u = n\pi Z_0/4Q_u$$

Resonant lines *continued*

c. Loaded Q of a resonant line (Fig. 5)

$$\frac{1}{Q} = \frac{1}{Q_u} + \frac{4R_b}{n\pi Z_0} + \frac{4G_a}{n\pi Y_0}$$

$$= (4/n\pi Z_0)\ (R_u + R_b + G_a/Y_0^2)$$

All external loads can be referred to one end and represented by either R_b or G_a as on Fig. 6.

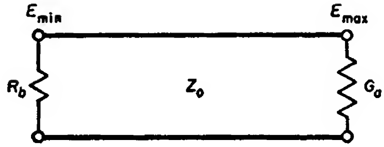

Fig. 5—Quarter-wave line with loadings at nominal short-circuit and open-circuit points.

The total loading is the sum of all the individual loadings.

General conditions:

$R_b/Z_0 = G_a/Y_0 \ll 1.0$
or, roughly, $Q > 5$

d. Input admittance and impedance:

The converse of the equations for Fig. 6 can be used at the resonance frequency. Then R or G is the input impedance or admittance, while

$R_b = n\pi Z_0/4Q_s$

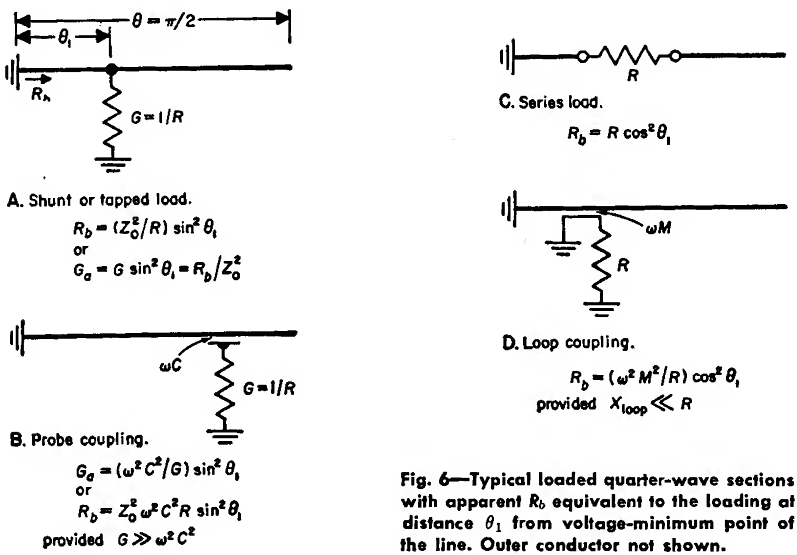

Fig. 6—Typical loaded quarter-wave sections with apparent R_b equivalent to the loading at distance θ_1 from voltage-minimum point of the line. Outer conductor not shown.

Resonant lines *continued*

where Q_s = singly loaded Q with the losses and all the loads considered except that at the terminals where input *R* or G is being measured.

In the vicinity of the resonance frequency, the input admittance when looking into a line at a tap point θ_1 in Fig. 7 is approximately

$$Y = G + jB = \frac{n\pi Y_0}{4 \sin^2 \theta_1}\left(\frac{1}{Q_s} + j2\frac{f - f_0}{f_0}\right)$$

Provided

$$|f - f_0|/f_0 \ll 1.0$$

and

$$\left|\theta \frac{f - f_0}{f_0} \cot \theta_1\right| \ll 1.0$$

where $\theta = n\pi/2$ = length of line at f_0. It is not valid when $\theta_1 \approx 0, \pi, 2\pi$, etc., except that it is good near the short-circuited end when $f - f_0 \approx 0$.

Such a resonant line is approximately equivalent to a lumped *LCG* parallel circuit, where

$$\omega_0{}^2L_1C_1 = (2\pi f_0)^2L_1C_1 = 1$$

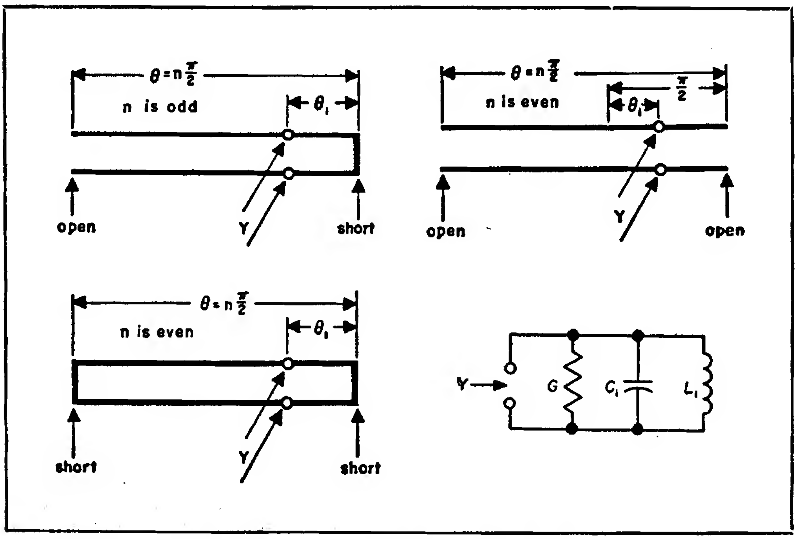

Fig. 7—Resonant transmission lines and their equivalent lumped circuit.

Resonant lines *continued*

Admittance of the equivalent circuit is

$$Y = G + j\left(\omega C_1 - \frac{1}{\omega L_1}\right)$$

$$\approx \omega_0 C_1 \left(\frac{1}{Q_s} + j2\,\frac{f - f_0}{f_0}\right)$$

Then, subject to the conditions stated above,

$$L_1 = \frac{4 \sin^2 \theta_1}{n\pi\omega_0 Y_0}$$

$$C_1 = \frac{n\pi Y_0}{4\omega_0 \sin^2 \theta_1} = \frac{nY_0}{8f_0 \sin^2 \theta_1}$$

$$G = \frac{n\pi Y_0}{4Q_s \sin^2 \theta_1}$$

$$Q_s = \frac{\omega_0 C_1}{G} = \frac{1}{\omega_0 L_1 G}$$

Similarly, the input impedance at a point in series with the line (Fig. 6C and D) is

$$Z = R + jX = \frac{n\pi Z_0}{4 \cos^2\theta_1}\left(\frac{1}{Q_s} + j2\,\frac{f - f_0}{f_0}\right)$$

Provided

$$|f - f_0|/f_0 \ll 1.0$$

and

$$\left|\theta\,\frac{f - f_0}{f_0}\tan\theta_1\right| \ll 1.0$$

It is not valid when $\theta_1 \approx \pi/2, 3\pi/2$, etc.

The voltage standing-wave ratio at resonance, on the generator (Fig. 8) is

$$S = \frac{R_2 + R_u}{R_1} = \frac{(R_2/R_1)\,Q_u + Q_d}{Q_u - Q_d}$$

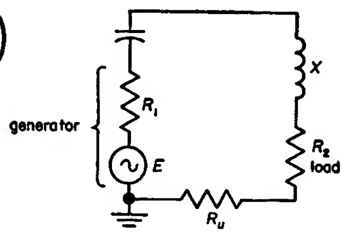

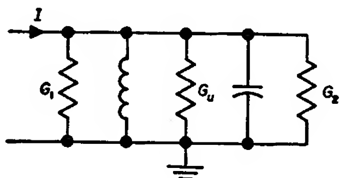

Fig. 8—Equivalent circuits of a resonant line (or a lumped tuned circuit) as seen at the short-circuited and open-circuited ends. All the power equations are good for either lumped or distributed parameters.

Resonant lines *continued*

When $R_1 = R_2$,

$$S = \frac{1 + Q_d/Q_u}{1 - Q_d/Q_u}$$

$$\rho = Q_d/Q_u$$

e. Insertion loss (Fig. 8)

At resonance, for either a distributed or a lumped-constant device:

$$\begin{aligned}
\text{(dissipation loss)} &= 10 \log_{10} (P_x/P_{\text{out}}) \\
&= 20 \log_{10} [1/(1 - Q_d/Q_u)] \\
&\approx 20 \log_{10} (1 + Q_d/Q_u) \\
&\approx 8.7\, Q_d/Q_u \text{ decibels} \\
\text{(mismatch loss)} &= 10 \log_{10} (P_m/P_x) \\
&= 10 \log_{10} [(1 + S_x)^2/4S_x] \text{ decibels}
\end{aligned}$$

The dissipation loss also includes a small additional mismatch loss due to the presence of the resonator. The error in the form $20 \log_{10} (1 + Q_d/Q_u)$ is about twice that of the form $8.7\, Q_d/Q_u$. The last expression $(8.7\, Q_d/Q_u)$ is in error compared to the first, $20 \log_{10} [1/(1 - Q_d/Q_u)]$, by roughly $-50\, (Q_d/Q_u)$ percent for $(Q_d/Q_u) < 0.2$.

The *selectivity* is given on page 242, where $Q = Q_d$. That equation is accurate over a smaller range of $(f - f_0)$ for a resonant line than it is for a single tuned circuit.

At resonance:

$$\frac{P_{\text{in}}}{P_{\text{out}}} = \frac{Q_u + (R_1/R_2)\, Q_d}{Q_u - Q_d}$$

The maximum power transfer, for fixed Q_u, Q_d and Z_0 occurs when $R_1 = R_2$. Then

$$P_{\text{in}}/P_{\text{out}} = (Q_u + Q_d)/(Q_u - Q_d)$$

$$P_{\text{out}}/P_m = (1 - Q_d/Q_u)^2$$

$$P_{\text{in}}/P_m = 1 - (Q_d/Q_u)^2$$

When the generator R_1 or G_1 is negligibly small (then $Q = Q_s = Q_d$):

$$(P_{\text{in}}/P_{\text{out}})_s = Q_u/(Q_u - Q)$$

Resonant lines *continued*

f. Power dissipation ($= P_c$).

$$\frac{P_c}{P_m} = \frac{4\,(Q_d/Q_u)\,(1 - Q_d/Q_u)}{1 + R_2/R_1}$$

For matched input and output ($R_1 = R_2$):

$$P_c/P_m = 2\,(Q_d/Q_u)\,(1 - Q_d/Q_u)$$

$$\approx 2\,Q_d/Q_u \text{ (for } Q_d \ll Q_u)$$

$$P_c/P_{\text{out}} = 2\,Q_d/(Q_u - Q_d)$$

$$P_c/P_{\text{in}} = 2\,Q_d/(Q_u + Q_d)$$

When the generator R_1 or G_1 is negligibly small:

$$(P_c/P_{\text{out}})_s = Q/(Q_u - Q)$$

g. Voltage and current

At the current-maximum point of an n-quarter-wavelength resonant line:

$$I_{sc} = 4\left[\frac{P_m Q_d\,(1 - Q_d/Q_u)}{(1 + R_2/R_1)\,n\pi Z_0}\right]^{1/2} \text{ root-mean-square amperes}$$

$$I = I_{sc} \cos \theta_1$$

and

$$E = Z_0 I_{sc} \sin \theta_1$$

The voltage and current are in quadrature time phase.

When $R_1 = R_2$ and $Q_d \ll Q_u$ and $n = 1$:

$$I_{sc} \approx (8\,P_m Q_d/\pi Z_0)^{1/2}$$

In a lumped-constant tuned circuit:

$$I = 2\left[\frac{P_m Q_d\,(1 - Q_d/Q_u)}{(1 + R_2/R_1)\,X}\right]^{1/2}$$

h. Pair of coupled resonators (Fig. 9):

With inductive coupling near the short-circuited end of a pair of quarter-wave resonant lines:

$$k = (4/\pi)\,\omega M/(Z_{10} Z_{20})^{1/2}$$

Resonant lines *continued*

For coupling through a lossless quarter-wavelength line, inductively coupled near the short-circuited ends of the resonators (Fig. 9D):

$$k = \frac{4\omega^2 M_1 M_2}{\pi Z_0 \, (Z_{10} \, Z_{20})^{1/2}}$$

Probe coupling near top (Fig. 9C):

$$k = (4/\pi)\ \omega C_{12}\ (Z_{10} Z_{20})^{1/2} \sin\theta_1 \sin\theta_2$$

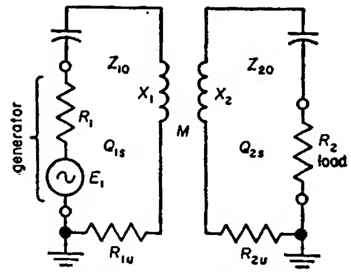

A. Equivalent circuit with resistances as seen at the short-circuited end.

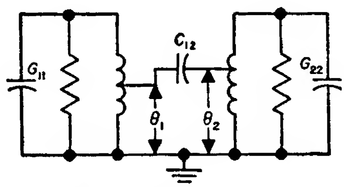

C. Probe-coupled resonators.

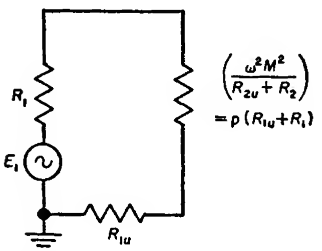

B. Equivalent circuit of first resonator at resonance frequency.

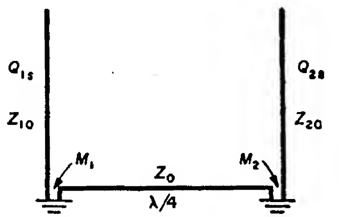

D. Quarter-wavelength line coupling.

Fig. 9—Two coupled resonators.

For lumped-constant coupled circuits, p and k are defined on pp. 236 and 242. In either lumped or distributed resonators:

$$\begin{aligned}
\text{(dissipation loss)} &= 10 \log_{10} (P_x/P_{\text{out}}) \\
&= 10 \log_{10} [1/(1 - Q_{1s}/Q_{1u})\ (1 - Q_{2s}/Q_{2u})] \\
&\approx 20 \log_{10} [1/(1 - Q_s/Q_u)] \\
&\approx 20 \log_{10} (1 + Q_s/Q_u) \\
&\approx 8.7\ Q_s/Q_u \text{ decibels}
\end{aligned}$$

where $Q_s/Q_u = [(Q_{1s}/Q_{1u})\ (Q_{2s}/Q_{2u})]^{1/2}$

Resonant lines *continued*

provided (Q_{1s}/Q_{1u}) and (Q_{2s}/Q_{2u}) do not differ by a ratio of more than 4 to 1, and neither exceeds 0.2.

$$(\text{mismatch loss at } f_0) = 10 \log_{10} (P_m/P_x) = 10 \log_{10} [(1 + p)^2/4p] \text{ decibels}$$

Equations and curves for *selectivity* are given on pp. 242, 243, and 245, where $Q = Q_s$.

At the peaks, when $p \geqslant 1$, the *mismatch loss* is zero, except for some that is included in the *dissipation loss*.

Input voltage standing-wave ratio at f_0 for equal or unequal resonators:

$$S = \frac{p + Q_{1s}/Q_{1u}}{1 - Q_{1s}/Q_{1u}}$$

At the peak frequencies $(p \geqslant 1)$ for equal or nearly equal resonators:

$$S = \frac{1 + Q_{1s}/Q_{1u}}{1 - Q_{1s}/Q_{1u}}$$

Similarly at the output, using subscript 2 instead of 1.

When the resonators are isolated, each one presents to the generator or load an swr of

$$S = (Q_u/Q_s) - 1$$

The power dissipation in either lumped or distributed (quarter-wave) devices, where the two resonators are not necessarily identical, but $Q_s \ll Q_u$ is:

$$P_{1c} = I_{1sc}{}^2 R_{1u} = [4/(1 + p)^2]\, P_m Q_{1s}/Q_{1u}$$

$$P_{2c} = [4p/(1 + p)^2]\, P_m Q_{2s}/Q_{2u}$$

These equations and those below for the currents assume that P_m is concentrated at f_0.

The currents in quarter-wave resonant lines, when $Q_s \ll Q_u$:

$$I_{1sc} = [4/(1 + p)]\, (P_m Q_{1s}/\pi Z_{10})^{1/2}$$

$$I_{2sc}/I_{1sc} = (p Z_{10} Q_{2s}/Z_{20} Q_{1s})^{1/2}$$

Similarly, for a pair of tuned circuits at resonance, when $Q_s \ll Q_u$:

$$I_1 = [2/(1 + p)]\, (P_m Q_{1s}/X_1)^{1/2}$$

$$I_2/I_1 = (p X_1 Q_{2s}/X_2 Q_{1s})^{1/2}$$

Quarter-wave matching sections

The accompanying figures show how voltage-reflection coefficient or standing-wave ratio (swr) vary with frequency f when quarter-wave matching lines are inserted between a line of characteristic impedance Z_0 and a load of resistance R. f_0 is the frequency for which the matching sections are exactly one-quarter wavelength ($\lambda/4$) long.

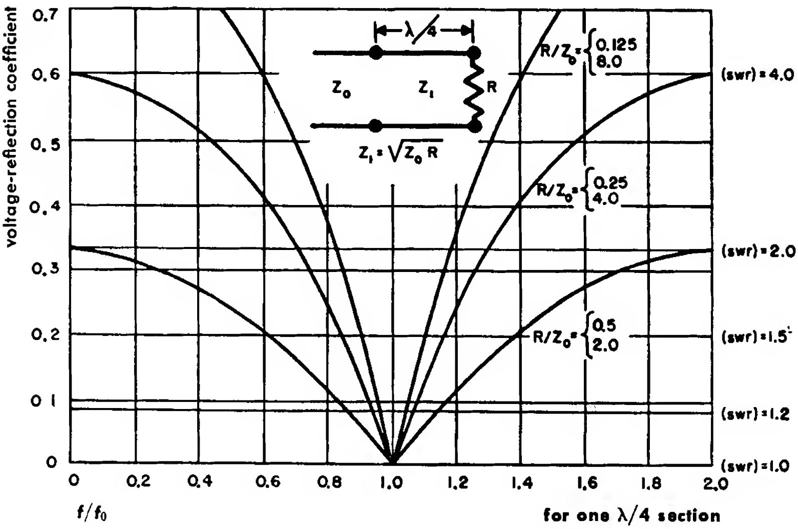

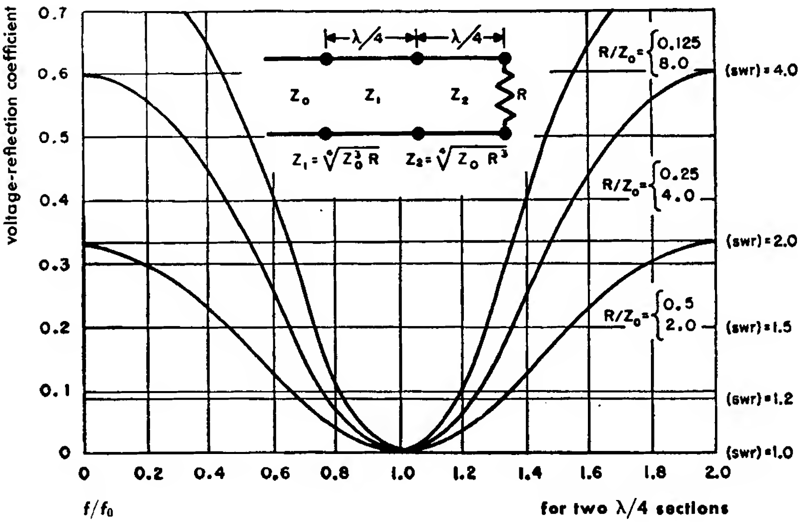

Impedance matching with shorted stub

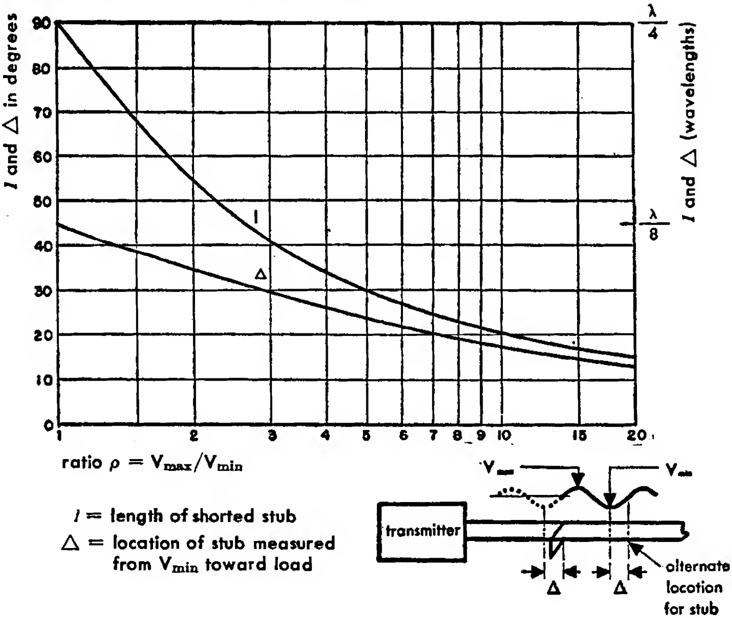

l = length of shorted stub

Δ = location of stub measured from V_{min} toward load

Impedance matching with open stub

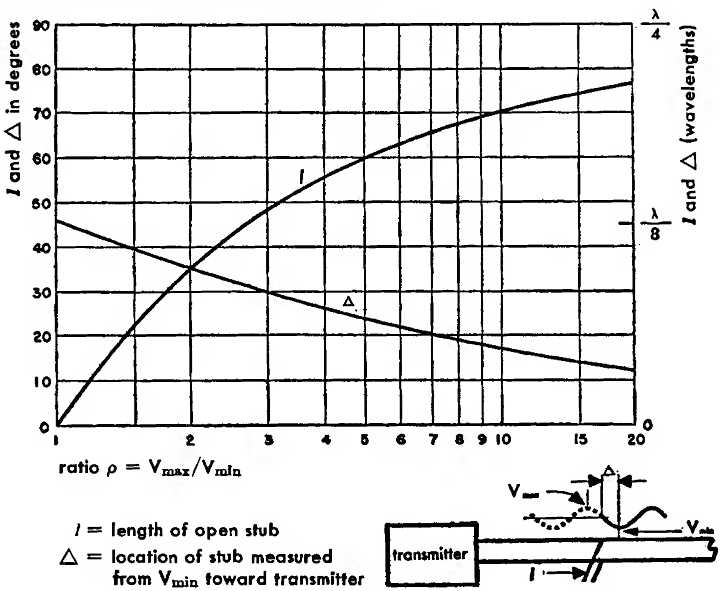

l = length of open stub

Δ = location of stub measured from V_{min} toward transmitter

Length of transmission line

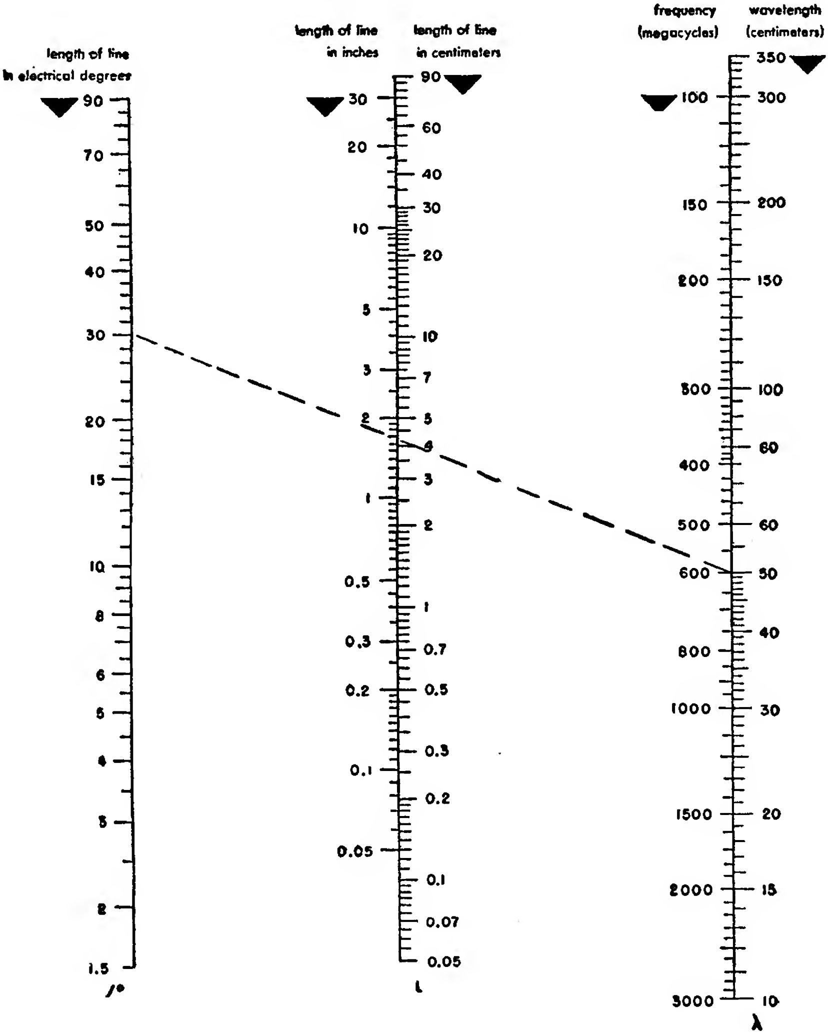

This chart gives the actual length of line in centimeters and inches when given the length in electrical degrees and the frequency, provided the velocity of propagation on the transmission line is equal to that in free space. The length is given on the L-scale intersection by a line between λ and $l°$, where $l° = \dfrac{360\ L \text{ in centimeters}}{\lambda \text{ in centimeters}}$

Example: $f = 600$ megacycles, $l° = 30$, Length $L = 1.64$ inches or 4.2 centimeters.

Measurement of impedance with slotted line

Symbols

Z_0 = characteristic impedance of line

Z = impedance of load (the unknown)

Z_1 = impedance at first V_{min}

k = velocity factor

= (velocity on line)/(velocity in free space)

λ = wavelength on line

χ = distance from load to first V_{min}

(swr) = V_{max}/V_{min}

$\theta° = 180 \dfrac{\chi}{\lambda/2} = 0.0120\, f\chi/k$

where f is in megacycles and χ in centimeters.

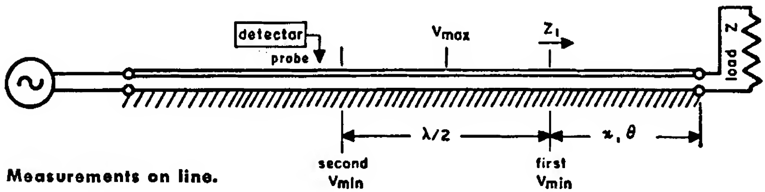

Measurements on line.

Procedure

Measure $\lambda/2$, χ, V_{max}, and V_{min}

Determine

$Z_1/Z_0 = 1/(\text{swr}) = V_{min}/V_{max}$

(wavelengths toward load) $= \chi/\lambda = 0.5\chi/(\lambda/2)$

Then Z/Z_0 may be found on an impedance chart. For example, suppose

$V_{min}/V_{max} = 0.60$ and $\chi/\lambda = 0.40$

Refer to the chart, such as the Smith chart reproduced in part here. Lay off with slider or dividers the distance on the vertical axis from the center point (marked 1.0) to 0.60. Pass around the circumference of the chart in a counterclockwise direction from the starting point 0 to the position 0.40, toward the load. Read off the resistance and reactance components of the normalized load impedance Z/Z_0 at the point of the dividers. Then it is found that

$Z = Z_0(0.77 + j0.39)$

Similarly, there may be found the admittance of the load. Determine

$Y_1/Y_0 = V_{max}/V_{min} = 1.67$

Measurement of impedance with slotted line *continued*

in the above example. Now pass around the chart counterclockwise through $\chi/\lambda = 0.40$, starting at 0.25 and ending at 0.15. Read off the components of the normalized admittance.

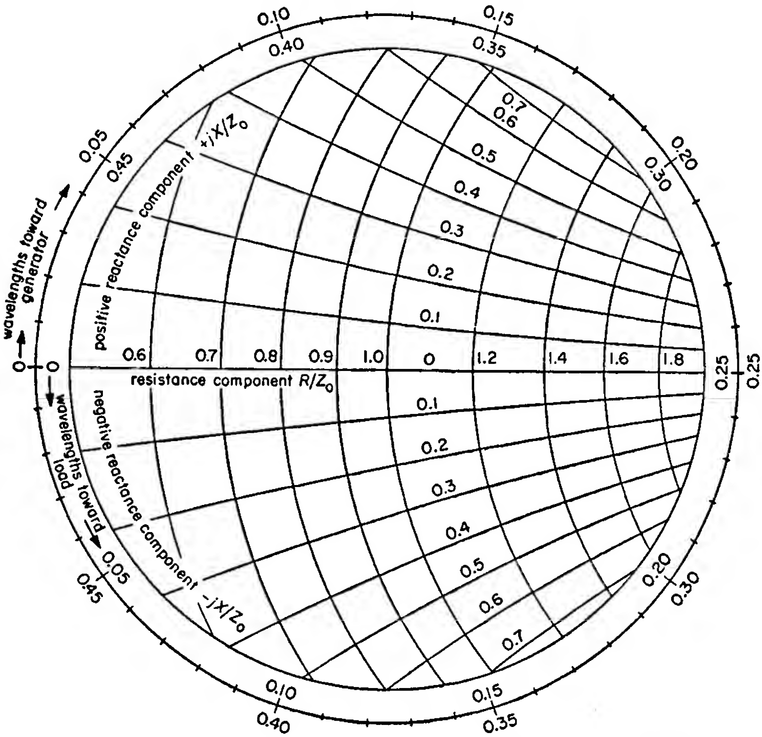

Smith chart—center portion.

$$Y = \frac{1}{Z} = \frac{1}{Z_0}(1.03 - j0.53)$$

Alternatively, these results may be computed as follows:

$$Z = R_s + jX_s = Z_0 \frac{1 - j(\text{swr}) \tan\theta}{(\text{swr}) - j\tan\theta} = Z_0 \frac{2(\text{swr}) - j[(\text{swr})^2 - 1]\sin 2\theta}{[(\text{swr})^2 + 1] + [(\text{swr})^2 - 1]\cos 2\theta}$$

$$Y = G + jB = \frac{1}{Z} = \frac{1}{R_p} - j\frac{1}{X_p} = Y_0 \frac{2(\text{swr}) + j[(\text{swr})^2 - 1]\sin 2\theta}{[(\text{swr})^2 + 1] - [(\text{swr})^2 - 1]\cos 2\theta}$$

where R_s and X_s are the series components of Z, while R_p and X_p are the parallel components.

Characteristic impedance of lines

0 to 220 ohms

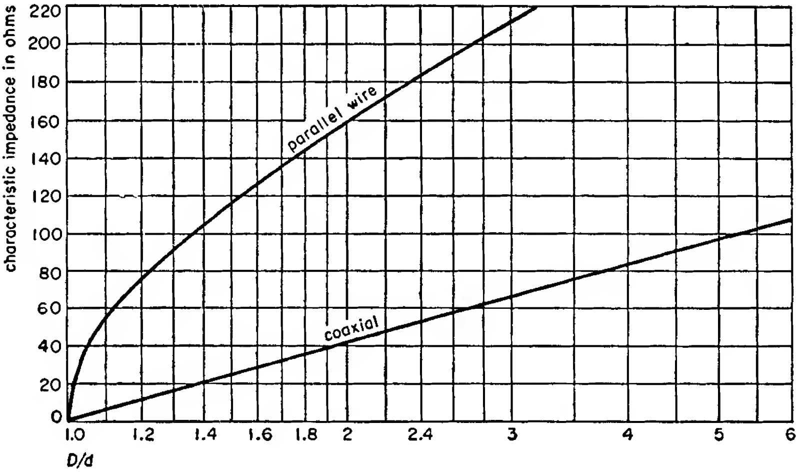

0 to 700 ohms

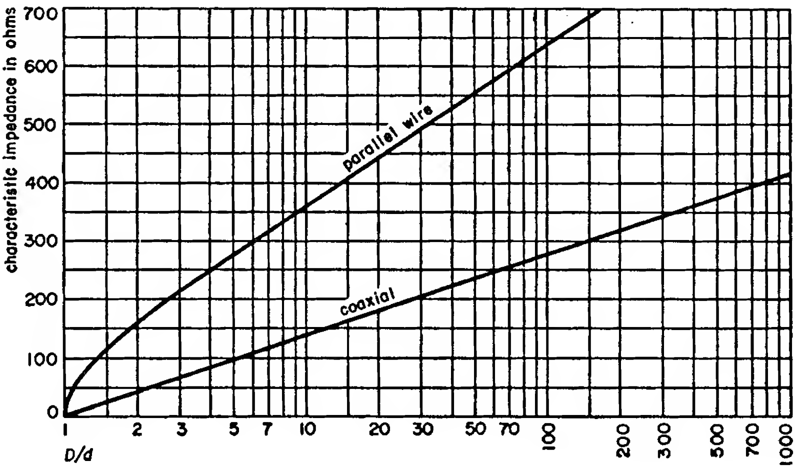

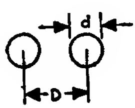

$Z_0 = 120 \cosh^{-1} \dfrac{D}{d}$

For $D \gg d$

$Z_0 \approx 276 \log_{10} \dfrac{2D}{d}$

parallel wires in air

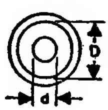

$Z_0 = \dfrac{138}{\sqrt{\epsilon}} \log_{10} \dfrac{D}{d}$

Curve is for $\epsilon = 1.00$

coaxial

Characteristic impedance of lines *continued*

type of line	characteristic impedance
A. Single coaxial line 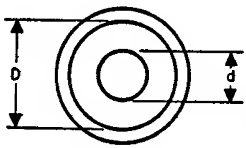 	$Z_0 = \frac{138}{\sqrt{\epsilon}} \log_{10} \frac{D}{d}$ $= \frac{60}{\sqrt{\epsilon}} \log_e \frac{D}{d}$ ϵ = dielectric constant = 1 in air
B. Balanced shielded line 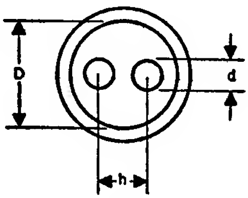 	For $D \gg d$, $h \gg d$, $Z_0 = \frac{276}{\sqrt{\epsilon}} \log_{10} \left[2v \frac{1-\sigma^2}{1+\sigma^2}\right]$ $= \frac{120}{\sqrt{\epsilon}} \log_e \left[2v \frac{1-\sigma^2}{1+\sigma^2}\right]$ $v = \frac{h}{d}$ $\quad\sigma = \frac{h}{D}$
C. Beads—dielectric ϵ_1 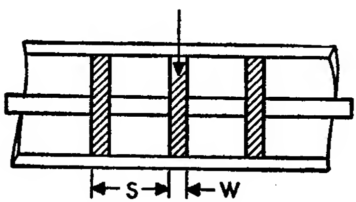 	For cases (A) and (B), if insulating beads are used at frequent intervals—call new characteristic impedance Z_0' $Z_0' = \frac{Z_0}{\sqrt{1 + \left(\frac{\epsilon_1}{\epsilon} - 1\right)\frac{W}{S}}}$ $W \ll S \ll \lambda/4$
D. Open two-wire line in air 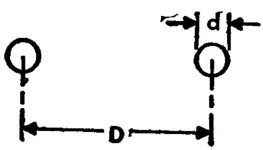 	$Z_0 = 120 \cosh^{-1} \frac{D}{d}$ $\approx 276 \log_{10} \frac{2D}{d}$ $\approx 120 \log_e \frac{2D}{d}$

Characteristic impedance of lines *continued*

type of line	characteristic impedance
E. Wires in parallel, near ground 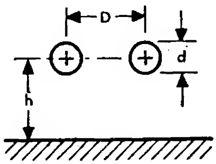	For $d \ll D, h,$ $Z_0 = \frac{69}{\sqrt{\epsilon}} \log_{10} \left[\frac{4h}{d} \sqrt{1 + \left(\frac{2h}{D} \right)^2} \right]$
F. Balanced, near ground 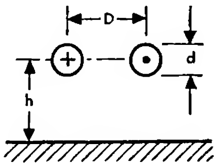	For $d \ll D, h,$ $Z_0 = \frac{276}{\sqrt{\epsilon}} \log_{10} \left[\frac{2D}{d} \frac{1}{\sqrt{1 + (D/2h)^2}} \right]$
G. Single wire, near ground 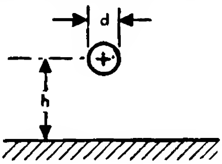	For $d \ll h,$ $Z_0 = \frac{138}{\sqrt{\epsilon}} \log_{10} \frac{4h}{d}$
H. Single wire, square enclosure 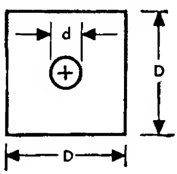	$Z_0 \approx [138 \log_{10} \rho + 6.48 - 2.34A - 0.48B - 0.12C]\epsilon^{-1/2}$ where $\rho = D/d$ $A = \frac{1 + 0.405\rho^{-4}}{1 - 0.405\rho^{-4}}$ $B = \frac{1 + 0.163\rho^{-8}}{1 - 0.163\rho^{-8}}$ $C = \frac{1 + 0.067\rho^{-12}}{1 - 0.067\rho^{-12}}$
I. Balanced 4-wire 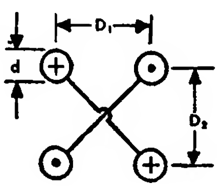	For $d \ll D_1, D_2$ $Z_0 = \frac{138}{\sqrt{\epsilon}} \log_{10} \frac{2D_2}{d\sqrt{1 + (D_2/D_1)^2}}$

Characteristic impedance of lines *continued*

type of line	characteristic impedance
J. Parallel-strip line 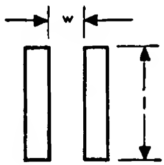	$\frac{w}{l} < 0.1$ $Z_0 \approx 377 \frac{w}{l}$
K. Five-wire line 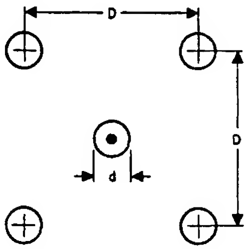	For $d \ll D$, $Z_0 = \frac{173}{\sqrt{\epsilon}} \log_{10} \frac{D}{0.933d}$
L. Wires in parallel—sheath return 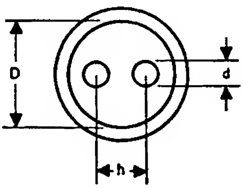	For $d \ll D, h$, $Z_0 = \frac{69}{\sqrt{\epsilon}} \log_{10} \left[\frac{\nu}{2\sigma^2} (1 - \sigma^4) \right]$ $\sigma = h/D$ $\nu = h/d$
M. Air coaxial with dielectric supporting wedge 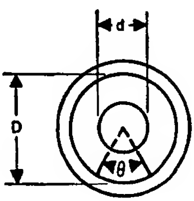	$Z_0 \approx \frac{138 \log_{10} (D/d)}{\sqrt{1 + (\epsilon - 1)(\theta/360)}}$ ϵ = dielectric constant of wedge θ = wedge angle in degrees

Characteristic impedance of lines *continued*

type of line	characteristic impedance
N. Balanced 2-wire — unequal diameters 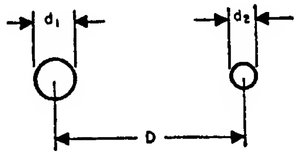	For d_1, $d_2 \ll D$, $Z_0 = \dfrac{276}{\sqrt{\epsilon}} \log_{10} \dfrac{2D}{\sqrt{d_1 d_2}}$
O. Balanced 2-wire near ground 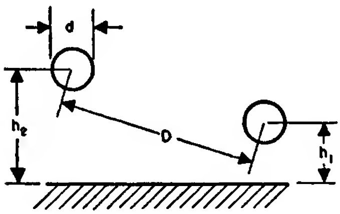	For $d \ll D$, h_1, h_2, $Z_0 = \dfrac{276}{\sqrt{\epsilon}} \log_{10} \left[\dfrac{2D}{d} \dfrac{1}{\sqrt{1 + \dfrac{D^2}{4h_1 h_2}}} \right]$ Holds also in either of the following special cases: $D = \pm(h_2 - h_1)$ or $h_1 = h_2$ (see F above)
P. Single wire between grounded parallel planes—ground return 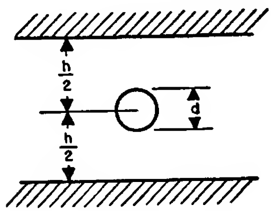	For $\dfrac{d}{h} < 0.75$, $Z_0 = \dfrac{138}{\sqrt{\epsilon}} \log_{10} \dfrac{4h}{\pi d}$
Q. Balanced line between grounded parallel planes 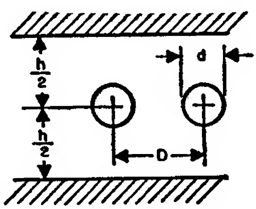	For $d \ll D$, h, $Z_0 = \dfrac{276}{\sqrt{\epsilon}} \log_{10} \left(\dfrac{4h \tanh \dfrac{\pi D}{2h}}{\pi d} \right)$

Characteristic impedance of lines *continued*

type of line	characteristic impedance

R. Balanced line between grounded parallel planes

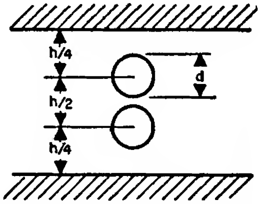

For $d \ll h$,

$$Z_0 = \frac{276}{\sqrt{\epsilon}} \log_{10} \frac{2h}{\pi d}$$

S. Single wire in trough

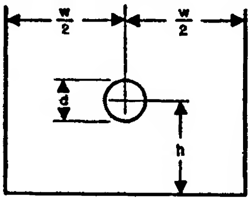

For $d \ll h, w$,

$$Z_0 = \frac{138}{\sqrt{\epsilon}} \log_{10} \left[\frac{4w \tanh \dfrac{\pi h}{w}}{\pi d} \right]$$

T. Balanced 2-wire line in rectangular enclosure

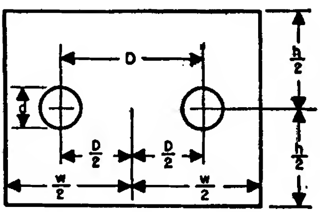

For $d \ll D, w, h$,

$$Z_0 = \frac{276}{\sqrt{\epsilon}} \left\{ \log_{10} \left[\frac{4h \tanh \dfrac{\pi D}{2h}}{\pi d} \right] - \sum_{m=1}^{\infty} \log_{10} \left[\frac{1 + u_m^2}{1 - v_m^2} \right] \right\}$$

where

$$u_m = \frac{\sinh \dfrac{\pi D}{2h}}{\cosh \dfrac{m\pi w}{2h}} \qquad v_m = \frac{\sinh \dfrac{\pi D}{2h}}{\sinh \dfrac{m\pi w}{2h}}$$

U. Eccentric line

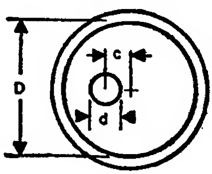

For $d \ll D$,

$$Z_0 = \frac{138}{\sqrt{\epsilon}} \log_{10} \left\{ \frac{D}{d} \left[1 - \left(\frac{2c}{D} \right)^2 \right] \right\}$$

For $c/D \ll 1$ this is the Z_0 of type A diminished by approximately

$$\frac{240}{\sqrt{\epsilon}} \left(\frac{c}{D} \right)^2 \text{ ohms}$$

Characteristic impedance of lines *continued*

type of line	characteristic impedance
V. Balanced 2-wire line in semi-infinite enclosure 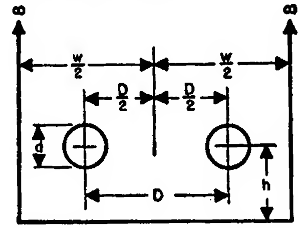 	For $d \ll D, w, h,$ $$Z_0 = \frac{276}{\sqrt{\epsilon}} \log_{10} \frac{2w}{\pi d\sqrt{A}}$$ where $$A = \operatorname{cosec}^2\left(\frac{\pi D}{w}\right) + \operatorname{cosech}^2\left(\frac{2\pi h}{w}\right)$$
W. Outer wires grounded, inner wires balanced to ground 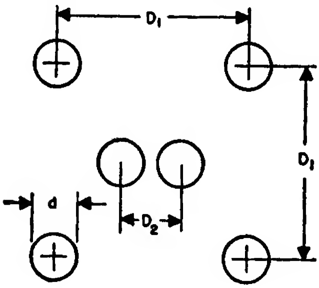 	$$Z_0 \approx \frac{276}{\sqrt{\epsilon}} \left\{ \log_{10} \frac{2D_2}{d} - \frac{\left[\log_{10} \frac{1 + (1 + D_2/D_1)^2}{1 + (1 - D_2/D_1)^2}\right]^2}{\log_{10} \frac{2D_1\sqrt{2}}{d}} \right\}$$
X. Split thin-walled cylinder 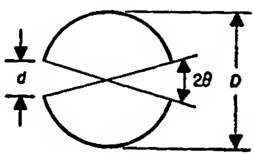 	$$Z_0 \approx \frac{129}{\log_{10}\left[\cot\frac{\theta}{2} + \left(\cot^2\frac{\theta}{2} - 1\right)^{1/2}\right]}$$ For θ small: $Z_0 \approx 129/\log_{10}(4D/d)$ *Courtesy of Electronic Engineering*
Y. Slotted air line 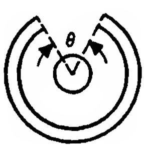 	When a slot is introduced into an air coaxial line for measuring purposes, the increase in characteristic impedance in ohms, compared with a normal coaxial line, is less than $\Delta Z = 0.03\theta^2$ where θ is the angular opening of the slot in radians

Voltage gradient in a coaxial line

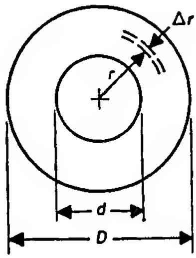

C' = capacitance in micromicrofarads/foot
D = diameter of inner surface of outer conductor in same units as d.
d = diameter of inner conductor
E = total voltage across line (E and ΔE both rms or both peak)
r = radius (r and Δr both in same units)
ϵ = net effective dielectric constant (= 1 for air); $1/\epsilon^{1/2}$ = velocity factor

$$\frac{\Delta E}{\Delta r} = \frac{0.434E}{r \log_{10} (D/d)} = \frac{0.059EC'}{r\epsilon} = \frac{60E}{rZ_0\epsilon^{1/2}} = \frac{6.10 \times 10^4 E}{rZ_0^2 C'}$$

At the voltage standing-wave maximum:

$$\text{(gradient at surface of inner conductor)} = \frac{5.37}{d}\left(\frac{SP_{\text{kw}}}{Z_0\epsilon}\right)^{1/2}$$

$$= \frac{5450\ (SP_{\text{kw}})^{1/2}}{d\ C'Z_0^{3/2}} \text{ peak volts/mil}$$

where d is in inches (1 mil = 0.001 inch). For amplitude or pulse modulation, let P_{kw} be the power in kilowatts at the crest of the modulation cycle. Thus, if the carrier is 1 kilowatt and modulation 100 percent, set

$P_{\text{kw}} = 4$ kilowatts

Example: What is the voltage gradient at inner conductor of a $6\frac{1}{8}$-inch rigid 50-ohm line with 500 kilowatts continuous-wave power, unity swr? Let $\epsilon = 1.00$ and $d = 2.60$ inches.

$$\text{(gradient)} = \frac{5.37}{2.60}\left(\frac{500}{50}\right)^{1/2} = 6.55 \text{ peak volts/mil}$$

The breakdown strength of air at atmospheric pressure is 29,000 peak volts/centimeter, or 74 peak volts/mil (experimental value, before derating).

Microstrip*

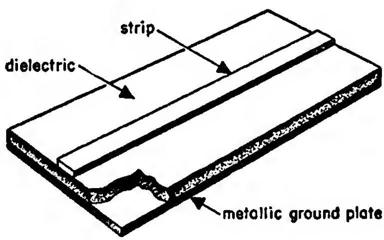

Microstrip consists of a wire above a ground plane, being analogous to a two-wire line in which one of the wires is represented by the image in

* See, D. D. Grieg and H. F. Engelmann, "Microstrip—A New Transmission Technique for the Kilomegacycle Range," and two accompanying papers in Proceedings of the IRE, vol. 40, pp. 1644–1663; December, 1952: also in *Electrical Communication*, vol. 30, pp. 26–54; March, 1953.

Microstrip *continued*

the ground plane of the wire that is physically present. On p. 595 is illustrated a short length of microstrip line, showing the metallic-strip conductor bonded to a dielectric sheet, to the other side of which is bonded a metallic ground plate.

Phase velocity

Theoretically, for the TEM mode with conductors completely immersed in the dielectric, the velocity of propagation is

$$v = c/(\epsilon_r)^{1/2}$$

where

c = velocity of light in vacuum

ϵ_r = dielectric constant relative to air

For Teflon-impregnated Fibreglas dielectric, this gives 604 feet per microsecond. Experimental measurements on a line with 7/32-inch strip width and dielectric sheet 1/16-inch thick give

$$v = 655 \text{ feet/microsecond.}$$

Typical measurements together with the theoretical TEM wavelength are plotted in Fig. 10.

Characteristic impedance

If it were not for fringing and leakage flux, the theoretical characteristic

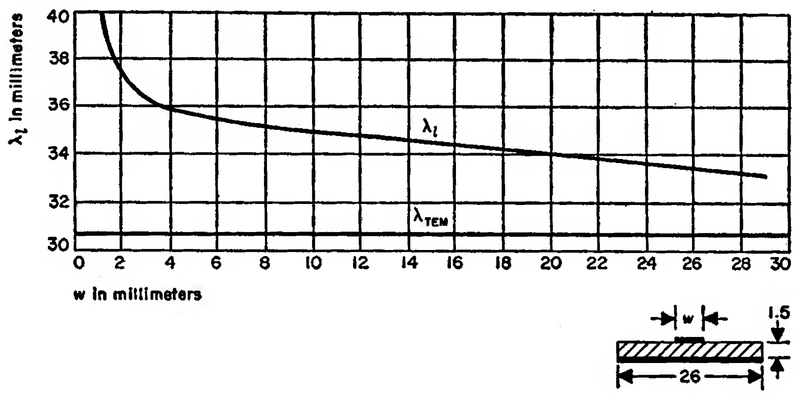

Fig. 10—Wavelength in microstrip versus width of strip conductor. The dimensions in the sketch at right are in millimeters. Dielectric was Fibreglas G-6. Measurements were taken at 4770 megacycles.

Microstrip *continued*

impedance would be

$$Z_0 = (h/w)\ (\mu/\epsilon)^{1/2}$$
$$= 377\ (h/w)\ (1/\epsilon_r)^{1/2}$$

where

h = thickness of dielectric
w = width of strip conductor
ϵ = dielectric constant in farads/meter
μ = permeability in henries/meter

Fig. 11 shows the experimentally determined Z_0 for typical microstrip lines.

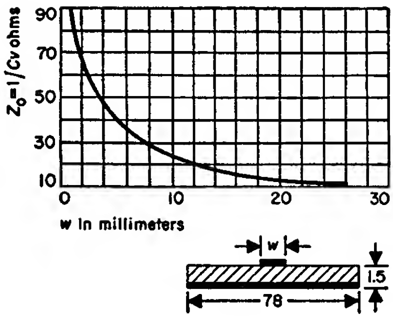

Fig. 11—Characteristic impedance for microstrip with Fibreglas G-6 dielectric. Dimensions in sketch are in millimeters. C is the measured electrostatic capacitance in farads per unit length and v is the phase velocity in units of length per second.

Attenuation

Conductor loss for copper, in decibels/foot:

$$\alpha_{cu} = 7.25 \times 10^{-5}\ (1/h)\ (f_{mc}\epsilon_r)^{1/2}$$

Dielectric loss in decibels/foot:

$$\alpha_d = 2.78 \times 10^{-2}\ f_{mc}F_p\ (\epsilon_r)^{1/2}$$

where

F_p = power factor or loss angle
h = dielectric thickness in inches

A correction factor for conductor attenuation is shown in Fig. 12 for use in the formula:

$$\alpha_c = \alpha_0 \times \Delta$$

where α_0 is, for copper conductors, given by α_{cu} above.

$$\alpha_0 = \alpha_{cu}\ (\mu_r\rho/\rho_{cu})^{1/2}$$

where

μ_r = relative permeability
ρ/ρ_{cu} = resistivity relative to copper.

The measured attenuation of a typical microstrip line is shown on the chart on p. 615. The relatively high attenuation is due to the small physical size of the line.

Microstrip *continued*

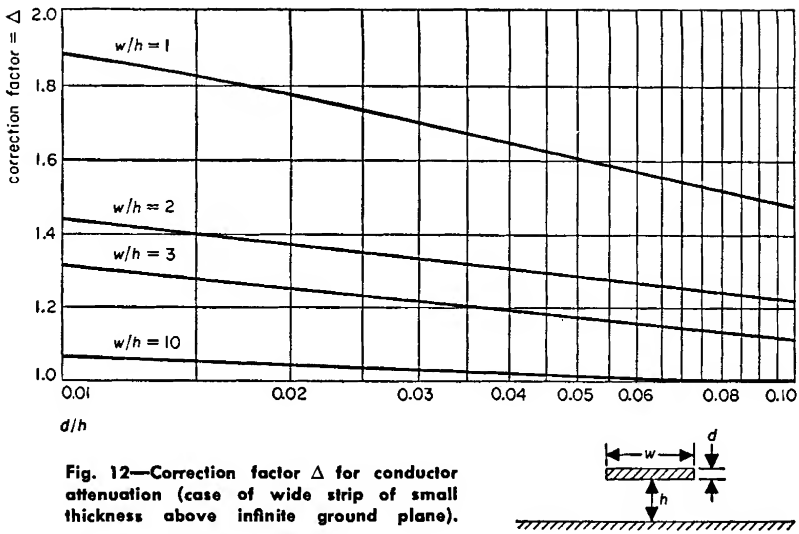

Fig. 12—Correction factor Δ for conductor attenuation (case of wide strip of small thickness above infinite ground plane).

Power-handling capacity

For a microstrip line composed of a strip 7/32-inch wide on a Teflon-impregnated Fibreglas base 1/16-inch thick:

a. At 3000 megacycles with 300 watts cw, the temperature under the strip conductor has been measured at 50° centigrade rise above 20° centigrade ambient.

b. Under pulse conditions, corona effects appear at the edge of the strip conductor for pulse power of roughly 10 kilowatts at 9000 megacycles.

Strip transmission lines*

Strip transmission lines differ from microstrip in that a second ground plane is placed above the conductor strip (see sketch below). The characteristic impedance is shown in Fig. 13 and the attenuation in Fig. 14.

Attenuation

Dielectric loss in decibels/unit length:

$\alpha_d = 27.3\ F_p \epsilon_r^{1/2}/\lambda_0$

where λ_0 = free-space wavelength.

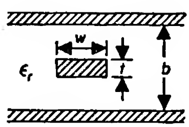

* See, S. B. Cohn, "Problems in Strip Transmission Lines," *Transactions of the IRE Professional Group on Microwave Theory and Techniques*, vol. MTT3, pp. 119–126; March 1955. Other papers on strip-type lines also appear in that issue of the journal.

Strip transmission lines *continued*

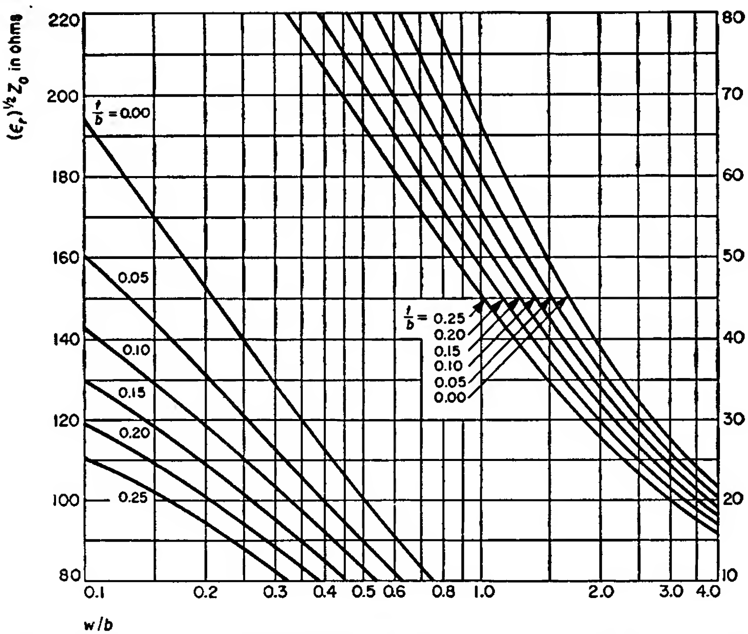

Fig. 13—Plot of strip-transmission-line Z_0 versus w/b for various values of t/b. For lower-left family of curves, refer to left-hand ordinate values; for upper-right curves, use right-hand scale. *Courtesy of Transactions of the IRE Professonal Group on Microwave Theory and Techniques.*

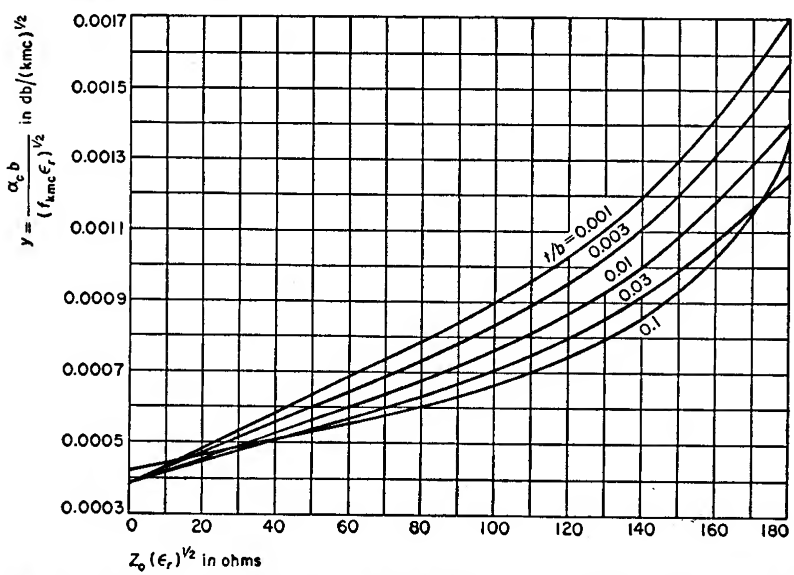

Fig. 14—Theoretical attenuation of copper-shielded strip transmission line in dielectric medium ϵ_r. *Courtesy of Transactions of the IRE Professional Group on Microwave Theory and Techniques.*

Strip transmission lines *continued*

Conductor loss in decibels/unit length:

$$\alpha_c = (y/b)\ (f_{\mathrm{kmo}}\epsilon_r\mu_r\rho/\rho_{cu})^{1/2}$$

where

y = ordinate from Fig. 14

ρ/ρ_{cu} = resistivity relative to copper

The unit of length in α_d is that of λ_0 and in α_c it is that of b.

Lines and resonators with helical inner conductor

Spiral delay line

For a transmission line with helical inner conductor (spiral delay line) where axial wavelength and length of line are both long compared to line diameter (similar to Fig. 15 in dimensional symbols):

$$L' = 0.30\ n^2d^2\ [1 - (d/D)^2]$$

microhenries/axial foot where d is in inches and

$n = 1/\tau$ = turns/inch.

$$C' = 7.4\ \epsilon_r/\log_{10}(D/d)$$

micromicrofarads/axial foot.

$$Z_0 = (L'/C')^{1/2} \times 10^3 \text{ ohms}$$

$$T = (L'C')^{1/2} \times 10^{-3}$$

microseconds/axial foot

$$\alpha_{\mathrm{db}} = 4.34R/Z_0 + 27.3\ F_p fT$$

decibels/axial foot where

R = total conductor resistance in ohms/axial foot

f = frequency in megacycles

F_p = power factor

ϵ_r = relative dielectric constant of medium between spiral and outer conductor

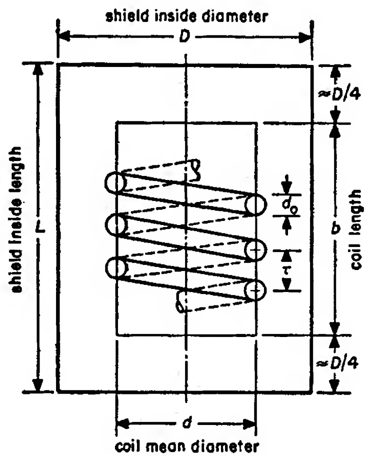

Fig. 15—Resonator with helical inner conductor. One end of the helix is grounded solidly to the shield; other end is open-circuited.

Lines and resonators with helical inner conductor *continued*

Resonator

In a quarter-wavelength resonator (Fig. 15), the mode of the fields is somewhat different from the above.

$L = 0.025\, n^2 d^2 [1 - (d/D)^2]$ microhenries/axial inch

where d is in inches and

$n = 1/\tau =$ turns/inch

Empirically, for air dielectric (and $b/d = 1.5$),

$C = 0.75/\log_{10}(D/d)$

micromicrofarads/axial inch.

These equations and all those below are good roughly for

$1.0 < b/d < 4.0$
$0.45 < d/D < 0.6$
$0.4 < d_0/\tau < 0.6$ at $b/d = 1.5$
$0.5 < d_0/\tau < 0.7$ at $b/d = 4.0$
$\tau < d/2$

where $d_0 =$ diameter of conductor

The axial length of the coil is approximately a quarter wavelength, but much shorter than that length in free space.

$b = 250/f\,(LC)^{1/2}$ inches

where f is the resonance frequency in megacycles.

$$n = \frac{1000}{fd^2\,(b/d)}\left[\frac{2.5/C}{1 - (d/D)^2}\right]^{1/2}$$

$$= \frac{1830}{fD^2\,(b/d)\,(d/D)^2}\left[\frac{\log_{10}(D/d)}{1 - (d/D)^2}\right]^{1/2} \text{ turns/inch}$$

$$Z_0 = 1000\,(L/C)^{1/2} = 0.25 \times 10^6/bfC$$

$$= \frac{10^6 \log_{10}(D/d)}{3\,fD\,(b/d)\,(d/D)}$$

$$= 183\, nd\left\{[1 - (d/D)^2]\log_{10}(D/d)\right\}^{1/2} \text{ ohms}$$

Lines and resonators with helical inner conductor *continued*

A practical working formula for the unloaded Q (not the theoretical maximum), for copper winding and shield, and negligible dielectric loss, is

$$Q_u \approx 220 \frac{(d/D) - (d/D)^3}{1.5 + (d/D)^3} Df^{1/2}$$

$$\approx 50\ Df^{1/2}$$

(with D in inches) provided d_0 exceeds 5 times the skin depth (page 128).

Example: A resonator is required for 10.0 megacycles with unloaded $Q_u = 1000$. The generator impedance is 10,000 ohms and the load is 50 ohms. They are matched through the resonator and provide a doubly loaded $Q_d = 100$. The power capability of the generator is 200 watts.

Suppose the proportions are set at $b/d = 1.5$ and $d/D = 0.55$. Then using the formulas and referring to Fig. 15, the following results are found.

$f = 10.0$ megacycles

$Q_u = 1000$

$D = 6.3$ inches

$d = 3.5$ inches

$b = 5.25$ inches

$L = b + D/2 = 8.4$ inches

$n = 6$ turns per inch

$nb = 31.5$ turns total

$\tau = 0.167$ inch

$d_0 = 0.067$ to 0.100 inch

$\delta = 0.0008$-inch skin depth (page 129)

$Z_0 = 1700$ ohms

Referring to the section on "Resonant lines" (pp. 574-582):

Lines and resonators with helical inner conductor *continued*

$R_b/Z_0 = (\pi/4)\ (1/Q_d - 1/Q_u) = 0.0071$

which is to be divided equally between generator and load and used in the formula in Fig. 6A.

$\theta_1 = 8.4$ degrees for 10,000-ohm generator

$(\text{tap}) = nb\theta_1/90$ degrees $= 2.9$ turns from short-circuited end

$\theta_1 = 0.6$ degrees for 50-ohm load

$(\text{tap}) = 0.2$ turn from short-circuited end

$S = 1.2$ on generator impedance

(dissipation loss) $= 0.9$ decibel

$=$ (insertion loss)

since (mismatch loss) $\approx$ zero

$P_m = 200$ watts

$P_c = 36$ watts

$I_{sc} = 5.3$ amperes

$E_{oc} = 9000$ volts

The envelope area of the coil is approximately 50 square inches, so the average dissipation is $P_c/(\text{area}) = 0.72$ watts per square inch. The power dissipation per unit area at the grounded end is twice the average value, due to the cosine distribution of current. Cooling is accomplished by radiation to the shield, and convection around the surface of the turns and from the coil supporting structure.

In many applications, the loaded Q required is much lower than 100, in which case the resonator will handle a proportionately higher generator power. On the other hand, suppose the generator power remains at 200 watts, but the loaded Q is allowed to be 12.5 (one-eighth its former value). Then the dimensions can be reduced to about one-half of those found in the example. The same values will result for power dissipation per unit area and voltage gradient between the open-circuited end and the shield.

Surface-wave transmission line*

The surface-wave transmission line is a single-conductor line having a relatively thick dielectric sheath (Fig. 16). The sheath diameter is often 3 or more times the conductor diameter. A mode of propagation that is practically nonradiating is excited on the line by means of a conical horn at each end as shown in Fig. 17. The mouth of the horn is roughly one-quarter to one wavelength in diameter. Losses are about half those of a two-wire line, but the surface-wave line has a practical lower frequency limit of about 50 megacycles.

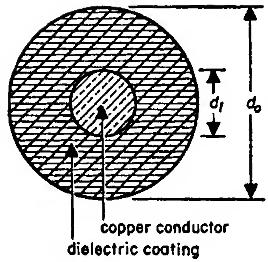

Fig. 16—Cross-section of surface-wave transmission line.

Design charts are given in Figs. 18–20 together with formulas herewith for attenuation losses.

The losses in the two launchers combined vary from less than 0.5 decibel to a little more than 1.0 decibel, according to their design.

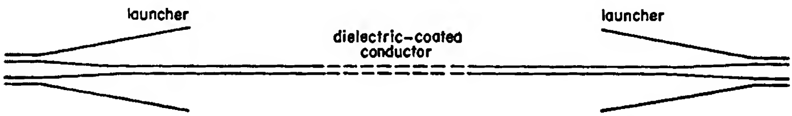

Fig. 17—Surface-wave transmission line with launchers at each end. These form transitions to coaxial line. Courtesy of *Electronics*

Conductor loss L_c by the formula below is 5 percent over the theoretical value for pure copper. Dielectric loss L_p for polyethylene at 100 megacycles is shown in Fig. 19. For other dielectrics and frequencies, find L_i by the formula.

$$L_c = 0.455\, f^{1/2}/Zd_i \text{ decibels/100 feet}$$

$$L_i = 26\, fF_pL_p/(\epsilon_r - 1) \text{ decibels/100 feet}$$

$$L_i = L_pf/100$$

for brown polyethylene (Fig. 19).

* Georg Goubau, "Designing Surface-Wave Transmission Lines," *Electronics*, vol. 27, pp. 180–184; April, 1954.

Surface-wave transmission line *continued*

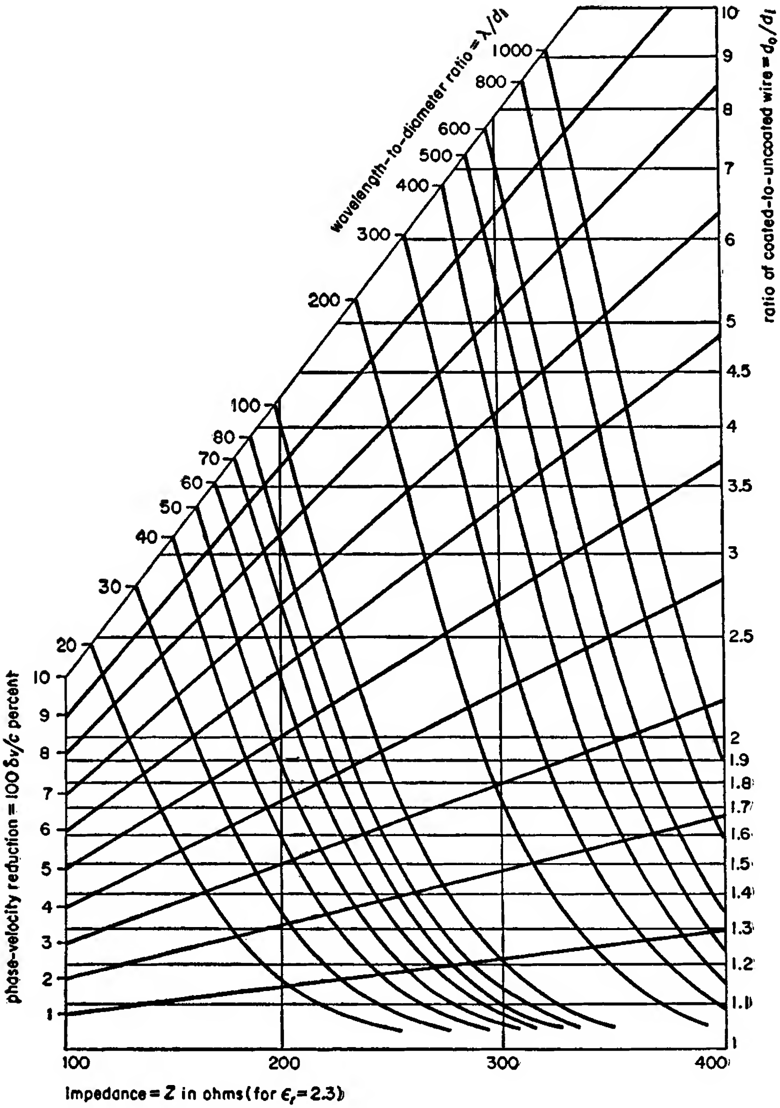

Fig. 18—Relationship among wire diameter, dielectric layer, phase-velocity reduction, and impedance (for brown polyethylene).

Courtesy of Electronics

Surface-wave transmission line *continued*

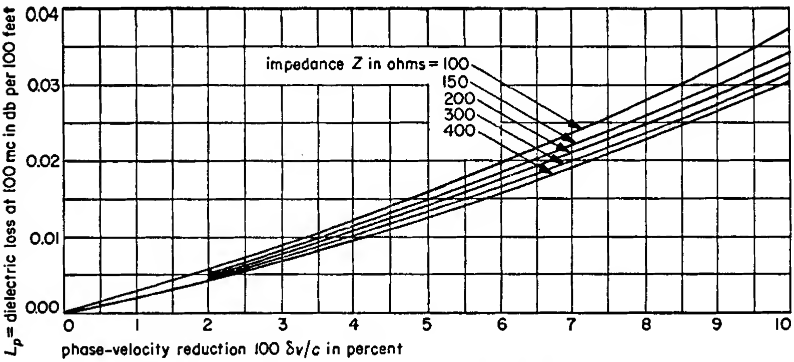

Fig. 19—Dielectric loss at 100 megacycles for brown polyethylene ($\epsilon_r = 2.3$ and $F_p = 5 \times 10^{-4}$).
Courtesy of Electronics

Symbols used in formulas and figures are:

c = velocity of propagation in free space
d_i = diameter of the conductor (inches in formula for L_c)
d_o = outside diameter of the dielectric coating
f = frequency in megacycles
F_p = power factor of dielectric
L_c = conductor loss in decibels/100 feet
L_i = dielectric loss in decibels/100 feet
L_p = dielectric loss shown in Fig. 19.
Z = waveguide impedance in ohms
δv = reduction in phase velocity
ϵ_r = dielectric constant relative to air
λ = free-space wavelength

Example: At 900 megacycles (λ = 0.333 meter), a 200-foot line is required having a permissible loss of 1.0 decibel/100 feet (not including the launcher losses). What are its dimensions?

Allowing 20 percent for dielectric loss, the conductor loss would be L_c = 0.8 decibel/100 feet. Assuming Z = 250 ohms as a first approximation, the formula for L_c gives d_i = 0.068 inch. Use no. 14 AWG wire (d_i = 0.064 and λ/d_i = 204). Now going to Fig. 18 and assuming that $100\ \delta v/c = 6$ percent is adequate, we find that $d_o/d_i = 3$ and Z = 270 ohms.

Recomputing, L_c = 0.79 decibel/100 feet. By Fig. 19, L_p = 0.017 at 100

Surface-wave transmission line *continued*

megacycles for brown polyethylene. Using the same material at 900 megacycles, the loss is $L_i = 0.15$ decibel/100 feet.

For 200 feet, the combined conductor and dielectric loss is 1.9 decibels, to which must be added the loss of 0.5 to 1.0 decibel total for the two launchers.

Dielectric other than polyethylene *(Fig. 20)*

Determine Z and $\delta v/c$ for polyethylene ($\epsilon_r = 2.3$) from Fig. 18. Then use Fig. 20 to find the value of d_o/d_i required for the same performance with actual dielectric constant ϵ_r. Make computation of new dielectric loss, using Fig. 19 and formula for L_i.

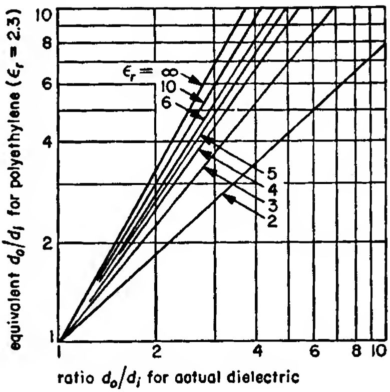

Fig. 20—Conversion chart for dielectric other than polyethylene. *Courtesy of Electronics*

Army-Navy list of standard radio-frequency cables*

The following notes apply to the table on pages 608-611:

* From "Guide to Selection of Standard RF Cables," Armed Services Electro-Standards Agency, Fort Monmouth, New Jersey, publication 49-2B, 1 November 1955 supplement.

† Diameter of strands given in inches. As, 7/0.0296 = 7 strands, each 0.0296-inch diameter.

‡ This value is the diameter over the outer layer of conducting or insulating synthetic rubber.

Note 1—Dielectric materials and approximate velocity factors (v = velocity of propagation in cable, c = velocity of light in free space):

A = Solid stabilized polyethylene ($v/c \approx 0.67$, except for RG–65A/U and RG–86/U).

A2 = Air-spaced polyethylene ($v/c \approx 0.84$).

D = Layer of insulating synthetic rubber between thin layers of conducting rubber ($v/c \approx 0.41$).

E = Inner layer conducting synthetic rubber, center layer insulating synthetic rubber, outer layer red insulating synthetic rubber ($v/c \approx 0.41$).

F = Solid polytetrafluoroethylene (teflon) ($v/c \approx 0.695$).

F2 = Taped polytetrafluoroethylene (teflon).

F3 = Air-spaced polytetrafluoroethylene (teflon).

Note 2—Composition of protective covering:

Y = Noncontaminating synthetic resin.

Z1 = Polytetrafluoroethylene- (teflon-) tape moisture seal, single Fiberglas braid, silicone-varnish impregnated.

Z2 = Polytetrafluoroethylene- (teflon-) tape moisture seal, double Fiberglas braid, silicone-varnish impregnated.

Note 3—For RG–65A/U, delay = 0.042 microsecond per foot at 5 megacycles; dc resistance = 7.0 ohms/foot.

Army-Navy list of standard radio-frequency cables* *continued*

class of cables		Army-Navy type RG–	inner conductor†	dielect material (note 1)	nominal diam of dielectric inches	shielding braid	protective covering (note 2)	nominal over-all diam inches	weight lb/ft	nominal impedance ohms	nominal capacitance $\mu\mu f/ft$	maximum operating voltage rms	remarks
50 ohms	Single braid	8A/U	7/0.0296 copper	A	0.285	Copper	Y	0.405	0.120	50.0	29.5	4,000	General-purpose medium-size flexible cable
		10A/U	7/0.0296 copper	A	0.285	Copper	Y Armor	0.475 (max)	0.160	50.0	29.5	4,000	Same as RG-8A/U, but armored
		17A/U	0.195 copper	A	0.680	Copper	Y	0.870	0.491	50.0	29.5	11,000	Large high-power low-attenuation transmission cable
		18A/U	0.195 copper	A	0.680	Copper	Y Armor	0.945 (max)	0.603	50.0	29.5	11,000	Same as RG-17A/U, but armored
		19A/U	0.260 copper	A	0.910	Copper	Y	1.120	0.745	50.0	29.5	14,000	Very large high-power low-attenuation transmission cable
		20A/U	0.260 copper	A	0.910	Copper	Y Armor	1.195 (max)	0.925	50.0	29.5	14,000	Same as RG-19A/U, but armored
		58C/U	19/0.0071 tinned copper	A	0.116	Tinned copper	Y	0.195	0.029	50.0	28.5	1,900	Small-size flexible cable
		122/U	27/0.005 tinned copper	A	0.096	Tinned copper	Synthetic resin	0.160	—	50.0	29.3	1,900	Small-size flexible lightweight cable
	Double braid	5B/U	0.053 silvered copper	A	0.181	Silvered copper	Y	0.328	0.093	50.0	28.5	3,000	Small microwave cable
		9B/U	7/0.0296 silvered copper	A	0.280	Silvered copper	Y	0.420	0.158	50.0	30.0	4,000	Special medium-size flexible cable
		14A/U	0.106 copper	A	0.370	Copper	Y	0.545	0.236	50.0	29.5	5,500	Medium-size power-transmission cable
		55A/U	0.035 silvered copper	A	0.116	Silvered copper	Y	0.216 (max)	0.032	50.0	28.5	1,900	Small-size flexible cable
		74A/U	0.106 copper	A	0.370	Copper	Y Armor	0.615 (max)	0.282	50.0	29.5	5,500	Same as RG-14A/U, but armored
75 ohms	Single braid	11A/U	7/0.0159 tinned copper	A	0.285	Copper	Y	0.405	0.096	75.0	20.5	4,000	Medium-size, flexible video and communication cable

		12A/U	7/0.0159 tinned copper	A	0.285	Copper	Y Armor	0.475 (max)	0.141	75.0	20.5	4,000	Same as RG–11A/U, but armored
		34A/U	7/0.0249 copper	A	0.455	Copper	Y	0.625	0.231	75.0	21.5	5,200	Large-size, high-power, low-attenuation, flexible cable
		35A/U	0.1045 copper	A	0.680	Copper	Y Armor	0.945 (max)	0.480	75.0	21.5	10,000	Large-size, high-power, low-attenuation video and communication cable
		59A/U	0.0230 copperweld	A	0.146	Copper	Y	0.242	0.032	75.0	21.0	2,300	General-purpose small-size video cable
		84A/U	0.1045 copper	A	0.680	Copper	Y Lead sheath	1.000	1.325	75.0	21.5	10,000	Same as RG–35A/U, but no armor; sheath for subterranean use
		85A/U	0.1045 copper	A	0.680	Copper	Y Lead sheath and armor	1.565 (max)	2.910	75.0	21.5	10,000	Same as RG–84A/U, with special armor
		164/U	0.1045 copper	A	0.680	Copper	Y	0.870	—	75.0	21.5	10,000	Same as RG–35A/U except without armor
	Double braid	6A/U	0.0285 copperweld	A	0.185	Inner—silver-coated copper. Outer—copper	Y	0.332	0.082	75.0	20.0	2,700	Small-size video and communication cable
		13A/U	7/0.0159 tinned copper	A	0.280	Copper	Y	0.420	0.126	75.0	20.5	4,000	Medium-size flexible video and communication cable
High temperature	Single braid	117/U	0.190 copper	F	0.620	Copper	Z2	0.730	0.450	50.0	29.0	5,000	Semiflexible cable for −55° to 250° C
		118/U	0.190 copper	F	0.620	Copper	Z2 Armor	0.780	0.600	50.0	29.0	5,000	Same as RG–117/U, but armored
		140/U	0.025 silvered copperweld	F	0.146	Silvered copper	Z1	0.241	0.045	75.0	21.0	2,300	Similar to RG–59A/U, but teflon insulation
		141/U	0.0359 silvered copperweld	F	0.116	Silvered copper	Z1	0.195	0.030	50.0	28.5	1,900	Similar to RG–58C/U, but teflon insulation
		144/U	7/0.0179 silvered copperweld	F	0.285	Silvered copper	Z2	0.405	0.120	75.0	20.5	4,000	Similar to RG–11A/U, but teflon insulation
		146/U	0.007 copperweld	F3	0.285	Copper	Z1	0.375	—	190.0	6.5	1,000	Special low-capacitance cable

*See notes on page 607.

continued **Army-Navy list of standard radio-frequency cables***

class of cables		Army-Navy type RG–	inner conductor†	dielect material (note 1)	nominal diam of dielectric inches	shielding braid	protective covering (note 2)	nominal over-all diam inches	weight lb/ft	nominal imped-ance ohms	nominal capaci-tance $\mu\mu f/ft$	maximum operating voltage rms	remarks
High temper-ature cont'd	Double braid	87A/U	7/0.0312 silvered copper	F	0.280	Silvered copper	Z2	0.425	0.176	50.0	29.5	4,000	Semiflexible cable for —55° to 250° C
		94A/U	19/0.0254 silvered copper	F2	0.370	Copper	Z2	0.470	—	50.0	29.0	5,000	For use where expansion and contraction are a major problem
		115/U	7/0.028 silvered copper	F2	0.250	Silvered copper	Z2	0.375	—	50.0	29.5	4,000	For use where expansion and contraction are a major problem
		116/U	7/0.0312 silvered copper	F	0.280	Silvered copper	Z2 Armor	0.475	0.224	50.0	29.5	4,000	Same as RG–87A/U, but armored
		142/U	0.0359 silvered copperweld	F	0.116	Silvered copper	Z1	0.206	0.045	50.0	28.5	1,900	Similar to RG–55/U, but teflon insulation
		143/U	0.057 silvered copperweld	F	0.185	Silvered copper	Z2	0.322	0.102	50.0	28.5	3,000	Similar to RG–58/U, but teflon insulation
Pulse	Single braid	26/U	19/0.0117 tinned copper	D	0.308 ‡	Tinned copper	Chloroprene. Armor	0.525 (max)	0.189	50.0	50.0	8,000 (peak)	Medium-size cable
		26A/U	19/0.0117 tinned copper	E	0.288 ‡	Tinned copper	Chloroprene. Armor	0.505	0.189	48.0	50.0	8,000 (peak)	High-voltage armored pulse cable
		27/U	19/0.0185 tinned copper	D	0.455 ‡	Tinned copper	Synthetic resin. Armor	0.675 (max)	0.304	48.0	50.0	15,000 (peak)	Large-size armored pulse cable
	Double braid	25/U	19/0.0117 tinned copper	D	0.308 ‡	Tinned copper	Chloroprene	0.565	0.205	50.0	50.0	8,000 (peak)	Special cable for twisting applications
		25A/U	19/0.0117 tinned copper	E	0.308 ‡	Tinned copper	Chloroprene	0.505	0.205	48.0	50.0	8,000 (peak)	Medium-size pulse cable
		28/U	19/0.0185 tinned copper	D	0.455 ‡	Inner—tinned copper. Outer—galvanized steel	Chloroprene	0.805	0.370	48.0	50.0	15,000 (peak)	Large-size pulse cable

		64A/U	19/0.0117 tinned copper	E	0.288 ‡	Tinned copper	Chloroprene	0.475	0.205	48.0	50.0	8,000 (peak)	Medium-size pulse cable
	Four braids	88B/U	19/0.0117 tinned copper	E	0.288 ‡	Tinned copper	Y	0.565 (max)	—	48.0	50.0	8,000 (peak)	Replaces RG-77/U in air-borne applications
Low capaci-tance	Single braid	62A/U	0.0253 copperweld	A2	0.146	Copper	Y	0.242	0.0382	93.0	13.5	750	Same as RG-71A/U except for braid
		62B/U	7/0.008 copperweld	A2	0.146	Copper	Y	0.242	0.040	93.0	13.5	750	Same as RG-62A/U, but stranded center conductor
		63B/U	0.0253 copperweld	A2	0.285	Copper	Y	0.405	0.082	125.0	10.0	1,000	Medium-size low-capacitance air-spaced cable
		79B/U	0.0253 copperweld	A2	0.285	Copper	Y Armor	0.475 (max)	0.138	125.0	10.0	1,000	Same as RG-63B/U, but armored
	Double braid	71A/U	0.0253 copperweld	A2	0.146	Tinned copper	Synthetic resin	0.250 (max)	0.046	93.0	13.5	750	Small-size low-capacitance air-spaced cable
High attenu-ation	Single braid	126/U	7/0.0203 Karma wire	F	0.180	Karma wire	Z2	0.275	0.076	50.0	29.0	3,000	High-attenuation cable
	Double braid	21A/U	0.053 resistance wire	A	0.185	Silvered copper	Y	0.332	0.093	50.0	29.0	2,700	High-attenuation cable. Small temperature coefficient of attenuation
High delay	Single braid	65A/U	0.008 Formex F. Helix diam 0.128	A	0.285	Copper	Y	0.405	0.096	950.0	44.0	1,000	High-impedence video cable. High-delay line (Note 3)
Twin con-ductor	No braid	86/U	2 cond. 7/0.0285 copper	A	0.300 × 0.650	None	None	0.300 × 0.650	—	200.0	7.8	—	For rhombic and doublet receiving antennas
	Single braid	130/U	2 cond. 7/0.0285 copper	A	0.472	Tinned copper	Synthetic resin	0.625	0.220	95.0	17.0	8,000	Large-size balanced cable. Inner conductors twisted for flexibility
		131/U	2 cond. 7/0.0285 copper	A	0.472	Tinned copper	Synthetic resin. Al. armor	0.710	0.295	95.0	17.0	8,000	Same as RG-130/U, but aluminum armored
	Double braid	22B/U	2 cond. 7/0.0152 copper	A	0.285	Tinned copper	Y	0.420	0.116	95.0	16.0	1,000	Small-size balanced cable
		111A/U	2 cond. 7/0.0152 copper	A	0.285	Tinned copper	Y Armor	0.490 (max)	1.145	95.0	16.0	1,000	Same as RG-22B/U, but armored

*See notes on page 607.

Attenuation and power rating of lines and cables

Attenuation: On pp. 614 and 615 is a chart that illustrates the attenuation of general-purpose radio-frequency lines and cables up to their practical upper frequency limit. Most of these are coaxial-type lines, but wave-guide and microstrip are included for comparison.

The following notes are applicable to this table.

a. For the RG-type cables, only the number is given (for instance, the curve for RG-14A/U is labeled only, 14). (See table on pages 607–611.) The data on RG-type cables taken mostly from, "Index of RF Lines and Fittings," Armed Services Electro-Standards Agency, Fort Monmouth, New Jersey, publication 49-2B, 1 November 1955 supplement, and from "Solid Dielectric Transmission Lines," Radio-Electronics-Television Manufacturer's Association Standard TR-143; February, 1956.

Some approximation is involved in order to simplify the chart. Thus, where a single curve is labeled with several type numbers, the actual attenuation of each individual type may be slightly different from that shown by the curve.

b. The curves for rigid copper coaxial lines are labeled with the diameter of the line only, as $\frac{7}{8}''$C. These have been computed for the standard 50-ohm-size lines listed in Radio-Electronics-Television Manufacturer's Association Standard TR-134; March, 1953. The computations considered the copper losses only, on the basis of a resistivity $\rho = 1.724$ microhm–centimeters; a derating of 20 percent has been applied to allow for imperfect surface, presence of fittings, etc., in long installed lengths. Relative attenuations of the different sizes are as follows:

$A_{6\frac{1}{8}''} \approx 0.13 A_{\frac{7}{8}''}$

$A_{3\frac{1}{8}''} \approx 0.26 A_{\frac{7}{8}''}$

$A_{1\frac{5}{8}''} \approx 0.51 A_{\frac{7}{8}''}$

c. Curves for three sizes of 50-ohm Styroflex cable are copied from a brochure of the manufacturer. These are labeled by size in inches as, $\frac{7}{8}''$S. The velocity factor of this type of cable is approximately $v/c = 0.91$.

d. The microstrip curve is for Teflon-impregnated Fiberglas dielectric 1/16-inch thick and conductor strip 7/32-inch wide.

e. Shown for comparison is the attenuation in the $TE_{1,0}$ mode of 5 sizes of brass waveguide. The resistivity of brass was taken as $\rho = 6.9$ microhm–centimeters, and no derating was applied. For copper or silver, attenuation is about half that for brass. For aluminum, attenuation is about 2/3 that for brass.

Attenuation and power rating of lines and cables *continued*

Power rating: On p. 616 is a chart of the approximate power-transmitting capabilities of various coaxial-type lines. The following notes are applicable.

f. Identification of the curves for the RG-type cables is as in note *a* above. The data for these cables are from the sources indicated in that note. For polyethylene cables, an inner-conductor maximum temperature of 80 degrees centigrade is specified (See note *l*). For high-temperature cables (types 87 and 116, the inner-conductor temperature is 250 degrees centigrade.

g. The curves for rigid coaxial line are labeled with the diameter of the line only, as $\frac{7}{8}''$C. These are rough estimates based largely on miscellaneous charts published in catalogs.

h. For Styroflex cables, see note c above.

i. The curves are for unity voltage standing-wave ratio. Safe operating power is inversely proportional to swr expressed as a numerical ratio greater than unity. Do not exceed maximum operating voltage (see pp. 595 and 607–611).

j. An ambient temperature of 40 degrees centigrade is assumed.

k. The 4 curves meeting the 100-watt abscissa may be extrapolated: at 3000 megacycles for RG-122, maximum average power is 20 watts; for 55,58, power is 28 watts; for 59, power is 44 watts; and for 5,6, power is 58 watts.

l. The Radio–Electronics–Television Manufacturer's Association Standard TR-143 states that operation of a polyethylene dielectric cable at a center-conductor temperature in excess of 80 degrees centigrade is likely to cause permanent damage to the cable. Where practicable, and particularly where continuous flexing is required, it is recommended that a cable be selected which, in regular operation, will produce a center-conductor temperature not greater than 65 degrees centigrade. Rating factors for various operating temperatures are given in the following table. Multiply points on the power-rating curve by the factors in the table to determine power rating at operating conditions.

ambient temperature in degrees centigrade	derating factor — maximum allowable center conductor temperature in degrees centergrade			
	80	75	70	65
40	1.0	0.86	0.72	0.59
50	0.72	0.59	0.46	0.33
60	0.46	0.33	0.22	0.10
70	0.20	0.09	0	—
80	0	—	—	—

Attenuation of cables

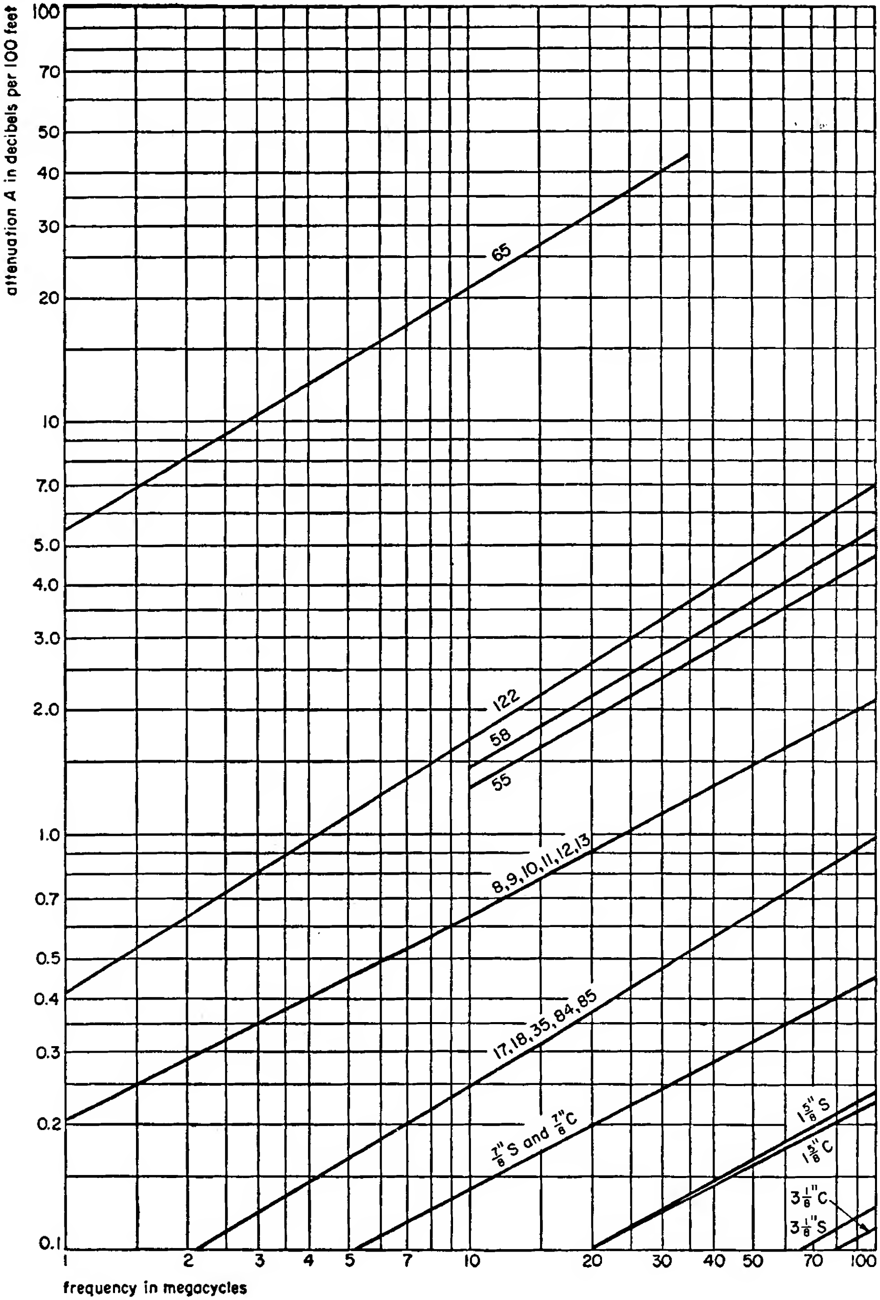

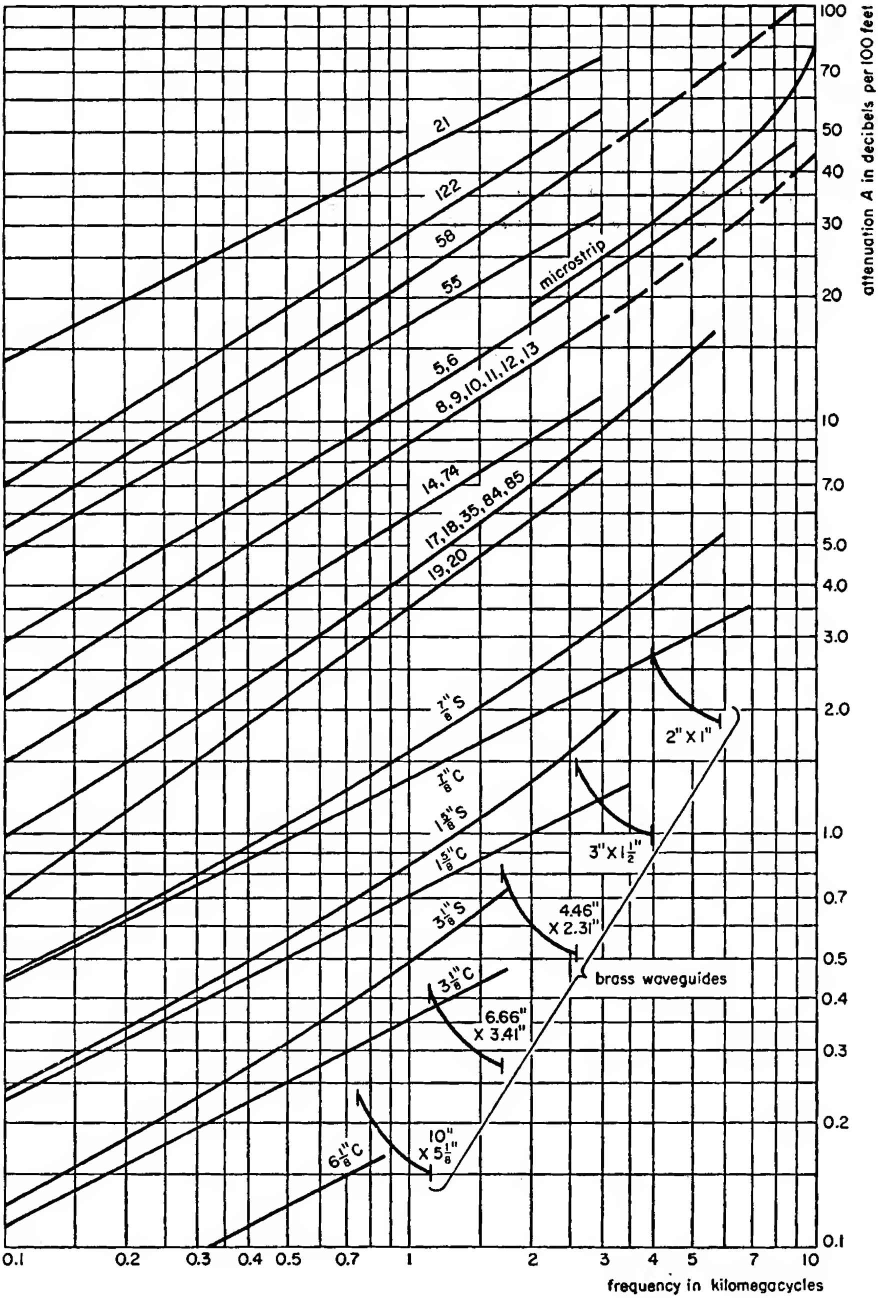

attenuation A in decibels per 100 feet
100
70
50
40
30
20
10
7.0
5.0
4.0
3.0
2.0
1.0
0.7
0.5
0.4
0.3
0.2
0.1
0.1
0.2
0.3
0.4
0.5
0.7
1
2
3
4
5
7
10
frequency in kilomegacycles
21
122
58
55
microstrip
5,6
8,9,10,11,12,13
14,74
17,18,35,84,85
19,20
7/8" S
7/8" C
1 5/8" S
1 5/8" C
3 1/8" S
3 1/8" C
6 1/8" C
2" X 1"
3" X 1 1/2"
4.46" X 2.31"
6.66" X 3.41"
10" X 5 1/8"
brass waveguides

Power rating of cables

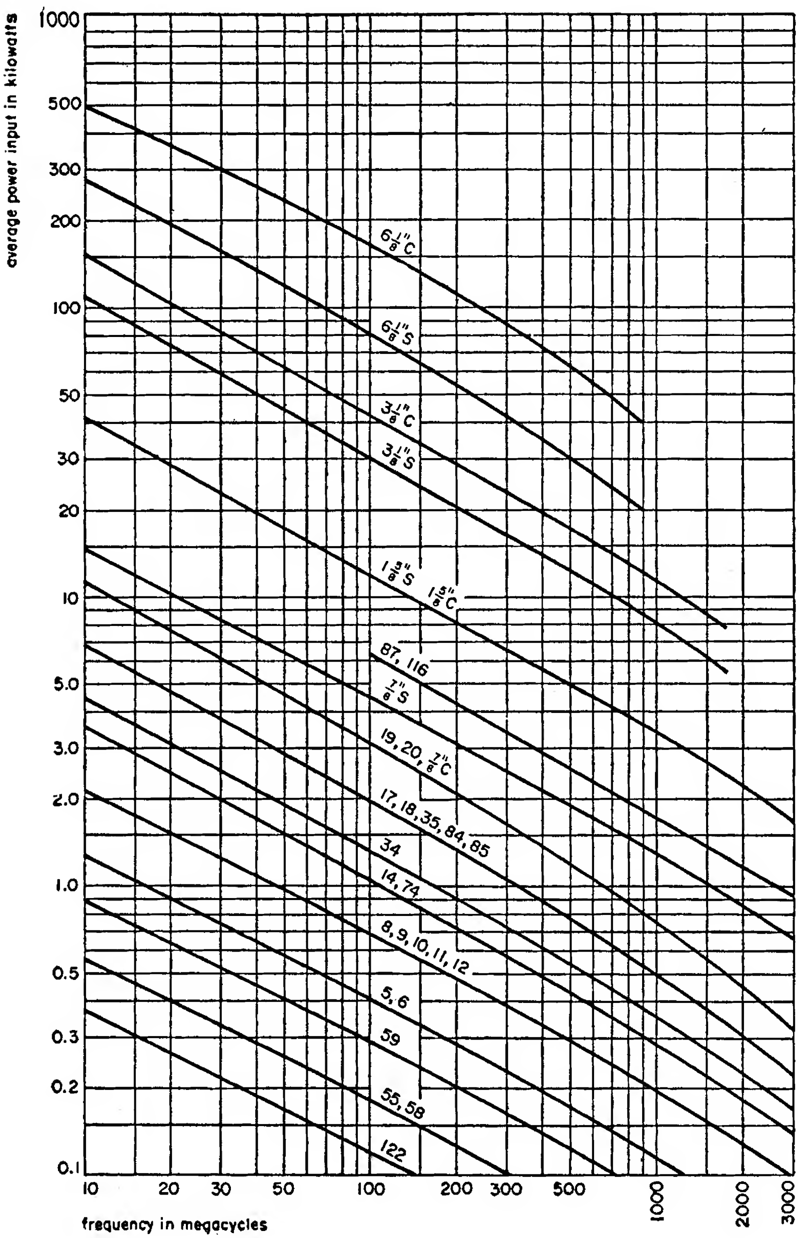

■ Waveguides and resonators

Propagation of electromagnetic waves in hollow waveguides

For propagation of energy at microwave frequencies through a hollow metal tube under fixed conditions, a number of different types of waves are available, namely:

TE waves: Transverse-electric waves, sometimes called H waves, characterized by the fact that the electric vector (*E* vector) is always perpendicular to the direction of propagation. This means that

$$E_z \equiv 0$$

where *z* is the direction of propagation.

TM waves: Transverse-magnetic waves, also called E waves, characterized by the fact that the magnetic vector (*H* vector) is always perpendicular to the direction of propagation.

This means that

$$H_z \equiv 0$$

where *z* is the direction of propagation.

Note—TEM waves: Transverse-electromagnetic waves. These waves are characterized by the fact that both the electric vector (*E* vector) and the magnetic vector (*H* vector) are perpendicular to the direction of propagation. This means that

$$E_z = H_z = 0$$

where *z* is the direction of propagation. This is the mode commonly excited in coaxial and open-wire lines. It cannot be propagated in a waveguide.

The solutions for the field configurations in waveguides are characterized by the presence of the integers *m* and *n* which can take on separate values from 0 or 1 to infinity. Only a limited number of these different *m,n* modes can be propagated, depending on the dimensions of the guide and the frequency of excitation. For each mode there is a definite lower limit or cutoff frequency below which the wave is incapable of being propagated. Thus, a waveguide is seen to exhibit definite properties of a high-pass filter.

The propagation constant $\gamma_{m,n}$ determines the amplitude and phase of each component of the wave as it is propagated along the length of the guide. With $z =$ (direction of propagation) and $\omega = 2\pi \times$ (frequency), the factor for each component is

$$\exp[j\omega t - \gamma_{m,n} z]$$

Propagation of electromagnetic waves in hollow waveguides *continued*

Thus, if $\gamma_{m,n}$ is real, the phase of each component is constant, but the amplitude decreases exponentially with z. When $\gamma_{m,n}$ is real, it is said that no propagation takes place. The frequency is considered below cutoff. Actually, propagation with high attenuation does take place for a small distance, and a short length of guide below cutoff is often used as a calibrated attenuator.

When $\gamma_{m,n}$ is imaginary, the amplitude of each component remains constant, but the phase varies with z. Hence, propagation takes place. $\gamma_{m,n}$ is a pure imaginary only in a lossless guide. In the practical case, $\gamma_{m,n}$ usually has both a real part $\alpha_{m,n}$, which is the attenuation constant, and an imaginary part $\beta_{m,n}$, which is the phase propagation constant. Then

$$\gamma_{m,n} = \alpha_{m,n} + j\beta_{m,n}$$

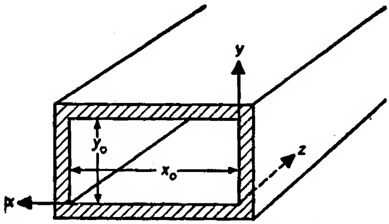

Fig. 1—Rectangular waveguide.

Rectangular waveguides

Fig. 1 shows a rectangular waveguide and a rectangular system of coordinates, disposed so that the origin falls on one of the corners of the waveguide; z is the direction of propagation along the guide, and the cross-sectional dimensions are y_o and x_o.

For the case of perfect conductivity of the guide walls with a nonconducting interior dielectric (usually air), the equations for the $TM_{m,n}$ or $E_{m,n}$ waves in the dielectric are:

$$E_x = -A\,\frac{\gamma_{m,n}}{\gamma^2_{m,n} + \omega^2\mu\epsilon}\left(\frac{m\pi}{x_o}\right)\sin\left(\frac{n\pi}{y_o}y\right)\cos\left(\frac{m\pi}{x_o}x\right)e^{j\omega t-\gamma_{m,n}z}$$

$$E_y = -A\,\frac{\gamma_{m,n}}{\gamma^2_{m,n} + \omega^2\mu\epsilon}\left(\frac{n\pi}{y_o}\right)\cos\left(\frac{n\pi}{y_o}y\right)\sin\left(\frac{m\pi}{x_o}x\right)e^{j\omega t-\gamma_{m,n}z}$$

$$E_z = A\sin\left(\frac{n\pi}{y_o}y\right)\sin\left(\frac{m\pi}{x_o}x\right)e^{j\omega t-\gamma_{m,n}z}$$

$$H_x = -A\,\frac{j\omega\epsilon}{\gamma^2_{m,n} + \omega^2\mu\epsilon}\left(\frac{n\pi}{y_o}\right)\cos\left(\frac{n\pi}{y_o}y\right)\sin\left(\frac{m\pi}{x_o}x\right)e^{j\omega t-\gamma_{m,n}z}$$

$$H_y = A\,\frac{j\omega\epsilon}{\gamma^2_{m,n} + \omega^2\mu\epsilon}\left(\frac{m\pi}{x_o}\right)\sin\left(\frac{n\pi}{y_o}y\right)\cos\left(\frac{m\pi}{x_o}x\right)e^{j\omega t-\gamma_{m,n}z}$$

$$H_z \equiv 0$$

Rectangular waveguides *continued*

where ϵ is the dielectric constant and μ the permeability of the dielectric material in meter-kilogram-second (rationalized) units.

Constant A is determined solely by the exciting voltage. It has both amplitude and phase. Integers *m* and *n* may individually take values from 1 to infinity. No TM waves of the 0,0 type or 1,0 type are possible in a rectangular guide so that neither *m* nor *n* may be 0.

Equations for the $TE_{m,n}$ waves or $H_{m,n}$ waves in a dielectric are:

$$E_x = -B \frac{j\omega\mu}{\gamma^2_{m,n} + \omega^2\mu\epsilon} \left(\frac{n\pi}{y_o}\right) \sin\left(\frac{n\pi}{y_o} y\right) \cos\left(\frac{m\pi}{x_o} x\right) e^{j\omega t - \gamma_{m,n}z}$$

$$E_y = B \frac{j\omega\mu}{\gamma^2_{m,n} + \omega^2\mu\epsilon} \left(\frac{m\pi}{x_o}\right) \cos\left(\frac{n\pi}{y_o} y\right) \sin\left(\frac{m\pi}{x_o} x\right) e^{j\omega t - \gamma_{m,n}z}$$

$$E_z \equiv 0$$

$$H_x = B \frac{\gamma_{m,n}}{\gamma^2_{m,n} + \omega^2\mu\epsilon} \left(\frac{m\pi}{x_o}\right) \cos\left(\frac{n\pi}{y_o} y\right) \sin\left(\frac{m\pi}{x_o} x\right) e^{j\omega t - \gamma_{m,n}z}$$

$$H_y = B \frac{\gamma_{m,n}}{\gamma^2_{m,n} + \omega^2\mu\epsilon} \left(\frac{n\pi}{y_o}\right) \sin\left(\frac{n\pi}{y_o} y\right) \cos\left(\frac{m\pi}{x_o} x\right) e^{j\omega t - \gamma_{m,n}z}$$

$$H_z = B \cos\left(\frac{n\pi}{y_o} y\right) \cos\left(\frac{m\pi}{x_o} x\right) e^{j\omega t - \gamma_{m,n}z}$$

where ϵ is the dielectric constant and μ the permeability of the dielectric material in meter-kilogram-second (rationalized) units.

Constant *B* depends only on the original exciting voltage and has both magnitude and phase; *m* and *n* individually may assume any integer value from 0 to infinity. The 0,0 type of wave where both *m* and *n* are 0 is not possible, but all other combinations are.

As stated previously, propagation only takes place when the propagation constant $\gamma_{m,n}$ is imaginary;

$$\gamma_{m,n} = \sqrt{\left(\frac{m\pi}{x_o}\right)^2 + \left(\frac{n\pi}{y_o}\right)^2 - \omega^2\mu\epsilon}$$

This means, for any *m,n* mode, propagation takes place when

$$\omega^2\mu\epsilon > \left(\frac{m\pi}{x_o}\right)^2 + \left(\frac{n\pi}{y_o}\right)^2$$

Rectangular waveguides *continued*

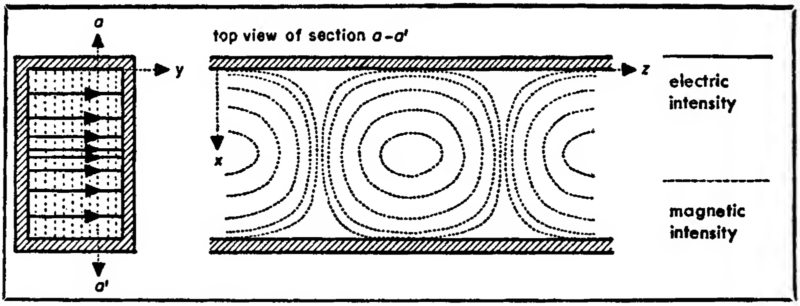

Fig. 2—Field configuration for $TE_{1,0}$ wave.

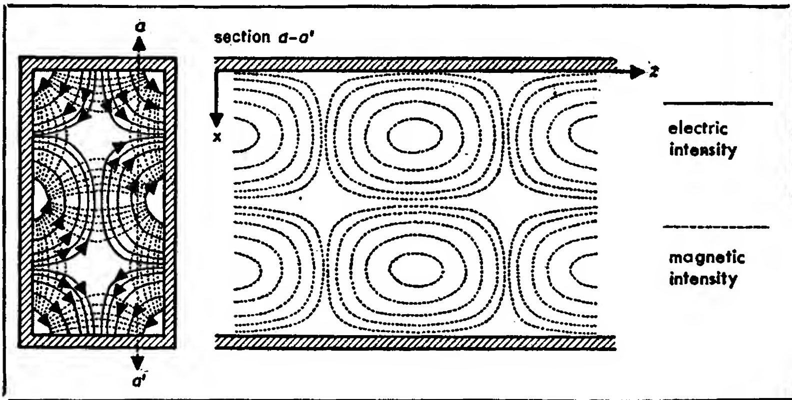

Fig. 3—Field configuration for a $TE_{2,1}$ wave.

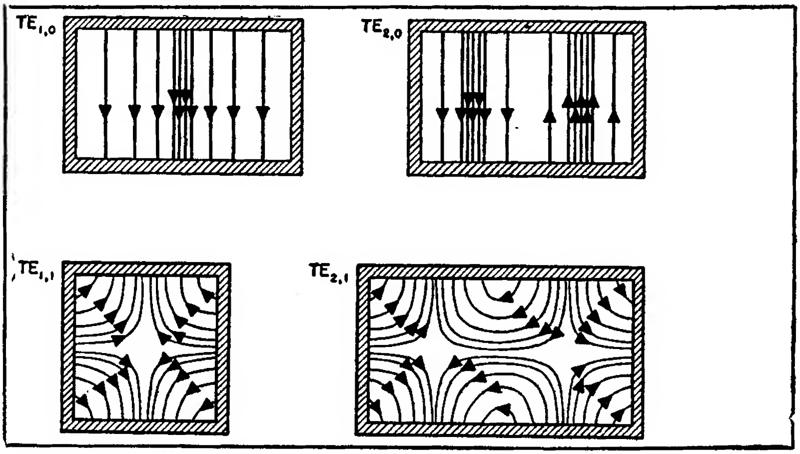

Fig. 4—Characteristic *E* lines for TE waves.

Rectangular waveguides *continued*

or, in terms of frequency f and velocity of light c, when

$$f > \frac{c}{2\pi\sqrt{\mu_1\epsilon_1}}\sqrt{\left(\frac{m\pi}{x_o}\right)^2 + \left(\frac{n\pi}{y_o}\right)^2}$$

where μ_1 and ϵ_1 are the relative permeability and relative dielectric constant, respectively, of the dielectric material with respect to free space.

The wavelength in the air-filled waveguide is always greater than the wavelength in free space. The wavelength in the dielectric-filled wave guide may be less than the wavelength in free space. If λ is the wavelength in free space and the medium filling the waveguide has a relative dielectric constant ϵ,

$$\lambda_{g(m,n)} = \frac{\lambda}{\sqrt{\epsilon - \left(\frac{m\lambda}{2x_o}\right)^2 - \left(\frac{n\lambda}{2y_o}\right)^2}} = \frac{\lambda}{\sqrt{\epsilon - \left(\frac{\lambda}{\lambda_c}\right)^2}}$$

where $(1/\lambda_c)^2 = (m/2x_0)^2 + (n/2y_0)^2$

The phase velocity within the guide is also always greater than in an unbounded medium. The phase velocity v and group velocity u are related by the following equation:

$$u = c^2/v$$

where the phase velocity is given by $v = c\lambda_g/\lambda$ and the group velocity is the velocity of propagation of the energy.

To couple energy into waveguides, it is necessary to understand the configuration of the characteristic electric and magnetic lines. Fig. 2 illustrates the field configuration for a $TE_{1,0}$ wave. Fig. 3 shows the instantaneous field configuration for a higher mode, a $TE_{2,1}$ wave.

In Fig. 4 are shown only the characteristic E lines for the $TE_{1,0}$, $TE_{2,0}$, $TE_{1,1}$, and $TE_{2,1}$ waves. The arrows on the lines indicate their instantaneous relative directions. In order to excite a TE wave, it is necessary to insert a probe to coincide with the direction of the E lines. Thus, for a $TE_{1,0}$ wave, a single probe projecting from the side of the guide parallel to the E lines would be sufficient to couple into it. Several means of coupling from a coaxial line to a rectangular waveguide to excite the $TE_{1,0}$ mode are shown in Fig. 5. With structures such as these, it is possible to make the standing-wave ratio due to the junction less than 1.15 over a 10- to 15-percent frequency band.

Fig. 6 shows the instantaneous configuration of a $TM_{1,1}$ wave; Fig. 7, the instantaneous field configuration for a $TM_{2,1}$ wave. Coupling to this type of wave may be accomplished by inserting a probe, which is parallel to the E lines, or by means of a loop so oriented as to link the lines of flux.

Rectangular waveguides *continued*

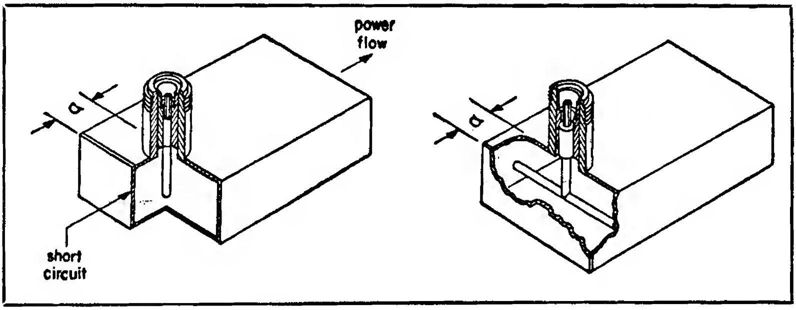

Fig. 5—Methods of coupling to $TE_{1,0}$ mode ($a \approx \lambda_g/4$).

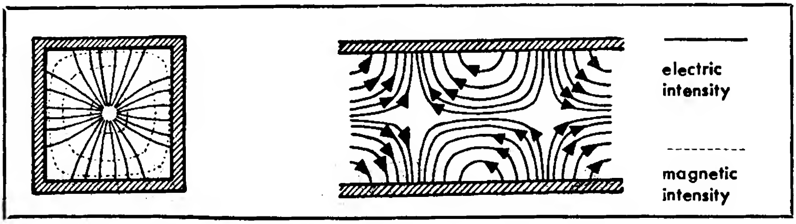

Fig. 6—Instantaneous field configuration for a $TM_{1,1}$ wave.

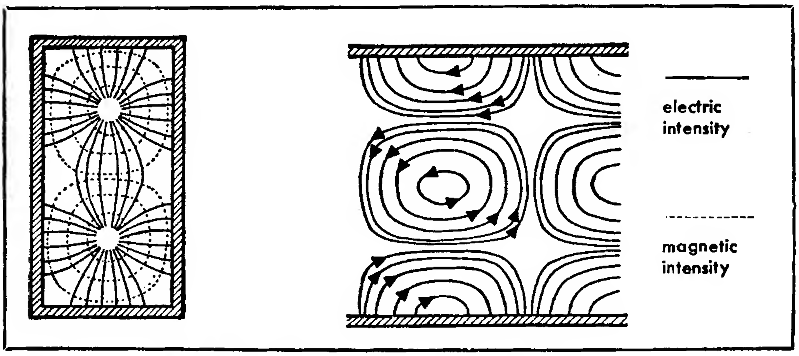

Fig. 7—Instantaneous field configuration for a $TM_{2,1}$ wave.

Circular waveguides

The usual coordinate system is ρ, θ, z, where ρ is in the radial direction; θ is the angle; z is in the longitudinal direction.

TM waves (E waves): $H_z \equiv 0$

$$E_\rho = H_\theta \, \eta \, \frac{\lambda}{\lambda_{g(m,n)}}$$

Circular waveguides *continued*

$$E_\theta = -H_\rho \eta \frac{\lambda}{\lambda_{g(m,n)}}$$

$$E_z = A\, J_n\, (k_{m,n}\, \rho)\, \cos n\, \theta\, e^{j\omega t - \gamma_{m,n} z}$$

$$H_\rho = -jA \frac{2\pi n}{\lambda k^2_{m,n} \eta \rho}\, J_n\, (k_{m,n} \rho)\, \sin n\, \theta\, e^{j\omega t - \gamma_{m,n} z}$$

$$H_\theta = -jA \frac{2\pi}{\lambda k_{m,n} \eta}\, J'_n\, (k_{m,n} \rho)\, \cos n\, \theta\, e^{-j\omega t - \gamma_{m,n} z}$$

where $\eta = (\mu/\epsilon)^{1/2}$ with μ and ϵ in absolute units.

By the boundary conditions, $E_z = 0$ when $\rho = a$, the radius of the guide. Thus, the only permissible values of k are those for which $J_n\, (k_{m,n}\, a) = 0$ because E_z must be zero at the boundary.

The numbers m, n take on all integral values from zero to infinity. The waves are seen to be characterized by the numbers, m and n, where n gives the order of the bessel functions, and m gives the order of the root of $J_n\, (k_{m,n}\, a)$. The bessel function has an infinite number of roots, so that there are an infinite number of k's that make $J_n\, (k_{m,n}\, a) = 0$.

TE waves (H waves): $E_z \equiv 0$

$$E_\rho = jB \frac{2\pi n \eta}{\lambda k^2_{m,n}\, \rho}\, J_n\, (k_{m,n} \rho)\, \sin n\, \theta\, e^{j\omega t - \gamma_{m,n} z}$$

$$E_\theta = jB \frac{2\pi \eta}{\lambda k_{m,n}}\, J'_n\, (k_{m,n} \rho)\, \cos n\, \theta\, e^{j\omega t - \gamma_{m,n} z}$$

$$H_\rho = -E_\theta \frac{\lambda_{g(m,n)}}{\eta \lambda}$$

$$H_\theta = E_\rho \frac{\lambda_{g(m,n)}}{\eta \lambda}$$

$$H_z = BJ_n\, (k_{m,n}\, \rho)\, \cos n\theta\, e^{j\omega t - \gamma_{m,n} z}$$

Again n takes on integral values from zero to infinity. The boundary condition $E_\theta = 0$ when $\rho = a$ still applies. To satisfy this condition k must be such as to make $J'_n\, (k_{m,n}\, a)$ equal to zero [where the superscript indicates the derivative of $J_n\, (k_{m,n}\, a)$]. It is seen that m takes on values from 1 to infinity since there are an infinite number of roots of $J'_n\, (k_{m,n}\, a)$.

Circular waveguides *continued*

For circular waveguides, the cutoff frequency for the *m,n* mode is

$$f_{c(m,n)} = c\, k_{m,n}/2\pi$$

where c = velocity of light and $k_{m,n}$ is evaluated from the roots of the bessel functions

$$k_{m,n} = U_{m,n}/a \quad \text{or} \quad U'_{m,n}/a$$

where a = radius of guide or pipe and $U_{m,n}$ is the root of the particular bessel function of interest (or its derivative).

The wavelength in any guide filled with a homogeneous dielectric ϵ (relative) is

$$\lambda_g = \lambda_0/[\epsilon - (\lambda_0/\lambda_c)^2]^{1/2}$$

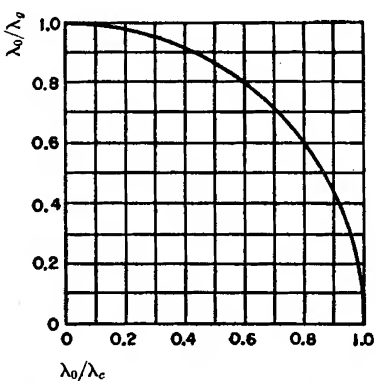

Fig. 8—Chart for determining guide wavelength.

where λ_0 is the wavelength in free space, and λ_c is the free-space cutoff wavelength for any mode under consideration.

The following tables are useful in determining the values of k. For TE waves the cutoff wavelengths are given in the following table.

Values of λ_c/a (where a = radius of guide)

n \ m	0	1	2
1	1.640	3.414	2.057
2	0.896	1.178	0.937
3	0.618	0.736	0.631

For TM waves the cutoff wavelengths are given in the following table.

Values of λ_c/a

n \ m	0	1	2
1	2.619	1.640	1.224
2	1.139	0.896	0.747
3	0.726	0.618	0.541

Circular waveguides *continued*

where n is the order of the bessel function and m is the order of the root.

Fig. 8 shows λ_0/λ_g as a function of λ_0/λ_c. From this, λ_g may be determined when λ_0 and λ_c are known.

The pattern of magnetic force of TM waves in a circular waveguide is shown in Fig. 9. Only the maximum lines are indicated. In order to excite this type of pattern, it is necessary to insert a probe along the length of the waveguide and concentric with the H lines. For instance, in the $TM_{0,1}$ type of wave, a probe extending down the length of the waveguide at the very center of the guide would provide the proper excitation. This method of excitation is shown in Fig. 10. Corresponding methods of excitation may be used for the other types of TM waves shown in Fig. 9.

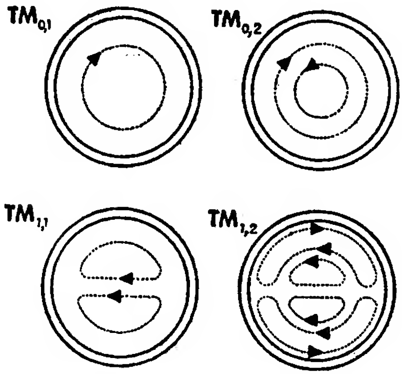

Fig. 9—Patterns of magnetic force of TM waves in circular waveguides.

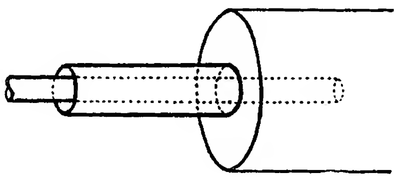

Fig. 10—Method of coupling to circular waveguide for $TM_{0,1}$ wave.

Fig. 11 shows the patterns of electric force for TE waves. Again only the maximum lines are indicated. This type of wave may be excited by an antenna that is parallel to the electric lines of force. The $TE_{1,1}$ wave may be excited by means of an antenna extending across the waveguide. This is illustrated in Fig. 12.

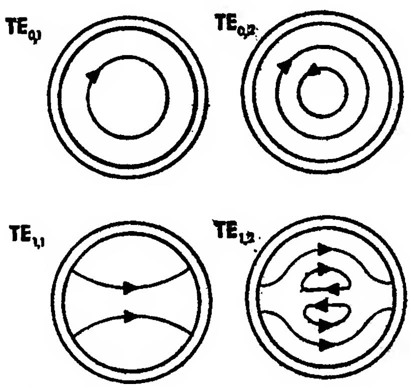

Fig. 11—Patterns of electric force of TE waves in circular waveguides.

Propagating E waves have a minimum attenuation at $(3)^{1/2} f_c$.

The $H_{1,1}$ wave has minimum attenuation at the frequency 2.6 $(3)^{1/2} f_c$.

Circular waveguides *continued*

The $H_{0,1}$ wave has the interesting and useful property that attenuation decreases as the frequency increases. The fact that this is true for all frequencies makes this transmission mode unique.

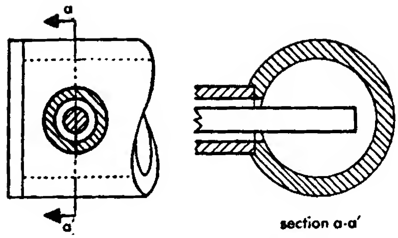

Fig. 12—Method of coupling to circular waveguide for $TE_{1,1}$ wave.

Ridged waveguides*

To lower the cutoff frequency of a waveguide for use over a wider-than-normal frequency band, ridges may be used. By proper choice of dimensions, it is possible to obtain as much as a four-to-one ratio between cutoff frequencies for the $TE_{2,0}$ and $TE_{1,0}$ modes.

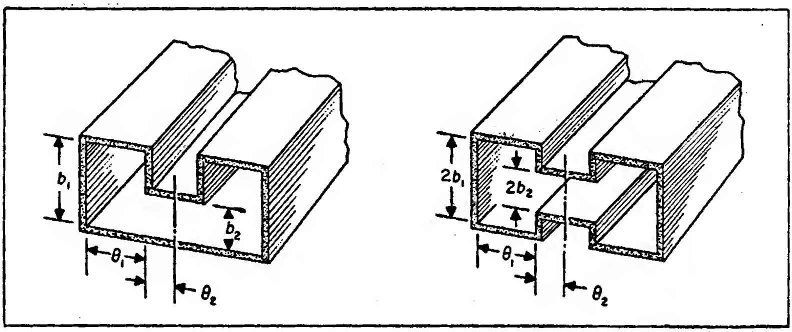

Fig. 13—Asymmetrical and symmetrical ridged waveguides.

Fig. 13 pictures two forms of commonly used ridged waveguide.

The value for the cutoff wavelength λ_c is

$$\lambda_c = \left(\frac{90^\circ}{\theta_1 + \theta_2}\right) \lambda_{c0}$$

where $\lambda_{c0} = 2a$ = cutoff wavelength without ridges and θ_1 and θ_2 satisfy the approximate equation

$$\cot \theta_1 + (b_1/b_2) \cot \theta_2 = 0.$$

The last equation is approximately true for small θ_1 and small b_1/b_2, since it assumes no discontinuity susceptance at the ridge edges.

* "Very-High-Frequency Techniques," McGraw-Hill Book Company Incorporated, New York, N. Y.; 1947: pp. 678–684.

Attenuation constants

Fig. 14—Cutoff wavelengths and attenuation factors; all dimensions are in meters.

Type of guide	coaxial cable TEM 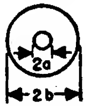	rectangular pipe $TE_{m,0}$ or $H_{m,0}$ 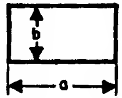	circular pipe 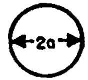 $TM_{0,1}$ or $E_{0,1}$	circular pipe $TE_{1,1}$ or $H_{1,1}$	circular pipe $TE_{0,1}$ or $H_{0,1}$
Cutoff wavelength λ_c	0	$\frac{2a}{m}$	$2.613a$	$3.412a$	$1.640a$
Attenuation constant $= \alpha$ (nepers/meter)	$\alpha_o \sqrt{\frac{c}{\lambda}} \frac{\left(\frac{1}{a} + \frac{1}{b}\right)}{\log_e \frac{b}{a}}$ (See also p. 574)	$\frac{4\alpha_o A}{a}\left(\frac{a}{2b} + \frac{\lambda^2}{\lambda_c^2}\right)$	$\frac{2\alpha_o}{a} A$	$\frac{2\alpha_o}{a} A \left(0.415 + \frac{\lambda^2}{\lambda_c^2}\right)$	$\frac{2\alpha_o}{a} A \left(\frac{\lambda}{\lambda_c}\right)^2$

where λ_c = cutoff wavelength $\quad A = \frac{\sqrt{c/\lambda}}{\sqrt{1 - (\lambda/\lambda_c)^2}} \quad \alpha_0 = \frac{1}{2}\sqrt{\frac{\mu_2\,\epsilon_1\pi}{\sigma_2\,\mu_1}}$ (M.K.S.)

Attenuation constants *continued*

All of the attenuation constants contain a common coefficient

$$\alpha_0 = \tfrac{1}{2}\,(\mu_2\epsilon_1\pi/\sigma_2\mu_1)^{1/2}$$

where

ϵ_1 = dielectric constant of insulator

μ_1 = magnetic permeability of insulator

σ_2 = electric conductivity of metal

μ_2 = magnetic permeability of metal

For air and copper,

$\alpha_0 = 0.35 \times 10^{-9}$ nepers/meter $= 0.3 \times 10^{-5}$ decibels/kilometer

To convert from nepers/meter to decibels/100 feet, multiply by 264. Fig. 14 summarizes some of the most important formulas. Dimensions a and b are measured in meters.

Attenuation in a waveguide beyond cutoff

When a waveguide is used at a wavelength greater than the cutoff wavelength, there is no real propagation and the fields are attenuated exponenially. The attenuation L in a length d is given by

$$L = 54.5\,\frac{d}{\lambda_c}\left[1 - \left(\frac{\lambda_c}{\lambda}\right)^2\right]^{1/2} \text{ decibels}$$

where

λ_c = cutoff wavelength

λ = operating wavelength

Note that for $\lambda \gg \lambda_c$, attenuation is essentially independent of frequency and

$L = 54.5\, d/\lambda_c$ decibels

λ_c is a function of geometry.

Standard waveguides

Fig. 15 presents a list of rectangular waveguides that have been adopted as standard with some of their properties.

Fig. 15—Standard waveguides.

Radio-Electronics Television Manufacturers Association designation	Army–Navy type number *	outer dimensions and wall thickness	frequency range in kilomegacycles for dominant ($TE_{1,0}$) mode	cutoff wavelength λ_c in centimeters for $TE_{1,0}$ mode	cutoff frequency f_c in kilomegacycles for $TE_{1,0}$ mode	theoretical attenuation, lowest to highest frequency in db/100 ft	theoretical power rating in megawatts for lowest to highest frequency ‡
WR1500		15.000 × 7.500 †	0.47 – 0.75	76.3	0.393		
WR1150		11.500 × 5.750 †	0.64 – 0.96	58.4	0.514		
WR975		10.000 × 5.125 × 0.125	0.75 – 1.12	49.6	0.605		
WR770		7.950 × 4.100 × 0.125	0.96 – 1.45	39.1	0.767		
WR650	RG–69/U	6.660 × 3.410 × 0.080	1.12 – 1.70	33.0	0.908	0.317– 0.212	11.9 –17.2
WR510		5.260 × 2.710 × 0.080	1.45 – 2.20	25.9	1.16		
WR430	RG–104/U	4.460 × 2.310 × 0.080	1.70 – 2.60	21.8	1.375	0.588– 0.385	5.2 – 7.5
WR340		3.560 × 1.860 × 0.080	2.20 – 3.30	17.3	1.735		
WR284	RG–48/U	3.000 × 1.500 × 0.080	2.60 – 3.95	14.2	2.08	1.102– 0.752	2.2 – 3.2
WR229		2.418 × 1.273 × 0.064	3.30 – 4.90	11.6	2.59		
WR187	RG–49/U	2.000 × 1.000 × 0.064	3.95 – 5.85	9.50	3.16	2.08 – 1.44	1.4 – 2.0
WR159		1.718 × 0.923 × 0.064	4.90 – 7.05	8.09	3.71		
WR137	RG–50/U	1.500 × 0.750 × 0.064	5.85 – 8.20	6.98	4.29	2.87 – 2.30	0.56 – 0.71
WR112	RG–51/U	1.250 × 0.625 × 0.064	7.05 – 10.00	5.70	5.26	4.12 – 3.21	0.35 – 0.46
WR90	RG–52/U	1.000 × 0.500 × 0.050	8.20 – 12.40	4.57	6.56	6.45 – 4.48	0.20 – 0.29
WR75		0.850 × 0.475 × 0.050	10.00 – 15.00	3.81	7.88		
WR62	RG–91/U	0.702 × 0.391 × 0.040	12.4 – 18.00	3.16	9.49	9.51 – 8.31	0.12 – 0.16
WR51		0.590 × 0.335 × 0.040	15.00 – 22.00	2.59	11.6		
WR42	RG–53/U	0.500 × 0.250 × 0.040	18.00 – 26.50	2.13	14.1	20.7 –14.8	0.043 – 0.058
WR34		0.420 × 0.250 × 0.040	22.00 – 33.00	1.73	17.3		
WR28	RG–96/U (*)	0.360 × 0.220 × 0.040	26.50 – 40.00	1.42	21.1	21.9 –15.0	0.022 – 0.031
WR22	RG–97/U (*)	0.304 × 0.192 × 0.040	33.00 – 50.00	1.14	26.35	31.0 –20.9	0.014 – 0.020
WR19		0.268 × 0.174 × 0.040	40.00 – 60.00	0.955	31.4		
WR15	RG–98/U (*)	0.228 × 0.154 × 0.040	50.00 – 75.00	0.753	39.9	52.9 –39.1	0.0063– 0.0090
WR12	RG–99/U (*)	0.202 × 0.141 × 0.040	60.00 – 90.00	0.620	48.4	93.3 –52.2	0.0042– 0.0060
WR10		0.180 × 0.130 × 0.040	75.00 –110.00	0.509	59.0		

* In this column, types marked with asterisk are silver; unmarked types are brass.

† Inner dimensions only are specified.

‡ For these computations, the breakdown strength of air was taken as 15,000 volts per centimeter. A safety factor of approximately 2 at sea level has been allowed.

Waveguide circuit elements*

Just as at low frequencies, it is possible to shape metallic or dielectric pieces to produce local concentrations of magnetic or electric energy within a waveguide and thus produce what are, essentially, lumped inductances or capacitances over a limited frequency bandwidth.

This behavior as a lumped element will be evident only at some distance from the obstacle in the guide, since the fields in the immediate vicinity are disturbed.

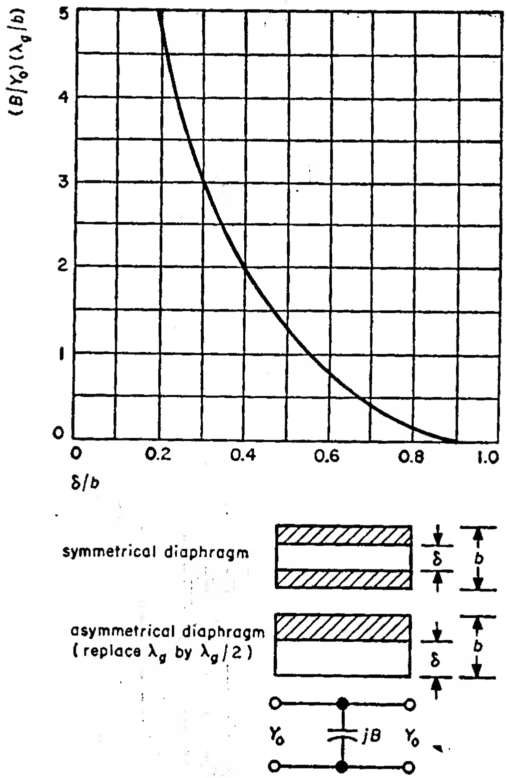

Fig. 16—Normalized susceptance of capacitive diaphragms.

Capacitive elements are formed from electric-field concentrating devices, such as screws or thin diaphragms inserted partially along electric-field lines. These are susceptible to breakdown under high power. Fig. 16 shows the relative susceptance B/Y_0 for symmetrical and asymmetrical diaphragms for small b/λ_g.

A common form of shunted lumped inductance is the diaphragm. Figs. 17 and 18 show the relative susceptance B/Y_0 for symmetrical and asymmetrical diaphragms in rectangular waveguides. These are computed for infinitely thin diaphragms. Finite thicknesses result in an increase in B/Y_0.

Another form of shunt inductance that is useful because of mechanical simplicity is a round post completely across the narrow dimension of a rectangular guide (for $TE_{1,0}$ mode). Figs. 19 and 20 give the normalized values of the elements of the equivalent 4-terminal network for several post diameters.

* For a more complete treatment, refer to C. G. Montgomery, R. H. Dicke, and E. M. Purcell, "Principles of Microwave Circuits," McGraw-Hill Book Company, Incorporated, New York, N. Y.; 1948: Chapters 1 and 6. Also N. Marcuvitz, "Waveguide Handbook," McGraw-Hill Book Company, Incorporated, New York, N. Y.; 1951.

Waveguide circuit elements *continued*

Frequency dependence of waveguide susceptances may be given approximately as follows:

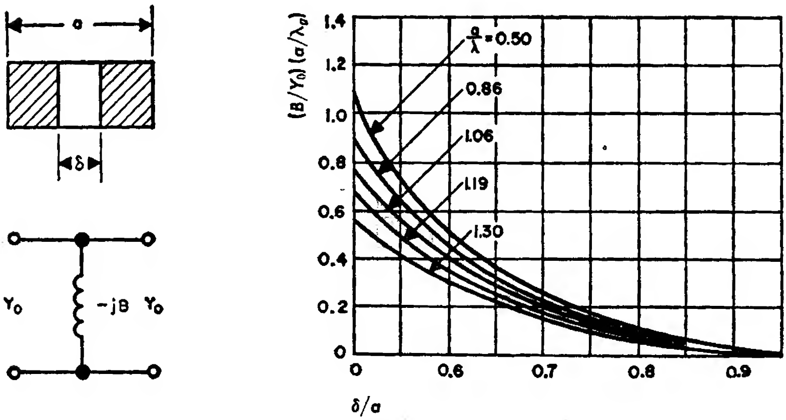

Reprinted from "Microwave Transmission Circuits," by George L. Ragan, 1st ed., 1948; by permission, McGraw-Hill Book Co., N. Y.

Fig. 17—Normalized susceptance of a symmetrical inductive diaphragm.

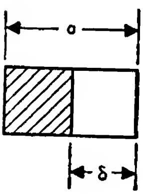

Reprinted from "Microwave Transmission Circuits," by George L. Ragan, 1st ed., 1948; by permission, McGraw-Hill Book Co., N. Y.

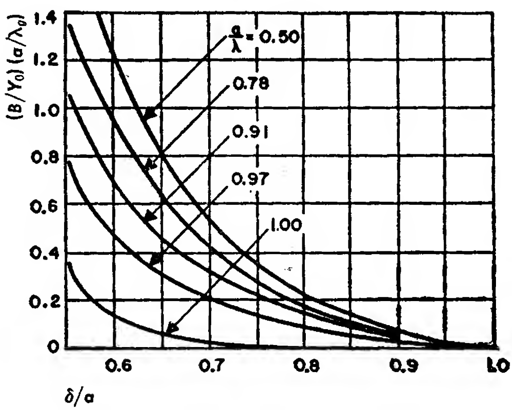

Fig. 18—Normalized susceptance of an asymmetrical inductive diaphragm.

Waveguide circuit elements *continued*

$$\text{Inductive} = B/Y_0 \propto \lambda_g$$

$$\text{Capacitative} = B/Y_0 \propto 1/\lambda_g \text{ (distributed)}$$
$$= B/Y_0 \propto \lambda_g/\lambda^2 \text{ (lumped)}$$

Distributed capacitances are found in junctions and slits, whereas tuning screws act as lumped capacitances.

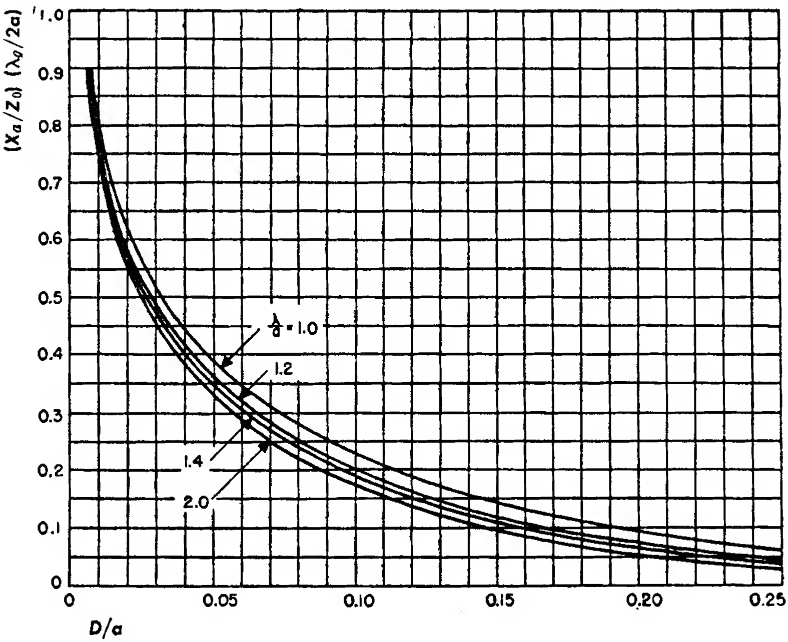

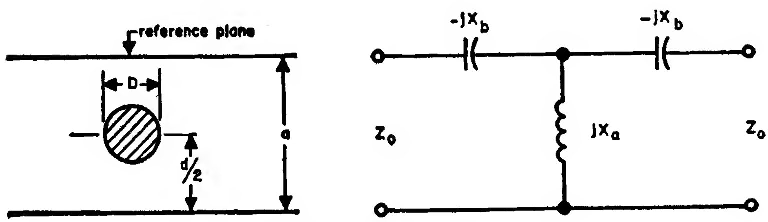

Fig. 19—Equivalent circuit for inductive cylindrical post.

Waveguide circuit elements *continued*

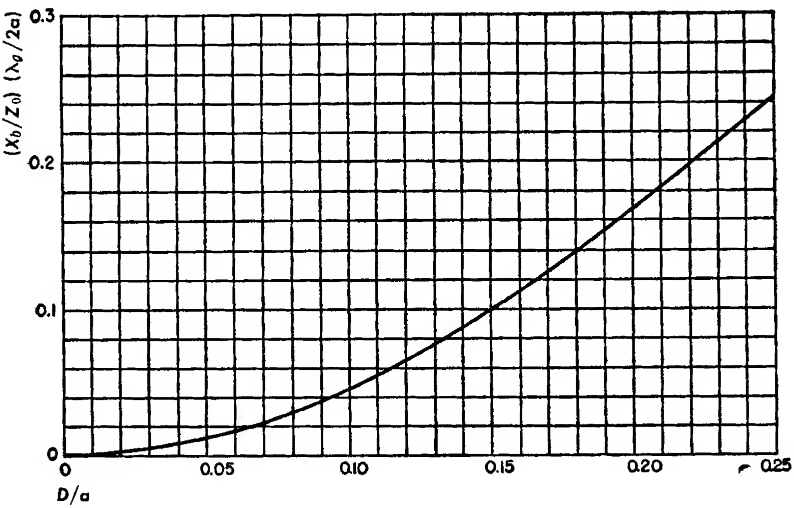

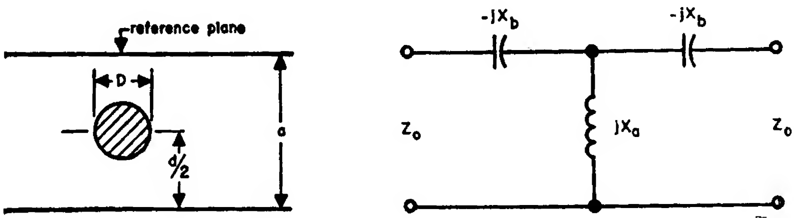

Fig. 20—Equivalent circuit for inductive cylindrical post.

Hybrid junctions*

The hybrid junction is illustrated in various forms in Fig. 21. An ideal junction is characterized by the fact that there is no direct coupling between arms 1 and 4 or between 2 and 3. Power flows from 1 to 4 only by virtue of reflections in arms 2 and 3. Thus, if arm 1 is excited, the voltage arriving at arm 4 is

$$E_4 = \frac{1}{2} E_1 \left(\Gamma_2 e^{j2\theta_2} - \Gamma_3 e^{j2\theta_3}\right)$$

* C. G. Montgomery, R. H. Dicke, and E. M. Purcell, "Principles of Microwave Circuits." McGraw-Hill Book Company, Incorporated, New York, N. Y.; 1948: Chapter 9.

Hybrid junctions *continued*

and the reflected voltage in arm 1 is

$$E_{r1} = \frac{1}{2} E_1 (\Gamma_2 e^{j2\theta_2} + \Gamma_3 e^{j2\theta_3})$$

where E_1 is the amplitude of the incident wave, Γ_2 and Γ_3 are the reflection coefficients of the terminations of arms 2 and 3, and θ_2 and θ_3 are the respective distances of the terminations from the junctions. In the case of the rings, θ is the distance between the arm-and-ring junction and the termination.

If the decoupled arms of the hybrid junction are independently matched

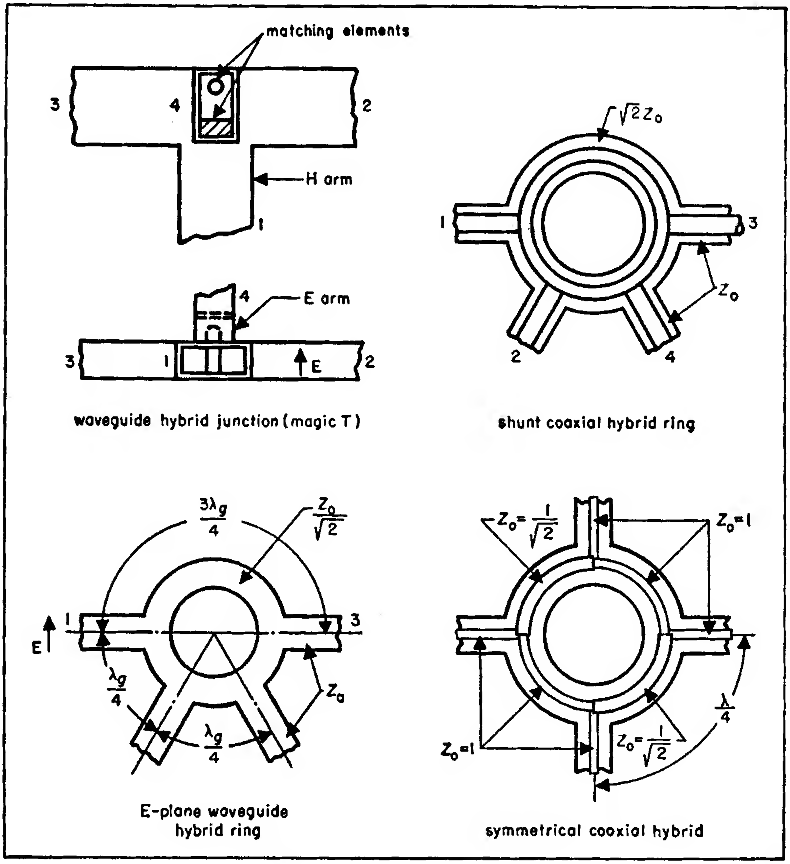

Fig. 21—Hybrid junctions.

Hybrid junctions *continued*

and the other arms are terminated in their characteristic impedances, then all four arms are matched at their inputs.

Resonant cavities

A cavity enclosed by metal walls will have an infinite number of natural frequencies at which resonance will occur. One of the more common types of cavity resonators is a length of transmission line (coaxial or waveguide) short-circuited at both ends.

Resonance occurs when

$2h = l(\lambda_g/2)$

where l is an integer and

$2h$ = length of the resonator

λ_g = guide wavelength in resonator

$= \lambda/[\epsilon - (\lambda/\lambda_c)^2]^{1/2}$

where

λ = free-space wavelength

λ_c = guide cutoff wavelength

ϵ = relative dielectric constant of medium in cavity

For $TE_{m,n}$ or $TM_{m,n}$ waves in a rectangular cavity with cross section a, b,

$\lambda_c = 2/[(m/a)^2 + (n/b)^2]^{1/2}$

where m and n are integers.

For $TE_{m,n}$ waves in a cylindrical cavity

$\lambda_c = 2\pi a/U'_{m,n}$

where a is the guide radius and $U'_{m,n}$ is the mth root of the equation $J'_n(U) = 0$.

For $TM_{m,n}$ waves in a cylindrical cavity

$\lambda_c = 2\pi a/U_{m,n}$

where a is the guide radius and $U_{m,n}$ is the mth root of the equation $J_n(U) = 0$.

For TM waves $l = 0, 1, 2 \ldots$

For TE waves $l = 1, 2 \ldots$, but not 0

Resonant cavities *continued*

Rectangular cavity of dimensions a, b, 2h

$\lambda = 2/[(l/2h)^2 + (m/a)^2 + (n/b)^2]^{1/2}$

where only one of l, m, n may be zero.

Cylindrical cavities of radius a and length 2h

$\lambda = 1/[(l/4h)^2 + (1/\lambda_c)^2]^{1/2}$

where λ_c is the guide cutoff wavelength.

Spherical resonators of radius a

$\lambda = 2\pi a/U_{m,n}$ for a TE wave

$\lambda = 2\pi a/U'_{m,n}$ for a TM wave

Values of $U_{m,n}$:

$U_{1,1} = 4.5, \quad U_{2,1} = 5.8, \quad U_{1,2} = 7.64$

Values of $U'_{m,n}$:

$U'_{1,1} = 2.75$ = lowest-order root

Additional cavity formulas

Note that resonant modes are characterized by three subscripts in the mode designations of Figs. 22–24.

Fig. 22—Formulas for a right-circular-cylindrical cavity.

mode	λ_0 resonant wavelength	Q (all dimensions in same units)
$TM_{0,1,1}$ (E_0)	$\dfrac{4}{\sqrt{\left(\frac{1}{h}\right)^2 + \frac{2.35}{a^2}}}$	$\dfrac{\lambda_0}{\delta}\dfrac{a}{\lambda_0}\dfrac{1}{1+\frac{a}{2h}}$
$TE_{0,1,1}$ (H_0)	$\dfrac{4}{\sqrt{\left(\frac{1}{h}\right)^2 + \frac{5.93}{a^2}}}$	$\dfrac{\lambda_0}{\delta}\dfrac{a}{\lambda_0}\left[\dfrac{1+0.168\left(\frac{a}{h}\right)^2}{1+0.168\left(\frac{a}{h}\right)^3}\right]$
$TE_{1,1,1}$ (H_1)	$\dfrac{4}{\sqrt{\left(\frac{1}{h}\right)^2 + \frac{1.37}{a^2}}}$	$\dfrac{\lambda_0}{\delta}\dfrac{h}{\lambda_0}\left[\dfrac{2.39h^2 + 1.73a^2}{3.39\frac{h^3}{a} + 0.73ah + 1.73a^2}\right]$

Resonant cavities *continued*

Fig. 23—Characteristics of various types of resonators.

type resonator		resonant wavelength, λ_0	Q
Square prism $TE_{1,0,1}$	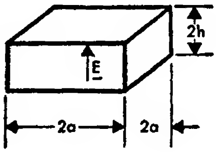	$2\sqrt{2}a$	$\frac{0.353\lambda}{\delta}\ \frac{1}{1+\frac{0.177\lambda}{h}}$
Circular cylinder $TM_{0,1,0}$	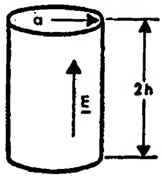	2.61a	$\frac{0.383\lambda}{\delta}\ \frac{1}{1+\frac{0.192\lambda}{h}}$
Sphere	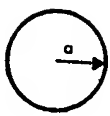	2.28a	$0.318\frac{\lambda}{\delta}$
Sphere with cones	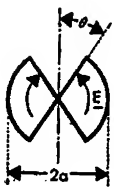	4a	Optimum Q for $\theta = 34°$ $0.1095\frac{\lambda}{\delta}$
Coaxial TEM	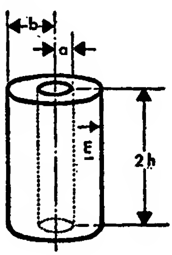	4h	Optimum Q for $\frac{b}{a} = 3.6$ $(Z_0 = 77$ ohms) $\frac{\lambda}{4\delta + 7.2\frac{h\delta}{b}}$

Skin depth in meters $= \delta = \sqrt{10^7/2\pi\omega\sigma}$
where σ = conductivity of wall in mhos/meter and $\omega = 2\pi \times$ frequency

Resonant cavities *continued*

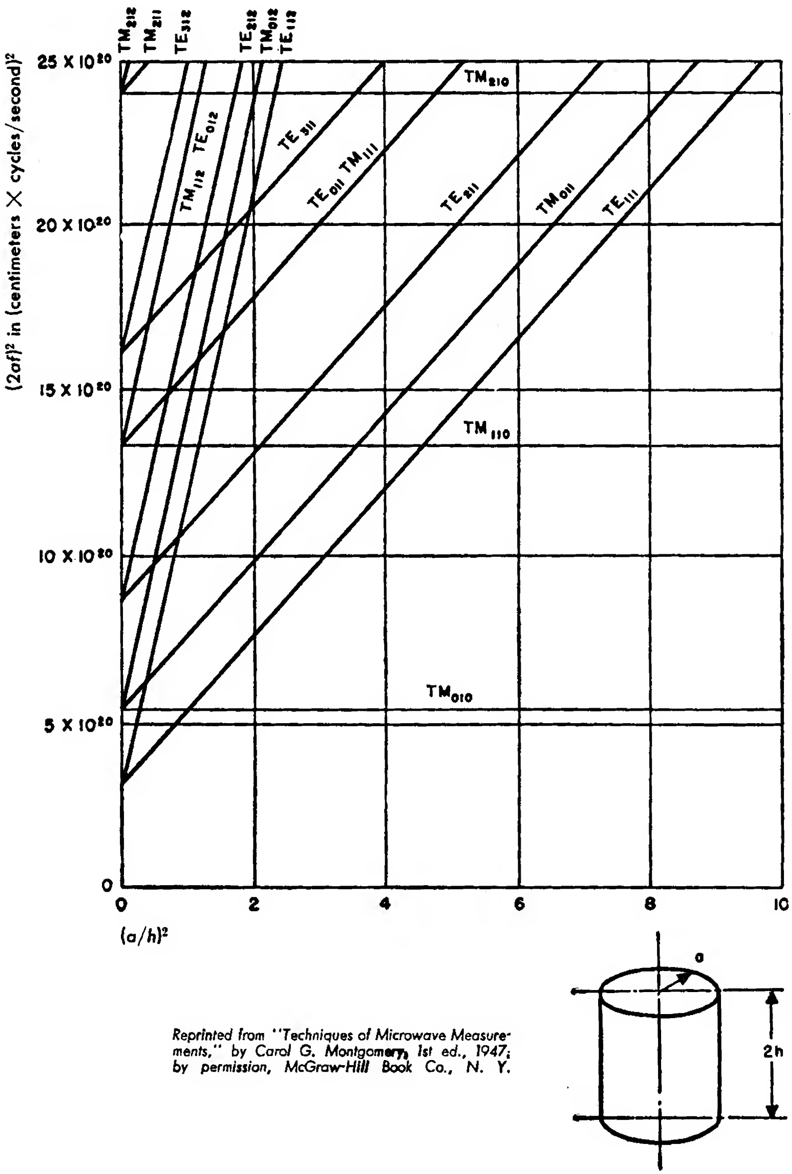

Reprinted from "Techniques of Microwave Measurements," by Carol G. Montgomery, 1st ed., 1947; by permission, McGraw-Hill Book Co., N. Y.

Fig. 24—Mode chart for right-circular-cylindrical cavity.

Resonant cavities *continued*

Fig. 24 is a mode chart for a right-circular-cylindrical resonator, showing the distribution of resonant modes with frequency as a function of cavity shape. With the aid of such a chart, one can predict the various possible resonances as the length ($2h$) of the cavity is varied by means of a movable piston.

Effect of temperature and humidity on cavity tuning

The resonant frequency of a cavity will change with temperature and humidity, due to changes in dielectric constant of the atmosphere, and with thermal expansion of the cavity. A homogeneous cavity made of one kind of metal will have a thermal-tuning coefficient equal to the linear coefficient of expansion of the metal, since the frequency is inversely proportional to the linear dimension of the cavity.

metal	linear coefficient of expansion/°C
Yellow brass	20×10^{-6}
Copper	17.6×10^{-6}
Mild steel	12×10^{-6}
Invar	1.1×10^{-6}

The relative dielectric constant of air (vacuum = 1) is given by

$$k_e = 1 + 210 \times 10^{-6} \frac{P_a}{T} + 180 \times 10^{-6} \left(1 + \frac{5580}{T}\right) \frac{P_w}{T}$$

where P_a and P_w are partial pressures of air and water vapor in millimeters of mercury and T is the absolute temperature. Fig. 25 is a nomograph showing change of cavity tuning relative to conditions at 25 degrees centigrade and 60 percent relative humidity (expansion is not included).

Coupling to cavities and loaded Q

Near resonance, a cavity may be represented as a simple shunt-resonant circuit, characterized by a loaded Q

$$\frac{1}{Q_l} = \frac{1}{Q_0} + \frac{1}{Q_{ext}}$$

where Q_0 is the unloaded Q characteristic of the cavity itself, and $1/Q_{ext}$

Resonant cavities *continued*

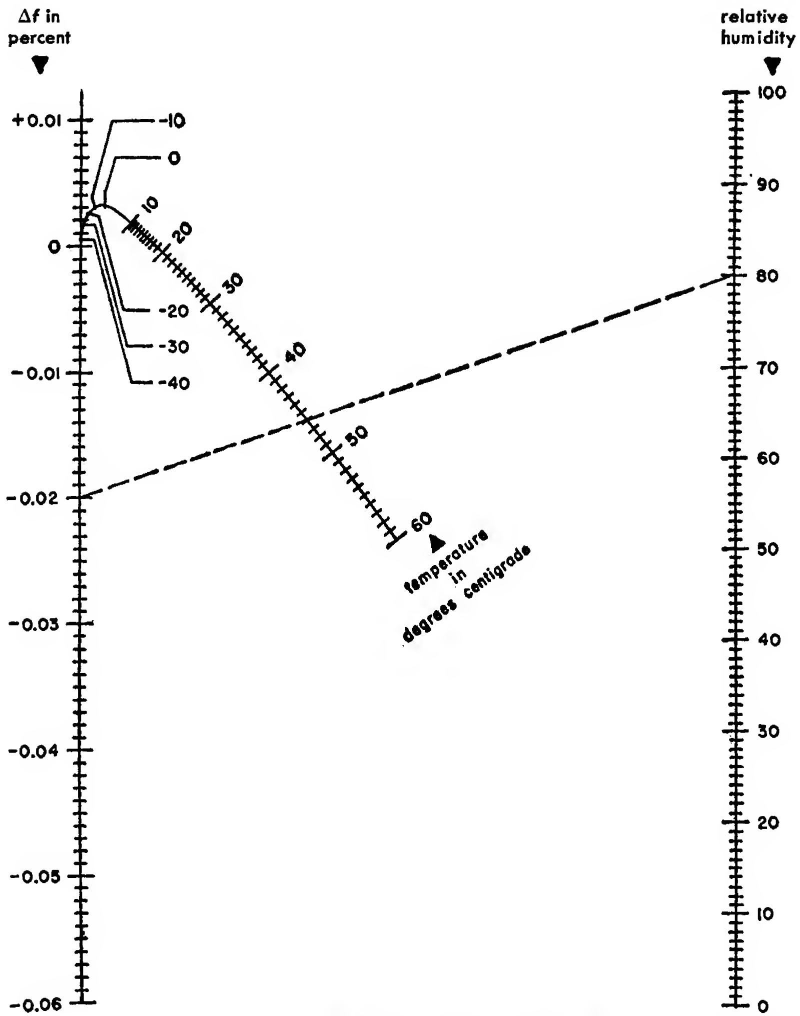

Reprinted from "Techniques of Microwave Measurements," by Carol G. Montgomery, 1st ed., 1947; by permission, McGraw-Hill Book Co., N. Y.

Fig. 25—Effect of temperature and humidity on cavity tuning.

Resonant cavities *continued*

is the loading due to the external circuits. The variation of Q_{ext} with size of the coupling is approximately as follows:

coupling	$1/Q_{ext}$ is proportional to
Small round hole	$(\text{diameter})^6$
Symmetrical inductive diaphragm	$(\delta)^4$ see Fig. 17
Small loop	$(\text{diameter})^4$

Summary of formulas for coupling through a cavity

In Fig. 26 are summarized some of the useful relationships in a 4-terminal cavity (transmission type) for three conditions of coupling: matched input (input resistance at resonance equals Z_0 of input line), equal coupling ($1/Q_{in} = 1/Q_{out}$), and matched output (resistance seen looking into output terminals at resonance equals output-load resistance). A matched generator is assumed.

Fig. 26—Coupling through a cavity.

	matched input	equal coupling	matched output
Input standing-wave ratio	1	$1 + g_c' = 2\left(\frac{1}{\sqrt{T}} - 1\right)$	$1 + 2g_c'$
Transmission ratio $= T$	$1 - g_c' = 1 - 2\rho$	$(1 + g_c'/2)^{-2} = (1 - \rho)^2$	$(1 + g_c')^{-1} = 1 - 2\rho$
$Q_l/Q_0 = \rho$	$\frac{g_c'}{2} = \frac{1 - T}{2}$	$\frac{g_c'}{2 + g_c'} = 1 - \sqrt{T}$	$\frac{g_c'}{2(1 + g_c')} = \frac{1 - T}{2}$

In Fig. 26, g_c' is the apparent conductance of the cavity at resonance, with no output load; the transmission T is the ratio of the actual output-circuit power delivered to the available power from the matched generator. The loaded Q is Q_l and unloaded Q is Q_0.

Cavity coupling techniques*

To couple power into or out of a resonant cavity, either waveguide or coaxial, loops, probes, or apertures may be used.

The essentially inductive loop (a certain amount of electric-field coupling exists) is inserted in the resonator at a desired point where it can couple to a strong magnetic field. The degree of coupling may be controlled by rotating the loop so that more or less loop area links this field. For a fixed location of the loop, the loaded Q of a loop-coupled coaxial resonator

* C. Montgomery, D. Dicke, and E. Purcell, "Principles of Microwave Circuits," McGraw-Hill Book Company, Incorporated, New York, N. Y.; 1948: chapter 7.

Resonant cavities *continued*

varies as the square of the effective loop area and inversely as the square of the distance of the loop center from the resonator axis of revolution.

The off-resonance input impedance of the loop is low, a feature that sometimes is helpful in series connections.

The capacitative probe is inserted in the resonator at a point where it is parallel to and can couple to strong electric fields. The degree of coupling is controlled by varying the length of the probe relative to the electric field.

The off-resonance input impedance of the probe-coupled resonator is high, which property is useful in parallel connections.

Aperture coupling is suitable when coupling waveguides to resonators or in coupling resonators together. In this case, the aperture must be located and shaped so as to excite the proper propagating modes.

For all means of coupling, the input impedance at resonance and the loaded Q may be adjusted by proper selection of the point of coupling and the degree of coupling.

Simple waveguide cavity*

A cavity may be made by enclosing a section of waveguide between a pair of large shunt susceptances, as shown in Fig. 27. Its loaded Q is given by

$$Q_l = \frac{1}{4}\,(\lambda_g/\lambda)^2\,(b^4 + 4b^2)^{1/2}\,\tan^{-1}(2/b)$$

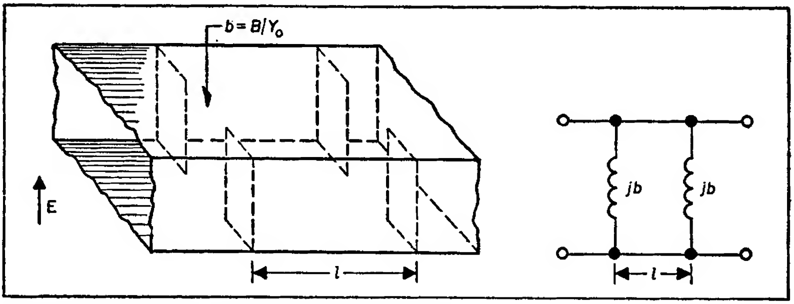

Fig. 27—Waveguide cavity and equivalent circuit.

and the resonant guide wavelength λ_{g0} is obtained from

$$2\pi l/\lambda_{g0} = \tan^{-1}(2/b)$$

* G. L. Ragan, "Microwave Transmission Circuits," McGraw-Hill Book Company, Incorporated, New York, N. Y.; 1948: chapter 10.

Resonant cavities *continued*

Resonant irises

Resonant irises may be used to obtain low values of loaded $Q(< 30)$. The simplest type is shown in Fig. 28. It consists of an inductive diaphragm and a capacitive screw located in the same plane across the waveguide. For $Q_l < 50$, the losses in the resonant circuit may be ignored and

$$1/Q_l \approx 1/Q_{ext}$$

To a good approximation, the loaded Q (matched load and matched generator) is given by

$$Q_l = (B_l/2Y_0)\ (\lambda_{g0}/\lambda)^2$$

where B_l is the susceptance of the inductive diaphragm. This value may be taken from charts such as Figs. 17 and 18 as a starting point, but because of the proximity of the elements, the susceptance value is modified. Exact Q's must be obtained experimentally. Other resonant structures are given in Figs. 29 and 30. These are often designed so that the capacitive gap will break down under high power levels for use as transmit-receive (tr) switches in radar systems.

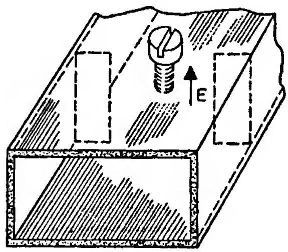

Fig. 28—Resonant iris in waveguide. The capacitive screw is tuned to resonance with the inductive diaphragm.

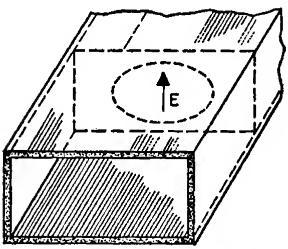

Fig. 29—Resonant element consisting of an oblong aperture in a thin transverse diaphragm.

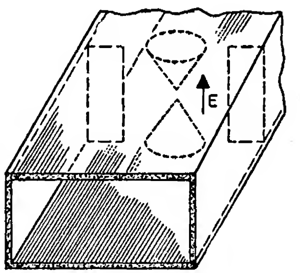

Fig. 30—Resonant structure consisting of cones with capacitive gap between apexes with thin symmetrical inductive diaphragm.

Scattering matrixes

Microwave structures are characterized by dimensions that are of the order of the wavelength of the propagated signal. The notions of current, voltage, and impedance, useful at lower frequencies, have been successfully extended to these structures, but these quantities are not as directly available for measurement: there are no voltmeters or ammeters and no apparent "terminal pair" between which to connect them. The electromagnetic field itself, distributed throughout a region, becomes the relevant quantity.

Within uniform structures, which are the usual form of waveguides, the *power flow* and the *phase* of the field at a cross section are the quantities of importance. The most usual form of measurement, that of the standing-wave pattern in a slotted section, is easily interpreted in terms of *traveling* waves and gives directly the *reflection coefficient*. The scattering description of waveguide junctions was introduced* to express this point of view. It is not, however, restricted to microwaves; a low-frequency network can be considered as a "waveguide junction" between transmission lines† connected to its terminal pairs and the scattering matrix is a useful complement to the impedance and admittance descriptions.

Amplitude of a traveling wave

In a uniform waveguide, a traveling wave is characterized, for a given mode and frequency, by the electromagnetic-field distribution in a transverse cross section and by a propagation constant h. The field in any other cross section, at a distance z in the direction of propagation, has the same pattern but is multiplied by $\exp(-jhz)$. A wave propagating in the opposite direction, for the same mode and frequency, varies with z as $\exp(jhz)$. When losses are negligible, h is real.

The *amplitude* of a traveling wave, at a given cross section in the waveguide, is a complex number a defined as follows. The square $|a^2|$ of the magnitude of a is the power flow,‡ that is, the integral of the Poynting vector over the waveguide cross section. The phase angle of a is that of the transverse field in the cross section.§

* C. G. Montgomery, R. H. Dicke, E. M. Purcell, "Principles of Microwave Circuits," McGraw-Hill Book Company, Inc., New York, N. Y.: 1948.

† Transmission lines are in fact considered as special cases of waveguides: see, "IRE Standards on Antennas and Waveguides: Definitions of Terms, 1953," The Institute of Radio Engineers, Inc.; New York, N. Y.: 1953. Published in *Proceedings of the IRE*, vol. 41, pp. 1721–1728; December, 1953.

‡ The amplitude is sometimes defined to make the power flow equal to $\frac{1}{2}|a|^2$ rather than to $|a|^2$. This would correspond to the use of peak values instead of root-mean-square values.

§ This phase is well defined for a pure mode, since the field has the same phase everywhere in the cross section.

Amplitude of a traveling wave *continued*

The amplitude of a given traveling wave varies with z as $\exp(-jhz)$.

The wave amplitude has the dimensions of the square root of a power. The meter–kilogram–second unit is therefore the $(\text{watt})^{1/2}$.

Reflection coefficient

Definition

At a cross section in a waveguide, the reflection coefficient is the ratio of the amplitudes of the waves traveling respectively in the negative and the positive directions.

The positive direction must be specified and is usually taken as toward the load. To give a definite phase to the reflection coefficient, a convention is necessary that describes how the phases of waves traveling in opposite directions are to be compared. The usual convention is to compare in the two waves the phases of the transverse electric-field vectors.*

For a short-circuit, produced, for instance, by a perfect conducting plane placed across the waveguide, the reflection coefficient is $W = -1$. For an open-circuit, it is $W = +1$ and for a matched load, $W = 0$.

When the cross section is displaced by z in the positive direction, the reflection coefficient W becomes

$$W' = W \exp(2jhz) \tag{1}$$

Measurement

In a slotted waveguide equipped with a sliding voltage† probe, the position of a maximum is one where the phase of the reflection coefficient is zero.

The ratio of the maximum to the minimum (the standing-wave ratio or swr) is

$$(\text{swr}) = (1 + |W|)/(1 - |W|)$$

Therefore,

$$W = [(\text{swr}) - 1]/[(\text{swr}) + 1] \tag{2}$$

is the value of W at the position of a maximum. At the position of a minimum,

* The dual convention, based on the magnetic-field vector, would give the "current" reflection coefficient, equal to minus the "voltage" reflection coefficient. The latter is used almost exclusively and the "voltage" qualification is implicit.

† A probe that gives a reading proportional to the electric field.

Reflection coefficient *continued*

which is easier to locate in practice, the reflection coefficient is [1 − (swr)]/[1 + (swr)].

At any other position, the value of W is obtained by applying (1). If the reflection coefficient is wanted in some waveguide connected to the slotted section, a good match must obtain at the transition or a correction must be applied as explained in problems a and b below, pages 654-655.

Scattering matrix of a junction

Definition

To define accurately the waves incident on a waveguide junction and those reflected (or scattered) from it, some reference locations must be chosen in the waveguides. These locations are called the *ports** of the junction. In a waveguide that can support several propagating modes, there should be as many ports as there are modes. (These ports may or may not have the same physical location in the multimode waveguide.)

At each port i of a junction, consider the amplitude a_i of the incident wave, traveling toward the junction, and the amplitude b_i of the scattered wave, traveling away from it. As a consequence of Maxwell's equations, there exists a linear relation between the b_i and the a_i. Considering the a_i (where i varies from 1 to n) as the components of a vector $\boldsymbol{a}$ and the b_i as the components of a vector $\boldsymbol{b}$, this relation can be expressed by

$$\boldsymbol{b} = \boldsymbol{S}\,\boldsymbol{a}$$

where $\boldsymbol{S} = (s_{ij})$ is an $n \times n$ matrix called the *scattering matrix* of the junction.

The s_{ii} is the *reflection coefficient* looking into port i and s_{ij} is the *transmission coefficient* from j to i, all other ports being terminated in matching impedances.

Properties

For a *reciprocal* junction, the transmission coefficient from i to j equals that from j to i; the matrix $\boldsymbol{S}$ is symmetrical,

$$\boldsymbol{S} = \tilde{\boldsymbol{S}}$$

where $\tilde{\boldsymbol{S}}$ denotes the transpose of $\boldsymbol{S}$.

* At lower frequencies, for a network connecting transmission lines, a port is a terminal pair.

Scattering matrix of a junction *continued*

The total power incident on the junction is

$$|\boldsymbol{a}|^2 = \sum_{i=1}^{i=n} |a_i|^2$$

The total power reflected is

$$|\boldsymbol{b}|^2 = \sum_{i=1}^{i=n} |b_i|^2$$

For a lossless junction, these two powers are equal,

$$|\boldsymbol{a}|^2 = |\boldsymbol{b}|^2$$

This implies that the matrix $\boldsymbol{S}$ is *unitary* (see page 1092):

$$\boldsymbol{S}^\dagger = \boldsymbol{S}^{-1}$$

For a *passive* junction with losses, $|\boldsymbol{b}|^2 < |\boldsymbol{a}|^2$ and hence the matrix $1 - \boldsymbol{S}\boldsymbol{S}^\dagger$ is definite positive (see page 1094).

Change of terminal plane

If the port in arm i is moved away from the junction by ϕ_i electrical radians, the scattering matrix becomes

$$\boldsymbol{S}' = \Phi \boldsymbol{S} \Phi \tag{5}$$

where

$$\Phi = \begin{bmatrix} \exp(-j\phi_1) & 0 & 0 & 0 & . & . & . \\ 0 & \exp(-j\phi_2) & 0 & 0 & . & . & . \\ 0 & 0 & \exp(-j\phi_3) & 0 & . & . & . \\ . & . & . & . & . & . & . \\ . & . & . & . & . & . & . \\ . & . & . & . & . & . & . \end{bmatrix} \tag{6}$$

Two-port junctions

The two-port junction includes the case of an obstacle or discontinuity placed in a waveguide as well as that of two essentially different waveguides connected to each other.

Two-port junctions *continued*

If reciprocity applies, the scattering matrix

$$\boldsymbol{S} = \begin{bmatrix} s_{11} & s_{12} \\ s_{21} & s_{22} \end{bmatrix} \tag{7}$$

is symmetrical:

$$s_{21} = s_{12}$$

For a lossless junction, the scattering coefficients can be expressed by

$$\left.\begin{aligned} s_{11} &= + \tanh (u/2) \exp (-2j\alpha) \\ s_{22} &= - \tanh (u/2) \exp (-2j\beta) \\ s_{12} &= + \operatorname{sech} (u/2) \exp [-j(\alpha + \beta)] \end{aligned}\right\} \tag{8}$$

in terms of three real parameters, u, α, and β.

This corresponds to the representation of the junction by an ideal transformer with transformer ratio $n = \exp(-u/2)$, of hyperbolic amplitude u, placed between two sections of transmission line with electrical lengths α and β, respectively.

The quantity $-20 \log_{10} |s_{12}|$ is the *insertion loss*.

Transformation matrix

For the purpose of finding the effect of successive obstacles in a waveguide or of combining two-port junctions placed in cascade, it is convenient to introduce the wave transformation matrix $\boldsymbol{T}$.

This matrix $\boldsymbol{T}$ relates the traveling waves on one side of the junction to those on the other side. Using the notations of Fig. 1,

$$\begin{bmatrix} A_1 \\ B_1 \end{bmatrix} = \boldsymbol{T} \begin{bmatrix} A_2 \\ B_2 \end{bmatrix} \tag{9}$$

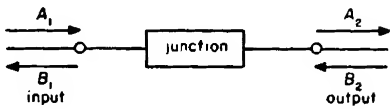

Fig. 1—Convention for wave transformation matrix *T*.

The 2×2 transformation matrix $\boldsymbol{T}$ may be deduced from the scattering matrix $\boldsymbol{S}$

$$\boldsymbol{T} = \frac{1}{s_{21}} \begin{bmatrix} 1 & -s_{22} \\ s_{11} & -\det \boldsymbol{S} \end{bmatrix} \tag{10}$$

Transformation matrix *continued*

Conversely, if $\boldsymbol{T} = (t_{ij})$, the scattering matrix is,

$$\boldsymbol{S} = \frac{1}{t_{11}} \begin{bmatrix} t_{21} & \det \boldsymbol{T} \\ 1 & -t_{12} \end{bmatrix} \tag{11}$$

When reciprocity applies to the junction,

$$\det \boldsymbol{T} = s_{12}/s_{21} \tag{12}$$

becomes unity.

The input reflection coefficient $W' = B_1/A_1$ is related to the load reflection coefficient $W = B_2/A_2$ by

$$W' = \frac{t_{21} + t_{22}\, W}{t_{11} + t_{12}\, W} \tag{13}$$

$$= s_{11} + \frac{s^2_{12} W}{1 - s_{22} W} \tag{14}$$

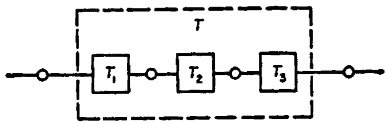

Fig. 2—Junctions in cascade.

When a number of junctions *1*, *2*, *3*, are placed in cascade (Fig. 2), the output port of each of them being the input port of the following one, the resulting junction has the transformation matrix

$$\boldsymbol{T} = \boldsymbol{T}_1 \boldsymbol{T}_2 \boldsymbol{T}_3$$

If n similar junctions with transformation matrix $\boldsymbol{T}$ are cascaded, the resulting transformation matrix is $\boldsymbol{T}^n$.

Letting trace $\boldsymbol{T} = t_{11} + t_{22} = 2 \cos \theta$

$$\boldsymbol{T}^n = \frac{\sin n\, \theta}{\sin \theta} \boldsymbol{T} - \frac{\sin (n - 1)\, \theta}{\sin \theta} \tag{15}$$

(see page 1097).

Measurement of the scattering matrix *

A slotted line is placed on side *1* of the junction (see Fig. 3). For any load with

* G. A. Deschamps "Determination of the Reflection Coefficients and Insertion Loss of a Waveguide Junction," *Journal of Applied Physics*, vol. 24, pp. 1046–1050; August, 1953: Also, *Electrical Communication*, vol. 31, pp. 57–62; March, 1954.

Measurement of the scattering matrix *continued*

reflection coefficient W, placed on side 2, the input reflection coefficient W' can be measured. W' is called the *image* of W. The images of various known loads can be plotted on a reflection chart and the scattering coefficients deduced by the following procedures.

a. With a matched load, one obtains directly s_{11} plotted as O' on Fig. 4. O' is called the iconocenter.

b. With a sliding short-circuit on side 2, or any variable reactive load, the input reflection coefficient describes a circle Γ', image of the unit circle Γ. This circle can be deduced from 3 or more measurements. Let C be its center and R its radius (Fig. 4). The magnitudes of the scattering coefficients result:

$$\left.\begin{aligned} |s_{11}| &= OO' \\ |s_{22}| &= O'C/R \\ |s_{12}|^2 &= R\,(1 - |s_{22}|^2) \end{aligned}\right\} \quad (16)$$

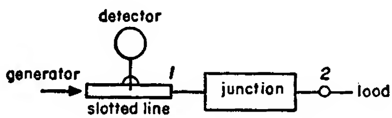

Fig. 3—Slotted-line set-up for scattering-matrix measurement.

The phases of these coefficients all follow from one more measurement

c. The input reflection coefficient is measured with an open-circuit load placed at port 2, or for a short-circuit placed a quarter-wave away from it. This may be one of the measurements taken in step *b*. It gives the point P', image of the point P ($W = +1$.)

A point P'' is constructed by projecting P' through O' onto Q on Γ', then Q through C onto P'' on Γ' (Fig. 5). Then,

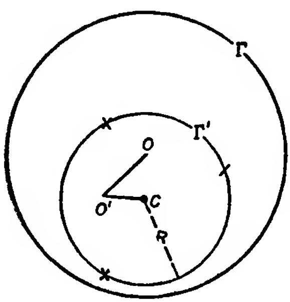

Fig. 4—Construction for the magnitudes of the scattering coefficients.

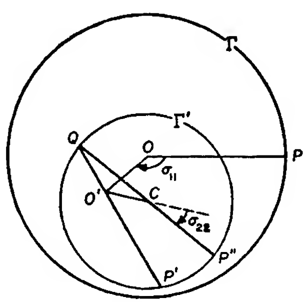

Fig. 5—Construction for the phases of the scattering coefficients.

Measurement of the scattering matrix *continued*

$$\left.\begin{array}{ll} \text{Phase of } s_{11} = & \text{angle } (OP, OO') \\ \text{Phase of } s_{22} = & \text{angle } (O'C, CP'') \\ \text{Phase of } s_{12} = & \tfrac{1}{2}\text{ angle } (OP, CP'') \end{array}\right\} \quad (17)$$

d. When no matched load is available, as was assumed in a, the iconocenter O' may be obtained as follows. Let P_1, P_2, P_3, P_4 represent the input reflection coefficients when a short-circuit is placed successively at port 2 and at distances $\lambda/8$, $\lambda/4$, and $3\lambda/8$ from it. These points define the circle Γ' (as in b) and the intersection I (the crossover point) of P_1P_3 and P_2P_4 may be used to find O': draw perpendiculars to CI at points C and I up to their intersections with Γ' at C' and I'; then O' is the intersection of CI and $C'I'$ (see Fig. 6).

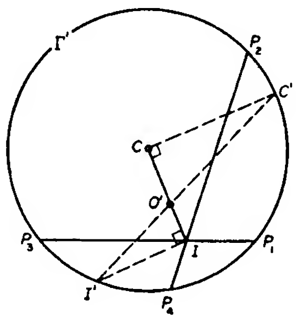

Fig. 6—Determination of O' from 4 measurements.

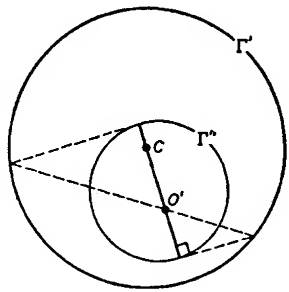

Fig. 7—Use of circles Γ'' and Γ' for determination of O'.

The point P_3 is identical to P' in c above, hence the 4 measurements give the complete scattering matrix by constructing P'' and applying (16) and (17).

e. The construction of O' in *d* above is valid with any sliding load not necessarily reactive. Taking a load with small standing-wave ratio increases the accuracy of the construction.

f. When exact measurements of the displacements of the sliding load are difficult to make; for instance if the wavelength is very short; the point O' may be obtained as follows. Using a reactive load, construct the circle Γ' as in *b* above, then using a sliding load as in e above, construct a circle Γ'', (see Fig. 7). The iconocenter O' is the hyperbolic midpoint of the

Measurement of the scattering matrix *continued*

diameter of Γ'' (through C) with respect to Γ'. It may be constructed by means of the hyperbolic protractor* (page 653), or by means of the dotted-line construction (Fig. 7).

Geometry of reflection charts

The following brief outline is complemented by the section on hyperbolic trigonometry on pp. 1050 to 1055.

Conformal chart

A reflection coefficient can be represented by a point in a plane just as any complex number is represented on the Argand diagram.

The passive loads, $|W| \leqslant 1$, are represented by points inside a unit circle Γ. Inside this circle, the lines of constant resistance and reactance may be drawn (Smith chart) or the lines of constant magnitude and phase of the impedance (Carter chart).

The transformation from a load reflection coefficient W to its image W' through a two-port junction, is bilinear, formulas (13) or (14). On the reflection chart, this transformation maps circles into circles and preserves the angle between curves and the cross ratio of 4 points: if

$$[W_1, W_2, W_3, W_4] = \frac{W_1 - W_3}{W_1 - W_4} : \frac{W_2 - W_3}{W_2 - W_4}$$

denotes the cross ratio of 4 reflection coefficients, W_1, W_2, W_3, and W_4, then

$$[W'_1, W'_2, W'_3, W'_4] = [W_1, W_2, W_3, W_4]$$

The transformation through a lossless junction preserves also the unit circle Γ and therefore leaves invariant the *hyperbolic distance* defined on p. 1050. The hyperbolic distance to the origin of the chart is the *mismatch*, i.e., the standing-wave ratio expressed in decibels: it may be evaluated by means of the proper graduation on the radial arm of the Smith chart. For two arbitrary points W_1, W_2, the hyperbolic distance between them may be interpreted as the mismatch that results from the load W_2 seen through a lossless network that matches W_1 to the input waveguide.

* G. A. Deschamps, "Hyperbolic Protractor for Microwave Impedance Measurements and Other Purposes," International Telephone and Telegraph Corporation, 67 Broad Street, New York 4, N. Y.; 1953.

Geometry of reflection charts *continued*

Projective chart

The reflection coefficient W is represented by the point $\overline{W}$ (Fig. 8) on the same radius of the circle Γ but at a distance

$$O\overline{W} = \frac{2\,OW}{1 + OW^2} \qquad (18)$$

from the origin.

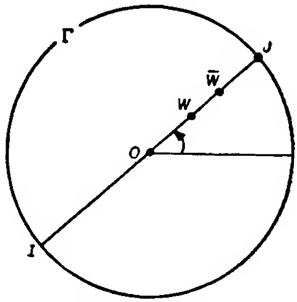

Fig. 8—Representation of a reflection coefficient by W on a Smith chart and $\overline{W}$ on the projective chart.

This is equivalent to using the standing-wave ratio squared instead of the direct ratio:

$$\frac{\overline{WJ}}{\overline{WI}} = \left(\frac{WJ}{WI}\right)^2 \qquad (19)$$

The transformation (13),(14), when the junction is lossless, is represented on this chart by a projective transformation; i.e., one that maps straight lines into straight lines and preserves the cross ratio of four points on a straight line. It therefore preserves the hyperbolic distance defined on p. 1050.

Evaluation of hyperbolic distance

On the projective chart, the hyperbolic distance $\langle AB \rangle$ between two points A and B inside the circle Γ can be evaluated by means of a hyperbolic protractor as shown in Fig. 9. The line AB is extended to its intersections I and J with Γ. The protractor is placed so that the sides OX,OY of the right angle go through I and J. (This can be done in many ways but does not affect the result.) The numbers read on the radial lines of the protractor going through A and B respectively, are added if A and B are on opposite sides of the radial line marked O; subtracted otherwise: This result divided by 2 is the distance $\langle AB \rangle$. In Fig. 9, for instance,

$$\langle AB \rangle = \tfrac{1}{2}\,(12 + 4) = 8 \text{ decibels.}$$

Evaluation of hyperbolic distance *continued*

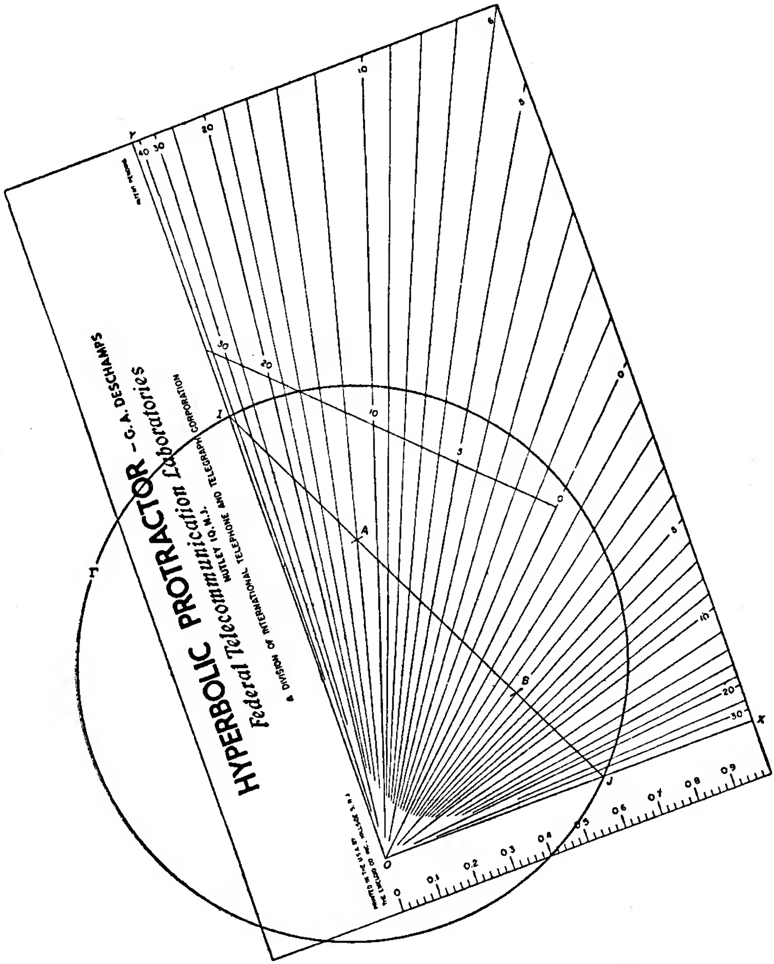

Fig. 9—Definition and evaluation of hyperbolic distance ⟨AB⟩ using hyperbolic protractor.

Problem a

A slotted line with 100-ohm characteristic impedance is used to make measurements on a 60-ohm coaxial line. The transition acts as an ideal transformer. Find the reflection coefficient W of an obstacle placed in the

Problem a *continued*

coaxial line, knowing that it produces a reflection coefficient

$$W' = 0.5 \exp(j\pi/2)$$

in the slotted line.

A match in the coaxial line appears in the slotted line as a normalized impedance of 0.6, hence the mismatch (standing-wave ratio in decibels) is 4.5 decibels. The corresponding point $\bar{O}'$ is plotted on the projective chart as in Fig. 10 at the distance $\langle O\bar{O}'\rangle = 4.5$. (On the Smith chart drawn inside the same unit circle Γ, the point would be O'.)

The point $\bar{W}'$ representing the unknown load is plotted at the hyperbolic distance

$$20 \log_{10} \frac{1 + 0.5}{1 - 0.5} = 9.5 \text{ decibels}$$

from the origin in the direction $+90°$. The hyperbolic distance

$$\langle \bar{O}'\bar{W}'\rangle = 11 \text{ decibels}$$

is measured with the protractor. This is the mismatch produced by the obstacle in the coaxial line. It corresponds to a magnitude of the reflection coefficient of 0.56.

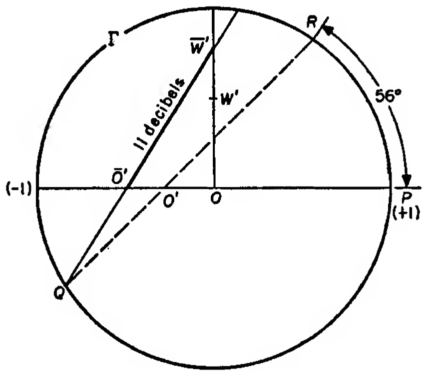

Fig. 10—Measurement of reflection coefficient with a mismatched slotted line.

The phase of this reflection coefficient is the elliptic angle $\langle \bar{O}'P, \bar{O}\bar{W}'\rangle$

It is evaluated as explained on p. 1051: extend QO' up to R on Γ and measure the arc

$$PR = 56°.$$

The answer is:

$$W = 0.56 \underline{/56°}$$

Problem b

If the transition between the slotted line and the waveguide is not an ideal transformer as in problem a, its properties may be found by the method described on p. 650. In particular, if the transition has no losses (the circle

Problem b *continued*

Γ' coincides with Γ), the point O' may be found as in *a*, *d*, *e*, or *f* above, the point P' as in *c* or *d* above, and this completes the calibration.

For any load placed in the waveguide and producing the reflection coefficient W' in the slotted line, the corrected standing-wave ratio in decibels is the hyperbolic distance $[O'W']$. This is evaluated by constructing $\overline{O',W'}$ on the projective chart and measuring $\langle \overline{O'W'} \rangle$ with the protractor. The phase angle is the elliptic angle $\langle \bar{O}'P', \bar{O}'\overline{W'} \rangle$ (see page 1051).

Problem c

A section of coaxial line 90 electrical degrees in length and with 100-ohm characteristic impedance is inserted between a 50-ohm coaxial line on one side and a 70-ohm coaxial line on the other (Fig. 11). Find the transformer ratio $n = \exp(-u/2)$ and the electrical lengths α, β of the representation (8), p. 648.

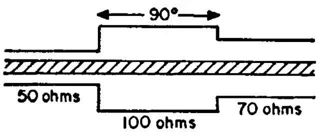

Fig. 11—Solution for transformation in transmission line.

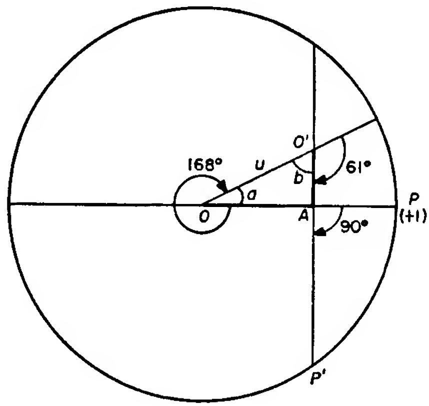

The two discontinuities are assumed to act as ideal transformers with hyperbolic amplitudes

$$20 \log_{10} \frac{100}{50} = 6 \text{ decibels} = 0.67 \text{ neper}$$

and

$$20 \log_{10} \frac{70}{100} = -3.1 \text{ decibels} = -0.36 \text{ neper}$$

Problem c *continued*

The characteristic polygon* on the projective chart is a triangle OAO′ wi h right angle A; hence, $u = \langle OO' \rangle$ is given by

$$\cosh u = \cosh 0.69 \cosh 0.36$$

$$u = 0.78 \text{ neper} = 6.8 \text{ decibels}$$

$$n = \exp(-u/2) = 1/1.48$$

The length of line α and β can be deduced from evaluating the elliptic angles $\langle OA,OO' \rangle = a$ and $\langle O'A,O'O \rangle = b$

$$\tan a = \frac{\tanh 0.36}{\sinh 0.69} = 0.46$$

$$a = 24°.7$$

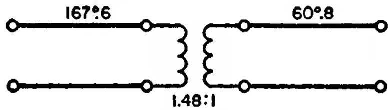

Fig. 12—Equivalent circuit for Fig. 11.

$$\tan b = \frac{\tanh 0.69}{\sinh 0.36} = 1.62$$

$$b = 58°.4$$

$$\alpha = \tfrac{1}{2}(360° - 24°.7) = 167.6°$$

$$\beta = \tfrac{1}{2}(180° - 58°.4) = 60.8°$$

The resulting equivalent network is shown in Fig. 12. It could also have been obtained by geometrical evaluation of the distance $\langle OO' \rangle$ with the hyperbolic protractor and of the elliptic angles a and b by constructions as described on pp. 653 and 1051.

Correspondances with current, voltage, and impedance viewpoint

Normalized current and voltage

In a waveguide, at a point where the amplitudes of the waves traveling in the positive and negative directions are respectively a and b, the normalized voltage v and the normalized current i are defined by

$$\left.\begin{aligned} v &= a + b \\ i &= a - b \end{aligned}\right\} \qquad (20)$$

* G. A. Deschamps, "Hyperbolic Protractor for Microwave Impedance Measurements and Other Purposes," International Telephone and Telegraph Corporation, New York 4, N. Y.; 1953: pp. 15–16 and p. 41.

Correspondances with current, voltage, and impedance viewpoint *continued*

The *net power flow* at that point in the positive direction is

$$|a|^2 - |b|^2 = \text{re } vi^* \tag{21}$$

Current and voltage not normalized

A more-general definition for current and voltage becomes possible when a meaning has been assigned to the *characteristic impedance* Z_0 of the waveguide

$$\left.\begin{aligned} V &= vZ_0^{1/2} \\ I &= iY_0^{1/2} \end{aligned}\right\} \tag{22}$$

where $Y_0 = 1/Z_0$ is the characteristic admittance and v and i are the normalized values defined above.

Conversely, if by some convention the voltage (or the current) has been defined, a characteristic impedance will result from (22). This is the case for a two-conductor waveguide supporting the TEM mode: the characteristic impedance is the ratio of voltage to current in a traveling wave.

If V and I are the voltage and the current at a point in a waveguide of characteristic impedance $Z_0 = 1/Y_0$, the amplitudes of the waves traveling in both directions at that point are

$$\left.\begin{aligned} a &= \tfrac{1}{2}\,(VY_0^{1/2} + IZ_0^{1/2}) \\ b &= \tfrac{1}{2}\,(VY_0^{1/2} - IZ_0^{1/2}) \end{aligned}\right\} \tag{23}$$

Normalized impedance and admittance

At a point in a waveguide, the normalized impedance is $Z = v/i$ and the normalized admittance is the inverse, $Y = 1/Z$.

They are related to the reflection coefficient $W = b/a$ by

$$\left.\begin{aligned} Z &= (1 + W)/(1 - W) \\ Y &= (1 - W)/(1 + W) \end{aligned}\right\} \tag{24}$$

hence

$$W = (1 - Y)/(1 + Y) = (Z - 1)/(Z + 1) \tag{25}$$

Correspondances with current, voltage, and impedance viewpoint *continued*

Impedance and admittance matrix of a junction

The $\boldsymbol{Z}$ and $\boldsymbol{Y}$ matrixes of a junction are defined in term of the scattering matrix $\boldsymbol{S}$ by

$$\left.\begin{aligned} \boldsymbol{Y} &= (\mathbf{1} - \boldsymbol{S})\ (\mathbf{1} + \boldsymbol{S})^{-1} \\ \boldsymbol{Z} &= (\mathbf{1} + \boldsymbol{S})\ (\mathbf{1} - \boldsymbol{S})^{-1} \end{aligned}\right\} \tag{26}$$

The matrixes $\boldsymbol{Y}$ and $\boldsymbol{Z}$ do not always exist since $\boldsymbol{S}$ may have eigenvalues $+1$ or -1, which means that $\det(\mathbf{1} - \boldsymbol{S})$ or $\det(\mathbf{1} + \boldsymbol{S})$ may be zero.

Conversely,

$$\boldsymbol{S} = (\mathbf{1} - \boldsymbol{Y})\ (\mathbf{1} + \boldsymbol{Y})^{-1} = (\boldsymbol{Z} - \mathbf{1})\ (\boldsymbol{Z} + \mathbf{1})^{-1} \tag{27}$$

These formulas may be used as definitions for the scattering matrix of lumped-constant networks with n terminal pairs. This is equivalent to considering the network as a junction between n transmission lines of unit characteristic impedance.

If the network or the junction is reciprocal, $\boldsymbol{Y}$ and $\boldsymbol{Z}$ are purely imaginary.

For a two-port junction, (26) becomes

$$\boldsymbol{Y} = \frac{\mathbf{1} - \boldsymbol{S}}{\mathbf{1} + \boldsymbol{S}} = \frac{1}{\det(\mathbf{1} + \boldsymbol{S})} \begin{bmatrix} 1 - \det \boldsymbol{S} + (s_{22} - s_{11}) & -2s_{12} \\ -2s_{21} & 1 - \det \boldsymbol{S} - (s_{22} - s_{11}) \end{bmatrix} \tag{28}$$

and

$$\boldsymbol{Z} = \frac{\mathbf{1} + \boldsymbol{S}}{\mathbf{1} - \boldsymbol{S}} = \frac{1}{\det(\mathbf{1} - \boldsymbol{S})} \begin{bmatrix} 1 - \det \boldsymbol{S} - (s_{22} - s_{11}) & 2s_{12} \\ 2s_{21} & 1 - \det \boldsymbol{S} + (s_{22} - s_{11}) \end{bmatrix} \tag{29}$$

$$\det(\mathbf{1} + \boldsymbol{S}) = 1 + \operatorname{tr} \boldsymbol{S} + \det \boldsymbol{S} = 1 + (s_{11} + s_{22}) + (s_{11}s_{22} - s_{12}^2)$$

$$\det(\mathbf{1} - \boldsymbol{S}) = 1 - \operatorname{tr} \boldsymbol{S} + \det \boldsymbol{S} = 1 - (s_{11} + s_{22}) + (s_{11}s_{22} - s_{12}^2)$$

The matrixes $\boldsymbol{Y}$ and $\boldsymbol{Z}$ relate normalized voltages and currents at both ports (Fig. 13) as follows

Correspondances with current, voltage, and impedance viewpoint *continued*

$$\begin{bmatrix} v_1 \\ v_2 \end{bmatrix} = \boldsymbol{Z} \begin{bmatrix} i_1 \\ i_2 \end{bmatrix}$$

$$\begin{bmatrix} i_1 \\ i_2 \end{bmatrix} = \boldsymbol{Y} \begin{bmatrix} v_1 \\ v_2 \end{bmatrix}$$

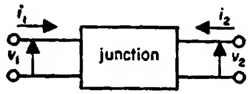

Fig. 13—Sign convention for defining the impedance and admittance of a 2-port junction.

Transformation matrix

A transformation matrix useful for composing two-port junctions in cascade relates the voltage and current on one side of the junction to the same quantities on the other side. With the notation in Fig. 14,

$$\begin{bmatrix} v' \\ i' \end{bmatrix} = \boldsymbol{U} \begin{bmatrix} v \\ i \end{bmatrix} \tag{30}$$

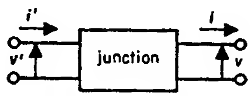

Fig. 14—Sign convention for voltages and currents related by the transformation matrix.

The matrix $\boldsymbol{U}$ sometimes called the *ABCD* matrix, has the same properties as $\boldsymbol{T}$ described above.

For a series element with normalized impedance Z,

$$\boldsymbol{U} = \begin{bmatrix} 1 & Z \\ 0 & 1 \end{bmatrix}$$

and for a shunt element with normalized admittance Y,

$$\boldsymbol{U} = \begin{bmatrix} 1 & 0 \\ Y & 1 \end{bmatrix}$$

A product of matrixes of these types gives the transformation matrix for any ladder network.

For the shunt-element Y, the scattering matrix is

$$\boldsymbol{S} = \frac{1}{2+Y} \begin{bmatrix} -Y & 2 \\ 2 & -Y \end{bmatrix} \tag{31}$$

Transformation matrix *continued*

hence,

$$\left.\begin{aligned} s_{11} &= s_{22} \\ s_{12} &= 1 + s_{11} \end{aligned}\right\} \tag{32}$$

For the series-element Z, the scattering matrix is

$$\boldsymbol{S} = \frac{1}{2+Z}\begin{bmatrix} Z & 2 \\ 2 & Z \end{bmatrix} \tag{33}$$

hence,

$$\left.\begin{aligned} s_{11} &= s_{22} \\ s_{12} &= 1 - s_{11} \end{aligned}\right\} \tag{34}$$

Relations (32) and (34) are characteristic, respectively, of a shunt and a series obstacle in a waveguide.

The matrix $\boldsymbol{T}$ can be deduced from $\boldsymbol{U}$ and vice versa:

$$\begin{aligned} \boldsymbol{T} &= \tfrac{1}{2}\begin{bmatrix} 1 & 1 \\ 1 & -1 \end{bmatrix}\boldsymbol{U}\begin{bmatrix} 1 & 1 \\ 1 & -1 \end{bmatrix} \\ &= \tfrac{1}{2}\begin{bmatrix} u_{11} + u_{12} + u_{21} + u_{22} & u_{11} - u_{12} + u_{21} - u_{22} \\ u_{11} + u_{12} - u_{21} - u_{22} & u_{11} - u_{12} - u_{21} + u_{22} \end{bmatrix} \end{aligned} \tag{35}$$

A similar formula will transform $\boldsymbol{T}$ into $\boldsymbol{U}$, since

$$\boldsymbol{U} = \tfrac{1}{2}\begin{bmatrix} 1 & 1 \\ 1 & -1 \end{bmatrix}\boldsymbol{T}\begin{bmatrix} 1 & 1 \\ 1 & -1 \end{bmatrix} \tag{36}$$

■ Antennas

The elementary dipole

Field intensity*

The elementary dipole forms the basis for many antenna computations. Since dipole theory assumes an antenna with current of constant magnitude and phase throughout its length, approximations to the elementary dipole are realized in practice only for antennas shorter than one-tenth wavelength. The theory can be applied directly to a loop whose circumference is less than one-tenth wavelength, thus forming a magnetic dipole. For larger antennas, the theory is applied by assuming the antenna to consist of a large number of infinitesimal dipoles with differences between individual dipoles of space position, polarization, current magnitude, and phase corresponding to the distribution of these parameters in the actual antenna. Field-intensity equations for large antennas are then developed by integrating or otherwise summing the field vectors of the many elementary dipoles.

The outline below concerns electric dipoles. It also can be applied to magnetic dipoles by installing the loop perpendicular to the *PO* line at the center of the sphere in Fig. 1. In this case, vector h becomes ϵ, the electric field; ϵ_t becomes the magnetic tangential field; and ϵ_r becomes the radial magnetic field.

Fig. 1 — Electric and magnetic components in spherical coordinates for electric dipoles.

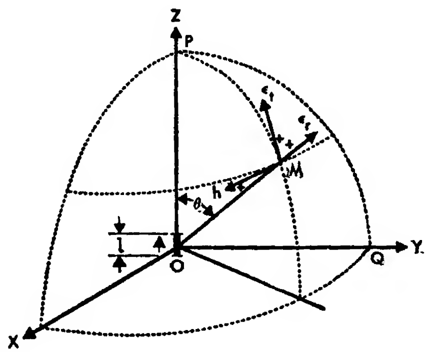

In the case of a magnetic dipole, the table, Fig. 2, showing variations of the field in the vicinity of the dipole, can also be used.

For electric dipoles, Fig. 1 indicates the electric and magnetic field components in spherical coordinates with positive values shown by the arrows.

* Based on R. Mesny, "Radio-Electricité Générale," Etienne Chiron, Paris, France; 1935.

The elementary dipole *continued*

r = distance OM
θ = angle POM measured from P toward M
I = current in dipole
λ = wavelength
f = frequency

$\omega = 2\pi f$
$\alpha = \dfrac{2\pi}{\lambda}$
c = velocity of light (see page 35)
$v = \omega t - \alpha r$
l = length of dipole

The following equations expressed in meter–kilogram–second units (in vacuum) result:

$$\left.\begin{aligned}\epsilon_r &= -\frac{30l\lambda I}{\pi}\,\frac{\cos\theta}{r^3}\,(\cos v - \alpha r \sin v)\\ \epsilon_t &= +\frac{30l\lambda I}{2\pi}\,\frac{\sin\theta}{r^3}\,(\cos v - \alpha r \sin v - \alpha^2 r^2 \cos v)\\ h &= +\frac{1}{4\pi}\,lI\,\frac{\sin\theta}{r^2}\,(\sin v - \alpha r \cos v)\end{aligned}\right\} \qquad (1)$$

Fig. 2—Variations of field in the vicinity of a dipole.

r/λ	$1/\alpha r$	A_r	ϕ_r	A_t	ϕ_t	A_h	ϕ_h
0.01	15.9	4,028	3°.6	4,012	3°.6	253	93°.6
0.02	7.96	508	7°.2	500	7°.3	64.2	97°.2
0.04	3.98	65	14°.1	61	15°.0	16.4	104°.1
0.06	2.65	19.9	20°.7	17.5	23°.8	7.67	110°.7
0.08	1.99	8.86	26°.7	7.12	33°.9	4.45	116°.7
0.10	1.59	4.76	32°.1	3.52	45°.1	2.99	122°.1
0.15	1.06	1.66	42°.3	1.14	83°.1	1.56	132°.3
0.20	0.80	0.81	51°.5	0.70	114°.0	1.02	141°.5
0.25	0.64	0.47	57°.5	0.55	133°.1	0.75	147°.5
0.30	0.56	0.32	62°.0	0.48	143°.0	0.60	152°.0
0.35	0.45	0.23	65°.3	0.42	150°.1	0.50	155°.3
0.40	0.40	0.17	68°.3	0.37	154°.7	0.43	158°.3
0.45	0.35	0.134	70°.5	0.34	158°.0	0.38	160°.5
0.50	0.33	0.106	72°.3	0.30	160°.4	0.334	162°.3
0.60	0.265	0.073	75°.1	0.26	164°.1	0.275	165°.1
0.70	0.228	0.053	77°.1	0.22	166°.5	0.234	167°.1
0.80	0.199	0.041	78°.7	0.196	168°.3	0.203	168°.7
0.90	0.177	0.032	80°.0	0.175	169°.7	0.180	170°.0
1.00	0.159	0.026	80°.9	0.157	170°.7	0.161	170°.9
1.20	0.133	0.018	82°.4	0.132	172°.3	0.134	172°.4
1.40	0.114	0.013	83°.5	0.114	173°.5	0.114	173°.5
1.60	0.100	0.010	84°.3	0.100	174°.3	0.100	174°.3
1.80	0.088	0.008	84°.9	0.088	174°.9	0.088	174°.9
2.00	0.080	0.006	85°.4	0.080	175°.4	0.080	175°.4
2.50	0.064	0.004	86°.4	0.064	176°.4	0.064	176°.4
5.00	0.032	0.001	88°.2	0.032	178°.2	0.032	178°.2

A_r = coefficient for radial electric field
A_t = coefficient for tangential electric field
A_h = coefficient for magnetic field
ϕ_r, ϕ_t, ϕ_h = phase angles corresponding to coefficients

The elementary dipole *continued*

These formulas are valid for the elementary dipole at distances that are large compared with the dimensions of the dipole. Length of the dipole must be small with respect to the wavelength, say $l/\lambda < 0.1$. The formulas are for a dipole in free space. If the dipole is placed vertically on a plane of infinite conductivity, its image should be taken into account, thus doubling the above values.

Field at great distance

When distance r exceeds five wavelengths, as is generally the case in radio applications, the radial electric field ϵ_r becomes negligible with respect to the tangential field and

$$\left.\begin{aligned} \epsilon_r &= 0 \\ \epsilon_t &= -\frac{60\pi l I}{\lambda r}\sin\theta\cos(\omega t - \alpha r) \\ h &= +\frac{\epsilon_t}{120\pi} \end{aligned}\right\} \qquad (2)$$

Field at short distance

In the vicinity of the dipole ($r/\lambda < 0.01$), αr is very small and only the first terms between parentheses in (1) remain. The ratio of the radial and tangential field is then

$$\frac{\epsilon_r}{\epsilon_t} = -2\cot\theta$$

Hence, the radial field at short distance has a magnitude of the same order as the tangential field. These two fields are in opposition. Further, the ratio of the magnetic and electric tangential field is

$$\frac{h}{\epsilon_t} = \frac{r \tan v}{60\lambda}$$

The magnitude of the magnetic field at short distances is, therefore, extremely small with respect to that of the tangential electric field, relative to their relationship at great distances. The two fields are in quadrature. Thus, at short distances, the effect of the dipole on an open circuit is much greater than on a closed circuit as compared with the effect at remote points.

The elementary dipole *continued*

Field at intermediate distance

At intermediate distance, say between 0.01 and 5.0 wavelengths, one should take into account all the terms of the equations (1). This case occurs, for instance, when studying reactions between adjacent antennas. To calculate the fields, it is convenient to transform the equations as follows:

$$\left.\begin{aligned} \epsilon_r &= -\,60\alpha^2 lI \cos\theta\, A_r \cos(v + \phi_r) \\ \epsilon_t &= +\,30\alpha^2 lI \sin\theta\, A_t \cos(v + \phi_t) \\ h &= -\,(1/4\pi)\alpha^2 lI \sin\theta\, A_h \cos(v + \phi_h) \end{aligned}\right\} \qquad (3)$$

where

$$\left.\begin{aligned} A_r &= \frac{\sqrt{1 + (\alpha r)^2}}{(\alpha r)^3} & \tan\phi_r &= \alpha r \\ A_t &= \frac{\sqrt{1 - (\alpha r)^2 + (\alpha r)^4}}{(\alpha r)^3} & \cot\phi_t &= \frac{1}{\alpha r} - \alpha r \\ A_h &= \frac{\sqrt{1 + (\alpha r)^2}}{(\alpha r)^2} & \cot\phi_h &= -\,\alpha r \end{aligned}\right\} \qquad (4)$$

Values of A's and ϕ's are given in Fig. 2 as a function of the ratio between the distance r and the wavelength λ. The second column contains values of $1/\alpha r$ that would apply if the fields ϵ_t and h behaved as at great distances.

Linear polarization

An electromagnetic wave is linearly polarized when the electric field lies wholly in one plane containing the direction of propagation.

Horizontal polarization: Is the case where the electric field lies in a plane parallel to the earth's surface.

Vertical polarization: Is the case where the electric field lies in a plane perpendicular to the earth's surface.

***E* plane:** Of an antenna is the plane in which the electric field lies. The principal E plane of an antenna is the E plane that also contains the direction of maximum radiation.

***H* plane:** Of an antenna is the plane in which the magnetic field lies. The H plane is normal to the E plane. The principal H plane of an antenna is the H plane that also contains the direction of maximum radiation.

Elliptical and circular polarization

Definitions

A plane electromagnetic wave, at a given frequency, is elliptically polarized when the extremity of the electric vector describes an ellipse in a plane perpendicular to the direction of propagation, making one complete revolution during one period of the wave. More generally, any field vector, electric, magnetic, or other, is elliptically polarized if it's extemity describes an ellipse.

Two perpendicular axes OX and OY are chosen for reference in the plane of the polarization ellipse, Fig. 3A. This plane is usually perpendicular to the direction of propagation. At a given frequency, the field components along these axes are represented by two complex numbers

$$\left.\begin{aligned} X &= |X| \exp j\varphi_1 \\ Y &= |Y| \exp j\varphi_2 \end{aligned}\right\} \tag{5}$$

Amplitude of elliptically polarized field: $E^2 = |X|^2 + |Y|^2$, so that the power density in free space for a plane wave is $E^2/240\pi$.

Axial ratio: The ratio r of the minor to the major axis of the polarization ellipse $= OB/OA$.

Ellipticity angle: $\alpha = \pm \tan^{-1} r$, where the sign is taken according to the sense of rotation.

Orientation angle: The angle β between OX and the major axis of the polarization ellipse (indeterminate for circular polarization).

Polarization of receiving antenna: For plane waves incident in a given direction, the polarization of the incident wave that, for a given amplitude, induces the maximum voltage across the antenna terminals. If this voltage is expressed as hE, then h is the effective length of the antenna for the given direction.

Polarization ratio: The ratio $P = Y/X$, a complex number with phase $\varphi = \varphi_2 - \varphi_1$ and magnitude $\tan \gamma = |Y| / |X|$.

Relative power received by an elliptically polarized receiving antenna as it is rotated in a plane normal to the direction of propagation of an elliptically polarized wave is given by

$$P_r = K \frac{(1 \pm r_1 r_2)^2 + (r_1 \pm r_2)^2 + (1 - r_1^2)(1 - r_2^2) \cos 2\theta}{(1 + r_1^2)(1 + r_2^2)} \tag{6}$$

Elliptical and circular polarization *continued*

where

K = constant
r_1 = axial ratio of elliptically polarized wave
r_2 = axial ratio of elliptically polarized antenna
θ = angle between the direction of maximum amplitude in the incident wave and the direction of maximum amplitude of the elliptically polarized antenna

The $+$ sign is to be used if both the receiving and transmitting antennas produce the same hand of polarization. The $(-)$ sign is to be used when one is left-handed and the other right-handed.

State of polarization is specified either by the polarization ratio P (angles γ and φ) or by the shape, orientation, and sense of the polarization ellipse (angles α and β).

Polarization charts

Problems on polarization can be solved by means of charts similar to those used for reflection coefficients and impedances.* These charts may be

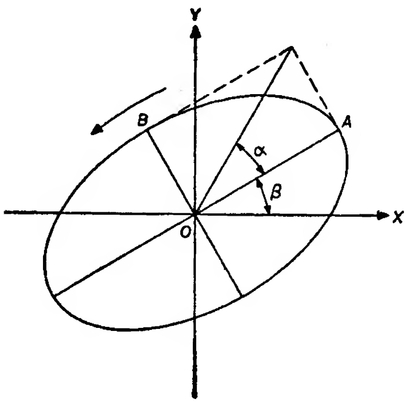

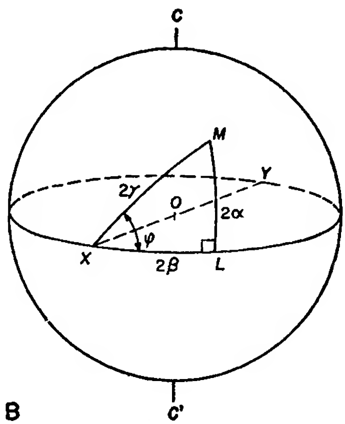

Fig. 3—Polarization ellipse at *A* and representation at *B* of a state of polarization by a point on a sphere.

related to the representation introduced in optics by H. Poincaré: The angles 2α and 2β are taken as the latitude and longitude of a point on a

* V. H. Rumsey, G. A. Deschamps, M. L. Kales, and J. I. Bohnert, "Techniques for Handling Elliptically Polarized Waves with Special Reference to Antennas," *Proceedings of the IRE*, vol. 39, pp. 533–552; May, 1951.

Elliptical and circular polarization *continued*

sphere, Fig. 3B. Each state of polarization is thus represented by a single point on the sphere and vice versa. Linear polarizations correspond to points on the equator and the two circular polarizations respectively to the poles C and C′. If X represents linear polarization along the reference axis, M some arbitrary polarization, and L the linear polarization along the major axis of the ellipse, the spherical triangle XLM has the following properties

$$\begin{aligned} XL &= 2\beta \\ LM &= 2\alpha \\ XM &= 2\gamma \\ L &= 90^\circ \\ X &= \varphi \end{aligned}$$

From these come the following relations

$$\left.\begin{aligned} \tan 2\beta &= \tan 2\gamma \cos \varphi \\ \sin 2\alpha &= \sin 2\gamma \sin \varphi \\ &\text{and} \\ \cos 2\gamma &= \cos 2\alpha \cos 2\beta \\ \tan \varphi &= \tan 2\alpha \csc 2\beta \end{aligned}\right\} \tag{7}$$

which convert from γ,φ (polarization ratio) to α,β (ellipse parameters) or vice versa.

These relations can be solved graphically on a chart (Fig. 4) that is a map of the sphere obtained by projection from pole C′ on the plane of the equator.* The circles for constant φ and constant γ are shown. β is read on the rim and α can be obtained by rotating the point about the center of the chart to bring it on the γ scale on the vertical diameter. A radial arm bearing the same graduations (standing-wave ratio and decibels) as on the Smith chart can also be used. Fig. 4 shows only the map of one hemisphere. Polarizations of the opposite sense can be plotted by considering the projection as taken from the pole C.

Example: Assume an axial ratio of 0.5 is measured with an angle of 15 degrees between the maximum field and the reference axis. The intersection M of the radial line $\beta = 15^\circ$ and a circle corresponding to $\alpha = 26.5^\circ$ (since $\tan 26.5^\circ = 0.5$) represents the measured polarization. This polariza-

* This is a standard geographic projection. Chart H.O. Misc., No. 7736-1 having a 20-centimeter radius, may be obtained at nominal charge from the United States Navy Department Hydrographic Office, Washington 25, D. C.

Elliptical and circular polarization *continued*

tion can be considered to be produced by two similar radiators normal to each other, the ratio of whose currents is tan $\gamma = 0.56$ (since the point lies on the $\gamma = 29°$ arc); the current in the radiator along the reference axis is larger and $\varphi = 69°$ ahead of the current in the other radiator.

Voltage induced by wave of arbitrary polarization: If the polarization of

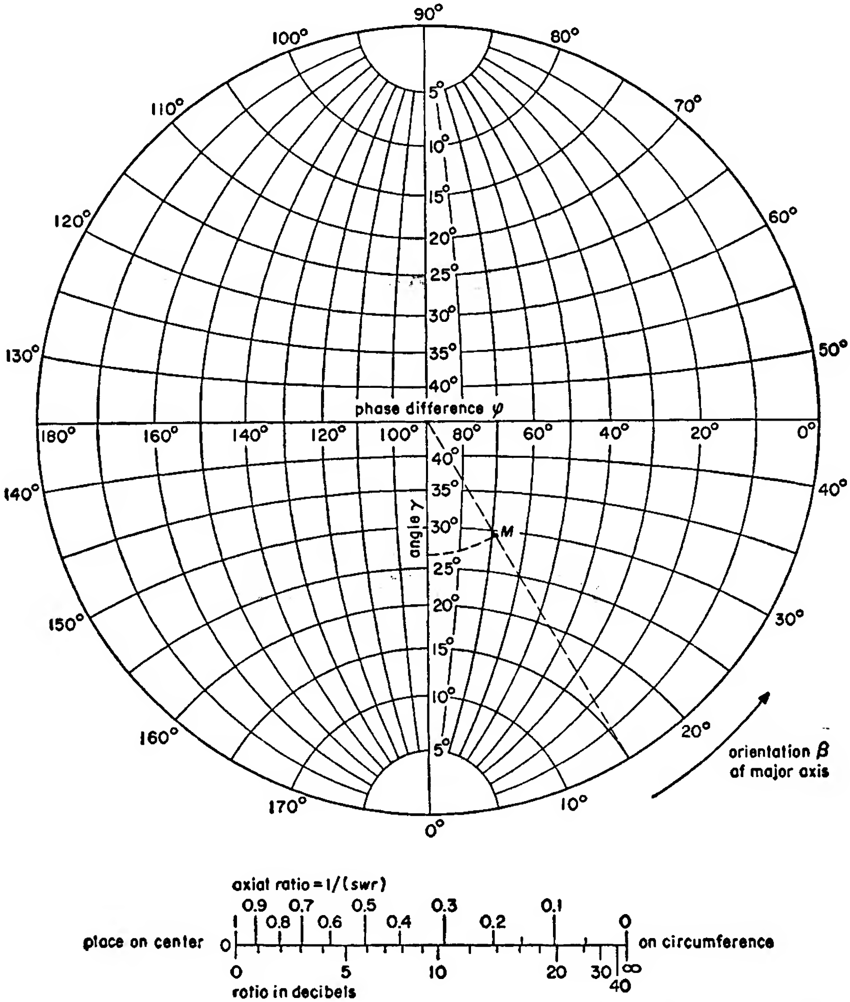

Fig. 4—Projection used in solving polarization problems. The dashed lines and point *M* are the construction for the example given in the text.

Elliptical and circular polarization *continued*

the antenna is represented by the point M on the Poincaré sphere and that of the incident wave by N, the voltage induced is

$$hE \cos \delta \tag{8}$$

where 2δ is the angular distance MN. On Fig. 4, the angle 2δ can be obtained by the following construction. Plot the points M and N on a transparent overlay, rotate the overlay about the center 0 until the points M and N fall on the same φ circle, and read the difference between the γ's.

Measurement of wave polarization

By comparing the signals received by a dipole oriented successively in the directions X and Y, the ratio $|Y|/|X|$ representing the polarization of the wave is found. On Fig. 4, the point M is on a known γ circle. To obtain another locus, compare the signals received with the same dipole oriented at 45° then 135° from OX. This gives a second circle that can be constructed as the first one with respect to points XY, then rotated by 90° by means of an overlay.

If many measurements are to be taken, the two systems of γ circles could be drawn in advance. This measurement leaves a sense ambiguity that can be resolved only by using receiving antennas with nonlinear polarization.*

Vertical radiators

Field intensity from a vertically polarized antenna with base close to ground

The following formula is obtained from elementary-dipole theory and is applicable to low-frequency antennas. It assumes that the earth is a perfect reflector, the antenna dimensions are small compared with λ, and the actual height does not exceed $\lambda/4$.

The vertical component of electric field radiated in the ground plane, at distances so short that ground attenuation may be neglected (usually when $D < 10\,\lambda$), is given by

$$E = \frac{377\, I\, H_e}{\lambda\, D} \tag{9}$$

where

E = field intensity in millivolts/meter

* Other methods using the projective chart are described by G. A. Deschamps in "Hyperbolic Protractor for Microwave Impedance Measurements and other Purposes," International Telephone and Telegraph Corporation, 67 Broad Street, New York 4, New York; 1953.

Vertical radiators *continued*

I = current at base of antenna in amperes
H_e = effective height of antenna
λ = wavelength in same units as H
D = distance in kilometers

The effective height of a grounded vertical antenna is equivalent to the height of a vertical wire producing the same field along the horizontal as the actual antenna, provided the vertical wire carries a current that is constant along its entire length and of the same value as at the base of the actual antenna. Effective height depends upon the geometry of the antenna and varies slowly with λ. For types of antennas normally used at low and medium frequencies, it is roughly one-half to two-thirds the actual height of the antenna.

For certain antenna configurations effective height can be calculated by the following formulas

Straight vertical antenna: $h \leqslant \lambda/4$

$$H_e = \frac{\lambda}{\pi \sin (2\pi h/\lambda)} \sin^2 \left(\frac{\pi h}{\lambda}\right)$$

where h = actual height

Loop antenna: $A < 0.001\ \lambda^2$

$$H_e = 2\pi n A/\lambda$$

where

A = mean area per turn of loop
n = number of turns

Adcock antenna

$$H_e = 2\pi ab/\lambda$$

where

a = height of antenna
b = spacing between antennas

In the above formulas, if H_e is desired in meters or feet, all dimensions h, A, a, b, and λ must be in meters or feet, respectively.

Practical vertical-tower antennas

The field intensity from a single vertical tower insulated from ground and either of self-supporting or guyed construction, such as is commonly used

Vertical radiators *continued*

for medium-frequency broadcasting, may be calculated by the following equation. This is more accurate than equation (9). Near ground level the formula is valid within the range $2\lambda < D < 10\lambda$.

$$E = \frac{60\,I}{D \sin\,(2\pi h/\lambda)} \left[\frac{\cos\,(2\pi\frac{h}{\lambda}\cos\theta) - \cos 2\pi\frac{h}{\lambda}}{\sin\theta} \right] \qquad (10)$$

where

E = field intensity in millivolts/meter

I = current at base of antenna in amperes

h = height of antenna

λ = wavelengths in same units as h

D = distance in kilometers

θ = angle from the vertical

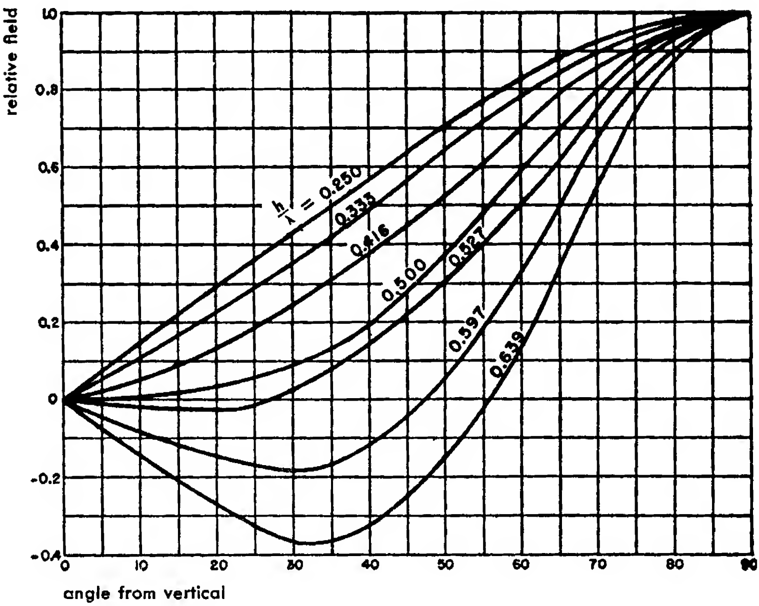

Fig. 5—Field strength as a function of angle of elevation for vertical radiators of different heights.

Vertical radiators *continued*

Radiation patterns in the vertical plane for antennas of various heights are shown in Fig. 5. Field intensity along the horizontal as a function of antenna height for one kilowatt radiated is shown in Fig. 6.

Both Figs. 5 and 6 assume sinusoidal distribution of current along the antenna and perfect ground conductivity. Current magnitudes for one-kilowatt power used in calculating Fig. 6 are also based on the assumption that the only resistance is the theoretical radiation resistance of a vertical wire with sinusoidal current.

Since inductance and capacitance are not uniformly distributed along the tower and since current is attenuated in traversing the tower, it is impossible to obtain sinusoidal current distribution in practice. Consequently actual radiation patterns and field intensities differ from Figs. 5 and 6.* The closest approximation to sinusoidal current is found on constant-cross-section towers.

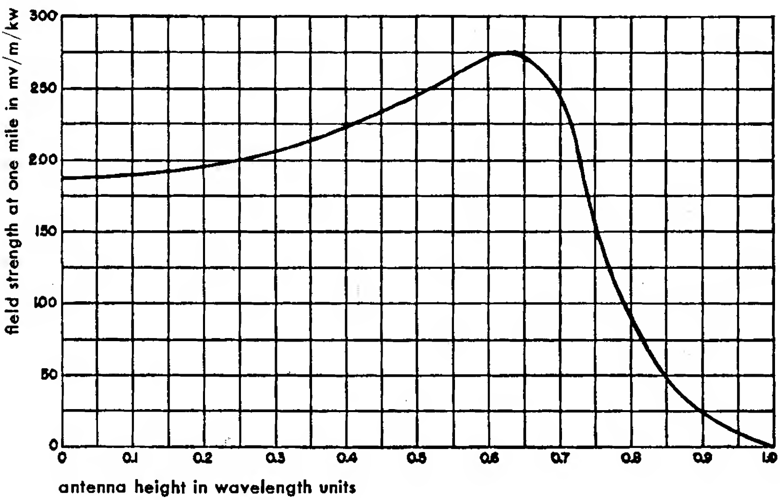

Fig. 6—Field strength along the horizontal as a function of antenna height for a vertical grounded radiator with one kilowatt radiated power.

In addition, antenna efficiencies vary from about 70 percent for 0.15 wavelength physical height to over 95 percent for 0.6 wavelength height. The input power must be multiplied by the efficiency to obtain the power radiated.

* For information on the effect of some practical current distributions on field intensities see H. E. Gihring and G. H. Brown, "General Considerations of Tower Antennas for Broadcast Use," *Proceedings of the IRE.*, vol. 23, pp. 311–356; April, 1935.

Vertical radiators *continued*

Average results of measurements of impedance at the base of several actual vertical radiators, as given by Chamberlain and Lodge*, are shown in Fig. 7.

* A. B. Chomberlain and W. B. Lodge, "The Broadcast Antenna," *Proceedings of the IRE*, vol. 24, pp. 11–35; January, 1936.

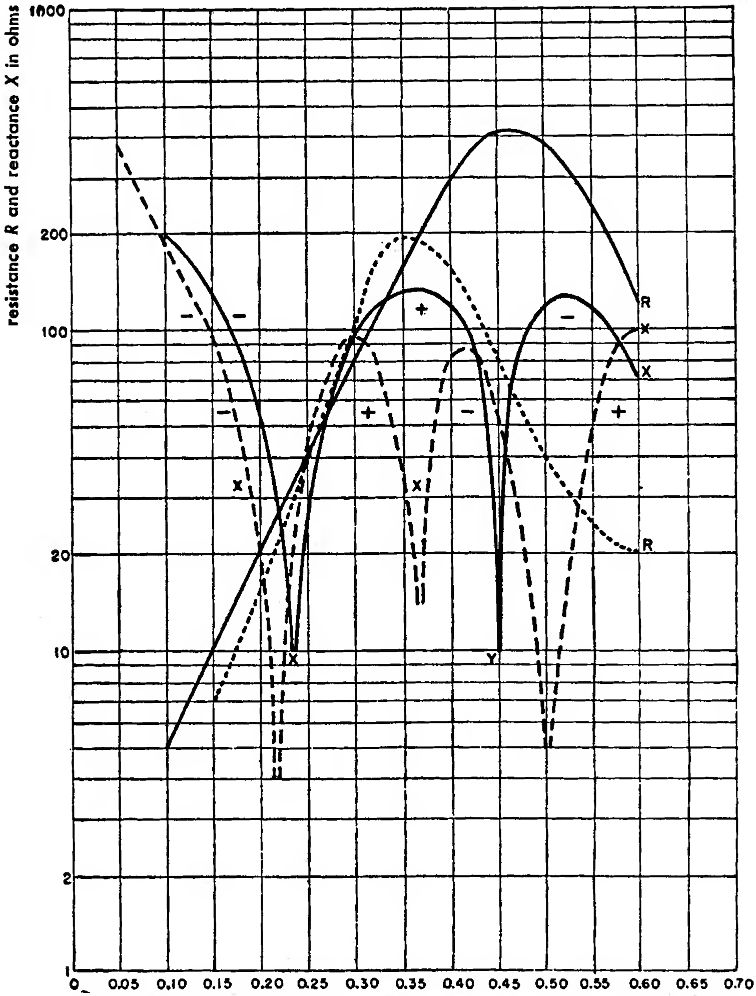

Courtesy of Proceedings of the IRE

Fig. 7—Resistance and reactance components of impedance between tower base and ground of vertical radiators as given by Chamberlain and Lodge. Solid lines show average results for 5 guyed towers; dashed lines show average results for 3 self-supporting towers.

Vertical radiators *continued*

For design purposes when actual resistance and current of the projected radiator are unknown, resistance values may be selected from Fig. 7 and the resulting effective current obtained from

$$I_e = (W\eta/R)^{1/2} \tag{11}$$

where

I_e = current effective in producing radiation in amperes

W = watts input

η = antenna efficiency, varying from 0.70 at $h/\lambda = 0.15$ to 0.95 at $h/\lambda = 0.6$

R = resistance at base of antenna in ohms

If I_e from (11) is substituted in (10), reasonable approximations to the field intensity at unit distances, such as one kilometer or one mile, will be obtained.

The practical equivalent of a higher tower may be secured by adding a capacitance "hat" with or without tuning inductance at the top of a lower tower.*

A good ground system is important with vertical-radiator antennas. It should consist of at least 120 radial wires, each one-half wavelength or longer, buried 6 to 12 inches below the surface of the soil. A ground screen of high-conductivity metal mesh, bonded to the ground system, should be used on or above the surface of the ground adjacent to the tower.

Field intensity and radiated power from antennas in free space

Isotropic radiator

The power density P at a point due to the power P_t radiated by an isotropic radiator is

$$P = P_t/4\pi R^2 \text{ watts/meter}^2 \tag{12}$$

* For additional information see G. H. Brown, "A Critical Study of the Characteristics of Broadcast Antennas as Affected by Antenna Current Distribution," *Proceedings of the IRE*, vol. 24, pp. 48–81; January, 1936. G. H. Brown and J. G. Leitch, "The Fading Characteristics of the Top-Loaded WCAU Antenna," *Proceedings of the IRE*, vol. 25, pp. 583–611; May, 1937. Also, C. E. Smith and E. M. Johnson, "Performance of Short Antennas," *Proceedings of the IRE*, vol. 35, pp. 1026–1038; October, 1947.

Field intensity and radiated power *continued*

where

R = distance in meters

P_t = transmitted power in watts

The electric-field intensity E in volts/meter and power density P in watts/meter^2 at any point are related by

$$P = E^2/120\pi$$

where 120π is known as the resistance of free space. From this

$$E = (120\pi P)^{1/2} = (30P_t)^{1/2}/R \text{ volts/meter} \qquad (13)$$

Half-wave dipole

For a half-wave dipole in the direction of maximum radiation

$$P = 1.64\ P_t/4\pi R^2 \qquad (14)$$

$$E = (49.2\ P_t)^{1/2}/R \qquad (15)$$

These relations are shown in Fig. 8.

Received power

To determine the power intercepted by a receiving antenna, multiply the power density from Fig. 8 by the receiving area. The receiving area is

$$\text{Area} = G\,\lambda^2/4\pi$$

where

G = gain of receiving antenna

λ = wavelength in meters

The receiving areas and gains of common antennas are given in Fig. 36.

Equation (16) can be used to determine the power received by an antenna of gain G_r when the transmitted power P_t is radiated by an antenna of gain G_t.

$$P_r = \frac{P_t G_r G_t \lambda^2}{(4\pi R)^2} \qquad (16)$$

G_t and G_r are the gains over an isotropic radiator. If the gains over a dipole are known, instead of gain over isotropic radiator, multiply each gain by 1.64 before inserting in (16).

Field intensity and radiated power *continued*

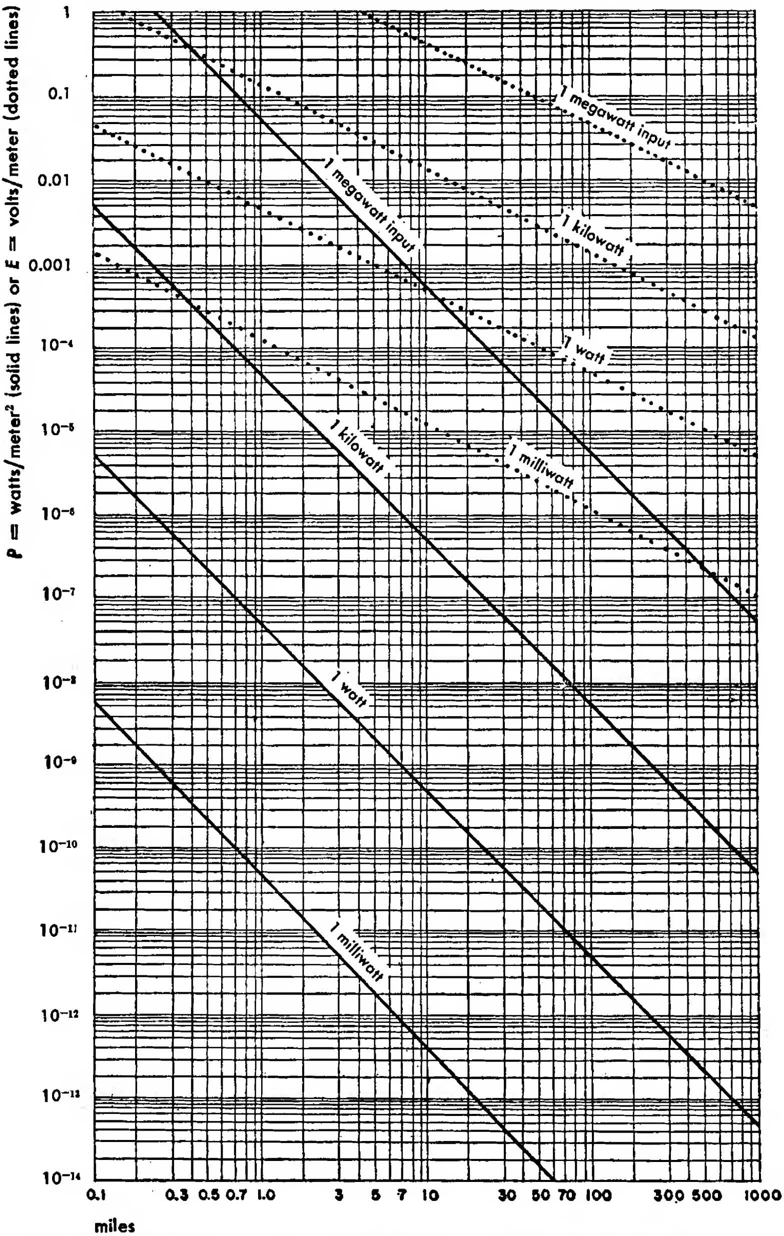

Fig. 8—Power density at various distances from a half-wave dipole.

Radiation from an end-fed conductor of any length

configuration (length of radiator)	expression for intensity $F(\theta)$
A. Half-wave, resonant	$F(\theta) = \dfrac{\cos\left(90^\circ \sin\theta\right)}{\cos\theta}$
B. Any odd number of half waves, resonant	$F(\theta) = \dfrac{\cos\left(\dfrac{l^\circ}{2}\sin\theta\right)}{\cos\theta}$
C. Any even number of half waves, resonant	$F(\theta) = \dfrac{\sin\left(\dfrac{l^\circ}{2}\sin\theta\right)}{\cos\theta}$
D. Any length, resonant	$F(\theta) = \dfrac{1}{\cos\theta}\Big[1 + \cos^2 l^\circ + \sin^2\theta \sin^2 l^\circ - 2\cos(l^\circ \sin\theta)\cos l^\circ - 2\sin\theta \sin(l^\circ \sin\theta)\sin l^\circ\Big]^{1/2}$
E. Any length, nonresonant	$F(\theta) = \tan\dfrac{\theta}{2}\sin\dfrac{l^\circ}{2}(1 - \sin\theta)$

where

$l^\circ = 360 l/\lambda$

$=$ length of radiator in electrical degrees, energy to flow from left-hand end of radiator.

$l =$ length of radiator in same units as λ

$\theta =$ angle from the normal to the radiator

$\lambda =$ wavelength

See also Fig. 9.

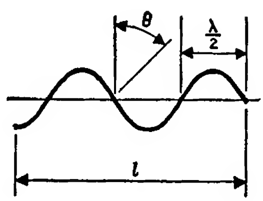

Radiation from an end-fed conductor of any length *continued*

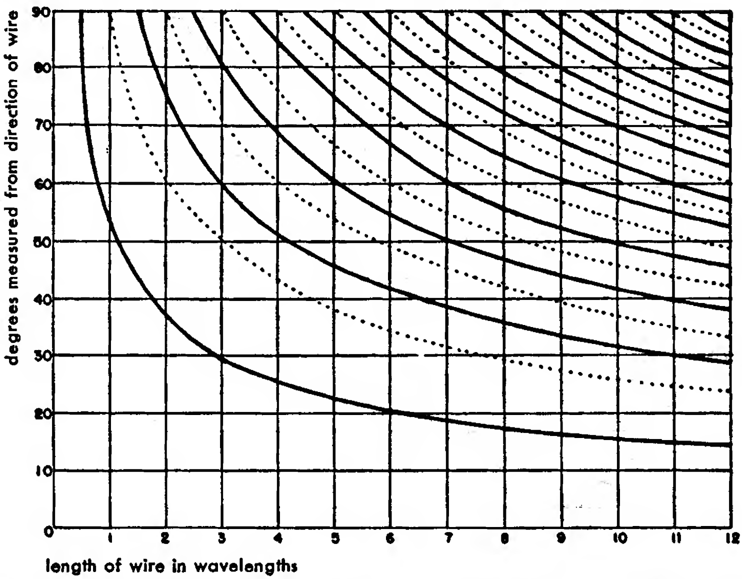

Fig. 9—Directions of maximum (solid lines) and minimum (dotted lines) radiation from a single-wire radiator. Direction given here is (90° — θ).

Rhombic antennas

Linear radiators may be combined in various ways to form antennas such as the horizontal vee, inverted vee, etc. The type most commonly used at high frequencies is the horizontal terminated rhombic shown in Fig. 10.

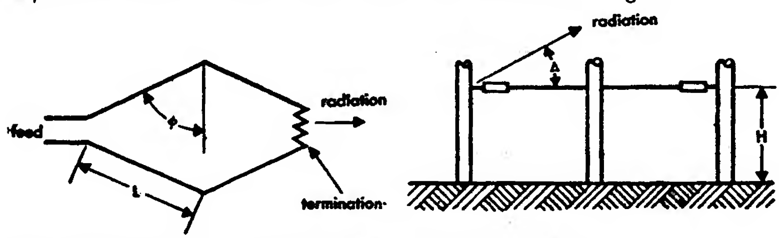

Fig. 10—Dimensions and radiation angles for rhombic antenna.

In designing rhombic antennas* for high-frequency radio circuits, the desired vertical angle Δ of radiation above the horizon must be known or assumed. When the antenna is to operate over a wide range of radiation angles or is to operate on several frequencies, compromise values of H, L, and ϕ must

* For more complete information see A. E. Harper, "Rhombic Antenna Design," D. Van Nostrand Company, New York, New York; 1941.

Rhombic antennas *continued*

be selected. Gain of the antenna increases as the length *L* of each side is increased; however, to avoid too-sharp directivity in the vertical plane, it is usual to limit *L* to less than six wavelengths.

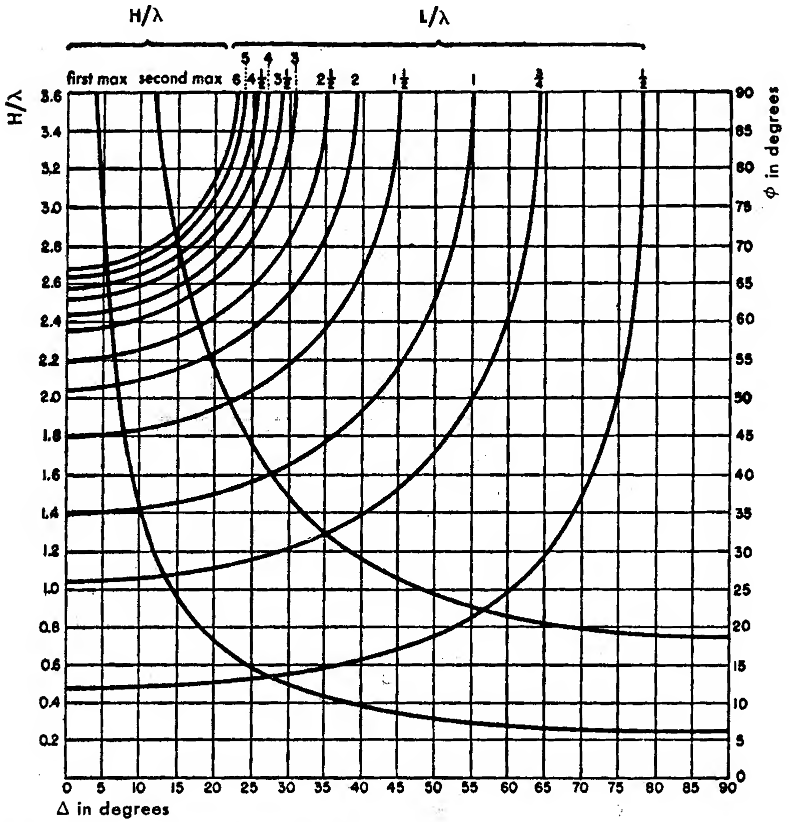

Fig. 11—Rhombic-antenna design chart.

Knowing the side length and radiation angle desired, the height *H* above ground and the tilt angle ϕ can be obtained from Fig. 11.

Example: Find *H* and ϕ if $\Delta = 20$ degrees and $L = 4\lambda$. On Fig. 11 draw a vertical line from $\Delta = 20$ degrees to meet $L/\lambda = 4$ curve and H/λ curves. From intersection at $L/\lambda = 4$, read on the right-hand scale $\phi = 71.5$ degrees. From intersection on H/λ curves, there are two possible values on the left-hand scale

a. $H/\lambda = 0.74$ or $H = 0.74\lambda$ **b.** $H/\lambda = 2.19$ or $H = 2.19\lambda$

Rhombic antennas *continued*

Similarly, with an antenna 4λ on the side and a tilt angle $\phi = 71.5°$, working backwards, it is found that the angle of maximum radiation Δ is 20°, if the antenna is 0.74λ or 2.19λ above ground.

Fig. 12 gives useful information for the calculation of the terminating resistance of rhombic antennas.

A—No. 14
B—No. 12
C—No. 10
D—No. 8
E—No. 6
(A–E: United States Steel Type "12" or American Iron and Steel Institute No. 410 Stainless Steel.)
F—No. 6 Iron wire
All sizes are American Wire Gauge

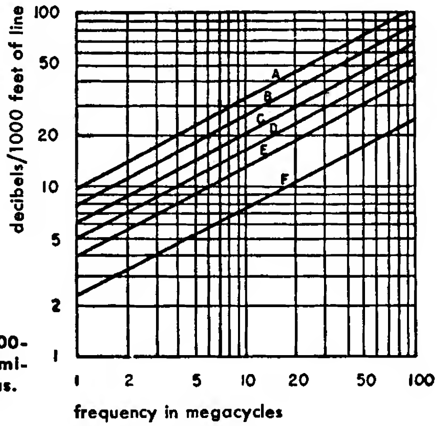

Fig. 12—Attenuation of balanced 600-ohm transmission lines for use as terminating networks for rhombic antennas.

Discones

The discone is a radiator whose impedance can be directly matched to a 50-ohm coaxial transmission line over a wide frequency band. The outer conductor of the transmission line is connected to the cone at the gap and the inner conductor to the center of the disc. The dimensions shown in Fig. 13 give the best impedance match over a wide band.* Since the bandwidth is inversely proportional to C_{min}, that dimension is usually made only slightly larger than the diameter of the coaxial transmission line. Dimensions S and D are determined from $S = 0.3\ C_{min}$ and $D = 0.7\ C_{max}$. L and ϕ determine how the standing-wave ratio varies with frequency at the low edge of the band, as shown in Fig. 14. A discone with $\phi = 60°$ and $C/L = 1/22$ had a standing-wave ratio of less than 1.5 over at least

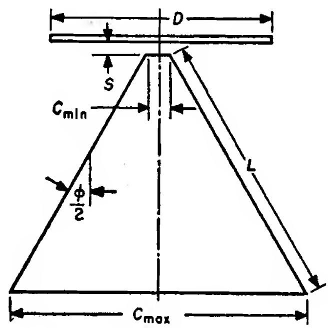

Courtesy of *Electronics*

Fig. 13—Optimum discone dimensions.

* J. J. Nail, "Designing Discone Antennas," *Electronics*, vol. 26, pp. 167–169; August, 1953.

Discones *continued*

a 7/1 frequency range and a standing-wave ratio of less than 2 over at least a 9/1 range in frequency.

The pattern is omnidirectional in the *H* plane, while the *E*-plane pattern varies somewhat with frequency as shown in Fig. 15.

Fig. 14—At right, standing-wave ratio versus ratio of frequency to the frequency at which slant height is $\lambda/4$.

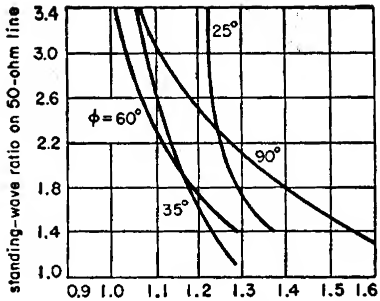

Courtesy of Electronics

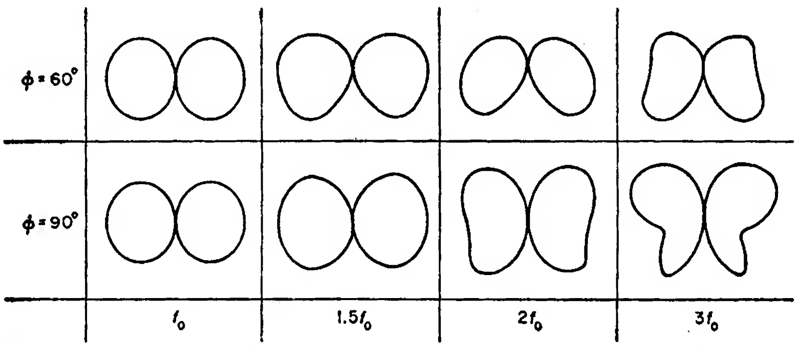

Fig. 15—Discone *E*-plane patterns.

Courtesy of Electronics

Helical antennas

Helical antennas can be classified either as to shape (such as cylindrical, flat, or conical) or as to type of pattern produced (such as normal or axial mode). Data will be given here only for the cylindrical helix radiating in the normal or axial mode.

Normal-mode helix

When the diameter is considerably less than a wavelength and the electrical length less than a wavelength, the helix radiates in the normal mode (peak of the pattern normal to the helix axis). In contrast with the ordinary dipole, where the radiating electromagnetic wave appears to travel on the dipole with the velocity of light in the surrounding medium, the velocity of the wave along the axis of the helix is lower and depends on the frequency, diameter, and number of turns per unit length. The velocity can be de-

Helical antennas *continued*

creased by large factors with a corresponding decrease in axial length for quarter-wave or half-wave resonance.

Velocity of propagation: The phase velocity along the helix axis is

$$(c/v)^2 = 1 + (M\lambda/\pi D)^2 \tag{17}$$

where

c = velocity of light in surrounding medium
v = axial velocity
λ = wavelength in surrounding medium
D = mean helix diameter (same units as λ)
M = value obtained from Fig. 16.

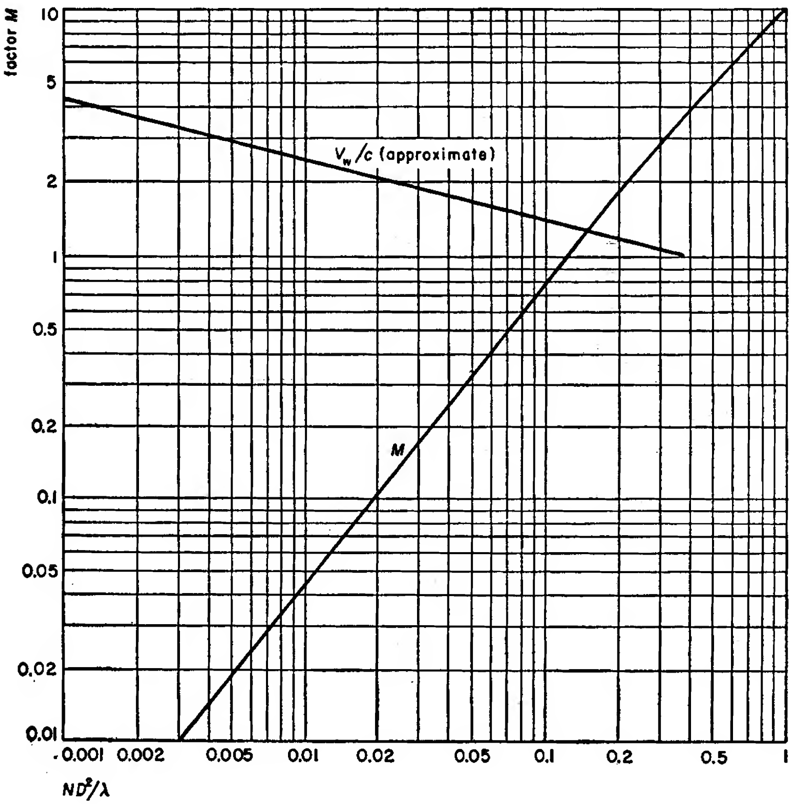

Fig. 16—Chart giving *M* for (17) and (18) and also showing apparent phase velocity V_w/c.

Helical antennas *continued*

The apparent phase velocity in the direction of the wire is equal to the axial velocity divided by the sine of the pitch angle, or

$$\left(\frac{V_w}{c}\right)^2 = \frac{1 + (N\pi D)^2}{1 + (M\lambda/\pi D)^2} \tag{18}$$

Where N is the number of turns per unit length. Fig. 16 shows the variation of V_w/c when the terms in (18) are much greater than unity. Fig. 17 shows, for a particular case, how the frequency for quarter-wave resonance varies with the number of turns per unit length for constant wire length. When $ND \geqslant 1$ and $ND^2/\lambda \leqslant 1/5$, this reduces to

$$V_w/c \approx (1.25)\ (h/D)^{1/5} \tag{18A}$$

where h = height of the quarter-wavelength helix.

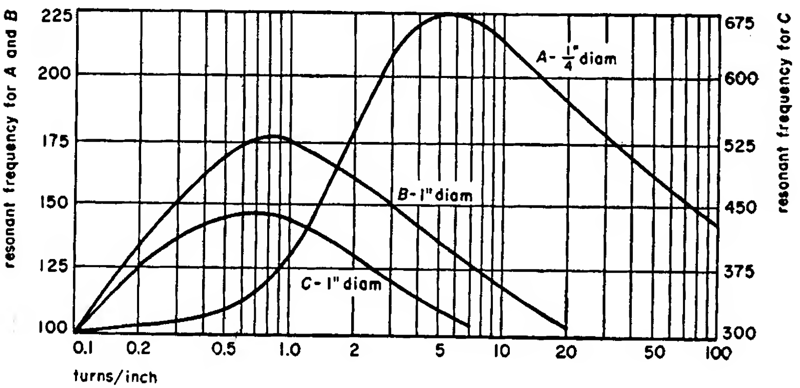

Fig. 17—Resonant frequency for various helix configurations with same length of wire.

To obtain a real input impedance (resonance), each half of the helical antenna must be a quarter-wavelength long at the velocity given above or for $ND^2/\lambda < 1/5$

$$\frac{h}{\lambda} = \frac{1}{4\,c/V} = \frac{1}{4\,[1 + 20\,(ND)^{5/2}\,(D/\lambda)^{1/2}]^{1/2}} \tag{19}$$

where h is the length of each half.

Effective Height: The effective height of a resonant helix above a perfect ground plane is $2\,h/\pi$ because the current distribution is similar to that of a quarter-wave monopole. A short monopole has an effective height of $h/2$ due to its triangular current distribution.

Helical antennas *continued*

Radiation resistance: The radiation resistance of a resonant helix above a perfect ground plane is $(25.3\ h/\lambda)^2$, while the radiation resistance of a short monopole is $(20\ h/\lambda)^2$.

Polarization: The radiated field is elliptically polarized and the ratio of the horizontally polarized field E_h to the vertically polarized field E_v is

$$\frac{E_h}{E_v} = \frac{(N\pi D)\ J_1\ (\pi D/\lambda)}{J_0\ (\pi D/\lambda)} \approx \frac{5\ ND^2}{\lambda} \tag{20}$$

where J_0, J_1 = Bessel functions* of the first kind.

The approximation is valid for diameters less than 0.1 wavelength. Circular polarization is obtained with a resonant helix when the height is about 0.9 times the diameter.

The horizontal polarization is decreased considerably when the helix is used with a ground plane. The vertical pattern of the horizontally polarized field then varies as $2\ (h/\lambda)\ \sin\theta\ \cos\theta$, while the vertical pattern of the vertically polarized field varies as $\cos\theta$.

Losses: For short resonant helixes, the loss may be appreciable because the wire diameter must be much smaller than the diameter of a dipole of the same height. Neglecting proximity effects, the ratio of the power dissipated P_l to the power radiated P_r is

$$\frac{P_l}{P_r} = \frac{2 \times 10^{-4}\ (V_w/c)}{d\ (h/\lambda)^2\ F_{mc}^{1/2}} \tag{21}$$

where

d = diameter of copper wire in inches

F_{mc} = frequency in megacycles/second

The efficiency is thus $1/(1 + P_l/P_r)$. Fig. 18 is a plot of height versus resonant frequency for three wire diameters for 50-percent efficiency, assuming that $V_w/c = 1$.

Q and tap point: The Q factor† can be calculated‡ approximately:

* Table of Bessel functions is given on p. 1118.

† Unloaded Q. When the antenna is driven by a zero-resistance generator, the 3-db bandwidth is f_0/Q. When driven by a generator whose resistance matches the resonant resistance of the antenna, the 3-db bandwidth is $2\ f_0/Q$.

‡ A. G. Kandoian and W. Sichak, "Wide-Frequency-Range Tuned Helical Antennas and Circuits," *Electrical Communication*, vol. 30, pp. 294–299; December, 1953: also, *Convention Record of the IRE 1953 National Convention*, Part 2—Antennas and Communication; pp. 42–47.

Helical antennas *continued*

$$Q = \pi Z_0/4R_{\text{base}} \tag{22}$$

where

Z_0 = characteristic impedance
$= 60\ (c/V)\ [\ln\ (4h/D) - 1]$
R_{base} = radiation resistance plus wire resistance
$= (25.3\ h/\lambda)^2 + 0.125\ (V_w/c)/dF_{\text{mc}}^{1/2}$

where d = wire diameter in inches.

The input resonant resistance R_{tap} with one end of the resonant helix connected to a perfectly conducting ground plane is

$$R_{\text{tap}} = (4/\pi)\ Q\ Z_0 \sin^2\theta \tag{23}$$

where θ = angular distance between tap point and the ground plane.

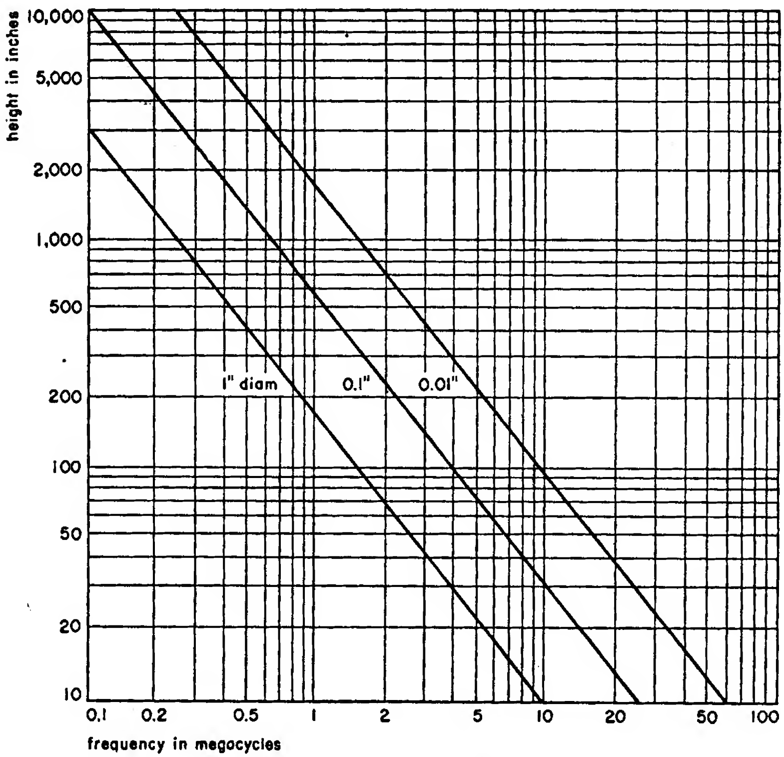

Fig. 18—Helix height versus frequency for 50-percent efficiency assuming $V_w/c = 1$.

Helical antennas *continued*

Axial-mode helix

When the helix circumference is of the order of a wavelength, an end-fire circularly polarized pattern (axial ratio less than 6 decibels) is obtained.*

Equations (24) give approximately the properties when the diameter in wavelengths is between 1/4 and 4/9, the pitch angle is between 12 and 15 degrees, the total number of turns is greater than 3, and the ground-plane diameter greater than a half-wavelength.

$$\left.\begin{aligned} \text{Half-power beamwidth} &= 17\lambda^{3/2}/D\,h^{1/2} \text{ degrees} \\ \text{Gain} &= 150\,d^2h/\lambda^3 \\ \text{Input resistance} &= 440\,D/\lambda \text{ ohms} \end{aligned}\right\} \quad (24)$$

Slot antennas

The properties of many slot antennas can be deduced from the properties of the complementary metallic antenna. The impedance Z_s of the slot antenna is related to the impedance Z_m of the metallic antenna by

$$Z_m Z_s = (60\pi)^2$$

The magnitude of the electric field E_s produced by the slot is proportional

* J. D. Kraus, "Antennas," McGraw-Hill Book Company, Incorporated, New York, New York; 1950: see p. 213.

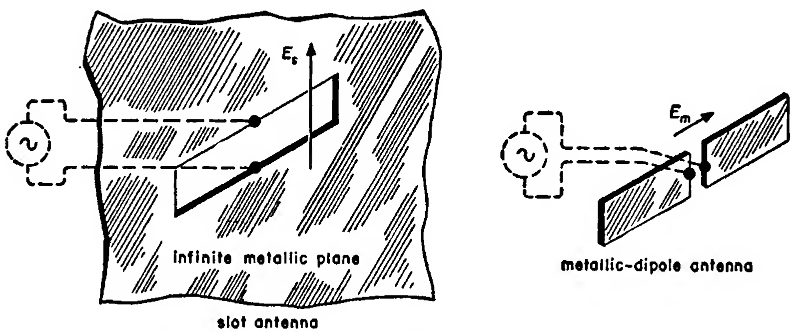

Fig. 19—Slot antenna and its metallic counterpart.

Slot antennas *continued*

to the magnitude of the magnetic field H_m of the metallic antenna and H_s is proportional to E_m. The electric- and magnetic-plane patterns of the slot are similar to the magnetic- and electric-plane patterns, respectively, of the metallic antenna.

Example: Slot antenna in an infinite metallic plane, Fig. 19. The complementary metallic antenna is a dipole. For a narrow slot a half-wavelength long, fed at the center, the impedance is $(60\pi)^2/73 = 494$ ohms if the slot radiates on both sides. (If a cavity is added to suppress radiation on one side, the impedance doubles.) The E-plane pattern of the slot and the H-plane pattern of the dipole are omnidirectional, while the slot H-plane pattern is the same as the dipole E-plane pattern.

Impedance of small annular slots: The annular-slot antenna, the complement of a loop, is often used as flush-mounted antenna to produce a pattern and polarization similar to that of a short dipole mounted on a large ground plane. When the outer diameter is less than about a tenth of a wavelength, the impedance* is given by Fig. 20.

* H. Levine and C. H. Papas, "Theory of the Circular Diffraction Antenna," *Journal of Applied Physics*, vol. 22, pp. 29–43; January, 1951.

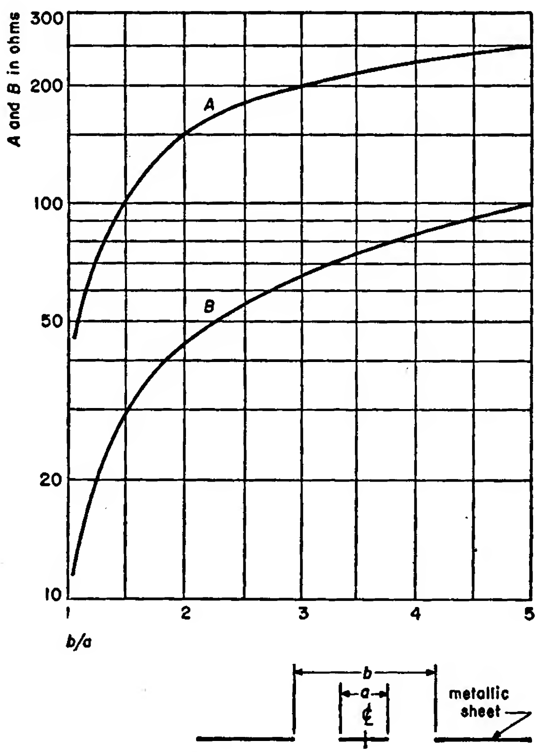

Fig. 20—Impedance of annular-slot antenna. $R = A\,(b/\lambda)^2$ and $X = B\,(\lambda/b)$ (capacitive).

Slot antennas *continued*

Axial slots on cylinders: Fig. 21 shows how the *E*-plane pattern* of an axial slot in the surface of a cylinder varies with diameter and wavelength.

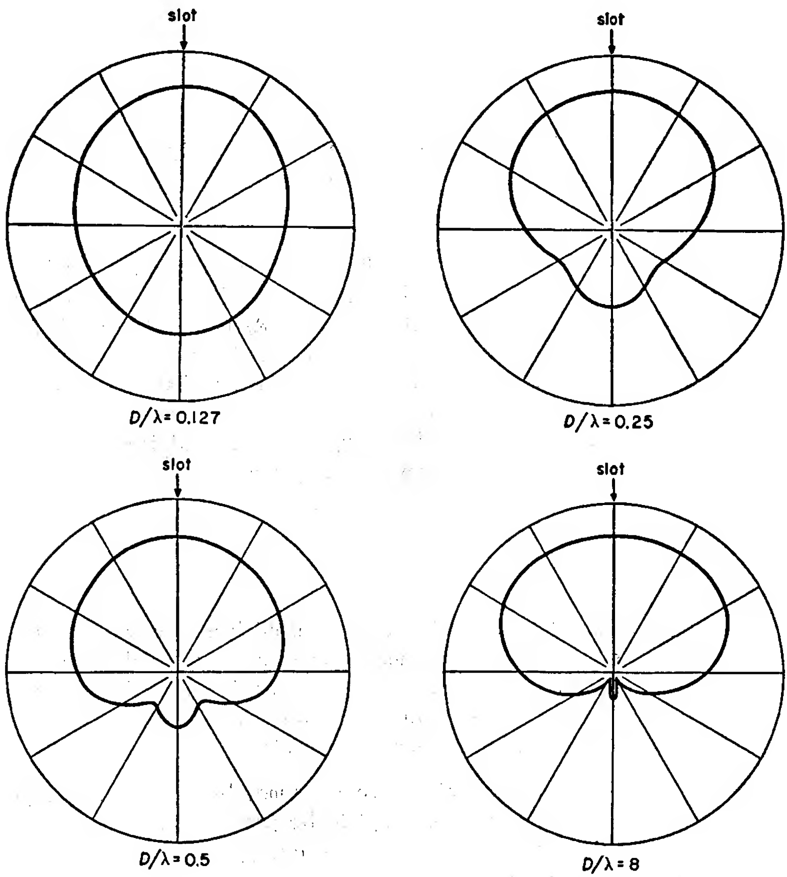

Courtesy of Proceedings of the IRE

Fig. 21—Radiation pattern for single axially slotted cylindrical antenna of diameter *D*.

Antenna arrays

The basis for all directivity control in antenna arrays is wave interference. By providing a large number of sources of radiation, it is possible with a fixed

* G. Sinclair, "Patterns of Slotted-Cylinder Antennas," *Proceedings of the IRE*, vol. 36, pp. 1487–1492; December, 1948.

Antenna arrays *continued*

amount of power greatly to reinforce radiation in a desired direction while suppressing the radiation in undesired directions. The individual sources may be any type of antenna.

Individual elements

Expressions for the radiation pattern of several common types of individual elements are shown in Fig. 22, but the array expressions are not limited to these. The expressions hold for linear radiators, rhombics, vees, horn radiators, or other complex antennas when combined into arrays, provided a suitable expression is used for A, the radiation pattern of the individual antenna. The array expressions are multiplying factors. Starting with an individual antenna having a radiation pattern given by A, the result of combining it with similar antennas is obtained by multiplying A by a suitable array factor, thus obtaining an A' for the group. The group may then be treated as a single source of radiation. The result of combining the group with similar groups or, for instance, of placing the group above ground, is obtained by multiplying A' by another of the array factors given.

Linear array

One of the most important arrays is the linear multielement array where a large number of equally spaced antenna elements are fed equal currents in phase to obtain maximum directivity in the forward direction. Fig. 23 gives expressions for the radiation pattern of several particular cases and the general case of any number of broadside elements.

In this type of array, a great deal of directivity may be obtained. A large number of minor lobes, however, are apt to be present and they may be undesirable under some conditions, in which case a type of array, called the binomial array, may be used.

Binomial array

Here again all the radiators are fed in phase but the current is not distributed equally among the array elements, the center radiators in the array being fed more current than the outer ones. Fig. 24 shows the configuration and general expression for such an array. In this case the configuration is made for a vertical stack of loop antennas in order to obtain single-lobe directivity

Antenna arrays *continued*

Fig. 22—Radiation patterns of several common types of antennas.

type of radiator	current distribution	directivity	
		horizontal E plane $A(\theta)$	vertical H plane $A(\beta)$
A Half-wave dipole	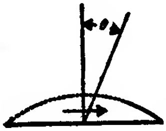	$A(\theta) = K \dfrac{\cos\left(\frac{\pi}{2}\sin\theta\right)}{\cos\theta} \approx K\cos\theta$	$A(\beta) = K(1)$
B Shortened dipole	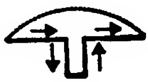	$A(\theta) \approx K\cos\theta$	$A(\beta) = K(1)$
C Lengthened dipole		$A(\theta) = K\left[\dfrac{\cos\left(\frac{\pi l}{\lambda}\sin\theta\right) - \cos\frac{\pi l}{\lambda}}{\cos\theta}\right]$	$A(\beta) = K(1)$
D Horizontal loop	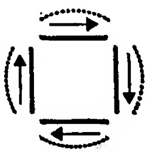	$A(\theta) \approx K(1)$	$A(\beta) = K\cos\beta$
E Horizontal turnstile	 i_1 and i_2 phased 90°	$A(\theta) \approx K'(1)$	$A(\beta) \approx K'(1)$

θ = horizontal angle measured from perpendicular bisecting plane

β = vertical angle measured from horizon

K and K' are constants and $K' \approx 0.7K$

Antenna arrays *continued*

in the vertical plane. If such an array were desired in the horizontal plane, say n dipoles end to end, with the specified current distribution the expression would be

$$F(\theta) = 2^{n-1}\left[\frac{\cos\left(\frac{\pi}{2}\sin\theta\right)}{\cos\theta}\right]\cos^{n-1}\left(\tfrac{1}{2}S^\circ\sin\theta\right) \qquad (25)$$

The term binomial results from the fact that the current intensity in the successive array elements is in accordance with the numerical coefficients of the terms in the binomial expansion $(a+b)^{n-1}$ where n is the number of elements in the array. This is shown in Fig. 24.

Fig. 23—Linear-multielement-array broadside directivity. See Fig. 22 to compare *A* for common antenna types.

	configuration of array	expression for intensity F(θ)
A	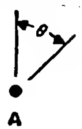	$F(\theta) = A[1]$
B	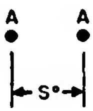	$F(\theta) = 2A\left[\cos\left(\frac{S^\circ}{2}\sin\theta\right)\right]$
C	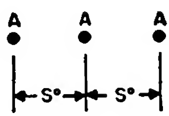	$F(\theta) = A + 2A\left[\cos\left(S^\circ\sin\theta\right)\right]$
D	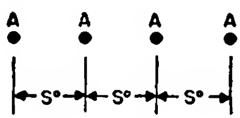	$F(\theta) = 4A\left[\cos\left(S^\circ\sin\theta\right)\cos\left(\frac{S^\circ}{2}\sin\theta\right)\right]$
E	*m* radiators (general case)	$F(\theta) = A\,\dfrac{\sin\left(m\frac{S^\circ}{2}\sin\theta\right)}{\sin\left(\frac{S^\circ}{2}\sin\theta\right)}$

Antenna arrays *continued*

Fig. 24—Development of the binomial array. The expression for the general case is given in E.

configuration of array	expression for intensity $F(\beta)$

A

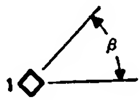

$$F(\beta) = \cos\beta[1]$$

B

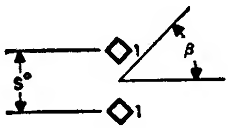

$$F(\beta) = 2\cos\beta\left[\cos\left(\frac{S^\circ}{2}\sin\beta\right)\right]$$

C

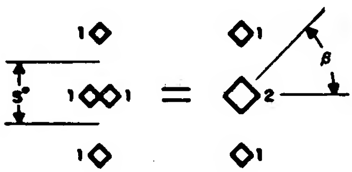

$$F(\beta) = 2^2\cos\beta\left[\cos^2\left(\frac{S^\circ}{2}\sin\beta\right)\right]$$

D

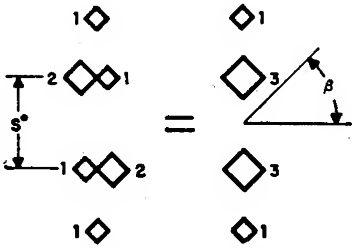

$$F(\beta) = 2^3\cos\beta\left[\cos^3\left(\frac{S^\circ}{2}\sin\beta\right)\right]$$

E

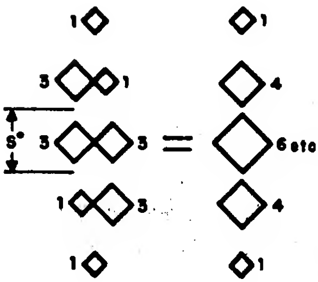

$$F(\beta) = 2^4\cos\beta\left[\cos^4\left(\frac{S^\circ}{2}\sin\beta\right)\right]$$

and in general:

$$F(\beta) = 2^{n-1}\cos\beta\left[\cos^{n-1}\left(\frac{S^\circ}{2}\sin\beta\right)\right]$$

where n = number of loops in the array

Antenna arrays *continued*

Optimum current distribution for broadside arrays*

It is the purpose here to give design equations and to illustrate a method of calculating the optimum current distribution in broadside arrays. The resulting current distribution is optimum in the sense that (a) if the side-lobe level is specified, the beam width is as narrow as possible, and (b) if the first null is specified, the side-lobe level is minimized. The current distribution for 4- through 12-; and 16-, 20-, and 24-element arrays can be calculated after either the side-lobe level or the position of the first null is specified.

Parameter Z: All design equations are given in terms of the parameter Z. To determine Z if the side-lobe level is specified, let

$$r = \frac{\text{(maximum amplitude of main lobe)}}{\text{(maximum amplitude of side lobe)}}$$

then

$$Z = \tfrac{1}{2}\left[\left(r + \sqrt{r^2 - 1}\right)^{1/M} + \left(r - \sqrt{r^2 - 1}\right)^{1/M}\right] = \cosh \rho/M \qquad (26)$$

where

M = (number of elements in the array) − 1

$\rho = \cosh^{-1} r$

To determine Z if the position of the first null is specified (Fig. 25), let θ_0 = position of first null. Then

$$Z = \frac{\cos(\pi/2M)}{\cos\left(\dfrac{\pi S}{\lambda}\sin\theta_0\right)} \qquad (27)$$

where S = spacing between elements.

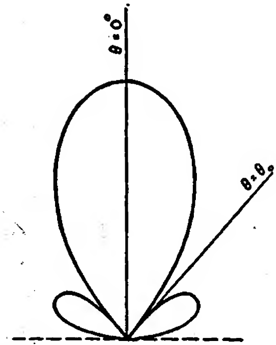

Fig. 25—Beam pattern for broadside array, showing first null at θ_0.

Design equations: The following are in Z. It is assumed that all elements are isotropic, are fed in phase, and are symmetrically arranged about the center. See Fig. 26 for designation of the respective elements to which the following currents I apply.

* C. L. Dolph, "A Current Distribution for Broadside Arrays Which Optimizes the Relationship Between Beam Width and Side-Lobe Level," *Proceedings of the IRE*, vol. 34, pp. 335–348; June, 1946. See also discussion on subject paper by H. J. Riblet and C. L. Dolph, *Proceedings of the IRE*, vol. 35, pp. 489–492; May, 1947.

Antenna arrays *continued*

4-element array

$$I_2 = Z^3$$
$$I_1 = 3(I_2 - Z)$$

8-element array

$$I_4 = Z^7$$
$$I_3 = 7(I_4 - Z^5)$$
$$I_2 = 5I_3 - 14I_4 + 14Z^3$$
$$I_1 = 3I_2 - 5I_3 + 7I_4 - 7Z$$

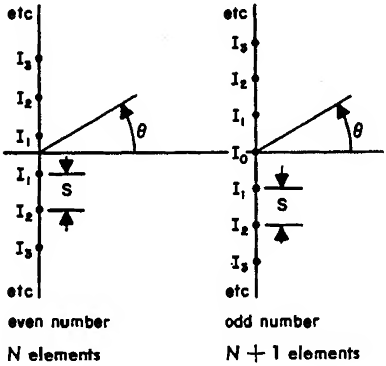

Fig. 26—Broadside array of even and odd number of elements showing nomenclature of radiators, spacing S, and beam-angular measurement θ.

12-element array

$$I_6 = Z^{11}$$
$$I_5 = 11(I_6 - Z^9)$$
$$I_4 = 9I_5 - 44I_6 + 44Z^7$$
$$I_3 = 7I_4 - 27I_5 + 77I_6 - 77Z^5$$
$$I_2 = 5I_3 - 14I_4 + 30I_5 - 55I_6 + 55Z^3$$
$$I_1 = 3I_2 - 5I_3 + 7I_4 - 9I_5 + 11I_6 - 11Z$$

16-element array

$$I_8 = Z^{15}$$
$$I_7 = 15I_8 - 15Z^{13}$$
$$I_6 = 13I_7 - 90I_8 + 90Z^{11}$$
$$I_5 = 11I_6 - 65I_7 + 275I_8 - 275Z^9$$
$$I_4 = 9I_5 - 44I_6 + 156I_7 - 450I_8 + 450Z^7$$
$$I_3 = 7I_4 - 27I_5 + 77I_6 - 182I_7 + 378I_8 - 378Z^5$$
$$I_2 = 5I_3 - 14I_4 + 30I_5 - 55I_6 + 91I_6 - 140I_8 + 140Z^3$$
$$I_1 = 3I_2 - 5I_3 + 7I_4 - 9I_5 + 11I_6 - 13I_7 + 15I_8 - 15Z$$

The relative current values necessary for optimum current distribution are plotted as a function of side-lobe level in decibels for 8-, 12-, and 16-element arrays (Figs. 27–29).

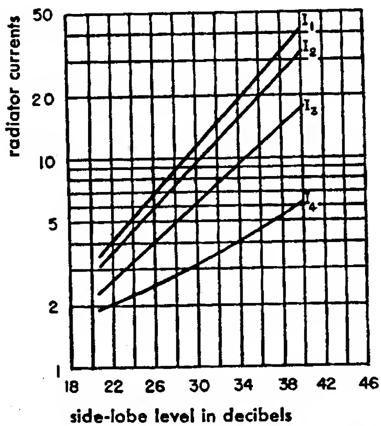

Courtesy of Proceedings of the IRE

Fig. 27—The relative current values for an 8-element array necessary for "the optimum current distribution" as a function of side-lobe level in decibels.

Antenna arrays *continued*

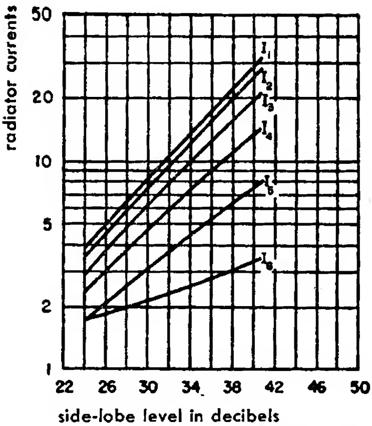

Courtesy of Proceedings of the IRE

Fig. 28—The relative current values for a 12-element array necessary for "the optimum current distribution" as a function of side-lobe level in decibels.

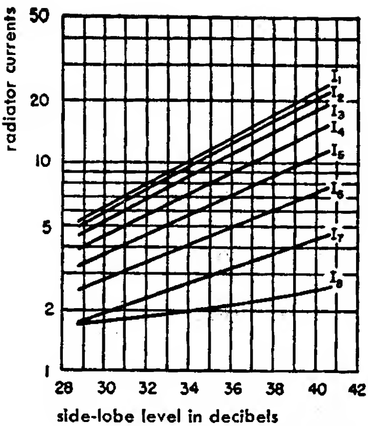

Courtesy of Proceedings of the IRE

Fig. 29—The relative current values for a 16-element array necessary for "the optimum current distribution" as a function of side-lobe level in decibels.

Effect of ground on antenna radiation at very-high and ultra-high frequencies

The behavior of the earth as a reflecting surface is considerably different for horizontal than for vertical polarization. For horizontal polarization the earth may be considered a perfect conductor, i.e., the reflected wave at all vertical angles β is substantially equal to the incident wave and 180 degrees out of phase with it. $F(\beta)$ in Fig. 30B was derived on this basis. The approximation is good for practically all types of ground.

For vertical polarization, however, the problem is much more complex as both the relative amplitude K and relative phase ϕ change with vertical angle β, and vary considerably with different types of ground. Fig. 31 is a set of curves that illustrate the problem. The subscripts to the amplitude and phase coefficients K and ϕ refer to the type of polarization.

It is to be noted particularly that at grazing incidence ($\beta = 0$) the reflection coefficient is the same for vertical and horizontal polarization. This is substantially true for practically all ground conditions.

Antenna arrays *continued*

Directivity of several miscellaneous arrays

Fig. 30—Directivity of several array problems that do not fall into any of the preceding classes.

<table>
<tr><th>configuration of array</th><th>expression for intensity</th></tr>
<tr><td>

A. Two radiators any phase ϕ

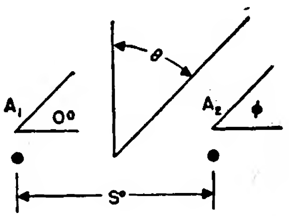

</td><td>

$F(\theta) =$

$[A_1^2 + A_2^2 + 2A_1A_2 \cos(S° \sin\theta + \phi)]^{\frac{1}{2}}$

When $A_1 = A_2$,

$F(\theta) = 2A \cos\left(\frac{S°}{2}\sin\theta + \frac{\phi}{2}\right)$

</td></tr>
<tr><td>

B. Radiator above ground (horizontal polarization)

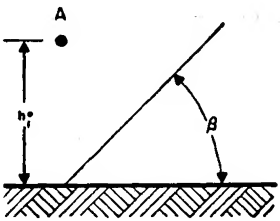

</td><td>

$F(\beta) = 2A \sin(h_1° \sin\beta)$

</td></tr>
<tr><td>

C. Radiator parallel to screen

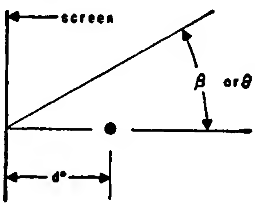

</td><td>

$F(\beta) = 2A \sin(d° \cos\beta)$

or

$F(\theta) = 2A \sin(d° \cos\theta)$

</td></tr>
</table>

$S°$ = spacing in electrical degrees

$h_1°$ = height of radiator in electrical degrees

$d°$ = spacing of radiator from screen in electrical degrees

Antenna arrays *continued*

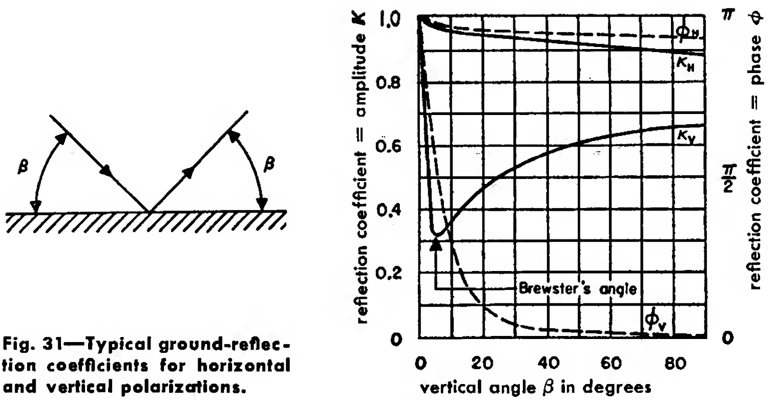

Fig. 31—Typical ground-reflection coefficients for horizontal and vertical polarizations.

Electromagnetic horns and parabolic reflectors

Radiation from a waveguide may be obtained by placing an electromagnetic horn of a particular size at the end of the waveguide.

Fig. 32 gives data for designing a horn to have a specified gain with the shortest length possible. The length L_1 is given by

$$L_1 = L\left(1 - \frac{a}{2A} - \frac{b}{2B}\right) \tag{28}$$

where

a = wide dimension of waveguide in the H plane

b = narrow dimension of waveguide in E plane

If $L \geqslant A^2/\lambda$, where A = longer dimension of aperture, the gain is given by

$$G = 10AB/\lambda^2 \tag{29}$$

The half-power width in the E plane is given by

$$51\ \lambda/B \text{ degrees} \tag{30}$$

and the half-power width in the H plane is given by

$$70\ \lambda/A \text{ degrees} \tag{31}$$

where

E = electric vector

H = magnetic vector

Fig. 33 shows how the angle between 10-decibel points varies with aperture.

Electromagnetic horns and parabolic reflectors *continued*

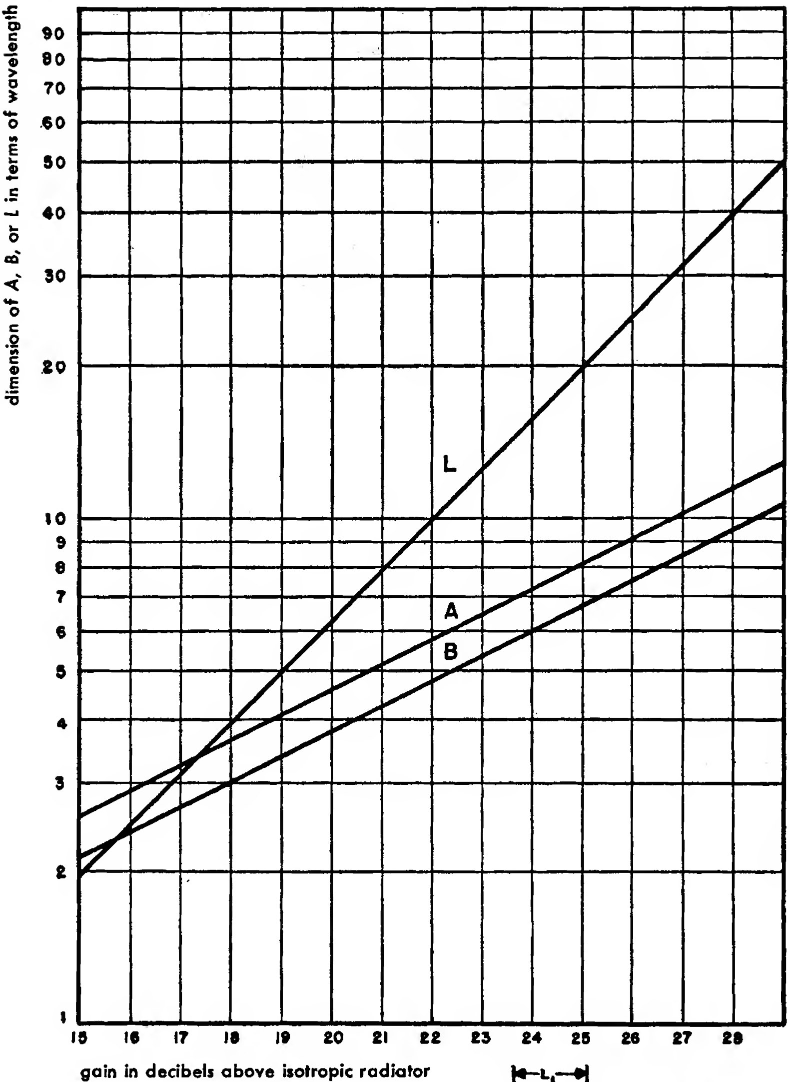

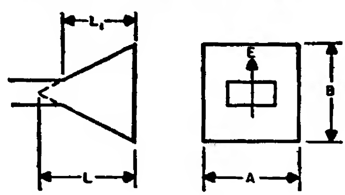

L = axial length to apex

A = width of aperture in *H* plane

B = width of aperture in *E* plane

Fig. 32—Design of electromagnetic-horn radiator.

Electromagnetic horns and parabolic reflectors *continued*

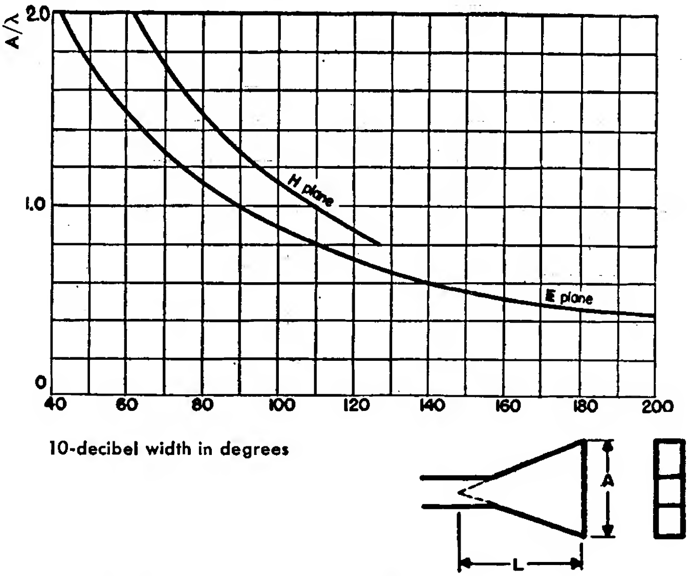

Fig. 33—10-decibel widths of horns. $L \geqslant A^2/\lambda$.

Parabolas

If the intensity across the aperture of the parabola is of constant phase and tapers smoothly from the center to the edges so that the intensity at the edges is 10 decibels down from that at the center, the gain is given by

$$G = 7A/\lambda^2 \tag{32}$$

where A = area of aperture. The half-power width is given by

$$70\ \lambda/D \text{ degrees} \tag{33}$$

where D = diameter of parabola. See nomograph, p. 754.

Passive reflectors

In some applications, an antenna and plane reflector are used instead of a directional antenna fed through a long transmission line. The main application is in microwave line-of-sight radio links where the antenna may be mounted up to 300 feet above the associated radio equipment. In some cases, the loss is less than that of a long transmission line. In addition, long-line effects, such as "pulling" of frequency-modulated oscillators, are minimized.

Passive reflectors *continued*

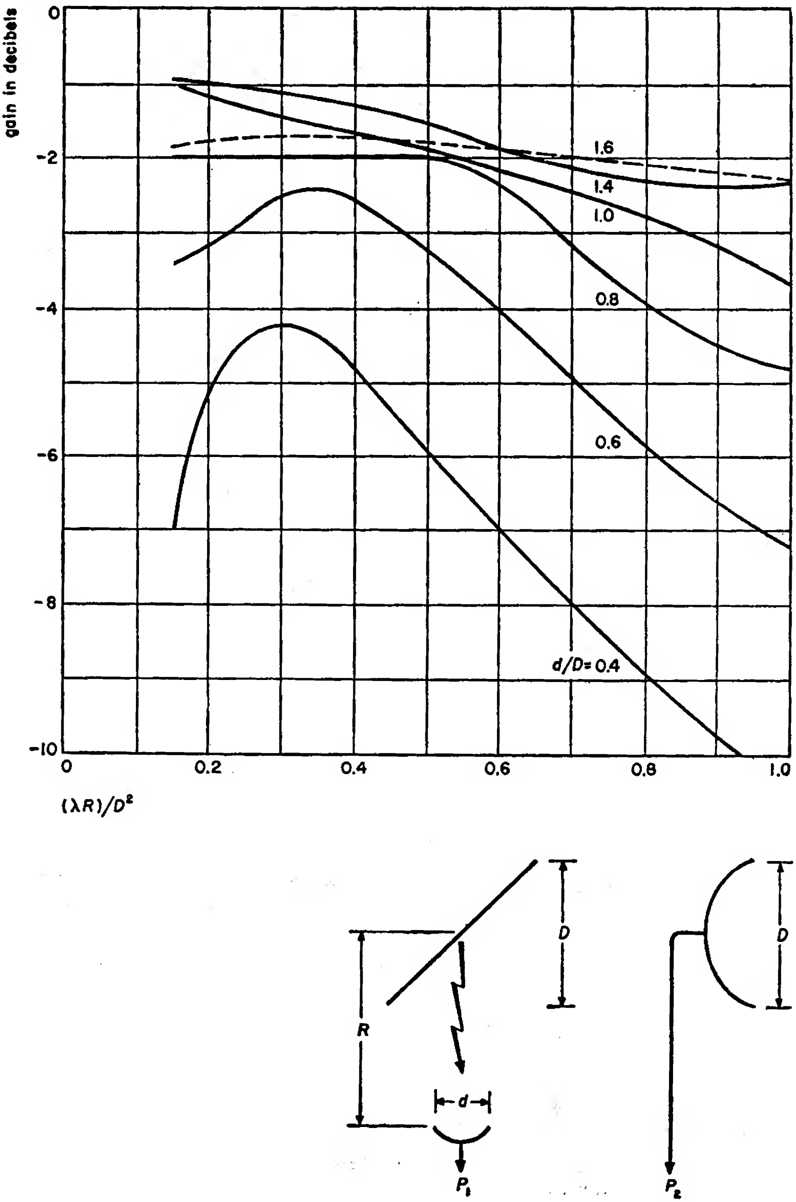

Fig. 34—Gain of antenna system incorporating a passive reflector. Diameter *D* of the parabolic antenna equals projected diameter *D* of the reflector.

Passive reflectors *continued*

Fig. 34 shows the gain relative to an antenna whose area is equal to the projected area of the reflector. (To obtain the gain relative to the antenna, add 20 log (D/d) to the gains shown.) The plane reflector is assumed to be of elliptical shape and the amplitude tapers parabolically across the aperture of the antenna so that the edge illumination is 10 decibels below the center.* Slightly more gain can be obtained if a rectangular reflector is used.†

Example: Compared to a 6-foot-diameter antenna, a reflector 6 feet in diameter mounted on a 200-foot tower has a loss of 3.5 decibels when fed with a 6-foot-diameter antenna at 6000 megacycles and a loss of 2.5 decibels when fed with an 8.5-foot-diameter antenna. The over-all system gain is larger if the transmission-line loss exceeds 3.5 or 2.5 decibels, respectively.

Corner reflectors

The corner reflector‡ is a simple directive antenna. The dimensions given in Fig. 35 will give a gain of 8 to 10 decibels over a dipole alone. If λ = wavelength,

$0.25\,\lambda \leqslant S \leqslant 0.7\,\lambda$

length of reflector $\geqslant \lambda$

height of reflector $\geqslant 5\,\lambda/8$

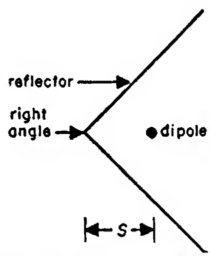

Fig. 35—Corner-reflector antenna.

Antenna gain and effective area

The gain of an antenna is a measure of how well the antenna concentrates its radiated power in a given direction. It is the ratio of the power radiated in a given direction to the power radiated in the same direction by a standard antenna (a dipole or isotropic radiator), keeping the input power constant. If the pattern of the antenna is known and there are no ohmic losses in the system, the gain G is defined by

* W. C. Jakes, Jr., "Theoretical Study of An Antenna–Reflector Problem," *Proceedings of the IRE*, vol. 41, pp. 272–274; February, 1953.

† R. E. Greenquist and A. J. Orlando, "Analysis of Passive Reflector Antenna Systems," *Proceedings of the IRE*, vol. 42, pp. 1173–1178; July, 1954.

‡ J. D. Kraus, "The Corner Reflector Antenna," *Proceedings of the IRE*, vol. 28, pp. 513–519; November, 1940.

Antenna gain and effective area *continued*

$$G = \left(\frac{\text{maximum power intensity}}{\text{average power intensity}}\right) = \frac{4\pi |E_0|^2}{\underset{\substack{\text{all}\\ \text{angles}}}{\int\int} |E|^2 \, d\Omega} \qquad (34)$$

where

$|E_0|$ = magnitude of the field at the maximum of the radiation pattern
$|E|$ = magnitude of the field in any direction

The effective area A_r of an antenna is defined by

$$A_r = \frac{G\lambda^2}{4\pi} \qquad (35)$$

where

G = gain of the antenna
λ = wavelength

The power delivered by a matched antenna to a matched load connected to its terminals is PA_r, where P is the power density in watts/meter^2 at the antenna and A_r is the effective area in meters^2.

The gains and receiving areas of some typical antennas are given in Fig. 36.

Fig. 36—Power gain G and effective area A of several common antennas.

radiator	gain above isotropic radiator	effective area
Isotropic radiator	1	$\lambda^2/4\pi$
Infinitesimal dipole or loop	1.5	1.5 $\lambda^2/4\pi$
Half-wave dipole	1.64	1.64 $\lambda^2/4\pi$
Optimum horn (mouth area = A)	10 A/λ^2	0.81 A
Horn (maximum gain for fixed length—see Fig. 33, mouth area = A)	5.6 A/λ^2	0.45 A
Parabola or metal lens	6.3 to 7.5 A/λ^2	0.5 to 0.6 A
Broadside array (area = A)	4π A/λ^2 (max)	A (max)
Omnidirectional stacked array (length = L, stack interval $\leqslant \lambda$)	$\approx 2L/\lambda$	$\approx L\ \lambda/2\pi$
Turnstile	1.15	1.15 $\lambda^2/4\pi$

Antenna gain and effective area *continued*

The gains and effective areas given in Fig. 36 apply in the receiving case only; when the polarizations are not the same, the gain is given by

$$G_\theta = G\cos^2\theta \tag{36}$$

where

G = gain of the antenna
θ = angle between plane of polarization of the antenna and the incident field

Equation (36) applies only to linear polarization. Equation (6) gives the variation for circular or elliptical polarization. If a circularly polarized antenna is used to receive power from an incident wave of the same screw sense, the gains and receiving areas in Fig. 36 are correct. If a circularly polarized antenna is used to receive power from a linearly polarized wave (or vice-versa) the gain or receiving area will be one-half those of Fig. 36.

If the half-power widths of a narrow-beam antenna are known, the approximate gain above an isotropic radiator may be computed from

$$G = \frac{30{,}000}{W_E W_H} \tag{37}$$

where

W_E = E-plane half-power width in degrees
W_H = H-plane half-power width in degrees

Equation (37) is not accurate if the half-power widths are greater than about 20 degrees, or if there are many large side lobes.

Vertically stacked horizontal loops

Radiation pattern for array of Fig. 37 is

$$F(\beta) = \frac{\sin\left(\frac{nS^\circ}{2}\sin\beta\right)}{\sin\left(\frac{S^\circ}{2}\sin\beta\right)}\cos\beta \tag{38}$$

where

n = number of loops
S° = spacing in electrical degrees

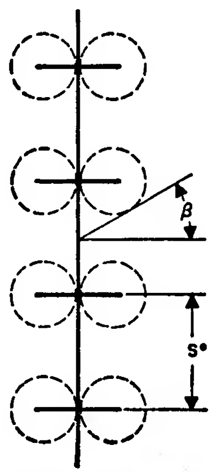

Fig. 37—Stacked loops.

Vertically stacked horizontal loops *continued*

If S = spacing in radians, the gain is

$$\text{gain} = \left\{\frac{1}{n} + \frac{6}{n^2}\sum_{1=k}^{n-1}(n-k)\left[\frac{\sin kS^\circ}{(kS)^3} - \frac{\cos kS^\circ}{(kS)^2}\right]\right\}^{-1} \tag{39}$$

The gain as a function of the number of loops and the electrical spacing s given in Fig. 38.

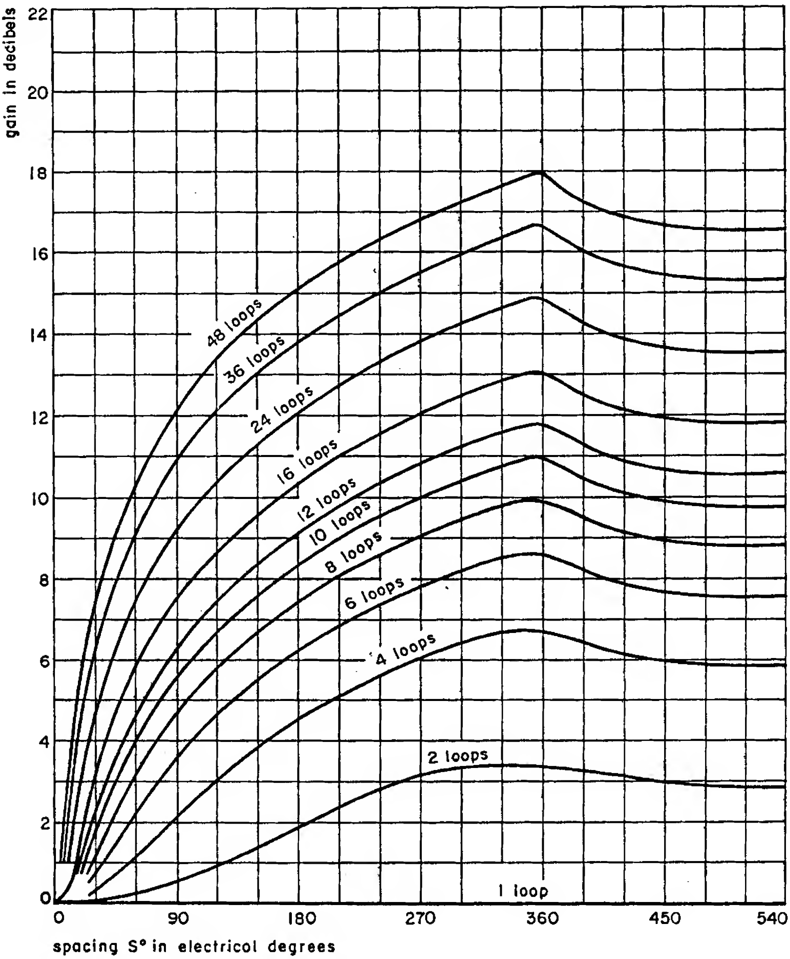

Fig. 38—Gain of linear array of horizontal loops vertically stacked.

Vertically stacked horizontal loops *continued*

The data are also directly applicable to stacked dipoles, discones, tripoles, etc., and all other antenna systems that have vertical directivity but are omnidirectional in the horizontal plane. Such antennas are widely used for frequency-modulation, television, and radio-beacon applications.

Examples in the solution of antenna-array problems

Problem 1: Find horizontal radiation pattern of four colinear horizontal dipoles, spaced successively $\lambda/2$, or 180 degrees.

Solution: From Fig. 23D, radiation from four radiators spaced 180 degrees is given by

$$F(\theta) = 4A \cos (180° \sin \theta) \cos (90° \sin \theta)$$

From Fig. 22A, the horizontal radiation of a half-wave dipole is given by

$$A = K \frac{\cos\left(\frac{\pi}{2} \sin \theta\right)}{\cos \theta}$$

therefore, the total radiation

$$F(\theta) = K \left[\frac{\cos\left(\frac{\pi}{2} \sin \theta\right)}{\cos \theta}\right] \cos (180° \sin \theta) \cos (90° \sin \theta)$$

Problem 2: Find vertical radiation pattern of four horizontal dipoles, stacked one above the other, spaced 180 degrees successively.

Solution: From Fig. 23D we obtain the general equation of four radiators, but since the spacing is vertical, the expression should be in terms of vertical angle β.

$$F(\beta) = 4A \cos (180° \sin \beta) \cos (90° \sin \beta)$$

From Fig. 22A we find that the vertical radiation from a horizontal dipole (in the perpendicular bisecting plane) is nondirectional. Therefore the vertical pattern is

Examples in the solution of antenna-array problems *continued*

$$F(\beta) = K(1) \cos (180^\circ \sin \beta) \cos (90^\circ \sin \beta)$$

Problem 3: Find horizontal radiation pattern of group of dipoles in problem 2.

Solution: From Fig. 22A.

$$F(\theta) = K \frac{\cos\left(\frac{\pi}{2} \sin \theta\right)}{\cos \theta} \approx K \cos \theta$$

Problem 4: Find the vertical radiation pattern of stack of five loops spaced $2\lambda/3$, or 240 degrees, one above the other, all currents equal in phase and amplitude.

Solution: From Fig. 23E, using vertical angle because of vertical stacking,

$$F(\beta) = A \frac{\sin [5(120^\circ) \sin \beta]}{\sin (120^\circ \sin \beta)}$$

From Fig. 22D, we find A for a horizontal loop in the vertical plane

$$A = F(\beta) = K \cos \beta$$

Total radiation pattern

$$F(\beta) = K \cos \beta \frac{\sin [5(120^\circ) \sin \beta]}{\sin (120^\circ \sin \beta)}$$

Problem 5: Find radiation pattern (vertical directivity) of the five loops in problem 4, if they are used in binomial array. Find also current intensities in the various loops.

Solution: From Fig. 24E

$$F(\beta) = K \cos \beta \, [\cos^4 (120^\circ \sin \beta)]$$

(all terms not functions of vertical angle β are combined in constant K)

Current distribution $(1 + 1)^4 = 1 + 4 + 6 + 4 + 1$, which represent the current intensities of successive loops in the array.

Examples in the solution of antenna-array problems *continued*

Problem 6: Find horizontal radiation pattern from two vertical dipoles spaced one-quarter wavelength apart when their currents differ in phase by 90 degrees.

Solution: From Fig. 30A

$s^\circ = \lambda/4 = 90^\circ = \text{spacing}$
$\phi = 90^\circ = \text{phase difference}$

Then,

$F(\theta) = 2A \cos (45 \sin \theta + 45^\circ)$

Problem 7: Find the vertical radiation pattern and the number of nulls in the vertical pattern $(0 \leqslant \beta \leqslant 90)$ from a horizontal loop placed three wavelengths above ground.

Solution

$h_1^\circ = 3(360) = 1080^\circ$

From Fig. 30B

$F(\beta) = 2A \sin (1080 \sin \beta)$

From Fig. 22D for loop antennas

$A = K \cos \beta$

Total vertical radiation pattern

$F(\beta) = K \cos \beta \sin (1080 \sin \beta)$

A null occurs wherever $F(\beta) = 0$.

The first term, $\cos \beta$, becomes 0 when $\beta = 90$ degrees.

The second term, $\sin (1080 \sin \beta)$, becomes 0 whenever the value inside the parenthesis becomes a multiple of 180 degrees. Therefore, number of nulls equals

$$1 + \frac{h_1^\circ}{180} = 1 + \frac{1080}{180} = 7$$

Problem 8: Find the vertical and horizontal patterns from a horizontal half-wave dipole spaced $\lambda/8$ in front of a vertical screen.

Solution:

$$d^\circ = \frac{\lambda}{8} = 45^\circ$$

Examples in the solution of antenna-array problems *continued*

From Fig. 30C

$F(\beta) = 2A \sin (45° \cos \beta)$

$F(\theta) = 2A \sin (45° \cos \theta)$

From Fig. 22A for horizontal half-wave dipole

Vertical pattern $A = K(1)$

Horizontal pattern $A = K \dfrac{\cos\left(\frac{\pi}{2} \sin \theta\right)}{\cos \theta}$

Total radiation patterns are

Vertical: $F(\beta) = K \sin (45° \cos \beta)$

Horizontal: $F(\theta) = K \dfrac{\cos\left(\frac{\pi}{2} \sin \theta\right)}{\cos \theta} \sin (45° \cos \theta)$

■ Radio-wave propagation

Very-low frequencies—up to 60 kilocycles

The received field intensity in microvolts/meter has been experimentally found to follow the Austin-Cohen equation for distances between 500 and 10,000 kilometers:

$$E = \frac{298 \times 10^3 (P)^{1/2}}{D} \left(\frac{\theta}{\sin \theta}\right)^{1/2} \exp\left(-\alpha \frac{D}{\lambda^{1/2}}\right) \tag{1}$$

where

D = kilometers between transmitter and receiver

E = received field intensity in microvolts/meter

P = radiated power from the transmitter antenna in kilowatts

R = effective radius of earth in kilometers = 6380

α = attenuation constant

exp = 2.718 to the exponent shown within parentheses

θ = angular distance in radians = D/R

λ = wavelength of radiation in kilometers = 300/(frequency in kilocycles)

The two nomograms, Figs. 1 and 2,* give solutions for the most important problems related to very-long-wave propagation. The first nomogram solves the following equations

$$(P)^{1/2} = \frac{H I}{\lambda} \cdot \frac{377}{298} \tag{2}$$

$$M = \frac{E}{298 \times 10^3 (P)^{1/2}} \tag{3}$$

where

H = radiation height (effective height) in meters

I = antenna current in amperes

M = quantity used in Fig. 2

Example

To effect a solution of the above equations:

a. On Fig. 1, draw two straight lines, the first connecting a value of H with a value of I, the second connecting a value of λ with a value of P; if both

* The nomograms, Figs. 1 and 2, are due to Mrs. M. Lindeman Phillips of the Central Radio Propagation Laboratory, National Bureau of Standards, Washington, D. C.

Very-low frequencies *continued*

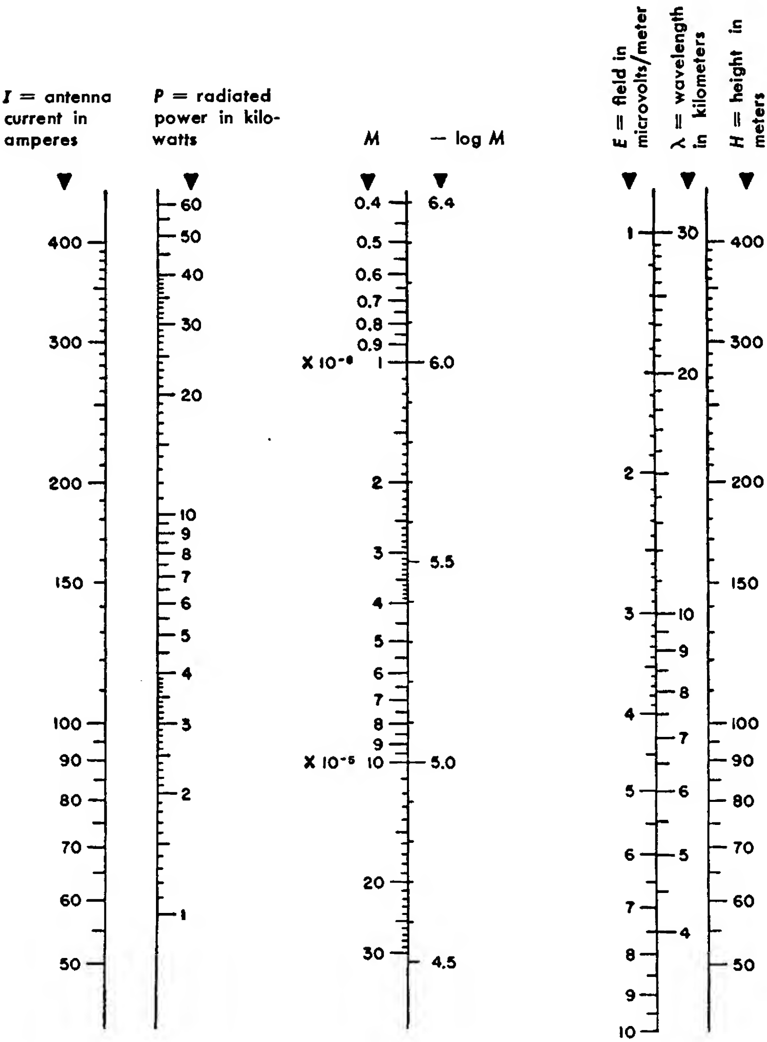

Fig. 1—First nomogram for the solution of very-long-wave field strength. For the solution of *P* and *M*, equations (2) and (3).

Very-low frequencies *continued*

lines intersect on the central *M* line of the nomogram, the values present a solution of (2). *Note:* This does *not* give a solution of (3), i.e., a solution for *M*.

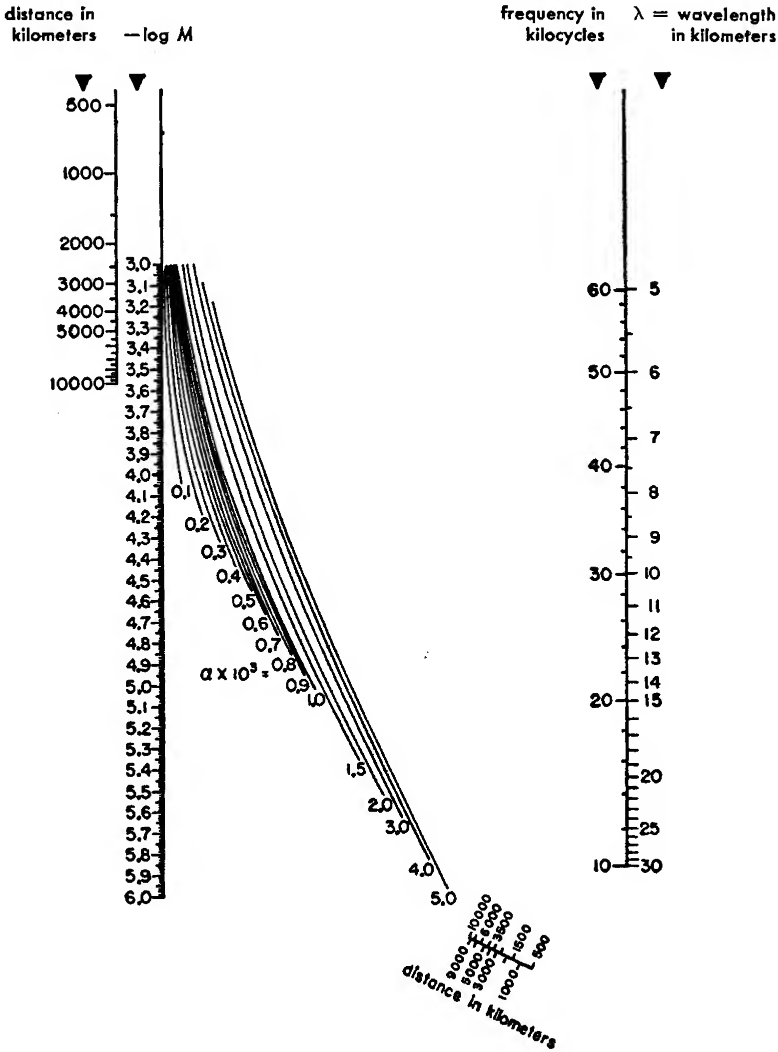

Fig. 2—Second nomogram for the determination of very-long-wave field strength by the Austin-Cohen equation (1). Value *M* is first determined from Fig. 1.

Very-low frequencies *continued*

b. Draw a straight line connecting values of P and E. The intersection of this line with the central nomographic scale M gives the corresponding value of M, as indicated in (3).

Fig. 2 represents the Austin-Cohen equation, affording the possibility of either determining or using various values for the attenuation constant α. To use,

c. Draw a straight line connecting points located on the two distance scales for the proper transmission distance.

d. Draw a second straight line connecting the proper values of wavelength (or frequency) and M; its intersection with the straight line in (c) above must lie at the proper value of α among the family of curves represented. The values of M, λ, D, and α thus indicated represent a solution of (1).

Low and medium frequencies—100 to 3000 kilocycles*

For low and medium frequencies, of approximately 100 to 3000 kilocycles, with a theoretical short vertical antenna over perfectly reflecting ground:

$E = 186\ (P_r)^{1/2}$ millivolts/meter at 1 mile

or,

$E = 300\ (P_r)^{1/2}$ millivolts/meter at 1 kilometer

where P_r = radiated power in kilowatts.

Actual inverse-distance fields at one mile for a given transmitter output power depend on the height and efficiency of the antenna and the efficiency of coupling devices.

Typical values found in practice for well-designed stations are:

Small L or T antennas as on ships: $25\ (P_t)^{1/2}$ millivolts/meter at 1 mile
Vertical radiators 0.15 to 0.25 λ high: $150\ (P_t)^{1/2}$ millivolts/meter at 1 mile
Vertical radiators 0.25 to 0.40 λ high: $175\ (P_t)^{1/2}$ millivolts/meter at 1 mile
Vertical radiators 0.40 to 0.60 λ high
or top-loaded vertical radiators: $220\ (P_t)^{1/2}$ millivolts/meter at 1 mile

where P_t = transmitter output power in kilowatts. These values can be increased by directive arrangements.

* For more exact methods of computation see F. E. Terman, "Radio Engineers' Handbook," 1st edition, McGraw-Hill Book Company, New York, New York, 1943; Section 10. Also, K. A. Norton, "The Calculation of Ground-Wave Field Intensities Over a Finitely Conducting Spherical Earth," *Proceedings of the IRE*, vol. 29, pp. 623–639; December, 1941.

Low and medium frequencies *continued*

The surface-wave field (commonly called *ground wave*) at greater distances can be found from Figs. 3–6.* Figs. 4–6 are based on a field strength of 186 millivolts/meter at one mile. The ordinates should be multiplied by the ratio of the actual field at 1 mile to 186 millivolts/meter.

* For additional curves of ground-wave field intensity versus distance, see chapter 22, "Broadcasting."

Fig. 3—Ground conductivity and dielectric constant for medium- and long-wave propagation to be used with Norton's, van der Pol's, Eckersley's, or other developments of Sommerfeld propagation formulas.

terrain	conductivity σ in emu	dielectric constant ϵ in esu
Sea water	4×10^{-11}	80
Fresh water	5×10^{-14}	80
Dry, sandy flat coastal land	2×10^{-14}	10
Marshy, forested flat land	8×10^{-14}	12
Rich agricultural land, low hills	1×10^{-13}	15
Pastoral land, medium hills and forestation	5×10^{-14}	13
Rocky land, steep hills	2×10^{-14}	10
Mountainous (hills up to 3000 feet)	1×10^{-14}	5
Cities, residential areas	2×10^{-14}	5
Cities, industrial areas	1×10^{-15}	3

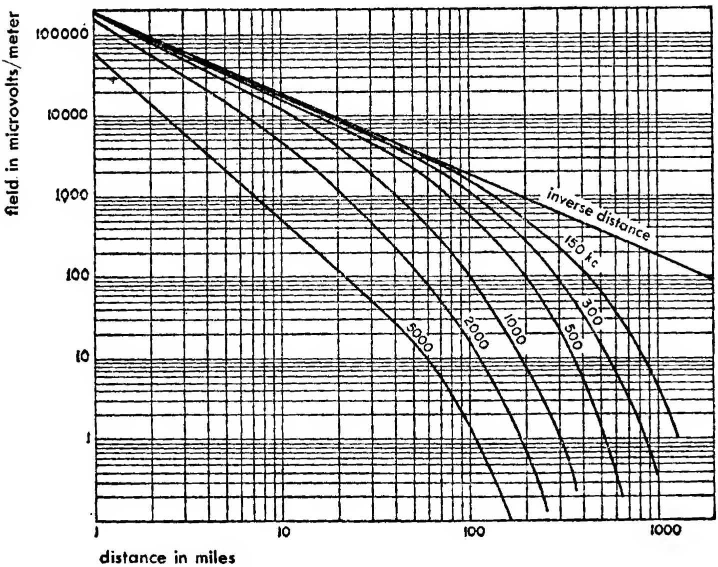

Fig. 4—Strength of surface waves as a function of distance with a vertical antenna for good earth ($\sigma = 10^{-13}$ emu and $\epsilon = 15$ esu).

Low and medium frequencies *continued*

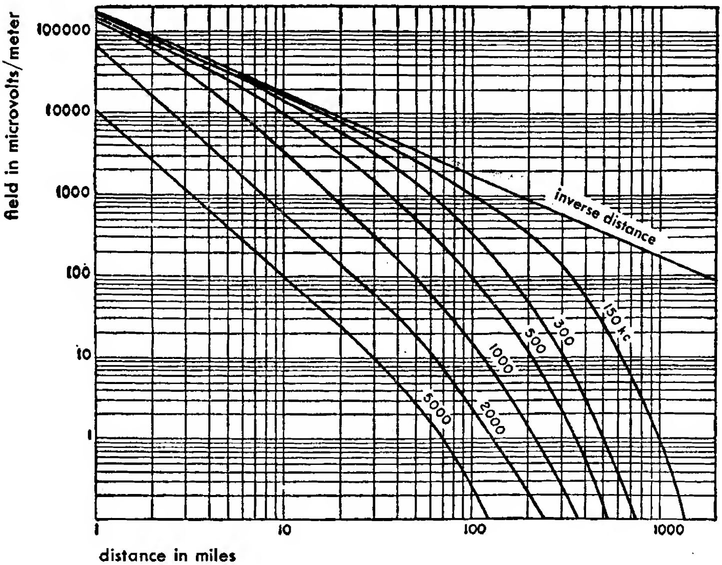

Fig. 5—As Fig. 4, for poor earth ($\sigma = 2 \times 10^{-14}$ emu and $\epsilon = 5$ esu).

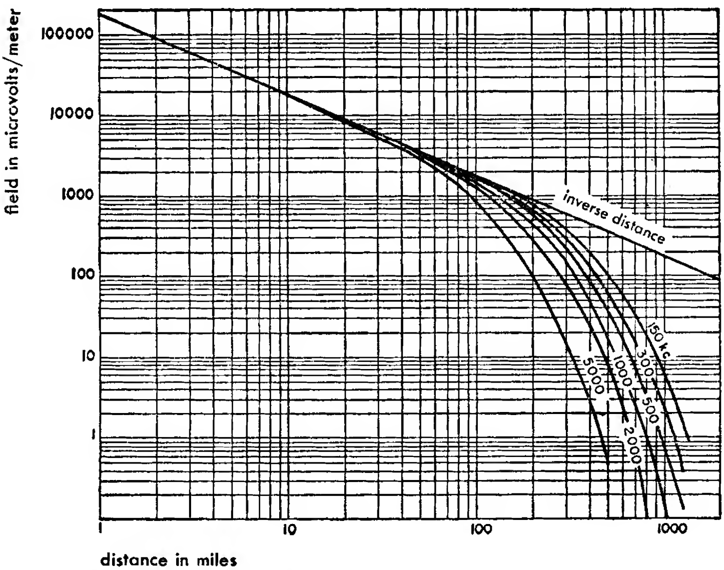

Fig. 6—As Fig. 4, for sea water ($\sigma = 4 \times 10^{-11}$ emu and $\epsilon = 80$ esu).

Low and medium frequencies *continued*

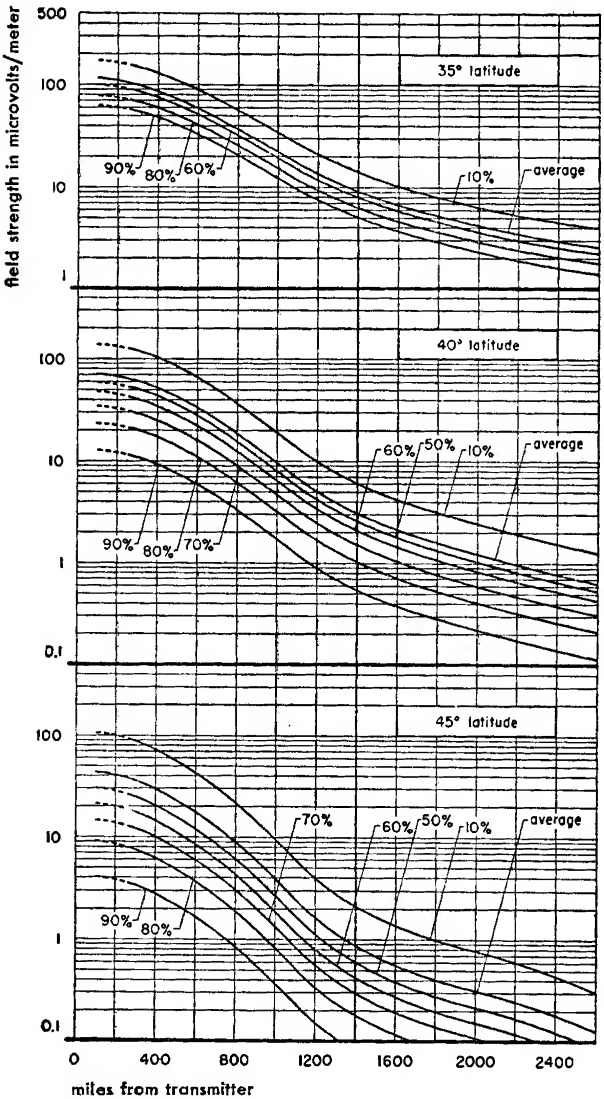

Fig. 7—Sky-wave signal range at medium frequencies for 1939 (typical of sunspot maximum). Shown are the values exceeded by field intensities (hourly median values) for various percentages of the nights per year per 100 millivolts/meter radiated at 1 mile. Annual average is also shown. For latitudes of 35, 40, and 45 degrees.

Low and medium frequencies *continued*

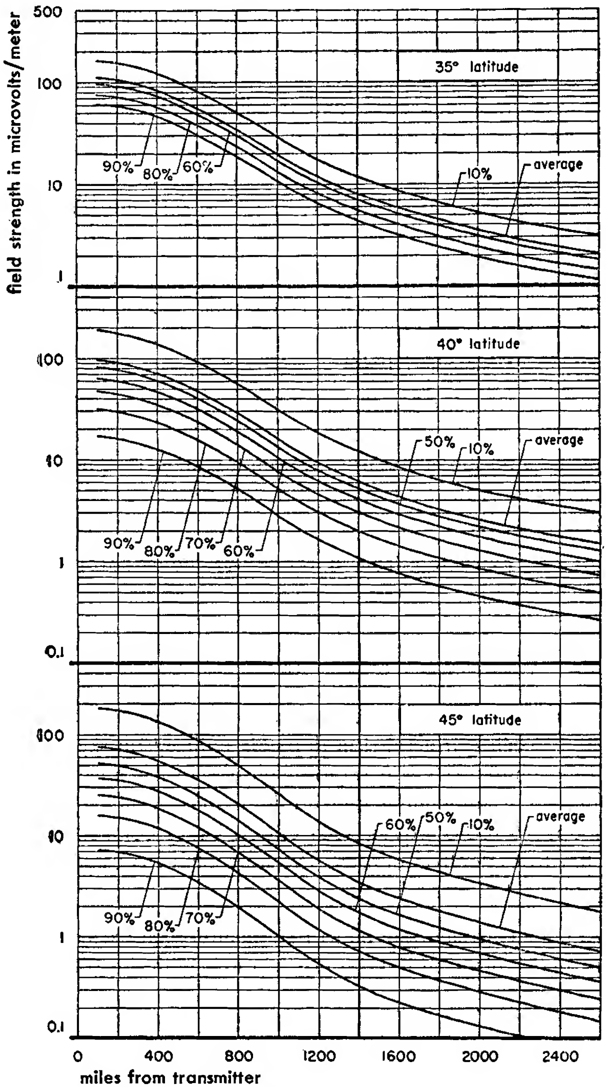

Fig. 8—Sky-wave signal range at medium frequencies for 1944 (sunspot minimum). Shown are the values exceeded by field intensities (hourly median values) for various percentages of the nights per year per 100 millivolts/meter radiated at 1 mile. Annual average is also shown. Values are given for latitudes of 35, 40, and 45 degrees.

Low and medium frequencies *continued*

Figs. 4, 5, and 6 do not include the effect of *sky* waves reflected from the ionosphere. Sky waves cause fading at medium distances and produce higher field intensities than the surface wave at longer distances, particularly at night and on the lower frequencies during the day. Sky-wave field intensity is subject to diurnal, seasonal, and irregular variations due to changing properties of the ionosphere.

The annual median field strengths are functions of the latitude, the frequency on which the transmission takes place, and the phase of the solar sunspot cycle at a given time.

The dependence of the annual median field for transmissions on frequencies around the middle of the United States standard broadcast band is shown on Fig. 7 for a period (1939) near sunspot maximum* and on Fig. 8, for a period of sunspot minimum (1944).

The curves are given for 35, 40, and 45 degrees latitude. The latitude used to characterize a path is that of a control point on the path. The control point is taken to be the midpoint of a path less than 1000 miles long; and for a longer path, the reflection point (for two-reflection transmission) that is at the higher latitude.

The curves are extracted from a report of the Federal Communications Commission in 1946.†

High frequencies—3 to 30 megacycles

At frequencies between about 3 and 25 megacycles and distances greater than about 100 miles, transmission depends entirely on sky waves reflected from the ionosphere. This is a region high above the earth's surface where the rarefied air is sufficiently ionized (primarily by ultraviolet sunlight) to reflect or absorb radio waves, such effects being controlled almost exclusively by the free-electron density. The ionosphere is usually considered as consisting of the following *layers*.

D layer: At heights from about 50 to 90 kilometers,‡ it exists only during daylight hours, and ionization density corresponds with the altitude of the sun.

This layer reflects very-low- and low-frequency waves, absorbs medium-frequency waves, and weakens high-frequency waves through partial absorption.

* Sunspot maximums occurred in 1938 and 1948; the next is expected in 1958. Sunspot minimums occurred in 1944 and 1954; the next is expected in 1964.

† Committee III—Docket 6,741, "Skywave Signal Range at Medium Frequencies," Federal Communications Commission, Washington, D. C.; 1946.

‡ 1 kilometer = 0.621 mile.

High frequencies *continued*

E layer: At height of about 110 kilometers, this layer is of importance for high-frequency daytime propagation at distances less than 1000 miles, and for medium-frequency nighttime propagation at distances in excess of about 100 miles. Ionization density corresponds closely with the altitude of the sun. Irregular cloud-like areas of unusually high ionization, called *sporadic E* may occur up to more than 50 percent of the time on certain days or nights. *Sporadic E* occasionally prevents frequencies that normally penetrate the *E* layer from reaching higher layers and also causes occasional long-distance transmission at very high frequencies. Some portion (perhaps the major part) of the sporadic-*E* ionization is ascribable to visible- and subvisible-wavelength bombardment of the atmosphere.

F_1 layer: At heights of about 175 to 250 kilometers, it exists only during daylight. This layer occasionally is the reflecting region for high-frequency transmission, but usually oblique-incidence waves that penetrate the *E* layer also penetrate the F_1 layer to be reflected by the F_2 layer. The F_1 layer introduces additional absorption of such waves.

F_2 layer: At heights of about 250 to 400 kilometers, F_2 is the principal reflecting region for long-distance high-frequency communication. Height and ionization density vary diurnally, seasonally, and over the sunspot cycle. Ionization does not follow the altitude of the sun in any simple fashion, since (at such extremely low air densities and molecular-collision rates) the medium can store received solar energy for many hours, and, by energy transformation, can even detach electrons during the night. At night, the F_1 layer merges with the F_2 layer at a height of about 300 kilometers. The absence of the F_1 layer, and reduction in absorption of the *E* layer, causes nighttime field intensities and noise to be generally higher than during daylight hours.

As indicated to the right on Fig. 10, these *layers* are contained in a thick region throughout which ionization generally increases with height. The layers are said to exist where the ionization gradient is capable of refracting waves back to earth. Obliquely incident waves follow a curved path through the ionosphere due to gradual refraction or bending of the wave front. When attention need be given only to the end result, the process can be assimilated to a reflection.

Depending on the ionization density at each layer, there is a *critical* or highest frequency f_c at which the layer reflects a vertically incident wave. Frequencies higher than f_c pass through the layer at vertical incidence. At oblique incidence, and distances such that the curvature of the earth and ionosphere can be neglected, the maximum usable frequency is given by

$$(\mathrm{muf}) = f_c \sec \phi$$

High frequencies *continued*

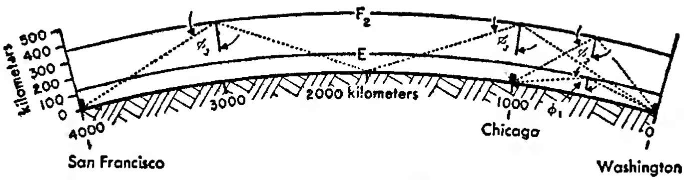

Fig. 9—Single- and two-hop transmission paths due to E and F_2 layers.

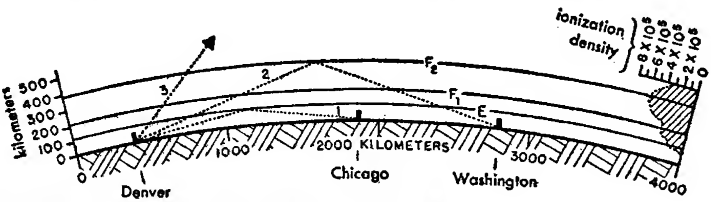

Fig. 10—Schematic explanation of skip-signal zones.

where

(muf) = maximum usable frequency for the particular layer and distance

ϕ = angle of incidence at reflecting layer

At greater distances, curvature is taken into account by the modification

$$(\text{muf}) = kf_c \sec \phi$$

where k is a correction factor that is a function of distance and vertical distribution of ionization.

f_c and height, and hence ϕ for a given distance, vary for each layer with local time of day, season, latitude, and throughout the eleven-year sunspot cycle. The various layers change in different ways with these parameters. In addition, ionization is subject to frequent abnormal variations.

The loss at reflection for each layer is a minimum at the maximum usable frequency and increases rapidly for frequencies lower than maximum usable frequency.

High frequencies travel from the transmitter to the receiver by reflection from the ionosphere and earth in one or more *hops* as indicated in Figs. 9 and 10. Additional reflections may occur along the path between the bottom edge of a higher layer and the top edge of a lower layer, the wave finally returning to earth near the receiver.

Fig. 9 illustrates single-hop transmission, Washington to Chicago, via the E layer (ϕ_1). At higher frequencies over the same distance, single-hop transmission would be obtained via the F_2 layer (ϕ_2). Fig. 9 also shows two-hop

High frequencies *continued*

transmission, Washington to San Francisco, via the F_2 layer (ϕ_3). Fig. 10 indicates transmission on a common frequency, (1) single-hop via *E* layer, Denver to Chicago, and, (2) single-hop via F_2, Denver to Washington, with, (3) the wave failing to reflect at higher angles, thus producing a *skip* region of no signal between Denver and Chicago.

Actual transmission over long distances is more complex than indicated by Figs. 9 and 10, because the layer heights and critical frequencies differ with time (and hence longitude) and with latitude. Further, scattered reflections occur at the various surfaces.

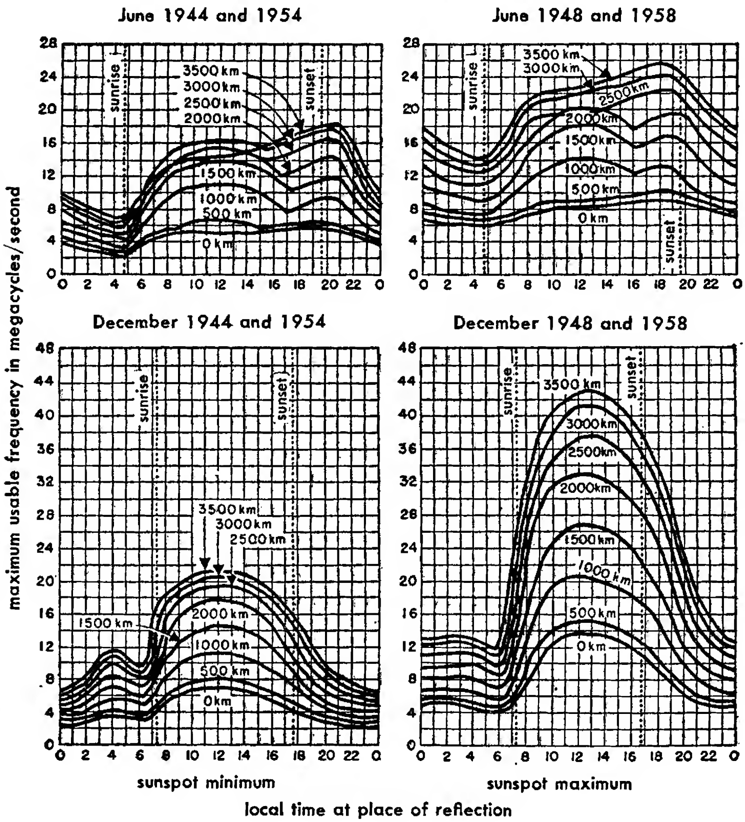

Fig. 11—Single-hop transmission at various frequencies.

High frequencies *continued*

Maximum usable frequencies (muf) for single-hop transmission at various distances throughout the day are given in Fig. 11. These approximate values apply to latitude 39° N for the minimum years (1944 and 1954) and maximum years (1948 and 1958) of the sunspot cycle. Since the maximum usable frequency and layer heights change from month to month, the latest predictions should be obtained whenever available.

This information is published (in the form of contour diagrams, similar to Fig. 15, supplemented by nomograms) by the National Bureau of Standards in the U. S. A., and equivalent predictions are supplied by similar organizations in other countries.

Preferably, operating frequencies should be selected from a specific frequency band that is bounded above and below by limits that are systematically determinable for the transmission path under consideration. The recommended upper limit is called the *optimum working frequency* (owf) and is defined as 85 percent of the *maximum usable frequency* (muf). The 85-percent limit provides some margin for ionospheric irregularities and turbulence, as well as statistical deviation of day-to-day ionospheric characteristics from the predicted monthly median value. So far as may be consistent with available frequency assignments, operation in reasonable proximity to the upper frequency limit is preferable, in order to reduce absorption loss.

The lower limit of the normally available band of frequencies is called the *lowest useful high frequency* (luhf). Below this limit ionospheric absorption is likely to be excessive, and radiated-power requirements quite uneconomical. For a given path, season, and time, the (luhf) may be predicted by a systematic graphical procedure. Unlike the (muf), the predicted (luhf) has to be corrected by a series of factors dependent on radiated power, directivity of transmitting and receiving antennas in azimuth and elevation, class of service, and presence of local noise sources. Available data include atmospheric-noise maps, field-intensity charts, contour diagrams for absorption factors, and nomograms facilitating the computation. The procedure is formidable but worth while.

The upper and lower frequency limits change continuously throughout the day, whereas it is ordinarily impractical to change operating frequencies correspondingly. Each operating frequency, therefore, should be selected to fall within the above limits for a substantial portion of the daily operating period.

If the operating frequency already has been dictated by outside considerations, and if this frequency has been found to be safely below the maximum

High frequencies *continued*

usable frequency, then the same noise maps, absorption contours, nomograms, and correction factors (mentioned above) may be applied to the systematic statistical determination of a *lowest required radiated power* (lrrp), which will just suffice to maintain the specified grade of service.

For single-hop transmission, frequencies should be selected on the basis of local time and other conditions existing at the midpoint of the path. In view of the layer heights and the fact that practical antennas do not operate effectively below angles of about three degrees, single-hop transmission cannot be achieved for distances in excess of about 2500 miles (4000 kilometers) via F_2 layer, or in excess of about 1250 miles (2000 kilometers) via the E layer. Multiple-hop transmission must occur for longer distances and, even at distances of less than 2500 miles, the major part of the received signal frequently arrives over a two- or more-hop path. In analyzing two-hop paths, each hop is treated separately and the lowest frequency required on either hop becomes the maximum usable frequency for the circuit.

It is usually impossible to predict accurately the course of radio waves on circuits involving more than two hops because of the large number of possible paths and the scattering that occurs at each reflection. When investigating F_2-layer transmission for such long-distance circuits, it is customary to consider the conditions existing at points 2000 kilometers (1250 miles) along the path from each end as the points at which the maximum usable frequencies should be calculated.

When investigating E-layer transmission, the corresponding control points are 1000 kilometers (620 miles) from each end. For practical purposes, F_1-layer transmission (usually of minor importance) is lumped with E-layer transmission and evaluated at the same control points.

Angles of departure and arrival

Angles of departure and arrival are of importance in the design of high-frequency antenna systems. These angles, for single-hop transmission, are obtained from the geometry of a triangular path over a curved earth with the apex of the triangle placed at the virtual height assumed for the altitude of the reflection. Fig. 12 is a family of curves showing radiation angle for different distances.

D = great-circle distance in statute miles

H = virtual height of ionosphere layer in kilometers

Δ = radiation angle in degrees

ϕ = semiangle of reflection at ionosphere

High frequencies *continued*

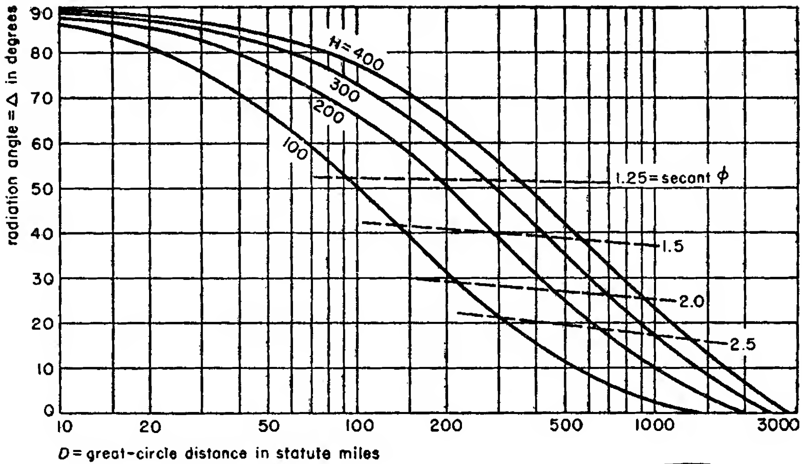

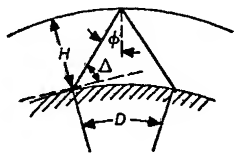

Fig. 12—Single-reflection radiation angle and great-circle distance.

Forecasts of high-frequency propagation

In addition to forecasts for ionospheric disturbances, the Central Radio Propagation Laboratories of the National Bureau of Standards issues monthly *Basic Radio Propagation Predictions* 3 months in advance used to determine the optimum working frequencies for shortwave communication. Indication of the general nature of the CRPL data and a much abbreviated example of their use follows:

Example

To determine working frequencies for use between San Francisco and Wellington, N. Z.

Method

a. Place a transparent sheet over Fig. 13 and mark thereon the equator, a line across the equator showing the meridian of time desired (viz., GCT or PST), and locations of San Francisco and Wellington.

b. Transfer sheet to Fig. 14, keeping equator lines of chart and transparency aligned. Slide from left to right until terminal points marked fall along a

Forecasts of high-frequency propagation *continued*

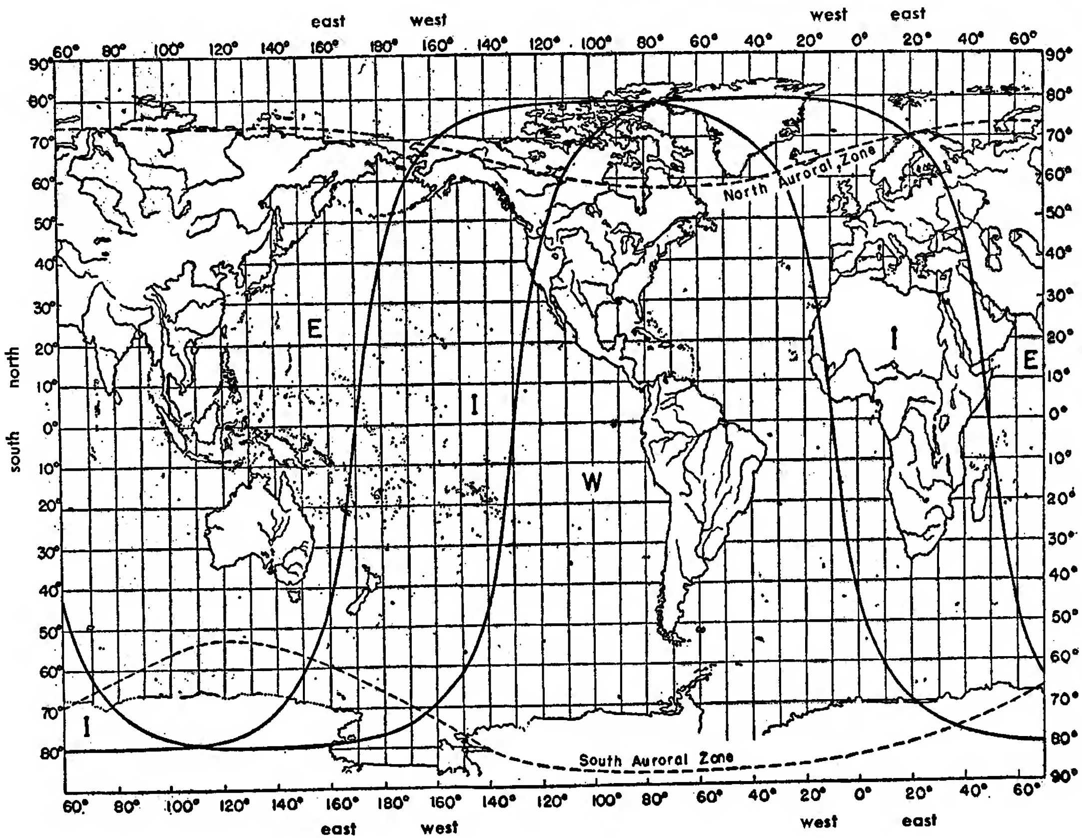

Fig. 13—World map showing zones covered by predicted charts and auroral zones. Zones shown are *E* = east, *I* = intermediate, and *W* = west.

Forecasts of high-frequency propagation *continued*

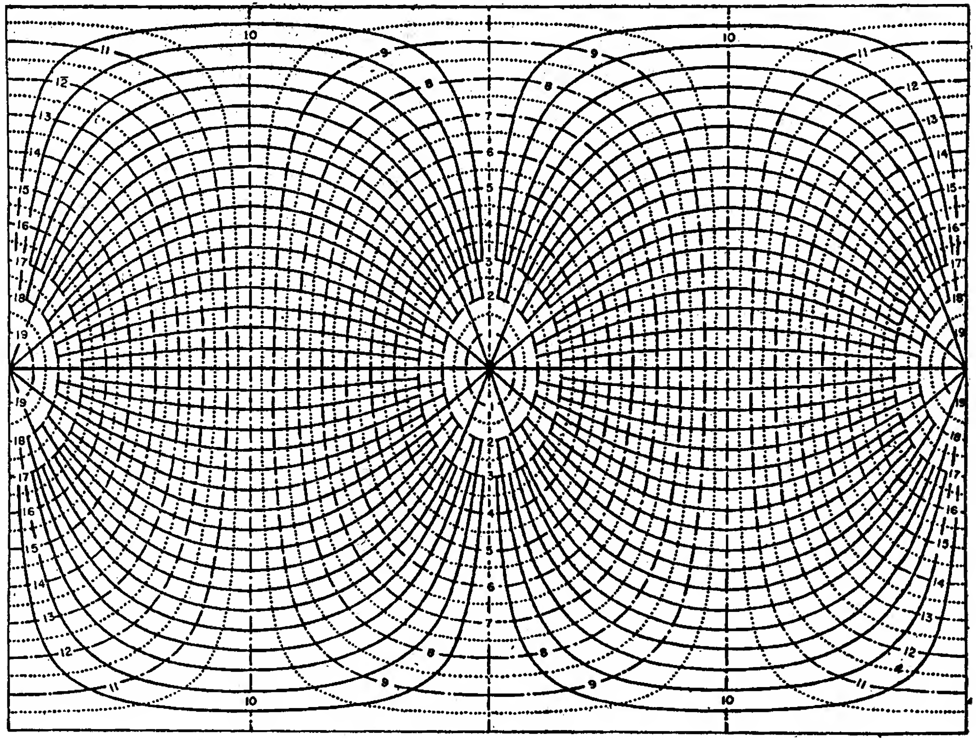

Fig. 14—Great circle chart centered on equator. Solid lines represent great circles. Dot-dash lines indicate distances in thousands of kilometers.

continued **Forecasts of high-frequency propagation**

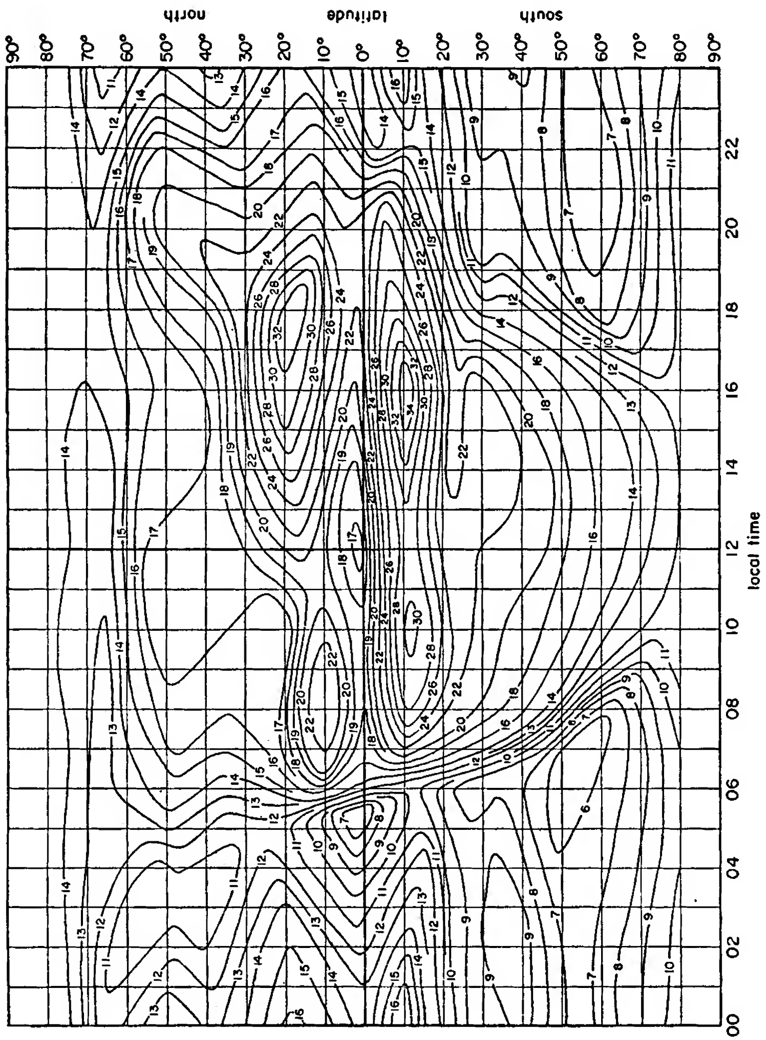

Fig. 15—F_2 4000-kilometer maximum usable frequency in megacycles. Zone *I* (see Fig. 13) predicted for July, 1955.

Forecasts of high-frequency propagation *continued*

Great Circle line. Sketch in this Great Circle between terminals and mark "control points" 2000 kilometers along this line from each end.

c. Transfer sheet to Fig. 15, showing muf for transmission via the F_2 layer. Align equator as before. Slide sheet from left to right placing meridian line on time desired and record frequency contours at control points. This illustration assumes that radio waves are propagated over this path via the F_2 layer. Eliminating all other considerations, 2 sets of frequencies, corresponding to the control points, are found as listed below, the lower of which is the (muf). The (muf), decreased by 15 percent, gives the optimum working frequency (Fig. 16).

Fig. 16—Maximum usable frequency.

GCT	at San Francisco control point (2000 km from San Francisco)	at Wellington, N. Z. control point (2000 km from Wellington)	optimum working frequency = lower of (muf) × 0.85
0000	27.0	22.0	18.7
0400	25.6	22.0	18.7
0800	16.6	9.7	8.3
1200	13.5	9.1	7.7
1600	16.5	8.5	7.2
2000	17.7	20.8	15.0

Transmission may also take place via other layers. For the purpose of illustration only and without reference to the problem above, Figs. 17 and 18 have been reproduced to show characteristics of the *E* and sporadic-*E* layers. The complete detailed step-by-step procedure, including special considerations in the use of this method, are contained in the complete CRPL forecasts.

continued **Forecasts of high-frequency propagation**

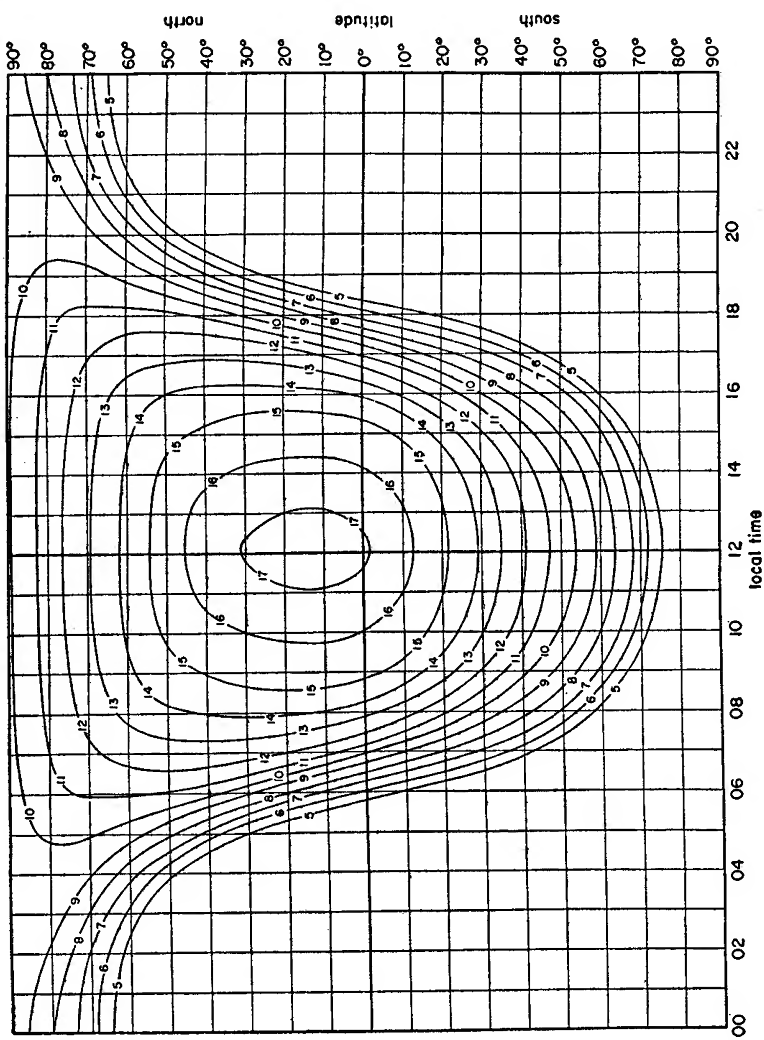

Fig. 17—*E*-layer 2000-kilometer maximum usable frequency in megacycles predicted for July, 1955.

Forecasts of high-frequency propagation *continued*

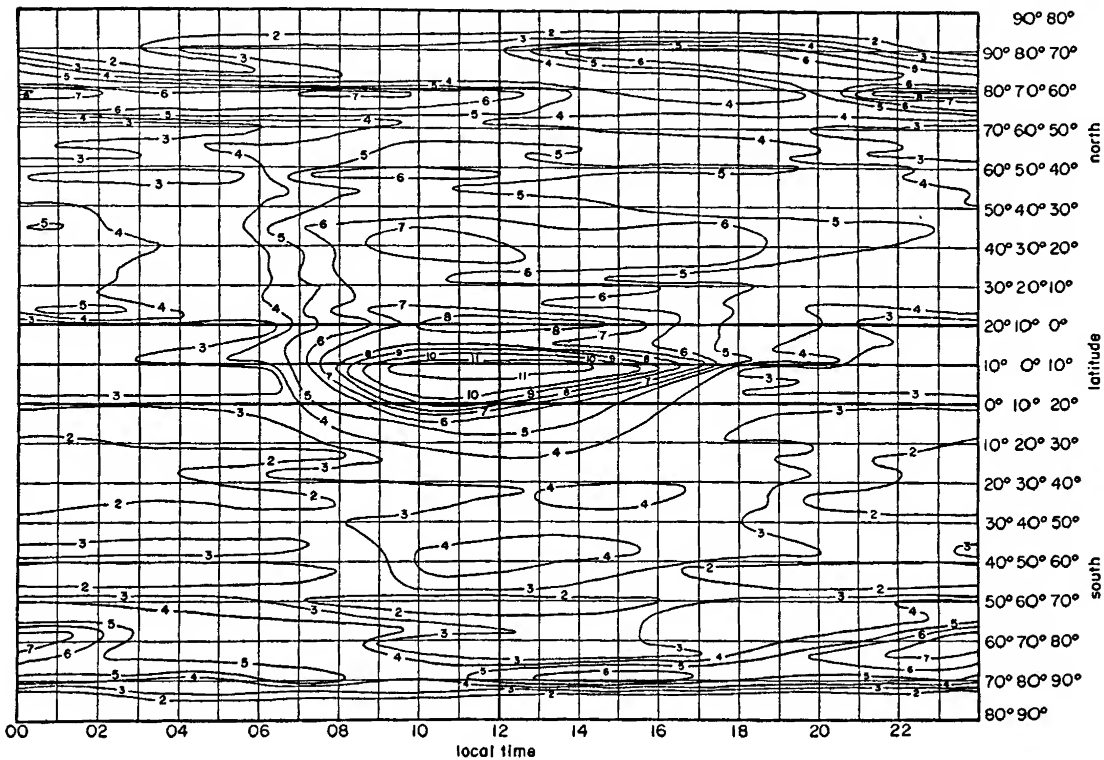

Fig. 18—Median fE_s in megacycles (sporadic-E layer) predicted for July, 1955.

Forecasts of high-frequency propagation *continued*

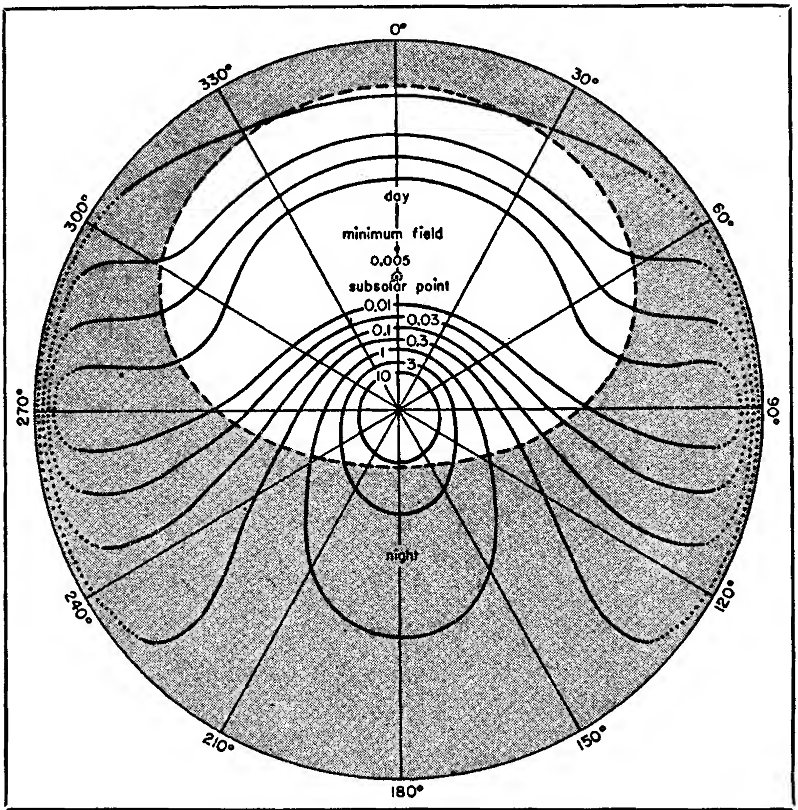

Fig. 19—Field-intensity contours in microvolts/meter for 1 kilowatt radiated at 6 megacycles. Azimuthal equidistant projection centered on station at 40 degrees south latitude. Time is noon of a June day during a sunspot-minimum year.

Contour charts of field intensity*

World-coverage field-intensity contours are useful for determining the strength of an interfering signal from a given transmitter, as compared with the wanted signal from another transmitter. A sample instance of such a field-intensity-contour chart is shown in Figs. 19 and 20. The field is given in microvolts/meter for a 1-kilowatt station at 6 megacycles. Fig. 19 is an azimuthal equidistant projection centered on the transmitter (periphery of figure represents antipodes). Fig. 20, at twice the scale, is centered on

* For sets of field-intensity contour charts, see "High-Frequency Radio Propagation Charts for Sunspot Minimum and Sunspot Maximum," Report CRPL—1-2, 3-1, National Bureau of Standards, Washington 25, D. C.; December 23, 1947.

Forecasts of high-frequency propagation *continued*

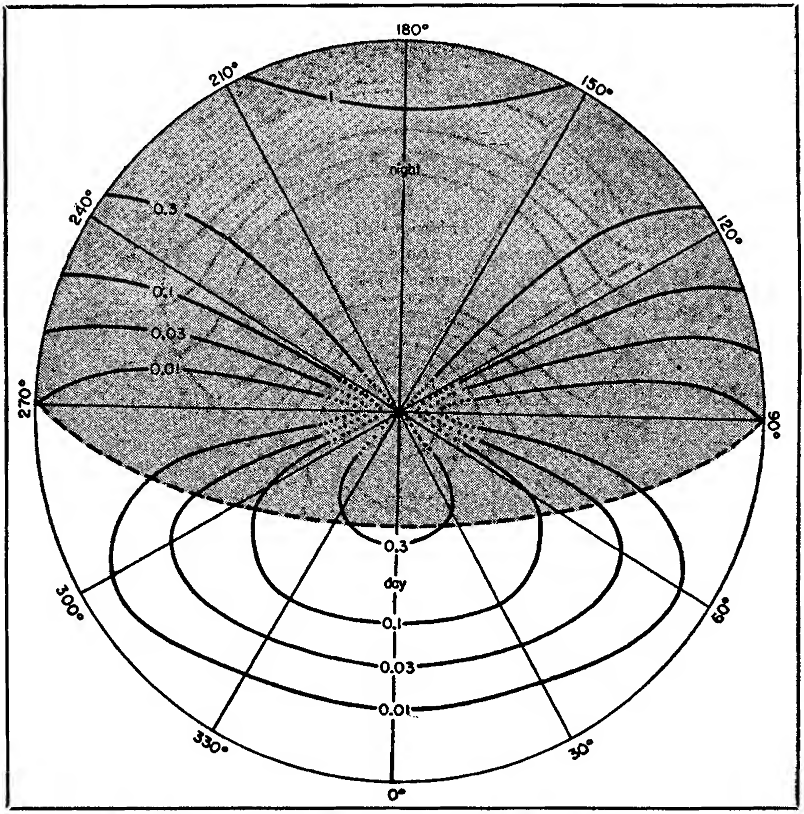

Fig. 20—Field intensity at antipodes, drawn to twice the scale of Fig. 19.

antipodes, but for a half-sphere only. These diagrams are useful in determining the point on the surface of the earth where the field intensity is a minimum, the so-called *dark spot.*

Great-circle calculations

Mathematical method

Referring to Fig. 21, A and B are two places on the earth's surface the latitudes and longitudes of which are known. The angles X and Y at A and B of the great circle passing through the two places and the distance Z between A and B along the great circle can be calculated as follows:

Great-circle calculations *continued*

B = place of greater latitude, i.e., nearer the pole, L_A = latitude of A, L_B = latitude of B, and C = difference of longitude between A and B,

Then,

$$\tan\frac{Y-X}{2} = \cot\frac{C}{2}\,\frac{\sin\frac{L_B-L_A}{2}}{\cos\frac{L_B+L_A}{2}} \quad \text{and} \quad \tan\frac{Y+X}{2} = \cot\frac{C}{2}\,\frac{\cos\frac{L_B-L_A}{2}}{\sin\frac{L_B+L_A}{2}}$$

give the values of $\frac{Y-X}{2}$ and $\frac{Y+X}{2}$,

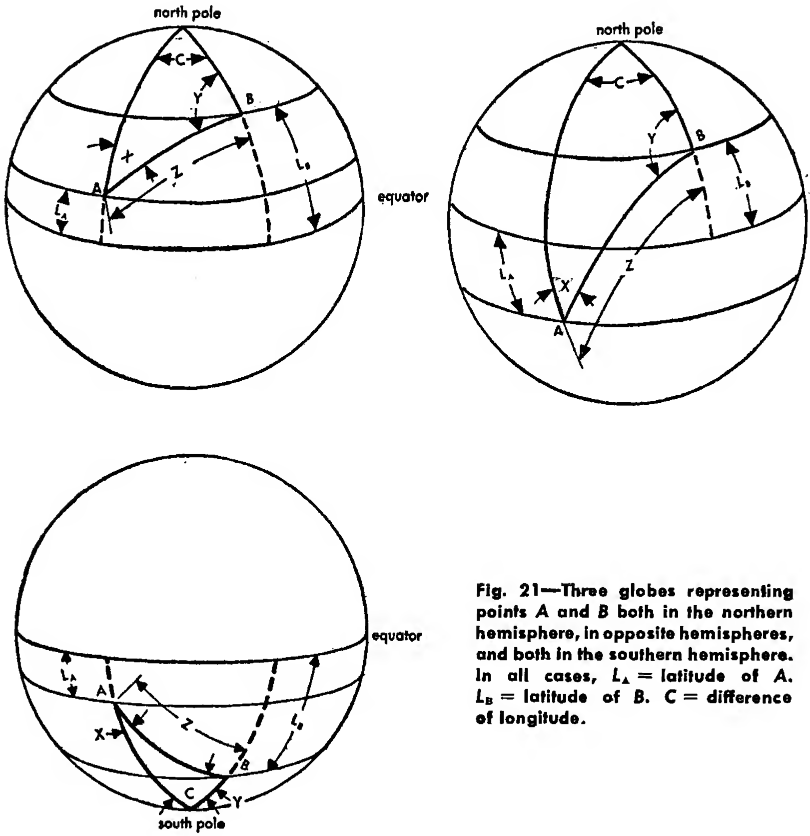

Fig. 21—Three globes representing points *A* and *B* both in the northern hemisphere, in opposite hemispheres, and both in the southern hemisphere. In all cases, L_A = latitude of *A*. L_B = latitude of *B*. C = difference of longitude.

Great-circle calculations *continued*

from which

$$\frac{Y+X}{2}+\frac{Y-X}{2}=Y \qquad \text{and} \qquad \frac{Y+X}{2}-\frac{Y-X}{2}=X$$

In the above formulas, north latitudes are taken as positive and south latitudes as negative. For example, if B is latitude 60° N and A is latitude 20° S,

$$\frac{L_B+L_A}{2}=\frac{60+(-20)}{2}=\frac{60-20}{2}=\frac{40}{2}=20°$$

$$\frac{L_B-L_A}{2}=\frac{60-(-20)}{2}=\frac{60+20}{2}=\frac{80}{2}=40°$$

If both places are in the southern hemisphere and L_B+L_A is negative, it is simpler to call the place of greater south latitude B and to use the above method for calculating bearings from true south and to convert the results afterwards to bearings east of north.

The distance Z (in degrees) along the great circle between A and B is given by the following:

$$\tan\frac{Z}{2}=\tan\frac{L_B-L_A}{2}\left(\sin\frac{Y+X}{2}\right)\Big/\left(\sin\frac{Y-X}{2}\right)$$

The angular distance Z (in degrees) between A and B may be converted to linear distance as follows:

Z (in degrees) $\times$ 111.12 = kilometers

Z (in degrees) $\times$ 69.05 = statute miles

Z (in degrees) $\times$ 60.00 = nautical miles

In multiplying, the minutes and seconds of arc must be expressed in decimals of a degree. For example, Z = 37° 45′ 36″ becomes 37.755°.

Example: Find the great-circle bearings at Brentwood, Long Island, Longitude 73° 15′ 10″ W, Latitude 40° 48′ 40″ N, and at Rio de Janeiro, Brazil Longitude 43° 22′ 07″ W, Latitude 22° 57′ 09″ S; and the great-circle distance in statute miles between the two points.

Great-circle calcu'ations *continued*

	longitude	latitude	
Brentwood	73° 15′ 10″ W	40° 48′ 40″ N	L_B
Rio de Janeiro	43° 22′ 07″ W	(−)22° 57′ 09″ S	L_A
C	29° 53′ 03″	17° 51′ 31″	$L_B + L_A$
		63° 45′ 49″	$L_B - L_A$

$\frac{C}{2} = 14° 56' 31''$ $\frac{L_B + L_A}{2} = 8° 55' 45''$ $\frac{L_B - L_A}{2} = 31° 52' 54''$

$$\begin{aligned}
\log \cot 14° 56' 31'' &= 10.57371 \\
\text{plus } \log \cos 31° 52' 54'' &= \underline{9.92898} \\
& 0.50269 \\
\text{minus } \log \sin 8° 55' 45'' &= \underline{9.19093} \\
\log \tan \frac{Y+X}{2} &= 1.31176 \\
\frac{Y+X}{2} &= 87° 12' 26''
\end{aligned}$$

$$\begin{aligned}
\log \cot 14° 56' 31'' &= 10.57371 \\
\text{plus } \log \sin 31° 52' 54'' &= \underline{9.72277} \\
& 0.29648 \\
\text{minus } \log \cos 8° 55' 45'' &= \underline{9.99471} \\
\log \tan \frac{Y-X}{2} &= 0.30177 \\
\frac{Y-X}{2} &= 63° 28' 26''
\end{aligned}$$

Bearing at Brentwood $= \frac{Y+X}{2} + \frac{Y-X}{2} = Y = 150° 40' 52''$ East of North

Bearing at Rio de Janeiro $= \frac{Y+X}{2} - \frac{Y-X}{2} = X = 23° 44' 00''$ West of North

$$\frac{L_B - L_A}{2} = 31° 52' 54''$$

$$\frac{Y+X}{2} = 87° 12' 26''$$

$$\frac{Y-X}{2} = 63° 28' 26''$$

$$\begin{aligned}
\log \tan 31° 52' 54'' &= 9.79379 \\
\text{plus } \log \sin 87° 12' 26'' &= \underline{9.99948} \\
& 9.79327 \\
\text{minus } \log \sin 63° 28' 26'' &= \underline{9.95170} \\
\log \tan \frac{Z}{2} &= 9.84157
\end{aligned}$$

$\frac{Z}{2} = 34° 46' 24''$ $Z = 69° 32' 48''$

$69° 32' 48'' = 69.547°$

Linear distance $= 69.547 \times 69.05 = 4802$ statute miles

Great-circle calculations *continued*

Use of nomogram, Fig. 23*

Note: Values near the ends of the nomogram scales of Fig. 23 are subject to error because the scales are compressed. If exact values are required in those regions, they should be calculated by means of the trigonometric formulas of the preceding section.

Method: In Fig. 22, Z and S are the locations of the transmitting and receiving stations, where Z is the west and S the east end of the path. *If a point lies in the southern hemisphere, its angle of latitude is always taken as negative. Northern-hemisphere latitudes are taken as positive.*

a. To obtain from Fig. 23 the great-circle distance ZS (short route):

1. Draw a slant line from (lat Z — lat S) measured up from the bottom on the left-hand scale to (lat Z + lat S) measured down from the top on the right-hand scale. If (lat Z — lat S) or (lat Z + lat S) is negative, regard it as positive.

2. Determine the separation in longitude of the stations. Regard as positive. If the angle so obtained is greater than 180 degrees, then subtract from 360 degrees. Measure this angle along the bottom scale, and erect a vertical line to the slant line obtained in (1).

3. From the intersection of the lines draw a horizontal line to the left-hand scale. This gives ZS in degrees.

4. Convert the distance ZS to kilometers, miles, or nautical miles, by using the scale at the bottom of Fig. 23.

Note: The *long great-circle route* in degrees is simply 360 — ZS. The value will always be greater than 180 degrees. Therefore, in order to obtain the dis-

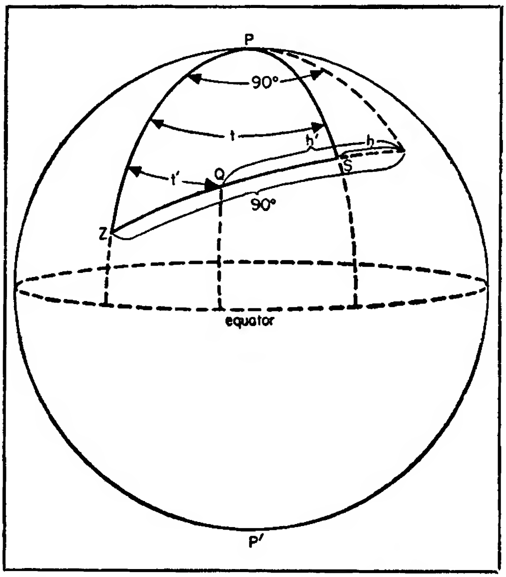

Fig. 22—Diagram of transmission between points Z and S. For use with Fig. 23.

* Taken from Bureau of Standards Radio Propagation Prediction Charts.

Great-circle calculations *continued*

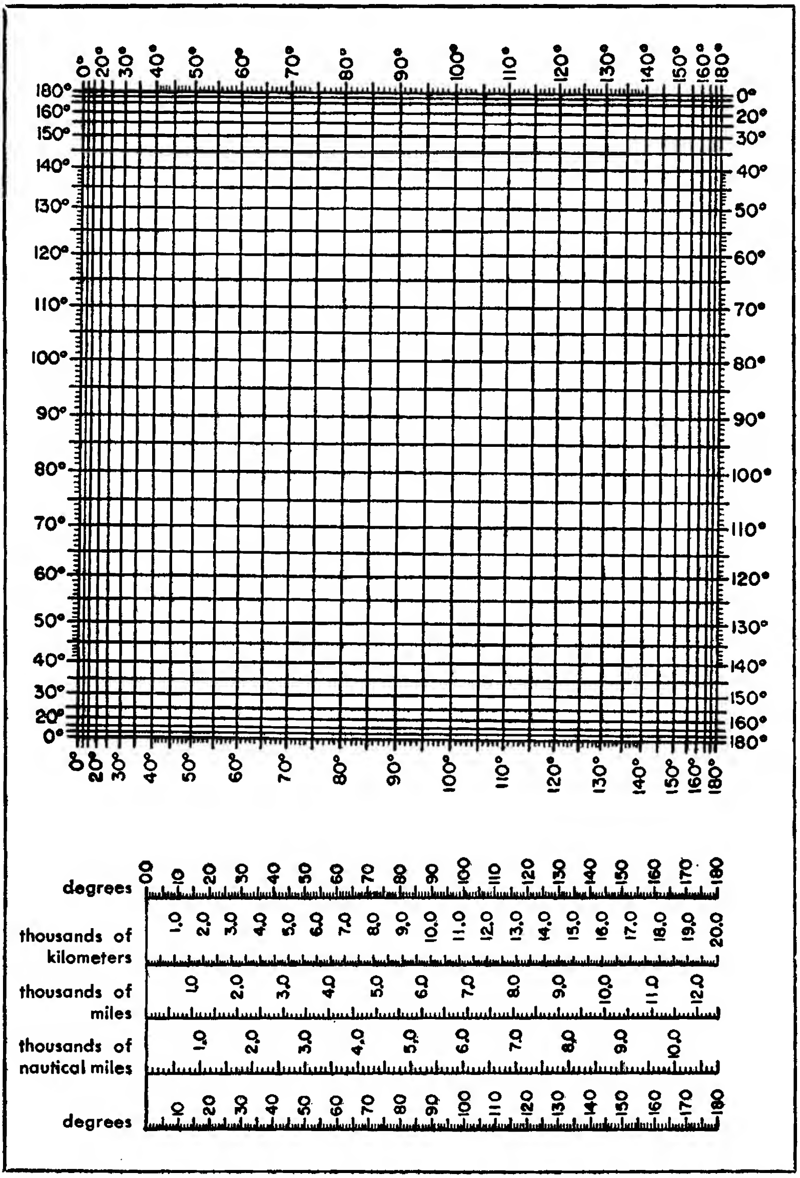

Fig. 23—Nomogram (after D'Ocagne) for obtaining great-circle distances, bearings, solar zenith angles, and latitude and longitude of transmission-control points. With conversion scale for various units.

Great-circle calculations *continued*

tance in miles from the conversion scale, the value for the degrees in excess of 180 degrees is added to the value for 180 degrees.

b. To obtain the bearing angle *PZS* (short route):

1. Subtract the short-route distance *ZS* in degrees obtained in (a) above from 90 degrees to get *h*. The value of *h* may be negative, but should always be regarded as positive.

2. Draw a slant line from (lat *Z* — *h*) measured up from the bottom on the left-hand scale to (lat *Z* + *h*) measured down from the top on the right-hand scale. If (lat *Z* — *h*) or (lat *Z* + *h*) is negative, regard it as positive.

3. From (90° — lat *S*) measured up from the bottom on the left-hand scale, draw a horizontal line until it intersects the previous slant line.

4. From the point of intersection draw a vertical line to the bottom scale. This gives the bearing angle *PZS*. The angle may be either east or west of north, and must be determined by inspection of a map.

c. To obtain the bearing angle *PSZ*:

1. Repeat steps (1), (2), (3), and (4) in (b) above, interchanging *Z* and *S* in all computations. The result obtained is the interior angle *PSZ*, in degrees.

2. The bearing angle *PSZ* is 360 degrees minus the result obtained in (1) (as bearings are customarily given clockwise from due north).

Note: The *long-route bearing angle* is simply obtained by adding 180 degrees to the short-route value as determined in (b) or (c) above.

d. To obtain the latitude of Q, the mid- or other point of the path (this calculation is in principle the converse of (b) above):

1. Obtain *ZQ* in degrees. If Q is the midpoint of the path, *ZQ* will be equal to one-half *ZS*. If Q is one of the 2000-kilometer control points, *ZQ* will be approximately 18 degrees, or *ZS* — 18°.

2. Subtract *ZQ* from 90 degrees to get *h'*. If *h'* is negative, regard it as positive.

3. Draw a slant line from (lat *Z* — *h'*) measured up from the bottom on the left-hand scale, to (lat *Z* + *h'*) measured down from the top on the right-hand scale. If (lat *Z* — *h'*) or (lat *Z* + *h'*) is negative, regard it as positive.

4. From the bearing angle *PZS* (taken always as less than 180 degrees) measured to the right on the bottom scale, draw a vertical line to meet the above slant line.

5. From this intersection draw a horizontal line to the left-hand scale.

Great-circle calculations *continued*

6. Subtract the reading given from 90 degrees to give the latitude of Q. (If the answer is negative, then Q is in the southern hemisphere.)

e. To obtain the longitude difference t' between Z and Q (this calculation is in principle the converse of (a) above):

1. Draw a straight line from (lat Z — lat Q) measured up from the bottom on the left-hand scale to (lat Z + lat Q) measured down from the top on the right-hand scale. If (lat Z — lat Q) or (lat Z + lat Q) is negative, regard it as positive.

2. From the left-hand side, at ZQ, in degrees, draw a horizontal line to the above slant line.

3. At the intersection drop a vertical line to the bottom scale, which gives t' in degrees.

Available maps and tables

Great-circle initial courses and distances are conveniently determined by means of navigation tables such as

a. Navigation Tables for Navigators and Aviators—HO No. 206.

b. Dead-Reckoning Altitude and Azimuth Table—HO No. 211.

c. Large Great-Circle Charts:

HO Chart No. 1280—North Atlantic
1281—South Atlantic
1282—North Pacific
1283—South Pacific
1284—Indian Ocean

The above tables and charts may be obtained at a nominal charge from United States Navy Department Hydrographic Office, Washington, D. C.

Ionospheric scatter propagation*

This type of transmission permits communication in the frequency range from approximately 25 to 60 megacycles and over distances from about 600 to 1200 miles. It is believed that this type of propagation is due to scattering from the lower E layer of the ionosphere and that the useful bandwidth is restricted to less than 10 kilocycles. The greatest use for this type of transmission has been for printing-telegraph channels.

* D. K. Bailey, R. Bateman, and R. C. Kirby, "Radio Transmission at VHF by Scattering and Other Processes in the Lower Ionosphere," *Proceedings of the IRE*, volume 43, pages 1181-1231; October, 1955.

Ionospheric scatter propagation *continued*

The median attenuation over paths of between 800 and 1000 miles in length is about 80 decibels below free-space path attenuation at 30 megacycles and about 90 decibels below free-space value at 50 megacycles.

Ultra-high-frequency line-of-sight conditions

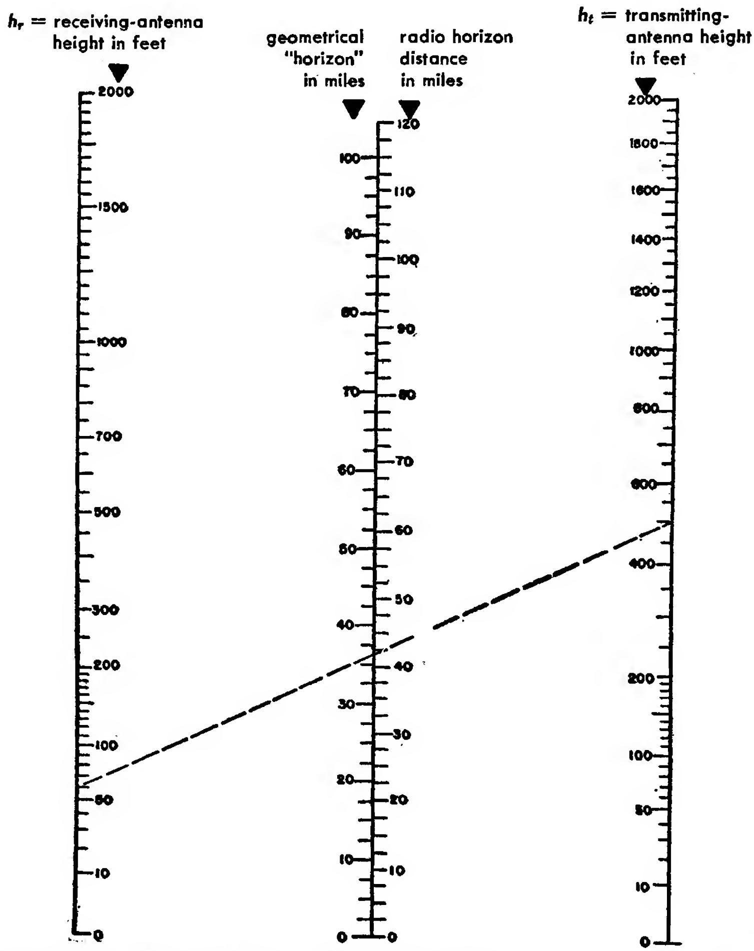

Example shown: Height of receiving antenna 60 feet, height of transmitting antenna 500 feet, and maximum radio-path length = 41.5 miles.

Fig. 24—Nomogram giving radio-horizon distance in miles when h_r and h_t are known.

Ultra-high-frequency line-of-sight conditions *continued*

Straight-line diagrams

The index of refraction of the normal lower atmosphere (troposphere) decreases with height so that radio rays follow a curved path, slightly bent downward toward the earth. If the real earth is replaced by a fictitious

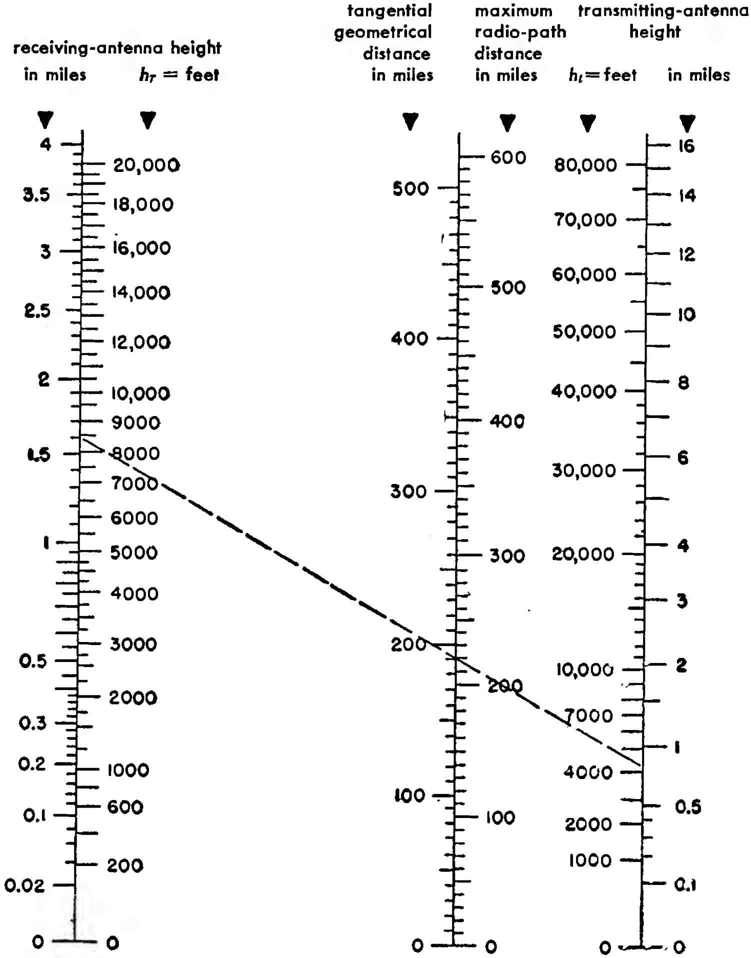

Example shown: Height of receiving-antenna airplane 8500 feet (1.6 miles), height of transmitting-antenna airplane 4250 feet (0.8 mile); maximum radio-path distance = 220 miles.

Fig. 25—Nomogram giving radio-path length and tangential distance for transmission between two airplanes at heights h_r and h_t.

Ultra-high-frequency line-of-sight conditions *continued*

earth having an enlarged radius 4/3 times the earth's true radius ($3963 \times 4/3 = 5284$ miles), the radio rays may be drawn on profiles as straight lines.

The radio distance to effective horizon is given with a good approximation by

$$d = (2h)^{1/2}$$

where

h = height in feet above sea level

d = radio distance to effective horizon in miles

when the height is very small compared to the earth's radius.

Over a smooth earth, a transmitter antenna at height h_t (feet) and a receiving antenna at height h_r (feet) are in radio line-of-sight provided the spacing in miles is less than $(2h_t)^{1/2} + (2h_r)^{1/2}$.

The nomogram in Fig. 24 gives the radio-horizon distance between a transmitter at height h_t and a receiver at height h_r. Fig. 25 extends the first nomogram to give the maximum radio-path length between two airplanes whose altitudes are known.

Path plotting and profile-chart construction

Path plotting: When laying out a microwave system, it is usually convenient to plot the path on a profile chart. This chart is scaled to indicate the departure of the curvature of the earth from a straight line. Referring to Fig. 26,

$$D^2 + R^2 = (h + R)^2 = h^2 + 2Rh + R^2$$
$$D^2 = h^2 + 2Rh$$

where

D = distance

R = radius of earth

h = altitude

Since $h \ll R$,

$$D = (2Rh)^{1/2}$$

and inserting the earth's radius, with R and D in statute miles and h in feet,

$$D = \left(\frac{2 \times 3900}{5280}\,h\right)^{1/2}$$

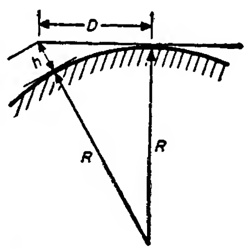

Fig. 26—Straight line tangent to earth's surface.

Ultra-high-frequency line-of-sight conditions *continued*

$$D = [(3/2)h]^{1/2}$$

$$h = (2/3)D^2$$

for true earth. Using 4/3-earth-radius correction factor,

$$D = [(3/2)h]^{1/2}\,(4/3)^{1/2} = (2h)^{1/2}$$

$$h = D^2/2$$

Other radius correction factors can be calculated accordingly.

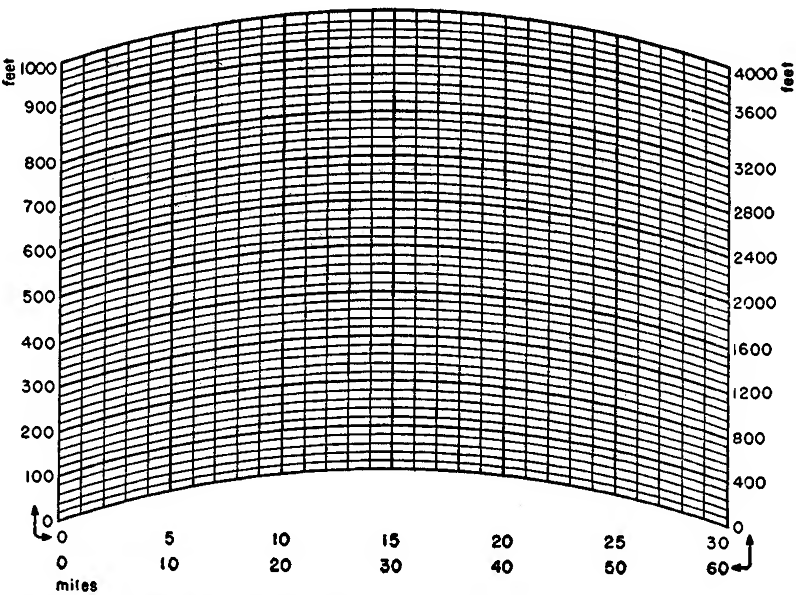

Fig. 27—Typical 4/3-earth profile paper, 1000-foot scale.

Profile paper: Using a 4/3-radius correction factor, the departure from a level tangent line is

$$h = D^2/2$$

where symbols are as above. Using this formula, a template can be made for convenient drawing of profile paper (Fig. 27). For instance, if the horizontal scale is 10 miles/inch, the vertical scale 100 feet/inch, and a

Ultra-high-frequency line-of-sight conditions *continued*

width corresponding to 40 miles is desired, the following points may be plotted:

distance from center (horizontal)		distance from level (vertical)
0 miles = 0 inches	and	0 feet = 0 inches
5 miles = $\frac{1}{2}$ inch	and	$12\frac{1}{2}$ feet = $\frac{1}{8}$ inch
10 miles = 1 inch	and	50 feet = $\frac{1}{2}$ inch
15 miles = $1\frac{1}{2}$ inches	and	$112\frac{1}{2}$ feet = $1\frac{1}{8}$ inches
20 miles = 2 inches	and	200 feet = 2 inches

A typical example of a template constructed according to these figures is given in Fig. 28. If it is desired to use a different scale than is provided

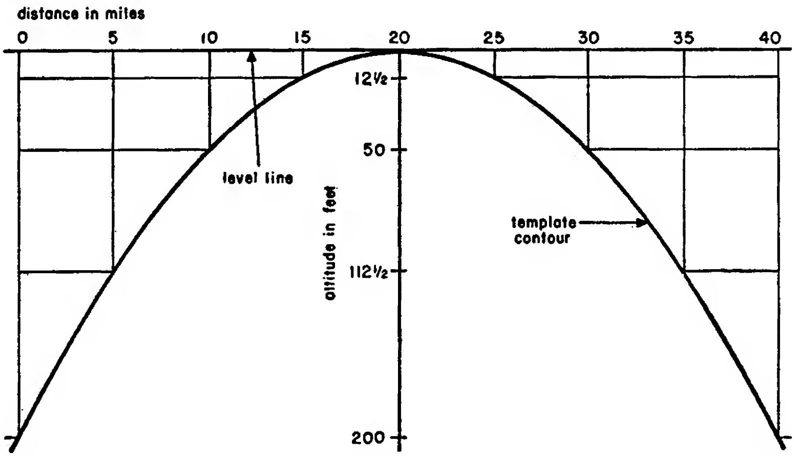

Fig. 28—Construction of a template for profile charts. Drawing is actual size.

on available profile-chart paper; for example, if a 50-mile hop is to be plotted on 30-mile paper, then the scale of miles may be doubled to extend the range of the paper to 60 miles. The vertical scale in feet must then be quadrupled; i.e., 100-foot divisions become 400-foot divisions. (Fig. 27)

Fresnel-zone clearance at uhf

A criterion to determine whether the earth is sufficiently removed from the radio line-of-sight ray to allow mean free-space propagation conditions to apply is to have the first Fresnel zone clear all obstacles in the path of the rays. This first zone is bounded by points for which the transmission path

Ultra-high-frequency line-of-sight conditions *continued*

from transmitter to receiver is greater by one-half wavelength than the direct path. Let d be the length of the direct path and d_1 and d_2 be the distances to transmitter and receiver. The radius of the first Fresnel zone corresponding to d_2 is approximately given by

$$R_1^2 = \lambda \frac{d_1 d_2}{d}$$

where all quantities are expressed in the same units.

The maximum occurs when $d_1 = d_2$ and is equal to

$$R_{1m} = \tfrac{1}{2}(\lambda d)^{1/2}$$

Expressing d in miles and frequency F in megacycles/second, the first Fresnel-zone radius at half distance is given in feet by

$$R_{1m} = 1140(d/F)^{1/2}$$

While a fictitious earth of 4/3 of true earth radius is generally accepted for determining first Fresnel-zone clearance under normal refraction condition, unusual conditions that occur in the atmosphere occasionally may make it desirable to allow Fresnel clearance of a fictitious earth radius of as little as 2/3 of the true radius.

Interference between direct and reflected uhf rays

Where there is one reflected ray combining with the direct ray at the receiving point (Fig. 29), the resulting field strength (neglecting the difference in angles of arrival, and assuming perfect reflection at T) is related to the free-space intensity by the following equation, irrespective of the polarization:

$$E = 2E_d \sin 2\pi \frac{\delta}{2\lambda}$$

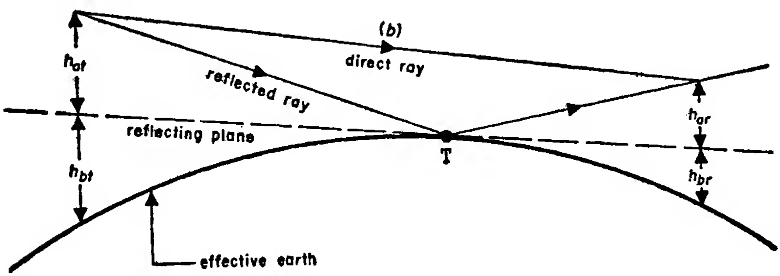

Fig. 29—Interference between direct and reflected rays.

Ultra-high-frequency line-of-sight conditions *continued*

where

$$\left.\begin{aligned} E &= \text{resulting field strength} \\ E_d &= \text{direct-ray field strength} \end{aligned}\right\} \text{same units}$$

δ = geometrical length difference between direct and reflected paths, which is given to a close approximation by

$\delta = 2h_{at}h_{ar}/d$

if h_{at} and h_{ar} are the heights of transmitter and receiver points above reflecting plane on effective earth.

The following cases are of interest:

$E = 0$ for $h_{at}h_{ar} = d\lambda/2$

$E = 2E_d$ for $h_{at}h_{ar} = d\lambda/4$

$E = E_d$ for $h_{at}h_{ar} = d\lambda/12$

In case $h_{at} = h_{ar} = h$,

$E = 0$ for $h = (d\lambda/2)^{1/2}$

$E = 2E_d$ for $h = (d\lambda/4)^{1/2}$

$E = E_d$ for $h = (d\lambda/12)^{1/2}$

All of these formulas are written with the same units for all quantities.

Space-diversity reception

When h_{ar} is varied, the field strength at the receiver varies approximately according to the preceding formula. The use of two antennas at different heights provides a means of compensating to a certain extent for changes in electrical-path differences between direct and reflected rays by selection of the stronger signal (space-diversity reception).

The spacing should be approximately such as to give a $\lambda/2$ variation between geometrical-path differences in the two cases. An approximate value of the spacing is given by $\lambda d/4h_{at}$ when all quantities are in the same units.

The spacing in feet for d in miles, h_{at} in feet, λ in centimeters, and f in megacycles is given by

$$\begin{aligned} \text{spacing} &= 43.4\ \lambda d/h_{at} \\ &= 1.3 \times 10^6\ d/fh_{at} \end{aligned}$$

Ultra-high-frequency line-of-sight conditions *continued*

Example: $\lambda = 3$ centimeters, $d = 20$ miles, and $h_{at} = 50$ feet; therefore

spacing = 52 feet

Assuming $h_{ar} = h_{at}$, the total height of the receiving point in this case would be $70 + 50 + 52 = 172$ feet

The value 70 (minimum for line-of-sight) is obtained from Fig. 24.

Variation of field strength with distance

Fig. 30 shows the variation of resulting field strength with distance and frequency; this effect is due to interference between the free-space wave and the ground-reflected wave as these two components arrive in or out of phase.

To compute the field accurately under these conditions, it is necessary to calculate the two components separately and to add them in correct phase relationship. The phase and amplitude of the reflected ray is determined by the geometry of the path and the change in magnitude and phase at ground reflection. For horizontally polarized waves, the reflection coefficient can be taken as approximately one, and the phase shift at reflection as 180 degrees, for nearly all types of ground and angles of incidence. For vertically polarized waves, the reflection coefficient and phase shift vary appreciably with the ground constants and angle of incidence. (See Fig. 31 of "Antennas" chapter.)

Measured field intensities usually show large deviations from point to point due to reflections from irregularities in the ground, buildings, trees, etc.

Fading at ultra-high frequencies

Line-of-sight propagation at ultra-high frequencies is affected both by signal-strength variations due to multipath transmission and by bending of the beam due to abnormal variation of refractive index with height in the lower atmosphere.

As previously noted, normal atmospheric refraction results in a moderate extension of the radio transmission path beyond the geometric horizon. It should be noted, however, that relatively stable and widespread departures from average refraction occur frequently and may be roughly predicted from a sufficiently detailed knowledge of local meteorological data. The atmospheric water-vapor gradient is of primary importance, with the vertical temperature gradient exerting a significant supplementary effect.

Ultra-high-frequency line-of-sight conditions *continued*

This can result either in a loss of signal on a line-of-sight path or in the production of "mirage" effects that may extend communication far beyond the normally expected range. The fading due to an upward bending of the beam may generally be minimized by allowing for Fresnel clearance over an earth of normal or perhaps reduced radius. The downward bending that results in interference to other systems in direct line can be minimized

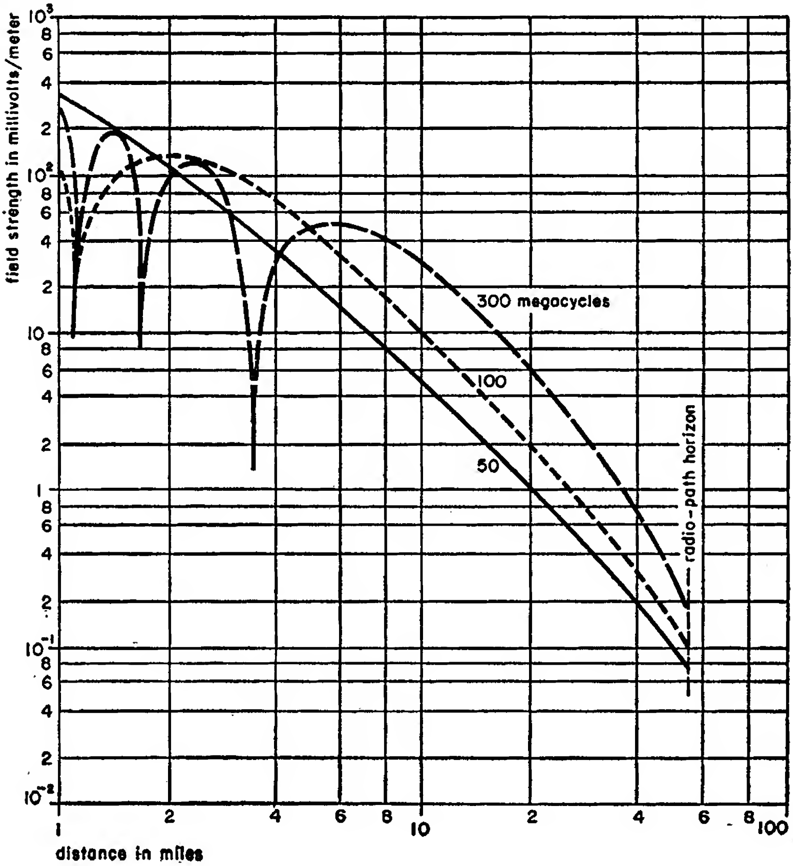

antenna heights: 1000 feet, 30 feet
power: 1 kilowatt
ground constants: $\sigma = 5 \times 10^{-14}$ emu
$\epsilon = 15$ esu
polarization: horizontal

Fig. 30—Variation of resultant field strength with distance and frequency. For information on ultra-high-frequency propagation beyond the horizon, see pp. 739 and 757.

Ultra-high-frequency line-of-sight conditions *continued*

by cross-polarizing the radiation on the interfering paths or eliminated by staggering the paths so that those on the same frequency are not in direct line.

Multipath fading is largely due to interference with the direct path of signals reflected from layers of abnormal water-vapor or temperature gradient. Continuity of communication service is greatly improved by the use of either space or frequency diversity.

For transmission paths of the order of 30 miles, good engineering practice should allow for possible increases of signal strength of +10 decibels with respect to free-space propagation and should allow a fading margin depending on the degree of reliability desired in accordance with the following:

10 decibels—90	percent
20 decibels—99	percent
30 decibels—99.9	percent
40 decibels—99.99	percent

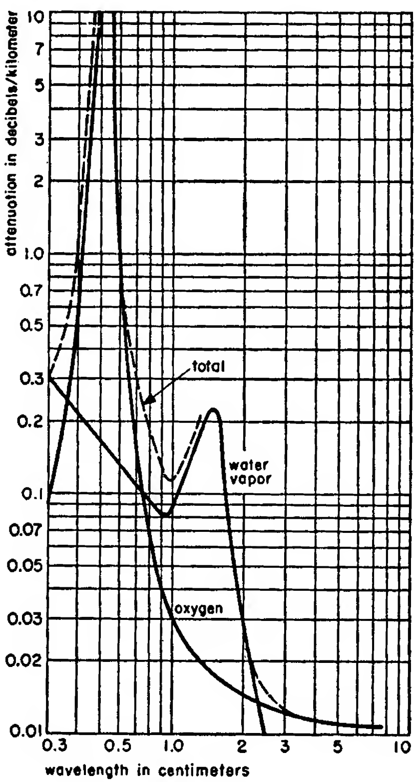

Fig. 31—Atmospheric absorption versus wavelength. The water-vapor curve is for 10 grams/meter^3 (66 percent relative humidity at 18° centigrade) and the oxygen curve was taken on a sample of gas at 15 centimeters mercury pressure.

Atmospheric absorption

Oxygen and water vapor may absorb energy from a radio wave by virtue of the permanent electric dipole moment of the water molecule and the permanent magnetic dipole moment of the oxygen molecule. Fig. 31 shows the water-vapor absoprtion and oxygen absorption as a function of wavelength. The water-vapor absorption curve is based on extensive measurements centered about a wavelength of 1.3 centimeters (frequency = 23,000 megacycles); the quantitative accuracy of the rest of this curve is less

Ultra-high-frequency line-of-sight conditions *continued*

certain. The oxygen absoprtion rises to a maximum at 5 millimeters wavelength; this has been quantitatively verified by direct measurements.

Free-space transmission formulas for uhf links

Free-space attenuation

Let the incoming wave be assimilated to a plane wave with a power flow per unit area equal to P_0. The available power at the output terminals of a receiving antenna may be expressed as

$$P_r = A_r P_0$$

where A_r is the effective area of the receiving antenna.

The free-space path attenuation is given by

$$\text{Attenuation} = 10 \log \frac{P_t}{P_r}$$

where P_t is the power radiated from the transmitting antenna (same units as for P_r). Then

$$\frac{P_r}{P_t} = \frac{A_r A_t}{d^2 \lambda^2}$$

where

A_r = effective area of receiving antenna

A_t = effective area of transmitting antenna

λ = wavelength

d = distance between antennas

The length and surface units in the formula should be consistent. This is valid provided $d \gg 2a^2/\lambda$, where a is the largest linear dimension of either of the antennas.

Effective areas of typical antennas

Hypothetical isotropic antenna (no heat loss)

$$A = \frac{1}{4\pi} \lambda^2 = 0.08\,\lambda^2$$

Free-space transmission formulas for uhf links *continued*

Small uniform-current dipole, short compared to wavelength (no heat loss)

$$A = \frac{3}{8\pi} \lambda^2 = 0.12\, \lambda^2$$

Half-wavelength dipole (no heat loss)

$$A \approx 0.13\, \lambda^2$$

Parabolic reflector of aperture area S (here, the factor 0.54 is due to nonuniform illumination of the reflector)

$$A \approx 0.54\, S$$

Very long horn with small aperture dimensions compared to length

$$A = 0.81\, S$$

Horn producing maximum field for given horn length

$$A = 0.45\, S$$

The aperture sides of the horn are assumed to be large compared to the wavelength.

Path attenuation between isotropic antennas

This is

$$\frac{P_t}{P_r} = 4.56 \times 10^3 f^2 d^2$$

where

f = megacycles/second

d = miles

Path attenuation α (in decibels) is

$$\alpha = 37 + 20 \log f + 20 \log d$$

A nomogram for the solution of α is given in Fig. 32.

Free-space transmission formulas for uhf links *continued*

Gain with respect to hypothetical isotropic antennas

Where directive antennas are used in place of isotropic antennas, the transmission formula becomes

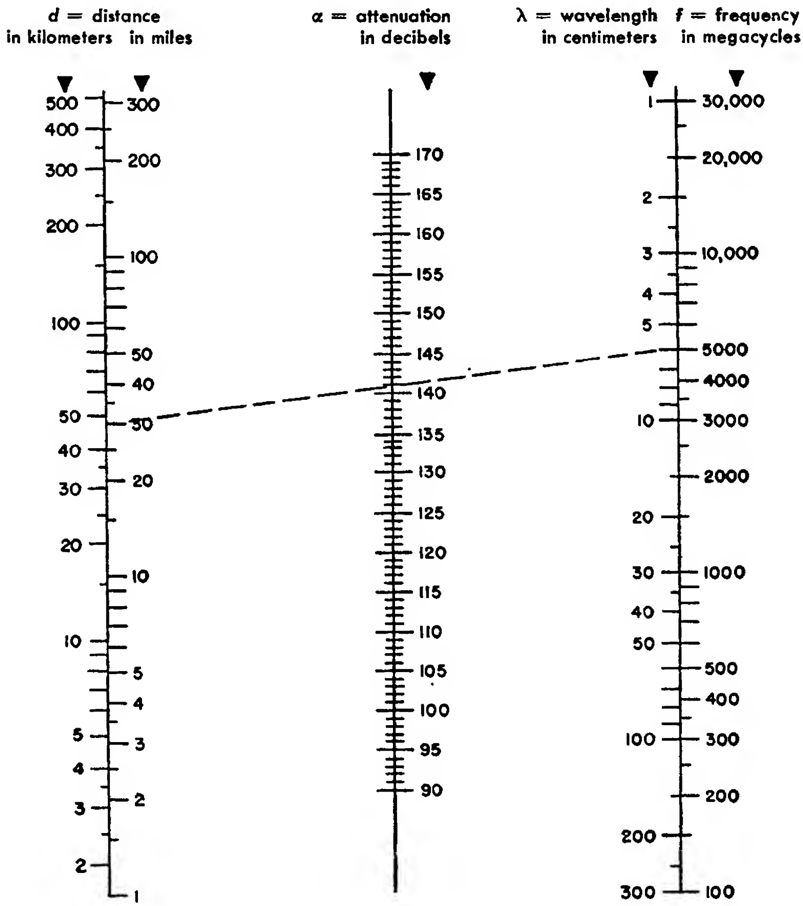

$\alpha = 37 + 20 \log f + 20 \log d$ decibels

Example shown: distance 30 miles, frequency 5000 megacycles; attenuation = 141 decibels

Fig. 32—Nomogram for solution of path attenuation α between isotropic antennas

Free-space transmission formulas for uhf links *continued*

$$\frac{P_r}{P_t} = G_t G_r \left[\frac{P_r}{P_t}\right]_{\text{isotropic}}$$

where G_t and G_r are the power gains due to the directivity of the transmitting and receiving antennas, respectively.

The apparent power gain is equal to the ratio of the effective area of the antenna to the effective area of the isotropic antenna (which is equal to $\lambda^2/4\pi \approx 0.08\,\lambda^2$).

The apparent power gain due to a parabolic reflector is thus

$$G = 0.54\left(\frac{\pi D}{\lambda}\right)^2$$

where D is the aperture diameter, and an illumination factor of 0.54 is assumed. In decibels, this becomes

$$G_{db} = 20 \log f + 20 \log D - 52.6$$

where

f = megacycles/second
D = aperture diameter in feet

The solution for G_{db} may be found in the nomogram, Fig. 33.

Beam angle

The beam angle θ in degrees is related to the apparent power gain G of a parabolic reflector with respect to isotropic antennas approximately by

$$\theta^2 \approx \frac{27{,}000}{G}$$

Since $G = 5.5 \times 10^{-6} D^2 f^2$, the beam angle becomes

$$\theta \approx \frac{7 \times 10^4}{fD}$$

Free-space transmission formulas for uhf links *continued*

where

θ = beam angle between 3-decibel points in degrees
f = frequency in megacycles
D = diameter of parabola in feet

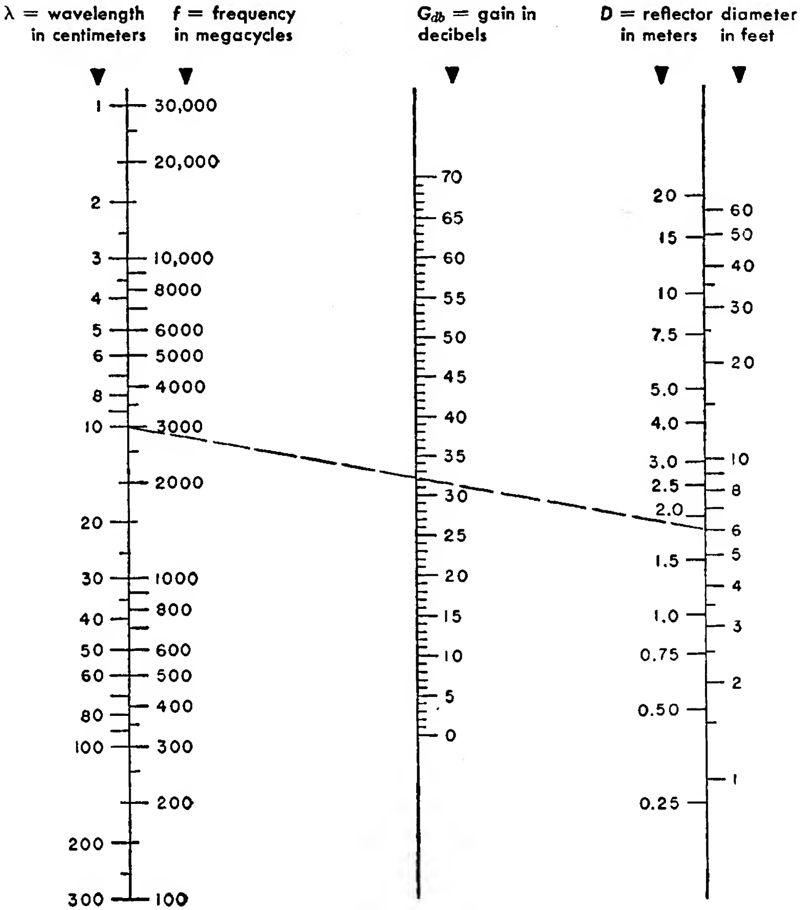

$10 \log G = 20 \log f + 20 \log D - 52.6$

Example shown: Frequency 3000 megacycles, diameter 6 feet; gain = 32 decibels

Fig. 33—Nomogram for determination of apparent power gain G_{db} (in decibels) of a parabolic reflector.

Free-space transmission formulas for uhf links *continued*

Transmitter power for a required output signal/noise ratio

Using the above expressions for path attenuation and reflector gain, the ratio of transmitted power to theoretical receiver noise, in decibels, is given by

$$10 \log \frac{P_t}{P_n} = A_p + \frac{S}{N} + (\mathrm{nf}) - G_t - G_r - \overline{(\mathrm{nif})}$$

where

S/N = required signal/noise ratio at receiver in decibels

(nf) = noise figure of receiver in decibels (see chapter "Radio noise and interference" for definition)

$\overline{(\mathrm{nif})}$ = noise improvement factor in decibels due to modulation methods where extra bandwidth is used to gain noise reduction (see chapter "Modulation" for definition)

P_n = theoretical noise power in receiver (see chapter "Radio noise and interference")

P_t = radiated transmitter power

G_t = gain of transmitting antenna in decibels

G_r = gain of receiving antenna in decibels

A_p = path attenuation in decibels

An equivalent way to compute the transmitter power for a required output signal/noise ratio is given below directly in terms of reflector dimensions and system parameters:

a. Normal free-space propagation,

$$P_t = \frac{\beta_1\beta_2}{40} \frac{BL^2}{f^2r^4} \frac{F}{K} \frac{S}{N}$$

b. With allowance for fading,

$$P_t = \frac{\beta_1\beta_2}{40} \frac{BL^2}{f^2r^4} \frac{F}{K} \sigma \left(\frac{S}{N}\right)_m$$

c. For multirelay transmission in n equal hops,

$$P_t = \frac{\beta_1\beta_2}{40} \frac{BL^2n}{f^2r^4} \frac{F}{K} \sigma \left(\frac{S}{N}\right)_{nm}$$

Free-space transmission formulas for uhf links *continued*

d. Signal/noise ratio for nonsimultaneous fading is

$$10 \log (S/N)_n = 10 \log \sigma (S/N)_{1m} - 10 \log \bar{n}$$

where

P_t = power in watts available at transmitter output terminals (kept constant at each repeater point)

β_1 = loss power ratio (numerical) due to transmission line at transmitter

β_2 = same as β_1 at receiver

B = root-mean-square bandwidth (generally approximated to bandwidth between 3-decibel attenuation points) in megacycles

L = total length of transmission in miles

f = carrier frequency in megacycles/second

r = radius of parabolic reflectors in feet

F = power-ratio noise figure of receiver (a numerical factor; see chapter "Radio noise and interference")

K = improvement in signal/noise ratio due to the modulation utilized. For instance, $K = 3m^2$ for frequency modulation, where m is the ratio of maximum frequency deviation to maximum modulating frequency. Note that this is the numerical power ratio.

σ = numerical ratio between available signal power in case of normal propagation to available signal power in case of maximum expected fading

S/N = required signal/noise power ratio at receiver

$(S/N)_m$ = minimum required signal/noise power ratio in case of maximum expected fading

$(S/N)_{nm}$ = same as above in case of n hops, at repeater number n

$(S/N)_{1m}$ = same as above at first repeater

$(S/N)_n$ = same as above at end of n hops

n = number of equal hops

m = number of hops where fading occurs

$$\bar{n} = n - m + \sum_{1}^{m} \sigma_k$$

σ_k = ratio of available signal power for normal conditions to available signal power in case of actual fading in hop number k (equation holds in case signal power is increased instead of decreased by abnormal propagation or reduced hop distance)

Free-space transmission formulas for uhf links *continued*

Passive reflectors distant from radiators

In some cases where obstacles in the path prevent line-of-sight conditions, it is feasible to reflect the signal from one antenna to the other by means of a plane surface located in the beam.

Under conditions in which the reflecting surface is at least 1000 feet from either antenna, the attenuation between the two radiators may be calculated by:

$$\text{(attenuation in decibels)} = 10 \log [1.25 \times 10^{17} (D_1 D_2/A)^2]$$

where

D_1, D_2 = distance in miles

A = effective area of reflector in feet^2

= projected area normal to path

Fig. 34 indicates the path attenuation between isotropic radiators for various common sizes of passive reflectors.

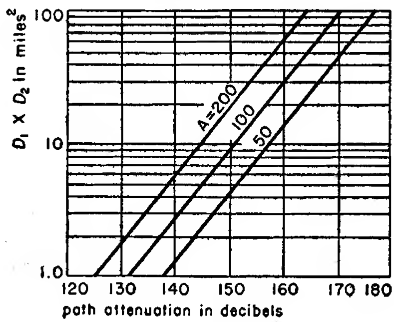

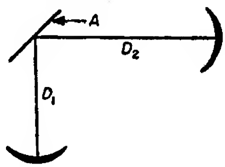

Fig. 34—Use of a passive reflector distant from both antennas.

Tropospheric scatter propagation

Weak but reliable fields are propagated several hundred miles beyond the horizon in the frequency band from about 40 to 4000 megacycles. The received power at these frequencies, and at points 30 miles or more beyond the horizon, is relatively independent of frequency and antenna height, but the hour-to-hour and day-to-day median carrier levels may be considerably influenced by atmospheric refraction.

With beyond-the-horizon propagation at these frequencies, there are two types of fading: In one, the amplitude has Rayleigh distribution over short periods when the tropospheric conditions can be considered constant. This fast fading is due to the existence of several paths differing slightly in length and may be considerably reduced by the use of diversity. The second type of fading is much slower and is caused chiefly by variations

Tropospheric scatter propagation *continued*

in the gradient of the refractive index of the atmosphere; this type of fading is little affected by diversity.

Design Chart*

A summary of several well-known factors and of propagation data available as of mid 1956 is given in Fig. 35 to facilitate the selection of equipment and for computing the carrier-to-noise ratio for tropospheric propagation beyond the horizon. Three sample computations are given in Fig. 36 to demonstrate the use of the appropriate curves to derive in an orderly fashion the necessary information. Certain data, such as antenna gain or receiver noise factor, may be available from other sources for the specific equipment to be used. The distribution of excess scatter loss L_{BH} represents winter hourly medians in the temperate zone so that considerable signal increase may be expected under more-favorable meteorological conditions. The 50 percent L_{BH} curve is for the median value that will be exceeded 50 percent of the time; or conversely, the design resulting from the use of this loss has a reliability of 50 percent. The additional margin required for a reliability of 99.9 percent is shown in the next to the bottom line of the table.

To simplify Fig. 35, it was designed to be entered with $10d_{ft}$ and $0.1P_w$.

* Reprinted from: F. J. Altmon, "Design Chart for Tropospheric Beyond-the-Horizon Propagation," *Electrical Communication*, vol. 33, pp. 165-167; June, 1956.

Tropospheric scatter propagation *continued*

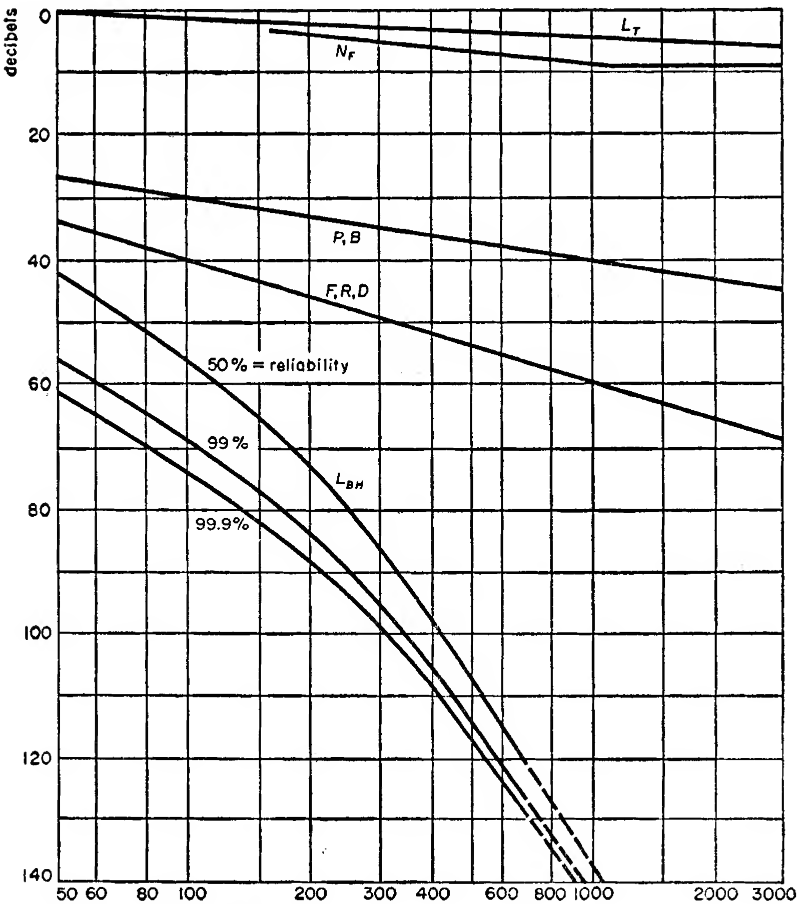

frequency in megacycles = f_{mc}

bandwidth in kilocycles = b_{kc}

range in miles = r_{ml}

divide scale by 10 for antenna diameter in feet = $10 d_{ft}$

multiply scale by 10 for power in watts = $0.1 p_w$

Fig. 35—Design chart for tropospheric scatter propagation.

Fig. 36—Computations for beyond-the-horizon links.

symbol and factor	equation	curve of Fig. 35	example 1		example 2		example 3	
			given	decibels	given	decibels	given	decibels
F = frequency	20 log f_{mc}	F	900 mc	59	2000 mc	66	300 mc	50
R = range	20 log r_{mi}	R	90 mi	39	200 mi	46	400 mi	52
K_p = propagation constant	See p. 751	—	—	37	—	37	—	37
L_{FS} = free-space loss	$F + R + K_p$	—	—	135	—	149	—	139
L_{BH} = median beyond-the-horizon loss	See note 1	L_{BH} 50%	90 mi	54	200 mi	72	400 mi	98
L_T = terminal loss	5 log $f_{mc} - 10$	L_T	900 mc	5	2000 mc	6	300 mc	3
L = total loss	$L_{FS} + L_{BH} + L_T$	—	—	194	—	227	—	240
D = antenna diameter	20 log 10 d_{ft}	D	28 ft	49	60 ft	55	100 ft	60
F = frequency	20 log f_{mc}	F	900 mc	59	2000 mc	66	300 mc	50
Sum	$D + F$	—	—	108	—	121	—	110
K_a = antenna constant	Use p. 753, add 20 db for $10d_{ft}$	—	—	73	—	73	—	73
G' = antenna gain, uncorrected	$D + F - K_a$	—	—	35	—	48	—	37
Gain for 2 antennas	$2G'$	—	—	70	—	96	—	74

L_c = antenna aperture-to-medium coupling loss	See note 2	—	—	2	—	4	—	2
G_N = net antenna gain	$2G' - L_c$	—	—	68	—	92	—	72
P = power ratio	$10 \log P_w$	P	500 w	27	10 kw	40	50 kw	47
G_T = total gain	$G_N + P$	—	—	95	—	132	—	119
C = median carrier at receiver in db below 1 watt	$G_T - L$	—	—	−99	—	−95	—	−121
B = bandwidth	$10 \log b_{kc} + 10$	B	200 kc	33	600 kc	38	60 kc	28
F_N = receiver noise	—	N_F	900 mc	9	2000 mc	9	300 mc	5
Sum	$B + F_N$	—	—	42	—	47	—	33
K_N = noise constant	$0.01\ kT°$		293°K	184	293°K	184	293°K	184
N = noise in db below 1 watt	$K_N - (B + F_N)$	—	—	−142	—	−137	—	−151
C/N = median carrier/noise	C–N	—	—	43	—	42	—	30
ΔL_{BH} = fading margin	50%–99.9%	L_{BH}	90 mi	18	200 mi	15	400 mi	10
Minimum long-term C/N	$(C - N) - \Delta L_{BH}$	—	—	25	—	27	—	20

Note 1: W. E. Morrow, "Ultra-High-Frequency Transmissions Over Paths of 300 to 600 Miles", presented at Symposium on Scatter Propagation of the New York Section of the Institute of Radio Engineers, New York, New York, on January 14, 1956.

Note 2: Aperture-to-medium coupling loss has been measured as being 4.5 decibels for 46-decibel-gain with antennas 150 miles apart. For much lower gains and for distances substantially shorter or longer, this loss may be negligible.

■ Radio noise and interference

Noise and its sources

Noise and interference from other communication systems are two factors limiting the useful operating range of all radio equipment.

The values of the main different sources of radio noise versus frequency are plotted in Fig. 1.

Atmospheric noise is shown in Fig. 1 as the average peaks read on the indicating instrument of an ordinary field-intensity meter. This is lower than the true peaks of atmospheric noise. Man-made noise is shown as the peak values that would be read on the radio noise meters specified in proposed American Standards C63.2 and C63.3. Receiver and antenna noise is that obtained with an energy-averaging device such as a thermo-ammeter.

Atmospheric noise

This noise is produced mostly by lightning discharges in thunderstorms. The noise level is thus dependent on frequency, time of day, weather, season of the year, and geographical location.

Subject to variations due to local stormy areas, noise generally decreases with increasing latitude on the surface of the globe. Noise is particularly severe during the rainy seasons in certain areas such as Caribbean, East Indies, equatorial Africa, northern India, etc. Fig. 1 shows median values of atmospheric noise for the U. S. A. and these values may be assumed to apply approximately to other regions lying between 30 and 50 degrees latitude north or south.

Rough approximations for atmospheric noise in other regions may be obtained by multiplying the values of Fig. 1 by the following factors:

degrees of latitude	nighttime		daytime	
	100 kc/s	10 mc/s	100 kc/s	10 mc/s
90–50	0.1	0.3	0.05	0.1
50–30	1	1	1	1
30–10	2	2	3	2
10– 0	5	4	6	3

Atmospheric noise is the principal limitation of radio service on the lower frequencies. At frequencies above about 30 megacycles, the noise falls to levels generally lower than receiver noise.

The peak amplitude of atmospheric noise usually may be assumed to be proportional to the square root of receiver bandwidth.

Noise and its sources *continued*

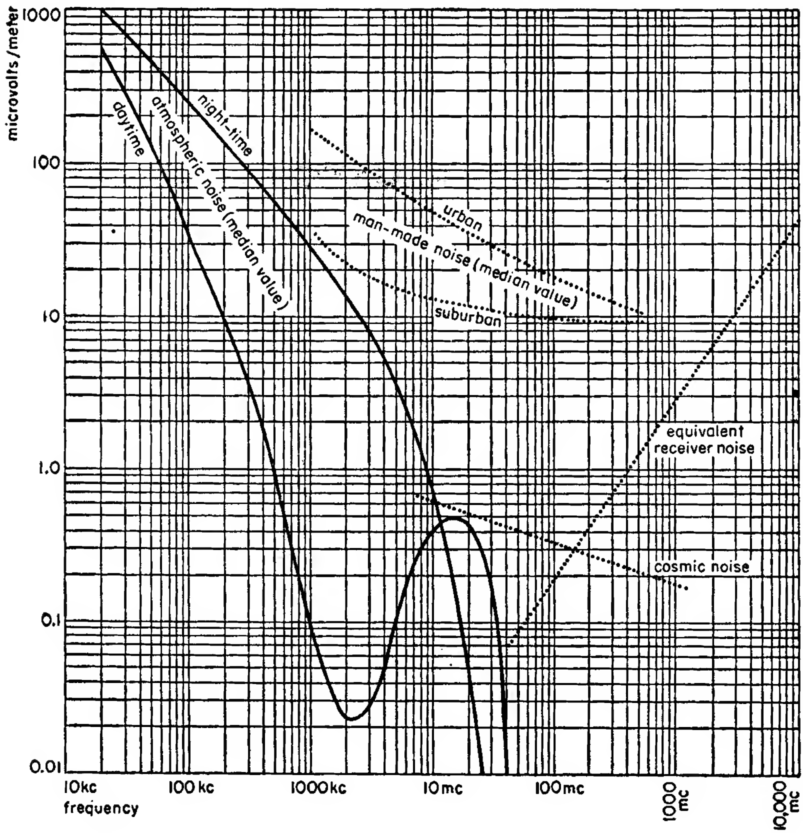

1. All curves assume a bandwidth of 10 kilocycles/second.
2. Refer to Fig. 3 for converting man-made-noise curves to bandwidths greater than 10 kilocycles. For all other curves, noise amplitude varies as the square root of bandwidth.
3. The curve of receiver noise shows the field intensities required to equal the receiver noise assuming
   a. The use of a half-wave-dipole antenna.
   b. A receiver noise level greater than the ideal receiver level by a factor varying from 2 decibels at 50 megacycles to 9 decibels at 1000 megacycles.
4. Transmission-line loss is not considered in the calculations.
5. For antennas having a gain with respect to a half-wave dipole, equivalent noise-field intensities are less than indicated above in proportion to the net gain of the antenna–transmission-line combination.

Fig. 1—Major sources of radio-frequency noise, showing amplitudes at various frequencies. For the U.S.A. and regions of similar latitude.

Noise and its sources *continued*

Cosmic and solar noise*

Fig. 2 shows the level of cosmic and solar noise relative to receiver noise when using a half-wave dipole. The noise levels shown in this figure refer to the following sources of cosmic and solar noise.

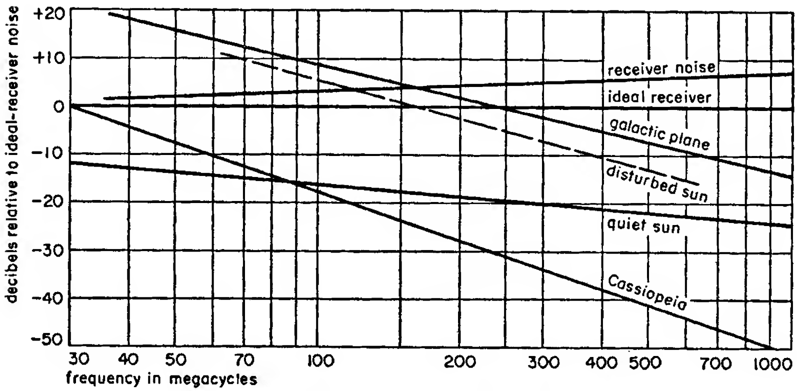

Fig. 2—Cosmic and solar noise levels for a half-wave-dipole receiving antenna.

Galactic plane: Cosmic noise from the galactic plane in the direction of the center of the galaxy. The noise levels from other parts of the galactic plane are between 10 and 20 decibels below the levels given in Fig. 2.

Quiet sun: Noise from the "quiet" sun; that is, solar noise at times when there is little or no sunspot activity.

Disturbed sun: Noise from the "disturbed" sun. The term disturbed refers to times of sunspot and solar-flare activity.

Cassiopeia: Noise from a high-intensity discrete source of cosmic noise known as Cassiopeia. This is one of more than a hundred known discrete sources, each of which subtends an angle at the earth's surface of less than 30 minutes of angle.

The levels of cosmic and solar noise received by an antenna directed at a noise source may be estimated by correcting the relative noise levels with a half-wave dipole (from Fig. 2) for the receiving-antenna gain realized on the noise source. Since the galactic plane is an extended nonuniform

* B. Lovell and J. A. Clegg, "Radio Astronomy," John Wiley & Sons, Inc., New York, N. Y., Chapman and Hall, Limited, London England: 1952. Also, J. L. Pawsey and R. N. Brocewell; "Radio Astronomy," Clarendon Press, Oxford, England; 1955.

Noise and its sources *continued*

noise source, free-space antenna gains cannot be realized and 10 to 15 decibels is approximately the maximum antenna gain that can be realized here. However, on the sun and other discrete sources of cosmic noise, antenna gains of 50 decibels or more can be had.

Man-made noise

This includes interference produced by sources such as motorcar ignition, electric motors, electric switching gear, high-tension line leakage, diathermy, industrial-heating generators. The field intensity from these sources is greatest in densely populated and industrial areas.

The nature of man-made noise is so variable that it is difficult to formulate a simple rule for converting 10-kilocycle-bandwidth receiver measurements to other bandwidth values. For instance, the amplitude of the field strength radiated by a diathermy device will be the same in a 100- as in a 10-kilocycle bandwidth receiver. Conversely, peak-noise field strength due to automobile ignition will be considerably greater with a 100- than with a 10-kilocycle bandwidth. According to the best available information, the peak field strengths of man-made noise (except diathermy and other narrow-band noise) increases as the receiver bandwidth is increased, substantially as shown in Fig. 3.

The man-made noise curves in Fig. 1 show typical median values for the U.S.A. In accordance with statistical practice, median values are interpreted to mean that 50 percent of all sites will have lower noise levels than the

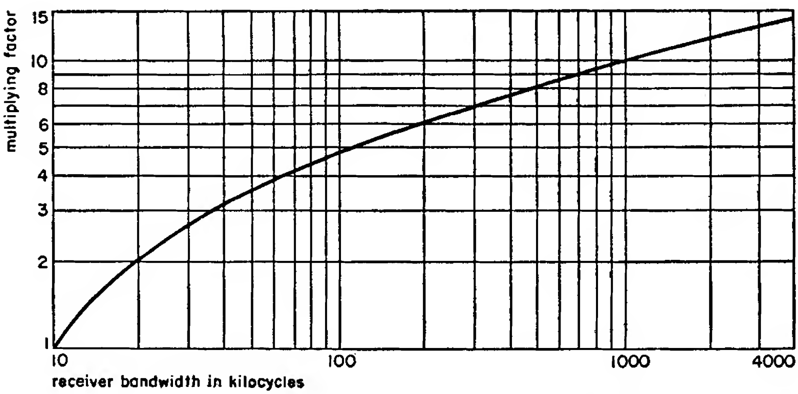

Fig. 3—Bandwidth factor. Multiply value of man-made noise from Fig. 1 by the factor above for receiver bandwidths greater than 10 kilocycles.

Noise and its sources *continued*

values of Fig. 1; 70 percent of all sites will have noise levels less than 1.9 times these values; and 90 percent of all sites, less than 7 times these values.

Thermal noise

Thermal noise is caused by the thermal agitation of electrons in resistances. Let R = resistive component in ohms of an impedance Z. The mean-square value of thermal-noise voltage is given by

$$E^2 = 4\,R\,kT \cdot \Delta f$$

where

k = Boltzmann's constant = 1.38×10^{-23} joules/degree Kelvin

T = absolute temperature in degrees Kelvin

Δf = bandwidth in cycles/second

E = root-mean-square noise voltage

The above equation assumes that thermal noise has a uniform distribution of power through the bandwidth Δf.

In case two impedances Z_1 and Z_2 with resistive components R_1 and R_2 are in series at the same temperature, the square of the resulting root-mean-square voltage is the sum of the squares of the root-mean-square noise voltages generated in Z_1 and Z_2;

$$E^2 = E_1^2 + E_2^2 = 4(R_1 + R_2)\,kT \cdot \Delta f$$

In case the same impedances are in parallel at the same temperature, the resulting impedance Z is calculated as is usually done for alternating-current circuits, and the resistive component R of Z is then determined. The root-mean-square noise voltage is the same as it would be for a pure resistance R.

It is customary in temperate climates to assign to T a value such that $1.38T = 400$, corresponding to about 17 degrees centigrade or 63 degrees Fahrenheit. Then

$$E^2 = 1.6 \times 10^{-20}\,R \cdot \Delta f$$

Noise in amplifiers

The ultimate sensitivity of an amplifier is set by the noise inherent to its input stage. For discussions of the noise produced in electron tubes and in transistors, refer to the pertinent chapters.

Noise measurements — noise figure

Measurement for broadcast receivers*

For standard broadcast receivers, the noise properties are determined by means of the equivalent noise sideband input (ensi). The receiver is connected as shown in Fig. 4.

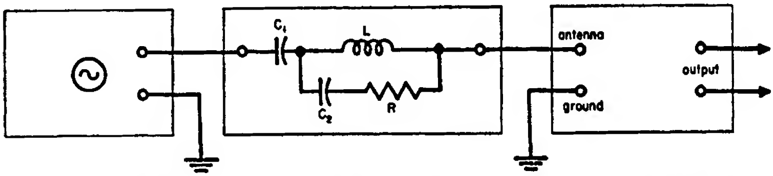

Fig. 4—Measurement of equivalent noise sideband input of a broadcast receiver.

Components of the standard dummy antenna are

C_1 = 200 micromicrofarads

C_2 = 400 micromicrofarads

L = 20 microhenries

R = 400 ohms

The equivalent noise sideband input

$$\text{(ensi)} = m\, E_s \sqrt{P'_n/P'_s}$$

where

E_s = root-mean-square unmodulated carrier-input voltage

m = degree of modulation of signal carrier at 400 cycles/second

P'_s = root-mean-square signal-power output when signal is applied

P'_n = root-mean-square noise-power output when signal input is reduced to zero

It is assumed that no appreciable noise is transferred from the signal generator to the receiver, and that m is small enough for the receiver to operate without distortion.

* "Standards on Radio Receivers: Methods of Testing Broadcast Radio Receivers, 1938," published by The Institute of Radio Engineers; 1942.

Noise measurements — noise figure *continued*

Noise figure of a receiver

A more precise evaluation of the quality of a receiver as far as noise is concerned is obtained by means of its *noise figure.**

It should be clearly realized that the noise figure evaluates only the linear part of the receiver, i.e., up to the demodulator.

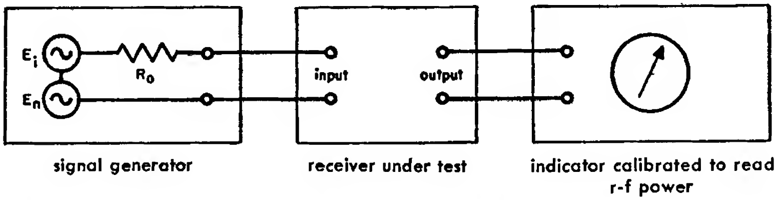

Fig. 5—Measurement of the noise figure of a receiver. The receiver is considered as a 4-terminal network. Output refers to last intermediate-frequency stage.

The equipment used for measuring noise figure is shown in Fig. 5. The incoming signal (applied to the receiver) is replaced by an unmodulated signal generator with

R_0 = internal resistive component

E_i = root-mean-square open-circuit carrier voltage

E_n = root-mean-square open-circuit noise voltage produced in signal generator

Then

$$E_n^2 = 4\,k\,T_0\,R_0\,\Delta f'$$

where

k = Boltzmann's constant = 1.38×10^{-23} joules/degree Kelvin

T_0 = temperature in degrees Kelvin

$\Delta f'$ = effective bandwidth of receiver (determined as below)

If the receiver does not include any other source of noise, the ratio E_i^2/E_n^2 is equal to the power carrier/noise ratio measured by the indicator:

$$\frac{E_i^2}{E_n^2} = \frac{E_i^2/4R_0}{k\,T_0\,\Delta f'} = \frac{P_i}{N_i}$$

* The definition of the noise figure was first given by H. T. Friis, "Noise Figures of Radio Receivers," *Proceedings of the IRE*, vol. 32, pp. 419–422; July, 1944.

Noise measurements — noise figure *continued*

The quantities $E_i^2/4R_0$ and $kT_0\Delta f'$ are called the *available* carrier and noise powers, respectively.

The output carrier/noise power ratio measured in a resistance R may be considered as the ratio of an available carrier-output power P_o to an available noise-output power N_o.

The noise figure F of the receiver is defined by

$$\frac{P_o}{N_o} = \frac{1}{F} \times \frac{P_i}{N_i}$$

$$F = \frac{N_o}{N_i} \times \frac{1}{P_o/P_i} = \frac{E^2{}_{i1:1}}{4k\,T_0\,R_0\,\Delta f'} = \frac{P_{i1:1}}{k\,T_0\,\Delta f'}$$

where

P_o/P_i = available gain G of the receiver

$P_{i1:1}$ = available power from the generator required to produce a carrier-to-noise ratio of one at the receiver output

Noise figure is often expressed in decibels:

$$F_{db} = 10 \log_{10} F$$

Effective bandwidth $\Delta f'$ of the receiver is

$$\Delta f' = \frac{1}{G}\int G_f\,df$$

where G_f is the differential available gain. $\Delta f'$ is generally approximated to the bandwidth of the receiver between those points of the response showing a 3-decibel attenuation with respect to the center frequency.

Noise figure of cascaded networks

The over-all noise figure of two networks a and b in cascade (Fig. 6) is

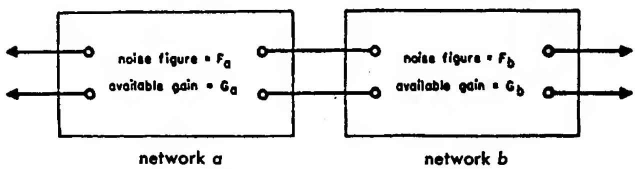

Fig. 6—Over-all noise figure F_{ab} of two networks, a and b, in cascade.

Noise measurements — noise figure *continued*

$$F_{ab} = F_a + \frac{F_b - 1}{G_a}$$

provided $\Delta f_b' \leqslant \Delta f_a'$

The value of F is a measure of the quality of the input tubes of the circuits. Up to some 300 megacycles, noise figures of 2 to 4 have been obtained. From 3000 to 6000 megacycles, the noise figure varies between 10 and 40 for the tubes at present available. It goes up to about 50 for 10,000-megacycle receivers.

The additional noise due to external sources influencing real antennas (such as cosmic noise), may be accounted for by an apparent antenna temperature, bringing the available noise-power input to $k\,T_a\,\Delta f'$ instead of $N_i = k\,T_0\,\Delta f'$ (the physical antenna resistance at temperature T_0 is generally negligible in high-frequency systems). The internal noise sources contribute $(F - 1)N_i$ as before, so that the new noise figure is given by

$$F'N_i = (F - 1)N_i + k\,T_0\,\Delta f'$$

$$F' = F - 1 + T_a/T_0$$

The average temperature of the antenna for a 6-megacycle equipment is found to be 3000 degrees Kelvin, approximately. The contribution of external sources is thus of the order of 10, compared with a value of $(F - 1)$ equal to 1 or 2, and becomes the limiting factor of reception. At 3000 megacycles, however, values of T_a may fall below T_0, while noise figures are of the order of 20.

Noise improvement factor

In case the receiver includes demodulation processes that produce a carrier/noise ratio improvement (nif), this improvement ratio must, of course, be considered when evaluating the carrier required to produce a desired output carrier/noise ratio. For a discussion of noise improvement factor in such systems as frequency modulation and pulse demodulation, see the chapter "Modulation."

Measurement of external radio noise

External noise fields, such as atmospheric, cosmic, and man-made, are measured in the same way as radio-wave field strengths, with the exception

Measurement of external radio noise *continued*

that peak, rather than average, values of noise are usually of interest, and that the over-all band-pass action of the measuring apparatus must be accurately known in measuring noise.* When measuring noise varying over wide limits with time, such as atmospheric noise, it is generally best to employ automatic recorders.

Interference effects in various systems

Besides noise, the efficiency of radio-communication systems can be limited by the interference produced by other radio-communication systems. The amount of tolerable signal/interference ratio, and the determination of conditions for entirely satisfactory service, are necessary for the specification of the amount of harmonic and spurious frequencies that can be allowed in transmitter equipments, as well as for the correct spacing of adjacent channels.

The following information has been extracted from "Final Acts of the International Telecommunication and Radio Conferences (Appendix 1)," Atlantic City, 1947.

Available information is not sufficient to give reliable rules in the cases of frequency modulation, pulse emission, and television transmission.

Simple telegraphy

It is considered that satisfactory radiotelegraph service is provided when the radio-frequency interference power available in the receiver, averaged over a cycle when the amplitude of the interfering wave is at a maximum, is at least 10 decibels below the available power of the desired signal averaged in the same manner, at the time when the desired signal is a minimum.

In order to determine the amount of interference produced by one telegraph channel on another, Figs. 7 and 8 will be found useful.

Frequency-shift telegraphy and facsimile

It is estimated that the interference level of —10 decibels as recommended

* For methods of measuring field strengths and, hence, noise, see "Standards on Radio Wave Propagation: Measuring Methods, 1942," published by the Institute of Radio Engineers. For information on suitable circuits to obtain peak values, particularly with respect to man-made noise, see C. V. Agger, D. E. Foster, and C. S. Young, "Instruments and Methods of Measuring Radio Noise," *Electrical Engineering*, vol. 59, pp. 178–192; March, 1940.

Interference effects in various systems *continued*

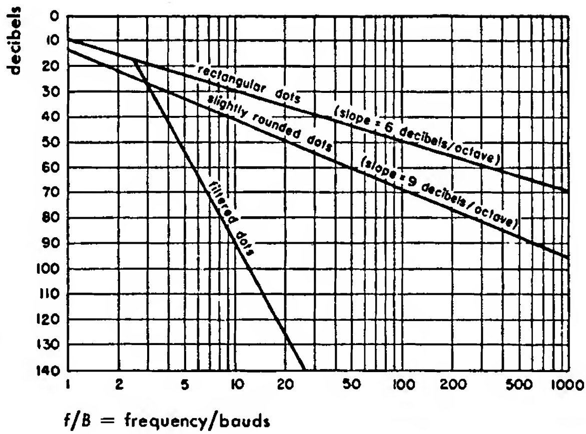

Fig. 7—Curves giving the envelopes for Fourier spectra of the emission resulting from several shapes of a single telegraph dot. For the upper curve the dot is taken to be rectangular and its length is ½ of the period T corresponding to the fundamental dotting frequency. The dotting speed in bauds is $B = 1/t = 2/T$. The bottom curve would result from the insertion of a filter with a pass band equal to 5 units on the f/B scale, and having a slope of 30 decibels/octave outside of the pass band.

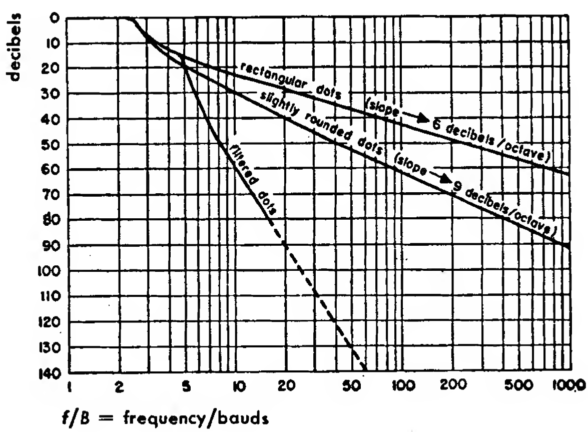

Fig. 8—Received power as a function of frequency separation between transmitter frequency and midband frequency of the receiver.

in the previous case will also be suitable for frequency-shift telegraphy and facsimile.

Double-sideband telephony

The multiplying factor for frequency separation between carriers as required for various ratios of signal/interference is given in the following table. This factor should be multiplied by the highest modulation frequency.

The acceptance band of the receiving filters in cycles/second is assumed to be 2 × (highest modulation frequency) and the cutoff characteristic is assumed to have a slope of 30 decibels/octave.

Interference effects in various systems *continued*

ratio of desired to interfering carriers in decibels	multiplying factor for various ratios of signal/interference			
	20 db	30 db	40 db	50 db
60	0	0	0	0
50	0	0	0	0.60
40	0	0	0.60	1.55
30	0	0.60	1.55	1.85
20	0.60	1.55	1.85	1.96
10	1.55	1.85	1.96	2.00
0	1.85	1.96	2.00	2.55
−10	1.96	2.00	2.55	2.85
−20	2.00	2.55	2.85	3.2
−30	2.55	2.85	3.2	3.6
−40	2.85	3.2	3.6	4.0
−50	3.2	3.6	4.0	4.5
−60	3.6	4.0	4.5	5.1
−70	4.0	4.5	5.1	5.7
−80	4.5	5.1	5.7	6.4
−90	5.1	5.7	6.4	7.2
−100	5.7	6.4	7.2	8.0

Broadcasting

As a result of a number of experiments, it is possible to set down the following results for carrier frequencies between 150 and 285 kilocycles/second and between 525 and 1560 kilocycles.

frequency separation between carriers in kilocycles	minimum ratio of desired and interfering carriers in decibels
11	0*
10	6†
9	14†
8	26‡
5 (or less)	60†

* extropolated † experimental ‡ interpolated

These experimental results agree reasonably well with the theoretical results of the preceding table with a highest modulation frequency of about 4500 cycles/second, and with a signal/interference ratio of 50 decibels.

Single-sideband telephony

Experience shows that the separation between adjacent channels need be only great enough to insure that the nearest frequency of the interfering signal is 40 decibels down on the receiver filter characteristic when due allowance has been made for the frequency instability of the carrier wave.

Spurious responses

In superheterodyne receivers, where a nonlinear element is used to get a desired intermediate-frequency signal from the mixing of the incoming signal and a local-oscillator signal, interference from spurious external signals results in a number of undesired frequencies that may fall within the intermediate-frequency band. Likewise, when two local oscillators are mixed in a transmitter or receiver to produce a desired output frequency, several unwanted components are produced at the same time due to the imperfections of the mixer characteristic. The following tables show how the location of the spurious frequencies can be determined.

Symbols

f_1 = signal frequency (or first source)

f_1' = spurious signal ($f_1' = f_1$ for mixing local sources, but when dealing with a receiver, usually $f_1' \neq f_1$)

f_2 = local-injection frequency (or second source)

f_x = desired mixer-output frequency

f_x' = spurious mixer-output frequency

$k = m + n$ = order of response, where m and n are positive integers

Coincidence is where $f_1' = f_1$ and $f_x' = f_x$

Defining and coincidence equations

mixing for difference frequency			mixing for sum frequency		
type	**defining equations**	**coincidence**	**type**	**defining equations**	**coincidence**
I	$f_x = \pm(f_1 - f_2)$ $f_x' = \pm(nf_2 - mf_1')$	$\left[\dfrac{f_2}{f_1}\right]_{co} = \dfrac{m+1}{n+1}$	IV	$f_x = f_1 + f_2$ $f_x' = mf_1' - nf_2$	$\left[\dfrac{f_2}{f_1}\right]_{co} = \dfrac{m-1}{n+1}$
II	$f_x = \pm(f_1 - f_2)$ $f_x' = \pm(mf_1' - nf_2)$	$\left[\dfrac{f_2}{f_1}\right]_{co} = \dfrac{m-1}{n-1}$	V	$f_x = f_1 + f_2$ $f_x' = nf_2 - mf_1'$	$\left[\dfrac{f_2}{f_1}\right]_{co} = \dfrac{m+1}{n-1}$
III	$f_x = f_1 - f_2$ $f_x' = mf_1' + nf_2$	$\left[\dfrac{f_2}{f_1}\right]_{co} = \dfrac{1-m}{n+1}$	VI	$f_x = f_1 + f_2$ $f_x' = mf_1' + nf_2$	$\left[\dfrac{f_2}{f_1}\right]_{co} = \dfrac{1-m}{n-1}$

In types I and II, both f_x and f_x' must use the same sign throughout.

Types III and VI are relatively unimportant except when $m = n = 1$.

Spurious responses *continued*

Image ($m = n = 1$)

kind of mixing	receiver ($f_x' = f_x$)	two local sources ($f_1' = f_1$)
Difference	$f_1' = \pm(2f_2 - f_1)$ $= \pm(f_1 - 2f_x)$ $f_2 < f_1$ $= f_1 + 2f_x$ $f_2 > f_1$	$f_x' = f_1 + f_2$
Sum	$f_1' = f_1 + 2f_2$ $= 2f_x - f_1$	$f_x' = \pm(f_1 - f_2)$

Intermediate-frequency rejection must be provided for spurious signa' $f_1' = f_x$ where $m = 1$, $n = 0$.

Selectivity equations

For types I, II, IV, and V only.

When $f_x' = f_x$

$$\frac{f_1' - f_1}{f_1} = \frac{A}{m}\left\{\frac{f_2}{f_1} - \left[\frac{f_2}{f_1}\right]_{co}\right\}$$

When $f_1' = f_1$

$$\frac{f_x' - f_x}{f_1} = B\left\{\frac{f_2}{f_1} - \left[\frac{f_2}{f_1}\right]_{co}\right\}$$

$$\frac{f_x' - f_x}{f_x} = C\,\frac{(f_2/f_1) - [f_2/f_1]_{co}}{1 \mp f_2/f_1}$$

Where the coefficients and the $\mp$ signs are

type	A	B		C	$\mp$ sign
		$f_2 < f_1$	$f_2 > f_1$		
I	$n + 1$	A	$-A$	A	$-$
II	$n - 1$	$-A$	A	$-A$	$-$
IV	$n + 1$	$-A$	$-A$	$-A$	$+$
V	$n - 1$	A	A	A	$+$

Variation of output frequency vs input-signal deviation

For any type

$\Delta f_x' = \pm m\,\Delta f_1'$

Use the $+$ or the $-$ sign according to defining equation for type in question:

Spurious responses *continued*

Table of spurious responses

Type I coincidences: $\left[\dfrac{f_2}{f_1}\right]_{co} = \dfrac{m+1}{n+1}$, where $f_x' = f_x$ and $f_1' = f_1$

frequency ratio $= [f_2/f_1]_{co}$			lowest order			
fraction	decimal	reciprocal	k_I	m_I	n_I	highest orders
1/1	1.000	1.000	2	1	1	All even orders $m =$ (See note *b*)
8/9	0.889	1.125	15	7	8	
7/8	0.875	1.143	13	6	7	
6/7	0.857	1.167	11	5	6	
5/6	0.833	1.200	9	4	5	
4/5	0.800	1.250	7	3	4	
7/9	0.778	1.286	14	6	8	
3/4	0.750	1.333	5	2	3	$\begin{cases} m_I = 5 \\ n_I = 7 \end{cases}$
5/7	0.714	1.400	10	4	6	
7/10	0.700	1.429	15	6	9	
2/3	0.667	1.500	3	1	2	$\begin{cases} m_I = 3 \\ n_I = 5 \end{cases}$ $\begin{cases} = 5 \\ = 8 \end{cases}$
5/8	0.625	1.600	11	4	7	
3/5	0.600	1.667	6	2	4	$\begin{cases} m_I = 5 \\ n_I = 9 \end{cases}$
4/7	0.571	1.750	9	3	6	
5/9	0.556	1.800	12	4	8	
6/11	0.545	1.833	15	5	10	
1/2	0.500	2.000	1	0	1	$\begin{cases} m_I = 1 \\ n_I = 3 \end{cases}$ $\begin{cases} = 2 \\ = 5 \end{cases}$ $\begin{cases} = 3 \\ = 7 \end{cases}$ $\begin{cases} = 4 \\ = 9 \end{cases}$

Types II, IV, and V coincidences: For each ratio $[f_2/f_1]_{co}$ there are also the following responses

type	k	m	n
II	$k_{II} = k_I + 4$	$m_{II} = m_I + 2$	$n_{II} = n_I + 2$
IV	$k_{IV} = k_I + 2$	$m_{IV} = m_I + 2$	$n_{IV} = n_I$
V	$k_V = k_I + 2$	$m_V = m_I$	$n_V = n_I + 2$

Notes:

a. When $f_2 > f_1$, use reciprocal column and interchange the values of m and n.

b. At $[f_2/f_1]_{co} = 1/1$, additional important responses are
type II: $m = n = 2$
type IV: $m = 2$, $n = 0$
type V: $m = 0$, $n = 2$

Spurious responses *continued*

Chart of spurious responses

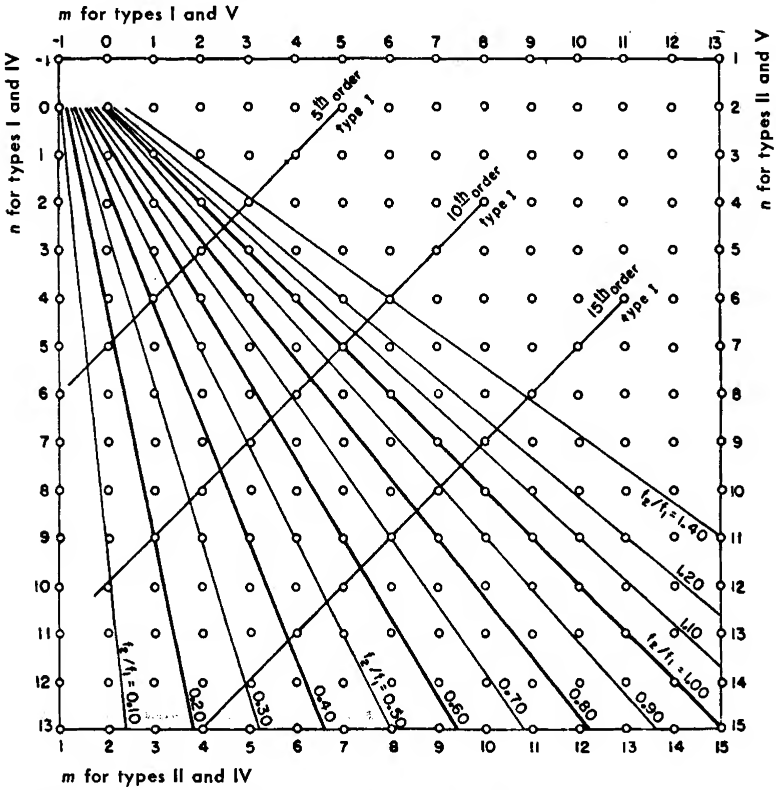

Each circle represents a spurious response coincidence, where $f_1' = f_1$ and $f_x' = f_x$.

Example: Suppose two frequencies whose ratio is $f_2/f_1 = 0.12$ are mixed to obtain the sum frequency. The spurious responses are found by laying a transparent straightedge on the chart, passing through the circle $-1, -1$ and lying a little to the right of the line marked $f_2/f_1 = 0.10$. It is observed that the straightedge passes near circles indicating the responses

$$\text{Type IV} \begin{cases} m = 1 \\ n = 0 \end{cases} \qquad \begin{cases} = 2 \\ = 7 \end{cases} \qquad \begin{cases} = 2 \\ = 8 \end{cases}$$

$$\text{Type V} \qquad \begin{cases} m = 0 \\ n = 9 \end{cases} \qquad \begin{cases} = 0 \\ = 10 \end{cases}$$

The actual frequencies of the responses f_x' or f_1' can be determined by substituting these coefficients m and n in the defining equations.

■ Broadcasting

Introduction

Radio broadcasting for public entertainment in the U.S.A. is at present of three general types.

Standard broadcasting: Utilizing amplitude modulation in the 535–1605-kilocycle/second band.

Frequency modulation: Broadcasting in the 88–108-megacycle/second band.

Television broadcasting: Utilizing amplitude-modulated video and frequency-modulated aural transmission in the (low) 54–88-megacycle band, the (high) 174–216-megacycle band, and in the (ultra-high-frequency) 470–890-megacycle band.

There is also

International broadcasting: On assigned frequencies in the region between 6000 and 21,700 kilocycles in accordance with international agreement.*

Operation in these bands in the U.S.A. is subject to licensing and technical regulations of the Federal Communications Commission.

Selected administrative and technical information and rules from F.C.C. publications applicable to each of these broadcast applications are given in this chapter.

General reference: "Rules Governing Radio Broadcast Services," Subparts A through G; January, 1956; Federal Communications Commission, Washington, D. C.

Standard broadcasting†

Standard-broadcast stations are licensed for operation on 10-kilocycle-spaced channels occupying the band 535–1605 kilocycles, inclusive, and are classified as indicated in Fig. 1.

* A more detailed explanation of international broadcasting frequency assignments and requirements is given in the chapter "Frequency data."

† See "Standards of Good Engineering Practice Concerning Standard Broadcast Stations August 1, 1939, revised to Oct. 30, 1947," Federal Communications Commission, Washington, D. C.; and, "Rules Governing Radio Broadcast Services," Subpart A; January, 1956.

Standard broadcasting *continued*

Fig. 1—Classification of standard-broadcast stations.*

class of station	class of channel	normal service	permissible power in kilowatts	signal-intensity contour in microvolts/meter of area protected from objectionable interference: day† (ground-wave)	night
Ia	Clear	Primary and secondary	50	SC = 100 AC = 500	Not duplicated
Ib	Clear	Primary and secondary	10 to 50	SC = 100 AC = 500	500 (50% sky wave)
II	Clear	Primary	0.25 to 50	500	2500 (Ground wave)
III–A	Regional	Primary	1 to 5	500	2500 (Ground wave)
III–B	Regional	Primary	Night = 0.5 to 1 Day = 5	500	4000 (Ground wave)
IV	Local	Primary	0.1 to 0.25	500	4000 (Ground wave)

* Taken from "Rules Governing Radio Broadcast Services," Subpart A; January, 1956. Federal Communications Commission, Washington, D. C.
† SC = same channel, AC = adjacent channel.

Field-intensity requirements

Primary service

City business, factory areas:	10	to	50	millivolts/meter, ground wave
City residential areas:	2	to	10	millivolts/meter, ground wave
Rural areas:	0.1	to	1.0	millivolt /meter, ground wave

Secondary service

All areas having sky-wave field intensity greater than 500 microvolts/meter for 50 percent or more of the time.

Coverage data

The charts of Figs. 2–4 show computed values of ground-wave field intensity as a function of the distance from the transmitting antenna. These are used for the determination of coverage and interference. They were computed for the frequencies indicated, a dielectric constant equal to 15 for ground and 80 for sea water (referred to air as unity), and for the surface conductivities noted. The curves are for radiation from a short vertical antenna at the surface of a uniformly conductive spherical earth, with an antenna power and efficiency such that the inverse-distance field is 100 millivolts/meter at one mile.

Standard broadcasting *continued*

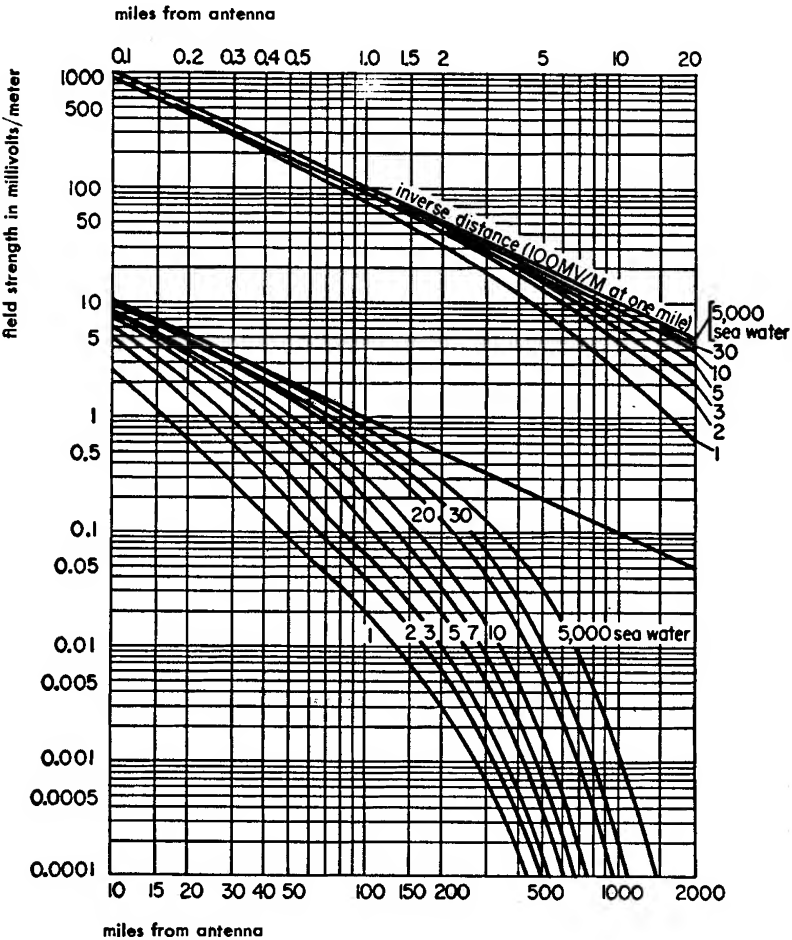

Fig. 2—Ground-wave field intensity plotted against distance. Computed for 550 kilocycles. Dielectric constant = 15. Ground-conductivity values above are emu $\times 10^{14}$.

Standard broadcasting *continued*

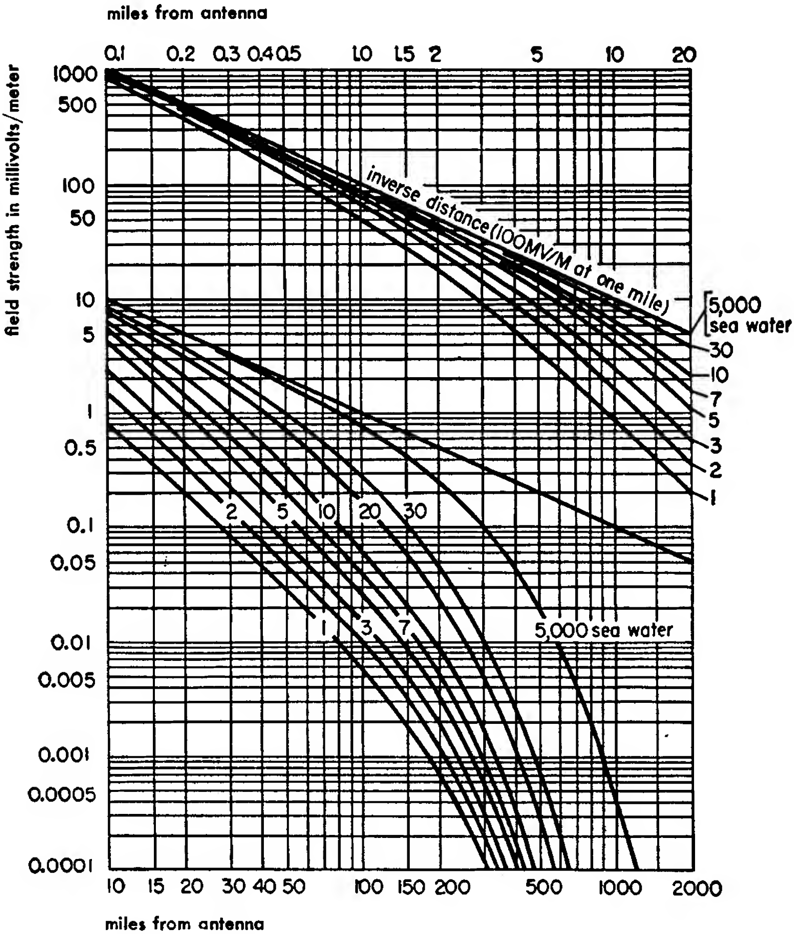

Fig. 3—Ground-wave field intensity plotted against distance. Computed for 1000 kilocycles. Dielectric constant = 15. Ground-conductivity values above are emu $\times 10^{14}$.

Standard broadcasting *continued*

The table of Fig. 5 gives data on ground inductivity and conductivity in the U.S.A.

Station performance requirements

Operation is maintained in accordance with the following specifications.

Modulation: Amplitude modulation of at least 85 to 95 percent.

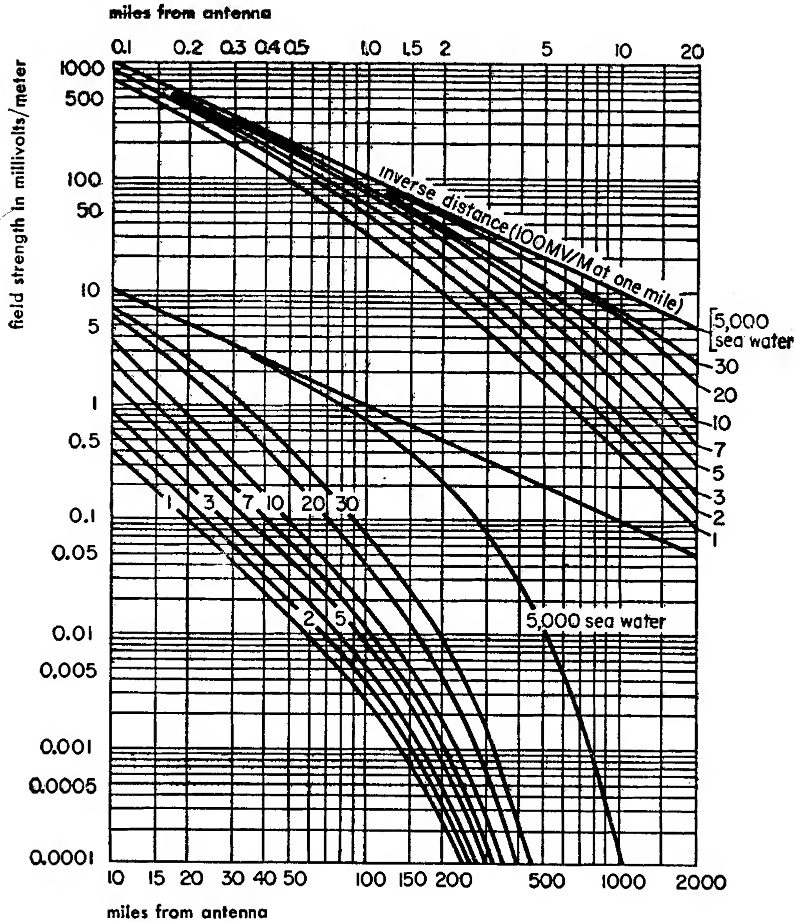

Fig. 4—Ground-wave field intensity plotted against distance. Computed for 1600 kilocycles. Dielectric constant = 15. Ground-conductivity values above are emu $\times 10^{14}$.

Standard broadcasting *continued*

Audio-frequency distortion: Harmonics less than 5 percent arithmetical sum or root-mean-square amplitude up to 85 percent modulation; less than 7.5 percent for 85 to 95 percent modulation.

Audio-frequency response: Transmission characteristic flat between 100 and 5000 cycles to within 2 decibels, referred to 1000 cycles.

Noise: At least 50 decibels, unweighted, below 100 percent modulation for the frequency band 150 to 5000 cycles, and at least 40 decibels down outside this range.

Carrier-frequency stability: Within 20 cycles of assigned frequency.

Fig. 5—Electrical characteristics of various types of terrain.*

type of terrain	inductivity referred to air = 1	conductivity in emu	absorption factor at 50 miles, 1000 kilocycles†
Sea water, minimum attenuation	81	4.64×10^{-11}	1.0
Pastoral, low hills, rich soil, typical of Dallas, Texas; Lincoln, Nebraska; and Wolf Point, Montana, areas	20	3×10^{-13}	0.50
Pastoral, low hills, rich soil, typical of Ohio and Illinois	14	10^{-13}	0.17
Flat country, marshy, densely wooded, typical of Louisiana near Mississippi River	12	7.5×10^{-14}	0.13
Pastoral, medium hills, and forestation, typical of Maryland, Pennsylvania, New York, exclusive of mountainous territory and sea coasts	13	6×10^{-14}	0.09
Pastoral, medium hills, and forestation, heavy clay soil, typical of central Virginia	13	4×10^{-14}	0.05
Rocky soil, steep hills, typical of New England	14	2×10^{-14}	0.025
Sandy, dry, flat, typical of coastal country	10	2×10^{-14}	0.024
City, industrial areas, average attenuation	5	10^{-14}	0.011
City, industrial areas, maximum attenuation	3	10^{-15}	0.003

* From "Standards of Good Engineering Practice Concerning Standard Broadcasting, August 1, 1939, revised October 30, 1947," Federal Communications Commission, Washington, D.C.

† This figure is stated for comparison purposes in order to indicate at a glance which values of conductivity and inductivity represent the higher absorption. It is the ratio between field intensity obtained with the soil constants given and with no absorption.

Frequency modulation*

Frequency-modulation broadcasting stations are authorized for operation on 100 allocated channels each 200 kilocycles wide extending consecutively from channel No. 201 on 88.1 megacycles to No. 300 on 107.9 megacycles.

Commercial broadcasting is authorized on channels No. 221 (92.1 megacycles) through No. 300. Noncommercial educational broadcasting is licensed on channels No. 201 through 220 (89.9 megacycles).

Station service classification

Class-*A* stations: Render service primarily to communities other than the principal city of an area. Provide coverage equivalent of effective rated power of 1 kilowatt and an antenna height of 250 feet. Class-*A* channel.

Class-*B* stations: Render service primarily to a metropolitan district or principal city and its surrounding rural area, or to primarily rural areas. In *FM Area I*, which includes New England and the North- and Middle-Atlantic-states areas, they are licensed for a coverage of not more than 20 kilowatts equivalent effective rated power and 300 feet minimum, 500 feet maximum, effective antenna height. In *FM Area II* (balance of U.S.A. outside of Area *I*), class-*B* stations are licensed for same coverage as class-*A* stations. However, greater coverage is encouraged where it would not result in undue interference to existing or probable assignments.

Coverage data

The frequency-modulation broadcasting service area is considered to be only that served by the ground wave. The median field intensity considered necessary for adequate service in city, business, or factory areas is 1 millivolt/meter; in rural areas, 50 microvolts/meter is specified. A median field intensity of 3000 to 5000 microvolts/meter is specified for the principal city to be served. The curves of Fig. 6 give data for determination of fm broadcast-station coverage as a function of rated power and antenna height.

Objectionable interference from other stations may limit the service area. Such interference is considered by the F.C.C. to exist when the ratio of desired to undesired signal values is as follows:

Same channel: 10/1

* See "Rules Governing Radio Broadcast Services," Part 3, Subparts B and C; January, 1956: Federal Communications Commission, Washington, D. C.

Frequency modulation *continued*

Adjacent channel (200-kc/s separation): 2/1

(400-kc/s separation): 1/10

(600-kc/s separation): 1/100

($\geqslant$800-kc/s separation): No restriction

Values are ground-wave median field for the desired signal, and the tropospheric-signal intensity exceeded for 1 percent of the time for the undesired signal. It is considered that stations having alternate-channel spacing (400-kilocycle separation) may be operated in the same coverage area without objectionable mutual interference.

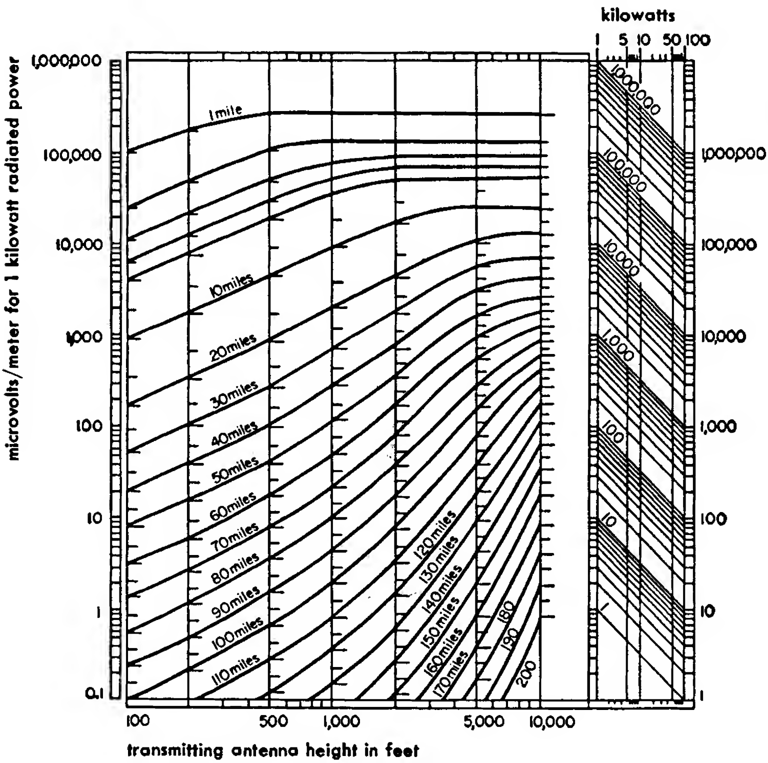

Fig. 6—Ground-wave signal range for frequency-modulation broadcasting band, 98 megacycles. Conductivity = 5 $\times$ 10^{-14} emu, and dielectric constant = 15. Receiving-antenna height = 30 feet. For horizontal (and approximately for vertical) polarization. These curves do not represent the best available propagation data. However, they are used to estimate expected coverage by a station filing for a license. It is recommended that Fig. 12 be used as a better engineering approximation.

Frequency modulation *continued*

Station performance requirements

Operation is maintained in accordance with the following specifications.

Audio-frequency response: Transmitting system capable of transmitting the band of frequencies 50 to 15,000 cycles. Pre-emphasis employed and response maintained within limits shown by curves of Fig. 7.

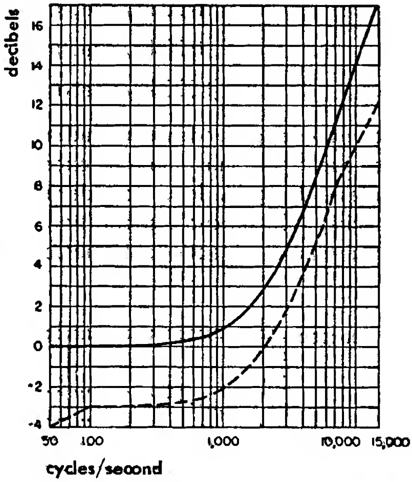

Fig. 7—Standard pre-emphasis curve for frequency-modulation and television aural broadcasting. Time constant = 75 microseconds (solid line). Frequency-response limits are set by the two lines.

Audio-frequency distortion: Maximum combined audiofrequency harmonic root-mean-square voltage in system output less than as shown below.

modulating frequency in cycles/second	percent harmonic
50–100	3.5
100–7500	2.5
7500–15000	3.0

Power output: Standard transmitter power output ratings are 10 watts for noncommercial stations, 250 watts, 1, 3, 5, 10, 25, 50, and 100 kilowatts.

Modulation: Frequency modulation with a modulating capability of 100 percent corresponding to a frequency swing of ±75 kilocycles.

Noise:

FM—In the band 50 to 15,000 cycles, at least 60 decibels below 100-percent swing at 400-cycle modulating frequency.

AM—In the band 50 to 15,000 cycles, at least 50 decibels below level representing 100-percent amplitude modulation.

Center-frequency stability: Within ±2000 cycles of assigned frequency.

Antenna polarization: Horizontal.

Television broadcasting*

Channel designations

Television-broadcast stations are authorized for commercial operation on 83 channels designated as in Fig. 8.

Fig. 8—Numerical designation of television channels.

channel number	band mc/s	channel number	band mc/s	channel number	band mc/s
2	54–60	29	560–566	57	728–734
3	60–66	30	566–572	58	734–740
4	66–72	31	572–578	59	740–746
5	76–82	32	578–584	60	746–752
6	82–88	33	584–590	61	752–758
7	174–180	34	590–596	62	758–764
8	180–186	35	596–602	63	764–770
9	186–192	36	602–608	64	770–776
10	192–198	37	608–614	65	776–782
11	198–204	38	614–620	66	782–788
12	204–210	39	620–626	67	788–794
13	210–216	40	626–632	68	794–800
14	470–476	41	632–638	69	800–806
15	476–482	42	638–644	70	806–812
16	482–488	43	644–650	71	812–818
17	488–494	44	650–656	72	818–824
18	494–500	45	656–662	73	824–830
19	500–506	46	662–668	74	830–836
20	506–512	47	668–674	75	836–842
21	512–518	48	674–680	76	842–848
22	518–524	49	680–686	77	848–854
23	524–530	50	686–692	78	854–860
24	530–536	51	692–698	79	860–866
25	536–542	52	698–704	80	866–872
26	542–548	53	704–710	81	872–878
27	548–554	54	710–716	82	878–884
28	554–560	55	716–722	83	884–890
		56	722–728		

Coverage data

Assignment of channels to specific areas has been made by the F.C.C. in such a manner as to facilitate maximum interference-free coverage within the available frequency spectrum. The radiated power of a particular station is fixed by several considerations.

Minimum power is 100 watts effective visual radiated power. No minimum antenna height is specified.

* See "Rules Governing Radio Broadcast Service," Part 3, Subpart E; January, 1956: Federal Communications Commission, Washington, D. C.

Television broadcasting *continued*

Interference: To avoid cochannel and adjacent-channel interference, a table of the channels assigned to listed communities in the United States has been designated in the referenced rules of the Federal Communications Commission.

Maximum power: (See Figs. 10 and 11.) Except as limited by antenna heights in excess of 1000 feet in *TV Zone I* and antenna heights in excess of 2000 feet in *TV Zones II* and *III*, the maximum visual estimated radiated power in decibels above 1 kilowatt is:

channel	maximum power
2–6	20 decibels = 100 kilowatts
7–13	25 decibels = 316 kilowatts
14–83	30 decibels = 1000 kilowatts

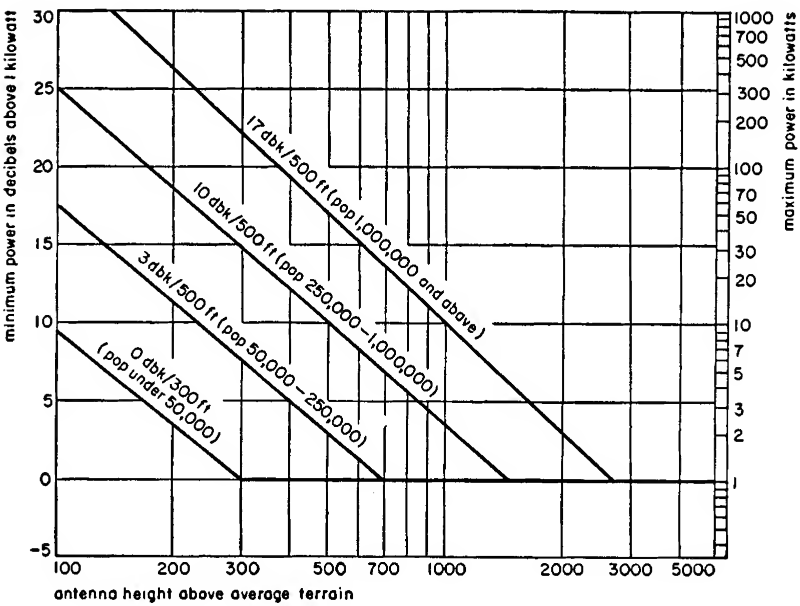

Fig. 9—Minimum television-station power in relation to population.

Television broadcasting *continued*

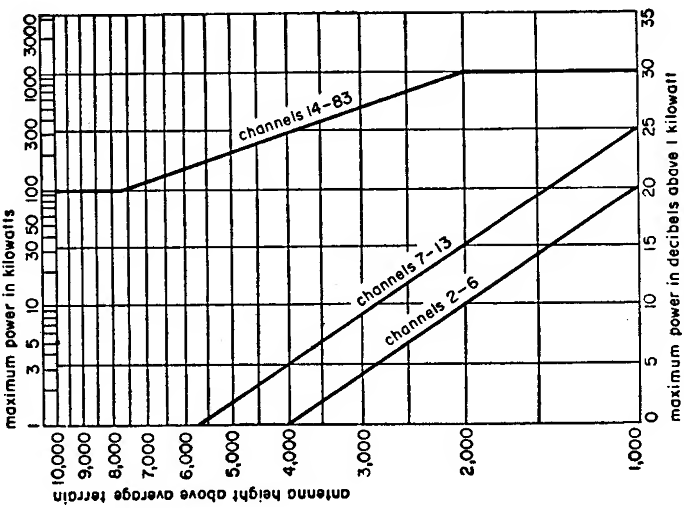

Fig. 10—Maximum television-station power versus antenna height for *TV Zone I*.

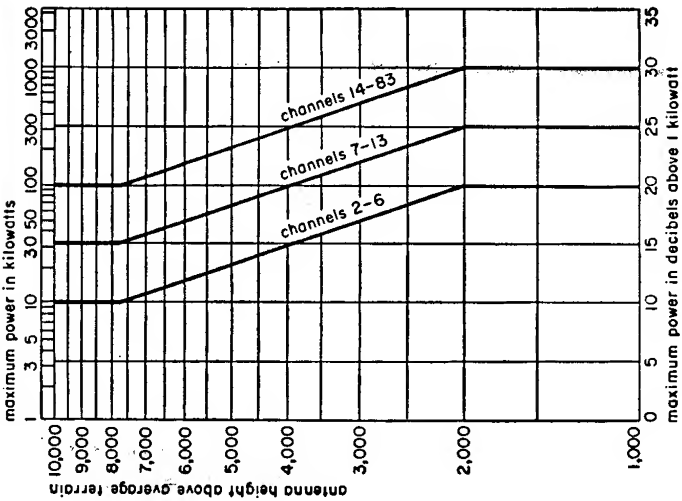

Fig. 11—Maximum television-station power versus antenna height for *TV Zones II and III*.

Television broadcasting *continued*

Grade of service: Two grades of service are designated *Grade A* and *Grade B*. The signal strength (in decibels above 1 microvolt/meter) specified for each service is:

channel	Grade A	Grade B
2–6	68 decibels = 2510 microvolts	47 decibels = 224 microvolts
7–13	71 decibels = 3550 microvolts	56 decibels = 631 microvolts
14–83	74 decibels = 5010 microvolts	64 decibels = 1585 microvolts

Transmitter location: The transmitter location must be so chosen that on the basis of effective radiated power and antenna height, the following

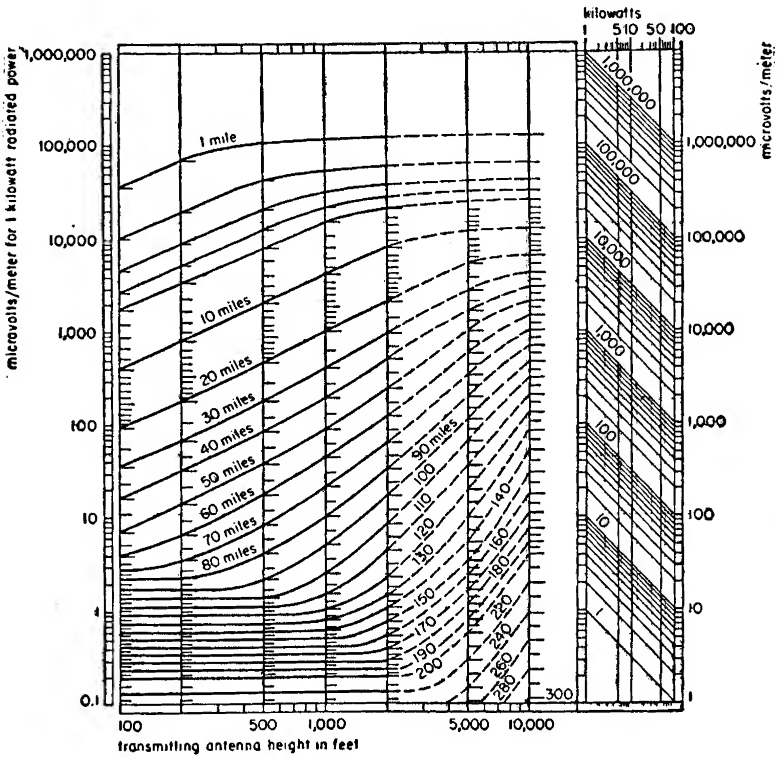

Fig. 12—Ground-wave signal range for television channels 2-6 and 14-83. Conductivity = 5 × 10^{-14} emu, and dielectric constant = 15. Receiving-antenna height = 30 feet. For horizontal (and approximately for vertical) polarization.

Television broadcasting *continued*

minimum field intensity in decibels above 1 microvolt/meter will be provided over the principal community to be served.

channel	signal
2–6	74 decibels = 5010 microvolts
7–13	77 decibels = 7080 microvolts
14–83	80 decibels = 10,000 microvolts

The curves of Figs. 12 and 13 give coverage distance through the allocated television-frequency bands as a function of radiated power and antenna height.

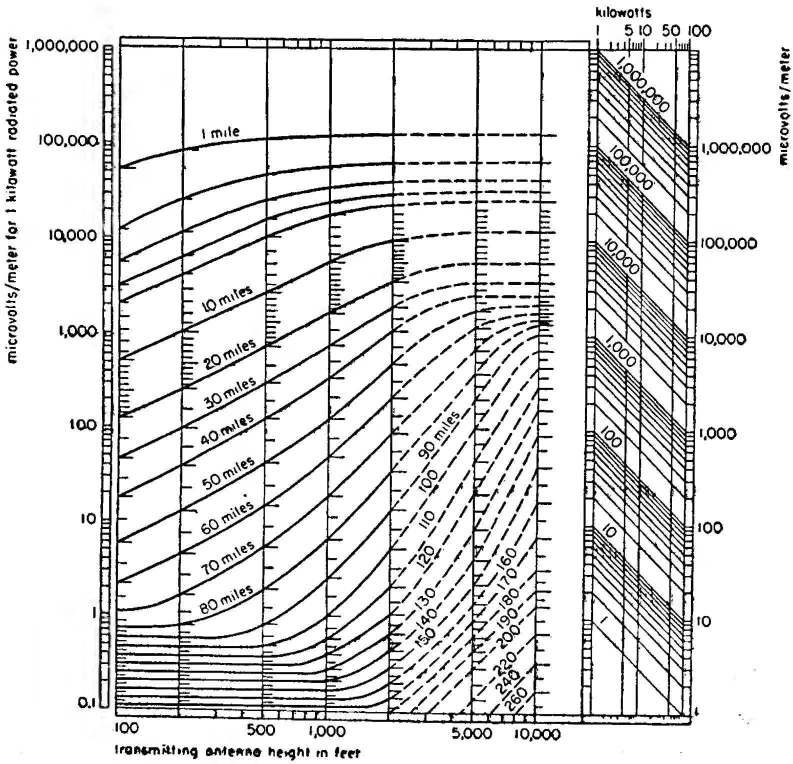

Fig. 13—Ground-wave signal range for television channels 7-13. Conductivity = 5 × 10^{-14} emu, and dielectric constant = 15. Receiving-antenna height = 30 feet. For horizontal (and approximately for vertical) polarization.

Television broadcasting *continued*

Over-all station performance requirements

F.C.C. television standards are

Channel width: 6 megacycles/second.

Picture carrier location: 1.25 megacycles above lower boundary of the channel.

Aural center frequency: 4.5 megacycles above visual carrier.

Polarization of radiation: Horizontal.

Modulation: Amplitude-modulated composite picture and synchronizing signal on visual carrier, together with frequency-modulated audio signal on aural carrier shall be included in a single television channel (Figs. 14 and 15).

Fig. 14—Radio-frequency amplitude characteristic of television picture transmission. Field intensity at points A shall not exceed 20 decibels below picture carrier. Drawing not to scale.

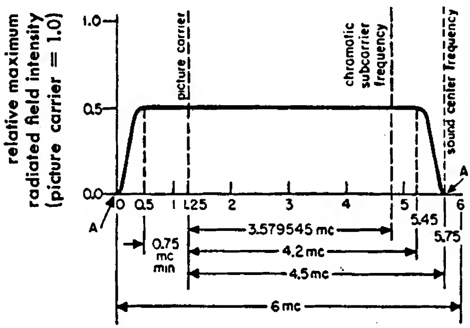

channel frequency spectrum in megacycles referred to lower frequency limit of channel

Visual transmission requirements

Modulation: Amplitude modulation.

Polarization: Horizontal.

Polarity of transmission: Negative—a decrease in initial light intensity causes an increase in radiated power.

Transmitter brightness response: For monochrome transmission, radio-frequency output varies in an inverse logarithmic relation to the brightness of the scene.

Aural-transmitter power: Maximum radiated power is 70 percent (minimum, 50 percent) of peak visual-transmitter power.

Television broadcasting *continued*

Scanning lines: 525 lines/frame interlaced two to one.

Scanning sequence: Horizontal from left to right, vertically from top to bottom.

Horizontal scanning frequency: 15,750 for monochrome or 2/455 times chrominance subcarrier frequency (15,734.264 $\pm$0.044 cycles/second).

Vertical scanning frequency: 60 cycles/second for monochrome or 2/525 times the horizontal scanning frequency (59.94 cycles/second) for color.

Aspect ratio: 4 units horizontal, 3 units vertical.

Chrominance subcarrier frequency: 3.579545 megacycles $\pm$10 cycles/second.

Reference black level: Black level is separated from the blanking level by 7.5 $\pm$2.5 percent of the video range from blanking level to reference white level.

Reference white level: Luminance signal of reference white is 12.5 $\pm$2.5 percent of peak carrier.

Peak-to-peak variation: Total permissible peak-to-peak variation in one frame due to all causes is less than 5 percent.

Color signal: The equation of the complete color signal is:

$$E_M = E_Y' + E_Q' \sin (\omega t + 33°) + E_I' \cos (\omega t + 33°)$$

where

$$E_Q' = +\,0.41\,(E_B' - E_Y') + 0.48\,(E_R' - E_Y')$$

$$E_I' = -\,0.27\,(E_B' - E_Y') + 0.74\,(E_R' - E_Y')$$

$$E_Y' = +\,0.30E_R' + 0.59E_G' + 0.11E_B'$$

For color-difference frequencies below 500 kilocycles, the signal can be represented by:

$$E_M = E_Y' + \left\{\frac{1}{1.14}\left[\frac{1}{1.78}\,(E_B' - E_Y')\sin \omega t + (E_R' - E_Y')\cos \omega t\right]\right\}$$

The symbols have the following significance:

E_M = total video voltage, corresponding to the scanning of a particular picture element applied to the modulator of the picture transmitter.

Television broadcasting *continued*

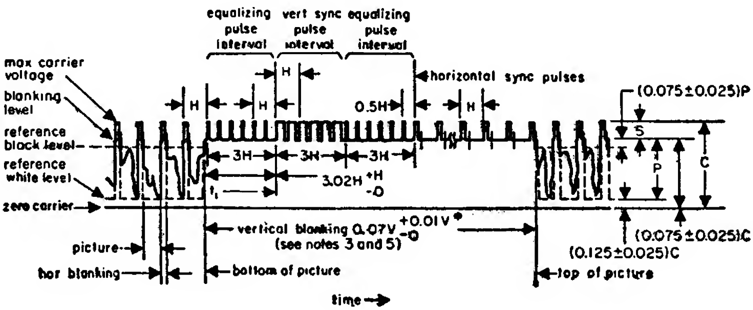

A

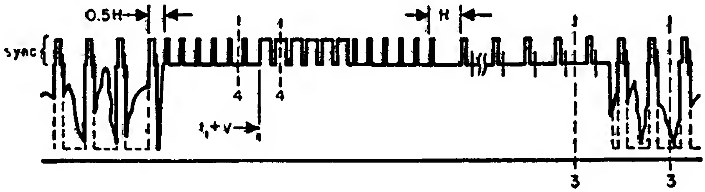

B

Notes:

1. H = time from start of one line to start of next line.
2. V = time from start of one field to start of next field.
3. Leading and trailing edges of vertical blanking should be complete in less than $0.1H$.
4. Leading and trailing shapes of horizontal blanking must be steep enough to preserve minimum and maximum values of $(x + y)$ and z under all conditions of picture content.
5. Dimensions marked with an asterisk indicate that tolerances given are permitted only for long-time variations, and not for successive cycles.
6. Equalizing pulse area shall be between 0.45 and 0.5 of the area of a horizontal synchronizing pulse.
7. Color burst follows each horizontal pulse but is omitted following the equalizing pulses and during the broad vertical pulses.
8. Color bursts to be omitted during monochrome transmission.
9. The burst frequency shall be 3.579545 megacycles. The tolerance on the frequency shall be ±10 cycles with a maximum rate of change of frequency not to exceed 1/10 cycle/second/second.
10. The horizontal scanning frequency shall be 2/455 times the burst frequency.
11. The dimensions specified for the burst determine the times of starting and stopping the burst but not its phase. The color burst consists of amplitude modulation of a continuous sine wave.

Fig. 15—(Above and at right.) Television composite-signal waveform data.

Television broadcasting *continued*

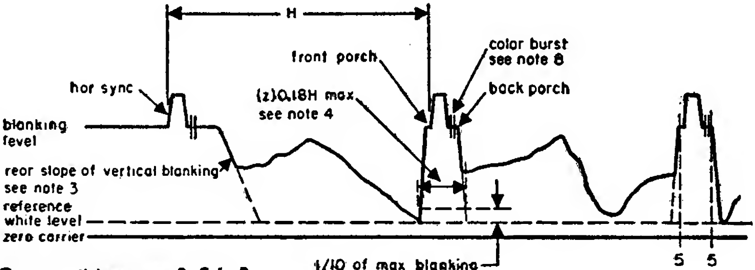

C—Detail between 3–3 in B

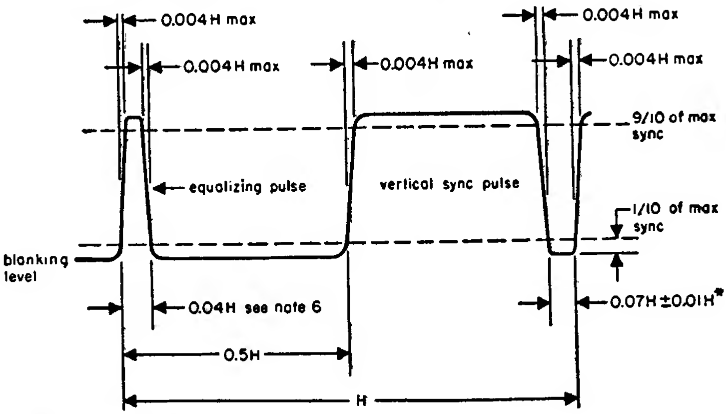

D—Detail between 4–4 in B

12. Dimension *P* represents the peak excursion of the luminance signal from blanking level but does not include the chrominance signal. Dimension *S* is the synchronizing amplitude above blanking level. Dimension C is the peak carrier amplitude.

13. Refer to F.C.C. standards for further explanations and tolerances.

14. Horizontal dimensions not to scale in *A*, *B*, and *C*.

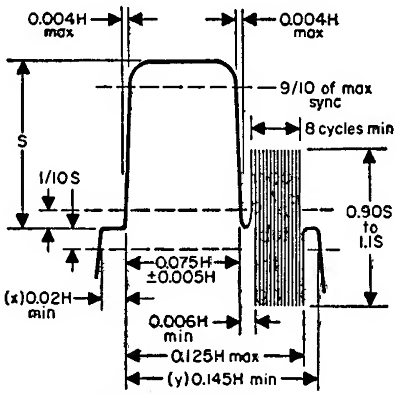

E—Detail between 5–5 in C

Fig. 15 — *continued*

Television broadcasting *continued*

E_Y' = gamma-corrected voltage of the monochrome (black-and-white) portion of the color picture signal, corresponding to the given picture element.

E_Q', E_I' = amplitudes of two orthogonal components of the chrominance signal corresponding respectively to narrow-band and wide-band axes.

E_R', E_G', E_B' = gamma-corrected voltage corresponding to red, green, and blue signals during the scanning of the given picture element.

ω = angular frequency = 2π times frequency of the chrominance subcarrier.

The portion of each expression between brackets represents the chrominance subcarrier signal that carries the chrominance information.

The phase reference in the E_M equation is the phase of the burst $+180°$, as shown in Fig. 16. The burst corresponds to amplitude modulation of a continuous sine wave.

The equivalent bandwidth assigned prior to modulation to the color difference signals E_Q' and E_I' are as follows:

Q-channel bandwidth:

At 400 kilocycles, less than 2 decibels down.
At 500 kilocycles, less than 6 decibels down.
At 600 kilocycles, at least 6 decibels down.

I-channel bandwidth:

At 1.3 megacycles, less than 2 decibels down.

At 3.6 megacycles, at least 20 decibels down.

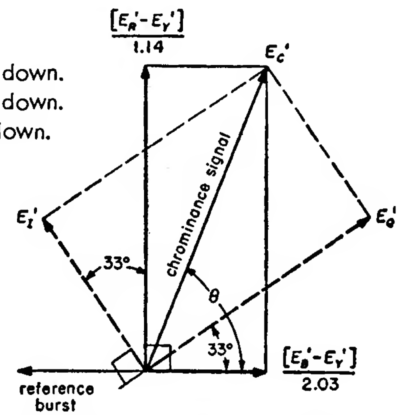

Fig. 16—Above, phases of color signal.

The gamma-corrected voltages E_R', E_G' and E_B' are suitable for a color picture tube having primary colors with the chromaticities listed at the right in the C.I.E. (Commission Internationale de l'Eclairage) system of specification.

color	x	y
Red (*R*)	0.61	0.33
Green (*G*)	0.21	0.71
Blue (*B*)	0.14	0.08

and having a transfer gradient (gamma exponent) of 2.2 associated with each primary color. The voltages E_R', E_G', and E_B' may be respectively of

Television broadcasting *continued*

the form $E_R^{1/2}$, $E_G^{1/2}$, and $E_B^{1/2}$, although other forms may be used with advances in the state of the art.

The radiated chrominance subcarrier vanishes on the reference white of the scene. The numerical values of the signal specification assume that this condition will be produced as C.I.E. Illuminant C ($x = 0.310$, $y = 0.316$).

E_Y', E_Q', E_I', and the components of these signals shall match each other in time to 0.05 microseconds.

The angles of the subcarrier measured with respect to the burst phase, when reproducing saturated primaries and their complements at 75 percent of full amplitude shall be within ± 10 degrees and their amplitudes within ±20 percent of the values specified above. The ratios of the measured amplitudes of the subcarrier to the luminance signal for the same saturated primaries and their complements must fall between the limits of 0.8 and 1.2 of the values specified for their ratios.

Visual transmitter design

Over-all frequency response: The output measured into the antenna after vestigial-sideband filters shall be within limits of +0 and

− 2 decibels	at 0.5 megacycles
− 2 decibels	at 1.25 megacycles
− 3 decibels	at 2.0 megacycles
− 6 decibels	at 3.0 megacycles
±12 decibels	at 3.5 megacycles

with respect to video amplitude characteristic of Fig. 17.

For color transmission, the following limits apply: +0 and

−2 decibels	at 0.5 megacycles
−2 decibels	at 1.25 megacycles
−2 decibels	from 1.25 to 4.18 megacycles

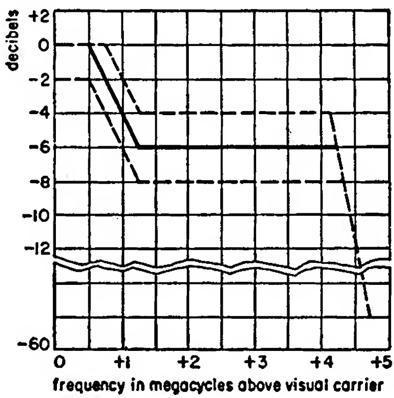

Fig. 17—Ideal demodulated amplitude characteristic of television transmitter. The dashed lines are F.C.C. limits.

This response is with respect to a 200-kilocycle modulating frequency.

Lower-sideband radiation: For modulating frequency of 1.25 megacycles or greater, radiation must be 20 decibels below carrier level. In addition, the

Television broadcasting *continued*

radiation of the lower sideband due to modulation by the color subcarrier (3.579545 megacycles) must be attenuated by a minimum of 42 decibels. For monochrome and color, the field strength of the upper sideband for a modulating frequency of 4.75 megacycles or greater shall be attenuated at least 20 decibels.

Spurious and harmonic emission: All emissions removed in frequency in excess of 3 megacycles above or below the respective channel edge shall be attenuated by no less than 60 decibels below visual-transmitter power.

Envelope delay: The modulated radiated signal shall have an envelope delay relative to the average envelope delay between 0.05 and 0.2 megacycle of zero microseconds up to a frequency of 3.0 megacycles; and then linearly decreasing to 4.18 megacycles to 0.17 microsecond at 3.58 megacycles. The tolerance on the envelope delay is ±0.05 microsecond at 3.58 megacycles and linearly increasing to ±0.1 microsecond down to 2.1 megacycles and up to 4.18 megacycles; and remain at ±0.1 microsecond down to 0.2 megacycles. See Fig. 18.

Radiated radio-frequency-signal envelope: Specified by Fig. 15 as modified by vestigial operation characteristic of Fig. 14.

Horizontal pulse-timing variations: Variation of time interval between successive pulse leading edges to be less than 0.5 percent of average interval.

Horizontal pulse-repetition stability: Rate of change of leading-edge recurrence frequency shall not exceed 0.15 percent/second.

Aural transmitter

Modulation: Frequency modulation with 100-percent swing of ±25 kilocycles. Required maximum swing = ±40 kilocycles.

Audio-frequency response: 50 to 15,000 cycles within limits and utilizing pre-emphasis as shown in Fig. 7.

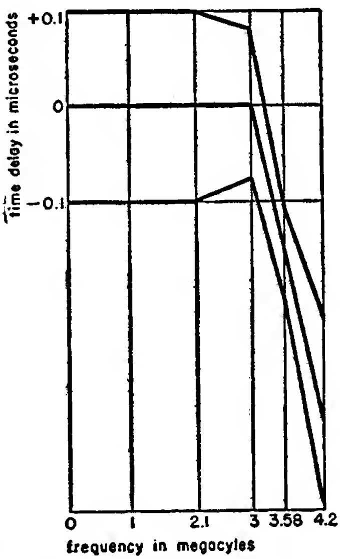

Fig. 18—Envelope delay curve for television transmitter.

Television broadcasting *continued*

Audio-frequency distortion: Maximum combined harmonic root-mean-square output voltage shall be less than

modulating frequency in cycles/second	percent harmonic
50– 100	3.5
100– 7500	2.5
7500–15000	3.0

Noise

FM—55 decibels below 100-percent swing.
AM—50 decibels below level corresponding to 100-percent modulation.

Radar fundamentals

General*

A simplified diagram of a set for radio direction and range finding is shown in Fig. 1. A pulsed high-power transmitter emits centimeter waves for approximately a microsecond through a highly directive antenna to

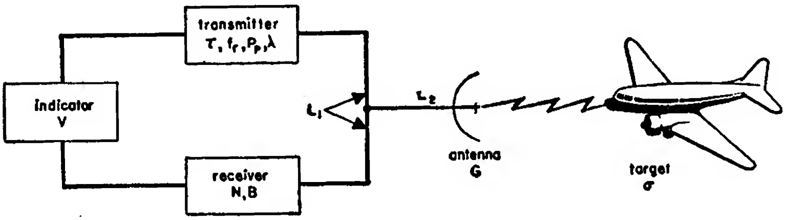

Fig. 1—Simplified diagram of a radar set.

illuminate the target. The returned echo is picked up by the same antenna, amplified by a high-gain wide-band receiver, and displayed on an indicator. Direction of a target is usually indicated by noting the direction of the narrow-beam antenna at the time the echo is received. The range is measured in terms of time because the radar pulse travels with the speed of light, 300 meters one way per microsecond, or approximately 10 microseconds per round-trip radar mile. Fig. 2 gives the range corresponding to a known echo time.

The factors characterizing the operation of each component are shown in Fig. 1. These are discussed below in turn and combined into the free-space range equation. The propagation factors modifying free-space range are presented.

Transmitter

Important transmitter factors are:

τ = pulse length in microseconds

f_r = pulse rate in cycles/second

d = duty ratio = $\tau f_r \times 10^{-6} = P_a/P_p$

P_a = average power in kilowatts

P_p = peak power in kilowatts

λ = carrier wavelength in centimeters

* "IRE Standards on Radio Aids to Navigation: Definitions of Terms, 1954," *Proceedings of the IRE*, vol. 43, pp. 189–209; February, 1955.

Transmitter *continued*

Pulse length is generally about one microsecond. A longer pulse may be used for greater range, if the oscillator power capacity permits. On the other hand, if a range resolution of ΔR feet is required, the pulse cannot be longer than $\Delta R/500$ microseconds.

The repetition frequency must be low enough to permit the desired maximum unambiguous range ($f_r < 90{,}000/R_u$). This is the range beyond which the echo returns after the next transmitter pulse and thus may be mistaken for a short-range echo of the next cycle. If this range is small, oscillator maximum average power may impose an upper limit.

The peak power required may be computed from the range equation (see below) after determination or assumption of the remaining factors. Peak and average power may be interconverted by use of Fig. 3. Pulse energy is $P_p\tau \times 10^{-3}$ joules.

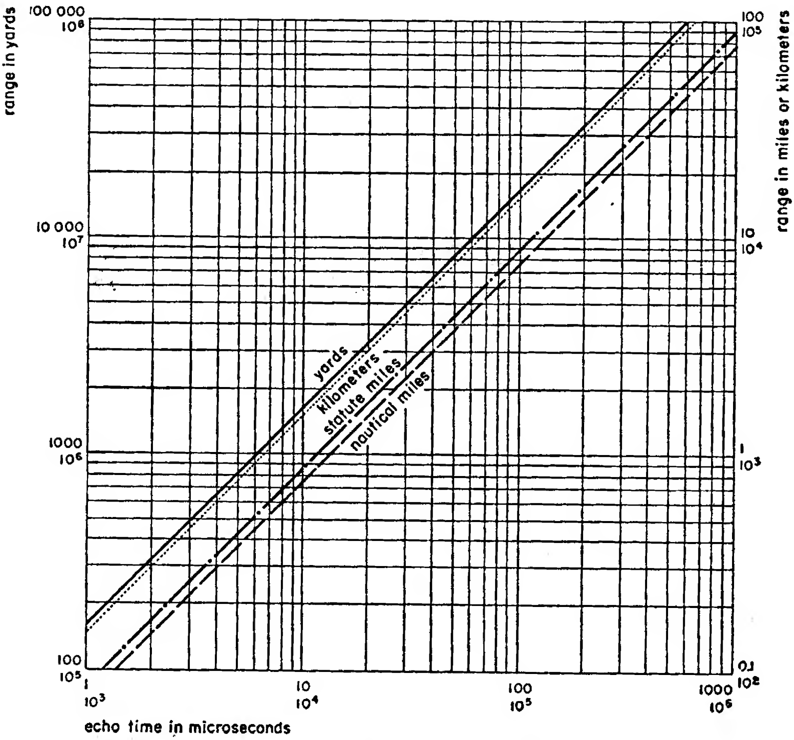

Fig. 2—Time between transmission and reception of a reflected signal.

Transmitter *continued*

The choice of carrier frequency is a complex one, often determined by available oscillators, antenna size, and propagation considerations. Frequency–wavelength conversions are facilitated by Fig. 4, which also defines the band nomenclature.

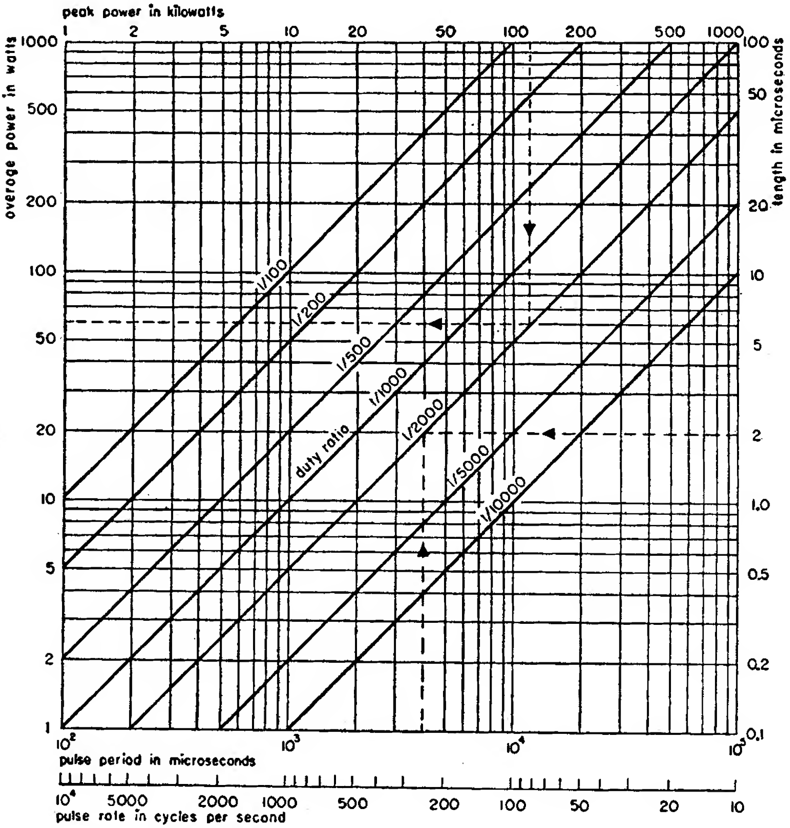

Fig. 3—Power-time relationships.

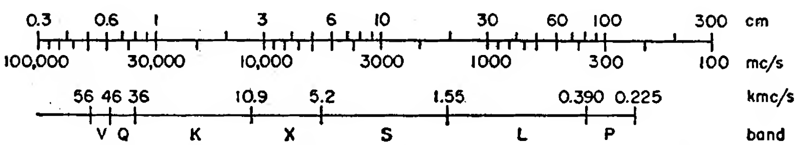

Fig. 4—Correlation between frequency, wavelength, and band nomenclature for radar.

Antenna

The beam width in radians of any antenna is approximately the reciprocal of its dimension in the plane of interest expressed in wavelength units. Beam width may be found readily from Fig. 5, which also shows gain of a paraboloid of revolution. The angular accuracy and resolution of a radar are roughly equal to the beam width; thus precision radars require high frequencies to avoid excessively cumbersome antennas.

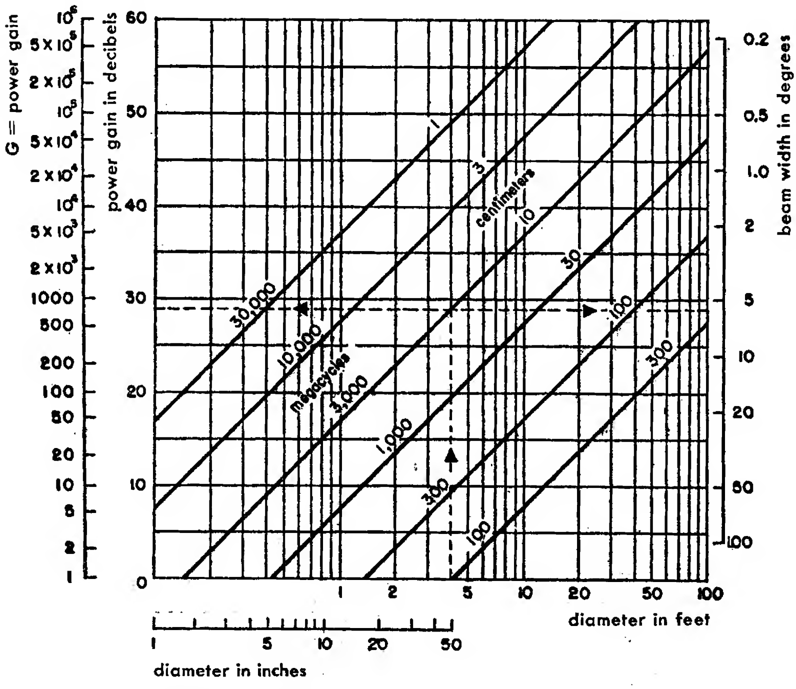

Fig. 5—Beam width and gain of a parabolic reflector.

Target echoing area

The radar cross section σ is defined as 4π times the ratio of the power per unit solid angle scattered back toward the transmitter, to the power per unit area striking the target. For large complex structures and short wavelengths, the values vary rapidly with aspect angle. The effective areas of several important configurations are listed in the following table.*

*L. N. Ridenour, "Radar System Engineering," v. 1, Radiation Laboratory Series, McGraw-Hill Book Company, New York, New York; 1947. See pp. 64–68, 78, 80.

Target echoing area *continued*

reflector	cross section $= \sigma$
Tuned $\lambda/2$ dipole	$0.22\lambda^2$
Small sphere with radius $= a$, where $a/\lambda < 0.15$	$9\pi a^2 (2\pi a/\lambda)^4$
Large sphere with radius $= a$, where $a/\lambda > 1$	πa^2
Corner reflector with one edge $= a$ (maximum)	$4\pi a^4/3\lambda^2$
Flat plate with area $= A$ (normal incidence)	$4\pi A^2/\lambda^2$
Cylinder with radius $= a$, length $= L$ (normal incidence)	$2\pi L^2 a/\lambda$
Small airplane (AT-11)	200 feet^2
Large airplane (B-17)	800 feet^2
Small cargo ship	1,500 feet^2
Large cargo ship	160,000 feet^2

Receiver

The receiver is characterized by an overall noise figure N, defined as the ratio of carrier power available from the antenna to theoretical noise

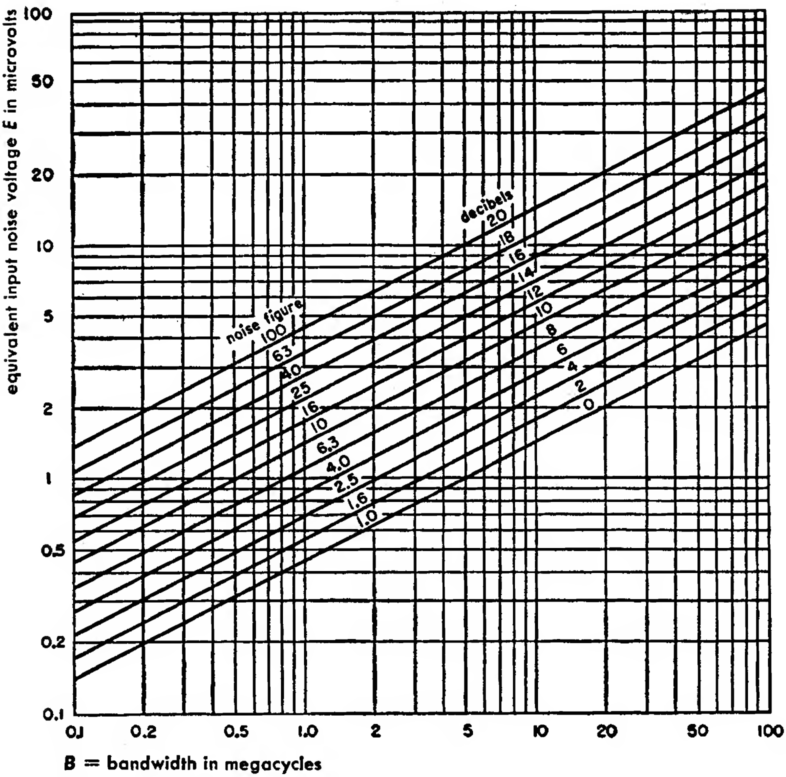

Fig. 6—Noise figure of a receiver of given bandwidth.

Receiver *continued*

power KTb, when the mean noise power and the carrier power are equal.* This equality must be observed at some stage in the receiver where both have been amplified so highly as to override completely any noise introduced by succeeding stages. $KT = 4.1 \times 10^{-21}$, and b = receiver bandwidth in cycles/second. The bandwidth in megacycles should be $1.2/\tau$, plus an allowance for frequency drift, thus usually about $2/\tau$. Fig. 6 enables the determination of the noise figure of a receiver operating from any source impedance, Z_g ohms. E is one-half the open-circuit voltage of a fifty-ohm source, adjusted for receiver output carrier-plus-noise 3 decibels above noise alone.

Thus, if the generator is calibrated for microvolts into Z_g ohms, use $\sqrt{50/Z_g}$ times the indicated voltage. If it is calibrated for voltage into an open circuit, multiply by $\frac{1}{2}\sqrt{50/Z_g}$, but add series resistance to make source $= Z_g$ ohms, for which the receiver input is designed.

Indicator

The many types of radar indicators are shown in Fig. 7. Type A is the first type used, and the best example of a deflection-modulated display. The PPI is the most common intensity-modulated type. For the purpose of determining maximum radar range, an indicator is characterized by a visibility factor V, defined† as follows:

$$V = \tau P_{\min} \times 10^{-6}/NKT$$

where $P_{\min}$ is the receiver input-signal power in watts for a 50-percent probability of detection.

For an A-scope presentation, V may be found from Fig. 8, where τ is in microseconds, and B is in megacycles. The values are conservative, but the effects of changing τB and f_r are shown correctly.

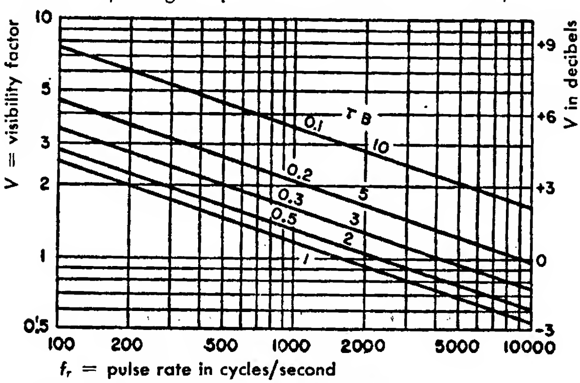

Fig. 8—Visibility factor for an A scope.

*Receiver noise figures are more completely discussed in the chapter "Radio noise and interference," p. 768–770.

† K. A. Norton, and A. C. Omberg, "The Maximum Range of a Radar Set," *Proceedings of the I.R.E.*, v. 35, pp. 4–24; January, 1947: p. 6.

type A

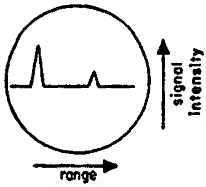

type B

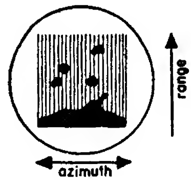

type C

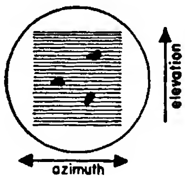

type D

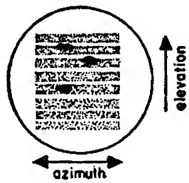

Coarse range information provided by position of signal in broad azimuthal trace. (Used in a prototype airborne interception set now obsolete.)

type E

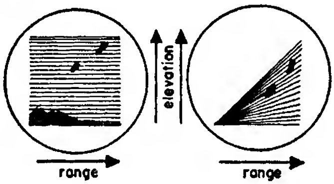

type F

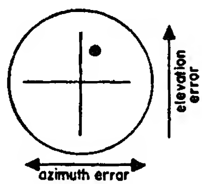

Single signal only. In the absence of a signal, the spot may be made to expand into a circle

type G

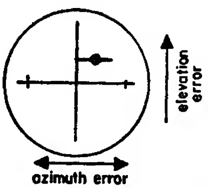

Single signal only. Signal appears as "wingspot," position giving azimuth and elevation errors. Length of wings inversely proportional to range

Fig. 7—Types of radar indicators are given on this and the facing page.

Courtesy of McGraw-Hill Book Company

type H

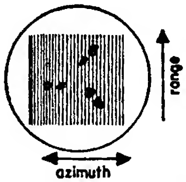

Signal appears as two dots. Left dot gives range and azimuth of target. Relative position of right dot gives rough indication of elevation

type I

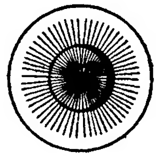

Antenna scan is conical. Signal is a circle, the radius proportional to range. Brightest part indicates direction from axis of cone to target

type J

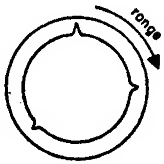

Same as type A, except time base is circular, and signals appear as radial pips

type K

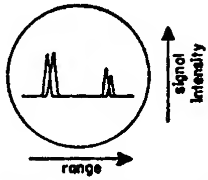

Type A with lobe-switching antenna. Spread voltage splits signals from two lobes. When pips are of equal size, antenna is on target

type L

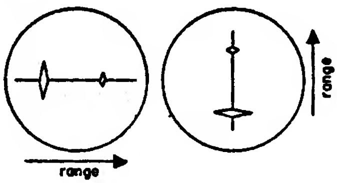

Same as type K, but signals from two lobes are placed back to back

type M

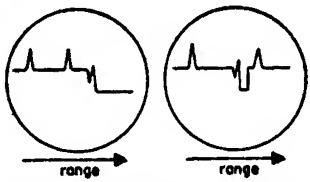

Type A with range step or range notch. When pip is aligned with step or notch, range can be read from dial or counter

type N

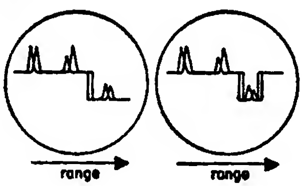

A combination of type K and type M

type P (PPI)

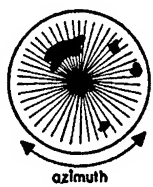

Range is measured radially from center

Range equation

The theoretical maximum free-space range of a radar using an isotropic common receiving and transmitting antenna, lossless transmission line, and a perfect receiver, may be found as follows:

Transmitted pulse energy $= P'$ (in peak watts) $\times\ \tau'$ (in seconds)

Energy incident on target $= P'\tau'/4\pi R^2$ per unit area

Energy returned to antenna $= P'\tau'\sigma/(4\pi R^2)^2$ per unit area

Energy at receiver input $= P'\tau'\sigma\lambda^2/(4\pi)^3R^4$

where σ, λ, and R are in the same units.

Receiver input-noise energy $= KT = 4.11 \times 10^{-21}$ joules. Assuming that the receiver adds no noise, and that the signal is visible on the indicator when signal and noise energies are equal, the maximum range is found to be

$$R^4 = \frac{P'\tau'\sigma\lambda^2}{(4\pi)^3KT}$$

The free-space range of an actual radar will be modified by several dimensionless factors, primarily antenna gain G, receiver noise figure N, and indicator visibility factor V, as discussed above.

Additional minor losses may be lumped under factors L_1 and L_2, one-way and two-way loss factors, respectively. L_1 includes losses in transmission lines running from the tr switch to both transmitter and receiver, as well as tr loss, usually about 1 decibel. L_2 includes loss of the transmission line between tr box and antenna, and atmospheric absorption.

The range equation, including these factors, and using convenient units, is

$$R_m = 0.1146\ \sqrt[4]{P_p\tau\sigma\lambda^2G^2L_1L_2^2/VN}$$

where

R_m = maximum free-space range in miles

P_p = peak power in kilowatts

τ = pulse width in microseconds

σ = effective target area in square feet

λ = wavelength in centimeters

The use of this equation is facilitated by use of decibels throughout, since many of the factors are readily found in this form. Thus, to find maximum radar range,

Range equation *continued*

a. From Fig. 9, find $(P_p + \tau + \sigma + \lambda^2)$ in decibels.

b. Add 2 $\times$ (gain in decibels of common antenna).

c. Subtract $(L_1 + 2L_2 + V + N)$ in decibels. Note: V may be negative.

d. From the net result and Fig. 9, find R_m in miles.

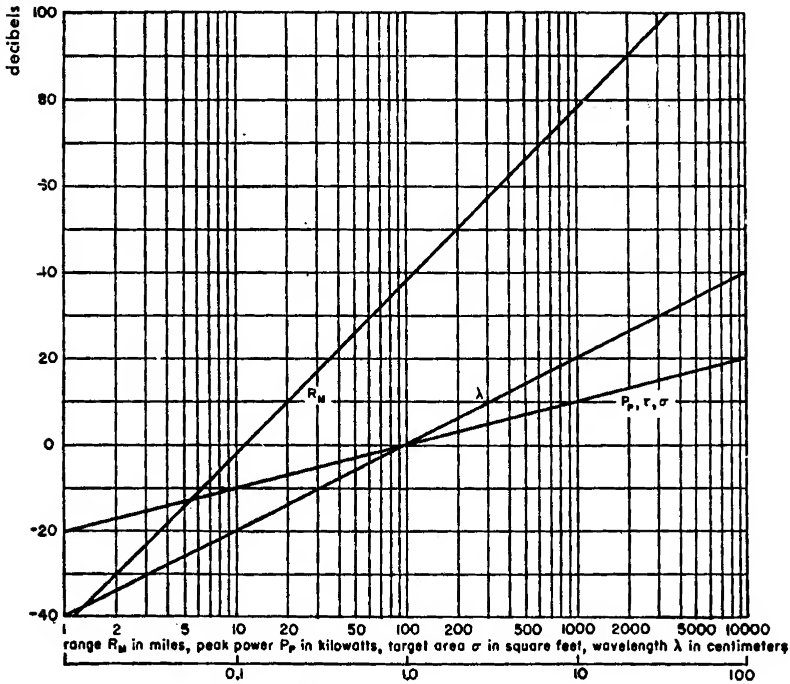

τ = pulse length in microseconds

Fig. 9—The radar range equation.

Reflection lobes

The maximum theoretical free-space range of a radar is often appreciably modified, especially for low-frequency sets, by reflections from the earth's surface. For low angles and a flat earth, the modifying factor is

$$F = 2 \sin \frac{(2\pi h_1 h_2)}{\lambda R}$$

where h_1, h_2, and R are defined in Fig. 10, all in the same units as λ. The result-

Reflection lobes *continued*

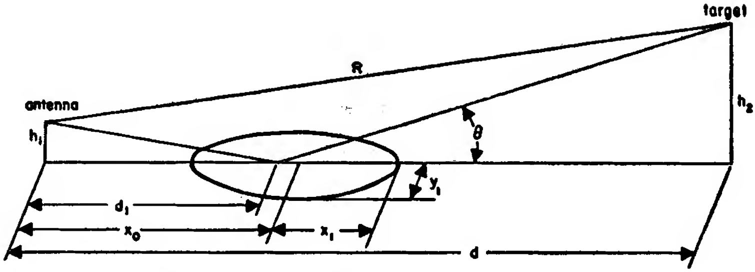

Fig. 10—Radar geometry, showing reflection from flat earth.

ing vertical pattern is shown in Fig. 11 for a typical case. The angles of the maxima of the lobes and the minima, or nulls, may be found from

$$\theta_m = \frac{h_2}{R} = \frac{n\lambda}{4h_1}$$

where

θ_m = angle of maximum in radians, when n = 1, 3, 5 . . . ;

= angle of minimum in radians, when n = 0, 2, 4 . . . .

This expression may be applied to the problem of finding the height of a maximum or null over the curved earth with the following approximate result:

$$H_2 = 44\, n\, \lambda\, D/H_1 + D^2/2$$

where

H = feet
λ = centimeters
D = miles

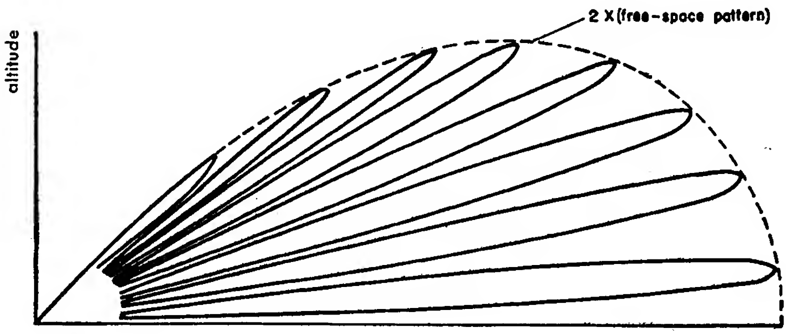

Fig. 11—Vertical-lobe pattern resulting from reflections from earth.

Reflection zone

The reflection from the ground occurs not at a point, but over an elliptical area, essentially the first Fresnel zone. The center of the ellipse and its dimensions may be found from

$x_0 = d_1(1 + 2a)$

$x_1 = 2d_1\sqrt{a(1 + a)}$

$y_1 = 2h_1\sqrt{a(1 + a)}$

where x_0, x_1, y_1, d, are shown in Fig. 10, and

$d_1 = h_1 d/h_2 = h_1/\sin\theta$

$a = \lambda/4h_1 \sin\theta$

In the maximum of the first lobe, $a = 1$, and the distances to the nearest and farthest points are

$x_0 - x_1 = 0.7h_1^2/\lambda$

$x_0 + x_1 = 23.3h_1^2/\lambda$

$y_1 = 2\sqrt{2}\,h_1$

These dimensions determine the extent of flat ground required to double the free-space range of a radar as above. The height limit of any large irregularity in the area is $h_1/4$. If the same area is available on a sloping site of angle ϕ, double range may be obtained on a target on the horizon. In this case

$x_0 + x_1 = 1.46\lambda/\sin^2\phi$

Continuous-wave Doppler radar

Echoes from stationary objects confuse or mask those from aircraft, especially on *ppi* scopes. This effect may be minimized by use of short pulses, narrow beams, and several circuit modifications, but it is still intolerable in many situations such as ground control of approach and aircraft detection. Discrimination between fixed and moving targets is possible by use of the Doppler principle.

In its simplest application, a cw transmitter is used and the return energy is detected by mixing with a portion of the transmitter power. Fixed targets produce a constant voltage, whereas a moving target produces an alternating voltage at the Doppler frequency difference between transmitted and received signals,

$$f_d = f_t\frac{c + v}{c - v} - f_t \approx \frac{2v}{c}f_t = 89.4\frac{v}{\lambda}$$

where

f_d = Doppler frequency in cycles/second

Continuous-wave Doppler radar *continued*

f_t = transmitted frequency in cycles/second

v = target radial velocity in miles/hour

c = speed of propagation in miles/hour

λ = transmitted wavelength in centimeters

Each cycle of Doppler frequency corresponds to a target radial motion of one-half transmitted wavelength. Thus, a target moving with a radial velocity of 300 miles/hour = 440 feet/second will move about 880 half-waves per second at 1000 megacycles ($\lambda \approx 1$ foot), resulting in a Doppler frequency of about 880 cycles. Target azimuth may be determined by rotating an antenna beam, but range cannot be found without modulation of the transmitter, so this type of radar is suitable only for measuring radial velocities of targets, and sentry applications to detect presence rather than accurate position of moving targets.

Pulsed Doppler radar—coherence

The straightforward way of obtaining range information is to pulse-modulate the transmitted carrier. If this is done in the simplified manner of Fig. 12, the received pulses will be small segments of the cw returns discussed above, as shown in Fig. 13. A fixed target produces uniform pulses, whereas moving-target pulses vary in amplitude periodically. An A-scope with one fixed and one moving target will appear as indicated. The basic cause of this distinction is phase coherence; that is, each time a fixed target echo returns, it is mixed with a voltage that has gone through the same difference in phase since the instant of transmission.

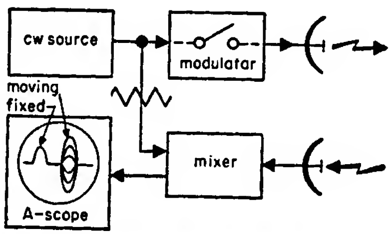

Fig. 12—Simple pulsed Doppler radar.

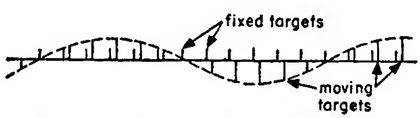

Fig. 13—Pulsed Doppler radar video signal.

To produce this same essential coherence in an actual radar using a magnetron, some complexity is required as in the upper circuits of Fig. 14. Here there is an extremely stable local oscillator, the stalo, that provides a relatively fixed reference, pulse after pulse, and a coherent oscillator, the coho, operating at if frequency, capable of being started in a phase related to each transmission and providing a coherent reference in the interval from pulse to pulse. It can be seen that at Doppler frequencies that are multiples of the repetition rate, the

Pulsed Doppler radar—coherence *continued*

resulting pulses will be of constant amplitude, so these are said to be produced by targets at

$$(\text{blind speeds}) = n\lambda f_r/89.4$$

Moving-target-indicator radar

Cancellation

To provide moving-target indication (mti) on a ppi-scope, the constant-amplitude fixed-target pulses must be cancelled by subtraction of successive pulse trains. A typical cancellation-circuit block diagram is shown in the lower part of Fig. 14. The delay element is an ultrasonic transmission line,

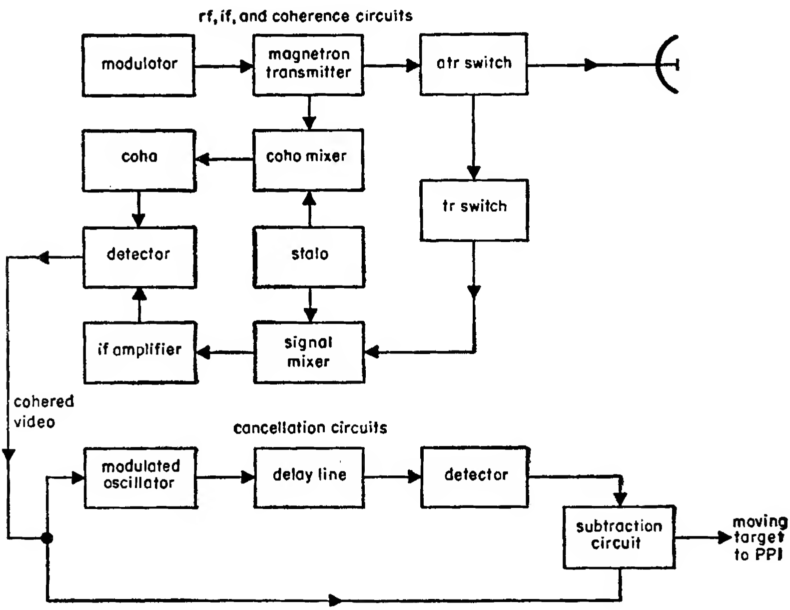

Fig. 14—Moving-target-indicator radar.

either mercury or quartz. These operate best in the region of 10 to 30 megacycles, so a carrier wave in this range is modulated by the video input.

Moving-target-indicator radar *continued*

After delay, the signal is detected, amplified, and subtracted from the next pulse train. Obviously, the delay must be $1/f_r$. For the mercury line, the length in inches determines the delay in microseconds,

$$D = L\,(17.42 + 0.0052T)$$

where T is centigrade temperature. For quartz, the length (with no reflections) is determined from

$$D = 4.84\,L$$

Limitations

There are three major limitations on the subclutter visibility (ratio of fixed target that can be cancelled to just-visible moving target).

Variation of fixed targets: Buildings and mountains do not vary, but vegetation and sea-echo fluctuations are a function of wind velocity. In low winds, cancellation of 50 db may be expected.

Antenna rotation: Antenna rotation modulates the fixed targets so that the visibility cannot be better than approximately

$$V_{sc} = 10^4\theta/r_{\max}\omega$$

where

V_{sc} = subclutter visibility (ratio)

θ = antenna horizontal beamwidth in degrees

$r_{\max}$ = range of farthest clutter in miles

ω = rotational rate in revolutions/minute

Thus for a beamwidth of one degree, maximum clutter range of 100 miles, and one antenna revolution per minute, V_{sc} is 100 or 40 db.

Equipment instabilities: The above limitations on maximum visibility must often be accepted as given. Then it is necessary to provide corresponding equipment stability, but there is no point in setting stability limits that would give performance exceeding the above two practical considerations. Permissible stalo and coho drift rated in kc/sec^2 are given by

$$df/dt = 20f_r/V_{sc}\,r_{\max}$$

Moving-target-indicator radar *continued*

The coho mistuning should not be greater than $1/4\tau$ megacycle where τ is pulse length in microseconds. Proper operation of the cancellation equipment requires an amplitude unbalance between the two channels of less than $100/V_{sc}$ percent. Likewise, temporal unbalance between delay time and pulse interval must not exceed $50/V_{sc}$ percent of the interval. These figures are usually achieved and maintained by automatic balance controls.

■ Wire transmission

Telephone transmission-line data

Line constants of copper open-wire pairs

8- and 12-inch spacing

Insulators:
 40 pairs toll and double-petticoat (DP) per mile
 53 pairs Pyrex glass (CS) per mile

Temperature 68° fahrenheit

freq in kc/s	resistance in ohms/loop mile						inductance in millihenries/loop mile					
	165 mil		128 mil		104 mil		165 mil		128 mil		104 mil	
	12″ DP	8″ CS	12″ DP	8″ CS	12″ DP	8″ CS	12″ DP	8″ CS	12″ DP	8″ CS	12″ DP	8″ CS
0.1	4.10	4.10	6.82	6.82	10.33	10.33	3.37	3.11	3.53	3.27	3.66	3.40
0.5	4.13	4.13	6.83	6.83	10.34	10.34	3.37	3.10	3.53	3.27	3.66	3.40
1.0	4.19	4.19	6.87	6.87	10.36	10.36	3.37	3.10	3.53	3.27	3.66	3.40
1.5	4.29	4.29	6.94	6.94	10.41	10.41	3.37	3.10	3.53	3.26	3.66	3.40
2.0	4.42	4.42	7.02	7.02	10.47	10.47	3.36	3.10	3.53	3.26	3.66	3.40
3.0	4.76	4.76	7.24	7.24	10.62	10.62	3.35	3.09	3.52	3.26	3.66	3.40
5.0	5.61	5.61	7.92	7.92	11.11	11.11	3.34	3.08	3.52	3.25	3.66	3.40
10	7.56	7.56	10.05	10.05	12.98	12.98	3.31	3.04	3.49	3.23	3.64	3.38
20	10.23	10.23	13.63	13.63	17.14	17.14	3.28	3.02	3.46	3.20	3.61	3.35
30	12.26	12.26	16.26	16.26	20.55	20.55	3.26	3.00	3.44	3.17	3.58	3.33
50	15.50	15.50	20.41	20.41	25.67	25.67	3.25	2.99	3.43	3.16	3.57	3.31
100	21.45	21.45	28.09	28.09	35.10	35.10	3.24	2.98	3.42	3.15	3.55	3.29
150	26.03	26.03	33.96	33.96	42.42	42.42	3.23	2.97	3.41	3.14	3.54	3.28
200	29.89	29.89	38.93	38.93	48.43	48.43	3.23	2.97	3.40	3.14	3.54	3.28
500	46.62	46.62	60.53	60.53	74.98	74.98	3.22	2.96	3.39	3.13	3.53	3.27
1000	65.54	65.54	84.84	84.84	104.9	104.9	3.22	2.96	3.38	3.12	3.52	3.26

freq in kc/s	leakage conductance in micromhos/loop mile			
	dry—all gauges		wet—all gauges	
	12″—DP	8″—CS	12″—DP	8″—CS
0.1	0.04	0.04	2.5	2.0
0.5	0.15	0.06	3.0	2.3
1.0	0.29	0.11	3.5	2.6
1.5	0.43	0.15	4.0	2.9
2.0	0.57	0.20	4.5	3.2
3.0	0.85	0.30	5.5	3.7
5.0	1.4	0.49	7.5	4.6
10	2.8	0.97	12.1	6.6
20	5.6	1.9	20.5	9.6
30	8.4	2.9	28.0	12.1
50	14.0	4.8	41.1	15.7

wire size	capacitance in microfarads/loop mile	
	12″	8″
In space		
165 mil	0.00898	0.00978
128 mil	0.00855	0.00928
104 mil	0.00822	0.00888
on 40-wire line, dry		
165 mil	0.00915	0.01000
128 mil	0.00871	0.00948
104 mil	0.00857	0.00908
on 40-wire line, wet		
165 mil	0.0093	0.0102
128 mil	0.0089	0.0097
104 mil	0.0085	0.0093

Telephone transmission-line data *continued*

Line constants of 40% Copperweld open-wire pairs

8- and 12-inch spacing

Insulators:
40 pairs toll and double-petticoat (DP) per mile
53 pairs Pyrex glass (CS) per mile

Temperature 68° fahrenheit

freq in kc/s	resistance in ohms/loop mile						inductance in millihenries/loop mile					
	165 mil		128 mil		104 mil		165 mil		128 mil		104 mil	
	12" DP	8" CS	12" DP	8" CS	12" DP	8" CS	12" DP	8" CS	12" DP	8" CS	12" DP	8" CS
0.0	9.8	9.8	16.2	16.2	24.6	24.6	—	—	—	—	—	—
0.1	10.0	10.0	16.3	16.3	24.6	24.6	3.37	3.11	3.53	3.27	3.66	3.40
0.5	10.0	10.0	16.4	16.4	24.7	24.7	3.37	3.10	3.53	3.27	3.66	3.40
1.0	10.1	10.1	16.6	16.6	24.8	24.8	3.37	3.10	3.53	3.27	3.66	3.40
1.5	10.1	10.1	16.7	16.7	24.9	24.9	3.37	3.10	3.53	3.26	3.66	3.40
2.0	10.2	10.2	16.8	16.8	25.2	25.2	3.36	3.10	3.53	3.26	3.66	3.40
3.0	10.4	10.4	17.1	17.1	25.4	25.4	3.35	3.09	3.52	3.26	3.66	3.40
5.0	10.6	10.6	17.4	17.4	26.0	26.0	3.34	3.08	3.52	3.25	3.66	3.40
10	10.8	10.8	17.7	17.7	26.5	26.5	3.31	3.04	3.49	3.23	3.64	3.38
20	11.4	11.4	18.2	18.2	27.1	27.1	3.28	3.02	3.46	3.20	3.61	3.35
30	12.3	12.3	18.8	18.8	27.5	27.5	3.26	3.00	3.44	3.17	3.58	3.33
50	14.5	14.5	20.4	20.4	28.7	28.7	3.25	2.99	3.43	3.16	3.57	3.31
100	20.8	20.8	26.5	26.5	33.3	33.3	3.24	2.98	3.42	3.15	3.55	3.29
150	25.9	25.9	32.5	32.5	39.6	39.6	3.23	2.97	3.41	3.14	3.54	3.28

freq in kc/s	leakage conductance in micromhos/loop mile			
	dry—all gauges		wet—all gauges	
	12"—DP	8"—CS	12"—DP	8"—CS
0.1	0.04	0.04	2.5	2.0
0.5	0.15	0.06	3.0	2.3
1.0	0.29	0.11	3.5	2.6
1.5	0.43	0.15	4.0	2.9
2.0	0.57	0.20	4.5	3.2
3.0	0.85	0.30	5.5	3.7
5.0	1.4	0.49	7.5	4.6
10	2.8	0.97	12.1	6.6
20	5.6	1.9	20.5	9.6
30	8.4	2.9	28.0	12.1
50	14.0	4.8	41.1	15.7

wire size	capacitance in microfarads/loop mile	
	12"	8"
in space		
165 mil	0.00898	0.00978
128 mil	0.00855	0.00928
104 mil	0.00822	0.00888
on 40-wire line, dry		
165 mil	0.00915	0.01000
128 mil	0.00871	0.00948
104 mil	0.00857	0.00908
on 40-wire line, wet		
165 mil	0.0093	0.0102
128 mil	0.0089	0.0097
104 mil	0.0085	0.0093

Telephone transmission-line data *continued*

Attenuation of copper open-wire pairs

8- and 12-inch spacing

Insulators:
40 pairs toll and double-petticoat (DP) per mile
53 pairs Pyrex glass (CS) per mile

Temperature 68° fahrenheit

dry weather

freq in kc/s	attenuation in decibels per mile								
	165 mil			128 mil			104 mil		
	12" DP	12" CS	8" CS	12" DP	12" CS	8" CS	12" DP	12" CS	8" CS
0.1	0.023	0.023	0.025	0.032	0.032	0.034	0.041	0.041	0.0425
0.5	0.029	0.029	0.0315	0.045	0.045	0.048	0.063	0.063	0.067
1.0	0.030	0.030	0.0325	0.047	0.047	0.0505	0.067	0.067	0.072
1.5	0.031	0.031	0.0335	0.048	0.048	0.051	0.068	0.068	0.073
2.0	0.0325	0.032	0.035	0.0485	0.048	0.052	0.069	0.069	0.074
3.0	0.036	0.034	0.038	0.051	0.050	0.054	0.071	0.070	0.076
5.0	0.044	0.041	0.0445	0.057	0.055	0.0595	0.076	0.074	0.080
10	0.061	0.056	0.0605	0.076	0.070	0.076	0.093	0.087	0.094
20	0.088	0.076	0.083	0.108	0.096	0.104	0.129	0.116	0.125
30	0.110	0.092	0.100	0.135	0.116	0.125	0.159	0.140	0.151
50	0.148	0.118	0.127	0.179	0.147	0.158	0.209	0.176	0.189
100	—	0.165	0.178	—	0.204	0.220	—	0.244	0.262
150	—	0.203	0.218	—	0.249	0.268	—	0.296	0.317
200	—	0.235	0.25	—	—	—	—	—	—
500	—	—	0.42±	—	—	—	—	—	—
1000	—	—	0.7±	—	—	—	—	—	—

wet weather

freq in kc/s	165 mil 12" DP	165 mil 12" CS	165 mil 8" CS	128 mil 12" DP	128 mil 12" CS	128 mil 8" CS	104 mil 12" DP	104 mil 12" CS	104 mil 8" CS
0.1	0.032	0.029	0.030	0.043	0.039	0.040	0.054	0.049	0.0505
0.5	0.037	0.034	0.036	0.053	0.050	0.053	0.072	0.069	0.0705
1.0	0.039	0.035	0.037	0.056	0.052	0.055	0.076	0.073	0.0775
1.5	0.041	0.037	0.0385	0.058	0.0535	0.0565	0.078	0.0745	0.0795
2.0	0.043	0.038	0.040	0.060	0.0545	0.058	0.0805	0.076	0.0805
3.0	0.0485	0.041	0.044	0.064	0.0575	0.061	0.0845	0.078	0.083
5.0	0.060	0.050	0.0525	0.075	0.0645	0.068	0.094	0.084	0.089
10	0.085	0.068	0.072	0.102	0.083	0.0885	0.120	0.101	0.106
20	0.127	0.095	0.101	0.150	0.116	0.123	0.173	0.137	0.144
30	0.161	0.118	0.124	0.188	0.142	0.150	0.216	0.168	0.176
50	0.220	0.154	0.162	0.253	0.185	0.195	0.287	0.217	0.227
100	—	0.228	0.237	—	0.271	0.283	—	0.313	0.326
150	—	0.288	0.299	—	0.339	0.353	—	0.390	0.405

Telephone transmission-line data *continued*

Attenuation of 40% Copperweld open-wire pairs

8- and 12-inch spacing

Insulators:
40 pairs toll and double-petticoat (DP) per mile
53 pairs Pyrex glass (CS) per mile

Temperature 68° fahrenheit

dry weather

freq in kc/s	attenuation in decibels per mile								
	165 mil			128 mil			104 mil		
	12″ DP	12″ CS	8″ CS	12″ DP	12″ CS	8″ CS	12″ DP	12″ CS	8″ CS
0.2	0.054	0.054	0.057	0.073	0.073	0.077	0.091	0.091	0.096
0.5	0.067	0.067	0.071	0.097	0.097	0.103	0.127	0.127	0.134
1.0	0.073	0.073	0.078	0.112	0.112	0.120	0.152	0.152	0.162
1.5	0.076	0.076	0.082	0.118	0.118	0.127	0.162	0.162	0.174
2.0	0.077	0.077	0.083	0.120	0.120	0.130	0.168	0.168	0.180
3.0	0.079	0.079	0.085	0.124	0.124	0.134	0.174	0.174	0.188
5.0	0.082	0.082	0.088	0.127	0.127	0.138	0.179	0.179	0.195
10	0.085	0.085	0.092	0.131	0.131	0.142	0.186	0.186	0.201
20	0.088	0.088	0.096	0.135	0.135	0.147	0.191	0.191	0.207
30	0.095	0.095	0.103	0.139	0.139	0.152	0.195	0.195	0.211
50	0.110	0.110	0.119	0.150	0.150	0.163	0.206	0.206	0.221
100	0.156	0.156	0.168	0.188	0.188	0.203	0.234	0.234	0.252
150	0.199	0.199	0.214	0.233	0.233	0.251	0.273	0.273	0.293

wet weather

0.2	0.066	0.060	0.063	0.089	0.081	0.084	0.111	0.101	0.105
0.5	0.077	0.072	0.076	0.111	0.104	0.110	0.145	0.136	0.142
1.0	0.083	0.078	0.084	0.126	0.119	0.126	0.168	0.160	0.169
1.5	0.088	0.082	0.087	0.130	0.124	0.133	0.178	0.170	0.181
2.0	0.089	0.083	0.089	0.136	0.128	0.137	0.184	0.176	0.188
3.0	0.093	0.086	0.092	0.140	0.132	0.142	0.192	0.183	0.196
5.0	0.100	0.091	0.097	0.147	0.137	0.148	0.201	0.190	0.205
10	0.111	0.098	0.104	0.159	0.145	0.155	0.214	0.200	0.215
20	0.126	0.107	0.115	0.175	0.155	0.166	0.233	0.212	0.228
30	0.145	0.120	0.127	0.197	0.168	0.177	0.253	0.224	0.238
50	0.184	0.147	0.153	0.230	0.190	0.199	0.288	0.247	0.261
100	0.282	0.219	0.227	0.314	0.254	0.265	0.372	0.303	0.317
150	0.370	0.285	0.295	0.415	0.324	0.336	0.461	0.367	0.382

continued **Telephone transmission-line data**

Characteristics of standard types of aerial copper-wire telephone circuits

1000 cycles per second

DP (double petticoat) insulators for all 12- and 18-inch spaced wires.

CS (special glass with steel pin) insulators for all 8-inch spaced wires.

type of circuit	gauge of wires mils	spacing of wires inches	primary constants per loop mile				propagation constant				line impedance				wavelength miles	velocity miles per second	attenuation db per mile
							polar		rectangular		polar		rectangular				
			R ohms	L henries	C μf	G μmho	magnitude	angle deg +	α	β	magnitude	angle deg −	R ohms	X ohms −			
Non-pole pair phys	165	8	4.11	.00311	.01000	.11	.0353	83.99	.00370	.0351	565	5.88	562	58	179.0	179,000	.0325
Non-pole pair side	165	12	4.11	.00337	.00915	.29	.0352	84.36	.00346	.0350	612	5.35	610	57	179.5	179,500	.030
Pole pair side	165	18	4.11	.00364	.00863	.29	.0355	84.75	.00325	.0353	653	5.00	651	57	178.0	178,000	.028
Non-pole pair phan	165	12	2.06	.00208	.01514	.58	.0355	85.34	.00288	.0354	373	4.30	372	28	177.5	177,500	.025
Non-pole pair phys	128	8	6.74	.00327	.00948	.11	.0358	80.85	.00569	.0353	603	8.97	596	94	178.0	178,000	.0505
Non-pole pair side	128	12	6.74	.00353	.00871	.29	.0356	81.39	.00533	.0352	650	8.32	643	94	178.5	178,500	.047
Pole pair side	128	18	6.74	.00380	.00825	.29	.0358	81.95	.00502	.0355	693	7.72	686	93	177.0	177,000	.044
Non-pole pair phan	128	12	3.37	.00216	.01454	.58	.0357	82.84	.00445	.0355	401	6.73	398	47	177.0	177,000	.039
Non-pole pair phys	104	8	10.15	.00340	.00908	.11	.0367	77.22	.00811	.0358	644	12.63	629	141	175.5	175,500	.072
Non-pole pair side	104	12	10.15	.00366	.00837	.29	.0363	77.93	.00760	.0355	692	11.75	677	141	177.0	177,000	.067
Pole pair side	104	18	10.15	.00393	.00797	.29	.0365	78.66	.00718	.0358	730	10.97	717	139	175.5	175,500	.063
Non-pole pair phan	104	12	5.08	.00223	.01409	.58	.0363	79.84	.00640	.0357	421	9.70	415	71	176.0	176,000	.056

Notes: 1. All values are for dry-weather conditions.
2. All capacitance values assume a line carrying 40 wires.
3. Resistance values are for temperature of 20° C (68° F).

continued **Telephone transmission-line data**

Representative values of toll-cable line and propagation constants

13, 16, and 19 AWG quadded toll cable
Nonloaded
All figures for loop-mile basis
Temperature 55° fahrenheit

freq in kc/s	resistance ohms/mile			inductance millihenries/mile			conductance micromhos/mile			capacitance μf/mile	characteristic impedance ohms			phase shift radians/mile			attenuation decibels/mile		
	13	16	19	13	16	19	13	16	19	13, 16, or 19	13	16	19	13	16	19	13	16	19
0	20.7	41.8	83.8	1.070	1.100	1.112	—	—	—	0.0610	—	—	—	—	—	—	—	—	—
0.1	20.7	41.8	83.8	1.069	1.100	1.112	0.40	0.25	0.10	0.0610	530–j505	745–j730	1050–j1040	0.020	0.027	0.040	0.17	0.24	0.35
0.5	20.7	41.9	83.9	1.065	1.099	1.112	1.4	0.75	0.40	0.0609	250–j210	345–j315	480– j460	0.050	0.064	0.092	0.36	0.51	0.77
1.0	20.8	42.0	84.0	1.060	1.098	1.111	2.5	1.5	1.0	0.0609	195–j140	255–j215	345– j319	0.075	0.092	0.133	0.47	0.69	1.06
1.5	20.9	42.1	84.1	1.057	1.097	1.111	3.5	2.0	1.6	0.0608	170–j105	225–j175	290– j255	0.100	0.116	0.17	0.53	0.79	1.27
2.0	21.0	42.2	84.2	1.053	1.096	1.110	4.5	2.65	2.35	0.0608	160– j85	205–j150	255– j215	0.120	0.140	0.20	0.58	0.87	1.44
3.0	21.3	42.4	84.3	1.046	1.095	1.110	6.5	4.15	4.05	0.0607	145– j63	180–j115	217– j170	0.170	0.189	0.25	0.63	1.00	1.68
5.0	22.0	43.0	84.5	1.035	1.093	1.109	10.5	7.6	8.0	0.0606	135– j42	155– j72	182– j120	0.26	0.28	0.35	0.70	1.16	2.03
10	24.0	44.5	85.3	1.007	1.085	1.105	21.0	18.5	20.0	0.0605	131– j23	142– j40	155– j73	0.50	0.52	0.59	0.80	1.32	2.43
20	29.1	49.5	89.0	0.968	1.066	1.095	47.0	46.2	50.0	0.0604	128– j15	137– j25	141– j41	0.97	1.00	1.07	1.04	1.55	2.77
30	35.5	55.4	94.0	0.945	1.047	1.085	78.0	80.5	87.5	0.0602	126– j12	135– j18	137– j30	1.43	1.48	1.57	1.27	1.78	3.02
50	47.5	67.0	105.5	0.910	1.015	1.065	150.	160.	180.	0.0600	124– j10	133– j13	134– j20	2.34	2.42	2.60	1.75	2.24	3.53
100	71.3	91.7	137.0	0.870	0.963	1.017	350.	400.	450.	0.0598	121– j7.3	130– j9	131– j13	4.54	4.71	5.00	2.72	3.31	4.80
150	90.0	111.2	165.0	0.850	0.935	0.980	600.	700.	800.	0.0595	119– j6.0	127– j7	129– j11	6.73	6.94	7.25	3.60	4.27	6.00
200	—	—	—	—	—	—	—	—	—	—	—	—	—	—	—	—	—	—	7.00
500	—	—	—	—	—	—	—	—	—	—	—	—	—	—	—	—	—	—	12±
1000	—	—	—	—	—	—	—	—	—	—	—	—	—	—	—	—	—	—	18±
For 0° F:																			
Increase by	—	—	—	—	—	—	50%	50%	50%	—	—	—	—	—	—	—	—	—	—
Decrease by	9%	9%	9%	0.5%	0.5%	0.5%	—	—	—	2%	—	—	—	2%	2%	2%	9%	9%	9%
For 110° F:																			
Increase by	8%	8%	8%	0.4%	0.4%	0.4%	—	—	—	2%	—	—	—	2%	2%	2%	9%	9%	9%
Decrease by	—	—	—	—	—	—	50%	50%	50%	—	—	—	—	—	—	—	—	—	—

Approximate characteristics of standard types of paper-insulated toll telephone cable circuits

1000 cycles per second

wire gauge AWG	type of load-ing*	spac-ing of load coils miles	constants assumed to be distributed per loop mile: R ohms	L henries	C μf	G μmho	propagation constant, polar: magni-tude	angle deg +	rectangular: α	β	line impedance, polar: magni-tude	angle deg −	rectangular: R ohms	X ohms	wave-length miles	velocity miles per second	cut-off fre-quency f_c	attenuation decibels per mile
side circuit																		
19	N.L.S.	—	84.0	0.001	0.061	1.0	0.183	47.0	0.1249	0.134	470	42.8	345	319.4	46.9	46900	—	1.06
19	H-31-S	1.135	87.2	0.028	0.061	1.0	0.277	76.6	0.0643	0.269	710	13.2	691	162.2	23.3	23300	6700	0.56
19	H-44-S	1.135	88.4	0.039	0.061	1.0	0.319	79.9	0.0561	0.314	818	9.9	806	140.8	20.0	20000	5700	0.49
19	H-88-S	1.135	91.2	0.078	0.061	1.0	0.441	84.6	0.0418	0.439	1131	5.2	1126	102.8	14.3	14300	4000	0.36
19	H-172-S	1.135	96.3	0.151	0.061	1.0	0.610	87.0	0.0323	0.609	1565	2.8	1563	76.9	10.3	10300	2900	0.28
19	B-88-S	0.568	97.7	0.156	0.061	1.0	0.620	87.0	0.0322	0.619	1590	2.8	1588	76.7	10.2	10200	5700	0.28
16	N.L.S.	—	42.1	0.001	0.061	1.5	0.129	49.1	0.0842	0.097	331	40.7	255	215.4	64.5	64500	—	0.69
16	H-31-S	1.135	44.5	0.028	0.061	1.5	0.266	82.8	0.0334	0.264	683	7.0	677	83.0	23.8	23800	6700	0.29
16	H-44-S	1.135	45.7	0.039	0.061	1.5	0.315	84.6	0.0296	0.313	808	5.2	805	72.8	20.1	20000	5700	0.26
16	H-88-S	1.135	48.5	0.078	0.061	1.5	0.438	87.6	0.0224	0.437	1124	2.7	1123	53.1	14.4	14400	4000	0.19
16	H-172-S	1.135	53.6	0.151	0.061	1.5	0.608	88.3	0.0183	0.608	1562	1.5	1562	41.1	10.3	10300	2900	0.16
16	B-88-S	0.568	54.9	0.156	0.061	1.5	0.618	88.3	0.0185	0.618	1587	1.5	1587	41.4	10.2	10200	5700	0.16
13	N.L.S.	—	20.8	0.001	0.061	2.5	0.094	52.9	0.0568	0.075	242	36.9	195	140.0	83.6	83600	—	0.47
phantom circuit																		
19	N.L.P.	—	42.0	0.0007	0.100	1.5	0.165	47.8	0.1106	0.122	262	42.0	195	175.2	51.5	51500	—	0.96
19	H-18-P	1.135	43.5	0.017	0.100	1.5	0.270	78.7	0.0529	0.264	429	11.1	421	82.6	23.8	23800	7000	0.46
19	H-25-P	1.135	44.2	0.023	0.100	1.5	0.308	81.3	0.0466	0.305	491	8.5	485	72.4	20.6	20600	5900	0.40
19	H-50-P	1.135	45.7	0.045	0.100	1.5	0.424	85.3	0.0351	0.423	675	4.5	673	53.3	14.9	14900	4200	0.30
19	H-63-P	1.135	47.8	0.056	0.100	1.5	0.472	86.0	0.0331	0.471	752	3.8	750	49.8	13.3	13300	3700	0.29
19	B-50-P	0.568	49.0	0.089	0.100	1.5	0.594	87.4	0.0273	0.593	945	2.4	944	39.8	10.6	10600	5900	0.24
16	N.L.P.	—	21.0	0.0007	0.100	2.4	0.116	50.0	0.0746	0.089	185	39.0	144	116.3	70.6	70600	—	0.65
16	H-18-P	1.135	22.2	0.017	0.100	2.4	0.262	84.0	0.0273	0.260	417	5.8	415	41.8	24.1	24100	7000	0.24
16	H-25-P	1.135	22.8	0.023	0.100	2.4	0.303	85.4	0.0243	0.302	483	4.4	481	36.8	20.8	20800	5900	0.21
16	H-50-P	1.135	24.3	0.045	0.100	2.4	0.422	87.4	0.0189	0.422	672	2.4	672	27.5	14.9	14900	4200	0.16
16	H-63-P	1.135	26.4	0.056	0.100	2.4	0.471	87.7	0.0185	0.471	749	2.0	749	26.6	13.4	13400	3700	0.16
16	B-50-P	0.568	27.5	0.089	0.100	2.4	0.593	88.5	0.0157	0.593	944	1.3	944	21.4	10.6	10600	5900	0.14
13	N.L.P.	—	10.4	0.0007	0.100	2.4	0.086	55.1	0.0442	0.071	137	33.9	114	76.3	89.1	89100	—	0.43
physical circuit																		
16	B-22	0.568	43.1	0.040	0.061	1.5	0.315	85.0	0.0273	0.314	809	4.8	806	67.1	20.0	20000	11300	0.24

* The letters H and B indicate loading-coil spacings of 6000 and 3000 feet, respectively.

continued **Telephone transmission-line data**

Approximate characteristics of standard types of paper-insulated exchange telephone cable circuits

1000 cycles per second

wire gauge AWG	code no	type of loading	loop mile constants: C µf	loop mile constants: G µmho	propagation constant, polar: mag	propagation constant, polar: angle deg	propagation constant, rectangular: α	propagation constant, rectangular: β	mid-section characteristic impedance, polar: mag	mid-section characteristic impedance, polar: angle deg	mid-section characteristic impedance, rectangular: Z_{01}	mid-section characteristic impedance, rectangular: Z_{02}	wave length miles	velocity miles per second	cut-off freq	atten db per mile
26	BST	NL	.083	1.6	—	—	—	—	910	—	—	—	—	—	—	2.9
	ST	NL	.069	1.6	.439	45.30	.307	.310	1007	44.5	719	706	20.4	20,400	—	2.67
24	DSM	NL	.085	1.9					725						—	2.3
	ASM	NL	.075	1.9	.355	45.53	.247	.251	778	44.2	558	543	25.0	25,000	—	2.15
		M88	.075	1.9	.448	70.25	.151	.421	987	23.7	904	396	14.9	14,900	3100	1.31
		H88	.075	1.9	.512	75.28	.130	.495	1160	14.6	1122	292	12.7	12,700	3700	1.13
		B88	.075	1.9	.684	81.70	.099	.677	1532	8.1	1515	215	9.3	9,270	5300	0.86
22	CSA	NL	.083	2.1	.297	45.92	.207	.213	576	43.8	416	399	29.4	29,400	—	1.80
		M88	.083	2.1	.447	76.27	.106	.434	905	13.7	880	214	14.5	14,500	2900	0.92
		H88	.083	2.1	.526	80.11	.0904	.519	1051	9.7	1040	177	12.1	12,100	3500	0.79
		H135	.083	2.1	.644	83.50	.0729	.640	1306	6.3	1300	144	9.8	9,800	2800	0.63
		B88	.083	2.1	.718	84.50	.0689	.718	1420	5.3	1410	130	8.75	8,750	5000	0.60
		B135	.083	2.1	.890	86.50	.0549	.890	1765	3.3	1770	102	7.05	7,050	4000	0.48
19	CNB	NL	.085	1.6	—	—	—	—	400	—	—	—	—	—	—	1.23
	DNB	NL	.066	1.6	.188	47.00	.128	.138	453	42.8	333	308	45.7	45,700	—	1.12
		M88	.066	1.6	.383	82.42	.0505	.380	950	8.9	939	146	16.6	16,600	3200	0.44
		H88	.066	1.6	.459	84.60	.0432	.459	1137	5.2	1130	103	13.7	13,700	3900	0.38
		H135	.066	1.6	.569	86.53	.0345	.570	1413	4.0	1410	99	11.0	11,000	3200	0.30
		H175	.066	1.6	.651	87.23	.0315	.651	1643	3.3	1640	95	9.7	9,700	2800	0.27
		B88	.066	1.6	.641	86.94	.0342	.641	1565	2.8	1560	77	9.8	9,800	5500	0.30
16	NH	NL	.064	1.5	.133	49.10	.0868	.1004	320	40.6	243	208	62.6	62,600	—	0.76
		M88	.064	1.5	.377	85.88	.0271	.377	937	4.6	934	76	16.7	16,700	3200	0.24
		H88	.064	1.5	.458	87.14	.0238	.458	1130	2.8	1130	55	13.7	13,700	3900	0.21

In the third column of the above table the letters M, H, and B indicate loading-coil spacings of 9000 feet, 6000 feet, and 3000 feet, respectively, and the figures show the inductance of the loading coils used.

Telephone transmission-line data *continued*

Representative values of line and propagation constants of miscellaneous cables

All figures for loop-mile basis

Nonloaded

Temperature 55° fahrenheit

16-gauge spiral-four (disc-insulated) toll-entrance cable

freq in kc/s	resistance ohms/mile	inductance mh/mile	conductance μmhos/mile	capacitance μf/mile	characteristic impedance ohms	phase shift radians/mile	attenuation db/mile
0.1	42.4	2.00	0.042	0.02491	—	0.024	0.18
0.5	42.9	1.98	0.053	0.02491	540–j460	0.045	0.32
1.0	43.4	1.94	0.074	0.02491	428–j324	0.067	0.44
1.5	43.9	1.89	0.102	0.02491	380–j275	0.085	0.49
2.0	44.4	1.82	0.127	0.02491	350–j230	0.101	0.55
3.0	45.5	1.74	0.186	0.02490	307–j157	0.145	0.64
5.0	47.5	1.64	0.320	0.02490	279–j107	0.218	0.74
10	50.8	1.56	0.72	0.02489	258–j63	0.405	0.85
20	56.9	1.53	1.95	0.02488	226–j36	0.78	0.99
30	63.0	1.52	3.54	0.02488	248–j26	1.15	1.10
50	73.0	1.51	7.1	0.02488	245–j19	1.90	1.31
100	94.8	1.46	16.9	0.02488	243–j13	3.80	1.71
150	113.5	1.44	27.1	0.02488	240–j10	5.65	2.08
200	130.0	1.43	38.0	0.02487	—	—	2.35

22 AWG emergency cable

side:							
0	166	1.00	—	—	—	—	—
1	—	—	1.3	0.063	468–j449	—	1.53
phant:							
0	83	0.69	—	—	—	—	—
1	—	—	2.1	0.100	265–j250	—	1.37

19 AWG CL emergency cable

side:							
dry 0	92	1.39	negligible	—	—	—	—
wet 0	92	1.39	negligible	—	—	—	—
dry 1	—	—	negligible	0.110	272–j244	—	1.48
wet 1	—	—	negligible	0.14	239–j214	—	1.69
phant:							
dry 0	46	0.5	negligible	—	—	—	—
wet 0	46	0.5	negligible	—	—	—	—
dry 1	—	—	negligible	0.25	124–j116	—	1.58
wet 1	—	—	negligible	0.28	117–j109	—	1.69

Telephone transmission-line data *continued*

Coaxial cable 0.27-inch diam (New York–Philadelphia 1936 type)

Temperature 68° fahrenheit

freq in kc/s	resistance ohms/mile	inductance mh/mile	conductance μmhos/mile	capacitance μf/mile	characteristic impedance ohms	phase shift radians/mile	attenuation db/mile
50	24	0.48	23	0.0773	78.5	—	1.3
100	32	0.47	46	0.0773	78	—	1.9
300	56	0.445	156	0.0772	76	—	3.2
1000	100±	0.43	570	0.0771	74.5	—	6.1

Coaxial cable 0.27-inch diam (Stevens Point–Minneapolis type)

Temperature 68° fahrenheit

freq in kc/s	resistance ohms/mile	inductance mh/mile	conductance μmhos/mile	capacitance μf/mile	characteristic impedance ohms	phase shift radians/mile	attenuation db/mile
10	—	—	—	—	—	—	0.75
20	—	—	—	—	—	—	0.92
30	—	—	—	—	—	—	1.10
50	—	—	—	—	79 $-j6$	—	1.38
100	—	—	—	—	77.8$-j4$	—	1.70
300	—	—	—	—	76.1$-j2$	—	3.00
1000	—	—	—	—	75 $-j1.3$	—	5.6
3000	—	—	—	—	74.5$-j1.1$	—	10
10000	—	—	—	—	—	—	18

Coaxial cable 0.375-inch diam (Polyethylene discs)

freq in kc/s	resistance ohms/mile	inductance mh/mile	conductance μmhos/mile	capacitance μf/mile	characteristic impedance ohms	phase shift radians/mile	attenuation db/mile
10	—	—	—	—	—	—	0.53
20	—	—	—	—	—	—	0.65
30	—	—	—	—	—	—	0.72
50	—	—	—	—	50±	—	0.90
100	—	—	—	—	—	—	1.18
300	—	—	—	—	—	—	2.1
1000	—	—	—	—	—	—	4.0
3000	—	—	—	—	—	—	7
10000	—	—	—	—	—	—	13

Telephone-set comparison*

The following graphs compare the 500-type telephone set (solid lines in the graphs) with the older 302-type set (dashed lines).

* W. F. Tuffnell, "500-Type Telephone Set," *Bell Laboratories Record*, vol. 29, pp. 414–418; September, 1951.

Comparison of over-all response

Courtesy of Bell Laboratories Record

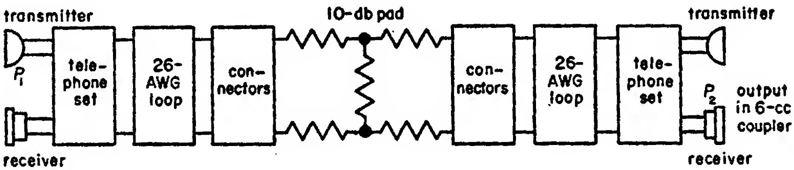

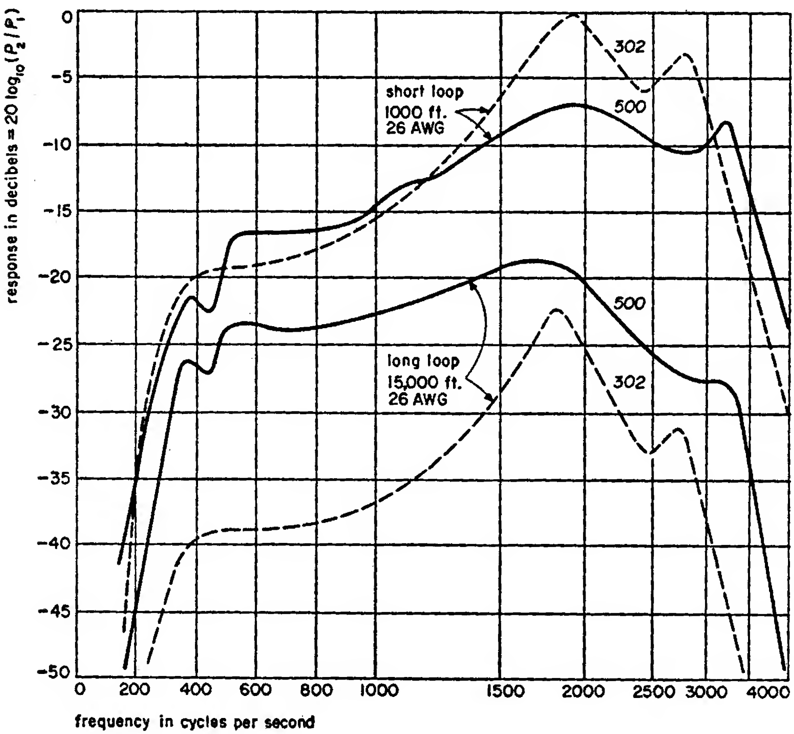

Telephone-set comparison *continued*

Relative volume levels

Courtesy of Bell Laboratories Record

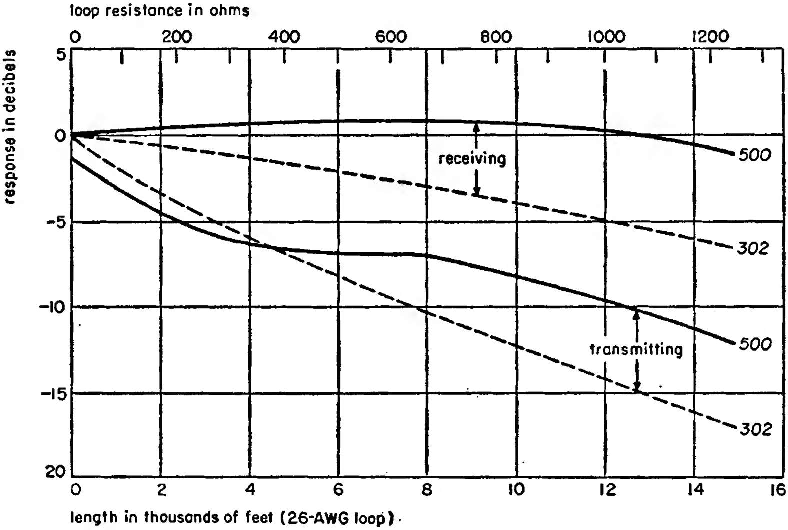

Comparative sidetone levels

Courtesy of Bell Laboratories Record

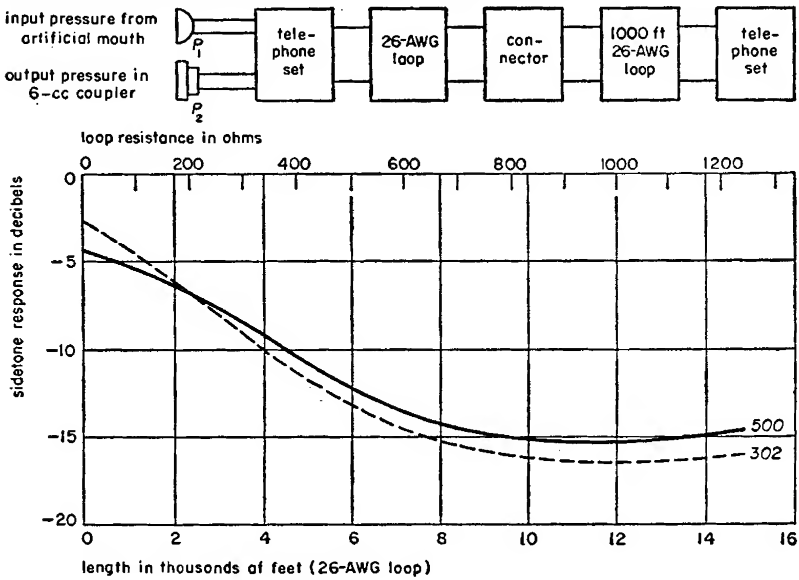

Negative-impedance telephone repeaters

characteristic	series type	shunt type
Generation of negative Z and Y	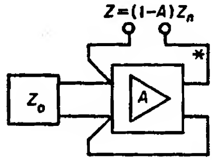 Typical $-Z$ generator * Positive feedback	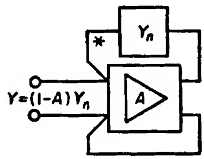 Typical $-Y$ generator * Positive feedback
Insertion gain between line A and line B	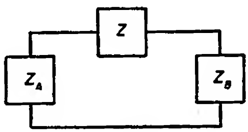 $\text{Gain} = 20\log_{10}\left\lvert 1+\frac{Z}{Z_A+Z_B}\right\rvert \text{db}$	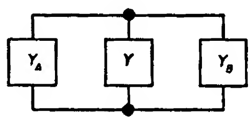 $\text{Gain} = -20\log_{10}\left\lvert 1+\frac{Y}{Y_A+Y_B}\right\rvert \text{db}$
Stability conditions	$Z_A + Z_B + Z > 0$	$Y_A + Y_B + Y > 0$
Typical network configurations for telephone lines	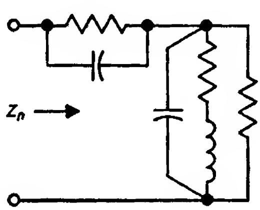 Z network for loaded cable	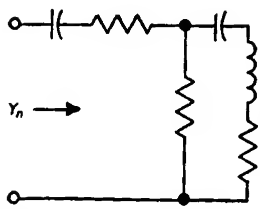 Y network for nonloaded cable and open wire
Maximum practical gain for a $-Z$ or $-Y$ repeater	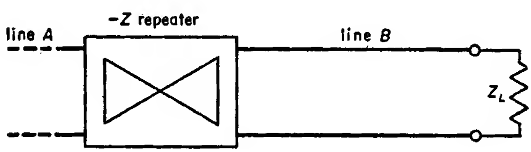 Characteristic impedance $= Z_0$ Propagation constant $= \gamma = \alpha + j\beta$ per unit length l	

Negative-impedance telephone repeaters *continued*

For a series (— Z-type) repeater

$$\text{Maximum gain} = -20 \log_{10} \left| 1 - M \left(\frac{N_A Z_{0,A} + N_B Z_{0,B}}{Z_{0,A} + Z_{0,B}} \right) \right| \text{db}$$

where

$$N = \frac{1 - |\Gamma|}{1 + |\Gamma|} = \text{minimum normalized impedance seen by repeater}$$

$$\Gamma = \left(\frac{Z_L - Z_0}{Z_L + Z_0} \right) \exp - 2\gamma l = \text{load reflection coefficient plus twice line loss}$$

M = stability factor, usually 0.9 (stability margin = $1 - M$)

For a shunt (— Y-type) repeater

Substitute $Y_{0,A}$ for $Z_{0,A}$ and $Y_{0,B}$ for $Z_{0,B}$

A negative-impedance telephone repeater is a voice-frequency repeater that provides effective gain by inserting a negative impedance into the line to cancel out the line impedances that cause transmission losses.

It is possible to generate two distinct types of negative impedances. The series type is stable when it is terminated in an open circuit and oscillates when connected to a low impedance. The shunt type is stable when short-circuited but will oscillate when terminated in a high impedance. The shunt type may be regarded as a negative admittance.

Because they represent lumped impedance discontinuities, series or shunt negative-impedance repeaters cause reflection at the point of insertion. These reflections produce echoes and limit the gain obtainable. To overcome these objections, series and shunt repeaters in combination are used.

The chart on these pages illustrates the characteristics of the two types of repeater. The chart assumes uniform lines. For nonuniform lines, reflections at all junctions must be computed and referred to the repeater location. In switched telephone trunks, Z_L is generally taken as zero or infinity.

Between lines having reasonably similar impedances, the bridged-T-configuration combination repeater may be used. Its insertion gain is

$$G_T = 20 \log_{10} \left| \frac{1 - ZY/4}{1 + \frac{ZY}{4} + \frac{Z}{Z_A + Z_B} + \frac{Y}{Y_A + Y_B}} \right|$$

Negative-impedance telephone repeaters *continued*

The characteristic impedance of the series-shunt repeater is

$$Z_0 = (Z/Y)^{1/2}$$

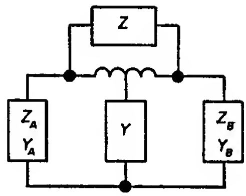

and its transmission is

$$\exp\gamma = \frac{1 - x/2}{1 + x/2}$$

where $x = (ZY)^{1/2} = Z/Z_0 = Y/Y_0$

The maximum gain obtainable from a bridged-T repeater is given by

$$20\log_{10}(\exp\gamma) < (RL_A/2) + (RL_B/2)$$

where RL_A and RL_B are the minimum return losses of the two lines relative to the characteristic impedance of the repeater. For best results, the characteristic impedance of the repeater should be matched to that of the line having the higher return loss.

In practice, the above gain must be reduced somewhat to allow a margin of stability.

In cases where the combination repeater is inserted between lines whose impedances differ by 3:1 or more, an "L" configuration (with the Z-type toward the higher impedance) may prove advantageous because of its impedance-matching properties.

Carrier telephone systems

Many types of carrier systems are available. These may be classified according to the following characteristics:

Speech bandwidth in cycles per second—300–2700, 250–2700, 250–3000, 250–3100, 250–3400*

Signaling method

By type:

Ringdown, dialing (E and M leads)

By frequency (c/s):

In-band—	Single frequency 1000, 1600, 2100, 2280, 2600 2700, 3000, interrupt carrier.
Out-of-band—	Single frequency 3400, 3550, 3700, 3850.
Frequency shift (2 tones),	3400 and 3550, 3450 and 3550, frequency shift of carrier.

* With in-band signaling.

Carrier telephone systems *continued*

Type of termination

2-wire, 4-wire, conditions for interconnection with other systems:

4-wire input levels vary from −13 to −17 dbm.

4-wire output levels vary from +4 to +10 dbm.

2-wire input level is zero dbm.

2-wire output level depends on circuit length, type of level stabilization, and hybrid balance. An average value is −9 dbm.

Length of system

Long haul, medium haul, short haul, subscriber carrier.

Terms commonly used in carrier telephone transmission

Four-wire termination: Separate wire pairs are employed to terminate the transmitting and receiving circuits at a terminal.

Two-wire termination: The transmitting and receiving circuits are terminated in a single wire pair by means of a four-wire terminating set.

Four-wire terminating set: A four-wire terminating set consists of a form of bridge circuit called a hybrid. The hybrid circuit may be made up of one or more transformers or it may be made up of resistors. The circuit is arranged so that the two-wire line and a balancing network form one pair of conjugate arms of the bridge. The four-wire input and output circuits are connected to form another pair of conjugate arms of the bridge. The amount of coupling between the input and output circuits at any frequency is determined by the degree of match between the impedances of the balancing network and the two-wire termination.

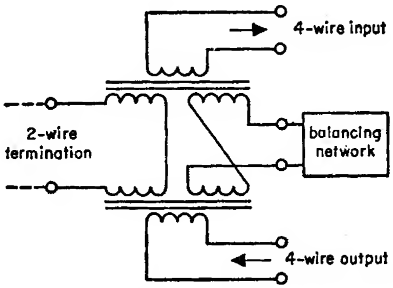

Two-coil hybrid; normal transmission loss = 3.5 to 4.0 db.

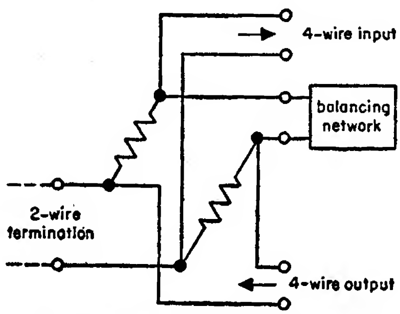

Simple resistance hybrid; normal transmission loss = 6 db.

Carrier telephone systems *continued*

Compromise network: The two-wire termination at a terminal is usually of varying impedance. It is therefore not practical to provide a network that will maintain a good hybrid balance under all conditions. A compromise network (usually a resistance in series with a capacitor, the values of which are determined by the general level of impedance) is employed to provide adequate average balance.

Transhybrid loss: The transhybrid loss is the transmission loss measured across the hybrid circuit for a given two-wire termination and balancing network at a given frequency.

Return loss: The return loss (*RL*) is the transhybrid loss less the sum of the losses from the two-wire path to each of the four-wire terminals.

$$(\text{Return loss}) = 20 \log_{10} \frac{Z_N + Z_L}{Z_N - Z_L}$$

where

Z_N = network impedance

Z_L = two-wire termination impedance

Crosstalk units: (*CU*)

$$(\text{Number of crosstalk units}) = 10^6 \times (P_R/P_S)^{1/2}$$

where

P_R = power in the disturbed circuit

P_S = power in the disturbing circuit

In decibels,

$$(\text{crosstalk}) = 20 \log_{10} (10^6/\text{crosstalk units}) = 10 \log_{10} (P_S/P_R)$$

Relative level: The relative power level at a point of the system, expressed in nepers, is one-half the natural logarithm of the ratio of the power at that point to the value of the power at the point of the system chosen as a reference point. Expressed in decibels, it is ten times the decimal logarithm of the above ratio. (*Note:* The reference point normally chosen is the test board at the transmitting end of the long-distance line.)

Carrier telephone systems *continued*

Net loss (equivalent): The net loss of a transmission system is the difference between the relative levels at the input and output of the system; in cases where the input corresponds to a point of zero relative level, it is equal in value, but opposite in sign, to the relative level at the output. 9 db is considered as a representative net circuit loss for a long circuit. Lower values may be employed provided satisfactory echo and singing margin are obtained.

Singing margin: The singing margin of a circuit is defined as the maximum amount by which the net loss of each of the two directions of transmission may be reduced simultaneously before singing occurs. A minimum value of 8 db is generally required for satisfactory transmission.

Intelligible crosstalk: In the coaxial case, a maximum length of parallel between any disturbing and disturbed channel is fixed by American Telephone and Telegraph Company at 1000 miles. Under this condition, the rms coupling in crosstalk units is required to be equal to at least 64 db between the zero level of the disturbing circuit and the −9-db level of the disturbed circuit. When crosstalk is unintelligible, it is treated as noise and the noise thus introduced should be consistent with the noise allowance. The American Telephone and Telegraph Company specifies that the crosstalk coupling in decibels corresponding to the root-mean-square value of all combinations, expressed in crosstalk units, shall be 55 db between equal-level points.

E and M leads: The *E* and *M* leads of a signaling system are the output and input leads, respectively. The *E* lead provides an open or ground. The *M* lead accepts open or ground, or battery or ground, as the circuit may require.

Frequency-allocation and level-comparison charts

The following notes apply to the charts of frequency allocation and level comparison (pp. 834-837) for the various commonly used wire and cable carrier telephone transmission systems.

Notes:

Solid arrows = carrier frequencies
Dotted arrows = pilot frequencies

↑ = east–west or *A–B* direction
↓ = west–east or *B–A* direction

 = channel No. 1

S = signalling frequency

FTR = Federal Telephone and Radio Company, a division of IT&T

STC = Standard Telephones and Cables, Limited

WECo = Western Electric Company

KSS = Kellogg Switchboard and Supply Company, a division of IT&T

Carrier telephone systems *continued*

Frequency allocations for open-wire carrier telephone systems

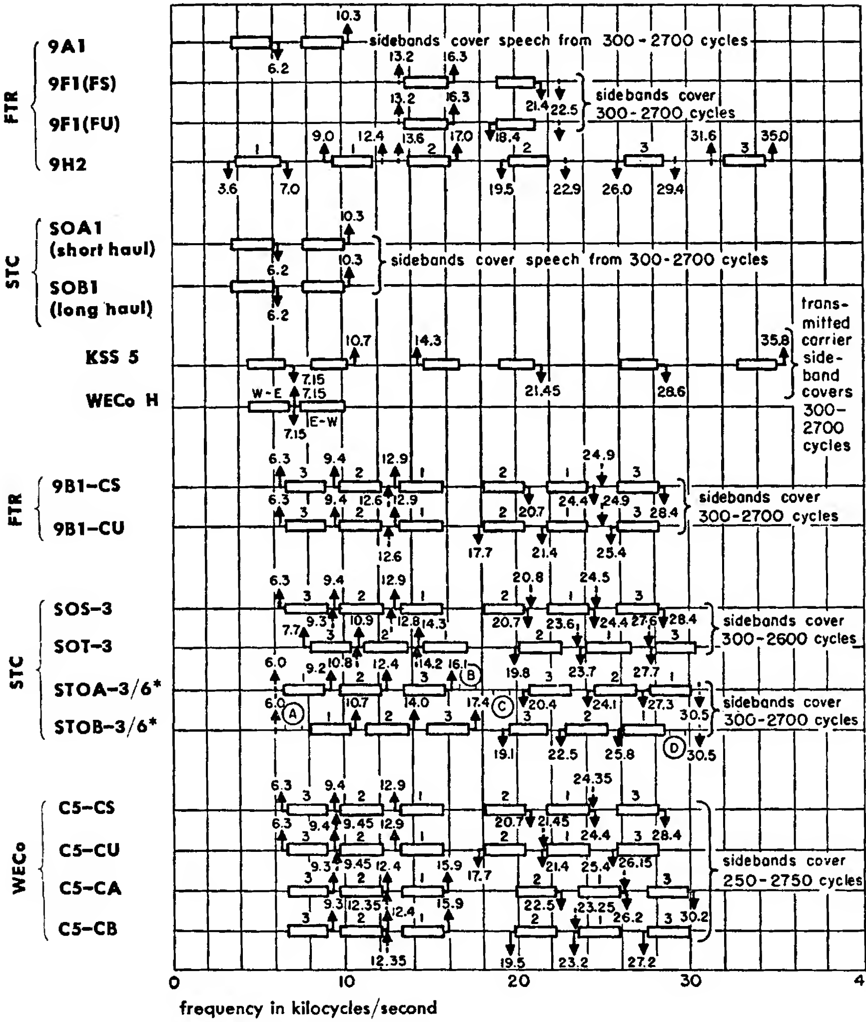

* Letters *A, B, C, D* designate 4 band locations in each of which 6 telegraph channels may be applied. See notes on p. 833.

continued **Carrier telephone systems**

Frequency allocations and level comparisons (WECo)

Courtesy of *Communications and Electronics*

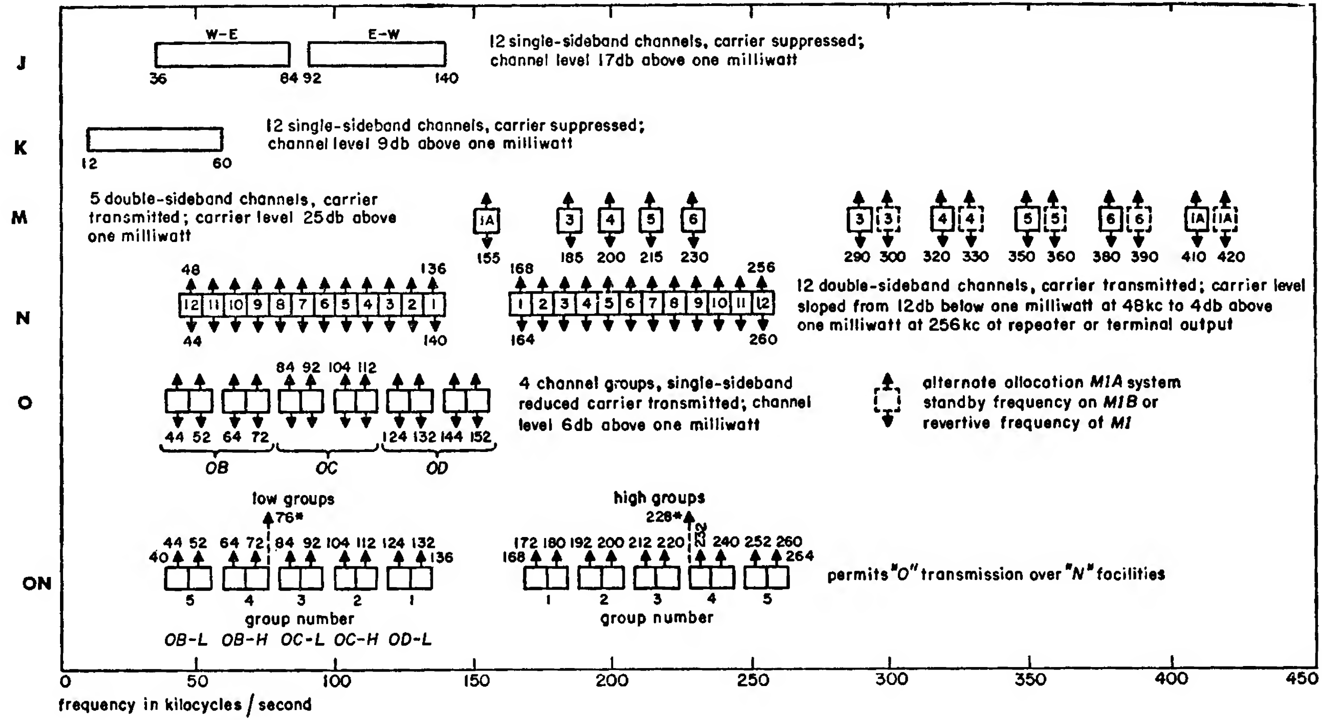

Frequency allocations for 12-channel open-wire and 12- or 24-channel cable-carrier systems

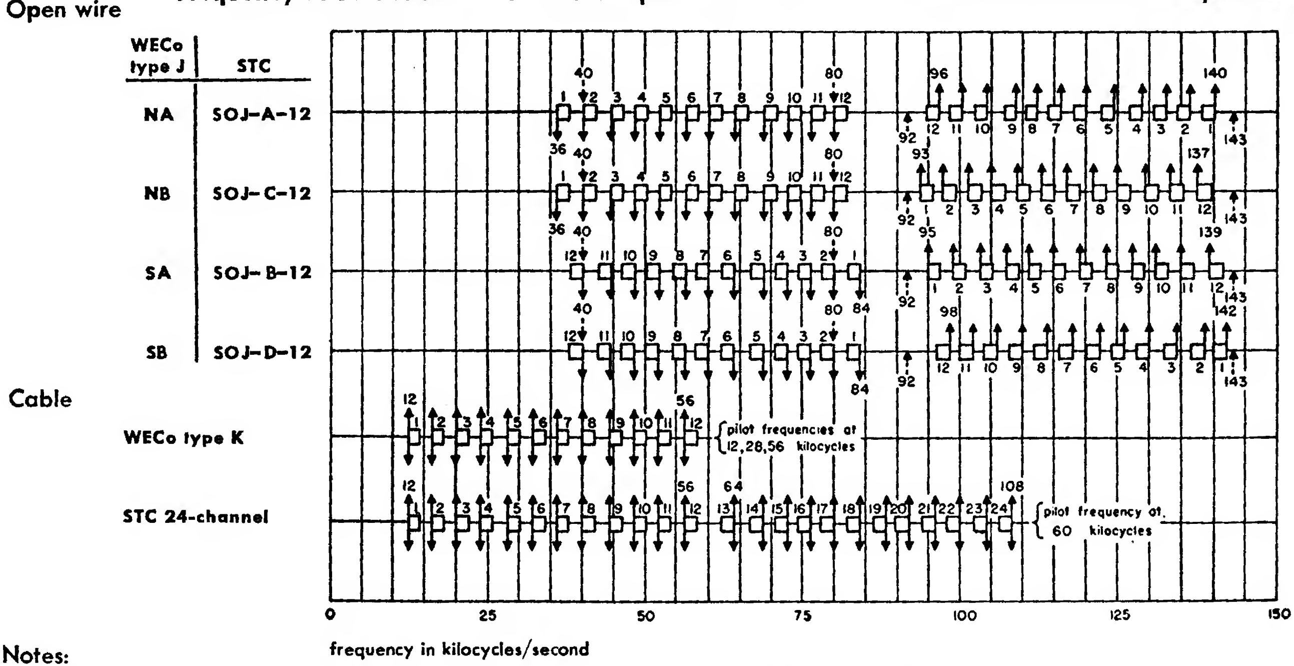

Notes:

Carriers spaced 4 kilocycles apart.
Sidebands include speech from 200 to 3300 cycles.
Frequencies shown are line frequencies obtained by two or more stages of modulation.

Channel numbers are shown at the base of each arrow.
See also notes on p. 833.

continued **Carrier telephone systems**

Frequency allocations and modulation steps for coaxial-cable carrier systems

Channel modulation

1st group modulation

2nd group modulation

Supergroup: STC and CCIF; WECo type L

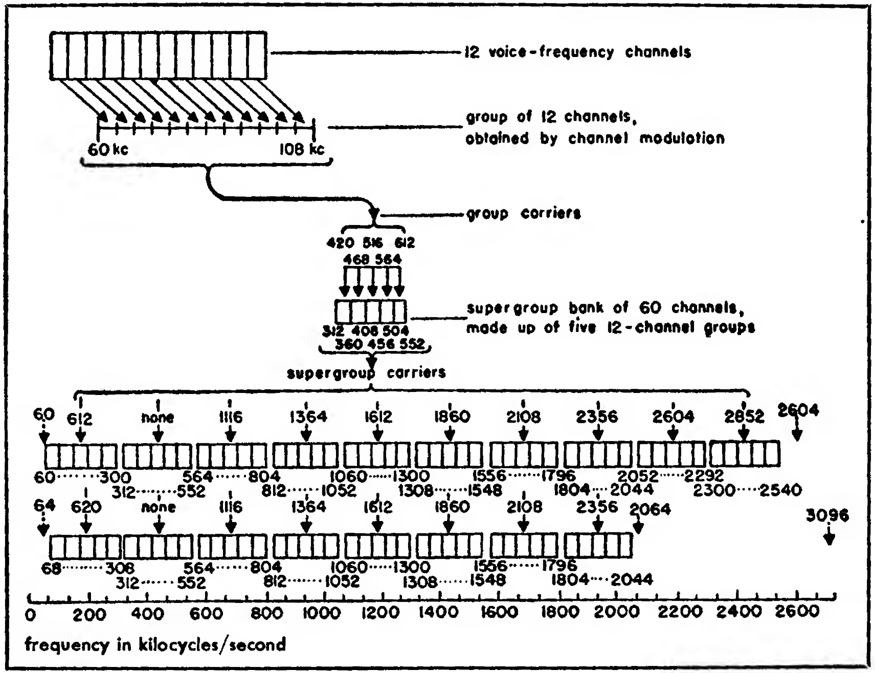

Notes:

Frequencies shown are line frequencies obtained by two or more stages of modulation.

See also notes on p. 833.

▯▯▯▯▯ = supergroup of 60 channels

CCIF = Comité Consultatif International Téléphonique

Compandors

Compandors are employed on a telephone channel to improve the noise and crosstalk quality of the channel.

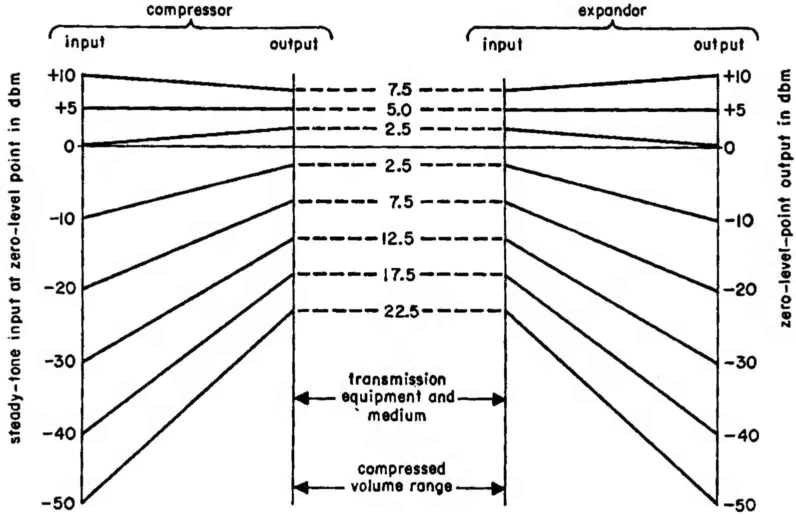

A compandor circuit includes a compressor at the transmitting end and an expander at the receiving end.

Syllabic type of compandors may be applied to any telephone channel.

The standard type of compandor employs a 2:1 compressor (output amplitude increases 1 db for each 2 db increase in input amplitude) and an expander that has the inverse characteristic. With this type of compandor, an effective signal-to-noise improvement of about 22 db may be expected.

Limitations to compandor application

Compandors, due to expander action, will double the decibels effective line-loss variations and variations in loss at the different frequencies.

Unusually high noise levels will not be materially reduced.

Telephone noise and noise measurement

Definitions

The following definitions are based upon those given in the Proceedings of the tenth Plenary Meeting (1934) of the *Comité Consultatif International Téléphonique* (C.C.I.F.).

Telephone noise and noise measurement *continued*

Note: The unit in which noise is expressed in many of the European countries differs from the two American standards, the *noise unit* and the *db above reference noise*. The European unit is referred to as the *psophometric electromotive force*.

Noise: Is a sound which tends to interfere with a correct perception of vocal sounds, desired to be heard in the course of a telephone conversation.

It is customary to distinguish between:

Room noise: Present in that part of the room where the telephone apparatus is used.

Frying noise (transmitter noise): Produced by the microphone, manifest even when conversation is not taking place.

Line noise: All noise electrically transmitted by the circuit, other than room noise and frying noise.

Reference noise: The reference power level for noise measurements in the United States has been standardized as 10^{-12} watts, or 90 db below 1 milliwatt at 1000 c/s. Noise power readings may be expressed in dbrn (db above reference noise).

Noise weighting: Noise weighting is employed to obtain a noise measurement that is representative of the relative disturbance effect of the noise frequencies in a communication system. The two types of weighting networks (*144* and *F1A*) used in the United States are based on the relative frequency response of the type-*144* and type-*F1A* telephone handsets, respectively. Noise measurements made with the *144* weighting network are expressed in dbrn or dba. Both are equal in value (db above −90 dbm). Noise measurements made with *F1A* weighting network are expressed in dba (db above −85 dbm). (Listening tests have indicated that the *F1A* handset is 5 db more sensitive than the *144* receiver.) An expression of noise in dba (db adjusted) is indicative of the disturbing effect independent of the network used.

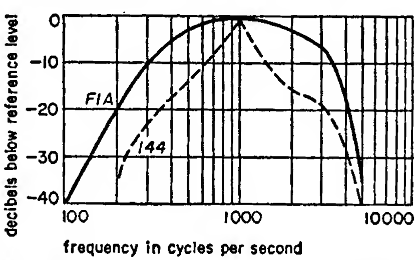

Noise weighting networks. Response relative to 1000 c/s.

Telephone noise and noise measurement *continued*

Psophometric electromotive force

The psophometric electromotive force is the electromotive force of a source having an internal resistance of 600 ohms and zero internal reactance that, when connected directly to a standard receiver of 600-ohms resistance and zero reactance, produces the same sinusoidal current as that of an 800-cycle generator of the same impedance as above.

A psophometer (includes a filter weighting network specified by C.C.I.F.) connected across the terminals of the 600-ohm receiver gives a reading of half of the psophometric electromotive force for the particular case considered. The term "psophometric voltage" between any two points refers to the instrument reading between these points.

Noise levels

The amount of noise found on different circuits, and even on the same circuit at different times, varies through quite wide limits. Further, there is no definite agreement as to what constitutes a *quiet* circuit, a *noisy* circuit, etc. The following values should therefore be regarded merely as a rough indication of the general levels that may be encountered under the different conditions:

Open-wire circuit	db above ref noise
Quiet	20
Average	35
Noisy	50
Cable circuit	
Quiet	15
Average	25
Noisy	40

Relationship of European and American noise units

The psophometric emf can be related to the American units: the *noise unit* and the *decibel above reference noise.*

The following chart shows this relationship together with correction factors for psophometric measurements on circuits of impedance other than 600 ohms.

Telephone noise and noise measurement *continued*

Relationship of European and American noise units

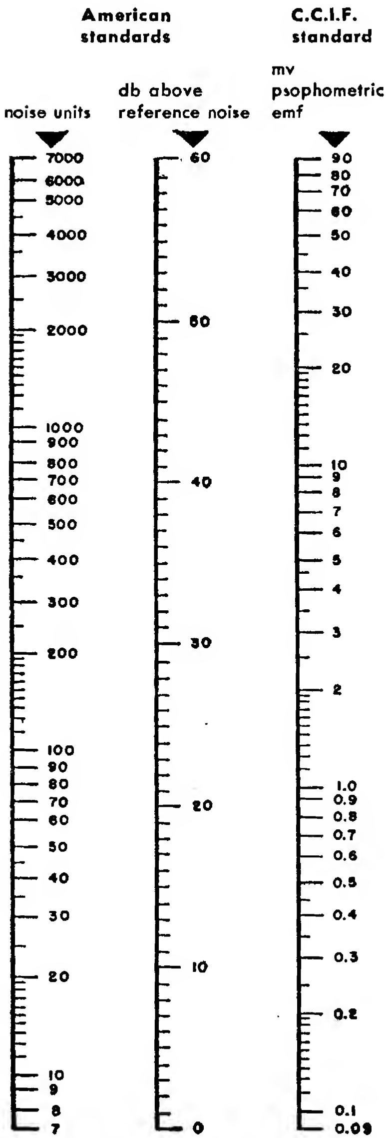

a. The relationship of noise units to decibels above reference noise is obtained from technical report No. 1B–5 of the joint subcommittee on development and research of the Bell Telephone System and the Edison Electric Institute.

b. The relationship of db above reference noise to psophometric emf is obtained from the Proceedings of Comité Consultatif International Téléphonique, 1934.

c. The C.C.I.F. expresses noise limits in terms of the psophometric emf for a circuit of 600 ohms resistance and zero reactance, terminated in a resistance of 600 ohms. Measurements made in terms of the potential difference across the terminations, or on circuits of impedance other than 600 ohms, should be corrected as follows:

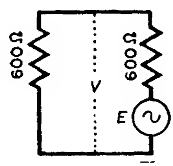

Psophometric emf $= E$

$E = 2V$

A psophometer measures V not E

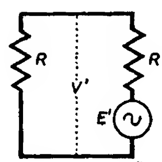

$$E = E' \sqrt{\frac{600}{R}}$$

$$= 2V' \sqrt{\frac{600}{R}}$$

d. Reference noise—with respect to which the American noise measuring set is calibrated—is a 1000-cycle/second tone 90 decibels below 1 milliwatt.

Telephone noise and noise measurement *continued*

Multichannel frequency-division loading*

The graph at the right shows the required single-tone capacity in dbm of a system at a point of zero transmission level as a function of the total number of telephone channels. The peak value of the single-frequency tone will not be exceeded by the peak value of the actual multichannel signal more than 1 percent of the time during the busy hour.

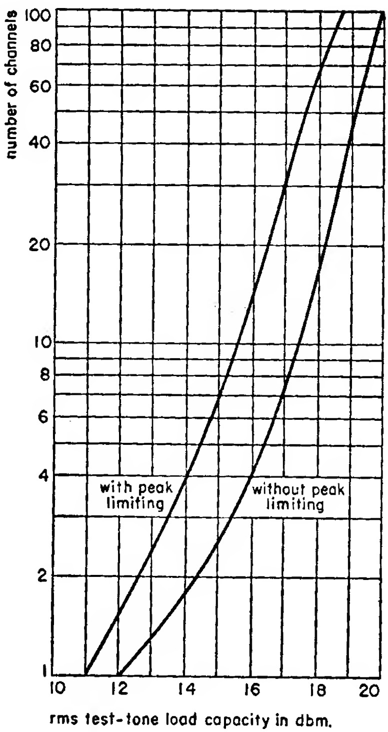

* B. D. Holbrook and J. T. Dixon, "Load Rating Theory for Multi-Channel Amplifiers," *Bell System Technical Journal,* vol. 18, pp. 624–644; October, 1939.

Telegraph facilities

International Morse and cable codes

International Morse code is determined by combinations of unipolar current pulses of short and long ($\approx$ 1:3) durations:

A =
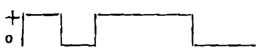

International cable code is determined by combinations of bipolar current pulses of the same length:

A =


Telegraph facilities *continued*

Code combinations

character	international Morse	international cable	character	international Morse	international cable
A	·—	+−	.	·—·—·—	Punctuations not shown because of many variations between systems.
B	—···	−+++	;	—·—·—·	
C	—·—·	−+−+	,	——··——	
D	—··	−++	:	———···	
E	·	+	?	··——··	
F	··—·	++−+	'	·————·	
G	——·	−−+	-	—····—	
H	····	++++	/	—··—·	
I	··	++	Ā	·—·—	
J	·———	+−−−	Á or Å	·——·—	
K	—·—	−+−	É	··—··	
L	·—··	+−++	CH	————	
M	——	−−	Ñ	——·——	
N	—·	−+	Ö	———·	
O	———	−−−	Ü	··——	
P	·——·	+−−+	(OR)	—·——·—	
Q	——·—	−−+−	"	·—··—·	
R	·—·	+−+	—	··——·—	
S	···	+++	=	—···—	
T	—	−	S O S	···———···	
U	··—	++−	Attention	—·—·—	
V	···—	+++−	CQ	—·—·——·—	
W	·——	+−−	DE	—·· ·	
X	—··—	−++−	Go ahead	—·—	
Y	—·——	−+−−	Wait	·—···	
Z	——··	−−++	Break	—···—	
1	·————	+−−−−	Understand	···—·	
2	··———	++−−−	Error	········	
3	···——	+++−−	OK	·—·	
4	····—	++++−	End message	·—·—·	+++−+
5	·····	+++++			
6	—····	−++++	End of work	···—·—	
7	——···	−−+++			
8	———··	−−−++			
9	————·	−−−−+			
0	—————	−−−−−			

Telegraph facilities *continued*

Printing-telegraph codes

lower-case character	Teletype 7-unit code st 1 2 3 4 5 stp	CCIT 2 5-unit code* 1 2 3 4 5	ARQ 7-unit Moore code 1 2 3 4 5 6 7
A	○ ● ● ○ ○ ○ ●	● ● ○ ○ ○	○ ○ ● ● ○ ● ○
B	○ ● ○ ○ ● ● ●	● ○ ○ ● ●	○ ○ ● ● ○ ○ ●
C	○ ○ ● ● ● ○ ●	○ ● ● ● ○	● ○ ○ ● ● ○ ○
D	○ ● ○ ○ ● ○ ●	● ○ ○ ● ○	○ ○ ● ● ● ○ ○
E	○ ● ○ ○ ○ ○ ●	● ○ ○ ○ ○	○ ● ● ● ○ ○ ○
F	○ ● ○ ● ● ○ ●	● ○ ● ● ○	○ ○ ● ○ ○ ● ●
G	○ ○ ● ○ ● ● ●	○ ● ○ ● ●	● ● ○ ○ ○ ○ ●
H	○ ○ ○ ● ○ ● ●	○ ○ ● ○ ●	● ○ ● ○ ○ ● ○
I	○ ○ ● ● ○ ○ ●	○ ● ● ○ ○	● ● ● ○ ○ ○ ○
J	○ ● ● ○ ● ○ ●	● ● ○ ● ○	○ ● ○ ○ ○ ● ●
K	○ ● ● ● ● ○ ●	● ● ● ● ○	○ ○ ○ ● ○ ● ●
L	○ ○ ● ○ ○ ● ●	○ ● ○ ○ ●	● ● ○ ○ ○ ● ○
M	○ ○ ○ ● ● ● ●	○ ○ ● ● ●	● ○ ● ○ ○ ○ ●
N	○ ○ ○ ● ● ○ ●	○ ○ ● ● ○	● ○ ● ○ ● ○ ○
O	○ ○ ○ ○ ● ● ●	○ ○ ○ ● ●	● ○ ○ ○ ● ● ○
P	○ ○ ● ● ○ ● ●	○ ● ● ○ ●	● ○ ○ ● ○ ● ○
Q	○ ● ● ● ○ ● ●	● ● ● ○ ●	○ ○ ○ ● ● ○ ●
R	○ ○ ● ○ ● ○ ●	○ ● ○ ● ○	● ● ○ ○ ● ○ ○
S	○ ● ○ ● ○ ○ ●	● ○ ● ○ ○	○ ● ○ ● ○ ● ○
T	○ ○ ○ ○ ○ ● ●	○ ○ ○ ○ ●	● ○ ○ ○ ● ○ ●
U	○ ● ● ● ○ ○ ●	● ● ● ○ ○	○ ● ● ○ ○ ● ○
V	○ ○ ● ● ● ● ●	○ ● ● ● ●	● ○ ○ ● ○ ○ ●
W	○ ● ● ○ ○ ● ●	● ● ○ ○ ●	○ ● ○ ○ ● ○ ●
X	○ ● ○ ● ● ● ●	● ○ ● ● ●	○ ○ ● ○ ● ● ○
Y	○ ● ○ ● ○ ● ●	● ○ ● ○ ●	○ ○ ● ○ ● ○ ●
Z	○ ● ○ ○ ○ ● ●	● ○ ○ ○ ●	○ ● ● ○ ○ ○ ●
Blank	○ ○ ○ ○ ○ ○ ●		
Space	○ ○ ○ ● ○ ○ ●	○ ○ ● ○ ○	● ● ○ ● ○ ○ ○
Carriage return	○ ○ ○ ○ ● ○ ●	○ ○ ○ ● ○	● ○ ○ ○ ○ ● ●
Line feed	○ ○ ● ○ ○ ○ ●	○ ● ○ ○ ○	● ○ ● ● ○ ○ ○
Figures	○ ● ● ○ ● ● ●	● ● ○ ● ●	○ ● ○ ○ ● ● ○
Letters	○ ● ● ● ● ● ●	● ● ● ● ●	○ ○ ○ ● ● ● ○
Idle			
Idle signal α			○ ● ○ ● ○ ○ ●
Idle signal β			○ ● ○ ● ● ○ ○
Request			○ ● ● ○ ● ○ ○
ff		○ ○ ○ ○ ○	○ ○ ○ ○ ● ● ●

* International Telegraph Alphabet 2 = space (start) + 5-unit Comite Consultatif International Telegraphique code 2 + mark (stop).

Telegraph facilities *continued*

Printing-telegraph code card

lower-case character	upper case: new U. S. Navy standard	Army, old Navy (Teletype A)	TWX (Teletype C)	British standard	Western Union 2B	Western Union 2C	Western Union 101 and 102	Western Union 101C and 102C	CCIT 2	American Cable & Radio
A	–	–	–	–	–	–	–	–	–	–
B	?	?	⅝	?	?	⅝	?	⅝	?	?
C	:	:	⅛	:	:	⅛	:	⅛	:	:
D	$	$	$	Who are you[1]	$	$	$	$	Who are you	XXX
E	3	3	3	3	3	3	3	3	3	3
F	!	!	¼	%		¼		¼		□
G	&	&	&	@	&	&	&	&		⊟
H	£	£	Stop	£	£	#	#	#		⧄
I	8	8	8	8	8	8	8	8	8	8
J	,	'	,	Bell[2]	Bell	'	Bell	,	Bell	Bell
K	(	(	½	(	(	½	(	½	(	(
L	)	)	¾	)	)	¾	)	¾	)	)
M	.	.	.	.	%	?	.	.	.	.
N	See note[3]	,	⅞	,	'	⅞	,	⅞	,	,
O	9	9	9	9	9	9	9	9	9	9
P	0	0	0	0	0	0	0	0	0	0
Q	1	1	1	1	1	1	1	1	1	1
R	4	4	4	4	4	4	4	4	4	4
S	Bell	Bell	Bell	'	¶	Bell	'	Bell	'	'
T	5	5	5	5	5	5	5	5	5	5
U	7	7	7	7	7	7	7	7	7	7
V	;	;	⅜	=	;	⅜	;	⅜	=	=
W	2	2	2	2	2	2	2	2	2	2
X	/	/	/	/	/	/	/	/	/	/
Y	6	6	6	6	6	6	6	6	6	6
Z	"	"	"	+	"	"	"	"	+	+
Line feed	Line feed	Line feed	Line feed	Line feed			Line feed	Line feed	Line feed	Line feed
Carriage return	Car ret	Car ret	Car ret	Car ret			Car ret	Car ret	Car ret	Car ret
Figures ↑	Figs	Figs	Figs	Figs	Figs	Figs	Figs	Figs	Figs	Figs
Letters[4] ↓	Ltrs	Ltrs	Ltrs	Ltrs	Ltrs	Ltrs	Ltrs	Ltrs	Ltrs	Ltrs
Space	Space	Space	Space	Space	Space	Space	Space	Space	Space	Space
Blank[4] 000	Blank	Blank	Blank	Blank	Blank	Blank	Blank	Blank	Blank	Blank
	Tape printers									
Car ret < or .	Car ret ,	Car ret ,	Car ret '		,					
Line feed ≡ or xx	Line feed .	Line feed .	Line ↑ feed ↑		#					
.	.					.				
,						,				
Figures ↑										

Notes
1. Not used on British Army field machines. Used on British national network.
2. Not used by British Army.
3. Key left blank but comma remains on type bar.
4. Symbols on lower-case line are used on certain monitoring sets.

Telegraph facilities *continued*

Signaling speeds and pulse lengths

The graph below shows the speeds of various telegraph systems. The American Morse curve is based on an average character of 8.5 units determined from actual count of representative traffic. The Continental Morse curve similarly on 9 units, and the Cable Morse on 3.7 units.

system	speed of usual types	
	frequency in cycles*	bauds
Grounded wire	75	150
Simplex (telephone)	50	100
Composite	15	30
Metallic telegraph	85	170
Carrier channel		
Narrow band	40	80
Wide band	75	150

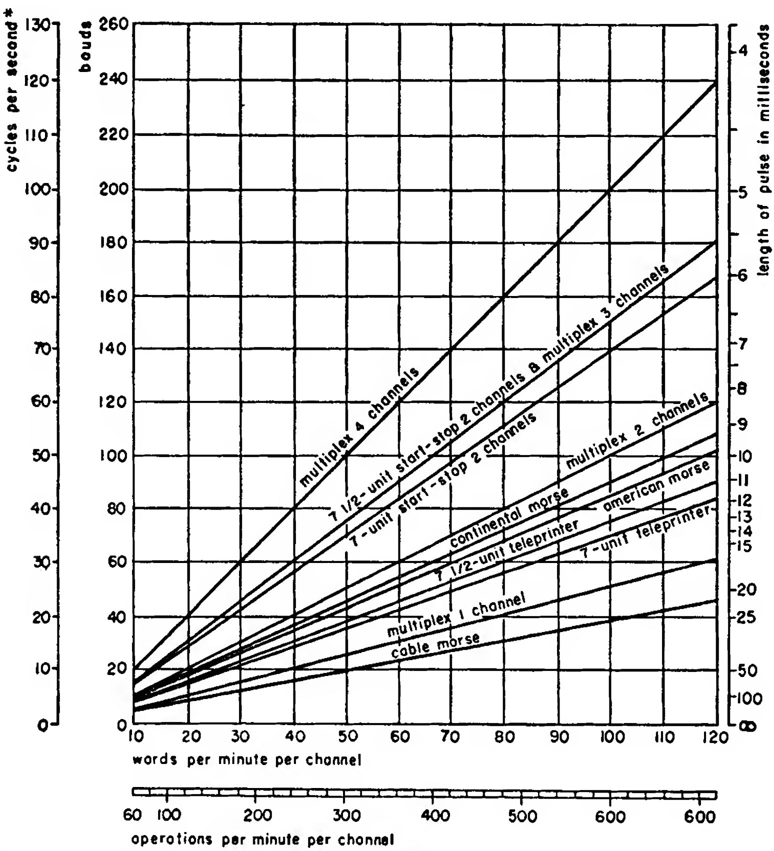

* Based on repetition rate of shortest signaling element.

Feed holes: For Morse, (number feed holes/second) = (number cycles/second). For multiplex and teleprinter, (number feed holes/second) = (words/minute)/10.

Telegraph facilities *continued*

International telegraph alphabet 2

The following notes are excerpts from the Comite Consultatif International Telegraphique regulations, Paris, 1949, revision pertaining to the International Telegraph Alphabet 2.

221. A number which includes a fraction shall be transmitted with the fraction linked to the whole number by a single hyphen. Examples:

1-3/4 and not 13/4; 3/4-8 and not 3/48;
363-1/2 4 5642 and not 3631/2 4 5642

222. The inverted commas sign (quotation mark) (" ") shall be signalled by transmitting the apostrophe sign (') twice, at the beginning and the end of the text within the inverted commas (quotation marks) (" ").

223. Accents on the letter E shall be made by hand when they are essential to the meaning (examples: achète, acheté). In this case the sending telegraphist shall repeat the word after the signature, signalling the accented E between two "blanks" so as to draw the attention of the receiving operator to it.

226. To indicate "wait": the combination MOM

227. To indicate the end of a telegram: the signal +

228. To indicate the end of the transmission: the two signals + ?

229. To indicate the end of work: the signal + transmitted twice by the office which has transmitted the last telegram.

231. In the interests of speed and efficiency in the movement of telegraph traffic and to further the development of a world-wide telecommunication network, the five-unit code, in accordance with the International Telegraph Alphabet 2, is recommended. However, this provision need not apply where Administrations or recognized private operating agencies have made other arrangements for particular circuits or networks. In such cases, the Administrations and recognized private operating agencies concerned could provide suitable facilities for converting from their method of operation to the five-unit code of International Telegraph Alphabet 2 whenever it becomes desirable to interconnect with offices using the latter system.

234. Signs:

Full stop (period)	.
Comma	,
Colon	:

Telegraph facilities *continued*

Question mark (note of interrogation)	?
Apostrophe	'
Cross	+
Hyphen or dash	—
Fraction bar	/
Double hyphen	=
Left-hand bracket (parenthesis)	(
Right-hand bracket (parenthesis)	)

240. Administrations and recognized private operating agencies desirous of confirming on a tape machine the reception or transmission of the signals "carriage return" and "line feed" shall effect this confirmation by printing:

241. The symbol < for the signal "carriage return";

242. The symbol ≡ for the signal "line feed".

243. The provisions regarding the transmission of words, whole numbers, fractional numbers, texts within inverted commas (quotation marks) and the letters è and é, which are applicable to instruments using International Telegraph Alphabet 1 (§2), shall also be applicable to instruments using International Telegraph Alphabet 2.

244. A group consisting of figures and letters shall be transmitted without space between figures and letters on these instruments.

245. To indicate the sign o/o or o/oo, the figure 0, the fraction bar (/) and the figures 0 and 00 shall be transmitted successively. Examples: 0/0, 0/00.

246. To indicate a "blank", the signal "space" shall be transmitted.

247. To indicate a transmission error, the letter E and the signal "space" shall be repeated alternately three times. Transmission shall be resumed beginning with the last word correctly sent. When transmitting with perforated tape and provision exists for eliminating incorrectly perforated characters, this method shall be used.

248. To indicate "wait", to show the end of a telegram, the end of a transmission or the end of work, the signals transmitted shall be the same as on instruments using the International Telegraph Alphabet 1 (§2).

Telegraph facilities *continued*

Carrier telegraph systems

Carrier telegraph systems may be classified as follows.

Modulation

Amplitude (am), freauency shift (fm)

am systems are less susceptible to carrier drift.

fm systems are less susceptible to noise and level variations.

Transmission speed: (5 characters per word) words per minute: 60, 75, 100

Channel spacing: (c/s) 120, 145, 170

Each of the three spacings is used in the United States. The 120-c/s spacing is standard outside the United States.

Carrier or midfrequencies generally used in 120- and 170-cps systems are:

Lowest 420 c/s increased by 120-c/s increments

Lowest 425 c/s increased by 170-c/s increments

Intercarrier-channel telegraphy: Carrier telegraph channels are applied in the available frequency spectrum between carrier telephone channels. The number applied is determined by the frequency spectrum available.

■ Electroacoustics

Theory of sound waves*

Sound (or a sound wave) is an alteration in pressure, stress, particle displacement, or particle velocity that is propagated in an elastic material; or the superposition of such propagated alterations. Sound (or sound sensation) is also the sensation produced through the ear by the above alterations.

Wave equation

Behavior of sound waves is given by the wave equation

$$\nabla^2 p = \frac{1}{c^2}\frac{\partial^2 p}{\partial t^2} \tag{1}$$

where p is the instantaneous pressure increment above and below a steady pressure (dynes/centimeter^2); p is a function of time and of the three coordinates of space. Also,

t = time in seconds

c = velocity of propagation in centimeters/second

∇^2 = the Laplacian, which for the particular case of rectangular coordinates x, y, and z (in centimeters), is given by

$$\nabla^2 \equiv \frac{\partial^2}{\partial x^2} + \frac{\partial^2}{\partial y^2} + \frac{\partial^2}{\partial z^2} \tag{2}$$

For a plane wave of sound, where variations with respect to y and z are zero, $\nabla^2 p = \partial^2 p/\partial x^2 = d^2p/dx^2$; the latter is approximately equal to the curvature of the plot of p versus x at some instant. Equation (1) states simply that, for variations in x only, the acceleration in pressure p (the second time derivative of p) is proportional to the curvature in p (the second space derivative of p).

Sinusoidal variations in time are usually of interest. For this case the usual procedure is to put p = (real part of $\bar{p}\epsilon^{j\omega t}$), where the phasor $\bar{p}$ now satisfies the equation.

$$\nabla^2 \bar{p} + (\omega/c)^2 \bar{p} = 0 \tag{3}$$

Velocity phasor $\bar{v}$ of the sound wave in the medium is related to the complex pressure phasor $\bar{p}$ by the formula

$$\bar{v} = -(1/j\omega\rho_0)\ \mathrm{grad}\ \bar{p} \tag{4}$$

* Lord Rayleigh, "Theory of Sound," vols. I and II, Dover Publications, New York, New York; 1945. P. M. Morse, "Vibration and Sound," 2nd edition, McGraw-Hill Book Company, New York, New York; 1948.

Theory of sound waves *continued*

Fig. 1—Table of solutions for various parameters.

factor	type of sound wave: plane wave	spherical wave
Equation for p	$\dfrac{\partial^2 p}{\partial x^2} = \dfrac{1}{c^2}\dfrac{\partial^2 p}{\partial t^2}$	$\dfrac{\partial^2 p}{\partial x^2} + \dfrac{2}{r}\dfrac{\partial p}{\partial r} = \dfrac{1}{c^2}\dfrac{\partial^2 p}{\partial t^2}$
Equation for $\bar{p}$	$\dfrac{d^2\bar{p}}{dx^2} + \left(\dfrac{\omega}{c}\right)^2 \bar{p} = 0$	$\dfrac{d^2\bar{p}}{dx^2} + \dfrac{2}{r}\dfrac{d\bar{p}}{dt} + \left(\dfrac{\omega}{c}\right)^2 \bar{p} = 0$
Solution for p	$p = F\left(t - \dfrac{x}{c}\right)$	$p = \dfrac{1}{r} F\left(t - \dfrac{x}{c}\right)$
Solution for $\bar{p}$	$\bar{p} = \bar{A}\epsilon^{-j\omega x/c}$	$\bar{p} = \dfrac{1}{r}\bar{A}\epsilon^{-j\omega r/c}$
Solution for $\bar{v}$	$\bar{v} = \dfrac{\bar{A}}{\rho_0 c}\epsilon^{-j\omega x/c}$	$\bar{v} = \dfrac{\bar{A}}{\rho_0 c r}\left(1 + \dfrac{c}{j\omega r}\right)\epsilon^{-j\omega r/c}$
$\bar{Z}$	$\bar{Z} = \rho_0 c$	$\bar{Z} = \rho_0 c \Big/ \left(1 + \dfrac{c}{j\omega r}\right)$
Equivalent electrical circuit for $\bar{Z}$	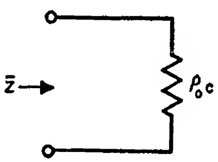	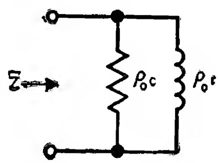

where

p = excess pressure in dynes/centimeter^2

$\bar{p}$ = complex excess pressure in dynes/centimeter^2

t = time in seconds

x = space coordinate for plane wave in centimeters

r = space coordinate for spherical wave in centimeters

$\bar{v}$ = complex velocity in centimeters/second

$\bar{Z}$ = specific acoustic impedance in dyne-seconds/centimeter^3

c = velocity of propagation in centimeters/second

$\omega = 2\pi f$; f = frequency in cycles/second

F = an arbitrary function

$\bar{A}$ = complex constant

ρ_0 = density of medium in grams/centimeter^3

Theory of sound waves *continued*

Specific acoustical impedance $\overline{Z}$ at any point in the medium is the ratio of the pressure phasor to the velocity phasor, or

$$\overline{Z} = \overline{p}/\overline{v} \tag{5}$$

Fig. 2—Table of intensity levels.

type of sound	intensity level in decibels above 10^{-16} watts/centimeter^2	intensity in microwatts/centimeter^2	root-mean-square sound pressure in dynes/centimeter^2	root-mean-square particle velocity in centimeters/second	peak-to-peak particle displacement for sinsuoidal tone at 1000 cycles in centimeters
Threshold of painful sound	130	1000	645	15.5	6.98×10^{-3}
Airplane, 1600 rpm, 18 feet	121	126	228	5.5	2.47×10^{-3}
Subway, local station, express passing	102	1.58	25.5	0.98	4.40×10^{-4}
Noisest spot at Niagara Falls	92	0.158	8.08	0.31	1.39×10^{-4}
Average automobile, 15 feet	70	10^{-3}	0.645	15.5×10^{-3}	6.98×10^{-6}
Average conversational speech 3¼ feet	70	10^{-3}	0.645	15.5×10^{-3}	6.98×10^{-6}
Average office	55	3.16×10^{-5}	0.114	2.75×10^{-3}	1.24×10^{-6}
Average residence	40	10^{-6}	20.4×10^{-3}	4.9×10^{-4}	2.21×10^{-7}
Quiet whisper, 5 feet	18	6.3×10^{-9}	1.62×10^{-3}	3.9×10^{-5}	1.75×10^{-8}
Reference level	0	10^{-10}	2.04×10^{-4}	4.9×10^{-6}	2.21×10^{-9}

Theory of sound waves *continued*

Spherical waves: The solutions of (1) and (3) take particularly simple and instructive forms for the case of one dimensional plane and spherical waves in one direction. Fig. 1 gives a summary of the pertinent information.

For example, the acoustical impedance for spherical waves has an equivalent electrical circuit comprising a resistance shunted by an inductance. In this form, it is obvious that a small spherical source (r is small) cannot radiate efficiently since the radiation resistance $\rho_0 c$ is shunted by a small inductance $\rho_0 r$. Efficient radiation begins approximately at the frequency where the resistance $\rho_0 r$ equals the inductive (mass) reactance $\rho_0 c$. This is the frequency at which the period $(= 1/f)$ equals the time required for the sound wave to travel the peripheral distance $2\pi r$.

Sound intensity

The sound intensity is the average rate of sound energy transmitted in a specified direction through a unit area normal to this direction at the point considered. In the case of a plane or spherical wave, the intensity in the direction of propagation is given by

$$I = p^2/\rho c \quad \text{ergs/second/centimeter}^2 \tag{6}$$

where

p = pressure (dynes/centimeter^2)

ρ = density of the medium (grams/centimeter^3) and

c = velocity of propagation (centimeters/second)

The sound intensity is usually measured in decibels, in which case it is known as the intensity level and is equal to 10 times the logarithm (to the base 10) of the ratio of the sound intensity (expressed in watts/centimeter^2) to the reference level of 10^{-16} watts/centimeter^2. Fig. 2 shows the intensity levels of some familiar sounds.

Sound in gases

The acoustical behavior of a medium is determined by its physical characteristics and, in the case of gases, by the density, pressure, temperature, specific heat, coefficients of viscosity, and the amount of heat exchange at the boundary surfaces.

Sound in gases *continued*

The velocity of propagation in a gas is a function of the equation of state ($PV = RT$ plus higher-order terms), the molecular weight, and the specific heat.*

For small displacements relative to the wavelength of sound, the velocity is given by

$$c = (\gamma p_0/\rho_0)^{1/2} \tag{7}$$

where

γ = ratio of the specific heat at constant pressure to that at constant volume

p_0 = the steady pressure of the gas in dynes/centimeter^2

ρ_0 = the steady or average density of the gas in grams/centimeter^3

The values of the velocity in a few gases are given in Fig. 3 for 0 degrees centigrade and 760 millimeters of mercury barometric pressure.

The velocity of sound c in dry air is given by the following experimentally verified equation

$$c = 33{,}145 \pm 5 \text{ centimeters/second}$$
$$= 1{,}087.42 \pm 0.16 \text{ feet/second}$$

for the audible-frequency range, at 0 degrees centigrade and 760 millimeters of mercury with 0.03-mole-percent content of CO_2.

The velocity in air for a range of about 20 degrees centigrade change in temperature is given by

$$c = 33{,}145 + 60.7T_c \text{ centimeters/second}$$
$$= 1{,}052.03 + 1.106T_f \text{ feet/second}$$

where T_c is the temperature in degrees centigrade and T_f in degrees fahrenheit. For values of T_c greater than 20 degrees, the following formula may be used

$$c = 33{,}145 \times (T_k/273)^{1/2} \text{ centimeters/second}$$

where T_k is the temperature in degrees kelvin.

For other corrections when extreme accuracy is desired, reference should be made to the literature.†

* H. C. Hardy, D. Telfair, and W. H. Pielemeier, "The Velocity of Sound in Air," *Journal of the Acoustical Society of America*, vol. 13, pp. 226–233; January, 1942. See also L. Beranek, "Acoustic Measurements," John Wiley & Sons, Inc., New York, New York; 1949: see p. 46.

† H. C. Hardy, D. Telfair, and W. H. Pielemeier, "The Velocity of Sound in Air," *Journal of the Acoustical Society of America*, vol. 13, pp. 226–233; January, 1942.

Sound in gases *continued*

Fig. 3—Velocity of sound in various gases.*

gas	symbol	velocity in meters/second	velocity in feet/second
Air	—	331.45	1087.42
Ammonia	NH_3	415	1361
Argon	A	319	1046
Carbon monoxide	CO	337.1	1106
Carbon dioxide	CO_2	268.6	881 (above 100 c/s)
Carbon disulfide	CS_2	189	606
Chlorine	Cl	205.3	674
Ethylene	C_2H_4	317	1040
Helium	He	970	3182
Hydrogen	H_2	1269.5	4165
Illuminating gas	—	490.4	1609
Methane	CH_4	432	1417
Neon	Ne	435	1427
Nitric oxide	NO	325	1066
Nitrous oxide	N_2O	261.8	859
Nitrogen	N_2	337	1096
Oxygen	O_2	317.2	1041
Steam (100° C)	H_2O	404.8	1328

* From, "Handbook of Chemistry and Physics," "International Critical Tables," and *Journal of the Acoustical Society of America.*

From (5) and Fig. 1, characteristic impedance is equal to the ratio of the sound pressure to the particle velocity.

$$\bar{Z} = \bar{p}/\bar{v} = \rho_0 c \cos \phi$$

where

For plane waves, $\phi = 0$ and $\cos \phi = 1$

For spherical waves, $\tan \phi = \lambda/2\pi r$

and

λ = wavelength of acoustical wave

r = distance from sound source

For r greater than a few wavelengths, $\cos \phi \approx 1$.

Characteristic impedance $\rho_0 c$ in dyne–seconds/centimeter^3 (rayls) for several gases at 0 degrees centigrade and 760 millimeters of mercury is given in Fig. 4.

Sound in gases *continued*

Fig. 4—Characteristic impedance $\rho_0 c$ for gases.

gas	symbol	$\rho_0 c$
Air	—	42.86
Argon	A	56.9
Carbon dioxide	CO_2	51.1
Carbon monoxide	CO	42.1
Helium	He	17.32
Hydrogen	H_2	11.40
Neon	Ne	38.3
Nitric Acid	NO	43.5
Nitrous oxide	N_2O	51.8
Nitrogen	N_2	41.8
Oxygen	O_2	45.3

Sound in liquids

In liquids, the velocity of sound is given by

$c = (1/K\rho_0)^{1/2}$ centimeters/second

where

K = compressibility in centimeters/second^2/gram and may be regarded as constant

Fig. 5—Velocity of sound in liquids.

liquid	temperature in °C	velocity in (cm/sec) $\times 10^5$
Alcohol, ethyl	12.5	1.24
	20	1.17
Benzene	20	1.32
Carbon disulfide	20	1.16
Chloroform	20	1.00
Ether, ethyl	20	1.01
Glycerin	20	1.92
Mercury	20	1.45
Pentaine	18	1.05
	20	1.02
Petroleum	15	1.33
Turpentine	3.5	1.37
	27	1.28
Water, fresh	17	1.43
Water, sea (36 parts/million salinity)	15	1.505

Sound in liquids *continued*

$K = (47 \times 10^{-9})/981$ for most liquids

Figures for the velocity of sound through some liquids in centimeters/second is given in Fig. 5.

Sound in solids

The velocity of sound in solids is determined by the shape and size of the bounded medium as compared with the wavelength of the excitation. For rods or square bars with unconstrained sides, the velocity of propagation varies with the ratio of thickness to wavelength, being, for a wavelength in diameter, about 0.65 times the zero-diameter-to-wavelength ratio.

Some experimental values are given in Fig. 6.

Fig. 6—Velocity c of sound in longitudinal direction for bar-shaped solids in centimeters/second.*

material	velocity c ($\times 10^5$)	material	velocity c ($\times 10^5$)
Aluminum	5.24	Crystals *continued*	
Antimony	3.40	Rochelle salt (sodium potassium	
Bismuth	1.79	tartrate, $KNaC_4H_4O_6 \cdot 4H_2O$)	
Brass	3.42	45° *Y*-cut	2.47
Cadmium	2.40	45° *X*-cut	2.47
Constantan	4.30	Calcium fluoride (CaF_2, fluorite)	
Copper	3.58	*X*-cut	6.74
German silver	3.58	Sodium chloride (NaCl, rock	
Gold	2.03	salt)	
Iridium	4.79	*X*-cut	4.51
Iron	5.17	Sodium bromide (NaBr)	
Lead	1.25	*X*-cut	2.79
Magnesium	4.90	Potassium chloride (KCl, sylvite)	
Manganese	3.83	*X*-cut	4.14
Nickel	4.76	Potassium bromide (KBr)	
Platinum	2.80	*X*-cut	3.38
Silver	2.64	Glasses	
Steel	5.05	Heavy flint	3.49
Tantalum	3.35	Extra-light flint	4.55
Tin	2.73	Crown	5.30
Tungsten	4.31	Heaviest crown	4.71
Zinc	3.81	Quartz	5.37
Cork	0.50	Granite	3.95
Crystals		Ivory	3.01
Quartz *X*-cut	5.44	Marble	3.81
Ammonium dihydrogen phos-		Slate	4.51
phate ($NH_4H_2PO_4$)		Wood	
45° *Z*-cut	3.28	Elm	1.01
		Oak	4.10

* B. W. Henvis, "Wavelengths of Sound," *Electronics*, vol. 20, pp. 134, 136; March, 1947.

Acoustical and mechanical networks and their electrical analogs*

The present advanced state of the art of electrical network theory suggests its advantageous application, by analogy, to equivalent acoustical and mechanical networks. Actually, Maxwell's initial work on electrical networks was based upon the previous work of Lagrange in dynamical systems. The following is a brief summary showing some of the network parameters available in acoustical and mechanical systems and their analysis using Lagrange's equations.

Fig. 7 shows the analogous behavior of electrical, acoustical, and mechanical systems. These are analogous in the sense that the equations (usually differential equations) formulating the various physical laws are alike.

Lagrange's equations

The Lagrangian equations are partial differential equations describing the stored and dissipated energy and the generalized coordinates of the system. They are

$$\frac{d}{dt}\left(\frac{\partial T}{\partial \dot{q}_v}\right) + \frac{\partial F}{\partial \dot{q}_v} + \frac{\partial V}{\partial q_v} = Q_\nu, \quad (\nu = 1, 2, \ldots, n,) \tag{9}$$

where T and V are, as in Fig. 7, the system's total kinetic and potential energy (in ergs), F is $\frac{1}{2}$ the rate of energy dissipation (in ergs/second, Rayleigh's dissipation function), Q_v the generalized forces (dynes), and q_v the generalized coordinates (which may be angles in radians, or displacements in centimeters). For most systems (and those considered herein) the generalized coordinates are equal in number to the number of degrees of freedom in the systems required to determine uniquely the values of T, V, and F.

Example

As an example of the application of these equations toward the design of electroacoustical transducers, consider the idealized crystal microphone in Fig. 8.

This system has 2 degrees of freedom since only 2 motions, namely the diaphragm displacement x_d and the crystal displacement x_c, are needed to specify the system's total energy and dissipation.

A sound wave impinging upon the microphone's diaphragm creates an excess pressure p (dynes/centimeter^2). The force on the diaphragm is then pA (dynes), where A is the effective area of the diaphragm. The diaphragm has

* E. G. Keller, "Mathematics of Modern Engineering," vol. 2, 1st ed., John Wiley, New York, New York; 1942. Also, H. F. Olson, "Dynamical Analogies," 1st ed., D. Van Nostrand, New York, New York; 1943.

Acoustical and mechanical networks and their electrical analogs *continued*

Fig. 7A—Table of analogous behavior of systems—parameter of energy dissipation (or radiation).

electrical	mechanical	acoustical
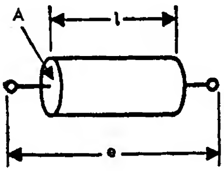	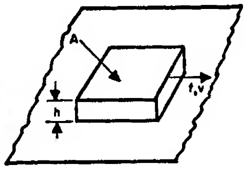	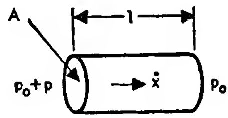
current in wire	viscous damping vane	gas flow in small pipe
$P = Ri^2$ $i = \frac{e}{R} = \frac{dq}{dt} = \dot{q}$ $R = \frac{\rho l}{A}$	$P = R_m v^2$ $v = \frac{f}{R_m} = \frac{dx}{dt} = \dot{x}$ $R_m = \frac{\mu A}{h}$	$P = R_a \dot{X}^2$ $\dot{X} = \frac{p}{R_a} = \frac{dX}{dt}$ $R_a = \frac{8\mu\pi l}{A^2}$
where i = current in amperes e = voltage in volts q = charge in coulombs t = time in seconds R = resistance in ohms ρ = resistivity in ohm-centimeters l = length in centimeters A = cross-sectional area of wire in centimeters^2 P = power in watts	where v = velocity in centimeters/second f = force in dynes x = displacement in centimeters t = time in seconds R_m = mechanical resistance in dyne-seconds/centimeter μ = coefficient of viscosity in poise h = height of damping vane in centimeters A = area of vane in centimeters^2 P = power in ergs/second	where $\dot{X}$ = volume velocity in centimeters^3/second p = excess pressure in dynes/centimeter^2 X = volume displacement in centimeters^3 t = time in seconds R_a = acoustic resistance in dyne-seconds/centimeter^5 μ = coefficient of viscosity in poise l = length of tube in centimeters A = area of circular tube in centimeters^2 P = power in ergs/second

Acoustical and mechanical networks and their electrical analogs *continued*

Fig. 7B—Table of analogous behavior of systems—parameter of energy storage (electrostatic or potential energy).

electrical	mechanical	acoustical
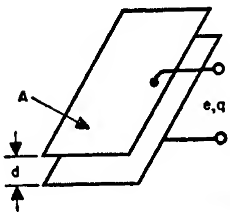	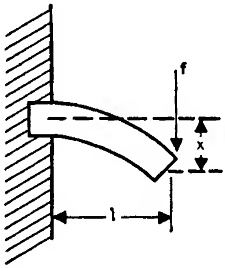	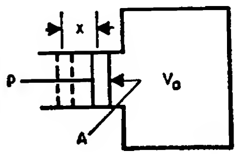
capacitor with closely spaced plates	clamped-free (cantilever beam)	piston acoustic compliance (at audio frequencies, adiabatic expansion)
$W_e = \frac{q^2}{2C} = \frac{Sq^2}{2}$ $q = Ce = \frac{e}{S}$ $C = \frac{kA}{36\pi d} \times 10^{-11}$	$V = \frac{x^2}{2C_m} = \frac{S_m x^2}{2}$ $x = C_m f = \frac{f}{S_m}$ $C_m = \frac{l^3}{3EI}$	$V = \frac{X^2}{2C_a} = \frac{S_a X^2}{2}$ $X = C_a p = \frac{p}{S_a} = xA$ $C_a = \frac{V_o}{c^2 \rho}$
where C = capacitance in farads S = stiffness = $1/C$ W_e = energy in watt-seconds k = relative dielectric constant (= 1 for air, numeric) A = area of plates in centimeters^2 d = separation of plates in centimeters	where C_m = mechanical compliance in centimeters/dyne S_m = mechanical stiffness = $1/C_m$ V = potential energy in ergs E = Young's modulus of elasticity in dynes/centimeter^2 I = moment of inertia of cross-section in centimeters^4 l = length of beam in centimeters	where C_a = acoustical compliance in centimeters^5/dyne S_a = acoustical stiffness = $1/C_a$ V = potential energy in ergs c = velocity of sound in enclosed gas in centimeters/second ρ = density of enclosed gas in grams/centimeter^3 V_o = enclosed volume in centimeters^3 A = area of piston in centimeters^2

Acoustical and mechanical networks and their electrical analogs *continued*

Fig. 7C—Table of analogous behavior of systems—parameter of energy storage (magnetostatic or kinetic energy).

electrical	mechanical	acoustical
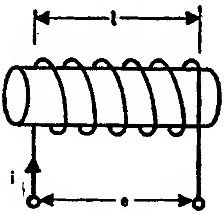 for a very long solenoid	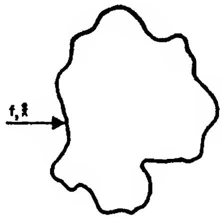 for translational motion in one direction m is the actual weight in grams	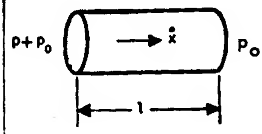 gas flow in a pipe
$W_m = \frac{Li^2}{2}$ $e = L\frac{di}{dt} = L\frac{d^2q}{dt^2} = L\ddot{q}$ $L = 4\pi l n^2 Ak \times 10^{-9}$	$T = \frac{mv^2}{2}$ $f = m\frac{dv}{dt} = m\frac{d^2x}{dt^2} = m\ddot{x}$	$T = \frac{M\dot{X}^2}{2}$ $p = M\frac{d\dot{X}}{dt} = M\frac{d^2X}{dt^2} = M\ddot{X}$ $M = \frac{\rho l}{A}$
where L = inductance in henries W_m = energy in watt-seconds l = length of solenoid in centimeters A = area of solenoid in centimeters^2 n = number of turns of wire/centimeter k = relative permeability of core (= 1 for air, numeric)	where m = mass in grams T = kinetic energy in ergs	where M = inertance in grams/centimeter^4 T = kinetic energy in ergs l = length of pipe in centimeters A = area of pipe in centimeters^2 ρ = density of gas in grams/centimeter^3

Acoustical and mechanical networks and their electrical analogs *continued*

an effective mass m_d, in the sense that the kinetic energy of all the parts associated with the diaphragm velocity $\dot{x}_d$ ($= dx_d/dt$) is given by $m_d\dot{x}_d^2/2$. The diaphragm is supported in place by the stiffness S_d. It is coupled to the crystal via the stiffness S_o. The crystal has a stiffness S_c, an effective mass of m_c (to be computed below), and is damped by the mechanical resistance R_c. The only other remaining parameter is the acoustical stiffness S_a introduced by compression of the air-tight pocket enclosed by the diaphragm and the case of the microphone.

The total potential energy V stored in the system for displacements x_d and x_c from equilibrium position, is

$$V = \tfrac{1}{2}S_d x_d^2 + \tfrac{1}{2}S_a(x_dA)^2 + \tfrac{1}{2}S_c x_c^2 + \tfrac{1}{2}S_o(x_d - x_c)^2 \tag{10}$$

The total kinetic energy T due to velocities $\dot{x}_d$ and $\dot{x}_c$ is

$$T = \tfrac{1}{2}m_c\dot{x}_c^2 + \tfrac{1}{2}m_d\dot{x}_d^2 \tag{11}$$

(This neglects the small kinetic energy due to motion of the air and that due to the motion of the spring S_o). If the total weight of the unclamped part of the crystal is w_c (grams), one can find the effective mass m_c of the crystal as soon as some assumption is made as to movement of the rest of the crystal when its end moves with velocity $\dot{x}_c$. Actually, the crystal is like a transmission line and has an infinite number of degrees of freedom. Practically, the crystal is usually designed so that its first resonant frequency is the highest passed by the microphone. In that case, the end of the crystal moves in phase with the rest, and in a manner that, for simplicity, is here taken as parabolically. Thus it is assumed that an element of the crystal located y centimeters away from its

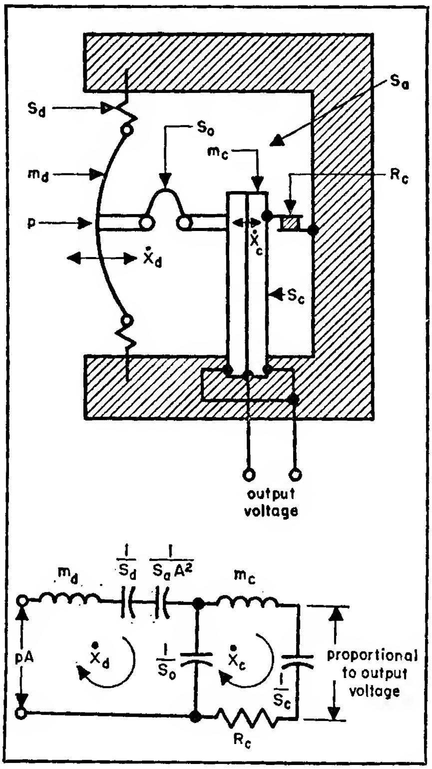

Fig. 8—Crystal microphone analyzed by use of Lagrange's equations.

Acoustical and mechanical networks and their electrical analogs *continued*

clamped end moves by the amount $(y/h)^2x_c$, where h is the length of the crystal. The kinetic energy of a length dy of the crystal due to its velocity of $(y/h)^2\dot{x}_c$ and its mass of $(dy/h)w_c$ is $\frac{1}{2}(dy/h)w_c(y/h)^4\dot{x}_c^2$. The kinetic energy of the whole crystal is the integral of the latter expression as y varies from 0 to h. The result is $\frac{1}{2}(w_c/5)\dot{x}_c^2$. This shows at once that the effective mass of the crystal is $m_c = w_c/5$, i.e., $\frac{1}{5}$ its actual weight.

The dissipation function is $F = \frac{1}{2}R_c\dot{x}_c^2$. Finally, the driving force associated with displacement x_d of the diaphragm is pA. Substitution of these expressions and (10) and (11) in Lagrange's equations (9) results in the force equations

$$\left.\begin{aligned} m_d\ddot{x}_d + S_dx_d + S_oA^2x_d + S_o(x_d - x_c) &= pA \\ m_c\ddot{x}_c + S_o(x_c - x_d) + S_cx_c + R_c\dot{x}_c &= 0 \end{aligned}\right\} \qquad (12)$$

These are the mechanical version of Kirchhoff's law that the sum of all the resisting forces (rather than voltages) are equal to the applied force. The equivalent electrical circuit giving these same differential equations is shown in Fig. 8. The crystal produces, by its piezoelectric effect, an open-circuit voltage proportional to the displacement x_c. By means of this equivalent circuit, it is now easy, by using the usual electrical-circuit techniques, to find the voltage generated by this microphone per unit of sound-pressure input, and also its amplitude- and phase-response characteristic as a function of frequency.

It is important to note that this process of analysis not only results in the equivalent electrical circuit, but also determines the effective values of the parameters in that circuit.

Sound in enclosed rooms*

Good acoustics—governing factors

Reverberation time or amount of reverberation: Varies with frequency and is measured by the time required for a sound, when suddenly interrupted, to die away or decay to a level 60 decibels (db) below the original sound.

The reverberation time and the shape of the reverberation-time/frequency curve can be controlled by selecting the proper amounts and varieties of

* F. R. Watson, "Acoustics of Buildings," 3rd ed., John Wiley and Sons, New York, New York; 1941.

Sound in enclosed rooms *continued*

sound-absorbent materials and by the methods of application. Room occupants must be considered inasmuch as each person present contributes a fairly definite amount of sound absorption.

Standing sound waves: Resonant conditions in sound studios cause standing waves by reflections from opposing parallel surfaces, such as ceiling-floor and parallel walls, resulting in serious peaks in the reverberation-time/frequency curve. Standing sound waves in a room can be considered comparable to standing electrical waves in an improperly terminated transmission line where the transmitted power is not fully absorbed by the load.

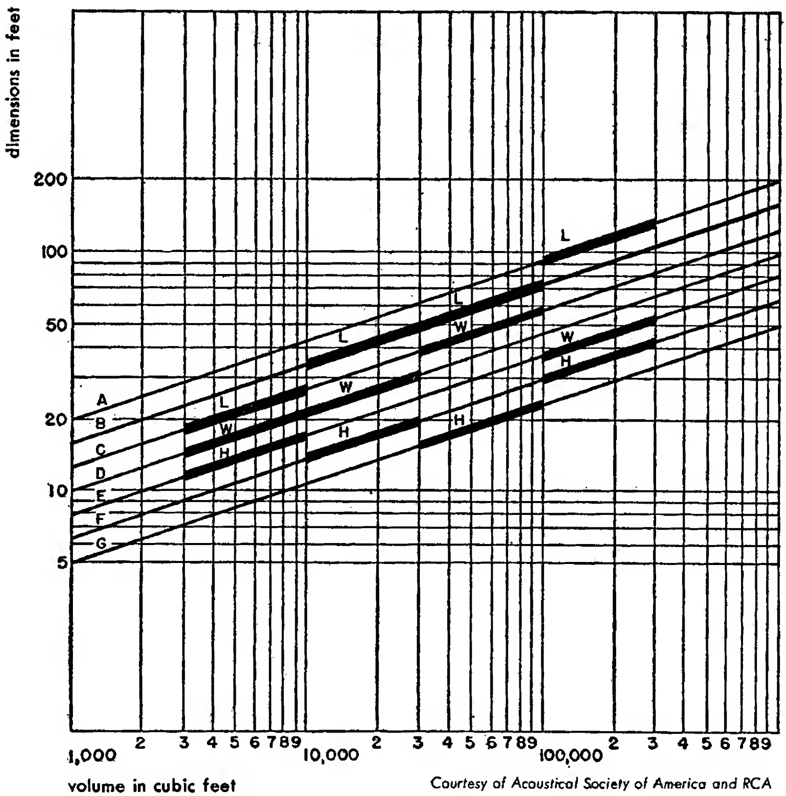

Courtesy of Acoustical Society of America and RCA

type room	H:W:L	chart designation
Small	1:1.25:1.6	E:D:C:
Average shape	1:1.60:2.5	F:D:B:
Low ceiling	1:2.50:3.2	G:C:B:
Long	1:1.25:3.2	F:E:A:

Fig. 9—Preferred room dimensions based on $2^{\frac{1}{3}}$ ratio. Permissible deviation ± 5 percent.

Sound in enclosed rooms *continued*

Room sizes and proportions for good acoustics

The frequency of standing waves is dependent on room sizes: frequency decreases with increase of distances between walls and between floor and ceiling. In rooms with two equal dimensions, the two sets of standing waves occur at the same frequency with resultant increase of reverberation time at resonant frequency. In a room with walls and ceilings of cubical contour this effect is tripled and elimination of standing waves is practically impossible.

The most advantageous ratio for height:width:length is in the proportion of $1:2^{1/3}:2^{2/3}$ or separated by $\frac{1}{3}$ or $\frac{2}{3}$ of an octave.

In properly proportioned rooms, resonant conditions can be effectively reduced and standing waves practically eliminated by introducing numerous surfaces disposed obliquely. Thus, large-order reflections can be avoided by breaking them up into numerous smaller reflections. The object is to prevent sound reflection back to the point of origin until after several re-reflections.

Most desirable ratios of dimensions for broadcast studios are given in Fig. 9.

Optimum reverberation time

Optimum, or most desirable reverberation time, varies with (1) room size, and (2) use, such as music, speech, etc. (see Figs. 10 and 11).

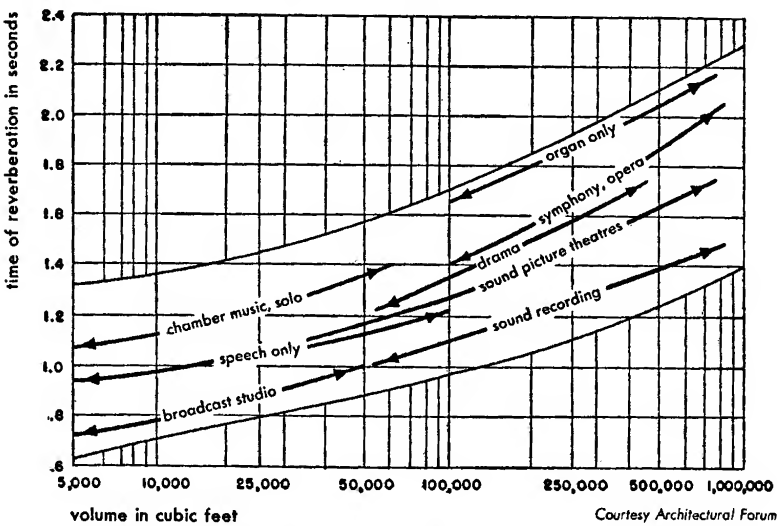

Fig. 10—Optimum reverberation time in seconds for various room volumes at 512 cycles per second.

Sound in enclosed rooms *continued*

These curves show the desirable ratio of the reverberation time for various frequencies to the reverberation time for 512 cycles. The desirable reverberation time for any frequency between 60 and 8000 cycles may be found by multiplying the reverberation time at 512 cycles (from Fig. 10) by the number in the vertical scale which corresponds to the frequency chosen.

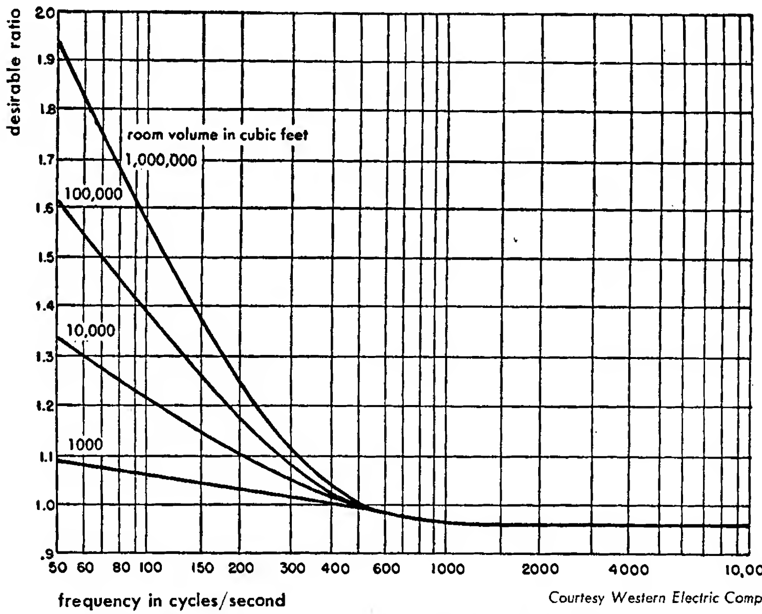

Courtesy Western Electric Company

Fig. 11—Desirable relative reverberation time versus frequency for various structures and auditoriums.

Computation of reverberation time

Reverberation time at different audio frequencies may be computed from room dimensions and average absorption. Each portion of the surface of a room has a certain absorption coefficient a dependent on the material of the surface, its method of application, etc. This absorption coefficient is equal to the ratio of the energy absorbed by the surface to the total energy impinging thereon at various audio frequencies. Total absorption for a given surface area in square feet S is expressed in terms of absorption units, the number of units being equal to $a_{av}S$.

$$a_{av} = \frac{\text{(total number of absorption units)}}{\text{(total surface in square feet)}}$$

Sound in enclosed rooms *continued*

One absorption unit provides the same amount of sound absorption as one square foot of open window. Absorption units are sometimes referred to as "open window" or "OW" units.

$$T = \frac{0.05V}{-S \log_e(1 - a_{av})}$$

where

T = reverberation time in seconds

V = room volume in cubic feet

S = total surface of room in square feet

a_{av} = average absorption coefficient of room at frequency under consideration.

For absorption coefficients a of some typical building materials, see Fig. 12. Fig. 13 shows absorption coefficients for some of the more commonly used materials for acoustical correction.

Fig. 12—Table of acoustical coefficients of materials and persons.*

description	sound absorption coefficients in cycles/second						authority
	128	256	512	1024	2048	4096	
Brick wall unpainted	0.024	0.025	0.031	0.042	0.049	0.07	W. C. Sabine
Brick wall painted	0.012	0.013	0.017	0.02	0.023	0.025	W. C. Sabine
Plaster + finish coat on wood lath—wood studs	0.020	0.022	0.032	0.039	0.039	0.028	P. E. Sabine
Plaster + finish coat on metal lath	0.038	0.049	0.060	0.085	0.043	0.056	V. O. Knudsen
Poured concrete unpainted	0.010	0.012	0.016	0.019	0.023	0.035	V. O. Knudsen
Poured concrete painted and varnished	0.009	0.011	0.014	0.016	0.017	0.018	V. O. Knudsen
Carpet, pile on concrete	0.09	0.08	0.21	0.26	0.27	0.37	Building Research Station
Carpet, pile on ⅛ in felt	0.11	0.14	0.37	0.43	0.27	0.25	Building Research Station
Draperies, velour, 18 oz per sq yd in contact with wall	0.05	0.12	0.35	0.45	0.38	0.36	P. E. Sabine
Ozite ⅜ in	0.051	0.12	0.17	0.33	0.45	0.47	P. E. Sabine
Rug, axminster	0.11	0.14	0.20	0.33	0.52	0.82	Wente and Bedell
Audience, seated per sq ft of area	0.72	0.89	0.95	0.99	1.00	1.00	W. C. Sabine
Each person, seated	1.4	2.25	3.8	5.4	6.6	—	Bureau of Standards, averages of 4 tests
Each person, seated	—	—	—	—	—	7.0	Estimated
Glass surfaces	0.05	0.04	0.03	0.025	0.022	0.02	Estimated

* Reprinted by permission from Architectural Acoustics by V. O. Knudsen, published by John Wiley and Sons, Inc.

Sound in enclosed rooms *continued*

Fig. 13—Table of acoustical coefficients of materials used for acoustical correction.

material	cycles/second 128	256	512	1024	2048	4096	noise-red coef *	manufactured by
Corkoustic—B4	0.08	0.13	0.51	0.75	0.47	0.46	0.45	Armstrong Cork Co.
Corkoustic—B6	0.15	0.28	0.82	0.60	0.58	0.38	0.55	Armstrong Cork Co.
Cushiontone A–3	0.17	0.58	0.70	0.90	0.76	0.71	0.75	Armstrong Cork Co.
Koustex	0.10	0.24	0.64	0.92	0.77	0.75	0.65	David E. Kennedy, Inc.
Sanacoustic (metal) tiles	0.25	0.56	0.99	0.99	0.91	0.82	0.85	Johns-Manville Sales Corp.
Permacoustic tiles ¾ in	0.19	0.34	0.74	0.76	0.75	0.74	0.65	Johns-Manville Sales Corp.
Low-frequency element	0.66	0.60	0.50	0.50	0.35	0.20	0.50	Johns-Manville Sales Corp.
Triple-tuned element	0.66	0.61	0.80	0.74	0.79	0.75	0.75	Johns-Manville Sales Corp.
High-frequency element	0.20	0.46	0.55	0.66	0.79	0.75	0.60	Johns-Manville Sales Corp.
Absorbatone A	0.15	0.28	0.82	0.99	0.87	0.98	0.75	Luse Stevenson Co.
Acoustex 60R	0.14	0.28	0.81	0.94	0.83	0.80	0.70	National Gypsum Co.
Econacoustic 1 in	0.25	0.40	0.78	0.76	0.79	0.68	0.70	National Gypsum Co.
Fiberglas acoustical tiletype TW–PF 9D	0.22	0.46	0.97	0.90	0.68	0.52	0.75	Owens-Corning Fiberglas Corp.
Acoustone D 11/16 in	0.13	0.26	0.79	0.88	0.76	0.74	0.65	U. S. Gypsum Company
Acoustone F 13/16 in	0.16	0.33	0.85	0.89	0.80	0.75	0.70	U. S. Gypsum Company
Acousti-celotex type C–6 1¼ in	0.30	0.56	0.94	0.96	0.69	0.56	0.80	The Celotex Corp.
Absorbex type A 1 in	0.41	0.71	0.96	0.88	0.85	0.96	0.85	The Celotex Corp.
Acousteel B metal facing 1⅝ in	0.29	0.57	0.98	0.99	0.85	0.57	0.85	The Celotex Corp.

Courtesy Acoustics Materials Association

* The noise-reduction coefficient is the average of the coefficients at frequencies from 256 to 2048 cycles inclusive, given to the nearest 5 percent. This average coefficient is recommended for use in comparing materials for noise-quieting purposes as in offices, hospitals, banks, corridors, etc.

Public-address systems*

Electrical power levels for public-address requirements

Indoor power-level requirements are shown in Fig. 14.

Outdoor power-level requirements are shown in Fig. 15.

Note: Curves are for an exponential trumpet-type horn. Speech levels above reference—average 70 db, peak 80 db. For a loudspeaker of 25-percent efficiency, 4 times the power output would be required or an equivalent of 6 decibels. For one of 10-percent efficiency, 10 times the power output would be required or 10 decibels.

* H. F. Olson, "Elements of Acoustical Engineering," 2nd ed., D. Van Nostrand, New York, New York; 1941.

Public-address systems *continued*

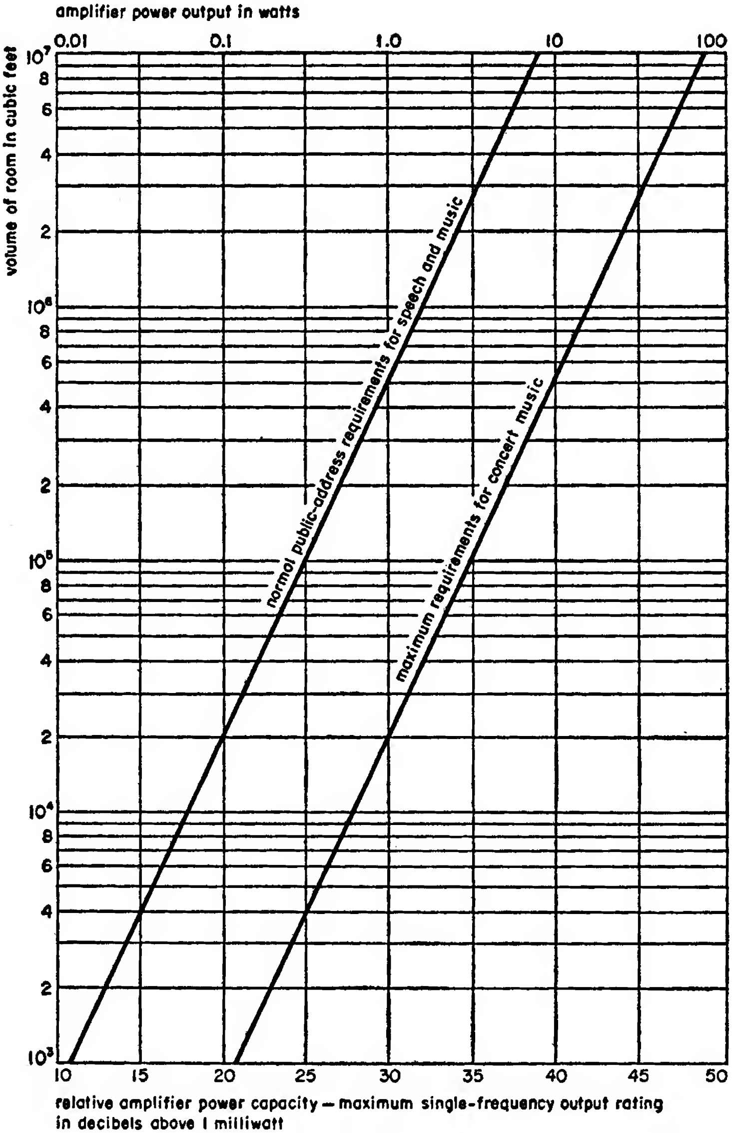

Fig. 14—Room volume and relative amplifier power capacity. To the indicated power level depending on loudspeaker efficiency, there must be added a correction factor that may vary from 4 decibels for the most efficient horn-type reproducers to 20 decibels for less efficient cone loudspeakers.

Public-address systems *continued*

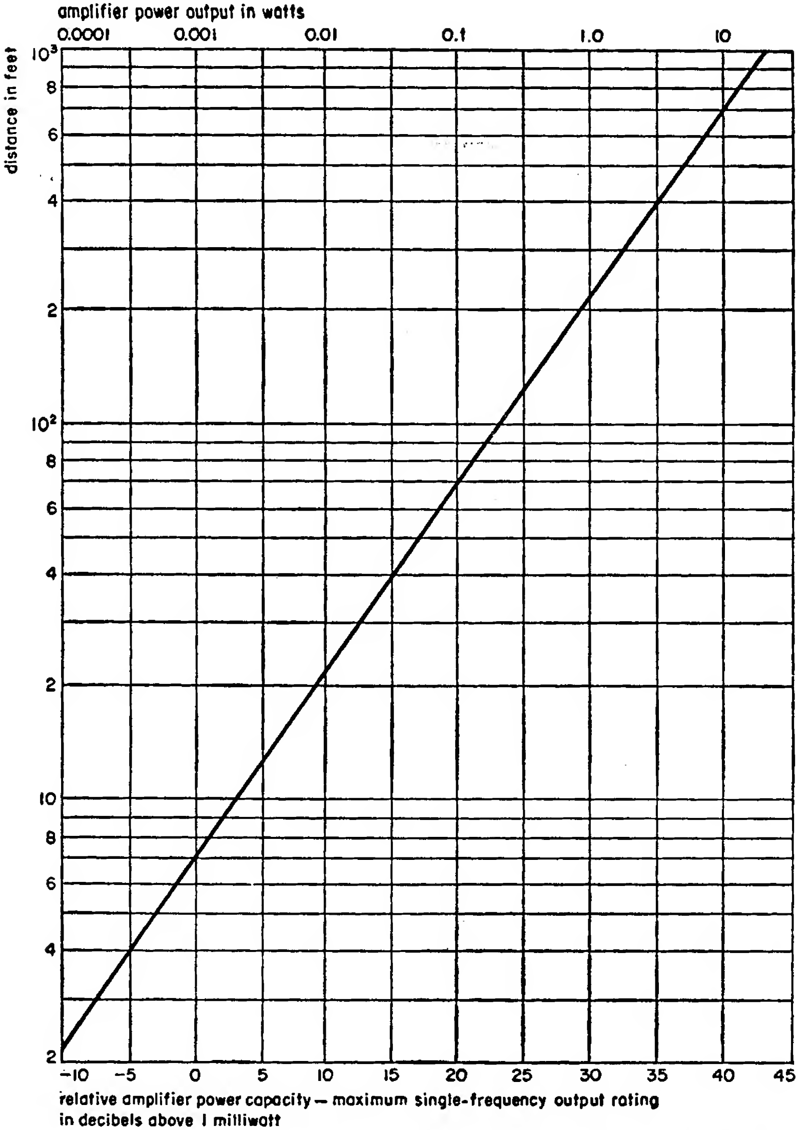

Fig. 15—Distance from loudspeaker and relative amplifier power capacity required for speech, average for 30° angle of coverage. For angles over 30°, more loudspeakers and proportional output power are required. Depending on loudspeaker efficiency, a correction factor must be added to the indicated power level, varying approximately from 4 to 7 decibels for the more-efficient type of horn loudspeakers.

Acoustic spectrum

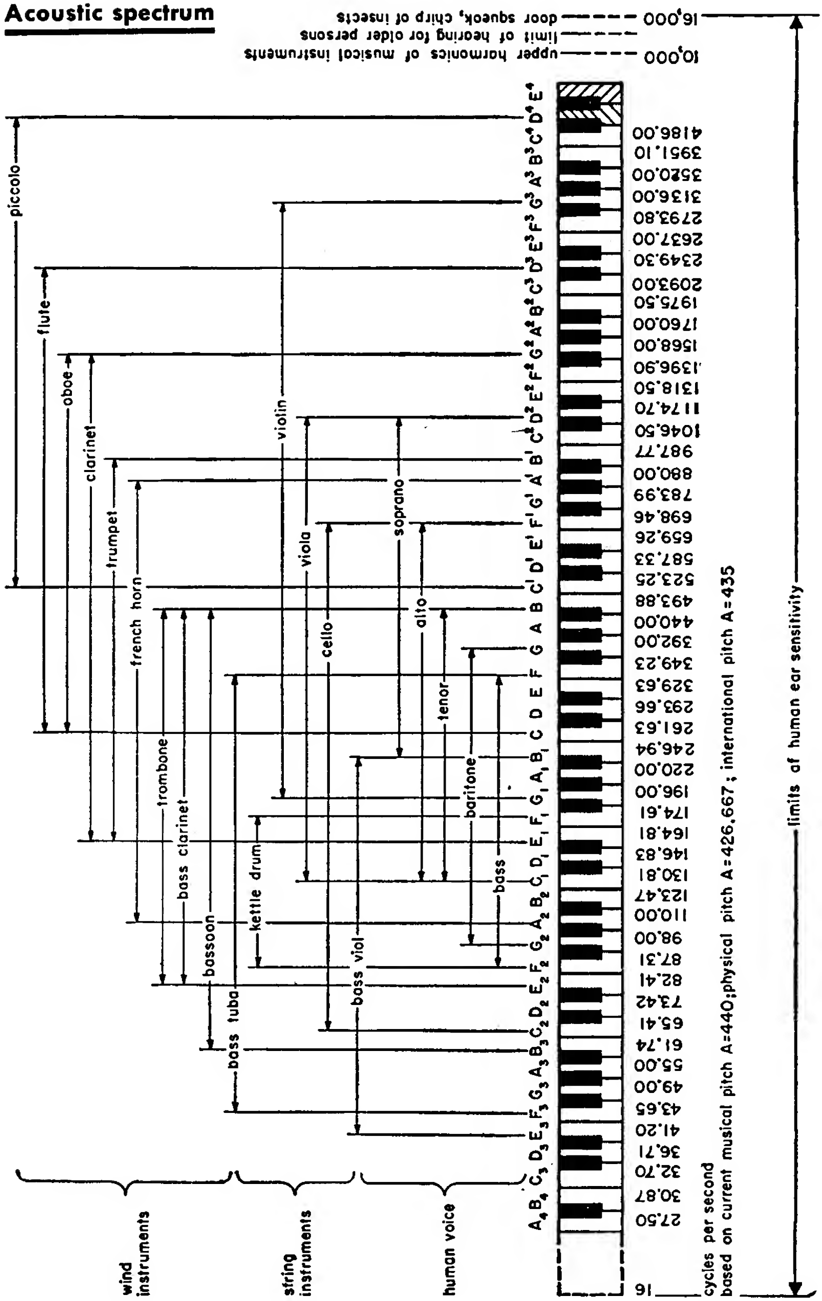

Sounds of speech and music*

A large amount of data are available regarding the wave shapes and statistical properties of the sounds of speech and music. Below are given some of these data that are of importance in the design of transmission systems.

Minimum-discernible-bandwidth changes

Fig. 16 gives the increase in high-frequency bandwidth required to produce a minimum discernible change in the output quality of speech and music.

Fig. 16—Table showing bandwidth increases necessary to give an even chance of quality improvement being noticeable. All figures are in kilocycles.

minus one limen		reference frequency	plus one limen	
speech	music		music	speech
—	—	3	3.0	3.3
3.4	3.3	4	4.8	4.8
4.1	4.1	5	6.0	6.9
4.6	5.0	6	7.4	9.4
5.1	5.8	7	9.3	12.8
5.5	6.4	8	11.0	—
5.8	6.9	9	12.2	—
6.2	7.4	10	13.4	—
6.4	8.0	11	15.0	—
7.0	9.8	13	—	—
7.6	11.0	15	—	—

These bandwidths are known as difference-limen units. For example, a system transmitting music and having an upper cutoff frequency of 6000 cycles would require a cutoff-frequency increase to 7400 cycles before there is a 50-percent chance that the change can be discerned. (Curve *B*, Fig. 17.)

Fig. 17 is based upon the data of Fig. 16. For any high-frequency cutoff along the abscissa, the ordinates give the next higher and next lower cutoff frequencies for which there is an even chance of discernment. As expected, one ob-

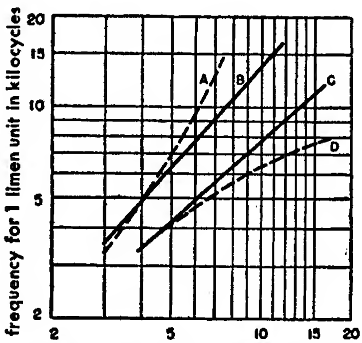

Courtesy of Bell System Technical Journal

Fig. 17 — Minimum-discernible-bandwidth changes. Curves show:

A—Plus 1 limen for speech
B—Plus 1 limen for music
C—Minus 1 limen for music
D—Minus 1 limen for speech

* H. Fletcher, "Speech and Hearing," 1st ed., D. Van Nostrand Company, New York, New York; 1929. S. S. Stevens, and H. Davis, "Hearing," J. Wiley and Sons, New York, New York; 1938.

Sounds of speech and music *continued*

serves that, for frequencies beyond about 4000 cycles, restriction of upper cutoff affects music more appreciably than speech.

Peak factor

One of the important factors in deciding upon the power-handling capacity of amplifiers, loudspeakers, etc., is the fact that in speech very large fluctuations of instantaneous level are present. Fig. 18 shows the peak factor (ratio of peak to root-mean-square pressure) for unfiltered (or wideband) speech, for separate octave bandwidths below 500 cycles, and for separate $\frac{1}{2}$-octave bandwidths above 500 cycles. The peak values for sound pressure of unfiltered speech, for example, rise 10 decibels higher than the averaged root-mean-square value over an interval of $\frac{1}{8}$ second, which corresponds roughly to a syllabic period. However, for a much longer interval of time, say the time duration of one sentence, the peak value reached by the sound pressure for unfiltered speech is about 20 decibels higher than the root-mean-square value averaged for the entire sentence.

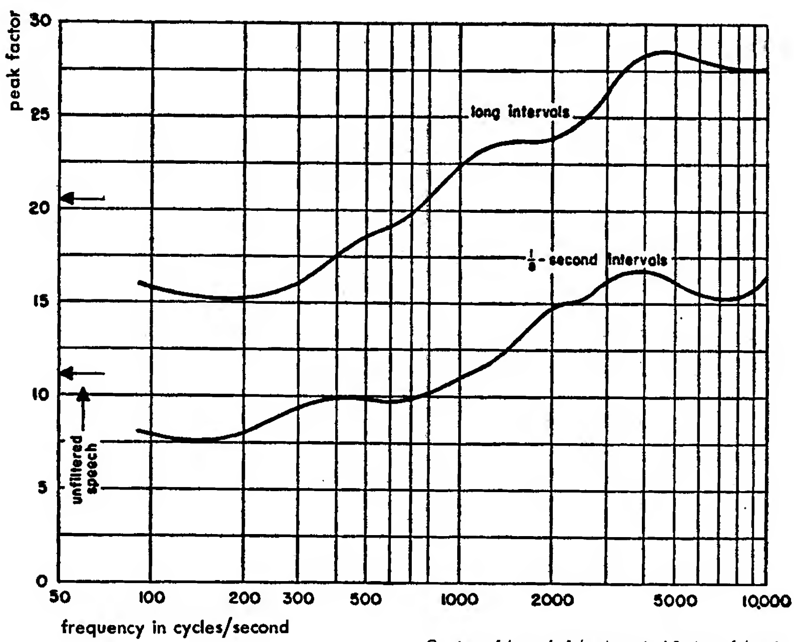

Courtesy of Journal of the Acoustical Society of America

Fig. 18—Peak factor (ratio of peak/root-mean-square pressures) in decibels for speech in 1- and 1/2-octave frequency bands, for 1/8- and 75-second time intervals.

Sounds of speech and music *continued*

Thus, if the required sound-pressure output demands a long-time average of, say, 1 watt of electrical power from an amplifier, then, to take care of the instantaneous peaks in speech, a maximum-peak-handling capacity of 100 watts is needed. If the amplifier is tested for amplitude distortion with a sine wave, 100 watts of peak-instantaneous power exists when the average power of the sine-wave output is 50 watts. This shows that if no amplitude distortion is permitted at the peak pressures in speech sounds, the amplifier should give no distortion when tested by a sine wave of an average power 50 times greater than that required to give the desired long-time-average root-mean-square pressure.

The foregoing puts a very stringent requirement on the amplifier peak power. In relaxing this specification, one of the important questions is what percentage of the time will speech overload an amplifier of lower power than that necessary to take care of all speech peaks. This is answered in Fig. 19; the abscissa gives the probability of the $\frac{\text{(peak)}}{\text{(long-time-average)}}$ powers exceeding the ordinates for continuous speech and white noise. When multiplied by 100, this probability gives the expected percent of time during which peak distortion occurs. If 1 percent is taken as a suitable criterion,

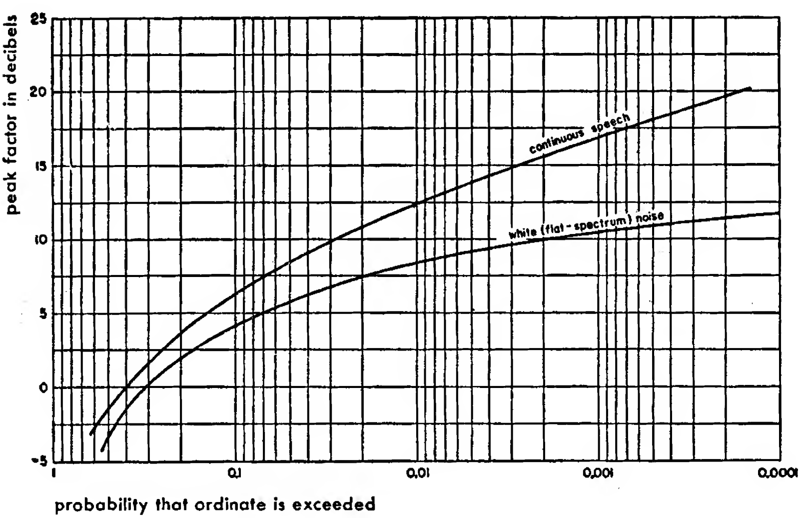

Fig. 19—Statistical properties of the peak factor in speech. The abscissa gives the probability (ratio of the time) that the peak factor in the uninterrupted speech of one person exceeds the ordinate value. Peak factor = (decibels instantaneous peak value) — (decibels root-mean-square long-time average).

Sounds of speech and music *continued*

then a 12-decibel ratio of $\frac{\text{(peak)}}{\text{(long-time-average)}}$ powers is sufficient. Thus, the amplifier should be designed with a power reserve of 16 in order that peak clipping may occur not more than about 1 percent of the time.

Speech-communication systems

In many applications of the transmission of information by speech sounds, a premium is placed on intelligibility rather than flawless reproduction. Especially important is the reduction of intelligibility as a function of both the background noise and the restriction of transmission-channel bandwidth. Intelligibility is usually measured by the percentage of correctly received monosyllabic nonsense words uttered in an uncorrelated sequence.

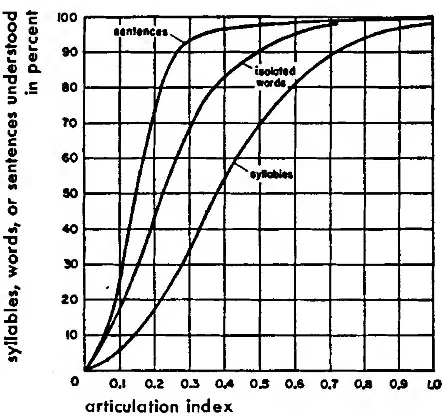

Fig. 20—Relations between various measures of speech intelligibility. Relations are approximate; they depend upon the type of material and the skill of the talkers and listeners.

This score is known as syllable articulation. Because the sounds are nonsense syllables, one part of the word is entirely uncorrelated with the remainder, so it is not consistently possible to guess the whole word correctly if only part of it is received intelligibly. Obviously, if the test speech were a commonly used word, or say a whole sentence with commonly used word sequences, the score would increase because of correct guessing from the context. Fig. 20 shows the inter-relationship between syllable, word, and sentence articulation. Also given is a quantity known as articulation index.

The concept and use of articulation index is obtained from Fig. 21. The abscissa is divided into 20 bandwidths of unequal frequency interval. Each of these bands will contribute 5 percent to the articulation index when the speech spectrum is not masked by noise and is sufficiently loud to be above the threshold of audibility. The ordinates give the root-mean-square peaks and minimums (in $\frac{1}{8}$-second intervals), and the average sound pressures created at 1 meter from a speaker's mouth in an anechoic (echo-free) chamber. The units are in decibels pressure per cycle relative to a pressure

Speech-communication systems *continued*

of 0.0002 dynes/centimeter^2. (For example, for a bandwidth of 100 cycles, rather than 1 cycle, the pressure would be that indicated plus 20 decibels; the latter figure is obtained by taking 10 times logarithm (to the base 10) of the ratio of the 100-cycle band to the indicated band of 1 cycle.)

An articulation index of 5 percent results in any of the 20 bands when a full 30-decibel range of speech-pressure peaks to speech-pressure minimums is obtained in that band. If the speech minimums are masked by noise of a higher pressure, the contribution to articulation is accordingly reduced to a value given by $\frac{1}{6}$ [(decibels level of speech peaks) − (decibels level of average noise)]. Thus, if the average noise is 30 decibels under the speech peaks, this expression gives 5 percent. If the noise is only 10 decibels below the speech peaks, the contribution to articulation index reduces to $\frac{1}{6} \times 10 = 1.67$ percent. If the noise is more than 30 decibels below the speech peaks, a value of 5 percent is used for the articulation index. Such a computation is made for each of the 20 bands of Fig. 21, and the results are added to give the expected articulation index.

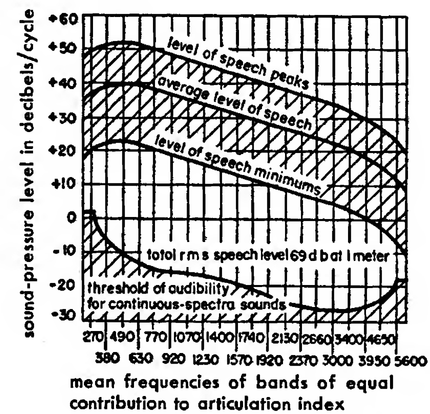

Courtesy of *Proceedings of the I.R.E.*

Fig. 21—Bands of equal articulation index. 0 decibels = 0.0002 dyne/centimeter^2.

A number of important results follow from Fig. 21. For example, in the presence of a large white (thermal-agitation) noise having a flat spectrum, an improvement in articulation results if pre-emphasis is used. A pre-emphasis rate of about 8 decibels/octave is sufficient.

Speech clipping

While the presence of peak clipping is detectable as distortion, particularly with consonants, the articulation is not appreciably affected by even large amounts of peak clipping.* The deterioration from clipping is determined

* J. C. R. Licklider and I. Pollack, "Effects of Differentiation, Integration, and Infinite Peak Clipping upon the Intelligibility of Speech," *Journal of the Acoustical Society of America*, vol. 20, pp. 42–51; January, 1946.

Speech-communication systems *continued*

apparently by the masking and smearing caused by the intermodulation frequencies produced by the nonlinear clipping circuit. Consequently, the articulation after clipping depends on whether the higher frequencies are preferentially amplified before (differentiation) or attenuated (similar to integration).

The articulation resulting from sequences of clipping, differentiation, and integration in various orders are shown in Fig. 22.

A—No distortion
B—Differentiation
C—Integration
D—Differentiation and clipping
E—Differentiation, clipping, and integration
F—Clipping and integration
G—Clipping
H—Clipping and differentiation
I—Integration and clipping
J—Integration, clipping, and differentiation

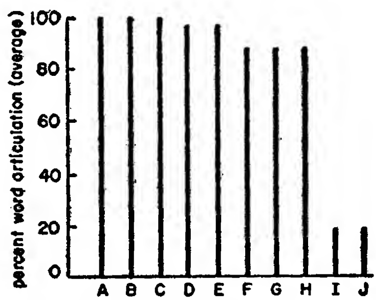

Courtesy of Journal of the Acoustical Society of America.

Fig. 22—Effects of various types of distortion on intelligibility of speech. The column diagram indicates the over-all averages for each of the 10 circuit arrangements.

Loudness

Equal loudness contours: Fig. 23 gives average hearing characteristics of the human ear at audible frequencies and at loudness levels of zero to 120 decibels versus intensity levels expressed in decibels above 10^{-16} watt per square centimeter. Ear sensitivity varies considerably over the audible range of sound frequencies at various levels. A loudness level of 120 decibels is heard fairly uniformly throughout the entire audio range but, as indicated in Fig. 23, a frequency of 1000 cycles at a 20-decibel level will be heard at very nearly the same intensity as a frequency of 60 cycles at a 60-decibel level. These curves explain why a loudspeaker operating at lower-than-normal-level sounds as though the higher frequencies were accentuated and the lower tones seriously attenuated or entirely lacking; also, why music, speech, and other sounds, when reproduced, should have very nearly the same intensity as the original rendition. To avoid perceptible deficiency of lower tones, a symphony orchestra, for example, should be reproduced at an acoustical level during the loud passages of 90 to 100 decibels.

Loudness *continued*

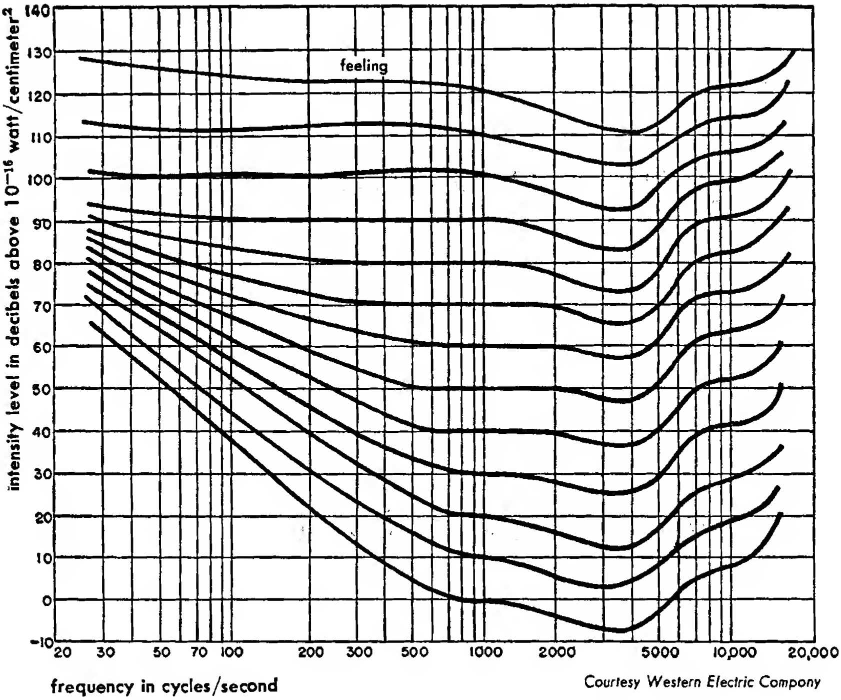

Fig. 23—Equal loudness contours.

Digital computers

Definition

A digital computing machine is a device employing numbers composed of digits or discrete units (integers) in the representation of quantities undergoing manipulation in the computing process. Numbers being symbolic representations of quantity, the computer is designed to manipulate these symbols in a logical manner so as to produce a symbolic representation of the logical result. The precision with which a result may be defined is proportional to the number of digits the machine can handle, provided the manipulations are performed accurately.

Numbers

A number is a quantity represented by an ordered group of symbols or digits.

A number system is made up of an ordered set of symbols, each representing an integer.

The number of individual symbols in a number system, including the representation for zero, is called the *radix* of the system. The relationship between a number N, the digits d and the radix R can be expressed by the following equation:

$$N = d_1 + d_2R + d_3R^2 + d_4R^3 + \dots d_nR^{n-1}$$

It is usual practice to write the digits of a number in decreasing order of significance as one reads from left to right. Thus a number expressed in the decimal system (radix 10) appears as:

$$1856 = (1 \times 10^3) + (8 \times 10^2) + (5 \times 10) + (6 \times 10^0)$$

Similarly the number 110110 expressed in the binary system (radix 2) appears as:

$$N = (1 \times 2^5) + (1 \times 2^4) + (0 \times 2^3) + (1 \times 2^2) + (1 \times 2^1) + (0 \times 2^0) = 54$$

Choice of radix

Computers may be built employing virtually any radix but only a very few radixes are considered significant from the standpoint of computer design. If the assumption is made that the number of electron tubes or quantity of apparatus necessary to represent a number is proportional to the radix used, it can be shown that a minimum number of elements will be required

Choice of radix *continued*

if the radix $R = e = 2.71828$. It is difficult to conceive an arithmetic built on such a radix. Since the assumption is tenuous at best, and if, as in many practical cases, the apparatus used is capable of assuming either of 2 stable conditions (as in relays, flip–flops, punched cards, punched tape, etc.), there is no radix more economical than radix 2, since none of the possible stable states is wasted. Radixes 4, 8, and 16 would be similarly economical.

In electronic machines, the usual method is to represent the 10 decimal digits by means of some form of binary code. Four binary symbols are required to represent all of the 10 symbols of the decimal system. Some computers have input and output devices that work in the decimal system, but have internal machinery and arithmetic units that operate in the binary system. The conversion is made internally before the computation is performed and the result is translated back into decimal notation upon completion of the computation. A certain amount of time is taken for the conversions, but this time is short compared to the time required to operate mechanical printing devices that are frequently used as outputs.

Coding

A code is a system of representation of a set of symbols by means of another different set of symbols.

A binary code consists of the two symbols, one and zero. It should be distinguished from a number system based on radix 2, since the element of position is not necessarily weighted in a code as it is in a number system. This difference is illustrated in Fig. 1, where the decimal number 347 is expressed as a binary number, as a binary coded decimal (radix 10), and as a binary coded octal (radix 8).

All of these numbers are representations of the same physical quantity. Because of the widespread use of the decimal system of numbers and because of the fact that most of the physical apparatus of computers is inherently binary or works best in a binary fashion (as in detecting the presence or absence of signal, the on or off condition of a tube, or the open or closed position of a relay), it has become common practice to represent the symbols of the decimal system in some form of binary code.

Fig. 1—Expression of a number in different codes.

system	code
Decimal	347
Binary (radix 2)	101011011
Binary coded decimal	0011 0100 0111
Binary coded octal	101 011 011
Octal (radix 8)	533

Since there are more than 2^3 symbols to be represented, it is

Coding *continued*

necessary that the binary representation of each decimal symbol employ a minimum of 4 binary symbols (the term *binary digit* or *bit* is frequently used) to avoid ambiguity. Also, since there are 16 possible combinations of the 4 binary symbols representing the decimal numbers in such a case and since any one of the combinations may be used to represent any decimal symbol, the number of possible codes is $16!/6!$, or slightly less than 3×10^{10}.

Fig. 2 shows the representation of the 10 decimal symbols 0 through 9 in a 4-bit code.

Fig. 2—Conversion of decimal system into binary code.

character	binary coded representation
0	0000
1	0001
2	0010
3	0011
4	0100
5	0101
6	0110
7	0111
8	1000
9	1001

Fig. 3—The excess-3 code.

character	excess-3 binary coded representation
0	0011
1	0100
2	0101
3	0110
4	0111
5	1000
6	1001
7	1010
8	1011
9	1100

In some applications it is not desirable to have the symbol 0 represented by the absence of signal, since it cannot then be distinguished from lost signals. This is avoided by choosing 10 of the possible representations that do not include the position 0000. Such a code is given in Fig. 3. This code uses the binary notation for 3 as the representation for 0. Each of the other 9 symbols is represented by the binary equivalent of the symbol plus 3. For that reason, it is known as an "excess-3" code. It has the further property that it is "self-complementing"; that is, the 9's complement of the decimal symbol is formed by changing 1's to 0's and the 0's to 1's in the coded representation of the symbol. This property is useful in performing many of the arithmetic operations within the computer.

The code given in Fig. 4 is one of a group of codes that is frequently used when mechanical analogs (position, shaft rotation, etc.) are converted into digital form for computer input purposes or for recording. This type of code obtains its usefulness from the property that one and only one digit

Coding *continued*

of the code changes in proceeding to the next higher or next lower number. The code shown is known as a reflected binary code, because of the inverted sequence in which the binary symbol 1 and 0 are used. Its conversion into the usual binary number is trivially easy. It will be noted that the most significant digit is the same as the binary number; a comparison is then made with the digit at the next least significant position; if the two are alike, the digit in that position in the binary number is a 0; if the two are unlike, the digit in that position in the binary number is a 1. This digit in the binary number is then compared with the next least significant position in the reflected code. Again if the two are alike, the digit in that position in the binary number is a 0; if the two are unlike, it is a 1. The operation is diagramed in Fig. 5. An electronic circuit for making the conversion is shown in Fig. 6.

Fig. 4—The reflected binary code.

character	reflected binary representation
0	0000
1	0001
2	0011
3	0010
4	0110
5	0111
6	0101
7	0100
8	1100
9	1101

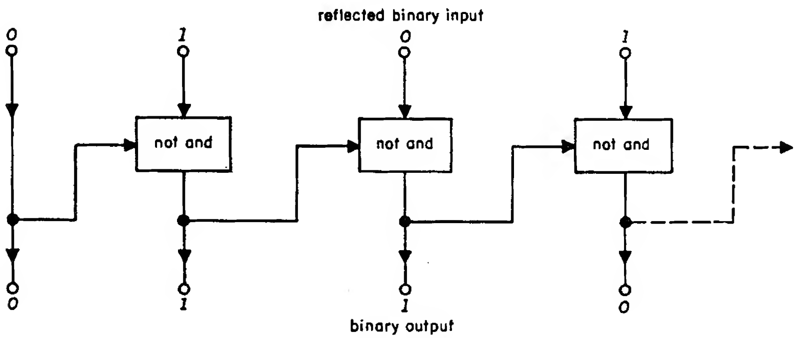

Fig. 5—Sequence for comparing binary and reflected binary codes.

The code given in Fig. 7 is a reflected binary, excess-3 representation of the 10 decimal symbols. This code, when converted into binary number, yields the binary excess-3 code given in Fig. 3. It has the property that only one digit change is required in advancing from the 9 to 0 representation, and that change occurs in the most significant position. This is a useful property for many applications.

continued **Coding**

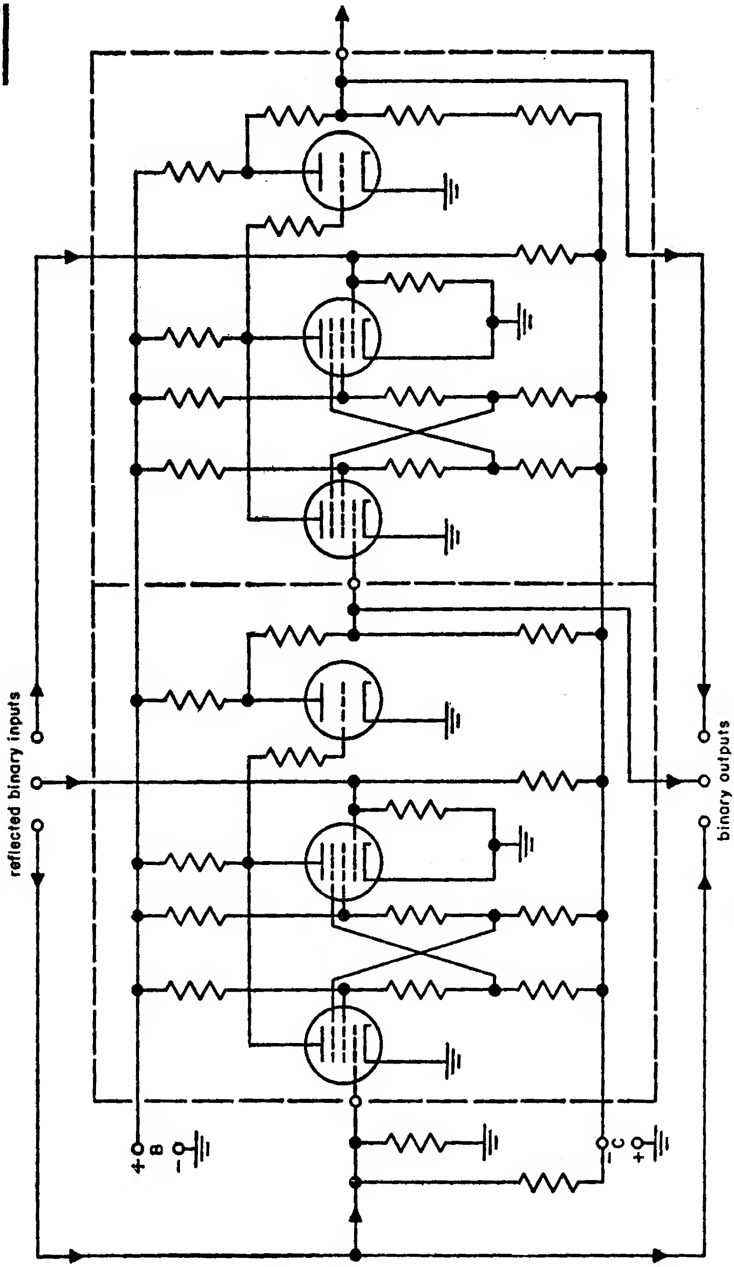

Fig. 6—Circuit for converting from reflected binary to binary code.

Coding *continued*

Computers in business applications particularly may be required to handle information other than numbers. To encode all of the letters of the alphabet plus all of the arabic numerals requires a minimum of 6 binary digits if ambiguity is to be avoided. A typical code of this type is given in Fig. 8.

Fig. 7—Reflected binary, excess-3 code.

character	reflected binary, excess-3 representation
0	0010
1	0110
2	0111
3	0101
4	0100
5	1100
6	1101
7	1111
8	1110
9	1010

Fig. 9—Code including check bits.

character	code
0	0010 001
1	0110 000
2	0111 001
3	0101 000
4	0100 001
5	1100 000
6	1101 001
7	1111 000
8	1110 001
9	1010 000

Fig. 8—Code including alphabet for business-machine applications.

character	coded representation	character	coded representation
0	0010 00	J	0110 01
1	0110 00	K	0111 01
2	0111 00	L	0101 01
3	0101 00	M	0100 01
4	0100 00	N	1100 01
5	1100 00	O	1101 01
6	1101 00	P	1111 01
7	1111 00	Q	1110 01
8	1110 00	R	1010 01
9	1010 00	S	0111 10
A	0110 11	T	0101 10
B	0111 11	U	0100 10
C	0101 11	V	1100 10
D	0100 11	W	1101 10
E	1100 11	X	1111 10
F	1101 11	Y	1110 10
G	1111 11	Z	1010 10
H	1110 11		
I	1010 11		

Coding *continued*

Additional bits are frequently used for the purpose of providing a check against errors. The 7-bit codes used in the Univac and the IBM machines are of this type. They are so constructed that the total number of 1's in the code for any character is either always odd or always even. For example, in the code of Fig. 8, a check bit (for even check) would make the code appear as in Fig. 9.

Switching circuits

In the circuits shown in Fig. 10, the following notation applies:

Only one of two states is permissible (1 or 0)

The $+$ symbol should be read "or"

The $\times$ symbol should be read "and"

Thus,

$A + B = A$ or B

$A \times B = A$ and B

$AB = A$ and B

$A(B + C) = A$ and either B or C

Since 1 and 0 are the only permissible representations, if

$A = 1$ and $B = 1$

Then:

$A + B = 1$	$A \times B = 1$
$A + 0 = 1$	$A \times 0 = 0$
$0 + B = 1$	$0 \times B = 0$

These functions are commutative and associative.

The zero or negative is written $\overline{A}$, read, "not A".

Thus,

$\overline{A} \times B = 0$

$\overline{A} \times \overline{B} = 0$

Switching circuits *continued*

Fig. 10—Typical computer circuits.

circuit	symbol
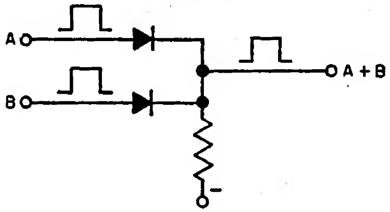 **A.** Logical "or" circuit using diodes.	
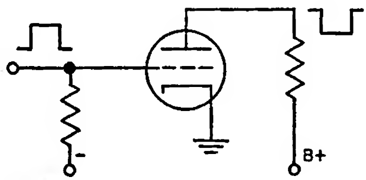 **B.** Inverter.	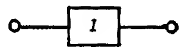
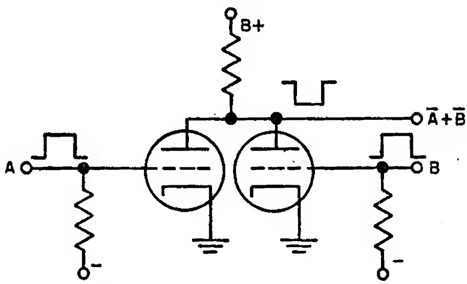 **C.** Logical "or" combined with inverter.	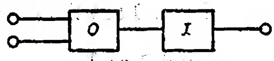
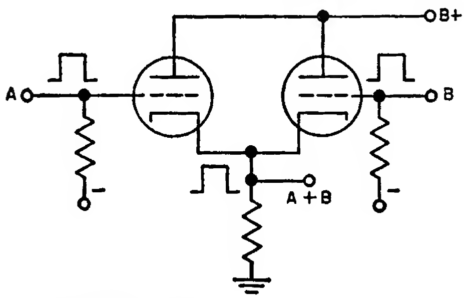 **D.** Logical "or" using dual triode.	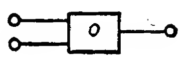

Switching circuits *continued*

Fig. 10—*Continued*

circuit	symbol

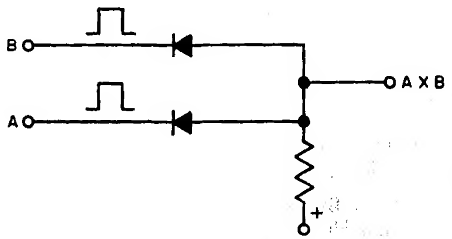

E. Logical "and" circuit using diodes.

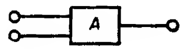

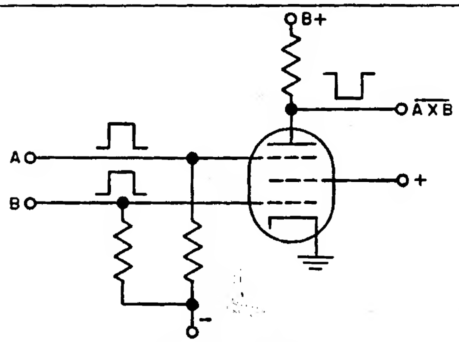

F. Logical "and" combined with inverter.

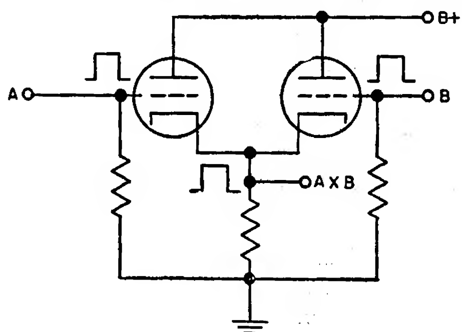

G. Logical "and" circuit using dual triode.

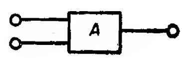

Nuclear physics

General

Atoms consist of a dense core or nucleus of particles surrounded by a "cloud" of negative electrons. The nucleus, the bulk of the atomic mass, has a radius of the order of 10^{-13} centimeter, as compared with 10^{-8} centimeter for the electronic shell. The nuclear particles are held together by forces very different from the well-known gravitational and electric forces: they are many orders of magnitude greater and come into play only when the interacting particles are extremely close together.

Detection of effects involving this combination of short distance and powerful force necessitates the use of tools of corresponding smallness: waves of extremely short wavelength (*X* rays, gamma rays) or nuclear particles themselves. Bombarding particles of this kind occur naturally as cosmic rays or are produced artificially by high-energy particle accelerators.

Fundamental particles

Fig. 1 is a table of subatomic particles based on present (1956) knowledge. The following are explanations of their constitution and qualities.

Electron: A particle with negative electric charge. Beta (β) particles emitted by certain radioactive materials are high-speed electrons. The electron mass is 9.1×10^{-28} gram.

Proton: A particle possessing a positive electric charge and a mass 1836 times the mass of an electron. The nucleus of a hydrogen atom consists of a single proton.

Neutron: A particle, electrically neutral, with mass slightly greater than that of a proton. In simplified form, the atom has been pictured as a relatively compact nucleus built up of protons and neutrons surrounded by a cloud of electrons whose number is equal to the number of protons in the nucleus. Uranium^{238}, for instance, contains 92 protons (balanced by its 92 electrons) and 146 neutrons. The chemical properties of the atom are determined only by the number and arrangement of the extranuclear electrons. The term *nucleon* is used to refer to either the neutron or proton when it is not necessary to distinguish between them.

Photon: Although electromagnetic disturbances (*X* rays, radio waves, heat rays, light, etc.) behave like waves, their energy is transmitted in discrete bundles called photons. The energy E ergs carried by each photon is related to the frequency ν cycles per second of the associated wave by $E = h\nu$ where h = Planck's constant = 6.62×10^{-27} erg–seconds. The high-energy photons emitted by some radioactive materials are called gamma (γ) rays.

Fig. 1—Table of the fundamental particles (1956).* continued

Fundamental particles

general classification	particle	symbol	charge	mass	equivalent energy mc^2 in (mev)	spin	mean life in seconds
	Photon	γ	0	0	0	1	∞
	Neutrino	ν	0	0	0	1/2	∞
	Electron	e	+, −	1	0.511	1/2	∞
Light mesons (*L* particles)	μ-meson	μ	+, −	206	105.3	1/2	$(2.22 \pm 0.02) \times 10^{-6}$
	Charged π meson	π	+, −	272.5	139.2	0	$(2.5 \pm 0.1) \times 10^{-8}$
	Neutral π meson	π^0	0	264	134.8	0	$\leqslant 5 \times 10^{-15}$
Heavy mesons (*K* particles)	$K_{\pi 3}$ particle or τ meson	τ	+, −	964 ± 3	493	Integer	$\approx 10^{-8}$
	$K_{\pi 2}$ particle or χ meson	χ	+, −	963 ± 5	492	Integer	10^{-8}
	$K_{\mu 2}$ particle	$K_{\mu 2}$	+ (−)	960 ± 5	490	Integer	$0.81 \pm 0.07 \times 10^{-8}$
	$K_{\mu 3}$ particle or κ meson	κ	+ (−)	952 ± 9	486	?	$\approx 10^{-8}$
	K_{e3} particle	K_{e3}	+ (−)	980 ± 25	500	?	$> 10^{-9}$
	θ^0 particle	θ^0	0	964 ± 10	492	Integer	$(1.5 \pm 0.5) \times 10^{-10}$
	(Neutral τ meson)	τ^0	0	?	?	Integer	?
Nucleons	Proton	p	+, −	1836.1	938.2	1/2	—
	Neutron	n	0	1838.6	939.5	1/2	$1.08 \times 10^3 \pm 240$
Hyperons	Λ^0 particle	Λ^0	0	2181 ± 2	1115 ± 1	Half integer	$(3.7 \pm 0.6) \times 10^{-10}$
	Σ particle	Σ	+, −	2327 ± 4	1189 ± 2	Half integer	$\approx 10^{-10}$
	(Neutral Σ particle)	(Σ^0)	0	?	?	(Half integer)	$\ll 10^{-10}$
	Cascade particle	Ξ	—	≈ 2583	≈ 1320	Half integer	$\approx 10^{-10}$

* Courtesy of B. B. Rossi.

Fundamental particles *continued*

Neutrino: A particle with negligible mass. The neutrino was hypothesized to account for certain features in the emission of the high-speed electrons—β particles—from radioactive nuclei. When a β-emitting nucleus disintegrates, it creates both an electron and a neutrino. The neutrino has never been detected directly, but its properties have been fairly well established by indirect experiment.

Positron: A particle with the same mass as an electron but having positive electric charge. Positrons do not exist in normal atoms. They may appear in radioactive decay or be materialized when high-energy photons interact with nuclei. The ultimate fate of every positron is its conversion into electromagnetic energy.

Negative proton: A particle with the same mass as the proton but having negative electrical charge. Like positrons, negative protons do not occur naturally but are produced as a result of high-energy interactions. They are converted into electromagnetic energy when they encounter normal protons.

Meson: Mesons are observed among the products of nuclear disintegration when very-high-energy particles strike nuclei. Most prominent of the meson family are the pi (π) and mu (μ) mesons. Three kinds of π mesons exist. Two are electrically charged ($\pm$) and decay into the lighter μ meson about 10^{-8} second after their formation. The third has no charge and decays into two photons. The μ meson is also unstable and decays into an electron and two neutrinos about 10^{-6} second after it appears.

Heavy elementary particles: Approximately a dozen different particles of this kind have been identified, classed as hyperons and heavy mesons; all are unstable, some being so short-lived that they decay even while in flight.

Deuteron; α particle: These "particles" are nuclei of deuterium and of helium, respectively. The deuteron consists of 1 proton and 1 neutron; the alpha (α) particle of 2 protons and 2 neutrons. The latter is a particle emitted by some naturally radioactive materials. Both are used as bombarding particles in high-energy accelerators.

Terminology

Atomic nucleus: Consists of protons and neutrons, Z and N in number. The number of protons Z is referred to as the *atomic number.*

Nuclear charge: Carried by the protons, each of which has charge $e = 1.6 \times 10^{-19}$ coulomb.

Mass number: An integer A equal to the total number of neutrons and protons in the nucleus. $A = N + Z$. The complete symbolic representation

Terminology *continued*

of a nucleus is ${}_ZX^A$ where X is the appropriate chemical symbol: carbon, with 6 protons and 6 neutrons, is written ${}_6C^{12}$.

Atomic mass unit, (amu): A unit of mass equal to 1.660×10^{-24} gram and equivalent to the mass of each of the particles of a fictitious substance whose molecular weight is 1 gram. One atomic mass unit is approximately the mass of the neutron or proton.

Isotopes: Nuclei with common Z. Isotopes are chemically indistinguishable: the three naturally occurring isotopes of oxygen are ${}_8O^{16}$, ${}_8O^{17}$, and ${}_8O^{18}$. Nuclei with common A are called *isobars;* with common N, *isotones*.

Mass defect: The masses of nuclei are less than the sum of the masses of their separated constituent neutrons and protons. The difference is the mass defect: the proton and neutron masses are respectively 1.6723×10^{-24} and 1.6746×10^{-24} gram, whereas the mass of the deuteron is 3.3430×10^{-24} gram; the mass defect of the deuteron is thus 0.0039×10^{-24} gram.

Binding energy: The energy required to separate all of the component neutrons and protons of the nucleus is called the total nuclear binding energy B. Binding energy and mass defect are equivalent according to the relativistic mass–energy relation. The fraction B/A is approximately 8×10^6 electron–volts for all but extremely light nuclei and represents on the average the energy required to remove a single neutron or proton from a nucleus.

Electron–volt: A unit convenient for representing the energy of charged particles accelerated by electric fields. The electron–volt (ev) is equal to 1.6×10^{-19} joule and is the kinetic energy acquired by a particle bearing one unit of electric charge (1.6×10^{-19} coulomb) that has been accelerated through a potential difference of 1 volt. According to the relativistic mass–energy equation 1 (amu) = 931 (mev), where 1 (mev) = 10^6 (ev).

Fission; fusion: The breakup of nuclei into nuclear fragments that are themselves nuclei is fission. The coalescing of two nuclei to form a heavier one is fusion. The mass defect for middle-weight nuclei is greater than that of light or heavy nuclei; light and heavy nuclei in general both have nucleons of average weights greater than those of medium-weight nuclei into which they might fission or fuse. Thus, when uranium breaks into its fission fragments, or two deuterium nuclei fuse to form helium, there is a net loss in mass. The mass lost appears as an equivalent amount of kinetic energy of the nuclei or their decay products. In the fission of U^{235}, for example, each fissioning nucleus releases approximately 200 mev $\approx 10^{-4}$ erg of energy.

Terminology *continued*

Nuclear radius of a nucleus of mass number A is given approximately by $R = r_0A^{1/3}$. Experimental values quoted for r_0 range from 1.1 to 1.5 $\times$ 10^{-13} centimeter. The unit of length, 10^{-13} centimeter is called the *fermi*.

Nuclear reaction: A process in which a nucleus struck by a fast-moving particle combines with it to form an energetic aggregate. This briefly formed compound nucleus breaks up almost immediately either into the original nucleus and particle or into a different nucleus and one or more secondary particles, effecting a *nuclear transmutation* in the second case. A typical reaction represented in detail is:

$$\underbrace{{}_1p^1}_{\substack{\text{bombarding}\\\text{particle}}} + \underbrace{{}_3Li^7}_{\substack{\text{target}\\\text{nucleus}}} \rightarrow \underbrace{({}_4Be^8)}_{\substack{\text{compound}\\\text{nucleus}}} \rightarrow \underbrace{{}_4Be^7}_{\substack{\text{residual}\\\text{nucleus}}} + \underbrace{{}_0n^1}_{\substack{\text{emitted}\\\text{particle}}}$$

or in abbreviated form, $Li^7(p,n)Be^7$. The bombarding and emitted particles in this reaction are a proton and neutron, respectively.

Cross section of a nuclear reaction is a measure of the probability of its occurrence. Quantitatively, the total cross section σ is the inverse of the number of particles that must strike 1 centimeter^2 of target material to induce a nuclear reaction in 1 nucleus of the target. If the number of target nuclei/centimeter^2 = N, and there are F bombarding particles incident on each centimeter^2 of the target/unit time, the number of nuclear events n (per centimeter^2/unit time) is given by $n = NF\sigma$. The *barn* = 10^{-24} centimeter^2 is commonly used to express cross-section values.

Stable nucleus: One that retains its identity indefinitely unless disturbed by external forces.

Radioactive nucleus or unstable nucleus: One which ultimately transforms spontaneously into a nucleus of a different kind. The transformation occurs through the emission of beta particles, alpha particles, or gamma rays (radioactive decay); through the breakup of the nucleus into one or more nuclear fragments (*spontaneous nuclear fission*); or through the absorption or capture of an extranuclear electron from the atomic shell (*electron capture*).

Activity of a radioactive material: The number of its nuclei that decay in unit time.

One Curie of a radioactive substance is that amount having an activity of 3.7×10^{10} disintegrations/second (= disintegration rate of 1 gram of radium).

Terminology *continued*

Radioactive decay constant λ: The *fraction* of nuclei of a radioactive material disintegrating in unit time. The radioactive nuclei remaining after time t in a material consisting originally of N_0 nuclei is given by $N = N_0 \exp(-\lambda t)$.

Half-life τ of a radioactive material is the time until its original activity is reduced by half and is given in terms of the decay constant by $\tau = 0.693/\lambda$.

Relativistic conceptions: Two concepts fundamental to the explanation of nuclear and atomic phenomena stem from the special theory of relativity.

These are:

a. *Relativistic mass:* The behavior of bodies moving at an appreciable fraction of the velocity of light can be explained only if they are assumed to have a mass that increases with velocity. The relativistic velocity-dependent mass,

$$m = m_0/(1 - v^2/c^2)^{1/2}$$

where

m_0 = mass of body at rest

v = velocity of the body

c = velocity of light

(all in consistent units), must be used in all accurate calculations of the behavior of energetic nuclear and atomic phenomena. The relativistic mass increase is important in the design of high-energy particle accelerators.

b. *Mass–energy equivalence.* The kinetic energy of a moving body is given accurately by $(m - m_0)c^2$. (The familiar expression $m_0v^2/2$ is an approximation applicable only at low velocities.) By inference, a body at rest has associated with it the so-called rest energy $E = m_0c^2$. A striking example is the tremendous quantity of energy released during nuclear fission.

Spin and magnetic moment. Fundamental particles appear to rotate about their axes like tops and, in addition, when grouped within the nucleus, move about each other continually. The angular momentum associated with these motions is called the *nuclear spin;* a measure of the magnetic effects produced by the rotating particles is the so-called nuclear *magnetic moment.*

Nuclear-physics bibliography

Introductory

1. G. Gamow, "Atomic Energy in Cosmic and Human Life", Cambridge University Press; Cambridge, England: 1947.
2. H. D. Smyth, "Atomic Energy for Military Purposes", revised edition, Princeton University Press; Princeton, N. J.: 1947.
3. K. K. Darrow, "Atomic Energy", John Wiley & Sons, Inc.; New York, N. Y.: 1948.
4. "The Effect of Atomic Weapons", U. S. Government Printing Office; Washington, D. C.: September, 1950.
5. S. Glasstone, "Sourcebook of Atomic Energy", D. Van Nostrand and Company, Inc.; New York, N. Y.: 1950.
6. W. Heisenberg, "Nuclear Physics", Methuen & Company; London, England: 1953.

Intermediate

1. J. D. Stranathan, "The Particles of Modern Physics", The Blakiston Company; Philadelphia, Pa.: 1942.
2. J. Mattauch and S. Fluegge, "Nuclear Physics Tables" and "An Introduction to Nuclear Physics", Interscience Publishers, Inc.; New York N. Y.: 1946.
3. F. Bitter, "Nuclear Physics", Addison-Wesley Publishing Company, Inc.; Cambridge, Mass.: 1950.
4. J. M. Cork, "Radioactivity and Nuclear Physics", 2nd edition, D. Van Nostrand & Company, Inc.; New York, N. Y.: 1950.
5. E. C. Pollard and W. L. Davidson, "Applied Nuclear Physics", 2nd edition, John Wiley & Sons, Inc.; New York, N. Y.: 1951.
6. E. Bleuler and G. J. Goldsmith, "Experimental Nucleonics", Rinehart & Company, Inc.; New York, N. Y.: 1952.
7. J. Chadwick, "Radioactivity and Radioactive Substances", 4th edition, Sir Isaac Pitman & Sons, Ltd.; London, England: 1953.
8. R. E. Lapp and H. L. Andrews, "Nuclear Radiation Physics", 2nd edition, Prentice-Hall, Inc.; New York, N. Y.: 1954.
9. A. E. S. Green, "Nuclear Physics", McGraw-Hill Book Company, Inc.; New York, N. Y.: 1955.
10. D. Halliday, "Introductory Nuclear Physics", 2nd edition, John Wiley & Sons, Inc.; New York, N. Y.: 1955.
11. I. Kaplan, "Nuclear Physics", Addison-Wesley Publishing Company, Inc.; Cambridge, Mass.: 1955.

Advanced and special

1. H. A. Bethe, "Elementary Nuclear Theory", John Wiley & Sons, Inc.; New York, N. Y.: 1947.
2. J. M. Blatt, and V. F. Weisskopf, "Theoretical Nuclear Physics", John Wiley & Sons, Inc.; New York, N. Y.: 1952.
3. B. B. Rossi, "High-Energy Particles", Prentice-Hall, Inc.; New York, N. Y.: 1952.
4. K. Siegbahn, Editor "Beta and Gamma-Ray Spectroscopy", Interscience Publishers, Inc.; New York, N. Y.: 1955.

High-energy particle accelerators

General

Particle accelerators use electric and magnetic fields to accelerate electrically charged particles or ionized atoms to high energy. Particle energies range from several hundred-thousand electron–volts (transformer–rectifier circuits) to several billion electron–volts (recently built proton synchrotrons).

Particles most commonly accelerated are electrons, produced from thermionic cathodes; and protons, deuterons, and alpha particles, from ionized hydrogen, deuterium, and helium gases. All these particles are used in the study of nuclear reactions induced when they strike nuclei directly. High-speed electrons are used also to produce high-energy *X* rays for bombarding nuclei. Electrons and *X* rays are in widespread medical and biological use and are also used in special chemical processes. Intense heavy-particle beams from cyclotrons are used to produce radioactive isotopes.

Since energy and mass are equivalent, it is possible for part of the energy of a bombarding particle to be converted into matter: Mesons are created when nuclei are struck by particles of energy $> \approx 150$ mev. Intense proton beams are used to produce large quantities of mesons, used, in turn, to bombard secondary targets for the study of interaction of mesons with nuclei. At extremely high energies in the billion-volt region, hyperons and *K*-particles are produced and intensive studies are currently directed toward understanding these particles.

Van de Graaff electrostatic generators

Electric charge is sprayed on a traveling insulated belt (Fig. 2) and carried to a rounded metallic terminal supported on an insulated column. Charged particles are introduced into the end of an evacuated tube in the charged terminal. The particles, progressively accelerated and focused as they pass through the tube away from the terminal, emerge from the machine in a sharp beam moving

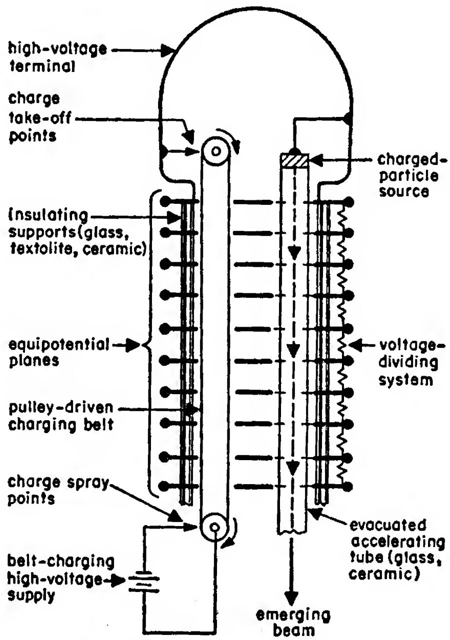

Fig. 2—A Van de Graaff generator.

High-energy particle accelerators *continued*

with high velocity. By pressurizing the atmosphere around the generator, the machine can be made very compact—a modern 2-million-volt generator can be housed in a tank less than 6 feet long. Voltages range from about 0.5- to 10-million volts. Beam currents up to 1 milliampere can be produced. The energy of the beam can be controlled to high precision ($\approx 1/10$ percent) and can be made highly monoenergetic (e.g., $(8 \times 10^6) \pm 10^4$ electron–volts). A practical upper limit to the voltage attainable by existing design standards seems to be in the region of 12- to 15-million volts. Representative generators of this type are listed in Fig. 3.

Fig. 3—Representative electrostatic accelerators.

characteristic	Massachusetts Institute of Technology; Cambridge, Mass.	University of Wisconsin; Madison, Wisc.
Column		
Length in feet	Vertical 18	Horizontal 11
Insulation	Vycor glass disks	Textolite tubes
Belt		
Material	Rubberized cotton	Woven cotton
Width in inches	20	26
Speed in feet/minute	3600	2700
Tank		
Size in feet	32 high $\times$ 12 diameter	20 long $\times$ 5.5 diameter
Filling	90 percent N_2, 10 percent CO_2 to 250 pounds/inch^2 (400 pounds/inch^2 maximum)	Air–freon, 100 pounds/inch^2 (maximum)
Voltage range in millions of electron–volts	3–8.5 (designed for 12)	0.150–4.6
Limited by	Discharge in accelerating tube	Sparking to tank wall
Beam current in microamperes	$\approx$ 1 for protons	$\lessdot$ 3 for protons
Energy resolution in percent	0.1	0.05 to 0.1

Cyclotrons

The cyclotron (Fig. 4) uses a combination of a strong unipolar magnetic field and a high-frequency electric field. The heart of the machine consists of two hollow metal electrodes called *dees*. The dees are connected to the terminals of a high-power radio-frequency oscillator and are housed in an evacuated chamber between the poles of a large electromagnet. Charged particles are produced by introducing gas (hydrogen, deuterium, or helium) into a small discharge tube at the center of the gap between the

High-energy particle accelerators *continued*

dees. The acceleration process begins with the extraction of charged particles from this ion source by the electric field across the dee gap. The particles receive an initial brief acceleration from the electric field, cross the gap, and enter one of the dees. The strong magnetic field causes the particles to move in a circular path. After traversing a semicircle they re-enter the gap, at which time, by proper choice of oscillator frequency, the electric field across the gap has been made to reverse; the particles are again accelerated, increasing their velocity further. This process is repeated over and over, the particles gaining in energy with each passage through the gap, moving in circles of ever increasing radius, and attaining very high energy, by the time they reach the outer circumference of the dees. At this point, the particles may be extracted from the dees by an electrostatic deflector and allowed to strike an external target. The time required for each semicircular traversal remains constant for particle velocities that are small compared to the velocity of light. This is the case in conventional cyclotrons of energy less than 20- to 30-million electron–volts, in which it is therefore possible to use a constant-frequency oscillator. At higher energies, the particle mass becomes appre-

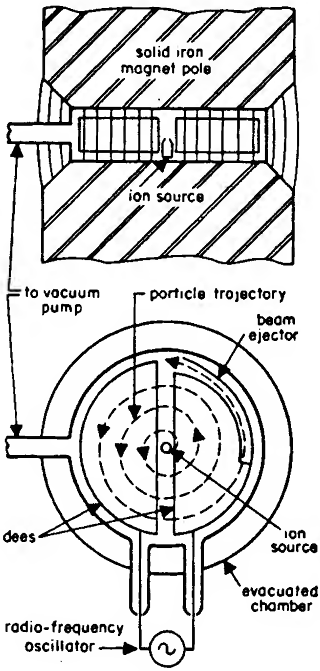

Fig. 4—A cyclotron.

Fig. 5—Representative cyclotrons.

characteristics	Massachusetts Institute of Technology; Cambridge, Mass.	University of California; Berkeley, Calif.	University of Chicago; Chicago, Ill.
Type	Conventional cyclotron	Synchrocyclotron	Synchrocyclotron
Magnet			
Pole diameter in inches	42	184	170
Weight of iron in tons	75	4,300	2,200
Field in gausses	18,000	15,000	18,600
Particle energy in millions of electron–volts	7.5 for protons 15 for deuterons 30 for α particles	350 for protons 195 for deuterons 390 for α particles	450 for protons

High-energy particle accelerators *continued*

ciably increased through the relativistic effect and the oscillator must be frequency modulated correspondingly. *Synchrocyclotrons* of this latter kind have been built to accelerate protons to very-high energies. Because of the relativistic effect, the cyclotron is a practical accelerator only for heavy charged particles and is not used to accelerate electrons. Beams of very-high intensity are produced (Fig. 5).

Betatrons

The betatron accelerates electrons through the use of a time-varying magnetic field (Fig. 6). A pulse of electrons is injected from an electron gun tangentially into a circular evacuated tube called the *doughnut*. A magnetic field perpendicular to the doughnut plane is simultaneously turned on and caused to rise rapidly to very-high intensity. This changing magnetic field induces a strong electric field that exerts a tangential force on the injected electrons. The magnetic field, which extends over the doughnut, acts also to constrain the moving electrons to circular paths. If the field strengths at and within the electron orbit are properly related, the orbit radius remains essentially constant through the acceleration cycle. The complete acceleration process involves several hundred thousand circular traversals and is accomplished in a fraction of a second. When the electrons have attained full energy, the magnetic field is purposely distorted, shifting the electron orbit and causing the electrons to strike a small target producing high-energy *X* rays. Techniques have also been developed for extracting part of the electron beam from the doughnut. Operation is usually at repetition rates ranging from 60 to 180 cycles/second. Machines of energy up to 300-million electron–volts are in use (Fig. 7).

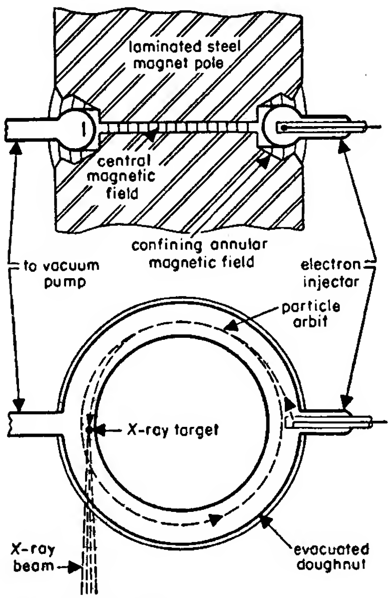

Fig. 6—A betatron.

High-energy particle accelerators *continued*

Fig. 7—Representative betatrons.

characteristics	General Electric Research Laboratory; Schenectady, N. Y.	University of Illinois; Urbana, Ill.
Orbit radius in inches	33	51
Injection		
Energy: in thousands of electron–volts	30–70	100
By	Electron gun	Electron gun
Magnet		
Over-all dimensions in feet	≈ 15 × 9 × 8.5 high	≈ 23 × 13 × 6 high
Weight in tons	130	400
Field at orbit (maximum in gausses)	4000	≈ 8000
Magnet power (full load in kilowatts)	200	170
Vacuum tube	Oval-shaped	Oval-shaped
Dimensions in inches	≈ 8 wide × 5 high	10 wide × 6 high
Repetition rate in cycles/second	60	6
Electron energy (maximum in millions of electron–volts)	100	312
X-ray output in roentgens/minute at 1 meter	≈ 2600 (at 100 mev)	≈ 12,000 (at 280 mev)

Synchrotrons

The synchrotron accelerates protons or electrons by combining a time-varying magnetic field with a radio-frequency electric field. The machine (Fig. 8) consists essentially of an evacuated accelerating "doughnut" placed between the poles of an annular electromagnet. Particles injected into the doughnut are constrained to a circular path by the magnetic field. As in the cyclotron, the particles are accelerated briefly by a radio-frequency field each time they pass an electric gap in the accelerating tube. In the case of protons, which become relativistic only at energies in the billion electron–volt region, the proton velocity increases continually

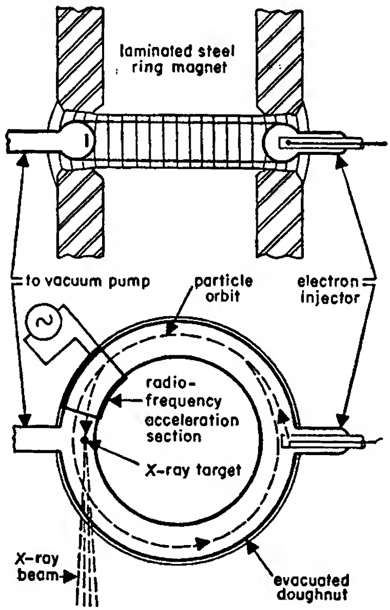

Fig. 8—Electron synchrotron.

High-energy particle accelerators *continued*

throughout the accelerating cycle. Successive revolutions around the doughnut occur in shorter times and the accelerating-field frequency must be increased correspondingly. Electrons, which are much lighter, are brought very quickly to the limiting velocity of light, becoming highly relativistic at energies of 2-million electron–volts or more. Above this energy, they revolve about the doughnut with essentially the same period. For this reason, electron synchrotrons are usually operated in two steps: an initial *betatron phase;* during which the electrons are accelerated by the time-changing magnetic field alone; and a *synchrotron phase,* after the electrons have reached the neighborhood of 2-million electron–volts when a constant-frequency accelerating field is turned on to carry out the remainder of the acceleration (and the magnetic field serves only to constrain the particles). An important advantage of the synchrotron over the betatron is the elimination of the central part of the magnetic field and the expensive and heavy magnetic material that this represents. Electron synchrotrons (Fig. 9) operate essentially in the same energy region as betatrons and have the same applications. Notable proton synchrotrons (Fig. 10) are the Brookhaven Cosmotron and the Berkeley Bevatron, which are used for the study of extremely high-energy phenomena in the billion-electron–volt region.

Fig. 9—Representative electron synchrotrons.

characteristics	University of California; Berkeley, Calif.	Cornell University; Ithaca, N. Y.
Orbit radius in inches	39.4	39.4
Magnet		
Weight of iron in tons	135	75
Weight of copper in tons	1.75	1.8
Peak field in gausses	14,000	10,000
Pole tip gap (pole-to-pole) in inches	3.7	3.25
Magnet power supply		
Type	Pulse	Alternator
Repetition rate in pulses/second	6	30
Peak voltage in kilovolts	19	11.2
Peak current in amperes	3060	3500
Oscillator		
Frequency in megacycles	47.7	47.5
Peak power in kilowatts	6	5.5
Electron energy (maximum in millions of electron–volts)	300	320
X-ray output in roentgens/minute at 1 meter	1000	1600

High-energy particle accelerators *continued*

Fig. 10—Representative protron synchrotrons.

characteristics	Brookhaven National Laboratory; Upton, N. Y.	University of California; Berkeley, Calif.
Orbit radius in feet	30	50
Injection Energy in millions of electron–volts By	 3.6 Electrostatic generator	 9.9 Linear accelerator
Magnet Weight in tons Peak field in gausses Pole tip gap in inches Peak current in amperes	 2,000 14,000 9.5 high $\times$ 48 radially 7,000	 10,000 15,000 $\approx$ 13 high $\times$ 52 radially 8,300
Frequency-modulated-oscillator frequency in kilocycles	370 to 4200	350 to 2500
Repetition rate in pulses/minute	12	4–10
Energy (maximum in billions of electron–volts)	3	6.1
Proton current (internal beam) in protons/pulse	5×10^{10}	10^{10}

Strong-focusing synchrotron: Charged particles accelerated in circular machines like the synchrotron experience perturbing forces that displace them from their ideal orbits. To confine the particles within the accelerating tube, it is necessary to shape the magnetic field of the machine so that restoring forces are exerted on particles so displaced. The particles thus perform oscillations about some average path and remain within the accelerating tube, provided this has sufficiently large cross-sectional area. At very-high energies, however, the required tube cross section is very large and the amount of magnetic material needed to surround it becomes prohibitively great. For example, a 30-billion-electron–volt proton synchrotron of conventional design would require at least 100,000 tons of iron.

Recent studies have revealed methods for shaping the confining magnetic field to reduce the amplitude of the oscillations by a large factor. It is expected that the *strong-focusing* or *alternating-gradient* fields so devised would permit the construction of a 100-billion-electron–volt synchrotron with a magnet weighing 6000 tons. Two strong-focusing machines are currently under construction to operate at about 25 billion electron–volts, one at the Brookhaven National Laboratory (Fig. 11) and the other at the

High-energy particle accelerators *continued*

European Council for Nuclear Research (CERN) in Geneva. The principles of strong-focusing design are currently being extended to radio-type vacuum tubes employing linear electron beams.*

Fig. 11—Preliminary design parameters for strong-focusing synchrotrons.

characteristics	Brookhaven National Laboratory; Upton, N. Y.	Harvard University, Massachusetts Institute of Technology; Cambridge, Mass. (tentative 1956)
Orbit radius in feet	280	91
Injection		
Energy: in millions of electron–volts	50	40
By	Linear accelerator	Linear accelerator
Magnet		
Weight of iron in tons	3000	323
Weight of copper in tons	35	65
Peak field in gausses	14,000	9000
Oscillator		
Frequency in megacycles	fm, 1.4–4.5	406
Repetition rate in pulses/minute	20	1800
Particle energy in billions of electron–volts	25–35 for protons	7.5 for electrons

Linear accelerators

The linear accelerator moves charged particles along a straight path by means of a radio-frequency electric field. The machine's essential element, the accelerating tube, is a long waveguide, loaded periodically along its length with suitable field-perturbing obstacles. High-power radio-frequency energy passes into the waveguide and builds up an oscillating electromagnetic field of high amplitude within it. If waveguide and obstacle dimensions are properly chosen, one of the travelling waves of which the field is composed will have the characteristics necessary for linear acceleration. Such a wave must have a strong electric component along the accelerating-tube axis and must move along this axis with the velocity of the particles being accelerated. As particle velocity increases along the tube,

* A. M. Clogston and H. Heffner, "Focusing of an Electron Beam by Periodic Fields, *Journal of Applied Physics*, vol. 25, pp. 436–447; April, 1954.

High-energy particle accelerators *continued*

the wave velocity must likewise change, and it is necessary, in general, to change the characteristics of the waveguide progressively along its length. For proton and other heavy-particle machines, this change is appreciable up to very-high energies. Electron accelerators, on the other hand, require a change in waveguide dimensions for, at most, only a very-short initial length of the accelerating tube.

Charged particles injected along the accelerating-tube axis in correct phase with respect to the accelerating wave are increased in velocity so as to keep in step with it. The field conditions surrounding the particles thus remain essentially constant and the particles move almost as though they were in an unvarying field.

Since accelerating-tube dimensions are proportional to the wavelength of the oscillator, operating frequencies in the very-high-frequency and micro-

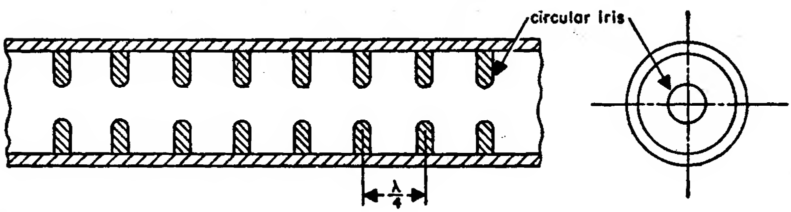

Fig. 12—Traveling-wave-type iris-loaded linear electron accelerator.

wave regions are used. For example, almost all electron accelerators use multimegawatt pulsed (1–5-microsecond) magnetrons or klystrons of about 3000-megacycle frequency to operate accelerating tubes with diameters of 3 to 4 inches. Peak accelerated electron-beam currents up to 100 milliamperes are easily obtained at duty cycles of from 10^{-4} to 10^{-3}, resulting in average beam currents of from 1 to 20 microamperes. Energies up to 4-million electron–volts/foot have been attained. A number of machines in the 10-to-40-million-electron–volt region are in use. The Stanford University linear electron accelerator (Fig. 13), 220-feet long, has already produced beams of 600-million, and will ultimately reach at least 1-billion electron–volts. The relatively high beam intensity of the linear accelerator and the ease with which the beam may be extracted from the accelerating tube are two of the machine's important advantages.

High-energy particle accelerators *continued*

Fig. 13—Representative linear accelerators.

characteristics	University of California; Berkeley, Calif.	Stanford University; Palo Alto, Calif.
Type	Proton—standing-wave	Electron—traveling-wave
Injection		
Energy in electron-volts	4×10^6	$5–8 \times 10^4$
By	Electrostatic generator	Electron gun
Accelerating tube		
Type	Cylindrical cavity	Disk-loaded circular waveguide
Length in feet	40	220
Excitation mode	*TM*	*TM*
Power supply	9 power oscillators	21 klystron power amplifiers
Frequency in megacycles	202.5	2856
Peak power/tube in megawatts	2.1	10–20
Repetition rate in pulses/second	15	60
Particle energy (maximum in millions of electron-volts	31.5	> 600
Beam current in microamperes		
Peak	60	50,000
Average	0.3	1

Particle-accelerator bibliography

Electrostatic generators

1. R. J. Van de Graaff, J. G. Trump, and W. W. Buechner, "Electrostatic Generators for the Acceleration of Charged Particles", *Reports on Progress in Physics*, vol. 11, The Physical Society, London, England: 1948.
2. B. Jennings, "Electronics and the Electrostatic Generator", *Proceedings of the IRE*, vol. 38, pp. 1126–1138; October, 1950.
3. R. L. Fortescue, "High-Voltage Direct-Current Generators", *Progress in Nuclear Physics* vol. 1, Academic Press; New York, N. Y.: 1950.

Cyclic accelerators

1. M. S. Livingston, "Particle Accelerators", *Advances in Electronics*, vol. 1, pp. 269–316, Academic Press, Inc.; New York, N. Y.: 1948.
2. J. H. Fremlin and J. S. Gooden, "Cyclic Accelerators", *Reports on Progress in Physics*, vol. 13, The Physical Society; London, England: 1950.
3. T. G. Pickavance, "Cyclotrons", *Progress in Nuclear Physics*, vol. 1, Academic Press; New York, N. Y.: 1950.
4. M. S. Livingston, J. E. Thomas, Jr., W. L. Kraushaar, and I. Halpern, "High Energy Accelerators", *Annual Review of Nuclear Science*, vol. 1, Annual Reviews, Inc.; Stanford, Cal.: 1952.
5. "Cosmotron Issue", *Review of Scientific Instruments*, vol. 24, pp. 723–870; September, 1953.
6. E. I. Chu and L. I. Schiff, "Recent Progress in Accelerators", *Annual Review of Nuclear Science*, vol. 2, Annual Reviews, Inc.; Stanford, Cal.: 1953.
7. M. S. Livingston, "High Energy Accelerators", Interscience Publishers, Inc., New York, N. Y.: 1954. (Also includes discussion of linear accelerators).

High-energy particle accelerators *continued*

Linear accelerators

1. J. C. Sloter, "The Design of Linear Accelerotors", *Reviews of Modern Physics*, vol. 20, pp. 473–518; July, 1948.
2. P. W. Fry and W. Walkinshaw, "Linear Accelerators", *Reports on Progress in Physics*, vol. 12, The Physical Society; London, England: 1949.
3. J. C. Slater, "High Energy Accelerators: The Linear Accelerator", *Annual Review of Nuclear Science*, vol. 1, Annual Reviews, Inc.; Stanford, Cal.: 1952.
4. "Linear Accelerator Issue", *Review of Scientific Instruments*, vol. 26, pp. 111-231; February, 1955.

General

1. T. P. Mittelman and H. H. Goldsmith, "Particle Accelerators", Report BNL-L-101, Brookhaven National Laboratory; Brookhaven, N. Y.: July 1, 1948.
2. F. E. Frost and J. M. Putnam, "Particle Accelerators", Report UCRL 2672, University of California Radiation Laboratory; Berkeley, Cal.: November 16, 1954.

Nuclear instrumentation

Particle detectors

Nuclear study is in large part carried out by observing the properties (e.g., number and kind, energy and angular distributions) of particles emitted by naturally radioactive nuclei, or by nuclei exposed to radiations of various kinds. The detection of such particles depends on the fact that a rapidly moving charged particle can produce an observable effect, such as fluorescence or ionization, in the medium through which it passes.

Particle track recorders: A group of detectors exists in which the path of the particle can be observed visually in the form of a track in a supersaturated vapor or liquid, or in a photographic emulsion.

Cloud chambers, either continuously or momentarily during an expansion phase, provide a gaseous atmosphere saturated with water vapor that condenses preferentially on molecules ionized by the particle. The vapor track is photographed stereoscopically. Energy and kind of ionizing particle are determined by the length, density, and shape of the track.

Bubble chambers maintain a volatile liquid at critical temperature and pressure. When the pressure is instantaneously reduced, the ionized molecules produced by the particle act as the centers of a line of briefly visible vapor bubbles.

Nuclear emulsions are thick photographic emulsions in which a track of developable silver-iodide grains marks the path of the ionizing particle. The developed tracks are viewed and measured by means of a microscope.

Nuclear instrumentation *continued*

Gas-filled counters are detectors in which the charged particle ionizes gas enclosed in an envelope containing two electrodes across which high voltage is maintained. The occurrence of the ionizing event is manifested as an electrical signal that is used to actuate various recording devices. Depending on the electric-field gradient and gas pressure, the counter is an *ionization chamber*, a *proportional counter*, or a *Geiger-Müller counter*.

Ionization chambers are designed so that the charge collected by the high-voltage electrodes is at most the small charge liberated in the initial ionization process. If the ionizing source is steady, the charge produced in the counter may be observed as an average current (Fig. 14A); or, with appropriate circuitry, single-particle ionization bursts may be used to produce small voltage pulses across the distributed capacitance of the chamber (Fig. 14B). The voltage pulses can be amplified electronically and recorded by auxiliary apparatus.

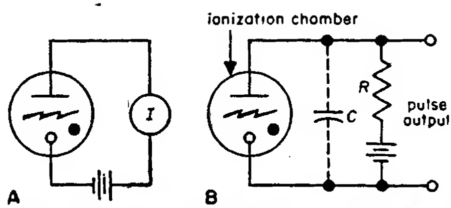

Fig. 14—Connections for an ionization chamber.

The *proportional counters* function similarly to ionization chambers, except that electrode-voltage and gas-pressure conditions are chosen that multiply by a large factor the charge initially liberated by the ionizing particle. The charge collected at the electrodes as a result of this "gas-multiplication" process is thus much greater than in the ionization chamber. Weaker radiations can be detected and voltage pulse amplifiers of lower gain can be used. Although larger, the collected charge and output pulse remain proportional to the initial ionization and serve as a measure of the particle energy.

Geiger-Müller counters use electrode voltage sufficiently great so that the gas multiplication factor is very large and an electric discharge is produced

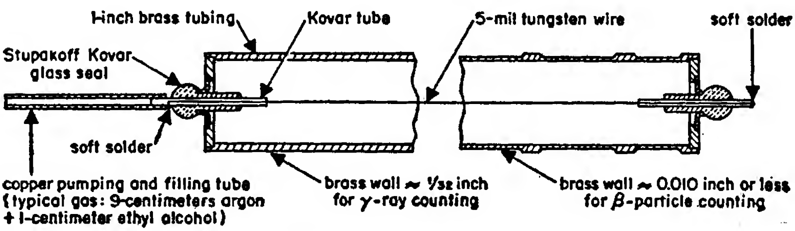

Fig. 15—Typical Geiger-Müller counter.

Nuclear instrumentation *continued*

in the counter whenever a charged particle enters, regardless of its energy. The counter (Fig. 15) is useful as an extremely sensitive detector of individual particles, producing large output pulses of uniform amplitude independent of the kind and energy of particle detected.

Voltage pulses produced by gas counters have rise times in the order of 10^{-6} second. Random particles arriving at an average rate of up to 10^5/second can be counted accurately by a carefully designed proportional counter. The Geiger-Müller counter, however, after producing its output pulse, requires up to 200 microseconds to restore itself to its original undischarged condition and cannot be used for counting rates much greater than 10^3/second.

Efficiency: All the gas counters detect charged particles with high efficiency. Counters with windows as thin as 2 or 3 milligrams/centimeter^2 are made which can be penetrated by charged particles of very low energy. X and γ rays penetrate thick-walled counters readily, but are detected only if they interact with one of the atoms in the counter gas or wall, releasing an energetic charged particle that is detected by the ionization it produces. Although *γ-ray counters* are purposely made thick-walled to increase the probability of this occurrence, which takes place infrequently, the efficiency of a typical gas-filled γ-ray counter is only 1 to 2 percent.

Neutron detection: Two common neutron detectors are the *neutron-recoil detector* and the *boron-trifluoride counter*. Both are proportional counters. The former is filled with a gas such as hydrogen whose charged nuclei recoil energetically when struck by neutrons and produce a typical proportional counter pulse. The pulse size decreases with decreasing energy of the incident neutron, so that the counter is not satisfactory for the detection of neutrons of very-low energy. The boron-trifluoride counter depends on a nuclear reaction for its effect. Neutrons of extremely low energy are very strongly absorbed by isotope B^{10} of boron. An unstable nucleus is produced that breaks into a lithium nucleus and an energetic α particle. The α particle is then detected by the counter in the usual way. Slow neutrons (< 1 electron–volt) may be detected directly by the boron-trifluoride counter. The detection of fast neutrons requires that these first be reduced in energy (thermalized) by passing through hydrogen-containing material, such as paraffin, surrounding the counter tube.

Crystal counters function qualitatively in the same way as an ionization chamber except that the medium between the high-voltage electrodes is a solid crystal instead of gas. The high density of the counter medium results in an advantageously small counter. A further advantage is the high velocity

Nuclear instrumentation *continued*

with wh ch electrons produced by ionization travel through the crystal, resu ting in fast counter pulses with rise time; n the neighborhood o 10^{-7} second. However, the reproducibility of pulses is, in general, not good; and the crystals become polarized electrically after long exposure to radiation Suitable crystals are silver chloride, zinc sulphide, diamond, cadmium sulphide, and the thallium halides.

Scintillation counters (Fig. 16) involve the use of a light-sensitive detector, such as a photomultiplier tube, that is actuated by the visible fluorescence produced when charged particles strike certain transparent materials. The

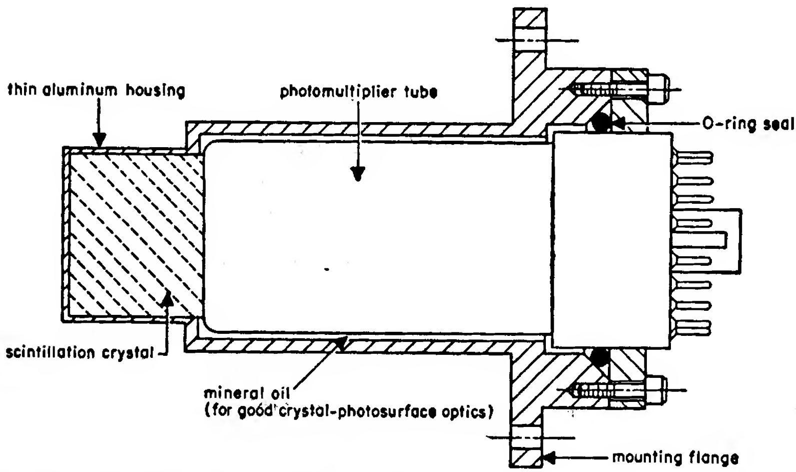

Fig. 16—Photomultiplier and scintillating-crystal assembly.

method has been developed in recent years into a highly superior counting technique following the discovery of crystals producing fluorescent scintillations of high intensity and very-short duration, and with the application of fast, sensitive, photomultiplier tubes. (Descriptions of photomultiplier tubes and their circuits are given in the chapter, "Electron tubes".) An important advantage is the very-fast decay time of the fluorescence, as short as 2 to 3×10^{-9} second, which allows the detection of events occurring very closely together in time. The light output is proportional to the energy of the exciting particle. Because the crystals are dense and can be used in comparatively large sizes, they are efficient as γ-ray detectors. Large inorganic crystals like sodium iodide can have γ-ray counting efficiencies approaching 100 percent. Large-volume scintillators have been constructed for the observation of particles and γ rays of very-high energy by using liquid solutions of organic scintillators. Solid plastic scintillators have been

Nuclear instrumentation *continued*

constructed by embedding scintillating material in clear plastic and possess the advantages of being easily machined and handled. See Fig. 17.

Cerenkov counters make use of the visible light emitted by relativistic charged particles when they enter media with high dielectric constant. A fast electron or proton entering a clear plastic material like polystyrene or lucite will emit visible light in a narrow cone in the direction in which the particle is moving. The light pulse can be detected in the usual manner with photosensitive devices. The duration of the pulse is extremely short ($< 10^{-9}$ second). The application of the counter is limited by the small intensity of the light pulse and the fact that only particles of a very-high energy produce Cerenkov radiation.

Fig. 17—Properties of some common scintillators.*

	scintillator	relative light yield for β particles	scintillation decay time at 25° C in 10^{-9} sec	emission spectrum bands in angstrom units	density	quality of crystals
Organic crystals	Anthracene	1.0	30–40 ($\approx$ 10 at −196°C)	4400	1.25	Good
	Stilbene	0.6	6–12	4200 (weak) 4080 (strong)	1.16	Good
	Terphenyl	0.65	5–12	3460 main band	1.23	Good
	Naphthalene	0.25	< 150	3450	1.15	Good, but crystals sublime
Inorganic crystals	NaI(Tl)	$\approx$ 2.0	250	4100	3.67	Excellent, but crystals hygroscopic
	ZnS(Ag)	$\approx$ 2.0	> 1000	Blue	4.10	Powder or small crystals only
Liquid and plastic scintillators	Toluene + 3–5 grams/liter terphenyl	0.3–0.4	< 3	3400	0.866	Liquid scintillator
	Polystyrene or polyvinyl toluene + 3% terphenyl + 0.02% tetraphenyl butadiene	$\approx$ 0.5	< 3	$\approx$ 4300	—	Plastic scintillator

* Data abstracted in large part from R. C. Sangster, "Technical Report No. 55", Massachusetts Institute of Technology Laboratory for Nuclear Science; Cambridge, Massachusetts; January 1, 1950. Also, R. F. Hofstadter, "Properties of Scintillation Materials", *Nucleonics*, vol. 6, pp. 70–73; May, 1950. Also, R. K. Swank and W. L. Buck, "Decay Times of Some Organic Scintillators", *Review of Scientific Instruments*, vol. 26, pp. 15–16; January, 1955.

Nuclear instrumentation *continued*

Electronic apparatus

The nature of radiations incident on particle counters is reflected, in general, by the magnitude of the counter outputs and the frequency with which they occur. An important part of nuclear experimentation is the recording of such signals in a manner that will facilitate their interpretation. The problem, intrinsically one of sorting and measuring the counter outputs, reduces usually to one or more of the following:

a. Measurement of the number of output pulses occurring in a given interval of time.

b. Sorting of the output pulses in terms of their amplitudes.

c. Determination of the time interval occurring between pulses associated with related events; for example, between the artificial creation of a short-lived particle or nucleus and its subsequent disintegration.

d. Selection of events of a particular kind from among other simultaneously occurring events; for example, the detection of particles emitted by a feebly radioactive source from among the normally occurring "background" of cosmic radiations.

Amplifiers: Pulse-recording instruments require input amplitudes in the 10-to-100-volt region for their operation. The output pulses of particle detectors are usually too small—fractions to hundreds of millivolts—and must be amplified electronically before being used to actuate such devices. Except where it is necessary to follow the rise times of extremely fast pulses, amplifiers in common use are of the resistance-coupled type employing negative feedback to enhance gain stability and linearity. Since the pulses passed are almost invariably of short duration, low-frequency amplification ($< 10^3$ cycles/second) is suppressed, greatly reducing the problems of microphonics and low-frequency pickup. Amplifier bandwidth is usually chosen to conform to the rise-time of the pulses amplified.

Scaling circuit: The total number of pulses observed during a given interval is recorded ultimately by some form of mechanically driven register, so that for very-high counting rates it is necessary to reduce the number of pulses to be counted by a known factor. The electronic scaling circuit is a system designed to produce 1 output pulse for every k pulses supplied to it. The two common basic designs are the decade circuit and the binary or scale-of-2 circuit.

Integral discriminator: A circuit designed to accept only pulses greater than a chosen minimum height. The circuit is usually designed to produce output pulses of constant amplitude for the actuation of further circuitry.

Nuclear instrumentation *continued*

The discriminator is often built as an integral part of other devices, such as scaling circuits.

Differential discriminator: This circuit consists basically of two integral discriminators that pass pulses differing in voltage by a chosen amount and is designed to produce an output pulse only when the circuit set for the lower amplitude is actuated. If the input pulse is large enough to operate both circuits, no output pulse results and only a selected range or *channel* of pulse heights is transmitted by the circuit.

Pulse-height analyzer: A circuit intended to select and record simultaneously the numbers of pulses of different height being produced by a particle detector. Most pulse-height analyzers are based on the straightforward use of a large number of differential discriminators each set to accept a different channel of pulse heights. Each of the channels usually actuates a separate scaling circuit. Multichannel differential discriminators using up to 100 channels are in common use.

Coincidence and anticoincidence circuits: These circuits are used to signal when two or more separate events under observation occur simultaneously in time. The coincidence circuit is designed to record such occurrences and the anticoincidence circuit to reject them. The most commonly used coincidence circuit is a set of normally conducting electron tubes connected through a common resistance to a power supply. Each of the events under observation (e.g., pulses from several particle detectors) goes to one of the tube inputs. Whenever an event occurs, it cuts off the associated tube. As long as any one of the tubes remains conducting, the voltage across the common resistor changes very little. However, if all of the tubes are actuated simultaneously, no current flows through the resistor and the large resulting voltage change is used to actuate further circuits that are insensitive to the smaller voltage changes produced when total coincidence does not occur. It is sometimes desirable, on the other hand, to exclude events from the data being recorded when these occur at the same time as some other kind of event. The anticoincidence circuit, actuated by the system observing the unwanted event, prevents the recording of such occurrences by applying a strong cutoff bias to some element of the recording system.

Nuclear-instrumentation bibliography

Particle detectors

1. S. C. Brown, "Theory and Operation of Geiger-Müller Counters", *Nucleonics*, vol. 2, pp. 10–22; June, 1948: vol. 3, pp. 50–64; August, 1948: pp. 46–61; October, 1948.
2. J. A. Victoreen, "Ionization Chambers", *Proceedings of the IRE* vol. 37, pp. 189–199; February, 1949.

Nuclear instrumentation *continued*

3. R. R. Wilson, D. R. Corson, and C. P. Baker, "Particle and Quantum Detectors", Preliminary Report No. 7, National Research Council; Washington, D. C.: January, 1950.
4. R. Hofstater, "Crystal Counters", *Proceedings of the IRE*, vol. 38, pp. 726–740; July, 1950.
5. J. Rotblat, "Photographic Emulsion Technique", *Progress in Nuclear Physics*, vol. 1, Academic Press; New York, N. Y.: 1950.
6. S. A. Korff, "Proportional Counters", *Nucleonics*, vol. 6, pp. 5–10, 36; June, 1950: vol. 7, pp. 46–52; November, 1950: vol. 8, pp. 38–43; January, 1951.
7. J. G. Wilson, "The Principles of Cloud-Chamber Technique", Cambridge University Press; Cambridge, England: 1951.
8. G. F. J. Garlick, "Luminescent Materials for Scintillation Counters", *Progress in Nuclear Physics*, vol. 2, Academic Press, Inc.; New York, N. Y.: 1952.
9. W. H. Jordan, "Detection of Nuclear Particles", *Annual Review of Nuclear Science*, vol. 1, Annual Reviews, Inc.; Stanford, Cal.: 1952.
10. J. B. Birks, "Scintillation Counters", McGraw-Hill Book Company, Inc.; New York, N. Y.: 1953.
11. F. C. Champion, "Solid Conduction Counters", *Progress in Nuclear Physics*, vol. 3, Academic Press; New York, N. Y.: 1953.
12. S. C. Curran, "Luminescence and the Scintillation Counter", Academic Press, Inc.; New York, N. Y.: 1953.
13. J. V. Jelley, "Cerenkov Radiation", *Progress in Nuclear Physics*, vol. 3, Academic Press, Inc., New York, N. Y.: 1953.
14. "Scintillation Counting Today", *Nucleonics*, vol. 12, pp. 13–56; March, 1954.
15. D. A. Glaser, "The Bubble Chamber", *Scientific American*, vol. 192, pp. 46–50; February, 1955:
16. W. B. Fretter, "Nuclear Particle Detection", *Annual Review of Nuclear Science*, vol. 5, pp. 145–178; Annual Reviews, Inc., Stanford, Cal.: 1955.

Electronic apparatus

1. W. C. Elmore, "Electronics for the Nuclear Physicist", *Nucleonics*, vol. 2, pp. 4–17; February. pp. 16–36; March: pp. 43–55; April: pp. 50–58; May: 1948.
2. W. C. Elmore and M. Sands, "Electronics: Experimental Techniques", McGraw-Hill Book Co., Inc.; New York, N. Y.: 1949.
3. J. S. Allen, "Recent Applications of Electron Multiplier Tubes", *Proceedings of the IRE*, vol. 38, pp. 346–358; April, 1950.
4. F. H. Wells, "Fast Pulse Circuit Techniques for Scintillation Counters", *Nucleonics*, vol. 10, pp. 28–33; April, 1952.
5. A. B. van Rennes, "Pulse Amplitude Analysis in Nuclear Research", *Nucleonics*, vol. 10, pp. 20–27; July: pp. 22–28; August: pp. 32–38; September: pp. 50–56; October: 1952.
6. A. B. Gillespie, "Signal, Noise and Resolution in Nuclear Counter Amplifiers", McGraw-Hill Book Company, Inc.; New York, N. Y.: 1953.
7. I. A. D. Lewis and F. H. Wells, "Millimicrosecond Pulse Techniques", McGraw-Hill Book Company, Inc.; New York, N. Y.: 1954.

General

1. "Nuclear Instrument Handbook", *Nucleonics*, vol. 4, pp. 97–152; May, 1949.
2. B. B. Rossi and H. H. Staub, "Ionization Chambers and Counters", McGraw-Hill Book Company, Inc.; New York, N. Y.: 1949.
3. D. H. Wilkinson, "Ionization Chambers and Counters", Cambridge University Press; Cambridge, England: 1950.
4. H. H. Staub, "Detection Methods", *Experimental Nuclear Physics*, vol. 1, John Wiley & Sons, Inc.; New York, N. Y.: 1953.
5. R. E. Bell, R. K. Swank, and J. Marshall, "Nuclear Particle Detection", *Annual Review of Nuclear Science*, vol. 5, pp. 145–178; Annual Reviews, Inc., Stanford, Cal.: 1955.
6. S. A. Korff, "Electron and Nuclear Counters", 2nd edition, D. Van Nostrand Company, Inc.; New York, N. Y.: 1955.

Radiation safety

Biological radiation damage

Damage to living tissues results from the physical and chemical changes that occur when energetic particles or photons dissipate energy in body tissue. Harmful results can occur either through brief, severe exposures that cause extensive tissue damage, or as the result of constant exposure to low-level radiation of sufficient intensity to destroy tissue cells faster than the body can replace them. It is important to note that these radiations are not detected by the senses and that symptoms of radiation sickness may not appear for hours or days after even severe exposures. It is therefore extremely important to monitor carefully all radiations to which personnel may be exposed and to adhere closely to established radioisotope handling procedures and radiation tolerance limits.

Hazardous radiations occur commonly in work involving the use of radioactive and fissionable materials, nuclear reactors, *X*-ray generators and high-energy particle accelerators. Radioisotopes emit energetic γ rays, β and α particles. High-energy accelerators can produce intense primary beams of protons, electrons, deuterons, α particles (and *X* rays and neutrons as secondary radiations when the beams are allowed to strike matter). The fissioning materials of nuclear reactors produce enormous amounts of all radiations, particularly neutrons, as well as large volumes of radioactive waste materials. Radiation intensities encountered range from those of small microcurie amounts of radioisotopes used in the laboratory to those of the megacurie radioactive wastes that must be removed periodically from nuclear reactors.

Radiation units

Roentgen: The accepted quantitative measure of energy dissipation in matter by *X* or γ rays is the roentgen *r*, which is defined in terms of the ionization produced by *X* radiation in a standard amount of air. (One roentgen is the amount of radiation that releases by ionization 1 electrostatic unit of charge of either sign in 1 centimeter^3 of air at normal temperature and pressure.) For biological purposes, the effects on body tissue of all radiations is expressed in terms of the radiation energy (in ergs) absorbed by 1 gram of tissue. Radiation dosage units are derived, in fact, on the basis of the energy absorption (93 ergs/gram) corresponding to the irradiation of body tissue by 1 roentgen of *X* radiation.

Roentgen equivalent physical (rep) unit, now *obsolete*, corresponds to energy absorption of 93 ergs/gram by tissue through which ionizing radiation passes.

Radiation safety *continued*

The rad unit replaces the rep unit, 1 (rad) = (100/93) (rep), and corresponds to energy absorption of 100 ergs/gram of body tissue.

Relative biolcgical effectiveness (rbe) is a weighting factor, equal to unity for X rays, that expresses how much more or less effectively a given radiation produces biological effects than do X rays of the same rad. The assignment of a number for rbe is clearly not straightforward, since a number of biological effects must be considered, and there are not as yet well established values of rbe in man. Some currently accepted qualitative values are tabulated in Fig. 18.

Fig. 18—Relative biological effectiveness (rbe).

particle	rbe
X and γ rays, β particles	1
Protons	5
α particles (low energy)	20
Neutrons	
Slow	5
Fast	10

Roentgen equivalent mammal (rem) unit, defined originally in terms of the rep, is the amount of any given radiation producing the same biological effect as 1 rep of X rays. The current definition is given properly as

$$1\ (\text{rem}) = [1/(\text{rbe})]\ (\text{rad})$$

but is for practical purposes unchanged because of the small difference (< 10 percent) between the rep and rad units.

Radiation dosimetry

A number* of calibrated portable radiation detection instruments have been designed using standard particle detectors in conjunction with count-integrating and count-rate circuitry. The devices are usually designed for specific applications, such as the detection of small amounts of radioactive contamination or the measurement of radiation from high-energy accelerators and use particle detectors (Geiger-Müller, ionization chamber, etc.) suited to the application. Pocket dosimeters and photographic films that may be worn on the body constitute very-important protection methods and are in almost universal use. The former are small ionization chambers, usually of the shape and size of a pocket pen, that can be charged from an external battery. The dosimeter charge leaks off in the presence of ionizing radiations and the amount of charge lost is a measure of the radiation to which the chamber has been exposed. The exposure is read on

* See, for example, "Annual Buyer's Guide", *Nucleonics*, vol. 12, p. D-26; November, 1954.

Radiation safety *continued*

a calibrated electrometer that is usually part of the dosimeter. Calibrated photographic film prepared by carefully controlled methods shows, by the amount of blackening, the amount of γ radiation to which it has been exposed. When used with suitable types and thicknesses of metal, the film also provides an estimate of the radiation spectrum and detects the presence of β particles. Neutrons can be detected by films that record the track of recoiling hydrogen nuclei. The films are examined by microscope to determine the neutron exposure. Film-badge services are provided by several of the national laboratories and in a number of areas by private agencies.

Handling radioactive isotopes

The hazard presented by radioisotopes is dependent on a number of factors. If the isotope is external to the body, important considerations—besides isotope amount, its distance from the body, and the area of the body irradiated—are the energy and kind of particle emitted. γ rays and neutrons can penetrate deeply into the body and affect vital organs. Charged particles cannot penetrate to great depths and constitute a hazard to the extent that they damage the body surface. In this respect, electrons are more damaging than α particles of the same energy. The human tolerances to external radiation exposure are indicated in Fig. 19.*

By far the greatest problem presented by radioisotopes is the possibility of their being taken into the body through inhalation, ingestion, or through breaks in the skin. Radiations originating within the body present an entirely different and more-serious problem; in particular, energetic α and β particles are very damaging. Important additional considerations are the lifetime of the radioisotope and its chemical character and form. These determine the extent to which it is absorbed, the organs to which it preferentially migrates, the ease with which it is excreted by the body, and its effective lifetime within the body. Certain isotopes, for example of radium, strontium, and plutonium, are long-lived and are also retained in critical body tissue for long periods. These isotopes are dangerous in very-small amounts: absorption into the body of 0.1 microcurie (10^{-13} gram) of radium is considered to be a maximum permissible amount and plutonium is estimated to be up to 10 times as hazardous.

Short-lived isotopes (minutes to days of half-life) are in general not of concern unless there is chronic daily exposure or they are handled in

* From, "Permissible Dose from External Sources of Ionizing Radiation", National Bureau of Standards Handbook No. 59, U. S. Government Printing Office; Washington 25, D. C.: September 24, 1954. It is recommended that this handbook be consulted for appropriate interpretation and extension of the data presented.

Radiation safety *continued*

Fig. 19—Maximum permissible exposure to external radiation.

radiation	exposure	magnitude
X, γ rays less than 3 mev	Long-term maximum permissible weekly dose	Whole body 0.3 roentgen measured in air at point of highest weekly dose in region occupied by person
	Accidental or emergency exposure (once in lifetime)	Whole body 25 roentgens—total dose measured in air Local Hands, forearms, feet, ankles: 100 roentgens—dose measured in air in addition to whole-body dose
	Planned emergency exposure (once in lifetime)	Dose not greater than one-half those specified under "Accidental"
X, γ rays, any energy	Long-term maximum permissible weekly dose	Local Hands, forearms, feet, ankles: 1.5 roentgens for skin Head, neck: 1.5 roentgens for skin 0.45 roentgen for lenses of eye
Neutrons, of energy $2.0–20 \times 10^6$ electron–volts $0.5–2 \times 10^6$ electron–volts Thermal ($<$ 1 electron–volt)	For 40-hour week	 30 neutrons/cm²/sec 50 neutrons/cm²/sec 1200 neutrons/cm²/sec
Radiation of very-low penetration power (half-value layer < 1 millimeter of tissue)	Long-term maximum permissible weekly dose	Whole body 1.5 rem for skin 0.3 rem for lenses of eye
Ionizing radiations, any type(s)	Long-term maximum permissible weekly dose	Whole body 0.3 rem for bloodforming organs, gonads, lenses of eye 0.6 rem for skin Local Hands, forearms, feet, ankles: 1.5 rem for skin Head, neck: 1.5 rem for skin 0.3 rem for lenses of eye
Any type	Weekly fluctuations	In 1 week, accumulated dose in any organ may exceed by 3 the basic permissible weekly dose, provided that total dose accumulated in any 13 consecutive weeks does not exceed by 10 the respective basic permissible weekly dose

Radiation safety *continued*

extremely large amounts. Caution should in any case be exercised in the handling of all radioisotopes. Isotopes with half-lives from a few years to about 100 years are especially dangerous, since they are long-lasting and because very small amounts possess high activities. Tolerances for internally absorbed radioactive material are indicated in Fig. 20. The general biological effects of radiation is shown in Fig. 21.

In general, it is to be stressed that no attempt should be made by untrained personnel to handle unsealed radioactive materials or perform any operations with them, either chemical or physical. Attention is drawn to the excellent detailed references and discussions listed in the following bibliography.

Fig. 20—Maximum permissible amounts of radioisotopes in total body.*

radioisotope	where concentrated	permissible amount in total body in microcuries
Ra^{226}	Bone	0.1
Sr^{90}	Bone	1.0
$Co^{60} + Y^{90}$	Liver	3.0
P^{32}	Bone	10.0
Ca^{45}	Bone	65.0
$Cs^{137} + Ba^{137}$	Muscle	90.0

* "Maximum Permissible Amounts of Radioisotopes in the Human Body and Maximum Permissible Concentrations in Air and Water", National Bureau of Standards Handbook No. 52, U. S. Government Printing Office; Washington, D. C.: March 20, 1953.

Health physics, radioisotopes, radioactivity bibliography

1. Handbooks of the National Bureau of Standards available by purchase from the Superintendent of Documents, U. S. Government Printing Office, Washington 25, D. C.
   - 23—Radium Protection: 1938.
   - 41—Medical X-ray Protection up to Two Million Volts: 1949.
   - 42—Safe Handling of Radioactive Isotopes: 1949.
   - 47—Recommendations of the International Commission on Radiological Protection and of the International Commission on Radiological Units: 1950.
   - 48—Control and Removal of Radioactive Contamination in Laboratories: 1951.
   - 50—X-ray Protection Design: 1952.
   - 51—Radiological Monitoring Methods and Instruments: 1952.
   - 52—Maximum Permissible Amounts of Radioisotopes in the Human Body and Maximum Permissible Concentrations in Air and Water: 1953.
   - 54—Protection Against Radiations from Radium, Cobalt-60, and Cesium-137: 1954.
   - 57—Photographic Dosimetry of X- and Gamma-Rays: 1954.
   - 59—Permissible Dose from External Sources of Ionizing Radiation: 1954.
2. R. D. Evans, "Fundamentals of Radioactivity and Its Instrumentation", *Advances in Biological and Medical Physics*, vol. 1, Academic Press, Inc.; New York, N. Y.: 1948.

Radiation safety *continued*

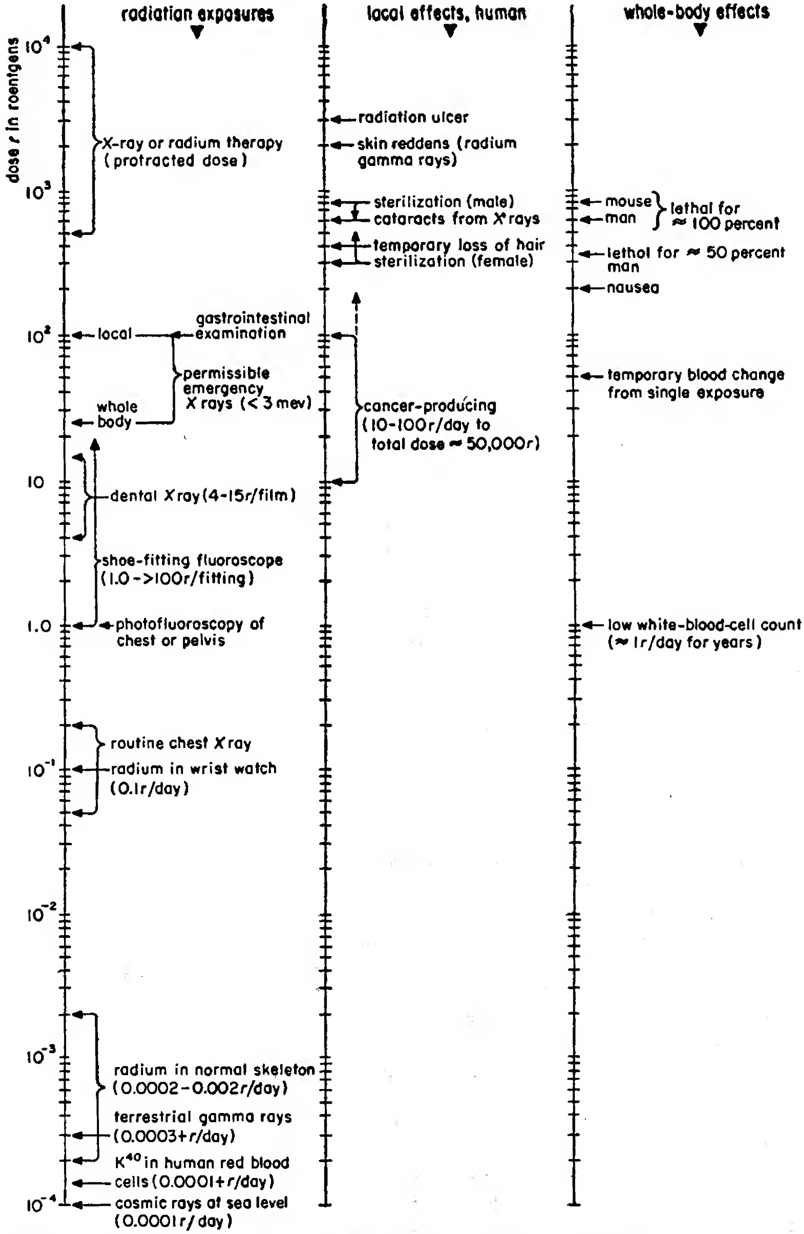

Fig. 21—Chart of radiation effects. **After R. D. Evans and C. R. Williams.**

Radiation safety *continued*

3. "Tabulation of Available Data Relative to Radiation Biology", Report 1019-1ER-17, NEPA Project, U. S. Atomic Energy Commission; Oak Ridge, Tenn.: 1949.
4. "Guide for Selection of Equipment for Radioactivity Laboratories", *Nucleonics*, vol. 7, p. R-1; November, 1950.
5. O. Glasser, Editor, "Medical Physics, II", Year Book Publishers, Inc.; Chicago, Ill.: 1950.
6. R. E. Zirkle, Editor, "Biological Effects of External Beta Radiation", McGraw-Hill Book Co., Inc.; New York, N. Y.: 1951.
7. A. Haddow, Editor, "Biological Hazards of Atomic Energy", Clarendon Press; Oxford, England: 1952.
8. J. R. Bradford, Editor, "Radioisotopes in Industry", Reinhold Publishing Corp.; New York, N. Y.: 1953.
9. F. G. Spear, "Radiation and Living Cells", John Wiley & Sons, Inc.; New York, N. Y.: 1953.
10. "General Handbook for Radiation Monitoring", Report LA1835, Los Alamos Scientific Laboratory; Los Alamos, N. M.: September, 1954.
11. H. A. Blair, Editor, "Biological Effects of External Radiation", McGraw-Hill Book Co., Inc.; New York, N. Y.: 1954.
12. L. D. Marinelli, "Radiation Dosimetry and Protection", *Annual Review of Nuclear Science*, vol. 3, Annual Reviews, Inc.; Stanford, Cal.: 1954.
13. R. E. Zirkle, Editor, "Biological Effects of External X- and Gamma Radiation, Part 1", McGraw-Hill Book Co., Inc.; New York, N. Y.: 1954.
14. C. L. Comar, "Radioisotopes in Biology and Agriculture", McGraw-Hill Book Company, Inc.; New York, N. Y.: 1955.

Miscellaneous data

Pressure–altitude graph

Design of electrical equipment for aircraft is somewhat complicated by the requirement of additional insulation for high voltages as a result of the decrease in atmospheric pressure. The extent of this effect may be determined from the chart below and the information on the opposite page.

1 inch mercury = 25.4 mm mercury = 0.4912 pounds/inch^2

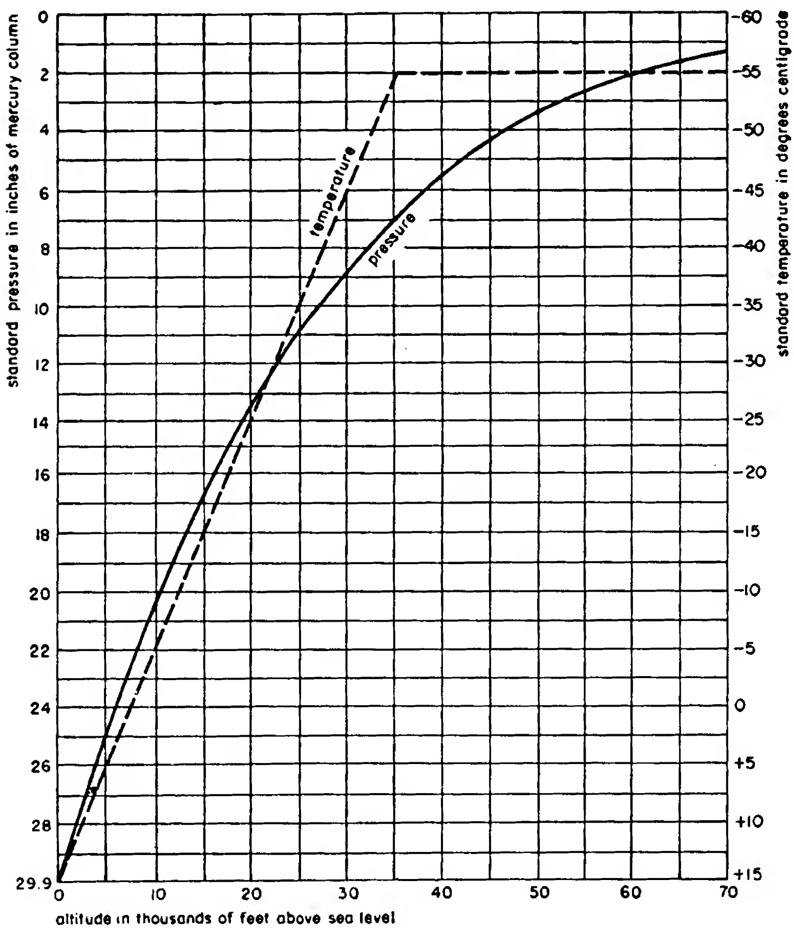

Sparkgap breakdown voltages

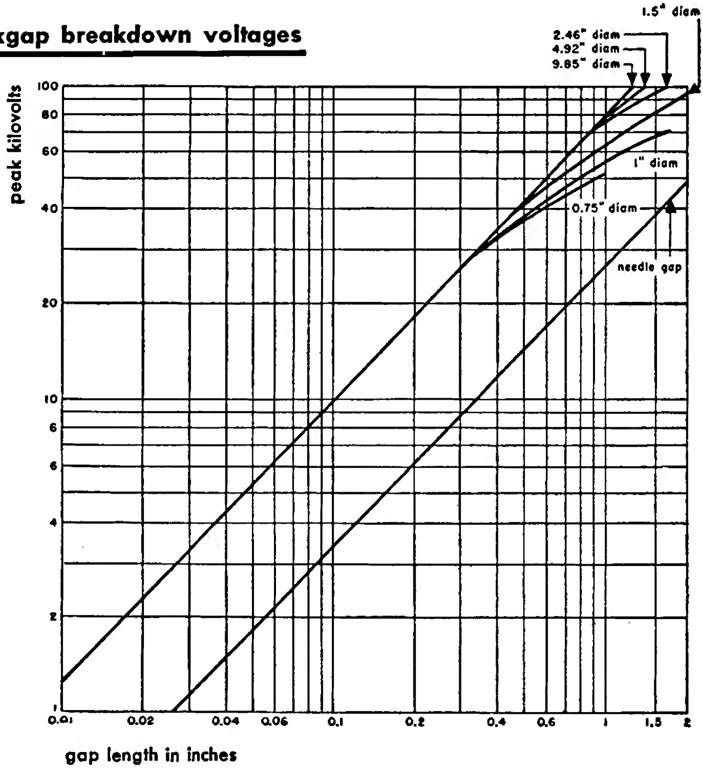

Table of multiplying factors.

pressure		temperature in degrees centigrade					
in Hg	mm Hg	−40	−20	0	20	40	60
5	127	0.26	0.24	0.23	0.21	0.20	0.19
10	254	0.47	0.44	0.42	0.39	0.37	0.34
15	381	0.68	0.64	0.60	0.56	0.53	0.50
20	508	0.87	0.82	0.77	0.72	0.68	0.64
25	635	1.07	0.99	0.93	0.87	0.82	0.77
30	762	1.25	1.17	1.10	1.03	0.97	0.91
35	889	1.43	1.34	1.26	1.19	1.12	1.05
40	1016	1.61	1.51	1.42	1.33	1.25	1.17
45	1143	1.79	1.68	1.58	1.49	1.40	1.31
50	1270	1.96	1.84	1.73	1.63	1.53	1.44
55	1397	2.13	2.01	1.89	1.78	1.67	1.57
60	1524	2.30	2.17	2.04	1.92	1.80	1.69

The graph above is for a voltage that is continuous or at a frequency low enough to permit complete deionization between cycles, between needle points, or clean, smooth spherical surfaces (electrodes ungrounded) in

Sparkgap breakdown voltages *continued*

dust-free dry air. Temperature is 25 degrees centigrade and pressure is 760 millimeters (29.9 inches) of mercury. Peak kilovolts shown in the chart should be multiplied by the factors given below it for atmospheric conditions other than the above.

An approximate rule for uniform fields at all frequencies up to at least 300 megacycles is that the breakdown gradient of air is 30 peak kilovolts/centimeter or 75 peak kilovolts/inch at sea level (760 millimeters of mercury) and normal temperature (25-degrees centigrade). The breakdown voltage is approximately proportional to pressure and inversely proportional to absolute (degrees-Kelvin) temperature.

Certain synthetic gases have higher dielectric strengths than air. Two such gases that appear to be useful for electrical insulation are sulfur hexafluoride (SF_6) and Freon 12 (CCl_2F_2), which both have about 2.5 times the dielectric strength of air. Mixtures of sulfur hexafluoride with helium and of perfluoromethylcyclohexane (C_7F_{14}) with nitrogen have good dielectric strength as well as other desirable properties.

Weather data*

Temperature extremes

United States

Lowest temperature	−70° F	Rodgers Pass, Montana (January 20, 1954)
Highest temperature	134° F	Greenland Ranch, Death Valley, California (July 10, 1933)

Alaska

Lowest temperature	−76° F	Tanana (January, 1886)
Highest temperature	100° F	Fort Yukon (June 27, 1915)

World

Lowest temperature	−90° F	Oimekon, Siberia (February, 1933)
Highest temperature	136° F	Azizia, Libya, North Africa (September 13, 1922)
Lowest mean temperature (annual)	−14° F	Framheim, Antarctica
Highest mean temperature (annual)	86° F	Massawa, Eritrea, Africa

* Compiled from "Climate and Man," Yearbook of Agriculture, U. S. Dept. of Agriculture, 1941. Obtainable from Superintendent of Documents, Government Printing Office, Washington 25, D. C.

Weather data *continued*

Precipitation extremes

United States

Wettest state	Louisiana—average annual rainfall 57.34 inches
Dryest state	Nevada—average annual rainfall 8.60 inches
Maximum recorded	Camp Leroy, California (January 22-23, 1943)—26.12 inches in 24 hours
Minimums recorded	Bagdad, California (1909–1913)—3.93 inches in 5 years
	Greenland Ranch, California—1.76 inches annual average

World

Maximums recorded	Cherrapunji, India (July, 1861)—366 inches in 1 month. (Average annual rainfall of Cherrapunji is 450 inches)
	Bagui, Luzon, Philippines, July 14–15, 1911—46 inches in 24 hours
Minimums recorded	Wadi Halfa, Anglo-Egyptian Sudan and Aswan, Egypt are in the "rainless" area; average annual rainfall is too small to be measured

World temperatures

territory	maximum °F	minimum °F	territory	maximum °F	minimum °F
NORTH AMERICA			ASIA *continued*		
Alaska	100	−76	India	120	−19
Canada	103	−70	Iraq	125	19
Canal Zone	97	63	Japan	101	−7
Greenland	86	−46	Malay States	97	66
Mexico	118	11	Philippine Islands	101	58
U. S. A.	134	−70	Siam	106	52
West Indies	102	45	Tibet	85	−20
			Turkey	111	−22
SOUTH AMERICA			U. S. S. R. (Russia)	109	−90
Argentina	115	−27			
Bolivia	82	25	AFRICA		
Brazil	108	21	Algeria	133	1
Chile	99	19	Anglo-Egyptian Sudan	126	28
Venezuela	102	45	Angola	91	33
			Belgian Congo	97	34
EUROPE			Egypt	124	31
British Isles	100	4	Ethiopia	111	32
France	107	−14	French Equatorial Africa	118	46
Germany	100	−16	French West Africa	122	41
Iceland	71	−6	Italian Somaliland	93	61
Italy	114	4	Libya	136	35
Norway	95	−26	Morocco	119	5
Spain	124	10	Rhodesia	112	18
Sweden	92	−49	Tunisia	122	28
Turkey	100	17	Union of South Africa	111	21
U. S. S. R. (Russia)	110	−61			
			AUSTRALASIA		
ASIA			Australia	127	19
Arabia	123	35	Hawaii	91	51
China	111	−10	New Zealand	94	23
East Indies	101	60	Samoan Islands	96	61
French Indo-China	113	33	Solomon Islands	97	70

Weather data *continued*

Wind-velocity and temperature extremes in North America

Maximum corrected wind velocity (fastest single mile).

station	wind miles/hour	temperature degrees fahrenheit maximum	minimum
UNITED STATES, 1871–1955			
Albany, New York	71	104	−26
Amarillo, Texas	84	108	−16
Buffalo, New York	91	99	−21
Charleston, South Carolina	76	104	7
Chicago, Illinois	87	105	−23
Bismarck, North Dakota	72	114	−45
Hatteras, North Carolina	110	97	8
Miami, Florida	132	95	27
Minneapolis, Minnesota	92	108	−34
Mobile, Alabama	87	104	−11
Mt. Washington, New Hampshire	188*	71	−46
Nantucket, Massachusetts	91	95	−6
New York, New York	99	102	−14
North Platte, Nebraska	72	112	−35
Pensacola, Florida	114	103	7
Washington, D.C.	62	106	−15
San Juan, Puerto Rico	149†	94	62
CANADA, 1955			
Banff, Alberta	52‡	97	−60
Kamloops, British Columbia	34‡	107	−37
Sable Island, Novia Scotia	64‡	86	−12
Toronto, Ontario	48‡	105	−46

* Gusts were recorded at 231 miles/hour (corrected).
† Estimated.
‡ For a period of 5 minutes.

Useful numerical data

1 cubic foot of water at 4° C (weight)	62.43 lb
1 foot of water at 4° C (pressure)	0.4335 lb/in²
Velocity of light in vacuum, c	186,280 mi/sec = 2.998×10^{10} cm/sec
Velocity of sound in dry air at 20° C, 76 cm Hg	1127 ft/sec
Degree of longitude at equator	69.173 miles
Acceleration due to gravity at sea-level, 40° Latitude, g	32.1578 ft/sec²
$\sqrt{2g}$	8.020
1 inch of mercury at 4° C	1.132 ft water = 0.4908 lb/in²
Base of natural logs ϵ	2.718
1 radian	$180° \div \pi = 57.3°$
360 degrees	2π radians
π	3.1416
Sine 1′	0.00029089
Arc 1°	0.01745 radian
Side of square	$0.707 \times$ (diagonal of square)

Centigrade table of relative humidity or percent of saturation

dry bulb degrees centigrade	difference between readings of wet and dry bulbs in degrees centigrade 0.5	1.0	1.5	2.0	2.5	3.0	3.5	4.0	4.5	5	6	7	8	9	10	11	12	13	14	15	16	18	20	22	24	26	28	30	32	34	36	38	40	dry bulb degrees centigrade
4	93	85	77	70	63	56	48	41	34	28	15																							4
8	94	87	81	74	68	62	56	50	45	39	28	17																						8
12	94	89	84	78	73	68	63	58	53	48	38	30	21	12	4																			12
16	95	90	85	81	76	71	67	62	58	54	45	37	29	21	14	7																		16
20	96	91	87	82	78	74	70	66	62	58	51	44	36	30	23	17	11																	20
22	96	92	87	83	79	75	72	68	64	60	53	46	40	34	27	21	16	11																22
24	96	92	88	85	81	77	74	70	66	63	56	49	43	37	31	26	21	14	10															24
26	96	92	89	85	81	77	74	71	67	64	57	51	45	39	34	28	23	18	13															26
28	96	92	89	85	82	78	75	72	68	65	59	53	47	42	37	31	26	21	17	13														28
30	96	93	89	86	82	79	76	73	70	67	61	55	50	44	39	35	30	24	20	16	12													30
32	96	93	90	86	83	80	77	74	71	68	62	56	51	46	41	36	32	27	23	19	15													32
34	97	93	90	87	84	81	77	74	71	69	63	58	53	48	43	38	34	30	26	22	18	10												34
36	97	93	90	87	84	81	78	75	72	70	64	59	54	50	45	41	36	32	28	24	21	13												36
38	97	94	90	87	84	81	79	76	73	70	65	60	56	51	46	42	38	34	30	26	23	16	10											38
40	97	94	91	88	85	82	79	76	74	71	66	61	57	52	48	44	40	36	32	29	25	19	13											40
44	97	94	91	88	86	83	80	77	75	73	68	63	59	54	50	47	43	39	36	32	29	23	17	12										44
48	97	94	92	89	86	84	81	78	76	74	69	65	61	56	53	49	45	42	39	35	33	27	21	16	12									48
52	97	94	92	89	87	84	82	79	77	75	70	66	62	58	55	51	48	44	41	38	35	30	25	20	16	11								52
56	97	95	92	90	87	85	83	80	78	76	72	68	64	60	57	53	50	46	43	40	38	32	27	23	19	15	11							56
60	98	95	93	90	88	86	83	81	79	77	73	69	65	62	58	55	52	48	45	43	40	35	30	26	21	18	14	11						60
70	98	96	93	91	89	87	85	83	81	79	75	71	68	65	61	58	55	52	50	47	44	40	35	31	27	23	20	17	14	11				70
80	98	96	94	92	90	88	86	84	83	81	77	74	71	67	64	61	58	56	53	50	48	43	39	35	31	28	24	22	19	16	14	11		80
90	98	97	95	93	91	89	87	85	84	82	79	76	73	69	67	64	61	58	56	53	51	47	42	39	35	32	28	26	23	20	18	16	14	90
100	99	97	95	93	92	90	88	86	85	83	80	77	74	71	68	66	63	60	58	56	54	49	45	42	38	35	32	29	26	24	22	19	17	100

Example: Assume dry-bulb reading (thermometer exposed directly to atmosphere) is 20° C and wet-bulb reading is 17° C, or a difference of 3° C. The relative humidity at 20° C is then 74%.

Materials and finishes for tropical and marine use

Corrosion

Ordinary finishing of equipment fails in meeting satisfactorily conditions encountered in tropical and marine use. Under these conditions corrosive influences are greatly aggravated by prevailing higher relative humidities, and temperature cycling causes alternate condensation on, and evaporation of moisture from, finished surfaces. Useful equipment life under adverse atmospheric influences depends largely on proper choice of base materials and finishes applied. Especially important in tropical and marine applications is avoidance of electrical contact between dissimilar metals.

Dissimilar metals, widely separated in the galvanic series,* should not be bolted, riveted, etc., without separation by insulating material at the facing surfaces. The only exception occurs when both surfaces have been coated with the same protective metal, e.g., electroplating, hot dipping, galvanizing, etc.

Aluminum, steel, zinc, and cadmium should never be used bare. Electrical contact surfaces should be given copper–nickel–chromium or copper–nickel finish, and, in addition, they should be silver plated. Variable-capacitor plates should be silver plated.

An additional 0.000015 to 0.000020 electroplating of hard, bright gold over the silver will greatly improve resistance to tarnish and oxidation and to attack by most chemicals; will lower electrical resistance; and will provide long-term solderability.

Fungus and decay

The value of fungicidal coatings or treatments is controversial. When

* The galvanic series is given on p. 42.

Finish application table†

material	finish	remarks
Aluminum alloy	Anodizing	An electrochemical-oxidation surface treatment, for improving corrosion resistance; not an electroplating process. For riveted or welded assemblies specify chromic acid anodizing. Do not anodize parts with nonaluminum inserts. Colors vary: Yellow-green, gray or black.
	"Alrok"	Chemical-dip oxide treatment. Cheap. Inferior in abrasion and corrosion resistance to the anodizing process, but applicable to assemblies of aluminum and nonaluminum materials.

† By Z. Fox. Reprinted by permission from *Product Engineering*, vol. 19, p. 161; January, 1948.

Materials and finishes for tropical and marine use *continued*

material	finish	remarks
Copper and zinc alloys	Bright acid dip	Immersion of parts in acid solution. Clear lacquer applied to prevent tarnish.
Brass, bronze, zinc die-casting alloys	Brass, chrome, nickel, tin	As discussed under steel.
Magnesium alloy	Dichromate treatment	Corrosion-preventive dichromate dip. Yellow color.
Stainless steel	Passivating treatment	Nitric-acid immunizing dip.
Steel	Cadmium	Electroplate, dull white color, good corrosion resistance, easily scratched, good thread antiseize. Poor wear and galling resistance.
	Chromium	Electroplate, excellent corrosion resistance and lustrous appearance. Relatively expensive. Specify hard chrome plate for exceptionally hard abrasion-resistive surface. Has low coefficient of friction. Used to some extent on nonferrous metals particularly when die-cast. Chrome plated objects usually receive a base electroplate of copper, then nickel, followed by chromium. Used for build-up of parts that are undersized. Do not use on parts with deep recesses.
	Blueing	Immersion of cleaned and polished steel into heated saltpeter or carbonaceous material. Part then rubbed with linseed oil. Cheap. Poor corrosion resistance.
	Silver plate	Electroplate, frosted appearance; buff to brighten. Tarnishes readily. Good bearing lining. For electrical contacts, reflectors.
	Zinc plate	Dip in molten zinc (galvanizing) or electroplate of low-carbon or low-alloy steels. Low cost. Generally inferior to cadmium plate. Poor appearance. Poor wear resistance: electroplate has better adherence to base metal than hot-dip coating. For improving corrosion resistance, zinc-plated parts are given special inhibiting treatments.
	Nickel plate	Electroplate, dull white. Does not protect steel from galvanic corrosion. If plating is broken, corrosion of base metal will be hastened. Finishes in dull white, polished, or black. Do not use on parts with deep recesses.
	Black oxide dip	Nonmetallic chemical black oxidizing treatment for steel, cast iron, and wrought iron. Inferior to electroplate. No buildup, Suitable for parts with close dimensional requirements as gears, worms, and guides. Poor abrasion resistance.
	Phosphate treatment	Nonmetallic chemical treatment for steel and iron products. Suitable for protection of internal surfaces of hollow parts. Small amount of surface buildup. Inferior to metallic electroplate. Poor abrasion resistance. Good paint base.
	Tin plate	Hot dip or electroplate. Excellent corrosion resistance, but if broken will not protect steel from galvanic corrosion. Also used for copper, brass, and bronze parts that must be soldered after plating. Tin-plated parts can be severely worked and deformed without rupture of plating.
	Brass plate	Electroplate of copper and zinc. Applied to brass and steel parts where uniform appearance is desired. Applied to steel parts when bonding to rubber is desired.
	Copper plate	Electroplate applied preliminary to nickel or chrome plates Also for parts to be brazed or protected against carburization Tarnishes readily.

Materials and finishes for tropical and marine use *continued*

equipment is to operate under tropical conditions, greater success can be achieved by the use of materials that do not provide a nutrient medium for fungus and insects. The following types or kinds of materials are examples of nonnutrient mediums that are generally considered acceptable.

Metals
Glass
Ceramics (steatite, glass-bonded mica)
Mica
Polyamide
Cellulose acetate
Rubber (natural or synthetic)
Plastic materials using glass, mica, or asbestos as a filler
Polyvinylchloride
Polytetrafluoroethylene
Monochlortrifluorethylene

The following types or kinds of materials should not be used, except where such materials are fabricated into completed parts and it has been determined that their use is acceptable to the customer concerned.

Linen
Cellulose nitrate
Regenerated cellulose
Wood
Jute
Leather
Cork
Paper and cardboard
Organic fiberboard
Hair or wool felts
Plastic materials using cotton, linen or wood flour as a filler

Wood should not be used as an electrical insulator and the use of wood for other purposes should be restricted to those parts for which a superior substitute is not known. When used, it should be pressure-treated and impregnated to resist moisture, insects, and decay with a water-borne preservative (as specified in Federal Specification *TT-W-571*), and should also be treated with a suitable fire-retardant chemical.

Principal low-voltage power supplies in foreign countries*

territory	dc volts	ac volts	frequency
NORTH AMERICA			
Alaska	—	**110**, 220	60
Bermuda	—	**110**, 220	60
British Honduras	110, 220	—	—
Canada	—	**110**, 115, 120, 220, 230	**60**, 25
Costa Rica	—	**110**, 220	60
El Salvador	110	**110**, 220	60
Guatemala	220	**110**, 220	**60**, 50
Honduras	120, 220	**110**, 220	60
Mexico	—	**110**, 115, 120, **125**, 220	**60**, 50
Nicaragua	110, 125	**110**, 220	60
Panama (Republic)	—	**110**, 220	**60**, 50
Panama (Canal Zone)	—	115	25, 60
WEST INDIES			
Antigua	220	—	—
Aruba	—	**115**, 220	60
Bahamas	—	110, **115**, 120, 220	60
Barbados	—	110	50
Cuba	—	**110**, 115, 220	60
Curacao	—	**115**, 125, 220	50
Dominican Republic	—	**110**, 120, 220, 240	60
Guadeloupe	—	110	50
Jamaica	—	**110**, 220	40, 60
Martinique	—	110, 220	50
Puerto Rico	—	**115**, 230	60
Trinidad	—	110, 230	60
Virgin Islands	—	**115**, 230	60
SOUTH AMERICA			
Argentina	**220**	**220**, 225	25, **50**, 60
Bolivia	110, 220	**110**, **220**, 230, 240	**50**, 60
Brazil	220	**110**, **120**, 127, 220	**50**, **60**
British Guiana	—	110, **115**, 230	**50**, 60
Chile	220	110, **220**	**50**, 60
Colombia	—	**110**, 115, **150**, 220, 230, 260	50, **60**
Ecuador	—	**110**, 220	60
French Guiana	—	110	50
Paraguay	220	**220**	50
Peru	220	110, **220**, 240	50, **60**
Surinam (Neth. Guiana)	—	**125**, 220	**50**, 60
Uruguay	—	220	50
Venezuela	—	**110**, 120, 220	**50**, 60
EUROPE			
Albania	—	125, **220**, 230	50
Austria	110	110, 120, **220**	50
Azores	220	110, **220**	**50**, 60
Balearic Islands	—	110, 125, 220	50
Belgium	110, 220	**110**, 115, 127, 130, 190, **220**	50
Bulgaria	—	150, **220**	50
Canary Islands	—	110, **115**, 190, 220	50
Cape Verde Islands	220, **230**, 240	—	—
Corsica	—	120, **127**, 200, 220	50
Crete	220	**127**, 220	50
Czechoslovakia	—	**110**, 200, 220	50
Denmark	110, **220**, 240	**220**	50
Dodecanese Islands	110	127, **220**	50
Estonia	110, 220	200, 220	50

* See footnotes on page 931.

Principal low-voltage power supplies in foreign countries* *continued*

territory	dc volts	ac volts	frequency
EUROPE—*continued*			
Finland	110, 127	110, 127, **220**, 230	50
France	110, 220	110, **115**, 120, 190, 200, 220	25, **50**
Germany	110, 240	110, 120, 127, **220**	50
Gibraltar	440	110, 240	50, 76
Greece	220	**127**, 220	50
Hungary	—	105, 110, 120, **220**	42, **50**
Iceland	—	220	50
Ionian Islands	220	**127**, 220	50
Ireland (Republic of)	—	200, **220**, 250	50
Italy	—	**127**, **150**, 160, 220, 260, 280	42, **50**
Latvia	—	220	50
Lithuania	220	**220**	50
Luxembourg	110, 220	110, 220	50, 60
Madeira Islands	110, 220	**220**	50
Malta	—	100, 220	50
Monaco	—	110	42
Netherlands	220	120, 127, 150, 208, **220**, 260	50
Norway	—	130, 150, **220**, 230	45, **50**
Poland	110, 120, **220**	110, **220**	50
Portugal	—	110, 190, **220**	50
Rumania	220	110, 150, 208, **220**	42, **50**
Spain	110, 130, 150, 220, 260	110, 127, 220	50
Sweden	127, 220	110, 127, 220	25, 50
Switzerland	160, 220	110, 125, 190, **220**, 250	50
Trieste	—	100, 120, 220	42, 50
Turkey	—	110, 190, **220**	50
United Kingdom	200, 220, **230**, 240	200, **230**, 240, 250	50
U.S.S.R. (Russia)	110, 220	110, 120, 127, 220	50
Yugoslavia	—	220	50
ASIA			
Aden	—	230	50
Afghanistan	—	115, 200, 220, 230	50, 60
Bahrein	—	230	50
Burma	—	220	50, 60
Cambodia	—	110, 190, 220	50
Ceylon	230	220, **230**, 240	50
China	—	**110**, 135, 190, **220**, 230	50, 60
Cyprus	220	110, 220	50
Formosa (Taiwan)	—	110	60
Hong Kong	—	200	**50**, 60
India	**220**, 230	220, **230**	50
Indonesia	—	**127**, 220	50
Iran	110	110, **220**	50, 60
Iraq	220	200, 220, 230	50
Israel	—	220	50
Japan	—	100, 110, 200, 220	40, 50, 60
Jordan	—	220	50
Korea	—	100, **110**, 200, 220	50, **60**
Kuwait	—	220, 240	50, 60
Laos	—	115	50
Lebanon	—	**110**, 190, 220	50
Malayan Federation	230	230	50
Nepal	—	120, 220	60
Okinawa	—	110	60
Pakistan	220	**220**, 230	50
Philippines	—	**110**, 220	60
Sarawak	—	230	50
Saudi Arabia	—	**110**, 220	60
Singapore	—	220	50
Syria	—	**110**, 190	**50**, 60
Thailand	110, 220	110, 220	50

Principal low-voltage power supplies in foreign countries* *continued*

territory	dc volts	ac volts	frequency
ASIA—*continued*			
Vietnam	—	115, 120, 208, 210	50
Yemen	—	**127,** 220	50
AFRICA			
Algeria	—	110, **127,** 220	50
Angola	—	220	50
Belgian Congo	220	220	50
Dahomey	220	230	50
Egypt	220	110, 200, 220	40, 42, **50**
Ethiopia	—	110, 127, 220	50
French Guinea	—	115, **230**	50
Gold Coast	220	230	50
Ivory Coast	220	230	50
Kenya	—	220, **240**	50
Liberia	—	110, 200, 220	50, 60
Libya	—	**125,** 130, 220	50
Madagascar	—	110, 115, 120, 200, 208, 220	50
Mauritania	—	115, 200	50
Mauritius	—	230	50
Morocco (French)	—	110, 115, 127, 220	50
Morocco (Spanish)	—	**127,** 220	50
Mozambique	240	220	50
Niger	—	230	50
Nigeria	—	230	50
Northern Rhodesia	—	220, 230	50
Nyasaland	—	230	50
Senegal	—	**115,** 127, 200, 220	50
Sierra Leone	—	230	50
Somaliland (British)	110	—	—
Somaliland (French)	220	—	—
Southern Rhodesia	—	220, 230	50
Sudan (French)	—	**115,** 200	50
Tanganyika	230	220, 230, 240	50
Tangier	—	**110,** 220	50
Tunisia	—	**110,** 127, 190, 220	50
Uganda	—	240	50
Union of South Africa	220, 230	120, 200, **220,** 240, 250	50
Upper Volta	—	230	50
OCEANIA			
Australia	220, 240	110, 230, **240,** 250	40, **50**
Fiji Islands	240	240	50
Hawaii	—	110, **120,** 208, 240	60
New Caledonia	—	110, 120	50
New Guinea (British)	—	**110,** 220, 240	50
New Zealand	230	220, **230**	50
Samoa	—	110, 220	50
Society Islands	—	110	60

* From "Electric Current Abroad" issued by the U. S. Department of Commerce, April 1954.

Bold numbers indicate the predominate voltages and types of supply where different kinds of supply exist.

Caution: The listings in these tables represent electrical supplies most generally used in each country. For power supply characteristics of particular cities, refer to the preceding reference, which may be obtained at nominal cost from the Superintendent of Documents, U. S. Government Printing Office, Washington 25, D. C.

Electric-motor data

Wiring and fusing data*

hp of motor	current rating amperes	minimum size wire AWG: type‡ R or T	minimum size wire AWG: type‡ RH	conduit internal diam in inches†: type‡ R or T	conduit internal diam in inches†: type‡ RH	maximum running fuse amperes	current rating amperes	minimum size wire AWG: type‡ R or T	minimum size wire AWG: type‡ RH	conduit internal diam in inches†: type‡ R or T	conduit internal diam in inches†: type‡ RH	maximum running fuse amperes
	single phase—115 volts						**single phase—230 volts**					
½	7.4	14	14	½	½	10	3.7	14	14	½	½	6
¾	10.2	14	14	½	½	15	5.1	14	14	½	½	8
1	13	12	12	½	½	20	6.5	14	14	½	½	10
1½	18.4	10	10	¾	¾	25	9.2	14	14	½	½	12
2	24	10	10	¾	¾	30	12	14	14	½	½	15
3	34	6	8	1	¾	45	17	10	10	¾	¾	25
5	56	4	4	1¼	1¼	70	28	8	8	¾	¾	35
7½	80	1	3	1½	1¼	100	40	6	6	1	1	50
10	100	1/0	1	1½	1½	125	50	4	6	1¼	1	60
	3-phase induction—220 volts						**3-phase induction—440 volts**					
½	2	14	14	½	½	3	1	14	14	½	½	2
¾	2.8	14	14	½	½	4	1.4	14	14	½	½	2
1	3.5	14	14	½	½	4	1.8	14	14	½	½	3
1½	5	14	14	½	½	8	2.5	14	14	½	½	4
2	6.5	14	14	½	½	8	3.3	14	14	½	½	4
3	9	14	14	½	½	12	4.5	14	14	½	½	6
5	15	12	12	½	½	20	7.5	14	14	½	½	10
7½	22	10	10	¾	¾	30	11	14	14	½	½	15
10	27	8	8	¾	¾	35	14	12	12	½	½	20
	direct current—115 volts						**direct current—230 volts**					
½	4.6	14	14	½	½	6	2.3	14	14	½	½	3
¾	6.6	14	14	½	½	10	3.3	14	14	½	½	4
1	8.6	14	14	½	½	12	4.3	14	14	½	½	6
1½	12.6	12	12	½	½	15	6.3	14	14	½	½	8
2	16.4	10	10	¾	¾	20	8.2	14	14	½	½	12
3	24	10	10	¾	¾	30	12	14	14	½	½	15
5	40	6	6	1	1	50	20	10	10	¾	¾	25
7½	58	3	4	1¼	1¼	70	29	8	8	¾	¾	40
10	76	2	3	1¼	1¼	100	38	6	6	1	1	50

* Reprinted by permission from General Electric Supply Corp. Catalog; 94WP. Adopted from 1947 National Electrical Code.

† Conduit size based on three conductors in one conduit for 3-phase alternating-current motors, and on two conductors in one conduit for direct-current and single-phase motors.

‡ **Cable types:**

R = tinned-copper conductor, natural- or synthetic-rubber insulation, 1 or 2 nonmetallic braids

RH = type *R* with special heat-resistant insulation

T = untinned-copper conductor, polyvinyl insulation, no jacket or braid

Electric-motor data *continued*

Torque and horsepower

Torque varies directly with power and inversely with rotating speed of the shaft, or

$$T = KP/N$$

where

T = torque in inch–pounds
P = horsepower
N = revolutions/minute
K = 63,000 (constant)

Transmission-line sag calculations*

For transmission-line work, with towers on the same or slightly different levels, the cables are assumed to take the form of a parabola, instead of their actual form of a catenary. The error is negligible and the computations are much simplified. In calculating sags, the changes in cables due to variations in loads and temperature must be considered.

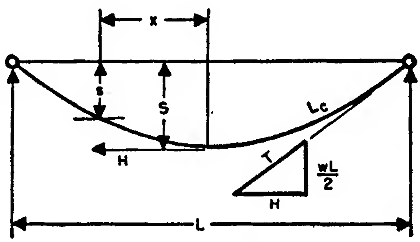

Supports at same elevations

For supports at same level: The formulas used in the calculations of sags are

$$H = WL^2/8S$$

$$S = WL^2/8H = [(L_c - L)\ 3L/8]^{1/2}$$

$$L_c = L + 8S^2/3L$$

* Reprinted by permission from "Transmission Towers," American Bridge Company, Pittsburgh, Pa.; 1923: p. 70.

Transmission-line sag calculations *continued*

where

L = length of span in feet
L_c = length of cable in feet
S = sag of cable at center of span in feet
H = tension in cable at center of span in pounds
= horizontal component af the tension at any point
W = weight of cable in pounds per lineal foot

Where cables are subject to wind and ice loads, W = the algebraic sum of the loads. That is, for ice on cables, W = weight of cables plus weight of ice; and for wind on bare or ice-covered cables, W = the square root of the sum of the squares of the vertical and horizontal loads.

For any intermediate point at a distance x from the center of the span, the sag is

$$S_x = S(1 - 4x^2/L^2)$$

For supports at different levels

$$S = S_0 = \frac{WL_0^2 \cos a}{8T} = \frac{WL^2}{8T \cos a}$$

$$S_1 = \frac{WL_1^2}{8H}$$

$$S_2 = \frac{WL_2^2}{8H}$$

$$\frac{L_1}{2} = \frac{L}{2} - \frac{hH \cos a}{WL}$$

$$\frac{L_2}{2} = \frac{L}{2} + \frac{hH \cos a}{WL}$$

$$L_c = L + \frac{4}{3}\left(\frac{S_1^2}{L_1} + \frac{S_2^2}{L_2}\right)$$

where

W = weight of cable in pounds per lineal foot between supports or in direction of L_0
T = tension in cable direction parallel with line between supports

Transmission-line sag calculations *continued*

The change l in length of cable L_c for varying temperature is found by multiplying the number of degrees n by the length of the cable in feet times the coefficient of linear expansion per foot per degree fahrenheit c. This is*

$$l = L_c \times n \times c$$

A short approximate method for determining sags under varying temperatures and loadings that is close enough for all ordinary line work is as follows:

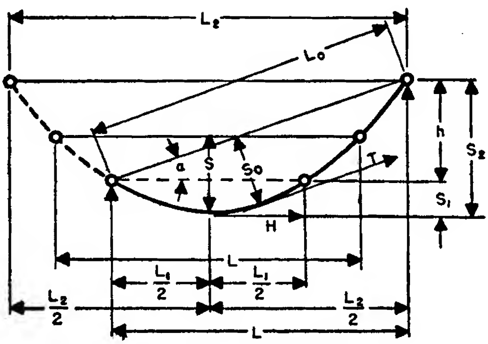

Supports at different elevations.

a. Determine sag of cable with maximum stress under maximum load at lowest temperature occurring at the time of maximum load, and find length of cable with this sag.

b. Find length of cable at the temperature for which the sag is required.

c. Assume a certain reduced tension in the cable at the temperature and under the loading combination for which the sag is required; then find the decrease in length of the cable due to the decrease of the stress from its maximum.

d. Combine the algebraic sum of (*b*) and (*c*) with (*a*) to get the length of the cable under the desired conditions, and from this length the sag and tension can be determined.

e. If this tension agrees with that assumed in (*c*), the sag in (*d*) is correct. If it does not agree, another assumption of tension in (*c*) must be made and the process repeated until (*c*) and (*d*) agree.

* Temperature coefficient of linear expansion is given on pp. 56-57.

Structural standards for steel radio towers *

Material

a. Structural steel shall conform to American Society for Testing Materials "Standard Specifications for Steel for Bridges and Buildings," Serial Designation A-7, as amended to date.

b. Steel pipe shall conform to American Society for Testing Materials standard specifications either for electric-resistance welded steel pipe, Grade *A* or Grade *B*, Serial Designation *A-135*, or for welded and seamless steel pipe, Grade *A* or Grade *B*, Serial Designation *A-53*, each as amended to date.

Loading

a. 20-Pound design: Structures up to 600 feet in height except if to be located within city limits shall be designed for a horizontal wind pressure of 20 pounds/foot^2 on flat surfaces and 13.3 pounds/foot^2 on cylindrical surfaces.

b. 30-pound design: Structures more than 600 feet in height and those of any height to be located within city limits shall be designed for a horizontal wind pressure of 30 pounds/foot^2 on flat surfaces and 20 pounds/foot^2 on cylindrical surfaces.

c. Other designs: Certain structures may be designed to resist loads greater than those described in paragraphs *a* and *b* just above. Fig. 1 of American Standard A58.1-1955 shows sections of the United States where greater wind pressures may occur. In all such cases, the pressure on cylindrical surfaces shall be computed as being 2/3 of that specified for flat surfaces.

d. For open-face (latticed) structures of square cross section, the wind pressure normal to one face shall be applied to 2.20 times the normal projected area of all members in one face, or 2.40 times the normal projected area of one face for wind applied to one corner. For open-faced (latticed) structures of triangular cross section, the wind pressure normal to one face shall be applied to 2.00 times the normal projected area of all members in one face, or 1.50 times the normal projected area for wind parallel to one face. For closed-face (solid) structures, the wind pressure

* Abstracted from "American Standard Minimum Design Loads in Buildings and Other Structures, A58.1-1955," American Standards Association; 70 East 45th Street; New York 17, N. Y.: $1.50 per copy. Also from Radio-Electronics-Television Manufacturers Association Standard TR—116; October, 1949. Sections on manufacture and workmanship, finish, and plans and marking of the standard are not reproduced here. The section on "Wind velocities and pressures" is not part of the standard.

Structural standards for steel radio towers *continued*

shall be applied to 1.00 times the normal projected area for square or rectangular shape, 0.80 for hexagonal or octagonal shape, or 0.60 for round or elliptical shape.

e. Provisions shall be made for all supplementary loadings caused by the attachment of guys, antennas, transmission and power lines, ladders, etc. The pressure shall be as described for the respective designs and shall be applied to the projected area of the construction.

f. The total load specified above shall be applied to the structure in the directions that will cause the maximum stress in the various members.

g. The dead weight of the structure and all material attached thereto, shall be included.

Unit stresses

a. All parts of the structure shall be so designed that the unit stresses resulting from the specified loads shall not exceed the following values in pounds/inch^2

Axial tension on net section = 20,000 pounds/inch^2

Axial compression on gross section:

For members with value of L/R not greater than 120,

$$= 17{,}000 - 0.485\, L^2/R^2 \text{ pounds/inch}^2$$

For members with value of L/R greater than 120,

$$= \frac{18{,}000}{1 + L^2/18{,}000\, R^2} \text{ pounds/inch}^2$$

where

L = unbraced length of the member
R = corresponding radius of gyration, both in inches.

Maximum L/R for main leg members = 140
Maximum L/R for other compression members with calculated stress = 200
Maximum L/R for members with no calculated stress = 250
Bending on extreme fibre = 20,000 pounds/inch^2
Single shear on bolts = 13,500 pounds/inch^2
Double shear on bolts = 27,000 pounds/inch^2

Structural standards for steel radio towers *continued*

Bearing on bolts (single shear) = 30,000 pounds/inch^2

Bearing on bolts (double shear) = 30,000 pounds/inch^2

Tension on bolts and other threaded parts, on nominal area at root of thread = 16,000 pounds/inch^2

Members subject to both axial and bending stresses shall be so designed that the calculated unit axial stress divided by the allowable unit axial stress, plus the calculated unit bending stress, divided by the allowable unit bending stress, shall not exceed unity.

b. Minimum thickness of material for structural members:

Painted structural angles and plates = 3/16 inch

Hot-dip galvanized structural angles and plates = 1/8 inch

Other structural members to mill minimum for standard shapes.

c. Where materials of higher quality than specified under "Material" above are used, the above unit stresses may be modified. The modified unit stresses must provide the same factor of safety based on the yield point of the materials.

Foundations

a. Standard foundations shall be designed for a soil pressure not to exceed 4000 pounds/foot^2 under the specified loading. In uplift, the foundations shall be designed to resist 100-percent more than the specified loading assuming that the base of the pier will engage the frustum of an inverted pyramid of earth whose sides form an angle of 30 degrees with the vertical. Earth shall be considered to weigh 100 pounds/foot^3 and concrete 140 pounds/foot^3.

b. Foundation plans shall ordinarily show standard foundations as defined in paragraph a just above. Where the actual soil conditions are not normal, requiring some modification in the standard design and complete soil information is provided to the manufacturer by the purchaser, the foundation plan shall show the required design.

c. Under conditions requiring special engineering such as pile construction, roof installations, etc., the manufacturer shall provide the necessary information so that proper foundations can be designed by the purchaser's engineer or architect.

d. In the design of guy anchors subject to submersion, the upward pressure of the water should be taken into account.

Structural standards for steel radio towers *continued*

Wind velocities and pressures

actual velocity V_a in miles/hour	indicated velocity V_i in miles/hour		pressure P in pounds/foot^2	
	3-cup anemometer	4-cup anemometer	cylindrical surfaces projected areas* $P = 0.0025\ V_a^2$	flat surfaces $P = 0.0042\ V_a^2$
10	9	10	0.25	0.42
20	20	23	1.0	1.7
30	31	36	2.3	3.8
40	42	50	4.0	6.7
50	54	64	6.3	10.5
60	65	77	9.0	15.1
70	76	91	12.3	20.6
80	88	105	16.0	26.8
90	99	119	20.3	34.0
100	110	132	25.0	42.0
110	121	146	30.3	50.8
120	133	160	36.0	60.5
130	144	173	42.3	71.0
140	155	187	49.0	82.3
150	167	201	56.3	94.5

* Although wind velocities are measured with cup anemometers, all data published by the U. S. Weather Bureau since January 1932 includes instrumental corrections and are actual velocities. Prior to 1932 indicated velocities were published.

In calculating pressures on structures, the "fastest single mile velocities" published by the Weather Bureau should be multiplied by a gust factor of 1.3 to obtain the maximum instantaneous actual velocities. See p. 924 for fastest single mile records at various places in the United States and Canada.

The American Bridge Company formulas given here are based on a ratio of 25/42 for pressures on cylindrical and flat surfaces, respectively, while the Radio-Electronics-Television Manufacturers Association specifies a ratio of 2/3. The actual ratio varies in a complex manner with Reynolds number, shape, and size of the exposed object.

Vibration and shock isolation

Symbols

b = damping factor

d = static deflection in inches

E = relative transmissibility

= (force transmitted by isolators)/(force transmitted by rigid mountings)

F = force in pounds

Vibration and shock isolation *continued*

F_0 = peak force in pounds

f = frequency in cycles per second (cps)

f_0 = resonant frequency of system in cycles per second

G = acceleration of gravity

$\approx$ 386 inches per second^2

g = peak acceleration in dimensionless gravitational units

$= \ddot{X}_0/G$

$j = (-1)^{1/2}$, vector operator

k = stiffness constant; force required to compress or extend isolators unit distance in pounds per inch

r = coefficient of viscous damping in pounds per inch per second

t = time in seconds

W = weight in pounds

x = displacement from equilibrium position in inches

X_0 = peak displacement in inches

$\dot{x}$ = velocity in inches per second

$= dx/dt$

$\dot{X}_0$ = peak velocity in inches per second

$\ddot{x}$ = acceleration in inches per second^2

$= d^2x/dt^2$

$\ddot{X}_0$ = peak acceleration in inches per second^2

ϕ = phase angle in radians

ω = angular velocity in radians per second

$= 2\pi f$

Equations

The following relations apply to simple harmonic motion in systems with one degree of freedom. Although actual vibration is usually more complex, the equations provide useful approximations for practical purposes.

Vibration and shock isolation *continued*

$$F = W(\ddot{x}/G) \tag{1}$$

$$F_0 = Wg \tag{2}$$

$$x = X_0 \sin (\omega t + \phi) \tag{3}$$

$$X_0 = 9.77g/f^2 \tag{4}$$

$$\dot{X}_0 = \omega X_0 = 6.28fX_0 = 61.4g/f \tag{5}$$

$$\ddot{X}_0 = \omega^2 X_0 = 39.5f^2X_0 = 386g \tag{6}$$

$$E = \left| \frac{r - j(k/\omega)}{r + j\,[(\omega W/G) - k/\omega]} \right| \tag{7}$$

$$f_0 = 3.13(k/W)^{1/2} \tag{8}$$

$$b = 9.77r/(kW)^{1/2} \tag{9}$$

For critical damping, $b = 1$.

Neglecting dissipation ($b = 0$), or at $f/f_0 = (2)^{1/2}$ for any degree of damping,

$$E = \left| \frac{1}{(f/f_0)^2 - 1} \right| \tag{10}$$

When damping is neglected,

$$k = W/d \tag{11}$$

$$f_0 = 3.13/d^{1/2} \tag{12}$$

$$E = 9.77/(df^2 - 9.77) \tag{13}$$

Acceleration

The intensity of vibratory forces is often defined in terms of g values. From (2), it is apparent, for example, that a peak acceleration of 10g on a body will result in a reactionary force by the body equal to 10 times its weight.

When an object is mounted on vibration isolators, the accelerations of the vehicle are transmitted to the object (or vice versa) in an amplitude and phase that depends on the elastic flexing of the isolators in the directions in which the accelerations (dynamic forces) are applied.

Vibration and shock isolation *continued*

Magnitudes

The relations between X_0, $\dot{X}_0$, $\ddot{X}_0$, and f are shown in Fig. 1. Any two of these parameters applied to the graph locates the other two. For example, suppose $f = 10$ cycles per second and peak displacement $X_0 = 1$ inch. From Fig. 1, peak velocity $\dot{X}_0 = 63$ inches per second and peak acceleration $\ddot{X}_0 = 10g$.

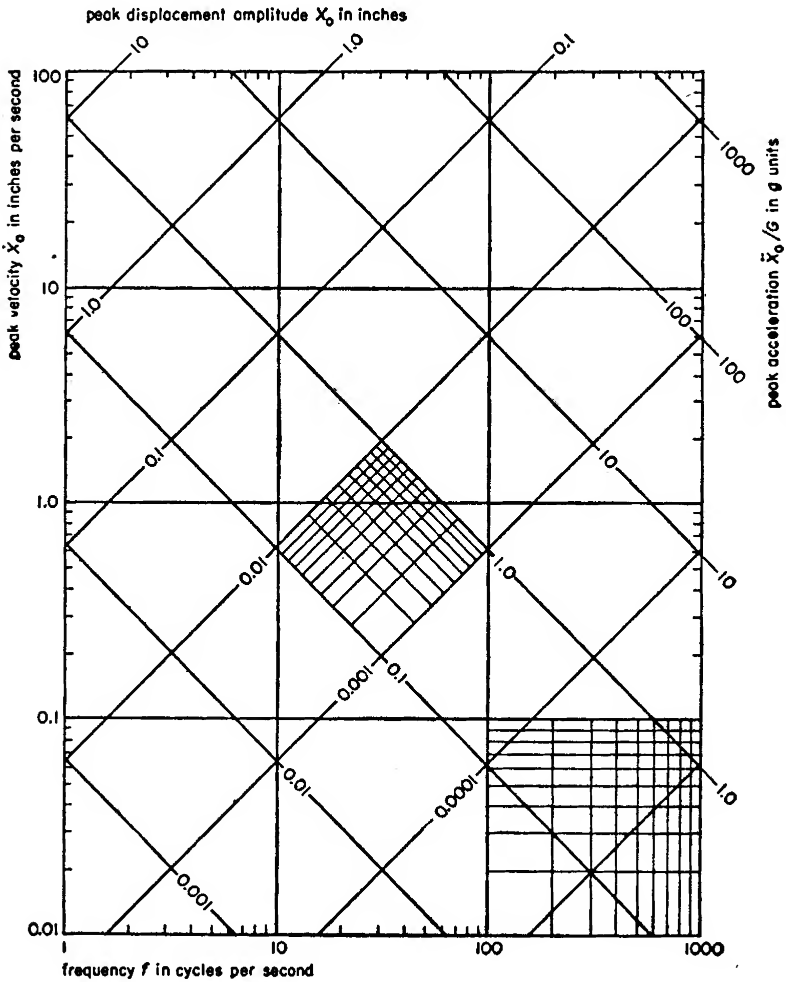

Fig. 1—Relation of frequency and peak values of velocity, displacement, and acceleration.

Vibration and shock isolation *continued*

Natural frequency

Neglecting damping, the natural frequency f_0 of vibration of an isolated system in the vertical direction can be calculated from (12) from the static deflection of the mounts. For example, suppose an object at rest causes a 0.25-inch deflection of its supporting springs. Then,

$f_0 = 3.13/(0.25)^2 = 6.3$ cycles per second

Resonance

In Fig. 2, E is plotted against f/f_0 for various damping factors. Note that resonance occurs when $f_0 \approx f$ and that the vibratory forces are then increased by the isolators. To reduce vibration, f_0 must be less than $0.7f$ and it should be as small as $0.3f$ for good isolation.

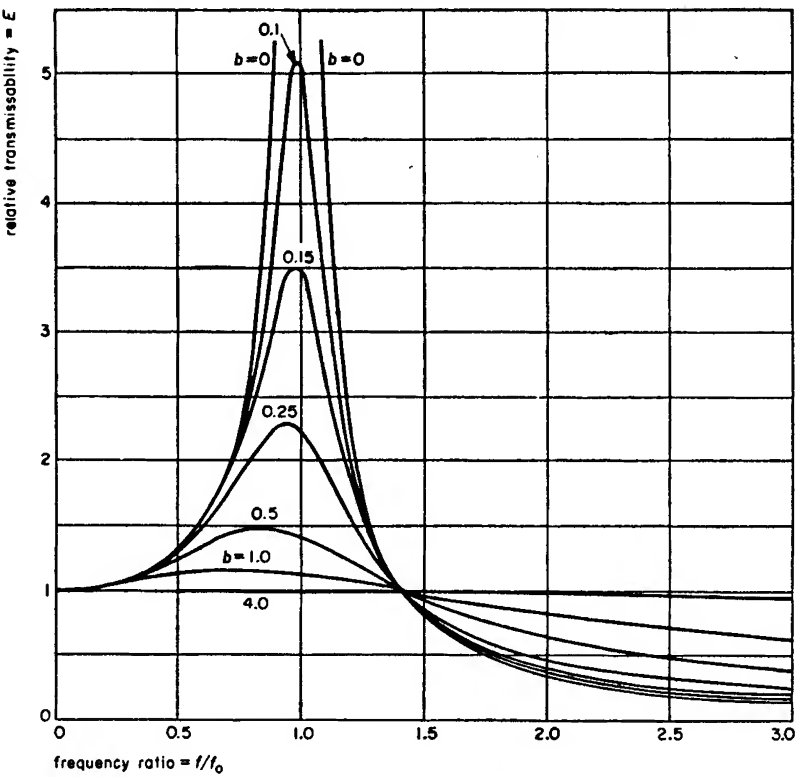

Fig. 2—Relative transmissability E as a function of the frequency ratio f/f_0 for various amounts of damping b. *By permission from "Vibration Analysis," by N. O. Myklestad. Copyright 1944. McGraw-Hill Book Company, Inc.*

Vibration and shock isolation *continued*

It is not possible to secure good isolation at all vibrational frequencies in vehicles and similar environments where several different and varying exciting frequencies are present and where the isolators may have to withstand shock as well as vibration. In such cases, f_0 is often selected as about 1.5 to 2 times the predominant f. Vibration in typical vehicles is shown in Fig. 3.

Although all supporting structures have compliance and may reduce the effects of vibration and shock, the apparent stiffness of many "rigid" mountings is merely a matter of degree, and in conjunction with the supported mass, they can also give rise to resonance effects, thus magnifying the amplitude of certain vibrations.

Damping

Damping is desirable in order to reduce vibration amplitude during such times as the exciting frequency is in the vicinity of f_0. This will occur occasionally in most installations. Any isolator that absorbs energy provides damping.

It is seldom practical to introduce damping as an independent variable in the design of vibration isolators for relatively small objects. The usual practice is to rely on the inherent damping characteristics of the rubber or other elastic material employed in the mounting. Damping achieved in this way seldom exceeds 5 percent of the amount needed to produce a critically damped system. In vibration isolators for large objects, such as variable-speed engines, the system often can be designed to produce nearly critical damping by employing fluid dash pots or similar devices.

Fig. 3—Vibration in typical vehicles.

vehicle	range of frequencies in cycles per second	approximate peak amplitude in inches	nature of excitation	usual choice of isolator resonant frequency
Ships	0 to 15	0.02	Engine vibration in diesel or reciprocating steam drive	6 cycles/second for vibration isolation in commercial vessels. 27 to 30 cycles/second for shock isolation on naval vessels. These latter mounts amplify most vibrations to some extent.
	0 to 33	0.01	Propeller-blade frequency = (propeller rpm) × (number of blades)/60	

Piston-engine aircraft	0 to 60	0.01	Engine vibrations	Above 20 cycles/second. Amplitude of vibrations varies with location in aircraft. Landing shock can be neglected
	0 to 100	0.01	Propeller vibrations. Aerodynamic vibrations due to buffeting	
Turboprop aircraft	0 to 60	0.01	Engine vibrations = (engine rpm)/60. Also aerodynamic vibrations due to buffeting and turbulence	9 cycles/second
	0 to 100	0.01	Propeller vibrations. Also aerodynamic vibrations due to buffeting and turbulence	
Jet Aircraft	Up to 500	0.001	Audible noise frequencies due to jet wake and combustion turbulence; very little engine vibration	9 cycles/second
Passenger automobiles	1	6	Suspension resonance	25 cycles/second will usually avoid resonance with wheel hop and suspension resonant frequencies
	8 to 12	0.02	Unsprung weight resonance (wheel hop)	
	20+	0.002	Irregular transient vibrations due to resonances of structural members with road roughnesses	
Automobile trucks	4	5	Suspension resonance	Above 20 cycles/second and should not correspond with any structural resonance. It is not advisable to attempt to isolate suspension and unsprung weight resonances
	20	0.05	Unsprung weight resonance	
	80+	0.005	Structural resonances	
Military tanks	1 to 3	2	Suspension resonance	Similar to automobile truck
	Depends on speed	—	Track-laying frequency $\approx 17.6 \dfrac{\text{(speed in mph)}}{\text{(tread spacing in inches)}}$	
	100+	0.001	Structural resonances	
Railroad trains	Broad and erratic		Similar to automobiles with additional excitations from rail joints and from side slop in rail trucks and draft gear	20 cycles/second has been successful in railroad applications. Shock with velocity changes up to 100 inches/second in direction of train occurs when coupling cars or starting freight trains

Vibration and shock isolation *continued*

Practical application

Vibration can be accurately precalculated only for the simplest systems. In other cases the actual vibration should be measured on experimental assemblies using electrical vibration pickups. Complex vibration is often described by a plot of the *g* values against frequency. These plots usually show several frequencies at which the largest accelerations are present. The patterns will vary from place to place in a complicated structure and will also depend on the direction in which the acceleration is measured.

After measuring and plotting vibration in this way, attention can be devoted to reduction of the predominant components using the equations and principles given above as guides in selecting the size, stiffness, damping characteristics, and location of isolators.

Shock

In many practical situations, vibration and shock occur simultaneously. The design of isolators for vibration should anticipate the effects of shock and vice versa.

When heavy shock is applied to a system using vibration isolators, there is usually a definite deflection at which the isolators snub or at which their stiffness suddenly becomes much greater. These actions may amplify the shock forces. To reduce this effect, it is generally desirable to use isolators that have smoothly increasing stiffness with increasing deflection.

Shock protection is improved by isolators that permit large deflections in all directions before the protected equipment is snubbed or strikes neighboring apparatus. The amplitude of vibration resulting from shock can be reduced by employing isolators that absorb energy and thus damp oscillatory movement.

Probabilities of damage to the apparatus itself from impact shock can be minimized by:

a. Making the weight of equipment components as small as possible and the strength of structural members as great as possible.

b. Distributing rather than concentrating the weights of equipment components and avoiding rigid connections between components.

Vibration and shock isolation *continued*

c. Employing structural members that have high ratios of stiffness to weight, such as tubes, I beams, etc.

d. Avoiding, so far as practical, stress concentrations at joints, supports, discontinuities, etc.

e. Using materials such as steel that yield rather than rupture under high stress.

Graphical symbols

American Standard Graphical Symbols for Electrical Diagrams Y32.2–1954* covers both the communication and power fields. Excerpts of primary interest to communications workers will be found on the following pages.

Diagram types

Block diagrams consist of simple rectangles and circles with names or other designations within or adjacent to them to show the general arrangement of apparatus to perform desired functions. The direction of power or signal flow is often indicated by arrows near the connecting lines or arrowheads on the lines.

Schematic diagrams show all major components and their interconnections. Single-line diagrams, as indicated by that name, use single lines to interconnect components even though two or more conductors are actually required. It is a shorthand form of schematic diagram. It is always used for waveguide diagrams.

Wiring diagrams are complete in that all conductors are shown and all terminal identifications are included. The contact numbers on electron-tube sockets, colors of transformer leads, rotors of variable capacitors, and other terminal markings are shown so that a workman having no knowledge of the operation of the equipment can wire it properly.

Orientation

Graphical symbols are no longer considered as being coarse pictures of specific pieces of equipment but are true symbols. Consequently, they may be rotated to any orientation with respect to each other without changing their meanings. Ground, chassis, and antenna symbols, for instance, may "point" in any direction that is convenient for drafting purposes.

*American Standards Association, 70 East 45th Street, New York 17, N. Y.; $1.25 per copy.

Graphical symbols *continued*

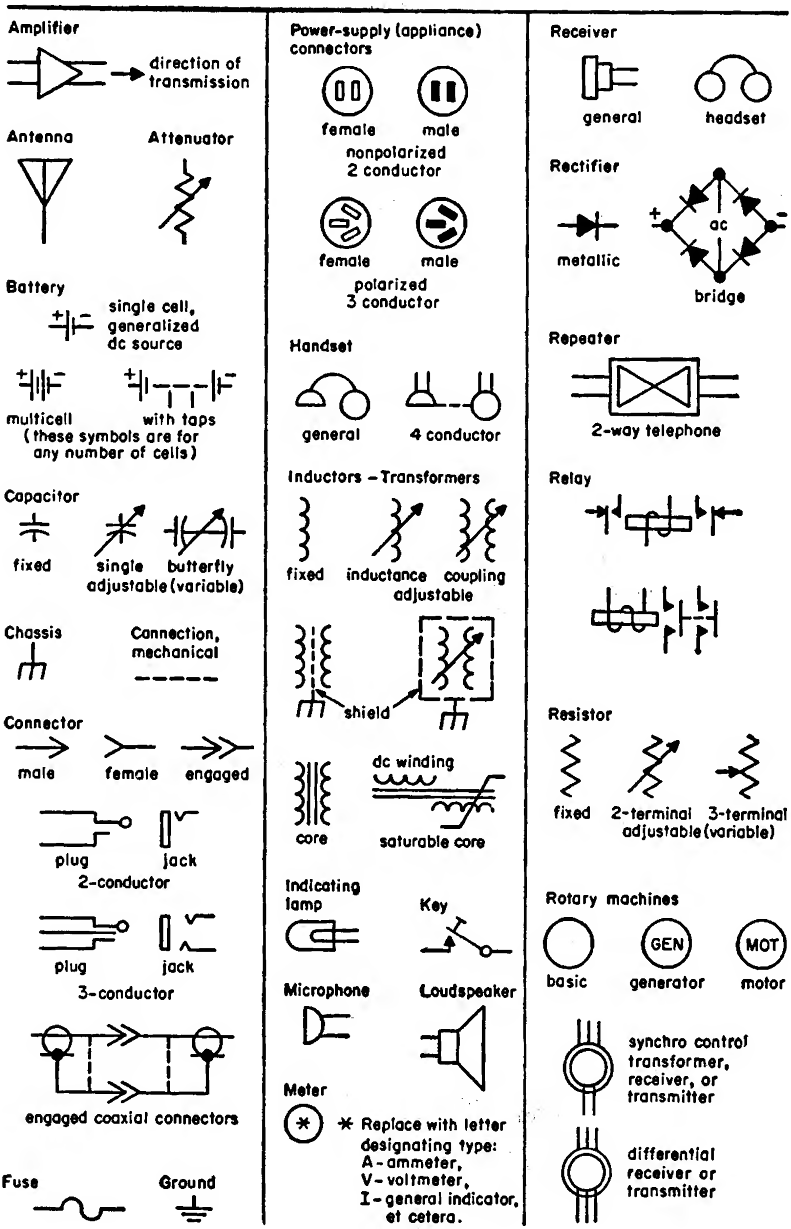

Graphical symbols *continued*

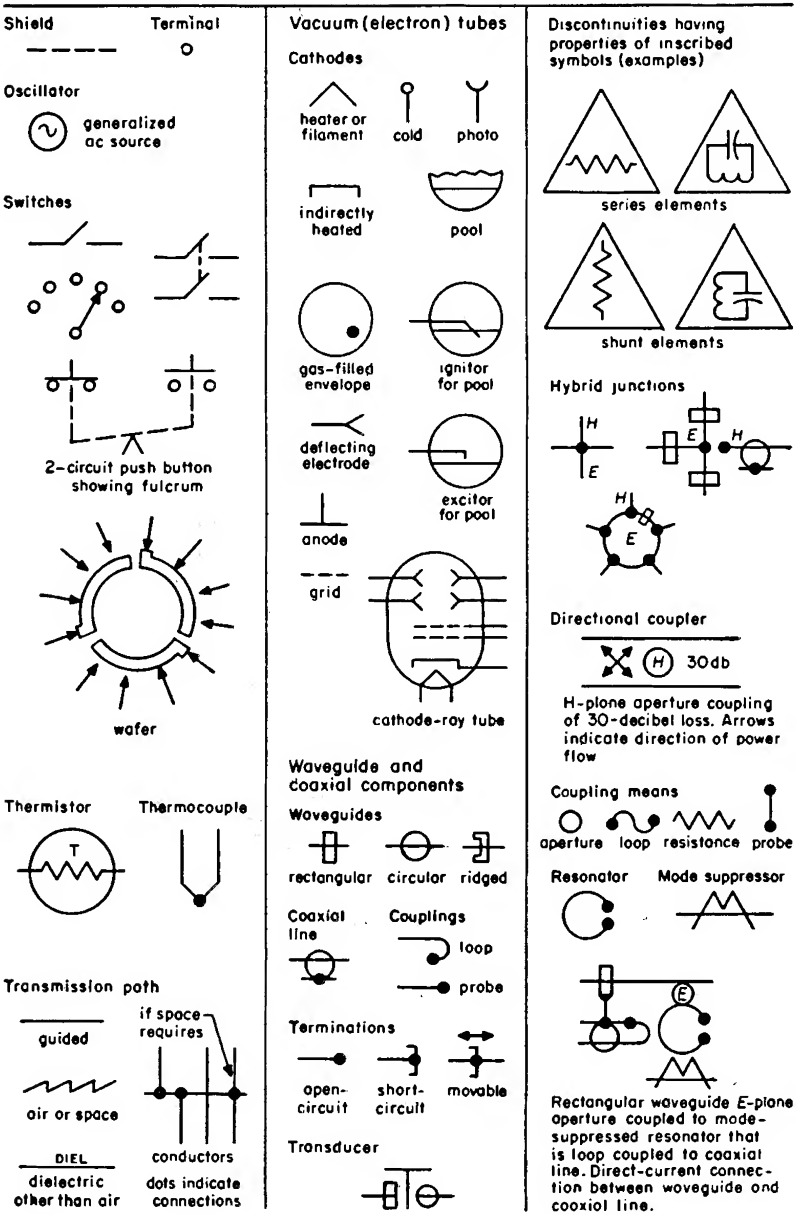

Graphical symbols *continued*

Detached elements

Switches and relays often have many sets of contacts and these may be separated and placed in the parts of the drawing to which they apply. Each separated element should be suitably identified. The winding of a relay may be labelled *K2/4* to indicate that relay *K2* has 4 sets of contacts separated from the winding symbol. Each separated set of contacts will then be designated *K2-1* through *K2-4* to permit individual identification.

Terminals

The terminal symbol need not be used unless it is needed. Thus, it may be omitted from relay and switch symbols. In particular, the terminal symbol often shown at the end of the movable element of a relay or switch should not be considered as the fulcrum or bearing but only as a terminal.

Associated or future equipment

Associated equipment, such as for measurement purposes, or additions that may be made later, are identified as such by using broken lines for both symbols and connections.

Radio-signal reporting codes *

The Comité Consultatif International Radio (CCIR) recommends that the SINPO and SINPFEMO codes be used instead of the older Q, FRAME, RAFISBENQO, and RISAFMONE codes.

A signal report consists of the code word SINPO or SINPFEMO followed by a 5- or 8-figure group respectively rating the 5 or 8 characteristics of the signal code.

The letter X is used instead of a numeral for characteristics not rated.

Although the code word SINPFEMO is intended for telephony, either code word may be used for telegraphy or telephony.

The over-all rating for telegraphy is interpreted as follows:

* From Recommendation number 141 of the Comité Consultatif International Radio, London, 1953.

Radio-signal reporting codes *continued*

symbol		mechanized operation	Morse operation
5	Excellent	4-channel time-division multiplex	High-speed Morse
4	Good	2-channel time-division multiplex	100 words/minute Morse
3	Fair	Marginal. Single start-stop printer	50 words/minute Morse
2	Poor	Equivalent to 25 words/minute Morse	25 words/minute Morse
1	Unusable	Possible breaks and repeats; call letters distinguishable	Possible breaks and repeats; call letters distinguishable

The over-all rating for telephony is interpreted as follows:

symbol		operating condition	quality
5	Excellent	Signal quality unaffected	Commercial
4	Good	Signal quality slightly affected	
3	Fair	Signal quality seriously affected. Channel usable by operators or by experienced subscribers	Marginally commercial
2	Poor	Channel just usable by operators	Not commercial
1	Unusable	Channel unusable by operators	

Sinpo signal-reporting code

	S	I	N	P	O
		degrading effect of			
rating scale	signal strength	interference (QRM)	noise (QRN)	propagation disturbance	over-all readability (QRK)
5	Excellent	Nil	Nil	Nil	Excellent
4	Good	Slight	Slight	Slight	Good
3	Fair	Moderate	Moderate	Moderate	Fair
2	Poor	Severe	Severe	Severe	Poor
1	Barely audible	Extreme	Extreme	Extreme	Unusable

Sinpfemo signal-reporting code

rating scale	S	I	N	P	F	E	M	O
		degrading effect of				modulation		
	signal strength	interference (QRM)	noise (QRN)	propagation disturbance	frequency of fading	quality	depth	over-all rating
5	Excellent	Nil	Nil	Nil	Nil	Excellent	Maximum	Excellent
4	Good	Slight	Slight	Slight	Slow	Good	Good	Good
3	Fair	Moderate	Moderate	Moderate	Moderate	Fair	Fair	Fair
2	Poor	Severe	Severe	Severe	Fast	Poor	Poor or nil	Poor
1	Barely audible	Extreme	Extreme	Extreme	Very fast	Very poor	Continuously overmodulated	Unusable

World time chart

Aleutian Islands Tutuila, Samoa	Hawaiian Islands Tahiti	San Francisco and Pacific Coast	Chicago, Central America (except Panama) Mexico, Winnipeg	Bogota, Bermuda, Havana Lima, Montreal New York, Panama	Santiago, Puerto Rico Lapaz, Asuncion	Buenos Aires* Rio de Janeiro, Santos Sao Paulo	Iceland Dakar	Algiers, Lisbon London, Paris Madrid	Greenwich Civil Time (GCT) or Universal Time (UT)	Bengasi, Berlin, Oslo Rome, Tunis, Tripoli Warsaw, Stockholm	Cairo, Capetown Istanbul, Moscow, Israel	Ethiopia, Iraq Madagascar	Bombay, Ceylon New Delhi	Chungking Chengtu, Kunming	Celebes, Hong Kong Manila, Shanghai	Korea, Japan Manchuria Adelaide	Brisbane, Guam Melbourne, New Guinea Sydney, Khabarovsk	Solomon Islands New Caledonia	Wellington* Auckland*
1:00pm	2:00pm	4:00pm	6:00pm	7:00pm	8:00pm	9:00pm	11:00pm	Midnite	0000	1:00am	2:00am	3:00am	5:30am	7:00am	8:00am	9:00am	10:00am	11:00am	11:30am
2:00pm	3:00pm	5:00pm	7:00pm	8:00pm	9:00pm	10:00pm	Midnite	1:00am	0100	2:00am	3:00am	4:00am	6:30am	8:00am	9:00am	10:00am	11:00am	Noon	12:30pm
3:00pm	4:00pm	6:00pm	8:00pm	9:00pm	10:00pm	11:00pm	1:00am	2:00am	0200	3:00am	4:00am	5:00am	7:30am	9:00am	10:00am	11:00am	Noon	1:00pm	1:30pm
4:00pm	5:00pm	7:00pm	9:00pm	10:00pm	11:00pm	Midnite	2:00am	3:00am	0300	4:00am	5:00am	6:00am	8:30am	10:00am	11:00am	Noon	1:00pm	2:00pm	2:30pm
5:00pm	6:00pm	8:00pm	10:00pm	11:00pm	Midnite	1:00am	3:00am	4:00am	0400	5:00am	6:00am	7:00am	9:30am	11:00am	Noon	1:00pm	2:00pm	3:00pm	3:30pm
6:00pm	7:00pm	9:00pm	11:00pm	Midnite	1:00am	2:00am	4:00am	5:00am	0500	6:00am	7:00am	8:00am	10:30am	Noon	1:00pm	2:00pm	3:00pm	4:00pm	4:30pm
7:00pm	8:00pm	10:00pm	Midnite	1:00am	2:00am	3:00am	5:00am	6:00am	0600	7:00am	8:00am	9:00am	11:30am	1:00pm	2:00pm	3:00pm	4:00pm	5:00pm	5:30pm
8:00pm	9:00pm	11:00pm	1:00am	2:00am	3:00am	4:00am	6:00am	7:00am	0700	8:00am	9:00am	10:00am	12:30pm	2:00pm	3:00pm	4:00pm	5:00pm	6:00pm	6:30pm
9:00pm	10:00pm	Midnite	2:00am	3:00am	4:00am	5:00am	7:00am	8:00am	0800	9:00am	10:00am	11:00am	1:30pm	3:00pm	4:00pm	5:00pm	6:00pm	7:00pm	7:30pm
10:00pm	11:00pm	1:00am	3:00am	4:00am	5:00am	6:00am	8:00am	9:00am	0900	10:00am	11:00am	Noon	2:30pm	4:00pm	5:00pm	6:00pm	7:00pm	8:00pm	8:30pm
11:00pm	Midnite	2:00am	4:00am	5:00am	6:00am	7:00am	9:00am	10:00am	1000	11:00am	Noon	1:00pm	3:30pm	5:00pm	6:00pm	7:00pm	8:00pm	9:00pm	9:30pm
Midnite	1:00am	3:00am	5:00am	6:00am	7:00am	8:00am	10:00am	11:00am	1100	Noon	1:00pm	2:00pm	4:30pm	6:00pm	7:00pm	8:00pm	9:00pm	10:00pm	10:30pm
1:00am	2:00am	4:00am	6:00am	7:00am	8:00am	9:00am	11:00am	Noon	1200	1:00pm	2:00pm	3:00pm	5:30pm	7:00pm	8:00pm	9:00pm	10:00pm	11:00pm	11:30pm
2:00am	3:00am	5:00am	7:00am	8:00am	9:00am	10:00am	Noon	1:00pm	1300	2:00pm	3:00pm	4:00pm	6:30pm	8:00pm	9:00pm	10:00pm	11:00pm	Midnite	12:30am
3:00am	4:00am	6:00am	8:00am	9:00am	10:00am	11:00am	1:00pm	2:00pm	1400	3:00pm	4:00pm	5:00pm	7:30pm	9:00pm	10:00pm	11:00pm	Midnite	1:00am	1:30am
4:00am	5:00am	7:00am	9:00am	10:00am	11:00am	Noon	2:00pm	3:00pm	1500	4:00pm	5:00pm	6:00pm	8:30pm	10:00pm	11:00pm	Midnite	1:00am	2:00am	2:30am
5:00am	6:00am	8:00am	10:00am	11:00am	Noon	1:00pm	3:00pm	4:00pm	1600	5:00pm	6:00pm	7:00pm	9:30pm	11:00pm	Midnite	1:00am	2:00am	3:00am	3:30am
6:00am	7:00am	9:00am	11:00am	Noon	1:00pm	2:00pm	4:00pm	5:00pm	1700	6:00pm	7:00pm	8:00pm	10:30pm	Midnite	1:00am	2:00am	3:00am	4:00am	4:30am
7:00am	8:00am	10:00am	Noon	1:00pm	2:00pm	3:00pm	5:00pm	6:00pm	1800	7:00pm	8:00pm	9:00pm	11:30pm	1:00am	2:00am	3:00am	4:00am	5:00am	5:30am
8:00am	9:00am	11:00am	1:00pm	2:00pm	3:00pm	4:00pm	6:00pm	7:00pm	1900	8:00pm	9:00pm	10:00pm	12:30am	2:00am	3:00am	4:00am	5:00am	6:00am	6:30am
9:00am	10:00am	Noon	2:00pm	3:00pm	4:00pm	5:00pm	7:00pm	8:00pm	2000	9:00pm	10:00pm	11:00pm	1:30am	3:00am	4:00am	5:00am	6:00am	7:00am	7:30am
10:00am	11:00am	1:00pm	3:00pm	4:00pm	5:00pm	6:00pm	8:00pm	9:00pm	2100	10:00pm	11:00pm	Midnite	2:30am	4:00am	5:00am	6:00am	7:00am	8:00am	8:30am
11:00am	Noon	2:00pm	4:00pm	5:00pm	6:00pm	7:00pm	9:00pm	10:00pm	2200	11:00pm	Midnite	1:00am	3:30am	5:00am	6:00am	7:00am	8:00am	9:00am	9:30am
Noon	1:00pm	3:00pm	5:00pm	6:00pm	7:00pm	8:00pm	10:00pm	11:00pm	2300	Midnite	1:00am	2:00am	4:30am	6:00am	7:00am	8:00am	9:00am	10:00am	10:30am
1:00pm	2:00pm	4:00pm	6:00pm	7:00pm	8:00pm	9:00pm	11:00pm	Midnite	2400	1:00am	2:00am	3:00am	5:30am	7:00am	8:00am	9:00am	10:00am	11:00am	11:30am

This chart is based on STANDARD TIME.
* Permanent DAYLIGHT SAVING TIME.

Passing heavy line denotes change of date. When passing the heavy line going to the right ADD one day. When passing the heavy line going to left SUBTRACT one day.

Patent coverage of inventions

A patent in the United States confers the right to the inventor for a period of 17 years to exclude all others from using his claimed invention. After the 17-year period the patented invention normally passes into the public domain and may be practiced by others thereafter without permission of the patentee. The issuance of a patent does not confer to the patentee the right to manufacture his invention, since an earlier unexpired patent may have claims dominating the later invention.

Besides the 17-year patent for invention, there are design patents for shorter periods that cover the outward artistic configuration of an article of manufacture and patents for new plants. The following material applies generally to patents for inventions and not to design patents nor to patents for horticultural plants.

What is patentable

A patent can be obtained on any new and useful process, machine, manufacture, or composition of matter, or any new and useful improvement thereof. The invention must not be obvious to one ordinarily skilled in the art to which the invention relates.

In his patent application the inventor must make the disclosure of his invention sufficiently clear and complete to enable one skilled in the art to build and practice the invention.

Recognizing inventions

If the improvement or other development is new to the originator and appears either basic or commercially feasible, he should submit a disclosure to his patent attorney for advice. This should include disclosures of new products in the mechanical, chemical, and electrical fields; of new combinations of new and/or old elements that produce a new result, or an old result but with fewer elements; and, in fact, any new improvement in these fields that appears to present a commercial advantage in either cost, durability, or operation. The question of whether the disclosure is a sufficient advancement to be the basis of patent claims depends on a novelty investigation and appraisal by a patent attorney.

Who may be an inventor

The inventor is the person who originates the idea and causes his mental picture of an embodiment to be reduced to physical form such as a written description or drawings or model. He may draw on the skill of others to

Patent coverage of inventions *continued*

complete this physical form of his invention so long as ideas, hints, and suggestions of others are in the regular course of their work as skilled technicians.

Contributions by others beyond ordinary mechanical skill make the contributor a coinventor. Employers or supervisors who do not contribute more than ordinary skill should not be identified as coinventors. On the other hand, a supervisor may convey an idea to another employee and direct its development into a patentable invention and do none of the physical work and yet he, the supervisor, is the true inventor. However, when two or more persons by cross-suggestion conceive and reduce an invention to a physical form, they thereby become joint inventors. Where there is real doubt as to whether an invention is sole or joint, the doubt should be resolved in favor of joint.

Making patentable inventions

The usual steps of making an invention are:

a. A desired result or problem is first recognized.

b. A conception of an embodiment capable of producing the desired result is visualized. This mental conception should then be followed with a written record of the physical form visualized (drawings and descriptions).

c. Reduction to practice. This may be "constructive" by filing a patent application, or "actual" by building a full-size working embodiment.

Obtaining a patent

For one to obtain a patent in the United States, the invention must have been made before:

a. It was known or used by others in this country, or

b. It was patented or described by others in any printed publication in this or any foreign country;

and an application for patent must be filed:

a. Within one year from the first date of public use or offer of sale of the invention in this country or any publication in this or any foreign country disclosing the invention, or

b. Prior to the issuance of a foreign patent based upon an application filed by the same inventor more than one year prior to his filing the application for U. S. patent.

Patent coverage of inventions *continued*

Assignment of inventions

The patent rights to an invention can be assigned and transferred and this may be done either before or after a patent application is filed or a patent is obtained.

Effect of publication—foreign patents

No public disclosure of an invention should be made before an application for patent is filed on it. The reason for this is that in certain foreign countries, e.g., France, Holland, and Brazil, the law provides that the publication or public use of the invention anywhere in the world before the date of filing of an application for patent makes the idea available to the public and thereby deprives the inventor of any right to a patent in those countries. However, in the United States, one year is allowed following the date of the first publication, or first public use or sale of the invention during which the application for patent may be filed. Since inventors or assignees are often interested in obtaining foreign patents as well as United States patents, the inventor should make certain as a general policy that no publication or public use is made of his invention before a patent application is filed.

The benefit of the United States filing date applies to the obtaining of patents in most important foreign countries, provided the foreign application is filed within one year of the date of filing of the United States application.

Interferences

Occasionally two or more applications are filed by different inventors claiming substantially the same patentable invention. Thus, while a patent application is pending, an interference may be declared by the Patent Office with respect to the application or patent of another inventor. This proceeding is to determine who is rightfully the first inventor and proof of dates, diligence, and reduction to practice must be established by recorded evidence, such as sketches, description, test data, models, and witnesses.

Engineer's notebook

The keeping of formal notebook records by engineers facilitates patent applications and prosecution of any subsequent interference cases. The permanently bound type of notebook is preferred and the engineer should make his original entries therein. Adherence to the following procedures will make the notebook more useful as evidence in legal proceedings:

Patent coverage of inventions *continued*

a. Make entries chronologically. Use ink.

b. Do not leave blank spaces. Draw a line diagonally across unused space on a page. Use both sides of each sheet. Do not skip or remove any notebook pages.

c. Do not erase. Draw a single line through any entries to be cancelled and initial and date changes made.

d. Make entries directly in notebook. If separate charts, graphs, etc., are a necessary part of an entry, they should be properly signed, witnessed, and dated as well as being referenced on the applicable pages of the notebook. These separate sheets should be securely fastened in the notebook.

e. Make each entry clear and complete.

f. Sign and date each entry on the day it is made.

g. Any entry believed to be sufficiently novel to become the subject of a patent application should be signed and dated by witnesses who understand the subject matter. Sketches, graphs, test data, or other materials related to the invention should be similarly witnessed.

Summary of military nomenclature system*

In the AN system for communication–electronic equipment, nomenclature consists of a name followed by a type number. The type number consists of indicator letters shown in the following tables and an assigned number.

The type number of an independent major unit, not part of or used with a specific set, consists of a component indicator, a number, the slant, and such of the set or equipment indicator letters as apply. Example: SB-5/PT would be the type number of a portable telephone switchboard for independent use.

The system indicator (AN) does not mean that the Army, Navy, and Air Force use the equipment, but simply that the type number was assigned in the AN system.

* Adapted from "Summary of Joint Nomenclature System ("AN") System for Communication Electronic Equipment," Communications–Electronics Nomenclature Subpanel of the Joint Communications–Electronics Committee; Washington 25, D. C.: January 30, 1955.

Summary of military nomenclature system *continued*

Nomenclature policy

AN nomenclature will be assigned to:

a. Complete sets of equipment and major components of military design.

b. Groups of articles of either commercial or military design that are grouped for a military purpose.

c. Major articles of military design that are not part of or used with a set.

d. Commercial articles when nomenclature will facilitate military identification and/or procedures.

AN nomenclature will not be assigned to:

a. Articles cataloged commercially except in accordance with paragraph (*d*) above.

b. Minor components of military design for which other adequate means of identification are available.

c. Small parts such as capacitors and resistors.

d. Articles having other adequate identification in joint military specifications.

Nomenclature assignments will remain unchanged regardless of later changes in installation and/or application.

Modification letters

Component modification suffix letters will be assigned for each modification of a component when detail, parts and subassemblies used therein are no longer interchangeable, but the component itself is interchangeable physically, electrically, and mechanically.

Set modification letters will be assigned for each modification not affecting interchangeability of the sets or equipment as a whole, except that in some special cases they will be assigned to indicate functional interchangeability and not necessarily complete electrical and mechanical interchangeability. Modification letters will only be assigned if the frequency coverage of the unmodified equipment is maintained.

The suffix letters X, Y, and Z will be used only to designate a set or equipment modified by changing the power input voltage, phase or frequency. X will indicate the first change, Y the second, Z the third, XX the fourth, etc., and these letters will be in addition to other modification letters applicable.

Summary of military nomenclature system *continued*

Set or equipment indicator letters

type of installation	type of equipment	purpose
A Airborne (installed and operated in aircraft)	A Invisible light, heat radiation	A Auxiliary assemblies (not complete operating sets used with or part of two or more sets or sets series)
B Underwater mobile, submarine	B Pigeon	B Bombing
C Air transportable (inactivated, do not use)	C Carrier	C Communications (receiving and transmitting)
D Pilotless carrier	D Radiac	D Direction finder and/or reconnaissance
	E Nupac	E Ejection and/or release
F Fixed	F Photographic	
G Ground, general ground use (includes two or more ground type installations)	G Telegraph or teletype	G Fire control or searchlight directing
		H Recording and/or reproducing (graphic meterological and sound)
	I Interphone and public address	
	J Electro-mechanical (not otherwise covered)	
K Amphibious	K Telemetering	
	L Countermeasures	L Searchlight control (inactivated, use "G")
M Ground, mobile (installed as operating unit in a vehicle which has no function other than transporting the equipment)	M Meterological	M Maintenance and test assemblies (including tools)
	N Sound in air	N Navigational aids (including altimeters, beacons, compasses, racons, depth sounding approach, and landing)
P Pack or portable (animal or man)	P Radar	P Peproducing (inactivated, do not use)
	Q Sonar and underwater sound	Q Special, or combination of purposes
	R Radio	R Receiving, passive detecting
S Water surface craft	S Special types, magnetic, etc., or combinations of types	S Detecting and/or range and bearing
T Ground, transportable	T Telephone (wire)	T Transmitting
U General utility (includes two or more general installation classes, airborne, shipboard, and ground)		
V Ground, vehicular (installed in vehicle designed for functions other than carrying electronic equipment, etc., such as tanks)	V Visual and visible light	
W Water surface and underwater	W Armament (peculiar to armament, not otherwise covered)	W Control
	X Facsimile or television	X Identification and recognition

Summary of military nomenclature system *continued*

Table of component indicators

indicator	family name	indicator	family name
AB	Supports, Antenna	OC	Oceonographic Devices
AM	Amplifiers	OS	Oscilloscope, Test
AS	Antennas, Complex	PD	Prime Drivers
AT	Antennas, Simple	PF	Fittings, Pole
BA	Battery, primary type	PG	Pigeon Articles
BB	Battery, secondary type	PH	Photographic Articles
BZ	Signal Devices, Audible	PP	Power Supplies
C	Controls	PT	Plotting Equipments
CA	Commutator Assemblies, Sonar	PU	Power Equipments
CB	Capacitor Bank	R	Receivers
CG	Cable Assemblies, rf	RC	Reels
CK	Crystal Kits	RD	Recorder—Reproducers
CM	Comparators	RE	Relay Assemblies
CN	Compensators	RF	Radio Frequency Component
CP	Computers	RG	Cables, rf, Bulk
CR	Crystals	RL	Reeling Machines
CU	Couplers	RO	Recorders
CV	Converters (electronic)	RP	Reproducers
CW	Covers	RR	Reflectors
CX	Cable Assemblies, non-rf	RT	Receiver and Transmitter
CY	Cases and Cabinets	S	Shelters
D	Dispensers	SA	Switching Devices
DA	Load, Dummy	SB	Switchboards
DT	Detecting Heads	SG	Generators, Signal
DY	Dynamotors	SM	Simulators
E	Hoists	SN	Synchronizers
F	Filters	ST	Straps
FN	Furniture	T	Transmitters
FR	Frequency Measuring Devices	TA	Telephone Apparatus
G	Generators, Power	TB	Towed Body
GO	Goniometers	TC	Towed Cable
GP	Ground Rods	TD	Timing Devices
H	Head, Hand, and Chest Sets	TF	Transformers
HC	Crystal Holder	TG	Positioning Devices
HD	Air Conditioning Apparatus	TH	Telegraph Apparatus
ID	Indicating Devices, non-crt	TK	Tool Kits
IL	Insulators	TL	Tools
IM	Intensity Measuring Devices	TN	Tuning Units
IP	Indicators, Cathode-Ray Tube	TR	Transducers
J	Junction Devices	TS	Test Items
KY	Keying Devices	TT	Teletypewriter and Facsimile App
LC	Tools, Line Construction	TV	Tester, Tube
LS	Loudspeakers	TW	Tapes, Recording Wires
M	Microphones	U	Connectors, Audio and Power
MA	Magazines	UG	Connectors, rf
MD	Modulators	V	Vehicles
ME	Meters	VS	Signaling Equipment, Visual
MF	Magnets or Mag-field Gens	WD	Cables, Two-Conductor
MK	Miscellaneous Kits	WF	Cables, Four-Conductor
ML	Meteorological Devices	WM	Cables, Multiple-Conductor
MT	Mountings	WS	Cables, Single-Conductor
MX	Miscellaneous	WT	Cables, Three-Conductor
O	Oscillators	ZM	Impedance Measuring Devices
OA	Operating Assemblies		

Summary of military nomenclature system *continued*

Additional indicators

Experimental sets: In order to identify a set or equipment of an experimental nature with the development organization concerned, the following indicators will be used within the parentheses:

XA Communications-Navigation Laboratory, Wright Air Development Center, Dayton, Ohio.

XB Naval Research Laboratory, Washington, D. C.

XC Coles Signal Laboratory, Fort Monmouth, N. J.

XD Cambridge Research Center, Cambridge, Mass.

XE Evans Signal Laboratory, Fort Monmouth, N. J.

XF Frankford Arsenal, Philadelphia, Pa.

XG U.S. Navy Electronic Laboratory, San Diego, Calif.

XH Aerial Reconnaissance Laboratory, Wright Air Development Center, Dayton, Ohio.

XJ Naval Air Development Center, Johnsville, Pa.

XK Flight Control Laboratory, Wright Air Development Center, Dayton, Ohio.

XL Signal Corps Electronics Research Unit, Mountain View, Calif.

XM Squier Signal Laboratory, Fort Monmouth, N. J.

XN Department of the Navy, Washington, D. C.

XO Redstone Arsenal, Huntsville, Ala.

XP Canadian Department of National Defense, Ottawa, Canada.

XR Engineer Research and Development Laboratory, Fort Belvoir, Va.

XS Electronic Components Laboratory, Wright Air Development Center, Dayton, Ohio.

XU U.S. Navy Underwater Sound Laboratory, Fort Trumbull, New London, Conn.

XW Rome Air Development Center, Rome, N. Y.

XY Armament Laboratory, Wright Air Development Center, Dayton, Ohio.

Summary of military nomenclature system *continued*

Example: Radio Set AN/ARC–3 ( ) might be assigned for a new airborne radio communication set under development. The cognizant development organization might then assign AN/ARC–3(XA–1), AN/ARC–3(XA–2), etc., type numbers to the various sets developed for test. When the set was considered satisfactory for use, the experimental indicator would be dropped and procurement nomenclature AN/ARC–3 would be officially assigned thereto.

Training sets: A set or equipment designed for training purposes will be assigned type numbers as follows:

a. A set to train for a specific basic set will be assigned the basic set type number followed by a dash, the letter T, and a number. Example: Radio Training Set AN/ARC–6A–T1 would be the first training set for Radio Set AN/ARC–6A.

b. A set to train for general types of sets will be assigned the usual set indicator letters followed by a dash, the letter T, and a number. Example: Radio Training Set AN/ARC–T1 would be the first training set for general airborne radio communication sets.

Parentheses indicator: A nomenclature assignment with parentheses, ( ) following the basic type number is made to identify an article generally, when a need exists for a more general identification than that provided by nomenclature assigned to specific designs of the article. Examples: AN/GRC–5( ), AM–6( )/GRC–5, SB–9( )/GG. A specific design is identified by the plain basic type number, the basic type number with a suffix letter, or the basic type number with an experimental symbol in parentheses. Examples: AN/GRC–5, AN/GRC–5A, AN/GRC–5(XC–1), AM–6B/GRC–5, SB–9(XE–3)/GG. The letter V within the parentheses is used to identify systems with varying parts list.

Examples of AN type numbers

AN/SRC–3( )	General reference set nomenclature for water surface craft radio communication set number 3.
AN/SRC–3	Original procurement set nomenclature applied against AN/SRC–3( ).
AN/SRC–3A	Modification set nomenclature applied against AN/SRC–3.
AN/APQ–13–T1( )	General reference training set nomenclature for the AN/APQ–13 set.

Summary of military nomenclature system *continued*

AN/APQ–13–T1	Original procurement training set nomenclature applied against AN/APQ–13–T1( ).
AN/APQ–13–T1A	Modification training set nomenclature applied against AN/APQ–13–T1.
AN/UPT–T3( )	General reference training set nomenclature for general utility radar transmitting training set number 3.
AN/UPT–T3	Original procurement training set nomenclature applied against AN/UPT–T3( ).
AN/UPT–T3A	Modification training set nomenclature applied against AN/UPT–T3.
T–51( )/ARQ–8	General reference component nomenclature for transmitter number 51, part of or used with airborne radio special set number 8.
T–51/ARQ–8	Original procurement component nomenclature applied against T–51( )/ARQ–8.
T–51A/ARQ–8	Modification component nomenclature applied against T–51/ARQ–8.
RD–31( )/U	General reference component nomenclature for recorder-reproducer number 31 for general utility use, not part of a specific set.
RD–31/U	Original procurement component nomenclature applied against RD–31( )/U.
RD–31A/U	Modification component nomenclature applied against RD–31/U.

Information theory

General

Information theory concerns the process of communication. The central problem is evaluation of the maximum speed and accuracy of communication that can be achieved with a given transmission facility.

The model of the communication process is depicted in Fig. 1.

Fig. 1—Process of communication.

The measure of information does not reflect meaning or purpose in communication: these are the domain of a user of a communication system; the relative frequency of a message and its reproduction are the domain of the system designer. The process of communication is:

a. *Sequential selection* of elements from a set of possible elements defined *a priori*: that is, in advance of communication.

b. *Encoding* of the selected elements as symbols or *signals* appropriate to the transmission system.

c. *Reception* and resolution of the symbols or signals into elements of the predefined set, though not always correctly.

Typical elements are words, letters, sounds, levels of light intensity, voltages. A set is usually composed of elements of the same kind, e.g., a set of letters. Some elements of a set are more likely to appear for communication than others. Successive selections of elements are not ordinarily independent—word selections are constrained to make meaningful phrases, sounds to fuse into words, levels of light to form recognizable images.

Sets composed only of discrete elements are considered in the following. A set such as a continuous range of amplitudes can usually be approximated to desired accuracy by considering an adequate number of discrete levels instead.

Symbols, messages

The elements of a set are denoted as $x_1 \ldots x_n$. The *a-priori* probabilities of $x_1 \ldots x_n$ are $p_1 \ldots p_n$, satisfying

General *continued*

$$\sum_{i=1}^{n} p_i = 1$$

The x_i will be called source symbols; sequences of x_i are called messages. A message formed of two elements is called a digram, and one formed of N elements an Ngram.

Ensemble: A set of elements together with their probabilities p_i. An ensemble with elements x_i is denoted by x.

Amount of information

Amount of information generated in any selection from the ensemble x:

$$H(x) = \sum_{i}^{n} p_i \log (1/p_i) = -\sum_{i}^{n} p_i \log p_i$$

a. If an element of x has unity probability, then $H(x) = 0$.

b. If all elements are equiprobable, $p_i = 1/n$, then $H(x)$ is maximum and equal to $\log n$.

Uncertainty: $H(x)$ is also called the uncertainty of x; uncertainty is greatest for equiprobable events; uncertainty is zero when any one event is certain.

Entropy: $H(x)$ is also called entropy by analogy with the quantity of the same mathematical form encountered in statistical mechanics. $H(x)$ and other quantities of this form are often referred to as ensemble entropies.

Information content of a symbol (or message): The information generated in the selection of a specific symbol (or message). It is equal to $(-\log p_i)$, where p_i is the symbol (or message) probability.

Average information content per symbol (or message): The average *information content* (above) of symbols (or messages). (Average information content per symbol is the same as $H(x)$, and equals the amount of information generated on the average in successive, independent selections from the ensemble.)

Information units

The amount of information $H(x)$ is measured in bits, hartleys, or nits according as logarithms are taken to the base 2, 10, or e.

1 bit (from binary digit) is defined by a choice between 2 equiprobable events.

Information units *continued*

1 hartley is defined by a choice among 10 equiprobable events (= 3.32 bits).

1 nit is defined by a choice among e equiprobable events (= 1.44 bits).

In Fig. 2 is plotted $(-p \log_2 p)$ bits and $-[p \log_2 p + (1-p) \log_2 (1-p)]$ bits versus p, probability expressed in percent from 1 to 99 percent. (Tables for $\log_2 x$ and 2^x are found on page 1110.)

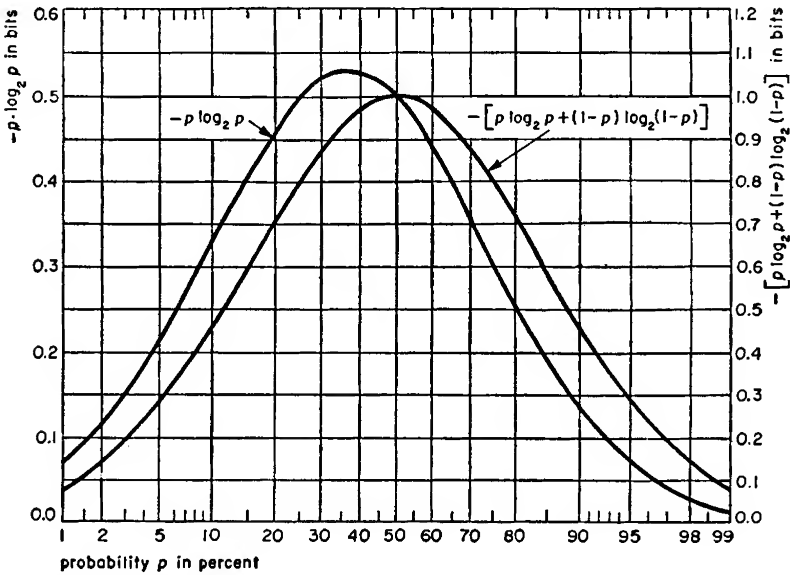

Fig. 2—Curves for computing entropies in bits.

Entropy of joint events

A pair of events x_i and y_j from the sets $(x_1 \ldots x_n)$ and $(y_1 \ldots y_m)$ may be considered as a composite event (x_i, y_j). Such pairs arise when successive symbols emitted by a single source are considered (digram), or when symbols from two sources are considered simultaneously (multiplexing), or when x represents the input to a channel or encoder and y the output.

Denoting the probability of (x_i, y_j) by p_{ij}, and the ensemble of joint events by x, y,

Entropy of x, y is

$$H(x, y) = -\sum_{i,j}^{n,m} p_{ij} \log p_{ij}$$

Entropy of joint events *continued*

If only x is observed, i.e., without regard to y, then probability of x_i is

$$p_i = \sum_{j=1}^{m} p_{ij}$$

and the entropy of x is

$$H(x) = -\sum_{i=1}^{n} p_i \log p_i$$

Similarly, the probability of y_j, with no regard to x, is

$$q_j = \sum_{i}^{n} p_{ij}$$

and the entropy of y is

$$H(y) = -\sum_{j=1}^{m} q_j \log q_j$$

Upon observing x_i, the probability (conditional probability) of y_j is

$c_{ij} = p_{ij}/p_i$

The entropy (uncertainty) of y when x_i is observed is

$$-\sum_{j}^{m} c_{ij} \log c_{ij}$$

which when averaged over x defines the

Conditional entropy of y given x:

$$H_x(y) = \sum_{i}^{n} p_i \left(-\sum_{j}^{m} c_{ij} \log c_{ij}\right) = -\sum_{i,j} p_{ij} \log c_{ij}$$

Similarly, denoting the probability of x_j given y_i as

$c_{ij}' = p_{ji}/q_i$

the conditional entropy

$$H_y(x) = -\sum_{i,j} p_{ji} \log c_{ij}'$$

Relation between these entropies:

$$H(x,y) = H(x) + H_x(y) = H(y) + H_y(x)$$

Entropy of joint events *continued*

Numerical example: Let $n = 3$, $m = 2$. Arranging the joint probabilities p_{ij} in a rectangular array or matrix as in Fig. 3, then,

Fig. 3—Joint probability matrix.

$$\begin{array}{c|ccc}
p_{ij} & y_1 & y_2 & y_3 \\
\hline
x_1 & 0.1 & 0.2 & 0.3 \rightarrow p_1 = 0.6 \\
x_2 & 0.2 & 0.0 & 0.2 \rightarrow p_2 = 0.4 \\
 & \downarrow & \downarrow & \downarrow \\
 & q_1 = 0.3 & q_2 = 0.2 & q_3 = 0.5
\end{array}$$

a. p_i is the sum of the elements in row i.

b. q_j is the sum of the elements in column j.

c. Dividing each element of the matrix by the p_i in the same row yields the matrix c_{ij}.

d. Dividing each element of the matrix by the q_j in the same column and transposing yields c_{ji}' (Bayes' theorem).

The entropies defined above may be obtained in bits from Fig. 2:

$$\begin{aligned}
H(x) &= -0.6 \log_2 0.6 - 0.4 \log_2 0.4 &&= 0.97 \\
H(y) &= -0.3 \log_2 0.3 - 0.2 \log_2 0.2 - 0.5 \log_2 0.5 &&= 1.49 \\
H(x, y) &= -0.1 \log_2 0.1 - 3(0.2) \log_2 0.2 - 0.3 \log_2 0.3 &&= 2.25 \\
H_x(y) &= H(x,y) - H(x) &&= 1.28 \\
H_y(x) &= H(x,y) - H(y) &&= 0.76
\end{aligned}$$

Statistical independence

The events x_i and y_j are said to be statistically independent when $p_{ij} = p_i q_j$. Then, $c_{ij} = q_j$ and $c_{ji}' = p_i$.

In terms of the entropies, independence means

$$H(x,y) = H(x) + H(y)$$
$$H_x(y) = H(y)$$
$$H_y(x) = H(x)$$

When there is dependence, these relations are replaced by inequalities

$$H(x,y) < H(x) + H(y)$$
$$H_x(y) < H(y)$$
$$H_y(x) < H(x)$$

Entropy of joint events *continued*

Multiple events

The preceding can be generalized to any number of events. Let, for instance, $(x_i\ y_j\ z_k)$ represent a composite event from the ensemble x, y, z and let p_{ijk} denote its probability.

The joint entropy is

$$H(x,y,z) = -\sum_{ijk} p_{ijk} \log p_{ijk}$$

From the array of numbers p_{ijk}, it is possible to deduce the probability of occurrence of any single event or of any pair of events and also the conditional probabilities.

For instance,

$$p_{ijk} \Big/ \sum_{k} p_{ijk}$$

is the probability that z_k will occur if x_i and y_j have been observed.

The conditional entropy $H_{xy}(z)$ is the average over all pairs $(x_i y_j)$ of the entropy of z given $x = x_i$ and $y = y_j$.

Alternatively, regarding x,y as a composite ensemble w, then from

$$H_w(z) = H(w,z) - H(w)$$

there results, on replacing w by x,y,

$$H_{x,y}(z) = H(x,y,z) - H(x,y)$$

Similarly, it can be found, for example, that

$$H_{x,y,z}(u,v) = H(x,y,z,u,v) - H(x,y,z)$$

Information source

A source of information is a system that produces messages by successive selections from an ensemble of symbols.

Information rate of a source

Information rate of a source is the amount of information generated per symbol or per second. The information per symbol (symbol entropy) is denoted by H. The information per second (time entropy) is $H' = rH$ where r is the average number of symbols selected per second.

Independent selections H = the entropy of the symbol ensemble, $H(x)$.

Selection dependent on preceding Ngram: H = the conditional entropy of x with respect to the ensemble of Ngrams.

Information source *continued*

Alternatively, when successive selections are not independent, the source may be regarded as changing state with each selection. If a selection depends only on the N preceding, then after a sequence of N selections, the source is said to be in a state S_i. With he next selection there is a transition to some state S_j determined by the element selected and the preceding $(N-1)$. The probability of transition from S_i to S_j is denoted by t_{ij} (transitional probability). (When $N = 1$, t_{ij} is the conditional probability c_{ij} and the number of states is the number of source symbols). Denoting the probability of state i as s_i,

$$H = \sum_i s_i \left(-\sum_j t_{ij} \log t_{ij}\right)$$

(From the latter standpoint, a source is said to be a Markoff process.)

Estimate of information rate: H is less than but approximately equal to $1/N$ times the information per Ngram generated by the source, the difference diminishing with N. In this way, information per letter of English may be approximated from information per word, information per Morse code symbol from information per letter, etc. Various approximations to the English language have been studied from this point of view.

Taking letters as the elementary source symbols; if letters were equiprobable and independent of each other, the rate would be $H_0 = 4.75$ bits per letter. Using the actual letter frequencies, it would be $H_1 = 4.03$ bits per letter. Using frequencies of occurrence of the digrams and trigrams, it becomes, respectively, $H_2 = 3.32$ and $H_3 = 3.1$ bits per letter.

If English words are ordered according to decreasing frequencies it is found that the probability of occurrence of the word in the mth position (rank m) is approximately $p_m \approx 1/10m$ (limiting m to 8727 to make $\Sigma p_m = 1$).

The resulting entropy is 11.82 bits per word or 2.14 bits per letter based on an average of 5.5 letters per word.

Binary encoding of information source

a. The output of every source with rate H bits per symbol can be encoded reversibly into sequences of binary digits averaging H binary digits per source symbol; no lesser average number of digits allows reversible encoding.

b. The time entropy of reversibly encoded source sequences cannot exceed H', the time entropy of the source.

Binary encoding of information source *continued*

c. If different sources have the same H', then messages from any one of them can be encoded into messages from any other without loss of information rate.

These are illustrated in Fig. 4. Typical messages in 4 different "languages" are shown "translated" into the same binary sequence. Each letter individually has its own binary code (rather than coding long sequences of letters as a whole). The notation A: $\frac{1}{2} \sim 0$, etc., means "A, of probability $\frac{1}{2}$, is encoded by 0."

Since all 4 messages are reversibly encoded into the same binary sequence, any one message is a reversible code for any other, though with no direct letter-for-letter correspondence. The method of forming the codes in the special cases illustrated is: The x_i are listed in order of decreasing probability p_i. The uppermost group of events with cumulative probability 1/2 is assigned 0; the lowermost group is assigned 1. Each group is further divided into upper and lower parts of equal cumulative probability, which are assigned respectively 0 and 1. This is continued until groups contain

I	II	III	IV
A: $\frac{1}{2} \sim 0$	W: $\frac{1}{4} \sim 00$	α: $\frac{1}{2} \sim 0$	a: $\frac{1}{2} \sim 0$
B: $\frac{1}{4} \sim 10$	X: $\frac{1}{4} \sim 01$	β: $\frac{1}{4} \sim 10$	b: $\frac{1}{8} \sim 100$
C: $\frac{1}{4} \sim 11$	Y: $\frac{1}{4} \sim 10$	γ: $\frac{1}{8} \sim 110$	c: $\frac{1}{8} \sim 101$
	Z: $\frac{1}{4} \sim 11$	δ: $\frac{1}{8} \sim 111$	d: $\frac{1}{8} \sim 110$
			e: $\frac{1}{8} \sim 111$

language	$\frac{\text{bits}}{\text{letter}}$	•	$\frac{\text{letters}}{\text{second}}$	=	$\frac{\text{bits}}{\text{second}}$	message	binary sequence
I	1.50	•	28	=	42	ABAABBCAACB	01000101011001110
II	2.00	•	21	=	42	XWXXXYXZ	
III	1.75	•	24	=	42	$\alpha\beta\alpha\alpha\beta\beta\gamma\alpha\delta\alpha$	Binary rate $= 1 \frac{\text{bit}}{\text{digit}} \bullet 42 \frac{\text{digits}}{\text{second}}$
IV	2.00	•	21	=	42	abacadaea	$= 42 \frac{\text{bits}}{\text{second}}$

Fig. 4—Four sources generating equal bits per second. A: ½ ~ 0 means "A, of probability ½ is encoded by 0".

Binary encoding of information source *continued*

only one event. The code is automatically reversible. It is efficient (nonredundant), in that more-probable events are assigned longer representations than less-probable ones in such a way that typical source sequences have the least possible number of binary digits.

The symbol probabilities are generally not integral powers of 1/2, and symbols generally not independent. An approximation to H code digits per symbol can still be obtained as outlined above if for "equal cumulative probability" is understood approximately equal cumulative probability.

To obtain a good approximation, it is usually required to apply the procedure to a list of *N*grams, rather than of the symbols. The *N*grams provide a smoother gradation of probabilities and lessen the effect of symbol dependences.

Redundancy

A source is redundant if H is less than the maximum entropy $H_M = \log n$ possible for the same number n of symbols. The selection of symbols in a redundant source is either not independent or, if independent, not equiprobable.

Amount of redundancy is the fractional departure of the source rate from this maximum: $(H_M - H)/H_M$.

From another viewpoint, redundancy indicates the predictability of the source: When the uncertainty H is zero, the redundancy is one and the symbols are completely predictable. Experimental trials at predicting English sentences give an estimated redundancy of at least 75 percent.

Compression by coding is the representation of information generated in source sequences by shorter sequences of code symbols. The maximum possible percent compression of source sequences when properly coded in an alphabet numbering the same as source events equals the source redundancy.

Languages II and III of Fig. 4 illustrate elimination of redundancy by coding into alphabets the same size. With language III as a source with entropy 1.75 bits per symbol, the redundancy is 1/8.

Encoding of III into II achieves the full reduction in redundancy since, on the average, in one second it takes 1/8 fewer symbols to convey 42 bits. This compression could mean a 1/8 bandwidth reduction factor for III. Or, II could be transmitted as the code for III with a saving of 1/8 of the time. Languages IV and II offer what may be called "amplitude compression", since information rate and symbol speed remain the same but the alphabet "range" is reduced from 5 to 4 symbols.

Channel

Communication channel: A transmission facility; defined by a set of constraints. These limit the rate and accuracy with which information can pass from a source to a destination.

Every physical facility is subject to random variations—component drift with temperature, crosstalk, mechanical imperfections, electrical noises, imperfect resolution.

Noiseless channel: One where these effects are negligible; the facility is essentially free of random error. In a noiseless channel, accuracy is not an issue. Every permissible channel input is at once identifiable at the output. The objective is to evaluate the maximum-possible rate of transfer of information through the channel in the presence of constraints of exactly specified nature (as opposed to random influences), often economic in origin, or attributable to limitations in the state of the art.

Noisy channel: One where randomness cannot be dismissed.

Constraints may be classified as those pertaining to the channel symbols (or signals) and those pertaining to the channel noise. The basic channel symbols available for transmission are limited in number and maximum speed of use. There are also restrictions on sequences formed of the basic symbols: e.g., a "spacing" symbol may be required between symbols. There may be an average-power limitation on sequences. The channel noise is a constraint on transmission in that no more than a certain maximum rate can be achieved if error-free reception is to be approached.

Noiseless channel

Binary channel: Transmission constrained to use of 2 symbols, 0 and 1, each of duration T_0. The maximum possible transmission rate is 1 selection between 2 possibilities every T_0 seconds. Thus the channel capacity is $C = 1/T_0$ bits per second. A binary source that produces 0's and 1's of duration T_0 can drive the channel directly. If, further, 0 and 1 are *equiprobably* produced at each selection, then the source rate equals the capacity and the source is said to be *matched* to the channel.

Channel with S available symbols all of duration T_0 can in time T handle any of $N(T) = S^{T/T_0}$ different sequences of symbols: capacity is

$C = (1/T) \log_2 N(T) = (1/T_0) \log_2 S$ bits per second.

If the minimum duration is the result of limited bandwidth $W = 1/2T_0$, then

$C = 2W \log_2 S$

Channel with dynamic range D quantized in steps of equal size d has $S = (D/d) + 1$ amplitude levels available for transmission:

Noiseless channel *continued*

$$C = 2W \log (1 + D/d)$$

or, in terms of average power in channel sequences, when D is centered on zero,

$$C = W \log_2 (1 + 12\, V^2/d^2),$$

where

V^2 = mean-square amplitude level, or "power"

$= d^2 (S^2 - 1)/12$

Capacity of the noiseless channel is defined in general as

$$C = \lim_{T \to \infty} \frac{1}{T} \log_2 N(T) \text{ bits per second}$$

$N(T)$ is the number of permissible channel sequences that can be formed in time T. Two cases are illustrated.

a. Binary channel, duration of 0 twice that of 1:

The $N(T)$ permissible sequences of length T terminate in 0 or 1. Letting the duration of 1 be 1 second, the number ending in 1 is $N(T - 1)$; number ending in 0 is $N(T - 2)$. Thus $N(T)$ satisfies the difference equation

$$N(T) = N(T - 1) + N(T - 2),$$

with characteristic (algebraic) equation

$$X^0 = X^{-1} + X^{-2}$$

or

$$X^2 - X - 1 = 0.$$

If X_{max} = largest real root of the characteristic equation, then

$$C = \log X_{max}$$

In this case $X_{max} = 1.62$, and $C = 0.70$ bits per second.

b. Binary channel, duration of 0 and 1 each second, with added constraint that after 1 is used then 0 must follow (though 1 or 0 can follow 0):

$N(T) = N(T - 1) + N(T - 2)$, as in a above.

$C = 0.70$ bits per second

These binary channels have the same capacity but can not handle the same binary sequences. If a proper encoder is placed between them, the over-all capacity of the two in series remains the same as either one alone.

Noiseless channel *continued*

Fundamental theorem for noiseless channel

Sequences of source symbols, of entropy H bits per symbol, when properly encoded in permissible sequences of a channel with capacity C bits per second, can be transmitted through the channel provided that the source does not produce symbols at an average number per second greater than C/H.

Noisy channel

Transmission through a noisy channel is subject to processes interfering at random with the channel symbols. The interference is itself a source of erroneous information. A noisy channel (or random transducer) is defined by: a set of input symbols x_i, a set of output symbols y_j, a matrix of probabilities c_{ij} that x_i is converted to y_j during transmission, and an average number of inputs per second.

An instance of a noisy channel is a facility for transmitting a 1-volt or 0-volt signal per second along a pair of wires, where the wires are short-circuited at random 10-percent of the time. The possible inputs are $x_0 = 0$, $x_1 = 1$, the outputs $y_0 = 0$, $y_1 = 1$ with $c_{00} = 1$, $c_{01} = 0$ and $c_{10} = 0.1$, $c_{11} = 0.9$.

If the channel interference produces symbols at the output that are not in the set of inputs, a decoder performing a "decision function" can be introduced to resolve all outputs into possible inputs. The decoder can be regarded as part of the channel.

Dispersion, equivocation

When x_i are used with probabilities u_i, then the joint probability of x_i, y_j ($p_{ij} = u_i\ c_{ij}$), the probability of y_j at the output, the ("inverse") probabilities c_{ij}', and associated entropies can be established as shown in the section on joint events.

Dispersion is the conditional entropy $H_x(y)$. It is a measure of the uncertainty of the output, on the average, given the input.

Equivocation is the conditional entropy $H_y(x)$. It is a measure of the uncertainty of the input, on the average, having observed the output.

When the channel is driven directly by a source (i.e., the input symbol probabilities u_i equal the source symbol probabilities p_i), then

$$R = H(x) - H_y(x) = H(y) - H_x(y)$$

is often referred to as the *rate of transmission* through the channel.

Noisy channel *continued*

Example: Binary source of rate 1 bit per digit driving *symmetric* binary channel defined by probabilities $c_{10} = c_{01} = p$ (1 and 0 are mistaken for each other with probability p).

$$R = 1 - \left[p \log_2 \frac{1}{p} + (1 - p) \log_2 \frac{1}{1 - p}\right] \text{ bits per digit}$$

The 1 is the source or channel symbol entropy and would be the information rate in the absence of errors. The bracketed term is the equivocation (and also dispersion in this symmetrical case).

Capacity of noisy channel

Of all possible assignments of probabilities u_i to the channel symbols, there is a set that results in a maximum value of the difference $H(x) - H_y(x)$. This maximum difference is defined as the capacity of the noisy channel:

$$C = \max_{u_i} [H(x) - H_y(x)]$$

where $\Sigma u_i = 1$ and $u_i \geqslant 0$.

(This maximization is sometimes described as matching the channel symbol usage to the channel noise).

Fundamental theorem for noisy channel

A channel of capacity C can be driven by any properly coded source of rate up to C with practically zero probability of error in recovering the input. This is not possible if the source rate exceeds C.

Underlying principle of theorem: Let long sequences, or blocks of input symbols be regarded as the basic transmission units (rather than the individual symbols), and let the symbols x_i within blocks be used with frequencies u_i. Each block will upon transmission give rise to one of a group of possible responses associated with it.

The groups of responses to all such blocks overlap. If there were no overlap at all, every such block would be ideal for transmission, since the noisy responses would fall into completely separable groups, each one identified with a definite input.

However, by limiting the number of possible input blocks to a certain number M, the response groups associated with these M become nearly separable, and still more so as the length of block considered increases. For any probabilities u_i, and number of symbols N per block, the number of blocks M must satisfy:

$$(1/N) \log M < R = H(x) - H_y(x)$$

Noisy channel *continued*

If such blocks of channel symbols are then associated with output sequences from a source of rate $H = (1/N) \log M$ (a noiseless coding procedure), then coded messages from the source can be identified at the channel output with virtually no error and at the rate H.

The maximum source rate for which this still holds is the maximum value of R, or the channel capacity.

The theorem does not define any specific encoding of the source but rather a class of codes that in general are difficult to apply.

There is presently much effort devoted to developing codes with a systematic structure, e.g., self-checking codes, and to evaluating explicit relations between code length and probability of error.

Channel with additive noise

Output y is the sum of the input x and channel noise n,

$$y = x + n$$

When n and x are statistically independent,

$$H_x(x + n) = H(n)$$

since probabilities of $(x + n)$ given x are the probabilities of n. Thus,

$$R = H(x + n) - H(n)$$

Since $H(n)$ is fixed by the channel, maximum R occurs when $H(x + n)$ is maximum.

Illustration: A binary facility for transmitting a $-$ 2- or $+$ 2-volt pulse once a second disturbed by crosstalk. The crosstalk consists of a $-$ 1- or $+$ 1-volt pulse occurring equally frequently at an average rate of 1 per second. The noise entropy $H(n)$ is 1 bit per second. If the $\pm$ 2-volt pulses are used equally frequently, $u_i = 1/2$, then the entropy of signal plus noise $H(x + n)$ is 2 bits per second, (4 equiprobable output levels: -3, -1, $+1$, $+3$). Thus, $R = 1$ bit per second. In this simple case, the rate R is easily achieved without error by noting that a positive output can only mean that $+2$ is intended and a minus output must mean -2. 1 bit per second is also the capacity of the channel, since $H(x + n)$ is already maximum.

Noisy binary channel

Defined by probabilities $c_{01} = p$ and $c_{10} = q$, these error probabilities implicitly determining the severity of interference present.

The channel capacity is

$$C = \log_2 \left\{ 2^{[qH_p - (1-p)H_q]/[1-(p+q)]} + 2^{[pH_q - (1-q)H_p]/[1-(p+q)]} \right\}$$

bits per digit where

Noisy channel *continued*

$H_p = -p \log_2 p - (1-p)\log_2(1-p)$

(A curve is given in Fig. 2.) H_q is obtained from H_p, replacing p by q.

C is symmetrical in p and q. The maximizing input digit probabilities are

$$u_1 = \frac{v_1 - q}{1 - (p+q)}$$

where v_1 = probability of 1 at the output

$$v_1 = \left\{1 + 2^{(H_p - H_q)/[1-(p+q)]}\right\}^{-1}$$

$$u_0 = \frac{v_2 - p}{1 - (p+q)}$$

where v_2 = probability of 0 at the output $= 1 - v_1$.

When $p = q$, the symmetric binary channel results. Further, let the binary digits be positive and negative pulses of equal amplitudes, equal durations $T = 1/2W$, and average power P. Let the channel noise be similar pulses with Gaussian distribution of amplitude of average power N, which add to the digit pulses. Then $C/W = 2(1 - H_p)$ bits per second per cycle of bandwidth, where the digit error-probability as a function of P/N is

$$p = \tfrac{1}{2}\operatorname{erfc}\left[(P/N)^{1/2}/(2)^{1/2}\right]$$

C/W versus P/N in decibels is given in Fig. 5.

Channel with additive noise

Signal limited in bandwidth and average power: A facility can handle pulses of all possible amplitudes, at a maximum rate of $1/2W$ per second and with the constraint that pulse sequences are limited to average power P. Noise pulses in the channel with Gaussian distribution of amplitude and of average power N (no direct-current component) add to the signal pulses. The capacity of the channel is

$$C = W \log_2 (1 + P/N) \text{ bits per second,}$$

showing explicit dependence on channel noise. A plot of C/W is given in Fig. 5. The capacity may be achieved arbitrarily closely if sequences of signal amplitudes are formed with Gaussian probability distribution and mean-square fluctuation P. The channel could be used with negligible probability of error by a binary or other source of rate up to C if long-enough source sequences are encoded into the Gaussian signals. If the Gaussian noise power varies directly with bandwidth, then letting W_0 be

Noisy channel *continued*

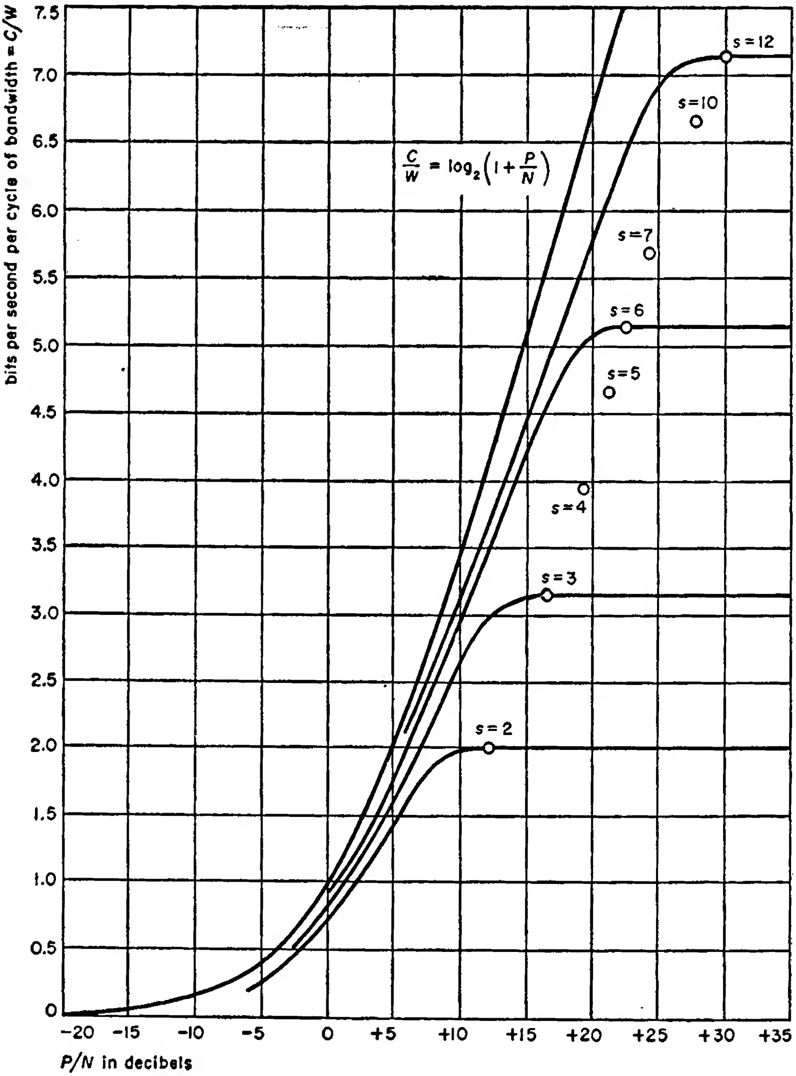

Fig. 5—Channel capacity versus P/N. The number of signal levels (equally spaced and centered on zero) is s. For a symmetrical binary channel, s = 2.

Noisy channel *continued*

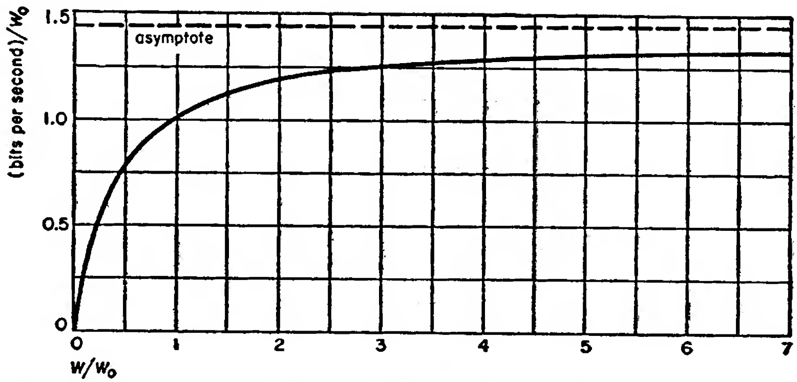

Fig. 6—Capacity of channel (limited in average power and bandwidth with Gaussian noise) as a function of bandwidth. W_0 = bandwidth for which signal power equals noise power ($P = N$).

that width for which $P = N$, the variation in C/W_0 is the curve given in Fig. 6.

The normalized capacity C/W_0 rises sharply to unity as bandwidth increases to W_0, then slowly approaches 1.44 bits = 1 nit with further increases in W. The quantity CT is the amount of information that can be transmitted a long-enough interval T. This quantity is referred to as an exchange relation indicating how T, W, P, and N can be "traded", that is, how constant capacity can be maintained by various channel adjustments.

Bibliography

1. C. E. Shannon, "A Mathematical Theory of Communication," *Bell System Technical Journal*, vol. 27, pp. 399–423; July: also, pp. 623–656; October, 1948.

2. P. L. Chessin, "A Bibliography on Noise," *IRE Transactions on Information Theory*, vol. IT-1, pp. 15–31; September, 1955.

3. F. L. H. M. Stumpers, "A Bibliography on Information Theory," *IRE Transactions on Information Theory*, vol. IT-1, pp. 31–47; September, 1955.

4. W. Jackson, editor, "Communication Theory," New York Academic Press and London Butterworths Scientific Publications; 1953: A collection of papers read at a symposium on "Applications of Communication Theory" held at the Institution of Electrical Engineers, London, England, September 22-26; 1952.

5. C. E. Shannon, "Communication in the Presence of Noise," *Proceedings of the IRE*, vol. 37, pp. 10–21; January, 1949.

6. L. Brillouin, "Science and Information Theory," Academic Press, Inc., New York, N. Y.; 1956.

7. C. E. Shannon, "Prediction and Entropy of Printed English," *Bell System Technical Journal*, vol. 30, pp. 50–64; January, 1951.

■ Probability and statistics

General

A *random experiment* is one that can be repeated a large number of times, under similar circumstances, but may yield different results at each trial.

For example, rolling of a die is a random experiment where the result is one of the numbers 1, 2, 3, 4, 5, or 6. Observing the noise voltage across a resistor is another random experiment that gives a number V dependent on the instant of observation. A random experiment may consist of observing or measuring elements taken from a set that is then known as a *population*.

The result of a random experiment is called a *random variable* or *variate*. This is usually a number, or a set of numbers, but it may also be an element of a given set such as a point within an area, or a color among a given group, or a quality such as good or bad.

A variate may be *discrete*, as in the case of the die, or *continuous* as in the case of a noise voltage.

Fluctuations of the result of a random experiment are due to causes that cannot be entirely controlled. However, if the conditions of the experiment are sufficiently uniform (for instance, if the same die is used in successive throws; if the resistor is at a constant temperature), some statistical regularity can be observed when results of a large number of experiments are considered. The statistical regularity is expressed by the law that gives the *probability* of obtaining a given result or a result falling within a given range of values. The law of probability is assumed to be the same for each performance of the experiment, independently of the results of other trials. When experiments done in time sequence are not independent, the whole sequence is considered as a single random experiment called a *stochastic* or *random process* (see p. 998).

A discrete variate, which may take values $x_1, x_2 \ldots x_n \ldots$ is described by $p(k)$, its *probability function*. $p(k)$ is the probability of obtaining x_k as the result of one trial.

$$0 \leqslant p(k) \leqslant 1$$

$$\sum_{\text{all } k} p(k) = 1$$

If the x_k are real numbers, the *cumulative probability function*

$$P(x) = \sum_{x_k < x} p(k)$$

also describes the variate. The p_k are the jumps of this function.

General *continued*

For a *continuous variate* that takes real numerical values, the probability that one trial of the experiment gives a result between x and $x + dx$ is $p(x)\,dx$ where $p(x)$ is the *probability density function*. The *cumulative distribution function* is

$$P(x) = \int_{-\infty}^{x} p(x)\,dx$$

$P(x)$ is the probability that the result is less than x.

$$P(-\infty) = 0$$

$$P(+\infty) = \int_{-\infty}^{+\infty} p(x)\,dx = 1$$

$$p(x) = dP/dx$$

For a continuous random variable with more than one dimension or *multivariate*, the probability density function p and the cumulative distribution function P can also be defined. For instance, if (x,y) are the coordinates of a random point in the plane, then $p(x,y)\,dx\,dy$ is the probability that the point has its abscissa between x and $x + dx$ and its ordinate between y and $y + dy$. The cumulative distribution function is

$$P(x,y) = \int_{-\infty}^{x} dx \int_{-\infty}^{y} dy\; p(x,y)$$

Definitions

Quantities often used to describe the location and spread of a random variable are listed below. The first formula in each case applies to a discrete variate with probability function $p(k) = p_k$. The second formula applies to a continuous variate x (real number) defined by its probability density function $p(x)$.

Average or mean

$$\mu = \sum_{\text{all } k} p_k x_k$$

$$\mu = \int_{-\infty}^{+\infty} x\, p(x)\,dx$$

Root-mean-square, rms

$$r = \left[\sum_{\text{all } k} p_k x_k^2\right]^{1/2}$$

Definitions *continued*

$$r = \left[\int_{-\infty}^{+\infty} x^2\, p(x)\, dx\right]^{1/2}$$

Moment of order r, about the origin

$$\nu_r = \sum_{\text{all } k} p_k\, x_k^{\,r}$$

$$\nu_r = \int_{-\infty}^{+\infty} x^r\, p(x)\, dx$$

Moment of order r, about the mean

$$\mu_r = \sum_{\text{all } k} p_k\, (x_k - \mu)^r$$

$$\mu_r = \int_{-\infty}^{+\infty} (x - \mu)^r\, p(x)\, dx$$

Variance

$$\sigma^2 = \mu_2 = \sum_{\text{all } k} p_k\, (x_k - \mu)^2$$

$$\sigma^2 = \mu_2 = \int_{-\infty}^{+\infty} (x - \mu)^2\, p(x)\, dx$$

Standard deviation or rms deviation from the mean

$$\sigma = \left[\sum_{\text{all } k} p_k\, (x_k - \mu)^2\right]^{1/2}$$

$$\sigma = \left[\int_{-\infty}^{+\infty} (x - \mu)^2\, p(x)\, dx\right]^{1/2}$$

Mean absolute deviation, mae

$$= \sum_{\text{all } k} p_k\, |x_k - \mu|$$

$$= \int_{-\infty}^{+\infty} |x - \mu|\, p(x)\, dx$$

Definitions *continued*

Median: A value m such that the variable x_k (or x) has equal probabilities of being larger or smaller than m.

For the continuous case

$$\int_{-\infty}^{m} p(x)\, dx = \int_{m}^{+\infty} p(x)\, dx$$

Mode: A value of x (or x_k) where the probability $p(x)$ (or p_k) is largest. There may be more than one mode.

p-percent value: A value of x exceeded only p-percent of the time; that is, with probability $p/100$. This applies mostly to continuous distributions where the p-percent value denoted by x_p satisfies

$$1 - P(x_p) = \int_{x_p}^{+\infty} p(x)\, dx = p/100$$

The median is the 50-percent value.

Quartile: The 25- and the 75-percent values.

Expected value or mathematical expectation: For any variable y equal to a given function $g(x)$ of the random variable x, the expected value is

$$E[y] = \sum_{\text{all } k} g(x_k)\, p_k$$

and for the continuous case,

$$E[y] = \int_{-\infty}^{+\infty} g(x)\, p(x)\, dx$$

Characteristic function

Continuous case

The characteristic function for a distribution defined by its probability density $p(x)$ or by its cumulative distribution function $P(x)$ is

$$C(u) = E[\exp jux] = \int (\exp jux)\, dP(x) = \int (\exp jux)\, p(x)\, dx$$

$$C(0) = 1$$

$$|C(u)| \leqslant 1$$

Characteristic function *continued*

$C(-u) = C^*(u)$

(Where the asterisk denotes the complex conjugate.) $C(u)$ can be expanded in term of the moments

$$C(u) = 1 + \sum \nu_r (ju)^r/r!$$

The function C is the Fourier transform of p, hence

$$p(x) = (1/2\pi) \int (\exp -jux)\, C(u)\, du$$

For a multivariate $\mathbf{x} = (x_1, x_2 \ldots x_n)$, the characteristic function is

$$C(u_1, u_2 \ldots u_n) = E\{\exp [j(u_1x_1 + u_2x_2 + \ldots + u_n x_n]\}$$

$$C(\mathbf{u}) = E[\exp j\mathbf{u}\cdot\mathbf{x}]$$

Discrete case

The characteristic function corresponding to the probability function p_k is

$$C(u) = \sum p_k \exp jux_k$$

Addition of statistically independent variables

If two independent variates x_1, x_2 have probability densities $p_1(x_1)$ and $p_2(x_2)$, the probability density function for their sum $x = x_1 + x_2$ is the convolution integral

$$p(x) = \int p_1(x - \xi)\, p_2(\xi)\, d\xi$$

or, in shortened form,

$$p = p_1 * p_2$$

Similarly the cumulative distribution function for the sum is

$$P(x) = P_1 * p_2 = \int P_1(x - \xi)\, dP_2(\xi)$$

Instead of computing these convolutions, it is simpler to use the corresponding property of the characteristic functions

$$C(u) = C_1(u)\, C_2(u)$$

and to deduce $p(x)$ as the Fourier transform of $C(u)$. This property extends to the sum of n independent variates.

Distributions

Binomial distribution

If the result of a random experiment is one of two alternatives, the statistics are completely defined by the probability p of one of the alternatives. The trial may be the flipping of a coin or the testing of an electron tube taken at random. The preferred alternative or "success" could be a head in the first case, an acceptable tube in the second case. The probability of failure in one trial is

$$q = 1 - p.$$

In n independent trials, the probability of exactly k "successes" is given by

$$C_k^n \, p^k \, (1 - p)^{n-k}$$

(definition of C_k^n appears on p. 1038). This is called the binomial distribution because $p(k)$ is the kth term in the development of the binomial $(p + q)^n$.

The average of k is np and the variance is

$$E[(k - np)^2] = npq$$

The standard deviation is

$$(npq)^{1/2}$$

The probability of at least one success in n independent trials is

$$1 - (1 - p)^n$$

Application: If 15 percent of the components from a given lot are defective, the probability of finding exactly 3 bad ones in a set of 10 is

$$C_3^{10} \, (0.15)^3 \, (0.85)^7 = \frac{10 \times 9 \times 8}{1 \times 2 \times 3} 15^3 \, 85^7 \, 10^{-20} = 13 \text{ percent}$$

The probability of finding at least one good component in a set of 3 is

$$1 - (0.15)^3 = 99.7 \text{ percent}$$

Poisson distribution

A random experiment that leads to the Poisson distribution might consist of counting, during a given time T, the electrons emitted by a cathode, the telephone calls received at a central office, or the noise pulses exceeding a threshold value. In all these cases the events are, in general, independent of each other and there is a constant probability νdt that one of them will occur during a short interval dt.

Distributions *continued*

The probability that exactly k events will occur during the time interval T is given by the Poisson frequency function

$$P_k = (m^k/k!) \exp(-m)$$

where the parameter $m = \nu T$ is the average number of events during the interval T.

The variance of k is

$$E[(k - \nu T)^2] = m$$

The standard deviation is

$$m^{1/2}$$

The characteristic function is

$$\exp\left\{m\left[(\exp ju) - 1\right]\right\}$$

The binomial distribution, when the product np is small and n is large, is approximately a Poisson distribution with parameter $m = np$.

Exponential distribution

In a Poisson process, the probability that the interval between two consecutive events lies between t and $t + dt$ is

$$\nu(\exp - \nu t)\, dt = d\,(1 - \exp - \nu t)$$

with $t \geqslant 0$. The average interval is

$$E[t] = 1/\nu$$

The root-mean-square is

$$(E[t^2])^{1/2} = 2/\nu$$

The standard deviation is

$$\left\{E[(t - 1/\nu)^2]\right\}^{1/2} = 1/\nu$$

The median is

$$(\log_e 2)/\nu = 0.6931/\nu$$

The cumulative distribution function is

$$1 - \exp(-\nu t)$$

The probability that an interval is larger than t is

$$\exp(-\nu t)$$

Distributions *continued*

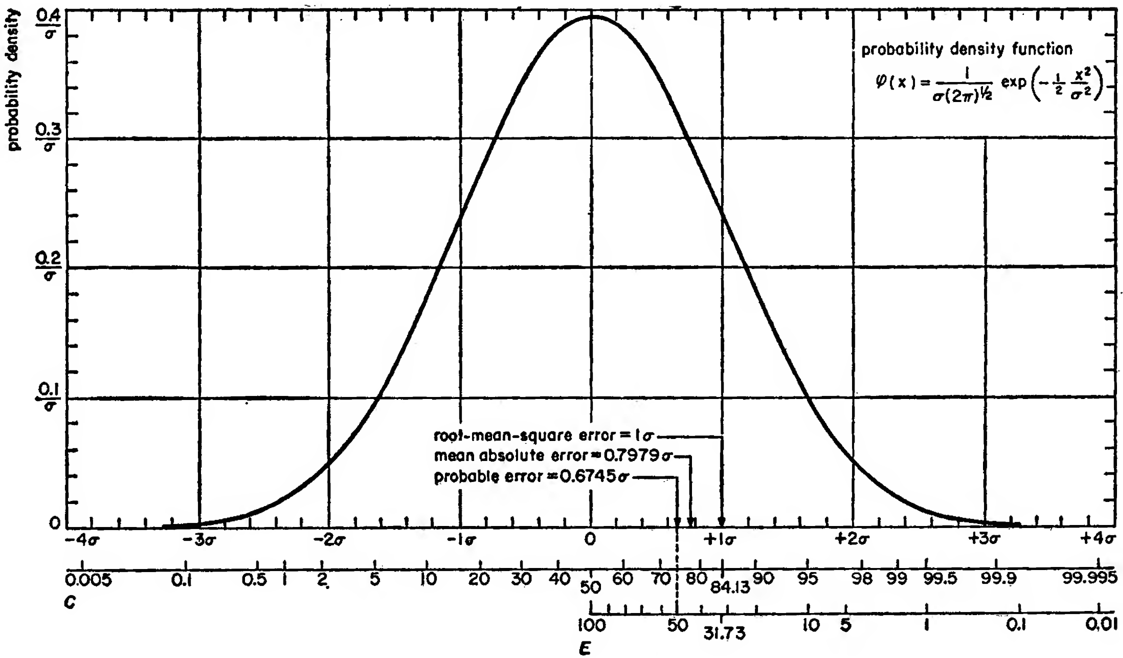

Fig. 1—The normal distribution. σ is the standard deviation. Scale C is the cumulative distribution function in percent = 100 Φ (x). For example, the probability of finding x between $-\sigma$ and $+2\sigma$ is 97 − 16 = 81 percent. Scale *E* is the probability that the error (absolute deviation) exceeds the value read on the axis. For example, if the deviation is larger than 2σ in either direction, probability is 4.5 percent.

Distributions *continued*

Problem: Pulses of noise, above a certain level, occur with an average density of 2 per millisecond. A device is triggered every time two pulses occur within the same 5-microsecond interval. How often does this happen? Since $\nu t = 0.01$, then $\exp - 0.01 = 0.990$ (from table on p. 1115) is the probability that one interval will exceed 5 microseconds. The device is triggered by 1 percent of the pairs of consecutive pulses, hence 20 times per second.

Normal distribution

The normal, or *Gaussian* distribution is often found in practice because it occurs whenever a large number of independent random causes, each producing small effects, act together on the quantity being measured (central limit theorem of the theory of probability).

The normal probability density function, for a mean of zero and a standard deviation σ, is

$$\varphi_\sigma(x) = [1/\sigma(2\pi)^{1/2}] \exp[-\tfrac{1}{2}(x/\sigma)^2]$$

(See Fig. 1 and table on p. 1116. When the mean value is μ instead of 0, the probability density becomes $\varphi_\sigma(x - \mu)$.

The cumulative distribution function

$$\Phi(x) = \int_{-\infty}^{x} \varphi_\sigma(x)\, dx$$

is given by scale C on Fig. 1 and more accurately by the table on p. 1117. Related to Φ are the error-function erf t and its complementary erfc t:

$$\text{erf } t = (2/\pi^{1/2}) \int_0^t \exp(-t^2)\, dt = 2\Phi[t\, 2^{1/2}] - 1$$

$$\text{erfc } t = 1 - \text{erf } t$$

The absolute deviation from the mean $|x - \mu|$, sometimes called the error, has the distribution given in the table on p. 1116 and scale E on Fig. 1. The median value, equal to $0.6745\,\sigma$, is called the *probable* error. It is exceeded 50 percent of the time. The average of $|x - \mu|$, equal to 0.7979σ, is the *mean absolute* error. The 3σ error is exceeded with probability of about 0.3 percent.

Additive property: The linear combination, with constant coefficients of n normal random variables is also a normal random variable. If

$$y = c_1x_1 + c_2x_2 + \ldots + c_nx_n$$

where x_i has mean μ_i and variance σ_i^2, then y has a mean

Distributions *continued*

$$\mu = \sum c_i \mu_i$$

and a variance

$$\sigma^2 = \sum c_i^2 \sigma_i^2$$

Multivariate normal distribution

The vector $\mathbf{x} = (x_1, x_2 \ldots x_n)$ is normally distributed about the origin if the probability density function is

$$\varphi_M(\mathbf{x}) = [(2\pi)^n \det M]^{-1/2} \exp[-\tfrac{1}{2}(\tilde{\mathbf{x}} M^{-1}\mathbf{x})]$$

where the *moment*, or *covariance* matrix $M = (\mu_{ij})$ is of order n. The coefficients μ_{ij} are the second-order moments

$$\mu_{ij} = E[x_i x_j]$$

Sometimes μ_{ii}, the *variance* of x_i, is denoted by σ_i^2 and μ_{ij}, the *covariance* of x_i and x_j, is expressed by $\sigma_i \sigma_j r_{ij}$. The r_{ij} are *correlation coefficients.*

Any linear function of x say, $y = Lx$, where L is a matrix of order $m \times n$ is normally distributed with the moment matrix

$$N = LM\tilde{L}$$

The characteristic function of the multivariate normal distribution is:

$$C(\mathbf{u}) = E[\exp(j\tilde{\mathbf{u}}\mathbf{x}) = \exp[-\tfrac{1}{2}(\tilde{\mathbf{u}}M\mathbf{u})]$$

The sum of two independent, normally distributed vectors $\mathbf{x},\mathbf{y}$ with covariance matrices M and N, respectively, is normally distributed with covariance matrix $M + N$

$$\varphi_M * \varphi_N = \varphi_{M+N}$$

Normal distribution in two dimensions: Let x,y be the coordinates of the random point, the probability density is

$$\varphi(x,y) = \frac{1}{2\pi\,\sigma_1\sigma_2\,(1-\rho^2)^{1/2}} \exp\left[-\frac{1}{2(1-\rho^2)}\left(\frac{x^2}{\sigma_1^2} - \frac{2\rho xy}{\sigma_1\sigma_2} + \frac{y^2}{\sigma_2^2}\right)\right]$$

where $\sigma^2{}_1$ and σ_2^2 are the variances of x and y and ρ is their correlation coefficient.

Distributions *continued*

Circular case—Rayleigh distribution: When the two variates have the same variance ($\sigma_1 = \sigma_2 = \sigma$) and are not correlated ($\rho = 0$),

$$\varphi(x,y) = \frac{1}{2\pi\sigma^2} \exp\left(-\tfrac{1}{2} \frac{x^2 + y^2}{\sigma^2} \right)$$

The distance R to the origin, $R^2 = x^2 + y^2$, is distributed according to the probability density function

$$p(R)\, dR = (R/\sigma^2) \exp(-R^2/2\sigma^2)\, dR$$

This is sometimes called the *Raleigh distribution*. When a large number of small independent random phasors with equiprobable phases are added, the extremity of the vector sum is distributed according to the circular normal bivariate distribution. The magnitude R of the sum has therefore the probability density $p(R)$. This applies to the electromagnetic field scattered by a large number of small scatterers. It also describes the distribution of the envelope of a narrow band of Gaussian noise.

Fig. 2 shows the function $p(R)$ and the scale C gives the probability that some given level will be exceeded. The rms of R is $\sigma(2)^{1/2}$. The average $\sigma(\pi/2)^{1/2} = 1.2533\sigma$ is the *mean radial* error. The *median* or 50-percent value, 1.1774σ is also called cep (circular error probable), because it is the radius of the 50-percent probability circle in the x,y plane.

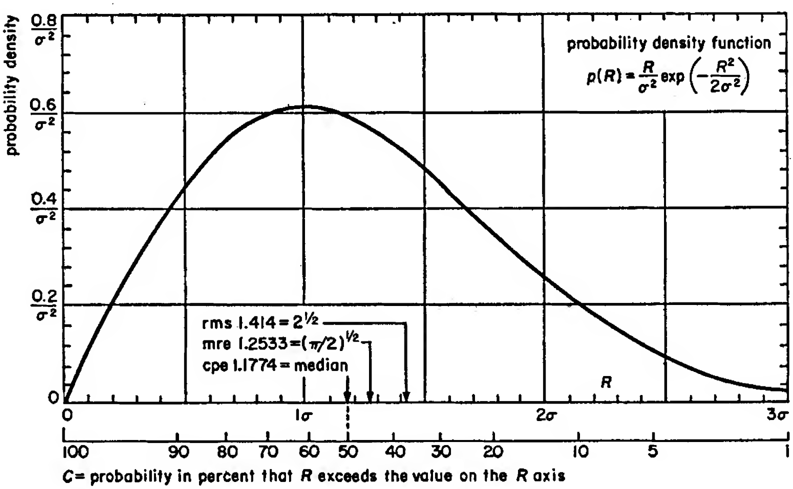

Fig. 2—Rayleigh distribution. R is the distance to the origin in a bivariate normal distribution. σ is the standard deviation for either component of the normal distribution.

Distributions *continued*

Using $X = R^2$ (power) as the variable,

$$p(R)\,dR = [\exp(-X/X_0)]\,d(X/X_0)$$

with $X_0 = 2\sigma^2$

When the circular normal distribution has its center at a distance S from the origin, the distance R to the origin is distributed according to

$$p(R)\,dR = \frac{R}{\sigma^2}\exp\left[-\frac{R^2+S^2}{2\sigma^2}\right] I_0\left(\frac{RS}{\sigma^2}\right) dR$$

where I_0 = Bessel function with imaginary argument. This is the distribution of the envelope of a sine wave plus some Gaussian noise. It also represents the distribution of the amplitude of a field that results from the addition of a fixed vector and a random component obtained, for instance, by scattering from a large number of small independent scatterers. See sketch at right.

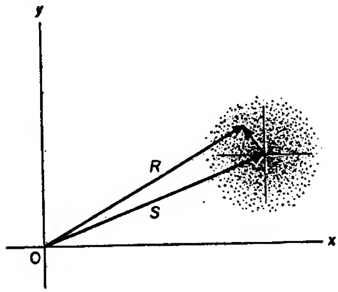

Chi-square distribution

The distribution of the sum of the squares of n independent normal variates, each having mean zero and variance unity, is called the chi-square distribution.

The probability density function for this sum x is

$$k_n(x) = \frac{x^{n/2-1}}{2^{n/2}\Gamma(n/2)}\exp(-x/2)$$

(x, being the sum of n squares, is positive.) The parameter n is called the *number of degrees of freedom*. The mean of x is n and its variance is $2n$.

The p-percent value of x (exceeded p percent of the time) is denoted, for n degrees of freedom, by $\chi_p^2(n)$

$$\int_{\chi_p^2}^{\infty} k_n(x)\,dx = p/100$$

Curves of χ_p^2 versus p are shown in Fig. 3.

The first functions k_n are:

$$k_1(x) = (2\pi x)^{-1/2}\exp(-x/2)$$

Distributions *continued*

where x is the square of the deviation in a normal distribution.

$k_2(x) = \frac{1}{2} \exp(-x/2)$

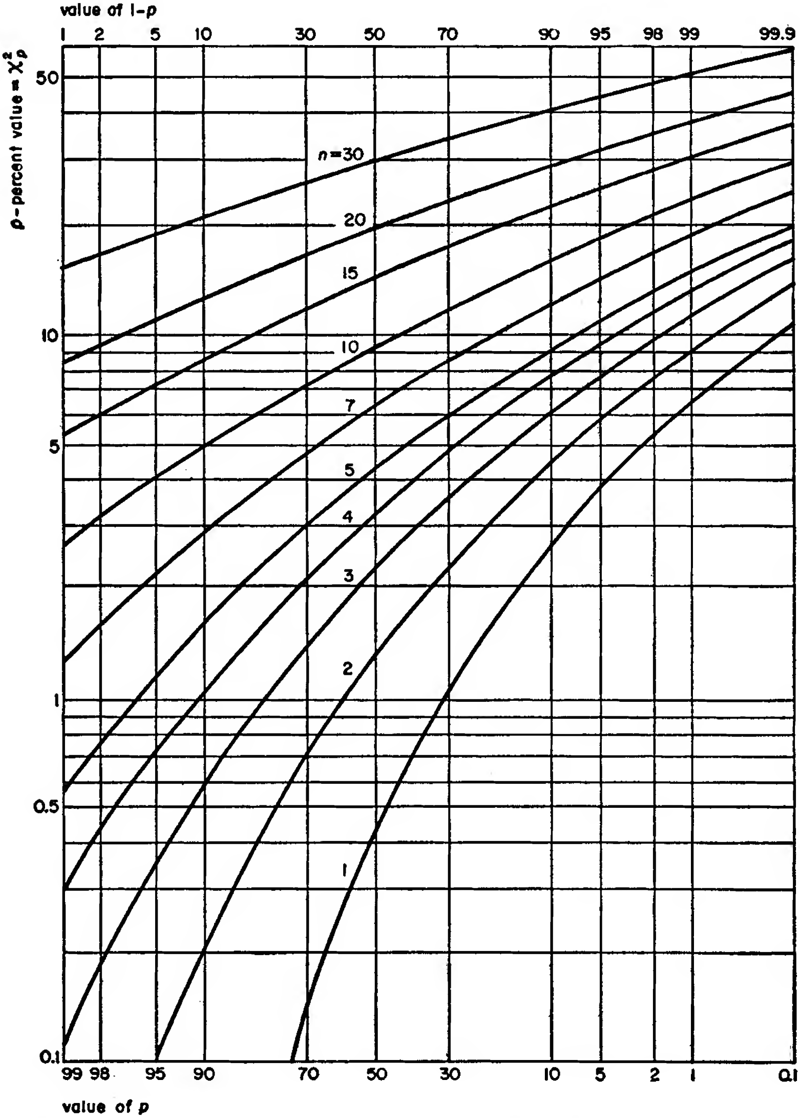

Fig. 3—Chi-square distribution. Function χ_p^2 (n) for n degrees of freedom.

Distributions *continued*

where x corresponds to R^2 in the Rayleigh distribution (see p. 991).

$$k_3(x) = (x/2\pi)^{1/2} \exp(-x/2)$$

where x is the square of the distance to the origin of a point in space having a normal distribution with spherical symmetry.

Sampling

If a random experiment is repeated n times, the results $x_1, x_2 \ldots x_n$ form a *sample* of size n. The distribution of x from which the sample is drawn is called the *parent distribution.*

The numbers $x_1 \ldots x_n$ may not all be different and may form a smaller set $x_1 \ldots x_k \ldots x_m$ where x_k occurs n_k times. The definitions on pp. 982–984 can be applied to a sample (or to an arbitrary set of numbers) by using the *relative frequencies* n_k/n in place of the probabilities p_k.

The *sample mean* is

$$\bar{x} = (1/n)(x_1 + x_2 + \ldots + x_n)$$

The *sample variance* is

$$s^2 = \frac{1}{n} \sum_{i=1}^{i=n} (x_i - \bar{x})^2$$

If the x_k are in such order that

$$x_1 \leqslant x_2 \leqslant x_3 \leqslant \ldots \leqslant x_n$$

the *sample median* is

$$\xi = x_{(n+1)/2}$$

if n is odd and

$$\xi = \tfrac{1}{2}\left[x_{n/2} + x_{(n/2)+1}\right]$$

if n is even.

Estimation of mean and variance of a normal variate

Given a sample of size n taken from a normal distribution, a frequent problem is to estimate the mean μ and the variance σ^2 of the parent population.

One estimate of μ is the sample mean $\bar{x}$. It is a normal random variable with average μ (the estimate is *unbiased*) and with variance σ^2/n. Another

Sampling *continued*

unbiased estimate of μ is the sample median ξ. It is easier to compute than $\bar{x}$ but has a larger standard deviation: $1.2\,\sigma/n^{1/2}$ for $n \leqslant 10$ and $1.25\,\sigma/n^{1/2}$ for n large. In the latter case, ξ becomes normally distributed.

The sample variance has an average of

$$[(n-1)/n]\sigma^2$$

and hence it is a biased estimate of the population variance. An unbiased estimate is

$$s'^2 = [1/(n-1)] \sum (x_i - \bar{x})^2 = [n/(n-1)]s^2$$

which differs appreciably from s^2 when n is small.

The standard deviation σ can also be deduced from the sample range; that is, from the difference between the largest and the smallest number in the sample. For a sample of size n, σ is obtained by dividing the range by the number c_n in the table*

n	c_n
5	2.33
10	3.08
20	3.73
30	4.09
100	5.02

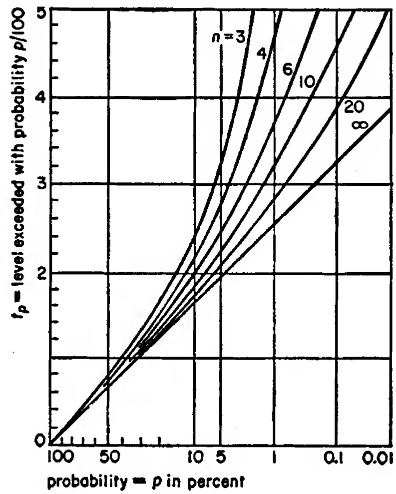

Fig. 4—Student's t distribution. For n degrees of freedom, the ordinate on the curve labelled n is the value t_p exceeded, in either direction, with a probability $p/100$.

A p-percent *confidence interval* is such that the quantity estimated falls within that interval p percent of the time. Intervals of this type can be deducted from a given sample for the mean μ and for the variance σ of the parent population.

For the mean:

$$\bar{x} - s'\,t_{1-p}\,(n-1) \leqslant \mu \leqslant \bar{x} + s'\,t_{1-p}\,(n-1)$$

The function $t_p\,(n)$ is shown in Fig. 4. For instance, for a sample of size 5,

*From: E. S. Pearson, "Percentage Limits for the Distribution of Range in Samples for a Normal Population," *Biometrika*, vol. 24, pp. 404–417; November, 1932: see p. 416. See also, E. S. Pearson and H. O. Hartley, "Biometrika Tables for Statisticians," volume 1, Cambridge University Press, London, England; 1954: see table 22.

Sampling *continued*

the 99-percent confidence interval is from

$\bar{x} - 4.6s'$ to $\bar{x} + 4.6s'$

since $t_{0.01}(4) = 4.6$

For the variance

$n\, s^2/\chi^2_{(1-p)/2}(n-1) \leqslant \sigma^2 \leqslant ns^2/\chi^2_{(1+p)/2}(n-1)$

The function $\chi^2_p(n)$ has been defined previously and is shown in Fig. 3.

For a sample of size 5, and a confidence of 90 percent, read on Fig. 3

$\chi^2_5(4) = 9.5$

$\chi^2_{95}(4) = 0.7$

Therefore the confidence interval is

$0.42s'^2 \leqslant \sigma^2 \leqslant 5.7s'^2$

in terms of the unbiased estimate s'^2 of σ^2:

$s'^2 = \frac{5}{4}s^2$

Chi-square test

The problem is to find how well a sample taken from a population agrees with some distribution function assumed for that population.

The range of x is divided into m regions and the number of sample points falling within each region is counted. Let $f_1, f_2 \ldots f_m$ be the result. From the assumed distribution and the size of the sample, the expected number of points in each region is computed: $g_1, g_2 \ldots g_m$. The deviation between this and the actual result is expressed by

$$D = \sum \frac{(f_i - g_i)^2}{g_i}$$

If the f_i are sufficiently large, say more than 10, this deviation is distributed according to the chi-square distribution with m-1 degrees of freedom. The curves of Fig. 3 can be used to evaluate in percent the significance of a given deviation.

If the assumed parent distribution is not completely known and r parameters defining it have been determined to fit the sample, the number of degrees of freedom is reduced to $m - 1 - r$.

Chi-square test *continued*

Application: During 3 successive one-hour periods the number of telephone calls received at a station was 11, 15, and 23, while during 2 nonoverlapping two-hour periods it was 40 and 37. How does this agree with a Poisson process?

Since the density ν (the number of calls per hour) has not been specified, it is deduced from the sample

$\nu = (11 + 15 + 23 + 40 + 37)/7 = 18$

The deviation from the expected number is

$7^2/18 + 3^2/18 + 5^2/18 + 4^2/36 + 1^2/36 = 5.1$

For $5 - 2 = 3$ degrees of freedom, this deviation is exceeded about 15 percent of the time. The assumption of a Poisson process is therefore very good. It would have been significantly doubtful only if the deviation obtained was exceeded as rarely as 5 percent or less of the time.

Monte Carlo method

The Monte Carlo method consists of solving statistical problems, or problems that can be interpreted as such, by substituting for the actual random experiment a simpler one where the desired probability laws are obtained by drawing random numbers.

Reading in order the digits in the table on p. 1114 is equivalent to successive trials where the result is one out of 10 equiprobable eventualities. Taking pairs of digits simulate 100 equiprobable eventualities. An event with probability of 63 percent may be simulated by the reading of successive pairs, considering as a "success," any pair from 00 to 62. The successive pairs divided by 100 approximate a random variable uniformly distributed over the 0-to-1 interval.

For a smoother approximation, 3 or 4 consecutive digits could be used.

Given any continuous variate defined by its cumulative distribution function $P(x)$, it can be simulated by solving $P(x) = r_i$, where r_i are successive random numbers uniformly distributed between 0 and 1. For instance, using pairs of digits read from p. 1114: 49, 31, 97, 45, 80 . . . , the table on p. 1117 gives successive values of x: 0, -0.5σ, 1.9σ, 0.1σ, 0.8σ that will be normally distributed about $x = 0$ with variance σ^2. This simulates the result of successive shots aimed at the point $x = 0$.

To obtain accurate numerical results by the Monte Carlo method, a large number of trials should be used and elaborate tables or the help of com-

Monte Carlo method *continued*

puting machines are necessary. There are cases, however, where only a crude evaluation is needed and it may be obtained even with a short table such as that on p. 1114.

Problem: Airplanes arrive over an airfield at random, independently of each other, at the average rate of one per minute. The landing operation takes 3/4 minute and only one airplane can be handled at a time. Will many airplanes have to wait before landing? The cumulative distribution function for the interval t minutes between arrival of successive airplanes is $1 - \exp - t$ (see p. 1115). The successive intervals, during an imaginary experiment, may therefore be taken as $t_i = -\log_e (1 - r_i)$, where r_i are the random numbers uniformly distributed between 0 and 1. This is equivalent to $t_i = -\log_e r_i$. Starting at the top left of the table of p. 1114 gives 0.71, 1.17, 0.03, 0.80, 0.22, 0.13, 0.25, 0.40, 0.37, 0.46, 0.17, 0.15, 0.37, 0.65, 3.91, 2.21, 0.17 . . . for the successive intervals in minutes. It is apparent that after a few minutes airplanes will be waiting. A few other trials using other parts of the table show that this situation is not exceptional. The traffic density is too high. The problem could be made more realistic by assuming a normal distribution of the landing times, simulated for instance, as explained above.

Random processes

A *random* or *stochastic* process is a random experiment for which the result is a whole function $y = f(t)$ instead of simply a number or a set of numbers. An example of *random function* is the continuous recording of the noise voltage across a resistor. When the independent variable t takes only discrete values 1, 2 . . . n . . . , the process is called a *random series*.

The probability law for a stochastic process is defined by all possible probability distributions obtained by sampling the random function at a finite number of points.

$$p(y_1, y_2 \ldots y_n; t_1, t_2 \ldots t_n)\, dy_1\, dy_2 \ldots dy_n$$

is the probability that at the instants t_k, for k from 1 to n, the value of the function is between y_k and $y_k + dy_k$.

The process is called *Gaussian* or *normal* when all these distributions are normal.

The process is stationary when all the distributions are invariant by a shift in time:

$$p(y_1, y_2 \ldots y_n; t + t_2 \ldots t + t_n) = p(y_1, y_2 \ldots y_n; t_1, t_2 \ldots t_n)$$

Random processes *continued*

If, furthermore, the process is *ergodic*,* any quantity $g\,[f]$ depending on the random function $f(t)$ has a statistical average $E\,[g\,[f]\,]$ equal to the time average

$$\text{av}\; g[f] = \lim_{T\to\infty} \frac{1}{T}\int_0^T g(f)\,dt$$

In this case, all properties of the process can be deduced from a single experiment giving the function $f(t)$ from $t = 0$ to $t = \infty$.

The process is *totally* or *purely random* if samples taken at different instants are statistically independent of each other

$$p(y_1, y_2 \ldots y_n;\, t_1, t_2 \ldots t_n) = p(y_1;\, t_1)\, p(y_2;\, t_2) \ldots p(y_n;\, t_n)$$

Power spectrum

For the power spectrum of a stationary random function, let

$$F_T(\nu) = \int_0^T f(t)\, \exp\,(-2\pi j\nu t)\, dt$$

be the Fourier transform of the given random function $f(t)$ limited to the interval 0 to T.

The power spectrum, or power density function is defined by

$$W(\nu) = \lim_{T\to\infty} \frac{1}{T}\,|F_T(\nu)|^2$$

The function W is defined for negative frequencies with

$$W(-\nu) = W(\nu)$$

since for a real function f,

$$F_T(-\nu) = F_T^*(\nu)$$

Sometimes the spectrum is limited to positive frequencies by considering

$$\begin{aligned} W'(\nu) &= 2\,W(\nu) \quad \text{for } \nu > 0 \\ &= 0 \qquad\quad\;\; \text{for } \nu < 0 \end{aligned}$$

The power in a band $\nu_1\nu_2$ is

$$\int_{\nu_1}^{\nu_2} W'(\nu)\, d\nu$$

*A process is ergodic if there is no subset of the functions generated that has a probability different from 0 and 1 and is stationary.

Random processes *continued*

Correlation function

The correlation function is defined by

$$\varphi(\tau) = \lim_{T \to \infty} \frac{1}{T} \int_0^T f(t)\, f(t+\tau)\, dt$$

The functions φ and W form a pair of Fourier transforms:

$$\varphi(t) = \int_{-\infty}^{+\infty} W(\nu) \exp(2\pi j\nu t)\, d\nu$$

$$W(\nu) = \int_{-\infty}^{+\infty} \varphi(t) \exp(-2\pi j\nu t)\, dt$$

or also

$$\varphi(t) = \int_0^{\infty} W'(\nu) \cos(2\pi\nu t)\, d\nu$$

$$W'(\nu) = 4 \int_0^{\infty} \varphi(t) \cos(2\pi\nu t)\, dt$$

The *mean square* of $f(t)$ is

$$\varphi(0) = \int_{-\infty}^{+\infty} W(\nu)\, d\nu = \int_0^{\infty} W'(\nu)\, d\nu$$

If the process is Gaussian it is entirely specified by its second-order properties: power spectrum or correlation function. For instance $p(y_1, y_2;\ 0, t)$ is a bivariate normal probability density function with $\mu_{11} = \mu_{22} = \varphi(0)$ and $\mu_{12} = \varphi(t)$

Effect of a linear filter

A linear filter is defined by its impulse response $h(t)$ or by its transfer function $H(\nu)$, Fourier transform of $h(t)$.

If the input to the filter is the random function $f_1(t)$, the output is the random function

$$f_2 = h * f_1$$

$$f_2(t) = \int_{-\infty}^{+\infty} h(t-\tau) f_1(\tau)\, d\tau$$

Random processes *continued*

Introducing the gain

$$G(\nu) = |H(\nu)|^2$$

the power spectrum of f_2 is

$$W_2 = GW_1$$

The correlation function of f_2 is

$$\varphi_2 = g * \varphi_1$$

where g is the Fourier transform of G or

$$g(t) = h(t) * h(-t) = \int_{-\infty}^{+\infty} h(\tau)\, h(\tau + t)\, d\tau$$

Fourier waveform analysis

Fourier transform of a function

The Fourier transform $F(y)$ of the function $f(x)$ is defined by the integral

$$F(y) = \int_{-\infty}^{+\infty} f(x) \exp(-2\pi jxy)\, dx$$

The function $f(x)$ can be deduced from $F(y)$ by the inverse Fourier transform,

$$f(x) = \int_{-\infty}^{+\infty} F(y) \exp(2\pi jxy)\, dy$$

When x represents time, y is the frequency. Sometimes the radian frequency $2\pi y = \omega$ is used as a variable instead of y and the Fourier transform is expressed as

$$F'(\omega) = \int_{-\infty}^{+\infty} f(x) \exp(-j\omega x)\, dx$$

Then

$$F'(\omega) = F(\omega/2\pi)$$

and

$$f(x) = \frac{1}{2\pi} \int_{-\infty}^{+\infty} F'(\omega) \exp(j\omega x)\, d\omega$$

The properties of the Fourier transform are listed in Fig. 1. For the Fourier transform of a random function see pages 998-999.

Fourier transform of a function *continued*

Fig. 1—Properties of Fourier transform.*

	function	Fourier transform
1. Definition	$f(x)$	$F(y) = \int_{-\infty}^{+\infty} f(x) \exp(-2\pi jxy)\, dx$
2. Inverse transform	$f(x) = \int_{-\infty}^{+\infty} F(y) \exp(2\pi jxy)\, dy$	$F(y)$
3. Linearity	$a\, f(x)$ $f_1(x) \pm f_2(x)$	$a\, F(y)$ $F_1(y) \pm F_2(y)$
4. Convolution	$h = f * g$ i.e., $h(x) = \int_{-\infty}^{+\infty} f(x-\tau)\, g(\tau)\, d\tau$	$H = F \cdot G$
4A. Product	$h = f \cdot g$	$H = F * G$
5. Unit impulse (or Dirac function defined on page 1081)	$\delta(x)$ $\Delta(x) = 1$ (for all x)	$\Delta(y) = 1$ (for all y) $\delta(y)$
6. Periodic train of equal impulses	$A \sum_{n=-\infty}^{n=+\infty} \delta(x - nT)$ (with n integer)	$\frac{A}{T} \sum_{n=-\infty}^{n=+\infty} \delta(y - n/T)$

* In the table, functions of x are denoted by lower-case letters and their transforms by the corresponding capital letters.

Fig. 1—*continued*

continued **Fourier transform of a function**

	function	Fourier transform
7. Translation or shifting theorem	$g(x) = f(x - x_0)$	$G(y) = \exp(-2\pi j x_0 y)\, F(x)$
	$g(x) = \exp(2\pi j y_0 x)\, f(x)$	$G(y) = F(y - y_0)$
8. Derivative	$g(x) = df/dx$	$G(y) = 2\pi j y\, F(y)$
	$g(x) = -2\pi j x\, f(x)$	$G(y) = dF/dy$
9. Integral	$g(x) = \int_{-\infty}^{x} f(x)\, dx$	$G(y) = [1/(2\pi j y)]\, F(y)$
	$g(x) = -[1/(2\pi j x)]\, f(x)$	$G(y) = \int_{-\infty}^{y} F(y)\, dy$
10. Change of unit	$g(x) = f(x/a) \qquad a>0$	$G(y) = a\, F(ay)$
	$g(x) = b\, f(bx) \qquad b>0$	$G(y) = F(y/b)$

11. Symmetry	$g(x) = f(-x)$ f even: $f(x) = f(-x)$ f odd: $f(x) = -f(-x)$	$G(y) = F(-y)$ F even: $F = 2\int_0^{\infty} f(x)\cos(2\pi xy)\,dx$ F odd: $F = -2j\int_0^{\infty} f(x)\sin(2\pi xy)\,dx$
12. Complex conjugate	$g(x) = f^*(x)$ if the function f is real	$G(y) = F^*(-y)$ $F(-y) = F^*(y)$
13. Area under the curve	$\int_{-\infty}^{+\infty} f(x)\,dx = F(0)$	$\int_{-\infty}^{+\infty} F(y)\,dy = f(0)$
14. Parseval's theorem	$\int_{-\infty}^{+\infty} f^*(x)\,g(x)\,dx$	$= \int_{-\infty}^{+\infty} F^*(y)\,G(y)\,dy$
14A. Alternative forms	$\int_{-\infty}^{+\infty} f(x)\,g(x)\,dx$	$= \int_{-\infty}^{+\infty} F(-y)\,G(y)\,dy$
	$\int_{-\infty}^{+\infty} f(u)\,G(u)\,du$	$= \int_{-\infty}^{+\infty} F(u)\,g(u)\,du$
14B. "Energy" relation	$\int_{-\infty}^{+\infty} \lvert f(x)\rvert^2\,dx$	$= \int_{-\infty}^{+\infty} \lvert F(y)\rvert^2\,dy$

Fourier series

Real form of Fourier series

For a periodic function with period 2π, defined by its values in the interval $-\pi$ to $+\pi$ or 0 to 2π, as illustrated in Fig. 2,

$$f(x) = \frac{A_0}{2} + \sum_{n=1}^{n=\infty} (A_n \cos nx + B_n \sin nx) \qquad x \text{ in radians}$$

$$= \frac{C_0}{2} + \sum_{n=1}^{n=\infty} C_n \cos (nx + \phi_n)$$

where

$$C_0 = A_0$$

$$C_n = \sqrt{A_n^2 + B_n^2}$$

$$\phi_n = \tan^{-1} (-B_n/A_n)$$

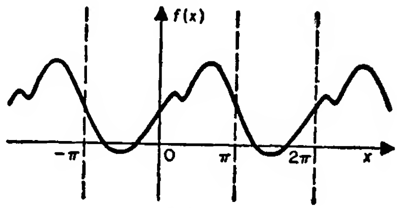

Fig. 2—Periodic wave.

The coefficients A_0, A_n, and B_n are determined by

$$A_0 = \frac{1}{\pi}\int_{-\pi}^{\pi} f(x)\, dx \qquad = \frac{1}{\pi}\int_{0}^{2\pi} f(x)\, dx$$

$$A_n = \frac{1}{\pi}\int_{-\pi}^{\pi} f(x) \cos nx\, dx = \frac{1}{\pi}\int_{0}^{2\pi} f(x) \cos nx\, dx$$

$$B_n = \frac{1}{\pi}\int_{-\pi}^{\pi} f(x) \sin nx\, dx = \frac{1}{\pi}\int_{0}^{2\pi} f(x) \sin nx\, dx$$

Arbitrary period

For a periodic function with period T, defined by its values in the intervals $-T/2$ to $+T/2$ or from 0 to T instead of from $-\pi$ to $+\pi$ or 0 to 2π, the Fourier expansion is given by

$$f(x) = \frac{A_0}{2} + \sum_{n=1}^{n=\infty} \left(A_n \cos 2n \frac{\pi}{T} x + B_n \sin 2n \frac{\pi}{T} x\right)$$

and the coefficients by

$$A_n = \frac{2}{T}\int_{-T/2}^{T/2} f(x) \cos \frac{2n\pi x}{T}\, dx = \frac{2}{T}\int_{0}^{T} f(x) \cos \frac{2n\pi x}{T}\, dx$$

Fourier series *continued*

$$B_n = \frac{2}{T}\int_{-T/2}^{T/2} f(x)\sin\frac{2n\pi x}{T}\,dx = \frac{2}{T}\int_0^T f(x)\sin\frac{2n\pi x}{T}\,dx$$

Complex form of Fourier series

For functions with period 2π,

$$f(x) = \sum_{n=-\infty}^{n=+\infty} D_n \exp(jnx)$$

where

$$D_n = \frac{1}{2\pi}\int_{-\pi}^{+\pi} f(x)\exp(-jnx)\,dx$$

and n takes on all positive and negative integral values including zero.

For real functions

$$D_n = \tfrac{1}{2}(A_n - jB_n) = \tfrac{1}{2}C_n\exp(j\phi_n)$$

$$D_{-n} = \tfrac{1}{2}(A_n + jB_n) = \tfrac{1}{2}C_n\exp(-j\phi_n) = D^*_n$$

$$D_0 = \tfrac{1}{2}A_0 = \tfrac{1}{2}C_0$$

For functions with an arbitrary period T

$$f(x) = \sum_{n=-\infty}^{n=+\infty} D_n \exp\left[j\frac{2n\pi x}{T}\right]$$

$$D_n = \frac{1}{T}\int_0^T f(x)\exp\left[-j\frac{2n\pi x}{T}\right]dx$$

Average power

The average power of the periodic waveform $f(x)$ is

$$\frac{1}{T}\int_0^T |f(x)|^2\,dx = \sum_{n=-\infty}^{n=+\infty} |D_n|^2$$

$$= \tfrac{1}{4}C_0^2 + \tfrac{1}{2}\sum_{n=1}^{n=\infty} C_n^2$$

$$= \tfrac{1}{4}A_0^2 + \tfrac{1}{2}\sum_{n=1}^{n=\infty}(A_n^2 + B_n^2)$$

Fourier series *continued*

Odd and even functions

If $f(x)$ is an odd function, i.e.,

$$f(x) = -f(-x)$$

then all the coefficients of the cosine terms (A_n) vanish and the Fourier series consists of sine terms alone.

If $f(x)$ is an even function, i.e.,

$$f(x) = f(-x)$$

then all the coefficients of the sine terms (B_n) vanish and the Fourier series consists of cosine terms alone, and a possible constant.

The Fourier expansions of functions in general include both cosine and sine terms. Every function capable of Fourier expansion consists of the sum of an even and an odd part:

$$f(x) = \underbrace{\frac{A_0}{2} + \sum_{n=1}^{n=\infty} A_n \cos nx}_{\text{even}} + \underbrace{\sum_{n=1}^{n=\infty} B_n \sin nx}_{\text{odd}}$$

To separate a general function $f(x)$ into its odd and even parts, use

$$f(x) \equiv \underbrace{\frac{f(x) + f(-x)}{2}}_{\text{even}} + \underbrace{\frac{f(x) - f(-x)}{2}}_{\text{odd}}$$

Whenever possible choose the origin so that the function to be expanded is either odd or even.

Odd or even harmonics

An odd or even function may contain odd or even harmonics. A condition that causes a function $f(x)$ of period 2π to have only odd harmonics in its Fourier expansion is

$$f(x) = -f(x + \pi)$$

A condition that causes a function $f(x)$ of period 2π to have only even harmonics in the Fourier expansion is

Fourier series *continued*

$f(x) = f(x + \pi)$

These conditions are sufficient but not necessary.

To separate a general function $f(x)$ into its odd and even harmonics use

$$f(x) \equiv \underbrace{\frac{f(x) + f(x+\pi)}{2}}_{\text{even harmonics}} + \underbrace{\frac{f(x) - f(x+\pi)}{2}}_{\text{odd harmonics}}$$

A periodic function may sometimes be changed from odd to even, and vice versa, by a shift of the origin but the presence of particular odd or even harmonics is unchanged by such a shift.

Numerical evaluation

If the function to be analyzed is not known analytically, a solution of the Fourier integral may be approximated by numerical integration. For instance, the period of the function is divided into 12 equal parts as indicated by Fig. 3.

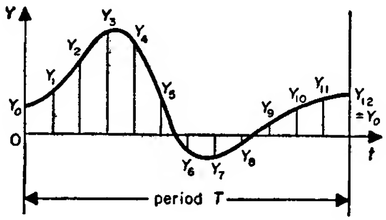

Fig. 3—Division of the period of the function for numerical solution.

The values of the ordinates at these 12 points are recorded and the following computations made:

	Y_0	Y_1	Y_2	Y_3	Y_4	Y_5	Y_6
		Y_{11}	Y_{10}	Y_9	Y_8	Y_7	
Sum	S_0	S_1	S_2	S_3	S_4	S_5	S_6
Difference		d_1	d_2	d_3	d_4	d_5	

Numerical evaluation *continued*

The sum terms are arranged as follows:

	S_0	S_1	S_2	S_3
	S_6	S_5	S_4	
Sum	$\overline{S_0}$	$\overline{S_1}$	$\overline{S_2}$	$\overline{S_3}$
Difference	D_0	D_1	D_2	

$\overline{S_0}$	$\overline{S_1}$
$\overline{S_2}$	$\overline{S_3}$
$\overline{S_7}$	$\overline{S_8}$

The difference terms are as follows:

	d_1	d_2	d_3
	d_5	d_4	
Sum	$\overline{S_4}$	$\overline{S_5}$	$\overline{S_6}$
Difference	D_3	D_4	

$\overline{S_4}$	D_0
$\overline{S_6}$	D_2
D_5	D_6

The coefficients of the Fourier series are now obtained as follows, where $A_0/2$ equals the average value, the $A_1 \ldots A_n$ expressions represent the coefficients of the cosine terms, and the $B_1 \ldots B_n$ expressions represent the coefficients of the sine terms:

$$\frac{A_0}{2} = \frac{\overline{S_7} + \overline{S_8}}{12}$$

$$A_1 = \frac{D_0 + 0.866\,D_1 + 0.5\,D_2}{6}$$

$$A_2 = \frac{\overline{S_0} + 0.5\,\overline{S_1} - 0.5\,\overline{S_2} - \overline{S_3}}{6}$$

$$A_3 = \frac{D_6}{6}$$

$$A_4 = \frac{\overline{S_0} - 0.5\,\overline{S_1} - 0.5\,\overline{S_2} + \overline{S_3}}{6}$$

$$A_5 = \frac{D_0 - 0.866\,D_1 + 0.5\,D_2}{6}$$

$$A_6 = \frac{\overline{S_7} - \overline{S_8}}{12}$$

Numerical evaluation *continued*

Also

$$B_1 = \frac{0.5\,\overline{S_4} + 0.866\,\overline{S_5} + \overline{S_6}}{6}$$

$$B_2 = \frac{0.866\,(D_3 + D_4)}{6}$$

$$B_3 = \frac{D_5}{6}$$

$$B_4 = \frac{0.866\,(D_3 - D_4)}{6}$$

$$B_5 = \frac{0.5\,\overline{S_4} - 0.866\,\overline{S_5} + \overline{S_6}}{6}$$

Common pulse forms and spectrums

Fig. 4—Time and frequency functions for commonly encountered pulse shapes.

time function	frequency function

A. Rectangular pulse

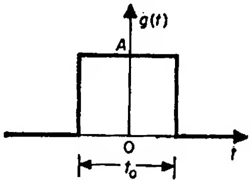

$g(t) = A$ for $-\frac{t_0}{2} < t < \frac{t_0}{2}$

$= 0$ otherwise

Area $\mathcal{A} = At_0$

$G(f) = \mathcal{A}(\sin \alpha)/\alpha$

where $\alpha = \pi t_0 f$

(See curve $(\sin x)/x$ below.)

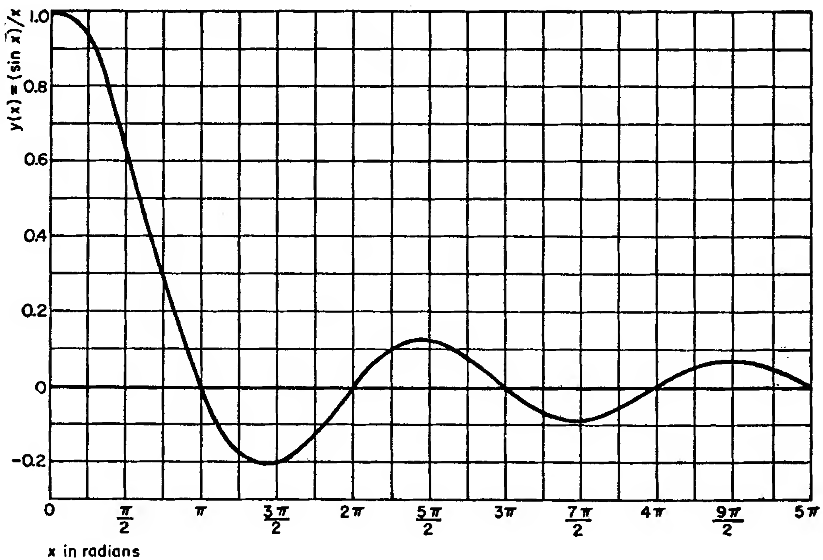

time function	frequency function
B. Isoceles-triangle pulse	

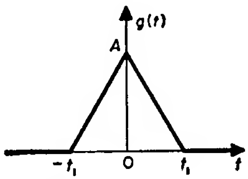

Area $\mathcal{A} = At_1$

$$g(t) = A\left(1 - \frac{t}{t_1}\right),\ 0 < t < t_1$$
$$= A\left(1 + \frac{t}{t_1}\right),\ -t_1 < t < 0$$
$$= 0,\ \text{otherwise}$$

$$G(f) = \mathcal{A}\left(\frac{\sin\alpha}{\alpha}\right)^2$$

where $\alpha = \pi t_1 f$

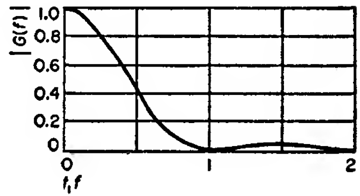

C. Sawtooth pulse

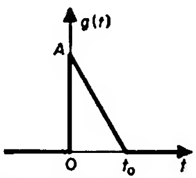

Area $\mathcal{A} = \frac{1}{2}At_0$

$$g(t) = A\left(1 - \frac{t}{t_0}\right),\ 0 < t < t_0$$
$$= 0,\ \text{otherwise}$$

$$G(f) = \mathcal{A}\,\frac{j}{\alpha}\left[\frac{\sin\alpha}{\alpha}\exp(-j\alpha) - 1\right]$$
$$= \mathcal{A}\,\frac{1 - \exp(-2j\alpha) - 2j\alpha}{2\alpha^2}$$

where $\alpha = \pi t_0 f$

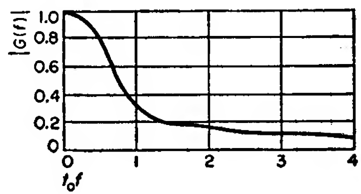

D. Any pulse of polygonal form may be represented as a linear combination of waveforms such as *A*, *B*, and C above eventually after some shifts in time. The pulse spectrum is the same linear combination of the corresponding spectrums (eventually modified according to property 7, Fig. 1).

Fig. 4—*Continued*

continued **Common pulse forms and spectrums**

time function	frequency function
E. Cosine pulse	

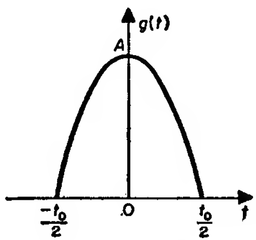

$$g(t) = A\cos\pi\frac{t}{t_0},\ -\frac{t_0}{2} < t < \frac{t_0}{2}$$
$$= 0, \text{ otherwise}$$
$$\text{Area } \mathcal{A} = \frac{2}{\pi}At_0$$

$$G(f) = \mathcal{A}\frac{\cos(\pi/2)\,\alpha}{1-\alpha^2}$$

where $\alpha = 2t_0 f$

For $\alpha = 1$,

$G(f) = \mathcal{A}\,\pi/4$

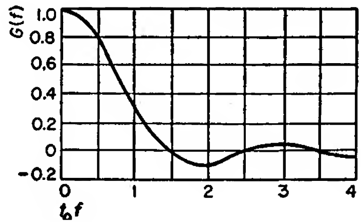

F. Cosine-squared pulse

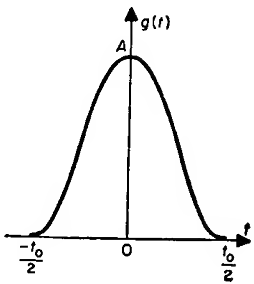

$$\left.\begin{aligned} g(t) &= A\cos^2\pi\frac{t}{t_0} \\ &= \tfrac{1}{2}A\left(1+\cos 2\pi\frac{t}{t_0}\right)\end{aligned}\right\}-\frac{t_0}{2}<t<\frac{t_0}{2}$$
$$=0, \text{ otherwise}$$
$$\text{Area } \mathcal{A} = \tfrac{1}{2}At_0$$

$$G(f) = \mathcal{A}\frac{\sin\pi\alpha}{\pi\alpha(1-\alpha^2)}$$

where $\alpha = t_0 f$

For $\alpha = 1$,

$G(f) = \tfrac{1}{2}\mathcal{A}$

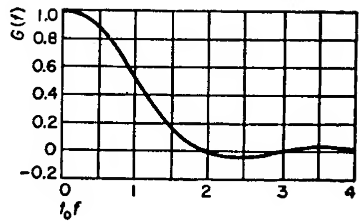

G. Gaussian pulse

Use curve on p. 988 with standard deviation $\sigma = t_1$

$$g(t) = A \exp - \tfrac{1}{2}\left(\frac{t}{t_1}\right)^2$$

Area $\mathcal{A} = At_1(2\pi)^{1/2}$

$$G(f) = \mathcal{A} \exp - \tfrac{1}{2}\left(\frac{f}{f_1}\right)^2$$

Use curve on p. 988 with standard deviation $\sigma = f_1 = 1/2\pi t_1$

H. Critically damped exponential pulse

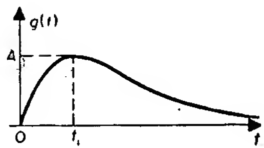

Area $\mathcal{A} = Aet_1$

$$g(t) = Ae\frac{t}{t_1}\exp\left(-\frac{t}{t_1}\right),\ t > 0$$

$$= 0,\ t < 0$$

$$e = 2.71828\ldots$$

$$G(f) = \mathcal{A}\frac{1}{(1 + j\alpha)^2}$$

where $\alpha = 2\pi t_1 f$

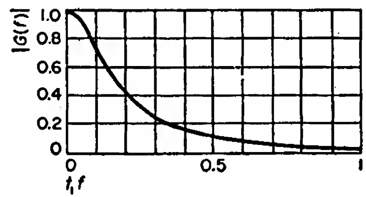

Pulse-train analysis

If the pulse defined by the function $g(t)$ is repeated every interval T, a periodic waveform

$$y(t) = \sum_{n=-\infty}^{n=+\infty} g(t - nT)$$

results with *period* T and *repetition frequency* $F = 1/T$ (see Fig. 5A, B).

This pulse train may be expressed as a convolution product

$$y(t) = \left[\sum_{n=-\infty}^{n=+\infty} \delta(t - nT)\right] * g(t)$$

and, applying properties 4 and 6 (Fig. 1), its Fourier transform is

$$Y(f) = \frac{1}{T}\left[\sum_{n=-\infty}^{n=+\infty} \delta(f - nF)\right].G(f)$$

The function $y(t)$ is represented by the Fourier series

$$y(t) = \sum_{-\infty}^{+\infty} D_n \exp(jnt)$$

where

$$D_n = (1/T)\, G(nF)$$

The coefficients D_n are obtained by sampling the pulse spectrum at frequencies multiple of the repetition frequency.

The amplitude C_n of the nth harmonic in the real representation (see p. 1006) is

$$C_n = 2\,|D_n| = (2/T)\,|G(nF)|$$

By a translation τ of the time origin, the D_n are multiplied by the factor $\exp(-2\pi jn\tau/T)$; the C_n are not changed.

The constant term of the series:

$$D_0 = A_0/2 = C_0/2$$

is the *average amplitude*

$$A_{av} = \mathcal{A}/T = G(0)/T$$

Pulse-train analysis *continued*

where

$$\mathcal{A} = \int_0^T g(t)\, dt$$

is the area under one pulse.

If the pulses do not overlap; i.e., if the function $g(t)$ is zero outside of some period a to $a + T$; the energy in a pulse is

Fig. 5—The spectrum for pulse trains. Spectrums are in general complex functions. They are represented here by real curves only to simplify the illustration.

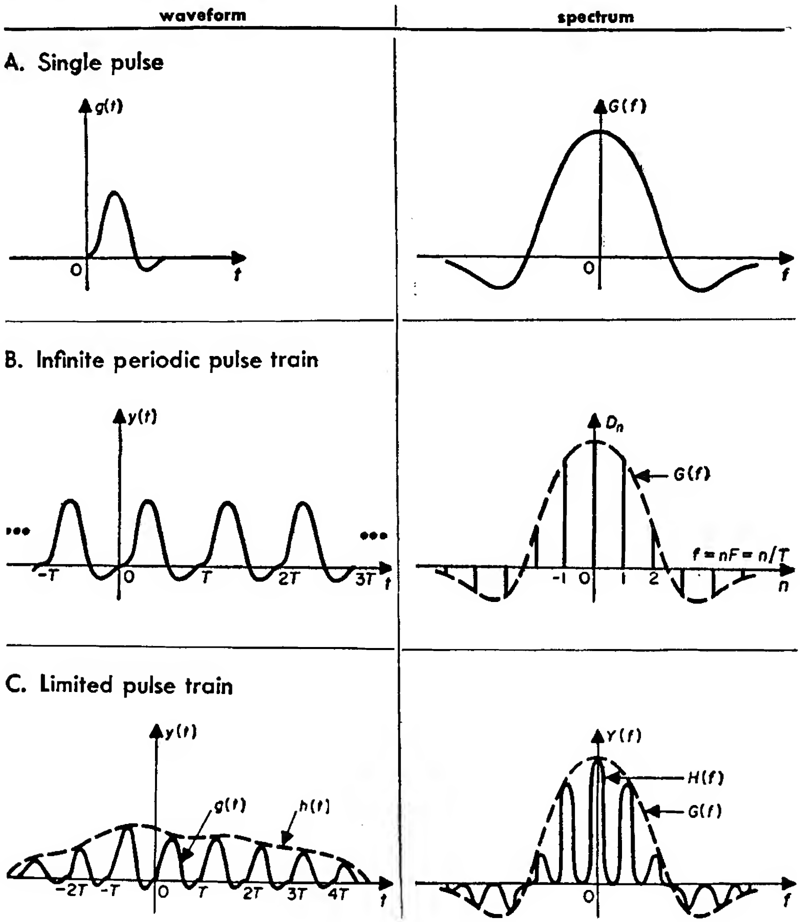

Pulse-train analysis *continued*

$$E = \int_{a}^{a+T} g^2(t)\, dt = \int_{-\infty}^{+\infty} |G(f)|^2\, df$$

The root-mean-square amplitude is

$$A_{rms} = (E/T)^{1/2}$$

The average power of the pulse train is

$$E/T = A^2_{rms} = \sum_{n=-\infty}^{n=+\infty} |D_n|^2 = \tfrac{1}{4} C_0^2 + \tfrac{1}{2} \sum_{1}^{\infty} C_n^2$$

A pulse train of finite extent, where all the pulses have the same shape and are spaced periodically may be represented as a product:

$$y(t) = h(t) \cdot \sum_{n=-\infty}^{n=+\infty} g(t - nT)$$

The function $h(t)$ defines the envelope of the pulse train.

The Fourier transform

$$Y(f) = \frac{1}{T} G(f) \cdot \sum_{n=-\infty}^{n=+\infty} H(f - nF)$$

may be interpreted, in the frequency domain, as a train of pulses having $G(f)$ as an envelope and a form defined by $H(f)$. See Fig. 5C.

When $h(t) = 1$, then $H(f)$ is the δ function. The pulse train is a periodic waveform having a line spectrum as explained above. See Fig. 5B.

The Fourier series coefficients for a number of commonly encountered pulse trains are given in Fig. 6.

When the pulse train is derived from a pulse listed in Fig. 6, the coefficients can also be read off the corresponding spectrum curve by sampling at values n/T of the frequency.

Pulse-train analysis *continued*

Fig. 6—Periodic waveforms and Fourier series.

waveform	coefficient of Fourier series
A. Rectangular wave 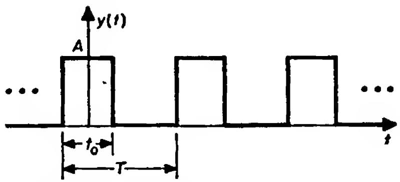 Derived from rectangular pulse, Fig. 4A $A_{av} = A\dfrac{t_0}{T}$ $\quad A_{rms} = A\left(\dfrac{t_0}{T}\right)^{1/2}$	$C_n = 2D_n = 2A_{av}\left\lvert\dfrac{\sin n\pi t_0/T}{n\pi t_0/T}\right\rvert$ Can be read off curve of $(\sin x)/x$, Fig. 4A, by sampling at $n\pi t_0/T$. Example: If $T = 2t_0$, $y(t) = 2A_{av}\left(\dfrac{1}{2} + \dfrac{2}{\pi}\cos\theta - \dfrac{2}{3\pi}\cos 3\theta + \dots\right)$ with $\theta = 2\pi t/T$
B. Isoceles-triangle wave 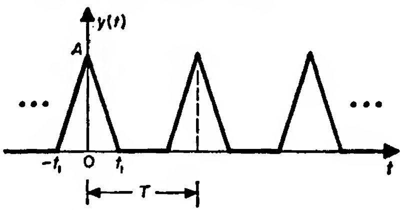 Derived from triangular pulse, Fig. 4B $A_{av} = A\dfrac{t_1}{T}$ $\quad A_{rms} = A\left(\dfrac{2t_1}{3T}\right)^{1/2}$	$C_n = 2A_{av}\left(\dfrac{\sin n\pi t_1/T}{n\pi t_1/T}\right)^2$ Example: If $T = 2t_1$, $y(t) = 2A_{av}\left[\dfrac{1}{2} + \left(\dfrac{2}{\pi}\right)^2\cos\theta + \left(\dfrac{2}{3\pi}\right)^2\cos 3\theta + \dots\right]$ with $\theta = 2\pi t/T$

Pulse-train analysis *continued*

Fig. 6—*continued*

waveform	coefficient of Fourier series
C. Sawtooth wave 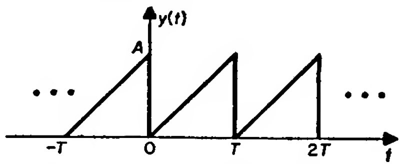 Derived from triangular pulse, Fig. 4C $A_{av} = \frac{A}{2}$ $\quad A_{rms} = A\ 3^{-1/2}$	$C_n = 2A_{av}\frac{1}{\pi n}$ $y(t) = 2A_{av}\left(\frac{1}{2} - \frac{1}{\pi}\sin\theta - \frac{1}{2\pi}\sin 2\theta - \dots\right)$
D. Clipped sawtooth wave 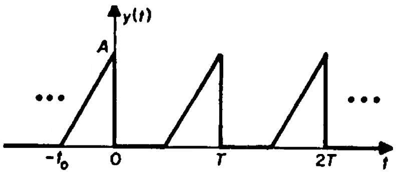 Derived from triangular pulse, Fig. 4C $A_{av} = A\frac{t_0}{2T}$ $\quad A_{rms} = A\left(\frac{t_0}{3T}\right)^{1/2}$	$C_n = 2A_{av}\frac{1}{\alpha^2}\left[\sin^2\alpha + \alpha(\alpha - \sin 2\alpha)\right]^{1/2}$ with $\alpha = n\pi t_0/T$

E. Sawtooth wave

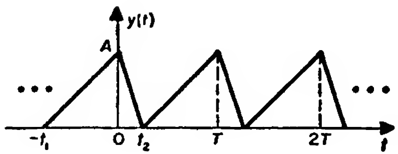

Derived from the sum of two triangular pulses, Fig. 4C

$A_{av} = \frac{A}{2}$ $\qquad$ $A_{rms} = A\,3^{-1/2}$

$$C_n = 2A_{av}\frac{T^2}{\pi^2 n^2 t_1 t_2}\sin n\pi\frac{t_1}{T}$$

with $t_1 + t_2 = T$

F. Symmetrical trapezoidal wave

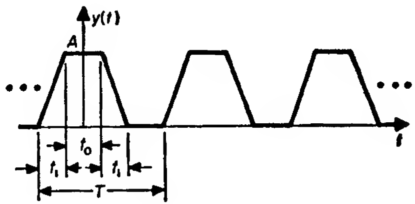

Derived as in Fig 4D.

$A_{av} = A\frac{t_0 + t_1}{T}$ $\qquad$ $A_{rms} = A\left(\frac{3t_0 + 2t_1}{3T}\right)^{1/2}$

$$D_n = A_{av}\frac{\sin \pi n t_1/T}{\pi n t_1/T}\,\frac{\sin \pi n(t_1 + t_0)/T}{\pi n(t_1 + t_0)/T}$$

$C_n = 2\,|\,D_n\,|$

Fig. 6—*continued*

waveform	coefficient of Fourier series

G. Train of cosine pulses

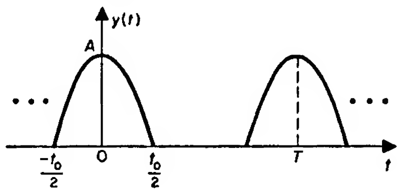

Derived from cosine pulse, Fig. 4E

$A_{av} = \frac{2}{\pi} A \frac{t_0}{T}$ $\qquad A_{rms} = A\left(\frac{t_0}{2T}\right)^{1/2}$

$$C_n = 2A_{av} \left| \frac{\cos(n\pi t_0/T)}{1 - (2nt_0/T)^2} \right|$$

For $nt_0/T = 1/2$, this becomes $\pi A_{av}/2$

H. Full-wave-rectified sine wave

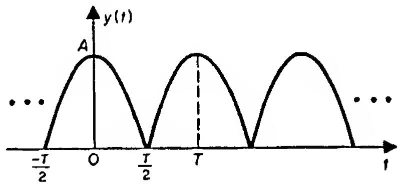

Derived from cosine pulse, Fig. 4E
(same as Fig. 6G with $t_0 = T$)

$A_{av} = \frac{2}{\pi} A$ $\qquad A_{rms} = A/(2)^{1/2}$

$$C_0 = 2A_{av}$$

$$C_n = 2A_{av} \frac{1}{4n^2 - 1} \qquad \text{for } n \neq 0$$

$$y(t) = 2A_{av} \left[\frac{1}{2} + \frac{1}{3}\cos\theta - \frac{1}{15}\cos 2\theta + \frac{1}{35}\cos 3\theta \ldots \right.$$

$$\left. \ldots - (-1)^n \frac{1}{4n^2 - 1} \cos n\theta \ldots \right]$$

with $\theta = 2\pi t/T$

I. Half-wave-rectified sine wave

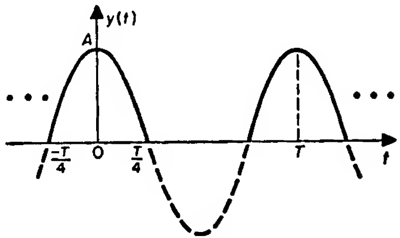

Derived from cosine pulse, Fig. 4E (same as Fig. 6G with $t_0 = T/2$

$$A_{av} = \frac{1}{\pi} A \qquad A_{rms} = \frac{A}{2}$$

$$C_0 = 2A_{av}$$

$$C_{2n+1} = 0, \text{ except for } C_1 = 2A_{av}\frac{\pi}{4}$$

$$C_{2n} = 2A_{av}\frac{1}{4n^2-1}$$

$$y(t) = 2A_{av}\left[\frac{1}{2} + \frac{\pi}{4}\cos\theta + \frac{1}{3}\cos 2\theta - \frac{1}{15}\cos 4\theta + \dots \right.$$
$$\left. \dots + (-1)^n \frac{1}{4n^2-1}\cos 2n\theta \dots \right]$$

J. Train of cosine-squared pulses

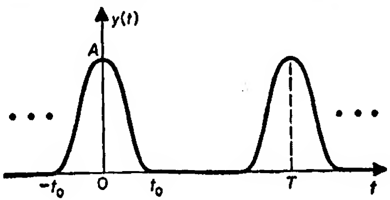

Derived from cosine-squared pulse, Fig. 4F

$$A_{av} = \frac{1}{2} A \frac{t_0}{T} \qquad A_{rms} = \frac{1}{2} A \left(\frac{3t_0}{2T}\right)^{1/2}$$

$$C_n = 2A_{av}\frac{\sin(n\pi t_0/T)}{(n\pi t_0/T)\,[1 - (nt_0/T)^2]}$$

continued **Pulse-train analysis**

Fig. 6—continued

waveform	coefficient of Fourier series

K. Fractional sine wave

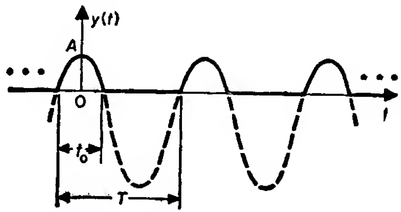

$$A_{av} = \frac{A}{\pi}\,\frac{\sin\alpha - \alpha\cos\alpha}{1-\cos\alpha}$$

$$A_{rms} = \frac{A}{(2\pi)^{1/2}}\,\frac{[2\alpha + \alpha\cos 2\alpha - (3/2)\sin 2\alpha]^{1/2}}{1-\cos\alpha}$$

with $\pi t_0/T = \alpha$

$$C_n = 2A_{av}\,\frac{\sin n\alpha\cos\alpha - n\sin\alpha\cos n\alpha}{n\,(n^2-1)\,(\sin\alpha - \alpha\cos\alpha)}$$

L. Critically damped exponential wave

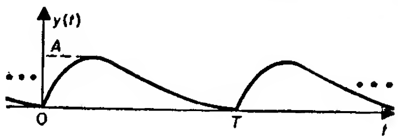

Derived from exponential pulse, Fig. 4H (period $T \gg$ period t_1 to make overlap negligible)

$$A_{av} = Ae\,\frac{t_1}{T} \qquad A_{rms} = \frac{Ae}{2}\left(\frac{t_1}{T}\right)^{1/2}$$

$e = 2.7182\ldots$

$$C_n = 2A_{av}\,\frac{1}{1+(2\pi n t_1/T)^2}$$

$$= 2A_{av}\cos^2\theta_n$$

with $\tan\theta_n = 2\pi n t_1/T$

Maxwell's equations

General*

The following four basic laws of electromagnetism for bodies at rest are derived from the fundamental, experimental, and theoretical work of Ampere and Faraday, and are valid for quantities determined by their average values in volumes that contain a very great number of molecules (macroscopic electromagnetism).

Statement of four basic laws *rationalized mks units*

a. The work required to carry a unit magnetic pole around a closed path is equal to the total current linking that path, that is, the total current passing through any surface that has the path for its periphery. This total current is the sum of the conduction current and the displacement current, the latter being equal to the derivative with respect to time of the electric induction flux passing through any surface that has the above closed path for its periphery.

b. The electromotive force (e.m.f.) induced in any fixed closed loop is equal to minus the time rate of change of the magnetic induction flux ϕ_B through that loop. By electromotive force is meant the work required to carry a unit positive charge around the loop.

c. The total flux of electric induction diverging from a charge Q is equal to Q in magnitude.

d. Magnetic-flux lines are continuous (closed) loops. There are no sources or sinks of magnetic flux.

Expression of basic laws in integral form

a. $$\int_0 \mathbf{H}\cdot\mathbf{ds} = I_{\text{total}} = I_{\text{conduction}} + \frac{\partial \phi_D}{\partial t}$$

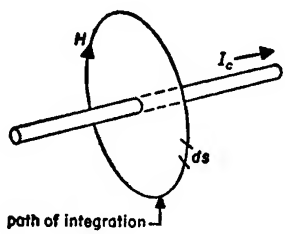

where

$\int_0$ = a line integral around a closed path
ds = vector element of length along path
H = magnetic-field vector
ϕ_D = electric induction flux

* Developed from: J. E. Hill, "Maxwell's Four Basic Equations," *Westinghouse Engineer*, vol. 6; p. 135; September, 1946.

Expression of basic laws in integral form *continued*

b. $\int_C \mathbf{E}\cdot d\mathbf{s} = -\dfrac{\partial \phi_B}{\partial t}$

The time rate of change of ϕ_B is written as a partial derivative to indicate that the loop does not move (the coordinates of each point of the loop remain fixed during integration). **E** is the electric-field vector.

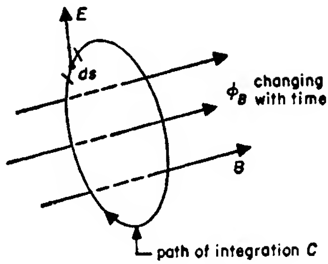

c. $\int_s \mathbf{D}\cdot d\mathbf{S} = Q$

where

S = any closed surface
dS = vector element of S
D = vector electric-flux density
Q = the net electric charge within S

and the integral indicates that $\mathbf{D}\cdot d\mathbf{S}$ is to be calculated for each element of S and summed.

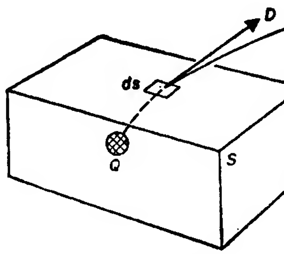

S = total surface
Q = total charge inside S

d. $\int_s \mathbf{B}\cdot d\mathbf{S} = 0$

where

B = vector magnetic-flux density.

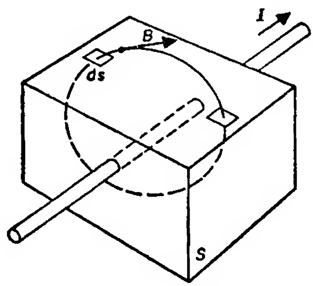

B lines are closed curves; as many enter region as leave it.

Basic laws in derivative form

	general form	static case	steady-state	quasi-steady-state	free-space	free-space single-frequency
a	$\left.\begin{matrix}\text{curl}\ \mathbf{H}\\ \nabla\times\mathbf{H}\end{matrix}\right\} = j_c + \frac{\partial \mathbf{D}}{\partial t}$ j_c = conduction current density	$\left.\begin{matrix}\text{curl}\ \mathbf{H}\\ \nabla\times\mathbf{H}\end{matrix}\right\} = 0$ $j_c = 0$ $\frac{\partial \mathbf{D}}{\partial t} = 0$	$\left.\begin{matrix}\text{curl}\ \mathbf{H}\\ \nabla\times\mathbf{H}\end{matrix}\right\} = j_c$ Conduction current exists but time derivatives are zero	$\left.\begin{matrix}\text{curl}\ \mathbf{H}\\ \nabla\times\mathbf{H}\end{matrix}\right\} \approx j_c$ $\partial\mathbf{D}/\partial t$ can be neglected except in capacitors (ac at industrial power frequencies)	$\left.\begin{matrix}\text{curl}\ \mathbf{H}\\ \nabla\times\mathbf{H}\end{matrix}\right\} = \frac{\partial \mathbf{D}}{\partial t} = \epsilon_0 \frac{\partial \mathbf{E}}{\partial t}$ $j_c = 0$ and ϵ_0 is the dielectric constant of free space	$\left.\begin{matrix}\text{curl}\ \mathbf{H}\\ \nabla\times\mathbf{H}\end{matrix}\right\} = j\omega\epsilon_0\mathbf{E}$ $\omega = 2\pi f$ = angular frequency, f = the frequency considered, and $j = \sqrt{-1}$
b	$\left.\begin{matrix}\text{curl}\ \mathbf{E}\\ \nabla\times\mathbf{E}\end{matrix}\right\} = -\frac{\partial \mathbf{B}}{\partial t}$	$\left.\begin{matrix}\text{curl}\ \mathbf{E}\\ \nabla\times\mathbf{E}\end{matrix}\right\} = 0$	$\left.\begin{matrix}\text{curl}\ \mathbf{E}\\ \nabla\times\mathbf{E}\end{matrix}\right\} = 0$	$\left.\begin{matrix}\text{curl}\ \mathbf{E}\\ \nabla\times\mathbf{E}\end{matrix}\right\} = -\frac{\partial \mathbf{B}}{\partial t}$	$\left.\begin{matrix}\text{curl}\ \mathbf{E}\\ \nabla\times\mathbf{E}\end{matrix}\right\} = -\frac{\partial \mathbf{B}}{\partial t} = -\mu_0\frac{\partial \mathbf{H}}{\partial t}$ μ_0 = magnetic permeability of free space	$\left.\begin{matrix}\text{curl}\ \mathbf{E}\\ \nabla\times\mathbf{E}\end{matrix}\right\} = -j\omega\mu_0\mathbf{H}$
c	$\left.\begin{matrix}\text{div}\ \mathbf{D}\\ \nabla\cdot\mathbf{D}\end{matrix}\right\} = \rho$ ρ = charge density = charge per unit volume	$\left.\begin{matrix}\text{div}\ \mathbf{D}\\ \nabla\cdot\mathbf{D}\end{matrix}\right\} = \rho$	$\left.\begin{matrix}\text{div}\ \mathbf{D}\\ \nabla\cdot\mathbf{D}\end{matrix}\right\} = \rho$	$\left.\begin{matrix}\text{div}\ \mathbf{D}\\ \nabla\cdot\mathbf{D}\end{matrix}\right\} = \rho$	$\left.\begin{matrix}\text{div}\ \mathbf{E}\\ \nabla\cdot\mathbf{E}\end{matrix}\right\} = 0$	$\left.\begin{matrix}\text{div}\ \mathbf{E}\\ \nabla\cdot\mathbf{E}\end{matrix}\right\} = 0$
d	$\left.\begin{matrix}\text{div}\ \mathbf{B}\\ \nabla\cdot\mathbf{B}\end{matrix}\right\} = 0$	$\left.\begin{matrix}\text{div}\ \mathbf{B}\\ \nabla\cdot\mathbf{B}\end{matrix}\right\} = 0$	$\left.\begin{matrix}\text{div}\ \mathbf{B}\\ \nabla\cdot\mathbf{B}\end{matrix}\right\} = 0$	$\left.\begin{matrix}\text{div}\ \mathbf{B}\\ \nabla\cdot\mathbf{B}\end{matrix}\right\} = 0$	$\left.\begin{matrix}\text{div}\ \mathbf{H}\\ \nabla\cdot\mathbf{H}\end{matrix}\right\} = 0$	$\left.\begin{matrix}\text{div}\ \mathbf{H}\\ \nabla\cdot\mathbf{H}\end{matrix}\right\} = 0$

Basic laws in derivative form *continued*

Notes:

For an explanation of the operator ∇ (del) and the associated vector operations see p. 1086 in the "Mathematical formulas" chapter.

$$\left.\begin{aligned}\epsilon_0 &= \frac{1}{36\pi \times 10^9}\ \text{farad/meter}\\ \mu_0 &= 4\pi \times 10^{-7}\ \text{henry/meter}\end{aligned}\right\}$$ in the rationalized meter-kilogram-second system of units.

Maxwell's equations result in the law of conservation of electric charges, the integral form of which is

$$I = -\,\partial Q_i/\partial t$$

Q_i = net sum of all electric charges within a closed surface S

I = outgoing conduction current

and the derivative form

$$\text{div}\ \boldsymbol{j}_c = -\,\partial\rho/\partial t$$

Boundary conditions at the surface of separation between two media 1 and 2 are

$$\mathbf{H}_{2T} - \mathbf{H}_{1T} = \boldsymbol{j}_s \times \mathbf{N}^\circ_{1,2} \qquad \mathbf{B}_{2N} - \mathbf{B}_{1N} = 0$$

$$\mathbf{E}_{2T} - \mathbf{E}_{1T} = 0 \qquad \mathbf{D}_{2N} - \mathbf{D}_{1N} = \sigma$$

Subscript T denotes a tangential, and subscript N a normal component.

$\mathbf{N}^\circ_{1,2}$ = unit normal vector from medium 1 to medium 2, which is the positive direction for normal vectors

$\boldsymbol{j}_s$ = current density on the surface, if any

σ = density of electric charge on the surface of separation

Retarded potentials *H. A. Lorentz*

Consider an electromagnetic system in free space in which the distribution of electric charges and currents is assumed to be known. From the four basic equations in derivative form:

$$\text{curl}\ \mathbf{H} = \boldsymbol{j}_c + \epsilon_0 \frac{\partial \mathbf{E}}{\partial t} \qquad \text{curl}\ \mathbf{E} = -\,\mu_0 \frac{\partial \mathbf{H}}{\partial t}$$

$$\text{div}\ \mathbf{H} = 0 \qquad \text{div}\ \mathbf{E} = \frac{\rho}{\epsilon_0}$$

Retarded potentials *continued*

two retarded potentials can be determined:

one scalar, $\phi = \frac{1}{4\pi\epsilon_0}\int_\infty \frac{\rho^* dV}{r}$ one vector, $\mathbf{A} = \frac{1}{4\pi}\int_\infty \frac{j_c^*}{r}\,dV$

The asterisks mean that the values of the quantities are taken at time $t - r/c$, where r is the distance from the location of the charge or current to the point P considered, and c = velocity of propagation = velocity of light $= 1/\sqrt{\epsilon_0\mu_0}$.

The electric and magnetic fields at point P are expressed by

$$\mathbf{H} = \text{curl } \mathbf{A} \qquad \mathbf{E} = -\textbf{grad } \phi - \mu_0 \frac{\partial \mathbf{A}}{\partial t}$$

Fields in terms of one vector only *Hertz vector*

The previous expressions imply a relation between ϕ and $\mathbf{A}$

$$\text{div } \mathbf{A} = -\epsilon_0 \frac{\partial \phi}{\partial t}$$

Consider a vector Π such that $\mathbf{A} = \partial\Pi/\partial t$. Then for all variable fields

$$\phi = -\frac{1}{\epsilon_0}\text{div } \Pi$$

The electric and magnetic fields can thus be expressed in terms of the vector Π only

$$\mathbf{H} = \text{curl } \frac{\partial \Pi}{\partial t}$$

$$\mathbf{E} = \frac{1}{\epsilon_0}\text{grad div } \Pi - \mu_0 \frac{\partial^2 \Pi}{\partial t^2}$$

Poynting vector

Consider any volume V of the previous electromagnetic system enclosed in a surface S. It can be shown that

$$-\int_V \mathbf{E}\cdot j_c\, dV = \frac{\partial}{\partial t}\int_V \left(\frac{\epsilon_0 E^2}{2} + \frac{\mu_0 H^2}{2}\right) dV + \text{flux}_S\, \mathbf{E} \times \mathbf{H}$$

The rate of change with time of the electromagnetic energy inside V is equal to the rate of change of the amount of energy localized inside V

Poynting vector *continued*

plus the flux of the vector $\mathbf{E} \times \mathbf{H}$ through the surface S enclosing said volume V. The vector product $\mathbf{E} \times \mathbf{H}$ is called the Poynting vector.

In the particular case of single-frequency phenomena, a complex Poynting vector $\mathbf{E} \times \mathbf{H}^*$ is often utilized ($\mathbf{H}^*$ is the complex conjugate of $\mathbf{H}$). It can be shown that

$$-\int_V \frac{\mathbf{E}\cdot j_c^*}{2}\, dV = 2j\omega \int_V \left(\mu_0 \frac{HH^*}{4} - \epsilon_0 \frac{EE^*}{4}\right) dV + \text{flux}_S \frac{\mathbf{E} \times \mathbf{H}^*}{2}$$

This shows that in case there is no conduction current inside V and the flux of the complex Poynting vector out of V is zero, then the mean value per period of the electric and magnetic energies inside V are equal.

Superposition theorem

The mathematical form of the four basic laws (linear differential equations with constant coefficients) shows that if two distributions $\mathbf{E}$, $\mathbf{H}$, j_c, ρ, and $\mathbf{E}'$, $\mathbf{H}'$, j_c', ρ', satisfy Maxwell's equations, they are also satisfied by any linear combination $\mathbf{E} + \lambda\mathbf{E}'$, $\mathbf{H} + \lambda\mathbf{H}'$, $j_c + \lambda j_c'$, and $\rho + \lambda\rho'$.

Reciprocity theorem

Let j_c be the conduction current resulting in any electromagnetic system from the action of an external electric field $\mathbf{E}_a$, and j_c' and $\mathbf{E}_a'$ be the corresponding quantities for another possible state; then

$$\int_\infty (\mathbf{E}_a \cdot j_c' - \mathbf{E}_a' \cdot j_c)\, dV = 0$$

This is the most useful way of expressing the general reciprocity theorem (Carson). It is valid provided all quantities vary simultaneously according to a linear law (excluding ferromagnetic substances, electronic space charge, and ionized-gas phenomena). A particular application of this general reciprocity theorem will be found on p. 132.

Maxwell's equations in different systems of coordinates

When a particular system of coordinates is advantageously used, such as cylindrical, spherical, etc., the components are derived from the vector equations by means of the formulas included in the chapter "Mathematical formulas," pages 1088 and 1089.

■ Mathematical formulas

Mensuration formulas

Areas of plane figures

figure	formula
Parallelogram 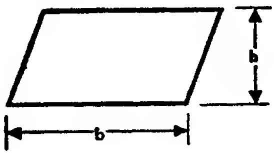	Area $= bh$
Trapezoid 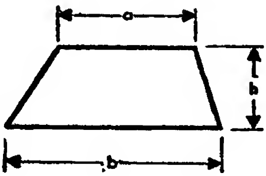	Area $= \frac{1}{2}h(a + b)$
Triangle 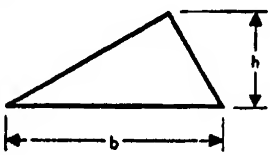	Area $= \frac{1}{2}bh$
Regular polygon 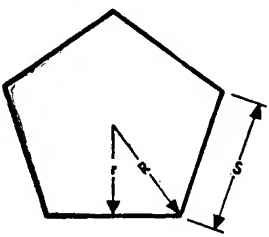	Area $= nr^2 \tan \frac{180°}{n}$ $= \frac{n}{4} S^2 \cot \frac{180°}{n}$ $= \frac{n}{2} R^2 \sin \frac{360°}{n}$ n = number of sides r = short radius S = length of one side R = long radius

Mensuration formulas *continued*

figure	formula
Circle 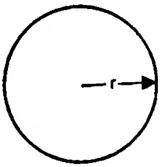	Area $= \pi r^2$ $r =$ radius $\pi = 3.141593$
Segment of circle 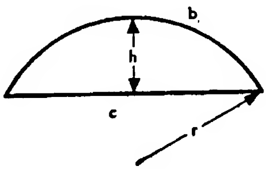	Area $= \frac{1}{2}[br - c(r-h)]$ $b =$ length of arc $c =$ length of chord $= \sqrt{4(2hr - h^2)}$
Sector of circle 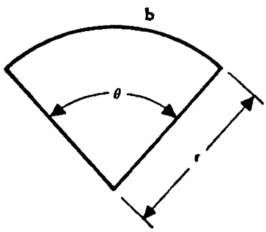	Area $= \dfrac{br}{2} = \pi r^2 \dfrac{\theta}{360°}$
Parabola 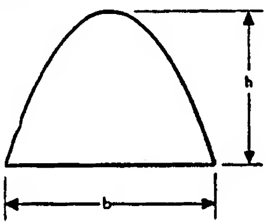	Area $= \frac{2}{3}bh$

Mensuration formulas *continued*

figure	formula
Ellipse 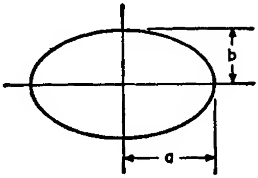	Area $= \pi ab$
Trapezium 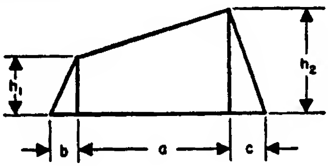	Area $= \frac{1}{2}[a(h_1 + h_2) + bh_1 + ch_2]$

Approximate area of irregular plane surface

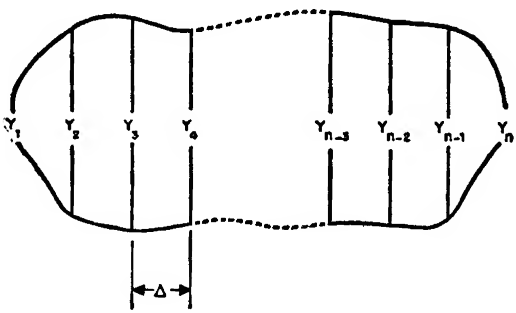

Trapezoidal rule

$$\text{Area} \approx \Delta\left(\frac{y_1}{2} + y_2 + y_3 + \ldots. + y_{n-2} + y_{n-1} + \frac{y_n}{2}\right)$$

Simpson's rule: *n* must be odd

$$\text{Area} \approx \frac{\Delta}{3}(y_1 + 4y_2 + 2y_3 + 4y_4 + 2y_5 + \ldots. + 2y_{n-2} + 4y_{n-1} + y_n)$$

$y_1, y_2, y_3 \ldots y_n$ = measured lengths of a series of equidistant parallel chords

Mensuration formulas *continued*

Surface areas and volumes of solid figures

figure	formula
Sphere 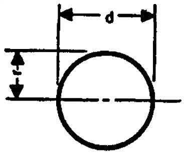	Surface $= 4\pi r^2 = 12.5664\, r^2 = \pi d^2$ Volume $= \dfrac{4\pi r^3}{3} = 4.1888\, r^3$
Sector of sphere 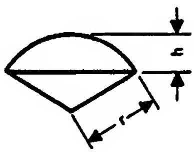	Total surface $= \dfrac{\pi r}{2}(4h + c)$ Volume $= \dfrac{2\pi r^2 h}{3} = 2.0944\, r^2 h$ $= \dfrac{2\pi r^2}{3}\left(r - \sqrt{r^2 - \dfrac{c^2}{4}}\right)$ $c = \sqrt{4\,(2hr - h^2)}$
Segment of sphere 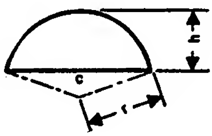	Spherical surface $= 2\pi rh = \dfrac{\pi}{4}(c^2 + 4h^2)$ Volume $= \pi h^2\left(r - \dfrac{h}{3}\right)$ $= \pi h^2\left(\dfrac{c^2 + 4h^2}{8h} - \dfrac{h}{3}\right)$
Cylinder 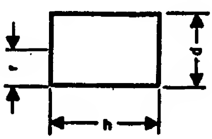	Cylindrical surface $= \pi dh = 3.1416\, dh$ Total surface $= 2\pi r(r + h)$ Volume $= \pi r^2 h = 0.7854\, d^2 h$ $= \dfrac{c^2 h}{4\pi} = 0.0796\, c^2 h$ $c =$ circumference

Mensuration formulas *continued*

figure	formula
Torus or ring of circular cross-section 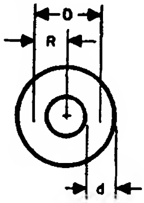	Surface $= 4\pi^2 Rr = 39.4784\, Rr = 9.8696\, Dd$ Volume $= 2\pi^2 Rr^2 = 19.74\, Rr^2$ $= 2.463\, Dd^2$ $D = 2R =$ diameter to centers of cross-section of material $r = d/2$
Pyramid 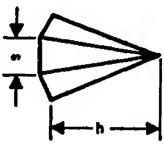	Volume $= \dfrac{Ah}{3}$ When base is a regular polygon: Volume $= \dfrac{h}{3}\left[nr^2\left(\tan\dfrac{360^\circ}{2n}\right)\right]$ $= \dfrac{h}{3}\left[\dfrac{ns^2}{4}\left(\cot\dfrac{360^\circ}{2n}\right)\right]$ $A =$ area of base $n =$ number of sides $r =$ short radius of base
Pyramidal frustum 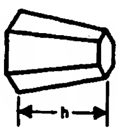	Volume $= \dfrac{h}{3}(a + A + \sqrt{aA})$ $A =$ area of base $a =$ area of top
Cone with circular base 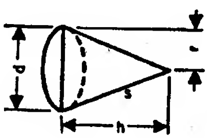	Conical area $= \pi rs = \pi r\sqrt{r^2 + h^2}$ Volume $= \dfrac{\pi r^2 h}{3} = 1.047\, r^2 h = 0.2618\, d^2 h$ $s =$ slant height

Mensuration formulas *continued*

figure	formula

Conic frustum

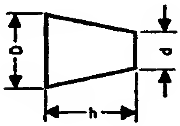

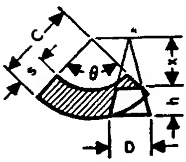

$$\text{Volume} = \frac{\pi h}{3}(R^2 + Rr + r^2)$$
$$= \frac{\pi h}{3}\left(\frac{R^3 - r^3}{R - r}\right)$$
$$= \frac{\pi h}{12}(D^2 + Dd + d^2)$$
$$= \frac{h}{3}(a + A + \sqrt{aA})$$

$$\text{Area of conic surface} = \frac{\pi s}{2}(D + d)$$

$$C = s + \frac{sd}{D - d} = s\left(1 + \frac{d}{D - d}\right)$$

$$\theta = \frac{180\,D}{C} = \frac{180\,(D - d)}{s}$$

A = area of base; a = area of top
$R = D/2$; $r = d/2$
s = slant height of frustum; C = slant height of full cone

Wedge frustum

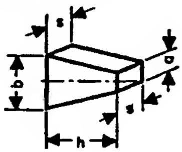

$$\text{Volume} = \frac{hs}{2}(a + b)$$

h = height between parallel bases

Ellipsoid

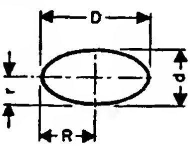

$$\text{Volume} = \frac{4\pi\, Rr^2}{3} = 4.1888\,Rr^2$$
$$= 0.053\,\pi^2\,Dd^2 = 0.5231\,Dd^2$$

Paraboloid

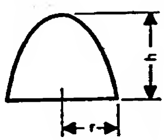

$$\text{Volume} = \frac{\pi r^2 h}{2} = 1.5707\,r^2 h$$

$$\text{Curved surface} = 0.5236\,\frac{r}{h^2}\left[(r^2 + 4\,h^2)^{3/2} - r^3\right]$$

Algebraic and trigonometric formulas *including complex quantities*

Quadratic equation

If $ax^2 + bx + c = 0$, then

$$x = \frac{-b \pm \sqrt{b^2 - 4ac}}{2a}$$

$$= -\frac{b}{2a} \pm \sqrt{\left(\frac{b}{2a}\right)^2 - \frac{c}{a}}$$

provided that $a \neq 0$

Arithmetic progression

$$l = a + (n - 1)\, d$$

$$S = \frac{n}{2}(a + l)$$

$$= \frac{2}{n}[2a + (n - 1)\, d]$$

where

a = first term

d = common difference

= value of any term minus value of preceding term

l = value of nth term

S = sum of n terms

Geometric progression

$$l = ar^{n-1}$$

$$S = \frac{a(r^n - 1)}{r - 1}$$

where

a = first term

l = value of the nth term

r = common ratio

= the value of any term divided by the preceding term

S = sum of n terms

Algebraic and trigonometric formulas *continued*

Combinations and permutations

The number of combinations of n things, all different, taken r at a time is

$$C^n_r = \frac{n!}{r!\,(n-r)!} = \frac{n\ (n-1)\ (n-2)\ \ldots (n-r+1)}{1\ \times 2\ \times 3\ \times \ldots\ \times r}$$

The number of permutations of n things r at a time is

$$P^n_r = n(n-1)\ (n-2) \ldots .\ (n-r+1) = \frac{n!}{(n-r)!}$$

$$P^n_n = n!$$

The number of combinations, with repetition, of n things taken r at a time is

$$D^n_r = \frac{(n+r-1)!}{r!(n-1)!} = \frac{n\ (n+1)\ (n+2)\ \ldots\ (n+r-1)}{1\ \times 2\ \times 3\ \times \ldots\ \times r}$$

Factorials

x	1	2	3	4	5	6	7	8	9	10
$x!$	1	2	6	24	120	720	5040	40,320	362,880	3,628,800

For $x > 10$, Stirling's formula may be used, with an error not exceeding 1 percent, as follows

$$x! = x^x e^{-x} \sqrt{2\pi x}$$

If common logarithms are used for computing $x!$,

$$\log (x!) = (x + \tfrac{1}{2}) \log x - 0.43429x + 0.3991$$

For example, if $x = 10$,

$$x + \tfrac{1}{2} = 10.5000$$

$$\log x = 1$$

$$\log (x!) = 10.5000 - 4.3429 + 0.3991 = 6.5562$$

$$x! = 3.599(10)^6 = 3,599,000$$

Algebraic and trigonometric formulas *continued*

Gamma function

$$x! = \Gamma\,(x+1)$$

$$\Gamma\,(x+1) = x\,\Gamma\,(x)$$

$$0! = \Gamma\,(1) = 1$$

$$(-\tfrac{1}{2})! = \Gamma(\tfrac{1}{2}) = \pi^{1/2} = 1.772$$

$$(\tfrac{1}{2})! = \Gamma(\tfrac{3}{2}) = \pi^{1/2}/2 = 0.886$$

$$(n+\tfrac{1}{2})! = \pi^{1/2}\,\frac{1.3.5\ldots(2n+1)}{2^{n+1}}$$

Binomial theorem

$$(a \pm b)^n = a^n \pm na^{n-1}b + \frac{n(n-1)}{2!}a^{n-2}b^2 \pm \frac{n(n-1)(n-2)}{3!}a^{n-3}b^3 + \ldots$$

If n is a positive integer, the series is finite and contains $n+1$ terms; otherwise, it is infinite, converging for $|b/a| < 1$, and diverging for $|b/a| > 1$.

Complex quantities

In the following formulas all quantities are real except $j = \sqrt{-1}$

$$(A+jB) + (C+jD) = (A+C) + j(B+D)$$

$$(A+jB)\,(C+jD) = (AC-BD) + j(BC+AD)$$

$$\frac{A+jB}{C+jD} = \frac{AC+BD}{C^2+D^2} + j\,\frac{BC-AD}{C^2+D^2}$$

$$\frac{1}{A+jB} = \frac{A}{A^2+B^2} - j\,\frac{B}{A^2+B^2}$$

$$A+jB = \rho(\cos\theta + j\sin\theta) = \rho\epsilon^{j\theta}$$

$$\sqrt{A+jB} = \pm\sqrt{\rho}\left(\cos\frac{\theta}{2} + j\sin\frac{\theta}{2}\right)$$

where

$$\rho = \sqrt{A^2+B^2} > 0$$

$$\cos\theta = A/\rho$$

$$\sin\theta = B/\rho$$

Algebraic and trigonometric formulas *continued*

Properties of e

$$e = 1 + 1 + 1/2! + 1/3! + \ldots. = 2.71828$$

$$1/e = 0.367879$$

$$e^{\pm jx} = \cos x \pm j \sin x = \exp(\pm jx)$$

$$\log_{10} e = 0.43429 \qquad \log_{10}(0.43429) = 9.63778-10$$

$$\log_e 10 = 2.30259 = 1/\log_{10} e \qquad \log_{10}(e^n) = n(0.43429)$$

$$\log_e N = \log_e 10 \times \log_{10} N$$

$$\log_{10} N = \log_{10} e \times \log_e N$$

Trigonometric identities

$$1 = \sin^2 A + \cos^2 A = \sin A \operatorname{cosec} A = \tan A \cot A = \cos A \sec A$$

$$\sin A = \frac{\cos A}{\cot A} = \frac{1}{\operatorname{cosec} A} = \cos A \tan A = \pm\sqrt{1 - \cos^2 A}$$

$$\cos A = \frac{\sin A}{\tan A} = \frac{1}{\sec A} = \sin A \cot A = \pm\sqrt{1 - \sin^2 A}$$

$$\tan A = \frac{\sin A}{\cos A} = \frac{1}{\cot A} = \sin A \sec A$$

$$\sin(A \pm B) = \sin A \cos B \pm \cos A \sin B$$

$$\cos(A \pm B) = \cos A \cos B \mp \sin A \sin B$$

$$\tan(A \pm B) = \frac{\tan A \pm \tan B}{1 \mp \tan A \tan B} = \frac{\tan A \cot B \pm 1}{\cot B \mp \tan A}$$

$$\cot(A \pm B) = \frac{\cot A \cot B \mp 1}{\cot B \pm \cot A} = \frac{\cot A \mp \tan B}{1 \pm \cot A \tan B}$$

$$\sin A = \frac{e^{jA} - e^{-jA}}{2j}$$

$$\cos A = \frac{e^{jA} + e^{-jA}}{2}$$

Algebraic and trigonometric formulas *continued*

$$\sin A + \sin B = 2 \sin \tfrac{1}{2}(A + B) \cos \tfrac{1}{2}(A - B)$$

$$\sin A - \sin B = 2 \cos \tfrac{1}{2}(A + B) \sin \tfrac{1}{2}(A - B)$$

$$\cos A + \cos B = 2 \cos \tfrac{1}{2}(A + B) \cos \tfrac{1}{2}(A - B)$$

$$\cos B - \cos A = 2 \sin \tfrac{1}{2}(A + B) \sin \tfrac{1}{2}(A - B)$$

$$\tan A \pm \tan B = \frac{\sin (A \pm B)}{\cos A \cos B}$$

$$\cot A \pm \cot B = \frac{\sin (B \pm A)}{\sin A \sin B}$$

$$\sin^2 A - \sin^2 B = \sin (A + B) \sin (A - B)$$

$$\cos^2 A - \sin^2 B = \cos (A + B) \cos (A - B)$$

$$\sin 2A = 2 \sin A \cos A$$

$$\cos 2A = \cos^2 A - \sin^2 A$$

$$\tan 2A = \frac{2 \tan A}{1 - \tan^2 A}$$

$$\sin 3A = 3 \sin A - 4 \sin^3 A = \sin A (4 \cos^2 A - 1)$$

$$\cos 3A = -3 \cos A + 4 \cos^3 A = \cos A (1 - 4 \sin^2 A)$$

$$\tan 3A = \frac{3 \tan A - \tan^3 A}{1 - 3 \tan^2 A}$$

$$\sin A + m \sin B = p \sin C$$

with $$p^2 = 1 + m^2 + 2m \cos (B - A)$$

and $$\tan (C - A) = \frac{m \sin (B - A)}{1 + m \cos (B - A)}$$

$$\sin \tfrac{1}{2} A = \pm\sqrt{\frac{1 - \cos A}{2}} \qquad \cos \tfrac{1}{2} A = \pm\sqrt{\frac{1 + \cos A}{2}}$$

$$\tan \tfrac{1}{2} A = \frac{\sin A}{1 + \cos A} \qquad \sin^2 A = \frac{1 - \cos 2A}{2}$$

$$\cos^2 A = \frac{1 + \cos 2A}{2} \qquad \tan^2 A = \frac{1 - \cos 2A}{1 + \cos 2A}$$

Algebraic and trigonometric formulas *continued*

$$\frac{\sin A \pm \sin B}{\cos A + \cos B} = \tan \tfrac{1}{2}(A \pm B)$$

$$\frac{\sin A \pm \sin B}{\cos B - \cos A} = \cot \tfrac{1}{2}(A \mp B)$$

$$\sin A \cos B = \tfrac{1}{2}[\sin(A+B) + \sin(A-B)]$$

$$\cos A \cos B = \tfrac{1}{2}[\cos(A+B) + \cos(A-B)]$$

$$\sin A \sin B = \tfrac{1}{2}[\cos(A-B) - \cos(A+B)]$$

$$\sin x + \sin 2x + \sin 3x + \dots + \sin mx = \frac{\sin \frac{1}{2}mx \sin \frac{1}{2}(m+1)x}{\sin \frac{1}{2}x}$$

$$\cos x + \cos 2x + \cos 3x + \dots + \cos mx = \frac{\sin \frac{1}{2}mx \cos \frac{1}{2}(m+1)x}{\sin \frac{1}{2}x}$$

$$\sin x + \sin 3x + \sin 5x + \dots + \sin(2m-1)x = \frac{\sin^2 mx}{\sin x}$$

$$\cos x + \cos 3x + \cos 5x + \dots + \cos(2m-1)x = \frac{\sin 2mx}{2 \sin x}$$

$$\tfrac{1}{2} + \cos x + \cos 2x + \dots + \cos mx = \frac{\sin(m+\frac{1}{2})x}{2 \sin \frac{1}{2}x}$$

angle	0	30°	45°	60°	90°	180°	270°	360°
sine	0	$\frac{1}{2}$	$\frac{1}{2}\sqrt{2}$	$\frac{1}{2}\sqrt{3}$	1	0	-1	0
cosine	1	$\frac{1}{2}\sqrt{3}$	$\frac{1}{2}\sqrt{2}$	$\frac{1}{2}$	0	-1	0	1
tangent	0	$\frac{1}{3}\sqrt{3}$	1	$\sqrt{3}$	$\pm\infty$	0	$\pm\infty$	0

versine: $\text{vers}\ \theta = 1 - \cos\theta$

haversine: $\text{hav}\ \theta = \frac{1}{2}(1 - \cos\theta) = \sin^2 \frac{1}{2}\theta$

Approximations for small angles

$$\left.\begin{aligned} \sin\theta &= (\theta - \theta^3/6 \dots) \\ \tan\theta &= (\theta + \theta^3/3 \dots) \\ \cos\theta &= (1 - \theta^2/2 \dots) \end{aligned}\right\} \theta \text{ in radians}$$

Algebraic and trigonometric formulas *continued*

$$\sin\theta = \theta \begin{cases} \text{with less than 1-percent error up} \\ \text{to } \theta = 0.24 \text{ radian} = 14.0^\circ \\ \\ \text{with less than 10-percent error up} \\ \text{to } \theta = 0.78 \text{ radian} = 44.5^\circ \end{cases}$$

$$\tan\theta = \theta \begin{cases} \text{with less than 1-percent error up} \\ \text{to } \theta = 0.17 \text{ radian} = 10.0^\circ \\ \\ \text{with less than 10-percent error up} \\ \text{to } \theta = 0.54 \text{ radian} = 31.0^\circ \end{cases}$$

Plane trigonometry

Right triangles $C = 90^\circ$

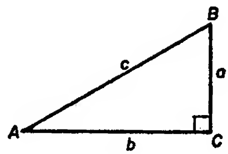

$$B = 90^\circ - A$$

$$\sin A = \cos B = a/c$$

$$\tan A = a/b$$

$$c^2 = a^2 + b^2$$

$$\text{area} = \tfrac{1}{2}ab = \tfrac{1}{2}a\,(c^2 - a^2)^{1/2} = \tfrac{1}{2}a^2 \cot A$$

$$= \tfrac{1}{2}\, b^2 \tan A = \tfrac{1}{4}\, c^2 \sin A \cos A$$

Oblique triangles

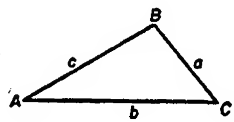

Sum of angles

$$A + B + C = 180^\circ \qquad (1)$$

Law of cosines

$$\left.\begin{aligned} a^2 &= b^2 + c^2 - 2\,bc\cos A \\ b^2 &= c^2 + a^2 - 2\,ca\cos B \\ c^2 &= a^2 + b^2 - 2\,ab\cos C \end{aligned}\right\} \qquad (2A)$$

$$\left.\begin{aligned} \cos A &= (b^2 + c^2 - a^2)/2\,bc \\ \cos B &= (c^2 + a^2 - b^2)/2\,ca \\ \cos C &= (a^2 + b^2 - c^2)/2\,ab \end{aligned}\right\} \qquad (2B)$$

Plane trigonometry *continued*

Law of sines

$$a/\sin A = b/\sin B = c/\sin C \tag{3}$$

Law of tangents

$$\left.\begin{aligned}\frac{a-b}{a+b} &= \frac{\tan\frac{1}{2}(A-B)}{\tan\frac{1}{2}(A+B)}\\ \frac{b-c}{b+c} &= \frac{\tan\frac{1}{2}(B-C)}{\tan\frac{1}{2}(B+C)}\\ \frac{c-a}{c+a} &= \frac{\tan\frac{1}{2}(C-A)}{\tan\frac{1}{2}(C+A)}\end{aligned}\right\} \tag{4}$$

Half-angle formulas

$$\left.\begin{aligned}\tan\frac{A}{2} &= \frac{r}{p-a}\\ \tan\frac{B}{2} &= \frac{r}{p-b}\\ \tan\frac{C}{2} &= \frac{r}{p-c}\end{aligned}\right\} \tag{5}$$

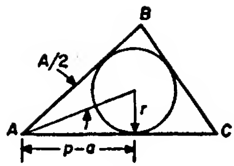

where

$$2p = a + b + c$$

$$r = [(p-a)(p-b)(p-c)/p]^{1/2}$$

Area

$$S = \tfrac{1}{2} bc \sin A = \tfrac{1}{2} ca \sin B = \tfrac{1}{2} ab \sin C \tag{6A}$$

$$S = [p(p-a)(p-b)(p-c)]^{1/2} \tag{6B}$$

$$\left.\begin{aligned}S &= \frac{a^2}{2}\frac{\sin B \sin C}{\sin A} = \frac{b^2}{2}\frac{\sin C \sin A}{\sin B}\\ &= \frac{c^2}{2}\frac{\sin A \sin B}{\sin C}\end{aligned}\right\} \tag{6C}$$

Plane trigonometry *continued*

To solve an oblique triangle

<table>
<tr><th>given</th><th>use</th><th colspan="2">to obtain</th></tr>
<tr><td rowspan="3">$a\ B\ C$</td><td>(1)</td><td colspan="2">A</td></tr>
<tr><td>(3)</td><td colspan="2">$b\ c$</td></tr>
<tr><td>(6C)</td><td colspan="2">S</td></tr>
<tr><td rowspan="3">$A\ b\ c$</td><td>(1)</td><td>$B + C$</td><td rowspan="2">hence B, C</td></tr>
<tr><td>(4)</td><td>$B - C$</td></tr>
<tr><td>(6A)</td><td colspan="2">S</td></tr>
<tr><td rowspan="2">$a\ b\ c$</td><td>(5) or (2B)</td><td colspan="2">$A\ B\ C$</td></tr>
<tr><td>(6B)</td><td colspan="2">S</td></tr>
<tr><td rowspan="2">$a\ b\ A$
ambiguous case</td><td>(3) and (1)</td><td colspan="2">$B\ C\ c$</td></tr>
<tr><td>(6A)</td><td colspan="2">S</td></tr>
</table>

Spherical trigonometry

Right spherical triangles ($\gamma = 90°$)

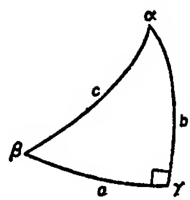

$$\cos c = \cos a \cos b = \cot \alpha \cot \beta$$

$$\cos \alpha = \sin \beta \cos a = \tan b \cot c$$
$$\cos \beta = \sin \alpha \cos b = \tan a \cot c$$

$$\sin a = \sin c \sin \alpha = \tan b \cot \beta$$
$$\sin b = \sin c \sin \beta = \tan a \cot \alpha$$

Oblique triangles

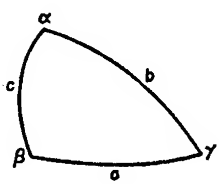

Law of cosines

$$\left.\begin{aligned} \cos a &= \cos b \cos c + \sin b \sin c \cos \alpha \\ \cos b &= \cos c \cos a + \sin c \sin a \cos \beta \\ \cos c &= \cos a \cos b + \sin a \sin b \cos \gamma \end{aligned}\right\} \text{(7A)}$$

Spherical trigonometry *continued*

$$\left.\begin{aligned}\cos\alpha &= -\cos\beta\cos\gamma + \sin\beta\sin\gamma\cos a\\ \cos\beta &= -\cos\gamma\cos\alpha + \sin\gamma\sin\alpha\cos b\\ \cos\gamma &= -\cos\alpha\cos\beta + \sin\alpha\sin\beta\cos c\end{aligned}\right\} \tag{7B}$$

Law of sines

$$\frac{\sin a}{\sin\alpha} = \frac{\sin b}{\sin\beta} = \frac{\sin c}{\sin\gamma} \tag{8}$$

Napier's analogies

$$\frac{\sin\frac{1}{2}(\alpha-\beta)}{\sin\frac{1}{2}(\alpha+\beta)} = \frac{\tan\frac{1}{2}(a-b)}{\tan\frac{1}{2}c} \tag{9A}$$

$$\frac{\cos\frac{1}{2}(\alpha-\beta)}{\cos\frac{1}{2}(\alpha+\beta)} = \frac{\tan\frac{1}{2}(a+b)}{\tan\frac{1}{2}c} \tag{9B}$$

$$\frac{\sin\frac{1}{2}(a-b)}{\sin\frac{1}{2}(a+b)} = \frac{\tan\frac{1}{2}(\alpha-\beta)}{\cot\frac{1}{2}\gamma} \tag{9C}$$

$$\frac{\cos\frac{1}{2}(a-b)}{\cos\frac{1}{2}(a+b)} = \frac{\tan\frac{1}{2}(\alpha+\beta)}{\cot\frac{1}{2}\gamma} \tag{9D}$$

Half-angle formulas

$$\tan\frac{\alpha}{2} = \frac{\tan r}{\sin(p-a)}$$

$$\tan\frac{\beta}{2} = \frac{\tan r}{\sin(p-b)}$$

$$\tan\frac{\gamma}{2} = \frac{\tan r}{\sin(p-c)} \tag{10A}$$

where

$$2p = a + b + c \text{ and}$$

$$\tan^2 r = \frac{\sin(p-a)\sin(p-b)\sin(p-c)}{\sin p}$$

Spherical trigonometry *continued*

$$\left.\begin{aligned}
\sin^2\frac{\alpha}{2} &= \frac{\sin(p-b)\sin(p-c)}{\sin b\sin c}\\
\cos^2\frac{\alpha}{2} &= \frac{\sin p\sin(p-a)}{\sin b\sin c}\\
\tan^2\frac{\alpha}{2} &= \frac{\sin(p-b)\sin(p-c)}{\sin p\sin(p-a)}
\end{aligned}\right\} \tag{10B}$$

and formulas obtained by permutation for β and γ.

Half-side formulas

$$\left.\begin{aligned}
\tan\tfrac{1}{2}a &= \tan R\sin(\alpha - E)\\
\tan\tfrac{1}{2}b &= \tan R\sin(\beta - E)\\
\tan\tfrac{1}{2}c &= \tan R\sin(\gamma - E)
\end{aligned}\right\} \tag{11A}$$

where

$$2E = \alpha + \beta + \gamma - \pi$$

is the spherical excess and

$$\tan^2 R = \frac{\sin E}{\sin(\alpha - E)\sin(\beta - E)\sin(\gamma - E)}$$

$$\left.\begin{aligned}
\sin^2\frac{a}{2} &= -\frac{\sin E\sin(E-\alpha)}{\sin\beta\sin\gamma}\\
\cos^2\frac{a}{2} &= \frac{\sin(E-\beta)\sin(E-\gamma)}{\sin\beta\sin\gamma}\\
\tan^2\frac{a}{2} &= -\frac{\sin E\sin(E-\alpha)}{\sin(E-\beta)\sin(E-\gamma)}
\end{aligned}\right\} \tag{11B}$$

and formulas obtained by permutation for b and c

Area

On a sphere of radius one, the area of a triangle is equal to the spherical excess $2E = \alpha + \beta + \gamma - \pi$

$$\tan^2\tfrac{1}{2}E = \tan\tfrac{1}{2}p\tan\tfrac{1}{2}(p-a)\tan\tfrac{1}{2}(p-b)\tan\tfrac{1}{2}(p-c) \tag{12}$$

Spherical trigonometry *continued*

To solve an oblique triangle*

given	use	to obtain
$a\ b\ c$	(10)	$\alpha\ \beta\ \gamma$
$\alpha\ \beta\ \gamma$	(11)	$a\ b\ c$
$a\ b\ \gamma$	(9)	$\alpha \pm \beta$, hence α, β, then c
$\alpha\ \beta\ c$	(9)	$a \pm b$, hence a, b, then γ
$a\ b\ \alpha$ ambiguous case	(8)	β
	(9)	$c\ \gamma$
$\alpha\ \beta\ a$ ambiguous case	(8)	b
	(9)	$c\ \gamma$

Hyperbolic functions†

$$\sinh x = \frac{e^x - e^{-x}}{2}$$

$$\cosh x = \frac{e^x + e^{-x}}{2}$$

$$\tanh x = \frac{\sinh x}{\cosh x} = \frac{1 - \exp(-2x)}{1 + \exp(-2x)} = \frac{1}{\coth x}$$

$$\operatorname{sech} x = 1/\cosh x$$

$$\operatorname{csch} x = 1/\sinh x$$

$$\sinh(-x) = -\sinh x$$

$$\cosh(-x) = \cosh x$$

*See also great-circle calculations on pp. 732-739.

†Tables of hyperbolic functions appear on pp. 1111-1113.

Hyperbolic functions *continued*

$\tanh(-x) = -\tanh x$

$\coth(-x) = -\coth x$

$\sinh jx = j \sin x$

$\cosh jx = \cos x$

$\tanh jx = j \tan x$

$\coth jx = -j \cot x$

$\cosh^2 x - \sinh^2 x = 1$

$1 - \tanh^2 x = 1/\cosh^2 x$

$\coth^2 x - 1 = 1/\sinh^2 x$

$\sinh 2x = 2 \sinh x \cosh x$

$\cosh 2x = \cosh^2 x + \sinh^2 x$

$\sinh(x \pm jy) = \sinh x \cos y \pm j \cosh x \sin y$

$\cosh(x \pm jy) = \cosh x \cos y \pm j \sinh x \sin y$

$$\tanh(x \pm y) = \frac{\tanh x \pm \tanh y}{1 \pm \tanh x \tanh y}$$

If $y = \operatorname{gd} x$ (gudermannian of x) is defined by

$$x = \log_e \tan\left(\frac{\pi}{4} + \frac{y}{2}\right)$$

then

$\sinh x = \tan y$

$\cosh x = \sec y$

$\tanh x = \sin y$

$\tanh(x/2) = \tan(y/2)$

Hyperbolic trigonometry

Hyperbolic (or pseudospherical) trigonometry applies to triangles drawn in the hyperbolic type of non-Euclidean space. Reflection charts, used in transmission-line theory and waveguide analysis are models of this hyperbolic space.*

Conformal model

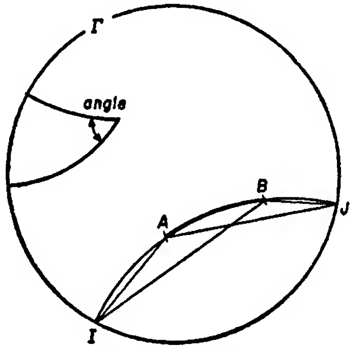

Conformal model.

The space is limited to the inside of a unit circle Γ. Geodesics (or "straight lines" for the model) are arcs of circle orthogonal to Γ as shown in sketch at right. The hyperbolic distance between two points A and B is defined by

$$[AB] = \log_e \frac{BI}{BJ} : \frac{AI}{AJ}$$

where I and J are the intersections with Γ of the geodesic AB. The distance $[AB]$ is expressed in nepers. For engineering purposes, a unit, corresponding to the decibel and equal to 1/8.686 neper, is sometimes used.

As this model is conformal, the angle between two lines is the ordinary angle between the tangents at their common point.

Projective model

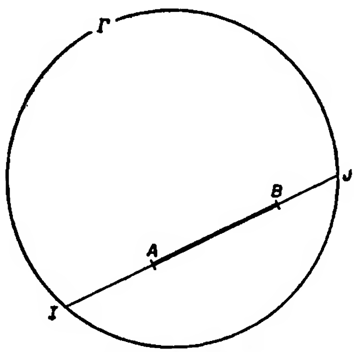

Projective model.

The space is again composed of the points inside of a circle Γ. Geodesics are straight-line segments limited to the inside of Γ. (JI in sketch at right.)

The hyperbolic distance $\langle AB \rangle$ is defined by

$$\langle AB \rangle = \tfrac{1}{2} \log_e \left(\frac{BI}{BJ} : \frac{AI}{AJ} \right)$$

* G. A. Deschamps, "Hyperbolic Protractor for Microwave Impedance Measurements and Other Purposes." International Telephone and Telegraph Corporation, 67 Broad Street, New York 4, New York; 1953.

Hyperbolic trigonometry *continued*

and can be measured directly by means of a hyperbolic protractor. The angles for this model do not appear in true size, except when at the center of Γ. An angle such as BAC, when it is considered in reference to the projective model, will be called an *elliptic* angle. It can be evaluated, as shown in the sketch at the right, by projecting B and C through the hyperbolic midpoint of OA onto B' and C' on the circle Γ, then measuring $B'OC'$ as in Euclidean geometry.

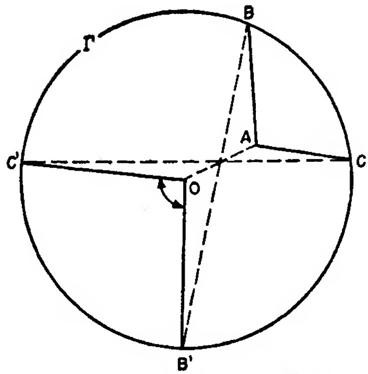

Construction of angle on projective model.

The two models drawn inside the same circle Γ can be set into a distance-preserving correspondance by the transformation: $\mathcal{B}(M) = M'$ defined by

$$[OM] = \langle OM' \rangle$$

or in terms of ordinary distances

$$OM' = 2\,OM/(1 + OM^2)$$

The hyperbolic distance to the center O being denoted by u:

$$OM = \tanh (u/2)$$

and

$$OM' = \tanh u$$

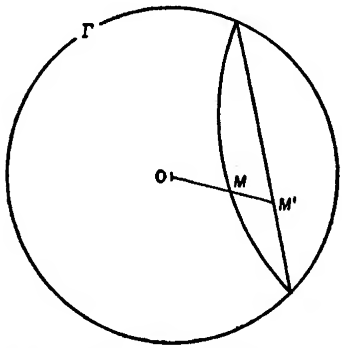

Correspondance between the two models.

The points on Γ are at an infinite distance from any point inside Γ.

In the following formulas, the sides are expressed in nepers, the angles in radians. The three points A,B,C are assumed to be inside the circle Γ.

Hyperbolic trigonometry *continued*

Right hyperbolic triangles ($\gamma = 90°$)

$$\cosh c = \cosh a \cosh b$$

$$\cosh c = \cot \alpha \cot \beta$$

$$\cos \alpha = \sin \beta \cosh a$$
$$= \tanh b \coth c$$

$$\cos \beta = \sin \alpha \cosh b$$
$$= \tanh a \coth c$$

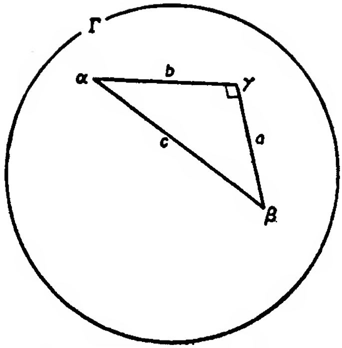

Projective representation of right hyperbolic triangle.

When B is at infinity, i.e., on Γ

$$\cos A = \tanh b$$

$$\cot A = \sinh b$$

$$\operatorname{cosec} A = \cosh b$$

$$\tan \tfrac{1}{2} A = \exp b$$

or

$$(\pi/2) - A = \operatorname{gd} b$$

(See definition of gd on p. 1049.)

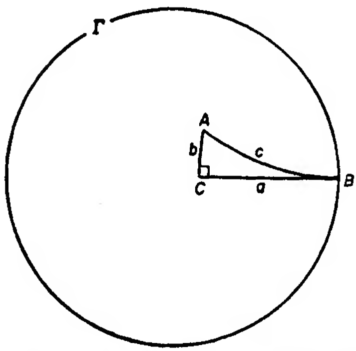

Conformal representation of right hyperbolic triangle with *B* at infinity.

CB and *AB* are "parallel," *A* is also called angle of parallelism and is noted by

$$A = \Pi(b)$$
$$= \pi/2 - \operatorname{gd} b$$

Hyperbolic trigonometry *continued*

Oblique hyperbolic triangles

Law of cosines

$$\cosh a = \cosh b \cosh c - \sinh b \sinh c \cos \alpha \text{ and permutations} \tag{13A}$$

$$\cos \alpha = -\cos \beta \cos \gamma + \sin \beta \sin \gamma \cosh a \text{ and permutations} \tag{13B}$$

Law of sines

$$\frac{\sinh a}{\sin \alpha} = \frac{\sinh b}{\sin \beta} = \frac{\sinh c}{\sin \gamma} \tag{14}$$

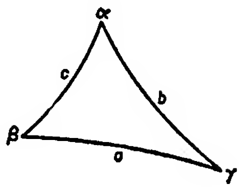

Napier's analogies

$$\frac{\sin \frac{1}{2}(\alpha - \beta)}{\sin \frac{1}{2}(\alpha + \beta)} = \frac{\tanh \frac{1}{2}(a - b)}{\tanh \frac{1}{2} c} \tag{15A}$$

$$\frac{\cos \frac{1}{2}(\alpha - \beta)}{\cos \frac{1}{2}(\alpha + \beta)} = \frac{\tanh \frac{1}{2}(a + b)}{\tanh \frac{1}{2} c} \tag{15B}$$

$$\frac{\sinh \frac{1}{2}(a - b)}{\sinh \frac{1}{2}(a + b)} = \frac{\tan \frac{1}{2}(\alpha - \beta)}{\cot \frac{1}{2} \gamma} \tag{15C}$$

$$\frac{\cosh \frac{1}{2}(a - b)}{\cosh \frac{1}{2}(a + b)} = \frac{\tan \frac{1}{2}(\alpha + \beta)}{\cot \frac{1}{2} \gamma} \tag{15D}$$

Half-angle formulas

$$\left.\begin{array}{l} \tan \dfrac{\alpha}{2} = \dfrac{\tanh r}{\sinh (p - \alpha)} \\ \text{and permutations where} \\ \qquad 2p = a + b + c \\ \text{and} \\ \tanh^2 r = \dfrac{\sinh (p - a) \sinh (p - b) \sinh (p - c)}{\sinh p} \end{array}\right\} \tag{16A}$$

Hyperbolic trigonometry *continued*

$$\left.\begin{aligned} \sin^2 \tfrac{1}{2}\alpha &= \frac{\sinh(p-b)\sinh(p-c)}{\sinh b \sinh c} \\ \cos^2 \tfrac{1}{2}\alpha &= \frac{\sinh p \sinh(p-a)}{\sinh b \sinh c} \\ \tan^2 \tfrac{1}{2}\alpha &= \frac{\sinh(p-b)\sinh(p-c)}{\sinh p \sinh(p-a)} \end{aligned}\right\} \tag{16B}$$

Half-side formulas

$$\coth \frac{a}{2} = \frac{\coth R}{\sin(\Delta + \alpha)}$$

and permutations where

$$2\Delta = \pi - \alpha - \beta - \gamma$$

is the hyperbolic defect and

$$\tanh^2 R = \frac{\sin \Delta}{\sin(\Delta+\alpha)\sin(\Delta+\beta)\sin(\Delta+\gamma)} \tag{17A}$$

$$\left.\begin{aligned} \sinh^2 \tfrac{1}{2}a &= \frac{\sin\Delta \sin(\Delta+\alpha)}{\sin\beta \sin\gamma} \\ \cosh^2 \tfrac{1}{2}a &= \frac{\sin(\Delta+\beta)\sin(\Delta+\gamma)}{\sin\beta\sin\gamma} \\ \tanh^2 \tfrac{1}{2}a &= \frac{\sin\Delta\sin(\Delta+\alpha)}{\sin(\Delta+\beta)\sin(\Delta+\gamma)} \end{aligned}\right\} \tag{17B}$$

Area

The hyperbolic area of a triangle is equal to the hyperbolic defect.

$$2\,\Delta = \pi - (\alpha + \beta + \gamma) \tag{18}$$

To solve an oblique hyperbolic triangle

Solution of an oblique hyperbolic triangle is analogous to that for an oblique spherical triangle, as follows.

Hyperbolic trigonometry *continued*

given	use	to obtain
$a\ b\ c$	(16)	$\alpha\ \beta\ \gamma$
$\alpha\ \beta\ \gamma$	(17)	$a\ b\ c$
$a\ b\ \gamma$	(15)	$\alpha \pm \beta$, hence α, β, then c
$\alpha\ \beta\ c$	(15)	$a \pm b$, hence a, b, then γ
$a\ b\ \alpha$ ambiguous case	(14)	β
	(15)	$c\ \gamma$
$\alpha\ \beta\ a$ ambiguous case	(14)	b
	(15)	$c\ \gamma$

Plane analytic geometry

In the following, x and y are coordinates of a variable point in a rectangular-coordinate system.

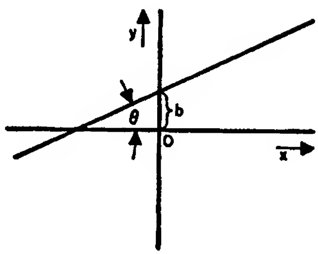

Slope-intercept

Straight line

General equation

$Ax + By + C = 0$
A, B, and C are constants.

Slope-intercept form

$y = sx + b$
b = y-intercept
$s = \tan\theta$

Intercept-intercept form

$$\frac{x}{a} + \frac{y}{b} = 1$$

a = x-intercept
b = y-intercept

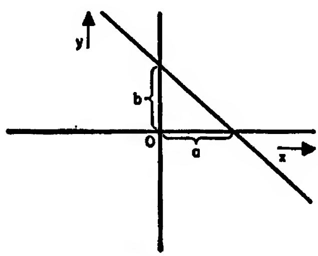

Intercept-intercept

Plane analytic geometry *continued*

Point-slope form

$$y - y_1 = s(x - x_1)$$

$s = \tan\theta$

(x_1,y_1) = coordinates of known point on line.

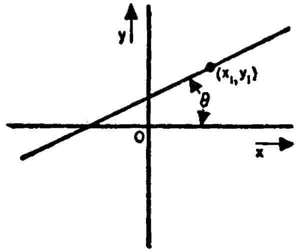

Point-slope

Point-point form

$$\frac{y - y_1}{y_1 - y_2} = \frac{x - x_1}{x_1 - x_2}$$

(x_1,y_1) and (x_2,y_2) are coordinates of two different points on the line.

Normal form

$$\frac{A}{\pm\sqrt{A^2+B^2}}x + \frac{B}{\pm\sqrt{A^2+B^2}}y + \frac{C}{\pm\sqrt{A^2+B^2}} = 0$$

the sign of the radical is chosen so that

$$\frac{C}{\pm\sqrt{A^2+B^2}} < 0$$

Distance from point (x_1,y_1) to a line

Substitute coordinates of the point in the normal form of the line. Thus,

$$\text{distance} = \frac{A}{\pm\sqrt{A^2+B^2}}x_1 + \frac{B}{\pm\sqrt{A^2+B^2}}y_1 + \frac{C}{\pm\sqrt{A^2+B^2}}$$

Angle between two lines

$$\tan\phi = \frac{s_1 - s_2}{1 + s_1 s_2}$$

where

ϕ = angle between the lines
s_1 = slope of one line
s_2 = slope of other line

When the lines are mutually perpendicular, $\tan\phi = \infty$, whence $s_1 = -1/s_2$

Plane analytic geometry *continued*

Transformation of rectangular coordinates

Translation

$x_1 = h + x_2$

$y_1 = k + y_2$

$x_2 = x_1 - h$

$y_2 = y_1 - k$

(h,k) = coordinates of new origin referred to old origin

Rotation

$x_1 = x_2 \cos\theta - y_2 \sin\theta$

$y_1 = x_2 \sin\theta + y_2 \cos\theta$

$x_2 = x, \cos\theta + y_1 \sin\theta$

$y_2 = -x_1 \sin\theta + y_1 \cos\theta$

(x_1,y_1) = "old" coordinates

(x_2,y_2) = "new" coordinates

θ = counterclockwise angle of rotation of axes

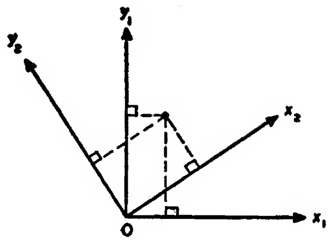

Circle

The equation of a circle of radius r with center at (m,n) is

$(x - m)^2 + (y - n)^2 = r^2$

Tangent line to a circle: At (x_1,y_1) is

$$y - y_1 = -\frac{x_1 - m}{y_1 - n}(x - x_1)$$

Normal line to a circle: At (x_1,y_1) is

$$y - y_1 = \frac{y_1 - n}{x_1 - m}(x - x_1)$$

Parabola

x-parabola

$(y - k)^2 = \pm 2p\,(x - h)$

where (h,k) are the coordinates of the vertex, and the sign used is plus or minus when the parabola is open to the right or to the left, respectively. The semilatus rectum is p.

Plane analytic geometry *continued*

y-parabola

$$(x - h)^2 = \pm 2p\,(y - k)$$

where (h,k) are the coordinates of the vertex. Use plus sign if parabola is open above, and minus sign if open below.

Tangent lines to a parabola

(x_1,y_1) = point of tangency

For x-parabola,

$$y - y_1 = \pm \frac{p}{y_1 - k}(x - x_1)$$

Use plus sign if parabola is open to the right, minus sign if open to the left.

For y-parabola,

$$y - y_1 = \pm \frac{x_1 - h}{p}(x - x_1)$$

Use plus sign if parabola is open above, minus sign if open below.

Normal lines to a parabola

(x_1,y_1) = point of contact

For x-parabola,

$$y - y_1 = \mp \frac{y_1 - k}{p}(x - x_1)$$

Use minus sign if parabola is open to the right, plus sign if open to the left.

For y-parabola,

$$y - y_1 = \mp \frac{p}{x_1 - h}(x - x_1)$$

Use minus sign if parabola is open above, plus sign if open below.

Plane analytic geometry *continued*

Ellipse

Figure shows ellipse centered at origin.

Foci: F, F'
Directrices: D, D'

e = eccentricity < 1
$2a = A'A$ = major axis
$2b = BB'$ = minor axis
$2c = FF'$ = focal distance

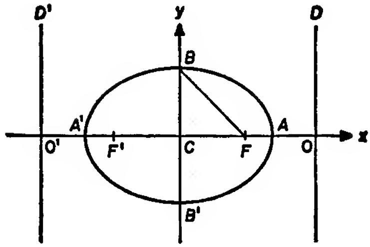

Then

$OC = a/e$
$BF = a$
$FC = ae$

$1 - e^2 = b^2/a^2$

Equation of ellipse

$$\frac{x^2}{a^2} + \frac{y^2}{b^2} = 1$$

Sum of the focal radii

To any point on ellipse $= 2a$

Equation of tangent line to ellipse

(x_1, y_1) = point of tangency

$$\frac{xx_1}{a^2} + \frac{yy_1}{b^2} = 1$$

Equation of normal line to an ellipse

$$y - y_1 = \frac{a^2 y_1}{b^2 x_1}(x - x_1)$$

Plane analytic geometry *continued*

Hyperbola

Figure shows x-hyperbola centered at origin.

Foci: F, F'

Directrices: D, D'

e = eccentricity > 1

$2a$ = transverse axis $= A'A$

$CO = a/e$

$CF = ae$

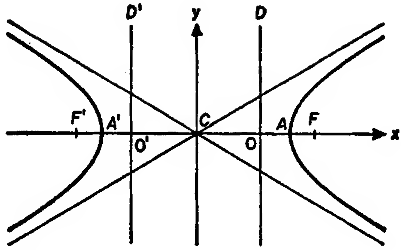

Equation of x-hyperbola

$$\frac{x^2}{a^2} - \frac{y^2}{b^2} = 1$$

where

$$b^2 = a^2 (e^2 - 1)$$

Equation of conjugate (y-) hyperbola

$$\frac{y^2}{b^2} - \frac{x^2}{a^2} = 1$$

Tangent line to x-hyperbola

(x_1, y_1) = point of tangency

$$a^2 y_1 y - b^2 x_1 x = -a^2 b^2$$

Normal line to x-hyperbola

$$y - y_1 = -\frac{a^2 y_1}{b^2 x_1}(x - x_1)$$

Asymptotes to hyperbola

$$y = \pm \frac{b}{a} x$$

Solid analytic geometry

In the following, x, y, and z are the coordinates of a variable point in space in a rectangular-coordinate system.

Distance between two points (x_1, y_1, z_1) and (x_2, y_2, z_2)

$$d = [(x_1 - x_2)^2 + (y_1 - y_2)^2 + (z_1 - z_2)^2]^{\frac{1}{2}}$$

Equations of the straight line

The straight line is specified in terms of its projections on two of the coordinate planes. For example, using the projections on the x-z and y-z planes respectively, the equations of the line are

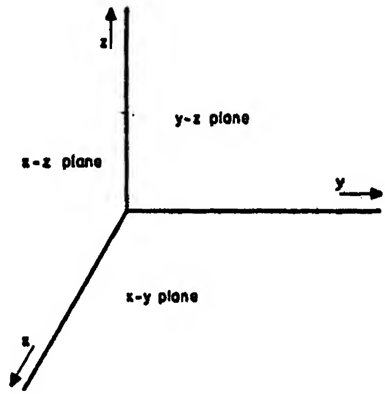

$$x = mz + \mu$$

$$y = nz + \nu$$

where

m = slope of x-z projection
n = slope of y-z projection
μ = intercept of x-z projection on x-axis
ν = intercept of y-z projection on y-axis

Equation of plane, intercept form

$$\frac{x}{a} + \frac{y}{b} + \frac{z}{c} = 1$$

where a, b, c are the intercepts of the plane on the x, y, and z axes, respectively.

Prolate spheroid

$$a^2(y^2 + z^2) + b^2x^2 = a^2b^2$$

where $a > b$, and x-axis = axis of revolution

Oblate spheroid

$$b^2(x^2 + z^2) + a^2y^2 = a^2b^2$$

where $a > b$, and y-axis = axis of revolution

Solid analytic geometry *continued*

Paraboloid of revolution

$y^2 + z^2 = 2px$

x-axis = axis of revolution

Hyperboloid of revolution

Revolving an x-hyperbola about the x-axis results in the hyperboloid of two sheets

$a^2 (y^2 + z^2) - b^2x^2 = -a^2b^2$

Revolving an x-hyperbola about the y-axis results in the hyperboloid of one sheet

$b^2 (x^2 + z^2) - a^2y^2 = a^2b^2$

Ellipsoid

$$\frac{x^2}{a^2} + \frac{y^2}{b^2} + \frac{z^2}{c^2} = 1$$

where a, b, c are the semiaxes of the ellipsoid or the intercepts on the x, y, and z axes, respectively.

Differential calculus

List of derivatives

In the following u, v, w are differentiable functions of x, and c is a constant.

General

$$\frac{dc}{dx} = 0$$

$$\frac{dx}{dx} = 1$$

$$\frac{d}{dx}(u + v - w) = \frac{du}{dx} + \frac{dv}{dx} - \frac{dw}{dx}$$

Differential calculus *continued*

$$\frac{d}{dx}(cv) = c\frac{dv}{dx}$$

$$\frac{d}{dx}(uv) = u\frac{dv}{dx} + v\frac{du}{dx}$$

$$\frac{d}{dx}(v^c) = cv^{c-1}\frac{dv}{dx}$$

$$\frac{d}{dx}\left(\frac{u}{v}\right) = \frac{v\frac{du}{dx} - u\frac{dv}{dx}}{v^2}$$

$$\frac{dy}{dx} = \frac{dy}{dv}\cdot\frac{dv}{dx} \quad \text{if } y = y(v)$$

$$\frac{dy}{dx} = \frac{1}{dx/dy} \quad \text{if } \frac{dx}{dy} \neq 0$$

Transcendental functions

$$\frac{d}{dx}(\log_e v) = \frac{1}{v}\frac{dv}{dx}$$

$$\frac{d}{dx}(c^v) = c^v \log_e c\frac{dv}{dx}$$

$$\frac{d}{dx}(e^v) = e^v\frac{dv}{dx}$$

$$\frac{d}{dx}(u^v) = vu^{v-1}\frac{du}{dx} + (\log_e u)u^v\frac{dv}{dx}$$

$$\frac{d}{dx}(\sin v) = \cos v\frac{dv}{dx}$$

$$\frac{d}{dx}(\cos v) = -\sin v\frac{dv}{dx}$$

$$\frac{d}{dx}(\tan v) = \sec^2 v\frac{dv}{dx}$$

$$\frac{d}{dx}(\cot v) = -\csc^2 v\frac{dv}{dx}$$

Differential calculus *continued*

$$\frac{d}{dx}(\sec v) = \sec v \tan v \frac{dv}{dx}$$

$$\frac{d}{dx}(\csc v) = -\csc v \cot v \frac{dv}{dx}$$

$$\frac{d}{dx}(\text{arc} \sin v) = \frac{1}{\sqrt{1 - v^2}} \frac{dv}{dx}$$

$$\frac{d}{dx}(\text{arc} \cos v) = -\frac{1}{\sqrt{1 - v^2}} \frac{dv}{dx}$$

$$\frac{d}{dx}(\text{arc} \tan v) = \frac{1}{1 + v^2} \frac{dv}{dx}$$

$$\frac{d}{dx}(\text{arc} \cot v) = -\frac{1}{1 + v^2} \frac{dv}{dx}$$

$$\frac{d}{dx}(\text{arc} \sec v) = \frac{1}{v\sqrt{v^2 - 1}} \frac{dv}{dx}$$

$$\frac{d}{dx}(\text{arc} \csc v) = -\frac{1}{v\sqrt{v^2 - 1}} \frac{dv}{dx}$$

Curvature of a curve

$$K = \frac{y''}{(1 + y'^2)^{3/2}} = \frac{1}{R}$$

where

K = curvature
R = radius of curvature
y', y'' = respectively, first and second derivatives of the function $y = f(x)$ representing the curve on rectangular coordinates

Bessel functions

A Bessel function of the nth order $y = Z_n(x)$ is any solution of the differential equation

$$y'' + (1/x)\, y' + (1 - n^2/x^2)\, y = 0$$

Special solutions are J_n (first kind), N_n (second kind), $H_n^{(1)}$ and $H_n^{(2)}$ (third kind).

Bessel functions *continued*

Derivative and recursion formulas

Z_n represents J_n, N_n, $H_n^{(1)}$, $H_n^{(2)}$ or any linear combination of these functions. Then,

$$dZ_n/dx = \tfrac{1}{2}(Z_{n-1} - Z_{n+1}) = -(n/x)\,Z_n + Z_{n-1} = (n/x)\,Z_n - Z_{n+1}$$

$$(n/x)\,Z_n = \tfrac{1}{2}(Z_{n-1} + Z_{n+1})$$

$$(d/dx)\,(x^n Z_n) = x^n Z_{n+1}$$

$$(d/dx)\,(x^{-n} Z_n) = -x^{-n}\,Z_{n-1}$$

$$dZ_0/dx = -Z_1$$

$$dZ_1/dx = Z_0 - Z_1/x$$

For n an integer,

$$Z_{-n}(x) = (-1)^n\,Z_n(x)$$

Bessel function of the first kind*

$$J_n(x) = \sum_{m=0}^{m=\infty} (-1)^m \frac{(x/2)^{n+2m}}{m!\,\Gamma(m+n+1)}$$

For n a positive integer,

$$J_n(x) = \frac{x^n}{2^n\,n!}\left[1 - \frac{x^2}{2\,(2n+2)} + \frac{x^4}{2.4\,(2n+2)\,(2n+4)} \cdots\right]$$

$$\exp(-ju\sin x) = \sum_{-\infty}^{+\infty} J_n(u)\,\exp(-jnx)$$

$$\cos(u\sin x) = J_0(u) + 2\sum_{1}^{\infty} J_{2n}(u)\cos 2nx$$

$$\sin(u\sin x) = 2\sum_{1}^{\infty} J_{2n-1}(u)\sin(2n-1)\,x$$

$$\cos(u\cos x) = J_0(u) + 2\sum_{1}^{\infty}(-1)^n J_{2n}(u)\cos 2nx$$

$$\sin(u\cos x) = 2\sum_{1}^{\infty}(-1)^{n+1} J_{2n-1}(u)\cos(2n-1)\,x$$

* See table in next chapter.

Bessel functions *continued*

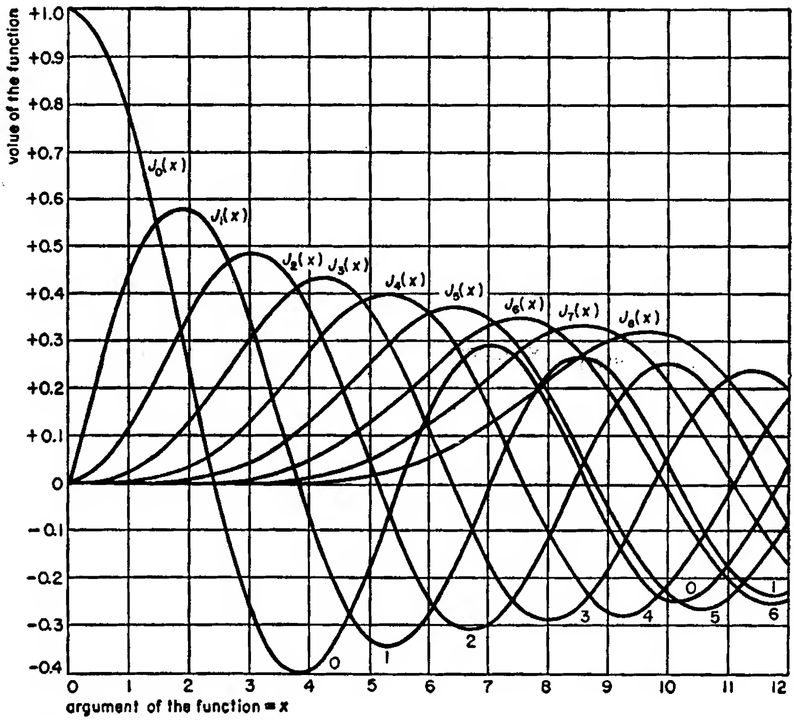

Bessel functions for the first 8 orders.

Bessel functions of the third kind

$H_n^{(1)}(x) = J_n(x) + j\,N_n(x)$

$H_n^{(2)}(x) = J_n(x) - j\,N_n(x)$

$N_{n-1} J_n - N_n J_{n-1} = 2/\pi x$

$[H_n^{(1)}(x)]^* = H_n^{(2)}(x^*)$

where (*) indicates the complex conjugate.

For x large,

$H_n^{(1)}(x) \approx (2/\pi x)^{1/2} \exp j\,[x - n\pi/2 - \pi/4]$

$H_n^{(2)}(x) \approx (2/\pi x)^{1/2} \exp -j\,[x - n\pi/2 - \pi/4]$

Bessel functions *continued*

Modified Bessel functions

$$I_n(x) = j^{-n} J_n(jx) = \sum_{m=0}^{m=\infty} \frac{(x/2)^{n+2m}}{m!\,\Gamma(n+m+1)}$$

$$K_n(x) = (\pi/2)\, j^{n+1} H_n^{(1)}(jx)$$

Modified Bessel functions are solutions of the differential equation

$$y'' + y'/x - (1 - n^2/x^2)\, y = 0$$

Integral calculus

Rational algebraic integrals

1. $$\int x^m\,dx = \frac{x^{m+1}}{m+1}, \qquad m \neq -1$$

2. $$\int \frac{dx}{x} = \log_e x$$

3. $$\int (ax+b)^m\,dx = \frac{(ax+b)^{m+1}}{a(m+1)}, \qquad m \neq -1$$

4. $$\int \frac{dx}{ax+b} = \frac{1}{a}\log_e(ax+b)$$

5. $$\int \frac{x\,dx}{ax+b} = \frac{1}{a^2}[ax+b - b\log_e(ax+b)]$$

6. $$\int \frac{x\,dx}{(ax+b)^2} = \frac{1}{a^2}\left[\frac{b}{ax+b} + \log_e(ax+b)\right]$$

7. $$\int \frac{dx}{x(ax+b)} = \frac{1}{b}\log_e\frac{x}{ax+b}$$

8. $$\int \frac{dx}{x(ax+b)^2} = \frac{1}{b(ax+b)} + \frac{1}{b^2}\log_e\frac{x}{ax+b}$$

9. $$\int \frac{dx}{x^2(ax+b)} = -\frac{1}{bx} + \frac{a}{b^2}\log_e\frac{ax+b}{x}$$

10. $$\int \frac{dx}{x^2(ax+b)^2} = -\frac{2ax+b}{b^2x(ax+b)} + \frac{2a}{b^3}\log_e\frac{ax+b}{x}$$

Integral calculus *continued*

11. $$\int \frac{dx}{x^2 + a^2} = \frac{1}{a} \tan^{-1} \frac{x}{a}$$

12. $$\int \frac{dx}{x^2 - a^2} = \frac{1}{2a} \log \frac{x - a}{x + a} = -\frac{1}{a} \tanh^{-1} \frac{a}{x}$$

13. $$\int \frac{dx}{(ax^2 + b)^m} = \frac{x}{2(m-1)\, b\, (ax^2 + b)^{m-1}} + \frac{2m - 3}{2(m-1)\, b} \int \frac{dx}{(ax^2 + b)^{m-1}}, \quad m \neq 1$$

14. $$\int \frac{x\, dx}{(ax^2 + b)^m} = -\frac{1}{2(m-1)\, a\, (ax^2 + b)^{m-1}}, \quad m \neq 1$$

15. $$\int \frac{x\, dx}{ax^2 + b} = \frac{1}{2a} \log_e (ax^2 + b)$$

16. $$\int \frac{x^2\, dx}{ax^2 + b} = \frac{x}{a} - \frac{b}{a} \int \frac{dx}{ax^2 + b}$$

17. $$\int \frac{x^2\, dx}{(ax^2 + b)^m} = -\frac{x}{2(m-1)\, a\, (ax^2 + b)^{m-1}} + \frac{1}{2(m-1)\, a} \int \frac{dx}{(ax^2 + b)^{m-1}}, \quad m \neq 1$$

18. $$\int \frac{dx}{ax^3 + b} = \frac{k}{3b} \left(\sqrt{3} \tan^{-1} \frac{2x - k}{k\sqrt{3}} + \log_e \frac{k + x}{\sqrt{k^2 - kx + x^2}} \right),$$

where $k = \sqrt[3]{b/a}$

19. $$\int \frac{x\, dx}{ax^3 + b} = \frac{1}{3ak} \left(\sqrt{3} \tan^{-1} \frac{2x - k}{k\sqrt{3}} - \log_e \frac{k + x}{\sqrt{k^2 - kx + x^2}} \right),$$

where $k = \sqrt[3]{b/a}$

20. $$\int \frac{dx}{x(ax^n + b)} = \frac{1}{bn} \log_e \frac{x^n}{ax^n + b}$$

Integral calculus *continued*

Let $X = ax^2 + bx + c$ and $q = b^2 - 4ac$

21. $$\int \frac{dx}{X} = \frac{1}{\sqrt{q}} \log_e \frac{2ax + b - \sqrt{q}}{2ax + b + \sqrt{q}}, \quad \text{when } q > 0$$

22. $$\int \frac{dx}{X} = \frac{2}{\sqrt{-q}} \tan^{-1} \frac{2ax + b}{\sqrt{-q}}, \quad \text{when } q < 0$$

For the case $q = 0$, use equation 3 with $m = -2$

23. $$\int \frac{dx}{X^n} = -\frac{2ax + b}{(n-1)\, q\, X^{n-1}} - \frac{2(2n-3)\, a}{q(n-1)} \int \frac{dx}{X^{n-1}}, \quad n \neq 1$$

24. $$\int \frac{x\, dx}{X} = \frac{1}{2a} \log_e X - \frac{b}{2a} \int \frac{dx}{X}$$

25. $$\int \frac{x^2\, dx}{X} = \frac{x}{a} - \frac{b}{2a^2} \log_e X + \frac{b^2 - 2ac}{2a^2} \int \frac{dx}{X}$$

Integrals involving $\sqrt{ax+b}$

26. $$\int x\sqrt{ax+b}\, dx = \frac{2(3ax - 2b)\sqrt{(ax+b)^3}}{15a^2}$$

27. $$\int x^2\sqrt{ax+b}\, dx = \frac{2(15a^2x^2 - 12abx + 8b^2)\sqrt{(ax+b)^3}}{105a^3}$$

28. $$\int x^m\sqrt{ax+b}\, dx = \frac{2}{a(2m+3)} \left[x^m\sqrt{(ax+b)^3} - mb \int x^{m-1}\sqrt{ax+b}\, dx \right]$$

29. $$\int \frac{\sqrt{ax+b}\, dx}{x} = 2\sqrt{ax+b} + \sqrt{b} \log_e \frac{\sqrt{ax+b} - \sqrt{b}}{\sqrt{ax+b} + \sqrt{b}}, \quad b > 0$$

$$= 2\sqrt{ax+b} - 2\sqrt{-b} \tan^{-1} \sqrt{\frac{ax+b}{-b}}, \quad b < 0$$

Integral calculus *continued*

30. $$\int \frac{\sqrt{ax+b}\,dx}{x^m} = -\frac{1}{(m-1)\,b}\left[\frac{\sqrt{(ax+b)^3}}{x^{m-1}} + \frac{(2m-5)\,a}{2}\int \frac{\sqrt{ax+b}\,dx}{x^{m-1}}\right], \quad m \neq 1$$

31. $$\int \frac{x\,dx}{\sqrt{ax+b}} = \frac{2(ax-2b)}{3a^2}\sqrt{ax+b}$$

32. $$\int \frac{x^2\,dx}{\sqrt{ax+b}} = \frac{2(3a^2x^2-4abx+8b^2)}{15a^3}\sqrt{ax+b}$$

33. $$\int \frac{x^m\,dx}{\sqrt{ax+b}} = \frac{2}{a(2m+1)}\left(x^m\sqrt{ax+b} - mb\int \frac{x^{m-1}\,dx}{\sqrt{ax+b}}\right), \quad m \neq \tfrac{1}{2}$$

34. $$\int \frac{dx}{x\sqrt{ax+b}} = \frac{1}{\sqrt{b}}\log_e \frac{\sqrt{ax+b}-\sqrt{b}}{\sqrt{ax+b}+\sqrt{b}}, \quad b > 0$$
$$= \frac{2}{\sqrt{-b}}\tan^{-1}\sqrt{\frac{ax+b}{-b}}, \quad b < 0$$

35. $$\int \frac{dx}{x^m\sqrt{ax+b}} = -\frac{\sqrt{ax+b}}{(m-1)\,bx^{m-1}} - \frac{(2m-3)\,a}{(2m-2)\,b}\int \frac{dx}{x^{m-1}\sqrt{ax+b}}, \quad m \neq 1$$

Integrals involving $\sqrt{x^2 \pm a^2}$ and $\sqrt{a^2 - x^2}$

36. $$\int \sqrt{x^2 \pm a^2}\,dx = \tfrac{1}{2}\left[x\sqrt{x^2 \pm a^2} \pm a^2 \log_e (x + \sqrt{x^2 \pm a^2})\right]$$

37. $$\int \sqrt{a^2 - x^2}\,dx = \tfrac{1}{2}\left(x\sqrt{a^2-x^2} + a^2 \sin^{-1}\frac{x}{a}\right)$$

38. $$\int \frac{dx}{\sqrt{x^2 \pm a^2}} = \log_e (x + \sqrt{x^2 \pm a^2})$$

39. $$\int \frac{dx}{\sqrt{a^2 - x^2}} = \sin^{-1}\frac{x}{a}$$

40. $$\int x\sqrt{x^2 \pm a^2}\,dx = \tfrac{1}{3}\sqrt{(x^2 \pm a^2)^3}$$

Integral calculus *continued*

41. $$\int x^2\sqrt{x^2 \pm a^2}\,dx = \frac{x}{4}\sqrt{(x^2 \pm a^2)^3} \mp \frac{a^2}{8}\left[x\sqrt{x^2 \pm a^2} \pm a^2 \log_e (x + \sqrt{x^2 \pm a^2})\right]$$

42. $$\int x\sqrt{a^2 - x^2}\,dx = -\tfrac{1}{3}\sqrt{(a^2 - x^2)^3}$$

43. $$\int x^2\sqrt{a^2 - x^2}\,dx = -\frac{x}{4}\sqrt{(a^2 - x^2)^3} + \frac{a^2}{8}\left(x\sqrt{a^2 - x^2} + a^2 \sin^{-1}\frac{x}{a}\right)$$

44. $$\int \frac{\sqrt{a^2 \pm x^2}}{x}\,dx = \sqrt{a^2 \pm x^2} - a \log_e \frac{a + \sqrt{a^2 \pm x^2}}{x}$$

45. $$\int \frac{\sqrt{x^2 - a^2}}{x}\,dx = \sqrt{x^2 - a^2} - a \cos^{-1}\frac{a}{x}$$

46. $$\int \frac{\sqrt{x^2 \pm a^2}}{x^2}\,dx = -\frac{\sqrt{x^2 \pm a^2}}{x} + \log_e (x + \sqrt{x^2 \pm a^2})$$

47. $$\int \frac{\sqrt{a^2 - x^2}}{x^2}\,dx = -\frac{\sqrt{a^2 - x^2}}{x} - \sin^{-1}\frac{x}{a}$$

48. $$\int \frac{x\,dx}{\sqrt{a^2 - x^2}} = -\sqrt{a^2 - x^2}$$

49. $$\int \frac{x\,dx}{\sqrt{x^2 \pm a^2}} = \sqrt{x^2 \pm a^2}$$

50. $$\int \frac{x^2\,dx}{\sqrt{x^2 \pm a^2}} = \frac{x}{2}\sqrt{x^2 \pm a^2} \mp \frac{a^2}{2}\log_e (x + \sqrt{x^2 \pm a^2})$$

51. $$\int \frac{x^2\,dx}{\sqrt{a^2 - x^2}} = -\frac{x}{2}\sqrt{a^2 - x^2} + \frac{a^2}{2}\sin^{-1}\frac{x}{a}$$

52. $$\int \frac{dx}{x\sqrt{x^2 - a^2}} = \frac{1}{a}\cos^{-1}\frac{a}{x}$$

53. $$\int \frac{dx}{x\sqrt{a^2 \pm x^2}} = -\frac{1}{a}\log_e\left(\frac{a + \sqrt{a^2 \pm x^2}}{x}\right)$$

Integral calculus *continued*

54. $$\int \frac{dx}{x^2\sqrt{x^2 \pm a^2}} = \pm \frac{\sqrt{x^2 \pm a^2}}{a^2x}$$

55. $$\int \frac{dx}{x^2\sqrt{a^2 - x^2}} = -\frac{\sqrt{a^2 - x^2}}{a^2x}$$

56. $$\int \sqrt{(x^2 \pm a^2)^3}\,dx = \tfrac{1}{4}\left[x\sqrt{(x^2 \pm a^2)^3} \pm \frac{3a^2x}{2}\sqrt{x^2 \pm a^2} + \frac{3a^4}{2}\log_e (x + \sqrt{x^2 \pm a^2})\right]$$

57. $$\int \sqrt{(a^2 - x^2)^3}\,dx = \tfrac{1}{4}\left[x\sqrt{(a^2 - x^2)^3} + \frac{3a^2x}{2}\sqrt{a^2 - x^2} + \frac{3a^4}{2}\sin^{-1}\frac{x}{a}\right]$$

58. $$\int \frac{dx}{\sqrt{(x^2 \pm a^2)^3}} = \frac{\pm x}{a^2\sqrt{x^2 \pm a^2}}$$

59. $$\int \frac{dx}{\sqrt{(a^2 - x^2)^3}} = \frac{x}{a^2\sqrt{a^2 - x^2}}$$

Integrals involving $\sqrt{ax^2 + bx + c}$

Let $X = ax^2 + bx + c$ and $q = b^2 - 4ac$

60. $$\int \frac{dx}{\sqrt{X}} = \frac{1}{\sqrt{a}}\log_e\left(\sqrt{X} + \frac{2ax + b}{2\sqrt{a}}\right), \quad a > 0$$

$$= \frac{1}{\sqrt{-a}}\sin^{-1}\frac{(-2ax - b)}{\sqrt{q}}, \quad a < 0$$

61. $$\int \frac{x\,dx}{\sqrt{X}} = \frac{\sqrt{X}}{a} - \frac{b}{2a}\int \frac{dx}{\sqrt{X}}$$

62. $$\int \frac{x^2dx}{\sqrt{X}} = \frac{(2ax - 3b)\sqrt{X}}{4a^2} + \frac{3b^2 - 4ac}{8a^2}\int \frac{dx}{\sqrt{X}}$$

63. $$\int \frac{dx}{x\sqrt{X}} = -\frac{1}{\sqrt{c}}\log_e\left(\frac{\sqrt{X} + \sqrt{c}}{x} + \frac{b}{2\sqrt{c}}\right), \quad c > 0$$

Integral calculus *continued*

64. $$\int \frac{dx}{x\sqrt{X}} = \frac{1}{\sqrt{-c}} \sin^{-1} \frac{bx + 2c}{x\sqrt{q}}, \quad c < 0$$

65. $$\int \frac{dx}{x\sqrt{X}} = -\frac{2\sqrt{X}}{bx}, \quad c = 0$$

66. $$\int \frac{dx}{(mx + n)\sqrt{X}} = \frac{1}{\sqrt{k}} \log_e \left[\frac{\sqrt{k} - m\sqrt{X}}{mx + n} + \frac{bm - 2an}{2\sqrt{k}}\right], \quad k > 0$$

$$= \frac{1}{\sqrt{-k}} \sin^{-1} \left[\frac{(bm - 2an)(mx + n) + 2k}{m(mx + n)\sqrt{q}}\right], \quad k < 0$$

67. $$\int \frac{dx}{(mx + n)\sqrt{X}} = -\frac{2m\sqrt{X}}{(bm - 2an)(mx + n)}, \quad k = 0$$

where $k = an^2 - bmn + cm^2$.

68. $$\int \frac{dx}{x^2\sqrt{X}} = -\frac{\sqrt{X}}{cx} - \frac{b}{2c} \int \frac{dx}{x\sqrt{X}}$$

69. $$\int \sqrt{X}\, dx = \frac{(2ax + b)\sqrt{X}}{4a} - \frac{q}{8a} \int \frac{dx}{\sqrt{X}}$$

70. $$\int x\sqrt{X}\, dx = \frac{X\sqrt{X}}{3a} - \frac{b(2ax + b)\sqrt{X}}{8a^2} + \frac{bq}{16a^2} \int \frac{dx}{\sqrt{X}}$$

71. $$\int x^2\sqrt{X}\, dx = \frac{(6ax - 5b)X\sqrt{X}}{24a^2} + \frac{(5b^2 - 4ac)(2ax + b)\sqrt{X}}{64a^3} - \frac{(5b^2 - 4ac)q}{128a^3} \int \frac{dx}{\sqrt{X}}$$

72. $$\int \frac{\sqrt{X}\, dx}{x} = \sqrt{X} + \frac{b}{2} \int \frac{dx}{\sqrt{X}} + c \int \frac{dx}{x\sqrt{X}}$$

73. $$\int \frac{\sqrt{X}\, dx}{mx + n} = \frac{\sqrt{X}}{m} + \frac{bm - 2an}{2m^2} \int \frac{dx}{\sqrt{X}} + \frac{an^2 - bmn + cm^2}{m^2} \int \frac{dx}{(mx + n)\sqrt{X}}$$

Integral calculus *continued*

74. $$\int \frac{\sqrt{X}\,dx}{x^2} = -\frac{\sqrt{X}}{x} + \frac{b}{2}\int \frac{dx}{x\sqrt{X}} + a\int \frac{dx}{\sqrt{X}}$$

75. $$\int \frac{dx}{X\sqrt{X}} = -\frac{2(2ax+b)}{q\sqrt{X}}$$

76. $$\int X\sqrt{X}\,dx = \frac{2(2ax+b)\,X\sqrt{X}}{8a} - \frac{3q(2ax+b)\sqrt{X}}{64a^2} + \frac{3q^2}{128a^2}\int \frac{dx}{\sqrt{X}}$$

Miscellaneous irrational integrals

77. $$\int \sqrt{2ax - x^2}\,dx = \frac{x-a}{2}\sqrt{2ax-x^2} + \frac{a^2}{2}\sin^{-1}\frac{x-a}{a}$$

78. $$\int \frac{dx}{\sqrt{2ax - x^2}} = \cos^{-1}\frac{a-x}{a}$$

79. $$\int \sqrt{\frac{mx+n}{ax+b}}\,dx = \int \frac{(mx+n)\,dx}{\sqrt{amx^2 + (bm+an)\,x + bn}}$$

Logarithmic integrals

80. $$\int \log_a x\,dx = x\log_a \frac{x}{a}$$

81. $$\int \log_e x\,dx = x(\log_e x - 1)$$

82. $$\int x^m \log_a x\,dx = x^{m+1}\left(\frac{\log_a x}{m+1} - \frac{\log_a e}{(m+1)^2}\right)$$

83. $$\int x^m \log_e x\,dx = x^{m+1}\left(\frac{\log_e x}{m+1} - \frac{1}{(m+1)^2}\right)$$

Exponential integrals

84. $$\int a^x\,dx = \frac{a^x}{\log_e a}$$

85. $$\int e^x\,dx = e^x$$

Integral calculus *continued*

86. $\int xe^x\,dx = e^x(x-1)$

87. $\int x^m e^x\,dx = x^m e^x - m\int x^{m-1}e^x\,dx$

Trigonometric integrals

In these equations m and n are *positive integers* unless otherwise indicated, and r and s are any integers.

88. $\int \sin x\,dx = -\cos x$

89. $\int \sin^2 x\,dx = \frac{1}{2}(x - \sin x\cos x)$

90. $\int \sin^n x\,dx = -\frac{\sin^{n-1}x\cos x}{n} + \frac{n-1}{n}\int \sin^{n-2}x\,dx$

91. $\int \frac{dx}{\sin^n x} = -\frac{\cos x}{(n-1)\sin^{n-1}x} + \frac{n-2}{n-1}\int \frac{dx}{\sin^{n-2}x}, \quad n \neq 1$

92. $\int \cos x\,dx = \sin x$

93. $\int \cos^2 x\,dx = \frac{1}{2}(x + \sin x\cos x)$

94. $\int \cos^n x\,dx = \frac{\cos^{n-1}x\sin x}{n} + \frac{n-1}{n}\int \cos^{n-2}x\,dx$

95. $\int \frac{dx}{\cos^n x} = \frac{\sin x}{(n-1)\cos^{n-1}x} + \frac{n-2}{n-1}\int \frac{dx}{\cos^{n-2}x}, \quad n \neq 1$

96. $\int \sin^n x\cos x\,dx = \frac{\sin^{n+1}x}{n+1}$

97. $\int \cos^n x\sin x\,dx = -\frac{\cos^{n+1}x}{n+1}$

Integral calculus *continued*

98. $\displaystyle\int \sin^2 x \cos^2 x\, dx = \frac{4x - \sin 4x}{32}$

99. $\displaystyle\int \frac{dx}{\sin x \cos x} = \log_e \tan x$

100. $$\int \sin^r x \cos^s x\, dx = \frac{\cos^{s-1} x \sin^{r+1} x}{r+s} + \frac{s-1}{r+s} \int \sin^r x \cos^{s-2} x\, dx, \quad r+s \neq 0$$

$$= -\frac{\sin^{r-1} x \cos^{s+1} x}{r+s} + \frac{r-1}{r+s} \int \sin^{r-2} x \cos^s x\, dx, \quad r+s \neq 0$$

$$= \frac{\sin^{r+1} x \cos^{s+1} x}{r+1} + \frac{s+r+2}{r+1} \int \sin^{r+2} x \cos^s x\, dx, \quad r \neq -1$$

$$= -\frac{\sin^{r+1} x \cos^{s+1} x}{s+1} + \frac{s+r+2}{s+1} \int \sin^r x \cos^{s+2} x\, dx, \quad s \neq -1$$

101. $\displaystyle\int \tan x\, dx = -\log_e \cos x$

102. $\displaystyle\int \tan^n x\, dx = \frac{\tan^{n-1} x}{n-1} - \int \tan^{n-2} x\, dx$

103. $\displaystyle\int \cot x\, dx = \log_e \sin x$

104. $\displaystyle\int \cot^n x\, dx = -\frac{\cot^{n-1} x}{n-1} - \int \cot^{n-2} x\, dx$

105. $\displaystyle\int \sec x\, dx = \log_e (\sec x + \tan x)$

106. $\displaystyle\int \sec^2 x\, dx = \tan x$

107. $\displaystyle\int \sec^n x\, dx = \frac{\sin x}{(n-1)\cos^{n-1} x} + \frac{n-2}{n-1} \int \sec^{n-2} x\, dx, \quad n \neq 1$

Integral calculus *continued*

108. $\int \csc^2 x\,dx = -\cot x$

109. $\int \csc x\,dx = \log_e (\csc x - \cot x)$

110. $\int \csc^n x\,dx = \dfrac{\cos x}{(n-1)\sin^{n-1} x} + \dfrac{n-2}{n-1}\int \csc^{n-2} x\,dx, \quad n \neq 1$

111. $\int \sec^n x \tan x\,dx = \dfrac{\sec^n x}{n}$

112. $\int \csc^n x \cot x\,dx = -\dfrac{\csc^n x}{n}$

n *is any constant* $\neq 0$ (111–112)

113. $\int \tan^n x \sec^2 x\,dx = \dfrac{\tan^{n+1} x}{n+1}$

114. $\int \cot^n x \csc^2 x\,dx = -\dfrac{\cot^{n+1} x}{n+1}$

n *is any constant* $\neq -1$ (113–114)

115. $$\int \frac{dx}{a + b\sin x} = \frac{-1}{\sqrt{a^2 - b^2}} \sin^{-1} \frac{b + a\sin x}{a + b\sin x}, \qquad a^2 > b^2$$

$$= \frac{+1}{\sqrt{b^2 - a^2}} \log_e \frac{b + a\sin x - \sqrt{b^2 - a^2}\,(\cos x)}{a + b\sin x}, \qquad b^2 > a^2$$

116. $$\int \frac{dx}{a + b\cos x} = -\frac{1}{\sqrt{a^2 - b^2}} \sin^{-1}\left(\frac{b + a\cos x}{a + b\cos x}\right), \qquad a > b > 0$$

$$= \frac{1}{\sqrt{a^2 - b^2}} \cdot \sin^{-1}\left(\frac{\sqrt{a^2 - b^2} \cdot \sin x}{a + b\cos x}\right), \quad a > b > 0$$

$$= \frac{1}{\sqrt{a^2 - b^2}} \cdot \tan^{-1}\left(\frac{\sqrt{a^2 - b^2} \cdot \sin x}{b + a\cos x}\right), \quad a > b > 0$$

$$= \frac{1}{\sqrt{b^2 - a^2}} \log_e \left(\frac{b + a\cos x + \sqrt{b^2 - a^2}\sin x}{a + b\cos x}\right)$$

when $b^2 > a^2$, $a < 0$

117. $\int \sqrt{1 - \cos x}\,dx = -2\sqrt{2}\cos\frac{x}{2}$

Integral calculus *continued*

118. $\int \sqrt{(1-\cos x)^3}\,dx = \frac{4\sqrt{2}}{3}\left(\cos^3\frac{x}{2} - 3\cos\frac{x}{2}\right)$

119. $\int x \sin x\,dx = \sin x - x\cos x$

120. $\int x^2 \sin x\,dx = 2x\sin x + (2 - x^2)\cos x$

121. $\int x\cos x\,dx = \cos x + x\sin x$

122. $\int x^2\cos x\,dx = 2x\cos x + (x^2 - 2)\sin x$

123. $\int x\sin nx\,dx = \frac{\sin nx}{n^2} - \frac{x\cos nx}{n}$

124. $\int x\cos nx\,dx = \frac{\cos nx}{n^2} + \frac{x\sin nx}{n}$

125. $\int x^2\sin nx\,dx = \frac{2x\sin nx}{n^2} - \left(\frac{x^2}{n} - \frac{2}{n^3}\right)\cos nx$

126. $\int x^2\cos nx\,dx = \frac{2x\cos nx}{n^2} - \left(\frac{x^2}{n} - \frac{2}{n^3}\right)\sin nx$

Inverse trigonometric integrals

127. $\int \sin^{-1} x\,dx = x\sin^{-1} x + \sqrt{1 - x^2}$

128. $\int \cos^{-1} x\,dx = x\cos^{-1} x - \sqrt{1 - x^2}$

129. $\int \tan^{-1} x\,dx = x\tan^{-1} x - \log_e \sqrt{1 + x^2}$

130. $\int \cot^{-1} x\,dx = x\cot^{-1} x + \log_e \sqrt{1 + x^2}$

131. $\int \sec^{-1} x\,dx = x\sec^{-1} x - \log_e (x + \sqrt{x^2 - 1})$
$= x\sec^{-1} x - \cosh^{-1} x$

132. $\int \csc^{-1} x\,dx = x\csc^{-1} x + \log_e (x + \sqrt{x^2 - 1})$
$= x\csc^{-1} x + \cosh^{-1} x$

Integral calculus *continued*

Definite integrals

133. $\int_0^\infty \frac{a\,dx}{a^2+x^2} = \frac{\pi}{2}$, if $a > 0$; $= 0$, if $a = 0$; $= -\frac{\pi}{2}$, if $a < 0$

134. $\int_0^\infty x^{n-1} e^{-x}\,dx = \int_0^1 \left[\log \frac{1}{x}\right]^{n-1} dx \equiv \Gamma(n)$ (*)

135. $\int_0^1 x^{m-1}(1-x)^{n-1}\,dx = \int_0^\infty \frac{x^{m-1}\,dx}{(1+x)^{m+n}} = \frac{\Gamma(m)\,\Gamma(n)}{\Gamma(m+n)}$ (*)

136. $\int_0^{\frac{\pi}{2}} \sin^n x\,dx = \int_0^{\frac{\pi}{2}} \cos^n x\,dx = \frac{1}{2}\sqrt{\pi}\,\frac{\Gamma\left(\frac{n+1}{2}\right)}{\Gamma\left(\frac{n}{2}+1\right)}$, $n > -1$

137. $\int_0^\infty \frac{\sin mx\,dx}{x} = \frac{\pi}{2}$, if $m > 0$; $= 0$, if $m = 0$; $= -\frac{\pi}{2}$, if $m < 0$

138. $\int_0^\infty \frac{\sin x \cdot \cos mx\,dx}{x} = 0$, if $m < -1$ or $m > 1$;

$= \frac{\pi}{4}$, if $m = -1$ or $m = 1$; $= \frac{\pi}{2}$, if $-1 < m < 1$

139. $\int_0^\infty \frac{\sin^2 x\,dx}{x^2} = \frac{\pi}{2}$

140. $\int_0^\infty \cos(x^2)\,dx = \int_0^\infty \sin(x^2)\,dx = \frac{1}{2}\sqrt{\frac{\pi}{2}}$

141. $\int_0^\infty \frac{\cos mx\,dx}{1+x^2} = \frac{\pi}{2} \cdot e^{-m}$, $m > 0$

142. $\int_0^\infty \frac{\cos x\,dx}{\sqrt{x}} = \int_0^\infty \frac{\sin x\,dx}{\sqrt{x}} = \sqrt{\frac{\pi}{2}}$

143. $\int_0^\infty e^{-a^2x^2}\,dx = \frac{1}{2a}\sqrt{\pi} = \frac{1}{2a}\Gamma(\frac{1}{2})$, $a > 0$ (*)

144. $\int_0^\infty x^{2n} e^{-ax^2}\,dx = \frac{1 \cdot 3 \cdot 5 \cdots (2n-1)}{2^{n+1} a^n}\sqrt{\frac{\pi}{a}}$

145. $\int_0^\infty e^{-x^2-a^2/x^2}\,dx = \frac{e^{-2a}\sqrt{\pi}}{2}$, $a > 0$

* $\Gamma(n)$ = gamma function

Integral calculus *continued*

146. $\int_0^\infty e^{-nx}\sqrt{x}\,dx = \frac{1}{2n}\sqrt{\frac{\pi}{n}}$

147. $\int_0^\infty \frac{e^{-nx}}{\sqrt{x}}\,dx = \sqrt{\frac{\pi}{n}}$

148. $\int_0^\infty e^{-a^2x^2}\cos bx\,dx = \frac{\sqrt{\pi}\cdot e^{-b^2/4a^2}}{2a}, \quad a > 0$

149. $\int_0^1 \frac{\log_e x}{1-x}\,dx = -\frac{\pi^2}{6}$

150. $\int_0^1 \frac{\log_e x}{1+x}\,dx = -\frac{\pi^2}{12}$

151. $\int_0^1 \frac{\log_e x}{1-x^2}\,dx = -\frac{\pi^2}{8}$

152. $\int_0^1 \log_e\left(\frac{1+x}{1-x}\right)\cdot\frac{dx}{x} = \frac{\pi^2}{4}$

153. $\int_0^1 \frac{\log_e x\,dx}{\sqrt{1-x^2}} = -\frac{\pi}{2}\log_e 2$

154. $\int_0^1 \frac{(x^p - x^q)\,dx}{\log_e x} = \log_e \frac{p+1}{q+1}, \; p+1 > 0,\; q+1 > 0$

155. $\int_0^1 (\log_e x)^n\,dx = (-1)^n \cdot n!$

156. $\int_0^1 \frac{dx}{\sqrt{\log_e\left(\frac{1}{x}\right)}} = \sqrt{\pi}$

157. $\int_0^1 x^m\left(\log_e \frac{1}{x}\right)^n dx = \frac{\Gamma(n+1)}{(m+1)^{n+1}}, \; m+1 > 0,\; n+1 > 0$ (*)

158. $\int_0^\infty \log_e\left(\frac{e^x+1}{e^x-1}\right)dx = \frac{\pi^2}{4}$

159. $\int_0^{\frac{\pi}{2}} \log_e \sin x\,dx = \int_0^{\frac{\pi}{2}} \log_e \cos x\,dx = -\frac{\pi}{2}\log_e 2$

* $\Gamma(n)$ = gamma function.

Integral calculus *continued*

160. $\int_0^{\pi} x \cdot \log_e \sin x \, dx = -\frac{\pi^2}{2} \log_e 2$

161. $\int_0^{\pi} \log_e (a \pm b \cos x)\, dx = \pi \log_e \left(\frac{a + \sqrt{a^2 - b^2}}{2}\right), \quad a \geqslant b$

162. $\int_{-\frac{\pi}{2}}^{\frac{\pi}{2}} \frac{\cos^2 \left(\frac{\pi}{2} \sin x\right) dx}{\cos x} = 1.22$

Table of Laplace transforms

Symbols

Constants are real unless otherwise specified.

$R(x)$ = "real part of x"
$j = \sqrt{-1}$
$f(t) = 0,\ t < 0$
$S_{-1}(t)$ = unit step, or Heaviside function
$= 0,\ t < 0$
$= 1,\ t > 0$
$S_0(t)$ = unit impulse, also called Dirac δ function
$= 0,\ t < 0$
$= 0,\ t > 0$
$= \infty$, if $t = 0$, and $\int_{-\infty}^{+\infty} S_0(t)\, dt = 1$

$$\int_{-\infty}^{+\infty} f(t)\, S_0(t)\, dt = f(0)$$

$\omega = 2\pi \times$ frequency
m,k = any positive integers
γ = period of a periodic function $(t > 0)$
$\Gamma(x)$ = gamma function
$= \int_0^{\infty} e^{-u} u^{x-1}\, du$
$\Gamma(k) = (k-1)!$, k = positive integer
$J_0(x)$ = Bessel function, first kind, zero order
$J_k(x)$ = Bessel function, first kind, kth order

Table of Laplace transforms *continued*

time function	transform
1. Definition $f(t)$	$F(p) = \int_0^\infty f(\lambda) e^{-p\lambda} d\lambda$, $R(p) > 0$
2. Inverse transform $f(t) = \frac{1}{j2\pi} \int_{c-j\infty}^{c+j\infty} F(z) e^{zt} dz$, $c > 0$ Note: No singularities to the right of path of integration.	$F(p)$
3. Shifting theorem $f(t-a)$	$e^{-ap} F(p)$, $a > 0$ (*)
4. Borel, or "convolution" theorem $\int_0^t f_1(\lambda) f_2(t-\lambda) d\lambda$	$F_1(p)\, F_2(p)$ (*)
5. Periodic function $f(t) = f(t - k\gamma)$, $t > k\gamma$	$\dfrac{\int_0^\gamma f(\lambda) e^{-p\lambda}\, d\lambda}{1 - e^{-p\gamma}}$
6. $f_1(t) + f_2(t)$	$F_1(p) + F_2(p)$ (*)
7. $\sum_{k=1}^{m} f_k(t)$	$\sum_{k=1}^{m} F_k(p)$ (*)
8. $f(t) e^{-at}$	$F(p + a)$ (*)
9. $f\left(\frac{t}{a}\right)$; a real, >0	$aF(ap)$ (*)
10. Derivative $\frac{d}{dt} f(t)$	$-f(0) + pF(p)$ (*)
11. Integral $\int f(t)\, dt$	$\frac{1}{p}\left[\int f\, dt\right]_{t=0} + \frac{F(p)}{p}$ (*)

* See pair 1 for definition of F.

Table of Laplace transforms *continued*

time function	transform
12. Unit step $S_{-1}(t)$	$\dfrac{1}{p}$
13. Unit impulse $S_0(t)$	1
14. Unit cisoid $e^{j\omega t}$	$\dfrac{1}{p - j\omega}$
15. t	$\dfrac{1}{p^2}$
16. t^k	$\dfrac{k!}{p^{k+1}}$
17. t^v, $R(v) > -1$	$\dfrac{\Gamma(v+1)}{p^{v+1}}$
18. $t^k e^{-at}$	$\dfrac{k!}{(p+a)^{k+1}}$
19. $1/\sqrt{\pi t}$	$1/\sqrt{p}$
20. $\dfrac{(2t)^k}{1\cdot 3\cdot 5 \cdots (2k-1)\sqrt{\pi t}}$	$\dfrac{1}{p^k\sqrt{p}}$
21. e^{at}	$\dfrac{1}{p-a}$
22. $\dfrac{1}{a}(e^{at}-1)$	$\dfrac{1}{p(p-a)}$
23. $\sin at$	$\dfrac{a}{p^2+a^2}$
24. $\cos at$	$\dfrac{p}{p^2+a^2}$
25. $J_0(at)$	$\dfrac{1}{\sqrt{p^2+a^2}}$
26. $J_k(at)$	$\dfrac{1}{r}\left(\dfrac{r-p}{a}\right)^k, \quad r^2 = p^2 + a^2$

Series

Maclaurin's theorem

$$f(x) = f(0) + xf'(0) + \frac{x^2}{2!} f''(0) + \ldots + \frac{x^n}{n!} f^n(0) + \ldots$$

Taylor's theorem

$$f(x) = f(x_0) + f'(x_0)(x - x_0) + \frac{f''(x_0)}{2!}(x - x_0)^2 + \ldots$$

$$f(x + h) = f(x) + f'(x) \cdot h + \frac{f''(x)}{2!} h^2 + \ldots + \frac{f^n(x)}{n!} h^n + \ldots$$

Miscellaneous

$$(1 \pm x)^n = 1 \pm nx + \frac{n(n-1)}{2!} x^2 \pm \frac{n(n-1)(n-2)}{3!} x^3 + \ldots$$

$$\log_e (1 + x) = x - \frac{x^2}{2} + \frac{x^3}{3} - \frac{x^4}{4} + \ldots, \quad |x| < 1$$

$$e^x = 1 + x + \frac{x^2}{2!} + \frac{x^3}{3!} + \ldots, \quad |x| < \infty$$

$$\left.\begin{aligned} \sin x &= x - \frac{x^3}{3!} + \frac{x^5}{5!} - \frac{x^7}{7!} + \ldots \\ \cos x &= 1 - \frac{x^2}{2!} + \frac{x^4}{4!} - \frac{x^6}{6!} + \ldots \end{aligned}\right\} |x| < \infty;\ x \text{ in radians}$$

See p. 1043 for accuracy of first-term approximation.

$$\left.\begin{aligned} \sinh x &= x + \frac{x^3}{3!} + \frac{x^5}{5!} + \frac{x^7}{7!} + \ldots \\ \cosh x &= 1 + \frac{x^2}{2!} + \frac{x^4}{4!} + \frac{x^6}{6!} + \ldots \end{aligned}\right\} |x| < \infty$$

$$\tan x = x + \frac{x^3}{3} + \frac{2x^5}{15} + \frac{17x^7}{315} + \frac{62x^9}{2835} + \ldots, \quad |x| < \frac{\pi}{2}$$

$$\cot x = \frac{1}{x} - \frac{x}{3} - \frac{x^3}{45} - \frac{2x^5}{945} - \frac{x^7}{4725} - \ldots, \quad |x| < \pi$$

$$\arcsin x = x + \frac{1}{2}\frac{x^3}{3} + \frac{1 \cdot 3}{2 \cdot 4}\frac{x^5}{5} + \frac{1 \cdot 3 \cdot 5}{2 \cdot 4 \cdot 6}\frac{x^7}{7} + \ldots, \quad |x| < 1$$

Series *continued*

$$\text{arc tan } x = x - \frac{x^3}{3} + \frac{x^5}{5} - \frac{x^7}{7} + \ldots, \qquad |x| < 1$$

$$\text{arc sinh } x = x - \frac{1}{2}\frac{x^3}{3} + \frac{1\cdot 3}{2\cdot 4}\frac{x^5}{5} - \frac{1\cdot 3\cdot 5}{2\cdot 4\cdot 6}\frac{x^7}{7} + \ldots, \quad |x| < 1$$

$$\text{arc tanh } x = x + \frac{x^3}{3} + \frac{x^5}{5} + \frac{x^7}{7} + \ldots, \qquad |x| < 1$$

For $n = 0$ or a positive integer, the expansion of the Bessel function of the first kind, nth order, is given by the convergent series,

$$J_n(x) = \frac{x^n}{2^n n!}\left[1 - \frac{x^2}{2\,(2n+2)} + \frac{x^4}{2\cdot 4\,(2n+2)\,(2n+4)} - \frac{x^6}{2\cdot 4\cdot 6\,(2n+2)\,(2n+4)\,(2n+6)} + \ldots\right]$$

and

$$J_{-n}(x) = (-1)^n J_n(x)$$

Note: $0! = 1$

Vector-analysis formulas

Rectangular coordinates

In the following, vectors are indicated in **bold-faced** type.

Associative law: For addition

$$\mathbf{a} + (\mathbf{b} + \mathbf{c}) = (\mathbf{a} + \mathbf{b}) + \mathbf{c} = \mathbf{a} + \mathbf{b} + \mathbf{c}$$

Commutative law: For addition

$$\mathbf{a} + \mathbf{b} = \mathbf{b} + \mathbf{a}$$

where

$\mathbf{a} = a\mathbf{a}_1$

a = magnitude of $\mathbf{a}$

$\mathbf{a}_1$ = unit vector in direction of $\mathbf{a}$

Scalar, or "dot" product

$$\mathbf{a}\cdot\mathbf{b} = \mathbf{b}\cdot\mathbf{a}$$

$$= ab\cos\theta$$

where θ = angle included by $\mathbf{a}$ and $\mathbf{b}$.

Vector-analysis formulas *continued*

Vector, or "cross" product

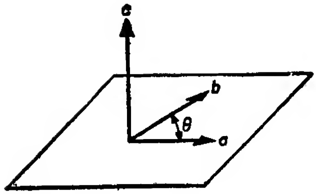

$$\boldsymbol{a} \times \boldsymbol{b} = -\boldsymbol{b} \times \boldsymbol{a}$$
$$= ab \sin \theta \cdot \boldsymbol{c}_1$$

where

θ = smallest angle swept in rotating $\boldsymbol{a}$ into $\boldsymbol{b}$

$\boldsymbol{c}_1$ = unit vector perpendicular to plane of $\boldsymbol{a}$ and $\boldsymbol{b}$, and directed in the sense of travel of a right-hand screw rotating from $\boldsymbol{a}$ to $\boldsymbol{b}$ through the angle θ.

Distributive law for scalar multiplication

$$\boldsymbol{a} \cdot (\boldsymbol{b} + \boldsymbol{c}) = \boldsymbol{a} \cdot \boldsymbol{b} + \boldsymbol{a} \cdot \boldsymbol{c}$$

Distributive law for vector multiplication

$$\boldsymbol{a} \times (\boldsymbol{b} + \boldsymbol{c}) = \boldsymbol{a} \times \boldsymbol{b} + \boldsymbol{a} \times \boldsymbol{c}$$

Scalar triple product

$$\boldsymbol{a} \cdot (\boldsymbol{b} \times \boldsymbol{c}) = (\boldsymbol{a} \times \boldsymbol{b}) \cdot \boldsymbol{c} = \boldsymbol{c} \cdot (\boldsymbol{a} \times \boldsymbol{b}) = \boldsymbol{b} \cdot (\boldsymbol{c} \times \boldsymbol{a})$$

Vector triple product

$$\boldsymbol{a} \times (\boldsymbol{b} \times \boldsymbol{c}) = (\boldsymbol{a} \cdot \boldsymbol{c})\boldsymbol{b} - (\boldsymbol{a} \cdot \boldsymbol{b})\boldsymbol{c}$$
$$(\boldsymbol{a} \times \boldsymbol{b}) \cdot (\boldsymbol{c} \times \boldsymbol{d}) = (\boldsymbol{a} \cdot \boldsymbol{c})(\boldsymbol{b} \cdot \boldsymbol{d}) - (\boldsymbol{a} \cdot \boldsymbol{d})(\boldsymbol{b} \cdot \boldsymbol{c})$$
$$(\boldsymbol{a} \times \boldsymbol{b}) \times (\boldsymbol{c} \times \boldsymbol{d}) = (\boldsymbol{a} \times \boldsymbol{b} \cdot \boldsymbol{d})\boldsymbol{c} - (\boldsymbol{a} \times \boldsymbol{b} \cdot \boldsymbol{c})\boldsymbol{d}$$

∇ = operator "del"

$$\equiv \boldsymbol{i} \frac{\partial}{\partial x} + \boldsymbol{j} \frac{\partial}{\partial y} + \boldsymbol{k} \frac{\partial}{\partial z}$$

where $\boldsymbol{i}, \boldsymbol{j}, \boldsymbol{k}$ are unit vectors in directions of x, y, z coordinates, respectively.

$$\text{grad } \phi = \nabla\phi = \boldsymbol{i} \frac{\partial \phi}{\partial x} + \boldsymbol{j} \frac{\partial \phi}{\partial y} + \boldsymbol{k} \frac{\partial \phi}{\partial z}$$

$$\text{grad } (\phi + \psi) = \text{grad } \phi + \text{grad } \psi$$
$$\text{grad } (\phi\psi) = \phi \text{ grad } \psi + \psi \text{ grad } \phi$$
$$\text{curl grad } \phi = 0$$
$$\text{div } \boldsymbol{a} = \nabla \cdot \boldsymbol{a} = \frac{\partial a_x}{\partial x} + \frac{\partial a_y}{\partial y} + \frac{\partial a_z}{\partial z}$$

Vector-analysis formulas *continued*

where a_x, a_y, a_z are the components of $\boldsymbol{a}$ in the directions of the respective coordinate axes.

$$\operatorname{div}(\boldsymbol{a}+\boldsymbol{b}) = \operatorname{div}\boldsymbol{a} + \operatorname{div}\boldsymbol{b}$$

$$\begin{aligned}\operatorname{curl}\boldsymbol{a} &= \nabla \times \boldsymbol{a}\\ &= \boldsymbol{i}\left(\frac{\partial a_z}{\partial y} - \frac{\partial a_y}{\partial z}\right) + \boldsymbol{j}\left(\frac{\partial a_x}{\partial z} - \frac{\partial a_z}{\partial x}\right) + \boldsymbol{k}\left(\frac{\partial a_y}{\partial x} - \frac{\partial a_x}{\partial y}\right)\\ &= \begin{vmatrix} \boldsymbol{i} & \boldsymbol{j} & \boldsymbol{k} \\ \dfrac{\partial}{\partial x} & \dfrac{\partial}{\partial y} & \dfrac{\partial}{\partial z} \\ a_x & a_y & a_z \end{vmatrix}\end{aligned}$$

$$\operatorname{curl}(\phi\boldsymbol{a}) = \operatorname{grad}\phi \times \boldsymbol{a} + \phi \operatorname{curl}\boldsymbol{a}$$

$$\operatorname{div}\operatorname{curl}\boldsymbol{a} = 0$$

$$\operatorname{div}(\boldsymbol{a}\times\boldsymbol{b}) = \boldsymbol{b}\cdot\operatorname{curl}\boldsymbol{a} - \boldsymbol{a}\cdot\operatorname{curl}\boldsymbol{b}$$

$\nabla^2 \equiv$ Laplacian

$$\nabla^2\phi = \frac{\partial^2\phi}{\partial x^2} + \frac{\partial^2\phi}{\partial y^2} + \frac{\partial^2\phi}{\partial z^2}$$

in rectangular coordinates.

$$\operatorname{curl}\operatorname{curl}\boldsymbol{a} = \operatorname{grad}\operatorname{div}\boldsymbol{a} - (\boldsymbol{i}\nabla^2 a_x + \boldsymbol{j}\nabla^2 a_y + \boldsymbol{k}\nabla^2 a_z)$$

In the following formulas τ is a volume bounded by a closed surface S. The unit vector $\boldsymbol{n}$ is normal to the surface S and directed positively outwards.

$$\int_\tau \nabla\phi\cdot d\tau = \int_S \phi\,\boldsymbol{n}\,dS$$

$$\int_\tau \nabla\cdot\boldsymbol{a}\,d\tau = \int_S \boldsymbol{a}\cdot\boldsymbol{n}\,dS \quad \text{(Gauss' theorem)}$$

$$\int_\tau \nabla\times\boldsymbol{a}\,d\tau = \int_S \boldsymbol{n}\times\boldsymbol{a}\,dS$$

$$\int_\tau (\psi\,\nabla^2\phi - \phi\,\nabla^2\psi)\,d\tau = \int_S\left(\psi\frac{\partial\phi}{\partial n} - \phi\frac{\partial\psi}{\partial n}\right)dS$$

where $\partial/\partial n$ is the derivative in the direction of the positive normal to S (Green's theorem).

Vector-analysis formulas *continued*

In the two following formulas S is an open surface bounded by a contour C, with distance along C represented by s.

$$\int_S \boldsymbol{n} \times \nabla\phi \, dS = \int_C \phi \, ds$$

$$\int_S \nabla \times \boldsymbol{a} \cdot \boldsymbol{n} \, dS = \int_C \boldsymbol{a} \cdot d\boldsymbol{s} \quad \text{(Stokes' theorem)}$$

where $\boldsymbol{s} = s\boldsymbol{s}_1$, and $\boldsymbol{s}_1$ is a unit vector in the direction of s.

Gradient, divergence, curl, and Laplacian in coordinate systems other than rectangular

Cylindrical coordinates: (ρ, ϕ, z), unit vectors $\boldsymbol{\rho}_1$, $\boldsymbol{\phi}_1$, $\boldsymbol{k}$, respectively,

$$\operatorname{grad} \psi = \nabla\psi = \frac{\partial\psi}{\partial\rho}\boldsymbol{\rho}_1 + \frac{1}{\rho}\frac{\partial\psi}{\partial\phi}\boldsymbol{\phi}_1 + \frac{\partial\psi}{\partial z}\boldsymbol{k}$$

$$\operatorname{div} \boldsymbol{a} = \nabla\cdot\boldsymbol{a} = \frac{1}{\rho}\frac{\partial}{\partial\rho}(\rho a_\rho) + \frac{1}{\rho}\left(\frac{\partial a_\phi}{\partial\phi}\right) + \frac{\partial a_z}{\partial z}$$

$$\operatorname{curl} \boldsymbol{a} = \nabla\times\boldsymbol{a} = \left(\frac{1}{\rho}\frac{\partial a_z}{\partial\phi} - \frac{\partial a_\phi}{\partial z}\right)\boldsymbol{\rho}_1 + \left(\frac{\partial a_\rho}{\partial z} - \frac{\partial a_z}{\partial\rho}\right)\boldsymbol{\phi}_1 + \left[\frac{1}{\rho}\frac{\partial}{\partial\rho}(\rho a_\phi) - \frac{1}{\rho}\frac{\partial a_\rho}{\partial\phi}\right]\boldsymbol{k}$$

$$\nabla^2\psi = \frac{1}{\rho}\frac{\partial}{\partial\rho}\left(\rho\frac{\partial\psi}{\partial\rho}\right) + \frac{1}{\rho^2}\frac{\partial^2\psi}{\partial\phi^2} + \frac{\partial^2\psi}{\partial z^2}$$

Spherical coordinates: (r, θ, ϕ), unit vectors $\boldsymbol{r}_1$, $\boldsymbol{\theta}_1$, $\boldsymbol{\phi}_1$

r = distance to origin
θ = polar angle
ϕ = azimuthal angle

$$\operatorname{grad} \psi = \nabla\psi = \frac{\partial\psi}{\partial r}\boldsymbol{r}_1 + \frac{1}{r}\frac{\partial\psi}{\partial\theta}\boldsymbol{\theta}_1 + \frac{1}{r\sin\theta}\frac{\partial\psi}{\partial\phi}\boldsymbol{\phi}_1$$

$$\operatorname{div} \boldsymbol{a} = \nabla\cdot\boldsymbol{a} = \frac{1}{r^2}\frac{\partial}{\partial r}(r^2 a_r) + \frac{1}{r\sin\theta}\frac{\partial}{\partial\theta}(a_\theta\sin\theta) + \frac{1}{r\sin\theta}\frac{\partial a_\phi}{\partial\phi}$$

$$\operatorname{curl} \boldsymbol{a} = \nabla\times\boldsymbol{a} = \frac{1}{r\sin\theta}\left[\frac{\partial}{\partial\theta}(a_\phi\sin\theta) - \frac{\partial a_\theta}{\partial\phi}\right]\boldsymbol{r}_1 + \frac{1}{r}\left[\frac{1}{\sin\theta}\frac{\partial a_r}{\partial\phi} - \frac{\partial}{\partial r}(r a_\phi)\right]\boldsymbol{\theta}_1 + \frac{1}{r}\left[\frac{\partial}{\partial r}(r a_\theta) - \frac{\partial a_r}{\partial\theta}\right]\boldsymbol{\phi}_1$$

Vector-analysis formulas *continued*

$$\nabla^2\psi = \frac{1}{r^2}\frac{\partial}{\partial r}\left(r^2\frac{\partial\psi}{\partial r}\right) + \frac{1}{r^2 \sin\theta}\frac{\partial}{\partial\theta}\left(\sin\theta\frac{\partial\psi}{\partial\theta}\right) + \frac{1}{r^2\sin^2\theta}\frac{\partial^2\psi}{\partial\phi^2}$$

Orthogonal curvilinear coordinates

Coordinates: u_1, u_2, u_3

Metric coefficients: h_1, h_2, h_3 $(ds^2 = h_1^2du_1^2 + h_2^2du_2^2 + h_3^2du_3^2)$

Unit vectors: $\mathbf{i}_1, \mathbf{i}_2, \mathbf{i}_3$ $(d\mathbf{s} = \mathbf{i}_1h_1du_1 + \mathbf{i}_2h_2du_2 + \mathbf{i}_3h_3du_3)$

$$\text{grad}\,\psi = \nabla\psi = \frac{1}{h_1}\frac{\partial\psi}{\partial u_1}\mathbf{i}_1 + \frac{1}{h_2}\frac{\partial\psi}{\partial u_2}\mathbf{i}_2 + \frac{1}{h_3}\frac{\partial\psi}{\partial u_3}\mathbf{i}_3$$

$$\text{div}\,\mathbf{a} = \nabla\cdot\mathbf{a} = \frac{1}{h_1h_2h_3}\left[\frac{\partial}{\partial u_1}(h_2h_3a_1) + \frac{\partial}{\partial u_2}(h_3h_1a_2) + \frac{\partial}{\partial u_3}(h_1h_2a_3)\right]$$

$$\begin{aligned}\text{curl}\,\mathbf{a} = \nabla\times\mathbf{a} &= \frac{1}{h_2h_3}\left[\frac{\partial}{\partial u_2}(h_3a_3) - \frac{\partial}{\partial u_3}(h_2a_2)\right]\mathbf{i}_1 \\ &\quad + \frac{1}{h_3h_1}\left[\frac{\partial}{\partial u_3}(h_1a_1) - \frac{\partial}{\partial u_1}(h_3a_3)\right]\mathbf{i}_2 \\ &\quad + \frac{1}{h_1h_2}\left[\frac{\partial}{\partial u_1}(h_2a_2) - \frac{\partial}{\partial u_2}(h_1a_1)\right]\mathbf{i}_3 \\ &= \frac{1}{h_1h_2h_3}\begin{vmatrix} h_1\mathbf{i}_1 & h_2\mathbf{i}_2 & h_3\mathbf{i}_3 \\ \dfrac{\partial}{\partial u_1} & \dfrac{\partial}{\partial u_2} & \dfrac{\partial}{\partial u_3} \\ h_1a_1 & h_2a_2 & h_3a_3\end{vmatrix}\end{aligned}$$

$$\nabla^2\psi = \frac{1}{h_1h_2h_3}\left[\frac{\partial}{\partial u_1}\left(\frac{h_2h_3}{h_1}\frac{\partial\phi}{\partial u_1}\right) + \frac{\partial}{\partial u_2}\left(\frac{h_3h_1}{h_2}\frac{\partial\phi}{\partial u_2}\right) + \frac{\partial}{\partial u_3}\left(\frac{h_1h_2}{h_3}\frac{\partial\phi}{\partial u_3}\right)\right]$$

Matrix algebra

Notations

A matrix of *order* $n \times m$ is a rectangular array of numbers consisting of n rows and m columns.

$$\begin{bmatrix} a_{11} & a_{12} & \cdots & a_{1j} & \cdots & a_{1m} \\ a_{21} & a_{22} & \cdots & a_{2j} & \cdots & a_{2m} \\ \cdots & \cdots & \cdots & \cdots & \cdots & \cdots \\ a_{i1} & a_{i2} & \cdots & a_{ij} & \cdots & a_{im} \\ a_{n1} & a_{n2} & \cdots & a_{nj} & \cdots & a_{nm} \end{bmatrix}$$

The element in row i and column j is designated by the subscripts ij in that order. When not written explicitly as above, a matrix can be noted by a single letter **A** or by its generic element between parenthesis (a_{ij}).

When $m = n$, the matrix is *square* and its order may be noted by n alone.

A matrix of order $n \times 1$ is a *vector* (or column vector) of dimension n. A matrix of order $1 \times n$ is a *row vector*. In both cases, the elements are called *coordinates* of the vector.

The *unit matrix* of order n is the square matrix

$\mathbf{1} = (\delta_{ij})$

where δ_{ij} is the *Kronecker index* equal to 1 for $j = i$ and otherwise equal to 0.

Operations

Illustrated for matrixes of order 2, pp. 1094–1097.

Sum and difference: The sum (or difference) of two matrixes **A** and **B**, of the same order $m \times n$, is a matrix **C**, of the same order, such that
$c_{ij} = a_{ij} \pm b_{ij}$

Multiplication by a number

$m\ (a_{ij}) = (m\ a_{ij})$

Matrix algebra *continued*

Product of two matrixes: Given $\mathbf{A} = (a_{ij})$ of order $m \times p$ and $\mathbf{B} = (b_{ki})$ of order $p \times n$, the product $\mathbf{AB} = \mathbf{C} = (c_{ij})$ is defined by

$$c_{ij} = \sum_{k=1}^{k=p} a_{ik}\, b_{kj}$$

It is a matrix of order $m \times n$.

In general the product $\mathbf{BA}$ is different from $\mathbf{AB}$.

Linear transformation

A linear transformation from a vector $\boldsymbol{u}$ of dimension m to a vector $\mathbf{v}$ of dimension n is represented by an $n \times m$ matrix $\mathbf{A}$

$$\mathbf{v} = \mathbf{A}\,\boldsymbol{u}$$

In expanded form,

$$v_1 = a_{11}\, u_1 + a_{12}\, u_2 + \ldots + a_{1m}\, u_m$$

$$v_2 = a_{21}\, u_1 + a_{22}\, u_2 + \ldots + a_{2m}\, u_m$$

$$\cdots\cdots\cdots\cdots\cdots\cdots\cdots\cdots$$

$$v_n = a_{n1}\, u_1 + a_{n2}\, u_2 + \ldots + a_{nm}\, u_m$$

Transposition: The transpose of matrix $\mathbf{A} = (a_{ij})$ is matrix $\mathbf{B} = (b_{ij})$ obtained by exchanging rows and columns

$$b_{ij} = a_{ji}$$

If $\mathbf{A}$ is of order $m \times n$, its transpose is of order $n \times m$. The transpose of $\mathbf{A}$ is noted by $\tilde{\mathbf{A}}$. When $\mathbf{A} = \tilde{\mathbf{A}}$, the matrix is *symmetric*.

The *complex conjugate* of $\mathbf{A}$ is the matrix $\mathbf{A}^*$ obtained by taking the complex conjugate of each element. When $\mathbf{A}^* = \mathbf{A}$, the matrix is real. The *hermitian conjugate* $\mathbf{A}^\dagger$ of $\mathbf{A}$ is the complex conjugate of the transpose. When $\mathbf{A}^\dagger = \mathbf{A}$, the matrix is *hermitian*.

The transpose of a product is equal to the product of the transpose taken in the reverse order

$$\widetilde{\mathbf{AB}} = \tilde{\mathbf{B}}\,\tilde{\mathbf{A}}$$

Matrix algebra *continued*

Similarly, for hermitian conjugate $(\boldsymbol{AB})^\dagger = \boldsymbol{B}^\dagger \boldsymbol{A}^\dagger$.

Scalar product: For two vectors $\boldsymbol{u}$ and $\mathbf{v}$ of same dimension, it is the number

$$\boldsymbol{u} \cdot \mathbf{v} = \tilde{\boldsymbol{u}}\, \mathbf{v} = \tilde{\mathbf{v}}\, \boldsymbol{u}.$$

The length $|\boldsymbol{u}|$ of a vector $\boldsymbol{u}$ is defined as $|\boldsymbol{u}| = (\boldsymbol{u} \cdot \boldsymbol{u})^{1/2}$

Hermitian product: For the two vectors $\boldsymbol{u},\mathbf{v}$ having n complex coordinates, the hermitian product is

$$(\boldsymbol{u},\mathbf{v}) = \boldsymbol{u}^\dagger\, \mathbf{v}.$$

The product $(\mathbf{v},\boldsymbol{u}) = (\boldsymbol{u},\mathbf{v})^*$. When the hermitian product is zero, the vectors are *orthogonal.*

The *norm* of a complex vector is

$$\|\boldsymbol{u}\|^2 = (\boldsymbol{u},\boldsymbol{u}) = \boldsymbol{u}^\dagger \boldsymbol{u}.$$

Determinant: (for a square matrix $\boldsymbol{A}$ of order n) is the sum of $n!$ terms

$$\det \boldsymbol{A} = \Sigma \pm a_{1i}\, a_{2j}\, a_{3k} \ldots a_{nl}$$

where the second subscripts $ijk \ldots l$, taken in order, form a permutation of the numbers $123 \ldots n$. For even permutations, which contain an even number of inversions, the sign is plus. For odd permutations, the sign is minus. The *cofactor* α_{ij} of the element a_{ij} is $(-1)^{i+j}$ times the determinant obtained from $\boldsymbol{A}$ by deleting the ith row and the jth column. The transpose of the matrix (α_{ij}) is the *adjugate* of $\boldsymbol{A}$; adj $\boldsymbol{A}$.

Inverse or reciprocal: of a square matrix $\boldsymbol{A}$ is a matrix $\boldsymbol{B}$ satisfying

$$\boldsymbol{AB} = \boldsymbol{BA} = \mathbf{1}$$

The inverse is noted by $\boldsymbol{A}^{-1}$. It exists only for *regular* matrixes that is, for those having their determinant different from zero.

The *Cramer's rule* to form the inverse is

$$\boldsymbol{A}^{-1} = \operatorname{adj} \boldsymbol{A}/\det \boldsymbol{A}$$

Orthogonal matrix: A matrix $\boldsymbol{A}$ is *orthogonal* if $\boldsymbol{A}\,\tilde{\boldsymbol{A}} = \mathbf{1}$. Orthogonal matrixes represent rotations: the linear transformation $\boldsymbol{y} = \boldsymbol{Ax}$ from the vector $\boldsymbol{x}$ into the vector $\boldsymbol{y}$ has the property $|\boldsymbol{y}| = |\boldsymbol{x}|$ and $\boldsymbol{y}_1 \cdot \boldsymbol{y}_2 = \boldsymbol{x}_1 \cdot \boldsymbol{x}_2$.

Unitary matrix: A matrix $\boldsymbol{A}$, with complex elements, is *unitary* when $\boldsymbol{A}^\dagger \boldsymbol{A} = \mathbf{1}$. The transformation $\boldsymbol{y} = \boldsymbol{Ax}$ preserves the *norm*, i.e., $\|\boldsymbol{y}\|^2 = \|\boldsymbol{x}\|^2$. The scattering matrix $\boldsymbol{S}$ of a passive, lossless network is unitary (see p. 647). When $\boldsymbol{x}$ represents incident waves, $\boldsymbol{y} = \boldsymbol{Sx}$ represent the reflected or

Matrix algebra *continued*

scattered waves and $\|\mathbf{y}\|^2 = \|\mathbf{x}\|^2$, invariance of the norm, means that the reflected power equals the incident power.

Trace (or *spur*) of a matrix is the sum of the terms in the main diagonal

$$\operatorname{tr} \mathbf{A} = \sum_{i=1}^{i=n} a_{ii}$$

Rules of operation

$$\mathbf{A} + \mathbf{B} = \mathbf{B} + \mathbf{A}$$

$$m(\mathbf{A} \pm \mathbf{B}) = m\mathbf{A} \pm m\mathbf{B}$$

$$\mathbf{A}(\mathbf{BC}) = (\mathbf{AB})\mathbf{C}$$

$$\mathbf{A}(\mathbf{B} \pm \mathbf{C}) = \mathbf{AB} \pm \mathbf{AC}$$

Exceptions: to the rules of ordinary algebra are as follows:

a. In general the product $\mathbf{AB}$ is different from $\mathbf{BA}$.

b. Division of the two members of an equation by a matrix is done by multiplying these members by the inverse matrix; care must be taken to place this inverse on the same side of both members.

Eigenvalue problem

Given a square matrix $\mathbf{A}$ of order n, the problem is to find vectors of dimension n that when multiplied by $\mathbf{A}$, give a vector of the same direction.

For such a vector

$$\mathbf{Au} = s\mathbf{u}$$

where s is a scalar. $\mathbf{u}$ is called an *eigenvector* (or characteristic vector) of the matrix $\mathbf{A}$ and s is the corresponding eigenvalue. The existence of a vector $\mathbf{u}$ ($\neq 0$) for a given s implies that s satisfies the characteristic equation

$$f(s) = \det(\mathbf{A} - s\mathbf{1}) = 0$$

$\mathbf{1}$ being the unit matrix (p. 1090). The trace of $\mathbf{A}$ is the sum of the eigenvalues and the determinant of $\mathbf{A}$ is their product.

$$\operatorname{tr} \mathbf{A} = \sum_{i=1}^{i=n} s_i$$

Matrix algebra *continued*

$$\det \boldsymbol{A} = \prod_{i=1}^{i=n} s_i$$

When the n roots $s_1\ s_2 \ldots s_n$ of the characteristic equation are distinct, the corresponding n eigenvectors are independent and $\boldsymbol{A}$ can be expressed as $\boldsymbol{A} = \boldsymbol{B}\ \boldsymbol{S}\ \boldsymbol{B}^{-1}$ where $\boldsymbol{S}$ is a diagonal matrix formed by the eigenvalues and $\boldsymbol{B}$ is regular.

A hermitian matrix has only real eigenvalues. When these eigenvalues are positive, the matrix is called *positive* (semidefinite). If none of them is equal to 0, the matrix is called *positive definite*. For a hermitian matrix $\boldsymbol{A}$, there exists a set of orthogonal eigenvectors; hence $\boldsymbol{A}$ can be represented by

$$\boldsymbol{A} = \boldsymbol{B}\,\boldsymbol{S}\,\boldsymbol{B}^{-1}$$

where $\boldsymbol{B}$ is unitary and $\boldsymbol{S}$ is diagonal and real.

A unitary matrix $\boldsymbol{U}$ has unitary eigenvalues (of the form exp $j\varphi$ with φ real) and also possesses a set of n orthogonal eigenvectors. It can be represented by

$$\boldsymbol{U} = \boldsymbol{B}\,\boldsymbol{S}\,\boldsymbol{B}^{-1}$$

where $\boldsymbol{B}$ is unitary and $\boldsymbol{S}$ is diagonal and formed with elements of magnitude 1

If the unitary matrix is also symmetrical (for instance, the scattering matrix of a lossless reciprocal network), there exist n real orthogonal eigenvectors, and $\boldsymbol{B}$ in the above formula is an orthogonal matrix.

Cayley–Hamilton theorem: The matrix $\boldsymbol{A}$ satisfies its own characteristic equation

$$f(\boldsymbol{A}) = 0$$

Matrixes of order 2

Let $\boldsymbol{A} = \begin{bmatrix} a & b \\ c & d \end{bmatrix}$ and $\boldsymbol{A}' = \begin{bmatrix} a' & b' \\ c' & d' \end{bmatrix}$

be two matrixes of order 2.

Sum

$$\boldsymbol{A} + \boldsymbol{A}' = \begin{bmatrix} a + a' & b + b' \\ c + c' & d + d' \end{bmatrix}$$

Matrix algebra *continued*

Difference

$$\mathbf{A} - \mathbf{A}' = \begin{bmatrix} a - a' & b - b' \\ c - c' & d - d' \end{bmatrix}$$

Multiplication by a number m

$$m\mathbf{A} = \begin{bmatrix} ma & mb \\ mc & md \end{bmatrix}$$

Product by a vector $\mathbf{x}$

If $\mathbf{x} = \begin{bmatrix} u \\ v \end{bmatrix}$ and $\mathbf{x}' = \begin{bmatrix} u' \\ v' \end{bmatrix}$, then

$$\mathbf{x}' = \mathbf{A}\mathbf{x}$$

expresses a linear transformation and means

$$u' = au + bv$$

$$v' = cu + dv$$

Products

$$\mathbf{A}\mathbf{A}' = \begin{bmatrix} aa' + bc' & ab' + bd' \\ ca' + dc' & cb' + dd' \end{bmatrix}$$

$$\mathbf{A}'\mathbf{A} = \begin{bmatrix} a'a + b'c & a'b + b'd \\ c'a + d'c & c'b + d'd \end{bmatrix}$$

Transpose

$$\tilde{\mathbf{A}} = \begin{bmatrix} a & c \\ b & d \end{bmatrix}$$

$\mathbf{A}$ is symmetric if $c = b$.

Matrix algebra *continued*

Complex conjugate

$$\mathbf{A}^* = \begin{bmatrix} a^* & b^* \\ c^* & d^* \end{bmatrix}$$

A is real if a, b, c, and d are real.

Hermitian conjugate

$$\mathbf{A}^\dagger = \begin{bmatrix} a^* & c^* \\ b^* & d^* \end{bmatrix}$$

A is hermitian if a and d are real and if b is the complex conjugate of c.

Determinant

$\det \mathbf{A} = ad - bc$

Trace

$\operatorname{tr} \mathbf{A} = a + d$

Adjugate

$$\operatorname{adj} \mathbf{A} = \begin{bmatrix} d & -b \\ -c & a \end{bmatrix}$$

Inverse

$$\mathbf{A}^{-1} = \frac{1}{ad - bc}\begin{bmatrix} d & -b \\ -c & a \end{bmatrix}$$

Characteristic equation

$\det(\mathbf{A} - s\mathbf{1}) = s^2 - s(a + d) + ad - bc = 0$

Eigenvalues

$$\left.\begin{matrix} s_1 \\ s_2 \end{matrix}\right\} = \frac{a+d}{2} \pm \left[\left(\frac{a+d}{2}\right)^2 - (ad - bc)\right]^{1/2}$$

Matrix algebra *continued*

Diagonal form

$$\mathbf{A} = \frac{1}{b(s_2 - s_1)} \begin{bmatrix} b & b \\ s_1 - a & s_2 - a \end{bmatrix} \begin{bmatrix} s_1 & 0 \\ 0 & s_2 \end{bmatrix} \begin{bmatrix} s_2 - a & -b \\ a - s_1 & b \end{bmatrix}$$

$s_2 \neq s_1$

Cayley–Hamilton theorem

$$\mathbf{A}^2 - \mathbf{A}\,(a + d) + ad - bc = 0$$

gives $\mathbf{A}^2$ in term of $\mathbf{A}$ and also gives by iteration the nth power $\mathbf{A}^n$ in terms of $\mathbf{A}$ and the unit matrix. A special case of importance (p. 649) is when det $\mathbf{A} = 1$ and θ is defined by tr $\mathbf{A} = 2 \cos \theta$

Then

$$s_1 = \exp j\theta$$

$$s_2 = \exp -j\theta$$

and

$$\mathbf{A}^n = \frac{\sin n\theta}{\sin \theta}\mathbf{A} - \frac{\sin (n - 1)\,\theta}{\sin \theta}$$

■ Mathematical tables

Common logarithms of numbers and proportional parts

	0	1	2	3	4	5	6	7	8	9	proportional parts 1	2	3	4	5	6	7	8	9
10	0000	0043	0086	0128	0170	0212	0253	0294	0334	0374	4	8	12	17	21	25	29	33	37
11	0414	0453	0492	0531	0569	0607	0645	0682	0719	0755	4	8	11	15	19	23	26	30	34
12	0792	0828	0864	0899	0934	0969	1004	1038	1072	1106	3	7	10	14	17	21	24	28	31
13	1139	1173	1206	1239	1271	1303	1335	1367	1399	1430	3	6	10	13	16	19	23	26	29
14	1461	1492	1523	1553	1584	1614	1644	1673	1703	1732	3	6	9	12	15	18	21	24	27
15	1761	1790	1818	1847	1875	1903	1931	1959	1987	2014	3	6	8	11	14	17	20	22	25
16	2041	2068	2095	2122	2148	2175	2201	2227	2253	2279	3	5	8	11	13	16	18	21	24
17	2304	2330	2355	2380	2405	2430	2455	2480	2504	2529	2	5	7	10	12	15	17	20	22
18	2553	2577	2601	2625	2648	2672	2695	2718	2742	2765	2	5	7	9	12	14	16	19	21
19	2788	2810	2833	2856	2878	2900	2923	2945	2967	2989	2	4	7	9	11	13	16	18	20
20	3010	3032	3054	3075	3096	3118	3139	3160	3181	3201	2	4	6	8	11	13	15	17	19
21	3222	3243	3263	3284	3304	3324	3345	3365	3385	3404	2	4	6	8	10	12	14	16	18
22	3424	3444	3464	3483	3502	3522	3541	3560	3579	3598	2	4	6	8	10	12	14	15	17
23	3617	3636	3655	3674	3692	3711	3729	3747	3766	3784	2	4	6	7	9	11	13	15	17
24	3802	3820	3838	3856	3874	3892	3909	3927	3945	3962	2	4	5	7	9	11	12	14	16
25	3979	3997	4014	4031	4048	4065	4082	4099	4116	4133	2	3	5	7	9	10	12	14	15
26	4150	4166	4183	4200	4216	4232	4249	4265	4281	4298	2	3	5	7	8	10	11	13	15
27	4314	4330	4346	4362	4378	4393	4409	4425	4440	4456	2	3	5	6	8	9	11	13	14
28	4472	4487	4502	4518	4533	4548	4564	4579	4594	4609	2	3	5	6	8	9	11	12	14
29	4624	4639	4654	4669	4683	4698	4713	4728	4742	4757	1	3	4	6	7	9	10	12	13
30	4771	4786	4800	4814	4829	4843	4857	4871	4886	4900	1	3	4	6	7	9	10	11	13
31	4914	4928	4942	4955	4969	4983	4997	5011	5024	5038	1	3	4	6	7	8	10	11	12
32	5051	5065	5079	5092	5105	5119	5132	5145	5159	5172	1	3	4	5	7	8	9	11	12
33	5185	5198	5211	5224	5237	5250	5263	5276	5289	5302	1	3	4	5	6	8	9	10	12
34	5315	5328	5340	5353	5366	5378	5391	5403	5416	5428	1	3	4	5	6	8	9	10	11
35	5441	5453	5465	5478	5490	5502	5514	5527	5539	5551	1	2	4	5	6	7	9	10	11
36	5563	5575	5587	5599	5611	5623	5635	5647	5658	5670	1	2	4	5	6	7	8	10	11
37	5682	5694	5705	5717	5729	5740	5752	5763	5775	5786	1	2	3	5	6	7	8	9	10
38	5798	5809	5821	5832	5843	5855	5866	5877	5888	5899	1	2	3	5	6	7	8	9	10
39	5911	5922	5933	5944	5955	5966	5977	5988	5999	6010	1	2	3	4	5	7	8	9	10
40	6021	6031	6042	6053	6064	6075	6085	6096	6107	6117	1	2	3	4	5	6	8	9	10
41	6128	6138	6149	6160	6170	6180	6191	6201	6212	6222	1	2	3	4	5	6	7	8	9
42	6232	6243	6253	6263	6274	6284	6294	6304	6314	6325	1	2	3	4	5	6	7	8	9
43	6335	6345	6355	6365	6375	6385	6395	6405	6415	6425	1	2	3	4	5	6	7	8	9
44	6435	6444	6454	6464	6474	6484	6493	6503	6513	6522	1	2	3	4	5	6	7	8	9
45	6532	6542	6551	6561	6571	6580	6590	6599	6609	6618	1	2	3	4	5	6	7	8	9
46	6628	6637	6646	6656	6665	6675	6684	6693	6702	6712	1	2	3	4	5	6	7	7	8
47	6721	6730	6739	6749	6758	6767	6776	6785	6794	6803	1	2	3	4	5	5	6	7	8
48	6812	6821	6830	6839	6848	6857	6866	6875	6884	6893	1	2	3	4	4	5	6	7	8
49	6902	6911	6920	6928	6937	6946	6955	6964	6972	6981	1	2	3	4	4	5	6	7	8
50	6990	6998	7007	7016	7024	7033	7042	7050	7059	7067	1	2	3	3	4	5	6	7	8
51	7076	7084	7093	7101	7110	7118	7126	7135	7143	7152	1	2	3	3	4	5	6	7	8
52	7160	7168	7177	7185	7193	7202	7210	7218	7226	7235	1	2	2	3	4	5	6	7	7
53	7243	7251	7259	7267	7275	7284	7292	7300	7308	7316	1	2	2	3	4	5	6	6	7
54	7324	7332	7340	7348	7356	7364	7372	7380	7388	7396	1	2	2	3	4	5	6	6	7

Common logarithms of numbers and proportional parts *continued*

	0	1	2	3	4	5	6	7	8	9	proportional parts 1	2	3	4	5	6	7	8	9
55	7404	7412	7419	7427	7435	7443	7451	7459	7466	7474	1	2	2	3	4	5	5	6	7
56	7482	7490	7497	7505	7513	7520	7528	7536	7543	7551	1	2	2	3	4	5	5	6	7
57	7559	7566	7574	7582	7589	7597	7604	7612	7619	7627	1	2	2	3	4	5	5	6	7
58	7634	7642	7649	7657	7664	7672	7679	7686	7694	7701	1	1	2	3	4	4	5	6	7
59	7709	7716	7723	7731	7738	7745	7752	7760	7767	7774	1	1	2	3	4	4	5	6	7
60	7782	7789	7796	7803	7810	7818	7825	7832	7839	7846	1	1	2	3	4	4	5	6	6
61	7853	7860	7868	7875	7882	7889	7896	7903	7910	7917	1	1	2	3	4	4	5	6	6
62	7924	7931	7938	7945	7952	7959	7966	7973	7980	7987	1	1	2	3	3	4	5	6	6
63	7993	8000	8007	8014	8021	8028	8035	8041	8048	8055	1	1	2	3	3	4	5	5	6
64	8062	8069	8075	8082	8089	8096	8102	8109	8116	8122	1	1	2	3	3	4	5	5	6
65	8129	8136	8142	8149	8156	8162	8169	8176	8182	8189	1	1	2	3	3	4	5	5	6
66	8195	8202	8209	8215	8222	8228	8235	8241	8248	8254	1	1	2	3	3	4	5	5	6
67	8261	8267	8274	8280	8287	8293	8299	8306	8312	8319	1	1	2	3	3	4	5	5	6
68	8325	8331	8338	8344	8351	8357	8363	8370	8376	8382	1	1	2	3	3	4	4	5	6
69	8388	8395	8401	8407	8414	8420	8426	8432	8439	8445	1	1	2	2	3	4	4	5	6
70	8451	8457	8463	8470	8476	8482	8488	8494	8500	8506	1	1	2	2	3	4	4	5	6
71	8513	8519	8525	8531	8537	8543	8549	8555	8561	8567	1	1	2	2	3	4	4	5	5
72	8573	8579	8585	8591	8597	8603	8609	8615	8621	8627	1	1	2	2	3	4	4	5	5
73	8633	8639	8645	8651	8657	8663	8669	8675	8681	8686	1	1	2	2	3	4	4	5	5
74	8692	8698	8704	8710	8716	8722	8727	8733	8739	8745	1	1	2	2	3	4	4	5	5
75	8751	8756	8762	8768	8774	8779	8785	8791	8797	8802	1	1	2	2	3	3	4	5	5
76	8808	8814	8820	8825	8831	8837	8842	8848	8854	8859	1	1	2	2	3	3	4	5	5
77	8865	8871	8876	8882	8887	8893	8899	8904	8910	8915	1	1	2	2	3	3	4	4	5
78	8921	8927	8932	8938	8943	8949	8954	8960	8965	8971	1	1	2	2	3	3	4	4	5
79	8976	8982	8987	8993	8998	9004	9009	9015	9020	9025	1	1	2	2	3	3	4	4	5
80	9031	9036	9042	9047	9053	9058	9063	9069	9074	9079	1	1	2	2	3	3	4	4	5
81	9085	9090	9096	9101	9106	9112	9117	9122	9128	9133	1	1	2	2	3	3	4	4	5
82	9138	9143	9149	9154	9159	9165	9170	9175	9180	9186	1	1	2	2	3	3	4	4	5
83	9191	9196	9201	9206	9212	9217	9222	9227	9232	9238	1	1	2	2	3	3	4	4	5
84	9243	9248	9253	9258	9263	9269	9274	9279	9284	9289	1	1	2	2	3	3	4	4	5
85	9294	9299	9304	9309	9315	9320	9325	9330	9335	9340	1	1	2	2	3	3	4	4	5
86	9345	9350	9355	9360	9365	9370	9375	9380	9385	9390	1	1	2	2	3	3	4	4	5
87	9395	9400	9405	9410	9415	9420	9425	9430	9435	9440	0	1	1	2	2	3	3	4	4
88	9445	9450	9455	9460	9465	9469	9474	9479	9484	9489	0	1	1	2	2	3	3	4	4
89	9494	9499	9504	9509	9513	9518	9523	9528	9533	9538	0	1	1	2	2	3	3	4	4
90	9542	9547	9552	9557	9562	9566	9571	9576	9581	9586	0	1	1	2	2	3	3	4	4
91	9590	9595	9600	9605	9609	9614	9619	9624	9628	9633	0	1	1	2	2	3	3	4	4
92	9638	9643	9647	9652	9657	9661	9666	9671	9675	9680	0	1	1	2	2	3	3	4	4
93	9685	9689	9694	9699	9703	9708	9713	9717	9722	9727	0	1	1	2	2	3	3	4	4
94	9731	9736	9741	9745	9750	9754	9759	9763	9768	9773	0	1	1	2	2	3	3	4	4
95	9777	9782	9786	9791	9795	9800	9805	9809	9814	9818	0	1	1	2	2	3	3	4	4
96	9823	9827	9832	9836	9841	9845	9850	9854	9859	9863	0	1	1	2	2	3	3	4	4
97	9868	9872	9877	9881	9886	9890	9894	9899	9903	9908	0	1	1	2	2	3	3	4	4
98	9912	9917	9921	9926	9930	9934	9939	9943	9948	9952	0	1	1	2	2	3	3	4	4
99	9956	9961	9965	9969	9974	9978	9983	9987	9991	9996	0	1	1	2	2	3	3	3	4

Natural trigonometric functions

for decimal fractions of a degree

deg	sin	cos	tan	cot	
0.0	.00000	1.0000	.00000	∞	90.0
.1	.00175	1.0000	.00175	573.0	.9
.2	.00349	1.0000	.00349	286.5	.8
.3	.00524	1.0000	.00524	191.0	.7
.4	.00698	1.0000	.00698	143.24	.6
.5	.00873	1.0000	.00873	114.59	.5
.6	.01047	0.9999	.01047	95.49	.4
.7	.01222	.9999	.01222	81.85	.3
.8	.01396	.9999	.01396	71.62	.2
.9	.01571	.9999	.01571	63.66	.1
1.0	.01745	0.9998	.01746	57.29	89.0
.1	.01920	.9998	.01920	52.08	.9
.2	.02094	.9998	.02095	47.74	.8
.3	.02269	.9997	.02269	44.07	.7
.4	.02443	.9997	.02444	40.92	.6
.5	.02618	.9997	.02619	38.19	.5
.6	.02792	.9996	.02793	35.80	.4
.7	.02967	.9996	.02968	33.69	.3
.8	.03141	.9995	.03143	31.82	.2
.9	.03316	.9995	.03317	30.14	.1
2.0	.03490	0.9994	.03492	28.64	88.0
.1	.03664	.9993	.03667	27.27	.9
.2	.03839	.9993	.03842	26.03	.8
.3	.04013	.9992	.04016	24.90	.7
.4	.04188	.9991	.04191	23.86	.6
.5	.04362	.9990	.04366	22.90	.5
.6	.04536	.9990	.04541	22.02	.4
.7	.04711	.9989	.04716	21.20	.3
.8	.04885	.9988	.04891	20.45	.2
.9	.05059	.9987	.05066	19.74	.1
3.0	.05234	0.9986	.05241	19.081	87.0
.1	.05408	.9985	.05416	18.464	.9
.2	.05582	.9984	.05591	17.886	.8
.3	.05756	.9983	.05766	17.343	.7
.4	.05931	.9982	.05941	16.832	.6
.5	.06105	.9981	.06116	16.350	.5
.6	.06279	.9980	.06291	15.895	.4
.7	.06453	.9979	.06467	15.464	.3
.8	.06627	.9978	.06642	15.056	.2
.9	.06802	.9977	.06817	14.669	.1
4.0	.06976	0.9976	.06993	14.301	86.0
.1	.07150	.9974	.07168	13.951	.9
.2	.07324	.9973	.07344	13.617	.8
.3	.07498	.9972	.07519	13.300	.7
.4	.07672	.9971	.07695	12.996	.6
.5	.07846	.9969	.07870	12.706	.5
.6	.08020	.9968	.08046	12.429	.4
.7	.08194	.9966	.08221	12.163	.3
.8	.08368	.9965	.08397	11.909	.2
.9	.08542	.9963	.08573	11.664	.1
5.0	.08716	0.9962	.08749	11.430	85.0
.1	.08889	.9960	.08925	11.205	.9
.2	.09063	.9959	.09101	10.988	.8
.3	.09237	.9957	.09277	10.780	.7
.4	.09411	.9956	.09453	10.579	.6
.5	.09585	.9954	.09629	10.385	.5
.6	.09758	.9952	.09805	10.199	.4
.7	.09932	.9951	.09981	10.019	.3
.8	.10106	.9949	.10158	9.845	.2
.9	.10279	.9947	.10334	9.677	.1
6.0	.10453	0.9945	.10510	9.514	84.0
	cos	sin	cot	tan	deg

deg	sin	cos	tan	cot	
6.0	.10453	0.9945	.10510	9.514	84.0
.1	.10626	.9943	.10687	9.357	.9
.2	.10800	.9942	.10863	9.205	.8
.3	.10973	.9940	.11040	9.058	.7
.4	.11147	.9938	.11217	8.915	.6
.5	.11320	9936	.11394	8.777	.5
.6	.11494	.9934	.11570	8.643	.4
.7	.11667	.9932	.11747	8.513	.3
.8	.11840	.9930	.11924	8.386	.2
.9	.12014	.9928	.12101	8.264	.1
7.0	.12187	0.9925	.12278	8.144	83.0
.1	.12360	.9923	.12456	8.028	.9
.2	.12533	.9921	.12633	7.916	.8
.3	.12706	.9919	.12810	7.806	.7
.4	.12880	.9917	.12988	7.700	.6
.5	.13053	.9914	.13165	7.596	.5
.6	.13226	.9912	.13343	7.495	.4
.7	.13399	.9910	.13521	7.396	.3
.8	.13572	.9907	.13698	7.300	.2
.9	.13744	.9905	.13876	7.207	.1
8.0	.13917	0.9903	.14054	7.115	82.0
.1	.14090	.9900	.14232	7.026	.9
.2	.14263	.9898	.14410	6.940	.8
.3	.14436	.9895	.14588	6.855	.7
.4	.14608	.9893	.14767	6.772	.6
.5	.14781	.9890	.14945	6.691	.5
.6	.14954	.9888	.15124	6.612	.4
.7	.15126	.9885	.15302	6.535	.3
.8	.15299	.9882	.15481	6.460	.2
.9	.15471	.9880	.15660	6.386	.1
9.0	.15643	0.9877	.15838	6.314	81.0
.1	.15816	.9874	.16017	6.243	.9
.2	.15988	.9871	.16196	6.174	.8
.3	.16160	.9869	.16376	6.107	.7
.4	.16333	.9866	.16555	6.041	.6
.5	.16505	.9863	.16734	5.976	.5
.6	.16677	.9860	.16914	5.912	.4
.7	.16849	.9857	.17093	5.850	.3
.8	.17021	.9854	.17273	5.789	.2
.9	.17193	.9851	.17453	5.730	.1
10.0	.1736	0.9848	.1763	5.671	80.0
.1	.1754	.9845	.1781	5.614	.9
.2	.1771	.9842	.1799	5.558	.8
.3	.1788	.9839	.1817	5.503	.7
.4	.1805	.9836	.1835	5.449	.6
.5	.1822	.9833	.1853	5.396	.5
.6	.1840	.9829	.1871	5.343	.4
.7	.1857	.9826	.1890	5.292	.3
.8	.1874	.9823	.1908	5.242	.2
.9	.1891	.9820	.1926	5.193	.1
11.0	.1908	0.9816	.1944	5.145	79.0
.1	.1925	.9813	.1962	5.097	.9
.2	.1942	.9810	.1980	5.050	.8
.3	.1959	.9806	.1998	5.005	.7
.4	.1977	.9803	.2016	4.959	.6
.5	.1994	.9799	.2035	4.915	.5
.6	.2011	.9796	.2053	4.872	.4
.7	.2028	.9792	.2071	4.829	.3
.8	.2045	.9789	.2089	4.787	.2
.9	.2062	.9785	.2107	4.745	.1
12.0	.2079	0.9781	.2126	4.705	78.0
	cos	sin	cot	tan	deg

Natural trigonometric functions

for decimal fractions of a degree *continued*

deg	sin	cos	tan	cot	
12.0	0.2079	0.9781	0.2126	4.705	**78.0**
.1	.2096	.9778	.2144	4.665	.9
.2	.2113	.9774	.2162	4.625	.8
.3	.2130	.9770	.2180	4.586	.7
.4	.2147	.9767	.2199	4.548	.6
.5	.2164	.9763	.2217	4.511	.5
.6	.2181	.9759	.2235	4.474	.4
.7	.2198	.9755	.2254	4.437	.3
.8	.2215	.9751	.2272	4.402	.2
.9	.2233	.9748	.2290	4.366	.1
13.0	0.2250	0.9744	0.2309	4.331	**77.0**
.1	.2267	.9740	.2327	4.297	.9
.2	.2284	.9736	.2345	4.264	.8
.3	.2300	.9732	.2364	4.230	.7
.4	.2317	.9728	.2382	4.198	.6
.5	.2334	.9724	.2401	4.165	.5
.6	.2351	.9720	.2419	4.134	.4
.7	.2368	.9715	.2438	4.102	.3
.8	.2385	.9711	.2456	4.071	.2
.9	.2402	.9707	.2475	4.041	.1
14.0	0.2419	0.9703	0.2493	4.011	**76.0**
.1	.2436	.9699	.2512	3.981	.9
.2	.2453	.9694	.2530	3.952	.8
.3	.2470	.9690	.2549	3.923	.7
.4	.2487	.9686	.2568	3.895	.6
.5	.2504	.9681	.2586	3.867	.5
.6	.2521	.9677	.2605	3.839	.4
.7	.2538	.9673	.2623	3.812	.3
.8	.2554	.9668	.2642	3.785	.2
.9	.2571	.9664	.2661	3.758	.1
15.0	0.2588	0.9659	0.2679	3.732	**75.0**
.1	.2605	.9655	.2698	3.706	.9
.2	.2622	.9650	.2717	3.681	.8
.3	.2639	.9646	.2736	3.655	.7
.4	.2656	.9641	.2754	3.630	.6
.5	.2672	.9636	.2773	3.606	.5
.6	.2689	.9632	.2792	3.582	.4
.7	.2706	.9627	.2811	3.558	.3
.8	.2723	.9622	.2830	3.534	.2
.9	.2740	.9617	.2849	3.511	.1
16.0	0.2756	0.9613	0.2867	3.487	**74.0**
.1	.2773	.9608	.2886	3.465	.9
.2	.2790	.9603	.2905	3.442	.8
.3	.2807	.9598	.2924	3.420	.7
.4	.2823	.9593	.2943	3.398	.6
.5	.2840	.9588	.2962	3.376	.5
.6	.2857	.9583	.2981	3.354	.4
.7	.2874	.9578	.3000	3.333	.3
.8	.2890	.9573	.3019	3.312	.2
.9	.2907	.9568	.3038	3.291	.1
17.0	0.2924	0.9563	0.3057	3.271	**73.0**
.1	.2940	.9558	.3076	3.251	.9
.2	.2957	.9553	.3096	3.230	.8
.3	.2974	.9548	.3115	3.211	.7
.4	.2990	.9542	.3134	3.191	.6
.5	.3007	.9537	.3153	3.172	.5
.6	.3024	.9532	.3172	3.152	.4
.7	.3040	.9527	.3191	3.133	.3
.8	.3057	.9521	.3211	3.115	.2
.9	.3074	.9516	.3230	3.096	.1
18.0	0.3090	0.9511	0.3249	3.078	**72.0**
	cos	sin	cot	tan	deg

deg	sin	cos	tan	cot	
18.0	0.3090	0.9511	0.3249	3.078	**72.0**
.1	.3107	.9505	.3269	3.060	.9
.2	.3123	.9500	.3288	3.042	.8
.3	.3140	.9494	.3307	3.024	.7
.4	.3156	.9489	.3327	3.006	.6
.5	.3173	.9483	.3346	2.989	.5
.6	.3190	.9478	.3365	2.971	.4
.7	.3206	.9472	.3385	2.954	.3
.8	.3223	.9466	.3404	2.937	.2
.9	.3239	.9461	.3424	2.921	.1
19.0	0.3256	0.9455	0.3443	2.904	**71.0**
.1	.3272	.9449	.3463	2.888	.9
.2	.3289	.9444	.3482	2.872	.8
.3	.3305	.9438	.3502	2.856	.7
.4	.3322	.9432	.3522	2.840	.6
.5	.3338	.9426	.3541	2.824	.5
.6	.3355	.9421	.3561	2.808	.4
.7	.3371	.9415	.3581	2.793	.3
.8	.3387	.9409	.3600	2.778	.2
.9	.3404	.9403	.3620	2.762	.1
20.0	0.3420	0.9397	0.3640	2.747	**70.0**
.1	.3437	.9391	.3659	2.733	.9
.2	.3453	.9385	.3679	2.718	.8
.3	.3469	.9379	.3699	2.703	.7
.4	.3486	.9373	.3719	2.689	.6
.5	.3502	.9367	.3739	2.675	.5
.6	.3518	.9361	.3759	2.660	.4
.7	.3535	.9354	.3779	2.646	.3
.8	.3551	.9348	.3799	2.633	.2
.9	.3567	.9342	.3819	2.619	.1
21.0	0.3584	0.9336	0.3839	2.605	**69.0**
.1	.3600	.9330	.3859	2.592	.9
.2	.3616	.9323	.3879	2.578	.8
.3	.3633	.9317	.3899	2.565	.7
.4	.3649	.9311	.3919	2.552	.6
.5	.3665	.9304	.3939	2.539	.5
.6	.3681	.9298	.3959	2.526	.4
.7	.3697	.9291	.3979	2.513	.3
.8	.3714	.9285	.4000	2.500	.2
.9	.3730	.9278	.4020	2.488	.1
22.0	0.3746	0.9272	0.4040	2.475	**68.0**
.1	.3762	.9265	.4061	2.463	.9
.2	.3778	.9259	.4081	2.450	.8
.3	.3795	.9252	.4101	2.438	.7
.4	.3811	.9245	.4122	2.426	.6
.5	.3827	.9239	.4142	2.414	.5
.6	.3843	.9232	.4163	2.402	.4
.7	.3859	.9225	.4183	2.391	.3
.8	.3875	.9219	.4204	2.379	.2
.9	.3891	.9212	.4224	2.367	.1
23.0	0.3907	0.9205	0.4245	2.356	**67.0**
.1	.3923	.9198	.4265	2.344	.9
.2	.3939	.9191	.4286	2.333	.8
.3	.3955	.9184	.4307	2.322	.7
.4	.3971	.9178	.4327	2.311	.6
.5	.3987	.9171	.4348	2.300	.5
.6	.4003	.9164	.4369	2.289	.4
.7	.4019	.9157	.4390	2.278	.3
.8	.4035	.9150	.4411	2.267	.2
.9	.4051	.9143	.4431	2.257	.1
24.0	0.4067	0.9135	0.4452	2.246	**66.0**
	cos	sin	cot	tan	deg

Natural trigonometric functions

for decimal fractions of a degree *continued*

deg	sin	cos	tan	cot	
24.0	0.4067	0.9135	0.4452	2.246	**66.0**
.1	.4083	.9128	.4473	2.236	.9
.2	.4099	.9121	.4494	2.225	.8
.3	.4115	.9114	.4515	2.215	.7
.4	.4131	.9107	.4536	2.204	.6
.5	.4147	.9100	.4557	2.194	.5
.6	.4163	.9092	.4578	2.184	.4
.7	.4179	.9085	.4599	2.174	.3
.8	.4195	.9078	.4621	2.164	.2
.9	.4210	.9070	.4642	2.154	.1
25.0	0.4226	0.9063	0.4663	2.145	**65.0**
.1	.4242	.9056	.4684	2.135	.9
.2	.4258	.9048	.4706	2.125	.8
.3	.4274	.9041	.4727	2.116	.7
.4	.4289	.9033	.4748	2.106	.6
.5	.4305	.9026	.4770	2.097	.5
.6	.4321	.9018	.4791	2.087	.4
.7	.4337	.9011	.4813	2.078	.3
.8	.4352	.9003	.4834	2.069	.2
.9	.4368	.8996	.4856	2.059	.1
26.0	0.4384	0.8988	0.4877	2.050	**64.0**
.1	.4399	.8980	.4899	2.041	.9
.2	.4415	.8973	.4921	2.032	.8
.3	.4431	.8965	.4942	2.023	.7
.4	.4446	.8957	.4964	2.014	.6
.5	.4462	.8949	.4986	2.006	.5
.6	.4478	.8942	.5008	1.997	.4
.7	.4493	.8934	.5029	1.988	.3
.8	.4509	.8926	.5051	1.980	.2
.9	.4524	.8918	.5073	1.971	.1
27.0	0.4540	0.8910	0.5095	1.963	**63.0**
.1	.4555	.8902	.5117	1.954	.9
.2	.4571	.8894	.5139	1.946	.8
.3	.4586	.8886	.5161	1.937	.7
.4	.4602	.8878	.5184	1.929	.6
.5	.4617	.8870	.5206	1.921	.5
.6	.4633	.8862	.5228	1.913	.4
.7	.4648	.8854	.5250	1.905	.3
.8	.4664	.8846	.5272	1.897	.2
.9	.4679	.8838	.5295	1.889	.1
28.0	0.4695	0.8829	0.5317	1.881	**62.0**
.1	.4710	.8821	.5340	1.873	.9
.2	.4726	.8813	.5362	1.865	.8
.3	.4741	.8805	.5384	1.857	.7
.4	.4756	.8796	.5407	1.849	.6
.5	.4772	.8788	.5430	1.842	.5
.6	.4787	.8780	.5452	1.834	.4
.7	.4802	.8771	.5475	1.827	.3
.8	.4818	.8763	.5498	1.819	.2
.9	.4833	.8755	.5520	1.811	.1
29.0	0.4848	0.8746	0.5543	1.804	**61.0**
.1	.4863	.8738	.5566	1.797	.9
.2	.4879	.8729	.5589	1.789	.8
.3	.4894	.8721	.5612	1.782	.7
.4	.4909	.8712	.5635	1.775	.6
.5	.4924	.8704	.5658	1.767	.5
.6	.4939	.8695	.5681	1.760	.4
.7	.4955	.8686	.5704	1.753	.3
.8	.4970	.8678	.5727	1.746	.2
.9	.4985	.8669	.5750	1.739	.1
30.0	0.5000	0.8660	0.5774	1.732	**60.0**
	cos	sin	cot	tan	deg

deg	sin	cos	tan	cot	
30.0	0.5000	0.8660	0.5774	1.7321	**60.0**
.1	.5015	.8652	.5797	1.7251	.9
.2	.5030	.8643	.5820	1.7182	.8
.3	.5045	.8634	.5844	1.7113	.7
.4	.5060	.8625	.5867	1.7045	.6
.5	.5075	.8616	.5890	1.6977	.5
.6	.5090	.8607	.5914	1.6909	.4
.7	.5105	.8599	.5938	1.6842	.3
.8	.5120	.8590	.5961	1.6775	.2
.9	.5135	.8581	.5985	1.6709	.1
31.0	0.5150	0.8572	0.6009	1.6643	**59.0**
.1	.5165	.8563	.6032	1.6577	.9
.2	.5180	.8554	.6056	1.6512	.8
.3	.5195	.8545	.6080	1.6447	.7
.4	.5210	.8536	.6104	1.6383	.6
.5	.5225	.8526	.6128	1.6319	.5
.6	.5240	.8517	.6152	1.6255	.4
.7	.5255	.8508	.6176	1.6191	.3
.8	.5270	.8499	.6200	1.6128	.2
.9	.5284	.8490	.6224	1.6066	.1
32.0	0.5299	0.8480	0.6249	1.6003	**58.0**
.1	.5314	.8471	.6273	1.5941	.9
.2	.5329	.8462	.6297	1.5880	.8
.3	.5344	.8453	.6322	1.5818	.7
.4	.5358	.8443	.6346	1.5757	.6
.5	.5373	.8434	.6371	1.5697	.5
.6	.5388	.8425	.6395	1.5637	.4
.7	.5402	.8415	.6420	1.5577	.3
.8	.5417	.8406	.6445	1.5517	.2
.9	.5432	.8396	.6469	1.5458	.1
33.0	0.5446	0.8387	0.6494	1.5399	**57.0**
.1	.5461	.8377	.6519	1.5340	.9
.2	.5476	.8368	.6544	1.5282	.8
.3	.5490	.8358	.6569	1.5224	.7
.4	.5505	.8348	.6594	1.5166	.6
.5	.5519	.8339	.6619	1.5108	.5
.6	.5534	.8329	.6644	1.5051	.4
.7	.5548	.8320	.6669	1.4994	.3
.8	.5563	.8310	.6694	1.4938	.2
.9	.5577	.8300	.6720	1.4882	.1
34.0	0.5592	0.8290	0.6745	1.4826	**56.0**
.1	.5606	.8281	.6771	1.4770	.9
.2	.5621	.8271	.6796	1.4715	.8
.3	.5635	.8261	.6822	1.4659	.7
.4	.5650	.8251	.6847	1.4605	.6
.5	.5664	.8241	.6873	1.4550	.5
.6	.5678	.8231	.6899	1.4496	.4
.7	.5693	.8221	.6924	1.4442	.3
.8	.5707	.8211	.6950	1.4388	.2
.9	.5721	.8202	.6976	1.4335	.1
35.0	0.5736	0.8192	0.7002	1.4281	**55.0**
.1	.5750	.8181	.7028	1.4229	.9
.2	.5764	.8171	.7054	1.4176	.8
.3	.5779	.8161	.7080	1.4124	.7
.4	.5793	.8151	.7107	1.4071	.6
.5	.5807	.8141	.7133	1.4019	.5
.6	.5821	.8131	.7159	1.3968	.4
.7	.5835	.8121	.7186	1.3916	.3
.8	.5850	.8111	.7212	1.3865	.2
.9	.5864	.8100	.7239	1.3814	.1
36.0	0.5878	0.8090	0.7265	1.3764	**54.0**
	cos	sin	cot	tan	deg

Natural trigonometric functions

for decimal fractions of a degree *continued*

deg	sin	cos	tan	cot	
36.0	0.5878	0.8090	0.7265	1.3764	**54.0**
.1	.5892	.8080	.7292	1.3713	.9
.2	.5906	.8070	.7319	1.3663	.8
.3	.5920	.8059	.7346	1.3613	.7
.4	.5934	.8049	.7373	1.3564	.6
.5	.5948	.8039	.7400	1.3514	.5
.6	.5962	.8028	.7427	1.3465	.4
.7	.5976	.8018	.7454	1.3416	.3
.8	.5990	.8007	.7481	1.3367	.2
.9	.6004	.7997	.7508	1.3319	.1
37.0	0.6018	0.7986	0.7536	1.3270	**53.0**
.1	.6032	.7976	.7563	1.3222	.9
.2	.6046	.7965	.7590	1.3175	.8
.3	.6060	.7955	.7618	1.3127	.7
.4	.6074	.7944	.7646	1.3079	.6
.5	.6088	.7934	.7673	1.3032	.5
.6	.6101	.7923	.7701	1.2985	.4
.7	.6115	.7912	.7729	1.2938	.3
.8	.6129	.7902	.7757	1.2892	.2
.9	.6143	.7891	.7785	1.2846	.1
38.0	0.6157	0.7880	0.7813	1.2799	**52.0**
.1	.6170	.7869	.7841	1.2753	.9
.2	.6184	.7859	.7869	1.2708	.8
.3	.6198	.7848	.7898	1.2662	.7
.4	.6211	.7837	.7926	1.2617	.6
.5	.6225	.7826	.7954	1.2572	.5
.6	.6239	.7815	.7983	1.2527	.4
.7	.6252	.7804	.8012	1.2482	.3
.8	.6266	.7793	.8040	1.2437	.2
.9	.6280	.7782	.8069	1.2393	.1
39.0	0.6293	0.7771	0.8098	1.2349	**51.0**
.1	.6307	.7760	.8127	1.2305	.9
.2	.6320	.7749	.8156	1.2261	.8
.3	.6334	.7738	.8185	1.2218	.7
.4	.6347	.7727	.8214	1.2174	.6
.5	.6361	.7716	.8243	1.2131	.5
.6	.6374	.7705	.8273	1.2088	.4
.7	.6388	.7694	.8302	1.2045	.3
.8	.6401	.7683	.8332	1.2002	.2
.9	.6414	.7672	.8361	1.1960	.1
40.0	0.6428	0.7660	0.8391	1.1918	**50.0**
.1	.6441	.7649	.8421	1.1875	.9
.2	.6455	.7638	.8451	1.1833	.8
.3	.6468	.7627	.8481	1.1792	.7
.4	.6481	.7615	.8511	1.1750	.6
40.5	0.6494	0.7604	0.8541	1.1708	**49.5**
	cos	sin	cot	tan	deg

deg	sin	cos	tan	cot	
40.5	0.6494	0.7604	0.8541	1.1708	**49.5**
.6	.6508	.7593	.8571	1.1667	.4
.7	.6521	.7581	.8601	1.1626	.3
.8	.6534	.7570	.8632	1.1585	.2
.9	.6547	.7559	.8662	1.1544	.1
41.0	0.6561	0.7547	0.8693	1.1504	**49.0**
.1	.6574	.7536	.8724	1.1463	.9
.2	.6587	.7524	.8754	1.1423	.8
.3	.6600	.7513	.8785	1.1383	.7
.4	.6613	.7501	.8816	1.1343	.6
.5	.6626	.7490	.8847	1.1303	.5
.6	.6639	.7478	.8878	1.1263	.4
.7	.6652	.7466	.8910	1.1224	.3
.8	.6665	.7455	.8941	1.1184	.2
.9	.6678	.7443	.8972	1.1145	.1
42.0	0.6691	0.7431	0.9004	1.1106	**48.0**
.1	.6704	.7420	.9036	1.1067	.9
.2	.6717	.7408	.9067	1.1028	.8
.3	.6730	.7396	.9099	1.0990	.7
.4	.6743	.7385	.9131	1.0951	.6
.5	.6756	.7373	.9163	1.0913	.5
.6	.6769	.7361	.9195	1.0875	.4
.7	.6782	.7349	.9228	1.0837	.3
.8	.6794	.7337	.9260	1.0799	.2
.9	.6807	.7325	.9293	1.0761	.1
43.0	0.6820	0.7314	0.9325	1.0724	**47.0**
.1	.6833	.7302	.9358	1.0686	.9
.2	.6845	.7290	.9391	1.0649	.8
.3	.6858	.7278	.9424	1.0612	.7
.4	.6871	.7266	.9457	1.0575	.6
.5	.6884	.7254	.9490	1.0538	.5
.6	.6896	.7242	.9523	1.0501	.4
.7	.6909	.7230	.9556	1.0464	.3
.8	.6921	.7218	.9590	1.0428	.2
.9	.6934	.7206	.9623	1.0392	.1
44.0	0.6947	0.7193	0.9657	1.0355	**46.0**
.1	.6959	.7181	.9691	1.0319	.9
.2	.6972	.7169	.9725	1.0283	.8
.3	.6984	.7157	.9759	1.0247	.7
.4	.6997	.7145	.9793	1.0212	.6
.5	.7009	.7133	.9827	1.0176	.5
.6	.7022	.7120	.9861	1.0141	.4
.7	.7034	.7108	.9896	1.0105	.3
.8	.7046	.7096	.9930	1.0070	.2
.9	.7059	.7083	.9965	1.0035	.1
45.0	0.7071	0.7071	1.0000	1.0000	**45.0**
	cos	sin	cot	tan	deg

Logarithms of trigonometric functions for decimal fractions of a degree

deg	L sin	L cos	L tan	L cot	
0.0	—∞	0.0000	—∞	∞	**90.0**
.1	7.2419	0.0000	7.2419	2.7581	.9
.2	7.5429	0.0000	7.5429	2.4571	.8
.3	7.7190	0.0000	7.7190	2.2810	.7
.4	7.8439	0.0000	7.8439	2.1561	.6
.5	7.9408	0.0000	7.9409	2.0591	.5
.6	8.0200	0.0000	8.0200	1.9800	.4
.7	8.0870	0.0000	8.0870	1.9130	.3
.8	8.1450	0.0000	8.1450	1.8550	.2
.9	8.1961	9.9999	8.1962	1.8038	.1
1.0	8.2419	9.9999	8.2419	1.7581	**89.0**
.1	8.2832	9.9999	8.2833	1.7167	.9
.2	8.3210	9.9999	8.3211	1.6789	.8
.3	8.3558	9.9999	8.3559	1.6441	.7
.4	8.3880	9.9999	8.3881	1.6119	.6
.5	8.4179	9.9999	8.4181	1.5819	.5
.6	8.4459	9.9998	8.4461	1.5539	.4
.7	8.4723	9.9998	8.4725	1.5275	.3
.8	8.4971	9.9998	8.4973	1.5027	.2
.9	8.5206	9.9998	8.5208	1.4792	.1
2.0	8.5428	9.9997	8.5431	1.4569	**88.0**
.1	8.5640	9.9997	8.5643	1.4357	.9
.2	8.5842	9.9997	8.5845	1.4155	.8
.3	8.6035	9.9996	8.6038	1.3962	.7
.4	8.6220	9.9996	8.6223	1.3777	.6
.5	8.6397	9.9996	8.6401	1.3599	.5
.6	8.6567	9.9996	8.6571	1.3429	.4
.7	8.6731	9.9995	8.6736	1.3264	.3
.8	8.6889	9.9995	8.6894	1.3106	.2
.9	8.7041	9.9994	8.7046	1.2954	.1
3.0	8.7188	9.9994	8.7194	1.2806	**87.0**
.1	8.7330	9.9994	8.7337	1.2663	.9
.2	8.7468	9.9993	8.7475	1.2525	.8
.3	8.7602	9.9993	8.7609	1.2391	.7
.4	8.7731	9.9992	8.7739	1.2261	.6
.5	8.7857	9.9992	8.7865	1.2135	.5
.6	8.7979	9.9991	8.7988	1.2012	.4
.7	8.8098	9.9991	8.8107	1.1893	.3
.8	8.8213	9.9990	8.8223	1.1777	.2
.9	8.8326	9.9990	8.8336	1.1664	.1
4.0	8.8436	9.9989	8.8446	1.1554	**86.0**
.1	8.8543	9.9989	8.8554	1.1446	.9
.2	8.8647	9.9988	8.8659	1.1341	.8
.3	8.8749	9.9988	8.8762	1.1238	.7
.4	8.8849	9.9987	8.8862	1.1138	.6
.5	8.8946	9.9987	8.8960	1.1040	.5
.6	8.9042	9.9986	8.9056	1.0944	.4
.7	8.9135	9.9985	8.9150	1.0850	.3
.8	8.9226	9.9985	8.9241	1.0759	.2
.9	8.9315	9.9984	8.9331	1.0669	.1
5.0	8.9403	9.9983	8.9420	1.0580	**85.0**
.1	8.9489	9.9983	8.9506	1.0494	.9
.2	8.9573	9.9982	8.9591	1.0409	.8
.3	8.9655	9.9981	8.9674	1.0326	.7
.4	8.9736	9.9981	8.9756	1.0244	.6
.5	8.9816	9.9980	8.9836	1.0164	.5
.6	8.9894	9.9979	8.9915	1.0085	.4
.7	8.9970	9.9978	8.9992	1.0008	.3
.8	9.0046	9.9978	9.0068	0.9932	.2
.9	9.0120	9.9977	9.0143	0.9857	.1
6.0	9.0192	9.9976	9.0216	0.9784	**84.0**
	L cos	L sin	L cot	L tan	deg

deg	L sin	L cos	L tan	L cot	
6.0	9.0192	9.9976	9.0216	0.9784	**84.0**
.1	9.0264	9.9975	9.0289	0.9711	.9
.2	9.0334	9.9975	9.0360	0.9640	.8
.3	9.0403	9.9974	9.0430	0.9570	.7
.4	9.0472	9.9973	9.0499	0.9501	.6
.5	9.0539	9.9972	9.0567	0.9433	.5
.6	9.0605	9.9971	9.0633	0.9367	.4
.7	9.0670	9.9970	9.0699	0.9301	.3
.8	9.0734	9.9969	9.0764	0.9236	.2
.9	9.0797	9.9968	9.0828	0.9172	.1
7.0	9.0859	9.9968	9.0891	0.9109	**83.0**
.1	9.0920	9.9967	9.0954	0.9046	.9
.2	9.0981	9.9966	9.1015	0.8985	.8
.3	9.1040	9.9965	9.1076	0.8924	.7
.4	9.1099	9.9964	9.1135	0.8865	.6
.5	9.1157	9.9963	9.1194	0.8806	.5
.6	9.1214	9.9962	9.1252	0.8748	.4
.7	9.1271	9.9961	9.1310	0.8690	.3
.8	9.1326	9.9960	9.1367	0.8633	.2
.9	9.1381	9.9959	9.1423	0.8577	.1
8.0	9.1436	9.9958	9.1478	0.8522	**82.0**
.1	9.1489	9.9956	9.1533	0.8467	.9
.2	9.1542	9.9955	9.1587	0.8413	.8
.3	9.1594	9.9954	9.1640	0.8360	.7
.4	9.1646	9.9953	9.1693	0.8307	.6
.5	9.1697	9.9952	9.1745	0.8255	.5
.6	9.1747	9.9951	9.1797	0.8203	.4
.7	9.1797	9.9950	9.1848	0.8152	.3
.8	9.1847	9.9949	9.1898	0.8102	.2
.9	9.1895	9.9947	9.1948	0.8052	.1
9.0	9.1943	9.9946	9.1997	0.8003	**81.0**
.1	9.1991	9.9945	9.2046	0.7954	.9
.2	9.2038	9.9944	9.2094	0.7906	.8
.3	9.2085	9.9943	9.2142	0.7858	.7
.4	9.2131	9.9941	9.2189	0.7811	.6
.5	9.2176	9.9940	9.2236	0.7764	.5
.6	9.2221	9.9939	9.2282	0.7718	.4
.7	9.2266	9.9937	9.2328	0.7672	.3
.8	9.2310	9.9936	9.2374	0.7626	.2
.9	9.2353	9.9935	9.2419	0.7581	.1
10.0	9.2397	9.9934	9.2463	0.7537	**80.0**
.1	9.2439	9.9932	9.2507	0.7493	.9
.2	9.2482	9.9931	9.2551	0.7449	.8
.3	9.2524	9.9929	9.2594	0.7406	.7
.4	9.2565	9.9928	9.2637	0.7363	.6
.5	9.2606	9.9927	9.2680	0.7320	.5
.6	9.2647	9.9925	9.2722	0.7278	.4
.7	9.2687	9.9924	9.2764	0.7236	.3
.8	9.2727	9.9922	9.2805	0.7195	.2
.9	9.2767	9.9921	9.2846	0.7154	.1
11.0	9.2806	9.9919	9.2887	0.7113	**79.0**
.1	9.2845	9.9918	9.2927	0.7073	.9
.2	9.2883	9.9916	9.2967	0.7033	.8
.3	9.2921	9.9915	9.3006	0.6994	.7
.4	9.2959	9.9913	9.3046	0.6954	.6
.5	9.2997	9.9912	9.3085	0.6915	.5
.6	9.3034	9.9910	9.3123	0.6877	.4
.7	9.3070	9.9909	9.3162	0.6838	.3
.8	9.3107	9.9907	9.3200	0.6800	.2
.9	9.3143	9.9906	9.3237	0.6763	.1
12.0	9.3179	9.9904	9.3275	0.6725	**78.0**
	L cos	L sin	L cot	L tan	deg

Logarithms of trigonometric functions for decimal fractions of a degree *continued*

deg	L sin	L cos	L tan	L cot	
12.0	9.3179	9.9904	9.3275	0.6725	78.0
.1	9.3214	9.9902	9.3312	0.6688	.9
.2	9.3250	9.9901	9.3349	0.6651	.8
.3	9.3284	9.9899	9.3385	0.6615	.7
.4	9.3319	9.9897	9.3422	0.6578	.6
.5	9.3353	9.9896	9.3458	0.6542	.5
.6	9.3387	9.9894	9.3493	0.6507	.4
.7	9.3421	9.9892	9.3529	0.6471	.3
.8	9.3455	9.9891	9.3564	0.6436	.2
.9	9.3488	9.9889	9.3599	0.6401	.1
13.0	9.3521	9.9887	9.3634	0.6366	77.0
.1	9.3554	9.9885	9.3668	0.6332	.9
.2	9.3586	9.9884	9.3702	0.6298	.8
.3	9.3618	9.9882	9.3736	0.6264	.7
.4	9.3650	9.9880	9.3770	0.6230	.6
.5	9.3682	9.9878	9.3804	0.6196	.5
.6	9.3713	9.9876	9.3837	0.6163	.4
.7	9.3745	9.9875	9.3870	0.6130	.3
.8	9.3775	9.9873	9.3903	0.6097	.2
.9	9.3806	9.9871	9.3935	0.6065	.1
14.0	9.3837	9.9869	9.3968	0.6032	76.0
.1	9.3867	9.9867	9.4000	0.6000	.9
.2	9.3897	9.9865	9.4032	0.5968	.8
.3	9.3927	9.9863	9.4064	0.5936	.7
.4	9.3957	9.9861	9.4095	0.5905	.6
.5	9.3986	9.9859	9.4127	0.5873	.5
.6	9.4015	9.9857	9.4158	0.5842	.4
.7	9.4044	9.9855	9.4189	0.5811	.3
.8	9.4073	9.9853	9.4220	0.5780	.2
.9	9.4102	9.9851	9.4250	0.5750	.1
15.0	9.4130	9.9849	9.4281	0.5719	75.0
.1	9.4158	9.9847	9.4311	0.5689	.9
.2	9.4186	9.9845	9.4341	0.5659	.8
.3	9.4214	9.9843	9.4371	0.5629	.7
.4	9.4242	9.9841	9.4400	0.5600	.6
.5	9.4269	9.9839	9.4430	0.5570	.5
.6	9.4296	9.9837	9.4459	0.5541	.4
.7	9.4323	9.9835	9.4488	0.5512	.3
.8	9.4350	9.9833	9.4517	0.5483	.2
.9	9.4377	9.9831	9.4546	0.5454	.1
16.0	9.4403	9.9828	9.4575	0.5425	74.0
.1	9.4430	9.9826	9.4603	0.5397	.9
.2	9.4456	9.9824	9.4632	0.5368	.8
.3	9.4482	9.9822	9.4660	0.5340	.7
.4	9.4508	9.9820	9.4688	0.5312	.6
.5	9.4533	9.9817	9.4716	0.5284	.5
.6	9.4559	9.9815	9.4744	0.5256	.4
.7	9.4584	9.9813	9.4771	0.5229	.3
.8	9.4609	9.9811	9.4799	0.5201	.2
.9	9.4634	9.9808	9.4826	0.5174	.1
17.0	9.4659	9.9806	9.4853	0.5147	73.0
.1	9.4684	9.9804	9.4880	0.5120	.9
.2	9.4709	9.9801	9.4907	0.5093	.8
.3	9.4733	9.9799	9.4934	0.5066	.7
.4	9.4757	9.9797	9.4961	0.5039	.6
.5	9.4781	9.9794	9.4987	0.5013	.5
.6	9.4805	9.9792	9.5014	0.4986	.4
.7	9.4829	9.9789	9.5040	0.4960	.3
.8	9.4853	9.9787	9.5066	0.4934	.2
.9	9.4876	9.9785	9.5092	0.4908	.1
18.0	9.4900	9.9782	9.5118	0.4882	72.0
	L cos	L sin	L cot	L tan	deg

deg	L sin	L cos	L tan	L cot	
18.0	9.4900	9.9782	9.5118	0.4882	72.0
.1	9.4923	9.9780	9.5143	0.4857	.9
.2	9.4946	9.9777	9.5169	0.4831	.8
.3	9.4969	9.9775	9.5195	0.4805	.7
.4	9.4992	9.9772	9.5220	0.4780	.6
.5	9.5015	9.9770	9.5245	0.4755	.5
.6	9.5037	9.9767	9.5270	0.4730	.4
.7	9.5060	9.9764	9.5295	0.4705	.3
.8	9.5082	9.9762	9.5320	0.4680	.2
.9	9.5104	9.9759	9.5345	0.4655	.1
19.0	9.5126	9.9757	9.5370	0.4630	71.0
.1	9.5148	9.9754	9.5394	0.4606	.9
.2	9.5170	9.9751	9.5419	0.4581	.8
.3	9.5192	9.9749	9.5443	0.4557	.7
.4	9.5213	9.9746	9.5467	0.4533	.6
.5	9.5235	9.9743	9.5491	0.4509	.5
.6	9.5256	9.9741	9.5516	0.4484	.4
.7	9.5278	9.9738	9.5539	0.4461	.3
.8	9.5299	9.9735	9.5563	0.4437	.2
.9	9.5320	9.9733	9.5587	0.4413	.1
20.0	9.5341	9.9730	9.5611	0.4389	70.0
.1	9.5361	9.9727	9.5634	0.4366	.9
.2	9.5382	9.9724	9.5658	0.4342	.8
.3	9.5402	9.9722	9.5681	0.4319	.7
.4	9.5423	9.9719	9.5704	0.4296	.6
.5	9.5443	9.9716	9.5727	0.4273	.5
.6	9.5463	9.9713	9.5750	0.4250	.4
.7	9.5484	9.9710	9.5773	0.4227	.3
.8	9.5504	9.9707	9.5796	0.4204	.2
.9	9.5523	9.9704	9.5819	0.4181	.1
21.0	9.5543	9.9702	9.5842	0.4158	69.0
.1	9.5563	9.9699	9.5864	0.4136	.9
.2	9.5583	9.9696	9.5887	0.4113	.8
.3	9.5602	9.9693	9.5909	0.4091	.7
.4	9.5621	9.9690	9.5932	0.4068	.6
.5	9.5641	9.9687	9.5954	0.4046	.5
.6	9.5660	9.9684	9.5976	0.4024	.4
.7	9.5679	9.9681	9.5998	0.4002	.3
.8	9.5698	9.9678	9.6020	0.3980	.2
.9	9.5717	9.9675	9.6042	0.3958	.1
22.0	9.5736	9.9672	9.6064	0.3936	68.0
.1	9.5754	9.9669	9.6086	0.3914	.9
.2	9.5773	9.9666	9.6108	0.3892	.8
.3	9.5792	9.9662	9.6129	0.3871	.7
.4	9.5810	9.9659	9.6151	0.3849	.6
.5	9.5828	9.9656	9.6172	0.3828	.5
.6	9.5847	9.9653	9.6194	0.3806	.4
.7	9.5865	9.9650	9.6215	0.3785	.3
.8	9.5883	9.9647	9.6236	0.3764	.2
.9	9.5901	9.9643	9.6257	0.3743	.1
23.0	9.5919	9.9640	9.6279	0.3721	67.0
.1	9.5937	9.9637	9.6300	0.3700	.9
.2	9.5954	9.9634	9.6321	0.3679	.8
.3	9.5972	9.9631	9.6341	0.3659	.7
.4	9.5990	9.9627	9.6362	0.3638	6
.5	9.6007	9.9624	9.6383	0.3617	.5
.6	9.6024	9.9621	9.6404	0.3596	.4
.7	9.6042	9.9617	9.6424	0.3576	.3
.8	9.6059	9.9614	9.6445	0.3555	.2
.9	9.6076	9.9611	9.6465	0.3535	.1
24.0	9.6093	9.9607	9.6486	0.3514	66.0
	L cos	L sin	L cot	L tan	deg

Logarithms of trigonometric functions for decimal fractions of a degree *continued*

deg	L sin	L cos	L tan	L cot	
24.0	9.6093	9.9607	9.6486	0.3514	66.0
.1	9.6110	9.9604	9.6506	0.3494	.9
.2	9.6127	9.9601	9.6527	0.3473	.8
.3	9.6144	9.9597	9.6547	0.3453	.7
.4	9.6161	9.9594	9.6567	0.3433	.6
.5	9.6177	9.9590	9.6587	0.3413	.5
.6	9.6194	9.9587	9.6607	0.3393	.4
.7	9.6210	9.9583	9.6627	0.3373	.3
.8	9.6227	9.9580	9.6647	0.3353	.2
.9	9.6243	9.9576	9.6667	0.3333	.1
25.0	9.6259	9.9573	9.6687	0.3313	65.0
.1	9.6276	9.9569	9.6706	0.3294	.9
.2	9.6292	9.9566	9.6726	0.3274	.8
.3	9.6308	9.9562	9.6746	0.3254	.7
.4	9.6324	9.9558	9.6765	0.3235	.6
.5	9.6340	9.9555	9.6785	0.3215	.5
.6	9.6356	9.9551	9.6804	0.3196	.4
.7	9.6371	9.9548	9.6824	0.3176	.3
.8	9.6387	9.9544	9.6843	0.3157	.2
.9	9.6403	9.9540	9.6863	0.3137	.1
26.0	9.6418	9.9537	9.6882	0.3118	64.0
.1	9.6434	9.9533	9.6901	0.3099	.9
.2	9.6449	9.9529	9.6920	0.3080	.8
.3	9.6465	9.9525	9.6939	0.3061	.7
.4	9.6480	9.9522	9.6958	0.3042	.6
.5	9.6495	9.9518	9.6977	0.3023	.5
.6	9.6510	9.9514	9.6996	0.3004	.4
.7	9.6526	9.9510	9.7015	0.2985	.3
.8	9.6541	9.9506	9.7034	0.2966	.2
.9	9.6556	9.9503	9.7053	0.2947	.1
27.0	9.6570	9.9499	9.7072	0.2928	63.0
.1	9.6585	9.9495	9.7090	0.2910	.9
.2	9.6600	9.9491	9.7109	0.2891	.8
.3	9.6615	9.9487	9.7128	0.2872	.7
.4	9.6629	9.9483	9.7146	0.2854	.6
.5	9.6644	9.9479	9.7165	0.2835	.5
.6	9.6659	9.9475	9.7183	0.2817	.4
.7	9.6673	9.9471	9.7202	0.2798	.3
.8	9.6687	9.9467	9.7220	0.2780	.2
.9	9.6702	9.9463	9.7238	0.2762	.1
28.0	9.6716	9.9459	9.7257	0.2743	62.0
.1	9.6730	9.9455	9.7275	0.2725	.9
.2	9.6744	9.9451	9.7293	0.2707	.8
.3	9.6759	9.9447	9.7311	0.2689	.7
.4	9.6773	9.9443	9.7330	0.2670	.6
.5	9.6787	9.9439	9.7348	0.2652	.5
.6	9.6801	9.9435	9.7366	0.2634	.4
.7	9.6814	9.9431	9.7384	0.2616	.3
.8	9.6828	9.9427	9.7402	0.2598	.2
.9	9.6842	9.9422	9.7420	0.2580	.1
29.0	9.6856	9.9418	9.7438	0.2562	61.0
.1	9.6869	9.9414	9.7455	0.2545	.9
.2	9.6883	9.9410	9.7473	0.2527	.8
.3	9.6896	9.9406	9.7491	0.2509	.7
.4	9.6910	9.9401	9.7509	0.2491	.6
.5	9.6923	9.9397	9.7526	0.2474	.5
.6	9.6937	9.9393	9.7544	0.2456	.4
.7	9.6950	9.9388	9.7562	0.2438	.3
.8	9.6963	9.9384	9.7579	0.2421	.2
.9	9.6977	9.9380	9.7597	0.2403	.1
30.0	9.6990	9.9375	9.7614	0.2386	60.0
	L cos	L sin	L cot	L tan	deg

deg	L sin	L cos	L tan	L cot	
30.0	9.6990	9.9375	9.7614	0.2386	60.0
.1	9.7003	9.9371	9.7632	0.2368	.9
.2	9.7016	9.9367	9.7649	0.2351	.8
.3	9.7029	9.9362	9.7667	0.2333	.7
.4	9.7042	9.9358	9.7684	0.2316	.6
.5	9.7055	9.9353	9.7701	0.2299	.5
.6	9.7068	9.9349	9.7719	0.2281	.4
.7	9.7080	9.9344	9.7736	0.2264	.3
.8	9.7093	9.9340	9.7753	0.2247	.2
.9	9.7106	9.9335	9.7771	0.2229	.1
31.0	9.7118	9.9331	9.7788	0.2212	59.0
.1	9.7131	9.9326	9.7805	0.2195	.9
.2	9.7144	9.9322	9.7822	0.2178	.8
.3	9.7156	9.9317	9.7839	0.2161	.7
.4	9.7168	9.9312	9.7856	0.2144	.6
.5	9.7181	9.9308	9.7873	0.2127	.5
.6	9.7193	9.9303	9.7890	0.2110	.4
.7	9.7205	9.9298	9.7907	0.2093	.3
.8	9.7218	9.9294	9.7924	0.2076	.2
.9	9.7230	9.9289	9.7941	0.2059	.1
32.0	9.7242	9.9284	9.7958	0.2042	58.0
.1	9.7254	9.9279	9.7975	0.2025	.9
.2	9.7266	9.9275	9.7992	0.2008	.8
.3	9.7278	9.9270	9.8008	0.1992	.7
.4	9.7290	9.9265	9.8025	0.1975	.6
.5	9.7302	9.9260	9.8042	0.1958	.5
.6	9.7314	9.9255	9.8059	0.1941	.4
.7	9.7326	9.9251	9.8075	0.1925	.3
.8	9.7338	9.9246	9.8092	0.1908	.2
.9	9.7349	9.9241	9.8109	0.1891	.1
33.0	9.7361	9.9236	9.8125	0.1875	57.0
.1	9.7373	9.9231	9.8142	0.1858	.9
.2	9.7384	9.9226	9.8158	0.1842	.8
.3	9.7396	9.9221	9.8175	0.1825	.7
.4	9.7407	9.9216	9.8191	0.1809	.6
.5	9.7419	9.9211	9.8208	0.1792	.5
.6	9.7430	9.9206	9.8224	0.1776	.4
.7	9.7442	9.9201	9.8241	0.1759	.3
.8	9.7453	9.9196	9.8257	0.1743	.2
.9	9.7464	9.9191	9.8274	0.1726	.1
34.0	9.7476	9.9186	9.8290	0.1710	56.0
.1	9.7487	9.9181	9.8306	0.1694	.9
.2	9.7498	9.9175	9.8323	0.1677	.8
.3	9.7509	9.9170	9.8339	0.1661	.7
.4	9.7520	9.9165	9.8355	0.1645	.6
.5	9.7531	9.9160	9.8371	0.1629	.5
.6	9.7542	9.9155	9.8388	0.1612	.4
.7	9.7553	9.9149	9.8404	0.1596	.3
.8	9.7564	9.9144	9.8420	0.1580	.2
.9	9.7575	9.9139	9.8436	0.1564	.1
35.0	9.7586	9.9134	9.8452	0.1548	55.0
.1	9.7597	9.9128	9.8468	0.1532	.9
.2	9.7607	9.9123	9.8484	0.1516	.8
.3	9.7618	9.9118	9.8501	0.1499	.7
.4	9.7629	9.9112	9.8517	0.1483	.6
.5	9.7640	9.9107	9.8533	0.1467	.5
.6	9.7650	9.9101	9.8549	0.1451	.4
.7	9.7661	9.9096	9.8565	0.1435	.3
.8	9.7671	9.9091	9.8581	0.1419	.2
.9	9.7682	9.9085	9.8597	0.1403	.1
36.0	9.7692	9.9080	9.8613	0.1387	54.0
	L cos	L sin	L cot	L tan	deg

Logarithms of trigonometric functions

for decimal fractions of a degree *continued*

deg	L sin	L cos	L tan	L cot	
36.0	9.7692	9.9080	9.8613	0.1387	**54.0**
.1	9.7703	9.9074	9.8629	0.1371	.9
.2	9.7713	9.9069	9.8644	0.1356	.8
.3	9.7723	9.9063	9.8660	0.1340	.7
.4	9.7734	9.9057	9.8676	0.1324	.6
.5	9.7744	9.9052	9.8692	0.1308	.5
.6	9.7754	9.9046	9.8708	0.1292	.4
.7	9.7764	9.9041	9.8724	0.1276	.3
.8	9.7774	9.9035	9.8740	0.1260	.2
.9	9.7785	9.9029	9.8755	0.1245	.1
37.0	9.7795	9.9023	9.8771	0.1229	**53.0**
.1	9.7805	9.9018	9.8787	0.1213	.9
.2	9.7815	9.9012	9.8803	0.1197	.8
.3	9.7825	9.9006	9.8818	0.1182	.7
.4	9.7835	9.9000	9.8834	0.1166	.6
.5	9.7844	9.8995	9.8850	0.1150	.5
.6	9.7854	9.8989	9.8865	0.1135	.4
.7	9.7864	9.8983	9.8881	0.1119	.3
.8	9.7874	9.8977	9.8897	0.1103	.2
.9	9.7884	9.8971	9.8912	0.1088	.1
38.0	9.7893	9.8965	9.8928	0.1072	**52.0**
.1	9.7903	9.8959	9.8944	0.1056	.9
.2	9.7913	9.8953	9.8959	0.1041	.8
.3	9.7922	9.8947	9.8975	0.1025	.7
.4	9.7932	9.8941	9.8990	0.1010	.6
.5	9.7941	9.8935	9.9006	0.0994	.5
.6	9.7951	9.8929	9.9022	0.0978	.4
.7	9.7960	9.8923	9.9037	0.0963	.3
.8	9.7970	9.8917	9.9053	0.0947	.2
.9	9.7979	9.8911	9.9068	0.0932	.1
39.0	9.7989	9.8905	9.9084	0.0916	**51.0**
.1	9.7998	9.8899	9.9099	0.0901	.9
.2	9.8007	9.8893	9.9115	0.0885	.8
.3	9.8017	9.8887	9.9130	0.0870	.7
.4	9.8026	9.8880	9.9146	0.0854	.6
.5	9.8035	9.8874	9.9161	0.0839	.5
.6	9.8044	9.8868	9.9176	0.0824	.4
.7	9.8053	9.8862	9.9192	0.0808	.3
.8	9.8063	9.8855	9.9207	0.0793	.2
.9	9.8072	9.8849	9.9223	0.0777	.1
40.0	9.8081	9.8843	9.9238	0.0762	**50.0**
.1	9.8090	9.8836	9.9254	0.0746	.9
.2	9.8099	9.8830	9.9269	0.0731	.8
.3	9.8108	9.8823	9.9284	0.0716	.7
.4	9.8117	9.8817	9.9300	0.0700	.6
40.5	9.8125	9.8810	9.9315	0.0685	**49.5**
	L cos	L sin	L cot	L tan	deg

deg	L sin	L cos	L tan	L cot	
40.5	9.8125	9.8810	9.9315	0.0685	**49.5**
.6	9.8134	9.8804	9.9330	0.0670	.4
.7	9.8143	9.8797	9.9346	0.0654	.3
.8	9.8152	9.8791	9.9361	0.0639	.2
.9	9.8161	9.8784	9.9376	0.0624	.1
41.0	9.8169	9.8778	9.9392	0.0608	**49.0**
.1	9.8178	9.8771	9.9407	0.0593	.9
.2	9.8187	9.8765	9.9422	0.0578	.8
.3	9.8195	9.8758	9.9438	0.0562	.7
.4	9.8204	9.8751	9.9453	0.0547	.6
.5	9.8213	9.8745	9.9468	0.0532	.5
.6	9.8221	9.8738	9.9483	0.0517	.4
.7	9.8230	9.8731	9.9499	0.0501	.3
.8	9.8238	9.8724	9.9514	0.0486	.2
.9	9.8247	9.8718	9.9529	0.0471	.1
42.0	9.8255	9.8711	9.9544	0.0456	**48.0**
.1	9.8264	9.8704	9.9560	0.0440	.9
.2	9.8272	9.8697	9.9575	0.0425	.8
.3	9.8280	9.8690	9.9590	0.0410	.7
.4	9.8289	9.8683	9.9605	0.0395	.6
.5	9.8297	9.8676	9.9621	0.0379	.5
.6	9.8305	9.8669	9.9636	0.0364	.4
.7	9.8313	9.8662	9.9651	0.0349	.3
.8	9.8322	9.8655	9.9666	0.0334	.2
.9	9.8330	9.8648	9.9681	0.0319	.1
43.0	9.8338	9.8641	9.9697	0.0303	**47.0**
.1	9.8346	9.8634	9.9712	0.0288	.9
.2	9.8354	9.8627	9.9727	0.0273	.8
.3	9.8362	9.8620	9.9742	0.0258	.7
.4	9.8370	9.8613	9.9757	0.0243	.6
.5	9.8378	9.8606	9.9772	0.0228	.5
.6	9.8386	9.8598	9.9788	0.0212	.4
.7	9.8394	9.8591	9.9803	0.0197	.3
.8	9.8402	9.8584	9.9818	0.0182	.2
.9	9.8410	9.8577	9.9833	0.0167	.1
44.0	9.8418	9.8569	9.9848	0.0152	**46.0**
.1	9.8426	9.8562	9.9864	0.0136	.9
.2	9.8433	9.8555	9.9879	0.0121	.8
.3	9.8441	9.8547	9.9894	0.0106	.7
.4	9.8449	9.8540	9.9909	0.0091	.6
.5	9.8457	9.8532	9.9924	0.0076	.5
.6	9.8464	9.8525	9.9939	0.0061	.4
.7	9.8472	9.8517	9.9955	0.0045	.3
.8	9.8480	9.8510	9.9970	0.0030	.2
.9	9.8487	9.8502	9.9985	0.0015	.1
45.0	9.8495	9.8495	0.0000	0.0000	**45.0**
	L cos	L sin	L cot	L tan	deg

Natural logarithms

	0	1	2	3	4	5	6	7	8	9	1	2	3	4	5	6	7	8	9
											mean differences								
1.0	0.0000	0100	0198	0296	0392	0488	0583	0677	0770	0862	10	19	29	38	48	57	67	76	86
1.1	0.0953	1044	1133	1222	1310	1398	1484	1570	1655	1740	9	17	26	35	44	52	61	70	78
1.2	0.1823	1906	1989	2070	2151	2231	2311	2390	2469	2546	8	16	24	32	40	48	56	64	72
1.3	0.2624	2700	2776	2852	2927	3001	3075	3148	3221	3293	7	15	22	30	37	44	52	59	67
1.4	0.3365	3436	3507	3577	3646	3716	3784	3853	3920	3988	7	14	21	28	35	41	48	55	62
1.5	0.4055	4121	4187	4253	4318	4383	4447	4511	4574	4637	6	13	19	26	32	39	45	52	58
1.6	0.4700	4762	4824	4886	4947	5008	5068	5128	5188	5247	6	12	18	24	30	36	42	48	56
1.7	0.5306	5365	5423	5481	5539	5596	5653	5710	5766	5822	6	11	17	23	29	34	40	46	51
1.8	0.5878	5933	5988	6043	6098	6152	6206	6259	6313	6366	5	11	16	22	27	32	38	43	49
1.9	0.6419	6471	6523	6575	6627	6678	6729	6780	6831	6881	5	10	15	20	26	31	36	41	46
2.0	0.6931	6981	7031	7080	7129	7178	7227	7275	7324	7372	5	10	15	20	24	29	34	39	44
2.1	0.7419	7467	7514	7561	7608	7655	7701	7747	7793	7839	5	9	14	19	23	28	33	37	42
2.2	0.7885	7930	7975	8020	8065	8109	8154	8198	8242	8286	4	9	13	18	22	27	31	36	40
2.3	0.8329	8372	8416	8459	8502	8544	8587	8629	8671	8713	4	9	13	17	21	26	30	34	38
2.4	0.8755	8796	8838	8879	8920	8961	9002	9042	9083	9123	4	8	12	16	20	24	29	33	37
2.5	0.9163	9203	9243	9282	9322	9361	9400	9439	9478	9517	4	8	12	16	20	24	27	31	35
2.6	0.9555	9594	9632	9670	9708	9746	9783	9821	9858	9895	4	8	11	15	19	23	26	30	34
2.7	0.9933	9969	1.0006	0043	0080	0116	0152	0188	0225	0260	4	7	11	15	18	22	25	29	33
2.8	1.0296	0332	0367	0403	0438	0473	0508	0543	0578	0613	4	7	11	14	18	21	25	28	32
2.9	1.0647	0682	0716	0750	0784	0818	0852	0886	0919	0953	3	7	10	14	17	20	24	27	31
3.0	1.0986	1019	1053	1086	1119	1151	1184	1217	1249	1282	3	7	10	13	16	20	23	26	30
3.1	1.1314	1346	1378	1410	1442	1474	1506	1537	1569	1600	3	6	10	13	16	19	22	25	29
3.2	1.1632	1663	1694	1725	1756	1787	1817	1848	1878	1909	3	6	9	12	15	18	22	25	28
3.3	1.1939	1969	2000	2030	2060	2090	2119	2149	2179	2208	3	6	9	12	15	18	21	24	27
3.4	1.2238	2267	2296	2326	2355	2384	2413	2442	2470	2499	3	6	9	12	15	17	20	23	26
3.5	1.2528	2556	2585	2613	2641	2669	2698	2726	2754	2782	3	6	8	11	14	17	20	23	25
3.6	1.2809	2837	2865	2892	2920	2947	2975	3002	3029	3056	3	5	8	11	14	16	19	22	25
3.7	1.3083	3110	3137	3164	3191	3218	3244	3271	3297	3324	3	5	8	11	13	16	19	21	24
3.8	1.3350	3376	3403	3429	3455	3481	3507	3533	3558	3584	3	5	8	10	13	16	18	21	23
3.9	1.3610	3635	3661	3686	3712	3737	3762	3788	3813	3838	3	5	8	10	13	15	18	20	23
4.0	1.3863	3888	3913	3938	3962	3987	4012	4036	4061	4085	2	5	7	10	12	15	17	20	22
4.1	1.4110	4134	4159	4183	4207	4231	4255	4279	4303	4327	2	5	7	10	12	14	17	19	22
4.2	1.4351	4375	4398	4422	4446	4469	4493	4516	4540	4563	2	5	7	9	12	14	16	19	21
4.3	1.4586	4609	4633	4656	4679	4702	4725	4748	4770	4793	2	5	7	9	12	14	16	18	21
4.4	1.4816	4839	4861	4884	4907	4929	4951	4974	4996	5019	2	5	7	9	11	14	16	18	20
4.5	1.5041	5063	5085	5107	5129	5151	5173	5195	5217	5239	2	4	7	9	11	13	15	18	20
4.6	1.5261	5282	5304	5326	5347	5369	5390	5412	5433	5454	2	4	6	9	11	13	15	17	19
4.7	1.5476	5497	5518	5539	5560	5581	5602	5623	5644	5665	2	4	6	8	11	13	15	17	19
4.8	1.5686	5707	5728	5748	5769	5790	5810	5831	5851	5872	2	4	6	8	10	12	14	16	19
4.9	1.5892	5913	5933	5953	5974	5994	6014	6034	6054	6074	2	4	6	8	10	12	14	16	18
5.0	1.6094	6114	6134	6154	6174	6194	6214	6233	6253	6273	2	4	6	8	10	12	14	16	18
5.1	1.6292	6312	6332	6351	6371	6390	6409	6429	6448	6467	2	4	6	8	10	12	14	16	18
5.2	1.6487	6506	6525	6544	6563	6582	6601	6620	6639	6658	2	4	6	8	10	11	13	15	17
5.3	1.6677	6696	6715	6734	6752	6771	6790	6808	6827	6845	2	4	6	7	9	11	13	15	17
5.4	1.6864	6882	6901	6919	6938	6956	6974	6993	7011	7029	2	4	5	7	9	11	13	15	17

Natural logarithms of 10^{+n}

n	1	2	3	4	5	6	7	8	9
$\log_e 10^n$	2.3026	4.6052	6.9078	9.2103	11.5129	13.8155	16.1181	18.4207	20.7233

Natural logarithms *continued*

	0	1	2	3	4	5	6	7	8	9	mean differences 1	2	3	4	5	6	7	8	9
5.5	1.7047	7066	7084	7102	7120	7138	7156	7174	7192	7210	2	4	5	7	9	11	13	14	16
5.6	1.7228	7246	7263	7281	7299	7317	7334	7352	7370	7387	2	4	5	7	9	11	12	14	16
5.7	1.7405	7422	7440	7457	7475	7492	7509	7527	7544	7561	2	3	5	7	9	10	12	14	16
5.8	1.7579	7596	7613	7630	7647	7664	7681	7699	7716	7733	2	3	5	7	9	10	12	14	15
5.9	1.7750	7766	7783	7800	7817	7834	7851	7867	7884	7901	2	3	5	7	8	10	12	13	15
6.0	1.7918	7934	7951	7967	7984	8001	8017	8034	8050	8066	2	3	5	7	8	10	12	13	15
6.1	1.8083	8099	8116	8132	8148	8165	8181	8197	8213	8229	2	3	5	6	8	10	11	13	15
6.2	1.8245	8262	8278	8294	8310	8326	8342	8358	8374	8390	2	3	5	6	8	10	11	13	14
6.3	1.8405	8421	8437	8453	8469	8485	8500	8516	8532	8547	2	3	5	6	8	9	11	13	14
6.4	1.8563	8579	8594	8610	8625	8641	8656	8672	8687	8703	2	3	5	6	8	9	11	12	14
6.5	1.8718	8733	8749	8764	8779	8795	8810	8825	8840	8856	2	3	5	6	8	9	11	12	14
6.6	1.8871	8886	8901	8916	8931	8946	8961	8976	8991	9006	2	3	5	6	8	9	11	12	14
6.7	1.9021	9036	9051	9066	9081	9095	9110	9125	9140	9155	1	3	4	6	7	9	10	12	13
6.8	1.9169	9184	9199	9213	9228	9242	9257	9272	9286	9301	1	3	4	6	7	9	10	12	13
6.9	1.9315	9330	9344	9359	9373	9387	9402	9416	9430	9445	1	3	4	6	7	9	10	12	13
7.0	1.9459	9473	9488	9502	9516	9530	9544	9559	9573	9587	1	3	4	6	7	9	10	11	13
7.1	1.9601	9615	9629	9643	9657	9671	9685	9699	9713	9727	1	3	4	6	7	8	10	11	13
7.2	1.9741	9755	9769	9782	9796	9810	9824	9838	9851	9865	1	3	4	6	7	8	10	11	12
7.3	1.9879	9892	9906	9920	9933	9947	9961	9974	9988	2.0001	1	3	4	5	7	8	10	11	12
7.4	2.0015	0028	0042	0055	0069	0082	0096	0109	0122	0136	1	3	4	5	7	8	9	11	12
7.5	2.0149	0162	0176	0189	0202	0215	0229	0242	0255	0268	1	3	4	5	7	8	9	11	12
7.6	2.0281	0295	0308	0321	0334	0347	0360	0373	0386	0399	1	3	4	5	7	8	9	10	12
7.7	2.0412	0425	0438	0451	0464	0477	0490	0503	0516	0528	1	3	4	5	6	8	9	10	12
7.8	2.0541	0554	0567	0580	0592	0605	0618	0631	0643	0656	1	3	4	5	6	8	9	10	11
7.9	2.0669	0681	0694	0707	0719	0732	0744	0757	0769	0782	1	3	4	5	6	8	9	10	11
8.0	2.0794	0807	0819	0832	0844	0857	0869	0882	0894	0906	1	3	4	5	6	7	9	10	11
8.1	2.0919	0931	0943	0956	0968	0980	0992	1005	1017	1029	1	2	4	5	6	7	9	10	11
8.2	2.1041	1054	1066	1078	1090	1102	1114	1126	1138	1150	1	2	4	5	6	7	9	10	11
8.3	2.1163	1175	1187	1199	1211	1223	1235	1247	1258	1270	1	2	4	5	6	7	8	10	11
8.4	2.1282	1294	1306	1318	1330	1342	1353	1365	1377	1389	1	2	4	5	6	7	8	9	11
8.5	2.1401	1412	1424	1436	1448	1459	1471	1483	1494	1506	1	2	4	5	6	7	8	9	11
8.6	2.1518	1529	1541	1552	1564	1576	1587	1599	1610	1622	1	2	3	5	6	7	8	9	10
8.7	2.1633	1645	1656	1668	1679	1691	1702	1713	1725	1736	1	2	3	5	6	7	8	9	10
8.8	2.1748	1759	1770	1782	1793	1804	1815	1827	1838	1849	1	2	3	5	6	7	8	9	10
8.9	2.1861	1872	1883	1894	1905	1917	1928	1939	1950	1961	1	2	3	4	6	7	8	9	10
9.0	2.1972	1983	1994	2006	2017	2028	2039	2050	2061	2072	1	2	3	4	6	7	8	9	10
9.1	2.2083	2094	2105	2116	2127	2138	2148	2159	2170	2181	1	2	3	4	5	7	8	9	10
9.2	2.2192	2203	2214	2225	2235	2246	2257	2268	2279	2289	1	2	3	4	5	6	8	9	10
9.3	2.2300	2311	2322	2332	2343	2354	2364	2375	2386	2396	1	2	3	4	5	6	7	9	10
9.4	2.2407	2418	2428	2439	2450	2460	2471	2481	2492	2502	1	2	3	4	5	6	7	8	10
9.5	2.2513	2523	2534	2544	2555	2565	2576	2586	2597	2607	1	2	3	4	5	6	7	8	9
9.6	2.2618	2628	2638	2649	2659	2670	2680	2690	2701	2711	1	2	3	4	5	6	7	8	9
9.7	2.2721	2732	2742	2752	2762	2773	2783	2793	2803	2814	1	2	3	4	5	6	7	8	9
9.8	2.2824	2834	2844	2854	2865	2875	2885	2895	2905	2915	1	2	3	4	5	6	7	8	9
9.9	2.2925	2935	2946	2956	2966	2976	2986	2996	3006	3016	1	2	3	4	5	6	7	8	9
0.0	2.3026																		

Natural logarithms of 10^{-n}

n	1	2	3	4	5	6	7	8	9
$\log_e 10^{-n}$	$\bar{3}.6974$	$\bar{5}.3948$	$\bar{7}.0922$	$\overline{10}.7897$	$\overline{12}.4871$	$\overline{14}.1845$	$\overline{17}.8819$	$\overline{19}.5793$	$\overline{21}.2767$

Logarithms to base 2 and powers of 2

x	$\log_2 x$
0.1	−3.32193
0.2	−2.32193
0.3	−1.73697
0.4	−1.32193
0.5	−1.00000
0.6	−0.73697
0.7	−0.51458
0.8	−0.32193
0.9	−0.15200
1.0	0.00000
1.1	0.13749
1.2	0.26303
1.3	0.37850
1.4	0.48543
1.5	0.58496
1.6	0.67807
1.7	0.76554
1.8	0.84798
1.9	0.92599
2.0	1.00000
10	3.32193
100	6.64386
1000	9.96578
2^y	y

$$\log_2 x = \log_2 10 \log_{10} x = \log_2 e \log_e x$$

$$2^y = e^{y \log_e 2} = 10^{y \log_{10} 2}$$

$$\log_2 10 = 3.32193 = 1/\log_{10} 2$$

$$\log_{10} 2 = 0.30103 = 1/\log_2 10$$

$$\log_2 e = 1.44269 = 1/\log_e 2$$

$$\log_e 2 = 0.69315 = 1/\log_2 e$$

y	2^y
0.1	1.072
0.2	1.149
0.3	1.231
0.4	1.320
0.5	1.414
0.6	1.515
0.7	1.625
0.8	1.741
0.9	1.866
1	2
2	4
3	8
4	16
5	32
6	64
7	128
8	256
9	512
10	1 024
11	2 048
12	4 096
13	8 192
14	16 384
15	32 768
16	65 536
17	131 072
18	262 144
19	524 288
20	1 048 576
21	2 097 152
22	4 194 304
23	8 388 608
24	16 777 216
25	33 554 432
26	67 108 864
27	134 217 728
28	268 435 456
29	536 870 912
30	1 073 741 824
31	2 147 483 648
32	4 294 967 296
$\log_2 x$	x

Hyperbolic sines [$\sinh x = \frac{1}{2}(e^{x} - e^{-x})$]

x	0	1	2	3	4	5	6	7	8	9	avg diff
0.0	0.0000	0.0100	0.0200	0.0300	0.0400	0.0500	0.0600	0.0701	0.0801	0.0901	100
.1	0.1002	0.1102	0.1203	0.1304	0.1405	0.1506	0.1607	0.1708	0.1810	0.1911	101
.2	0.2013	0.2115	0.2218	0.2320	0.2423	0.2526	0.2629	0.2733	0.2837	0.2941	103
.3	0.3045	0.3150	0.3255	0.3360	0.3466	0.3572	0.3678	0.3785	0.3892	0.4000	106
.4	0.4108	0.4216	0.4325	0.4434	0.4543	0.4653	0.4764	0.4875	0.4986	0.5098	110
0.5	0.5211	0.5324	0.5438	0.5552	0.5666	0.5782	0.5897	0.6014	0.6131	0.6248	116
.6	0.6367	0.6485	0.6605	0.6725	0.6846	0.6967	0.7090	0.7213	0.7336	0.7461	122
.7	0.7586	0.7712	0.7838	0.7966	0.8094	0.8223	0.8353	0.8484	0.8615	0.8748	130
.8	0.8881	0.9015	0.9150	0.9286	0.9423	0.9561	0.9700	0.9840	0.9981	1.012	138
.9	1.027	1.041	1.055	1.070	1.085	1.099	1.114	1.129	1.145	1.160	15
1.0	1.175	1.191	1.206	1.222	1.238	1.254	1.270	1.286	1.303	1.319	16
.1	1.336	1.352	1.369	1.386	1.403	1.421	1.438	1.456	1.474	1.491	17
.2	1.509	1.528	1.546	1.564	1.583	1.602	1.621	1.640	1.659	1.679	19
.3	1.698	1.718	1.738	1.758	1.779	1.799	1.820	1.841	1.862	1.883	21
.4	1.904	1.926	1.948	1.970	1.992	2.014	2.037	2.060	2.083	2.106	22
1.5	2.129	2.153	2.177	2.201	2.225	2.250	2.274	2.299	2.324	2.350	25
.6	2.376	2.401	2.428	2.454	2.481	2.507	2.535	2.562	2.590	2.617	27
.7	2.646	2.674	2.703	2.732	2.761	2.790	2.820	2.850	2.881	2.911	30
.8	2.942	2.973	3.005	3.037	3.069	3.101	3.134	3.167	3.200	3.234	33
.9	3.268	3.303	3.337	3.372	3.408	3.443	3.479	3.516	3.552	3.589	36
2.0	3.627	3.665	3.703	3.741	3.780	3.820	3.859	3.899	3.940	3.981	39
.1	4.022	4.064	4.106	4.148	4.191	4.234	4.278	4.322	4.367	4.412	44
.2	4.457	4.503	4.549	4.596	4.643	4.691	4.739	4.788	4.837	4.887	48
.3	4.937	4.988	5.039	5.090	5.142	5.195	5.248	5.302	5.356	5.411	53
.4	5.466	5.522	5.578	5.635	5.693	5.751	5.810	5.869	5.929	5.989	58
2.5	6.050	6.112	6.174	6.237	6.300	6.365	6.429	6.495	6.561	6.627	64
.6	6.695	6.763	6.831	6.901	6.971	7.042	7.113	7.185	7.258	7.332	71
.7	7.406	7.481	7.557	7.634	7.711	7.789	7.868	7.948	8.028	8.110	79
.8	8.192	8.275	8.359	8.443	8.529	8.615	8.702	8.790	8.879	8.969	87
.9	9.060	9.151	9.244	9.337	9.431	9.527	9.623	9.720	9.819	9.918	96
3.0	10.02	10.12	10.22	10.32	10.43	10.53	10.64	10.75	10.86	10.97	11
.1	11.08	11.19	11.30	11.42	11.53	11.65	11.76	11.88	12.00	12.12	12
.2	12.25	12.37	12.49	12.62	12.75	12.88	13.01	13.14	13.27	13.40	13
.3	13.54	13.67	13.81	13.95	14.09	14.23	14.38	14.52	14.67	14.82	14
.4	14.97	15.12	15.27	15.42	15.58	15.73	15.89	16.05	16.21	16.38	16
3.5	16.54	16.71	16.88	17.05	17.22	17.39	17.57	17.74	17.92	18.10	17
.6	18.29	18.47	18.66	18.84	19.03	19.22	19.42	19.61	19.81	20.01	19
.7	20.21	20.41	20.62	20.83	21.04	21.25	21.46	21.68	21.90	22.12	21
.8	22.34	22.56	22.79	23.02	23.25	23.49	23.72	23.96	24.20	24.45	24
.9	24.69	24.94	25.19	25.44	25.70	25.96	26.22	26.48	26.75	27.02	26
4.0	27.29	27.56	27.84	28.12	28.40	28.69	28.98	29.27	29.56	29.86	29
.1	30.16	30.47	30.77	31.08	31.39	31.71	32.03	32.35	32.68	33.00	32
.2	33.34	33.67	34.01	34.35	34.70	35.05	35.40	35.75	36.11	36.48	35
.3	36.84	37.21	37.59	37.97	38.35	38.73	39.12	39.52	39.91	40.31	39
.4	40.72	41.13	41.54	41.96	42.38	42.81	43.24	43.67	44.11	44.56	43
4.5	45.00	45.46	45.91	46.37	46.84	47.31	47.79	48.27	48.75	49.24	47
.6	49.74	50.24	50.74	51.25	51.77	52.29	52.81	53.34	53.88	54.42	52
.7	54.97	55.52	56.08	56.64	57.21	57.79	58.37	58.96	59.55	60.15	58
.8	60.75	61.36	61.98	62.60	63.23	63.87	64.51	65.16	65.81	66.47	64
.9	67.14	67.82	68.50	69.19	69.88	70.58	71.29	72.01	72.73	73.46	71
5.0	74.20										

If $x > 5$, $\sinh x = \frac{1}{2}(e^{x})$ and $\log_{10} \sinh x = (0.4343)x + 0.6990 - 1$, correct to four significant figures.

Hyperbolic cosines [$\cosh x = \frac{1}{2}(e^{x} + e^{-x})$]

x	0	1	2	3	4	5	6	7	8	9	avg diff
0.0	1.000	1.000	1.000	1.000	1.001	1.001	1.002	1.002	1.003	1.004	1
.1	1.005	1.006	1.007	1.008	1.010	1.011	1.013	1.014	1.016	1.018	2
.2	1.020	1.022	1.024	1.027	1.029	1.031	1.034	1.037	1.039	1.042	3
.3	1.045	1.048	1.052	1.055	1.058	1.062	1.066	1.069	1.073	1.077	4
.4	1.081	1.085	1.090	1.094	1.098	1.103	1.108	1.112	1.117	1.122	5
0.5	1.128	1.133	1.138	1.144	1.149	1.155	1.161	1.167	1.173	1.179	6
.6	1.185	1.192	1.198	1.205	1.212	1.219	1.226	1.233	1.240	1.248	7
.7	1.255	1.263	1.271	1.278	1.287	1.295	1.303	1.311	1.320	1.329	8
.8	1.337	1.346	1.355	1.365	1.374	1.384	1.393	1.403	1.413	1.423	10
.9	1.433	1.443	1.454	1.465	1.475	1.486	1.497	1.509	1.520	1.531	11
1.0	1.543	1.555	1.567	1.579	1.591	1.604	1.616	1.629	1.642	1.655	13
.1	1.669	1.682	1.696	1.709	1.723	1.737	1.752	1.766	1.781	1.796	14
.2	1.811	1.826	1.841	1.857	1.872	1.888	1.905	1.921	1.937	1.954	16
.3	1.971	1.988	2.005	2.023	2.040	2.058	2.076	2.095	2.113	2.132	18
.4	2.151	2.170	2.189	2.209	2.229	2.249	2.269	2.290	2.310	2.331	20
1.5	2.352	2.374	2.395	2.417	2.439	2.462	2.484	2.507	2.530	2.554	23
.6	2.577	2.601	2.625	2.650	2.675	2.700	2.725	2.750	2.776	2.802	25
.7	2.828	2.855	2.882	2.909	2.936	2.964	2.992	3.021	3.049	3.078	28
.8	3.107	3.137	3.167	3.197	3.228	3.259	3.290	3.321	3.353	3.385	31
.9	3.418	3.451	3.484	3.517	3.551	3.585	3.620	3.655	3.690	3.726	34
2.0	3.762	3.799	3.835	3.873	3.910	3.948	3.987	4.026	4.065	4.104	38
.1	4.144	4.185	4.226	4.267	4.309	4.351	4.393	4.436	4.480	4.524	42
.2	4.568	4.613	4.658	4.704	4.750	4.797	4.844	4.891	4.939	4.988	47
.3	5.037	5.087	5.137	5.188	5.239	5.290	5.343	5.395	5.449	5.503	52
.4	5.557	5.612	5.667	5.723	5.780	5.837	5.895	5.954	6.013	6.072	58
2.5	6.132	6.193	6.255	6.317	6.379	6.443	6.507	6.571	6.636	6.702	64
.6	6.769	6.836	6.904	6.973	7.042	7.112	7.183	7.255	7.327	7.400	70
.7	7.473	7.548	7.623	7.699	7.776	7.853	7.932	8.011	8.091	8.171	78
.8	8.253	8.335	8.418	8.502	8.587	8.673	8.759	8.847	8.935	9.024	86
.9	9.115	9.206	9.298	9.391	9.484	9.579	9.675	9.772	9.869	9.968	95
3.0	10.07	10.17	10.27	10.37	10.48	10.58	10.69	10.79	10.90	11.01	11
.1	11.12	11.23	11.35	11.46	11.57	11.69	11.81	11.92	12.04	12.16	12
.2	12.29	12.41	12.53	12.66	12.79	12.91	13.04	13.17	13.31	13.44	13
.3	13.57	13.71	13.85	13.99	14.13	14.27	14.41	14.56	14.70	14.85	14
.4	15.00	15.15	15.30	15.45	15.61	15.77	15.92	16.08	16.25	16.41	16
3.5	16.57	16.74	16.91	17.08	17.25	17.42	17.60	17.77	17.95	18.13	17
.6	18.31	18.50	18.68	18.87	19.06	19.25	19.44	19.64	19.84	20.03	19
.7	20.24	20.44	20.64	20.85	21.06	21.27	21.49	21.70	21.92	22.14	21
.8	22.36	22.59	22.81	23.04	23.27	23.51	23.74	23.98	24.22	24.47	23
.9	24.71	24.96	25.21	25.46	25.72	25.98	26.24	26.50	26.77	27.04	26
4.0	27.31	27.58	27.86	28.14	28.42	28.71	29.00	29.29	29.58	29.88	29
.1	30.18	30.48	30.79	31.10	31.41	31.72	32.04	32.37	32.69	33.02	32
.2	33.35	33.69	34.02	34.37	34.71	35.06	35.41	35.77	36.13	36.49	35
.3	36.86	37.23	37.60	37.98	38.36	38.75	39.13	39.53	39.93	40.33	39
.4	40.73	41.14	41.55	41.97	42.39	42.82	43.25	43.68	44.12	44.57	43
4.5	45.01	45.47	45.92	46.38	46.85	47.32	47.80	48.28	48.76	49.25	47
.6	49.75	50.25	50.75	51.26	51.78	52.30	52.82	53.35	53.89	54.43	52
.7	54.98	55.53	56.09	56.65	57.22	57.80	58.38	58.96	59.56	60.15	58
.8	60.76	61.37	61.99	62.61	63.24	63.87	64.52	65.16	65.82	66.48	64
.9	67.15	67.82	68.50	69.19	69.89	70.59	71.30	72.02	72.74	73.47	71
5.0	74.21										

If $x > 5$, $\cosh x = \frac{1}{2}(e^{x})$, and $\log_{10} \cosh x = (0.4343)x + 0.6990 - 1$, correct to four significant figures.

Hyperbolic tangents [tanh $x = (e^{x} - e^{-x})/(e^{x} + e^{-x}) = \sinh x/\cosh x$]

x	0	1	2	3	4	5	6	7	8	9	avg diff
0.0	.0000	.0100	.0200	.0300	.0400	.0500	.0599	.0699	.0798	.0898	100
.1	.0997	.1096	.1194	.1293	.1391	.1489	.1587	.1684	.1781	.1878	98
.2	.1974	.2070	.2165	.2260	.2355	.2449	.2543	.2636	.2729	.2821	94
.3	.2913	.3004	.3095	.3185	.3275	.3364	.3452	.3540	.3627	.3714	89
.4	.3800	.3885	.3969	.4053	.4136	.4219	.4301	.4382	.4462	.4542	82
0.5	.4621	.4700	.4777	.4854	.4930	.5005	.5080	.5154	.5227	.5299	75
.6	.5370	.5441	.5511	.5581	.5649	.5717	.5784	.5850	.5915	.5980	67
.7	.6044	.6107	.6169	.6231	.6291	.6352	.6411	.6469	.6527	.6584	60
.8	.6640	.6696	.6751	.6805	.6858	.6911	.6963	.7014	.7064	.7114	52
.9	.7163	.7211	.7259	.7306	.7352	.7398	.7443	.7487	.7531	.7574	45
1.0	.7616	.7658	.7699	.7739	.7779	.7818	.7857	.7895	.7932	.7969	39
.1	.8005	.8041	.8076	.8110	.8144	.8178	.8210	.8243	.8275	.8306	33
.2	.8337	.8367	.8397	.8426	.8455	.8483	.8511	.8538	.8565	.8591	28
.3	.8617	.8643	.8668	.8693	.8717	.8741	.8764	.8787	.8810	.8832	24
.4	.8854	.8875	.8896	.8917	.8937	.8957	.8977	.8996	.9015	.9033	20
1.5	.9052	.9069	.9087	.9104	.9121	.9138	.9154	.9170	.9186	.9202	17
.6	.9217	.9232	.9246	.9261	.9275	.9289	.9302	.9316	.9329	.9342	14
.7	.9354	.9367	.9379	.9391	.9402	.9414	.9425	.9436	.9447	.9458	11
.8	.9468	.9478	.9488	.9498	.9508	.9518	.9527	.9536	.9545	.9554	9
.9	.9562	.9571	.9579	.9587	.9595	.9603	.9611	.9619	.9626	.9633	8
2.0	.9640	.9647	.9654	.9661	.9668	.9674	.9680	.9687	.9693	.9699	6
.1	.9705	.9710	.9716	.9722	.9727	.9732	.9738	.9743	.9748	.9753	5
.2	.9757	.9762	.9767	.9771	.9776	.9780	.9785	.9789	.9793	.9797	4
.3	.9801	.9805	.9809	.9812	.9816	.9820	.9823	.9827	.9830	.9834	4
.4	.9837	.9840	.9843	.9846	.9849	.9852	.9855	.9858	.9861	.9863	3
2.5	.9866	.9869	.9871	.9874	.9876	.9879	.9881	.9884	.9886	.9888	2
.6	.9890	.9892	.9895	.9897	.9899	.9901	.9903	.9905	.9906	.9908	2
.7	.9910	.9912	.9914	.9915	.9917	.9919	.9920	.9922	.9923	.9925	2
.8	.9926	.9928	.9929	.9931	.9932	.9933	.9935	.9936	.9937	.9938	1
.9	.9940	.9941	.9942	.9943	.9944	.9945	.9946	.9947	.9949	.9950	1
3.0	.9951	.9959	.9967	.9973	.9978	.9982	.9985	.9988	.9990	.9992	4
4.0	.9993	.9995	.9996	.9996	.9997	.9998	.9998	.9998	.9999	.9999	1
5.0	.9999										

If $x > 5$, tanh x = 1.0000 to four decimal places.

Multiples of 0.4343 [0.43429448 = $\log_{10} e$]

x	0	1	2	3	4	5	6	7	8	9
0.0	0.0000	0.0434	0.0869	0.1303	0.1737	0.2171	0.2606	0.3040	0.3474	0.3909
1.0	0.4343	0.4777	0.5212	0.5646	0.6080	0.6514	0.6949	0.7383	0.7817	0.8252
2.0	0.8686	0.9120	0.9554	0.9989	1.0423	1.0857	1.1292	1.1726	1.2160	1.2595
3.0	1.3029	1.3463	1.3897	1.4332	1.4766	1.5200	1.5635	1.6069	1.6503	1.6937
4.0	1.7372	1.7806	1.8240	1.8675	1.9109	1.9543	1.9978	2.0412	2.0846	2.1280
5.0	2.1715	2.2149	2.2583	2.3018	2.3452	2.3886	2.4320	2.4755	2.5189	2.5623
6.0	2.6058	2.6492	2.6926	2.7361	2.7795	2.8229	2.8663	2.9098	2.9532	2.9966
7.0	3.0401	3.0835	3.1269	3.1703	3.2138	3.2572	3.3006	3.3441	3.3875	3.4309
8.0	3.4744	3.5178	3.5612	3.6046	3.6481	3.6915	3.7349	3.7784	3.8218	3.8652
9.0	3.9087	3.9521	3.9955	4.0389	4.0824	4.1258	4.1692	4.2127	4.2561	4.2995

Multiples of 2.3026 [2.3025851 = 1/0.4343 = $\log_e 10$]

x	0	1	2	3	4	5	6	7	8	9
0.0	0.0000	0.2303	0.4605	0.6908	0.9210	1.1513	1.3816	1.6118	1.8421	2.0723
1.0	2.3026	2.5328	2.7631	2.9934	3.2236	3.4539	3.6841	3.9144	4.1447	4.3749
2.0	4.6052	4.8354	5.0657	5.2959	5.5262	5.7565	5.9867	6.2170	6.4472	6.6775
3.0	6.9078	7.1380	7.3683	7.5985	7.8288	8.0590	8.2893	8.5196	8.7498	8.9801
4.0	9.2103	9.4406	9.6709	9.9011	10.131	10.362	10.592	10.822	11.052	11.283
5.0	11.513	11.743	11.973	12.204	12.434	12.664	12.894	13.125	13.355	13.585
6.0	13.816	14.046	14.276	14.506	14.737	14.967	15.197	15.427	15.658	15.888
7.0	16.118	16.348	16.579	16.809	17.039	17.269	17.500	17.730	17.960	18.190
8.0	18.421	18.651	18.881	19.111	19.342	19.572	19.802	20.032	20.263	20.493
9.0	20.723	20.954	21.184	21.414	21.644	21.875	22.105	22.335	22.565	22.796

Table of random digits*

49	31	97	45	80	57	47	01	46	00	57	16	83	04	58	23	89	20	78	25	18	53	20	38	74	66	22	07	90	50	29	22	37	05	41	67	11	58	45	84
88	78	67	69	63	12	12	72	50	14	71	88	66	53	34	38	01	30	93	79	22	93	62	20	58	49	17	11	10	27	22	68	18	01	10	31	59	50	92	46
84	86	69	52	02	43	98	37	26	55	40	41	85	95	04	52	38	30	72	32	66	39	77	65	10	81	15	00	07	04	74	58	09	03	54	43	74	42	21	78
11	84	92	64	82	20	46	19	94	50	28	83	37	66	61	47	27	79	29	35	89	73	02	32	72	65	42	03	50	91	69	09	37	13	64	08	10	79	69	52
54	96	61	75	94	57	39	37	32	67	37	88	36	21	24	62	19	94	95	42	81	82	17	53	23	96	06	89	17	24	40	45	69	12	34	58	09	06	53	42
10	95	93	33	49	80	71	99	67	51	44	88	23	35	92	66	23	41	38	21	94	37	78	25	54	53	58	61	14	32	72	92	76	73	49	83	96	25	89	12
22	78	40	77	83	35	90	30	00	91	19	08	21	38	73	07	18	42	15	66	68	48	54	99	91	53	16	51	98	65	61	86	93	30	93	81	12	90	64	81
86	03	76	17	91	33	81	56	39	68	45	31	62	92	83	89	31	85	58	06	07	33	00	71	84	86	78	86	45	77	40	04	81	65	20	07	63	81	07	97
80	03	76	50	89	85	91	97	43	91	22	78	85	54	33	31	18	87	48	82	10	99	31	49	30	35	07	23	64	29	68	77	39	76	69	28	65	68	99	38
72	75	18	43	59	15	76	91	36	15	08	29	38	61	93	05	02	62	12	55	20	80	11	51	78	64	45	38	33	57	09	77	43	07	51	49	74	01	13	85
79	24	13	53	47	66	85	17	92	47	46	13	93	66	89	82	58	71	35	86	93	36	91	30	44	69	68	67	81	62	66	37	80	29	19	34	01	25	00	80
43	59	33	95	55	97	34	55	84	94	26	56	69	53	23	32	99	38	99	88	19	36	05	50	49	94	95	17	63	41	84	01	93	06	90	25	65	67	29	96
29	52	26	27	13	33	70	11	71	86	06	76	55	71	41	48	61	71	82	82	47	79	88	98	90	06	89	36	54	83	17	70	12	12	92	14	88	01	53	86
88	83	64	72	90	67	27	47	83	62	35	38	49	03	80	12	31	78	97	02	69	22	33	20	07	03	51	36	11	49	32	54	69	20	72	62	52	22	15	04
65	90	56	62	53	91	48	23	06	89	49	33	37	84	82	36	19	91	13	55	34	51	15	07	21	84	85	03	41	59	97	13	86	19	19	97	78	92	85	75
44	79	86	93	71	07	86	59	17	56	45	59	51	40	44	56	80	69	91	26	54	03	15	93	29	58	96	35	22	20	35	29	22	79	24	55	46	74	30	36
35	51	09	91	39	32	03	12	79	25	79	81	91	50	54	76	17	41	22	06	66	72	28	55	15	04	72	39	24	11	02	73	70	81	68	30	04	36	34	50
50	12	59	32	23	64	20	94	97	14	11	97	16	22	34	74	85	74	64	01	71	05	90	74	96	38	40	41	81	26	28	26	13	78	44	12	54	31	43	98
25	17	39	00	38	63	87	14	04	18	11	45	28	93	18	53	08	42	19	93	45	47	88	60	66	31	13	53	32	43	80	57	33	06	06	48	64	45	30	08
68	45	99	00	94	44	99	59	37	18	38	74	68	12	71	96	26	09	81	37	97	24	69	11	21	89	43	72	03	93	77	15	38	85	52	26	84	31	28	44
22	98	22	59	36	96	41	73	48	45	85	14	95	75	04	15	05	93	68	49	84	98	36	83	12	25	51	95	61	58	86	30	00	76	89	14	00	67	77	53
48	24	36	29	93	47	13	28	52	48	35	22	97	28	37	36	75	27	16	55	35	55	40	29	35	72	88	96	87	72	19	85	03	96	50	65	22	21	55	63
93	51	41	49	15	67	96	08	22	03	40	11	72	43	46	32	18	98	70	74	04	36	81	76	32	50	96	27	19	08	94	46	46	64	32	62	24	31	36	74
69	70	79	83	03	93	06	91	62	16	60	87	59	75	45	68	65	29	21	60	81	31	16	04	79	69	98	53	09	52	23	92	14	97	30	21	71	89	23	14
87	46	79	17	94	70	81	41	27	43	03	76	93	25	51	74	80	14	16	92	03	82	38	98	87	55	82	87	44	52	72	77	52	37	16	42	85	37	47	93
81	00	68	14	98	59	37	53	05	02	94	07	79	22	09	31	50	66	96	06	80	42	26	54	37	38	79	75	62	61	27	81	64	67	04	82	73	50	33	39
15	45	88	14	81	50	18	74	33	75	94	37	60	06	66	94	14	52	23	99	61	30	74	94	68	43	34	44	37	00	20	20	77	70	88	17	16	72	45	31
33	46	91	25	10	23	09	54	80	16	42	35	41	13	47	90	92	00	38	64	83	87	38	25	57	10	00	28	00	93	59	28	30	44	94	60	72	52	14	31
67	19	80	71	76	65	99	61	83	17	81	14	94	32	91	10	81	74	43	48	38	11	01	68	55	28	92	29	37	58	88	73	13	63	16	51	38	35	76	19
58	03	79	22	61	85	50	45	56	90	10	63	17	82	38	00	15	74	62	59	43	89	29	11	89	87	22	65	69	35	84	76	26	79	36	75	00	00	17	95
93	68	30	96	64	53	92	74	98	85	20	75	49	23	55	57	95	51	09	40	14	95	42	22	99	40	15	65	26	85	29	22	33	83	83	30	31	57	09	99
32	74	80	21	21	11	97	29	69	14	28	06	56	95	64	06	83	55	68	45	01	71	19	84	39	09	44	63	39	37	49	09	54	02	38	81	69	71	24	74
49	21	19	29	63	38	62	56	53	12	62	17	57	33	53	84	97	21	77	26	62	32	85	53	28	45	73	89	39	40	27	46	62	69	27	53	34	51	13	79
63	36	56	42	24	69	47	55	75	12	11	04	45	04	83	68	82	19	74	26	73	00	46	21	09	81	90	77	10	77	57	46	37	00	45	65	12	34	90	70
63	57	62	63	73	44	61	04	37	48	00	33	16	34	22	99	62	27	67	57	34	21	88	94	45	05	60	95	23	36	50	55	89	22	42	52	73	28	15	02
41	07	84	70	36	65	52	46	84	66	67	15	72	64	19	37	97	81	65	11	99	15	90	19	68	45	88	68	68	75	28	41	39	59	18	44	15	64	69	59
70	84	68	95	58	64	17	31	53	81	87	71	35	08	41	46	27	02	65	08	92	85	82	99	49	15	81	79	33	72	56	65	74	31	93	58	13	05	42	73
68	80	06	44	92	20	16	23	27	07	10	28	18	25	25	74	15	58	67	49	27	39	69	74	77	65	55	47	16	01	13	12	16	88	67	95	76	35	96	67
44	97	78	95	25	51	26	96	37	47	91	36	77	40	33	67	02	06	90	92	37	10	34	53	09	30	12	94	33	80	96	99	68	93	56	22	78	46	01	84
79	35	46	38	47	24	39	55	36	79	40	56	03	69	14	69	17	63	19	18	57	34	79	70	12	48	42	82	06	06	60	74	22	22	26	89	99	32	45	97

* Reprinted by permission from "The Compleat Strategyst," by J. D. Williams. Copyright, 1954. McGraw-Hill Book Company, Inc.

Exponentials [e^n and e^{-n}]

n	e^n	diff	n	e^n	diff	n	e^n (*)	n	e^{-n}	diff	n	e^{-n}	n	e^{-n} (*)
0.00	1.000	10	**0.50**	1.649	16	**1.0**	2.718	**0.00**	1.000	−10	**0.50**	.607	**1.0**	.368
.01	1.010	10	.51	1.665	17	.1	3.004	.01	0.990	−10	.51	.600	.1	.333
.02	1.020	10	.52	1.682	17	.2	3.320	.02	.980	−10	.52	.595	.2	.301
.03	1.030	11	.53	1.699	17	.3	3.669	.03	.970	− 9	.53	.589	.3	.273
.04	1.041	10	.54	1.716	17	.4	4.055	.04	.961	−10	.54	.583	.4	.247
0.05	1.051	11	**0.55**	1.733	18	**1.5**	4.482	**0.05**	.951	− 9	**0.55**	.577	**1.5**	.223
.06	1.062	11	.56	1.751	17	.6	4.953	.06	.942	−10	.56	.571	.6	.202
.07	1.073	10	.57	1.768	18	.7	5.474	.07	.932	− 9	.57	.566	.7	.183
.08	1.083	11	.58	1.786	18	.8	6.050	.08	.923	− 9	.58	.560	.8	.165
.09	1.094	11	.59	1.804	18	.9	6.686	.09	.914	− 9	.59	.554	.9	.150
0.10	1.105	11	**0.60**	1.822	18	**2.0**	7.389	**0.10**	.905	− 9	**0.60**	.549	**2.0**	.135
.11	1.116	11	.61	1.840	19	.1	8.166	.11	.896	− 9	.61	.543	.1	.122
.12	1.127	12	.62	1.859	19	.2	9.025	.12	.887	− 9	.62	.538	.2	.111
.13	1.139	11	.63	1.878	18	.3	9.974	.13	.878	− 9	.63	.533	.3	.100
.14	1.150	12	.64	1.896	20	.4	11.02	.14	.869	− 8	.64	.527	.4	.0907
0.15	1.162	12	**0.65**	1.916	19	**2.5**	12.18	**0.15**	.861	− 9	**0.65**	.522	**2.5**	.0821
.16	1.174	11	.66	1.935	19	.6	13.46	.16	.852	− 8	.66	.517	.6	.0743
.17	1.185	12	.67	1.954	20	.7	14.88	.17	.844	− 9	.67	.512	.7	.0672
.18	1.197	12	.68	1.974	20	.8	16.44	.18	.835	− 8	.68	.507	.8	.0608
.19	1.209	12	.69	1.994	20	.9	18.17	.19	.827	− 8	.69	.502	.9	.0550
0.20	1.221	13	**0.70**	2.014	20	**3.0**	20.09	**0.20**	.819	− 8	**0.70**	.497	**3.0**	.0498
.21	1.234	12	.71	2.034	20	.1	22.20	.21	.811	− 8	.71	.492	.1	.0450
.22	1.246	13	.72	2.054	21	.2	24.53	.22	.803	− 8	.72	.487	.2	.0408
.23	1.259	12	.73	2.075	21	.3	27.11	.23	.795	− 8	.73	.482	.3	.0369
.24	1.271	13	.74	2.096	21	.4	29.96	.24	.787	− 8	.74	.477	.4	.0334
0.25	1.284	13	**0.75**	2.117	21	**3.5**	33.12	**0.25**	.779	− 8	**0.75**	.472	**3.5**	.0302
.26	1.297	13	.76	2.138	22	.6	36.60	.26	.771	− 8	.76	.468	.6	.0273
.27	1.310	13	.77	2.160	21	.7	40.45	.27	.763	− 7	.77	.463	.7	.0247
.28	1.323	13	.78	2.181	22	.8	44.70	.28	.756	− 8	.78	.458	.8	.0224
.29	1.336	14	.79	2.203	23	.9	49.40	.29	.748	− 7	.79	.454	.9	.0202
0.30	1.350	13	**0.80**	2.226	22	**4.0**	54.60	**0.30**	.741	− 8	**0.80**	.449	**4.0**	.0183
.31	1.363	14	.81	2.248	22	.1	60.34	.31	.733	− 7	.81	.445	.1	.0166
.32	1.377	14	.82	2.270	23	.2	66.69	.32	.726	− 7	.82	.440	.2	.0150
.33	1.391	14	.83	2.293	23	.3	73.70	.33	.719	− 7	.83	.436	.3	.0136
.34	1.405	14	.84	2.316	24	.4	81.45	.34	.712	− 7	.84	.432	.4	.0123
0.35	1.419	14	**0.85**	2.340	23	**4.5**	90.02	**0.35**	.705	− 7	**0.85**	.427	**4.5**	.0111
.36	1.433	15	.86	2.363	24			.36	.698	− 7	.86	.423		
.37	1.448	14	.87	2.387	24	**5.0**	148.4	.37	.691	− 7	.87	.419	**5.0**	.00674
.38	1.462	15	.88	2.411	24	**6.0**	403.4	.38	.684	− 7	.88	.415	**6.0**	.00248
.39	1.477	15	.89	2.435	25	**7.0**	1097.	.39	.677	− 7	.89	.411	**7.0**	.000912
0.40	1.492	15	**0.90**	2.460	24	**8.0**	2981.	**0.40**	.670	− 6	**0.90**	.407	**8.0**	.000335
.41	1.507	15	.91	2.484	25	**9.0**	8103.	.41	.664	− 7	.91	.403	**9.0**	.000123
.42	1.522	15	.92	2.509	26	**10.0**	22026.	.42	.657	− 6	.92	.399	**10.0**	.000045
.43	1.537	16	.93	2.535	25			.43	.651	− 7	.93	.395		
.44	1.553	15	.94	2.560	26	$\pi/2$	4.810	.44	.644	− 6	.94	.391	$\pi/2$	.208
						$2\pi/2$	23.14						$2\pi/2$	.0432
0.45	1.568	16	**0.95**	2.586	26	$3\pi/2$	111.3	**0.45**	.638	− 7	**0.95**	.387	$3\pi/2$	.00898
.46	1.584	16	.96	2.612	26	$4\pi/2$	535.5	.46	.631	− 6	.96	.383	$4\pi/2$	.00187
.47	1.600	16	.97	2.638	26	$5\pi/2$	2576.	.47	.625	− 6	.97	.379	$5\pi/2$	.000388
.48	1.616	16	.98	2.664	27	$6\pi/2$	12392.	.48	.619	− 6	.98	.375	$6\pi/2$	.000081
.49	1.632	17	.99	2.691	27	$7\pi/2$	59610.	.49	.613	− 6	.99	.372	$7\pi/2$	.000017
						$8\pi/2$	286751.						$8\pi/2$	.000003
0.50	1.649		**1.00**	2.718				**0.50**	0.607		**1.00**	.368		

* Note: Do not interpolate in this column.

Properties of e are listed on p. 1040.

Normal probability density function

$$\varphi(x) = \frac{1}{(2\pi)^{1/2}} \exp - \frac{x^2}{2}$$

(Standard deviation $\sigma = 1$)

x	$\varphi(x)$	x	$\varphi(x)$	x	$\varphi(x)$	x	$\varphi(x)$
0.0	0.3989	1.0	0.2420	2.0	0.0540	3.0	0.0044
0.1	0.3970	1.1	0.2179	2.1	0.0440	3.1	0.0033
0.2	0.3910	1.2	0.1942	2.2	0.0355	3.2	0.0024
0.3	0.3814	1.3	0.1714	2.3	0.0283	3.3	0.0017
0.4	0.3683	1.4	0.1497	2.4	0.0224	3.4	0.0012
0.5	0.3521	1.5	0.1295	2.5	0.0175	3.5	0.0009
0.6	0.3332	1.6	0.1109	2.6	0.0136	3.6	0.0006
0.7	0.3123	1.7	0.0940	2.7	0.0104	3.7	0.0004
0.8	0.2897	1.8	0.0790	2.8	0.0079	3.8	0.0003
0.9	0.2661	1.9	0.0656	2.9	0.0060	3.9	0.0002
						4.0	0.0001

Probability of deviation from mean in normal distribution

The probability that the absolute deviation from the mean $|x - \mu|$ exceeds t times the standard deviation σ is $p/100$.

t	$p(t)$	t	$p(t)$
0.0	100.000	2.2	2.781
0.2	84.148	2.4	1.640
0.4	68.916	2.6	0.932
0.6	54.851	2.8	0.511
0.8	42.371	3.0	0.270
1.0	31.731	3.2	0.137
1.2	23.014	3.4	0.067
1.4	16.151	3.6	0.032
1.6	10.960	3.8	0.014
1.8	7.186	4.0	0.006
2.0	4.550		

p	$t(p)$	p	$t(p)$
100	0.0000	40	0.8416
95	0.0627	35	0.9346
90	0.1257	30	1.0364
85	0.1891	25	1.1503
80	0.2533	20	1.2816
75	0.3186	15	1.4395
70	0.3853	10	1.6449
65	0.4538	5	1.9600
60	0.5244	1	2.5758
55	0.5978	0.1	3.2905
50	0.6745	0.01	3.8906
45	0.7554	0.001	4.4172

Cumulative normal distribution function

$$\Phi(x) = \frac{1}{\sigma(2\pi)^{1/2}} \int_{-\infty}^{x} \exp - \tfrac{1}{2} \left(\frac{x-\mu}{\sigma} \right)^2 dx$$

x	Φ(x)	x	Φ(x)	x	Φ(x)
$\mu - 4.0\sigma$	3×10^{-5}	$\mu - 1.3\sigma$	0.0968	$\mu + 1.4\sigma$	0.9192
$\mu - 3.9\sigma$	5×10^{-5}	$\mu - 1.2\sigma$	0.1151	$\mu + 1.5\sigma$	0.9332
$\mu - 3.8\sigma$	7×10^{-5}	$\mu - 1.1\sigma$	0.1357	$\mu + 1.6\sigma$	0.9452
$\mu - 3.7\sigma$	0.0001	$\mu - 1.0\sigma$	0.1587	$\mu + 1.7\sigma$	0.9554
$\mu - 3.6\sigma$	0.0002	$\mu - 0.9\sigma$	0.1841	$\mu + 1.8\sigma$	0.9641
$\mu - 3.5\sigma$	0.0002	$\mu - 0.8\sigma$	0.2119	$\mu + 1.9\sigma$	0.9713
$\mu - 3.4\sigma$	0.0003	$\mu - 0.7\sigma$	0.2420	$\mu + 2.0\sigma$	0.9772
$\mu - 3.3\sigma$	0.0005	$\mu - 0.6\sigma$	0.2743	$\mu + 2.1\sigma$	0.9821
$\mu - 3.2\sigma$	0.0007	$\mu - 0.5\sigma$	0.3085	$\mu + 2.2\sigma$	0.9861
$\mu - 3.1\sigma$	0.0010	$\mu - 0.4\sigma$	0.3446	$\mu + 2.3\sigma$	0.9893
$\mu - 3.0\sigma$	0.0013	$\mu - 0.3\sigma$	0.3821	$\mu + 2.4\sigma$	0.9918
$\mu - 2.9\sigma$	0.0019	$\mu - 0.2\sigma$	0.4207	$\mu + 2.5\sigma$	0.9938
$\mu - 2.8\sigma$	0.0026	$\mu - 0.1\sigma$	0.4602	$\mu + 2.6\sigma$	0.9953
$\mu - 2.7\sigma$	0.0035	μ	0.5000	$\mu + 2.7\sigma$	0.9965
$\mu - 2.6\sigma$	0.0047	$\mu + 0.1\sigma$	0.5398	$\mu + 2.8\sigma$	0.9974
$\mu - 2.5\sigma$	0.0062	$\mu + 0.2\sigma$	0.5793	$\mu + 2.9\sigma$	0.9981
$\mu - 2.4\sigma$	0.0082	$\mu + 0.3\sigma$	0.6179	$\mu + 3.0\sigma$	0.9987
$\mu - 2.3\sigma$	0.0107	$\mu + 0.4\sigma$	0.6554	$\mu + 3.1\sigma$	0.9990
$\mu - 2.2\sigma$	0.0139	$\mu + 0.5\sigma$	0.6915	$\mu + 3.2\sigma$	0.9993
$\mu - 2.1\sigma$	0.0179	$\mu + 0.6\sigma$	0.7257	$\mu + 3.3\sigma$	0.9995
$\mu - 2.0\sigma$	0.0228	$\mu + 0.7\sigma$	0.7580	$\mu + 3.4\sigma$	0.9997
$\mu - 1.9\sigma$	0.0287	$\mu + 0.8\sigma$	0.7881	$\mu + 3.5\sigma$	0.9998
$\mu - 1.8\sigma$	0.0359	$\mu + 0.9\sigma$	0.8159	$\mu + 3.6\sigma$	0.9998
$\mu - 1.7\sigma$	0.0446	$\mu + 1.0\sigma$	0.8413	$\mu + 3.7\sigma$	0.9999
$\mu - 1.6\sigma$	0.0548	$\mu + 1.1\sigma$	0.8643	$\mu + 3.8\sigma$	$1 - (7 \times 10^{-5})$
$\mu - 1.5\sigma$	0.0668	$\mu + 1.2\sigma$	0.8849	$\mu + 3.9\sigma$	$1 - (5 \times 10^{-5})$
$\mu - 1.4\sigma$	0.0808	$\mu + 1.3\sigma$	0.9032	$\mu + 4.0\sigma$	$1 - (3 \times 10^{-5})$

Bessel functions*

Table I—$J_0(z)$

z	0	0.1	0.2	0.3	0.4	0.5	0.6	0.7	0.8	0.9
0	1.0000	0.9975	0.9900	0.9776	0.9604	0.9385	0.9120	0.8812	0.8463	0.8075
1	0.7652	0.7196	0.6711	0.6201	0.5669	0.5118	0.4554	0.3980	0.3400	0.2818
2	0.2239	0.1666	0.1104	0.0555	0.0025	−0.0484	−0.0968	−0.1424	−0.1850	−0.2243
3	−0.2601	−0.2921	−0.3202	−0.3443	−0.3643	−0.3801	−0.3918	−0.3992	−0.4026	−0.4018
4	−0.3971	−0.3887	−0.3766	−0.3610	−0.3423	−0.3205	−0.2961	−0.2693	−0.2404	−0.2097
5	−0.1776	−0.1443	−0.1103	−0.0758	−0.0412	−0.0068	+0.0270	0.0599	0.0917	0.1220
6	0.1506	0.1773	0.2017	0.2238	0.2433	0.2601	0.2740	0.2851	0.2931	0.2981
7	0.3001	0.2991	0.2951	0.2882	0.2786	0.2663	0.2516	0.2346	0.2154	0.1944
8	0.1717	0.1475	0.1222	0.0960	0.0692	0.0419	0.0146	−0.0125	−0.0392	−0.0653
9	−0.0903	−0.1142	−0.1367	−0.1577	−0.1768	−0.1939	−0.2090	−0.2218	−0.2323	−0.2403
10	−0.2459	−0.2490	−0.2496	−0.2477	−0.2434	−0.2366	−0.2276	−0.2164	−0.2032	−0.1881
11	−0.1712	−0.1528	−0.1330	−0.1121	−0.0902	−0.0677	−0.0446	−0.0213	+0.0020	0.0250
12	0.0477	0.0697	0.0908	0.1108	0.1296	0.1469	0.1626	0.1766	0.1887	0.1988
13	0.2069	0.2129	0.2167	0.2183	0.2177	0.2150	0.2101	0.2032	0.1943	0.1836
14	0.1711	0.1570	0.1414	0.1245	0.1065	0.0875	0.0679	0.0476	0.0271	0.0064
15	−0.0142	−0.0346	−0.0544	−0.0736	−0.0919	−0.1092	−0.1253	−0.1401	−0.1533	−0.1650

* See also discussion and graph on Bessel functions on p. 1066.

Table II—$J_1(z)$ *continued*

Bessel functions

x	0	0.1	0.2	0.3	0.4	0.5	0.6	0.7	0.8	0.9
0	0.0000	0.0499	0.0995	0.1483	0.1960	0.2423	0.2867	0.3290	0.3688	0.4059
1	0.4401	0.4709	0.4983	0.5220	0.5419	0.5579	0.5699	0.5778	0.5815	0.5812
2	0.5767	0.5683	0.5560	0.5399	0.5202	0.4971	0.4708	0.4416	0.4097	0.3754
3	0.3391	0.3009	0.2613	0.2207	0.1792	0.1374	0.0955	0.0538	0.0128	−0.0272
4	−0.0660	−0.1033	−0.1386	−0.1719	−0.2028	−0.2311	−0.2566	−0.2791	−0.2985	−0.3147
5	−0.3276	−0.3371	−0.3432	−0.3460	−0.3453	−0.3414	−0.3343	−0.3241	−0.3110	−0.2951
6	−0.2767	−0.2559	−0.2329	−0.2081	−0.1816	−0.1538	−0.1250	−0.0953	−0.0652	−0.0349
7	−0.0047	+0.0252	0.0543	0.0826	0.1096	0.1352	0.1592	0.1813	0.2014	0.2192
8	0.2346	0.2476	0.2580	0.2657	0.2708	0.2731	0.2728	0.2697	0.2641	0.2559
9	0.2453	0.2324	0.2174	0.2004	0.1816	0.1613	0.1395	0.1166	0.0928	0.0684
10	0.0435	0.0184	−0.0066	−0.0313	−0.0555	−0.0789	−0.1012	−0.1224	−0.1422	−0.1603
11	−0.1768	−0.1913	−0.2039	−0.2143	−0.2225	−0.2284	−0.2320	−0.2333	−0.2323	−0.2290
12	−0.2234	−0.2157	−0.2060	−0.1943	−0.1807	−0.1655	−0.1487	−0.1307	−0.1114	−0.0912
13	−0.0703	−0.0489	−0.0271	−0.0052	+0.0166	0.0380	0.0590	0.0791	0.0984	0.1165
14	0.1334	0.1488	0.1626	0.1747	0.1850	0.1934	0.1999	0.2043	0.2066	0.2069
15	0.2051	0.2013	0.1955	0.1879	0.1784	0.1672	0.1544	0.1402	0.1247	0.1080

Index

A

B

L

M

N

O

Q

R

S

T

U

V